

1N-22070

NASA Technical Memorandum 87263

# Bibliography of Lewis Research Center Technical Publications Announced in 1985

(NASA-TM-87263) BIBLIOGRAPHY OF LEWIS  
RESEARCH CENTER TECHNICAL PUBLICATIONS  
ANNOUNCED IN 1985 (NASA) 307 p CSCL 05B  
N86-32336  
Unclas  
G3/82 43097

May 1986

**NASA**

## **PREFACE**

In 1985, Lewis Research Center's 1127 research authors published 422 technical publications which were announced to and reached the worldwide scientific community. The 422 papers included 197 symposium/seminar presentations and 74 articles sent directly to journals for publication. In 1985, Lewis authors published approximately 65 percent of their research contributions in outside publications and the remainder as NASA research reports. Sixty percent of Lewis-authored society presentations and journal articles were addressed to members of the following technical societies: AIAA, 65 papers; ASME, 62 papers; SAE, 24 papers; IEEE, 18 papers; ACS (American Ceramic Society), 17 papers; ASM, 17 papers; ASLE, 13 papers; AVS (American Vacuum Society), 12 papers.

In 1985, 220 contractor-authored research reports were produced. In addition, 6 patent applications were filed and 25 patents were issued.

Many Lewis authors have received awards for their contributions; among them are the following:

The 1985 Lewis Distinguished Paper Award was presented to Robert A. Miller for his paper entitled "An Oxidation-Based Model for Thermal Barrier Coating Life" which was published in the Journal of the American Ceramic Society. James A. DiCarlo's paper "Fibers for Structurally Reliable Metal and Ceramic Composites" was the most popular technical article in 1985 according to the Journal of Metals.

A few Lewis-authored publications are not included in this compilation due to FEDD (For Early Domestic Dissemination) and ITAR (International Traffic in Arms Regulations) considerations which limit their announcement and distribution.

All the publications in this collection were announced in the 1985 issues of STAR (Scientific and Technical Aerospace Reports) and IAA (International Aerospace Abstracts).

The arrangement of the material is by NASA subject category, as noted in the Contents. The various indexes will help locate specific publications by subject, author, contractor organization, contract number, and report number.

George Mandel  
Chief, Technical Information Services Division



# TABLE OF CONTENTS

## PREFACE

Includes aeronautics (general); aerodynamics; air transportation and safety; aircraft communications and navigation; aircraft design, testing and performance; aircraft instrumentation; aircraft propulsion and power; aircraft stability and control; and research and support facilities (air).

For related information see also *Astronautics*.

## 01 AERONAUTICS (GENERAL) 1

## 02 AERODYNAMICS 1

Includes aerodynamics of bodies, combinations, wings, rotors, and control surfaces; and internal flow in ducts and turbomachinery.

For related information see also *34 Fluid Mechanics and Heat Transfer*.

## 03 AIR TRANSPORTATION AND SAFETY 10

Includes passenger and cargo air transport operations; and aircraft accidents.

For related information see also *16 Space Transportation and 85 Urban Technology and Transportation*.

## 04 AIRCRAFT COMMUNICATIONS AND NAVIGATION N.A.

Includes digital and voice communication with aircraft; air navigation systems (satellite and ground based); and air traffic control.

For related information see also *17 Spacecraft Communications, Command and Tracking and 32 Communications*.

## 05 AIRCRAFT DESIGN, TESTING AND PERFORMANCE 12

Includes aircraft simulation technology.

For related information see also *18 Spacecraft Design, Testing and Performance and 39 Structural Mechanics*.

## 06 AIRCRAFT INSTRUMENTATION 13

Includes cockpit and cabin display devices; and flight instruments.

For related information see also *19 Spacecraft Instrumentation and 35 Instrumentation and Photography*.

## 07 AIRCRAFT PROPULSION AND POWER 13

Includes prime propulsion systems and systems components, e.g., gas turbine engines and compressors; and on-board auxiliary power plants for aircraft.

For related information see also *20 Spacecraft Propulsion and Power, 28 Propellants and Fuels, and 44 Energy Production and Conversion*.

## 08 AIRCRAFT STABILITY AND CONTROL 34

Includes aircraft handling qualities; piloting; flight controls; and autopilots.

## 09 RESEARCH AND SUPPORT FACILITIES (AIR) 34

Includes airports, hangars and runways; aircraft repair and overhaul facilities; wind tunnels; shock tube facilities; and engine test blocks.

For related information see also *14 Ground Support Systems and Facilities (Space)*.

## ASTRONAUTICS

Includes astronautics (general); astrodynamics; ground support systems and facilities (space); launch vehicles and space vehicles; space transportation; spacecraft communications, command and tracking; spacecraft design, testing and performance; spacecraft instrumentation; and spacecraft propulsion and power.

For related information see also *Aeronautics*.

## 12 ASTRONAUTICS (GENERAL) 35

For extraterrestrial exploration see *91 Lunar and Planetary Exploration*.

## 13 ASTRODYNAMICS 36

Includes powered and free-flight trajectories; and orbit and launching dynamics.

## 14 GROUND SUPPORT SYSTEMS AND FACILITIES (SPACE) N.A.

Includes launch complexes, research and production facilities; ground support equipment, e.g., mobile transporters; and simulators.

For related information see also *09 Research and Support Facilities (Air)*.

## 15 LAUNCH VEHICLES AND SPACE VEHICLES 36

Includes boosters; manned orbital laboratories; reusable vehicles; and space stations.

## 16 SPACE TRANSPORTATION 38

Includes passenger and cargo space transportation, e.g., shuttle operations; and rescue techniques.

For related information see also *03 Air Transportation and Safety and 85 Urban Technology and Transportation*.

## 17 SPACECRAFT COMMUNICATION, COMMAND AND TRACKING 38

Includes telemetry; space communications networks; astromavigation; and radio blackout.

For related information see also *04 Aircraft Communications and Navigation and 32 Communications*.

## 18 SPACECRAFT DESIGN, TESTING AND PERFORMANCE 38

Includes spacecraft thermal and environmental control; and attitude control.

For life support systems see *54 Man/System Technology and Life Support*. For related information see also *05 Aircraft Design, Testing and Performance and 39 Structural Mechanics*.

## 19 SPACECRAFT INSTRUMENTATION 41

For related information see also *06 Aircraft Instrumentation and 35 Instrumentation and Photography*.

## 20 SPACECRAFT PROPULSION AND POWER 41

Includes main propulsion systems and components, e.g., rocket engines; and spacecraft auxiliary power sources.

For related information see also *07 Aircraft Propulsion and Power, 28 Propellants and Fuels, and 44 Energy Production and Conversion*.

## CHEMISTRY AND MATERIALS

Includes chemistry and materials (general); composite materials; inorganic and physical chemistry; metallic materials; nonmetallic materials; and propellants and fuels.

### 23 CHEMISTRY AND MATERIALS (GENERAL) 53

Includes biochemistry and organic chemistry.

### 24 COMPOSITE MATERIALS 54

Includes laminates.

### 25 INORGANIC AND PHYSICAL CHEMISTRY 59

Includes chemical analysis, e.g., chromatography; combustion theory; electrochemistry; and photochemistry.

For related information see also *77 Thermodynamics and Statistical Physics*.

### 26 METALLIC MATERIALS 64

Includes physical, chemical, and mechanical properties of metals, e.g., corrosion; and metallurgy.

### 27 NONMETALLIC MATERIALS 78

Includes physical, chemical, and mechanical properties of plastics, elastomers, lubricants, polymers, textiles, adhesives, and ceramic materials.

### 28 PROPELLANTS AND FUELS 92

Includes rocket propellants, igniters, and oxidizers; storage and handling; and aircraft fuels.

For related information see also *07 Aircraft Propulsion and Power*, *20 Spacecraft Propulsion and Power*, and *44 Energy Production and Conversion*.

## ENGINEERING

Includes engineering (general); communications; electronics and electrical engineering; fluid mechanics and heat transfer; instrumentation and photography; lasers and masers; mechanical engineering; quality assurance and reliability; and structural mechanics.

For related information see also *Physics*.

### 31 ENGINEERING (GENERAL) 94

Includes vacuum technology; control engineering; display engineering; and cryogenics.

### 32 COMMUNICATIONS 95

Includes land and global communications; communications theory; and optical communications.

For related information see also *04 Aircraft Communications and Navigation* and *17 Spacecraft Communications, Command and Tracking*.

### 33 ELECTRONICS AND ELECTRICAL ENGINEERING 100

Includes test equipment and maintainability; components, e.g., tunnel diodes and transistors; microminiaturization; and integrated circuitry.

For related information see also *60 Computer Operations and Hardware* and *76 Solid-State Physics*.

### 34 FLUID MECHANICS AND HEAT TRANSFER 106

Includes boundary layers; hydrodynamics; fluidics; mass transfer; and ablation cooling.

For related information see also *02 Aerodynamics* and *77 Thermodynamics and Statistical Physics*.

### 35 INSTRUMENTATION AND PHOTOGRAPHY 120

Includes remote sensors; measuring instruments and gages; detectors; cameras and photographic supplies; and holography.

For aerial photography see *43 Earth Resources*. For related information see also *06 Aircraft Instrumentation* and *19 Spacecraft Instrumentation*.

### 36 LASERS AND MASERS 126

Includes parametric amplifiers.

### 37 MECHANICAL ENGINEERING 126

Includes auxiliary systems (non-power); machine elements and processes; and mechanical equipment.

### 38 QUALITY ASSURANCE AND RELIABILITY 137

Includes product sampling procedures and techniques; and quality control.

### 39 STRUCTURAL MECHANICS 139

Includes structural element design and weight analysis; fatigue; and thermal stress.

For applications see *05 Aircraft Design, Testing and Performance* and *18 Spacecraft Design, Testing and Performance*.

## GEOSCIENCES

Includes geosciences (general); earth resources; energy production and conversion; environment pollution; geophysics; meteorology and climatology; and oceanography.

For related information see also *Space Sciences*.

### 42 GEOSCIENCES (GENERAL) N.A.

### 43 EARTH RESOURCES 153

Includes remote sensing of earth resources by aircraft and spacecraft; photogrammetry; and aerial photography.

For instrumentation see *35 Instrumentation and Photography*.

### 44 ENERGY PRODUCTION AND CONVERSION 153

Includes specific energy conversion systems, e.g., fuel cells and batteries; global sources of energy; fossil fuels; geophysical conversion; hydroelectric power; and wind power.

For related information see also *07 Aircraft Propulsion and Power*, *20 Spacecraft Propulsion and Power*, *28 Propellants and Fuels*, and *85 Urban Technology and Transportation*.

### 45 ENVIRONMENT POLLUTION 165

Includes air, noise, thermal and water pollution; environment monitoring; and contamination control.

**46 GEOPHYSICS** 166  
Includes aeronomy; upper and lower atmosphere studies; ionospheric and magnetospheric physics; and geomagnetism.  
For space radiation see *93 Space Radiation*.

**47 METEOROLOGY AND CLIMATOLOGY** 166  
Includes weather forecasting and modification.

**48 OCEANOGRAPHY** N.A.  
Includes biological, dynamic and physical oceanography; and marine resources.

## LIFE SCIENCES

Includes sciences (general); aerospace medicine; behavioral sciences; man/system technology and life support; and planetary biology.

**51 LIFE SCIENCES (GENERAL)** 168  
Includes genetics.

**52 AEROSPACE MEDICINE** N.A.  
Includes physiological factors; biological effects of radiation; and weightlessness.

**53 BEHAVIORAL SCIENCES** N.A.  
Includes psychological factors; individual and group behavior; crew training and evaluation; and psychiatric research.

**54 MAN/SYSTEM TECHNOLOGY AND LIFE SUPPORT** 168  
Includes human engineering; biotechnology; and space suits and protective clothing.

**55 PLANETARY BIOLOGY** N.A.  
Includes exobiology; and extraterrestrial life.

## MATHEMATICAL AND COMPUTER SCIENCES

Includes mathematical and computer sciences (general); computer operations and hardware; computer programming and software; computer systems; cybernetics; numerical analysis; statistics and probability; systems analysis; and theoretical mathematics.

**59 MATHEMATICAL AND COMPUTER SCIENCES (GENERAL)** 168

**60 COMPUTER OPERATIONS AND HARDWARE** 168  
Includes computer graphics and data processing.  
For components see *33 Electronics and Electrical Engineering*.

**61 COMPUTER PROGRAMMING AND SOFTWARE** 169  
Includes computer programs, routines, and algorithms.

**62 COMPUTER SYSTEMS** 170  
Includes computer networks.

**63 CYBERNETICS** 171  
Includes feedback and control theory.  
For related information see also *54 Man/System Technology and Life Support*.

**64 NUMERICAL ANALYSIS** 171  
Includes iteration, difference equations, and numerical approximation.

**65 STATISTICS AND PROBABILITY** N.A.  
Includes data sampling and smoothing; Monte Carlo method; and stochastic processes.

**66 SYSTEMS ANALYSIS** N.A.  
Includes mathematical modeling; network analysis; and operations research.

**67 THEORETICAL MATHEMATICS** N.A.  
Includes topology and number theory.

## PHYSICS

Includes physics (general); acoustics; atomic and molecular physics; nuclear and high-energy physics; optics; plasma physics; solid-state physics; and thermodynamics and statistical physics.  
For related information see also *Engineering*.

**70 PHYSICS (GENERAL)** N.A.  
For geophysics see *46 Geophysics*. For astrophysics see *90 Astrophysics*. For solar physics see *92 Solar Physics*.

**71 ACOUSTICS** 172  
Includes sound generation, transmission, and attenuation.  
For noise pollution see *45 Environment Pollution*.

**72 ATOMIC AND MOLECULAR PHYSICS** 177  
Includes atomic structure and molecular spectra.

**73 NUCLEAR AND HIGH-ENERGY PHYSICS** 177  
Includes elementary and nuclear particles; and reactor theory.  
For space radiation see *93 Space Radiation*.

**74 OPTICS** 178  
Includes light phenomena.

**75 PLASMA PHYSICS** 178  
Includes magnetohydrodynamics and plasma fusion.  
For ionospheric plasmas see *46 Geophysics*. For space plasmas see *90 Astrophysics*.

**76 SOLID-STATE PHYSICS** 180  
Includes superconductivity.  
For related information see also *33 Electronics and Electrical Engineering* and *36 Lasers and Masers*.

**77 THERMODYNAMICS AND STATISTICAL PHYSICS** 184  
Includes quantum mechanics; and Bose and Fermi statistics.  
For related information see also *25 Inorganic and Physical Chemistry* and *34 Fluid Mechanics and Heat Transfer*.

## SOCIAL SCIENCES

Includes social sciences (general); administration and management; documentation and information science; economics and cost analysis; law and political science; and urban technology and transportation.

**80 SOCIAL SCIENCES (GENERAL)** N.A.  
Includes educational matters.

**81 ADMINISTRATION AND MANAGEMENT** N.A.  
Includes management planning and research.

**82 DOCUMENTATION AND INFORMATION SCIENCE** 184  
Includes information storage and retrieval technology; micrography; and library science.  
For computer documentation see 61 *Computer Programming and Software*.

**83 ECONOMICS AND COST ANALYSIS** N.A.  
Includes cost effectiveness studies.

**84 LAW AND POLITICAL SCIENCE** N.A.  
Includes space law; international law; international cooperation; and patent policy.

**85 URBAN TECHNOLOGY AND TRANSPORTATION** 184  
Includes applications of space technology to urban problems; technology transfer; technology assessment; and surface and mass transportation.  
For related information see 03 *Air Transportation and Safety*, 16 *Space Transportation*, and 44 *Energy Production and Conversion*.

## SPACE SCIENCES

Includes space sciences (general); astronomy; astrophysics; lunar and planetary exploration; solar physics; and space radiation.

For related information see also *Geosciences*.

**88 SPACE SCIENCES (GENERAL)** N.A.

**89 ASTRONOMY** N.A.  
Includes radio and gamma-ray astronomy; celestial mechanics; and astrometry.

**90 ASTROPHYSICS** N.A.  
Includes cosmology; and interstellar and interplanetary gases and dust.

**91 LUNAR AND PLANETARY EXPLORATION** N.A.  
Includes planetology; and manned and unmanned flights.

For spacecraft design see 18 *Spacecraft Design, Testing and Performance*. For space stations see 15 *Launch Vehicles and Space Vehicles*.

**92 SOLAR PHYSICS** N.A.  
Includes solar activity, solar flares, solar radiation and sunspots.

**93 SPACE RADIATION** N.A.  
Includes cosmic radiation; and inner and outer earth's radiation belts.  
For biological effects of radiation see 52 *Aerospace Medicine*. For theory see 73 *Nuclear and High-Energy Physics*.

## GENERAL

**99 GENERAL**

186

Note: N.A. means that no abstracts were assigned to this category for this issue.

SUBJECT INDEX .....	A-1
PERSONAL AUTHOR INDEX .....	B-1
CORPORATE SOURCE INDEX .....	C-1
CONTRACT NUMBER INDEX .....	D-1
REPORT/ACCESSION NUMBER INDEX .....	E-1

# Bibliography of Lewis Research Center Technical Publications Announced in 1985

01

## AERONAUTICS (GENERAL)

**N85-15658\*#** National Aeronautics and Space Administration. Lewis Research Center, Cleveland, Ohio.

### TEMPERATURE DISTORTION GENERATOR FOR TURBOSHAFT ENGINE TESTING

G. A. KLANN, R. L. BARTH, and T. J. BIESIADNY Dec. 1984 34 p refs Presented at the SAE Aerospace Congr. and Exposition, Long Beach, Calif., 15-18 Oct. 1984 (NASA-TM-83748; USAAVSCOM-TR-84-C-12; E-2197; NAS 1.15:83748) Avail: NTIS HC A03/MF A01 CSCL 01B

The procedures and unique hardware used to conduct an experimental investigation into the response of a small-turboshaft-engine compression system to various hot gas ingestion patterns are presented. The temperature distortion generator described herein uses gaseous hydrogen to create both steady-state and time-variant, or transient, temperature distortion at the engine inlet. The range of transient temperature ramps produced by the distortion generator during the engine tests was from less than 111 deg K/sec (200 deg R/sec) to above 611 deg K/sec (1100 deg R/sec); instantaneous temperatures to 422 deg K (760 deg R) above ambient were generated. The distortion generator was used to document the maximum inlet temperatures and temperature rise rates that the compression system could tolerate before the onset of stall for various circumferential distortions as well as the compressor system response during stall. Author

**N85-17935\*#** National Aeronautics and Space Administration. Lewis Research Center, Cleveland, Ohio.

### DESIGN DESCRIPTION OF A MICROPROCESSOR BASED ENGINE MONITORING AND CONTROL UNIT (EMAC) FOR SMALL TURBOSHAFT

A. N. BAEZ Jan. 1985 30 p refs (NASA-TM-86860; E-2324; NAS 1.15:86860) Avail: NTIS HC A03/MF A01 CSCL 01B

Research programs have demonstrated that digital electronic controls are more suitable for advanced aircraft/rotorcraft turbine engine systems than hydromechanical controls. Commercially available microprocessors are believed to have the speed and computational capability required for implementing advanced digital control algorithms. Thus, it is desirable to demonstrate that off-the-shelf microprocessors are indeed capable of performing real time control of advanced gas turbine engines. The engine monitoring and control (EMAC) unit was designed and fabricated specifically to meet the requirements of an advanced gas turbine engine control system. The EMAC unit is fully operational in the Army/NASA small turboshaft engine digital research program. Author

**N85-23685\*#** National Aeronautics and Space Administration. Lewis Research Center, Cleveland, Ohio.

### FUTURE DIRECTIONS IN AEROPROPULSION TECHNOLOGY

N. T. SAUNDERS and A. J. GLASSMAN 6 Sep. 1985 39 p refs Proposed for presentation at 7th Intern. Symp. on Air Breathing Eng., Beijing, China, 2-6 Sep. 1985 (NASA-TM-87010; E-2553; NAS 1.15:87010) Avail: NTIS HC A03/MF A01 CSCL 01B

Future directions in aeropropulsion technology that have been identified in a series of studies recently sponsored by the U.S. Government are discussed. Advanced vehicle concepts that could become possible by the turn of the century are presented along with some of their projected capabilities. Key building-block propulsion technologies that will contribute to making these vehicle concepts a reality are discussed along with projections of their status by the year 2000. Some pertinent highlights of the NASA aeropropulsion program are included in the discussion. Author

02

## AERODYNAMICS

Includes aerodynamics of bodies, combinations, wings, rotors, and control surfaces; and internal flow in ducts and turbomachinery.

**A85-10352\*** National Aeronautics and Space Administration. Lewis Research Center, Cleveland, Ohio.

### GENERATION OF INSTABILITY WAVES IN FLOWS SEPARATING FROM SMOOTH SURFACES

M. E. GOLDSTEIN (NASA, Lewis Research Center, Cleveland, OH) Journal of Fluid Mechanics (ISSN 0022-1120), vol. 145, Aug. 1984, p. 71-94. refs

This paper analyses the coupling between an imposed disturbance and an instability wave that propagates downstream on a shear layer which emanates from a separation point on a smooth surface. Since the wavelengths of the most-amplified instability waves will generally be small compared with the streamwise body dimensions, the analysis is restricted to this 'high-frequency' limit and the solution is obtained by using matched asymptotic expansions. An 'inner' solution, valid near the separation point, is matched onto an outer solution, which represents an instability wave on a slowly diverging mean flow. The analysis relates the amplitude of this instability to that of the imposed disturbance. Author

**A85-10357\*** National Aeronautics and Space Administration. Lewis Research Center, Cleveland, Ohio.

### RESONANCE IN FLOWS WITH VORTEX SHEETS AND EDGES

P. A. DURBIN (NASA, Lewis Research Center, Cleveland, OH) Journal of Fluid Mechanics (ISSN 0022-1120), vol. 145, Aug. 1984, p. 275-285. refs

It is shown that the vortex sheet in a slot between two semi-infinite plates does not admit incompressible resonant perturbations. The semi-infinite vortex sheet entering a duct does admit incompressible resonance. These results indicate that the vortex-sheet approximation is less useful for impinging shear flows than for non-impinging flows. They also suggest an important role

## 02 AERODYNAMICS

of downstream vortical disturbances in resonant flows. The general solution for perturbations to flow with a vortex sheet and edges is written in terms of a Cauchy integral. Requirements on the behavior of this solution at edges and at downstream infinity fix the criteria for resonance. Author

**A85-10870\*#** National Aeronautics and Space Administration. Lewis Research Center, Cleveland, Ohio.

### **ACOUSTIC PRESSURES EMANATING FROM A TURBOMACHINE STAGE**

S. M. RAMACHANDRA (NASA, Lewis Research Center, Cleveland, OH) American Institute of Aeronautics and Astronautics and NASA, Aeroacoustics Conference, 9th, Williamsburg, VA, Oct. 15-17, 1984. 13 p. Previously announced in STAR as N84-30224. refs

(AIAA PAPER 84-2325)

A knowledge of the acoustic energy emission of each blade row of a turbomachine is useful for estimating the overall noise level of the machine and for determining its discrete frequency noise content. Because of the close spacing between the rotor and stator of a compressor stage, the strong aerodynamic interactions between them have to be included in obtaining the resultant flow field. This paper outlines a three-dimensional theory for determining the discrete frequency noise content of an axial compressor consisting of a rotor and a stator each with a finite number of blades. The lifting surface theory and the linearized equation of an ideal, nonsteady compressible fluid motion are used for thin blades of arbitrary cross section. The combined pressure field at a point of the fluid is constructed by linear addition of the rotor and stator solutions together with an interference factor obtained by matching them for net zero vorticity behind the stage. Author

**A85-11646\*#** National Aeronautics and Space Administration. Lewis Research Center, Cleveland, Ohio.

### **ANALYTICAL STUDY OF BLOWING BOUNDARY LAYER CONTROL FOR SUBSONIC V/STOL INLETS**

D. P. HWANG (NASA, Lewis Research Center, Cleveland, OH) IN: Computation of internal flows; Methods and applications; Proceedings of the Energy Sources Technology Conference, New Orleans, LA, February 12-16, 1984. New York, American Society of Mechanical Engineers, 1983, p. 151-157. refs

The analytical methods used to study blowing boundary-layer control (BLC) for subsonic V/STOL inlets at the NASA Lewis Research Center are briefly described. The methods are then shown to give good agreement with experimental results, both with and without blowing BLC. Finally, because of this good agreement, the methods have been used to determine analytically the optimum (minimum blowing power required) location and height for a blowing slot within a subsonic V/STOL inlet. Results of this analytical study are presented. Author

**A85-18679\*#** National Aeronautics and Space Administration. Lewis Research Center, Cleveland, Ohio.

### **EFFICIENT SOLUTION OF THE EULER AND NAVIER-STOKES EQUATIONS WITH A VECTORIZED MULTIPLE-GRID ALGORITHM**

R. C. CHIMA (NASA, Lewis Research Center, Cleveland, OH) and G. M. JOHNSON (Colorado State University, Fort Collins, CO) (Computational Fluid Dynamics Conference, 6th, Danvers, MA, July 13-15, 1983, Collection of Technical Papers, p. 72-89) AIAA Journal (ISSN 0001-1452), vol. 23, Jan. 1985, p. 23-32. Previously cited in issue 18, p. 2634, Accession no. A83-39359. refs

**A85-19489\*#** National Aeronautics and Space Administration. Lewis Research Center, Cleveland, Ohio.

### **ACCELERATED CONVERGENCE FOR INCOMPRESSIBLE FLOW CALCULATIONS**

G. M. NEELY and R. W. CLAUS (NASA, Lewis Research Center, Cleveland, OH) American Institute of Aeronautics and Astronautics, Aerospace Sciences Meeting, 23rd, Reno, NV, Jan. 14-17, 1985. 8 p. Previously announced in STAR as N85-10949. refs

(AIAA PAPER 85-0058)

Two improved algorithms which solve the steady-state Navier-Stokes equations, PISO and SIMPLER, are studied. Computations were carried out on progressively finer grids for the driven cavity and flow over a backward-facing step. The effects of relaxation factor, number of grid nodes and number of sweeps through the pressure equations are studied to evaluate the performance of the PISO and SIMPLER schemes. Results show that these improved schemes accelerate the convergence rate of the solution generally by a factor of two as compared to the SIMPLE method. Author

**A85-19490\*#** Texas Technological Univ., Lubbock.

### **FLOW VISUALIZATION OF LATERAL JET INJECTION INTO SWIRLING CROSSFLOW**

G. B. FERRELL (Texas Tech University, Lubbock, TX; Oklahoma State University, Stillwater, OK), K. AOKI (Oklahoma State University, Stillwater, OK; Tokai University, Hiratsuka, Japan), and D. G. LILLEY (Oklahoma State University, Stillwater, OK) American Institute of Aeronautics and Astronautics, Aerospace Sciences Meeting, 23rd, Reno, NV, Jan. 14-17, 1985. 12 p. refs (Contract NAG3-159)

(AIAA PAPER 85-0059)

Flow visualization experiments have been conducted to characterize the time-mean flowfield of a deflected turbulent jet in a confining cylindrical crossflow. Jet-to-crossflow velocity ratios of 2, 4, and 6 were investigated, under crossflow inlet swirler vane angles of 0 (swirler removed), 45 and 70 degrees. Smoke, neutrally-buoyant helium-filled soap bubbles, and multi-spark flow visualization were employed to highlight interesting features of the deflected jet, as well as the trajectory and spread pattern of the jet. Gross flowfield characterization was obtained for a range of lateral jet-to-crossflow velocity ratios and a range of inlet swirl strengths in the main flow. The flow visualization results agree well with the measurements obtained elsewhere with the six-orientation single hot-wire method. Author

**A85-19510\*#** United Technologies Research Center, East Hartford, Conn.

### **THREE-DIMENSIONAL INVISCID FLOW ANALYSIS OF TURBOFAN FORCED MIXERS**

T. J. BARBER, G. L. MULLER, S. M. RAMSAY (United Technologies Research Center, East Hartford, CT), and E. M. MURMAN (MIT, Cambridge, MA) American Institute of Aeronautics and Astronautics, Aerospace Sciences Meeting, 23rd, Reno, NV, Jan. 14-17, 1985. 14 p. refs

(Contract NAS3-23039)

(AIAA PAPER 85-0086)

A three-dimensional potential analysis has been formulated and applied to the inviscid flow over a turbofan forced mixer. The method uses a unique small disturbance formulation to analytically uncouple the circumferential flow from the radial and axial flow problem, thereby reducing the analysis to the solution of a series of axisymmetric problems. These equations are discretized using a flux volume formulation along a Cartesian grid. The method extends earlier applications of the Cartesian method to complex cambered geometries. The effects of power addition are also included within the potential formulation. Good agreement is obtained with an alternate small disturbance analysis for a symmetric mixer in a planar duct. In addition calculations showing pressure distributions and induced secondary vorticity fields are presented for practical turbofan mixer configurations, and where possible, comparison has been made with available experimental data. Author

**A85-19731\*#** Akron Univ., Ohio.

**PROGRESS IN DEVELOPMENT OF A NAVIER-STOKES SOLVER FOR EVALUATION OF ICED AIRFOIL PERFORMANCE**

M. G. POTAPCZUK (Akron, University, Akron, OH) and P. M. GERHART (Evansville, University, Evansville, IN; Akron, University, Akron, OH) American Institute of Aeronautics and Astronautics, Aerospace Sciences Meeting, 23rd, Reno, NV, Jan. 14-17, 1985. 19 p. refs

(Contract NAG3-416)

(AIAA PAPER 85-0410)

A method is being developed for evaluation of the flow field behavior about an airfoil with significant ice accretion on the leading edge. The computer code, being evaluated for this purpose, solves the Navier-Stokes equations in a body-fitted curvilinear coordinate system. This requires the use of a grid generation code to transform the x-y coordinates of the physical space into xi-eta coordinates of the computational space. Evaluation of the suitability of these two codes for predicting iced airfoil performance is presently being carried out in anticipation of use in an overall icing analysis effort. Results of this evaluation to date indicate good correlation with known information on clean airfoils. Preliminary results for rime and glaze, iced airfoil shapes are also presented. Author

**A85-20744\*** United Technologies Corp., East Hartford, Conn.

**A LINEARIZED UNSTEADY AERODYNAMIC ANALYSIS FOR TRANSONIC CASCADES**

J. M. VERDON and J. R. CASPAR (United Technologies Research Center, East Hartford, CT) Journal of Fluid Mechanics (ISSN 0022-1120), vol. 149, Dec. 1984, p. 403-429. refs (Contract NAS3-23696)

The unsteady airloads generated by the vibrations of turbomachine blades operating at transonic Mach numbers are predicted by a linearized potential flow analysis whose unsteady aerodynamics model encompasses the effects of blade geometry, nonzero mean pressure variation across the blade row, high frequency blade motion, and shock motion, all within the framework of a linearized frequency-domain formulation. A numerical solution for the entire unsteady flow field is determined by matching a solution covering an extended blade passage region to another covering, and extending beyond, the supersonic region(s) adjacent to a blade surface. Results are given for cascades of double circular arc and flat plate blades, in order to demonstrate the unsteady analysis and to partially illustrate the effects of blade geometry, inlet Mach number, vibration frequency and shock motion on unsteady response. O.C.

**A85-25135\*#** Ohio State Univ., Columbus.

**PREDICTING RIME ICE ACCRETION ON AIRFOILS**

M. B. BRAGG (Ohio State University, Columbus, OH) AIAA Journal (ISSN 0001-1452), vol. 23, March 1985, p. 381-387. refs (Contract NAG3-28)

A method for predicting the droplet impingement and resulting rime ice accretion on airfoils in an incompressible, inviscid flowfield is presented. The governing equations for the water droplet trajectories are described briefly and the appropriate similarity parameters presented. Droplet impingement parameters are described for both monodisperse and arbitrary droplet size distributions. A time-stepping ice accretion process is presented where the flowfield and droplet impingement characteristics are updated periodically to model the time-dependent nature of the process. The method compares well to experimental results of both droplet impingement and rime ice shapes. The time stepping improves the accuracy of the ice shape predictions. Recommendations are given for further research. Author

**A85-25928\*#** Tennessee Univ. Space Inst., Tullahoma.

**FLOW CONTROL IN A DIFFUSING S-DUCT**

A. D. VAKILI, J. M. WU, P. LIVER, and M. K. BHAT (Tennessee, University, Space Institute, Tullahoma, TN) American Institute of Aeronautics and Astronautics, Shear Flow Control Conference, Boulder, CO, Mar. 12-14, 1985. 8 p. refs

(Contract NAG3-364)

(AIAA PAPER 85-0524)

Accurate measurements have been made of secondary flow in a 1.51 area ratio diffusing 30 deg - 30 deg S-Duct with circular cross section. Turbulent flow was entering the duct at Mach number of 0.6, the boundary layer thickness at the duct entrance was ten percent of the duct inlet diameter. Through measurements made, local flow velocity vector as well as static and total pressures mapping of the flow at several stations were obtained. Strong secondary flow was measured in the first bend which continued into the second bend with new vorticity produced in there in the opposite direction. Surface oil flow visualization and wall pressures indicated a region of separated flow starting at theta approximately equal to 22 deg on the inside of the first bend up to theta approximately equal to 44 deg on the outside of the second bend. The flow separated in 'cyclone' form and never reattached in the duct. As a result of the secondary flow and the flow separation, significant total pressure distortion was observed at the exit of the duct. Using flow control devices the separation was eliminated while the exit distortion was improved. Author

**A85-26389\*#** National Aeronautics and Space Administration. Lewis Research Center, Cleveland, Ohio.

**ANALYTICAL MODELING OF CIRCUIT AERODYNAMICS IN THE NEW NASA LEWIS ALTITUDE WIND TUNNEL**

C. E. TOWNE, L. A. POVINELLI, W. G. KUNIK, K. K. MURAMOTI, C. E. HUGHES (NASA, Lewis Research Center, Cleveland, OH), and R. LEVY (Scientific Research Associates, Inc., Glastonbury, CT) American Institute of Aeronautics and Astronautics, Aerospace Sciences Meeting, 23rd, Reno, NV, Jan. 14-17, 1985. 21 p. Previously announced in STAR as N85-15688. refs

(AIAA PAPER 85-0380)

Rehabilitation and extension of the capability of the altitude wind tunnel (AWT) was analyzed. The analytical modelling program involves the use of advanced axisymmetric and three dimensional viscous analyses to compute the flow through the various AWT components. Results for the analytical modelling of the high speed leg aerodynamics are presented; these include: an evaluation of the flow quality at the entrance to the test section, an investigation of the effects of test section bleed for different model blockages, and an examination of three dimensional effects in the diffuser due to reentry flow and due to the change in cross sectional shape of the exhaust scoop. E.A.K.

**A85-28899\*#** National Aeronautics and Space Administration. Lewis Research Center, Cleveland, Ohio.

**FEEDBACK IN SEPARATED FLOWS OVER SYMMETRIC AIRFOILS**

H. M. ATASSI (NASA, Lewis Research Center, Cleveland, OH; Notre Dame, University, Notre Dame, IN) American Institute of Aeronautics and Astronautics and NASA, Aeroacoustics Conference, 9th, Williamsburg, VA, Oct. 15-17, 1984. 14 p. NASA-USAF-supported research. Previously announced in STAR as N84-31091. refs

(AIAA PAPER 84-2297)

For a flow over an airfoil with laminar separation, a feedback cycle may exist whereby a Kelvin-Helmholtz instability wave emanating from the separation point on the airfoil surface grows along the shear layer and is diffracted as it interacts with the sharp trailing edge of the airfoil, causing acoustic radiation which, in turn, propagates upstream and regenerates the initial instability wave. The analysis is restricted to the high frequency limit. Solutions to the boundary-value problem are obtained using the slowly varying approximation and the method of matched asymptotic expansions. Resonant solutions exist for certain discrete values of the Reynolds and Strouhal numbers. The results are discussed and compared with available data. Author

## 02 AERODYNAMICS

**A85-29126\*#** National Aeronautics and Space Administration. Lewis Research Center, Cleveland, Ohio.

### **REVIEW - COMPUTATIONAL METHODS FOR INTERNAL FLOWS WITH EMPHASIS ON TURBOMACHINERY**

W. D. MCNALLY and P. M. SOCKOL (NASA, Lewis Research Center, Cleveland, OH) ASME, Transactions, Journal of Fluids Engineering (ISSN 0098-2202), vol. 107, March 1985, p. 6-22. Previously announced in STAR as N82-13113. refs

Current computational methods for analyzing flows in turbomachinery and other related internal propulsion components are presented. The methods are divided into two classes. The inviscid methods deal specifically with turbomachinery applications. Viscous methods, deal with generalized duct flows as well as flows in turbomachinery passages. Inviscid methods are categorized into the potential, stream function, and Euler approaches. Viscous methods are treated in terms of parabolic, partially parabolic, and elliptic procedures. Various grids used in association with these procedures are also discussed. Author

**A85-29259\*#** Pennsylvania State Univ., University Park. **COMPUTATION OF THREE-DIMENSIONAL VISCOUS FLOWS USING A SPACE-MARCHING METHOD**

K. N. S. MURTHY and B. LAKSHMINARAYANA (Pennsylvania State University, University Park, PA) Journal of Aircraft (ISSN 0021-8669), vol. 22, April 1985, p. 311-317. Previously cited in issue 17, p. 2418, Accession no. A84-36971. refs (Contract NSG-3266)

**A85-30175\*** Virginia Polytechnic Inst. and State Univ., Blacksburg.

### **VORTEX INDUCED LIFT ON A FLAT PLATE WITH A CURVED FORWARD-FACING FLAP**

S. TANVEER (Virginia Polytechnic Institute and State University, Blacksburg, VA; California Institute of Technology, Pasadena, CA) Studies in Applied Mathematics (ISSN 0022-2526), vol. 72, April 1985, p. 173-187. Navy-supported research. refs (Contract NAG3-179)

Free streamline solutions are obtained for two-dimensional inviscid incompressible flow past a flat plate with a forward-facing curved flap. It is shown that it is possible to shape the curved flap to make the adverse pressure gradient on top of the flap less severe than for a straight flap and thus increase the prospects of making the flow experimentally realizable. Author

**A85-32961\*#** National Aeronautics and Space Administration. Lewis Research Center, Cleveland, Ohio.

### **ASSESSMENT OF THREE-DIMENSIONAL INVISCID CODES AND LOSS CALCULATIONS FOR TURBINE AERODYNAMIC COMPUTATIONS**

L. A. POVINELLI (NASA, Lewis Research Center, Cleveland, OH) ASME, Transactions, Journal of Engineering for Gas Turbines and Power (ISSN 0022-0825), vol. 107, April 1985, p. 265-275; Discussion, p. 275, 276; Author's Closure, p. 276. Previously announced in STAR as N84-16142. refs (ASME PAPER 84-GT-187)

An assessment of several three dimensional inviscid turbine aerodynamic computer codes and loss models used at the NASA Lewis Research Center is presented. Five flow situations are examined, for which both experimental data and computational results are available. The five flows form a basis for the evaluation of the computational procedures. It was concluded that stator flows may be calculated with a high degree of accuracy, whereas, rotor flow fields are less accurately determined. Exploitation of contouring, leaning, bowing, and sweeping will require a three dimensional viscous analysis technique. Author

**A85-32963\*#** National Aeronautics and Space Administration. Lewis Research Center, Cleveland, Ohio.

### **INVESTIGATION OF FLOW PHENOMENA IN A TRANSONIC FAN ROTOR USING LASER ANEMOMETRY**

A. J. STRAZISAR (NASA, Lewis Research Center, Cleveland, OH) ASME, Transactions, Journal of Engineering for Gas Turbines and Power (ISSN 0022-0825), vol. 107, April 1985, p. 427-435. Previously announced in STAR as N84-17143. refs (ASME PAPER 84-GT-199)

Several flow phenomena including flowfield periodicity, rotor shock oscillation, and rotor shock system geometry were investigated in a transonic low aspect ratio fan rotor using laser anemometry. Flow periodicity is found to increase with increasing rotor pressure rise, and to correlate with blade geometry variations. Analysis of time-accurate laser anemometer data indicates that the rotor shock oscillates about its mean location with an amplitude of 3 to 4 percent of rotor chord. The shock surface is nearly two-dimensional for levels of rotor pressure rise at and above the peak efficiency level but becomes more complex for lower levels of pressure rise. Spanwise shock lean generates radial flows due to streamline deflection in the hub-to-shroud streamsurface. Author

**A85-32964\*#** National Aeronautics and Space Administration. Lewis Research Center, Cleveland, Ohio.

### **DESIGN AND PERFORMANCE OF A FIXED, NONACCELERATING GUIDE VANE CASCADE THAT OPERATES OVER AN INLET FLOW ANGLE RANGE OF 60 DEG**

J. M. SANZ (NASA, Lewis Research Center, Cleveland, OH; Universities Space Research Association, Columbia, MD), E. R. MCFARLAND, N. L. SANGER, T. F. GELDER, and R. H. CAVICCHI (NASA, Lewis Research Center, Cleveland, OH) ASME, Transactions, Journal of Engineering for Gas Turbines and Power (ISSN 0022-0825), vol. 107, April 1985, p. 477-484. Previously announced in STAR as N84-14120. refs (ASME PAPER 84-GT-75)

A unique set of wind tunnel guide vanes are designed with an inverse design code and analyzed with a panel method and an integral boundary layer code developed at the NASA Lewis Research Center. The fixed guide vanes, 80 feet long with 6-foot chord length, were designed for the NASA Ames 40 x 80/80 x 120 ft Wind Tunnel. Low subsonic flow is accepted over a 60-deg range of inlet angle from either the 40 x 80 leg or the 80 x 120 leg of the wind tunnel, and directed axially into the main leg of the tunnel where drive fans are located. Experimental tests of 1/10-scale models were conducted to verify design calculations. Author

**A85-32965\*#** Iowa State Univ. of Science and Technology, Ames.

### **A NOTE ON BLADE WAKE INTERACTION INFLUENCE ON COMPRESSOR STATOR ROW AERODYNAMIC PERFORMANCE**

T. H. OKIISHI, J. L. HANSEN (Iowa State University of Science and Technology, Ames, IA), and M. D. HATHAWAY (U.S. Army, Propulsion Laboratory, Cleveland, OH) ASME, Transactions, Journal of Engineering for Gas Turbines and Power (ISSN 0022-0825), vol. 107, April 1985, p. 549-551. refs (Contract F49620-83-K-0023; NAG3-356)

Attention is given to the effect of blade wake interactions on the performance of an axial flow compressor's stator row, for the case of compressor and fan stator flows without shocks. The measured midspan loss of total pressure can be related to stator surface boundary layers, the chopped rotor wakes passing through the stator row, and the interaction between these flows. The interaction between rotor blade wake segments and stator blade surface boundary layers generates much higher losses than expected in both the stator wake and in the region of flow between stator boundary layers/wakes, if interaction effects are ignored. O.C.



**A85-39728\*#** National Aeronautics and Space Administration. Lewis Research Center, Cleveland, Ohio.

**APPLICATION OF RUNGE KUTTA TIME MARCHING SCHEME FOR THE COMPUTATION OF TRANSONIC FLOWS IN TURBOMACHINES**

S. V. SUBRAMANIAN (NASA, Lewis Research Center, Cleveland, OH; Avco Corp., Avco Lycoming Div., Stratford, CT) and R. BOZZOLA (Avco Corp., Avco Lycoming Div., Stratford, CT) AIAA, SAE, ASME, and ASEE, Joint Propulsion Conference, 21st, Monterey, CA, July 8-10, 1985. 8 p. refs (AIAA PAPER 85-1332)

Numerical solutions of the unsteady Euler equations are obtained using the classical fourth order Runge Kutta time marching scheme. This method is fully explicit and is applied to the governing equations in the finite volume, conservation law form. In order to determine the efficiency of this scheme for solving turbomachinery flows, steady blade-to-blade solutions are obtained for compressor and turbine cascades under subsonic and transonic flow conditions. Computed results are compared with other numerical methods and wind tunnel measurements. The present study also focuses on other important numerical aspects influencing the performance of the algorithm and the solution accuracy such as grid types, boundary conditions, and artificial viscosity. For this purpose, H, O, and C type computational grids as well as characteristic and extrapolation type boundary conditions are included in the solution procedure. Author

**A85-39767\*#** National Aeronautics and Space Administration. Lewis Research Center, Cleveland, Ohio.

**CALCULATION OF THREE-DIMENSIONAL, VISCOUS FLOW THROUGH TURBOMACHINERY BLADE PASSAGES BY PARABOLIC MARCHING**

T. KATSANIS (NASA, Lewis Research Center, Cleveland, OH) AIAA, SAE, ASME, and ASEE, Joint Propulsion Conference, 21st, Monterey, CA, July 8-10, 1985. 14 p. Previously announced in STAR as N85-23711. refs (AIAA PAPER 85-1408)

The three-dimensional compressible Navier-Stokes equations are formulated in a rotating coordinate system, so as to include centrifugal and Coriolis forces. The equations are parabolized by using a previously calculated inviscid static pressure field. The thin layer Navier-Stokes approximation, which neglects streamwise diffusion, is used. A body-fitted coordinate system is used. The streamwise momentum equation is uncoupled from the cross-stream momentum equation by using contravariant momentum components, and then using the contravariant velocity components as primary unknowns. To reduce problems with small separating regions, the Reyhner and Flugge-Lotz approximation is used. The energy equation is included to allow for calculation of heat transfer. The flow may be laminar, or a simple eddy-viscosity turbulence may be used. A number of curved ducts and an axial stator were analyzed, including cases for which experimental data are available. Author

**A85-40691\*#** Washington Univ., Seattle.

**AN EXPERIMENTAL STUDY OF THREE-DIMENSIONAL SHOCK WAVE/TURBULENT BOUNDARY LAYER INTERACTIONS IN A SUPERSONIC FLOW**

J. H. CHOU, M. E. CHILDS (Washington, University, Seattle), and R. S. WONG (TRW, Inc., Redondo Beach, CA) American Institute of Aeronautics and Astronautics, Fluid Dynamics and Plasmadynamics and Lasers Conference, 18th, Cincinnati, OH, July 16-18, 1985. 9 p. refs (Contract NAG3-256)

(AIAA PAPER 85-1566)

Wall static pressure distributions, surface flow patterns, pitot pressures, and yaw angle profiles were measured in a skewed three-dimensional shock wave/turbulent boundary layer interaction region. The test section was axisymmetric with a constant diameter. The nominal freestream Mach number was 4. Upstream of the interaction, the boundary layer thickness was 0.31 in. (0.787 cm). The three-dimensional flow was produced by azimuthal pressure gradients which were generated by an 8-degree cone aligned with

the primary flow direction, but with the cone axis displaced 0.3 in. (0.76 cm) from the channel centerline. The yaw angle was found to be a function of both the azimuthal angle and the distance from the beginning of the interaction. It was observed that yaw angle increased substantially near the wall. The maximum yaw angle for the whole flow field was obtained in the 90 degree azimuthal plane. Author

**A85-40817\*#** Douglas Aircraft Co., Inc., Long Beach, Calif.

**CALCULATION OF COMPRESSIBLE FLOW ABOUT THREE-DIMENSIONAL INLETS WITH AUXILIARY INLETS, SLATS AND VANES BY MEANS OF A PANEL METHOD**

J. L. HESS, D. M. FRIEDMAN, and R. W. CLARK (Douglas Aircraft Co., Long Beach, CA) AIAA, SAE, ASME, and ASEE, Joint Propulsion Conference, 21st, Monterey, CA, July 8-10, 1985. 9 p. refs

(Contract NAS3-22250)

(AIAA PAPER 85-1196)

An efficient and user-oriented method has been constructed for calculating flow in and about complex inlet configurations. Efficiency is attained by: the use of a panel method, a technique of superposition for obtaining solutions at any inlet operating condition, and employment of an advanced matrix-iteration technique for solving large full systems of equations, including the nonlinear equations for the Kutta condition. User concerns are addressed by the provision of several novel graphical output options that, taken together, yield a more complete comprehension of the flowfield than had been possible previously. Examples of these features are presented for some complicated configurations, and where possible, comparisons are made between calculation and experiment. Author

**A85-40819\*#** Douglas Aircraft Co., Inc., Long Beach, Calif.

**LOW-SPEED AERODYNAMIC TEST OF AN AXISYMMETRIC SUPERSONIC INLET WITH VARIABLE COWL SLOT**

A. G. POWELL, H. R. WELGE (Douglas Aircraft Co., Long Beach, CA), and C. J. TREFNY (NASA, Lewis Research Center, Cleveland, OH) AIAA, SAE, ASME, and ASEE, Joint Propulsion Conference, 21st, Monterey, CA, July 8-10, 1985. 5 p. Previously announced in STAR as N85-26710.

(AIAA PAPER 85-1210)

The experimental low-speed aerodynamic characteristics of an axisymmetric mixed-compression supersonic inlet with variable cowl slot are described. The model consisted of the NASA P-inlet centerbody and redesigned cowl with variable cowl slot powered by the JT8D single-stage fan simulator and driven by an air turbine. The model was tested in the NASA Lewis Research Center 9- by 15-foot low-speed tunnel at Mach numbers of 0, 0.1, and 0.2 over a range of flows, cowl slot openings, centerbody positions, and angles of attack. The variable cowl slot was effective in minimizing lip separation at high velocity ratios, showed good steady-state and dynamic distortion characteristics, and had good angle-of-attack tolerance. Author

**A85-41814\*** Politecnico di Torino (Italy).

**TIME DEPENDENT COMPUTATION OF THE EULER EQUATIONS FOR DESIGNING 2-D CASCADES, INCLUDING THE CASE OF TRANSONIC SHOCK FREE DESIGN**

L. ZANNETTI (Torino, Politecnico, Turin, Italy) IN: 1983 Tokyo International Gas Turbine Congress, Tokyo, Japan, October 23-29, 1983, Proceedings. Volume 2. Tokyo, Gas Turbine Society of Japan, 1984, p. 423-429. refs

(Contract NAS3-22772)

A numerical method to solve the inverse problem for airfoil cascades is described. The case of compressible, inviscid flow is considered. The proposed method is based on the finite difference approximation of the time-dependent Euler equations. Numerical examples show the capability of the method to design subsonic or transonic shockless blades. Author

## 02 AERODYNAMICS

**A85-41826\*** Cincinnati Univ., Ohio.

### **THE THREE-DIMENSIONAL COMPRESSIBLE FLOW IN A RADIAL INFLOW TURBINE SCROLL**

A. HAMED, W. TABAKOFF, and M. MALAK (Cincinnati University, OH) IN: 1983 Tokyo International Gas Turbine Congress, Tokyo, Japan, October 23-29, 1983, Proceedings. Volume 2. Tokyo, Gas Turbine Society of Japan, 1984, p. 515-521. refs (Contract NAG3-52; NAG3-26)

This work presents the results of an analytical study and an experimental investigation of the three-dimensional flow in a turbine scroll. The finite element method is used in the iterative numerical solution of the locally linearized governing equations for the three-dimensional velocity potential field. The results of the numerical computations are compared with the experimental measurements in the scroll cross sections, which were obtained using laser Doppler velocimetry and hot wire techniques. The results of the computations show a variation in the flow conditions around the rotor periphery which was found to depend on the scroll geometry. Author

**A85-42954\*** Grumman Aerospace Corp., Bethpage, N.Y.

### **THE COMPUTATION OF VISCID/INVISCID INTERACTION ON AIRFOILS WITH SEPARATED FLOW**

R. E. MELNIK and J. W. BROOK (Grumman Research and Development Center, Bethpage, NY) IN: Symposium on Numerical and Physical Aspects of Aerodynamic Flows, 3rd, Long Beach, CA, January 21-24, 1985, Proceedings. Long Beach, CA, California State University, 1985, p. 1-21 to 1-37. Research supported by the Grumman Aerospace Independent Research and Development Program. refs (Contract NAS3-24082)

Attention is given to the computation of viscous subsonic and transonic flow over two-dimensional airfoils at high Reynolds numbers, where the boundary layers are thin and turbulent over most of the airfoil and its wake. An attempt is made to develop a fast viscid/invicid interaction method for the computation of viscous flows over airfoils with extensive low separation regions, which can be used as the basis of predictions of the stalling characteristics of airfoils with reasonable accuracy. These insights are applied in the form of changes to the GRUMFOIL computer code, in order to improve separated flow prediction capabilities. O.C.

**A85-42988\*** National Aeronautics and Space Administration. Langley Research Center, Hampton, Va.

### **A THREE-DIMENSIONAL BOUNDARY-LAYER ANALYSIS INCLUDING HEAT-TRANSFER AND BLADE-ROTATION EFFECTS**

V. N. VATSA (NASA, Langley Research Center, Hampton, VA) IN: Symposium on Numerical and Physical Aspects of Aerodynamic Flows, 3rd, Long Beach, CA, January 21-24, 1985, Proceedings. Long Beach, CA, California State University, 1985, p. 10-45 to 10-59. refs

(Contract NAS3-23716)

An analysis has been developed for calculating three-dimensional viscous flows over arbitrary bodies through the solution of complete three-dimensional boundary-layer equations. The governing equations include the effect of blade rotation and are written in nonorthogonal surface-fitted coordinates to allow maximum flexibility. A coupled finite-difference numerical scheme is used for solving the governing equations. The accuracy of this scheme has been assessed through comparisons with known analytical/experimental results for several test cases. The present analysis has then been applied to compute viscous flows over a turbine endwall and airfoil suction surface, and fairly good correlation has been obtained with available experimental data for surface heat transfer and viscous streamline skewing. Author

**A85-43974\*#** Army Propulsion Lab., Cleveland, Ohio.

### **ROTOR WAKE CHARACTERISTICS OF A TRANSONIC AXIAL FLOW FAN**

M. D. HATHAWAY (U.S. Army, Propulsion Laboratory, Cleveland, OH), J. GERTZ, A. EPSTEIN (MIT, Cambridge, MA), and A. J. STRAZISAR (NASA, Lewis Research Center, Cleveland, OH) AIAA, SAE, ASME, and ASEE, Joint Propulsion Conference, 21st, Monterey, CA, July 8-10, 1985. 12 p. refs (AIAA PAPER 85-1133)

State of the art turbomachinery flow analysis codes are not capable of predicting the viscous flow features within turbomachinery blade wakes. Until efficient 3D viscous flow analysis codes become a reality there is therefore a need for models which can describe the generation and transport of blade wakes and the mixing process within the wake. To address the need for experimental data to support the development of such models, high response pressure measurements and laser anemometer velocity measurements have been obtained in the wake of a transonic axial flow fan rotor. Author

**A85-43977\*#** National Aeronautics and Space Administration. Lewis Research Center, Cleveland, Ohio.

### **INVISCID ANALYSIS OF ADVANCED TURBOPROP PROPELLER FLOW FIELDS**

J. M. BARTON, O. YAMAMOTO (Sverdrup Technology, Inc., Middleburg Heights, OH), and L. J. BOBER (NASA, Lewis Research Center, Cleveland, OH) AIAA, SAE, ASME, and ASEE, Joint Propulsion Conference, 21st, Monterey, CA, July 8-10, 1985. 12 p. refs (Contract NAS3-24105) (AIAA PAPER 85-1263)

A three-dimensional Euler code, previously developed for high speed propellers, was rewritten and vectorized for the Cray computer. Calculations were compared with previous results and measurements. The new code requires less memory and is more than two times faster than its predecessor. The new boundary conditions produced more accurate results and improved stability. The accuracy and stability characteristics also resulted in reduced manual intervention required to obtain solutions. The code is a useful tool for examining the fluid dynamics and performance of propellers. Author

**A85-47023\*#** National Aeronautics and Space Administration. Lewis Research Center, Cleveland, Ohio.

### **APPLICATION OF COMPUTATIONAL FLUID DYNAMICS TO COMPLEX INLET DUCTS**

C. E. TOWNE (NASA, Lewis Research Center, Cleveland, OH) and E. F. SCHUM (Rockwell International Corp., Columbus, OH) AIAA, SAE, ASME, and ASEE, Joint Propulsion Conference, 21st, Monterey, CA, July 8-10, 1985. 14 p. Previously announced in STAR as N85-30247. refs (AIAA PAPER 85-1213)

A three-dimensional parabolic Navier-Stokes code, PEPSIG, was used to analyze the flow in the subsonic diffuser section of a typical modern inlet design. The effect of curvature of the diffuser centerline and transitioning cross sections was studied to determine the primary cause of flow distortion in the duct. Total pressure values at the engine compressor face are reported. M. G.

**A85-47025\*#** National Aeronautics and Space Administration. Lewis Research Center, Cleveland, Ohio.

### **WIND TUNNEL RESULTS OF ADVANCED HIGH SPEED PROPELLERS IN THE TAKEOFF, CLIMB, AND LANDING OPERATING REGIMES**

G. L. STEFKO and R. J. JERACKI (NASA, Lewis Research Center, Cleveland, OH) AIAA, SAE, ASME, and ASEE, Joint Propulsion Conference, 21st, Monterey, CA, July 8-10, 1985. 22 p. Previously announced in STAR as N85-29925. refs (AIAA PAPER 85-1259)

Low speed wind tunnel performance tests of two advanced propellers were completed. The 62.2 cm diameter adjustable pitch models were tested at Mach numbers typical of takeoff, initial climbout, and landing speeds in the 10 by 10 ft Supersonic Wind

Tunnel. Both models had eight blades and a cruise design point operating condition of 0.80 Mach number, 10,668 km S.A. altitude, 243.8 m/s tip speed and a high power loading of 301 kW sq m. No adverse or unusual low speed operating conditions were found during the test with either the straight blade SR-2 or the 45 deg swept SR-3 propellers. The 45 deg swept propeller efficiency exceeded the straight blade efficiency by 4 to 5 percent. Typical net efficiencies of the straight and 45 deg swept propeller at a Mach 0.20 takeoff condition were 50.2 and 54.9 percent respectively. At a Mach 0.34 climb condition, the efficiencies were 53.7 and 59.1 percent. Reverse thrust data indicates that these propellers are capable of producing more reverse thrust at Mach 0.20 than a high bypass turbofan engine at Mach 0.20. E.A.K.

**A85-48539\*** National Aeronautics and Space Administration. Lewis Research Center, Cleveland, Ohio.

**INVISCID AND VISCOUS FLOWS IN CASCADES WITH AN EXPLICIT MULTIGRID ALGORITHM**

R. V. CHIMA (NASA, Lewis Research Center, Cleveland, OH) AIAA Journal (ISSN 0001-1452), vol. 23, Oct. 1985, p. 1556-1563. Previously cited in issue 17, p. 2427, Accession no. A84-38043. refs

**A85-50106\*** National Aeronautics and Space Administration. Lewis Research Center, Cleveland, Ohio.

**NOISE CONSTRAINTS EFFECTING OPTIMAL PROPELLER DESIGNS**

C. J. MILLER (NASA, Lewis Research Center, Cleveland, OH) and J. P. SULLIVAN (Purdue University, West Lafayette, IN) SAE, General Aviation Aircraft Meeting and Exposition, Wichita, KS, Apr. 16-19, 1985. 11 p. Previously announced in STAR as N85-19923. refs (SAE PAPER 850871)

A preliminary design tool for advanced propellers was developed combining a fast vortex lattice aerodynamic analysis, a fast subsonic point source noise analysis, and an optimization scheme using a conjugate directions method. Twist, chord and sweep distributions are optimized to simultaneously improve both the aerodynamic performance and the noise observed at a fixed relative position. The optimal, noise/performance tradeoffs for straight and advanced concept blades are presented. The techniques used include increasing the blade number, blade sweep, reducing the rotational speed, shifting the spanwise loading and diameter changes. E.A.K.

**N85-10919\*** Ohio State Univ., Columbus.  
**DESIGN AND WIND TUNNEL EVALUATION OF A SYMMETRIC AIRFOIL SERIES FOR LARGE WIND TURBINE APPLICATIONS**  
**Final Report**

G. M. GREGOREK May 1984 27 p refs  
(Contract NAG3-330; DE-A101-76ET-20320)  
(NASA-CR-174764; DOE/NASA/0330-1; NAS 1.26:174764)  
Avail: NTIS HC A03/MF A01 CSCL 01A

A family of symmetric airfoils with thickness to chord ratios of 0.21, 0.25, and 0.29 was designed for applications to large wind turbines using the Eppler analytic design methodology. The airfoil series, designed for Reynolds numbers above  $4 \times 1,000,000$ , has a contour that maintains its thickness to the 0.7 chord position, allowing use of a deep aft spar for structural integrity. Wind tunnel tests of the 21 percent thick airfoil conducted in the Ohio State University Airfoil Test Facilities at  $M = 0.25$  and  $Re = 2, 4$  and  $8 \times 1,000,000$  showed good agreement with predicted surface pressures and lift and drag coefficients when the angle of attack was low and the Reynolds number was  $8 \times 1,000,000$ . At the lowest Reynolds number, both the measured lift curve slope and the maximum lift coefficient differ significantly from theory. In the post stall region, agreement with theory and experiment is poor, at all Reynolds numbers, verifying the need for improved analytic methods in this important flow regime. Author

**N85-12008\*** GMAF, Inc., Freeport, N.Y.

**INVERSE DESIGN TECHNIQUE FOR CASCADES** Final Report  
L. ZANNETTI and M. PANDOLFI Washington NASA Nov. 1984 33 p refs  
(Contract NAS3-22772)  
(NASA-CR-3836; E-2275; NAS 1.26:3836) Avail: NTIS HC A03/MF A01 CSCL 01A

A numerical technique to generate cascades is presented. The basic prescribed parameters are: inlet angle, exit pressure, and distribution of blade thickness and lift along a blade. Other sets of parameters are also discussed. The technique is based on the lambda scheme. The problem of stability of the computation as a function of the prescribed set of parameters and the treatment of boundary conditions is discussed. A one dimensional analysis to indicate a possible way for assuring stability for any two dimensional calculation is provided. E.A.K.

**N85-12036\*** National Aeronautics and Space Administration. Lewis Research Center, Cleveland, Ohio.

**MODEL EQUATION FOR SIMULATING FLOWS IN MULTISTAGE TURBOMACHINERY**

J. J. ADAMCZYK Nov. 1984 37 p refs  
(NASA-TM-86869; E-2291; NAS 1.15:86869) Avail: NTIS HC A03/MF A01 CSCL 01A

A steady, three-dimensional average-passage equation system is derived for use in simulating multistage turbomachinery flows. These equations describe a steady, viscous flow that is periodic from blade passage to blade passage. From this system of equations, various reduced forms can be derived for use in simulating the three-dimensional flow field within multistage machinery. It is suggested that a properly scaled form of the average-passage equation system would provide an improved mathematical model for simulating the flow in multistage machines at design and, in particular, at off-design conditions. Author

**N85-12039\*** National Aeronautics and Space Administration. Lewis Research Center, Cleveland, Ohio.

**INCOMPRESSIBLE LIFTING-SURFACE AERODYNAMICS FOR A ROTOR-STATOR COMBINATION**

S. M. RAMACHANDRA Oct. 1984 32 p refs  
(NASA-TM-83767; E-2258; NAS 1.15:83767) Avail: NTIS HC A03/MF A01 CSCL 01A

Current literature on the three dimensional flow through compressor cascades deals with a row of rotor blades in isolation. Since the distance between the rotor and stator is usually 10 to 20 percent of the blade chord, the aerodynamic interference between them has to be considered for a proper evaluation of the aerothermodynamic performance of the stage. A unified approach to the aerodynamics of the incompressible flow through a stage is presented that uses the lifting surface theory for a compressor cascade of arbitrary camber and thickness distribution. The effects of rotor stator interference are represented as a linear function of the rotor and stator flows separately. The loading distribution on the rotor and stator flows separately. The loading distribution on the rotor and stator blades and the interference factor are determined concurrently through a matrix iteration process. Author

**N85-14798\*** National Aeronautics and Space Administration. Lewis Research Center, Cleveland, Ohio.

**A THREE-DIMENSIONAL AXISYMMETRIC CALCULATION PROCEDURE FOR TURBULENT FLOWS IN A RADIAL VANELESS DIFFUSER**

L. F. SCHUMANN 1984 17 p refs Proposed for presentation at the 30th Intern. Gas Turbine Conf. and Exhibit, Houston, Tex., 17-21 Mar. 1985; sponsored by the American Society of Mechanical Engineers  
(NASA-TM-86903; E-2387; NAS 1.15:86903; USAAVSCOM-TR-84-C-21; AD-A157113) Avail: NTIS HC A02/MF A01 CSCL 01A

An analytical model is proposed to calculate the three-dimensional axisymmetric turbulent flowfield in a radial vaneless diffuser. The model assumes that the radial and tangential

## 02 AERODYNAMICS

boundary layer profiles are approximated by power law profiles. Then, using the integrated radial and tangential momentum and continuity equations for the boundary layer and corresponding inviscid equations for the core flow, there results six ordinary differential equation in six unknowns which are easily solved using a Runge-Kutta technique. A model is also proposed for fully developed flow. The results using this technique were compared with the results from a three-dimensional viscous, axisymmetric duct code and with experimental data and good quantitative agreement was obtained. Author

**N85-15688\*#** National Aeronautics and Space Administration. Lewis Research Center, Cleveland, Ohio.

### **ANALYTICAL MODELING OF CIRCUIT AERODYNAMICS IN THE NEW NASA LEWIS WIND TUNNEL**

C. E. TOWNE, L. A. POVINELLI, W. G. KUNIK, K. K. MURAMOTO, C. E. HUGHES, and R. LEVY (Scientific Research Associates) 1985 22 p refs Presented at the 23rd Aerospace Sci. Meeting, Reno, Nev., 14-17 Jan. 1985; sponsored by AIAA (NASA-TM-86912; E-2405; NAS 1.15:86912; AIAA-85-0380) Avail: NTIS HC A02/MF A01 CSCL 01A

Rehabilitation and extension of the capability of the altitude wind tunnel (AWT) was analyzed. The analytical modeling program involves the use of advanced axisymmetric and three dimensional viscous analyses to compute the flow through the various AWT components. Results for the analytical modeling of the high speed leg aerodynamics are presented; these include: an evaluation of the flow quality at the entrance to the test section, an investigation of the effects of test section bleed for different model blockages, and an examination of three dimensional effects in the diffuser due to reentry flow and due to the change in cross sectional shape of the exhaust scoop. E.A.K.

**N85-15689\*#** National Aeronautics and Space Administration. Lewis Research Center, Cleveland, Ohio.

### **UNSTEADY PRESSURE MEASUREMENTS ON A BICONVEX AIRFOIL IN A TRANSONIC OSCILLATING CASCADE**

L. M. SHAW, D. R. BOLDMAN, A. E. BUGGELE, and D. H. BUFFUM (Purdue Univ.) 1985 18 p refs Proposed for presentation at the 30th Intern. Gas Turbine Conf. and Exhibit, Houston, Tex., 17-21 Mar. 1985; sponsored by the American Society of Mechanical Engineering (NASA-TM-86914; E-2408; NAS 1.15:86914) Avail: NTIS HC A02/MF A01 CSCL 01A

Flush-mounted dynamic pressure transducers were installed on the center airfoil of a transonic oscillating cascade to measure the unsteady aerodynamic response as nine airfoils were simultaneously driven to provide 1.2 deg of pitching motion about the midchord. Initial tests were performed at an incidence and angle of 0 deg and A Mach number of 0.65 in order to obtain results in a shock-free compressible flowfield. Subsequent tests were performed at an incidence angle of 7 deg and Mach number of 0.8 in order to observe the surface pressures with an oscillating shock near the leading edge of the airfoil. Results are presented for interblade phase angles of 90 and -90 deg and at blade oscillatory frequencies of 200 and 500 Hz (semi-chord reduced frequencies up to about 0.5 at a Mach number of 0.8). Results from the zero-incidence cascade are compared with a classical unsteady flat-plate analysis. Flow visualization results depicting the shock motion on the airfoils in the high-incidence cascade are discussed. The airfoil pressure data are tabulated. Author

**N85-19923\*#** National Aeronautics and Space Administration. Lewis Research Center, Cleveland, Ohio.

### **NOISE CONSTRAINTS EFFECTING OPTIMAL PROPELLER DESIGNS**

C. J. MILLER and J. P. SULLIVAN 1985 15 p refs To be presented at the Soc. of Automotive Engr. Gen. Aviation Aircraft Meeting and Exposition, Wichita, Kan., 16-19 Apr. 1985 (NASA-TM-86967; E-2449; NAS 1.15:86967) Avail: NTIS HC A02/MF A01 CSCL 01A

A preliminary design tool for advanced propellers was developed combining a fast vortex lattice aerodynamic analysis, a fast

subsonic point source noise analysis, and an optimization scheme using a conjugate directions method. Twist, chord and sweep distributions are optimized to simultaneously improve both the aerodynamic performance and the noise observed at a fixed relative position. The optimal noise/performance tradeoffs for straight and advanced concept blades are presented. The techniques used include increasing the blade number, blade sweep, reducing the rotational speed, shifting the spanwise loading and diameter changes. E.A.K.

**N85-21114\*#** National Aeronautics and Space Administration. Lewis Research Center, Cleveland, Ohio.

### **PRELIMINARY ANALYSIS OF TONE-EXCITED TWO-STREAM JET VELOCITY DECAY**

U. H. VONGLAHN 1985 22 p refs Presented at the 109th Meeting of the Acoustical Society of America, Austin, Tex., 8-12 Apr. 1985 (NASA-TM-86951; E-2473; NAS 1.15:86951) Avail: NTIS HC A02/MF A01 CSCL 01A

Acoustic research related to jet flows has established that sound, by amplifying the naturally occurring large-scale structures in turbulent shear layers, can cause a more rapidly decay of the jet plume velocity and temperature and an increase in jet spreading rate. One possible application of this sound-flow interaction phenomenon is to future STOL aircraft that may require modified jet plume characteristics in order to reduce the loads and temperatures on the deflected flaps during take-off and landing operations. The tone-excitation effect on the velocity decay of model-scale, two-stream jet plumes is analyzed. Measured data are correlated in terms of parameters that include excitation sound level and outer-to-inner stream velocity ratio. The effect of plume tone-excitation on far-field jet noise is examined and its implication for large-scale two-stream jets is discussed. A.R.H.

**N85-21115\*#** National Aeronautics and Space Administration. Lewis Research Center, Cleveland, Ohio.

### **ADVANCED LINER-COOLING TECHNIQUES FOR GAS TURBINE COMBUSTORS**

C. T. NORNGREN and S. M. RIDDLEBAUGH 1985 21 p refs Proposed for presentation at the 21st Joint Propulsion Conf., Monterey, Calif., 8-10 Jul. 1985; sponsored by AIAA, SAE and ASME (NASA-TM-86952; E-2475; NAS 1.15:86952) Avail: NTIS HC A02/MF A01 CSCL 21E

Component research for advanced small gas turbine engines is currently underway at the NASA Lewis Research Center. As part of this program, a basic reverse-flow combustor geometry was being maintained while different advanced liner wall cooling techniques were investigated. Performance and liner cooling effectiveness of the experimental combustor configuration featuring counter-flow film-cooled panels is presented and compared with two previously reported combustors featuring: splash film-cooled liner walls; and transpiration cooled liner walls (Lamilloy). Author

**N85-21117\*#** Cornell Univ., Ithaca, N.Y. School of Mechanics and Aerospace Engineering.

### **A THEORY OF POST-STALL TRANSIENTS IN MULTISTAGE AXIAL COMPRESSION SYSTEMS Final Report**

F. K. MOORE and E. M. GREITZER Washington NASA Mar. 1985 115 p refs Prepared in cooperation with M.I.T., Cambridge)

(Contract NAG3-34; NSG-3208)

(NASA-CR-3878; NAS 1.26:3878) Avail: NTIS HC A06/MF A01 CSCL 01A

A theory is presented for post stall transients in multistage axial compressors. The theory leads to a set of coupled first-order ordinary differential equations capable of describing the growth and possible decay of a rotating-stall cell during a compressor mass-flow transient. These changing flow features are shown to have a significant effect on the instantaneous compressor pumping characteristic during unsteady operation, and hence on the overall system behavior. It is also found from the theory that the ultimate mode of system response, stable rotating stall or surge, depends

not only on the B parameter but also on other parameters, such as the compressor length-to-diameter ratio. Small values of this latter quantity tend to favor the occurrence of surge, as do large values of B. A limited parametric study is carried out to show the impact of the different system features on transient behavior. Based on analytical and numerical results, several specific topics are suggested for future research on post-stall transients. M.G.

**N85-22368\*#** Hamilton Standard, Windsor Locks, Conn.  
**LARGE-SCALE ADVANCED PROPFAN (LAP) PERFORMANCE, ACOUSTIC AND WEIGHT ESTIMATION, JANUARY, 1984**  
D. PARZYCH, A. SHENKMAN, and S. COHEN Feb. 1985 61 p  
(Contract NAS3-23051)  
(NASA-CR-174782; NAS 1.26:174782; SP-06A83) Avail: NTIS HC A04/MF A01 CSCL 01A

In comparison to turbo-prop applications, the Prop-Fan is designed to operate in a significantly higher range of aircraft flight speeds. Two concerns arise regarding operation at very high speeds: aerodynamic performance and noise generation. This data package covers both topics over a broad range of operating conditions for the eight (8) bladed SR-7L Prop-Fan. Operating conditions covered are: Flight Mach Number 0 - 0.85; blade tip speed 600-800 ft/sec; and cruise power loading 20-40 SHP/D2. Prop-Fan weight and weight scaling estimates are also included.

Author

**N85-23711\*#** National Aeronautics and Space Administration. Lewis Research Center, Cleveland, Ohio.  
**CALCULATION OF THREE-DIMENSIONAL, VISCOUS FLOW THROUGH TURBOMACHINERY BLADE PASSAGES BY PARABOLIC MARCHING**  
T. KATSANIS 11 Jul. 1985 29 p refs Proposed for presentation at 21st Joint Propulsion Conf., Monterey, Calif., 8-11 Jul. 1985; sponsored by AIAA, SAE and ASME  
(NASA-TM-86984; E-2527; NAS 1.15:86984) Avail: NTIS HC A03/MF A01 CSCL 01A

The three-dimensional compressible Navier-Stokes equations are formulated in a rotating coordinate system, so as to include centrifugal and Coriolis forces. The equations are parabolized by using a previously calculated inviscid static pressure field. The thin layer Navier-Stokes approximation, which neglects streamwise diffusion, is used. A body-fitted coordinate system is used. The streamwise momentum equation is uncoupled from the cross-stream momentum equation by using contravariant momentum components, and then using the contravariant velocity components as primary unknowns. To reduce problems with small separated regions, the Reyhner and Flugge-Lotz approximation is used. The energy equation is included to allow for calculation of heat transfer. The flow may be laminar, or a simple eddy-viscosity turbulence may be used. A number of curved ducts and an axial stator were analyzed, including cases for which experimental data are available.

Author

**N85-26668\*#** General Electric Co., Cincinnati, Ohio. Aircraft Engine Business Group.  
**DEVELOPMENT OF A ROTOR WAKE-VORTEX MODEL, VOLUME 1 Final Technical Report**  
R. K. MAJJIGI and P. R. GLIEBE Jun. 1984 171 p refs  
(Contract NAS3-23681)  
(NASA-CR-174849; NAS 1.26:174849) Avail: NTIS HC A08/MF A01 CSCL 01A

Certain empirical rotor wake and turbulence relationships were developed using existing low speed rotor wake data. A tip vortex model was developed by replacing the annulus wall with a row of image vortices. An axisymmetric turbulence spectrum model, developed in the context of rotor inflow turbulence, was adapted to predicting the turbulence spectrum of the stator gust upwash.

G.L.C.

**N85-26670\*#** National Aeronautics and Space Administration. Lewis Research Center, Cleveland, Ohio.  
**AERODYNAMIC DETUNING ANALYSIS OF AN UNSTALLED SUPERSONIC TURBOFAN CASCADE**  
D. HOYNIK and S. FLEETER 21 Mar. 1985 25 p refs  
Presented at the 30th Intern. Gas Turbine Conf. and Exhibit, Houston, Tex., 17-21 Mar. 1985; sponsored by ASME  
(NASA-TM-87001; E-2546; NAS 1.15:87001) Avail: NTIS HC A02/MF A01 CSCL 01A

An approach to passive flutter control is aerodynamic detuning, defined as designed passage-to-passage differences in the unsteady aerodynamic flow field of a rotor blade row. Thus, aerodynamic detuning directly affects the fundamental driving mechanism for flutter. A model to demonstrate the enhanced supersonic aeroelastic stability associated with aerodynamic detuning is developed. The stability of an aerodynamically detuned cascade operating in a supersonic inlet flow field with a subsonic leading edge locus is analyzed, with the aerodynamic detuning accomplished by means of nonuniform circumferential spacing of adjacent rotor blades. The unsteady aerodynamic forces and moments on the blading are defined in terms of influence coefficients in a manner that permits the stability of both a conventional uniformly spaced rotor configuration as well as the detuned nonuniform circumferentially spaced rotor to be determined. With Verdon's uniformly spaced Cascade B as a baseline, this analysis is then utilized to demonstrate the potential enhanced aeroelastic stability associated with this particular type of aerodynamic detuning.

Author

**N85-29916\*#** Toledo Univ., Ohio. Dept. of Mechanical Engineering.  
**AERODYNAMIC ANALYSIS OF A HORIZONTAL AXIS WIND TURBINE BY USE OF HELICAL VORTEX THEORY. VOLUME 1: THEORY Final Report**  
D. R. JENG, T. G. KEITH, JR., and A. ALIABARKHANAFJEH Dec. 1982 88 p refs  
(Contract NCC3-5; DE-AI01-76ET-20320)  
(NASA-CR-168054; DOE/NASA/0005-1; NAS 1.26:168054)  
Avail: NTIS HC A05/MF A01 CSCL 01A

The theoretical development of a method of analysis for prediction of the aerodynamic performance of horizontal axis wind turbines is presented. The method is based on the assumption that a helical vortex emanates from each blade element. Collectively these vortices form a vortex system that extends infinitely far downstream of the blade. Velocities induced by this vortex system are found by applying the Biot-Savart law. Accordingly, this method avoids the use of any interference factors which are used in many of the momentum theories. The method can be used to predict the performance of wind turbines with a small number of blades. The wind turbine performance of a two-bladed rotor is determined and compared to existing experimental data and to corresponding values computed from the widely used PROP code. It was found that the present method compared favorably with experimental data, especially for low wind velocities. The wind turbine performance of a single-bladed rotor is determined subject to the condition that there was no lift on the counterweight or support span. Output power for a one-bladed wind turbine was compared to that of a two-bladed machine.

R.J.F.

**N85-29925\*#** National Aeronautics and Space Administration. Lewis Research Center, Cleveland, Ohio.  
**WIND TUNNEL RESULTS OF ADVANCED HIGH SPEED PROPELLERS IN THE TAKEOFF, CLIMB AND LANDING OPERATING REGIMES**  
G. L. STEFKO and R. J. JERACKI 1985 23 p refs Prepared for the 21st Joint Propulsion Conf., Monterey, Calif., 8-10 Jul. 1985; sponsored in part by AIAA, SAE, ASME and ASEE  
Previously announced in IAA as A85-47025  
(NASA-TM-87054; E-2621; NAS 1.15:87054; AIAA-85-1259)  
Avail: NTIS HC A02/MF A01 CSCL 01A

Low speed wind tunnel performance tests of two advanced propellers were completed. The 62.2 cm diameter adjustable pitch

## 02 AERODYNAMICS

models were tested at Mach numbers typical of takeoff, initial climbout, and landing speeds in the 10 by 10 ft Supersonic Wind Tunnel. Both models had eight blades and a cruise design point operating condition of 0.80 Mach number, 10.668 km S.A. altitude, 243.8 m/s tip speed and a high power loading of 301 kW sq m. No adverse or unusual low speed operating conditions were found during the test with either the straight blade SR-2 or the 45 deg swept SR-3 propellers. The 45 deg swept propeller efficiency exceeded the straight blade efficiency by 4 to 5%. Typical net efficiencies of the straight and 45 deg swept propeller at a Mach 0.20 takeoff condition were 50.2 and 54.9% respectively. At a Mach 0.34 climb condition, the efficiencies were 53.7 and 59.1%. Reverse thrust data indicates that these propellers are capable of producing more reverse thrust at Mach 0.20 than a high bypass turbofan engine at Mach 0.20. E.A.K.

**N85-35158\*#** Braun (Willis H.), Berea, Ohio.  
**UNSTEADY FLOW IN A SUPERSONIC CASCADE WITH TWO IN-PASSAGE SHOCKS** Final Report  
W. H. BRAUN Sep. 1985 90 p refs  
(Contract NAS3-24100)  
(NASA-CR-3925; E-2129; NAS 1.26:3925) Avail: NTIS HC A05/MF A01 CSCL 01A

A model for a supersonic blade row with two in-passage shock waves is developed. It accounts for three-dimensional effects in real flows by using an altered blade shape in a two-dimensional cascade. There is enough flexibility in the choice of blade shape to accommodate a desired entrance angle, exit angle, boundary-layer thickness and stage pressure ratio at a given entrance Mach number. The model divides the mean flow into regions of uniform or one-dimensional flow in which the solutions for the unsteady flow may be formed successively. The analysis makes use of previous solutions for unsteady flow in cascades and over an oscillation wedge. Six flow conditions are chosen in the range of parameters for which the two-shock model is valid for studies of flutter in torsion and bending. It is found, in keeping with previous results from a single-shock model, that in each case there is increasing instability with decreasing frequency. Author

**N85-35159\*#** Stanitz (John D.), University Heights, Ohio.  
**GENERAL DESIGN METHOD FOR 3-DIMENSIONAL, POTENTIAL FLOW FIELDS. PART 2: COMPUTER PROGRAM DIN3D1 FOR SIMPLE, UNBRANCHED DUCTS** Final Report  
J. D. STANITZ Washington NASA Sep. 1985 88 p refs  
(Contract NAS3-21991)  
(NASA-CR-3926; E-2388; NAS 1.26:3926) Avail: NTIS HC A05/MF A01 CSCL 01A

The general design method for three-dimensional, potential, incompressible or subsonic-compressible flow developed in part 1 of this report is applied to the design of simple, unbranched ducts. A computer program, DIN3D1, is developed and five numerical examples are presented: a nozzle, two elbows, an S-duct, and the preliminary design of a side inlet for turbomachines. The two major inputs to the program are the upstream boundary shape and the lateral velocity distribution on the duct wall. As a result of these inputs, boundary conditions are overprescribed and the problem is ill posed. However, it appears that there are degrees of compatibility between these two major inputs and that, for reasonably compatible inputs, satisfactory solutions can be obtained. By not prescribing the shape of the upstream boundary, the problem presumably becomes well posed, but it is not clear how to formulate a practical design method under this circumstance. Nor does it appear desirable, because the designer usually needs to retain control over the upstream (or downstream) boundary shape. The problem is further complicated by the fact that, unlike the two-dimensional case, and irrespective of the upstream boundary shape, some prescribed lateral velocity distributions do not have proper solutions. Author

**N85-35162\*#** Douglas Aircraft Co., Inc., Long Beach, Calif.  
**CALCULATION OF COMPRESSIBLE FLOW ABOUT THREE-DIMENSIONAL INLETS WITH AUXILIARY INLETS, SLATS AND VANES BY MEANS OF A PANEL METHOD** Final Contractor Report, 17 Feb. 1983 - 15 Aug. 1985  
J. L. HESS, D. M. FRIEDMAN, and R. W. CLARK Jun. 1985 197 p refs  
(Contract NAS3-22250)  
(NASA-CR-174975; NAS 1.26:174975; MDC-J3789) Avail: NTIS HC A09/MF A01 CSCL 01A

An efficient and user oriented method was constructed for calculating flow in and about complex inlet configurations. Efficiency is attained by: (1) the use of a panel method; (2) a technique of superposition for obtaining solutions at any inlet operating condition; and (3) employment of an advanced matrix iteration technique for solving large full systems of equations, including the nonlinear equations for the Kutta condition. User concerns are addressed by the provision of several novel graphical output options that yield a more complete comprehension of the flowfield than was possible previously. E.A.K.

## 03

### AIR TRANSPORTATION AND SAFETY

Includes passenger and cargo air transport operations; and aircraft accidents.

**A85-10653\*#** National Aeronautics and Space Administration. Lewis Research Center, Cleveland, Ohio.  
**PROGRESS TOWARD THE DEVELOPMENT OF AN AIRCRAFT ICING ANALYSIS CAPABILITY**  
R. J. SHAW (NASA, Lewis Research Center, Cleveland, OH) American Institute of Aeronautics and Astronautics, Aerospace Sciences Meeting, 22nd, Reno, NV, Jan. 9-12, 1984. 36 p. Previously announced in STAR as N84-20490. refs  
(AIAA PAPER 84-0105)

An overview of the NASA efforts to develop an aircraft icing analysis capability is presented. Discussions are included of the overall and long term objectives of the program as well as current capabilities and limitations of the various computer codes being developed. Descriptions are given of codes being developed to analyze two and three dimensional trajectories of water droplets, airfoil ice accretion, aerodynamic performance degradation of components and complete aircraft configurations, electrothermal deicer, and fluid freezing point depressant deicer. The need for bench mark and verification data to support the code development is also discussed. Author

**A85-20872\*#** Wichita State Univ., Kans.  
**ICING TUNNEL TESTS OF ELECTRO-IMPULSE DE-ICING OF AN ENGINE INLET AND HIGH-SPEED WINGS**  
G. W. ZUMWALT (Wichita State University, Wichita, KS) American Institute of Aeronautics and Astronautics, Aerospace Sciences Meeting, 23rd, Reno, NV, Jan. 14-17, 1985. 8 p. refs  
(Contract NAG3-284)  
(AIAA PAPER 85-0466)

A brief review is given of four earlier tests in the NASA Lewis Icing Research Tunnel and of flight tests in NASA's Icing Research Aircraft and in a Cessna 206 airplane. Details are given of recent icing tunnel tests of thicker-skinned wings, a Gates Learjet, a composite leading edge, and a Boeing 767, and of a Falcon Fanjet engine inlet. These were tested at speeds from 87 to 220 knots, air temperatures from -2 to -15 C, LWC values of 0.6 to 2.4 grams/cu meter, and median droplet diameters from 12 to 20 microns. Energy requirements are reported, as well as conclusions from comparisons of several Electro-Impulse De-Icing coil system designs. Fundamental studies of the structural dynamics and ice shedding of a 12.7 cm (5 inch) diameter semicylinder are described. Some potential problem areas are discussed: fatigue of skin and



coil mountings, system weight and cost, electro-magnetic interference and noise. Author

**A85-28898\*#** National Aeronautics and Space Administration. Lewis Research Center, Cleveland, Ohio.

**THE UH-1H HELICOPTER ICING FLIGHT TEST PROGRAM - AN OVERVIEW**

R. J. SHAW and G. P. RICHTER (NASA, Lewis Research Center, Cleveland, OH) American Institute of Aeronautics and Astronautics, Aerospace Sciences Meeting, 23rd, Reno, NV, Jan. 14-17, 1985. 25 p. Previously announced in STAR as N85-15702. refs (AIAA PAPER 85-0338)

An ongoing joint NASA/Army program to study the effects of ice accretion on unprotected helicopter rotor aerodynamic performance is discussed. This program integrates flight testing, wind tunnel testing, and analytical modeling. Results are discussed for helicopter flight testing in the Canadian NRC hover spray rig facility to measure rotor aero performance degradation and document rotor ice accretion characteristics. The results of dry wind tunnel testing of airfoil sections with artificial ice accretions and predictions of rotor performance degradation using available rotor performance codes and the wind tunnel data are presented. An alternative approach to conducting future helicopter icing flight programs is discussed. Author

**A85-30192\*#** National Aeronautics and Space Administration. Lewis Research Center, Cleveland, Ohio.

**ICING FLIGHT RESEARCH - AERODYNAMIC EFFECTS OF ICE AND ICE SHAPE DOCUMENTATION WITH STEREO PHOTOGRAPHY**

K. L. MIKKELSEN, R. C. MCKNIGHT, R. J. RANAUDO (NASA, Lewis Research Center, Cleveland, OH), and P. J. PERKINS, JR. (Sverdrup Technology, Inc., Middleburg Heights, OH) American Institute of Aeronautics and Astronautics, Aerospace Sciences Meeting, 23rd, Reno, NV, Jan. 14-17, 1985. 31 p. Previously announced in STAR as N85-18049. refs (AIAA PAPER 85-0468)

Aircraft icing flight research was performed in natural icing conditions. A data base consisting of icing cloud measurements, ice shapes, and aerodynamic measurements is being developed. During research icing encounters the icing cloud was continuously measured. After the encounter, the ice accretion shapes on the wing were documented with a stereo camera system. The increase in wing section drag was measured with a wake survey probe. The overall aircraft performance loss in terms of lift and drag coefficient changes were obtained by steady level speed/power measurements. Selective deicing of the airframe components was performed to determine their contributions to the total drag increase. Engine out capability in terms of power available was analyzed for the iced aircraft. It was shown that the stereo photography system can be used to document ice shapes in flight and that the wake survey probe can measure increases in wing section drag caused by ice. On one flight, the wing section drag coefficient ( $c_{sub d}$ ) increased approximately 120 percent over the uniced baseline at an aircraft angle of attack of 6 deg. On another flight, the aircraft drag coefficient ( $c_{sub d}$ ) increased by 75 percent over the uniced baseline at an aircraft lift coefficient ( $c_{sub d}$ ) of 0.5. Author

**A85-42937\*#** Texas A&M Univ., College Station. **PERFORMANCE DEGRADATION OF HELICOPTER ROTOR IN FORWARD FLIGHT DUE TO ICE**

K. D. KORKAN (Texas A & M University, College Station), L. DADONE (Boeing Vertol Co., Philadelphia, PA), and R. J. SHAW (NASA, Lewis Research Center, Cleveland, OH) Journal of Aircraft (ISSN 0021-8669), vol. 22, Aug. 1985, p. 713-718. refs (Contract NAG3-242)

This study addresses the analytical assessment of the degradation in the forward flight performance of the front rotor Boeing Vertol CH47D helicopter in a rime ice natural icing encounter. The front rotor disk was divided into 24 15-deg sections and the local Mach number and angle of attack were evaluated as a function of azimuthal and radial location for a specified flight condition. Profile drag increments were then calculated as a function of azimuthal and radial position for different times of exposure to icing, and the rotor performance was re-evaluated including these drag increments. The results of the analytical prediction method, such as horsepower required to maintain a specific flight condition, as a function of icing time have been generated. The method to illustrate the value of such an approach in assessing performance changes experienced by a helicopter rotor as a result of rime ice accretion is described. Author

**N85-15702\*#** National Aeronautics and Space Administration. Lewis Research Center, Cleveland, Ohio.

**THE UH-1H HELICOPTER ICING FLIGHT TEST PROGRAM: AN OVERVIEW**

R. J. SHAW and G. P. RICHTER 1985 26 p refs Presented at the 23rd Aerospace Sci. Meeting, Reno, Nevada, 14-17 Jan. 1985; sponsored by AIAA, 14-17 Jan. 1985 (NASA-TM-86925; E-2421; NAS 1.15:86925; AIAA-85-0338) Avail: NTIS HC A03/MF A01 CSCL 01C

An ongoing joint NASA/Army program to study the effects of ice accretion on unprotected helicopter rotor aerodynamic performance is discussed. This program integrates flight testing, wind tunnel testing, and analytical modeling. Results are discussed for helicopter flight testing in the Canadian NRC hover spray rig facility to measure rotor aero performance degradation and document rotor ice accretion characteristics. The results of dry wind tunnel testing of airfoil sections with artificial ice accretions and predictions of rotor performance degradation using available rotor performance codes and the wind tunnel data are presented. An alternative approach to conducting future helicopter icing flight programs is discussed. B.W.

**N85-27839\*#** National Aeronautics and Space Administration. Lewis Research Center, Cleveland, Ohio.

**ICE SHAPES AND THE RESULTING DRAG INCREASE FOR A NACA 0012 AIRFOIL**

W. OLSEN, R. J. SHAW, and J. NEWTON 12 Jan. 1984 31 p refs Presented at the 22nd Aerospace Sci. Meeting, Reno, Nev., 9-12 Jan. 1984; sponsored by AIAA (NASA-TM-83556; E-1935; NAS 1.15:83556) Avail: NTIS HC A03/MF A01 CSCL 01C

Experimental measurements of the ice shapes and resulting drag increases were measured in the NASA-Lewis Icing Research Tunnel. The measurements were made over a large range of conditions (e.g., airspeed and temperature, drop size and liquid water content of the cloud, and the angle of attack of the airfoil). The measured drag increase did not agree with the existing correlation. Additional results were given which are helpful in understanding the ice structure and the way it forms, and in improving the ice accretion modeling theories. There are data on the ice surface roughness, on the effect of the ice shape on the local droplet catch, and on the relative importance of various parts of the ice shape on the drag increase. Experimental repeatability is also discussed. Author

# AIRCRAFT DESIGN, TESTING AND PERFORMANCE

Includes aircraft simulation technology.

## A85-21844\*# Texas A&M Univ., College Station. EXPERIMENTAL AERODYNAMIC CHARACTERISTICS OF AN NACA 0012 AIRFOIL WITH SIMULATED ICE

K. D. KORKAN, E. J. CROSS, JR., and C. C. CORNELL (Texas A&M University, College Station, TX) Journal of Aircraft (ISSN 0021-8669), vol. 22, Feb. 1985, p. 130-134. Previously cited in issue 06, p. 719, Accession no. A84-17937. refs (Contract NAG3-242)

## A85-40811\*# Wichita State Univ., Kans. ELECTRO-IMPULSE DE-ICING OF A TURBOFAN ENGINE INLET

G. W. ZUMWALT (Wichita State University, KS) AIAA, SAE, ASME, and ASEE, Joint Propulsion Conference, 21st, Monterey, CA, July 8-10, 1985. 8 p. refs (Contract NAG3-284) (AIAA PAPER 85-1118)

The application of electromagnetic impulse deicing (EIDI) systems to turbofan engine inlets on business aircraft has been investigated experimentally. The tests were performed in the Icing Research Tunnel at NASA's Lewis Research Center. The deicing system testbed was a Falcon Fanjet 20 engine nacelle. The effectiveness of various deicing coil configurations and mount designs were compared, and design parameters were developed specifically for EIDI systems in turbofan engines. Flight tests were also carried out at altitudes in the range 3000-6000 ft corresponding to a temperature range of -3 to -8 C. It is shown that the ice particles removed from the engine inlet by the deicing system were small enough for the engine to ingest. Tentative design specifications are given with respect to the optimum coil configuration, and operating power of a EIDI production candidate. I.H.

## N85-12887\*# National Aeronautics and Space Administration. Lewis Research Center, Cleveland, Ohio. INITIAL FEASIBILITY GROUND TEST OF A PROPOSED PHOTOGRAMMETRIC SYSTEM FOR MEASURING THE SHAPES OF ICE ACCRETIONS ON HELICOPTER ROTOR BLADES DURING FORWARD FLIGHT Final Report, 1 Oct. - 31 Dec. 1983

R. L. PALKO (Calspan Field Services, Inc., Arnold Air Force Station, Tenn.), P. L. CASSADY (Calspan Field Services, Inc., Arnold Air Force Station, Tenn.), R. C. MCKNIGHT, and R. J. FREEDMAN Aug. 1984 45 p (NASA-TM-87391; NAS 1.15:87391; AD-A146051; AEDC-TR-84-10) Avail: NTIS HC A03/MF A01 CSCL 01C

A ground test was accomplished to determine if a combination of standard photographic system parameters could be chosen that would allow stereophotographs to be made of the main rotor of a UH-1H helicopter in forward flight. The photographs would be used to measure the shape of ice accretions on the rotor in forward flight. During the ground test, 83 photographic pairs were obtained at three camera shutter speeds for a range of ambient light conditions from dark to complete daylight. Twenty-seven of these photographic pairs were evaluated on the AEDC analytical stereocompiler for readability. The test showed that quality photographs could be taken using standard equipment with shutter speeds of 1/30 and 1/60 sec for up to three hours per day. The test also showed that the addition of a specifically designed control circuit for synchronization at 1/500-sec shutter speed would allow testing for the complete day for most winter days. GRA

N85-18049\*# National Aeronautics and Space Administration. Lewis Research Center, Cleveland, Ohio.

## ICING FLIGHT RESEARCH: AERODYNAMIC EFFECTS OF ICE AND ICE SHAPE DOCUMENTATION WITH STEREO PHOTOGRAPHY

K. L. MIKKELSEN, R. C. MCKNIGHT, R. J. RANAUDO, and P. J. PERKINS, JR. (Sverdrup Technology, Inc., Middleburg Heights, Ohio) 1985 32 p refs Presented at the 23rd Aerospace Sci. Meeting, Reno, Nevada, 14-17 Jan. 1985; sponsored by AIAA (NASA-TM-86906; E-2395; NAS 1.15:86906; AIAA-85-0468) Avail: NTIS HC A03/MF A01 CSCL 01C

Aircraft icing flight research was performed in natural icing conditions. A data base consisting of icing cloud measurements, ice shapes, and aerodynamic measurements is being developed. During research icing encounters the icing cloud was continuously measured. After the encounter, the ice accretion shapes on the wing were documented with a stereo camera system. The increase in wing section drag was measured with a wake survey probe. The overall aircraft performance loss in terms of lift and drag coefficient changes was obtained by steady level speed/power measurements. Selective deicing of the airframe components was performed to determine their contributions to the total drag increase. Engine out capability in terms of power available was analyzed for the iced aircraft. It was shown that the stereo photography system can be used to document ice shapes in flight and that the wake survey probe can measure increases in wing section drag caused by ice. On one flight, the wing section drag coefficient ( $C_{sub d}$ ) increased approximately 120 percent over the uniced baseline at an aircraft angle of attack of 6 deg. On another flight, the aircraft drag coefficient ( $C_{sub d}$ ) increased by 75 percent over the uniced baseline at an aircraft lift coefficient ( $C_{sub l}$ ) of 0.5. Author

N85-19978\*# General Electric Co., Cincinnati, Ohio. Aircraft Engine Business Group.

## STUDY OF ADVANCED FUEL SYSTEM CONCEPTS FOR COMMERCIAL AIRCRAFT

G. A. COFFINBERRY Jan. 1985 256 p refs (Contract NAS3-23267) (NASA-CR-174751; NAS 1.26:174751; R85AEB166) Avail: NTIS HC A12/MF A01 CSCL 01C

An analytical study was performed in order to assess relative performance and economic factors involved with alternative advanced fuel systems for future commercial aircraft operating with broadened property fuels. The DC-10-30 wide-body tri-jet aircraft and the CF6-80X engine were used as a baseline design for the study. Three advanced systems were considered and were specifically aimed at addressing freezing point, thermal stability and lubricity fuel properties. Actual DC-10-30 routes and flight profiles were simulated by computer modeling and resulted in prediction of aircraft and engine fuel system temperatures during a nominal flight and during statistical one-day-per-year cold and hot flights. Emergency conditions were also evaluated. Fuel consumption and weight and power extraction results were obtained. An economic analysis was performed for new aircraft and systems. Advanced system means for fuel tank heating included fuel recirculation loops using engine lube heat and generator heat. Environmental control system bleed air heat was used for tank heating in a water recirculation loop. The results showed that fundamentally all of the three advanced systems are feasible but vary in their degree of compatibility with broadened-property fuel. B.W.

## N85-35185\*# SKF Industries, Inc., King of Prussia, Pa. PLANETARY-GEAR-SUPPORT BEARING TEST RIG DESIGN Contractor Report, 8 Feb. 1983 - 8 Jan. 1985

J. W. ROSENLIEN Mar. 1985 81 p (Contract NAS3-23702) (NASA-CR-174927; NAS 1.26:174927; AT85T004) Avail: NTIS HC A05/MF A01 CSCL 01C

A test rig was designed to evaluate the performance of a spherical roller bearing with a geared outer ring operating under conditions similar to those of a planet bearing in a helicopter



transmission. The configuration is an extension of the widely accepted four-square gearbox arrangement. It provides for testing of two bearings simultaneously with outer ring rotation, misalignment, diametrically opposed loading through the gear teeth, and under race lubrication. Instrumentation permits the measurement of inner and outer ring temperature, bearing drag torque, degree of misalignment, outer ring speed, cage speed, and applied load. Author

## 06

### AIRCRAFT INSTRUMENTATION

Includes cockpit and cabin display devices; and flight instruments.

**A85-16098\*#** Army Propulsion Lab., Cleveland, Ohio.  
**COMPARISON OF ICING CLOUD INSTRUMENTS FOR 1982-1983 ICING SEASON FLIGHT PROGRAM**  
 R. F. IDE (U.S. Army, Propulsion Laboratory, Cleveland, OH) and G. P. RICHTER (NASA, Lewis Research Center, Cleveland, OH) American Institute of Aeronautics and Astronautics, Aerospace Sciences Meeting, 22nd, Reno, NV, Jan. 9-12, 1984. 24 p. Previously announced in STAR as N84-29870. refs (AIAA PAPER 84-0020)

A number of modern and old style liquid water content (LWC) and droplet sizing instruments were mounted on a DeHavilland DHC-6 Twin Otter and operated in natural icing clouds in order to determine their comparative operating characteristics and their limitations over a broad range of conditions. The evaluation period occurred during the 1982-1983 icing season from January to March 1983. Time histories of all instrument outputs were plotted and analyzed to assess instrument repeatability and reliability. Scatter plots were also generated for comparison of instruments. The measured LWC from four instruments differed by as much as 20 percent. The measured droplet size from two instruments differed by an average of three microns. The overall effort demonstrated the need for additional data, and for some means of calibrating these instruments to known standards. Author

## 07

### AIRCRAFT PROPULSION AND POWER

Includes prime propulsion systems and systems components, e.g., gas turbine engines and compressors; and on-board auxiliary power plants for aircraft.

**A85-13627\*#** National Aeronautics and Space Administration. Lewis Research Center, Cleveland, Ohio.  
**THE ROLE OF MODERN CONTROL THEORY IN THE DESIGN OF CONTROLS FOR AIRCRAFT TURBINE ENGINES**  
 W. MERRILL, B. LEHTINEN, and J. ZELLER (NASA, Lewis Research Center, Cleveland, OH) Journal of Guidance, Control, and Dynamics (ISSN 0731-5090), vol. 7, Nov.-Dec. 1984, p. 652-661. Previously cited in issue 11, p. 1707, Accession no. A82-26526. refs

**A85-13630\*#** National Aeronautics and Space Administration. Lewis Research Center, Cleveland, Ohio.  
**IDENTIFICATION OF MULTIVARIABLE HIGH-PERFORMANCE TURBOFAN ENGINE DYNAMICS FROM CLOSED-LOOP DATA**  
 W. MERRILL (NASA, Lewis Research Center, Aerodynamics and Engine Systems Div., Cleveland, OH) (Identification and system parameter estimation 1982; Proceedings of the Sixth Symposium, Washington, DC, June 7-11, 1982. Volume 1, p. 427-434) Journal of Guidance, Control, and Dynamics (ISSN 0731-5090), vol. 7, Nov.-Dec. 1984, p. 677-683. Previously cited in issue 06, p. 723, Accession no. A84-18582. refs

**A85-13953\*#** General Electric Co., Cincinnati, Ohio.  
**COMPARISON OF SCALED MODEL DATA TO FULL SIZE ENERGY EFFICIENT ENGINE TEST RESULTS**  
 S. P. LAVIN, P. Y. HO (General Electric Co., Aircraft Engine Business Group, Cincinnati, OH), and R. CHAMBERLIN (NASA, Lewis Research Center, Cleveland, OH) American Institute of Aeronautics and Astronautics and NASA, Aeroacoustics Conference, 9th, Williamsburg, VA, Oct. 15-17, 1984. 15 p. refs (Contract NAS3-20643) (AIAA PAPER 84-2281)

Acoustic tests of a subscale fan and a subscale mixer nozzle were conducted in anechoic chambers over a variety of operating conditions. The subscale fan test was an investigation into the effects of vane/blade ratio and spacing on fan generated noise. A turbulence control structure (TCS) was used to simulate the 'turbulence-free' condition in flight. The subscale mixer nozzle test investigated the acoustic properties of several different forced mixer designs. A tertiary flow was utilized on the mixer model to simulate the forward velocity effects on the jet. The results were scaled up to full size conditions and compared with measured engine data. The comparisons showed good agreement between the component scaled model results and the full scale engine data. Author

**A85-13954\*#** General Electric Co., Cincinnati, Ohio.  
**MEASUREMENT AND PREDICTION OF ENERGY EFFICIENT ENGINE NOISE**  
 S. P. LAVIN, P. Y. HO (General Electric Co., Aircraft Engine Business Group, Cincinnati, OH), and R. CHAMBERLIN (NASA, Lewis Research Center, Cleveland, OH) American Institute of Aeronautics and Astronautics and NASA, Aeroacoustics Conference, 9th, Williamsburg, VA, Oct. 15-17, 1984. 11 p. refs (AIAA PAPER 84-2284)

The NASA/GE Energy Efficient Engine (E3) static noise levels were measured in an acoustic arena on the Integrated Core and Low Spool Test System. These measured levels were scaled to the appropriate size to power four study aircraft and were projected to flight for evaluation of noise levels relative to FAR36, Stage III limits. As a result of these evaluations, it is predicted that the NASA/GE E3 engine with a wide spacing cut-on blade/vane ratio fan and a forced mixer nozzle can meet FAR36 Stage III limits with sufficient design margin. Author

**A85-16097\*#** National Aeronautics and Space Administration. Lewis Research Center, Cleveland, Ohio.  
**SENSOR FAILURE DETECTION FOR JET ENGINES USING ANALYTICAL REDUNDANCY**  
 W. C. MERRILL (NASA, Lewis Research Center, Cleveland, OH) AIAA, SAE, and ASME, Joint Propulsion Conference, 20th, Cincinnati, OH, June 11-13, 1984. 23 p. Previously announced in STAR as N84-24585. refs (AIAA PAPER 84-1452)

Analytical redundant sensor failure detection, isolation and accommodation techniques for gas turbine engines are surveyed. Both the theoretical technology base and demonstrated concepts are discussed. Also included is a discussion of current technology needs and ongoing Government sponsored programs to meet those needs. Author

## 07 AIRCRAFT PROPULSION AND POWER

### **A85-18792\*#** General Electric Co., Cincinnati, Ohio. **CONSIDERATIONS FOR DAMAGE ANALYSIS OF GAS TURBINE HOT SECTION COMPONENTS**

T. S. COOK and J. H. LAFLEN (General Electric Co., Cincinnati, OH) American Society of Mechanical Engineers, Pressure Vessels and Piping Conference and Exhibition, San Antonio, TX, June 17-21, 1984. 7 p. refs

(Contract NAS3-22534)

(ASME PAPER 84-PVP-77)

The hot flowpath of a gas turbine engine contains static and rotating components operating in a very hostile environment. Since the reliable operation of these components is critical to the safe and efficient performance of the engine, structural life analysis of these members is carried out with great care. However, the complex nature of the strain-temperature-time cycle affecting the engine makes a general analysis procedure difficult and usually leads to separating the damage into regimes where one damage mode dominates. In particular, cycle dependent, time dependent, and thermomechanical fatigue regimes have been identified and some general considerations of each region are discussed. This discussion includes both the damage models themselves and the application of the models. Specific examples of several models are given and important factors affecting each are presented.

Author

### **A85-21866\*#** Pennsylvania State Univ., University Park. **EFFECTS OF FRICTION DAMPERS ON AERODYNAMICALLY UNSTABLE ROTOR STAGES**

A. SINHA (Pennsylvania State University, University Park, PA) and J. H. GRIFFIN (Carnegie-Mellon University, Pittsburgh, PA) AIAA Journal (ISSN 0001-1452), vol. 23, Feb. 1985, p. 262-270. Previously cited in issue 14, p. 1976, Accession no. A83-32791. refs

(Contract NAG3-231)

### **A85-25442\*** Washington Univ., Seattle. **AN EXPERIMENTAL INVESTIGATION AND NUMERICAL PREDICTION OF THERMOMECHANICAL PHENOMENA IN HIGH SPEED ROTOR TIP RUBBING**

A. F. EMERY, S. ETEMAD, J. WOLAK, and S. R. CHOI (Washington University, Seattle, WA) IN: Numerical methods in thermal problems. Volume 3 Proceedings of the Third International Conference, Seattle, WA, August 2-5, 1983. Swansea, Wales, Pineridge Press, 1983, p. 1040-1049. refs

(Contract NAG3-7)

A thermomechanical study of the intermittent rubbing of a rotor blade tip and a casing seal is carried out taking into account the existence of thermal contact resistance. The effect of the thermal properties of a plasma sprayed coating on the blade tip is studied. The influence of a variable heat generation and variable thermal contact resistance at the blade tip as it passes along the path of rubbing is also discussed.

Author

### **A85-25984\*** General Electric Co., Cincinnati, Ohio. **ALTITUDE TESTING OF A FLIGHT WEIGHT, SELF-COOLED, 2D THRUST VECTORING EXHAUST NOZZLE**

W. H. WOOTEN, J. T. BLOZY, D. W. SPEIR (General Electric Co., Cincinnati, OH), and R. A. LOTTIG (NASA, Lewis Research Center, Cleveland, OH) Society of Automotive Engineers, Aerospace Congress and Exposition, Long Beach, CA, Oct. 15-18, 1984. 11 p.

(SAE PAPER 841557)

The Augmented Deflector Exhaust Nozzle (ADEN) was tested in PSL-3 at NASA-Lewis Research Center using an F404 engine. The ADEN is a flight weight Single Expansion Ramp Nozzle with thrust vectoring, an internal cooling system utilizing the available engine fan flow, and a variable area throat controlled by the engine control system. Test conditions included dry and max A/B operation at nozzle pressure ratios from 2.0 to 15.0. High nozzle pressure loading was simulated to verify structural integrity at near maximum design pressure. Nozzle settings covered the full range in throat area and + or - 15 deg deflection angle. Test results demonstrated expected aerodynamic performance, cooling system effectiveness, control system stability, and mechanical integrity.

Author

### **A85-30378\*#** National Aeronautics and Space Administration. **THE EFFECT OF AERODYNAMIC AND STRUCTURAL DETUNING ON TURBOMACHINE SUPERSONIC UNSTALLED TORSIONAL FLUTTER**

D. HOYNIK (NASA, Lewis Research Center, Cleveland, OH) and S. FLEETER (Purdue University, West Lafayette, IN) IN: Structures, Structural Dynamics, and Materials Conference, 26th, Orlando, FL, April 15-17, 1985, Technical Papers. Part 2. New York, American Institute of Aeronautics and Astronautics, 1985, p. 500-514. refs (AIAA PAPER 85-0761)

The effects of alternate-blade structural detuning and adjacent-blade alternate-circumferential-spacing aerodynamic detuning on the supersonic unstalled torsional flutter stability of a turbomachine rotor are investigated analytically. An unsteady aerodynamic model employing influence coefficients is constructed for the case of a flat-plate-airfoil cascade in torsion-mode harmonic oscillation in a supersonic inviscid isentropic adiabatic irrotational perfect-gas inlet flow with a subsonic leading-edge locus. The influence coefficients and equations of motion are derived; the model is verified by applying it to the 12-blade cascade-B flow geometry studied by Verdon and McCune (1975); and the results are presented graphically. It is found that the rotor can be stabilized

### **A85-19509\*#** National Aeronautics and Space Administration. **COMPUTATIONAL THERMO-FLUID DYNAMICS CONTRIBUTIONS TO ADVANCED GAS TURBINE ENGINE DESIGN**

R. W. GRAHAM, J. J. ADAMCZYK, and H. E. ROHLIK (NASA, Lewis Research Center, Cleveland, OH) American Institute of Aeronautics and Astronautics, Aerospace Sciences Meeting, 23rd, Reno, NV, Jan. 14-17, 1985. 10 p. Previously announced in STAR as N85-10069. refs

(AIAA PAPER 85-0083)

The design practices for the gas turbine are traced throughout history with particular emphasis on the calculational or analytical methods. Three principal components of the gas turbine engine will be considered: namely, the compressor, the combustor and the turbine.

B.W.

### **A85-20867\*#** Texas A&M Univ., College Station. **ANALYTICAL DETERMINATION OF PROPELLER PERFORMANCE DEGRADATION DUE TO ICE ACCRETION**

T. L. MILLER (Sverdrup Technology, Inc., Middleburg Heights, OH), K. D. KORKAN (Texas A&M University, College Station, TX), and R. J. SHAW (NASA, Lewis Research Center, Cleveland, OH) American Institute of Aeronautics and Astronautics, Aerospace Sciences Meeting, 23rd, Reno, NV, Jan. 14-17, 1985. 42 p. refs (Contract NAG3-242)

(AIAA PAPER 85-0339)

It is pointed out that ice accretion on aircraft produces an adverse effect on aircraft performance in terms of decreased lift and increased drag of the lifting surface. Ice on the surface of a propeller may also cause a decrease in thrust, increase in the required power, and a resultant decrease in propeller efficiency. During the past years, a number of attempts have been made to analyze the effects of ice accretion on both fixed wings and propellers. The present investigation is concerned with the development of a single user-oriented computer code which makes it possible to calculate propeller performance degradation due to ice accretion for specified flight conditions, atmospheric conditions, and propeller geometry. This development is based on a combination of several of the codes and correlations considered in earlier studies.

G.R.

over the entire reduced frequency range by applying a combination of structural and aerodynamic detuning as the passive flutter-control mechanism. T.K.

**A85-32005\*#** General Electric Co., Lynn, Mass.  
**CONTINGENCY POWER CONCEPTS FOR HELICOPTER TURBOSHAFT ENGINE**

R. HIRSCHKRON, R. H. DAVIS, D. N. GOLDSTEIN, J. F. HAYNES (General Electric Co., Lynn, MA), and J. W. GAUNTNER (NASA, Lewis Research Center, Cleveland, OH) IN: American Helicopter Society, Annual Forum, 40th, Arlington, VA, May 16-18, 1984, Proceedings. Alexandria, VA, American Helicopter Society, 1984, p. 597-608. Previously announced in STAR as N84-23648. (Contract NAS3-23705)

Twin helicopter engines are often sized by power requirement of safe mission completion after the failure of one of the two engines. This study was undertaken for NASA Lewis by General Electric Co. to evaluate the merits of special design features to provide a 2-1/2 minute Contingency Power rating, permitting an engine size reduction. The merits of water injection, cooling flow modulation, throttle push and an auxiliary power plant were evaluated using military life cycle cost (LCC) and commercial helicopter direct operating cost (DOC) merit factors in a rubber engine/rubber aircraft scenario. Author

**A85-32006\*#** General Electric Co., Lynn, Mass.  
**TF34 CONVERTIBLE ENGINE CONTROL SYSTEM DESIGN**

D. R. GILMORE, JR. (General Electric Co., Aircraft Engine Business Group, Lynn, MA) IN: American Helicopter Society, Annual Forum, 40th, Arlington, VA, May 16-18, 1984, Proceedings. Alexandria, VA, American Helicopter Society, 1984, p. 609-620. refs (Contract NAS3-22752)

The characteristics of the TF34 convertible engine, capable of producing shaft power, thrust, or a combination of both, is investigated with respect to the control system design, development, bench testing, and the anticipated transient response during engine testing at NASA. The modifications to the prototype standard TF34-GE-400 turbofan, made primarily in the fan section, consist of the variable inlet guide vanes and variable exit guide vanes. The control system was designed using classical frequency domain techniques and was based on the anticipated convertible/VTOL airframe requirements. The engine has been run in the fan mode and in the shaft mode, exhibiting a response of 0.14 second to a 5-percent thrust change. L.T.

**A85-34013\*#** National Aeronautics and Space Administration.  
 Lewis Research Center, Cleveland, Ohio.

**PREDICTED TURBINE STAGE PERFORMANCE USING QUASI-THREE-DIMENSIONAL AND BOUNDARY-LAYER ANALYSES**

R. J. BOYLE, J. E. HAAS (NASA, Lewis Research Center, Cleveland, OH), and T. KATSANIS (NASA, Lewis Research Center; U.S. Army, Research and Technology Laboratories, Cleveland, OH) Journal of Propulsion and Power (ISSN 0748-4658), vol. 1, May-June 1985, p. 242-251. Previously cited in issue 17, p. 2432, Accession no. A84-36972. refs

**A85-39065\*** Army Propulsion Lab., Cleveland, Ohio.  
**TEMPERATURE DISTORTION GENERATOR FOR TURBOSHAFT ENGINE TESTING**

G. A. KLANN (U.S. Army, Propulsion Laboratory, Cleveland, OH), R. L. BARTH, and T. J. BIESIADNY (NASA, Lewis Research Center, Cleveland, OH) IN: Advances in aerospace propulsion; Proceedings of the Aerospace Congress and Exposition, Long Beach, CA, October 15-18, 1984. Warrendale, PA, Society of Automotive Engineers, Inc., 1984, p. 89-99. Previously announced in STAR as N85-15659. refs (SAE PAPER 841541)

The procedures and unique hardware used to conduct an experimental investigation into the response of a small-turboshaft-engine compression system to various hot gas ingestion patterns are presented. The temperature distortion generator described herein uses gaseous hydrogen to create both

steady-state and time-variant, or transient, temperature distortion at the engine inlet. The range of transient temperature ramps produced by the distortion generator during the engine tests was from less than 111 deg K/sec (200 deg R/sec) to above 611 deg K/sec (1100 deg R/sec); instantaneous temperatures to 422 deg K (760 deg F) above ambient were generated. The distortion generator was used to document the maximum inlet temperatures and temperature rise rates that the compression system could tolerate before the onset of stall for various circumferential distortions as well as the compressor system response during stall. Author

**A85-39580\*#** National Aeronautics and Space Administration.  
 Lewis Research Center, Cleveland, Ohio.

**FLAME RADIATION AND LINEAR HEAT TRANSFER IN A TUBULAR-CAN COMBUSTOR**

R. W. CLAUS, G. M. NEELY, and F. M. HUMENIK (NASA, Lewis Research Center, Cleveland, OH) Journal of Propulsion and Power (ISSN 0748-4658), vol. 1, July-Aug. 1985, p. 270-278. Previously cited in issue 07, p. 872, Accession no. A84-21300. refs

**A85-39606\*#** National Aeronautics and Space Administration.  
 Lewis Research Center, Cleveland, Ohio.

**EXPERIMENTS IN DILUTION JET MIXING - EFFECTS OF MULTIPLE ROWS AND NON-CIRCULAR ORIFICES**

J. D. HOLDEMAN (NASA, Lewis Research Center, Modeling and Verification Branch, Cleveland, OH), R. SRINIVASAN, E. B. COLEMAN, G. D. MEYERS, and C. D. WHITE (Garrett Turbine Engine Co., Phoenix, AZ) AIAA, SAE, ASME, and ASEE, Joint Propulsion Conference, 21st, Monterey, CA, July 8-10, 1985. 12 p. Previously announced in STAR as N85-25266. refs (AIAA PAPER 85-1104)

Experimental and empirical model results are presented that extend previous studies of the mixing of single-sided and opposed rows of jets in a confined duct flow to include effects of non-circular orifices and double rows of jets. Analysis of the mean temperature data obtained in this investigation showed that the effects of orifice shape and double rows are significant only in the region close to the injection plane, provided that the orifices are symmetric with respect to the main flow direction. The penetration and mixing of jets from 45-degree slanted slots is slightly less than that from equivalent-area symmetric orifices. The penetration from two-dimensional slots is similar to that from equivalent-area closely-spaced rows of holes, but the mixing is slower for the 2-D slots. Calculated mean temperature profiles downstream of jets from non-circular and double rows of orifices, made using an extension developed for a previous empirical model, are shown to be in good agreement with the measured distributions. Author

**A85-39703\*#** National Aeronautics and Space Administration.  
 Lewis Research Center, Cleveland, Ohio.

**ADVANCED LINER-COOLING TECHNIQUES FOR GAS TURBINE COMBUSTORS**

C. T. NORGREN and S. M. RIDDLEBAUGH (NASA, Lewis Research Center, Cleveland, OH) AIAA, SAE, ASME, and ASEE, Joint Propulsion Conference, 21st, Monterey, CA, July 8-10, 1985. 13 p. Previously announced in STAR as N85-21115. refs (AIAA PAPER 85-1290)

Component research for advanced small gas turbine engines is currently underway at the NASA Lewis Research Center. As part of this program, a basic reverse-flow combustor geometry was being maintained while different advanced liner wall cooling techniques were investigated. Performance and liner cooling effectiveness of the experimental combustor configuration featuring counter-flow film-cooled panels is presented and compared with two previously reported combustors featuring: splash film-cooled liner walls; and transpiration cooled liner walls (Lamilloy). Author

## 07 AIRCRAFT PROPULSION AND POWER

**A85-39717\*#** National Aeronautics and Space Administration. Lewis Research Center, Cleveland, Ohio.

### **SMALL GAS TURBINE COMBUSTOR STUDY - FUEL INJECTOR PERFORMANCE IN A TRANSPARATION-COOLED LINER**

S. M. RIDDLEBAUGH and C. T. NORGRÉN (NASA, Lewis Research Center, Cleveland, OH) AIAA, SAE, ASME, and ASEE, Joint Propulsion Conference, 21st, Monterey, CA, July 8-10, 1985. 12 p. refs

(AIAA PAPER 85-1312)

The effect of fuel injection technique on the performance of an advanced reverse flow combustor liner constructed of Lamilloy (a multilaminate transpiration type material) was determined. Performance and emission levels are documented over a range of simulated flight conditions using simplex pressure atomizing, spill return, and splash cone airblast injectors. A parametric evaluation of the effect of increased combustor loading with each of the fuel injector types is obtained. E.A.K.

**A85-40841\*#** General Electric Co., Cincinnati, Ohio.

### **STALL RECOVERY CONTROL STRATEGY METHODOLOGY AND RESULTS**

W. R. HOPF and W. G. STEENKEN (General Electric Co., Cincinnati, OH) AIAA, SAE, ASME, and ASEE, Joint Propulsion Conference, 21st, Monterey, CA, July 8-10, 1985. 14 p. refs

(Contract NAS3-23540)

(AIAA PAPER 85-1433)

The nonrecoverable stall condition in high performance turbofan engines is characterized by thrust loss, rising turbine temperatures, high pressure compressor rotating stall, and loss of engine control. Stall recovery control is presently investigated by means of an engine system computer model capable of either surge or rotating stall postinstability operation. Several techniques are examined which can yield rapid recovery from stall; a composite strategy which involves reduction of engine speed to idle while simultaneously opening the 10th- and 14th-stage compressor bleed ports allowed recovery to speeds slightly higher than idle while combustor fuel flow continued. O.C.

**A85-41778\*** National Aeronautics and Space Administration. Lewis Research Center, Cleveland, Ohio.

### **THE TREND OF FUTURE GAS TURBINE TECHNOLOGY**

M. J. HARTMANN (NASA, Lewis Research Center, Cleveland, OH) IN: 1983 Tokyo International Gas Turbine Congress, Tokyo, Japan, October 23-29, 1983, Proceedings. Volume 1. Tokyo, Gas Turbine Society of Japan, 1984, p. S-19 to S-25.

Future gas turbine technology will be based on contributions to the technology base being made today. At the NASA Lewis Research Center in Cleveland, OH, research is being conducted on turbomachinery system components and in a number of associated disciplines to advance the technology of aviation turbofan and turbojet engines. Areas of research include compressors, turbines, internal flow analysis, combustion, fuels, materials, structures, bearings, seals, lubrication, dynamics and controls, and instrumentation. A review of the research directions being taken in these areas and the steady advances being made provides a reasonable glimpse at gas turbine technology of the future. Author

**A85-42365\*#** Virginia Polytechnic Inst. and State Univ., Blacksburg.

### **OPTIMIZATION OF CASCADE BLADE MISTUNING. I - EQUATIONS OF MOTION AND BASIC INHERENT PROPERTIES**

E. NISSIM (Virginia Polytechnic Institute and State University, Blacksburg) AIAA Journal (ISSN 0001-1452), vol. 23, Aug. 1985, p. 1213-1222. refs

(Contract NAG3-347)

Attention is given to the derivation of the equations of motion of mistuned compressor blades, interpolating aerodynamic coefficients by means of quadratic expressions in the reduced frequency. If the coefficients of the quadratic expressions are permitted to assume complex values, excellent accuracy is obtained and Pade rational expressions are obviated. On the basis of the

resulting equations, it is shown analytically that the sum of all the real parts of the eigenvalues is independent of the mistuning introduced into the system. Blade mistuning is further treated through the aerodynamic energy approach, and the limiting vibration modes associated with alternative mistunings are identified. O.C.

**A85-42671\*#** National Aeronautics and Space Administration. Lewis Research Center, Cleveland, Ohio.

### **FUTURE FUNDAMENTAL COMBUSTION RESEARCH FOR AEROPROPULSION SYSTEMS**

E. J. MULARZ (NASA, Lewis Research Center; U.S. Army, Propulsion Laboratory, Cleveland, OH) AIAA, SAE, ASME, and ASEE, Joint Propulsion Conference, 21st, Monterey, CA, July 8-10, 1985. 7 p. Army-supported research. Previously announced in STAR as N85-27870. refs

(AIAA PAPER 85-1398)

Physical fluid mechanics, heat transfer, and chemical kinetic processes which occur in the combustion chamber of aeropropulsion systems were investigated. With the component requirements becoming more severe for future engines, the current design methodology needs the new tools to obtain the optimum configuration in a reasonable design and development cycle. Research efforts in the last few years were encouraging but to achieve these benefits research is required into the fundamental aerothermodynamic processes of combustion. It is recommended that research continues in the areas of flame stabilization, combustor aerodynamics, heat transfer, multiphase flow and atomization, turbulent reacting flows, and chemical kinetics. Associated with each of these engineering sciences is the need for research into computational methods to accurately describe and predict these complex physical processes. Research needs in each of these areas are highlighted. E.A.K.

**A85-45715\*#** Virginia Polytechnic Inst. and State Univ., Blacksburg.

### **OPTIMIZATION OF CASCADE BLADE MISTUNING. II - GLOBAL OPTIMUM AND NUMERICAL OPTIMIZATION**

E. NISSIM and R. T. HAFTKA (Virginia Polytechnic Institute and State University, Blacksburg) AIAA Journal (ISSN 0001-1452), vol. 23, Sept. 1985, p. 1402-1410.

(Contract NAG3-347)

The values of the mistuning which yield the most stable eigenvectors are analytically determined, using the simplified equations of motion which were developed in Part I of this work. It is shown that random mistunings, if large enough, may lead to the maximal stability, whereas the alternate mistunings cannot. The problem of obtaining maximum stability for minimal mistuning is formulated, based on numerical optimization techniques. Several local minima are obtained using different starting mistuning vectors. The starting vectors which lead to the global minimum are identified. It is analytically shown that all minima appear in multiplicities which are equal to the number of compressor blades. The effect of mistuning on the flutter speed is studied using both an optimum mistuning vector and an alternate mistuning vector. Effects of mistunings in elastic axis locations are shown to have a negligible effect on the eigenvalues. Finally, it is shown that any general two-dimensional bending-torsion system can be reduced to an equivalent uncoupled torsional system. Author

**A85-45854\*#** National Aeronautics and Space Administration. Lewis Research Center, Cleveland, Ohio.

### **VIBRATION AND FLUTTER OF MISTUNED BLADED-DISK ASSEMBLIES**

K. R. V. KAZA and R. E. KIELB (NASA, Lewis Research Center, Cleveland, OH) Journal of Propulsion and Power (ISSN 0748-4658), vol. 1, Sept.-Oct. 1985, p. 336-344. Previously cited in issue 05, p. 602, Accession no. A85-16095. refs

**A85-47021\*#** National Aeronautics and Space Administration. Lewis Research Center, Cleveland, Ohio.

**LARGE-SCALE ADVANCED PROPFAN (LAP) PROGRAM PROGRESS REPORT**

D. A. SAGERSEER (NASA, Lewis Research Center, Cleveland, OH) and S. G. LUDEMANN (United Technologies Corp., Hamilton Standard Div., Windsor Locks, CT) AIAA, SAE, ASME, and ASEE, Joint Propulsion Conference, 21st, Monterey, CA, July 8-10, 1985. 26 p. Previously announced in STAR as N85-29964. refs (AIAA PAPER 85-1187)

The propfan is an advanced propeller concept which maintains the high efficiencies traditionally associated with conventional propellers at the higher aircraft cruise speeds associated with jet transports. The large-scale advanced propfan (LAP) program extends the research done on 2 ft diameter propfan models to a 9 ft diameter article. The program includes design, fabrication, and testing of both an eight bladed, 9 ft diameter propfan, designated SR-7L, and a 2 ft diameter aeroelastically scaled model, SR-7A. The LAP program is complemented by the propfan test assessment (PTA) program, which takes the large-scale propfan and mates it with a gas generator and gearbox to form a propfan propulsion system and then flight tests this system on the wing of a Gulfstream 2 testbed aircraft. Author

**A85-49021\*** National Aeronautics and Space Administration. Lewis Research Center, Cleveland, Ohio.

**A GENERALIZED COMPUTER CODE FOR DEVELOPING DYNAMIC GAS TURBINE ENGINE MODELS (DIGTEM)**

C. J. DANIELE (NASA, Lewis Research Center, Cleveland, OH) IN: Aerospace simulation; Proceedings of the Conference, San Diego, CA, February 2-4, 1984. La Jolla, CA, Society for Computer Simulation, 1984, p. 212-221. Previously announced in STAR as N84-12166. refs

This paper describes DIGTEM (digital turbofan engine model), a computer program that simulates two spool, two stream (turbofan) engines. DIGTEM was developed to support the development of a real time multiprocessor based engine simulator being designed at the Lewis Research Center. The turbofan engine model in DIGTEM contains steady state performance maps for all the components and has control volumes where continuity and energy balances are maintained. Rotor dynamics and duct momentum dynamics are also included. DIGTEM features an implicit integration scheme for integrating stiff systems and trims the model equations to match a prescribed design point by calculating correction coefficients that balance out the dynamic equations. It uses the same coefficients at off design points and iterates to a balanced engine condition. Transients are generated by defining the engine inputs as functions of time in a user written subroutine (TMRSP). Closed loop controls can also be simulated. DIGTEM is generalized in the aerothermodynamic treatment of components. This feature, along with DIGTEM's trimming at a design point, make it a very useful tool for developing a model of a specific turbofan engine. B.W.

**N85-10064\*#** National Aeronautics and Space Administration. Lewis Research Center, Cleveland, Ohio.

**COMBUSTION GAS PROPERTIES I-ASTM JET A FUEL AND DRY AIR**

R. E. JONES, A. M. TROUT, J. D. WEAR, and B. J. MCBRIDE Oct. 1984 12 p refs Document incl. microfiche supplement (NASA-TP-2359; NAS 1.60:2359) Avail: NTIS HC E03/MF A01 CSCL 21E

A series of computations was made to produce the equilibrium temperature and gas composition for ASTM jet A fuel and dry air. The computed tables and figures provide combustion gas property data for pressures from 0.5 to 50 atmospheres and equivalence ratios from 0 to 2.0. S.B.

**N85-10065\*#** National Aeronautics and Space Administration. Lewis Research Center, Cleveland, Ohio.

**COMPARISON OF NUMERICAL TECHNIQUES FOR INTEGRATION OF STIFF ORDINARY DIFFERENTIAL EQUATIONS ARISING IN COMBUSTION CHEMISTRY**

K. RADHAKRISHNAN Oct. 1984 41 p refs Sponsored in part by Michigan Univ. and NRC (Contract NAG3-147; NAG3-294) (NASA-TP-2372; E-2149; NAS 1.60:2372) Avail: NTIS HC A03/MF A01 CSCL 21E

The efficiency and accuracy of several algorithms recently developed for the efficient numerical integration of stiff ordinary differential equations are compared. The methods examined include two general-purpose codes, EPISODE and LSODE, and three codes (CHEMEQ, CREK1D, and GCKP84) developed specifically to integrate chemical kinetic rate equations. The codes are applied to two test problems drawn from combustion kinetics. The comparisons show that LSODE is the fastest code currently available for the integration of combustion kinetic rate equations. An important finding is that an interactive solution of the algebraic energy conservation equation to compute the temperature does not result in significant errors. In addition, this method is more efficient than evaluating the temperature by integrating its time derivative. Significant reductions in computational work are realized by updating the rate constants ( $k = A \exp(-E/RT)$ ) only when the temperature change exceeds an amount  $\Delta T$  that is problem dependent. An approximate expression for the automatic evaluation of  $\Delta T$  is derived and is shown to result in increased efficiency. Author

**N85-10067\*#** National Aeronautics and Space Administration. Lewis Research Center, Cleveland, Ohio.

**EFFECT OF COMBINED PRESSURE AND TEMPERATURE DISTORTION ORIENTATION ON HIGH-BYPASS-RATIO TURBOFAN ENGINE STABILITY**

R. H. SOEDER and C. M. MEHALIC Washington Oct. 1984 37 p refs (NASA-TM-83771; E-2262; NAS 1.15:83771) Avail: NTIS HC A03/MF A01 CSCL 21E

Total-temperature, static-pressure and total-pressure distributions were measured in the inlet duct upstream of the engine inlet and within the fan and compressor of a YTF34 turbofan engine. Free-stream and boundary layer yaw angle variations were measured between a rotatable screen assembly and the engine inlet. Total pressure distortions were generated using three 180 deg extent screens and total temperature distortions were generated using a rotatable hydrogen burner. Reynolds number index upstream of the rotatable screen assembly was maintained at 0.5 (based on the undistorted sectors at station 1, the inlet flow measuring station). The engine mechanical fan speed at sea level condition was rated at 7005 rpm. The engine was tested at a corrected fan speed of 90 percent of rated condition. Yaw angle increased between the rotatable screen assembly and the engine inlet. The largest variation in free-stream and boundary layer yaw angle occurs when the combined distortions are 180 deg out-of-phase. Static-pressure distortion increased exponentially as flow approached the engine. Total-pressure distortions were attenuated between the engine inlet and the compressor exit. Total-temperature distortion persisted through the compressor for all four combined distortions investigated. Author

**N85-10068\*#** National Aeronautics and Space Administration. Lewis Research Center, Cleveland, Ohio.

**CREKID: A COMPUTER CODE FOR TRANSIENT, GAS-PHASE COMBUSTION OF KINETICS**

D. T. PRATT (Washington Univ., Seattle) and K. RADHAKRISHNAN Washington Oct. 1984 38 p refs (Contract NAG3-147) (NASA-TM-83806; E-2176; NAS 1.15:83806) Avail: NTIS HC A03/MF A01 CSCL 21B

A new algorithm was developed for fast, automatic integration of chemical kinetic rate equations describing homogeneous, gas-phase combustion at constant pressure. Particular attention is

## 07 AIRCRAFT PROPULSION AND POWER

paid to the distinguishing physical and computational characteristics of the induction, heat-release and equilibration regimes. The two-part predictor-corrector algorithm, based on an exponentially-fitted trapezoidal rule, includes filtering of ill-posed initial conditions, automatic selection of Newton-Jacobi or Newton iteration for convergence to achieve maximum computational efficiency while observing a prescribed error tolerance. The new algorithm was found to compare favorably with LSODE on two representative test problems drawn from combustion kinetics.

B.W.

**N85-10069\*#** National Aeronautics and Space Administration. Lewis Research Center, Cleveland, Ohio.

### **COMPUTATIONAL THERMO-FLUID DYNAMICS CONTRIBUTIONS TO ADVANCED GAS TURBINE ENGINE DESIGN**

R. W. GRAHAM, J. J. ADAMCZYK, and H. E. ROHLIK Washington 1984 13 p refs Proposed for presentation at the 23d Aerospace Sciences Meeting, Reno, Nev., 14-17 Jan. 1985; sponsored by AIAA Previously announced in IAA as A85-19509

(NASA-TM-86865; E-2194; NAS 1.15:86865) Avail: NTIS HC A02/MF A01 CSCL 21E

The design practices for the gas turbine are traced throughout history with particular emphasis on the calculational or analytical methods. Three principal components of the gas turbine engine will be considered: namely, the compressor, the combustor and the turbine.

B.W.

**N85-10947\*#** United Technologies Corp., East Hartford, Conn. Engineering Div.

### **ENERGY EFFICIENT ENGINE FLIGHT PROPULSION SYSTEM PRELIMINARY ANALYSIS AND DESIGN REPORT Final Update Report**

J. W. BISSET and D. C. HOWE Sep. 1983 166 p refs

(Contract NAS3-20646)

(NASA-CR-174701; NAS 1.26:174701; PWA-5594-248) Avail: NTIS HC A06/MF A01 CSCL 21E

The final design and analysis of the flight propulsion system is presented. This system is the conceptual study engine defined to meet the performance, economic and environmental goals established for the Energy Efficient Engine Program. The design effort included a final definition of the engine, major components, internal subsystems, and nacelle. Various analytical representations and results from component technology programs are used to verify aerodynamic and structural design concepts and to predict performance. Specific design goals and specifications, reflecting future commercial aircraft propulsion system requirements for the mid-1980's, are detailed by NASA and used as guidelines during engine definition. Information is also included which details salient results from a separate study to define a turbofan propulsion system, known as the maximum efficiency engine, which reoptimized the advanced fuel saving technologies for improved fuel economy and direct operating costs relative to the flight propulsion system.

M.A.C.

**N85-10948\*#** Washington Univ., Seattle.

### **AN INTERACTIVE COMPUTER CODE FOR CALCULATION OF GAS-PHASE CHEMICAL EQUILIBRIUM (EQLBRM) Final Report**

B. S. PRATT and D. T. PRATT Oct. 1984 22 p refs

(Contract NAG3-277)

(NASA-CR-168337; NAS 1.26:168337) Avail: NTIS HC A02/MF A01 CSCL 21E

A user friendly, menu driven, interactive computer program known as EQLBRM which calculates the adiabatic equilibrium temperature and product composition resulting from the combustion of hydrocarbon fuels with air, at specified constant pressure and enthalpy is discussed. The program is developed primarily as an instructional tool to be run on small computers to allow the user to economically and efficiently explore the effects of varying fuel type, air/fuel ratio, inlet air and/or fuel temperature, and operating pressure on the performance of continuous combustion devices

such as gas turbine combustors, Stirling engine burners, and power generation furnaces.

M.A.C.

**N85-10949\*#** National Aeronautics and Space Administration. Lewis Research Center, Cleveland, Ohio.

### **ACCELERATED CONVERGENCE FOR INCOMPRESSIBLE FLOW CALCULATIONS**

G. M. NEELY and R. W. CLAUS 1984 13 p refs Proposed for presentation at the 23rd Aerospace Sci. Meeting, Reno, Nev., 14-17 Jan. 1985; sponsored by the American Inst. of Aeronautics and Astronautics

(NASA-TM-86863; E-2327; NAS 1.15:86863) Avail: NTIS HC A02/MF A01 CSCL 21E

Two improved algorithms which solve the steady-state Navier-Stokes equations, PISO and SIMPLER, are studied. Computations were carried out on progressively finer grids for the driven cavity and flow over a backward-facing step. The effects of relaxation factor, number of grid nodes and number of sweeps through the pressure equations are studied to evaluate the performance of the PISO and SIMPLER schemes. Results show that these improved schemes accelerate the convergence rate of the solution generally by a factor of two as compared to the SIMPLE method.

Author

**N85-10950\*#** United Technologies Corp., East Hartford, Conn. **ENERGY EFFICIENT ENGINE COMBUSTOR TEST HARDWARE DETAILED DESIGN REPORT**

M. H. ZEISSER, W. GREENE, and D. J. DUBIEL Mar. 1982 105 p refs

(Contract NAS3-20646)

(NASA-CR-167945; NAS 1.26:167945; PWA-5594-197) Avail: NTIS HC A06/MF A01 CSCL 21E

The combustor for the Energy Efficient Engine is an annular, two-zone component. As designed, it either meets or exceeds all program goals for performance, safety, durability, and emissions, with the exception of oxides of nitrogen. When compared to the configuration investigated under the NASA-sponsored Experimental Clean Combustor Program, which was used as a basis for design, the Energy Efficient Engine combustor component has several technology advancements. The prediffuser section is designed with short, strutless, curved-walls to provide a uniform inlet airflow profile. Emissions control is achieved by a two-zone combustor that utilizes two types of fuel injectors to improve fuel atomization for more complete combustion. The combustor liners are a segmented configuration to meet the durability requirements at the high combustor operating pressures and temperatures. Liner cooling is accomplished with a counter-parallel FINWALL technique, which provides more effective heat transfer with less coolant.

Author

**N85-10951\*#** National Aeronautics and Space Administration. Lewis Research Center, Cleveland, Ohio.

### **TURBINE ENGINE HOT SECTION TECHNOLOGY (HOST)**

Washington Oct. 1982 356 p refs Workshop held in Cleveland, 19-20 Oct. 1982

(NASA-TM-83022; E-1458; NAS 1.15:83022) Avail: NTIS HC A16/MF A01 CSCL 21E

Research and plans concerning aircraft gas turbine engine hot section durability problems were discussed. Under the topics of structural analysis, fatigue and fracture, surface protective coatings, combustion, turbine heat transfer, and instrumentation specific points addressed were the thermal and fluid environment around liners, blades, and vanes, material coatings, constitutive behavior, stress-strain response, and life prediction methods for the three components.

**N85-10954\*#** National Aeronautics and Space Administration. Lewis Research Center, Cleveland, Ohio.

## **NONLINEAR STRUCTURAL AND LIFE ANALYSES OF A TURBINE BLADE**

A. KAUFMAN *In its* Turbine Eng. Hot Sect. Technol. (HOST) p 39-44 Oct. 1982

Avail: NTIS HC A16/MF A01 CSCL 21E

The most critical structural requirements that aircraft gas turbine engines must meet result from the diversity of extreme environmental conditions in the turbine section components. Accurate life assessment of the components under these conditions requires sound analytical tools and techniques. The utility of advanced structural analysis techniques and advanced life prediction techniques in the life assessment of hot-section components was evaluated. The extent to which a three-dimensional cyclic isoparametric finite element analysis of a hot-section component would improve the accuracy of component life predictions was assessed. At the same time, high temperature life prediction theories such as strainrange partitioning and the frequency modified approaches were applied and their efficiency judged. A stress analysis was performed on a commercial air-cooled turbine blade. The evaluation of the life prediction methods indicated that none of those studied were satisfactory. R.S.F.

**N85-10955\*#** National Aeronautics and Space Administration. Lewis Research Center, Cleveland, Ohio.

## **NONLINEAR STRUCTURAL AND LIFE ANALYSES OF A COMBUSTOR LINER**

A. KAUFMAN *In its* Turbine Eng. Hot Sect. Technol. (HOST) p 45-53 Oct. 1982

Avail: NTIS HC A16/MF A01 CSCL 21E

Three-dimensional, nonlinear, finite element structural analyses were performed for a simulated aircraft combustor liner specimen in order to assess the capability of nonlinear analyses using classical inelastic material models to represent the thermoplastic-creep response of the component. In addition, the computed stress-strain history at the critical location was input into life prediction methods in order to evaluate the ability of these procedures to predict crack initiation life. It is concluded that: (1) elastic analysis is adequate for obtaining strain range and critical location; (2) inelastic analyses did not accurately represent cyclic behavior of materials; and (3) none of the crack initiation life prediction methods were satisfactory. R.S.F.

**N85-10956\*#** National Aeronautics and Space Administration. Lewis Research Center, Cleveland, Ohio.

## **PRE-HOST HIGH TEMPERATURE CRACK PROPAGATION**

T. W. ORANGE *In its* Turbine Eng. Hot Sect. Technol. (HOST) p 55-63 Oct. 1982

Avail: NTIS HC A16/MF A01 CSCL 21E

The highlights of NASA contract CR-167896, Fracture Mechanics Criteria for Turbine Engine Hot Section Components, are presented. The five technical tasks of the program are reviewed. Results of several tasks are presented. R.S.F.

**N85-10957\*#** National Aeronautics and Space Administration. Lewis Research Center, Cleveland, Ohio.

## **HOST INSTRUMENTATION R AND D PROGRAM OVERVIEW**

N. C. WENGER *In its* Turbine Eng. Hot Sect. Technol. (HOST) p 65-68 Oct. 1982

Avail: NTIS HC A16/MF A01 CSCL 21E

The turbine hot-section technology (HOST) Instrumentation R&D program focuses on two main classes of instrumentation: (1) those that characterize the environment around the turbine engine components, which include gas flows measurement, gas temperatures, and heat fluxes; (2) to characterize the effect of the environment on the turbine engine components, which include strain measurements and an optical system to structural responses such as cracking, buckling, spalling, carbon buildup. The HOST Instrumentation R&D program concentrates on the critical measurements that can not be made by commercially available instruments or with instruments that are already in development. The measurements of strain and gas flow are emphasized, these

measurements are extremely critical to the success of the HOST program and the HOST requirements differ from the current state of the art by a considerable margin. E.A.K.

**N85-10959\*#** United Technologies Research Center, East Hartford, Conn.

## **HIGH TEMPERATURE STATIC STRAIN SENSOR DEVELOPMENT PROGRAM**

C. HULSE, F. LEMKEY, R. BAILEY, and H. GRANT *In* NASA. Lewis Research Center Turbine Eng. Hot Sect. Technol. (HOST) p 83-91 Oct. 1982

(Contract NAS3-23169)

Avail: NTIS HC A16/MF A01 CSCL 21E

The development of resistance strain gages which are useful for static strain measurements on nickel or cobalt superalloy parts inside a gas turbine engine on a test stand were examined. These measurements of a strain gage alloy development program which to be followed by an optional investigation of complete strain gage systems which will use the best of the alloys developed together with other system improvements is reviewed. The specific goal for the complete system is to make measurements to 2,000 micro epsilon with error of only + or - 10% over a 50 hour period. In addition to simple survival and stability, attaining a low thermal coefficient to resistivity, of order 100 ppm/K or less, is also a major goal. The first task was to select candidate alloys or alloy systems using a search of the literature and the available metallurgical theory. Alloy candidates were evaluated and compared by a grading system. Equipment and techniques were developed which are suitable for iterative studies of a variety of compositions. Many compositions were examined and significantly improved alloys were identified. E.A.K.

**N85-10962\*#** National Aeronautics and Space Administration. Lewis Research Center, Cleveland, Ohio.

## **HOT SECTION LASER ANEMOMETRY**

W. C. NIEBERDING *In its* Turbine Eng. Hot Sect. Technol. (HOST) p 109-112 Oct. 1982 refs

Avail: NTIS HC A16/MF A01 CSCL 21E

The objectives and problems faced in the development of a laser anemometry system for hot section applications was discussed. The goal was to map the flow profiles through and between the vanes and between the rotating blades of a turbine. A laser anemometer system was developed which measures the Doppler shift directly along the optical axis. Some testing is being conducted in a small bench top combustor facility. The cost involved in this testing was also discussed. E.R.

**N85-10964\*#** National Aeronautics and Space Administration. Lewis Research Center, Cleveland, Ohio.

## **TURBINE HEAT TRANSFER**

J. E. ROHDE *In its* Turbine Eng. Hot Sect. Technol. (HOST) p 119-136 Oct. 1982

Avail: NTIS HC A16/MF A01 CSCL 21E

Objectives and approaches to research in turbine heat transfer are discussed. Generally, improvements in the method of determining the hot gas flow through the turbine passage is one area of concern, as is the cooling air flow inside the airfoil, and the methods of predicting the heat transfer rates on the hot gas side and on the coolant side of the airfoil. More specific areas of research are: (1) local hot gas recovery temperatures along the airfoil surfaces; (2) local airfoil wall temperature; (3) local hot gas side heat transfer coefficients on the airfoil surfaces; (4) local coolant side heat transfer coefficients inside the airfoils; (5) local hot gas flow velocities and secondary flows at real engine conditions; and (6) local delta strain range of the airfoil walls. E.R.



## 07 AIRCRAFT PROPULSION AND POWER

**N85-10968\*#** National Aeronautics and Space Administration. Lewis Research Center, Cleveland, Ohio.

### **COOLANT PASSAGE HEAT TRANSFER WITH ROTATION**

J. E. ROHDE *In its* Turbine Eng. Hot Sect. Technol. (HOST) p 175-179 Oct. 1982

Avail: NTIS HC A16/MF A01 CSCL 21E

Although the effects of the coriolis and buoyancy forces due to rotation on coolant-side heat transfer are generally not included in the design methods for blades, the influence of these forces could be large. Comparisons of nonrotating heat transfer data and extrapolations of available correlation for the average heat transfer coefficients with radial outflow of cooling air showed that neglecting rotation at gas turbine engine conditions result in variations in the heat transfer coefficient by as much as 45 percent. This, in effect, results in blade metal temperatures running as much as 100 F different from predicted values. This also may explain why rotating blade metal temperatures in engine tests are often higher than expected from results obtained in nonrotating cascade tests. B.G.

**N85-10969\*#** National Aeronautics and Space Administration. Lewis Research Center, Cleveland, Ohio.

### **STRUCTURAL ANALYSIS**

R. H. JOHNS *In its* Turbine Eng. Hot Sect. Technol. (HOST) p 181-184 Oct. 1982

Avail: NTIS HC A16/MF A01 CSCL 21E

Hot section components of aircraft gas turbine engines are subjected to severe thermal-structural loading conditions, especially during the start-up and take-off portions of the engine cycle. The most severe and damaging stresses and strains are those induced by the steep thermal gradients induced during the start-up transient. These transient stresses and strains are also the most difficult to predict, in part because the temperature gradients and distributions are not well known or predictable, and also because the cyclic elasto-viscoplastic behavior of the materials at these extremes of temperature and strain are not well known or predictable. One element of the structures program will develop improved time-varying thermal-mechanical load models for the entire engine mission cycle from start-up to shutdown. The thermal model refinements will be consistent with those required by the structural code including considerations of mesh-point density, strain concentrations, and thermal gradients. Models will be developed for the burner liner, turbine vane and turbine blade. B.G.

**N85-10971\*#** National Aeronautics and Space Administration. Lewis Research Center, Cleveland, Ohio.

### **COMPONENT-SPECIFIC MODELING**

M. S. HIRSCHBEIN *In its* Turbine Eng. Hot Sect. Technol. (HOST) p 197-202 Oct. 1982

Avail: NTIS HC A16/MF A01 CSCL 21E

The ability to accurately structurally analyze engine components to assure that they can survive for their designed lifetime in an increasingly harsh environment is discussed. Under the HOST (HOT Section Technology) program, advanced component-specific modeling methods, with built-in analysis capability, will be developed separately for burner liners, turbine blades and vanes. These modeling methods will make maximum use of, but will not rely solely on, existing analysis methods and techniques, to analyze the three identified components. Nor will the complete structural analysis of a component necessarily be performed as a single analysis. The approach to be taken will develop complete software analysis packages with internal, component-specific, self-adaptive solution strategies. Each package will contain a set of modeling and analysis tools. The selection and order of specific methods and techniques within the set to be applied will depend on the specific-component, the current thermo-mechanical loading, and the current state of the component. All modeling and analysis decisions will be made internally based on developed decision criteria within the solution strategies; minimal user intervention will be required. B.W.

**N85-10972\*#** National Aeronautics and Space Administration. Lewis Research Center, Cleveland, Ohio.

### **THE 3-D INELASTIC ANALYSIS METHODS FOR HOT SECTION COMPONENTS: BRIEF DESCRIPTION**

C. C. CHAMIS *In its* Turbine Eng. Hot Sect. Technol. (HOST) p 203-208 Oct. 1982

Avail: NTIS HC A16/MF A01

Advanced 3-D inelastic structural/stress analysis methods and solution strategies for more accurate yet more cost-effective analysis of components subjected to severe thermal gradients and loads in the presence of mechanical loads, with steep stress and strain gradients are being developed. Anisotropy, time and temperature dependent plasticity and creep effects are also addressed. The approach is to develop four different theories, one linear and three higher order theories (polynomial function, special function, general function). The theories are progressively more complex from linear to general function in order to provide streamlined analysis capability with increasing accuracy for each hot section component and for different parts of the same component according to the severity of the local stress, strain and temperature gradients associated with hot spots, cooling holes and surface coating cracks. To further enhance the computational effectiveness, the higher order theories will have embedded singularities (cooling passages, for example) in the generic modeling region. Each of the four theories consists of three formulation models derivable from independent theoretical formulations. These formulation models are based on: (1) mechanics of materials; (2) special finite elements; and (3) an advanced formulation to be recommended by the contractor. B.W.

**N85-10973\*#** National Aeronautics and Space Administration. Lewis Research Center, Cleveland, Ohio.

### **LIFE PREDICTION AND CONSTITUTIVE BEHAVIOR: OVERVIEW**

G. R. HALFORD *In its* Turbine Eng. Hot Sect. Technol. (HOST) p 209-212 Oct. 1982

Avail: NTIS HC A16/MF A01 CSCL 21E

The evolution of programs to investigate high temperature constitutive behavior and develop cyclic life prediction methods is reviewed. Contracts granted for developing and verifying workable engineering methods for the calculation, in advance of service, of the local stress-strain response at the critical life governing location in typical hot section components as well as the resultant cyclic crack initiation and crack growth lifetimes are listed. The Langley fatigue facility is being upgraded to include: (1) a servocontrolled testing machine for high temperature crack growth; (2) three servocontrolled tension/torsion machines for biaxial studies; (3) a HOST/satellite computer for data acquisition, processing, storage, and retrieval; and (4) HCV/LCF machines for cumulative damage studies. A.R.H.

**N85-10975\*#** National Aeronautics and Space Administration. Lewis Research Center, Cleveland, Ohio.

### **CONSTITUTIVE MODEL DEVELOPMENT FOR ISOTROPIC MATERIALS**

A. KAUFMAN *In its* Turbine Eng. Hot Sect. Technol. (HOST) p 215-221 Oct. 1982

Avail: NTIS HC A16/MF A01 CSCL 21E

The objective is to develop a unified constitutive model for finite-element structural analysis of turbine engine hot section components. This effort constitutes a different approach for nonlinear finite-element computer codes which were heretofore based on classical inelastic methods. A unified constitutive theory will avoid the simplifying assumptions of classical theory and should more accurately represent the behavior of superalloy materials under cyclic loading conditions and high temperature environments. Model development will be directed toward isotropic, cast nickel-base alloys used for aircooled turbine blades and vanes. The contractor will select a base material for model development and an alternate material for verification purposes from a list of three alloys specified by NASA. The candidate alloys represent a cross-section of turbine blade and vane materials of interest to



both large and small size engine manufacturers. Material stock for the base and alternate materials will be supplied to the Contractor by the government. R.J.F.

**N85-10977\*#** National Aeronautics and Space Administration. Lewis Research Center, Cleveland, Ohio.

### **HOST HIGH TEMPERATURE CRACK PROPAGATION**

T. W. ORANGE *In its* Turbine Eng. Hot Sect. Technol. (HOST) p 227-229 Oct. 1982

Avail: NTIS HC A16/MF A01 CSCL 21E

Methods for characterizing and predicting crack growth at elevated temperatures are discussed. Nonlinear behavior, thermal gradients, and thermomechanical cycling are discussed. R.J.F.

**N85-10978\*#** National Aeronautics and Space Administration. Lewis Research Center, Cleveland, Ohio.

### **SURFACE PROTECTION OVERVIEW**

S. R. LEVINE *In its* Turbine Eng. Hot Sect. Technol. (HOST) p 231-239 Oct. 1982

Avail: NTIS HC A16/MF A01 CSCL 21E

A first-cut integrated environmental attack life prediction methodology for hot section components is addressed. The HOST program is concerned with oxidation and hot corrosion attack of metallic coatings as well as their degradation by interdiffusion with the substrate. The effects of the environment and coatings on creep/fatigue behavior are being addressed through a joint effort with the Fatigue sub-project. An initial effort will attempt to scope the problem of thermal barrier coating life prediction. Verification of models will be carried out through benchmark rig tests including a 4 atm. replaceable blade turbine and a 50 atm. pressurized burner rig. B.W.

**N85-10979\*#** National Aeronautics and Space Administration. Lewis Research Center, Cleveland, Ohio.

### **AIRFOIL DEPOSITION MODEL**

F. J. KOHL *In its* Turbine Eng. Hot Sect. Technol. (HOST) p 241-257 Oct. 1982 refs

Avail: NTIS HC A16/MF A01 CSCL 21E

The methodology to predict deposit evolution (deposition rate and subsequent flow of liquid deposits) as a function of fuel and air impurity content and relevant aerodynamic parameters for turbine airfoils is developed in this research. The spectrum of deposition conditions encountered in gas turbine operations includes the mechanisms of vapor deposition, small particle deposition with thermophoresis, and larger particle deposition with inertial effects. The focus is on using a simplified version of the comprehensive multicomponent vapor diffusion formalism to make deposition predictions for: (1) simple geometry collectors; and (2) gas turbine blade shapes, including both developing laminar and turbulent boundary layers. For the gas turbine blade the insights developed in previous programs are being combined with heat and mass transfer coefficient calculations using the STAN 5 boundary layer code to predict vapor deposition rates and corresponding liquid layer thicknesses on turbine blades. A computer program is being written which utilizes the local values of the calculated deposition rate and skin friction to calculate the increment in liquid condensate layer growth along a collector surface. B.W.

**N85-10980\*#** National Aeronautics and Space Administration. Lewis Research Center, Cleveland, Ohio.

### **EFFECTS OF SURFACE CHEMISTRY ON HOT CORROSION LIFE: OVERVIEW**

J. MERUTKA *In its* Turbine Eng. Hot Sect. Technol. (HOST) p 263-267 Oct. 1982

Avail: NTIS HC A16/MF A01 CSCL 21E

This program concentrates on analyzing a limited number of hot corroded components from the field and the carrying out of a series of controlled laboratory experiments to establish the effects of oxide scale and coating chemistry on hot corrosion life. This is to be determined principally from the length of the incubation period, the investigation of the mechanisms of hot corrosion attack,

and the fitting of the data generated from the test exposure experiments to an empirical life prediction model. Author

**N85-10984\*#** National Aeronautics and Space Administration. Lewis Research Center, Cleveland, Ohio.

### **DILUTION ZONE MIXING STUDIES**

J. D. HOLDEMAN *In its* Turbine Eng. Hot Sect. Technol. (HOST) p 307-314 Oct. 1982 refs

Avail: NTIS HC A16/MF A01 CSCL 21E

The objectives and status of a project to investigate various aspects of the jet in a confined cross flow problem are outlined. The experiments performed thus far dealt primarily with a single row of jets mixing into an isothermal flow in a constant cross section duct. Variations in the mixing were observed as a function of jet to mainstream momentum ratio, orifice size, and spacing. The current experiments examine perturbations of this problem characteristic to gas turbine combustion chambers, namely: flow area convergence, nonisothermal mainstream flow, and opposed in line and staggered injection. An empirical model was developed to describe the observed temperature distributions. The current interactive code provides a 3-D pictorial representation of the temperature, as given by these correlations, for any user specified downstream location, flow, and orifice parameters. M.G.

**N85-10986\*#** National Aeronautics and Space Administration. Lewis Research Center, Cleveland, Ohio.

### **COMBUSTION SYSTEM FOR RADIATION INVESTIGATIONS**

J. D. WEAR *In its* Turbine Eng. Hot Sect. Technol. (HOST) p 331-334 Oct. 1982

Avail: NTIS HC A16/MF A01 CSCL 21E

An inlet interface flange, inlet diffuser, fuel struts and nozzles, combustor liner, liner housing and exhaust flange comprise a system to be installed in an existing test facility. The system was designed for operation at 40 atmospheres inlet pressure, 900 K inlet temperature, and air flow to 80 kg/sec. Six penetrations are provided in the outer pressure housing. Adapters at the penetrations, permit use of various types of radiation instrumentation. Five total radiation radiometers and two heat flux gases were installed. Rotating exhaust instrumentation can also be used to determine combustor performance. Data are presented showing total radiation at three axial positions of the combustor, and comparison of total radiation with data from a heat flux gage. A.R.H.

**N85-10987\*#** National Aeronautics and Space Administration. Lewis Research Center, Cleveland, Ohio.

### **VALIDATION OF STRUCTURAL ANALYSIS METHODS USING THE IN-HOUSE LINER CYCLIC RIGS**

R. L. THOMPSON *In its* Turbine Eng. Hot Sect. Technol. (HOST) p 335-344 Oct. 1982

Avail: NTIS HC A16/MF A01 CSCL 21E

Test conditions and variables to be considered in each of the test rigs and test configurations, and also used in the validation of the structural predictive theories and tools, include: thermal and mechanical load histories (simulating an engine mission cycle; different boundary conditions; specimens and components of different dimensions and geometries; different materials; various cooling schemes and cooling hole configurations; several advanced burner liner structural design concepts; and the simulation of hot streaks. Based on these test conditions and test variables, the test matrices for each rig and configurations can be established to verify the predictive tools over as wide a range of test conditions as possible using the simplest possible tests. A flow chart for the thermal/structural analysis of a burner liner and how the analysis relates to the tests is shown schematically. The chart shows that several nonlinear constitutive theories are to be evaluated. A.R.H.

## 07 AIRCRAFT PROPULSION AND POWER

**N85-10988\*#** National Aeronautics and Space Administration. Lewis Research Center, Cleveland, Ohio.

**HOST LINER CYCLIC FACILITIES: FACILITY DESCRIPTION**  
D. SCHULTZ *In its* Turbine Eng. Hot Sect. Technol. (HOST) p 345-360 Oct. 1982

Avail: NTIS HC A16/MF A01 CSCL 21E

A quartz lamp box, a quartz lamp annular rig, and a low pressure liner cyclic can rig planned for liner cyclic tests are described. Special test instrumentation includes an IR-TV camera system for measuring liner cold side temperatures, thin film thermocouples for measuring liner hot side temperatures, and laser and high temperature strain gages for obtaining local strain measurements. A plate temperature of 2,000 F was obtained in an initial test of an apparatus with three quartz lamps. Lamp life, however, appeared to be limited for the standard commercial quartz lamps available. The design of vitiated and nonvitiated preheaters required for the quartz lamp annular rig and the cyclic can test rigs is underway.

A.R.H.

**N85-10989\*#** General Electric Co., Cincinnati, Ohio. Aircraft Engine Business Group.

**ENERGY EFFICIENT ENGINE COMPONENT DEVELOPMENT AND INTEGRATION PROGRAM Semiannual Report, 1 Oct. 1981 - 31 Mar. 1982**

Apr. 1982 346 p

(Contract NAS3-20643)

(NASA-CR-169496; NAS 1.26:169496; R82AEB285; SAR-8)

Avail: NTIS HC A15/MF A01 CSCL 21E

The development of the technology to improve energy efficiency of propulsion systems for subsonic commercial aircrafts was examined. Goals established include: (1) fuel consumption, reduction in flight propulsion system; (2) direct operation cost; (3) noise, with provision for engine growth corresponding to future engine application; and (4) emissions, EPA new engine standards.

E.A.K.

**N85-10990\*#** General Electric Co., Cincinnati, Ohio. Aircraft Engine Business Group.

**ENERGY EFFICIENT ENGINE COMPONENT DEVELOPMENT AND INTEGRATION PROGRAM Semiannual Report, 1 Apr. - 30 Sep. 1981**

30 Oct. 1981 338 p

(Contract NAS3-20643)

(NASA-CR-170034; NAS 1.26:170034; R81AEG709; SAR-7)

Avail: NTIS HC A15/MF A01 CSCL 21E

Accomplishments in the Energy Efficient Engine Component Development and Integration program during the period of April 1, 1981 through September 30, 1981 are discussed. The major topics considered are: (1) propulsion system analysis, design, and integration; (2) engine component analysis, design, and development; (3) core engine tests; and (4) integrated core/low spool testing.

R.S.F.

**N85-10991\*#** TRW, Inc., Cleveland, Ohio. Materials Technology.

**ENERGY EFFICIENT ENGINE. VOLUME 2. APPENDIX A: COMPONENT DEVELOPMENT AND INTEGRATION PROGRAM Final Semiannual Status Report, 1 Apr. - 30 Sep. 1981**

D. J. MORACZ and C. R. COOK East Hartford, Conn. Pratt and Whitney Aircraft 30 Oct. 1981 200 p refs Prepared for Pratt and Whitney Aircraft, East Hartford, Conn. 2 Vol.

(Contract NAS3-20646)

(NASA-CR-173085; NAS 1.26:173085;

PWA-5594-179-VOL-2-APP-A; ER-8050-F-VOL-2-APP-A;

SASR-7-VOL-2-APP-A) Avail: NTIS HC A09/MF A01 CSCL 21E

The large size and the requirement for precise lightening cavities in a considerable portion of the titanium fan blades necessitated the development of a new manufacturing method. The approach which was selected for development incorporated several technologies including HIP diffusion bonding of titanium sheet laminates containing removable cores and isothermal forging of the blade form. The technology bases established in HIP/DB for

composite blades and in isothermal forging for fan blades were applicable for development of the manufacturing process. The process techniques and parameters for producing and inspecting the cored diffusion bonded titanium laminate blade preform were established. The method was demonstrated with the production of twelve hollow simulated blade shapes for evaluation. Evaluations of the critical experiments conducted to establish procedures to produce hollow structures by a laminate/core/diffusion bonding approach are included. In addition the transfer of this technology to produce a hollow fan blade is discussed.

B.G.

**N85-10992\*#** Pratt and Whitney Aircraft, East Hartford, Conn. Commercial Products Div.

**ENERGY EFFICIENT ENGINE. VOLUME 1: COMPONENT DEVELOPMENT AND INTEGRATION PROGRAM Semiannual Status Report, 1 Apr. - 30 Sep. 1981**

30 Oct. 1981 228 p 2 Vol.

(Contract NAS3-20646)

(NASA-CR-173084; NAS 1.26:173084; PWA-5594-179-VOL-1;

SASR-7-VOL-1) Avail: NTIS HC A11/MF A01 CSCL 21E

Technology for achieving lower installed fuel consumption and lower operating costs in future commercial turbofan engines are developed, evaluated, and demonstrated. The four program objectives are: (1) propulsion system analysis; (2) component analysis, design, and development; (3) core design, fabrication, and test; and (4) integrated core/low spool design, fabrication, and test.

B.G.

**N85-10993\*#** General Electric Co., Cincinnati, Ohio. Aircraft Engine Business Group.

**ENERGY EFFICIENT ENGINE ICLS NACELLE DETAIL DESIGN REPORT**

R. R. ESKRIDGE, A. P. KUCHAR, and C. L. STOTLER Jul.

1982 125 p refs

(Contract NAS3-20643)

(NASA-CR-167870; NAS 1.26:167870; R81AEG700) Avail:

NTIS HC A06/MF A01 CSCL 21E

The results of the detail design of the Nacelle for the General Electric Energy Efficient Engine (E3) Integrated Core Low Spool (ICLS) test vehicles are presented. A slave nacelle is designed for the ICLS test. Cost and reliability are the important factors considered. The slave nacelle simulates the internal flow lines of the actual Flight Propulsion System (FPS) but has no external fairing. The aerodynamic differences between the ICLS and FPS nacelles are presented, followed by the structural description and analysis of the various nacelle components.

M.A.C.

**N85-10994\*#** General Electric Co., Cincinnati, Ohio. Aircraft Engine Business Group.

**ENERGY EFFICIENT ENGINE. LOW PRESSURE TURBINE TEST HARDWARE DETAILED DESIGN REPORT**

D. G. CHERRY, C. H. GAY, and D. T. LENAHAAN Aug. 1982 186 p

(Contract NAS3-20643)

(NASA-CR-167956; NAS 1.26:167956; R81AEG597) Avail:

NTIS HC A09/MF A01 CSCL 21E

The low pressure turbine for the energy efficient engine is a five-stage configuration with moderate aerodynamic loading incorporating advanced features of decambered airfoils and extended blade overlaps at platforms and shrouds. Mechanical integrity of 18,000 hours on flowpath components and 36,000 hours on all other components is achieved along with no aeromechanical instabilities within the steady-state operating range. Selection of a large number (156) of stage 4 blades, together with an increased stage 4 vane-to-blade gap, assists in achieving FAR 36 acoustic goals. Active clearance control (ACC) of gaps at blade tips and interstage seals is achieved by fan air cooling judiciously applied at responsive locations on the casing. This ACC system is a major improvement in preventing deterioration of the 0.0381 cm (0.015 in.) clearances required to meet the integrated-core/low-spool turbine efficiency goal of 91.1% and the light propulsion system efficiency goal of 91.7%.

Author

**N85-10995\*#** General Electric Co., Cincinnati, Ohio. Aircraft Engine Business Group.

**ENERGY EFFICIENT ENGINE HIGH PRESSURE TURBINE TEST HARDWARE DETAILED DESIGN REPORT**

E. E. HALILA, D. T. LENAHA, and T. T. THOMAS Jun. 1982 194 p refs

(Contract NAS3-20643)

(NASA-CR-167955; NAS 1.26:167955; R81AEG284) Avail:

NTIS HC A09/MF A01 CSCL 21E

The high pressure turbine configuration for the Energy Efficient Engine is built around a two-stage design system. Moderate aerodynamic loading for both stages is used to achieve the high level of turbine efficiency. Flowpath components are designed for 18,000 hours of life, while the static and rotating structures are designed for 36,000 hours of engine operation. Both stages of turbine blades and vanes are air-cooled incorporating advanced state of the art in cooling technology. Direct solidification (DS) alloys are used for blades and one stage of vanes, and an oxide dispersion system (ODS) alloy is used for the Stage 1 nozzle airfoils. Ceramic shrouds are used as the material composition for the Stage 1 shroud. An active clearance control (ACC) system is used to control the blade tip to shroud clearances for both stages. Fan air is used to impinge on the shroud casing support rings, thereby controlling the growth rate of the shroud. This procedure allows close clearance control while minimizing blade tip to shroud rubs. Author

**N85-10996\*#** General Electric Co., Cincinnati, Ohio. Aircraft Engine Business Group.

**ENERGY EFFICIENT ENGINE HIGH PRESSURE TURBINE CERAMIC SHROUD SUPPORT TECHNOLOGY REPORT**

W. A. NELSON and R. G. CARLSON Nov. 1982 56 p refs

(Contract NAS3-20643)

(NASA-CR-168036; NAS 1.26:168036; R82AEB399) Avail: NTIS

HC A04/MF A01 CSCL 21E

This work represents the development and fabrication of ceramic HPT (high pressure turbine) shrouds for the Energy Efficient Engine (E3). Details are presented covering the work performed on the ceramic shroud development task of the NASA/GE Energy Efficient Engine (E3) component development program. The task consists of four phases which led to the selection of a ZrO<sub>2</sub>-BY2O<sub>3</sub> ceramic shroud material system, the development of an automated plasma spray process to produce acceptable shroud structures, the fabrication of select shroud systems for evaluation in laboratory, component, and CF6-50 engine testing, and finally, the successful fabrication of ZrO<sub>2</sub>-8Y2O<sub>3</sub>/superpeg, engine quality shrouds for the E3 engine. Author

**N85-10997\*#** General Electric Co., Cincinnati, Ohio. Aircraft Engine Business Group.

**ENERGY EFFICIENT ENGINE ICLS ENGINE BEARINGS, DRIVES AND CONFIGURATION: DETAIL DESIGN REPORT**

C. L. BROMAN Jun. 1982 76 p refs

(Contract NAS3-20643)

(NASA-CR-167871; NAS 1.26:167871; R81AEG821) Avail:

NTIS HC A05/MF A01 CSCL 21E

The detailed design of the forward and aft sumps, the accessory drive system, the lubrication system, and the piping/manifold configuration to be employed in the ICLS engine test of the Energy Efficient Engine is addressed in the report. The design goals for the above components were established based on the requirements of the test cell engine. Author

**N85-10998\*#** General Electric Co., Cincinnati, Ohio. Aircraft Engine Business Group.

**ENERGY EFFICIENT ENGINE. HIGH PRESSURE COMPRESSOR DETAIL DESIGN REPORT**

P. R. HOLLOWAY, C. C. KOCH, G. L. KNIGHT, and S. L. SHAFFER May 1982 168 p refs

(Contract NAS3-20643)

(NASA-CR-165558; NAS 1.26:165558; R81AEG710) Avail:

NTIS HC A08/MF A01 CSCL 21E

A compressor optimization study defined a 10-stage configuration with a 22.6:1 pressure ratio, and adiabatic efficiency goal of 86.1%, and a polytropic efficiency of 90.6%; the corrected airflow is 53.5 kg/sec. Subsequent component testing included three full-scale tests: a six-stage rig test, and another 10-stage rig test completed in the second quarter of 1982. Information from these tests is being used to select the configuration for a core engine test scheduled for July 1982 and an integrated core/low spool test slated for early 1983. The test results will also provide data base for the flight propulsion system. Author

**N85-10999\*#** General Electric Co., Cincinnati, Ohio. Aircraft Engine Business Group.

**ADVANCED BLADE TIP SEAL SYSTEM, VOLUME 2 Final Report**

J. W. ZELAHY and N. P. FAIRBANKS Feb. 1982 28 p

(Contract NAS3-20074)

(NASA-CR-167851; NAS 1.26:167851; TIS-R82AEB403-VOL-2)

Avail: NTIS HC A03/MF A01 CSCL 21E

The results of the endurance and performance engine tests conducted on monocrystal/abrasive-tipped CF6-50 Stage 1 HPT blades fabricated in Task VII of MATE Project 3 are presented. Two engine tests are conducted. The endurance engine test is conducted for 1000 C cycles. The performance engine test is conducted on a variable cycle core engine. Posttest evaluation and analyses of the blades and shrouds included visual, dimensional, and destructive evaluations. M.A.C.

**N85-12059\*#** General Electric Co., Cincinnati, Ohio. Aircraft Engine Engineering Div.

**MATERIALS FOR ADVANCED TURBINE ENGINES. PROJECT 2: RENE 150 DIRECTIONALLY SOLIDIFIED SUPERALLOY TURBINE BLADES, VOLUME 2 Final Report**

G. J. DEBOER Feb. 1982 39 p 2 Vol.

(Contract NAS3-20074)

(NASA-CR-167993; NAS 1.26:167993; R82AEB540-VOL-2)

Avail: NTIS HC A03/MF A01 CSCL 21E

The results of the engine testing of Rene 150 Stage 1 high pressure turbine blades in CF6-50 core and fan engines are presented. The core engine test was conducted for 233 hours with a variety of test cycles, and the fan engine test was conducted for 1000 C cycles. Post-test analysis of the core engine test data confirmed the suitability of the Rene 150 HPT blade for fan engine testing. Post-test evaluation and analysis of the fan engine test blades included visual and dimensional inspection as well as metallographic examination of selected blades. The Rene 150 HPT blade met the target goal of this project by demonstrating increased metal temperature capability; however, the post-test analysis revealed several areas that would have to be addressed in designing a long-life Rene 150 CF6-50 HPT blade. R.S.F.

**N85-13798\*#** National Aeronautics and Space Administration. Lewis Research Center, Cleveland, Ohio.

**NEW INTEGRATION TECHNIQUES FOR CHEMICAL KINETIC RATE EQUATIONS. 2: ACCURACY COMPARISON**

K. RADHAKRISHNAN (Michigan Univ., Ann Arbor) 1985 15 p

refs Proposed for presentation at the 30th Intern. Gas Turbine Conf. and Exhibit, Houston, 17-21 Mar. 1985; sponsored by ASME

(NASA-TM-86893; E-2366; NAS 1.15:86893) Avail: NTIS HC A02/MF A01 CSCL 21E

A comparison of the accuracy of several techniques recently developed for solving stiff differential equations is presented. The techniques examined include two general purpose codes

## 07 AIRCRAFT PROPULSION AND POWER

EEPIISODE and LODE developed for an arbitrary system of ordinary differential equations, and three specialized codes CHEMEQ, CREKID, and GCKP84 developed specifically to solve chemical kinetic rate equations. The accuracy comparisons are made by applying these solution procedures to two practical combustion kinetics problems. Both problems describe adiabatic, homogeneous, gas phase chemical reactions at constant pressure, and include all three combustion regimes: induction, heat release, and equilibration. The comparisons show that LODE is the most efficient code - in the sense that it requires the least computational work to attain a specified accuracy level. An important finding is that an iterative solution of the algebraic enthalpy conservation equation for the temperature can be more accurate and efficient than computing the temperature by integrating its time derivative.

M.G.

**N85-14840\*#** National Aeronautics and Space Administration. Lewis Research Center, Cleveland, Ohio.

### **REDUCING NUMERICAL DIFFUSION FOR INCOMPRESSIBLE FLOW CALCULATIONS**

R. W. CLAUS, G. M. NEELY, and S. A. SYED (United Technologies, East Hartford, Conn.) 1984 20 p refs Presented at the Western States Meeting of the Combustion Inst., Boulder, Colo., 2-3 Apr. 1984

(NASA-TM-83621; E-2055; NAS 1.15:83621) Avail: NTIS HC A03/MF A01 CSCL 21E

A number of approaches for improving the accuracy of incompressible, steady-state flow calculations are examined. Two improved differencing schemes, Quadratic Upstream Interpolation for Convective Kinematics (QUICK) and Skew-Upwind Differencing (SUD), are applied to the convective terms in the Navier-Stokes equations and compared with results obtained using hybrid differencing. In a number of test calculations, it is illustrated that no single scheme exhibits superior performance for all flow situations. However, both SUD and QUICK are shown to be generally more accurate than hybrid differencing. Author

**N85-15724\*#** Tuskegee Inst., Ala. School of Engineering and Architecture.

### **AN IMPROVED COMPUTER MODEL FOR PREDICTION OF AXIAL GAS TURBINE PERFORMANCE LOSSES Final Report**

R. M. JENKINS Aug. 1984 119 p refs

(Contract NSG-3295)

(NASA-CR-174246; NAS 1.26:174246) Avail: NTIS HC A03/MF A01 CSCL 21E

The calculation model performs a rapid preliminary pitchline optimization of axial gas turbine annular flowpath geometry, as well as an initial estimate of blade profile shapes, given only a minimum of thermodynamic cycle requirements. No geometric parameters need be specified. The following preliminary design data are determined: (1) the optimum flowpath geometry, within mechanical stress limits; (2) initial estimates of cascade blade shapes; and (3) predictions of expected turbine performance. The model uses an inverse calculation technique whereby blade profiles are generated by designing channels to yield a specified velocity distribution on the two walls. Velocity distributions are then used to calculate the cascade loss parameters. Calculated blade shapes are used primarily to determine whether the assumed velocity loadings are physically realistic. Model verification is accomplished by comparison of predicted turbine geometry and performance with an array of seven NASA single-stage axial gas turbine configurations. B.W.

**N85-15725\*#** National Aeronautics and Space Administration. Lewis Research Center, Cleveland, Ohio.

### **EFFECT OF STEADY-STATE TEMPERATURE DISTORTION ON INLET FLOW TO A HIGH-BYPASS-RATION TURBOFAN ENGINE**

R. H. SOEDER, C. M. MEHALIC, and K. STANCIK (AFSC) Jan. 1985 32 p refs

(NASA-TM-86896; E-2369; NAS 1.15:86896) Avail: NTIS HC A03/MF A01 CSCL 21E

The effects of circumferential inlet temperature distortion on the flow characteristics between a distortion generator and a high bypass ratio turbofan engine and through its compression system were evaluated to support the effort to generate analytical models. The flow characteristics are defined by the inlet duct, the flow angles, and the total temperature, total pressure, and static pressure profiles in the inlet duct and through the fan and compressor. The effects of Reynolds number, rotor speed, and distortion extent are also considered. E.A.K.

**N85-15726\*#** National Aeronautics and Space Administration. Lewis Research Center, Cleveland, Ohio.

### **INTEGRATING CHEMICAL KINETIC RATE EQUATIONS BY SELECTIVE USE OF STIFF AND NONSTIFF METHODS**

K. RADHAKRISHNAN 1985 15 p refs Presented at the 23rd Aerospace Sci. Meeting, Reno, Nev., 14-17 Jan. 1985; sponsored by AIAA Previously announced in IAA as A85-19607 (NASA-TM-86923; E-2418; NAS 1.15:86923; AIAA-85-0237)

Avail: NTIS HC A02/MF A01 CSCL 21E

The effect of switching between nonstiff and stiff methods on the efficiency of algorithms for integrating chemical kinetic rate equations was examined. Different integration methods were tested by application of the packaged code LODE to four practical combustion kinetics problems. The problems describe adiabatic, and homogeneous gas phase combustion reactions. It is shown that selective use of nonstiff and stiff methods in different regimes of a typical batch combustion problem is faster than the use of either method for the entire problem. The implications which result in the development of fast integration techniques for combustion kinetic rate equations are discussed. E.A.K.

**N85-15727\*#** National Aeronautics and Space Administration. Lewis Research Center, Cleveland, Ohio.

### **EXPERIMENTAL STUDY OF THE SPRAY CHARACTERISTICS OF A RESEARCH AIRBLAST ATOMIZER**

W. A. ACOSTA 1985 16 p refs Proposed for presentation

at the 30th Intern. Gas Turbine Conf. and Exhibit, Houston, Tex., 17-21 Mar. 1985; sponsored by ASME

(NASA-TM-86911; E-2404; NAS 1.15:86911;

USAAVSCOM-TR-84-C-18) Avail: NTIS HC A02/MF A01

CSCL 21E

Airblast atomization was studied using a especially designed atomizer in which the liquid first impinges on a splash plate, then is directed radially outward and is atomized by the air passing through two concentric, vaned swirlers that swirl the air in opposite directions. The effect of flow conditions, air mass velocity (mass flow rate per unit area) and liquid to air ratio on the mean drop size was studied. Seven different ethanol solutions were used to simulate changes in fuel physical properties. The range of atomizing air velocities was from 30 to 80 m/s. The mean drop diameter was measured at ambient temperature (295 K) and atmospheric pressure. Author

**N85-15728\*#** Pennsylvania State Univ., University Park. **THE STRUCTURE OF DILUTE COMBUSTING SPRAYS Final Report**

J. S. SHUEN, A. S. P. SOLOMON, and F. M. FAETH Jan. 1985 124 p refs

(Contract NAG3-190)

(NASA-CR-174838; NAS 1.26:174838) Avail: NTIS HC A06/MF A01 CSCL 21E

An experimental and theoretical study of drop processes in a turbulent flame is described. The experiments involved a monodisperse (105 and 180 micro m initial diameter) stream of

methanol drops injected at the base of a turbulent methane-fueled diffusion flame burning in still air. The following measurements were made: mean and fluctuating phase velocities, mean drop number flux, drop-size distributions and mean gas-phase temperatures. Measurements were compared with predictions of two separated flow models: (1) deterministic separated flow, where drop-turbulence interactions are ignored; and (2) stochastic separated flow, where drop-turbulence interactions are considered using random-walk computations. The stochastic separated flow analysis yielded best agreement with measurements, since it provides for turbulent dispersion of drops which was important for present test conditions (and probably for most combustor sprays as well). Distinguishing the presence or absence of envelope flames around the drops, however, was relatively unimportant for present test conditions, since the drops spent most of their lifetime in fuel-rich regions of the flow where this distinction is irrelevant.

Author

**N85-15744\*#** National Aeronautics and Space Administration. Lewis Research Center, Cleveland, Ohio.

**ENGINE CYCLIC DURABILITY BY ANALYSIS AND MATERIAL TESTING**

A. KAUFMAN and G. R. HALFORD *In* AGARD Eng. Cyclic Durability by Analysis and Testing 12 p Sep. 1984 refs Previously announced as N84-18683

Avail: NTIS HC A12/MF A01 CSCL 21E

The problem of calculating turbine engine component durability is addressed. Nonlinear, finite-element structural analyses, cyclic constitutive behavior models, and an advanced creep-fatigue life prediction method called strainrange partitioning were assessed for their applicability to the solution of durability problems in hot-section components of gas turbine engines. Three different component or subcomponent geometries are examined: a stress concentration in a turbine disk; a lower lip of a half-scale combustor liner; and a squealer tip of a first-stage high-pressure turbine blade. Cyclic structural analyses were performed for all three problems. The computed strain-temperature histories at the critical locations of the combustor liner and turbine blade components were imposed on smooth specimens in uniaxial, strain-controlled, thermomechanical fatigue tests of evaluate the structural and life analysis methods.

Author

**N85-18057\*#** National Aeronautics and Space Administration. Lewis Research Center, Cleveland, Ohio.

**EXPERIMENTAL AND ANALYTICAL STUDY OF CERAMIC-COATED TURBINE-TIP SHROUD SEALS FOR SMALL TURBINE ENGINES**

T. J. BIESIADNY, G. E. MCDONALD, R. C. HENDRICKS, J. K. LITTLE, R. A. ROBINSON (AVSCOM Research and Technology Labs, Cleveland, Ohio), G. A. KLANN (AVSCOM Research and Technology Labs, Cleveland, Ohio), and E. S. LASSOW (Howmet Turbine Components Corp., Whitehall, Mich.) Jan. 1985 32 p refs

(NASA-TM-86881; E-2343; NAS 1.15:86881;

USAAVSCOM-TR-84-C-19) Avail: NTIS HC A03/MF A01 CSCL 21E

The results of an experimental and analytical evaluation of ceramic turbine tip shrouds within a small turbine engine operating environment are presented. The ceramic shrouds were subjected to 1001 cycles between idle and high power and steady-state conditions for a total of 57.8 engine hr. Posttest engine inspection revealed mud-flat surface cracking, which was attributed to microcracking under tension with crack penetration to the ceramic and bond coat interface. Sections and micrographs tend to corroborate the thesis. The engine test data provided input to a thermomechanical analysis to predict temperature and stress profiles throughout the ceramic gas-path seal. The analysis predicts cyclic thermal stresses large enough to cause the seal to fail. These stresses are, however, mitigated by inelastic behavior of the shroud materials and by the microfracturing that tensile stresses produce. Microfracturing enhances shroud longevity during early life but provides the failure mechanism during life but provides

the failure mechanism during extended life when coupled with the time dependent inelastic materials effects.

Author

**N85-18058\*#** Pratt and Whitney Aircraft Group, East Hartford, Conn. Commercial Engineering.

**STUDY OF CONTROLLED DIFFUSION STATOR BLADING Final Report**

R. F. BEHLKE, J. D. BROOKY, and E. CANAL Mar. 1983 134 p refs

(Contract NAS3-22008)

(NASA-CR-167995; NAS 1.26:167995; PWA-5698-77) Avail:

NTIS HC A07/MF A01 CSCL 21E

Tests were conducted on a high tip speed, highly loaded front compressor stage having low aspect ratio rotor and stator airfoils. The stator airfoils were designed by the controlled diffusion procedure recently developed by P&WA for designing transonic cascade airfoils. The rotor blades consisted of multiple-circular-arc airfoil sections. The stage had a tip speed of 442 m/sec (1450 ft/sec), a hub/tip ratio of 0.597, a rotor aspect ratio of 1.3, and a stator aspect ratio of 1.45. At design speed the rotor-stator stage achieved an adiabatic efficiency of 89.1% at design flow and pressure ratio. Surge margin was 14%. The stage efficiency exceeded the design goal by 0.6 percentage points. The rotor efficiency was 92.4%, exceeding design by 0.3 percentage points. The controlled diffusion stator demonstrated a lower minimum loss over the multiple-circular-arc stator from the root to 70 percent span. A surge diffusion factor of 0.72 was reached at both the rotor tip and the stator root. The NAS3-22008 program demonstrated its intent: high efficiency and loading levels with low aspect ratio blades and the controlled diffusion stator in the unfavorable front stage environment.

Author

**N85-21162\*#** National Aeronautics and Space Administration. Lewis Research Center, Cleveland, Ohio.

**A COMPARISON OF THE EFFICIENCY OF NUMERICAL METHODS FOR INTEGRATING CHEMICAL KINETIC RATE EQUATIONS**

K. RADHAKRISHNAN 1984 18 p refs Presented at JANNAP Propulsion Meeting, New Orleans, 7-9 Feb. 1984 Previously announced as N84-31280

(Contract NAG3-147)

(NASA-TM-83590; E-1988; NAS 1.15:83590) Avail: NTIS HC

A02/MF A01 CSCL 21E

A comparison of the efficiency of several algorithms recently developed for the efficient numerical integration of stiff ordinary differential equations is presented. The methods examined include two general-purpose codes EPISODE and LSODE and three codes (CHEMEQ, CREK1D, and GCKP84) developed specifically to integrate chemical kinetic rate equations. The codes are applied to two test problems drawn from combustion kinetics. The comparisons show that LSODE is the fastest code currently available for the integration of combustion kinetic rate equations. An important finding is that an iterative solution of the algebraic energy conservation equation to compute the temperature can be more efficient than evaluating the temperature by integrating its time-derivative.

Author

**N85-21163\*#** John Deere Technologies International, Inc., Wood-Ridge, N.J. Rotary Engine Div.

**STRATIFIED CHARGE ROTARY AIRCRAFT ENGINE TECHNOLOGY ENABLEMENT PROGRAM Final Report**

P. R. BADGLEY, C. E. IRION, and D. M. MYERS 31 Jan. 1985 110 p refs

(Contract NAS3-23056)

(NASA-CR-174812; NAS 1.26:174812; JDTI-RED-85-1) Avail:

NTIS HC A06/MF A01 CSCL 21E

The multifuel stratified charge rotary engine is discussed. A single rotor, 0.7L/40 cu in displacement, research rig engine was tested. The research rig engine was designed for operation at high speeds and pressures, combustion chamber peak pressure providing margin for speed and load excursions above the design requirement for a high is advanced aircraft engine. It is indicated that the single rotor research rig engine is capable of meeting the

## 07 AIRCRAFT PROPULSION AND POWER

established design requirements of 120 kW, 8,000 RPM, 1,379 KPA BMEP. The research rig engine, when fully developed, will be a valuable tool for investigating, advanced and highly advanced technology components, and provide an understanding of the stratified charge rotary engine combustion process. E.A.K.

**N85-21164\*#** National Aeronautics and Space Administration. Lewis Research Center, Cleveland, Ohio.

### **COMBUSTION RESEARCH FOR GAS TURBINE ENGINES**

E. J. MULARZ and R. W. CLAUS 1985 19 p refs To be presented at the 7th Intern. Symp. on Air Breathing Engines, Peking, 2-6 Sep. 1985

(NASA-TM-86963; E-2490; NAS 1.15:86963; AD-A153977) Avail: NTIS HC A02/MF A01 CSCL 21E

Research on combustion is being conducted at Lewis Research Center to provide improved analytical models of the complex flow and chemical reaction processes which occur in the combustor of gas turbine engines and other aeropropulsion systems. The objective of the research is to obtain a better understanding of the various physical processes that occur in the gas turbine combustor in order to develop models and numerical codes which can accurately describe these processes. Activities include in-house research projects, university grants, and industry contracts and are classified under the subject areas of advanced numerics, fuel sprays, fluid mixing, and radiation-chemistry. Results are high-lighted from several projects. Author

**N85-21165\*#** Massachusetts Inst. of Tech., Cambridge. Dept. of Aeronautics and Astronautics.

### **ADVANCED STRESS ANALYSIS METHODS APPLICABLE TO TURBINE ENGINE STRUCTURES Final Report**

T. H. H. PIAN Mar. 1985 44 p refs

(Contract NAG3-33)

(NASA-CR-175573; NAS 1.26:175573) Avail: NTIS HC A03/MF A01 CSCL 21E

Advanced stress analysis methods applicable to turbine engine structures are investigated. Constructions of special elements which containing traction-free circular boundaries are investigated. New versions of mixed variational principle and version of hybrid stress elements are formulated. A method is established for suppression of kinematic deformation modes. semiLoof plate and shell elements are constructed by assumed stress hybrid method. An elastic-plastic analysis is conducted by viscoplasticity theory using the mechanical subelement model. B.W.

**N85-21166\*#** Illinois Univ., Urbana-Champaign.

### **THE MECHANISMS OF FLAME HOLDING IN THE WAKE OF A BLUFF BODY Final Report**

R. A. STREHLOW and S. MALIK Mar. 1985 196 p refs

(Contract NAG3-60)

(NASA-CR-3866; NAS 1.26:3866) Avail: NTIS HC A09/MF A01 CSCL 21E

The flame holding mechanism for lean methane- and lean propane-air flames is examined under conditions where the recirculation zone is absent. The main objective of this work is to study the holding process in detail in an attempt to determine the mechanism of flame holding and also the conditions where this mechanism is viable and when it fails and blow-off occurs. Inverted flames held in the wake of a flat strip were studied. Experiments with different sizes of flame holders were performed. The velocity flow field was determined using a laser Doppler velocimetry technique. Equation of continuity was used to calculate the flame temperature from the change in area of flow streamlines before and after the flame. Observations of the inverted flame itself were obtained using schlieren and direct photography. Results show that there are different mechanisms operative at the time of blow-off for lean propane and methane flames. Blow-off or extinction occurs for lean propane-air flame in spite of the reaction going to completion and the disparity between the heat loss and the gain in mass diffusion in the reaction zone i.e.,  $Le = 1.0$  causes the flame to blow-off. For methane-air flame the controlling factor or blow-off is incomplete reaction due to higher blowing rate leading to reduced residence time in the reaction zone. M.G.

**N85-21167\*#** Oklahoma State Univ., Stillwater. School of Mechanical and Aerospace Engineering.

### **INVESTIGATION OF FLOWFIELDS FOUND IN TYPICAL COMBUSTOR GEOMETRIES Final Report**

D. G. LILLEY Washington NASA Feb. 1985 192 p refs Sponsored in part by AF

(Contract NAG3-74)

(NASA-CR-3869; NAS 1.26:3869) Avail: NTIS HC A09/MF A01 CSCL 21E

Activities undertaken during the entire course of research are summarized. Studies were concerned with experimental and theoretical research on 2-D axisymmetric geometries under low speed nonreacting, turbulent, swirling flow conditions typical of gas turbine and ramjet combustion chambers. They included recirculation zone characterization, time-mean and turbulence simulation in swirling recirculating flow, sudden and gradual expansion flowfields, and further complexities and parameter influences. The study included the investigation of: a complete range of swirl strengths; swirler performance; downstream contraction nozzle sizes and locations; expansion ratios; and inlet side-wall angles. Their individual and combined effects on the test section flowfield were observed, measured and characterized. Experimental methods included flow visualization (with smoke and neutrally-buoyant helium-filled soap bubbles), five-hole pitot probe time-mean velocity field measurements, and single-, double-, and triple-wire hot-wire anemometry measurements of time-mean velocities, normal and shear Reynolds stresses. Computational methods included development of the STARPIC code from the primitive-variable TEACH computer code, and its use in flowfield prediction and turbulence model development. M.G.

**N85-21168\*#** National Aeronautics and Space Administration. Lewis Research Center, Cleveland, Ohio.

### **COMBUSTION GAS PROPERTIES. 2: NATURAL GAS FUEL AND DRY AIR**

J. D. WEAR, R. E. JONES, A. M. TROUT, and B. J. MCBRIDE Apr. 1985 12 p refs

(NASA-TP-2435; E-2435; NAS 1.60:2435) Avail: NTIS HC A02/MF A01 CSCL 21E

A series of computations has been made to produce the equilibrium temperature and gas composition for natural gas fuel and dry air. The computed tables and figures provide combustion gas property data for pressures from 0.5 to 50 atmospheres and equivalence ratios from 0 to 2.0. Only samples tables and figures are provided in this report. The complete set of tables and figures is provided on four microfiche films supplied with this report.

Author

**N85-22390\*#** Oklahoma State Univ., Stillwater. School of Mechanical and Aerospace Engineering.

### **DEFLECTED JET EXPERIMENTS IN A TURBULENT COMBUSTOR FLOWFIELD Ph.D. Thesis Final Report**

G. B. FERRELL and D. G. LILLEY Feb. 1985 273 p refs

(Contract NAG3-549)

(NASA-CR-174863; NAS 1.26:174863) Avail: NTIS HC A12/MF A01 CSCL 21E

Experiments were conducted to characterize the time-mean and turbulent flow field of a deflected turbulent jet in a confining cylindrical crossflow. Jet-to-crossflow velocity ratios of 2, 4, and 6 were investigated, under crossflow inlet swirler vane angles of 0 (swirler removed), 45 and 70 degrees. Smoke, neutrally buoyant helium-filled soap bubbles, and multi-spark flow visualization were employed to highlight interesting features of the deflected jet, as well as the trajectory and spread pattern of the jet. A six-position single hot-wire technique was used to measure the velocities and turbulent stresses in nonswirling crossflow cases. In these cases, measurements confirmed that the deflected jet is symmetrical about the vertical plan passing through the crossflow axis, and the jet penetration was found to be reduced from that of comparable velocity ratio infinite crossflow cases. In the swirling crossflow cases, the flow visualization techniques enabled gross flow field characterization to be obtained for a range of lateral jet-to-crossflow

velocity ratios and a range of inlet swirl strengths in the main flow. Author

**N85-22391\*#** Massachusetts Inst. of Tech., Cambridge. Gas Turbine Lab.

**STRUCTURAL RESPONSE OF A ROTATING BLADED DISK TO ROTOR WHIRL Final Report**

E. F. CRAWLEY Apr. 1985 140 p refs

(Contract NAG3-200)

(NASA-CR-175605; NAS 1.26:175605) Avail: NTIS HC A07/MF A01 CSCL 21E

A set of high speed rotating whirl experiments were performed in the vacuum of the MIT Blowdown Compressor Facility on the MIT Aeroelastic Rotor, which is structurally typical of a modern high bypass ratio turbofan stage. These tests identified the natural frequencies of whirl of the rotor system by forcing its response using an electromagnetic shaker whirl excitation system. The excitation was slowly swept in frequency at constant amplitude for several constant rotor speeds in both a forward and backward whirl direction. The natural frequencies of whirl determined by these experiments were compared to those predicted by an analytical 6 DOF model of a flexible blade-rigid disk-flexible shaft rotor. The model is also presented in terms of nondimensional parameters in order to assess the importance of the interaction between the bladed disk dynamics and the shaft-disk dynamics. The correlation between the experimental and predicted natural frequencies is reasonable, given the uncertainty involved in determining the stiffness parameters of the system. Author

**N85-22392\*#** Case Western Reserve Univ., Cleveland, Ohio. Dept. of Mechanical and Aerospace Engineering.

**DILUTION JET CONFIGURATIONS IN A REVERSE FLOW COMBUSTOR M.S. Thesis Final Report**

J. ZIZELMAN Apr. 1985 214 p refs

(Contract NSG-3206)

(NASA-CR-174888; NAS 1.26:174888) Avail: NTIS HC A10/MF A01 CSCL 21E

Results of measurements of both temperature and velocity fields within a reverse flow combustor are presented. Flow within the combustor is acted upon by perpendicularly injected cooling jets introduced at three different locations along the inner and outer walls of the combustor. Each experiment is typified by a group of parameters: density ratio, momentum ratio, spacing ratio, and confinement parameter. Measurements of both temperature and velocity are presented in terms of normalized profiles at azimuthal positions through the turn section of the combustion chamber. Jet trajectories defined by minimum temperature and maximum velocity give a qualitative indication of the location of the jet within the cross flow. Results of a model from a previous temperature study are presented in some of the plots of data from this work.

Author

**N85-25261\*#** National Aeronautics and Space Administration. Lewis Research Center, Cleveland, Ohio.

**PERFORMANCE AND SURGE LIMITS OF A TF30-P-3 TURBOFAN ENGINE/AXISYMMETRIC MIXED-COMPRESSION INLET PROPULSION SYSTEM AT MACH 2.5**

J. F. WASSERBAUER, H. E. NEUMANN, and R. J. SHAW May 1985 21 p refs

(NASA-TP-2461; E-2412; NAS 1.60:2461) Avail: NTIS HC A02/MF A01 CSCL 21E

Steady-state performance and inlet-engine compatibility were investigated with a low-bleed inlet. The inlet had minimum internal contraction, consistent with high total pressure recovery and low cowl drag. The inlet-engine combination displayed good performance with only about 2% of inlet performance bleed. The inlet-engine combination had 5.58 deg angle-of-attack capability with 6% bleed. Author

**N85-25262\*#** Michigan State Univ., East Lansing. Coll. of Engineering.

**DEVELOPMENT OF A TEMPERATURE MEASUREMENT SYSTEM WITH APPLICATION TO A JET IN A CROSS FLOW EXPERIMENT Final Report**

C. WARK and J. F. FOSS Apr. 1985 123 p refs

(Contract NAG3-245)

(NASA-CR-174896; NAS 1.26:174896; FSFL-R-85-002) Avail: NTIS HC A06/MF A01 CSCL 21E

A temperature measurement system, which allows the simultaneous sampling of up to 80 separate thermocouples, was developed. The minimum resolution for the system corresponds to  $\pm 0.16$  C per least significant bit of the A/D converter. The time constant values  $\lambda$ , for each of the 64 thermocouples, were determined experimentally at 7 mps. Software routines were used to correct the measured temperatures for the effect of  $\lambda$  for each thermocouple. The temperature measurement system was utilized to study the thermal field of a heated jet discharging perpendicularly into a low and a high disturbance level cross stream for a given momentum flux ratio and for three overheated values. The peak instantaneous temperatures reveal that strong molecular diffusion was operative. Various measures of the thermal field, for the disturbed case, suggest that the jet column remains relatively compact while being buffeted by the ambient turbulence field and that its penetration, into the cross wind, is inhibited by the presence of the strong disturbance field. E.A.K.

**N85-25263\*#** National Aeronautics and Space Administration. Lewis Research Center, Cleveland, Ohio.

**NUMERICAL CALCULATION OF SUBSONIC JETS IN CROSSFLOW WITH REDUCED NUMERICAL DIFFUSION**

R. W. CLAUS 1985 19 p refs Presented at the 21st Joint Propulsion Conf., Monterey, Calif., 8-10 Jul. 1985; sponsored by AIAA, SAE and ASME

(NASA-TM-87003; E-2548; NAS 1.15:87003) Avail: NTIS HC A02/MF A01 CSCL 21E

A series of calculations are reported for two, subsonic jet in crossflow geometries. The parametric variation examined are the lateral spacing of a row of jets. The first series of calculations corresponds to a widely spaced jet geometry,  $S/D = 4$ , and the second series corresponds to closely spaced jets,  $S/D = 2$ . The calculations are done with alternate differencing schemes to illustrate the impact of numerical diffusion. The calculated jet trajectories agreed well with experimental data in the widely spaced jet geometry, but not in the closely spaced geometry. E.A.K.

**N85-25264\*#** National Aeronautics and Space Administration. Lewis Research Center, Cleveland, Ohio.

**SMALL GAS TURBINE COMBUSTOR STUDY: FUEL INJECTOR PERFORMANCE IN A TRANSPARATION-COOLED LINER**

S. M. RIDDLEBAUGH and C. T. NORNGREN 1985 20 p refs Proposed for presentation at the 21st Joint Propulsion Conf., Monterey, Calif., 8-10 Jul. 1985; sponsored by AIAA, SAE and ASME

(NASA-TM-86989; E-2533; NAS 1.15:86989) Avail: NTIS HC A02/MF A01 CSCL 21E

The effect of fuel injection technique on the performance of an advanced reverse flow combustor liner constructed of Lamilloy (a multilaminate transpiration type material) was determined. Performance and emission levels are documented over a range of simulated flight conditions using simplex pressure atomizing, spill return, and splash cone airblast injectors. A parametric evaluation of the effect of increased combustor loading with each of the fuel injector types is obtained. E.A.K.



## 07 AIRCRAFT PROPULSION AND POWER

**N85-25265\*#** Arizona State Univ., Tempe. Dept. of Mechanical and Aerospace Engineering.

### **BEHAVIOR OF TURBULENT GAS JETS IN AN AXISYMMETRIC CONFINEMENT Final Report**

R. M. C. SO and S. A. AHMED Jan. 1985 95 p refs

(Contract NAG3-260)

(NASA-CR-174829; NAS 1.26:174829; CR-R-84041) Avail:

NTIS HC A05/MF A01 CSCL 20D

The understanding of the mixing of confined turbulent jets of different densities with air is of great importance to many industrial applications, such as gas turbine and Ramjet combustors. Although there have been numerous studies on the characteristics of free gas jets, little is known of the behavior of gas jets in a confinement. The jet, with a diameter of 8.73 mm, is aligned concentrically in a tube of 125 mm diameter, thus giving a confinement ratio of approximately 205. The arrangement forms part of the test section of an open-jet wind tunnel. Experiments are carried out with carbon dioxide, air and helium/air jets at different jet velocities. Mean velocity and turbulence measurements are made with a one-color, one-component laser Doppler velocimeter operating in the forward scatter mode. Measurements show that the jets are highly dissipative. Consequently, equilibrium jet characteristics similar to those found in free air jets are observed in the first two diameters downstream of the jet. These results are independent of the fluid densities and velocities. Decay of the jet, on the other hand, is a function of both the jet fluid density and momentum. In all the cases studied, the jet is found to be completely dissipated in approximately 30 jet diameters, thus giving rise to a uniform flow with a very high but constant turbulence field across the confinement.

Author

**N85-25266\*#** National Aeronautics and Space Administration. Lewis Research Center, Cleveland, Ohio.

### **EXPERIMENTS IN DILUTION JET MIXING EFFECTS OF MULTIPLE ROWS AND NON-CIRCULAR ORIFICES**

J. D. HOLDEMAN, R. SRINIVASAN (Garrett Turbine Engine Co.), E. B. COLEMAN (Garrett Turbine Engine Co.), G. D. MEYERS (Garrett Turbine Engine Co.), and C. D. WHITE (Garrett Turbine Engine Co.) 1985 16 p refs Presented at the 21st Joint Propulsion Conf., Monterey, Calif., 8-10 Jul. 1985; sponsored by AIAA, SAE and ASME

(NASA-TM-86996; E-2542; NAS 1.15:86996) Avail: NTIS HC

A02/MF A01 CSCL 21E

Experimental and empirical model results are presented that extend previous studies of the mixing of single-sided and opposed rows of jets in a confined duct flow to include effects of non-circular orifices and double rows of jets. Analysis of the mean temperature data obtained in this investigation showed that the effects of orifice shape and double rows are significant only in the region close to the injection plane, provided that the orifices are symmetric with respect to the main flow direction. The penetration and mixing of jets from 45-degree slanted slots is slightly less than that from equivalent-area symmetric orifices. The penetration from 2-dimensional slots is similar to that from equivalent-area closely-spaced rows of holes, but the mixing is slower for the 2-D slots. Calculated mean temperature profiles downstream of jets from non-circular and double rows of orifices, made using an extension developed for a previous empirical model, are shown to be in good agreement with the measured distributions.

Author

**N85-26709\*#** Detroit Diesel Allison, Indianapolis, Ind. Allison Gas Turbine Div.

### **ANALYTICAL FUEL PROPERTY EFFECTS--SMALL COMBUSTORS Final Report**

R. D. SUTTON, D. L. TROTH, and G. A. MILES Oct. 1984 224 p refs

(Contract NAS3-23165)

(NASA-CR-174738; EDR-11683; NAS 1.26:174738;

AVSCOM-TR-84-C-14) Avail: NTIS HC A10/MF A01 CSCL

21E

The consequences of using broad-property fuels in both conventional and advanced state-of-the-art small gas turbine combustors are assessed. Eight combustor concepts were selected

for initial screening, of these, four final combustor concepts were chosen for further detailed analysis. These included the dual orifice injector baseline combustor (a current production 250-C30 engine combustor) two baseline airblast injected modifications, short and piloted prechamber combustors, and an advanced airblast injected, variable geometry air staged combustor. Final predictions employed the use of the STAC-I computer code. This quasi 2-D model includes real fuel properties, effects of injector type on atomization, detailed droplet dynamics, and multistep chemical kinetics. In general, fuel property effects on various combustor concepts can be classified as chemical or physical in nature. Predictions indicate that fuel chemistry has a significant effect on flame radiation, liner wall temperature, and smoke emission. Fuel physical properties that govern atomization quality and evaporation rates are predicted to affect ignition and lean-blowout limits, combustion efficiency, unburned hydrocarbon, and carbon monoxide emissions.

Author

**N85-26710\*#** National Aeronautics and Space Administration. Lewis Research Center, Cleveland, Ohio.

### **LOW-SPEED AERODYNAMIC TEST OF AN AXISYMMETRIC SUPERSONIC INLET WITH VARIABLE COWL SLOT**

A. G. POWELL (Douglas Aircraft Co., Long Beach, Calif.), H. R. WELGE (Douglas Aircraft Co., Long Beach, Calif.), and C. J. TREFNY 1985 6 p refs Proposed for presentation at the 21st Joint Propulsion Conf., Monterey, Calif., 8-10 Jul. 1985; sponsored by AIAA, SAE and ASME

(Contract NAS1-16147)

(NASA-TM-87039; E-2595; NAS 1.15:87039;

DOUGLAS-PAPER-7551) Avail: NTIS HC A02/MF A01 CSCL 21E

The experimental low-speed aerodynamic characteristics of an axisymmetric mixed-compression supersonic inlet with variable cowl slot are described. The model consisted of the NASA P-inlet centerbody and redesigned cowl with variable cowl slot powered by the JT8D single-stage fan simulator and driven by an air turbine. The model was tested in the NASA Lewis Research Center 9- by 15-foot low-speed tunnel at Mach numbers of 0, 0.1, and 0.2 over a range of flows, cowl slot openings, centerbody positions, and angles of attack. The variable cowl slot was effective in minimizing lip separation at high velocity ratios, showed good steady-state and dynamic distortion characteristics, and had good angle-of-attack tolerance.

Author

**N85-26711\*#** General Electric Co., Cincinnati, Ohio. Aircraft Engine Business Group.

### **EFFECTS OF SURFACE CHEMISTRY ON HOT CORROSION LIFE Annual Report, 2 May 1984 - 2 May 1985**

R. E. FRYXELL Jun. 1985 47 p refs

(Contract NAS3-23926)

(NASA-CR-174915; NAS 1.26:174915; R85AEB307; AR-2) Avail:

NTIS HC A03/MF A01 CSCL 21E

Burner rig tests were conducted under the following conditions: 900 C, hourly thermal cycling, 0.5 ppm sodium as NaCl in the gas stream, velocity 0.3 Mach. The alloys are Udiment 700, Rene 80, uncoated and with RT21, Codep, or NiCoCrAlY coatings. These tests were completed for specimens in the as-processed condition and after aging at 1100 C in oxidizing or inert environments for time up to 600 hours. Coil inductance changes used for periodic nondestructive inspection of specimens were useful in following the course of corrosion. Typical sulfidation was observed in all cases, structurally similar to that observed for service-run turbine components. Aging at caused a severe decrease in hot corrosion life of RT21 and Codep coatings and a significant but less decrease in the life of the NiCoCrAlY coating. The extent of these decreases was much greater for all three coatings on U700 substrates than on Rene 80 substrates. Coating/substrate interdiffusion rather than by surface oxidation.

M.G.



**N85-26712\*#** Virginia Polytechnic Inst. and State Univ., Blacksburg. Dept. of Mechanical Engineering.  
**THERMODYNAMIC EVALUATION OF TRANSONIC COMPRESSOR ROTORS USING THE FINITE VOLUME APPROACH** Semiannual Status Report, 20 Dec. 1985 - 31 May 1985

S. NICHOLSON and J. MOORE 1985 42 p refs  
 (Contract NAG3-593)  
 (NASA-CR-175811; NAS 1.26:175811; JM/85-6) Avail: NTIS HC A03/MF A01 CSCL 21E

Progress made in extending the finite volume explicit time marching method to laminar and turbulent flow during the time period from January to May 1985 is documented. Previously, extensions were made to the finite volume method to improve the accuracy of the calculation of total pressure in compressible inviscid flow. The current work extends these ideas and develops new ideas which allow the calculation of laminar and turbulent boundary layers in internal flows. The method is verified using four test cases with free-stream Mach numbers ranging from .075 to 1.20.

R.J.F.

**N85-26713\*#** Notre Dame Univ., Ind. Dept. of Electrical Engineering.

**ALTERNATIVES FOR JET ENGINE CONTROL** Technical Progress Report, 1 Nov. 1983 - 31 Oct. 1984

M. K. SAIN 31 Oct. 1984 266 p refs  
 (Contract NSG-3048)  
 (NASA-CR-175831; NAS 1.26:175831) Avail: NTIS HC A12/MF A01 CSCL 21E

The technical progress of researches Alternatives for Jet Engine Control is reported. A numerical study employing feedback tensors for optimal control of nonlinear systems was completed. It is believed that these studies are the first of their kind. State regulation, with a decrease in control power is demonstrated. A detailed treatment follows.

E.A.K.

**N85-26714\*#** Notre Dame Univ., Ind. Dept. of Electrical Engineering.

**ALTERNATIVES FOR JET ENGINE CONTROL** Technical Progress Report, 1 Oct. 1982 - 31 Oct. 1983

M. K. SAIN 31 Oct. 1983 140 p refs  
 (Contract NSG-3048)  
 (NASA-CR-175832; NAS 1.26:175832) Avail: NTIS HC A07/MF A01 CSCL 21E

The technical progress of researches on alternatives for jet engine control, is reported. The principal new activities involved the initial testing of an input design method for choosing the inputs to a non-linear system to aid the approximation of its tensor parameters, and the beginning of order reduction studies designed to remove unnecessary monomials from tensor models.

E.A.K.

**N85-26715\*#** Notre Dame Univ., Ind. Dept. of Electrical Engineering.

**ALTERNATIVES FOR JET ENGINE CONTROL** Semiannual Status Report, 1 Nov. 1983 - 30 Apr. 1984

M. K. SAIN 30 Apr. 1984 271 p refs  
 (Contract NSG-3048)  
 (NASA-CR-175833; NAS 1.26:175833) Avail: NTIS HC A12/MF A01 CSCL 21E

The technical progress of researches on alternatives for jet engine control is reported. Extensive numerical testing is included. It is indicated that optimal inputs contribute significantly to the process of calculating tensor approximations for nonlinear systems, and that the resulting approximations may be order-reduced in a systematic way.

E.A.K.

**N85-26716\*#** Oklahoma State Univ., Stillwater. School of Mechanical and Aerospace Engineering.

**CONFINED TURBULENT SWIRLING RECIRCULATING FLOW PREDICTIONS** Ph.D. Thesis. Final Report

M. T. ABUJELALA and D. G. LILLEY May 1985 226 p refs  
 (Contract NAG3-74)  
 (NASA-CR-174917; NAS 1.26:174917) Avail: NTIS HC A11/MF A01 CSCL 21E

The capability and the accuracy of the STARPIC computer code in predicting confined turbulent swirling recirculating flows is presented. Inlet flow boundary conditions were demonstrated to be extremely important in simulating a flowfield via numerical calculations. The degree of swirl strength and expansion ratio have strong effects on the characteristics of swirling flow. In a nonswirling flow, a large corner recirculation zone exists in the flowfield with an expansion ratio greater than one. However, as the degree of inlet swirl increases, the size of this zone decreases and a central recirculation zone appears near the inlet. Generally, the size of the central zone increased with swirl strength and expansion ratio. Neither the standard k-epsilon turbulence mode nor its previous extensions show effective capability for predicting confined turbulent swirling recirculating flows. However, either reduced optimum values of three parameters in the mode or the empirical C sub mu formulation obtained via careful analysis of available turbulence measurements, can provide more acceptable accuracy in the prediction of these swirling flows.

Author

**N85-26717\*#** Oklahoma State Univ., Stillwater. School of Mechanical and Aerospace Engineering.

**TURBULENCE CHARACTERISTICS OF SWIRLING FLOWFIELDS** Ph.D. Thesis. Final Report

T. W. JACKSON and D. G. LILLEY May 1985 266 p refs  
 (Contract NAG3-74)  
 (NASA-CR-174918; NAS 1.26:174918) Avail: NTIS HC A13/MF A01 CSCL 21E

The time mean and turbulence properties of a confined swirling jet using the six orientation, single hot wire technique were obtained. The effect of swirl on a confined, expanding jet is to reduce the size of the corner recirculation zone and generate a central recirculation zone followed by a precessing vortex core. The effect of introducing a contraction nozzle of area ratio four, located two test section diameters downstream of the inlet, is to dramatically reduce the size and shape of the central recirculation zone for the swirling flows considered. The shear stresses are found to increase by an order of magnitude in the region of the contraction nozzle because of large radial gradients of axial velocity. Reduction of the expansion ratio to  $D/o = 1$  causes the time mean flow field to be homogeneous throughout the entire test section with the tangential velocity dominating in the swirling cases. No recirculation zones were observed for these particular flows. Turbulence levels and dissipation rates were found to be low except in the entrance regions and in areas of acceleration in the swirling flow cases.

Author

**N85-27867\*#** Oklahoma State Univ., Stillwater. School of Mechanics and Aerospace Engineering.

**PREDICTIONS AND MEASUREMENTS OF ISOTHERMAL FLOWFIELDS IN AXISYMMETRIC COMBUSTOR GEOMETRIES** Ph.D. Thesis. Final Report

D. L. RHODES and D. G. LILLEY May 1985 169 p refs  
 (Contract NAG3-74)  
 (NASA-CR-174916; NAS 1.26:174916) Avail: NTIS HC A08/MF A01 CSCL 21E

Numerical predictions, flow visualization experiments and time-mean velocity measurements were obtained for six basic nonreacting flowfields (with inlet swirl vane angles of 0 (swirler removed), 45 and 70 degrees and sidewall expansion angles of 90 and 45 degrees) in an idealized axisymmetric combustor geometry. A flowfield prediction computer program was developed which solves appropriate finite difference equations including a conventional two equation k-epsilon eddy viscosity turbulence model. The wall functions employed were derived from previous swirling flow measurements, and the staircase approximation was

## 07 AIRCRAFT PROPULSION AND POWER

employed to represent the sloping wall at the inlet to the test chamber. Recirculation region boundaries have been sketched from the entire flow visualization photograph collection. Tufts, smoke, and neutrally buoyant helium filled soap bubbles were employed as flow tracers. A five hole pitot probe was utilized to measure the axial, radial, and swirl time mean velocity components.

Author

**N85-27868\*#** Ohio State Univ., Columbus. Dept. of Engineering Mechanics.

**A STUDY OF INTERNAL AND DISTRIBUTED DAMPING FOR VIBRATING TURBOMACHINE BLADES Final Report, 15 Apr. 1983 - 15 Apr. 1985**

A. W. LEISSA Jun. 1985 24 p refs

(Contract NAG3-424)

(NASA-CR-175901; NAS 1.26:175901) Avail: NTIS HC A02/MF A01 CSCL 21E

Internal and distributed damping as possible methods for reducing the vibration response of turbomachine blades and theoretical methods for analyzing damped vibration were studied. It is demonstrated how the Ritz-Galerkin methods may be used to straightforwardly to analyze forced vibrations with damping. This is done directly without requiring the free vibration eigenfunctions. The Galerkin method is an effective technique for these types of problems. The Ritz method has the further advantage of not needing to satisfy the force type boundary conditions, which is particularly important for plates and shells. But proper functionals representing the forcing and damping terms must be developed, and this is done. Two types of damping--viscous and material (hysteretic) are considered. Both distributed and concentrated exciting forces are treated. Numerical results are obtained for cantilevered beams and rectangular plates. Studies showing the rates of convergence of the solutions are made. In the case of the cantilever beam, approximate solutions from the present methods are compared with the exact solutions. R.J.F.

**N85-27869\*#** Princeton Univ., N. J. Dept. of Mechanical and Aerospace Engineering.

**THE ROLE OF SURFACE GENERATED RADICALS IN CATALYTIC COMBUSTION Final Report**

D. A. SANTAVICCA, Y. STEIN, and B. S. H. ROYCE Jun. 1985 24 p refs

(Contract NAG3-353)

Avail: NTIS HC A02/MF A01 CSCL 21B

Experiments were conducted to better understand the role of catalytic surface reactions in determining the ignition characteristics of practical catalytic combustors. Hydrocarbon concentrations, carbon monoxide and carbon dioxide concentrations, hydroxyl radical concentrations, and gas temperature were measured at the exit of a platinum coated, stacked plate, catalytic combustor during the ignition of lean propane-air mixtures. The substrate temperature profile was also measured during the ignition transient. Ignition was initiated by suddenly turning on the fuel and the time to reach steady state was of the order of 10 minutes. The gas phase reaction, showed no pronounced effect due to the catalytic surface reactions, except the absence of a hydroxyl radical overshoot. It is found that the transient ignition measurements are valuable in understanding the steady state performance characteristics. E.A.K.

**N85-27870\*#** National Aeronautics and Space Administration. Lewis Research Center, Cleveland, Ohio.

**FUTURE FUNDAMENTAL COMBUSTION RESEARCH FOR AEROPROPULSION SYSTEMS**

E. J. MULARZ 1985 8 p refs Presented at the 21st Joint Propulsion Conf., Monterey, Calif.; sponsored by AIAA, SAE, ASME and ASEE

(NASA-TM-87049; E-2612; NAS 1.15:87049; AIAA-85-1398; USAVSCOM-TR-85-C-11) Avail: NTIS HC A02/MF A01 CSCL 21E

Physical fluid mechanics, heat transfer, and chemical kinetic processes which occur in the combustion chamber of aeropropulsion systems were investigated. With the component

requirements becoming more severe for future engines, the current design methodology needs the new tools to obtain the optimum configuration in a reasonable design and development cycle. Research efforts in the last few years were encouraging but to achieve these benefits research is required into the fundamental aerothermodynamic processes of combustion. It is recommended that research continues in the areas of flame stabilization, combustor aerodynamics, heat transfer, multiphase flow and atomization, turbulent reacting flows, and chemical kinetics. Associated with each of these engineering sciences is the need for research into computational methods to accurately describe and predict these complex physical processes. Research needs in each of these areas are highlighted. E.A.K.

**N85-28944\*#** National Aeronautics and Space Administration. Lewis Research Center, Cleveland, Ohio.

**ADVANCED SECONDARY POWER SYSTEM FOR TRANSPORT AIRCRAFT**

A. C. HOFFMAN, I. G. HANSEN, R. F. BEACH, R. M. PLENCNER, R. P. DENGLER, K. S. JEFFERIES, and R. J. FRYE May 1985 38 p refs

(NASA-TP-2463; E-2434; NAS 1.60:2463) Avail: NTIS HC A03/MF A01 CSCL 21E

A concept for an advanced aircraft power system was identified that uses 20-kHz, 440-V, sin-wave power distribution. This system was integrated with an electrically powered flight control system and with other aircraft systems requiring secondary power. The resulting all-electric secondary power configuration reduced the empty weight of a modern 200-passenger, twin-engine transport by 10 percent and the mission fuel by 9 percent. Author

**N85-28945\*#** National Aeronautics and Space Administration. Lewis Research Center, Cleveland, Ohio.

**DEAN: A PROGRAM FOR DYNAMIC ENGINE ANALYSIS**

G. G. SADLER and K. J. MELCHER 1985 18 p refs Proposed for presentation at the 21st Joint Propulsion Conf., Monterey, Calif., 8-10 Jul. 1985; sponsored by AIAA, SAE and ASME Prepared in cooperation with Army Research and Technology Labs.

(NASA-TM-87033; E-2588; NAS 1.15:87033; USAVSCOM-TR-85-C-10) Avail: NTIS HC A02/MF A01 CSCL 21E

The Dynamic Engine Analysis program, DEAN, is a FORTRAN code implemented on the IBM/370 mainframe at NASA Lewis Research Center for digital simulation of turbofan engine dynamics. DEAN is an interactive program which allows the user to simulate engine subsystems as well as a full engine systems with relative ease. The nonlinear first order ordinary differential equations which define the engine model may be solved by one of four integration schemes, a second order Runge-Kutta, a fourth order Runge-Kutta, an Adams Predictor-Corrector, or Gear's method for stiff systems. The numerical data generated by the model equations are displayed at specified intervals between which the user may choose to modify various parameters affecting the model equations and transient execution. Following the transient run, versatile graphics capabilities allow close examination of the data. DEAN's modeling procedure and capabilities are demonstrated by generating a model of simple compressor rig. Author

**N85-29955\*#** Pratt and Whitney Aircraft Group, East Hartford, Conn. Engineering Div.

**ENERGY EFFICIENT ENGINE HIGH-PRESSURE TURBINE COMPONENT RIG PERFORMANCE TEST REPORT**

K. P. LEACH May 1983 249 p refs

(Contract NAS3-20646)

(NASA-CR-168189; NAS 1.26:168189; PWA-5594-243) Avail: NTIS HC A11/MF A01 CSCL 21E

A rig test of the cooled high-pressure turbine component for the Energy Efficient Engine was successfully completed. The principal objective of this test was to substantiate the turbine design point performance as well as determine off-design performance with the interaction of the secondary flow system. The measured efficiency of the cooled turbine component was 88.5 percent, which surpassed the rig design goal of 86.5 percent. The secondary

flow system in the turbine performed according to the design intent. Characterization studies showed that secondary flow system performance is insensitive to flow and pressure variations. Overall, this test has demonstrated that a highly-loaded, transonic, single-stage turbine can achieve a high level of operating efficiency. B.W.

**N85-29956\*#** Pratt and Whitney Aircraft Group, East Hartford, Conn.

**ENERGY EFFICIENT ENGINE INTEGRATED CORE/LOW SPOOL TEST HARDWARE DESIGN REPORT**

J. W. BISSET and D. C. HOWE Mar. 1983 223 p refs  
(Contract NAS3-20646)  
(NASA-CR-168137; NAS 1.26:168137; PWA-5594-231) Avail: NTIS HC A10/MF A01 CSCL 21E

The National Aeronautics and Space Administration is sponsoring the Energy Efficient Engine Program to identify and verify the technology required to significantly lower fuel consumption and operating cost for commercial gas-turbine engines. A major task that has been completed under this program is the design and analysis of test hardware for the integrated core/low spool. The integrated core/low spool is a test simulation of the conceptual study engine defined to meet the performance, economic and environmental goals of the Energy Efficient Engine Program. It is intended to permit evaluation and verification of critical technologies in a full engine operating environment. This report describes the design and results of design-related analyses for the integrated core/low spool and its subsystems. The design effort included a definition of the engine, major components, internal and external subsystems, test ducting, and test instrumentation. Various analytical representations, in addition to results acquired from supporting component rig and subscale model tests, have been used to verify aerodynamic and structural design concepts as well as to predict performance. Author

**N85-29957\*#** General Electric Co., Cincinnati, Ohio. Aircraft Engine Business Group.

**ENERGY EFFICIENT ENGINE (E3) CONTROLS AND ACCESSORIES DETAIL DESIGN REPORT**

R. S. BEITLER and J. P. LAVASH Dec. 1982 158 p refs  
(Contract NAS3-20643)  
(NASA-CR-168017; NAS 1.26:168017; R82AEB400) Avail: NTIS HC A08/MF A01 CSCL 21E

An Energy Efficient Engine program has been established by NASA to develop technology for improving the energy efficiency of future commercial transport aircraft engines. As part of this program, a new turbofan engine was designed. This report describes the fuel and control system for this engine. The system design is based on many of the proven concepts and component designs used on the General Electric CF6 family of engines. One significant difference is the incorporation of digital electronic computation in place of the hydromechanical computation currently used. Author

**N85-29958\*#** Pratt and Whitney Aircraft, East Hartford, Conn. Commercial Products Div.

**ENERGY EFFICIENT ENGINE COMPONENT DEVELOPMENT AND INTEGRATION PROGRAM Semiannual Status Report, 1 Oct. 1981 - 31 Mar. 1982**

30 Apr. 1982 160 p refs  
(Contract NAS3-20646)  
(NASA-CR-172846; NAS 1.26:172846; PWA-5594-202; SASR-8) Avail: NTIS HC A08/MF A01 CSCL 21E

The objective of the Energy Efficient Engine Component Development and Integration program is to develop, evaluate, and demonstrate the technology for achieving lower installed fuel consumption and lower operating costs in future commercial turbofan engines. Minimum goals have been set for a 12 percent reduction in thrust specific fuel consumption (TSFC), 5 percent reduction in direct operating cost (DOC), and 50 percent reduction in performance degradation for the Energy Efficient Engine (flight propulsion system) relative to the JT9D-7A reference engine. The Energy Efficient Engine features a twin spool, direct drive, mixed

flow exhaust configuration, utilizing an integrated engine nacelle structure. A short, stiff, high rotor and a single stage high pressure turbine are among the major enhancements in providing for both performance retention and major reductions in maintenance and direct operating costs. Improved clearance control in the high pressure compressor and turbines, and advanced single crystal materials in turbine blades and vanes are among the major features providing performance improvement. Highlights of work accomplished and programs modifications and deletions are presented. B.W.

**N85-29960\*#** Scientific Systems, Inc., Cambridge, Mass.

**NONLINEAR GLOBAL STABILITY ANALYSIS OF COMPRESSOR STALL PHENOMENA**

H. RAZAVI Jun. 1985 105 p refs  
(Contract NAS3-24089)  
(NASA-CR-174908; NAS 1.26:174908; SSI-24089) Avail: NTIS HC A06/MF A01 CSCL 21E

Compressor stall phenomena are analyzed from the point of view of nonlinear control theory, based on bifurcation-catastrophe techniques. This new approach appears promising and offers insight into such well-known compressor instability problems as surge and rotating stall and suggests strategies for recovery. Three interlocking dynamic nonlinear state space models are developed. It is shown that the problem of rotating stall can be viewed as an induced bifurcation of solution of the unstalled model. Hysteresis effects are shown to exist in the stall/recovery process. Surge cycles are observed for some critical parameter values. The oscillatory behavior is seen to be due to development of limit cycles, generated by Hopf bifurcation of solutions. More specifically, it is observed that at certain critical values of parameters, a family of stable limit cycles with growing and then diminishing amplitudes is generated, then giving rise to an unstable family of limit cycles. This unstable family in turn bifurcates into other unstable families. To further illustrate the utility of the methodology, some partial computation of domains is carried out, and parameter sensitivity analysis is performed. Author

**N85-29961#** Detroit Diesel Allison, Indianapolis, Ind. Engineering Dept.

**ADVANCED GAS TURBINE (AGT) TECHNOLOGY PROJECT Semiannual Report**

Mar. 1984 94 p  
(Contract DEN3-168; DE-AE01-77CS-51040)  
(NASA-CR-174798; DOE/NASA/0168-8; NAS 1.26:174798; EDR-11682) Avail: NTIS HC A05/MF A01 CSCL 21E

Significant development activity occurred during the July to December 1983 period in the Allison-Pontiac AGT 100 Advanced Gas Turbine Technology Project. Two engines were evaluated through dynamometer testing. Through 1983, total accumulated engine test time (burning) was 41 hr 19 min. Engine D-2 incorporated a modification to the interface system between the ceramic regenerator bulkhead and power turbine scroll assembly, solving the problem of cracked bulkheads experienced on the last builds of engine D-1. A design modification was defined to eliminate the tendency to leak hot gas from the engine flow path into the gearbox vent cavity. Compressor aerodynamic analyses that identified impeller modifications for improved performance were completed. These near-term improvements will be tested next period on a compressor rig. Two turbine aerodynamic improvements were designed for 1984 implementation: improved gasifier vane shape and a reduced capacity power turbine. Combustor development included rig changes to better simulate the engine flow path and to provide viewing stations for use of optical pyrometers. Rig testing was conducted to proof-test ceramic units, to examine starting and igniter relocations, and to map stability limits. Regenerator testing evaluated 23 disk/seal combinations in 145 hr of hot rig testing. Advanced concepts included a silicone leaf seal, polyimide integral wearface and seal platform, different crossarm cooling systems, low-leakage aluminum silicate risks, and an extruded magnesium-aluminum silicate disk. Ceramic turbine rotor development experienced improvement in molding, baking, and sintering engine configuration rotors. Nineteen sintered alpha

## 07 AIRCRAFT PROPULSION AND POWER

silicon carbide rotors were cold-spin tested to failure. Average burst speed was 94,930 rpm. R.J.F.

**N85-29964\*#** National Aeronautics and Space Administration. Lewis Research Center, Cleveland, Ohio.

### **LARGE-SCALE ADVANCED PROPFAN (LAP) PROGRAM Progress Report**

D. A. SAGERSE and S. G. LUDEMANN (Hamilton Standard, Windsor Locks, Conn.) 1985 28 p refs Presented at the 21st Joint Propulsion Conf., Monterey, Calif., 8-10 Jul. 1985; sponsored by AIAA, SAE, ASME, and ASEE (NASA-TM-87067; E-2637; NAS 1.15:87067; AIAA-85-1187) Avail: NTIS HC A03/MF A01 CSCL 21E

The propfan is an advanced propeller concept which maintains the high efficiencies traditionally associated with conventional propellers at the higher aircraft cruise speeds associated with jet transports. The large-scale advanced propfan (LAP) program extends the research done on 2 ft diameter propfan models to a 9 ft diameter article. The program includes design, fabrication, and testing of both an eight bladed, 9 ft diameter propfan, designated SR-7L, and a 2 ft diameter aeroelastically scaled model, SR-7A. The LAP program is complemented by the propfan test assessment (PTA) program, which takes the large-scale propfan and mates it with a gas generator and gearbox to form a propfan propulsion system and then flight tests this system on the wing of a Gulfstream 2 testbed aircraft. E.A.K.

**N85-29965\*#** Pratt and Whitney Aircraft, West Palm Beach, Fla. Government Products Div.

### **CONVOLUTED NOZZLE DESIGN FOR THE RL10 DERIVATIVE 2B ENGINE Final Report**

1 Jul. 1985 113 p refs Prepared in cooperation with Textron Bell Aerospace Co., Buffalo, N.Y. (Contract NAS3-22902)

(NASA-CR-174953; NAS 1.26:174953; PWA-FR-18323-2; REPT-8881-933004) Avail: NTIS HC A06/MF A01 CSCL 21E

The convoluted nozzle is a conventional refractory metal nozzle extension that is formed with a portion of the nozzle convoluted to show the extendible nozzle within the length of the rocket engine. The convoluted nozzle (CN) was deployed by a system of four gas driven actuators. For spacecraft applications the optimum CN may be self-deployed by internal pressure retained, during deployment, by a jettisonable exit closure. The convoluted nozzle is included in a study of extendible nozzles for the RL10 Engine Derivative 2B for use in an early orbit transfer vehicle (OTV). Four extendible nozzle configurations for the RL10-2B engine were evaluated. Three configurations of the two position nozzle were studied including a hydrogen dump cooled metal nozzle and radiation cooled nozzles of refractory metal and carbon/carbon composite construction respectively. E.A.K.

**N85-31057\*#** Pratt and Whitney Aircraft, East Hartford, Conn. Commercial Products Div.

### **CREEP FATIGUE LIFE PREDICTION FOR ENGINE HOT SECTION MATERIALS (ISOTROPIC) Annual Report**

V. MORENO Aug. 1983 89 p refs (Contract NAS3-23288)

(NASA-CR-168228; NAS 1.26:168228; PWA-5894-17; AR-1) Avail: NTIS HC A05/MF A01 CSCL 21E

The Hot Section Technology (HOST) program, creep fatigue life prediction for engine hot section materials (isotropic), is reviewed. The program is aimed at improving the high temperature crack initiation life prediction technology for gas turbine hot section components. Significant results include: (1) cast B1900 and wrought IN 718 selected as the base and alternative materials respectively; (2) fatigue test specimens indicated that measurable surface cracks appear early in the specimen lives, i.e., 15% of total life at 871 C and 50% of life at 538 C; (3) observed crack initiation sites are all surface initiated and are associated with either grain boundary carbides or local porosity, transgranular cracking is observed at the initiation site for all conditions tested; and (4) an initial evaluation of two life prediction models, representative of macroscopic (Coffin-Manson) and more microscopic (damage rate) approaches,

was conducted using limited data generated at 871 C and 538 C. It is found that the microscopic approach provides a more accurate regression of the data used to determine crack initiation model constants, but overpredicts the effect of strain rate on crack initiation life for the conditions tested. E.A.K.

**N85-31058\*#** National Aeronautics and Space Administration. Lewis Research Center, Cleveland, Ohio.

### **COMBUSTION GAS PROPERTIES. PART 3: HYDROGEN GAS FUEL AND DRY AIR**

J. D. WEAR, R. E. JONES, B. J. MCBRIDE, and R. A. BEYERLE (Sverdrup Technology, Inc.) Jun. 1985 12 p refs Doc. includes microfiche supplement

(Contract NAS3-24105) (NASA-TP-2477; E-2545; NAS 1.60:2477) Avail: NTIS HC A02/MF A01 CSCL 07D

A series of computations has been made to produce the equilibrium temperature and gas composition for hydrogen gas fuel and dry air. The computed tables and figures provide combustion gas property data for pressures from 0.5 to 50 atmospheres and equivalence ratios from 0 to 2.0. Only sample tables and figures are provided in this report. Author

**N85-31060\*#** National Aeronautics and Space Administration. Lewis Research Center, Cleveland, Ohio.

### **SPIRAL BEVEL AND CIRCULAR ARC HELICAL GEARS: TOOTH CONTACT ANALYSIS AND THE EFFECT OF MISALIGNMENT ON CIRCULAR ARC HELICAL GEARS**

F. L. LITVIN (Illinois Univ. at Chicago), W. T. TSUNG (Illinois Univ. at Chicago), C. B. TSAY (Illinois Univ. at Chicago), J. J. COY, and R. F. HANDSCHUH 1985 15 p refs Presented at the 21st Joint Propulsion Conf., Monterey, Calif. 8-10 Jul. 1985; sponsored in part by AIAA, SAE and ASME

(NASA-TM-87013; E-2557; NAS 1.15:87013; USAVSCOM-TR-85-C-6) Avail: NTIS HC A02/MF A01 CSCL 21E

A computer aided method for tooth contact analysis was developed and applied. Optimal machine-tool settings for spiral bevel gears are proposed and when applied indicated that kinematic errors can be minimized while maintaining a desirable bearing contact. The effect of misalignment for circular arc helical gears was investigated and the results indicated that directed pinion refinishing can compensate the kinematic errors due to misalignment. Author

**N85-32119\*#** General Electric Co., Cincinnati, Ohio. Aircraft Engine Business Group.

### **COMPONENT-SPECIFIC MODELING Annual Status Report, 1 Jan. - 31 Dec. 1984**

R. L. MCKNIGHT 1985 131 p (Contract NAS3-23687)

(NASA-CR-174925; NAS 1.26:174925; ASR-2) Avail: NTIS HC A07/MF A01 CSCL 21E

Accomplishments are described for the second year effort of a 3-year program to develop methodology for component specific modeling of aircraft engine hot section components (turbine blades, turbine vanes, and burner liners). These accomplishments include: (1) engine thermodynamic and mission models; (2) geometry model generators; (3) remeshing; (4) specialty 3-D inelastic structural analysis; (5) computationally efficient solvers, (6) adaptive solution strategies; (7) engine performance parameters/component response variables decomposition and synthesis; (8) integrated software architecture and development, and (9) validation cases for software developed. Author

**N85-34138\*#** General Electric Co., Cincinnati, Ohio. Aircraft Engine Business Group.  
**HIGH PRESSURE COMPRESSOR COMPONENT PERFORMANCE REPORT**

S. J. CLINE, W. FESLER, H. S. LIU, R. C. LOVELL, and S. J. SHAFFER Sep. 1983 170 p  
 (Contract NAS3-20643)  
 (NASA-CR-168245; NAS 1.26:168245; R82AEB437) Avail: NTIS HC A08/MF A01 CSCL 21E

A compressor optimization study defined a 10 stage configuration with a 22.6:1 pressure ratio, an adiabatic efficiency goal of 86.1%, and a polytropic efficiency of 90.6%; the corrected airflow is 53.5 kg/s. Subsequent component testing included three full scale tests: a six stage rig test, a 10 stage rig test, and another 10 stage rig test completed in the second quarter of 1982. Information from these tests is used to select the configuration for a core engine test and an integrated core/low spool test. The test results will also provide data base for the flight propulsion system. The results of the test series with both aerodynamic and mechanical performance of each compressor build are presented. The second 10 stage compressor adiabatic efficiency was 0.848 at a cruise operating point versus a test goal of 0.846. E.A.K.

**N85-34140\*#** General Electric Co., Cincinnati, Ohio. Aircraft Engine Business Group.

**COMPONENT-SPECIFIC MODELING Annual Status Report**

R. L. MCKNIGHT May 1985 162 p refs  
 (Contract NAS3-23687)  
 (NASA-CR-174765; NAS 1.26:174765; ASR-1) Avail: NTIS HC A08/MF A01 CSCL 21E

A series of interdisciplinary modeling and analysis techniques that were specialized to address three specific hot section components are presented. These techniques will incorporate data as well as theoretical methods from many diverse areas including cycle and performance analysis, heat transfer analysis, linear and nonlinear stress analysis, and mission analysis. Building on the proven techniques already available in these fields, the new methods developed will be integrated into computer codes to provide an accurate, and unified approach to analyzing combustor burner liners, hollow air cooled turbine blades, and air cooled turbine vanes. For these components, the methods developed will predict temperature, deformation, stress and strain histories throughout a complete flight mission. Author

**N85-34141\*#** General Electric Co., Cincinnati, Ohio. Aircraft Engine Business Group.

**ENERGY EFFICIENT ENGINE. FAN AND QUARTER-STAGE COMPONENT PERFORMANCE REPORT**

S. J. CLINE, P. H. HALTER, J. T. KUTNEY, JR., and T. J. SULLIVAN Jan. 1983 71 p refs  
 (Contract NAS3-20643)  
 (NASA-CR-168070; NAS 1.26:168070; R82AEB408) Avail: NTIS HC A04/MF A01 CSCL 21E

The fan configuration for the general Electric/NASA Energy Efficient Engine was selected following an extensive preliminary design study. The fan has an inlet radius ratio of 0.342 and a specific flowrate of 208.9 Kg/sec/sq. m (42.8 lbm/sec/sq. ft). The design corrected tip speed is 411.5 m/sec (1350 ft/sec) producing a bypass flow total-pressure ratio of 1.65 and a core flow total-pressure ratio of 1.6. The design bypass ratio is 6.8. The aerodynamic design point corresponds to the maximum climb power setting at Mach 0.8 and 10.67 Km (35,000 ft) altitude. The fully-instrumented fan component was tested in the Lynn Large Fan Test Facility in 1981. The overall performance results, reported herein, showed excellent fan performance with the fan meeting all of its component test goals of flow, efficiency and stall margin. Author

**N85-35195\*** National Aeronautics and Space Administration. Lewis Research Center, Cleveland, Ohio.

**FLOW MODIFYING DEVICE Patent**

J. S. KELM (General Electric Co., Cincinnati), E. C. VICKERS (General Electric Co., Cincinnati), J. J. WILLIAMS (General Electric Co., Cincinnati), and J. R. TAYLOR, inventors (to NASA) (General Electric Co., Cincinnati) 13 Aug. 1985 10 p Continuation of abandoned US-Patent-Appl-SN-192677 filed 1 Oct. 1980  
 (NASA-CASE-LEW-13562-2; US-PATENT-4,534,166;  
 US-PATENT-APPL-SN-500651; US-PATENT-CLASS-60-39.23;  
 US-PATENT-CLASS-60-748; US-PATENT-CLASS-239-402.5)  
 Avail: US Patent and Trademark Office CSCL 21E

A swirler for a gas turbine engine combustor is disclosed for simultaneously controlling combustor flow rate, swirl angle, residence time and fuel-air ratio to provide three regimes of operation. A first regime is provided in which fuel-air ratio is less than stoichiometric, NOx is produced at one level, and combustor flow rate is high. In a second regime, fuel-air ratio is nearly stoichiometric, NOx production is less than that of the first regime, and combustor flow rate is low. In a third regime, used for example at highoff, fuel-air ratio is greater than stoichiometric and the combustor flow rate is less than in either of the other regimes. Author

**N85-35197\*#** Pratt and Whitney Aircraft, East Hartford, Conn. Engineering Div.

**ENERGY EFFICIENT ENGINE PROGRAM TECHNOLOGY BENEFIT/COST STUDY, VOLUME 1 Executive Summary**

D. E. GRAY and W. B. GARDNER Oct. 1983 19 p 2 Vol.  
 (Contract NAS3-20646)  
 (NASA-CR-174766-VOL-1; NAS 1.26:174766-VOL-1;  
 PWA-5594-258-VOL-1) Avail: NTIS HC A02/MF A01 CSCL 21E

Turbofan engine technologies required for the years 2000 to 2010 were studied, to assess the benefits of those technologies, and to formulate programs for developing the technologies required for that time period. Preliminary technology concepts that might be amenable to future development were ranked. Cycle studies, flowpath definition studies, and mechanical configuration studies were used to identify and establish the feasibility of the technologies that would be required in the 2000 to 2010 time frame. It is shown that a turbofan engine with advancements in aerodynamics, mechanical arrangements, and materials offer significant performance improvements over 1988 technology. The benefits of technologies are assessed using fuel burn and direct operating cost plus interest (DOC+I). The concepts could yield thrust specific fuel consumption benefits of almost 16%, fuel burn benefits of up to 24% and DOC+I benefits up to 14% in a long-range airplane relative to energy efficient engine technology levels. Technology development programs are formulated and recommended to realize those benefits E.A.K.

**N85-35198\*#** Pratt and Whitney Aircraft, East Hartford, Conn. Engineering Div.

**ENERGY EFFICIENT ENGINE PROGRAM TECHNOLOGY BENEFIT/COST STUDY, VOLUME 2**

D. E. GRAY and W. B. GARDNER Oct. 1983 109 p refs 2 Vol.  
 (Contract NAS3-20646)  
 (NASA-CR-174766-VOL-2; NAS 1.26:174766-VOL-2;  
 PWA-5594-251-VOL-2) Avail: NTIS HC A06/MF A01 CSCL 21E

The benefit/cost study to identify turbofan engine technologies required for the years 2000 to 2010, the benefits of those technologies were formulated, and programs for developing the technologies required for that time period were formulated. It is shown that there are still many potential benefits to be realized from the advancement of gas turbine engine technology. Preliminary technology concepts that might be amenable to future development were ranked. Cycle studies, flowpath definition studies, and mechanical configuration studies were used to identify and establish the feasibility of the technologies that would be required in the 2000 to 2010 time frame. It is shown that a turbofan engine with

## 07 AIRCRAFT PROPULSION AND POWER

advancements in aerodynamics, mechanical arrangements, and materials offers significant performance improvements over 1988 technology. The benefits of the technologies are assessed using fuel burn and direct operating cost plus interest (DOC+I). E.A.K.

**N85-35199\*#** General Electric Co., Cincinnati, Ohio. Aircraft Engine Business Group.

### **ENERGY EFFICIENT ENGINE, HIGH PRESSURE TURBINE THERMAL BARRIER COATING. SUPPORT TECHNOLOGY REPORT**

E. C. DUDERSTADT and P. AGARWAL May 1983 128 p refs

(Contract NAS3-20643)

(NASA-CR-168037; NAS 1.26:168037; R82AEB293) Avail: NTIS HC A07/MF A01 CSCL 21E

This report describes the work performed on a thermal barrier coating support technology task of the Energy Efficient Engine Component Development Program. A thermal barrier coating (TBC) system consisting of a Ni-Cr-Al-Y bond coat layer and ZrO<sub>2</sub>-Y<sub>2</sub>O<sub>3</sub> ceramic layer was selected from eight candidate coating systems on the basis of laboratory tests. The selection was based on coating microstructure, crystallographic phase composition, tensile bond and bend test results, erosion and impact test results, furnace exposure, thermal cycle, and high velocity dynamic oxidation test results. Procedures were developed for applying the selected TBC to CF6-50, high pressure turbine blades and vanes. Coated HPT components were tested in three kinds of tests. Stage 1 blades were tested in a cascade cyclic test rig, Stage 2 blades were component high cycle fatigue tested to qualify thermal barrier coated blades for engine testing, and Stage 2 blades and Stage 1 and 2 vanes were run in factory engine tests. After completion of the 1000 cycle engine test, the TBC on the blades was in excellent condition over all of the platform and airfoil except at the leading edge above midspan on the suction side of the airfoil. The coating damage appeared to be caused by particle impingement; adjacent blades without TBC also showed evidence of particle impingement. B.W.

## 08

### **AIRCRAFT STABILITY AND CONTROL**

Includes aircraft handling qualities; piloting; flight controls; and autopilots.

**N85-12901\*#** United Technologies Research Center, East Hartford, Conn.

### **HIGH-TEMPERATURE OPTICALLY ACTIVATED GAAS POWER SWITCHING FOR AIRCRAFT DIGITAL ELECTRONIC CONTROL**

J. M. BERAKE, D. H. GRANTHAM, J. L. SWINDAL, J. F. BLACK, and L. B. ALLEN May 1983 201 p refs

(Contract NAS3-22535)

(NASA-CR-174711; NAS 1.26:174711; UTRC-R83-925312-25)

Avail: NTIS HC A10/MF A01 CSCL 01C

Gallium arsenide high-temperature devices were fabricated and assembled into an optically activated pulse-width-modulated power control for a torque motor typical of the kinds used in jet engine actuators. A bipolar heterojunction phototransistor with gallium aluminum arsenide emitter/window, a gallium arsenide junction field-effect power transistor and a gallium arsenide transient protection diode were designed and fabricated. A high-temperature fiber optic/phototransistor coupling scheme was implemented. The devices assembled into the demonstrator were successfully tested at 250 C, proving the feasibility of actuator-located switching of control power using optical signals transmitted by fibers. Assessments of the efficiency and technical merits were made for extension of this high-temperature technology to local conversion of optical power to electrical power and its control at levels useful for driving actuators. Optical power sources included

in the comparisons were an infrared light-emitting diode, an injection laser diode, tungsten-halogen lamps and arc lamps. Optical-to-electrical power conversion was limited to photovoltaics located at the actuator. Impedance matching of the photovoltaic array to the load was considered over the full temperature range, -55 C to 260 C. Loss of photovoltaic efficiency at higher temperatures was taken into account. Serious losses in efficiency are: (1) in the optical source and the cooling which they may require in the assumed 125 C ambient, (2) in the decreased conversion efficiency of the gallium arsenide photovoltaic at 260 C, and (3) in impedance matching. Practical systems require improvements in these areas. Author

## 09

### **RESEARCH AND SUPPORT FACILITIES (AIR)**

Includes airports, hangars and runways; aircraft repair and overhaul facilities; wind tunnels; shock tube facilities; and engine test blocks.

**A85-19661\*#** National Aeronautics and Space Administration. Lewis Research Center, Cleveland, Ohio.

### **THE ALTITUDE WIND TUNNEL (AWT) - A UNIQUE FACILITY FOR PROPULSION SYSTEM AND ADVERSE WEATHER TESTING**

R. CHAMBERLIN (NASA, Lewis Research Center, Cleveland, OH) American Institute of Aeronautics and Astronautics, Aerospace Sciences Meeting, 23rd, Reno, NV, Jan. 14-17, 1985. 12 p. refs (AIAA PAPER 85-0314)

A need has arisen for a new wind tunnel facility with unique capabilities for testing propulsion systems and for conducting research in adverse weather conditions. New propulsion system concepts, new aircraft configurations with an unprecedented degree of propulsion system/aircraft integration, and requirements for aircraft operation in adverse weather dictate the need for a new test facility. Required capabilities include simulation of both altitude pressure and temperature, large size, full subsonic speed range, propulsion system operation, and weather simulation (i.e., icing, heavy rain). A cost effective rehabilitation of the NASA Lewis Research Center's Altitude Wind Tunnel (AWT) will provide a facility with all these capabilities. Author

**A85-19709\*#** National Aeronautics and Space Administration. Lewis Research Center, Cleveland, Ohio.

### **ANALYTICAL AND PHYSICAL MODELING PROGRAM FOR THE NASA LEWIS RESEARCH CENTER'S ALTITUDE WIND TUNNEL (AWT)**

J. M. ABBOTT, J. H. DIEDRICH, J. F. GROENEWEG, L. A. POVINELLI, L. REID, J. J. REINMANN, and J. R. SZUCH (NASA, Lewis Research Center, Cleveland, OH) American Institute of Aeronautics and Astronautics, Aerospace Sciences Meeting, 23rd, Reno, NV, Jan. 14-17, 1985. 13 p. refs (AIAA PAPER 85-0379)

An effort is currently underway at the NASA Lewis Research Center to rehabilitate and extend the capabilities of the Altitude Wind Tunnel (AWT). This extended capability will include a maximum test section Mach number of about 0.9 at an altitude of 55,000 ft and a -20 F stagnation temperature (octagonal test section, 20 ft across the flats). In addition, the AWT will include an icing and acoustic research capability. In order to insure a technically sound design, an AWT modeling program (both analytical and physical) was initiated to provide essential input to the AWT final design process. This paper describes the modeling program, including the rationale and criteria used in program definition, and presents some early program results. Author

**A85-26381\*#** National Aeronautics and Space Administration. Lewis Research Center, Cleveland, Ohio.

**THE NASA ALTITUDE WIND TUNNEL - ITS ROLE IN ADVANCED ICING RESEARCH AND DEVELOPMENT**

B. J. BLAHA and R. J. SHAW (NASA, Lewis Research Center, Cleveland, OH) American Institute of Aeronautics and Astronautics, Aerospace Sciences Meeting, 23rd, Reno, NV, Jan. 14-17, 1985. 20 p. Previously announced in STAR as A85-15758. refs

(AIAA PAPER 85-0090)

Currently experimental aircraft icing research is severely hampered by limitations of ground icing simulation facilities. Existing icing facilities do not have the size, speed, altitude, and icing environment simulation capabilities to allow accurate studies to be made of icing problems occurring for high speed fixed wing aircraft and rotorcraft. Use of the currently dormant NASA Lewis Altitude Wind Tunnel (AWT), as a proposed high speed propulsion and adverse weather facility, would allow many such problems to be studied. The characteristics of the AWT related to adverse weather simulation and in particular to icing simulation are discussed, and potential icing research programs using the AWT are also included. Author

**N85-15757\*#** National Aeronautics and Space Administration. Lewis Research Center, Cleveland, Ohio.

**ANALYTICAL AND PHYSICAL MODELING PROGRAM FOR THE NASA LEWIS RESEARCH CENTER'S ALTITUDE WIND TUNNEL (AWT)**

J. M. ABBOTT, J. H. DEIDRICH, J. F. GROENEWEG, L. A. POVINELLI, L. REID, J. J. REINMANN, and J. R. SZUCH 1985 21 p refs Presented at the 23rd Aerospace Sci. Meeting, Reno, Nevada, 14-17 Jan. 1985; sponsored by AIAA (NASA-TM-86919; E-2413; NAS 1.15:86919; AIAA-85-0379) Avail: NTIS HC A02/MF A01 CSCL 14B

An effort is currently underway at the NASA Lewis Research Center to rehabilitate and extend the capabilities of the Altitude Wind Tunnel (AWT). This extended capability will include a maximum test section Mach number of about 0.9 at an altitude of 55,000 ft and a -20 F stagnation temperature (octagonal test section, 20 ft across the flats). In addition, the AWT will include an icing and acoustic research capability. In order to insure a technically sound design, an AWT modeling program (both analytical and physical) was initiated to provide essential input to the AWT final design process. This paper describes the modeling program, including the rationale and criteria used in program definition, and presents some early program results. Author

**N85-15758\*#** National Aeronautics and Space Administration. Lewis Research Center, Cleveland, Ohio.

**THE NASA ALTITUDE WIND TUNNEL (AWT): ITS ROLE IN ADVANCED ICING RESEARCH AND DEVELOPMENT**

B. J. BLAHA and R. J. SHAW 1985 21 p refs Presented at the 23rd Aerospace Sci. Meeting, Reno, Nevada, 14-17 Jan. 1985; sponsored by AIAA (NASA-TM-86920; E-2414; NAS 1.15:86920; AIAA-85-0090) Avail: NTIS HC A02/MF A01 CSCL 14B

Currently experimental aircraft icing research is severely hampered by limitations of ground icing simulation facilities. Existing icing facilities do not have the size, speed, altitude, and icing environment simulation capabilities to allow accurate studies to be made of icing problems occurring for high speed fixed wing aircraft and rotorcraft. Use of the currently dormant NASA Lewis Altitude Wind Tunnel (AWT), as a proposed high speed propulsion and adverse weather facility, would allow many such problems to be studied. The characteristics of the AWT related to adverse weather simulation and in particular to icing simulation are discussed, and potential icing research programs using the AWT are also included. Author

**N85-18067\*#** National Aeronautics and Space Administration. Lewis Research Center, Cleveland, Ohio.

**THE ALTITUDE WIND TUNNEL (AWT): A UNIQUE FACILITY FOR PROPULSION SYSTEM AND ADVERSE WEATHER TESTING**

R. CHAMBERLIN 1985 21 p refs Presented at the 23rd Aerospace Sci. Meeting, Reno, Nevada, 14-17 Jan. 1985; sponsored by AIAA Previously announced in IAA as A85-19661 (NASA-TM-86921; E-2415; NAS 1.15:86921; AIAA-85-0314) Avail: NTIS HC A02/MF A01 CSCL 14B

A need has arisen for a new wind tunnel facility with unique capabilities for testing propulsion systems and for conducting research in adverse weather conditions. New propulsion system concepts, new aircraft configurations with an unprecedented degree of propulsion system/aircraft integration, and requirements for aircraft operation in adverse weather dictate the need for a new test facility. Required capabilities include simulation of both altitude pressure and temperature, large size, full subsonic speed range, propulsion system operation, and weather simulation (i.e., icing, heavy rain). A cost effective rehabilitation of the NASA Lewis Research Center's Altitude Wind Tunnel (AWT) will provide a facility with all these capabilities. Author

**N85-22400\*#** Mechanical Technology, Inc., Latham, N. Y. **DEVELOPMENT OF A MULTIPLANE MULTISPEED BALANCING SYSTEM FOR TURBINE SYSTEMS**

M. R. MARTIN 19 Jul. 1984 114 p refs (Contract NAS3-20609) (NASA-CR-174750; NAS 1.26:174750; MTI-84TR39) Avail: NTIS HC A06/MF A01 CSCL 14B

A prototype high speed balancing system was developed for assembled gas turbine engine modules. The system permits fully assembled gas turbine modules to be operated and balanced at selected speeds up to full turbine speed. The balancing system is a complete stand-alone system providing all necessary lubrication and support hardware for full speed operation. A variable speed motor provides the drive power. A drive belt and gearbox provide rotational speeds up to 21,000 rpm inside a vacuum chamber. The heart of the system is a dedicated minicomputer with attendant data acquisition, storage and I/O devices. The computer is programmed to be completely interactive with the operator. The system was installed at CCAD and evaluated by testing 20 T55 power turbines and 20 T53 power turbines. Engine test results verified the performance of the high speed balanced turbines. B.W.

## ASTRONAUTICS (GENERAL)

**N85-12071\*#** Battelle Columbus Labs., Ohio.

**PRELIMINARY ANALYSIS OF SPACE MISSION APPLICATIONS FOR ELECTROMAGNETIC LAUNCHERS Final Technical Report**

L. A. MILLER, E. E. RICE, R. W. EARHART, and R. J. CONLON 30 Aug. 1984 326 p refs (Contract NAS3-23354) (NASA-CR-174067; NAS 1.26:174067) Avail: NTIS HC A15/MF A01 CSCL 22A

The technical and economic feasibility of using electromagnetically launched EML payloads propelled from the Earth's surface to LEO, GEO, lunar orbit, or to interplanetary space was assessed. Analyses of the designs of rail accelerators and coaxial magnetic accelerators show that each is capable of launching to space payloads of 800 KG or more. A hybrid launcher in which EML is used for the first 2 KM/sec followed by chemical rocket stages was also tested. A cost estimates study shows that one to two EML launches per day are needed to break even,



## 12 ASTRONAUTICS (GENERAL)

compared to a four-stage rocket. Development models are discussed for: (1) Earth orbital missions; (2) lunar base supply mission; (3) solar system escape mission; (4) Earth escape missions; (5) suborbital missions; (6) electromagnetic boost missions; and (7) space-based missions. Safety factors, environmental impacts, and EML systems analysis are discussed. Alternate systems examined include electrothermal thrusters, an EML rocket gun; an EML theta gun, and Soviet electromagnetic accelerators. A.R.H.

**N85-13886\*#** National Aeronautics and Space Administration. Lewis Research Center, Cleveland, Ohio.

### MISSIONS/PLANNING PANEL

J. S. FORDYCE *In its Space Power* p 57 Apr. 1984

Avail: NTIS HC A14/MF A01 CSCL 22A

A panel discussion was held to develop a viewpoint of space power technology needs and state of readiness for future mission scenarios. Among the points made in the discussion, it was agreed that missions, particularly the far term ones, do serve to drive technology; however, as the missions become nearer term, issues of schedule and cost severely limit the willingness to accept risk. There are, in fact, no rewards to a mission manager for introducing new technology. Mission downscaling is the usual response to technology limitations. All panelists agreed that there exists a serious gap between when technologists feel their job is done and what mission managers need for decision. Typically a two to three year engineering development gap exists. It is essential to take technologies to the engineering model level and conduct a flight demonstration to close this gap. All agreed that increased effort should be made to achieve stronger interactions between planners and technologists and that workshops like the present one are a step in the right direction. Technologists need mission credibility and vice versa. R.J.F.

**N85-27922\*#** Stanford Univ., Calif.

### FREE-SURFACE PHENOMENA UNDER LOW- AND ZERO-GRAVITY CONDITIONS Final Technical Report

L. HESSELINK Jun. 1985 8 p

(Contract NAG3-557)

(NASA-CR-175885; NAS 1.26:175885) Avail: NTIS HC A02/MF A01 CSCL 22A

A free surface experiment using a liquid doped with a fluorescent dye under sheet illumination is summarized. The work includes the selection of a CCD camera for use during the design stages of the experiment as well as a preliminary demonstration of this technique in the production of a contour map of a liquid-liquid interface with better than 0.1 mm resolution. With a different data sampling and storage procedure, the image processing is reduced to a simple thresholding procedure which can be done in hardware. Author

## 13

### ASTRODYNAMICS

Includes powered and free-flight trajectories; and orbit and launching dynamics.

**N85-21228\*#** National Aeronautics and Space Administration. Lewis Research Center, Cleveland, Ohio.

### RADIATION EXPOSURE AND PERFORMANCE OF MULTIPLE BURN LEO-GEO ORBIT TRANSFER TRAJECTORIES

S. H. GORLAND 1985 14 p refs Presented at the JANNAF Propulsion Meeting, San Diego, Calif., 9-12 Apr. 1985

(NASA-TM-86946; E-2465; NAS 1.15:86946) Avail: NTIS HC A02/MF A01 CSCL 22A

Many potential strategies exist for the transfer of spacecraft from low Earth orbit (LEO) to geosynchronous (GEO) orbit. One strategy has generally been utilized, that being a single impulsive burn at perigee and a GEO insertion burn at apogee. Multiple

burn strategies were discussed for orbit transfer vehicles (OTVs) but the transfer times and radiation exposure, particularly for potentially manned missions, were used as arguments against those options. Quantitative results concerning the trip time and radiation encountered by multiple burn orbit transfer missions in order to establish the feasibility of manned missions, the vulnerability of electronics, and the shielding requirements are presented. The performance of these multiple burn missions is quantified in terms of the payload and propellant variances from the minimum energy mission transfer. The missions analyzed varied from one to eight perigee burns and ranged from a high thrust, 1 g acceleration, cryogenic hydrogen-oxygen chemical propulsion system to a continuous burn, 0.001 g acceleration, hydrogen fueled resistojet propulsion system with a trip time of 60 days. Author

## 15

### LAUNCH VEHICLES AND SPACE VEHICLES

Includes boosters; manned orbital laboratories; reusable vehicles; and space stations.

**A85-23200\*#** National Aeronautics and Space Administration. Lewis Research Center, Cleveland, Ohio.

### A HIGH ENERGY STAGE FOR THE NATIONAL SPACE TRANSPORTATION SYSTEM

A. J. STOFAN (NASA, Lewis Research Center, Cleveland, OH) International Astronautical Federation, International Astronautical Congress, 35th, Lausanne, Switzerland, Oct. 7-13, 1984. 12 p. Previously announced in STAR as N84-32411. (IAF PAPER 84-15)

The Shuttle/Centaur is an expendable hydrogen/oxygen cryogenic upper stage for use with the National Space Transportation System. It is a modification of the existing Atlas/Centaur which was used by NASA since 1966 to launch interplanetary and earth orbital payloads for numerous organizations. Two configurations of the Shuttle/Centaur are being developed. Vehicle capability includes placing approximately 4500 kg (10,000 lb) in geostationary orbit, and initial applications will be for the interplanetary Galileo and Ulysses Missions in 1986. The Shuttle/Centaur development program is discussed, the configurations and performance are described, and the unique integration and operations requirements related to the Shuttle are indicated. Design changes to the current Atlas/Centaur required for Shuttle operation are described here, and include those related to Orbiter cargo bay dimensions, environment, and safety considerations. Author

**A85-39730\*#** Martin Marietta Aerospace, Denver, Colo.

### MAIN PROPULSION SYSTEM DESIGN RECOMMENDATIONS FOR AN ADVANCED ORBIT TRANSFER VEHICLE

L. REDD (Martin Marietta Aerospace, Denver, CO) AIAA, SAE, ASME, and ASEE, Joint Propulsion Conference, 21st, Monterey, CA, July 8-10, 1985. 9 p.

(Contract NAS3-23858)

(AIAA PAPER 85-1336)

Various main propulsion system configurations of an advanced OTV are evaluated with respect to the probability of nonindependent failures, i.e., engine failures that disable the entire main propulsion system. Analysis of the life-cycle cost (LCC) indicates that LCC is sensitive to the main propulsion system reliability, vehicle dry weight, and propellant cost; it is relatively insensitive to the number of missions/overhaul, failures per mission, and EVA and IVA cost. In conclusion, two or three engines are recommended in view of their highest reliability, minimum life-cycle cost, and fail operational/fail safe capability. L.T.

**N85-16989\*#** National Aeronautics and Space Administration. Lewis Research Center, Cleveland, Ohio.

## OTV PROPULSION ISSUES

Washington Apr. 1984 296 p refs Conf. held in Cleveland, 3-4 Apr. 1984

(NASA-CP-2347; E-2171; NAS 1.55:2347) Avail: NTIS HC

A13/MF A01 CSCL 22B

The statistical technology needs of aero-assist maneuvering, propulsion, and usage of cryogenic fluids were presented. Industry panels discussed the servicing of reusable space based vehicles and propulsion-vehicle interaction.

**N85-16991\*#** National Aeronautics and Space Administration. Lewis Research Center, Cleveland, Ohio.

## SHUTTLE/CENTAUR PROJECT PERSPECTIVE

E. T. MUCKLEY *In its* OTV Propulsion Issues p 15-27 Apr. 1984 refs

Avail: NTIS HC A13/MF A01 CSCL 22B

The shuttle/Centaur vehicle is being developed as an expendable, cryogenic high energy upper stage for use with the National Space Transportation System (NSTS). The stage is expected to meet the demands of a wide range of users. The shuttle/Centaur will be a modification of the highly successful Centaur stage, used extensively with the Atlas and Titan boosters since 1966 to launch planetary, geosynchronous and Earth orbital missions. The design changes required for use with the NSTS are described. These are primarily related to: (1) tank resizing to take advantage of the orbiter payload bay dimensions; (2) provisions for physically adopting Centaur to the orbiter; and, (3) accommodating safety requirements of the manned NSTS. The expected performance capabilities of two versions of the shuttle/Centaur are also described. The initial version, designated G-prime, is the larger of the two, with a length of about 9.1m (30 ft.). This vehicle will be used to launch the Galileo and International Solar Polar Mission to Jupiter in May 1986. B.G.

**N85-16997\*#** National Aeronautics and Space Administration. Lewis Research Center, Cleveland, Ohio.

## OTV PROPULSION TECHNOLOGY PROGRAMMATIC OVERVIEW

L. P. COOPER *In its* OTV Propulsion Issues p 97-102 Apr. 1984 refs

Avail: NTIS HC A13/MF A01 CSCL 22B

An advanced orbit transfer vehicles (OTV) which will be an integral part of the national space transportation system to carry men and cargo between low Earth orbit and geosynchronous orbit will perform planetary transfers and deliver large acceleration limited space structures to high Earth orbits is reviewed. The establishment of an advanced propulsion technology base for an OTV for the mid 1990's is outlined. The program supports technology for three unique engine concepts. Work is conducted to generic technologies which benefit all three concepts and specific technology which benefits only one of the concepts. Concept and technology definitions to identify propulsion innovations, and subcomponent research to explore and validate their potential benefits are included. E.A.K.

**N85-17008\*#** National Aeronautics and Space Administration. Lewis Research Center, Cleveland, Ohio.

## VEHICLE/ENGINE INTEGRATION

L. P. COOPER, T. J. VINOPAL (Boeing Aerospace Co., Seattle), D. E. FLORENCE (General Electric Corp., Fairfield, Conn.), R. W. MICHEL (Aerojet TechSystems Co.), J. R. BROWN (Pratt and Whitney Aircraft, East Hartford, Conn.), R. P. BERGERON (Rockwell International Corp., Pittsburgh), and V. A. WELDON *In its* OTV Propulsion Issues p 229-245 Apr. 1984 refs

Avail: NTIS HC A13/MF A01 CSCL 22B

VEHICLE/ENGINE Integration Issues are explored for orbit transfer vehicles (OTV's). The impact of space basing and aeroassist on VEHICLE/ENGINE integration is discussed. The AOTV structure and thermal protection subsystem weights were scaled as the vehicle length and surface was changed. It is concluded that for increased allowable payload lengths in a

ground-based system, lower length-to-diameter (L/D) is as important as higher mixture ratio (MR) in the range of mid L/D ATOV's. Scenario validity, geometry constraints, throttle levels, reliability, and servicing are discussed in the context of engine design and engine/vehicle integration. R.S.F.

**N85-21231\*#** National Aeronautics and Space Administration. Lewis Research Center, Cleveland, Ohio.

## ADVANCED RESEARCH AND TECHNOLOGY PROGRAMS FOR ADVANCED HIGH-PRESSURE OXYGEN-HYDROGEN ROCKET PROPULSION

S. J. MARSIK and S. F. MOREA (NASA. Marshall Space Flight Center) 1985 14 p refs Proposed for presentation at the 1985 JANNAF Propulsion Meeting, San Diego, Calif., 9-12 Apr. 1985

(NASA-TM-86969; E-2495; NAS 1.15:86969) Avail: NTIS HC A02/MF A01 CSCL 20H

A research and technology program for advanced high pressure, oxygen-hydrogen rocket propulsion technology is presently being pursued by the National Aeronautics and Space Administration (NASA) to establish the basic discipline technologies, develop the analytical tools, and establish the data base necessary for an orderly evolution of the staged combustion reusable rocket engine. The need for the program is based on the premise that the USA will depend on the Shuttle and its derivative versions as its principal Earth-to-orbit transportation system for the next 20 to 30 yr. The program is focused in three principal areas of enhancement: (1) life extension, (2) performance, and (3) operations and diagnosis. Within the technological disciplines the efforts include: rotor-dynamics, structural dynamics, fluid and gas dynamics, materials fatigue/fracture/life, turbomachinery fluid mechanics, ignition/combustion processes, manufacturing/productibility/nondestructive evaluation methods and materials development/evaluation. An overview of the Advanced High Pressure Oxygen-Hydrogen Rocket Propulsion Technology Program Structure and Working Groups objectives are presented with highlights of several significant achievements. Author

**N85-21233\*#** Ohio State Univ., Columbus. Dept. of Electrical Engineering.

## ENGINEERING CALCULATIONS FOR COMMUNICATIONS SATELLITE SYSTEMS PLANNING Interim Report, 15 Jul. 1983 - 14 Jul. 1984

C. A. LEVIS, C. H. MARTIN, C. H. REILLY, D. J. GONSALVEZ, and Y. YAMAURA Mar. 1985 59 p refs (Contract NAG3-159)

(NASA-CR-175552; NAS 1.26:175552; ESL-713533-5) Avail: NTIS HC A04/MF A01 CSCL 22B

An extended gradient search code for broadcasting satellite service (BSS) spectrum/orbit assignment synthesis is discussed. Progress is also reported on both single-entry and full synthesis computational aids for fixed satellite service (FSS) spectrum/orbit assignment purposes. Author

**N85-22520\*#** National Aeronautics and Space Administration. Lewis Research Center, Cleveland, Ohio.

## PRELIMINARY ASSESSMENT OF POWER-GENERATING TETHERS IN SPACE AND OF PROPULSION FOR THEIR ORBIT MAINTENANCE

R. E. ENGLISH and P. M. FINNEGAN *In its* Spacecraft Environ. Interactions Technol., 1983 p 637-647 Mar. 1985 refs

Avail: NTIS HC A99/MF E03 CSCL 22B

The concept of generating power in space by means of a conducting tether deployed from a spacecraft was studied. Using hydrogen and oxygen as the rocket propellant to overcome the drag of such a power-generating tether would yield more benefit than if used in a fuel cell. The mass consumption would be 25 percent less than the reactant consumption of fuel cells. Residual hydrogen and oxygen in the external tank and in the orbiter could be used very effectively for this purpose. Many other materials (such as waste from life support) could be used as the propellant. Electrical propulsion using tether generated power can compensate for the drag of a power-generating tether, half the power going to

## 16 SPACE TRANSPORTATION

the useful load and the rest for electric propulsion. In addition, the spacecraft's orbital energy is a large energy reservoir that permits load leveling and a ratio of peak to average power equal to 2. Critical technologies to be explored before a power-generating tether can be used in space are delineated. Author

### 16

#### SPACE TRANSPORTATION

Includes passenger and cargo space transportation, e.g., shuttle operations; and rescue techniques.

**N85-29987\*#** National Aeronautics and Space Administration. Lewis Research Center, Cleveland, Ohio.

#### **TECHNOLOGY REQUIREMENTS TO BE ADDRESSED BY THE NASA LEWIS RESEARCH CENTER CRYOGENIC FLUID MANAGEMENT FACILITY PROGRAM**

J. C. AYDELOTT and R. S. RUDLAND (Martin Marietta Aerospace, Denver) 1985 25 p refs Presented at the 21st Joint Propulsion Conf., Monterey, Calif., 8-10 Jul. 1985; sponsored in part by AIAA, SAE, ASME and ASEE Previously announced in IAA as A85-47024

(NASA-TM-87048; E-2610; NAS 1.15:87048; AIAA-85-1229)

Avail: NTIS HC A02/MF A01 CSCL 14B

The NASA Lewis Research Center is responsible for the planning and execution of a scientific program which will provide advance in space cryogenic fluid management technology. A number of future space missions were identified that require or could benefit from this technology. These fluid management technology needs were prioritized and a shuttle attached reusable test bed, the cryogenic fluid management facility (CFMF), is being designed to provide the experimental data necessary for the technology development effort. Author

### 17

#### SPACECRAFT COMMUNICATION, COMMAND AND TRACKING

Includes telemetry; space communications networks; astronavigation; and radio blackout.

**A85-36663\*** Toledo Univ., Ohio.

#### **MODELING OF NASA'S 30/20 GHZ SATELLITE COMMUNICATIONS SYSTEM**

S. C. KWATRA, B. W. MAPLES (Toledo, University, Toledo, OH), and G. A. STEVENS (NASA, Lewis Research Center, Cleveland, OH) IN: ICC '84 - Links for the future: Science, systems and services for communications; Proceedings of the International Conference on Communications, Amsterdam, Netherlands, May 14-17, 1984. Volume 3. New York/Amsterdam, Institute of Electrical and Electronics Engineers, Inc./North-Holland, 1984, p. 1102-1106. refs

(Contract NAG3-157)

NASA is in the process of developing technology for a 30/20 GHz satellite communications link. Currently hardware is being assembled for a test transponder. A simulation package is being developed to study the link performance in the presence of interference and noise. This requires developing models for the components of the system. This paper describes techniques used to model the components for which data is available. Results of experiments performed using these models are described. A brief overview of NASA's 30/20 GHz communications satellite program is also included. Author

**N85-15779\*#** National Aeronautics and Space Administration. Lewis Research Center, Cleveland, Ohio.

#### **CHARACTERIZATION OF MMIC DEVICES FOR ACTIVE ARRAY ANTENNAS**

J. SMETANA, E. FARR (Illinois Univ., Urbana), and R. MITTRA (Illinois Univ., Urbana) 1984 17 p refs Presented at the Antenna Appl. Symp., Monticello, Ill., 19-21 Sep. 1984; sponsored by Illinois Univ. and RADC

(NASA-TM-86907; E-2396; NAS 1.15:86907) Avail: NTIS HC A02/MF A01 CSCL 09F

Certain aspects of monolithic microwave integrated circuit (MMIC) interconnectivity were investigated. Considerations that lead to preserving the inherently reproducible characteristics of the MMIC are proposed. It is shown that at radio frequencies (RF) greater than 20 GHz, the transition from the MMIC device to other transmission media must be an accurate RF match. It is proposed that the RF match is sufficiently critical to include the transition as part of the delivered MMIC package. The model to analyze several transitions is presented. This model consists of a succession of abrupt discontinuities in printed circuit transmission lines. The analysis of these discontinuities is achieved by the Spectral Galerkin technique, to establish the modes and mode matching, to generate the generalized S parameters of the individual discontinuities. Preliminary results achieved with this method are presented. It is concluded that special effects should be coordinated by the active array antenna industry toward standardization of MMIC packaging and characterization. E.A.K.

**N85-34150\*#** National Aeronautics and Space Administration. Lewis Research Center, Cleveland, Ohio.

#### **TELECOMMUNICATIONS FORECAST FOR ITU REGION 2 TO THE YEAR 1995**

J. E. HOLLANSWORTH, J. A. SALZMAN, and J. R. RAMLER Aug. 1985 131 p refs

(NASA-TM-87077; E-2653; NAS 1.15:87077) Avail: NTIS HC A07/MF A01 CSCL 17B

Telecommunications activity was studied. The primary objective was to forecast the need for fixed service satellites (FSS) by countries within ITU Region 2 excluding the United States and Greenland. Forecasts of telecommunications equipment needs were developed as a yardstick of the relative level of telecommunications activity among developing countries within the region. A likely scenario for the implementation of domestic and regional communications satellites is forecasted to provide services to and among countries in ITU Region 2. By 1995, it is forecast that 15 fixed service satellites will be implemented. A forecast of the countries requirements indicates that, with the possible exception of Canada, this constellation of satellites will meet these countries' needs to beyond the year 2000. E.A.K.

### 18

#### SPACECRAFT DESIGN, TESTING AND PERFORMANCE

Includes spacecraft thermal and environmental control; and attitude control.

**A85-30303\*#** Analox Corp., Cleveland, Ohio.

#### **INTERDISCIPLINARY DESIGN ANALYSIS OF A PRECISION SPACECRAFT ANTENNA**

R. E. STEINBACH (Analox Corp., Cleveland, OH) and S. R. WINEGAR (NASA, Lewis Research Center, Cleveland, OH) IN: Structures, Structural Dynamics, and Materials Conference, 26th, Orlando, FL, April 15-17, 1985, Technical Papers. Part 1. New York, American Institute of Aeronautics and Astronautics, 1985, p. 704-712.

(AIAA PAPER 85-0804)

The Advanced Communications Technology Satellite (ACTS) will operate in the 20/30 GHz range (Ka Band), and will include a

multi-beam antenna (MBA) capable of 0.3 degree scanning spot beams with very high beam-to-beam isolation. The antenna Radio Frequency (RF) performance requirements lead to stringent requirements on the antenna reflector surface shape. A prediction of RF performance of a potential flight model antenna reflector operating under space environmental conditions is made using a radiant heat input model (TRASYS), a thermal analyzer (SINDA), a structural model (NASTRAN), and RF far field pattern simulation. Interfacing software has been written to pass thermal model temperature results to the structural model, and structural model thermal deformation results to the RF far field pattern simulation. A complete analysis can be performed in a single computer run, and potential changes in design can be quickly and easily evaluated using this interdisciplinary design analysis tool. Author

**A85-35379\*** # Alabama Univ., Huntsville.

**EXPERIMENTS IN CHARGE CONTROL AT GEOSYNCHRONOUS ORBIT - ATS-5 AND ATS-6**

R. C. OLSEN (Alabama, University, Huntsville, AL) Journal of Spacecraft and Rockets (ISSN 0022-4650), vol. 22, May-June 1985, p. 254-264. refs  
(Contract NSG-3150; NAS5-23481; NAS8-33982)

In connection with existing theoretical concepts, it was difficult to explain the negative potentials found in sunlight, first on Applied Technology Satellite-5 (ATS-5) and then on ATS-6. The problem became important when an association between spacecraft charging and anomalies in spacecraft behavior was observed. A study of daylight charging phenomena on ATS-6 was conducted, and an investigation was performed with the objective to determine effective methods of charge control, taking into account the feasibility to utilize the ATS-5 and ATS-6 ion engines as current sources. In the present paper, data and analysis for the ion engine experiments on ATS-5 and ATS-6 are presented. It is shown that electron emission from a satellite with insulating surfaces is not an effective method of charge control because the increase in differential charging which results limits the effectiveness of electron emitters and increases the possibility of electrostatic discharges between surfaces at different potentials. G.R.

**N85-14858\*** # National Aeronautics and Space Administration, Lewis Research Center, Cleveland, Ohio.

**CIRCUIT TRANSIENTS DUE TO NEGATIVE BIAS ARCS ON A HIGH-VOLTAGE SOLAR ARRAY IN LOW EARTH ORBIT**

R. N. METZ (Colby Coll., Waterville, Maine) Jan. 1985 12 p refs  
(NASA-TP-2407; E-2239; NAS 1.60:2407) Avail: NTIS HC A02/MF A01 CSCL 22B

Arcing to negatively biased, exposed solar cell interconnects on solar arrays placed in plasma environments was established. Arcing, however, may cause damaging interference with the operation of electrical power systems in spacecraft planned to be driven with high-voltage solar arrays. An analytical model was developed to estimate the effects of negative bias arcs on solar array power system performance. Solar cell characteristics, plasma interactions, and power system features are modeled by a linear, lumped element transient circuit, and the time domain equations are solved. Numerical results for solar array common mode and load voltage transients are calculated for typical conditions. Acceptable load transients are found for a range of arc current amplitudes and time constants. E.A.K.

**N85-21250\*** # Pennsylvania State Univ., University Park. Dept. of Physics.

**MASS ANALYSIS OF NEUTRAL PARTICLES AND IONS RELEASED DURING ELECTRICAL BREAKDOWNS ON SPACECRAFT SURFACES** Final Report, 1 Sep. 1979 - 31 Dec. 1984

B. R. F. KENDALL 16 Mar. 1985 32 p refs  
(Contract NSG-3301)  
(NASA-CR-175585; NAS 1.26:175585) Avail: NTIS HC A03/MF A01 CSCL 22B

Charged-particle fluxes from breakdown events were studied. Methods to measure mass spectra and total emitted flux of neutral

particles were developed. The design and construction of the specialized mass spectrometer was completed. Electrical breakdowns were initiated by a movable blunt contact touching the insulating surface. The contact discharge apparatus was used for final development of two different high-speed recording systems and for measurements of the composition of the materials given off by the discharge. It was shown that intense instantaneous fluxes of neutral particles were released from the sites of electrical breakdown events. A laser micropulse mass analyzer showed that visible discoloration at breakdown sites were correlated with the presence of iron on the polymer side of the film, presumably caused by punch-through to the Inconel backing. Kapton samples irradiated by an oxygen ion beam were tested. The irradiated samples were free of surface hydrocarbon contamination but otherwise behaved in the same way as the Kapton samples tested earlier. Only the two samples exposed to oxygen ion bombardment were relatively clean. This indicates an additional variable that should be considered when testing spacecraft materials in the laboratory. E.A.K.

**N85-22470\*** # National Aeronautics and Space Administration, Lewis Research Center, Cleveland, Ohio.

**SPACECRAFT ENVIRONMENTAL INTERACTIONS TECHNOLOGY, 1983**

Washington Mar. 1985 673 p refs Conf. held in Colorado Springs, 4-6 Oct. 1983 Prepared in cooperation with AFGL, Hanscom AFB, Mass.  
(NASA-CP-2359; E-2186; NAS 1.55:2359; AFGL-TR-85-0018)  
Avail: NTIS HC A99/MF E03 CSCL 22B

State of the art of environment interactions dealing with low-Earth-orbit plasmas; high-voltage systems; spacecraft charging; materials effects; and direction of future programs are contained in over 50 papers.

**N85-22474\*** # National Aeronautics and Space Administration, Washington, D.C.

**ELECTRON AND ION DENSITY DEPLETIONS MEASURED IN THE STS-3 ORBITER WAKE**

G. B. MURPHY (Iowa Univ., Iowa City), J. S. PICKETT (Iowa Univ., Iowa City), W. S. RAITT (Utah State Univ., Logan), and S. D. SHAWHAN /in NASA, Lewis Research Center Spacecraft Environ. Interactions Technol., 1983 p 33-42 Mar. 1985 refs  
(Contract NAG3-449)  
Avail: NTIS HC A99/MF E03 CSCL 22B

The third Space Shuttle flight on Columbia carried instrumentation to measure thermal plasma density and temperature. Two separate investigations, the Plasma Diagnostics Package (PDP) and the Vehicle Charging and Potential Experiment (VCAP), carried a Langmuir Probe, and the VCAP also included a Spherical Retarding Potential Analyzer (SRPA). Only those measurements made while the PDP is in the payload bay are discussed here since the VCAP instrumentation remains in the payload bay at all times and the two measurements are compared. The wake behind a large structure (in this case the Space Shuttle Orbiter) flying through the ionospheric plasma is discussed. Much theoretical work was done regarding plasma wakes. The instrumentation on this mission gives the first data taken with a large vehicle in the ionospheric laboratory. First, the PDP Langmuir Probe and its data set will be presented, then the VCAP Langmuir Probe and SRPA with associated data. The agreement between the two data sets is discussed and then followed by some other PDP data which infers an even lower wake density. B.G.

**N85-22478\*** # National Aeronautics and Space Administration, Lewis Research Center, Cleveland, Ohio.

**ELECTRON BEAM CHARGING OF SPACE SHUTTLE THERMAL PROTECTION SYSTEM TILES**

J. V. STASKUS /in its Spacecraft Environ. Interactions Technol., 1983 p 91-102 Mar. 1985 refs  
Avail: NTIS HC A99/MF E03 CSCL 22B

Six space shuttle reusable surface insulation tiles were tested in the NASA Lewis Research Center's electron bombardment test facility. The 30-cm-square specimens were assembled by using

## 18 SPACECRAFT DESIGN, TESTING AND PERFORMANCE

the same materials and techniques used to apply the tiles to the space shuttle and were composed to 15-cm- and 20-cm-square tiles and pieces on 0.6-cm-thick aluminum substrates. There were two specimens of each of three thicknesses. One specimen of each thickness had gaps of less than 0.1 cm between tiles, and the other had gaps of approximately 0.15 cm. The specimens were exposed to monoenergetic electron beams (2 to 25 keV) with nominal fluxes of 0.1 and 1 nA/sq. cm. Tests were conducted with both grounded and floating substrates. The data presented include charging rates, equilibrium potentials, and substrate currents. There is evidence that discharging occurred. Author

**N85-22486\*#** National Aeronautics and Space Administration. Lewis Research Center, Cleveland, Ohio.

### THREE-DIMENSIONAL CALCULATION OF SHUTTLE CHARGING IN POLAR ORBIT

D. L. COOKE, I. KATZ, M. J. MANDELL, J. R. LILLEY, JR., and A. J. RUBIN (AFGL) *In* NASA. Lewis Research Center Spacecraft Environ. Interactions Technol., 1983 p 205-227 Mar. 1985 refs

(Contract F19628-82-C-0081)

Avail: NTIS HC A99/MF E03 CSCL 22B

The charged particles environment in polar orbit can be of sufficient intensity to cause spacecraft charging. In order to gain a quantitative understanding of such effects, the Air Force is developing POLAR, a computer code which simulates in three dimensions the electrical interaction of large space vehicles with the polar ionospheric plasma. It models the physical processes of wake generation, ambient ion collection, precipitating auroral electron fluxes, and surface interactions, including secondary electron generation and backscattering, which lead to vehicle charging. These processes may be followed dynamically on a subsecond timescale so that the rapid passage through intense auroral arcs can be simulated. POLAR models the ambient plasma as isotropic Maxwellian electrons and ions ( $0+$ ,  $H+$ ), and allows for simultaneous precipitation of power-law, energetic Maxwellian, and accelerated Gaussian distributions of electrons. Magnetic field effects will be modeled in POLAR but are currently ignored.

G.L.C.

**N85-22487\*#** National Aeronautics and Space Administration. Lewis Research Center, Cleveland, Ohio.

### POLAR ORBIT ELECTROSTATIC CHARGING OF OBJECTS IN SHUTTLE WAKE

I. KATZ, D. E. PARKS, D. L. COOKE, M. J. MANDELL (AFGL), and A. J. RUBIN *In* NASA. Lewis Research Center Spacecraft Environ. Interactions Technol., 1983 p 229-234 Mar. 1985 refs

(Contract F19628-82-C-0081)

Avail: NTIS HC A99/MF E03 CSCL 22B

A survey of DMSP data has uncovered several cases where precipitating auroral electron fluxes are both sufficiently intense and energetic to charge spacecraft materials such as teflon to very large potentials in the absence of ambient ion currents. Analytical bounds are provided which show that these measured environments can cause surface potentials in excess of several hundred volts to develop on objects in the orbiter wake for particular vehicle orientations.

G.L.C.

### N85-22493\*# Systems Science and Software, La Jolla, Calif. SURFACE INTERACTIONS AND HIGH-VOLTAGE CURRENT COLLECTION

M. J. MANDELL and I. KATZ *In* NASA. Lewis Research Center Spacecraft Environ. Interactions Technol., 1983 p 305-320 Mar. 1985 refs

(Contract NAS3-23058)

Avail: NTIS HC A99/MF E03 CSCL 22B

Spacecraft of the future will be larger and have higher power requirements than any flown to date. For several reasons, it is desirable to operate a high power system at high voltage. While the optimal voltages for many future missions are in the range 500 to 5000 volts, the highest voltage yet flown is approximately 100 volts. The NASCAP/LEO code is being developed to embody

the phenomenology needed to model the environmental interactions of high voltage spacecraft. Some plasma environment are discussed. The treatment of the surface conductivity associated with emitted electrons and some simulations by NASCAP/LEO of ground based high voltage interaction experiments are described.

Author

**N85-22500\*#** National Aeronautics and Space Administration. Lewis Research Center, Cleveland, Ohio.

### DESIGN GUIDELINES FOR ASSESSING AND CONTROLLING SPACECRAFT CHARGING EFFECTS Abstract Only

C. K. PURVIS, H. B. GARRETT (JPL, California Inst. of Tech., Pasadena), A. WHITTLESEY (JPL, California Inst. of Tech., Pasadena), and N. J. STEVENS (Hughes Aircraft Co., El Segundo, Calif.) *In* its Spacecraft Environ. Interactions Technol. p 389 Mar. 1985 Previously announced as N84-33452

Avail: NTIS HC A99/MF E03 CSCL 22B

The need for uniform criteria, or guidelines, to be used in all phases of spacecraft design is discussed. Guidelines were developed for the control of absolute and differential charging of spacecraft surfaces by the lower energy space charged particle environment. Interior charging due to higher energy particles is not considered. A guide to good design practices for assessing and controlling charging effects is presented. Uniform design practices for all space vehicles are outlined.

E.A.K.

**N85-22512\*#** Case Western Reserve Univ., Cleveland, Ohio.

### ELECTRON YIELDS FROM SPACECRAFT MATERIALS

K. YANG, W. L. GORDON, and R. W. HOFFMAN *In* NASA. Lewis Research Center Spacecraft Environ. Interactions Technol., 1983 p 537-545 Mar. 1985 refs

(Contract NSG-3197)

Avail: NTIS HC A99/MF E03 CSCL 22B

Photoyields and secondary electron emission (SEE) characteristics were determined under UHV conditions for a group of insulating materials used in spacecraft applications. The SEE studies were carried out with a pulsed primary beam while photoyields were obtained with a chopped photon beam from a Kr resonance source with major emission at 123.6 nm. This provides a photon flux close to that of the Lyman alpha in the space environment. Yields per incident photon are obtained relative to those from a freshly evaporated and air oxidized Al surface. Results are presented for Kapton, FEP Teflon, the borosilicate glass covering of a shuttle tile, and spacesuit outer fabric.

E.A.K.

**N85-22517\*#** National Aeronautics and Space Administration. Lewis Research Center, Cleveland, Ohio.

### SPACECRAFT ENVIRONMENTAL INTERACTIONS: A JOINT AIR FORCE AND NASA RESEARCH AND TECHNOLOGY PROGRAM

C. P. PIKE (AFGL), C. K. PURVIS, and W. R. HUDSON (NASA, Washington) *In* its Spacecraft Environ. Interactions Technol., 1983 p 599-608 Mar. 1985

Avail: NTIS HC A99/MF E03 CSCL 22B

A joint Air Force/NASA comprehensive research and technology program on spacecraft environmental interactions to develop technology to control interactions between large spacecraft systems and the charged-particle environment of space is described. This technology will support NASA/Department of Defense operations of the shuttle/IUS, shuttle/Centaur, and the force application and surveillance and detection missions, planning for transatmospheric vehicles and the NASA space station, and the AFSC military space system technology model. The program consists of combined contractual and in-house efforts aimed at understanding spacecraft environmental interaction phenomena and relating results of ground-based tests to space conditions. A concerted effort is being made to identify project-related environmental interactions of concern. The basic properties of materials are being investigated to develop or modify the materials as needed. A group simulation investigation is evaluating basic plasma interaction phenomena to provide inputs to the analytical

modeling investigation. Systems performance is being evaluated by both groundbased tests and analysis. B.W.

**N85-23904\*#** National Aeronautics and Space Administration, Lewis Research Center, Cleveland, Ohio.

**LINEARIZATION OF DIGITAL DERIVED RATE ALGORITHM FOR USE IN LINEAR STABILITY ANALYSIS**

R. E. GRAHAM and T. W. PORADA 21 Jun. 1985 13 p refs  
Proposed for presentation at 4th Am. Control Conf., Boston, 19-21 Jun. 1985

(NASA-TM-87000; E-2522; NAS 1.15:87000) Avail: NTIS HC A02/MF A01 CSCL 22B

The digital derived rate (DDR) algorithm is used to calculate the rate of rotation of the Centaur upper-stage rocket. The DDR is highly nonlinear algorithm, and classical linear stability analysis of the spacecraft cannot be performed without linearization. The performance of this rate algorithm is characterized by a gain and phase curve that drop off at the same frequency. This characteristic is desirable for many applications. A linearization technique for the DDR algorithm is investigated. The linearization method is described. Examples of the results of the linearization technique are illustrated, and the effects of linearization are described. A linear digital filter may be used as a substitute for performing classical linear stability analyses, while the DDR itself may be used in time response analysis. Author

**N85-29997\*#** Case Western Reserve Univ., Cleveland, Ohio. Dept. of Physics.

**STUDY OF KAPTON UNDER SIMULATED SHUTTLE ENVIRONMENT Annual Report, 1 May 1984 - 30 Apr. 1985**

T. G. ECK and R. W. HOFFMAN Jul. 1985 10 p

(Contract NAG3-426)

(NASA-CR-176003; NAS 1.26:176003) Avail: NTIS HC A02/MF A01 CSCL 22B

Weight loss and severe degradation of the surface of Kapton that occurs in low Earth orbit is studied. Atomic oxygen, the major ambient species at low Earth altitude and incident with approximately 5 eV energy in ram conditions, is the primary suspect, but a thorough study of oxygen-Kapton interactions has not yet been carried out. A low-energy ion source is used to simulate the shuttle low Earth orbit environment. This source, together with diagnostic tools including surface analysis and mass spectroscopic capability, is being used to carry out experiments from which quantum yields may be obtained. R.J.F.

## 19

### SPACECRAFT INSTRUMENTATION

**N85-27968\*#** National Aeronautics and Space Administration, Lewis Research Center, Cleveland, Ohio.

**THIN-FILM SENSORS FOR SPACE PROPULSION TECHNOLOGY Abstract Only**

W. S. KIM and D. R. ENGLUND *In its* Struct. Integrity and Durability of Reusable Space Propulsion Systems p 183-188 May 1985 refs

Avail: NTIS HC A09/MF A01 CSCL 22B

SSME components such as the turbine blades of the high pressure fuel turbopump are subjected to rapid and extreme thermal transients that contribute to blade cracking and subsequent failure. The objective was to develop thin film sensors for SSME components. The technology established for aircraft gas turbine engines was adopted to the materials and environment encountered in the SSME. Specific goals are to expand the existing thin film sensor technology, to continue developing improved sensor processing techniques, and to test the durability of aircraft gas turbine engine technology in the SSME environment. A thin film sensor laboratory is being installed in a refurbished clean room,

and new sputtering and photoresist exposure equipment is being acquired. Existing thin film thermocouple technology in an SSME environment are being tested. Various coatings and their insulating films are being investigated for use in sensor development. E.R.

**N85-27970\*#** National Aeronautics and Space Administration, Lewis Research Center, Cleveland, Ohio.

**HEAT FLUX SENSOR CALIBRATOR Abstract Only**

C. H. LIEBERT *In its* Struct. Integrity and Durability of Reusable Space Propulsion Systems p 195-198 May 1985 refs

Avail: NTIS HC A09/MF A01 CSCL 22B

The heat flux to space shuttle main engine (SSME) turbopump turbine blades may be as high as 10 to the 7th power. The heat flux causes thermal transients that are of the order of 1 sec as temperature varies from perhaps 1500 K to 100 K. It is suspected that these transients cause durability problems in the turbine blades. To quantitatively evaluate the effect of these transients, heat flux sensors or gauges were developed to obtain data to verify analytical models. The objective is to design and fabricate a system for steady state and transient calibration and durability testing of heat flux sensors for use in SSME turbine blades. The calibrator consists of: (1) the arc lamp, (2) a high speed positioning table for placing standard and special heat flux sensors in the incident beam of radiant heat flux, (3) provision for cooling the blade and special sensors inserted in the blade, (4) a computer for controlling the positioning table, storing electrical output values from sensors, and calculating heat flux from these values, and (5) a pyrometer for measuring sensor surface temperatures. E.R.

**N85-27971\*#** Rockwell International Corp., Canoga Park, Calif.  
**FEASIBILITY OF MAPPING VELOCITY FLOW FIELDS IN SSME POWERHEAD BY LASER ANEMOMETRY TECHNIQUES Abstract Only**

D. G. PELACCIO, L. K. SHARMA, T. V. FERGUSON, J. M. MARAM, and S. PINKOWSKI *In* NASA. Lewis Research Center Struct. Integrity and Durability of Reusable Space Propulsion Systems p 199 May 1985

(Contract NAS3-24356)

Avail: NTIS HC A09/MF A01 CSCL 22B

Because of the flow environment associated with the SSME powerhead pressure (3000 psia), temperature (1800 R), and mechanical complexity and the high vibration test stand environment, detailed flow measurements are difficult to make. The feasibility of using laser anemometry techniques to map velocity flow fields in an SSME powerhead is studied. In the study three engine powerhead component flow environments: (1) the high pressure fuel turbopump preburner, (2) the fuel turbopump turbine rotor and stator region, and (3) the 180 deg turnaround duct - are being considered. Flow parameters measured by the anemometry techniques are time averaged values of the velocity magnitude and flow direction, turbulence intensity, velocity component correlation, integral time scale, and turbulence spectrum. E.R.

## 20

### SPACECRAFT PROPULSION AND POWER

Includes main propulsion systems and components, e.g., rocket engines; and spacecraft auxiliary power sources.

**A85-15512\*#** Colorado State Univ., Fort Collins.

**THEORY OF ION ACCELERATION WITH CLOSED ELECTRON DRIFT**

H. R. KAUFMAN (Colorado State University, Fort Collins, CO) *Journal of Spacecraft and Rockets* (ISSN 0022-4650), vol. 21, Nov.-Dec. 1984, p. 558-562. Previously cited in issue 2, p. 241, Accession no. A83-12490. refs

(Contract NSG-3011)



## 20 SPACECRAFT PROPULSION AND POWER

**A85-16406\*#** Hughes Research Labs., Malibu, Calif.

### **IAPS (8-CM) ION THRUSTER CYCLIC ENDURANCE TEST**

C. R. DULGEROFF, J. R. BEATTIE, R. L. POESCHEL, and J. HYMAN, JR. (Hughes Research Laboratories, Malibu, CA) IN: International Electric Propulsion Conference, 17th, Tokyo, Japan, May 28-31, 1984, Proceedings . Tokyo, Japan Society for Aeronautical and Space Sciences, 1984, p. 250-260. refs (Contract NAS3-21741)

Attention is given to the cyclic endurance qualification test, performed in a vacuum facility with a liquid nitrogen-cooled cryosurface and a frozen mercury target, to which a mercury-ion thruster representative of Ion Auxiliary Propulsion System (IAPS) thrusters was subjected. At the time that the endurance test was successfully concluded, upon consumption of the IAPS propellant tank's mercury, 8,471 hours of 'beam-on time' and 599 cycles had been accumulated. The system's Power Electronics Unit accumulated 10,268 hours of test time with high voltage applied to the operating thruster or dummy load. O.C.

**A85-16408\*#** National Aeronautics and Space Administration. Lewis Research Center, Cleveland, Ohio.

### **GROUND CORRELATION INVESTIGATION OF THRUSTER/SPACECRAFT INTERACTIONS TO BE MEASURED ON THE IAPS FLIGHT TEST**

J. L. POWER (NASA, Lewis Research Center, Cleveland, OH) IN: International Electric Propulsion Conference, 17th, Tokyo, Japan, May 28-31, 1984, Proceedings . Tokyo, Japan Society for Aeronautical and Space Sciences, 1984, p. 266-285. Previously announced in STAR as N84-23691. refs

Preliminary ground correlation testing has been conducted with an 8 cm mercury ion thruster and diagnostic instrumentation replicating to a large extent the IAPS flight test hardware, configuration, and electrical grounding/isolation. Thruster efflux deposition retained at 25 C was measured and characterized. Thruster ion efflux was characterized with retarding potential analyzers. Thruster-generated plasma currents, the spacecraft common (SCC) potential, and ambient plasma properties were evaluated with a spacecraft potential probe (SPP). All the measured thruster/spacecraft interactions or their IAPS measurements depend critically on the SCC potential, which can be controlled by a neutralizer ground switch and by the SPP operation. Author

**A85-16412\*#** Hughes Research Labs., Malibu, Calif.

### **ION PROPULSION FOR COMMUNICATIONS SATELLITES**

R. L. POESCHEL (Hughes Research Laboratories, Malibu, CA) IN: International Electric Propulsion Conference, 17th, Tokyo, Japan, May 28-31, 1984, Proceedings . Tokyo, Japan Society for Aeronautical and Space Sciences, 1984, p. 306-313. refs (Contract NAS3-23258)

In a recent study of potential applications for electric propulsion, it was determined that ion propulsion can provide North-South stationkeeping (NSSK) for communication satellites in geosynchronous orbit with appreciably less mass than chemical propulsion. While this finding is not new, the margin of benefit over advanced chemical propulsion technology depends strongly on the ion propulsion system specifications. Full advantage must be taken of the under-utilized stored energy available from the communication satellite's batteries. This paper describes a methodology for evaluating the benefits obtained in using ion propulsion for NSSK, both in terms of the mass reduction and its economic value. Author

**A85-16438\*#** Hughes Research Labs., Malibu, Calif.

### **RING-CUSP ION THRUSTERS**

J. R. BEATTIE and R. L. POESCHEL (Hughes Research Laboratories, Malibu, CA) IN: International Electric Propulsion Conference, 17th, Tokyo, Japan, May 28-31, 1984, Proceedings . Tokyo, Japan Society for Aeronautical and Space Sciences, 1984, p. 496-505. refs (Contract NAS3-21943)

The high performance ion thruster technology presented is suitable for either geostationary satellite north-south stationkeeping or interplanetary spacecraft primary propulsion. The thruster

employs a ring-cusp magnetic field arrangement for plasma confinement, incurring an ion production cost which at about 100 eV/ion, is approximately half the value for the state-of-the-art J-series mercury ion thruster. A comparison of the average plasma properties existing within the ion-production volumes indicates that the improved performance of the ring-cusp configuration is due to higher electron temperature, confirming the superiority of this design in confining the energetic electrons emitted by the cathode. O.C.

**A85-16439\*#** National Aeronautics and Space Administration. Lewis Research Center, Cleveland, Ohio.

### **PERFORMANCE CAPABILITIES OF THE 12-CENTIMETER XENON ION THRUSTER**

M. MANTENIEKS and M. SCHATZ (NASA, Lewis Research Center, Cleveland, OH) IN: International Electric Propulsion Conference, 17th, Tokyo, Japan, May 28-31, 1984, Proceedings . Tokyo, Japan Society for Aeronautical and Space Sciences, 1984, p. 506-523. Previously announced in STAR as N84-27825. refs

The 8- and 12-cm mercury ion thruster systems were developed primarily to provide N-S station keeping of satellites with masses up to about 1800 to 3600 kg respectively. The on-orbit propulsion requirements of recently proposed Large Space Systems (LSS) are beyond the thrust capabilities of the baseline 8- and 12-cm thruster systems. This paper presents a characterization of the performance capabilities of the 12-cm Xenon ion thruster to enable an evaluation of its application to LSS auxiliary propulsion requirements. With minor thruster modifications and simplifications the thrust was increased to 64 mN, a factor of six over the baseline 12-cm mercury thruster performance. The thruster was operated over a range of specific impulse of about 2000 to 4000 seconds and at total efficiencies up to 68.0 percent. The operating levels reached in this study were found to be close to the operating limits of the thruster design in terms of perveance, grid breakdown voltage and thruster component temperatures such as those of the magnets and cathode baffle. Author

**A85-16440\*#** TRW, Inc., Redondo Beach, Calif.

### **ELECTROTHERMAL THRUSTER DIAGNOSTICS**

S. ZAFRAN (TRW, Inc., TRW Space and Technology Group, Redondo Beach, CA) IN: International Electric Propulsion Conference, 17th, Tokyo, Japan, May 28-31, 1984, Proceedings . Tokyo, Japan Society for Aeronautical and Space Sciences, 1984, p. 524-528. refs (Contract NAS3-23265)

A flight-qualified electrothermal thruster demonstrated its adaptability to a variety of propellants. Originally qualified for operation with hydrazine propellant, it was operated with nitrogen, hydrogen, and ammonia propellants, demonstrating 73, 61, and 52 percent overall efficiency with these propellants, respectively, when tested over a wide range of operating conditions. By introducing a preheater to admit hot, rather than cold, propellant inlet gases to the thruster's augmentation heat exchanger, delivered specific impulse closer to theoretical performance limits should be achieved. Author

**A85-16441\*#** Michigan State Univ., East Lansing.

### **EXPERIMENTS WITH A MICROWAVE ELECTROTHERMAL THRUSTER CONCEPT**

J. ASMUSSEN, S. WHITEHAIR (Michigan State University, East Lansing, MI), and S. NAKANISHI (NASA, Lewis Research Center, Cleveland, OH) IN: International Electric Propulsion Conference, 17th, Tokyo, Japan, May 28-31, 1984, Proceedings . Tokyo, Japan Society for Aeronautical and Space Sciences, 1984, p. 529-540. refs (Contract NAG3-305)

The design and test of two microwave electrothermal thrusters is described. The coaxial and cylindrical cavity concepts are tested in nitrogen gas with 200-2,000 W of 2.45 GHz input power. Experimental measurements and calculations of thrust, specific impulse and energy efficiency are presented for different gas flow rates and discharge pressures. Measured energy efficiencies varied between 10-60 percent and the performance compared favorably



with other electrothermal thrusters operating in nitrogen gas. The experimental performance demonstrated the feasibility of the concept. Author

**A85-16445\*** National Aeronautics and Space Administration. Lewis Research Center, Cleveland, Ohio.

**CATHODE DEGRADATION AND EROSION IN HIGH PRESSURE ARC DISCHARGES**

T. L. HARDY and S. NAKANISHI (NASA, Lewis Research Center, Cleveland, OH) IN: International Electric Propulsion Conference, 17th, Tokyo, Japan, May 28-31, 1984, Proceedings. Tokyo, Japan Society for Aeronautical and Space Sciences, 1984, p. 560-573. Previously announced in STAR as N84-22631. refs

The various processes which control cathode erosion and degradation were identified and evaluated. A direct current arc discharge was established between electrodes in a pressure-controlled gas flow environment. The cathode holder was designed for easy testing of various cathode materials. The anode was a water cooled copper collector electrode. The arc was powered by a dc power supply with current and voltage regulated cross-over control. Nitrogen and argon were used as propellants and the materials used were two percent thoriated tungsten, barium oxide impregnated porous tungsten, pure tungsten and lanthanum hexaboride. The configurations used were cylindrical solid rods, wire bundles supported by hollow molybdenum tubes, cylindrical hollow tubes, and hollow cathodes of the type used in ion thrusters. The results of the mass loss tests in nitrogen indicated that pure tungsten eroded at a rate more than 10 times faster than the rates of the impregnated tungsten materials. It was found that oxygen impurities of less than 0.5 percent in the nitrogen increased the mass loss rate by a factor of 4 over high purity nitrogen. At power levels less than 1 kW, cathode size and current level did not significantly affect the mass loss rate. The hollow cathode was found to be operable in argon and in nitrogen only at pressures below 400 and 200 torr, respectively. M.A.C.

**A85-18584\*** Hughes Aircraft Co., El Segundo, Calif.  
**ENVIRONMENTALLY-INDUCED VOLTAGE LIMITATIONS IN LARGE SPACE POWER SYSTEMS**

N. J. STEVENS (Hughes Aircraft Co., El Segundo, CA) (IEEE, U.S. Defense Nuclear Agency, U.S. Department of Energy, and NASA, Annual Conference on Nuclear and Space Radiation Effects, 21st, Colorado Springs, CO, July 23-25, 1984) IEEE Transactions on Nuclear Science (ISSN 0018-9499), vol. NS-31, Dec. 1984, p. 1381-1386. refs

(Contract NAS3-23869)

Large power systems proposed for future space missions imply higher operating voltage requirements which, in turn, will interact with the space plasma environment. The effects of these interactions can only be inferred because of the limited data base of ground simulations, small test samples, and two space flight experiments. This report evaluates floating potentials for a 100 kW power system operating at 300, 500, 750, and 1000 volts in relation to this data base. Of primary concern is the possibility of discharging to space. The implications of such discharges were studied at the 500 volt operational setting. It was found that discharging can shut down the power system if the discharge current exceeds the array short circuit current. Otherwise, a power oscillation can result that ranges from 2 to 20 percent, depending upon the solar array area involved in the discharge. Means of reducing the effect are discussed. Author

**A85-19713\*** National Aeronautics and Space Administration. Lewis Research Center, Cleveland, Ohio.

**THE EFFECT OF PLASMA ON SOLAR CELL ARRAY ARC CHARACTERISTICS**

D. B. SNYDER (NASA, Lewis Research Center, Cleveland, OH) and E. TYREE (NASA, Lewis Research Center; Case Western Reserve University, Cleveland, OH) American Institute of Aeronautics and Astronautics, Aerospace Sciences Meeting, 23rd, Reno, NV, Jan. 14-17, 1985. 10 p. Previously announced in STAR as N85-11133. refs

(AIAA PAPER 85-0384)

The influence from the ambient plasma on the arc characteristics of a negatively biased solar cell array was investigated. The arc characteristics examined were the peak current during an arc, the decay time as the arc terminates, and the charge lost during the arc. These arc characteristics were examined in a nitrogen plasma with charge densities ranging from 15,000 to 45,000 cu cm. Background gas pressures ranged from 8x1,000,000 to 6x100,000 torr. Over these ranges of parameters no significant effect on the arc characteristics were seen. Arc characteristics were also examined for three gas species: helium, nitrogen and argon. The helium arcs have higher peak currents and shorter decay times than nitrogen and argon arcs. There are slight differences in the arc characteristics between nitrogen and argon. These differences may be caused by the differences in mass of the respective species. Also, evidence is presented for an electron emission mechanism appearing as a precursor to solar array arcs. Occasionally the plasma generator could be turned off, and currents could still be detected in the vacuum system. When these currents are presented, arcs may occur. Author

**A85-19715\*** System Science and Software, San Diego, Calif.  
**COMPUTER SIMULATION OF PLASMA ELECTRON COLLECTION BY PIX-II**

M. J. MANDELL, I. KATZ, G. A. JONGEWARD (System Science and Software, La Jolla, CA), and J. C. ROCHE (NASA, Lewis Research Center, Cleveland, OH) American Institute of Aeronautics and Astronautics, Aerospace Sciences Meeting, 23rd, Reno, NV, Jan. 14-17, 1985. 9 p. refs

(Contract NAS3-23881)

(AIAA PAPER 85-0386)

A wake model was defined for the NASCAP/LEO finite element model for the plasma interaction experiment (PIX-II) launched to study the interaction between high-voltage large solar arrays with the space plasma environment. The cell surface model considers the individual cells, distances between interconnects, and the fraction of surface covered by interconnects. Account is taken of the electrostatic potential around the spacecraft, which travels at 7500 mps, over five times the speed of thermal ions. Ram ions are produced ahead of the array and the wake ion density is described with a geometric shadowing model. The model correctly predicted the currents in high and low bias voltages when compared to orbital data. The panel snapover, however, was projected to occur at 100 V and instead occurred at 300 V, which indicates that the snapover state is bistable. Finally, a low potential was both predicted and measured in the wake. M.S.K.

**A85-29310\*** Loral Electro-Optical Systems, Inc., Pasadena, Calif.

**INERT GAS TEST OF TWO 12-CM MAGNETOSTATIC THRUSTERS**

W. D. RAMSEY (Loral Corp., Pasadena, CA) Journal of Spacecraft and Rockets (ISSN 0022-4650), vol. 22, Mar.-Apr. 1985, p. 162-165. Previously cited in issue 02, p. 145, Accession no. A83-12494. refs

(Contract NAS3-22876)

## 20 SPACECRAFT PROPULSION AND POWER

**A85-29314\*#** O'Donnell and Associates, Inc., Pittsburgh, Pa.  
**SIMPLIFIED DESIGN AND LIFE PREDICTION OF ROCKET THRUST CHAMBERS**

J. S. POROWSKI, W. J. O'DONNELL, M. L. BADLANI, B. KASRAIE, and H. J. KASPER. *Journal of Spacecraft and Rockets* (ISSN 0022-4650), vol. 22, Mar.-Apr. 1985, p. 181-187. Previously cited in issue 17, p. 2708, Accession no. A82-35087. refs

**A85-33144\*** Wisconsin Univ., Madison.  
**A ROTATING SUPERCONDUCTING SOLENOID FOR 100 KWH ENERGY STORAGE**

J. WAYNERT, Y. M. EYSSA, G. E. MCINTOSH, and Z. FENG (Wisconsin, University, Madison, WI) *IEEE Transactions on Magnetics* (ISSN 0018-9464), vol. MAG-21, March 1985, p. 664-667. refs  
(Contract NAG3-359)

Two concentric superconducting solenoids, one rotating, the other stationary are analyzed for energy storage in space. Energy is transferred from the rotating mass through a shaft coupled to a motor-generator. The inner windings interact with the magnetic field of the outer solenoid to cancel the centrifugal and self-field forces of the flywheel rim. Current is induced in the inner solenoid thus requiring no separate power supply, while the current in the outer solenoid must vary with the angular velocity of the flywheel. The effect of the gap and scaling laws are developed. The efficiency in energy per unit mass is marginally attractive. Author

**A85-39267\*** Rockwell International Corp., Canoga Park, Calif.  
**REUSABLE ROCKET ENGINE TURBOPUMP CONDITION MONITORING**

M. E. HAMPSON (Rockwell International Corp., Rocketdyne Div., Canoga Park, CA) IN: *Space systems technology; Proceedings of the Aerospace Congress and Exposition, Long Beach, CA, October 15-18, 1984*. Warrendale, PA, Society of Automotive Engineers, Inc. (SAE SP-593), 1984, p. 157-165.  
(Contract NAS3-23349)  
(SAE PAPER 841619)

Significant improvements in engine readiness with reductions in maintenance costs and turn-around times can be achieved with an engine condition monitoring systems (CMS). The CMS provides health status of critical engine components, without disassembly, through monitoring with advanced sensors. Engine failure reports over 35 years were categorized into 20 different modes of failure. Rotor bearings and turbine blades were determined to be the most critical in limiting turbopump life. Measurement technologies were matched to each of the failure modes identified. Three were selected to monitor the rotor bearings and turbine blades: the isotope wear detector and fiberoptic deflectometer (bearings), and the fiberoptic pyrometer (blades). Signal processing algorithms were evaluated for their ability to provide useful health data to maintenance personnel. Design modifications to the Space Shuttle Main Engine (SSME) high pressure turbopumps were developed to incorporate the sensors. Laboratory test fixtures have been designed for monitoring the rotor bearings and turbine blades in simulated turbopump operating conditions. Author

**A85-39626\*#** National Aeronautics and Space Administration.  
Lewis Research Center, Cleveland, Ohio.

**SPACE STATION PROPULSION - THE ADVANCED DEVELOPMENT PROGRAM AT LEWIS**

R. E. JONES (NASA, Lewis Research Center, Cleveland, OH) AIAA, SAE, ASME, and ASEE, Joint Propulsion Conference, 21st, Monterey, CA, July 8-10, 1985. 9 p. Previously announced in STAR as N85-25386.  
(AIAA PAPER 85-1154)

A reference configuration was established for the initial operating capability (IOC) station. The reference configuration has assumed hydrazine fueled thrusters as the propulsion system. This was to establish costing and as a reference for comparison when other propulsion systems are considered. An integral part of the plan to develop the Space Station is the advanced development program. The objective of this program is to provide advanced technology alternatives for the initial and evolutionary Space Station

which optimize the system's functional characteristics in terms of performance, cost, and utilization. The portion of the Advanced Development Program that is concerned with auxiliary propulsion and the research and programmatic activities conducted are discussed. E.A.K.

**A85-39628\*#** Rocket Research Corp., Redmond, Wash.  
**PERFORMANCE CHARACTERIZATION TESTS OF A 1-KW RESISTOJET USING HYDROGEN, NITROGEN AND AMMONIA AS PROPELLANTS**

C. I. MIYAKE and F. X. MCKEVITT (Rocket Research Co., Redmond, WA) AIAA, SAE, ASME, and ASEE, Joint Propulsion Conference, 21st, Monterey, CA, July 8-10, 1985. 8 p. refs  
(Contract NAS3-23868)  
(AIAA PAPER 85-1159)

A performance mapping test of a 1 kW radiatively heated resistojet demonstrated high specific impulse and efficiency with hydrogen, nitrogen and ammonia as propellants. The resistojet was based on an unmodified augmentation section of the flight-qualified Rocket Research Company Augmented Catalytic Thruster. Peak specific impulse values of 686.9 sec for hydrogen, 191.6 sec for nitrogen, and 342 sec for ammonia were demonstrated. A maximum specific impulse efficiency of 94.3 percent was demonstrated with hydrogen. Testing covered a thrust range of 27 to 112 mlbf with augmentation powers ranging from 300 to 1000 watts. A total of 83 runs accumulating 25 hours of operation were conducted with the three propellants. Comparison of specific impulse efficiency to other published resistojet performance data showed the radiatively heated resistojet compares favorably to other design concepts. Author

**A85-39733\*#** Rockwell International Corp., Canoga Park, Calif.  
**CRYOGENIC UPPER STAGE TEST BED ENGINE**

R. PAUCKERT, A. ZACHARY, E. DEGAETANO, and R. SUTTON (Rockwell International Corp., Rocketdyne Div., Canoga Park, CA) AIAA, SAE, ASME, and ASEE, Joint Propulsion Conference, 21st, Monterey, CA, July 8-10, 1985. 11 p.  
(Contract NAS3-23773)  
(AIAA PAPER 85-1339)

A vehicle system with unique characteristics will be needed in connection with the extension of the Space Transportation System (STS) from Low Earth Orbit (LEO) to Geosynchronous Equatorial Orbit (GEO) and beyond. These characteristics are determined by NASA missions related to the deployment of large space structures, satellite servicing, and manned sorties to geosynchronous orbit. Advances in vehicle design and operation will be required along with significant advances in engine technologies. A versatile, well-instrumented test bed engine will be needed for the evaluation of the required technologies. Developments leading to the fabrication and assembly of the first high chamber pressure expander cycle test bed engine are discussed. The test bed engine, which is called Integrated Component Evaluator (ICE), is required for the development of an advanced, cryogenic, upperstage engine. G.R.

**A85-39735\*#** Aerojet Techsystems Co., Sacramento, Calif.  
**PROGRESS REPORT - ADVANCED CRYOGENIC OTV ENGINE TECHNOLOGY**

L. SCHOENMAN (Aerojet TechSystems Co., Sacramento, CA) AIAA, SAE, ASME, and ASEE, Joint Propulsion Conference, 21st, Monterey, CA, July 8-10, 1985. 11 p. refs  
(Contract NAS3-23772)  
(AIAA PAPER 85-1341)

New technologies for space-based, reusable, throttleable, cryogenic orbit transfer propulsion are being evaluated. A variable-thrust (200 to 3000 lbf), 2000 psi chamber pressure, LO2/LH2 engine has been selected to demonstrate the 20-hour, 500-restart life goal, and a specific impulse in excess of 480 lbf-sec/lbm. The results of recent vehicle-engine integration analyses and the progress in design, fabrication, and testing are provided. Emphasis is placed on the following technology areas being investigated in support of the advanced engine design: LOX hydrostatic bearings; burn-resistant materials for high-pressure GOX

turbines and valves; high surface-low flux annular combustion chambers for the dual propellant expander cycle; improved cooling approaches for high-pressure combustion chambers, new concepts in integrated controls; and engine health diagnostics. Author

**A85-42922\*** # Xerox Electro-Optical Systems, Pasadena, Calif.  
**DEVELOPMENT OF A LARGE INSERT GAS ION THRUSTER**  
 G. STEINER (Xerox Electro-Optical Systems, Pasadena, CA) Journal of Spacecraft and Rockets (ISSN 0022-4650), vol. 22, July-Aug. 1985, p. 465-468. Previously cited in issue 02, p. 146, Accession no. A83-12496. refs  
 (Contract NAS3-22444)

**A85-43975\*** # Boeing Aerospace Co., Seattle, Wash.  
**SPACE STATION PROPULSION OPTIONS**  
 C. L. WILKINSON, S. M. BRENNAN (Boeing Aerospace Co., Seattle, WA), and M. E. VALGORA (NASA, Lewis Research Center, Cleveland, OH) AIAA, SAE, ASME, and ASEE, Joint Propulsion Conference, 21st, Monterey, CA, July 8-10, 1985. 9 p. refs  
 (Contract NAS3-23353)  
 (AIAA PAPER 85-1155)

The selection of the propulsion system for the Space Station represents a complex issue. The present paper provides a summary of the Station design factors which dictate the propulsion requirements, taking into account approaches for meeting these requirements. Factors which affect propulsion system selection are related to thrusting strategy, volume and mass limitations, safety and contamination, electrical power, time phasing, synergistic opportunities, propellant scavenging, water electrolysis, and free-flyers. In a discussion of propulsion systems, attention is given to monopropellant options, bipropellant options, and resistojets.

G.R.

**A85-43976\*** # Jet Propulsion Lab., California Inst. of Tech., Pasadena.  
**AN EVALUATION OF OXYGEN/HYDROGEN PROPULSION SYSTEMS FOR THE SPACE STATION**  
 R. W. KLEMETSON, P. W. GARRISON (California Institute of Technology, Jet Propulsion Laboratory, Pasadena), and N. P. HANNUM (NASA, Lewis Research Center, Cleveland, OH) AIAA, SAE, ASME, and ASEE, Joint Propulsion Conference, 21st, Monterey, CA, July 8-10, 1985. 27 p. NASA-supported research. Previously announced in STAR as N85-28971. refs  
 (AIAA PAPER 85-1156)

Conceptual designs for O<sub>2</sub>/H<sub>2</sub> chemical and resistojets propulsion systems for the Space Station was developed and evaluated. The evolution of propulsion requirements was considered as the Space Station configuration and its utilization as a space transportation node change over the first decade of operation. The characteristics of candidate O<sub>2</sub>/H<sub>2</sub> auxiliary propulsion systems are determined, and opportunities for integration with the OTV tank farm and the Space Station life support, power and thermal control subsystems are investigated. OTV tank farm boiloff can provide a major portion of the growth station impulse requirements and CO<sub>2</sub> from the life support system can be a significant propellant resource, provided it is not denied by closure of that subsystem. Waste heat from the thermal control system is sufficient for many propellant conditioning requirements. It is concluded that the optimum level of subsystem integration must be based on higher level Space Station studies. Author

**A85-43978\*** # Rockwell International Corp., Canoga Park, Calif.  
**SMALL CENTRIFUGAL PUMPS FOR LOW THRUST ROCKETS**  
 N. C. GULBRANDSEN, R. B. FURST, R. M. BURGESS (Rockwell International Corp., Rocketdyne Div., Canoga Park, CA), and D. D. SCHEER (NASA, Lewis Research Center, Cleveland, OH) AIAA, SAE, ASME, and ASEE, Joint Propulsion Conference, 21st, Monterey, CA, July 8-10, 1985. 12 p.  
 (Contract NAS3-23164)  
 (AIAA PAPER 85-1302)

This paper presents the results of a combined analytical and experimental investigation of low specific speed pumps for potential use as components of propellant feed systems for low thrust rocket

engines. Shrouded impellers and open face impellers were tested in volute type and vaned diffuser type pumps. Full- and partial-emission diffusers and full- and partial-admission impellers were tested. Axial and radial loads, head and efficiency versus flow, and cavitation tests were conducted. Predicted performance of two pumps are compared when pumping water and liquid hydrogen. Detailed pressure loss and parasitic power values are presented for two pump configurations. Partial-emission diffusers were found to permit use of larger impeller and diffuser passages with a minimal performance penalty. Normal manufacturing tolerances were found to result in substantial power requirement variation with only a small pressure rise change. Impeller wear ring leakage was found to reduce pump pressure rise to an increasing degree as the pump flowrate was decreased. Author

**A85-45370\*** National Aeronautics and Space Administration. Lewis Research Center, Cleveland, Ohio.  
**HIGH VOLTAGE-HIGH POWER COMPONENTS FOR LARGE SPACE POWER DISTRIBUTION SYSTEMS**

D. D. RENZ (NASA, Lewis Research Center, Cleveland, OH) IN: IECEC '84: Advanced energy systems - Their role in our future; Proceedings of the Nineteenth Intersociety Energy Conversion Engineering Conference, San Francisco, CA, August 19-24, 1984. Volume 1. La Grange Park, IL, American Nuclear Society, 1984, p. 176-184. Previously announced in STAR as N84-22615. refs

Space power components including a family of bipolar power switching transistors, fast switching power diodes, heat pipe cooled high frequency transformers and inductors, high frequency conduction cooled transformers, high power-high frequency capacitors, remote power controllers and rotary power transfer devices were developed. Many of these components such as the power switching transistors, power diodes and the high frequency capacitor are commercially available. All the other components were developed to the prototype level. The dc/dc series resonant converters were built to the 25 kW level. S.L.

**A85-45371\*** National Aeronautics and Space Administration. Lewis Research Center, Cleveland, Ohio.  
**PRELIMINARY DESIGN OF A 10 KW THERMOPHOTOVOLTAIC SYSTEM FOR SPACE APPLICATIONS**

M. F. PISZCZOR, JR. (NASA, Lewis Research Center, Cleveland, OH) and M. GHALLA-GORADIA (Cleveland State University, OH) IN: IECEC '84: Advanced energy systems - Their role in our future; Proceedings of the Nineteenth Intersociety Energy Conversion Engineering Conference, San Francisco, CA, August 19-24, 1984. Volume 1. La Grange Park, IL, American Nuclear Society, 1984, p. 185-190. Previously announced in STAR as N84-32427. refs

A very high degree of reflection of sub-bandgap energy photons from the cell back to the emitter was found to be crucial in achieving high efficiencies for a TPV system. Results show that small increases in reflectance above 0.85 lead to progressively larger increases in cell efficiency. In general, for a required power output, the radiator area, emitter temperature, emitter material and cell temperature may be chosen to satisfy various external constraints. The results can then be used to determine the optimum cell material and its operating temperature. Author

**A85-45377\*** Chronos Research Labs., Inc., Olivehain, Calif.  
**PYROELECTRIC CONVERSION IN SPACE**

R. B. OLSEN (Chronos Research Laboratories, Inc., Olivehain, CA) IN: IECEC '84: Advanced energy systems - Their role in our future; Proceedings of the Nineteenth Intersociety Energy Conversion Engineering Conference, San Francisco, CA, August 19-24, 1984. Volume 1. La Grange Park, IL, American Nuclear Society, 1984, p. 224-228. refs  
 (Contract NAS3-23052)

Pyroelectric conversion in space deserves a close look as preliminary calculations indicate that a system specific power of 350 to 850 watts per kilogram will be feasible. This power-to-weight ratio far exceeds state-of-the-art photovoltaic systems (40 to 66 watts/kg) and surpasses proposed thin blanket photovoltaics (about 300 watts/kg). In addition to its high specific power, the pyroelectric

## 20 SPACECRAFT PROPULSION AND POWER

approach promises to be far less expensive than photovoltaics.

Author

**A85-45387\*** National Aeronautics and Space Administration. Lewis Research Center, Cleveland, Ohio.

### **A 37.5-KW POINT DESIGN COMPARISON OF THE NICKEL-CADMIUM BATTERY, BIPOLAR NICKEL-HYDROGEN BATTERY, AND REGENERATIVE HYDROGEN-OXYGEN FUEL CELL ENERGY STORAGE SUBSYSTEMS FOR LOW EARTH ORBIT**

M. A. MANZO and M. A. HOBERECHT (NASA, Lewis Research Center, Cleveland, OH) IN: IECEC '84: Advanced energy systems - Their role in our future; Proceedings of the Nineteenth Intersociety Energy Conversion Engineering Conference, San Francisco, CA, August 19-24, 1984. Volume 1. La Grange Park, IL, American Nuclear Society, 1984, p. 287-294. Previously announced in STAR as N84-23022.

Nickel-cadmium batteries, bipolar nickel-hydrogen batteries, and regenerative fuel cell storage subsystems were evaluated for use as the storage subsystem in a 37.5 kW power system for Space Station. Design requirements were set in order to establish a common baseline for comparison purposes. The storage subsystems were compared on the basis of effective energy density, round trip electrical efficiency, total subsystem weight and volume, and life.

Author

**A85-45388\*** National Aeronautics and Space Administration. Lewis Research Center, Cleveland, Ohio.

### **DILUTE PLASMA COUPLING CURRENTS TO A HIGH VOLTAGE SOLAR ARRAY IN WEAK MAGNETIC FIELDS**

N. T. GRIER (NASA, Lewis Research Center, Cleveland, OH) IN: IECEC '84: Advanced energy systems - Their role in our future; Proceedings of the Nineteenth Intersociety Energy Conversion Engineering Conference, San Francisco, CA, August 19-24, 1984. Volume 1. La Grange Park, IL, American Nuclear Society, 1984, p. 295-302. Previously announced in STAR as N84-24708. refs

The plasma coupling current to an approximately 2000 sq cm array was measured for externally biased positive and negative voltages on the array to 1000 V in applied magnetic field strengths from 0 to 0.93 G. The plasma density varied from 2,000 to 1.3 million electrons/cu cm. It was found that the magnetic field primarily increased the plasma coupling current for negative biases. For positive bias, the current could increase or decrease depending on the voltage, field strength, and plasma density. It was also found that the plasma coupling current was not very sensitive to how the plane of the array was oriented relative to the magnetic field.

Author

**A85-45429\*** Boeing Aerospace Co., Seattle, Wash. **HIGH VOLTAGE REQUIREMENTS AND ISSUES FOR THE 1990'S**

W. G. DUNBAR (Boeing Aerospace Co., Seattle, WA) and K. A. FAYMON (NASA, Lewis Research Center, Cleveland, OH) IN: IECEC '84: Advanced energy systems - Their role in our future; Proceedings of the Nineteenth Intersociety Energy Conversion Engineering Conference, San Francisco, CA, August 19-24, 1984. Volume 1. La Grange Park, IL, American Nuclear Society, 1984, p. 570-575. refs

The development of high-power high-voltage space systems will require advances in power generation and processing. The systems must be reliable, adaptable, and durable for space mission success. The issues, which must be resolved in order to produce a high power system, are weight and volume reduction of components and modules and the creation of a reliable high repetition pulse power processor. Capacitor energy density must be increased by twice the present capacity and packaging must be reduced by a factor of 10 to 20 times. The packaging must also protect the system from interaction with the natural space environment and the induced environment, produced from spacecraft systems and environment interaction.

I.F.

**A85-47042\*#** National Aeronautics and Space Administration. Lewis Research Center, Cleveland, Ohio.

### **ELECTRIC POWER - PHOTOVOLTAIC OR SOLAR DYNAMIC?**

R. L. THOMAS (NASA, Lewis Research Center, Cleveland, OH), G. J. HALLINAN (Rockwell International Corp., Rocketdyne Div., Canoga Park, CA), and J. L. HIEATT (TRW, Inc., TRW Space and Technology Group, Redondo Beach, CA) Aerospace America (ISSN 0740-722X), vol. 23, Sept. 1985, p. 60-62.

The design of the power system for supplying the Space Station with insolation-generated electricity is the main Phase B task at NASA-Lewis Center. The advantages and limitations of two types of power systems, the photovoltaic arrays (PV) and the solar dynamic system (SD), are discussed from the points of view of cost, overall systems integration, and growth. Subsystems of each of these options are described, and a sketch of a projected SD system is shown. The PV technology is well developed and proven, but its low efficiency calls for solar arrays of large areas, which affect station dynamics, control, and drag compensation. The SD systems would be less costly to operate than PV, and are more efficient, needing less deployed area. The major drawback of the SD is its infancy. The conservative and forgiving designs for some of its components must still be created and tested, and the development risks assessed.

I.S.

**N85-11131\*#** Hughes Research Labs., Malibu, Calif. **CHARACTERIZATION OF 8-CM ENGINEERING MODEL THRUSTER Final Report, 12 Apr. 1978 - 12 Sep. 1982**

W. S. WILLIAMSON Mar. 1984 87 p  
(Contract NAS3-21358; NAS3-21036)  
(NASA-CR-174673; NAS 1.26:174673) Avail: NTIS HC A05/MF A01 CSCL 21C

Development of 8 cm ion thruster technology which was conducted in support of the Ion Auxiliary Propulsion System (IAPS) flight contract (Contract NAS3-21055) is discussed. The work included characterization of thruster performance, stability, and control; a study of the effects of cathode aging; environmental qualification testing; and cyclic lifetesting of especially critical thruster components.

R.J.F.

**N85-11132\*#** GT-Devices, Alexandria, Va. **INVESTIGATION OF A PULSED ELECTROTHERMAL THRUSTER SYSTEM**

R. L. BURTON, S. A. GOLDSTEIN, B. K. HILKO, D. A. TIDMAN, and N. K. WINSOR 31 Oct. 1984 64 p refs  
(Contract NAS3-23866)  
(NASA-CR-174768; NAS 1.26:174768; GTD-84-4) Avail: NTIS HC A04/MF A01 CSCL 21C

The performance of an ablative wall Pulsed Electrothermal (PET) thruster is accurately characterized on a calibrated thrust stand, using polyethylene propellant. The thruster is tested for four configurations of capillary length and pulse length. The exhaust velocity is determined with twin time-of-flight photodiode stagnation probes, and the ablated mass is measured from the loss over ten shots. Based on the measured thrust impulse and the ablated mass, the specific impulse varies from 1000 to 1750 seconds. The thrust to power varies from .05 N/kW (quasi-steady mode) to .10 N/kW (unsteady mode). The thruster efficiency varies from .56 at 1000 seconds to .42 at 1750 seconds. A conceptual design is presented for a 40 kW PET propulsion system. The point design system performance is .62 system efficiency at 1000 seconds specific impulse. The system's reliability is enhanced by incorporating 20, 20 kW thruster modules which are fired in pairs. The thruster design is non-ablative, and uses water propellant, from a central storage tank, injected through the cathode.

M.A.C.

**N85-11133\*#** National Aeronautics and Space Administration. Lewis Research Center, Cleveland, Ohio.

### **THE EFFECT OF PLASMA ON SOLAR CELL ARRAY ARC CHARACTERISTICS**

D. B. SNYDER and E. TYREE 1984 17 p refs Proposed for presentation at the 23rd Aerospace Sci. Meeting, Reno, Nev., 14-17 Jan. 1985; sponsored by the American Inst. of Aeronautics and Astronautics Previously announced in IAA as A85-19713 (NASA-TM-86887; E-2351; NAS 1.15:86887) Avail: NTIS HC A02/MF A01 CSCL 10A

The influence from the ambient plasma on the arc characteristics of a negatively biased solar cell array was investigated. The arc characteristics examined were the peak current during an arc, the decay time as the arc terminates, and the charge lost during the arc. These arc characteristics were examined in a nitrogen plasma with charge densities ranging from 15,000 to 45,000 cu cm. Background gas pressures ranged from 8x1,000,000 to 6x100,000 torr. Over these ranges of parameters no significant effect on the arc characteristics were seen. Arc characteristics were also examined for three gas species: helium, nitrogen and argon. The helium arcs have higher peak currents and shorter decay times than nitrogen and argon arcs. There are slight differences in the arc characteristics between nitrogen and argon. These differences may be caused by the differences in mass of the respective species. Also, evidence is presented for an electron emission mechanism appearing as a precursor to solar array arcs. Occasionally the plasma generator could be turned off, and currents could still be detected in the vacuum system. When these currents are presented, arcs may occur. Author

**N85-12937\*#** Hughes Research Labs., Malibu, Calif.  
**ION THRUSTER SYSTEM (8-CM) CYCLIC ENDURANCE TEST Final Report, 20 Sep. 1978 - 31 Jan. 1984**

C. R. DULGEROFF, J. R. BEATTIE, R. L. POESCHEL, and J. HYMAN, JR. Oct. 1984 138 p refs (Contract NAS3-21741) (NASA-CR-174745; NAS 1.26:174745) Avail: NTIS HC A07/MF A01 CSCL 21C

This report describes the qualification test of an Engineering-Model 5-mN-thrust 8-cm-diameter mercury ion thruster which is representative of the Ion Auxiliary Propulsion System (IAPS) thrusters. Two of these thrusters are scheduled for future flight test. The cyclic endurance test described herein was a ground-based test performed in a vacuum facility with a liquid-nitrogen-cooled cryo-surface and a frozen mercury target. The Power Electronics Unit, Beam Shield, Gimal, and Propellant Tank that were used with the thruster in the endurance test are also similar to those of the IAPS. The IAPS thruster that will undergo the longest beam-on-time during the actual space test will be subjected to 7,055 hours of beam-on-time and 2,557 cycles during the flight test. The endurance test was successfully concluded when the mercury in the IAPS Propellant Tank was consumed. At that time, 8,471 hours of beam-on-time and 599 cycles had been accumulated. Subsequent post-test-evaluation operations were performed (without breaking vacuum) which extended the test values to 652 cycles and 9,489 hours of beam-on-time. The Power Electronic Unit (PEU) and thruster were in the same vacuum chamber throughout the test. The PEU accumulated 10,268 hr of test time with high voltage applied to the operating thruster or dummy load. Author

**N85-13877\*#** National Aeronautics and Space Administration. Lewis Research Center, Cleveland, Ohio.

### **DEVELOPMENTS IN SPACE POWER COMPONENTS FOR POWER MANAGEMENT AND DISTRIBUTION**

D. D. RENZ /n NASA. Langley Research Center An Assessment of Integrated Flywheel System Technol. p 369-387 Nov. 1984 refs

Avail: NTIS HC A18/MF A01 CSCL 10B

Advanced power electronic components development for space applications is discussed. The components described include transformers, inductors, semiconductor devices such as transistors

and diodes, remote power controllers, and transmission lines.

M.G.

**N85-13880\*#** National Aeronautics and Space Administration. Lewis Research Center, Cleveland, Ohio.

### **SPACE POWER**

Washington Apr. 1984 322 p refs Workshop held in Cleveland, 10-12 Apr. 1984 (NASA-CP-2352; E-2305; NAS 1.55:2352) Avail: NTIS HC A14/MF A01 CSCL 22B

Appropriate directions for the applied research and technology programs that will develop space power systems for U.S. future space missions beyond 1995 are explored. Spacecraft power supplies; space stations, space power reactors, solar arrays, thermoelectric generators, energy storage, and communication satellites are among the topics discussed.

**N85-13910\*#** Cleveland State Univ., Ohio. Coll. of Engineering.  
**A HISTORICAL OVERVIEW OF THE ELECTRICAL POWER SYSTEMS IN THE US MANNED AND SOME US UNMANNED SPACECRAFT Final Report, Apr. 1984 - Jan. 1985**

J. E. MAISEL Nov. 1984 158 p refs (Contract NAG3-547) (NASA-CR-174806; NAS 1.26:174806; MAI-R4) Avail: NTIS HC A08/MF A01 CSCL 22B

A historical overview of electrical power systems used in the U.S. manned spacecraft and some of the U.S. unmanned spacecraft is presented in this investigation. A time frame of approximately 25 years, the period for 1959 to 1984, is covered in this report. Results indicate that the nominal bus voltage was 28 volts dc in most spacecraft and all other voltage levels were derived from this voltage through such techniques as voltage inversion or rectification, or a combination. Most spacecraft used solar arrays for the main source of power except for those spacecraft that had a relatively short flight duration, or deep space probes that were designed for very long flight duration. Fuel cells were used on Gemini, Apollo, and Space Shuttle (short duration flights) while radioisotope thermoelectric generators were employed on the Pioneer, Jupiter/Saturn, Viking Lander, and Voyager spacecraft (long duration flights). The main dc bus voltage was unregulated on the manned spacecraft with voltage regulation provided at the user loads. A combination of regulated, semiregulated, and unregulated buses were used on the unmanned spacecraft depending on the type of load. For example, scientific instruments were usually connected to regulated buses while fans, relays, etc. were energized from an unregulated bus. Different forms of voltage regulation, such as shunt, buck/boot, and pulse-width modulated regulators, were used. This report includes a comprehensive bibliography on spacecraft electrical power systems for the space programs investigated. Author

**N85-15804\*#** Little (Arthur D.), Inc., Cambridge, Mass.  
**PRELIMINARY EVALUATION OF A LIQUID BELT RADIATOR FOR SPACE APPLICATIONS Final Report**

W. P. TEAGAN and K. FITZGERALD Dec. 1984 180 p refs (Contract NAS3-22253) (NASA-CR-174807; NAS 1.26:174807) Avail: NTIS HC A09/MF A01 CSCL 10B

The liquid belt radiator (LBR) is discussed. The LBR system operates either in the sensible heat mode or in the latent heat mode. Parametric analysis shows that the LBR may reduce the mass of heat pipe radiators by 70 to 90% when the LBR surface has a total emissivity in excess of 0.3. It is indicated that the diffusion pump oils easily meet this criteria with emissivities greater than 0.8. Measurements on gallium indicate that its emissivity is probably in excess of 0.3 in the solid state when small amounts of impurities are on the surface. The point design exhibits a characteristic mass of 3.1 kg/kW of power dissipation, a mass per unit prime radiating area of approximately 0.9 kg/sq m and a total package volume of approximately 2.50 cubic m. This compares favorably with conventional technologies which have weights on the order of 4 kg/sq m. E.A.K.

## 20 SPACECRAFT PROPULSION AND POWER

**N85-15806\*#** Hughes Research Labs., Malibu, Calif.  
**EXTENDED PERFORMANCE TECHNOLOGY STUDY 30-CM THRUSTER Final Report, 26 Jun. 1979 - 26 Oct. 1982**

J. R. BEATTIE Jun. 1983 201 p refs

(Contract NAS3-21943)

(NASA-CR-168259; NAS 1.26:168259) Avail: NTIS HC A10/MF A01 CSCL 21C

The extended performance technology study was an investigation of advanced discharge chambers and thruster components that were designed to operate under conditions which result in an increase in the thrust and thrust to power ratio of the state of the art J-series thruster. The high level of performance was achieved by a discharge chamber that employs a ring cusp magnetic confinement arrangement and a three grid ion extraction assembly. It is shown that the ring cusp magnetic field geometry confines the plasma to the volume immediately adjacent to the ion extraction assembly. A high emission current hollow cathode that demonstrated operation at an emission current as high as J sub E = 40 A, and measurements which show the breakdown voltage of individual sections of the J-series propellant flow electrical isolator is about 340 V per section are investigated.

E.A.K.

**N85-17023\*#** TRW Space Technology Labs., Redondo Beach, Calif. Energy Technology Div.

**HIGH FREQUENCY PLASMA GENERATOR FOR ION THRUSTERS Final Report, Sep. 1980 - Apr. 1983**

H. GOEDE, W. F. DIVERGILIO, V. V. FOSNIGHT, and G. KOMATSU Jul. 1984 74 p refs

(Contract NAS3-22473)

(NASA-CR-174772; NAS 1.26:174772) Avail: NTIS HC A04/MF A01 CSCL 21C

The results of a program to experimentally develop two new types of plasma generators for 30 cm electrostatic argon ion thrusters are presented. The two plasma generating methods selected for this study were by radio frequency induction (RFI), operating at an input power frequency of 1 MHz, and by electron cyclotron heating (ECH) at an operating frequency of 5.0 GHz. Both of these generators utilize multiline cusp permanent magnet configurations for plasma confinement and beam profile optimization. The program goals were to develop a plasma generator possessing the characteristics of high electrical efficiency (low eV/ion) and simplicity of operation while maintaining the reliability and durability of the conventional hollow cathode plasma sources. The RFI plasma generator has achieved minimum discharge losses of 120 eV/ion while the ECH generator has obtained 145 eV/ion, assuming a 90% ion optical transparency of the electrostatic acceleration system. Details of experimental tests with a variety of magnet configurations are presented. Author

**N85-18084\*#** Creare, Inc., Hanover, N.H.

**ANALYTICAL AND EXPERIMENTAL INVESTIGATION OF RUBBING INTERACTION IN LABYRINTH SEALS FOR A LIQUID HYDROGEN FUEL PUMP Final Report**

F. X. DOLAN, F. E. KENNEDY, and E. M. SCHULSON Aug. 1984 200 p

(Contract NAS3-23276)

(NASA-CR-174657; NAS 1.26:174657; CREARE-TN-371) Avail: NTIS HC A09/MF A01 CSCL 21H

Cracking of the titanium knife edges on the labyrinth seals of the liquid hydrogen fuel pump in the Space Shuttle main engine is considered. Finite element analysis of the thermal response of the knife edge in sliding contact with the wear ring surface shows that interfacial temperatures can be quite high and they are significantly influenced by the thermal conductivity of the surfaces in rubbing contact. Thermal shock experiments on a test specimen similar to the knife edge geometry demonstrate that cracking of the titanium alloy is possible in a situation involving repeated thermal cycles over a wide temperature range, as might be realized during a rub in the liquid hydrogen fuel pump. High-speed rub interaction tests were conducted using a representative knife edge and seal geometry over a broad range of interaction rates and alternate materials were experimentally evaluated. Plasma-sprayed

aluminum-graphite was found to be significantly better than presently used aluminum alloy seals from the standpoint of rub performance. Ion nitriding the titanium alloy knife-edges also improved rub performance compared to the untreated baseline.

A.B.H.

**N85-19020\*#** Pratt and Whitney Aircraft, West Palm Beach, Fla. Government Products Div.

**DESIGN AND ANALYSIS REPORT FOR THE RL10-2B BREADBOARD LOW THRUST ENGINE Final Report**

J. R. BROWN, R. R. FOUST, D. E. GALLER, P. G. KANIC, T. D. KMIEC, C. D. LIMERICK, R. J. PECKHAM, and T. SWARTWOUT 12 Dec. 1984 138 p

(Contract NAS3-24238)

(NASA-CR-174857; NAS 1.26:174857; FR-18046-3) Avail: NTIS HC A07/MF A01 CSCL 21H

The breadboard low thrust RL10-2B engine is described. A summary of the analysis and design effort to define the multimode thrust concept applicable to the requirements for the upper stage vehicles is provided. Baseline requirements were established for operation of the RL10-2B engine under the following conditions: (1) tank head idle at low propellant tank pressures without vehicle propellant conditioning or settling thrust; (2) pumped idle at a ten percent thrust level for low G deployment and/or vehicle tank pressurization; and (3) full thrust (15,000 lb.). Several variations of the engine configuration were investigated and results of the analyses are included. Author

**N85-21256\*** National Aeronautics and Space Administration. Lewis Research Center, Cleveland, Ohio.

**RING-CUSP ION THRUSTER WITH SHELL ANODE Patent**

J. S. SOVEY, V. K. RAWLIN, and R. F. ROMAN, inventors (to NASA) 21 Aug. 1984 6 p Filed 9 Mar. 1983 Supersedes N83-21903 (21 - 11, p 1783)

(NASA-CASE-LEW-13881-1; NAS 1.71:LEW-13881-1;

US-PATENT-4,466,242; US-PATENT-APPL-SN-473498;

US-PATENT-CLASS-60-202) Avail: US Patent and Trademark Office CSCL 21C

An improved ion thruster for low specific impulse operation in the 1500 sec to 6000 sec range has a multicusp boundary field provided by high strength magnets on an iron anode shell which lengthens the paths of electrons from a hollow cathode assembly. A downstream anode pole piece in the form of an iron ring supports a ring of magnets to provide a more uniform beam profile. A cylindrical cathode magnet can be moved selectively in an axial direction along a feed tube to produce the desired magnetic field at the cathode tip. Author

**N85-21258\*#** National Aeronautics and Space Administration. Lewis Research Center, Cleveland, Ohio.

**RAIL ACCELERATOR TECHNOLOGY AND APPLICATIONS**

L. M. ZANA and W. R. KERSLAKE 25 Mar. 1985 18 p refs Presented at the JANNAF Propulsion Meeting, San Diego, Calif., 9-12 Apr. 1985; sponsored by the JANNAF Interagency Propulsion Committee

(NASA-TM-86947; E-2466; NAS 1.15:86947) Avail: NTIS HC A02/MF A01 CSCL 21H

Rail accelerators offer a viable means of launching ton-size payloads from the Earth's surface to space. The results of two mission studies which indicate that an Earth-to-Space Rail Launcher (ESRL) system is not only technically feasible but also economically beneficial, particularly when large amounts of bulk cargo are to be delivered to space are given. An in-house experimental program at the Lewis Research Center (LeRC) was conducted in parallel with the mission studies with the objective of examining technical feasibility issues. A 1 m long - 12.5 by 12.5 mm bore rail accelerator as designed with clear polycarbonate sidewalls to visually observe the plasma armature acceleration. The general character of plasma/projectile dynamics is described for a typical test firing.

R.J.F.



**N85-21259\*#** National Aeronautics and Space Administration. Lewis Research Center, Cleveland, Ohio.

**VACUUM CHAMBER PRESSURE EFFECTS ON THRUST MEASUREMENTS OF LOW REYNOLDS NUMBER NOZZLES**

J. S. SOVEY, P. F. PENKO, S. P. GRISNIK, and M. V. WHALEN 1985 12 p refs Presented at the 1985 JANNAF Propulsion Meeting, San Diego, Calif., 9-12 Apr. 1985 (NASA-TM-86955; E-2440; NAS 1.15:86955) Avail: NTIS HC A02/MF A01 CSCL 21H

Tests were conducted to investigate the effect of vacuum facility pressure on the performance of small thruster nozzles. Thrust measurements of two converging-diverging nozzles with an area ratio of 140 and an orifice plate flowing unheated nitrogen and hydrogen were taken over a wide range of vacuum facility pressures and nozzle throat Reynolds numbers. In the Reynolds number range of 2200 to 12 000 there was no discernable viscous effect on thrust below an ambient to total pressure ratio of 1000. In nearly all cases, flow separation occurred at a pressure ratio of about 1000. This was the upper limit for obtaining an accurate thrust measurement for a conical nozzle with an area ratio of 140. Author

**N85-21260\*#** National Aeronautics and Space Administration. Lewis Research Center, Cleveland, Ohio.

**COMPATIBILITY EXPERIMENTS OF FACILITIES, MATERIALS, AND PROPELLANTS FOR ELECTROTHERMAL THRUSTERS**

M. V. WHALEN, S. P. GRISNIK, and J. S. SOVEY 1985 16 p refs Presented at the 1985 JANNAF Propulsion Meeting, San Diego, Calif., 9-12 Apr. 1985 (NASA-TM-86956; E-2479; NAS 1.15:86956) Avail: NTIS HC A02/MF A01 CSCL 21H

Experiments were performed to determine the compatibility of materials and propellants for electro-thermal thrusters. Candidate propellants for resistojet propulsion include carbon dioxide, methane, hydrogen, ammonia, and hydrazine. The materials being examined are grain stabilized platinum for resistojets for Space station and rhenium for high performance resistojets for satellites. Heater mass loss and deterioration of materials were evaluated. A coiled tube of platinum, with yttria dispersed throughout the base material to inhibit grain growth, was tested in carbon dioxide at 1300 C for 2000 hr. Post-test examination indicated the platinum-yttria heater would last over 100 000 hr with less than 10 percent mass loss. Short-term compatibility tests were conducted to test the integrity of the platinum-yttria in hydrogen, methane, carbon dioxide/methane mixtures and ammonia environments. In each of these 100 hr tests, the platinum-yttria mass change indicated a minimum coil life of 100 000 hr. Facility related effects were investigated in materials tests using rhenium heated to high temperatures. Vacuum facility water reduction was monitored using a mass spectrometer. In vacuum environments obtained using only diffusion pumping and those obtained with the assistance of cryogenic equipment there were mass gains in the rhenium heaters. These mass gains were the result of the high amount of oxygen and water contained in the gas. Propellant purity and preferred test facility environments are discussed.

G.L.C.

**N85-21261\*#** National Aeronautics and Space Administration. Lewis Research Center, Cleveland, Ohio.

**GAAS AND 3-5 COMPOUND SOLAR CELLS STATUS AND PROSPECTS FOR USE IN SPACE**

D. J. FLOOD and D. J. BRINKER 1984 13 p refs Presented at the 4th European Symp. on Photovoltaic Generators in Space, Cannes, France, 18-20 Sep. 1984 (NASA-TM-86960; E-2485; NAS 1.15:86960) Avail: NTIS HC A02/MF A01 CSCL 10B

Gallium arsenide solar cells equal or surpass the best silicon solar cells in efficiency, radiation resistance, annealability, and in the capability to produce usable power output at elevated temperatures. NASA has been involved in a long range research and development program to capitalize on these manifold advantages, and to explore alternative III-V compounds for additional potential improvements. The current status and future

prospects for research and development in this area are reviewed and the progress being made toward development of GaAs cells suitable for variety of space missions is discussed. Cell types under various stages of development include n(+)/p shallow homojunction thin film GaAs cells, x100 concentration ratio p/n and n/p GaAs small area concentrator cells, mechanically-stacked, two-junction tandem cells, and three-junction monolithic cascade cells, among various other cell types. Author

**N85-21263\*#** National Aeronautics and Space Administration. Lewis Research Center, Cleveland, Ohio.

**HIGH-VOLTAGE, HIGH-POWER, SOLID-STATE REMOTE POWER CONTROLLERS FOR AEROSPACE APPLICATIONS**

J. C. STURMAN Mar. 1985 34 p refs (NASA-TP-2437; E-2359; NAS 1.60:2437) Avail: NTIS HC A03/MF A01 CSCL 10B

Two general types of remote power controller (RPC) that combine the functions of a circuit breaker and a switch were developed for use in direct-current (dc) aerospace systems. Power-switching devices used in these designs are the relatively new gate-turnoff thyristor (GTO) and power metal-oxide-semiconductor field-effect transistors (MOSFET). The various RPC's can switch dc voltages to 1200 V and currents to 100 A. Seven different units were constructed and subjected to comprehensive laboratory and thermal vacuum testing. Two of these were dual units that switch both positive and negative voltages simultaneously. The RPC's using MOSFET's have slow turnon and turnoff times to limit voltage spiking from high di/dt. The GTO's have much faster transition times. All RPC's have programmable overload tripout and microsecond tripout for large overloads. The basic circuits developed can be used to build switchgear limited only by the ratings of the switching device used. Author

**N85-22569\*#** National Aeronautics and Space Administration. Lewis Research Center, Cleveland, Ohio.

**THE HIGH VOLTAGE SILICON CELL: A COMPARATIVE ANALYSIS**

V. G. WEIZER, C. K. SWARTZ, R. E. HART, and M. P. GODLEWSKI /n ESA Photovoltaic Generators in Space p 25-29 Nov. 1984 refs Avail: NTIS HC A20/MF A01 CSCL 21H

An experimental technique capable of resolving the dark saturation current into its base and emitter components is used in an analysis in which the voltage limiting mechanisms for high voltage, low resistivity silicon solar cells were determined. Hi-low emitter cells, multistep diffused cells, ion-implanted emitter cell, MINMIS and MINP cells were studied. The results are at variance with prior expectations: the MINP and the MINMIS voltage improvements are due, to a considerable extent, to an optimization of the base component of the saturation current. This result is substantiated by an independent analysis of the material used to fabricate the devices. Author (ESA)

**N85-22580\*#** National Aeronautics and Space Administration. Lewis Research Center, Cleveland, Ohio.

**GAAS AND 3-5 COMPOUND SOLAR CELLS STATUS AND PROSPECTS FOR USE IN SPACE**

D. J. FLOOD and D. J. BRINKER /n ESA Photovoltaic Generators in Space p 89-94 Nov. 1984 refs Avail: NTIS HC A20/MF A01 CSCL 21H

The status and prospects of GaAs and 3-5 compound thin film and heterojunction solar cells for space missions are reviewed. Cell types considered include n+/p shallow homojunction thin film GaAs cells, 100x concentration ratio p/n and n/p GaAs small area concentrator cells; mechanically-stacked, two-junction tandem cells; and three-junction monolithic cascade cells. Author (ESA)



## 20 SPACECRAFT PROPULSION AND POWER

**N85-22586#** National Aeronautics and Space Administration. Lewis Research Center, Cleveland, Ohio.

### **THE EFFECTS OF LITHIUM COUNTERDOPING ON RADIATION DAMAGE AND ANNEALING IN N(+)-P SILICON SOLAR CELLS**

I. WEINBERG, H. W. BRANDHORST, JR., S. MEHTA, and C. K. SWARTZ *In* ESA Photovoltaic Generators in Space p 131-136 Nov. 1984 refs

Avail: NTIS HC A20/MF A01 CSCL 21H

Boron-doped silicon solar cells were counterdoped with lithium and the resultant n+p cells irradiated by 1 MeV electrons. Lithium counterdoped cells exhibit significantly increased radiation resistance with considerable annealing occurring at 100 C; DLTS studies indicate that the annealing behavior is controlled by a single defect at  $E_v + 0.43$  eV. It is concluded that the increased radiation resistance of the counterdoped cells is due primarily to the interaction of lithium with oxygen, single vacancies and divacancies. It is speculated that the lithium-oxygen interaction is the most effective in contributing to the increased radiation resistance.

Author (ESA)

**N85-23926\*#** National Aeronautics and Space Administration. Lewis Research Center, Cleveland, Ohio.

### **FABRICATION OF CERAMIC SUBSTRATE-REINFORCED AND FREE FORMS**

R. J. QUENTMEYER, G. McDONALD, and R. C. HENDRICKS 19 Apr. 1985 26 p refs Presented at 12th Intern. Conf. on Met. Coatings, Los Angeles, 15-19 Apr. 1985; sponsored by American Vacuum Society

(NASA-TM-86994; E-2540; NAS 1.15:86994) Avail: NTIS HC A03/MF A01 CSCL 21H

Components fabricated of, or coated with, ceramics have lower parasitic cooling requirements. Techniques are discussed for fabricating thin-shell ceramic components and ceramic coatings for applications in rocket or jet engine environments. Thin ceramic shells with complex geometric forms involving convolutions and reentrant surfaces were fabricated by mandrel removal. Mandrel removal was combined with electroplating or plasma spraying and isostatic pressing to form a metal support for the ceramic. Rocket engine thrust chambers coated with 0.08 mm (3 mil) of  $ZrO_2-8Y_2O_3$  had no failures and a tenfold increase in engine life. Some measured mechanical properties of the plasma-sprayed ceramic are presented.

B.G.

**N85-25384\*#** United Technologies Corp., South Windsor, Conn. Power Systems Div.

### **LONG-LIFE HIGH PERFORMANCE FUEL CELL PROGRAM Interim Report, 28 May 1981 - 31 Oct. 1984**

R. E. MARTIN Feb. 1985 187 p refs

(Contract NAS3-22234)

(NASA-CR-174874; NAS 1.26:174874; FCR-6853) Avail: NTIS HC A09/MF A01 CSCL 10B

A multihundred kilowatt Regenerative Fuel Cell for use in a space station is envisioned. Three 0.508 sq ft (471.9 cm) active area multicell stacks were assembled and endurance tested. The long term performance stability of the platinum on carbon catalyst configuration suitability of the lightweight graphite electrolyte reservoir plate, the stability of the free standing butyl bonded potassium titanate matrix structure, and the long life potential of a hybrid polysulfone cell edge frame construction were demonstrated. A 18,000 hour demonstration test of multicell stack to a continuous cyclical load profile was conducted. A total of 12,000 cycles was completed, confirming the ability of the alkaline fuel cell to operate to a load profile simulating Regenerative Fuel Cell operation. An orbiter production hydrogen recirculation pump employed in support of the cyclical load profile test completed 13,000 hours of maintenance free operation. Laboratory endurance tests demonstrated the suitability of the butyl bonded potassium matrix, perforated nickel foil electrode substrates, and carbon ribbed substrate anode for use in the alkaline fuel cell. Corrosion testing of materials at 250 F (121.1 C) in 42% wgt. potassium identified ceria, zirconia, strontium titanate, strontium zirconate and lithium cobaltate as candidate matrix materials.

A.R.H.

**N85-25385\*#** National Aeronautics and Space Administration. Lewis Research Center, Cleveland, Ohio.

### **MANRATING ORBITAL TRANSFER VEHICLE PROPULSION**

L. P. COOPER 1985 14 p refs Proposed for presentation at the 21st Joint Propulsion Conf., Monterey, Calif., 8-10 Jul. 1985; sponsored by AIAA, SAE and ASME

(NASA-TM-87019; E-2570; NAS 1.15:87019) Avail: NTIS HC A02/MF A01 CSCL 21H

The expended capabilities for Orbital Transfer Vehicles (OTV) which will be needed to meet increased payload requirements for transporting materials and men to geosynchronous orbit are discussed. The requirement to provide manrating offers challenges and opportunities to the propulsion system designers. The propulsion approaches utilized in previous manned space vehicles of the United States are reviewed. The principals of reliability analysis are applied to the Orbit Transfer Vehicle. Propulsion system options are characterized in terms of the test requirements to demonstrate reliability goals and are compared to earlier vehicle approaches.

E.A.K.

**N85-25386\*#** National Aeronautics and Space Administration. Lewis Research Center, Cleveland, Ohio.

### **SPACE STATION PROPULSION: THE ADVANCED DEVELOPMENT PROGRAM AT LEWIS**

R. E. JONES 1985 14 p refs Proposed for presentation at the 21st Joint Propulsion Conf., Monterey, Calif., 8-10 Jul. 1985; sponsored by AIAA, SAE and ASME

(NASA-TM-86999; E-2544; NAS 1.15:86999) Avail: NTIS HC A02/MF A01 CSCL 21H

A reference configuration was established for the initial operating capability (IOC) station. The reference configuration has assumed hydrazine fueled thrusters as the propulsion system. This was to establish costing and as a reference for comparison when other propulsion systems are considered. An integral part of the plan to develop the Space Station is the advanced development program. The objective of this program is to provide advanced technology alternatives for the initial and evolutionary Space Station which optimize the system's functional characteristics in terms of performance, cost, and utilization. The portion of the Advanced Development Program that is concerned with auxiliary propulsion and the research and programmatic activities conducted are discussed.

E.A.K.

**N85-26900\*#** National Aeronautics and Space Administration. Lewis Research Center, Cleveland, Ohio.

### **FUEL AND OXIDIZER TURBINE LOSS ANALYSIS**

J. E. HAAS *In* NASA. Marshall Space Flight Center Advan. High Pressure O<sub>2</sub>/H<sub>2</sub> Technol. p 560-570 Apr. 1985

Avail: NTIS HC A99/MF E03; SOD HC CSCL 21H

The turbine losses for the fuel and oxidizer turbines at the FPL condition were assessed by a quasi-3D loss analysis method. This loss analysis method uses two flow codes - MERIDL and TSONIC - to calculate the flow velocities along the blade surfaces and endwalls. The velocities are then used as input to the boundary layer code - BLAYER - to calculate the friction losses due to incidence, secondary flow, and tip clearance. The loss analysis for the fuel turbine indicated an overall two-stage efficiency of about 90%. The largest loss was due to rotor tip clearance. The loss analysis for the oxidizer turbine is nearly completed. Results for the first stage of the two-stage design indicates an efficiency of about 80%, with high losses due to rotor incidence and blade and endwall friction.

E.A.K.

**N85-26901\*#** National Aeronautics and Space Administration. Lewis Research Center, Cleveland, Ohio.

### **REDISTRIBUTION OF THE INLET TEMPERATURE PROFILE THROUGH THE SSME FUEL TURBINE**

J. R. SCHWAB *In* NASA. Marshall Space Flight Center Advan. High Pressure O<sub>2</sub>/H<sub>2</sub> Technol. p 571-578 Apr. 1985 refs

Avail: NTIS HC A99/MF E03; SOD HC CSCL 21H

A three-dimensional Euler code was used to predict radial inlet temperature profile redistribution through the two-stage fuel turbopump turbine. The calculation was made at the FPL condition

using a turbine inlet radial temperature profile. This same calculation was made earlier on single-stage turbine. There was a redistribution of the temperature profile such that the hotter gas that originated at the midspan region at the turbine inlet was shifted to the hub and tip regions on the blade pressure surface at the rotor exit. For the SSME fuel turbine, however, there was no redistribution of the inlet temperature profile. No strong secondary flow patterns were identified. It is indicated that this trend is attributed to the high solidity SSME blading. E.A.K.

**N85-26907\*#** Rockwell International Corp., Canoga Park, Calif. Rocketdyne Div.

### REUSABLE ROCKET ENGINE TURBOPUMP CONDITION MONITORING

M. E. HAMPSON and S. BARKHOUDARIAN /in NASA. Marshall Space Flight Center Advan. High Pressure O<sub>2</sub>/H<sub>2</sub> Technol. p 654-673 Apr. 1985 refs (Contract NAS3-23349)

Avail: NTIS HC A99/MF E03; SOD HC CSCL 21H

Significant improvements in engine readiness with attendant reductions in maintenance costs and turnaround times can be achieved with an engine condition monitoring system (CMS). The CMS provides real time health status of critical engine components, without disassembly, through component monitoring with advanced sensor technologies. Three technologies were selected to monitor the rotor bearings and turbine blades: the isotope wear detector and fiber optic deflectometer (bearings), and the fiber optic pyrometer (blades). Signal processing algorithms were evaluated and ranked for their utility in providing useful component health data to unskilled maintenance personnel. Design modifications to current configuration Space Shuttle Main Engine (SSME) high pressure turbopumps and the MK48-F turbopump were developed to incorporate the sensors. Author

**N85-26912\*#** National Aeronautics and Space Administration. Lewis Research Center, Cleveland, Ohio.

### TETHERED NUCLEAR POWER FOR THE SPACE STATION

D. J. BENTS 1985 27 p refs Proposed for presentation at the 20th Intersoc. Energy Conversion Eng. Conf. (IECEC), Miami Beach, Fla., 18-23 Aug. 1985; sponsored by SAE, ANS, ASME, IEEE, AIAA, ACS, and AICHE (NASA-TM-87023; E-2572; NAS 1.15:87023) Avail: NTIS HC A03/MF A01 CSCL 18L

A nuclear space power system the SP-100 is being developed for future missions where large amounts of electrical power will be required. Although it is primarily intended for unmanned spacecraft, it can be adapted to a manned space platform by tethering it above the station through an electrical transmission line which isolates the reactor far away from the inhabited platform and conveys its power back to where it is needed. The transmission line, used in conjunction with an instrument rate shield, attenuates reactor radiation in the vicinity of the space station to less than one-one hundredth of the natural background which is already there. This combination of shielding and distance attenuation is less than one-tenth the mass of boom-mounted or onboard man-rated shields that are required when the reactor is mounted nearby. This paper describes how connection is made to the platform (configuration, operational requirements) and introduces a new element the coaxial transmission tube which enables efficient transmission of electrical power through long tethers in space. Design methodology for transmission tubes and tube arrays is discussed. An example conceptual design is presented that shows SP-100 at three power levels 100 kWe, 300 kWe, and 1000 kWe connected to space station via a 2 km HVDC transmission line/tether. Power system performance, mass, and radiation hazard are estimated with impacts on space station architecture and operation. B.W.

**N85-27941\*#** National Aeronautics and Space Administration. Lewis Research Center, Cleveland, Ohio.

### STRUCTURAL INTEGRITY AND DURABILITY OF REUSABLE SPACE PROPULSION SYSTEMS

Washington May 1985 191 p refs Conf. held in Cleveland, Ohio, 4-5 Jun. 1985; sponsored by NASA, Washington and NASA. Lewis Research Center (NASA-CP-2381; E-2554; NAS 1.55:2381) Avail: NTIS HC A09/MF A01 CSCL 21H

The space shuttle main engine (SSME), a reusable space propulsion system, is discussed. The advances in high pressure oxygen hydrogen rocket technology are reported to establish the basic technology and to develop new analytical tools for the evaluation in reusable rocket systems.

**N85-27942\*#** National Aeronautics and Space Administration. Lewis Research Center, Cleveland, Ohio.

### OVERVIEW OF AEROTHERMODYNAMIC LOADS DEFINITION STUDY Abstract Only

L. A. POVINELLI /in its Struct. Integrity and Durability of Reusable Space Propulsion Systems p 3-5 May 1985 refs Avail: NTIS HC A09/MF A01 CSCL 21H

The Aerothermodynamic Loads Definition were studied to develop methods to more accurately predict the operating environment in the space shuttle main engine (SSME) components. Development of steady and time-dependent, three-dimensional viscous computer codes and experimental verification and engine diagnostic testing are considered. The steady, nonsteady, and transient operating loads are defined to accurately predict powerhead life. Improvements in the structural durability of the SSME turbine drive systems depends on the knowledge of the aerothermodynamic behavior of the flow through the preburner, turbine, turnaround duct, gas manifold, and injector post regions. E.A.K.

**N85-27943\*#** National Aeronautics and Space Administration. Lewis Research Center, Cleveland, Ohio.

### SSME FUEL PREBURNER TWO-DIMENSIONAL ANALYSIS

T. J. VANOVERBEKE /in its Struct. Integrity and Durability of Reusable Space Propulsion Systems p 7-14 May 1985 Avail: NTIS HC A09/MF A01 CSCL 21H

The durability of the SSME turbine is strongly affected by the temperature profile leaving the preburner. A reacting flow computer model to predict the turbine inlet temperature profile was used. Calculations were made by using a reacting flow code, to assess the sensitivity of the turbine inlet temperature profile to variations in the flow entering the SSME preburner. E.A.K.

**N85-27972\*#** National Aeronautics and Space Administration. Lewis Research Center, Cleveland, Ohio.

### PRIMARY PROPULSION OF ELECTROTHERMAL, ION AND CHEMICAL SYSTEMS FOR SPACE-BASED RADAR ORBIT TRANSFER

S. Y. WANG and P. J. STAIGER 1985 16 p refs Presented at 21st Joint Propulsion Conf., Monterey, Calif., 8-10 Jul. 1985; sponsored by AIAA, SAE and ASME (NASA-TM-87043; E-2603; NAS 1.15:87043) Avail: NTIS HC A02/MF A01 CSCL 21C

An orbit transfer mission concept has been studied for a Space-Based Radar (SBR) where 40 kW required for radar operation is assumed available for orbit transfer propulsion. Arcjet, pulsed electrothermal (PET), ion, and storable chemical systems are considered for the primary propulsion. Transferring two SBR per shuttle flight to 1112 km/60 deg using electrical propulsion systems offers an increased payload at the expense of increased trip time, up to 2000 kg each, which may be critical for survivability. Trade offs between payload mass, transfer time, launch site, inclination, and height of parking orbits are presented. Author

## 20 SPACECRAFT PROPULSION AND POWER

**N85-28971\*#** National Aeronautics and Space Administration. Lewis Research Center, Cleveland, Ohio.

### **AN EVALUATION OF OXYGEN-HYDROGEN PROPULSION SYSTEMS FOR THE SPACE STATION**

R. W. KLEMETSON, P. W. GARRISON, and N. P. HANNUM 1985 28 p refs Presented at the 21st Joint Propulsion Conf., Monterey, Calif., 8-10 Jul. 1985; sponsored in part by AIAA, SAE, ASME, and ASEE Previously announced in IAA as A85-43976 Prepared in cooperation with JPL, Pasadena, Calif. (NASA-TM-87059; E-2628; NAS 1.15:87059) Avail: NTIS HC A03/MF A01 CSCL 21H

Conceptual designs for O<sub>2</sub>/H<sub>2</sub> chemical and resistojet propulsion systems for the space station was developed and evaluated. The evolution of propulsion requirements was considered as the space station configuration and its utilization as a space transportation node change over the first decade of operation. The characteristics of candidate O<sub>2</sub>/H<sub>2</sub> auxiliary propulsion systems are determined, and opportunities for integration with the OTV tank farm and the space station life support, power and thermal control subsystems are investigated. OTV tank farm boiloff can provide a major portion of the growth station impulse requirements and CO<sub>2</sub> from the life support system can be a significant propellant resource, provided it is not denied by closure of that subsystem. Waste heat from the thermal control system is sufficient for many propellant conditioning requirements. It is concluded that the optimum level of subsystem integration must be based on higher level space station studies. Author

**N85-34176\*#** National Aeronautics and Space Administration. Lewis Research Center, Cleveland, Ohio.

### **OPTICAL ANALYSIS OF PARABOLIC DISH CONCENTRATORS FOR SOLAR DYNAMIC POWER SYSTEMS IN SPACE**

K. S. JEFFERIES Aug. 1985 27 p refs (NASA-TM-87080; E-2659; NAS 1.15:87080) Avail: NTIS HC A03/MF A01 CSCL 10B

An optical analysis of a parabolic solar collection system operating in Earth orbit was performed using ray tracing techniques. The analysis included the effects of: (1) solar limb darkening, (2) parametric variation of mirror surface error, (3) parametric variation of mirror rim angle, and (4) parametric variation of alignment and pointing error. This ray tracing technique used numerical integration to combine the effects of rays emanating from different parts of the sun at different intensities with the effects of normally distributed mirror-surface errors to compute the angular intensity distribution of rays leaving the mirror surface. A second numerical integration was then performed over the surface of the parabolic mirror to compute the radial distribution of brightness at the mirror focus. Major results of the analysis included: (1) solar energy can be collected at high temperatures with high efficiency, (2) higher absorber temperatures can be achieved at lower efficiencies, or higher efficiencies can be achieved at lower temperatures, and (3) collection efficiency is near its maximum level across a broad plateau of rim angles from 40 deg to 70 deg. Author

**N85-34177\*#** National Aeronautics and Space Administration. Lewis Research Center, Cleveland, Ohio.

### **HEATERLESS IGNITION OF INERT GAS ION THRUSTER HOLLOW CATHODES**

M. F. SCHATZ 1985 23 p refs Presented at the 18th Intern. Elec. Propulsion Conf., Alexandria, Va., 30 Sep. - 2 Oct. 1985; sponsored by AIAA, JSASS and DGLR (NASA-TM-87086; E-2672; NAS 1.15:87086) Avail: NTIS HC A02/MF A01 CSCL 21C

Heaterless inert gas ion thruster hollow cathodes were investigated with the aim of reducing ion thruster complexity and increasing ion thruster reliability. Cathodes heated by glow discharges are evaluated for power requirements, flowrate requirements, and life limiting mechanisms. An accelerated cyclic life test is presented. E.A.K.

**N85-34178\*#** National Aeronautics and Space Administration. Lewis Research Center, Cleveland, Ohio.

### **ELECTRODE EROSION IN ARC DISCHARGES AT ATMOSPHERIC PRESSURE**

T. L. HARDY 1985 21 p refs Presented at the 18th Intern. Elec. Propulsion Conf., Alexandria, Va., 30 Sep. - 2 Oct. 1985; sponsored by AIAA, JSASS and DGLR (NASA-TM-87087; E-2673; NAS 1.15:87087) Avail: NTIS HC A02/MF A01 CSCL 21C

An experimental investigation was performed in an effort to measure and increase lifetime of electrodes in an arcjet thruster. The electrode erosion of various anode and cathode materials was measured after tests in an atmospheric pressure nitrogen arc discharge at powers less than 1 kW. A free-burning arc configuration and a constricted arc configuration were used to test the materials. Lanthanum hexaboride and thoriated tungsten had low cathode erosion rates while thoriated tungsten and pure tungsten had the lowest anode erosion rates of the materials tested. Anode cooling, reverse gas flow, and external magnetic fields were all found to reduce electrode mass loss. Author

**N85-34179\*#** National Aeronautics and Space Administration. Lewis Research Center, Cleveland, Ohio.

### **HOLLOW CATHODES IN HIGH PRESSURE ARC DISCHARGES**

T. L. HARDY and F. M. CURRAN 1985 9 p refs Presented at the 18th Intern. Elec. Propulsion Conf., Alexandria, Va., 30 Sep. - 2 Oct. 1985; sponsored by AIAA, JSASS and DGLR (NASA-TM-87098; E-2689; NAS 1.15:87098) Avail: NTIS HC A02/MF A01 CSCL 21C

An orified hollow cathode was tested at high pressure to improve lifetime and efficiency in arcjet thrusters. It is indicated that the arc would not operate with emission from the insert above 200 torr in nitrogen regardless of insert material, orifice diameter, or gas flow direction. Emission occurred from the insert in argon and xenon although it could not be ascertained whether diffuse or spot emission existed within the cathode. Over the extended range of configurations and operating parameters explored the desired diffuse emission mode could not be obtained at high enough pressures for orified hollow cathodes to operate in the range which is considered for arcjet applications. E.A.K.

**N85-35225\*#** National Aeronautics and Space Administration. Lewis Research Center, Cleveland, Ohio.

### **STATUS OF ADVANCED ORBITAL TRANSFER PROPULSION**

L. P. COOPER 1985 26 p refs Proposed for presentation at the 36th Intern. Astronautics Federation Congr., Stockholm, 7-12 Oct. 1985 (NASA-TM-87069; E-2638; NAS 1.15:87069; IAF-85-164) Avail: NTIS HC A03/MF A01 CSCL 21H

A new Orbital Transfer Vehicle (OTV) propulsion system that will be used in conjunction with the Space Shuttle, Space Station and Orbit Maneuvering Vehicle is discussed. The OTV will transfer men, large space structures and conventional payloads between low Earth and higher energy orbits. Space probes carried by the OTV will continue the exploration of the solar system. When lunar bases are established, the OTV will be their transportation link to Earth. Critical engine design considerations based upon the need for low cost payload delivery, space basing, reusability, aeroassist maneuvering, low g transfers of large space structures and man rating are described. The importance of each of these to propulsion design is addressed. Specific propulsion requirements discussed are: (1) high performance H<sub>2</sub>/O<sub>2</sub> engine; (2) multiple engine configurations totalling no more than 15,000 lbf thrust 15 to 20 hr life; (3) space maintainable modular design; (4) health monitoring capability; and (5) safety and mission success with backup auxiliary propulsion. E.A.K.

## CHEMISTRY AND MATERIALS (GENERAL)

Includes biochemistry and organic chemistry.

**A85-36694\*** Sandia National Labs., Albuquerque, N. Mex.

**PROPERTIES OF COATED AND MODIFIED SURFACES**

D. M. MATTOX (Sandia National Laboratory, Albuquerque, NM), J. E. GREENE (Illinois, University, Urbana, IL), D. H. BUCKLEY (NASA, Lewis Research Center, Cleveland, OH), and G. A. SOMORJAI (California, University, Berkeley, CA) Materials Science and Engineering (ISSN 0025-5416), vol. 70, April 1985, p. 79-89. refs

The ability to create surface and near-surface properties distinct from the bulk properties of a material by means of coating or surface modification techniques is an important new field of development for engineering materials, encompassing ion implantation, plasma processing, reactive deposition methods, ion beam deposition and modification, molecular beam epitaxy, and fast quench thermal processing. Attention is given to specific areas of process control which illustrate (1) the use of process development to control material properties, (2) the importance of surface modification and coating to the tribology and ion-surface interactions of semiconductor film growth, and (3) recent findings in surface science which exemplify potential applications of ion-surface interactions that generate novel material qualities.

O.C.

**N85-10105\*** National Aeronautics and Space Administration. Lewis Research Center, Cleveland, Ohio.

**DYNAMICS OF GRAPHITE FIBER INTERCALATION: IN SITU RESISTIVITY MEASUREMENTS WITH A FOUR POINT PROBE**

D. A. JAWORSKE 1984 14 p refs Presented at the Mater. Res. Soc. Symp. on Intercalated Graphite, Boston, 28-30 Nov. 1984; sponsored by American Physical Society (NASA-TM-86858; E-2321; NAS 1.15:86858) Avail: NTIS HC A02/MF A01 CSCL 11D

The dynamics of ferric chloride intercalation of single graphite fibers were studied, in situ, using a four point dc bridge. Measurements before, during and after the intercalation showed that the intercalation occurred within minutes at 200 C. Changes in fiber resistivity after exposure to air suggested hydration of the graphite intercalation compound. Deintercalation of the ferric chloride was initiated at temperatures in excess of 400 C. cycling the intercalant into and out of the graphite fiber gave no improvements in fiber resistivity. The activation energy of the ferric chloride intercalation reaction was found to be  $17 \pm 4$  kcal/mol consistent with the concept of a preliminary nucleation step in the intercalation reaction. Author

**N85-14864\*** National Aeronautics and Space Administration. Lewis Research Center, Cleveland, Ohio.

**EFFECT OF WATER ON HYDROGEN PERMEABILITY**

D. D. HULLIGAN (Sverdrup Technology, Middleburg Heights, Ohio) and W. A. TOMAZIC 1984 14 p refs Presented at the 22nd Automotive Technol. Develop. Contractors' Coordination meeting, Dearborn, Mich., 26 Oct. - 2 Nov. 1984; sponsored by DOE (Contract DE-AI01-77CS-51040) (NASA-TM-86904; E-2389; DOE/NASA/51040-59; NAS 1.15:86904) Avail: NTIS HC A02/MF A01 CSCL 07D

Doping of hydrogen with CO or CO<sub>2</sub> was developed to reduce hydrogen permeation in Stirling engines by forming low permeability oxide coatings in the heater tubes. An end product of this process is water - which can condense in the cold parts of the engine system. If the water vapor is reduced to a low enough level, the hydrogen can reduce the oxide coating resulting in increased permeability. The equilibrium level of water (oxygen bearing gas) required to avoid reduction of the oxide coating was investigated. Results at 720 C and 13.8 MPa have shown that: (1) pure hydrogen will reduce the coating; (2) 500 ppm CO (500 ppm water equivalent)

does not prevent the reduction; and (3) 500 ppm CO<sub>2</sub> (1000 ppm water) appears to be close to the equilibrium level. Further tests are planned to define the equilibrium level more precisely and to extend the data to 820 C and 3.4, 6.9, and 13.8 MPa. R.S.F.

**N85-21264\*** National Aeronautics and Space Administration. Lewis Research Center, Cleveland, Ohio.

**A COMPUTER SIMULATION OF THIN FILM NUCLEATION AND GROWTH: THE VOLMER-WEBER CASE**

J. SALIK and H. M. GHOSE (Cuyahoga Community Coll.) 1985 12 p refs Proposed for presentation at the 12th Intern. Conf. on Met. Coatings, Los Angeles, 15-19 Apr. 1985; sponsored by the American Vacuum Society (NASA-TM-86968; E-2493; NAS 1.15:86968) Avail: NTIS HC A02/MF A01 CSCL 07A

The computer simulation of thin film nucleation and growth, which was previously performed for the case of single monolayer, was modified to include multilayer growth via the Volmer-Weber mechanism. The simulation results show that: (1) the kinetics of multilayer film growth is nearly identical to that of monolayer growth; (2) when no reevaporation takes place, the cluster density resulting from multilayer growth is higher at high coverage than that resulting from monolayer growth; (3) when reevaporation does take place, the cluster density resulting from multilayer growth is nearly identical to that resulting from monolayer growth. This is not due, however, to similarity in microstructure. E.A.K.

**N85-26921\*** National Aeronautics and Space Administration. Lewis Research Center, Cleveland, Ohio.

**GRAPHITE FIBER INTERCALATION: DYNAMICS OF THE BROMINE INTERCALATION PROCESS**

D. A. JAWORSKE and R. ZINOLABEDINI (Cleveland State Univ.) 21 Jun. 1985 10 p refs Presented at 17th Biennial Conf. Carbon, Lexington, Ky., 16-21 Jun. 1985; sponsored by American Carbon Society (NASA-TM-87015; E-2441; NAS 1.15:87015) Avail: NTIS HC A02/MF A01 CSCL 11D

The resistance of pitch-based graphite fibers was monitored, in situ, during a series of bromine intercalation experiments. The threshold pressure for the bromine intercalation of pitch-based fibers was estimated to be 102 torr. When the bromine atmosphere was removed from the reaction chamber, the resistivity of the intercalated graphite fibers increased consistently. This increase was attributed to loss of bromine from the perimeter of the fiber. The loss was confirmed by mapping the bromine concentration across the diameter of single intercalated fibers with either energy dispersive spectroscopy or scanning Auger microscopy. A statistical study comparing fibers intercalated in bromine vapor with fibers intercalated in bromine liquid showed that similar products were obtained with both methods of intercalation. Author

**N85-30011\*** National Aeronautics and Space Administration. Lewis Research Center, Cleveland, Ohio.

**BURNER RIG CORROSION OF SiC AT 1000 DEG C**

N. S. JACOBSON, C. A. STEARNS, and J. L. SMIALEK 1985 27 p refs Presented at the 87th Ann. Meeting of the Am. Ceram. Soc., Cincinnati, 5-9 May 1985 (NASA-TM-87061; E-2512; NAS 1.15:87061) Avail: NTIS HC A03/MF A01 CSCL 11B

Sintered alpha-SiC was examined in both oxidation and hot corrosion with a burner rig at 400 kPa (4 atm) and 1000 C with a flow velocity of 310 ft/sec. Oxidation tests for times to 46 hr produced virtually no attack, whereas tests with 4 ppm Na produced extensive corrosion in 13-1/2 hr. Thick glassy layers composed primarily of sodium silicate formed in the salt corrosion tests. This corrosion attack caused severe pitting of the silicon carbide substrate which led to a 32 percent strength decrease below the as-received material. Parallel furnace tests of Na<sub>2</sub>SO<sub>4</sub>/air induced attacked yielded basically similar results with some slight product composition differences. The differences are explained in terms of the continuous sulfate deposition which occurs in a burner rig. Author

## COMPOSITE MATERIALS

Includes laminates.

**A85-11926\*** Ohio State Univ., Columbus.

**ULTRASONIC WAVE PROPAGATION IN TWO-PHASE MEDIA - SPHERICAL INCLUSIONS**

L. S. FU and Y. C. SHEU (Ohio State University, Columbus, OH) Composite Structures (ISSN 0263-8223), vol. 2, no. 4, 1984, p. 289-303. Previously announced in STAR as N83-36500. refs (Contract NAG3-340)

The scattering theory, recently developed via the extended method of equivalent inclusion, is used to study the propagation of time-harmonic waves in two-phase media of elastic matrix with randomly distributed elastic spherical inclusion materials. The elastic moduli and mass density of the composite medium are determined as functions of frequencies when given properties and concentration of the spheres and the matrix. Velocity and attenuation of ultrasonic waves in two-phase media are determined for cases of distributed spheres and localized damage. An averaging theorem that requires the equivalence of the strain energy and the kinetic energy between the effective medium and the original matrix with spherical inhomogeneities is employed to derive the effective moduli and mass density. The functional dependency of these quantities upon frequencies and concentration provides a method of data analysis in ultrasonic evaluation of material properties. Numerical results or moduli, velocity and/or attenuation as functions of concentration of inclusion material, or porosity, are graphically displayed. Author

**A85-15632\*#** National Aeronautics and Space Administration. Lewis Research Center, Cleveland, Ohio.

**HYGROTHERMOMECHANICAL EVALUATION OF TRANSVERSE FILAMENT TAPE EPOXY/POLYESTER FIBERGLASS COMPOSITES**

R. F. LARK and C. C. CHAMIS (NASA, Lewis Research Center, Cleveland, OH) IN: Reinforced Plastics/Composites Institute, Annual Conference, 38th, Houston, TX, February 7-11, 1983, Preprints. New York, Society of the Plastics Industry, Inc., 1984, p. 12-C-1 to 12-C-15. refs

Transverse filament tape (TFT) fiberglass/epoxy and TFT polyester composites intended for low cost wind turbine blade fabrication have been subjected to static and cyclic load behavior tests whose results are presently evaluated on the basis of an integrated hygrothermomechanical response theory. Laminate testing employed simulated filament winding procedures. The results obtained show that the predicted hygrothermomechanical environmental effects on TFT composites are in good agreement with measured data for various properties, including fatigue at different R-ratio values. O.C.

**A85-15636\*#** National Aeronautics and Space Administration. Lewis Research Center, Cleveland, Ohio.

**DESIGN PROCEDURES FOR FIBER COMPOSITE STRUCTURAL COMPONENTS - RODS, BEAMS, AND BEAM COLUMNS**

C. C. CHAMIS (NASA, Lewis Research Center, Cleveland, OH) IN: Reinforced Plastics/Composites Institute, Annual Conference, 38th, Houston, TX, February 7-11, 1983, Preprints. New York, Society of the Plastics Industry, Inc., 1984, p. 16-C-1 to 16-C-9. Previously announced in STAR as N83-24559. refs

Step by step procedures are described which are used to design structural components (rods, columns, and beam columns) subjected to steady state mechanical loads and hydrothermal environments. Illustrative examples are presented for structural components designed for static tensile and compressive loads, and fatigue as well as for moisture and temperature effects. Each example is set up as a sample design illustrating the detailed steps that are used to design similar components. Author

**A85-16040\*** National Aeronautics and Space Administration. Lewis Research Center, Cleveland, Ohio.

**SELECT FIBER COMPOSITES FOR SPACE APPLICATIONS - A MECHANISTIC ASSESSMENT**

C. A. GINTY and C. C. CHAMIS (NASA, Lewis Research Center, Cleveland, OH) IN: Technology vectors; Proceedings of the Twenty-ninth National SAMPE Symposium and Exhibition, Reno, NV, April 3-5, 1984. Covina, CA, Society for the Advancement of Material and Process Engineering, 1984, p. 979-993. Previously announced in STAR as N84-22702. refs

Three fiber composites (graphite-fiber epoxy, graphite-fiber aluminum, and graphite-fiber magnesium) are evaluated for their possible use in space applications. Using the composite mechanics theories for thermomechanical behavior embodied in the ICAN (Integrated Composites Analyzer) computer code, select composite thermal and mechanical properties are predicted and also their response to cryogenic temperatures, resembling those which occur in space applications. The predicted results are presented in graphical form as a function of the composite's laminate configuration, fiber volume ratio and the selected use temperature. These results are suitable for preliminary design purposes only and should serve as an aid in selecting controlled experiments for obtaining corresponding measured data. Author

**A85-16094\*#** National Aeronautics and Space Administration. Lewis Research Center, Cleveland, Ohio.

**ICAN - INTEGRATED COMPOSITES ANALYZER**

P. L. N. MURTHY and C. C. CHAMIS (NASA, Lewis Research Center, Cleveland, OH) AIAA, ASME, ASCE, and AHS, Structures, Structural Dynamics and Materials Conference, 25th, Palm Springs, CA, May 14-16, 1984. 24 p. Previously announced in STAR as N84-26755. refs (AIAA PAPER 84-0974)

The ICAN computer program performs all the essential aspects of mechanics/analysis/design of multilayered fiber composites. Modular, open-ended and user friendly, the program can handle a variety of composite systems having one type of fiber and one matrix as constituents as well as intraply and interply hybrid composite systems. It can also simulate isotropic layers by considering a primary composite system with negligible fiber volume content. This feature is specifically useful in modeling thin interply matrix layers. Hygrothermal conditions and various combinations of in-plane and bending loads can also be considered. Usage of this code is illustrated with a sample input and the generated output. Some key features of output are stress concentration factors around a circular hole, locations of probable delamination, a summary of the laminate failure stress analysis, free edge stresses, microstresses and ply stress/strain influence coefficients. These features make ICAN a powerful, cost-effective tool to analyze/design fiber composite structures and components. A.R.H.

**A85-16096\*#** National Aeronautics and Space Administration. Lewis Research Center, Cleveland, Ohio.

**INTERPLY LAYER DEGRADATION EFFECTS ON COMPOSITE STRUCTURAL RESPONSE**

C. C. CHAMIS (NASA, Lewis Research Center, Cleveland, OH) and G. C. WILLIAMS (Arizona, University, Tucson, AZ) AIAA, ASME, ASCE, and AHS, Structures, Structural Dynamics and Materials Conference, 25th, Palm Springs, CA, May 14-16, 1984. 29 p. Previously announced in STAR as N84-26756. (AIAA PAPER 84-0849)

Recent research activities at NASA Lewis Research Center to computationally evaluate the effects of interply layer progressive weakening (degradation) on the structural response of a composite beam are summarized. The structural responses of interest include: (1) bending, (2) buckling, (3) free vibrations, (4) periodic excitation, and (5) impact. Finite element analysis was used for the computational evaluations. The interply layer degradation effects on the various structural responses were determined and assessed as a function of the interply layer modulus varying from 1 million psi down to 1000 psi and even lower for some limiting cases. The results obtained show that the interply layer degradation has

generally negligible effects on composite structural response and, therefore, structural integrity, unless the interply layer modulus degrades to about 10,000 psi or less. Author

**A85-21520\*** National Aeronautics and Space Administration. Lewis Research Center, Cleveland, Ohio.

**PMR POLYIMIDE COMPOSITES FOR AEROSPACE APPLICATIONS**

T. T. SERAFINI (NASA, Lewis Research Center, Cleveland, OH) IN: Polyimides: Synthesis, characterization, and applications. Volume 2. New York, Plenum Press, 1984, p. 957-975. refs

A novel class of addition-type polyimides has been developed in response to the need for high temperature polymers with improved processability. The new plastic materials are known as PMR (for in situ polymerization of monomer reactants) polyimides. The highly processable PMR polyimides have made it possible to realize much of the potential of high temperature resistant polymers. Monomer reactant combinations for several PMR polyimides have been identified. The present investigation is concerned with a review of the current status of PMR polyimides. Attention is given to details of PMR polyimide chemistry, the processing of composites and their properties, and aerospace applications of PMR-15 polyimide composites. G.R.

**A85-29133\*#** Drexel Univ., Philadelphia, Pa.

**USE OF STATICAL INDENTATION LAWS IN THE IMPACT ANALYSIS OF LAMINATED COMPOSITE PLATES**

T. M. TAN (Drexel University, Philadelphia, PA; Purdue University, West Lafayette, IN) and C. T. SUN (Purdue University, West Lafayette, IN) ASME, Transactions, Journal of Applied Mechanics (ISSN 0021-8936), vol. 52, March 1985, p. 6-12. (Contract NSG-3185)

The low-velocity impact response of graphite/epoxy laminates was investigated theoretically and experimentally. A nine-node isoparametric plate finite element in conjunction with an empirical contact law was used for the theoretical investigation. Theoretical results are in good agreement with strain-gage experimental data. The results of the investigation indicate that the present theoretical procedure describes the impact response of laminate for low-impact velocities. Author

**A85-37421\*#** National Aeronautics and Space Administration. Lewis Research Center, Cleveland, Ohio.

**ANALYSIS OF STRESS-STRAIN, FRACTURE, AND DUCTILITY BEHAVIOR OF ALUMINUM MATRIX COMPOSITES CONTAINING DISCONTINUOUS SILICON CARBIDE REINFORCEMENT**

D. L. MCDANIELS (NASA, Lewis Research Center, Cleveland, OH) Metallurgical Transactions A - Physical Metallurgy and Materials Science (ISSN 0360-2133), vol. 16A, June 1985, p. 1105-1115. refs

Mechanical properties and stress-strain behavior were evaluated for several types of commercially fabricated aluminum matrix composites, containing up to 40 vol pct discontinuous SiC whisker, nodule, or particulate reinforcement. The elastic modulus of the composites was found to be isotropic, to be independent of type of reinforcement, and to be controlled solely by the volume percentage of SiC reinforcement present. The yield/tensile strengths and ductility were controlled primarily by the matrix alloy and temper condition. Type and orientation of reinforcement had some effect on the strengths of composites, but only for those in which the whisker reinforcement was highly oriented. Ductility decreased with increasing reinforcement content; however, the fracture strains observed were higher than those reported in the literature for this type of composite. This increase in fracture strain was probably attributable to cleaner matrix powder, better mixing, and increased mechanical working during fabrication. Comparison of properties with conventional aluminum and titanium structural alloys showed that the properties of the low-cost, lightweight composites demonstrated very good potential for application to aerospace structures. Author

**A85-37483\*** National Aeronautics and Space Administration. Lewis Research Center, Cleveland, Ohio.

**HIGH TEMPERATURE METAL AND CERAMIC COMPOSITES**

R. A. SIGNORELLI and J. A. DICARLO (NASA, Lewis Research Center, Cleveland, OH) Journal of Metals (ISSN 0148-6608), vol. 37, June 1985, p. 41, 42.

The Materials Division at NASA Lewis is engaged in research and development efforts on behalf of fiber-reinforced composite materials that are lighter, stiffer, and more structurally reliable than conventional monolithic alloys and ceramics in applications that range from the cryogenic to the refractory. Attention is presently given to metal matrix composites, in which high performance depends on stiff, strong and thermally stable large diameter fibers, with chemically stable interfacial bonding and good coefficient of thermal expansion matching between fibers and matrices, and to ceramic matrix composites, in which intermediate strength interfacial bonds must allow cracks to propagate through the matrix only, while retaining good load transfer characteristics between fiber and matrix. O.C.

**A85-37484\*** National Aeronautics and Space Administration. Lewis Research Center, Cleveland, Ohio.

**FIBERS FOR STRUCTURALLY RELIABLE METAL AND CERAMIC COMPOSITES**

J. A. DICARLO (NASA, Lewis Research Center, Ceramics Systems Branch, Cleveland, OH) Journal of Metals (ISSN 0148-6608), vol. 37, June 1985, p. 44-49. refs

In their current state of development, commercially available reinforcing fibers fail to meet the requirements formulated for metal or ceramic matrix composites of sufficient strength and toughness. Attention is presently given to criteria for high strength and toughness in metal and ceramic matrix composites, as well as the approach adopted in fiber evaluation as a result of studies at the NASA Lewis Research Center. Two areas of special interest have been strength improvement in large diameter boron fibers for tough, impact-resistant boron/aluminum composites, and the evaluation of SiC fibers as reinforcement in tough ceramic-matrix composites with service temperatures of the order of 1400 C. O.C.

**A85-39215\*#** National Aeronautics and Space Administration. Lewis Research Center, Cleveland, Ohio.

**INTERPLY LAYER DEGRADATION EFFECTS ON COMPOSITE STRUCTURAL RESPONSE**

C. C. CHAMIS (NASA, Lewis Research Center, Cleveland, OH) and G. C. WILLIAMS Journal of Aircraft (ISSN 0021-8669), vol. 22, July 1985, p. 573-580. Previously cited in issue 05, p. 571, Accession no. A85-16096.

**A85-41127\*** National Aeronautics and Space Administration. Lewis Research Center, Cleveland, Ohio.

**A STUDY OF INTERPLY LAYER EFFECTS ON THE FREE EDGE STRESS FIELD OF ANGLEPLY LAMINATES**

P. L. N. MURTHY and C. C. CHAMIS (NASA, Lewis Research Center, Cleveland, OH) (George Washington University and NASA, Symposium on Advances and Trends in Structures and Dynamics, Washington, DC, Oct. 22-25, 1984) Computers and Structures (ISSN 0045-7949), vol. 20, no. 1-3, 1985, p. 431-441. Previously announced in STAR as N85-15822. refs

The general-purpose finite-element program MSC/NASTRAN is used to study the interply layer effects on the free-edge stress field of symmetric angleply laminates subjected to uniform tensile stress. The free-edge region is modeled as a separate substructure (superelement) which enables easy mesh refinement and provides the flexibility to move the superelement along the edge. The results indicate that the interply layer reduces the stress intensity significantly at the free edge. Another important observation of the study is that the failures observed near free edges of these types of laminates could have been caused by the interlaminar shear stresses. Author



## 24 COMPOSITE MATERIALS

**A85-46543\*** National Aeronautics and Space Administration. Lewis Research Center, Cleveland, Ohio.

### **IMPACT RESISTANCE OF FIBER COMPOSITES - ENERGY-ABSORBING MECHANISMS AND ENVIRONMENTAL EFFECTS**

C. C. CHAMIS and J. H. SINCLAIR (NASA, Lewis Research Center, Cleveland, OH) IN: Recent advances in composites in the United States and Japan; Proceedings of the Symposium, Hampton, VA, June 6-8, 1983. Philadelphia, PA, ASTM, 1985, p. 326-345. Previously announced in STAR as N84-24712. refs

Energy absorbing mechanisms were identified by several approaches. The energy absorbing mechanisms considered are those in unidirectional composite beams subjected to impact. The approaches used include: mechanic models, statistical models, transient finite element analysis, and simple beam theory. Predicted results are correlated with experimental data from Charpy impact tests. The environmental effects on impact resistance are evaluated. Working definitions for energy absorbing and energy releasing mechanisms are proposed and a dynamic fracture progression is outlined. Possible generalizations to angle-ply laminates are described. E.A.K.

**A85-47022\*#** National Aeronautics and Space Administration. Lewis Research Center, Cleveland, Ohio.

### **TEN YEAR ENVIRONMENTAL TEST OF GLASS FIBER/EPOXY PRESSURE VESSELS**

J. R. FADDOL (NASA, Lewis Research Center, Cleveland, OH) AIAA, SAE, ASME, and ASEE, Joint Propulsion Conference, 21st, Monterey, CA, July 8-10, 1985. 10 p. Previously announced in STAR as N85-30034. refs (AIAA PAPER 85-1198)

By the beginning of the 1970's composite pressure vessels had received a significant amount of development effort, and applications were beginning to be investigated. One of the first applications grew out of NASA Johnson Space Center efforts to develop a superior emergency breathing system for firemen. While the new breathing system provided improved wearer comfort and an improved mask and regulator, the primary feature was low weight which was achieved by using a glass fiber reinforced aluminum pressure vessel. Part of the development effort was to evaluate the long term performance of the pressure vessel and as a consequence, some 30 bottles for a test program were procured. These bottles were then provided to NASA Lewis Research Center where they were maintained in an outdoor environment in a pressurized condition for a period of up to 10 yr. During this period, bottles were periodically subjected to cyclic and burst testing. There was no protective coating applied to the fiberglass/epoxy composite, and significant loss in strength did occur as a result of the environment. Similar bottles stored indoors showed little, if any, degradation. This report contains a description of the pressure vessels, a discussion of the test program, data for each bottle, and appropriate plots, comparisons, and conclusions. Author

**A85-47970\*** Martin Marietta Aerospace, Denver, Colo. **FIBERGLASS EPOXY LAMINATE FATIGUE PROPERTIES AT 300 AND 20 K**

J. M. TOTH, JR., W. J. BAILEY, and D. A. BOYCE (Martin Marietta Aerospace, Denver, CO) IN: Fatigue at low temperatures; Proceedings of the Symposium, Louisville, KY, May 10, 1983. Philadelphia, PA, ASTM, 1985, p. 163-172. (Contract NAS3-23245)

A subcritical liquid hydrogen orbital storage and supply experiment is being designed for flight in the Space Shuttle cargo bay. The Cryogenic Fluid Management Experiment (CFME) includes a liquid hydrogen tank supported in a vacuum jacket by two fiberglass epoxy composite trunnion mounts. The ability of the CFME to last for the required seven missions depends primarily on the fatigue life of the composite trunnions at cryogenic temperatures. To verify the trunnion design and test the performance of the composite material, fatigue property data at 300 and 20 K were obtained for the specific E-glass fabric/S-glass unidirectional laminate that will be used for the CFME trunnions.

The fatigue life of this laminate was greater at 20 K than at 300 K, and was satisfactory for the intended application. Author

**N85-12095\*#** National Aeronautics and Space Administration. Lewis Research Center, Cleveland, Ohio.

### **HIGH PERFORMANCE FIBERS FOR STRUCTURALLY RELIABLE METAL AND CERAMIC COMPOSITES**

J. A. DICARLO 1984 16 p refs Presented at a Conf. on High Performance Textiles Structures, Philadelphia, 6-8 Jun. 1984; sponsored by The Fiber Soc. and SAMPE (NASA-TM-86878; E-2339; NAS 1.15:86878) Avail: NTIS HC A02/MF A01 CSCL 11D

Very few of the commercially available high performance fibers with low densities, high Young's moduli, and high tensile strengths possess all the necessary property requirements for providing either metal matrix composites (MMC) or ceramic matrix composites (CMC) with high structural reliability. These requirements are discussed in general and examples are presented of how these property guidelines are influencing fiber evaluation and improvement studies at NASA aimed at developing structurally reliable MMC and CMC for advanced gas turbine engines. A.R.H.

**N85-12948\*#** National Aeronautics and Space Administration. Lewis Research Center, Cleveland, Ohio.

### **FUNDAMENTAL STUDIES OF COMPOSITE TOUGHNESS**

K. J. BOWLES IN NASA. Langley Research Center Tough Composite Mater. p 125-136 Dec. 1984 Avail: NTIS HC A17/MF A01 CSCL 11D

Evaluation of drop weight impact testing of neat resin and crossplied graphite fiber reinforced composites resulted in three conclusions: (1) during impact of cross-ply laminates, resin properties appear to influence the extent and mechanism of damage propagation; (2) by itself, neat resin strain to fracture is not a controlling influence on resin or composite fracture toughness; and (3) impact failure energy of neat resin plates can give a misleading indication of the resin contribution to composite impact behavior because of differences in the magnitude of diaphragm action in the two systems. Both geometric and composite constituent materials properties influence the drop weight impact resistance of crossplied composite plates. The matrix influence appears to be reflected in the incipient damage mechanism and the propagation of damage. M.G.

**N85-14878\*#** National Aeronautics and Space Administration. Lewis Research Center, Cleveland, Ohio.

### **CREEP OF CHEMICALLY VAPOR DEPOSITED SiC FIBERS**

J. A. DICARLO 1984 21 p refs Presented at the 8th Ann. Conf. on Composites and Advan. Ceram. Mater., Cocoa Beach, Fla., 15-18 Jan. 1984; sponsored by American Ceramic Society (NASA-TM-86897; E-2372; NAS 1.15:86897) Avail: NTIS HC A02/MF A01 CSCL 11D

The creep, thermal expansion, and elastic modulus properties for chemically vapor deposited SiC fibers were measured between 1000 and 1500 C. Creep strain was observed to increase logarithmically with time, monotonically with temperature, and linearly with tensile stress up to 600 MPa. The controlling activation energy was 480 + or - 20 kJ/mole. Thermal pretreatments near 1200 and 1450 C were found to significantly reduce fiber creep. These results coupled with creep recovery observations indicate that below 1400 C fiber creep is anelastic with negligible plastic component. This allowed a simple predictive method to be developed for describing fiber total deformation as a function of time, temperature, and stress. Mechanistic analysis of the property data suggests that fiber creep is the result of beta-SiC grain boundary sliding controlled by a small percent of free silicon in the grain boundaries. Author



**N85-14882\*#** National Aeronautics and Space Administration. Lewis Research Center, Cleveland, Ohio.

**FABRICATION AND QUALITY ASSURANCE PROCESSES FOR SUPERHYBRID COMPOSITE FAN BLADES**

R. F. LARK and C. C. CHAMIS 1983 15 p refs Presented at the 15th Ann. SAMPE Tech. Conf., Cincinnati, 4-5 Oct. 1983 (NASA-TM-83354; E-1611; NAS 1.15:83354) Avail: NTIS HC A02/MF A01 CSCL 11D

The feasibility of fabricating full-scale fan blades from superhybrid composites (SHC) for use large, commercial gas turbine engines was evaluated. The type of blade construction selected was a metal-spar/SHC-shell configuration, in which the outer shell was adhesively bonded to a short, internal, titanium spar. Various aspects of blade fabrication, inspection, and quality assurance procedures developed in the investigation are described. It is concluded that the SHC concept is feasible for the fabrication of prototype, full-scale, metal-spar/SHC-shell fan blades that have good structural properties and meet dimensional requirements.

R.S.F.

**N85-15822\*#** National Aeronautics and Space Administration. Lewis Research Center, Cleveland, Ohio.

**A STUDY OF INTERPLY LAYER EFFECTS ON THE FREE-EDGE STRESS FIELD OF ANGLEPLY LAMINATES**

P. L. N. MURTHY and C. C. CHAMIS 1984 31 p refs Presented at the Symp. on Adv. and Trends in Struct. Dyn., Washington, D.C., 22-25 Oct. 1984; sponsored by NASA and George Washington Univ. (NASA-TM-86924; E-2201; NAS 1.15:86924) Avail: NTIS HC A03/MF A01 CSCL 11D

The general-purpose finite-element program MSC/NASTRAN is used to study the interply layer effects on the free-edge stress field of symmetric angleply laminates subjected to uniform tensile stress. The free-edge region is modeled as a separate substructure (superelement) which enables easy mesh refinement and provides the flexibility to move the superelement along the edge. The results indicate that the interply layer reduces the stress intensity significantly at the free edge. Another important observation of the study is that the failures observed near free edges of these types of laminates could have been caused by the interlaminar shear stresses.

Author

**N85-15823\*#** National Aeronautics and Space Administration. Lewis Research Center, Cleveland, Ohio.

**DESIGN PROCEDURES FOR FIBER COMPOSITE STRUCTURAL COMPONENTS: PANELS SUBJECTED TO COMBINED IN-PLANE LOADS**

C. C. CHAMIS 1985 29 p refs Presented at the 40th Ann. Conf. of the Society of the Plastics Industry (SPI) Reinforced Plastics/Composites Inst., Atlanta, 28 Jan. - 1 Feb. 1985 (NASA-TM-86909; E-2319; NAS 1.15:86909) Avail: NTIS HC A03/MF A01 CSCL 11D

Step by step procedures are described which can be used to design panels made from fiber composite angleply laminates and subjected to combined in plane loads. The procedures are set up as a multistep sample design. Steps in the sample design procedure range from selection of the laminate configuration to the subsequent analyses required to check design requirements for: (1) displacement, (2) ply stresses, and (3) buckling. The sample design steps are supplemented with appropriate tabular and graphical data which can be used to expedite the design process.

Author

**N85-21266\*** National Aeronautics and Space Administration. Lewis Research Center, Cleveland, Ohio.

**THERMAL BARRIER COATING SYSTEM Patent**

S. STECURA, inventor (to NASA) 27 Nov. 1984 7 p Filed 16 Aug. 1983 Supersedes N83-34014 (21 - 22, p 3601) Continuation-in-part of abandoned US Patent Appl. SN-375784, filed 6 May 1982

(NASA-CASE-LEW-13324-2; NAS 1.71:LEW-13324-2; US-PATENT-4,485,151; US-PATENT-APPL-SN-523297; US-PATENT-CLASS-428-633; US-PATENT-CLASS-428-656; US-PATENT-CLASS-428-678; US-PATENT-CLASS-428-679; US-PATENT-CLASS-428-680; US-PATENT-CLASS-428-681; US-PATENT-CLASS-428-682; US-PATENT-CLASS-428-683; US-PATENT-CLASS-428-684; US-PATENT-APPL-SN-375784) Avail: US Patent and Trademark Office CSCL 11D

A high temperature oxidation resistant, thermal barrier coating system is disclosed for a nickel cobalt, or iron base alloy substrate. An inner metal bond coating contacts the substrate, and a thermal barrier coating covers the bond coating. NiCrAlR, FeCrAlR, and CoCrAlR alloys are satisfactory as bond coating compositions where R=Y or Yb. These alloys contain, by weight, 24.9-36.7% chromium, 5.4-18.5% aluminum, and 0.05 to 1.55% yttrium or 0.05 to 0.53% ytterbium. The coatings containing yttrium are preferred over those containing yttrium. An outer thermal barrier coating of partial stabilized zirconium oxide (zirconia) which is between 6% and 8%, by weight, of yttrium oxide (yttria) covers the bond coating. Partial stabilization provides a material with superior durability. Partially stabilized zirconia consists of mixtures of cubic, tetragonal, and monoclinic phases.

Official Gazette of the U.S. Patent and Trademark Office

**N85-21267\*** National Aeronautics and Space Administration. Lewis Research Center, Cleveland, Ohio.

**DIAMONDLIKE FLAKES Patent**

B. A. BANKS, inventor (to NASA) 22 Jan. 1985 6 p Filed 19 Mar. 1984 Supersedes N84-22696 (22 - 13, p 1953) Continuation-in-part of US Patent-4,437,962, US Patent Appl. SN-495381, filed 17 May 1983

(NASA-CASE-LEW-13837-2; NAS 1.71:LEW-13837-2; US-PATENT-4,495,044; US-PATENT-APPL-SN-591089; US-PATENT-CLASS-204-192C; US-PATENT-CLASS-204-192R; US-PATENT-CLASS-204-192N; US-PATENT-CLASS-423-445; US-PATENT-CLASS-423-446; US-PATENT-CLASS-423-449; US-PATENT-CLASS-427-39; US-PATENT-4,437,962; US-PATENT-APPL-SN-495381) Avail: US Patent and Trademark Office CSCL 11D

A carbon coating was vacuum arc deposited on a smooth surface of a target which was simultaneously ion beam sputtered. The bombarding ions have sufficient energy to create diamond bonds. Spalling occurs as the carbon deposit thickens. The resulting diamond like carbon flakes improve thermal, electrical, mechanical, and tribological properties when used in aerospace structures and components.

Official Gazette of the U.S. Patent and Trademark Office

**N85-21273\*#** National Aeronautics and Space Administration. Lewis Research Center, Cleveland, Ohio.

**NONLINEAR ANALYSIS FOR HIGH-TEMPERATURE MULTILAYERED FIBER COMPOSITE STRUCTURES M.S. Thesis**

D. A. HOPKINS Aug. 1984 120 p refs (NASA-TM-83754; E-2242; NAS 1.15:83754) Avail: NTIS HC A06/MF A01 CSCL 11D

A unique upward-integrated top-down-structured approach is presented for nonlinear analysis of high-temperature multilayered fiber composite structures. Based on this approach, a special purpose computer code was developed (nonlinear COBSTRAN) which is specifically tailored for the nonlinear analysis of tungsten-fiber-reinforced superalloy (TFRS) composite turbine blade/vane components of gas turbine engines. Special features of this computational capability include accounting of: micro- and macro-heterogeneity, nonlinear (stress-temperature-time dependent) and anisotropic material behavior, and fiber degradation. A

## 24 COMPOSITE MATERIALS

demonstration problem is presented to manifest the utility of the upward-integrated top-down-structured approach, in general, and to illustrate the present capability represented by the nonlinear COBSTRAN code. Preliminary results indicate that nonlinear COBSTRAN provides the means for relating the local nonlinear and anisotropic material behavior of the composite constituents to the global response of the turbine blade/vane structure.

Author

**N85-27978\*#** National Aeronautics and Space Administration. Lewis Research Center, Cleveland, Ohio.  
**DESIGNING FOR FIBER COMPOSITE STRUCTURAL DURABILITY IN HYGROTHERMOMECHANICAL ENVIRONMENT**

C. C. CHAMIS 1985 23 p refs Proposed for presentation at the 5th Intern. Conf. on Composite Mater., San Diego, Calif., 30 Jul. - 1 Aug. 1985; sponsored by American Society of Mining Engineers  
(NASA-TM-87045; E-2606; NAS 1.15:87045) Avail: NTIS HC A02/MF A01 CSCL 11D

A methodology is described which can be used to design/analyze fiber composite structures subjected to complex hygrothermomechanical environments. This methodology includes composite mechanics and advanced structural analysis methods (finite element). Select examples are described to illustrate the application of the available methodology. The examples include: (1) composite progressive fracture; (2) composite design for high cycle fatigue combined with hot-wet conditions; and (3) general laminate design.

E.A.K.

**N85-30027\*** National Aeronautics and Space Administration. Lewis Research Center, Cleveland, Ohio.  
**ARC SPRAY FABRICATION OF METAL MATRIX COMPOSITE MONOTAPE Patent**

L. J. WESTFALL, inventor (to NASA) 21 May 1985 7 p Filed 9 Dec. 1983  
(NASA-CASE-LEW-13828-1; US-PATENT-4,518,625; US-PATENT-APPL-SN-560035; US-PATENT-CLASS-427-37; US-PATENT-CLASS-219-76.14; US-PATENT-CLASS-427-178; US-PATENT-CLASS-427-422) Avail: US Patent and Trademark Office CSCL 11D

Arc metal spraying is used to spray liquid metal onto an array of high strength fibers that were previously wound onto a large drum contained inside a controlled atmosphere chamber. This chamber is first evacuated to remove gaseous contaminants and then backfilled with a neutral gas up to atmospheric pressure. This process is used to produce a large size metal matrix composite monotape.

Official Gazette of the U.S. Patent and Trademark Office

**N85-30034\*#** National Aeronautics and Space Administration. Lewis Research Center, Cleveland, Ohio.  
**TEN YEAR ENVIRONMENTAL TEST OF GLASS FIBER/EPOXY PRESSURE VESSELS**

J. R. FADDIOL 1985 18 p refs Presented at the 21st Joint Propulsion Conf., Monterey, Calif., 8-10 Jul. 1985; sponsored by AIAA, SAE, ASME, and ASEE  
(NASA-TM-87058; E-2625; NAS 1.15:87058) Avail: NTIS HC A02/MF A01 CSCL 11D

By the beginning of the 1970's composite pressure vessels had received a significant amount of development effort, and applications were beginning to be investigated. One of the first applications grew out of NASA Johnson Space Center efforts to develop a superior emergency breathing system for firemen. While the new breathing system provided improved wearer comfort and an improved mask and regulator, the primary feature was low weight which was achieved by using a glass fiber reinforced aluminum pressure vessel. Part of the development effort was to evaluate the long term performance of the pressure vessel and as a consequence, some 30 bottles for a test program were procured. These bottles were then provided to NASA Lewis Research Center where they were maintained in an outdoor environment in a pressurized condition for a period of up to 10 yr.

During this period, bottles were periodically subjected to cyclic and burst testing. There was no protective coating applied to the fiberglass/epoxy composite, and significant loss in strength did occur as a result of the environment. Similar bottles stored indoors showed little, if any, degradation. This report contains a description of the pressure vessels, a discussion of the test program, data for each bottle, and appropriate plots, comparisons, and conclusions.

R.J.F.

**N85-30035\*#** Virginia Polytechnic Inst. and State Univ., Blacksburg.  
**A STUDY OF THE STRESS WAVE FACTOR TECHNIQUE FOR THE CHARACTERIZATION OF COMPOSITE MATERIALS Final Report**

A. K. GOVADA, J. C. DUKE, JR., E. G. HENNEKE, II, and W. W. STINCHCOMB Feb. 1985 103 p refs  
(Contract NAG3-172)  
(NASA-CR-174870; NAS 1.26:174870; CCMS-84-13) Avail: NTIS HC A06/MF A01 CSCL 11D

This study has investigated the potential of the Stress Wave Factor as an NDT technique for thin composite laminates. The conventional SWF and an alternate method for quantifying the SWF were investigated. Agreement between the initial SWF number, ultrasonic C-scan, inplane displacements as obtained by full field moire interferometry, and the failure location have been observed. The SWF number was observed to be the highest when measured along the fiber direction and the lowest when measured across the fibers. The alternate method for quantifying the SWF used square root of the zeroth moment (square root of  $M_{00}$ ) of the frequency spectrum of the received signal as a quantitative parameter. From this study it therefore appears that the stress wave factor has an excellent potential to monitor damage development in thin composite laminates.

B.W.

**N85-30037\*#** Massachusetts Inst. of Tech., Cambridge. Dept. of Materials Science and Engineering.  
**STRUCTURAL CHARACTERISTICS OF HIGH TEMPERATURE COMPOSITES Progress Report, Mar. 1984 - Feb. 1985**

J. F. MANDELL 1985 23 p refs  
(Contract NAG3-377)  
(NASA-CR-175998; NAS 1.26:175998) Avail: NTIS HC A02/MF A01 CSCL 11D

A progress report is presented for research carried from March 1984 through February 1985. A tensile test method has been developed which should give tensile and simulated shear (+ or - 45 deg) data for fiber composites up to 1000 C. Longitudinal and some transverse stress-strain data have been obtained for a glass matrix/Nicalon fiber system up to the matrix limiting temperature of 600 C. This demonstrates the functioning of the test method and the high temperature test facility which has been established on this grant. Transverse and longitudinal compression tests have been run, mostly in an end loaded configuration. A more satisfactory compression test is still required, and is under development.

B.W.

**N85-32148\*#** National Aeronautics and Space Administration. Lewis Research Center, Cleveland, Ohio.  
**GRAPHITE/PMR POLYIMIDE COMPOSITES WITH IMPROVED TOUGHNESS**

R. D. VANNUCCI and K. J. BOWLES 1985 15 p refs  
Proposed for presentation at the 17th Natl. SAMPE Tech. Conf., Kiamasha Lake, N.Y., 22-24 Oct. 1985  
(NASA-TM-87081; E-2661; NAS 1.15:87081) Avail: NTIS HC A02/MF A01 CSCL 11D

The toughness of composites made with modified PMR (polymerization of monomer reactants) polyimides and Celion 6000 graphite fibers was studied. Various types/levels of monomer reactants containing flexible links were incorporated into PMR resin compositions used to prepare composites. The composites were evaluated for toughness using instrumented drop weight and 10 deg off axis tensile tests at room temperature, and for strength using flexure and short beam shear tests at room temperature and at elevated temperature. The effect of resin composition on

composite processability, thermo-oxidative stability, toughness and mechanical properties are discussed. Author

**N85-34223\*** National Aeronautics and Space Administration. Lewis Research Center, Cleveland, Ohio.

**MECHANICAL PROPERTIES OF SiC FIBER-REINFORCED REACTION-BONDED Si<sub>3</sub>N<sub>4</sub> COMPOSITES**

R. T. BHATT 1985 14 p refs Presented at the 21st Univ. Conf. on Ceram. Sci., University Park, Pa., 17-19 Jul. 1985; sponsored by Pennsylvania State Univ. Prepared in cooperation with Army Aviation Research and Development Command, Cleveland (NASA-TM-87085; E-2671; NAS 1.15:87085; USAVSCOM-TR-85-C-14) Avail: NTIS HC A02/MF A01 CSCL 11D

The room temperature mechanical and physical properties of silicon carbide fiber reinforced reaction-bonded silicon nitride composites (SiC/RBSN) have been evaluated. The composites contained 23 and 40 volume fraction of aligned 140 micro m diameter chemically vapor deposited SiC fibers. Preliminary results for composite tensile and bend strengths and fracture strain indicate that the composites displayed excellent properties when compared with unreinforced RBSN of comparable porosity. Fiber volume fraction showed little influence on matrix first cracking strain but did influence the stressed required for matrix first cracking and for ultimate composite fracture strength. It is suggested that by reducing matrix porosity and by increasing the volume fraction of the large diameter SiC fiber, it should be possible to further improve the composite stress at which the matrix first cracks. Author

**N85-35233\*** National Aeronautics and Space Administration. Lewis Research Center, Cleveland, Ohio.

**THERMAL BARRIER COATING SYSTEM Patent**

S. STECURA, inventor (to NASA) 13 Aug. 1985 5 p Filed 14 Aug. 1984 Supersedes N84-33595 (22 - 23, p 3724) Continuation-in-part of US Patent-4,485,151, US Patent-Appl-SN-523297, filed 16 Aug. 1983, and continuation-in-part of abandoned US Patent-Appl-SN-375784, filed 6 May 1982

(NASA-CASE-LEW-14057-1; US-PATENT-4,535,033; US-PATENT-4,485,151; US-PATENT-APPL-SN-640712; US-PATENT-APPL-SN-523297; US-PATENT-APPL-SN-375784; US-PATENT-CLASS-428-633; US-PATENT-CLASS-428-656; US-PATENT-CLASS-428-678; US-PATENT-CLASS-428-679; US-PATENT-CLASS-428-680; US-PATENT-CLASS-428-681; US-PATENT-CLASS-428-682) Avail: US Patent and Trademark Office CSCL 11D

An oxide thermal barrier coating comprises ZrO<sub>3</sub>-Yb<sub>2</sub>O<sub>3</sub> that is plasma sprayed onto a previously applied bond coating. The zirconia is partially stabilized with about 124 w/c ytterbia to insure cubic, monoclinic, and terragonal phases.

Official Gazette of the U.S. Patent and Trademark Office

## 25

## INORGANIC AND PHYSICAL CHEMISTRY

Includes chemical analysis, e.g., chromatography; combustion theory; electrochemistry; and photochemistry.

**A85-11892\*** EIC, Inc., Norwood, Mass.

**MODERATE TEMPERATURE SODIUM CELLS. V - DISCHARGE REACTIONS AND RECHARGEABILITY OF NIS AND NIS<sub>2</sub> POSITIVE ELECTRODES IN MOLTEN NaAlCl<sub>4</sub>**

K. M. ABRAHAM and J. E. ELLIOT (EIC Laboratories, Inc., Norwood, MA) Electrochemical Society, Journal (ISSN 0013-4651), vol. 131, Oct. 1984, p. 2211-2217. refs (Contract NAS3-21726)

NiS<sub>2</sub> and NiS have been characterized as high energy density rechargeable positive electrodes for moderate-temperature Na

batteries of the configuration, Na(1)/beta double prime-Al<sub>2</sub>O<sub>3</sub>/NaAlCl<sub>4</sub>(1), NiS<sub>x</sub>. The batteries operate in the temperature range 170 - 190 C. Positive electrode reactions during discharge/charge cycles have been characterized. Excellent rechargeability of the batteries has been demonstrated by extended cell cycling. A Na/NiS<sub>2</sub> cell, operating at 190 C, exceeded 600 deep discharge/charge cycles with practically no capacity deterioration. The feasibility of secondary Na/NiS<sub>x</sub> batteries with specific energies equal to or greater than 50 Wh/lb and cycle lives exceeding 1000 deep discharge/charge cycles has been demonstrated. Author

**A85-11897\*** National Aeronautics and Space Administration. Lewis Research Center, Cleveland, Ohio.

**REACTIONS OF NaCl WITH GASEOUS SO<sub>3</sub>, SO<sub>2</sub>, AND O<sub>2</sub>**

W. L. FIELDER, C. A. STEARNS, and F. J. KOHL (NASA, Lewis Research Center, Cleveland, OH) Electrochemical Society, Journal (ISSN 0013-4651), vol. 131, Oct. 1984, p. 2414-2417. Previously announced in STAR as N83-29358. refs

Hot corrosion of gas turbine engine components involves deposits of Na<sub>2</sub>SO<sub>4</sub> which are produced by reactions between NaCl and oxides of sulfur. For the present investigation, NaCl single crystals were exposed at 100 to 850 C to gaseous mixtures of SO<sub>3</sub>, SO<sub>2</sub>, and O<sub>2</sub>. The products formed during this exposure depend, primarily, on the temperatures. The four product films were: NaCl-SO<sub>3</sub>; Na<sub>2</sub>S<sub>2</sub>O<sub>7</sub>; Na<sub>2</sub>SO<sub>4</sub>; and NaCl-Na<sub>2</sub>SO<sub>4</sub>. The kinetics of the reactions were measured. Author

**A85-12713\*** General Electric Co., Schenectady, N. Y.

**PREDICTION OF AN AXISYMMETRIC COMBUSTING FLOW**

S. M. CORREA (General Electric Co., Schenectady, NY) AIAA Journal (ISSN 0001-1452), vol. 22, Nov. 1984, p. 1602-1608. Previously cited in issue 16, p. 2326, Accession no. A83-36315. refs (Contract NAS3-23525)

**A85-12890\*** Louisiana State Univ., Baton Rouge.

**SYSTEMATIC OPTIMIZATION OF A DETAILED KINETIC MODEL USING A METHANE IGNITION EXAMPLE**

M. FRENKLACH (Louisiana State University, Baton Rouge, LA) Combustion and Flame (ISSN 0010-2180), vol. 58, Oct. 1984, p. 69-72. refs (Contract NAG3-477)

An approach to the systematic optimization of a large-scale dynamic model is proposed which consists in parameterization of simulation results as response surfaces. The optimization procedure is carried out using a second-order orthogonal design. The approach proposed here is demonstrated by an example involving the shock-initiated ignition of methane. V.L.

**A85-13092\*** Kentucky Univ., Lexington.

**GRAVITATIONAL EFFECTS ON FLAMES SPREADING OVER THICK SOLID SURFACES**

M. VEDHA-NAYAGAM and R. A. ALTENKIRCH (Kentucky, University, Lexington, KY) International Astronautical Federation, International Astronautical Congress, 35th, Lausanne, Switzerland, Oct. 7-13, 1984. 8 p. refs (Contract NAG3-258) (IAF PAPER 84-154)

A theoretical model for the downward spread of a flame in the gas over a semi-infinitely thick fuel bed is presented. Gas-phase chemistry is assumed to proceed at an infinite rate while the fuel bed is taken to pyrolyze at the surface in an Arrhenius fashion. Spread rates and flame shapes are computed for two different ambient oxygen concentrations for gravitational accelerations both below and above that of the earth. Predicted spread rates decrease and actual flame size increases with decreasing gravity. Results agree favorably with available, experimental results and expected results from reduced gravity experimentation. Author

## 25 INORGANIC AND PHYSICAL CHEMISTRY

**A85-15614\*** Stonehart Associates, Inc., Madison, Conn.  
**ELECTROCATALYST ADVANCES FOR HYDROGEN OXIDATION IN PHOSPHORIC ACID FUEL CELLS**

P. STONEHART (Stonehart Associates, Inc., Madison, CT) International Journal of Hydrogen Energy (ISSN 0360-3199), vol. 9, no. 11, 1984, p. 921-928.

(Contract DE-AC03-78ET-15365; DEN3-176)

The important considerations that presently exist for achieving commercial acceptance of fuel cells are centered on cost (which translates to efficiency) and lifetime. This paper addresses the questions of electrocatalyst utilization within porous electrode structures and the preparation of low-cost noble metal electrocatalyst combinations with extreme dispersions of the metal. Now that electrocatalyst particles can be prepared with dimensions of 10 Å, either singly or in alloy combinations, a very large percentage of the noble metal atoms in a crystallite are available for reaction. The cost savings for such electrocatalysts in the present commercially driven environment are considerable.

Author

**A85-19548\*#** Washington Univ., Seattle.  
**DIRECT NUMERICAL SIMULATIONS OF A REACTING MIXING LAYER WITH CHEMICAL HEAT RELEASE**

P. A. MCMURTRY, W.-H. JOU, R. W. METCALFE (Flow Industries, Inc., Kent, WA), and J. J. RILEY (Flow Industries, Inc., Kent; Washington, University, Seattle, WA) American Institute of Aeronautics and Astronautics, Aerospace Sciences Meeting, 23rd, Reno, NV, Jan. 14-17, 1985. 9 p. refs

(Contract NAS3-24229)

(AIAA PAPER 85-0143)

In order to study the coupling between chemical heat release and fluid dynamics, direct numerical simulations of a chemically reacting mixing layer with heat release are performed. The fully compressible equations as well as an approximate set of equations that is asymptotically valid for low-Mach-number flows are treated. These latter equations have the computational advantage that high-frequency acoustic waves have been filtered out, allowing much larger time steps to be taken in the numerical solution procedure. A detailed derivation of these equations along with an outline of the numerical solution technique is given. Simulation results indicate that the rate of chemical product formed, the thickness of the mixing layer, and the amount of mass entrained into the layer all decrease with increasing rates of heat release.

Author

**A85-19550\*#** National Aeronautics and Space Administration. Lewis Research Center, Cleveland, Ohio.

**FLAME FLASHBACK IN A PREMIXED DUMP COMBUSTOR**

M. P. PROCTOR (Sverdrup Technology, Inc., Cleveland, OH), D. N. ANDERSON (NASA, Lewis Research Center, Cleveland, OH), and J. S. TIEN (Case Western Reserve University, Cleveland, OH) American Institute of Aeronautics and Astronautics, Aerospace Sciences Meeting, 23rd, Reno, NV, Jan. 14-17, 1985. 11 p. refs

(Contract NAG3-290)

(AIAA PAPER 85-0145)

A stainless steel, rectangular center-dump, premixed-prevapaporized combustor was used at the NASA Lewis Research Center to study flashback in controlled conditions simulating gas turbine combustor operations under steady-state and transient conditions. The combustor allowed visual access to the combustion area, and was operated at inlet air temperatures from 600 to 850 K, premixer wall temperatures from 450 to 900 K, and average premixer velocity from 40 to 80 ft/s. A parametric study revealed a slight decrease in the flashback equivalence ratio as the inlet air temperatures increased. It also indicated that the premixer wall temperature and premixer velocity are not governing parameters of flashback. It is suggested that flashback occurs through the premixer wall boundary layer flow reversal caused by combustion instability.

L.T.

**A85-19607\*#** National Aeronautics and Space Administration. Lewis Research Center, Cleveland, Ohio.

**INTEGRATING CHEMICAL KINETIC RATE EQUATIONS BY SELECTIVE USE OF STIFF AND NONSTIFF METHODS**

K. RADHAKRISHNAN (NASA, Lewis Research Center, Cleveland, OH; Michigan, University, Ann Arbor, MI) American Institute of Aeronautics and Astronautics, Aerospace Sciences Meeting, 23rd, Reno, NV, Jan. 14-17, 1985. 11 p. refs

(AIAA PAPER 85-0237)

The effect of switching between nonstiff and stiff methods on the efficiency of algorithms for integrating chemical kinetic rate equations is presented. Different integration methods are tested by application of the packaged code LSODE to four practical combustion kinetics problems. The problems describe adiabatic, homogeneous gas-phase combustion reactions. It is shown that selective use of nonstiff and stiff methods in different regimes of a typical batch combustion problem is faster than the use of either method for the entire problem. The implications of this result to the development of fast integration techniques for combustion kinetic rate equations are discussed.

Author

**A85-19665\*#** Pennsylvania State Univ., University Park.  
**DROP-TURBULENCE INTERACTIONS IN A DIFFUSION FLAME**

J.-S. SHUEN (Sverdrup Technology, Inc., Cleveland, OH; Pennsylvania State University, University Park, PA), A. S. P. SOLOMON (GM Research Laboratories, Warren, MI; Pennsylvania State University, University Park, PA), and G. M. FAETH (Pennsylvania State University, University Park, PA) American Institute of Aeronautics and Astronautics, Aerospace Sciences Meeting, 23rd, Reno, NV, Jan. 14-17, 1985. 12 p. refs

(Contract NAG3-190)

(AIAA PAPER 85-0319)

A monodisperse stream of methanol drops injected along the axis of a turbulent, methane-fueled diffusion flame burning in still air is studied experimentally and theoretically, in order to determine mean and fluctuating phase velocities, mean drop number flux, drop size distributions, and mean gas phase temperature. Measured values were compared with the predictions of two separated flow analyses, namely deterministic separated flow and stochastic separated flow. The stochastic analysis yielded the best agreement with measurements, due to its providing for the turbulent dispersion of drops.

O.C.

**A85-19666\*#** Flow Research, Inc., Kent, Wash.  
**DIRECT SIMULATIONS OF CHEMICALLY REACTING TURBULENT MIXING LAYERS**

J. J. RILEY (Flow Research Co., Kent; Washington, University, Seattle, WA) and R. W. METCALFE (Flow Research Co., Kent, WA) American Institute of Aeronautics and Astronautics, Aerospace Sciences Meeting, 23rd, Reno, NV, Jan. 14-17, 1985. 16 p. refs

(Contract NAS3-23531)

(AIAA PAPER 85-0321)

The results of direct numerical simulations of chemically reacting mixing layers are presented. The reaction considered is a binary, irreversible reaction with no heat release, so that only the effect of the turbulence on the chemical reaction is investigated. The simulation results are shown to be consistent with similarity theory, and are found to be in approximate agreement with laboratory data, even though there are no adjustable constants in the method.

Author

**A85-23192\*#** Massachusetts Inst. of Tech., Cambridge.  
**METHANOL AS A SOOT REDUCER IN A TURBULENT SWIRLING BURNER**

A. J. IZQUIERDO (Intevep, S. A., Venezuela) and D. P. HOULT (MIT, Cambridge, MA) American Society of Mechanical Engineers and Institute of Electrical and Electronics Engineers, Joint Power Generation Conference, Toronto, Canada, Oct. 1-4, 1984. 6 p. Research supported by Intevep, S.A. refs (Contract NCC3-15) (ASME PAPER 84-JPGC-GT-2)

The combined effect of using methanol as a fuel additive together with a prototype multifuel injector has been evaluated with regard to soot formation in a tubular laboratory burner with a turbulent swirl stabilized diffusion flame. Kerosene, ERBS fuel and Blending Stock with approximately 14,12.8 and 10.3 wt pct of hydrogen respectively were characterized in terms of soot loading at the axial positions  $Z/D = 2.5$  and  $4.0$  and normalized radius  $r/R = +$  or  $0.67$ . Mixtures of ERBS fuel and Blending Stock with 15 and 7.5 wt pct of methanol were also characterized in the same way. Measurements with the plain fuels showed a drastic reduction in soot formation, in the order of one hundred and fifty fold decrease, due to the new injector design. Further reductions by a factor of 2 and 1.5 were accomplished with the mixtures of 15 and 7.5 wt pct of methanol respectively. Author

**A85-23199\*#** National Aeronautics and Space Administration. Lewis Research Center, Cleveland, Ohio.  
**EFFECT OF GRAVITY ON HALOGENATED HYDROCARBON FLAME RETARDANT EFFECTIVENESS**

P. D. RONNEY (NASA, Lewis Research Center, Cleveland, OH) International Astronautical Federation, International Astronautical Congress, 35th, Lausanne, Switzerland, Oct. 7-13, 1984. 13 p. Previously announced in STAR as N84-33536. refs (IAF PAPER 84-156)

Flammability limits, burning velocities, and minimum ignition energies under initially quiescent conditions were measured for stoichiometric and fuel-lean methane-, ethane-, and propane-air mixtures containing varying concentrations of Halon 1301. The characteristics of near-limit flames were strongly affected by fuel type but not Halon concentration. The conclusions were that the mechanism of the flammability limits was affected by fuel type but not Halon concentration, that the zero-g flammability limit is probably related to a stability criterion which is affected mostly by the molecular diffusion characteristics of the reactant gases and is mostly independent of chemical kinetics, and that the one-g upward flammability and ignition limits provide adequate criteria for safety at one-g and zero-g for both uninhibited and inhibited mixtures. Author

**A85-33570\*** National Aeronautics and Space Administration. Lewis Research Center, Cleveland, Ohio.

**HIGH TEMPERATURE OXIDATION OF PROPENE**

A. BURCAT (NASA, Lewis Research Center, Cleveland, OH; Technion Israel Institute of Technology, Haifa, Israel) and K. RADHAKRISHNAN (NASA, Lewis Research Center, Cleveland, OH; Michigan, University, Ann Arbor, MI) Combustion and Flame (ISSN 0010-2180), vol. 60, May 1985, p. 157-169. refs (Contract NAG3-147; NAG3-294)

An ignition delay correlation is established for propene-oxygen-argon mixtures on the basis of over 100 experiments with component concentrations being in the ranges of 0.6-1.6 percent for propene and 2.7-14.4 percent for oxygen diluted in argon. Temperatures in the range of 1274-1840 K were achieved, with average initial pressures ranging from 50 to 133 torr. Furthermore, standard numerical solutions were obtained using LSODE and CHEMEQ integration techniques, covering 59 reactions and 29 species. The partial agreement between the results indicates that the scheme used is adequate but incomplete. Two possible oxidative path-determining loops were identified, though neither was found conclusively superior to the other. L.T.

**A85-33785\*** Spring Arbor Coll., Mich.

**CHEMICAL AND ELECTROCHEMICAL BEHAVIOR OF THE CR(III)/CR(II) HALF-CELL IN THE IRON-CHROMIUM REDOX ENERGY STORAGE SYSTEM**

D. A. JOHNSON (Spring Arbor College, Spring Arbor, MI) and M. A. REID (NASA, Lewis Research Center, Cleveland, OH) Electrochemical Society, Journal (ISSN 0013-4651), vol. 132, May 1985, p. 1058-1062. refs (Contract DE-A104-80AL-12726)

The Cr(III) complexes present in the acidified chromium solutions used in the iron-chromium redox energy storage system have been isolated and identified as  $\text{Cr}(\text{H}_2\text{O})_6(3+)$  and  $\text{Cr}(\text{H}_2\text{O})_5\text{Cl}(2+)$  by ion-exchange chromatography and visible spectrophotometry. The cell reactions during charge-discharge cycles have been followed by means of visible spectrophotometry. The spectral bands were resolved into component peaks and concentrations of the Cr(III) species calculated using Beer's law. During the charge mode,  $\text{Cr}(\text{H}_2\text{O})_5\text{Cl}(2+)$  is reduced to  $\text{Cr}(\text{H}_2\text{O})_5\text{Cl}(+)$ , and during the discharge mode  $\text{Cr}(\text{H}_2\text{O})_5\text{Cl}(+)$  is oxidized back to  $\text{Cr}(\text{H}_2\text{O})_5\text{Cl}(2+)$ . Electrode potential measurements also support this interpretation. Hysteresis effects in the charge-discharge curves can be explained by the slow attainment of equilibrium between  $\text{Cr}(\text{H}_2\text{O})_6(3+)$  and  $\text{Cr}(\text{H}_2\text{O})_5\text{Cl}(2+)$ . Author

**A85-41633\*** National Aeronautics and Space Administration. Lewis Research Center, Cleveland, Ohio.

**AES AND LEED STUDY OF THE ZINC BLENDE SiC(100) SURFACE**

M. DAYAN (NASA, Lewis Research Center, Cleveland, OH) Journal of Vacuum Science and Technology A (ISSN 0734-2101), vol. 3, Mar.-Apr. 1985, p. 361-366. refs

Auger and LEED measurements have been carried out on the (100) surface of zinc blende SiC. Two different phases of the clean surface, in addition to two kinds of oxygen-covered surfaces, have been obtained, identified, and discussed. In the oxygen-covered surface, the oxygen is bonded to the Si. The carbon-rich phase is reconstructed ( $2 \times 1$ ), similar to the (100) clean surfaces of Si, Ge, and diamond. The Si-topped surface is reconstructed. A model of alternating Si dimers is suggested for this surface. Author

**A85-42571\*#** Cornell Univ., Ithaca, N.Y.

**COMBUSTION EFFICIENCY OF A PREMIXED CONTINUOUS FLOW COMBUSTOR**

M. S. ANAND and F. C. GOULDIN (Cornell University, Ithaca, NY) ASME, Transactions, Journal of Engineering for Gas Turbines and Power (ISSN 0022-0825), vol. 107, July 1985, p. 695-705. refs (Contract NSG-3019)

Exhaust gas temperature, velocity, and composition measurements at various radial locations at the combustor exit are presented for a swirling-flow continuous combustor of a confined concentric jet configuration operating on premixed propane or methane and air. The main objective of the study is to determine the effect of fuel substitution and of changes in outer flow swirl conditions on the combustor performance. It is found that there is no difference in observed properties for propane and methane firing; the use of either of the fuels results in nearly the same exit temperature and velocity profiles and the same efficiency for a given operating condition. A mechanism for combustion is proposed which explains qualitatively the changes in efficiency and pollutant emissions observed with changing swirl. V.L.

**A85-47320\*** California Inst. of Tech., Pasadena.

**GROWTH OF A DIFFUSION FLAME IN THE FIELD OF A VORTEX**

F. E. MARBLE (California Institute of Technology, Pasadena) IN: Recent advances in the aerospace sciences. New York, Plenum Press, 1985, p. 395-413. refs (Contract AF-FOSR-80-0265; NAG3-70)

In the present study of the growth of a diffusion flame in the field of a vortex, the motion in the core is converted into a solid

body rotation. The flame extension and distortion kinematics are presented, and the effect of the local flow field on local flame structure is analyzed in detail. The combustion field is found to consist of a totally reacted core region whose radius is time-dependent, and an external flame region which consists of a pair of spiral arms that extend at large radii toward their original positions on the horizontal axis. Two similarity rules are formulated which are independent of kinematic viscosity. O.C.

**A85-48493\*** Case Western Reserve Univ., Cleveland, Ohio.  
**MECHANISM FOR CHELATED SULFATE FORMATION FROM SO<sub>2</sub> AND BIS (TRIPHENYLPHOSPHINE) PLATINUM**

S. P. MEHANDRU and A. B. ANDERSON (Case Western Reserve University, Cleveland, OH) *Inorganic Chemistry* (ISSN 0020-1669), vol. 24, no. 16, 1985, p. 2570-2573. refs  
 (Contract NAG3-341)

Structure and energy surface calculations using the atom superposition and electron delocalization molecular orbital theory show that the first step in the reaction between SO<sub>2</sub> and the dioxygen complex (PPh<sub>3</sub>)<sub>2</sub>PtO<sub>2</sub> is the coordination of SO<sub>2</sub> with one oxygen atom of the complex, followed by metal-oxygen bond breaking and reorientation, leading to a five-membered cyclic structure. This then rearranges to form the bidentate coordinated sulfate. Alternative pathways are considered and are found to be less favorable. Author

**A85-48513\*** Case Western Reserve Univ., Cleveland, Ohio.  
**MECHANISM FOR FORMING HYDROGEN CHLORIDE AND SODIUM SULFATE FROM SULFUR TRIOXIDE, WATER, AND SODIUM CHLORIDE**

A. B. ANDERSON (Case Western Reserve University, Cleveland, OH) *American Chemical Society, Journal* (ISSN 0002-7863), vol. 106, no. 21, 1984, p. 6262-6265. refs  
 (Contract NAG3-341)

A molecular orbital study of sodium sulfate and hydrogen chloride formation from sulfur trioxide, water, and sodium chloride shows no activation barrier, in agreement with recent experimental work of Kohl, Fielder, and Stearns. Two overall steps are found for the process. First, gas-phase water reacts with sulfur trioxide along a pathway involving a linear O-H-O transition state yielding closely associated hydroxyl and bisulfite which rearrange to become a hydrogen sulfate molecule. Then the hydrogen sulfate molecule transfers a hydrogen atom to a surface chloride in solid sodium chloride while an electron and a sodium cation simultaneously transfer to yield sodium bisulfate and gas-phase hydrogen chloride. This process repeats. Both of these steps represent well-known reactions for which mechanisms have not been previously determined. Author

**N85-10138\*** National Aeronautics and Space Administration.  
 Lewis Research Center, Cleveland, Ohio.

**ANALYSIS OF GLOW DISCHARGES FOR UNDERSTANDING THE PROCESS OF FILM FORMATION**

M. VENUGOPALAN (Univ. of Western Illinois, Macomb) and R. AVNI Washington Oct. 1984 127 p refs Submitted for publication  
 (NASA-TM-83750; E-2231; NAS 1.15:83750) Avail: NTIS HC A07/MF A01 CSCL 07D

The physical and chemical processes which occur during the formation of different types of films in a variety of glow discharge plasmas are discussed. Emphasis is placed on plasma diagnostic experiments using spectroscopic methods, probe analysis, mass spectrometric sampling and magnetic resonance techniques which are well suited to investigate the neutral and ionized gas phase species as well as some aspects of plasma surface interactions. The results on metallic, semi-conducting and insulating films are reviewed in conjunction with proposed models and the problem encountered under film deposition conditions. It is concluded that the understanding of film deposition process requires additional experimental information on plasma surface interactions of free radicals and the synergetic effects where photon, electron and ion bombardment change the reactivity of the incident radical with the surface. Author

**N85-11149\*** Illinois Univ., Urbana-Champaign. Dept. of Aeronautical and Astronautical Engineering.

**THE MECHANISMS OF FLAME HOLDING IN THE WAKE OF A BLUFF BODY Final Report**

R. A. STREHLOW and S. MALIK 30 Oct. 1984 194 p refs  
 (Contract NAG3-60)  
 (NASA-CR-174058; NAS 1.26:174058) Avail: NTIS HC A09/MF A01 CSCL 21B

The flame holding mechanism for lean methane and lean propane air flames is examined under conditions where the recirculation zone is absent. The holding process is studied in detail in an attempt to determine the mechanism of flame holding and also the conditions where this mechanism is viable and when it fails and blow off occurs. Inverted flames held in the wake of a flat strip are studied. The velocity flow field is determined using a Laser Doppler Velocimetry technique. Equation of continuity is used to calculate the flame temperature from the change in area of flow streamlines before and after the flame. For methane air flame the controlling factor for blow off is incomplete reaction due to higher blowing rate leading to reduced residence time in the reaction zone. M.A.C.

**N85-13889\*** National Aeronautics and Space Administration.  
 Lewis Research Center, Cleveland, Ohio.

**ELECTROCHEMISTRY AND STORAGE**

L. H. THALLER *In its Space Power* p 95-99 Apr. 1984  
 Avail: NTIS HC A14/MF A01 CSCL 07D

The term electrochemistry implies the use of devices that convert chemical energy into electrical energy and sometimes vice versa. These devices are usually composed of some number of individual cells that are connected together to form a battery. In the cases where these devices cannot be electrically recharged they are usually referred to as primary batteries, whereas if these batteries can be charged and recharged repeatedly, they are called secondary batteries. The past and present uses of primary and secondary batteries in aerospace applications are discussed. R.J.F.

**N85-21283\*** Illinois Univ., Urbana. Dept. of Aeronautical and Astronautical Engineering.

**BEHAVIOR OF THE LEAN METHANE-AIR FLAME AT ZERO-GRAVITY Final Report, Nov. 1983 - Dec. 1984**

K. A. NOE and R. A. STREHLOW Feb. 1985 48 p refs  
 (Contract NCC3-35)  
 (NASA-CR-175586; NAS 1.26:175586; AAE-85-2; UILU-ENG-85-0502) Avail: NTIS HC A03/MF A01 CSCL 21B

A special rig was designed and constructed to be compatible with the NASA Lewis Research Center Airborne Research Laboratory to allow the study of the effect of gravity on the behavior of lean limit in a standard 50.4 mm (2 in.) internal diameter tube when the mixtures are ignited at the open end and propagate towards the closed end of the tube. The lean limit at zero gravity was found to be 5.10% methane and the flame was found to extinguish in a manner previously observed for downward propagating flames at one g. It was observed that g-jitter could be maintained at less than + or 0.04 g on most zero g trajectories. All of propagating lean limit flames were found to be sporadically cellularly unstable at zero g. There was no observable correlation between the occurrence of g-jitter and the lean limit, average propagation speed of the flame through the tube or the occurrence of cellular instability. B.W.

**N85-22644\*** National Aeronautics and Space Administration.  
 Lewis Research Center, Cleveland, Ohio.

**FORMATION OF HIGH MOLECULAR WEIGHT PRODUCTS FROM BENZENE DURING BOUNDARY LUBRICATION**

W. MORALES Apr. 1985 18 p refs  
 (NASA-TM-86966; E-2433; NAS 1.15:86966) Avail: NTIS HC A02/MF A01 CSCL 07D

High molecular weight products were detected on the wear track of an iron disk at the end of a sliding friction and wear test using benzene as a lubricant. Size exclusion chromatography in conjunction with UV analysis gave evidence that the high molecular



weight products are polyphenyl ether type substances. Organic electrochemistry was used to elucidate the possible surface reaction mechanisms. Author

**N85-23941\*#** National Aeronautics and Space Administration. Lewis Research Center, Cleveland, Ohio.

**APPLICATIONS OF HIGH PRESSURE DIFFERENTIAL SCANNING CALORIMETRY TO AVIATION FUEL THERMAL STABILITY RESEARCH Final Report**

M. C. NEVEU (State Univ. of New York, Fredonia) and D. P. STOCKER Apr. 1985 25 p refs (NASA-TM-87002; E-2547; NAS 1.15:87002) Avail: NTIS HC A02/MF A01 CSCL 21D

High pressure differential scanning calorimetry (DSC) was studied as an alternate method for performing high temperature fuel thermal stability research. The DSC was used to measure the heat of reaction versus temperature of a fuel sample heated at a programmed rate in an oxygen pressurized cell. Pure hydrocarbons and model fuels were studied using typical DSC operating conditions of 600 psig of oxygen and a temperature range from ambient to 500 C. The DSC oxidation onset temperature was determined and was used to rate the fuels on thermal stability. Kinetic rate constants were determined for the global initial oxidation reaction. Fuel deposit formation is measured, and the high temperature volatility of some tetralin deposits is studied by thermogravimetric analysis. Gas chromatography and mass spectrometry are used to study the chemical composition of some DSC stressed fuels. E.A.K.

**N85-25444\*#** Louisiana State Univ., Baton Rouge. Dept. of Chemical Engineering.

**SHOCK TUBE STUDY OF THE FUEL STRUCTURE EFFECTS ON THE CHEMICAL KINETIC MECHANISMS RESPONSIBLE FOR SOOT FORMATION, PART 2 Final Report**

M. FRENKLACH, D. W. CLARY, and M. K. RAMACHANDRA May 1985 171 p refs (Contract NAG3-477) (NASA-CR-174880; NAS 1.26:174880) Avail: NTIS HC A08/MF A01 CSCL 21B

Soot formation in oxidation of allene, 1,3-butadiene, vinylacetylene and chlorobenzene and in pyrolysis of ethylene, vinylacetylene, 1-butene, chlorobenzene, acetylen-hydrogen, benzene-acetylene, benzene-butadiene and chlorobenzene-acetylene argon-diluted mixtures was studied behind reflected shock waves. The results are rationalized within the framework of the conceptual models. It is shown that vinylacetylene is much less sooty than allene, which indicates that conjugation by itself is not a sufficient factor for determining the sooting tendency of a molecule. Structural reactivity in the context of the chemical kinetics is the dominant factor in soot formation. Detailed chemical kinetic modeling of soot formation in pyrolysis of acetylene is reported. The main mass growth was found to proceed through a single dominant route composed of conventional radical reactions. The practically irreversible formation reactions of the fused polycyclic aromatics and the overshoot by hydrogen atom over its equilibrium concentration are the g-driving kinetic forces for soot formation. E.A.K.

**N85-28982\*** National Aeronautics and Space Administration. Lewis Research Center, Cleveland, Ohio.

**CHEMICAL CONTROL OF NADIMIDE CURE TEMPERATURE AND RATE Patent**

R. W. LAUVER, inventor (to NASA) 30 Apr. 1985 9 p Filed 22 Jul. 1983 Division of US Patent Appl-SN-404809, filed 3 Aug. 1982, US Patent-4,455,418 (NASA-CASE-LEW-13770-2; US-PATENT-4,514,557; US-PATENT-4,455,418; US-PATENT-APPL-SN-516217; US-PATENT-APPL-SN-404809; US-PATENT-CLASS-528-342; US-PATENT-CLASS-526-262; US-PATENT-CLASS-528-322) Avail: US Patent and Trademark Office CSCL 07D

Polyimide resins suitable for use as composite matrix materials are formed by copolymerization of maleic and norbornenyl endcapped monomers and oligomers. The copolymers can be

cured at temperatures under about 300 C by controlling the available concentration of the maleic end-capped reactant. This control can be achieved by adding sufficient amounts of said maleic reactant, or by chemical modification of either copolymer, so as to either increase Diels-Alder retrogression of the norbornenyl capped reactant and/or holding initiation and polymerization to a rate compatible with the availability of the maleic-capped reactant.

Official Gazette of the U.S. Patent and Trademark Office

**N85-28983\*#** National Aeronautics and Space Administration. Lewis Research Center, Cleveland, Ohio.

**FUEL RICH CATALYTIC COMUSTION: THE FIRST STAGE OF A TWO-STAGE COMBUSTOR**

T. A. BRABBS and S. L. OLSON 1984 12 p refs Presented at Fall Meeting of the Eastern Sect. of the Combust. Inst., Clearwater Beach, Fla., 3-5 Dec. 1984 (NASA-TM-87042; E-2601; NAS 1.15:87042) Avail: NTIS HC A02/MF A01 CSCL 21B

An experimental program demonstrated that fuel-rich catalytic combustion can be accomplished soot free as long as the combustion temperature is less than the temperature at the rich limit of combustion. Although soot was not measured directly, three pieces of data strongly suggest that it was not present: (1) the product gases were completely transparent and produced no radiation characteristic of soot, (2) measured reaction temperatures followed closely those calculated for equilibrium with no soot present, and (3) over 99 percent of the carbon was accounted for in the measured reaction products. Data for two catalyst configurations were taken along with gas samples at two locations downstream of the catalyst bed. Author

**N85-30039\*** National Aeronautics and Space Administration. Lewis Research Center, Cleveland, Ohio.

**CHEMICAL APPROACH FOR CONTROLLING NADIMIDE CURE TEMPERATURE AND RATE Patent**

R. W. LAUVER, inventor (to NASA) 22 Jun. 1985 8 p Filed 14 Dec. 1983 Division of abandoned US Patent Appl-SN-516217, filed 22 Jul. 1983 (NASA-CASE-LEW-13770-6; US-PATENT-4,495,339; US-PATENT-APPL-SN-561434; US-PATENT-APPL-SN-516217; US-PATENT-CLASS-526-262; US-PATENT-CLASS-526-204; US-PATENT-CLASS-526-217; US-PATENT-CLASS-528-314; US-PATENT-CLASS-528-322) Avail: US Patent and Trademark Office CSCL 07D

Polyimide resins suitable for use as composite matrix materials are formed by copolymerization of maleic and norbornenyl end-capped monomers and oligomers. The copolymers can be cured at temperatures under about 300 C. by controlling the available concentration of the maleic end-capped reactant. This control can be achieved by adding sufficient amounts of said maleic reactant, or by chemical modification of either copolymer, to increase Diels-Alder retrogression of the norbornenyl-capped reactant and/or holding initiation and polymerization to a rate compatible with the availability of the maleic-capped reactant.

Official Gazette of the U.S. Patent and Trademark Office

**N85-31244\*#** National Aeronautics and Space Administration. Lewis Research Center, Cleveland, Ohio.

**FUEL-RICH CATALYTIC COMBUSTION: A SOOT-FREE TECHNIQUE FOR IN SITU HYDROGEN-LIKE ENRICHMENT**

T. A. BRABBS and S. L. OLSON Jul. 1985 12 p refs Presented at the Fall Meeting of the Eastern Sect. of the Combust. Inst., Clearwater Beach, Fla., 3-5 Dec. 1984 (NASA-TP-2498; E-2604; NAS 1.60:2498) Avail: NTIS HC A02/MF A01 CSCL 21B

An experimental program on the catalytic oxidation of iso-octane demonstrated the feasibility of the two-stage combustion system for reducing particulate emissions. With a fuel-rich ( $\phi = 4.8$  to 7.8) catalytic combustion preburner as the first stage the combustion process was soot free at reactor outlet temperatures of 1200 K or less. Although soot was not measured directly, its absence was indicated. Reaction products collected at two



## 25 INORGANIC AND PHYSICAL CHEMISTRY

positions downstream of the catalyst bed were analyzed on a gas chromatograph. Comparison of these products indicated that pyrolysis of the larger molecules continued along the drift tube and that benzene formation was a gas-phase reaction. The effective hydrogen-carbon ratio calculated from the reaction products increased by 20 to 68 percent over the range of equivalence ratios tested. The catalytic partial oxidation process also yielded a large number of smaller-containing molecules. The fraction of fuel carbon in compounds having two or fewer carbon atoms ranged from 30 percent at 1100 K to 80 percent at 1200 K. F.M.R.

**N85-32156\*** National Aeronautics and Space Administration. Lewis Research Center, Cleveland, Ohio.

### **SHOCK TUBE MEASUREMENTS OF GROWTH CONSTANTS IN THE BRANCHED-CHAIN ETHANE-CARBON MONOXIDE-OXYGEN SYSTEM**

R. S. BROKAW, T. A. BRABBS, and C. A. SNYDER Jul. 1985 15 p refs

(NASA-TM-87068; E-2574; NAS 1.15:87068) Avail: NTIS HC A02/MF A01 CSCL 07D

Exponential free radical growth constants have been measured for ethane carbon monoxide oxygen mixtures by monitoring the growth of oxygen atom concentration as manifested by CO flame band emission. Data were obtained over the temperature range of 1200 to 1700 K. The data were analyzed using an ethane oxidation mechanism involving seven elementary reaction steps. Calculated growth constants were close to experimental values at lower temperatures, up to about 1400 K, but at higher temperatures computed growth constants were considerably smaller than experiment. In attempts to explain these results additional branching reactions were added to the mechanism. However, these additional reactions did not appreciably change calculated growth constants.

Author

## 26

### **METALLIC MATERIALS**

Includes physical, chemical, and mechanical properties of metals, e.g., corrosion; and metallurgy.

**A85-11058\*** National Aeronautics and Space Administration. Lewis Research Center, Cleveland, Ohio.

### **DEFORMATION AND FRACTURE BEHAVIOR OF NI-MO-AL(GAMMA/GAMMA PRIME-ALPHA) IN SITU COMPOSITE**

A. M. SRIRAMAMURTHY (Defence Metallurgical Research Laboratory, Hyderabad, India) and S. N. TEWARI (NASA, Lewis Research Center, Materials Processing Science Section, Cleveland, OH; Defence Metallurgical Research Laboratory, Hyderabad, India) Metallurgical Transactions A - Physical Metallurgy and Materials Science (ISSN 0360-2133), vol. 15A, Oct. 1984, p. 1905-1919. Research supported by the Ministry of Defence of India. refs

Tensile properties of a directionally solidified (DS) eutectic alloy of the nominal composition Ni-33 Mo-5.7 Al (weight percent) have been investigated both at room temperature and elevated temperatures. The microstructure-mechanical property relationship has been studied for the alloy both in the as-DS and heat-treated conditions. Changes in the yield strength, the work hardening behavior, and the fracture morphology have been explained in terms of the microstructural changes due to the heat treatment. The yield drops observed have been attributed to the microdebonding due to the possible segregation of impurities at the fiber-matrix interface, and partly to the strain aging. The deformation mechanism has been identified to be the cutting of gamma prime particles.

Author

**A85-11070\*** Rensselaer Polytechnic Inst., Troy, N.Y.

### **TOPOLOGICAL REACTION RATE MEASUREMENTS RELATED TO SCUFFING**

J. L. LAUER, S. S. FUNG (Rensselaer Polytechnic Institute, Troy, NY), and W. R. JONES, JR. (NASA, Lewis Research Center, Cleveland, OH) ASLE Transactions, vol. 27, Oct. 1984, p. 288-293; Discussion, p. 293, 294; Authors' Closure, p. 294. Previously announced in STAR as N84-14288. refs

(Contract AF-AFOSR-81-0005; NSG-3180)

A ball-on-plate (both consisting of hardened M-50 steel) sliding elastohydrodynamic contact was run with trimethylolpropane triheptanoate (TMPTH) with and without tricresyl phosphate (TCP). The contact area of the plate was optically profiled with a phase-locked interference microscope (PLIM) both before and after exposure to alcoholic hydrochloric acid. As scuffing was approached, the profile within the contact region changed more rapidly after the acid treatment; after scuffing, it assumed a constant high value. A metallurgical phase found in the scuff mark was apparently responsible for the high reactivity. The microscopic profile changes (sensitivity, + or - 3 nm (+ or - A) in depth) involved primarily the small asperities (radius, 3 microns); the larger ones were unaffected. Soaking the steel in TCP smoothed the fine structure of the surface profile but increased its reactivity toward alcoholic hydrochloric acid before sliding was started. Thus it would appear that PLIM examination could be used for screening potentially scuff-resistant materials.

Author

**A85-11071\*** National Aeronautics and Space Administration. Lewis Research Center, Cleveland, Ohio.

### **FRICTION AND WEAR OF SOME FERROUS-BASE METALLIC GLASSES**

K. MIYOSHI and D. H. BUCKLEY (NASA, Lewis Research Center, Cleveland, OH) ASLE Transactions, vol. 27, Oct. 1984, p. 295-303; Discussion, p. 303; Authors' Closure, p. 303, 304. Previously announced in STAR as N83-19886. refs

Sliding friction experiments, X-ray photoelectron spectroscopy (XPS) analysis, and electron microscopy and diffraction studies were conducted with ferrous base metallic glasses (amorphous alloys) in contact with aluminium oxide at temperatures to 750 C in a vacuum. Sliding friction experiments were also conducted in argon and air atmospheres. The results of the investigation indicate that the coefficient of friction increases with increasing temperature to 350 C in vacuum. The increase in friction is due to an increase in adhesion resulting from surface segregation of boron oxide and/or silicon oxide to the surface of the foil. Above 500 C the coefficient of friction decreased rapidly. The decrease correlates with the segregation of boron nitride to the surface. Contaminants can come from the bulk of the material to the surface upon heating and impart boron oxide and/or silicon oxide at 350 C and boron nitride above 500 C. The segregation of contaminants is responsible for the friction behavior. The amorphous alloys have superior wear resistance to crystalline 304 stainless steel. The relative concentrations of the various constituents at the surfaces of the amorphous alloys are very different from the nominal bulk compositions.

Author

**A85-11603\*** National Aeronautics and Space Administration. Lewis Research Center, Cleveland, Ohio.

### **STRAINRANGE PARTITIONING - A TOTAL STRAIN RANGE VERSION**

G. R. HALFORD and J. F. SALTSMAN (NASA, Lewis Research Center, Cleveland, OH) IN: International Conference on Advances in Life Prediction Methods, Albany, NY, April 18-20, 1983, Proceedings. New York, American Society of Mechanical Engineers, 1983, p. 17-26. Previously announced in STAR as N83-14246. refs

Procedures are presented for expressing the Strainrange Partitioning (SRP) method for creep fatigue life prediction in terms of total strain range. Inelastic and elastic strain-range - life relations are summed to give total strain-range - life relations. The life components due to inelastic strains are dealt with using conventional SRP procedures while the life components due to elastic strains are expressed as families of time-dependent terms

for each type of SRP cycle. Cyclic constitutive material behavior plays an important role in establishing the elastic strain-range life relations as well as the partitioning of the inelastic strains. To apply the approach, however, it is not necessary to have to determine the magnitude of the inelastic strain range. The total strain SRP approach is evaluated and verified using two nickel base superalloys, AF2-1DA and Rene 95. Excellent agreement is demonstrated between observed and predicted cyclic lifetimes with 70 to 80 percent of the predicted lives falling within factors of two of the observed lives. The total strain-range SRP approach should be of considerable practical value to designers who are faced with creep-fatigue problems for which the inelastic strains cannot be calculated with sufficient accuracy to make reliable life predictions by the conventional inelastic strain range SRP approach. Author

**A85-11935\*** National Aeronautics and Space Administration. Lewis Research Center, Cleveland, Ohio.

#### **CAVITATION EROSION SIZE SCALE EFFECTS**

P. V. RAO and D. H. BUCKLEY (NASA, Lewis Research Center, Cleveland, OH) *Wear* (ISSN 0043-1648), vol. 96, July 9, 1984, p. 239-253. refs  
(Contract NCC3-21)

Size scaling in cavitation erosion is a major problem confronting the design engineers of modern high speed machinery. An overview and erosion data analysis presented in this paper indicate that the size scale exponent  $n$  in the erosion rate relationship as a function of the size or diameter can vary from 1.7 to 4.9 depending on the type of device used. There is, however, a general agreement as to the values of  $n$  if the correlations are made with constant cavitation number. Author

**A85-12098\*** Max-Planck-Inst. fuer Metallforschung, Stuttgart (West Germany).

#### **A STUDY OF FATIGUE DAMAGE MECHANISMS IN WASPALOY FROM 25 TO 800 C**

B. A. LERCH (Max-Planck-Institut fuer Metallforschung, Stuttgart, West Germany; Cincinnati, University, Cincinnati, OH), N. JAYARAMAN (Cincinnati, University, Cincinnati, OH), and S. D. ANTOLOVICH (Georgia Institute of Technology, Atlanta, GA) *Materials Science and Engineering* (ISSN 0025-5416), vol. 66, Sept. 15, 1984, p. 151-166. refs  
(Contract NSG-3263)

The objective of the study was to examine the effect of various microstructures on the fatigue and damage accumulation behavior of Waspaloy, a nickel-base alloy commonly used in aircraft engines. Shearing was the dominant deformation mode in specimens with coarse grains and small (50-80 Å) gamma prime particles, whereas Orowan looping was dominant in fine-grained specimens with large (about 900 Å) gamma prime particles. At temperatures up to 500 C, cracks initiated transgranularly, while at 800 C the failure process was intergranular for both coarse-grained and fine-grained specimens. At temperatures above 500 C, a significant decrease in the fatigue life was observed for both coarse-grained and fine-grained material. V.L.

**A85-12789\*** National Aeronautics and Space Administration. Lewis Research Center, Cleveland, Ohio.

#### **DEFORMATION AND EROSION OF F.C.C. METALS AND ALLOYS UNDER CAVITATION ATTACK**

B. C. S. RAO and D. H. BUCKLEY (NASA, Lewis Research Center, Cleveland, OH) *Materials Science and Engineering* (ISSN 0025-5416), vol. 67, Oct. 1984, p. 55-67. refs

Experimental investigations have been conducted to determine the early stages of cavitation attack on 6061-T6 aluminum alloy, electrolytic tough pitch copper, brass, and bronze, all having polycrystalline fcc matrices. The surface profiles and scanning electron micrographs show that the pits are initially formed at the grain boundaries, while the grain surfaces are progressively roughened by multiple slip and twinning. The initial erosion is noted to have occurred from the material in the grain boundaries, as well as by fragmentation of part of the grains. Further erosion occurred by shearing and necking of the surface undulations caused

by plastic deformation. The mean penetration depth, computed on the basis of mass loss, was lowest on the bronze and greatest on the copper. Attention is given to the relation of cavitation attack to grain size, glide stress and stacking fault energy. O.C.

**A85-14959\*** Columbia Univ., New York.

#### **MODELING OF GAMMA/GAMMA-PRIME PHASE EQUILIBRIUM IN THE NICKEL-ALUMINUM SYSTEM**

J. M. SANCHEZ, J. R. BAREFOOT, R. N. JARRETT, and J. K. TIEN (Columbia University, New York, NY) *Acta Metallurgica* (ISSN 0001-6160), vol. 32, Sept. 1984, p. 1519-1525. refs  
(Contract NSF DMR-82-06195; NAG3-57)

A theoretical model is proposed for the determination of phase equilibrium in alloys, taking into consideration dissimilar lattice parameters. Volume-dependent pair interactions are introduced by means of phenomenological Lennard-Jones potentials and the configurational entropy of the system is treated in the tetrahedron approximation of the cluster variation method. The model is applied to the superalloy-relevant, nickel-rich, gamma/gamma-prime phase region of the Ni-Al phase diagram. The model predicts reasonable values for the lattice parameters and the enthalpy of formation as a function of composition, and the calculated phase diagram closely approximates the experimental diagram. Author

**A85-15603\*** National Aeronautics and Space Administration. Lewis Research Center, Cleveland, Ohio.

#### **EFFECTS OF SO<sub>2</sub> AND SO<sub>3</sub> ON THE Na<sub>2</sub>SO<sub>4</sub> INDUCED CORROSION OF NICKEL**

A. K. MISRA (NASA, Lewis Research Center, Materials Div., Cleveland, OH; California, University, Berkeley, CA) and D. P. WHITTLE *Oxidation of Metals* (ISSN 0030-770X), vol. 22, Aug. 1984, p. 1-33. refs  
(Contract DE-AC03-76SF-00098)

The effects of SO<sub>2</sub> and SO<sub>3</sub> in the environment on the hot-corrosion behavior of Ni in the temperature range 750-950 C has been studied. Below the melting point of Na<sub>2</sub>SO<sub>4</sub> (884 C), rapid corrosion takes place by formation of a Na<sub>2</sub>SO<sub>4</sub>-NiSO<sub>4</sub> melt which can penetrate the porous oxide scale and give rise to sulfide information by coming in contact with the metal. The distribution of the sulfides depends on the SO<sub>2</sub> level in the ambient gas. Continued corrosion occurs by a sulfidation-oxidation mechanism. At temperatures above the melting point of Na<sub>2</sub>SO<sub>4</sub>, accelerated degradation occurs via dissolution of the surface scale, followed by reprecipitation of the oxide in a nonprotective form. Author

**A85-19084\*** National Aeronautics and Space Administration. Lewis Research Center, Cleveland, Ohio.

#### **MECHANICAL-CONTACT-INDUCED TRANSFORMATION FROM THE AMORPHOUS TO THE PARTIALLY CRYSTALLINE STATE IN METALLIC GLASS**

K. MIYOSHI and D. H. BUCKLEY (NASA, Lewis Research Center, Cleveland, OH) *Thin Solid Films* (ISSN 0040-6090), vol. 118, 1984, p. 363-373. Previously announced in STAR as N84-20673. refs

Friction and wear tests were conducted with 3.2- and 6.4-millimeter-diameter aluminum oxide spheres sliding, in reciprocating motion, on a Fe<sub>67</sub>Co<sub>18</sub>B<sub>14</sub>Si<sub>1</sub> metallic foil. Crystallites with a size range of 10 to 150 nanometers were produced on the wear surface of the amorphous alloy. A strong interaction between transition metals and metalloids such as silicon and boron results in strong segregation during repeated sliding, provides preferential transition metal-metalloid clustering in the amorphous alloy, and subsequently produces the diffused honeycomb structure formed by dark grey bands and primary crystals, that is, alpha-Fe in the matrix. Large plastic flow occurs on an amorphous alloy surface with sliding and the flow film of the alloy transfers to the aluminum oxide pin surface. Multiple slip bands due to shear deformation are observed on the side of the wear track. Two distinct types of wear debris were observed as a result of sliding: an alloy wear debris, and/or powdery-whiskery oxide debris. A.R.H.

**A85-24667\*** National Aeronautics and Space Administration. Lewis Research Center, Cleveland, Ohio.

# **ION-BEAM NITRIDING OF STEELS**

J. SALIK (NASA, Lewis Research Center, Cleveland, OH) Journal of Applied Physics (ISSN 0021-8979), vol. 57, Feb. 15, 1985, p. 1328-1331. Previously announced in STAR as N84-21719. refs

The application of the ion beam technique to the nitriding of steels is described. It is indicated that the technique can be successfully applied to nitriding. Some of the structural changes obtained by this technique are similar to those obtained by ion nitriding. The main difference is the absence of the iron nitride diffraction lines. It is found that the dependence of the resultant microhardness on beam voltage for super nitralloy is different from that of 304 stainless steel. E.A.K.

**A85-25835\*** Ball Aerospace Systems Div., Boulder, Colo.

# **FRACTURE TOUGHNESS OF HOT-PRESSED BERYLLIUM**

D. D. LEMON (Ball Corp., Ball Aerospace Systems Div., Boulder, CO) and W. F. BROWN, JR. (NASA, Lewis Research Center, Cleveland, OH) Journal of Testing and Evaluation (ISSN 0090-3973), vol. 13, March 1985, p. 152-161. refs

This paper presents the results of an investigation into the fracture toughness, sustained-load flaw growth, and fatigue-crack propagation resistance of S200E hot-pressed beryllium at room temperature. It also reviews the literature pertaining to the influence of various factors on the fracture toughness of hot-pressed beryllium determined using fatigue-cracked specimens. Author

**A85-26158\*** National Aeronautics and Space Administration. Lewis Research Center, Cleveland, Ohio.

# **DUCTILITY IN RAPIDLY SOLIDIFIED NIAL**

D. J. GAYDOSH, R. W. JECH, and R. H. TITRAN (NASA, Lewis Research Center, Cleveland, OH) Journal of Materials Science Letters (ISSN 0261-8028), vol. 4, Feb. 1985, p. 138-140. refs

An attempt is made to refine the grain structure of equiatomic NiAl by means of rapid solidification processing, and to examine the effect of small grain size on room temperature ductility. Free melt spinning was used to produce the rapidly solidified material. Room temperature bend testing of both as-spun and heat-treated NiAl ribbon was conducted by free bending the ribbon around a mandrel of successively smaller diameter until failure occurred. Room-temperature plastic deformation was exhibited both before and after a 1-h heat treatment at 1000 C. Heat treatment increased the observed ductility. O.C.

**A85-27808\*** Virginia Polytechnic Inst. and State Univ., Blacksburg.

# **NEW EUTECTIC ALLOYS AND THEIR HEATS OF TRANSFORMATION**

D. FARKAS (Virginia Polytechnic Institute and State University, Blacksburg, VA) and C. E. BIRCHENALL (Delaware University, Newark, DE) Metallurgical Transactions A - Physical Metallurgy and Materials Science (ISSN 0360-2133), vol. 16A, March 1985, p. 323-328. refs

(Contract NSG-3184)

Eutectic compositions and congruently melting intermetallic compounds in binary and multicomponent systems among common elements such as Al, Ca, Cu, Mg, P, Si, and Zn may be useful for high temperature heat storage. In this work, heats of fusion of new multicomponent eutectics and intermetallic phases are reported, some of which are competitive with molten salts in heat storage density at high temperatures. The method used to determine unknown eutectic compositions combined results of differential thermal analysis, metallography, and microprobe analysis. The method allows determination of eutectic compositions in no more than three steps. The heats of fusion of the alloys were measured using commercial calorimeters, a differential thermal analyzer, and a differential scanning calorimeter. Author

**A85-27812\*#** National Aeronautics and Space Administration. Lewis Research Center, Cleveland, Ohio.

# **ELEVATED TEMPERATURE CREEP-RUPTURE BEHAVIOR OF THE SINGLE CRYSTAL NICKEL-BASE SUPERALLOY NASAIR 100**

M. V. NATHAL (NASA, Lewis Research Center, Cleveland, OH) and L. J. EBERT (Case Western Reserve University, Cleveland, OH) Metallurgical Transactions A - Physical Metallurgy and Materials Science (ISSN 0360-2133), vol. 16A, March 1985, p. 427-439. refs

The creep and rupture behavior of 001-line-oriented single crystals of the nickel-base superalloy NASAIR 100 was investigated at temperatures of 925 and 1000 C. In the stress and temperature ranges studied, the steady state creep rate, time to failure, time to the onset of secondary creep, and the time to the onset of tertiary creep all exhibited power law dependencies on the applied stress. The creep rate exponents for this alloy were between seven and eight, and the modulus-corrected activation energy for creep was approximately 350 kJoule/mole, which was comparable to the measured activation energy for Ostwald ripening of the gamma-prime precipitates. Oriented gamma-prime coarsening to form lamellae perpendicular to the applied stress was very prominent during creep. At 1000 C, the formation of a continuous gamma-gamma-prime lamellar structure was completed during the primary creep stage. Shear through the gamma-gamma-prime interface is considered to be the rate limiting step in the deformation process. Gradual thickening of the lamellae appeared to be the cause of the onset of tertiary creep. At 925 C, the fully developed lamellar structure was not achieved until the secondary or tertiary creep stages. At this temperature, the gamma-gamma-prime lamellar structure did not appear to be as beneficial for creep resistance as at the higher temperature. Author

**A85-31688\*** National Aeronautics and Space Administration. Lewis Research Center, Cleveland, Ohio.

# **CHEMICAL REACTIONS INVOLVED IN THE INITIATION OF HOT CORROSION OF IN-738**

G. C. FRYBURG, F. J. KOHL, and C. A. STEARNS (NASA, Lewis Research Center, Cleveland, OH) Electrochemical Society, Journal (ISSN 0013-4651), vol. 131, Dec. 1984, p. 2985-2997. Previously announced in STAR as N84-28958. refs

Sodium-sulfate-induced hot corrosion of preoxidized IN-738 was studied at 975 C with special emphasis placed on the processes occurring during the long induction period. Thermogravimetric tests were run for predetermined periods of time, and then one set of specimens was washed with water. Chemical analysis of the wash solutions yielded information about water soluble metal salts and residual sulfate. A second set of samples was cross sectioned dry and polished in a nonaqueous medium. Element distributions within the oxide scale were obtained from electron microprobe X-ray micrographs. Evolution of SO was monitored throughout the thermogravimetric tests. Kinetic rate studies were performed for several pertinent processes; appropriate rate constants were obtained from the following chemical reactions:  $\text{Cr}_2\text{O}_3 + 2 \text{Na}_2\text{SO}_4(1) + 3/2 \text{O}_2$  yields  $2 \text{Na}_2\text{CrO}_4(1) + 2 \text{SO}_3(\text{g})$ ;  $\text{TiO}_2 + \text{Na}_2\text{SO}_4(1)$  yields  $\text{Na}_2\text{O}(\text{T}102)\text{n} + 503(\text{g})$ ;  $\text{n T}102 + \text{Na}_2\text{CrO}_4(1)$  yields  $\text{Na}_2(\text{T}102)\text{n} + \text{CrO}_3(\text{g})$ . Author

**A85-32387\*** National Aeronautics and Space Administration. Lewis Research Center, Cleveland, Ohio.

# **INFLUENCE OF COMPOSITION ON THE MICROSTRUCTURE AND MECHANICAL PROPERTIES OF A NICKEL-BASE SUPERALLOY SINGLE CRYSTAL**

M. V. NATHAL (NASA, Lewis Research Center, Cleveland, OH) and L. J. EBERT (Case Western Reserve University, Cleveland, OH) IN: Superalloys 1984; Proceedings of the Fifth International Symposium, Champion, PA, October 7-11, 1984. Warrendale, PA, Metallurgical Society of AIME, 1984, p. 125-133. Previously announced in STAR as N84-17354. refs

(Contract NSG-330)

The effects of cobalt, tantalum, and tungsten contents on the microstructure and mechanical properties of single crystal Mar-M247 were investigated. Elevated temperature tensile and

creep-rupture properties of 001 oriented single crystals were related to microstructural features of the alloys. Substitution of Ni for Co in the high refractory metal alloys increased the lattice mismatch, which was considered to be the cause of the increases in tensile and creep strength. Substitution of Ni for Ta caused large decreases in tensile strength and creep life, consistent with decreases in gamma prime volume fraction, lattice mismatch, and solid solution hardening. Substitution of W for Ta resulted in decreased life at high stresses, which was related to small decreases in mismatch and volume fraction. However, the W substitution resulted in improved life at low stresses, which was related to solid solution strengthening by W. Author

**A85-32388\*** National Aeronautics and Space Administration. Lewis Research Center, Cleveland, Ohio.  
**FACTORS WHICH INFLUENCE DIRECTIONAL COARSENING OF GAMMA-PRIME DURING CREEP IN NICKEL-BASE SUPERALLOY SINGLE CRYSTALS**

R. A. MACKAY (NASA, Lewis Research Center, Cleveland, OH) and L. J. EBERT (Case Western Reserve University, Cleveland, OH) IN: Superalloys 1984; Proceedings of the Fifth International Symposium, Champion, PA, October 7-11, 1984. Warrendale, PA, Metallurgical Society of AIME, 1984, p. 135-144. Previously announced in STAR as N84-17355. refs (Contract NSG-3246)

Changes in the morphology of the gamma prime precipitate were examined as a function of the time during creep at 982 C in 001 oriented single crystals of a Ni-Al-Mo-Ta superalloy. In this alloy, which has a large negative misfit of -0.80 pct., the gamma prime particles link together during creep to form platelets, or rafts, which are aligned with their broad faces perpendicular to the applied tensile axis. The effects of initial microstructure and alloy composition of raft development and creep properties were investigated. Directional coarsening of gamma prime begins during primary creep and continues well after the onset of second state creep. The thickness of the rafts remains constant up through the onset of tertiary creep, a clear indication of the stability of the finely-spaced gamma/gamma prime lamellar structure. The thickness of the rafts which formed was equal to the initial gamma prime size which was present prior to testing. The single crystals with the finest gamma prime size exhibited the longest creep lives, because the resultant rafted structure had a larger number of gamma/gamma prime interfaces per unit volume of material. Reducing the Mo content by only 0.73 wt. pct. increased the creep life by a factor of three, because the precipitation of a third phase was eliminated. Author

**A85-32399\*** Rockwell International Corp., Canoga Park, Calif.  
**THE EFFECT OF MICROSTRUCTURE, TEMPERATURE, AND HOLD-TIME ON LOW-CYCLE FATIGUE OF AS HIP P/M RENE 95**

S. BASHIR (Rockwell International Corp., Rocketdyne Div., Canoga Park, CA) and S. D. ANTOLOVICH (Georgia Institute of Technology, Atlanta, GA) IN: Superalloys 1984; Proceedings of the Fifth International Symposium, Champion, PA, October 7-11, 1984. Warrendale, PA, Metallurgical Society of AIME, 1984, p. 295-307. refs (Contract NSG-3147)

The effects of microstructure, temperature, plastic strain range, and hold time on the low-cycle fatigue (LCF) life were studied for Rene 95, an important Ni base superalloy used in jet engine disks. It was shown that the life could be varied by approximately an order of magnitude at elevated temperatures by simple heat treatments. The life was largest for the microstructure that promoted the most homogeneous deformation mode. The results are explained using the concept of a synergistic interaction between the deformation mode and boundary oxidation. Author

**A85-32400\*** Rensselaer Polytechnic Inst., Troy, N.Y.  
**THE INFLUENCE OF HOLD TIMES ON LCF AND FCG BEHAVIOR IN A P/M NI-BASE SUPERALLOY**

S. J. CHOE, S. V. GOLWALKER, D. J. DUQUETTE, and N. S. STOLOFF (Rensselaer Polytechnic Institute, Troy, NY) IN: Superalloys 1984; Proceedings of the Fifth International Symposium, Champion, PA, October 7-11, 1984. Warrendale, PA, Metallurgical Society of AIME, 1984, p. 309-318. refs (Contract NAG3-22)

The relative importance of creep and environmental interactions in high temperature fatigue behavior has been investigated for as-HIP Rene 95. Strain-controlled low cycle fatigue and load-controlled fatigue crack growth tests were performed at elevated temperatures in argon, followed by fractographic analyses of the fracture surfaces by scanning electron microscopy. Fatigue lives were drastically reduced and crack growth rates increased one hundred fold as a result of superposition of hold times on continuous cycling. A change in fracture mode with hold time also was noted. Chromium oxide was detected on the fracture surface by Auger electron spectroscopy. The drastic changes in fatigue resistance due to hold times were attributed primarily to environmental interactions with fatigue processes. Author

**A85-32412\*** Columbia Univ., New York.  
**EFFECTS OF COBALT ON THE HOT WORKABILITY OF NICKEL-BASE SUPERALLOYS**

R. N. JARRETT, J. P. COLLIER, and J. K. TIEN (Columbia University, New York, NY) IN: Superalloys 1984; Proceedings of the Fifth International Symposium, Champion, PA, October 7-11, 1984. Warrendale, PA, Metallurgical Society of AIME, 1984, p. 455-466. refs (Contract NAG3-57)

The effect of cobalt on the workability of nickel-base superalloys is examined with reference to experimental results for four heats of alloys based on the Nimonic 115 composition with varying amounts of nickel substituted for the nominal 14 percent cobalt. It is shown that Co lowers the gamma-prime solvus, which in turn lowers the Cr<sub>23</sub>C<sub>6</sub> carbide solvus. It is further shown that these solvus temperatures bracket the hot working range for the alloys. However, thermomechanical processing modifications reflecting the effect of Co on the gamma-prime and carbide solvi are shown to restore the workability and the properties of alloys with little or no cobalt. V.L.

**A85-32414\*** Illinois Univ., Urbana.  
**RAPID SOLIDIFICATION AND DYNAMIC COMPACTION OF NI-BASE SUPERALLOY POWDERS**

R. D. FIELD, S. J. HALES, W. O. POWERS, and H. L. FRASER (Illinois, University, Urbana, IL) IN: Superalloys 1984; Proceedings of the Fifth International Symposium, Champion, PA, October 7-11, 1984. Warrendale, PA, Metallurgical Society of AIME, 1984, p. 487-496. Research supported by the United Technologies Corp. and DARPA. refs (Contract NAG3-325)

A Ni-base superalloy containing 13Al-9Mo-2Ta (in at. percent) has been characterized in both the rapidly solidified condition and after dynamic compaction. Dynamically compacted specimens were examined in the as-compacted condition and observations related to current theories of interparticle bonding. In addition, the recrystallization behavior of the compacted material at relatively low temperature (about 0.5-0.75 T<sub>m</sub>) was investigated. Author

**A85-32431\*** National Aeronautics and Space Administration. Lewis Research Center, Cleveland, Ohio.

**CYCLIC OXIDATION BEHAVIOR OF BETA+GAMMA OVERLAY COATINGS ON GAMMA AND GAMMA+GAMMA-PRIME ALLOYS**

J. A. NESBITT (NASA, Lewis Research Center, Cleveland, OH; Michigan Technological University, Houghton, MI), B. H. PILSNER, L. A. CAROL, and R. W. HECKEL (Michigan Technological University, Houston, MI) IN: Superalloys 1984; Proceedings of the Fifth International Symposium, Champion, PA, October 7-11, 1984. Warrendale, PA, Metallurgical Society of AIME, 1984, p. 699-710. refs

(Contract NAG3-244; NAG3-216)

Detailed experimental studies of the cyclic oxidation behavior of low-pressure plasma sprayed beta+gamma coating on gamma-phase Ni-Cr-Al alloys have shown the correlation of weight change, oxide type, and Cr and Al concentration-distance profiles as a function of oxidation time. Of special interest was the transition to breakaway oxidation due to the loss of the Al flux to the oxide and the failure of the coated alloy to form an Al<sub>2</sub>O<sub>3</sub>-rich oxide scale. The experimental results on beta+gamma/gamma coating systems were used as the basis of a numerical model (ternary, semi-infinite, finite-difference analysis) which accurately predicted changes in Cr and Al concentration-distance profiles. The model was used to study parameters critical to enhancing the life of coatings which fail by a combination of Al loss in forming the oxide scale and Al loss via interdiffusion with the substrate alloy. Comparisons of beta+gamma/gamma coating behavior are made to the oxidation of coated gamma+gamma-prime substrates, both ternary Ni-Cr-Al alloys and Mar-M 247-type alloys. Author

**A85-32434\*** National Aeronautics and Space Administration. Lewis Research Center, Cleveland, Ohio.

**ON THE FATIGUE CRACK PROPAGATION BEHAVIOR OF SUPERALLOYS AT INTERMEDIATE TEMPERATURES**

J. GAYDA, R. V. MINER, and T. P. GABB (NASA, Lewis Research Center, Cleveland, OH) IN: Superalloys 1984; Proceedings of the Fifth International Symposium, Champion, PA, October 7-11, 1984. Warrendale, PA, Metallurgical Society of AIME, 1984, p. 731-740. refs

Two superalloys used in gas-turbine disks, Rene 95 and IN-100 were tested in several forms at 0.33 Hz in air, and the results were compared with earlier data on Astroloy to gain a better understanding of the effects of grain size, strength, and alloy composition on the fatigue crack propagation behavior. In addition, selected forms of Rene 95 were tested at 0.33 Hz in vacuum and in air using a cycle with a 120-sec tensile dwell to evaluate the effects of environment and creep. Results of the study emphasize the beneficial effect of large grain size on the fatigue and creep-fatigue crack growth resistance of the superalloys in the temperature range corresponding to the operating temperatures of aircraft gas-turbine engine disk rims. V.L.

**A85-32440\*** Garrett Turbine Engine Co., Phoenix, Ariz. **DEVELOPMENT OF COATED SINGLE-CRYSTAL SUPERALLOY SYSTEMS FOR GAS TURBINE APPLICATIONS**

T. E. STRANGMAN, M. FUJII, and X. NGUYEN-DINH (Garrett Turbine Engine Co., Phoenix, AZ) IN: Superalloys 1984; Proceedings of the Fifth International Symposium, Champion, PA, October 7-11, 1984. Warrendale, PA, Metallurgical Society of AIME, 1984, p. 795-804. refs  
(Contract NAS3-20073)

**A85-37415\*#** National Aeronautics and Space Administration. Lewis Research Center, Cleveland, Ohio.

**THE SUBSTITUTION OF NICKEL FOR COBALT IN HOT ISOSTATICALLY PRESSED POWDER METALLURGY UDIMET 700 ALLOYS**

F. H. HARF (NASA, Lewis Research Center, Cleveland, OH) Metallurgical Transactions A - Physical Metallurgy and Materials Science (ISSN 0360-2133), vol. 16A, June 1985, p. 993-1003. refs

Nickel was substituted in various proportions for cobalt in a series of five hot-isostatically-pressed powder metallurgy alloys based on the UDIMET 700 composition. These alloys were given 5-step heat treatments appropriate for use in turbine engine disks. The resultant microstructures displayed three distinct sizes of gamma-prime particles in a gamma matrix. The higher cobalt-content alloys contained larger amounts of the finest gamma-prime particles, and had the lowest gamma-gamma-prime lattice mismatch. While all alloys had approximately the same tensile properties at 25 and 650 gamma C, the rupture lives at 650 and 760 C peaked in the alloys with cobalt contents between 12.7 and 4.3 pct. Minimum creep rates increased as cobalt contents were lowered, suggesting their correlation with the gamma-prime particle size distribution and the gamma-gamma-prime mismatch. It was also found that, on overaging at temperatures higher than suitable for turbine disk use, the high cobalt-content alloys were prone to sigma phase formation. Author

**A85-39284\*** Garrett Turbine Engine Co., Phoenix, Ariz. **PROGRESS IN THE UTILIZATION OF AN OXIDE-DISPERSION-STRENGTHENED ALLOY FOR SMALL ENGINE TURBINE BLADES**

T. G. BEATTY and P. P. MILLAN (Garrett Turbine Engine Co., Phoenix, AZ) IN: Advanced aerospace materials technology; Proceedings of the Aerospace Congress and Exposition, Long Beach, CA, October 15-18, 1984. Warrendale, PA, Society of Automotive Engineers, Inc., 1984, p. 1-9. refs  
(Contract NAS3-20073)  
(SAE PAPER 841512)

The conventional means of improving gas turbine engine performance typically involves increasing the turbine inlet temperature; however, at these higher operational temperatures the high pressure turbine blades require air-cooling to maintain durability. Air-cooling imposes design, material, and economic constraints not only on the turbine blades but also on engine performance. The use of uncooled turbine blades at increased operating temperatures can offer significantly improved performance in small gas turbine engines. A program to demonstrate uncooled MA6000 high pressure turbine blades in a GTEC TFE731 turbofan engine is being conducted. The project goals include demonstration of the advantages of using uncooled MA6000 turbine blades as compared with cast directionally solidified MAR-M 247 blades. Author

**A85-40275\*** Negev Univ., Beersheva (Israel). **SURFACE HARDENING OF STEEL BY BORIDING IN A COLD RF PLASMA**

I. FINBERG, R. AVNI, A. GRILL (Negev, University, Beersheba, Israel), T. SPALVINS, and D. H. BUCKLEY (NASA, Lewis Research Center, Surface Science Branch, Cleveland, OH) Materials Letters (ISSN 0167-577X), vol. 3, April 1985, p. 187-190. Sponsorship: U.S. - Israel Binational Science Foundation. refs  
(Contract USIBSF-2813/82)

Scanning electron spectroscopy, X-ray diffractometry, Auger electron spectroscopy, and microhardness measurements, are used to study the surfaces of 4340-steel samples that have been borided in a cold RF plasma which had been initiated in a gas mixture of 2.7 percent diborane in Ar. As a result of the dislocation of the diborane in the plasma, boron is deposited on the surface of the steel substrate and two crystalline phases, tetragonal Fe<sub>2</sub>B and orthorhombic FeB, are formed. The formation of boride phases then increases the surface microhardness from 2650 MPa to a maximum value of 7740 MPa. O.C.

**A85-42568\***# National Aeronautics and Space Administration. Lewis Research Center, Cleveland, Ohio.

**EFFECT OF SURFACE CONFIGURATION DURING SOLID PARTICLE IMPINGEMENT EROSION**

P. V. RAO and D. H. BUCKLEY (NASA, Lewis Research Center, Cleveland, OH) ASME, Transactions, Journal of Engineering for Gas Turbines and Power (ISSN 0022-0825), vol. 107, July 1985, p. 661-668. refs

A study of the progression of erosion and its detrimental effects due to solid particle impingement requires a detailed understanding of the erosion process and morphology of real surfaces of ductile metals. A series of experiments was conducted to investigate the erosion characteristics of aluminum alloy surfaces during spherical glass bead and angular crushed glass particle impingement. The effects of particle shape on cylindrical surfaces and surfaces with pre-existing holes and slits were determined. An attempt was made to understand the relationship between erosion rate and pit morphology. Based on the experimental observations, an empirical relationship between erosion rate and volume loss is presented. This technique provides an improved prediction method for a wide spectrum of ductile materials. Author

**A85-42569\***# National Aeronautics and Space Administration. Lewis Research Center, Cleveland, Ohio.

**CHARACTERIZATION OF SOLID PARTICLE EROSION RESISTANCE OF DUCTILE METALS BASED ON THEIR PROPERTIES**

P. V. RAO and D. H. BUCKLEY (NASA, Lewis Research Center, Cleveland, OH) ASME, Transactions, Journal of Engineering for Gas Turbines and Power (ISSN 0022-0825), vol. 107, July 1985, p. 669-678. refs

This paper presents experimental results pertaining to spherical glass bead and angular crushed glass particle impingement. A concept of energy absorption to explain the failure of material is proposed and is correlated with the erosion characteristics of several pure metals. Analyses of extensive erosion data indicate that the properties - surface energy, specific melting energy, strain energy, melting point, bulk modulus, hardness, atomic volume - and the product of the parameters - linear coefficient of thermal expansion x bulk modulus x temperature rise required for melting, and ultimate resilience x hardness - exhibit the best correlations. The properties of surface energy and atomic volume are suggested for the first time for correlation purposes and are found to correlate well with erosion rates at different angles of impingement. It further appears that both energy and thermal properties contribute to the total erosion. Author

**A85-43551\*** National Aeronautics and Space Administration. Lewis Research Center, Cleveland, Ohio.

**DIFFUSION WELDING OF MA 6000 AND A CONVENTIONAL NICKEL-BASE SUPERALLOY**

T. J. MOORE and T. K. GLASGOW (NASA, Lewis Research Center, Cleveland, OH) Welding Journal, Research Supplement (ISSN 0043-2296), vol. 64, Aug. 1985, p. 219-s to 226-s. refs

A feasibility study of diffusion welding the oxide dispersion strengthened (ODS) alloy MA 6000 to itself and to conventional Ni-base superalloy Udimet 700 was conducted. Butt joints between MA 6000 pieces and lap joints between Udimet 700 and the ODS alloy were produced by hot pressing for 1.25 hr at temperatures ranging from 1000 to 1200 C (1832-2192 F) in vacuum. Following pressing, all weldments were heat treated and machined into mechanical property test specimens. While three different combinations of recrystallized and unrecrystallized MA 6000 butt joints were produced, the unrecrystallized to unrecrystallized joint was most successful as determined by mechanical properties and microstructural examination. Failure to weld the recrystallized material probably related to a lack of adequate deformation at the weld interface. While recrystallized MA 6000 could be diffusion welded to Udimet 700 in places, complete welding over the entire lap joint was not achieved, again due to the lack of sufficient deformation at the faying surfaces. Several methods are proposed to promote the intimate contact necessary for diffusion welding MA 6000 to itself and to superalloys. Author

**A85-43979\***# Pratt and Whitney Aircraft Group, East Hartford, Conn.

**APPLICATION OF TWO CREEP FATIGUE LIFE MODELS FOR THE PREDICTION OF ELEVATED TEMPERATURE CRACK INITIATION OF A NICKEL BASE ALLOY**

V. MORENO, D. M. NISSLEY (United Technologies Corp., Pratt and Whitney Group, East Hartford, CT), G. R. HALFORD, and J. F. SALTSMAN (NASA, Lewis Research Center, Cleveland, OH) AIAA, SAE, ASME, and ASEE, Joint Propulsion Conference, 21st, Monterey, CA, July 8-10, 1985. 15 p. refs  
(Contract NAS3-23288)  
(AIAA PAPER 85-1420)

Cyclic Damage Accumulation (CDA) and Total Strain-Strain Range Partitioning (TS-SRP) models for predicting the creep-fatigue crack initiation life of high temperature alloys are presented. The models differ in their fundamental assumptions regarding the controlling parameters for fatigue crack initiation and in the amount of data required to determine model constants. The CDA model represents a ductility exhaustion approach and uses stress quantities to calculate the cyclic fatigue damage. The TS-SRP model is based on the use of total mechanical strain and earlier concepts of the Strain Range Partitioning Method. Both models were applied to a well controlled fatigue data set at a high temperature nickel base alloy, B1900 + Hf, tested at 1600 F and 1800 F. The tests were divided into a baseline data set required to determine model constants and a verification data set for evaluation of the predictive capability of the models. Both models correlated the baseline data set to within factors of two in life, and predicted the verification data set to within a factor of three or better. In addition, sample calculations to demonstrate the application of each model and discussions of the predictive capabilities and areas requiring further development are presented. Author

**A85-44703\*** National Aeronautics and Space Administration. Lewis Research Center, Cleveland, Ohio.

**DENDRITIC SOLIDIFICATION. III - SOME FURTHER REFINEMENTS TO THE MODEL FOR DENDRITIC GROWTH UNDER AN IMPOSED THERMAL GRADIENT**

V. LAXMANAN (NASA, Lewis Research Center, Cleveland, OH) Acta Metallurgica (ISSN 0001-6160), vol. 33, Aug. 1985, p. 1475-1480. refs  
(Contract NAG3-417)

Some further refinements to a simple model for dendritic solidification in a binary alloy melt under an imposed positive thermal gradient are presented. Two new expressions for the dendrite tip undercooling have been obtained and shown to yield a limiting value of  $\Delta T_{sub 0}$  and very small growth rates. Here  $\Delta T_{sub 0}$  is the equilibrium solidification range of the alloy. At very large growth rates, all three tip undercooling expressions reach the same limiting value depending on the value of a dimensionless parameter  $\lambda$  which is related to the effective diffusion distance ahead of the dendrite tip. The predicted tip undercoolings are, however, somewhat lower at intermediate growth rates. An improved calculation for the solute buildup at the dendrite tip due to curvature effects is also included. Author

**A85-44772\*** National Aeronautics and Space Administration. Lewis Research Center, Cleveland, Ohio.

**PM SUPERALLOYS - A TROUBLED ADOLESCENT?**

R. L. DRESHFIELD and H. R. GRAY (NASA, Lewis Research Center, Cleveland, OH) Metal Powder Report (ISSN 0026-0657), vol. 40, March 1985, 6 p. Previously announced in STAR as N84-26785. refs

The history of powder metallurgy P/M superalloy technology is reviewed with a comment on the state of the art, and speculates on the technology's future potential growth and maturity. M.A.C.



**A85-47972\*** Lockheed-California Co., Burbank.

**EFFECT OF LOW TEMPERATURE ON FATIGUE AND FRACTURE PROPERTIES OF Ti-5Al-2.5Sn(ELI) FOR USE IN ENGINE COMPONENTS**

J. T. RYDER (Lockheed-California Co., Burbank) and W. E. WITZELL (General Dynamics Corp., Convair Div., San Diego, CA)  
IN: Fatigue at low temperatures; Proceedings of the Symposium, Louisville, KY, May 10, 1983. Philadelphia, PA, ASTM, 1985, p. 210-237. refs

(Contract NAS3-18896)

Experiments were conducted to evaluate the characteristics of the Ti-5Al-2.5Sn (ELI) alloy used in a fuel pump impeller at cryogenic temperatures. Tension, fracture toughness, and fatigue crack propagation data were collected determining the effect of frequency and load ratio on crack propagation. The results revealed that tensile strength increased significantly at 20 K compared to room temperature and fracture toughness was reduced at cryogenic temperatures. The fatigue crack growth rate was not sensitive to experimental conditions and there were only minimal crack orientation effects. Different frequencies produced no effect. At various temperatures and frequencies a load ratio increase resulted in higher crack growth rates. At low stress intensity levels the fatigue rate for both temperatures was the same; however, at high stress intensity levels the crack growth rate at 20 K increased because of the decrease in fracture toughness. The results correlated well with previous data. I.F.

**N85-10165\*#** National Aeronautics and Space Administration. Lewis Research Center, Cleveland, Ohio.

**MORPHOLOGICAL CHANGES OF GAMMA PRIME PRECIPITATES IN NICKEL-BASE SUPERALLOY SINGLE CRYSTALS Ph.D. Thesis - Case Western Reserve Univ., May 1984**

R. A. MACKAY Jul. 1984 232 p refs

(Contract NSG-3246)

(NASA-TM-83698; E-2156; NAS 1.15:83698) Avail: NTIS HC A11/MF A01 CSCL 11F

Changes in the morphology of the gamma prime precipitate were examined during tensile creep at temperatures between 927 and 1038 C in 001-oriented single crystals of a Ni-Al-Mo-Ta superalloy. In this alloy, which has a large negative misfit of -0.80%, the gamma prime particles link together during creep to form platelets, or rafts, which are aligned with their broad faces perpendicular to the applied tensile axis. The dimensions of the gamma and gamma prime phases were measured as directional coarsening developed in an attempt to trace the changing morphology under various stress levels. In addition, the effects of initial microstructure, as well as slight compositional variations, were related to raft development and creep properties. The results showed that directional coarsening of gamma prime began during primary creep, and under certain conditions, continued to develop after the onset of steady-state creep. The length of the rafts increased linearly with time up to a plateau region. The thickness of the rafts, however, remained equal to the initial gamma prime size at least up through the onset of tertiary creep; this is a clear indication of the stability of the finely-spaced gamma-gamma prime lamellar structure. It was found that the single crystals with the finest gamma prime size exhibited the longest creep lives, because the resultant rafted structure had a larger number of gamma-gamma prime interfaces per unit volume of material. R.J.F.

**N85-10166\*#** Purdue Univ., West Lafayette, Ind.

**EFFECTS OF COBALT, BORON, AND ZIRCONIUM ON THE MICROSTRUCTURE OF UDIMET 738 M.S. Thesis. Final Report**

T. G. NAKANISHI Sep. 1984 76 p refs

(Contract NAG3-59)

(NASA-CR-174762; NAS 1.26:174762) Avail: NTIS HC A05/MF A01 CSCL 11F

A structural study was carried out on Co modified Udimet 738 alloys containing 0.04, 0.10, and 0.20 wt % Zr at 0.01 and 0.03 wt % B levels. Samples in the as-cast and solution-treated conditions were exposed at 843 C to study structural stability.

The structures produced by the interactions of Co, Zr, and B were studied by SEM, X-ray diffraction, and dispersive analysis techniques. The additions of large amounts of Zr and B were found to increase the solidification range of the U-738. Structural changes involved eutectic gamma prime islands, formation of low melting point compounds, and precipitation of borides and Zr rich phases. Boron and zirconium additions did not show substantial changes in mechanical properties. Removal of Co from the alloys resulted in reduction of the matrix solubility for carbon and increase in the gamma prime solvus. Structural instabilities found were continuous grain boundary M23C6 films, MC breakdown, and plate-like phases. Removal of cobalt resulted in a slight decrease in tensile and stress rupture properties. Detailed structural results presented. R.S.F.

**N85-10168\*#** National Aeronautics and Space Administration. Lewis Research Center, Cleveland, Ohio.

**THE EFFECTS OF SEVEN ALLOYING ELEMENTS ON THE MICROSTRUCTURE AND STRESS-RUPTURE BEHAVIOR OF NICKEL-BASE SUPERALLOYS**

D. R. HULL, R. V. MINER, and C. A. BARRETT Oct. 1984 28 p refs

(NASA-TM-83791; E-2287; NAS 1.15:83791) Avail: NTIS HC A03/MF A01 CSCL 11F

Seven alloying elements: Al, Cr, Ti, Nb, Ta, Mo, and W were added at two levels of concentration to produce a series of experimental nickel-base superalloys. Fifty alloys, representing a fraction of a 2 to the 7th power factorial design, were cast, tested, and analyzed. Each alloy's microstructure was characterized by phase extractions, X-ray diffraction, metallography and energy dispersive X-ray spectroscopy. Regression analysis was used to determine the effect of alloying element content on microstructure and stress-rupture life. Author

**N85-11217\*#** National Aeronautics and Space Administration. Lewis Research Center, Cleveland, Ohio.

**THE REACTIONS OF COBALT, IRON AND NICKEL IN SO-2 ATMOSPHERES: SIMILARITIES AND DIFFERENCES**

N. S. JACOBSON and W. L. WORRELL (Pennsylvania Univ., Philadelphia) Jun. 1984 13 p refs Presented at the 3rd Intern. Conf. on Transport in Non-Stoichiometric Compounds, University Park, Pa., 11-15 Jun. 1984

(Contract NSF DMR-79-23647)

(NASA-TM-86868; E-2331; NAS 1.15:86868) Avail: NTIS HC A02/MF A01 CSCL 11F

The reactions of cobalt, iron and nickel in SO<sub>2</sub> atmospheres are reviewed and compared. A mixed oxide-sulfide product layer is observed in all cases. Cobalt and nickel exhibits similar behavior. The observed rates are near the sulfidation rates, and the reaction rate is strongly influenced by the outward diffusion of metal through an interconnected sulfide network. A continuous interconnected sulfide is not observed in the oxide-sulfide scales formed on iron, and the reaction rates are more difficult to summarize. The differences and similarities among the three metals are explained in terms of the absence of scale-gas equilibrium and the ratio of the metal diffusivity in the corresponding oxide and sulfide.

Author

**N85-11221\*#** Case Western Reserve Univ., Cleveland, Ohio. Dept. of Metallurgy and Materials Science.

**THE TRANSIENT OXIDATION OF SINGLE CRYSTAL NIAL+ZR M.S. Thesis. Final Report**

J. K. DOYCHAK Sep. 1983 243 p refs

(Contract NAG3-58)

(NASA-CR-174756; NAS 1.26:174756) Avail: NTIS HC A11/MF A01 CSCL 11F

The 800 C oxidation of oriented single crystals of Zr doped beta-NiAl was studied using transmission electron microscopy. The oxide phases and metal-oxide orientation relationships were determined to characterize the transient stages of oxidation prior to the transformation to or formation of alpha-Al<sub>2</sub>O<sub>3</sub>. On (001) and (012) metal orientations, NiAl<sub>2</sub>O<sub>4</sub> was the first oxide to form followed by delta-Al<sub>2</sub>O<sub>3</sub> which becomes the predominant oxide



phase. All oxides were highly epitaxially related to the metal; the orientation relationships being function of parallel cation close-packed directions in the metal and oxide. On (011) and (111) metal orientations, gamma-Al<sub>2</sub>O<sub>3</sub> became the predominant oxide phase rather than delta-Al<sub>2</sub>O<sub>3</sub>, indicating a structural stability from the highly epitaxial oxides. The relative concentration of aluminum in the oxide scales increased with time indicating preferential gamma- or delta-Al<sub>2</sub>O<sub>3</sub> growth. The striking feature common to the orientation relationships is the alignment of 100 m and 110 ox directions, believed to result from the minimal 3 percent mismatch between the corresponding (100)m and (110)ox planes.

M.G.

**N85-11223\*#** Michigan Technological Univ., Houghton.  
**THE EFFECT OF TANTALUM AND CARBON ON THE STRUCTURE/PROPERTIES OF A SINGLE CRYSTAL NICKEL-BASE SUPERALLOY M.S. Thesis. Final Report**

H. C. NGUYEN Oct. 1984 100 p refs

(Contract NAG3-216)

(NASA-CR-174779; NAS 1.26:174779) Avail: NTIS HC A05/MF A01 CSCL 11F

The microstructure, phase chemistry, and creep and hot tensile properties were studied as a function of tantalum and carbon levels in Mar-M247 type single crystal alloys. Microstructural studies showed that several types of carbides (MC, M<sub>2</sub>3C<sub>6</sub> and M<sub>5</sub>C) are present in the normal carbon (0.10 wt % C) alloys after heat treatment. In general, the composition of the MC carbides changes from titanium rich to tantalum rich as the tantalum level in the alloy increases. Small M<sub>2</sub>3C<sub>6</sub> carbides are present in all alloys. Tungsten rich M<sub>6</sub>C carbides are also observed in the alloy containing no tantalum. No carbides are present in the low carbon (0.01 wt % C) alloy series. The morphology of gamma prime is observed to be sensitive to heat treatment and tantalum level in the alloy. Cuboidal gamma prime is present in all the as cast structures. After heat treatment, the gamma prime precipitates tend to have a more spheroidal like morphology, and this tendency increases as the tantalum level decreases. On prolonged aging, the gamma prime reverts back to a cuboidal morphology or under stress at high temperatures, forms a rafted structure. The weight fraction and lattice parameter of the spheroidal gamma prime increases with increasing tantalum content. Changes in the phase chemistry of the gamma prime matrix and gamma prime have also been analyzed using phase extraction techniques. The partitioning ratio decreases for tungsten and aluminum and increases for tantalum as the tantalum content increases for both alloy series; no significant changes occur in the partitioning ratios of the other alloying elements. A reduction in secondary creep rate and an increase in rupture time result from increasing the tantalum content and decreasing the carbon level.

R.J.F.

**N85-11224\*#** National Aeronautics and Space Administration. Lewis Research Center, Cleveland, Ohio.

**STUDIES ON THE HOT CORROSION OF A NICKEL-BASE SUPERALLOY, UDIMET 700**

A. K. MISRA Nov. 1984 47 p refs

(Contract NCC3-43)

(NASA-TM-86882; E-2314; NAS 1.15:86882) Avail: NTIS HC A03/MF A01 CSCL 11F

The hot corrosion of a nickel-base superalloy, Udimet 700, was studied in the temperature range of 884 to 965 C and with different amounts of Na<sub>2</sub>SO<sub>4</sub>. Two different modes of degradation were identified: (1) formation of Na<sub>2</sub>MoO<sub>4</sub> - MoO<sub>3</sub> melt and fluxing by this melt, and (2) formation of large interconnected sulfides. The dissolution of Cr<sub>2</sub>O<sub>3</sub>, TiO<sub>2</sub> in the Na<sub>2</sub>SO<sub>4</sub> melt does not play a significant role in the overall corrosion process. The conditions for the formation of massive interconnected sulfides were identified and a mechanism of degradation due to sulfide formation is described. The formation of Na<sub>2</sub>MoO<sub>4</sub> - MoO<sub>3</sub> melt requires an induction period and various physiochemical processes during the induction period were identified. The factors affecting the length of the induction period were also examined. The melt penetration through the oxide appears to be the prime mode of

degradation whether the degradation is due to the formation of sulfides or the formation of the Na<sub>2</sub>MoO<sub>4</sub> - MoO<sub>3</sub> melt. Author

**N85-11225\*#** Pratt and Whitney Aircraft, East Hartford, Conn.  
**HOT ISOSTATICALLY PRESSED MANUFACTURE OF HIGH STRENGTH MERL 76 DISK AND SEAL SHAPES Final Report**

D. J. EVANS Jul. 1982 12 p 2 Vol.

(Contract NAS3-20072)

(NASA-CR-165550; NAS 1.26:165550; PWA-5574-149) Avail:

NTIS HC A02/MF A01 CSCL 11F

The performance of a HIP MERL 76 disk installed in an experimental engine and exposed to realistic operating conditions in a 150 hour, 1500 cycle endurance test is examined. Post test analysis, based on visual, fluorescence penetrant and dimensional inspection, indicates that the disk performs satisfactorily. M.A.C.

**N85-12129\*#** National Aeronautics and Space Administration. Lewis Research Center, Cleveland, Ohio.

**EFFECTS OF TIN ON MICROSTRUCTURE AND MECHANICAL BEHAVIOR OF INCONEL 718**

R. L. DRESHFIELD, W. A. JOHNSON, and G. A. MAURER 1984 13 p refs Presented at the TMS-AIME Fall Meeting, Detroit, 17-20 Sep. 1984

(NASA-TM-86866; E-2329; NAS 1.15:86866) Avail: NTIS HC A02/MF A01 CSCL 11F

Columbium, for which the United States is 100 percent import reliant, is of strategic importance to the U.S. aerospace industry. A major amount of the Cb is used in Inconel 718. Should Cb sources be disrupted, it may be desired to use a grade of Cb melting stock having greater Sn content than the preferred vacuum grade. Additions of Sn to Inconel 718 were varied from none added to 1 wt %. The Sn additions below 800 ppm had no detrimental effects on 650 C stress rupture behavior; however, 1-wt % Sn severely degraded both life and ductility. Additions of Sn in excess of 200 ppm were slightly detrimental to the 425 C tensile yield strength and ductility. The Sn additions had no effect on the microstructure of Inconel 718 even after stress rupture testing for over 6000 hr at 650 C.

R.S.F.

**N85-12131\*#** National Aeronautics and Space Administration. Lewis Research Center, Cleveland, Ohio.

**THE EFFECTS OF CR, CO, AL, MO AND TA ON THE CYCLIC OXIDATION BEHAVIOR OF A PROTOTYPE CAST NI-BASE SUPERALLOY BASED ON A 2(5) COMPOSITE STATISTICALLY DESIGNED EXPERIMENT**

C. A. BARRETT 1984 20 p refs Presented at the High Temp. Corrosion in Energy Systems 7, Detroit, 17 Sep. 1984; sponsored by AIME and ASM

(NASA-TM-83784; E-2280; NAS 1.15:83784) Avail: NTIS HC A02/MF A01 CSCL 11F

A series of cast Ni-base superalloys were systematically varied at selected levels of Co, Cr, Mo, Ta, and Al. The elemental levels varied were Mo, 0 to 4 percent; Cr, 6 to 18 percent; Co, 0 to 20 percent; Ta, 0 to 8 percent; and Al, 3.25 to 6.25 percent. The cyclic oxidation resistance was determined from specific weight change data as a function of time for 1 hr cycles in static air at 1100 C. The significant terms in decreasing order of their importance were Al, Ta, Cr<sub>2</sub>, Al-Cr, Cr-Co, Co<sub>2</sub>, Al-Mo, Cr-Mo, Al-Al, and Mo-Ta. The Al term alone accounted for close to 82 percent of the explained variability. The estimating equation showed that the Al level was the most important and should be at its 6.25 wt % maximum value. The Mo and Ta levels should also be at their maximum 4 and 8 wt % respectively. The cobalt composition should be as low as possible, i.e., 0 wt %. The Cr level optimum varies depending on the other 4 levels. The X-ray diffraction results indicate the most protective scales are alumina/aluminate spinel stabilized with a tri-rutile oxide high in Ta and Mo.

R.S.F.

**N85-12132\*#** National Aeronautics and Space Administration. Lewis Research Center, Cleveland, Ohio.

**UNIVERSAL BINDING ENERGY RELATIONS IN METALLIC ADHESION**

J. FERRANTE, J. R. SMITH (General Motors Research Labs.), and J. J. ROSE (Iowa State Univ., Ames) 1984 14 p refs Presented at the Materials Research Society Ann. Meeting, Boston, 27-29 Nov. 1984

(NASA-TM-86889; E-2354; NAS 1.15:86889) Avail: NTIS HC A02/MF A01 CSCL 11F

Rose, Smith, and Ferrante have discovered scaling relations which map the adhesive binding energy calculated by Ferrante and Smith onto a single universal binding energy curve. These binding energies are calculated for all combinations of Al(111), Zn(0001), Mg(0001), and Na(110) in contact. The scaling involves normalizing the energy by the maximum binding energy and normalizing distances by a suitable combination of Thomas-Fermi screening lengths. Rose et al. have also found that the calculated cohesive energies of K, Ba, Cu, Mo, and Sm scale by similar simple relations, suggesting the universal relation may be more general than for the simple free electron metals for which it was derived. In addition, the scaling length was defined more generally in order to relate it to measurable physical properties. Further this universality can be extended to chemisorption. A simple and yet quite accurate prediction of a zero temperature equation of state (volume as a function of pressure for metals and alloys) is presented. Thermal expansion coefficients and melting temperatures are predicted by simple, analytic expressions, and results compare favorably with experiment for a broad range of metals. B.W.

**N85-13006\*#** National Aeronautics and Space Administration. Lewis Research Center, Cleveland, Ohio.

**EFFECT OF HUMIDITY ON FRETTING WEAR OF SEVERAL PURE METALS**

H. GOTO (Cleveland State Univ., Ohio) and D. H. BUCKLEY Dec. 1984 12 p refs

(NASA-TP-2403; E-2184; NAS 1.60:2403) Avail: NTIS HC A02/MF A01 CSCL 11F

Fretting wear experiments with several pure metals were conducted in air at various relative humidity levels. The materials used were iron, aluminum, copper, silver, chromium, titanium, and nickel. Each pure metal had a maximum fretting wear volume at a specific humidity level RH sub max that was not dependent on mechanical factors such as contact load, fretting amplitude, and frequency in the ranges studied. The weight loss due to fretting wear at RH sub max for each pure metal decreased with increasing heat of oxygen adsorption on the metal, indicating that adhesive wear dominated at RH sub max. R.J.F.

**N85-13007\*#** National Aeronautics and Space Administration. Lewis Research Center, Cleveland, Ohio.

**STIRLING MATERIAL TECHNOLOGY**

R. H. TITRAN, J. R. STEPHENS, and C. M. SCHEUERMANN 1984 22 p refs Presented at the 22nd Automotive Technol. Develop. Contractors' Conf. Coord. Meeting, Dearborn, Mich., 29 Oct. - 2 Nov. 1984; sponsored by the Society of Automotive Engineers

(Contract DE-AI01-77CS-51040)

(NASA-TM-86888; DOE/NASA/51040-57; E-2352; NAS 1.15:86888) Avail: NTIS HC A02/MF A01 CSCL 11F

The Stirling engine is an external combustion engine that offers the advantage of high fuel economy, low emissions, low noise, and low vibrations compared to current internal combustion automotive engines. The most critical component from a materials viewpoint is the heater head consisting of the cylinders, heating tubes, and regenerator housing. Materials requirements for the heater head include compatibility with hydrogen, resistance to hydrogen permeation, high temperature oxidation/corrosion resistance, and high temperature creep-rupture and fatigue properties. A materials research and technology program identified the wrought alloys CG-27 and 12RN72 and the cast alloys XF-818, NASAUT 4G-A1, and NASACC-1 as candidate replacements for

the cobalt containing alloys used in current prototype engines. It is concluded that manufacture of the engine is feasible from low cost iron-base alloys rather than the cobalt alloys used in prototype engines. Results of research that lead to this conclusion are presented. R.S.F.

**N85-15877\*#** Massachusetts Inst. of Tech., Cambridge. Dept. of Materials Science and Engineering.

**THERMAL-MECHANICAL FATIGUE CRACK GROWTH IN INCONEL X-750 Final Report**

N. MARCHAND and R. M. PELLOUX Oct. 1984 17 p refs (Contract NAG3-280)

(NASA-CR-174740; NAS 1.26:174740) Avail: NTIS HC A02/MF A01 CSCL 11F

Thermal-mechanical fatigue crack growth (TMFCG) was studied in a gamma-gamma' nickel base superalloy Inconel X-750 under controlled load amplitude in the temperature range from 300 to 650 C. In-phase (T sub max at sigma sub max), out-of-phase (T sub min at sigma sub max), and isothermal tests at 650 C were performed on single-edge notch bars under fully reversed cyclic conditions. A dc electrical potential method was used to measure crack length. The electrical potential response obtained for each cycle of a given wave form and R value yields information on crack closure and crack extension per cycle. The macroscopic crack growth rates are reported as a function of delta K and the relative magnitude of the TMFCG are discussed in the light of the potential drop information and of the fractographic observations. R.S.F.

**N85-15878\*#** National Aeronautics and Space Administration. Lewis Research Center, Cleveland, Ohio.

**OPTIMIZATION OF THE NICRAL-Y/ZRO-Y2O3 THERMAL BARRIER SYSTEM**

S. STECURA 1985 24 p refs Presented at the 87th Ann. Meeting of the American Ceramic Society, Cincinnati, 5-9 May 1985

(NASA-TM-86905; E-2394; NAS 1.15:86905) Avail: NTIS HC A02/MF A01 CSCL 11F

The effects of bond and thermal barrier coating compositions, thicknesses, and densities on air plasma spray deposited Ni-Cr-Al-Y/ZrO2-Y2O3 life were evaluated in cyclic furnace oxidation tests at temperatures from 1110 to 1220 C. An empirical relation was developed to give life as a function of the above parameters. The thermal barrier system tested which had the longest life consisted of Ni-35.0 wt% Cr-5.9 wt% Al-0.95 wt% Y bond coating and ZrO2-6.1 wt% Y2O3 thermal barrier coating. Author

**N85-18124\*#** National Aeronautics and Space Administration. Lewis Research Center, Cleveland, Ohio.

**A STUDY OF SPECTRUM FATIGUE CRACK PROPAGATION IN TWO ALUMINUM ALLOYS. 1: SPECTRUM SIMPLIFICATION**

J. TELESMA and S. D. ANTOLOVICH (Georgia Inst. of Technology) Jan. 1985 16 p refs 2 Vol.

(NASA-TM-86929; E-2348; NAS 1.15:86929) Avail: NTIS HC A02/MF A01 CSCL 11F

The fatigue crack propagation behavior of two commercial Al alloys was studied using spectrum loading conditions characteristics of those encountered at critical locations in high performance fighter aircraft. A tension dominated (TD) and tension compression (TC) spectrum were employed for each alloy. Using a mechanics-based analysis, it was suggested that negative loads could be eliminated for the TC spectrum for low to intermediate maximum stress intensities. The suggestion was verified by subsequent testing. Using fractographic evidence, it was suggested that a further simplification in the spectra could be accomplished by eliminating low and intermediate peak load points resulting in near or below threshold maximum peak stress intensity values. It is concluded that load interactions become more important at higher stress intensities and more plasticity at the crack tip. These results suggest that a combined mechanics/fractographic mechanisms approach can be used to simplify other complex spectra. M.G.

**N85-18125\*#** National Aeronautics and Space Administration. Lewis Research Center, Cleveland, Ohio.

**A STUDY OF SPECTRUM FATIGUE CRACK PROPAGATION IN TWO ALUMINUM ALLOYS. 2: INFLUENCE OF MICROSTRUCTURES**

J. TELESMA and S. D. ANTOLOVICH (Georgia Inst. of Technology) Jan. 1985 19 p refs 2 Vol. (NASA-TM-86930; E-2439; NAS 1.15:86930) Avail: NTIS HC A02/MF A01 CSCL 11F

The important metallurgical factors that influence both constant amplitude and spectrum crack growth behavior in aluminum alloys were investigated. The effect of microstructural features such as grain size, inclusions, and dispersoids was evaluated. It was shown that a lower stress intensities, the I/M 7050 alloy showed better fatigue crack propagation (FCP) resistance than P/M 7091 alloy for both constant amplitude and spectrum testing. It was suggested that the most important microstructural variable accounting for superior FCP resistance of 7050 alloy is its large grain size. It was further postulated that the inhomogeneous planar slip and large grain size of 7050 limit dislocation interactions and thus increase slip reversibility which improves FCP performance. The hypothesis was supported by establishing that the cyclic strain hardening exponent for the 7091 alloy is higher than that of 7050. M.G.

**N85-18126\*#** National Aeronautics and Space Administration. Lewis Research Center, Cleveland, Ohio.

**REPLACEABLE BLADE TURBINE AND STATIONARY SPECIMEN CORROSION TESTING FACILITY**

G. J. SANTORO and F. D. CALFO Jan. 1985 21 p refs (NASA-TM-86931; E-2371; NAS 1.15:86931) Avail: NTIS HC A02/MF A01 CSCL 11F

A facility was constructed to provide relatively low cost testing of hot section turbine blade and vane materials under hot corrosion conditions more akin to service environments. The facility consists of a small combustor whose pressurized gas flow can be directed to either a test section consisting of three small cascaded specimens or to a partial admittance single-stage axial flow turbine. The turbine rotor contains 28 replaceable turbine blades. The combustion gases resulting from the burning of Jet A-I fuel can be seeded with measured amounts of alkali salts. This facility is described here along with preliminary corrosion test results obtained during the final checkout of the facility. Author

**N85-18127\*#** Michigan Technological Univ., Houghton. **THE EFFECT OF TANTALUM ON THE STRUCTURE/PROPERTIES OF TWO POLYCRYSTALLINE NICKEL-BASE SUPERALLOYS: B-1900 + HF MAR-M247 M.S. Thesis, Final Report**

G. M. JANOWSKI Washington Feb. 1985 109 p refs (Contract NAG3-216) (NASA-CR-174847; NAS 1.26:174847) Avail: NTIS HC A06/MF A01 CSCL 11F

The microstructure, phase compositions, and phase fractions were studied in conventionally cast B-1900 + Hf and both conventionally cast and directionally solidified MAR-M247 as a function of tantalum concentration. The hot tensile and creep rupture properties of the solutionized and aged MAR-M247-type alloys were also determined as a function of tantalum level. The effects of tantalum on the microstructure and phase compositions of B-1900 + Hf and MAR-M247 (conventionally cast and directionally solidified) were found to be very similar. The addition of tantalum to the as cast and heat treated alloys was shown to cause the partial replacement of the Hf in the MC carbides by Ta, although the degree of replacement was decreased by the solutionizing and aging heat treatment. The gamma prime and minor phase fractions (primarily MC type carbides) both increased approximately linearly with tantalum concentration. The gamma prime phase compositions were relatively insensitive to tantalum variations with the exception of the tantalum and/or hafnium levels. Bulk tantalum additions increased the tantalum, chromium, and cobalt levels of the gamma phase in both alloy series. The increase in the concentrations of the latter two elements in the gamma phase was a result of the decrease in the gamma phase fraction

with increasing bulk tantalum concentration and constant gamma/gamma prime partitioning ratio. Tantalum additions increased the yield stress and ultimate tensile strength of the directionally solidified MAR-M247 type alloys and had no significant effect on ductility. B.W.

**N85-19072\*#** National Aeronautics and Space Administration. Lewis Research Center, Cleveland, Ohio.

**HIGH TEMPERATURE PROPERTIES OF EQUIATOMIC FEAL WITH TERNARY ADDITIONS**

R. H. TITRAN, K. M. VEDULA (Case Western Reserve Univ.), and G. G. ANDERSON (Case Western Reserve Univ.) 1984 14 p refs Presented at the Fall Meeting of the Mater. Res. Soc., Boston, 26-30 Nov. 1984 (NASA-TM-86938; E-2452; NAS 1.15:86938) Avail: NTIS HC A02/MF A01 CSCL 11F

The aluminide intermetallic compounds are considered potential structural materials for aerospace applications. The B2 binary aluminide FeAl has a melting point in excess of 1500 K, is of simple cubic structure, exists over a wide range of composition with solubility for third elements and is potentially self-protecting in extreme environments. The B2 FeAl compound has been alloyed with 1 to 5 at % ternary additions of Si, Ti, Zr, Hf, Cr, Ni, Co, Nb, Ta, Mo, W, and Re. The alloys were prepared by blending a third elemental powder with prealloyed binary FeAl powder. Consolidation was by hot extrusion at 1250 K. Annealing studies on the extruded rods showed that the third element addition can be classified into three categories based upon the amount of homogenization and the extent of solid solutioning. Constant strain rate compression tests were performed to determine the flow stress as a function of temperature and composition. The mechanical strength behavior was dependent upon the third element homogenization classification. Author

**N85-19073\*#** Michigan Technological Univ., Houghton. **EFFECTS OF MAR-M247 SUBSTRATE (MODIFIED) COMPOSITION ON COATING OXIDATION COATING/SUBSTRATE INTERDIFFUSION M.S. Thesis, Final Report**

B. H. PILSNER Feb. 1985 126 p refs (Contract NAG3-216) (NASA-CR-174851; NAS 1.26:174851) Avail: NTIS HC A07/MF A01 CSCL 11F

The effects of gamma+gamma' Mar-M247 substrate composition on gamma+beta Ni-Cr-Al-Zr coating oxidation and coating/substrate interdiffusion were evaluated. These results were also compared to a prior study for a Ni-Cr-Al-Zr coated gamma Ni-Cr-Al substrate with equivalent Al and Cr atomic percentages. Cyclic oxidation behavior at 1130 C was investigated using change in weight curves. Concentration/distance profiles were measured for Al, Cr, Co, W, and Ta. The surface oxides were examined by X-ray diffraction and scanning electron microscopy. The results indicate that variations of Ta and C concentrations in the substrate do not affect oxidation resistance, while additions of grain boundary strengthening elements (Zr, Hf, B) increase oxidation resistance. In addition, the results indicate that oxidation phenomena in gamma+beta/gamma+gamma' Mar-M247 systems have similar characteristics to the gamma+beta/gamma Ni-Cr-Al system. Author

## 26 METALLIC MATERIALS

**N85-19074\*#** National Aeronautics and Space Administration. Lewis Research Center, Cleveland, Ohio.

### **LOW CYCLE FATIGUE OF MAR-M 200 SINGLE CRYSTALS AT 760 AND 870 DEG C**

W. W. MILLIGAN (Georgia Inst. of Tech., Atlanta), N. JAYARAMAN (Cincinnati Univ.), and R. C. BILL 1984 31 p refs Presented at the TMS-AIME Fall Meeting, Detroit, 17-19 Sep. 1984 Prepared in cooperation with Army Research and Technology Labs., Cleveland

(Contract DA PROJ. 1L1-61101-AH-45)

(NASA-TM-86933; E-2444; NAS 1.15:86933;

USAAVSCOM-TR-85-C-1) Avail: NTIS HC A03/MF A01 CSCL 11F

Fully reversed low cycle fatigue tests were conducted on single crystals of the nickel-base superalloys Mar-M 200 at 760 C and 870 C. At 760 C, planar slip (octahedral) lead to orientation-dependent strain hardening and cyclic lives. Multiple slip crystals strain hardened the most, resulting in relatively high stress ranges and low lives. Single slip crystals strain hardened the least, resulting in relatively low stress ranges and higher lives. A preferential crack initiation site which was related to slip plane geometry was observed in single slip orientated crystals. At 870 C, the trends were quite different, and the slip character was much more homogeneous. As the tensile axis orientation deviated from 001, the stress ranges increased and the cyclic lives decreased. Two possible mechanisms were proposed to explain the behavior: one is based on Takeuchi and Kuramoto's cube cross-slip model, and the other is based on orientation-dependent creep rates. E.A.K.

**N85-19075\*#** National Aeronautics and Space Administration. Lewis Research Center, Cleveland, Ohio.

### **CHARACTERIZATION OF EROSION OF METALLIC MATERIALS UNDER CAVITATION ATTACK IN A MINERAL OIL**

B. C. S. RAO (Case Western Reserve Univ.) and D. H. BUCKLEY 1985 24 p refs Proposed for presentation at the Tribology Conf., Atlanta, 8-10 Oct. 1985; sponsored by the American Society of Lubrication Engineers and the American Society of Mechanical Engineers

(NASA-TM-86934; E-2049-1; NAS 1.15:86934) Avail: NTIS HC A02/MF A01 CSCL 11F

Cavitation erosion and erosion rates of eight metallic materials representing three crystal structures were studied. The erosion experiments were conducted with a 20-kHz ultrasonic magnetostrictive oscillator in a viscous mineral oil. The erosion rates of the metals with an fcc matrix were 10 to 100 times higher than that of an hcp-matrix titanium alloy. The erosion rates of iron and molybdenum, with bcc matrices, were higher than that of the titanium alloy but lower than those of those of the fcc materials. Studies with scanning electron microscopy indicated that the cavitation pits were initially formed at the grain boundaries and precipitates and that the pits formed at the junction of grain boundaries grew faster than the others. Transcrystalline craters formed by cavitation attack over the surface of grains and roughened the surfaces by multiple slip and twinning. Surface roughness measurements showed that the pits that formed over the grain boundaries deepened faster than pits. Computer analysis revealed that a geometric expression describes the nondimensional erosion curves during the time period 0.5 t (sub 0) t 2.5 t (sub 0), where t (sub 0) is the incubation period. The fcc metals had very short incubation periods; the titanium alloy had the longest incubation period. Author

**N85-19076\*#** National Aeronautics and Space Administration. Lewis Research Center, Cleveland, Ohio.

### **THE B2 ALUMINIDES AS ALTERNATIVE MATERIALS**

J. R. STEPHENS 1984 26 p refs Presented at the Fall Meeting of the Mater. Res. Soc., Boston, 26-30 Nov. 1984

(NASA-TM-86937; E-2451; NAS 1.15:86937) Avail: NTIS HC A03/MF A01 CSCL 11F

The potential of the B2 aluminides as structural material alternatives for the strategic element containing superalloys currently used in gas turbine engines is being explored with

emphasis on the equiatomic Fe and Ni aluminides. Although Co is a strategic material, the equiatomic Co aluminide is also being studied to gain a more complete understanding of these fourth period intermetallics. Research focuses on initial processing techniques such as ingot melting, power metallurgy, and rapid solidification with and without additional thermomechanical processing; high temperature deformation - primarily compressive creep; compositional effects within the binary B2 aluminides; third-element alloying addition effects on high temperature strength and oxidation resistance, and near room temperature ductility as influenced by processing, alloying, and grain size. Various programs now underway are reviewed and some highlights of research results are presented. A.R.H.

**N85-19078\*#** IIT Research Inst., Chicago, Ill.

### **CREEP-RUPTURE BEHAVIOR OF IRON SUPERALLOYS IN HIGH-PRESSURE HYDROGEN Quarterly Narrative Report, 7 Dec. 1982 - 28 Feb. 1983**

S. BHATTACHARYYA and W. PETERMAN Jun. 1984 44 p (Contract DEN3-303)

(NASA-CR-174411; NAS 1.26:174411; IITRI-M06116-3; QNR-1)

Avail: NTIS HC A03/MF A01 CSCL 11F

The creep-rupture properties of five iron-base and one cobalt-base high temperature alloys were investigated to assess the feasibility of using the alloys as construction materials in a Stirling engine. The alloys were heat treated and hardness measurements were taken. Typical microstructures of the alloys are shown. The creep-rupture properties of the alloys were determined at 760 and 815 C in 15.0 MPa H<sub>2</sub> for 200 to 1000 hours. Plots of rupture life versus stress for the six superalloys are presented along with creep strain-time plots. R.S.F.

**N85-20041\*#** Michigan Technological Univ., Houghton.

### **A STUDY OF INTERDIFFUSION IN BETA + GAMMA/GAMMA + GAMMA PRIME NI-CR-AL M.S. Thesis. Final Report**

L. A. CAROL Feb. 1985 191 p refs

(Contract NAG3-244)

(NASA-CR-174852; NAS 1.26:174852) Avail: NTIS HC A09/MF A01 CSCL 11F

Ternary diffusion in the NiCrAl system at 1200 C was studied with beta + gamma/gamma + gamma prime infinite diffusion couples. Interdiffusion resulted in the formation of complex, multiphase diffusion zones. Concentration/distance profiles for Cr and Al in the phases present in the diffusion zone were measured after 200 hr. The Ni-rich portion of the NiCrAl phase diagram (1200 C) was also determined. From these data, bulk Cr and Al profiles were calculated and translated to diffusion paths on the ternary isotherm. Growth layer kinetics of the layers present in the diffusion zone were also measured. B.G.

**N85-20042\*#** National Aeronautics and Space Administration. Lewis Research Center, Cleveland, Ohio.

### **RAPIDLY SOLIDIFIED NIAL AND FEAL**

D. J. GAYDOSH and M. A. CRIMP 1984 10 p refs

(NASA-TM-86941; E-2289; NAS 1.15:86941) Avail: NTIS HC A02/MF A01 CSCL 11F

Melt spinning was used to produce rapidly solidified ribbons of the B2 intermetallics NiAl and FeAl. Both Fe-40Al and Fe-45Al possessed some bend ductility in the as spun condition. The bend ductility of Fe-40Al, Fe-45Al, and equiatomic NiAl increased with subsequent heat treatment. Heat treatment at approximately 0.85 T (sub m) resulted in significant grain growth in equiatomic FeAl and in all the NiAl compositions. Low bend ductility in both FeAl and NiAl generally coincided with intergranular failure, while increased bend ductility was characterized by increasing amounts of transgranular cleavage fracture. Author

**N85-20043\*#** National Aeronautics and Space Administration.  
Lewis Research Center, Cleveland, Ohio.  
**THE RESPONSE OF COBALT-FREE UDIMET 700 TYPE ALLOY  
TO MODIFIED HEAT TREATMENTS**

F. H. HARF 28 Feb. 1985 27 p refs Presented at the  
114th Ann. Meeting of the Am. Inst. of Mining, Met. and Petrol.  
Engr., New York, 24-28 Feb. 1985  
(NASA-TM-86942; E-2335; NAS 1.15:86942) Avail: NTIS HC  
A03/MF A01 CSCL 11F

A superalloy based on Udimet 700, in which all of the cobalt was replaced by nickel, was prepared from hot isostatically pressed prealloyed powders. This material was given various heat treatments consisting of partial solutioning and aging in a sequence of four different temperatures. Comparisons were made of microstructures and mechanical properties. Best results were obtained by partially solutioning at 1145 deg C and aging through a sequence of 870, 1030, 650 and 760 deg C. This heat treatment also provided significantly improved properties for wrought material of the same composition. The results suggest that cobalt free Udimet 700 should be considered as a substitute for Udimet 700 with the standard 17 percent cobalt content. R.J.F.

**N85-21320\*#** Case Western Reserve Univ., Cleveland, Ohio.  
**EFFECT OF REDUCTION OF STRATEGIC COLUMBIUM  
ADDITION IN 718 ALLOY ON THE STRUCTURE AND  
PROPERTIES Final Report**

K. R. ZIEGLER and J. F. WALLACE Jan. 1985 179 p refs  
(Contract NAG3-268)  
(NASA-CR-174841; NAS 1.26:174841) Avail: NTIS HC A09/MF  
A01 CSCL 11F

A series of alloys was developed having a base composition similar to Inconel 718, with reduced Cb levels of 3.00 and 1.10 wt% Cb. Substitutions of 3.0% W, 3.0W + 0.9V or Mo increased from 3.0% to 5.8% were made for the Cb in these alloys. Two additional alloys, one containing 3.49% Cb and 1.10% Ti and another containing 3.89% Cb and 1.29% Ti were also studied. Tensile properties at room and elevated temperatures, stress-rupture tests, and an analysis of extracted phases were carried out for each of the alloys. Additions of solid solution elements to a reduced Cb alloy had no significant effect on the properties of the alloys under either process condition. The solution and age alloys with substitutions of 1.27% i at 3.89% Cb had tensile properties similar to those of the original alloy and stress-rupture properties superior to the original alloy. The improved stress-rupture properties were the result of significant precipitation of Ni<sub>3</sub>Ti-gamma prime in the alloy, which is more stable than gamma' at the elevated temperatures. At lower temperatures, the new alloy benefits from gamma' strengthening. With more precise control and proper processing, the reduced Cb direct-age alloy could substitute for Alloy 718 in high strength applications. A.R.H.

**N85-21321\*#** National Aeronautics and Space Administration.  
Lewis Research Center, Cleveland, Ohio.  
**DIGITAL TEMPERATURE AND VELOCITY CONTROL OF MACH  
0.3 ATMOSPHERIC PRESSURE DURABILITY TESTING BURNER  
RIGS IN LONG TIME, UNATTENDED CYCLIC TESTING**

D. L. DEADMORE Mar. 1985 37 p refs  
(NASA-TM-86959; E-2484; NAS 1.15:86959) Avail: NTIS HC  
A03/MF A01 CSCL 11F

Hardware and software were developed to implement the hybrid digital control of two Jet A-1 fueled Mach 0.3 burners from startup to completion of a preset number of hot corrosion flame durability cycle tests of materials at 1652 F. This was accomplished by use of a basic language programmable microcomputer and data acquisition and control unit connected together by the IEEE-488 Bus. The absolute specimen temperature was controlled to + or - 3 F by use of digital adjustment of the fuel flow using a P-I-D (Proportional-Integral-Derivative) control algorithm. The specimen temperature was within + or - 2 F of the set point more than 90 percent of the time. Pressure control was achieved by digital adjustment of the combustion air flow using a proportional control algorithm. The burner pressure was controlled at 1.0 + or - 0.02

psig. Logic schemes were incorporated into the system to protect the test specimen from abnormal test conditions in the event of a hardware or software malfunction. Author

**N85-21322\*#** National Aeronautics and Space Administration.  
Lewis Research Center, Cleveland, Ohio.

**ALLOYS BASED ON NIAL FOR HIGH TEMPERATURE  
APPLICATIONS**

K. M. VEDULA (Case Western Reserve Univ.), V. PATHARE, I. ASLANIDIS (Case Western Reserve Univ.), and R. H. TITRAN 1984 13 p refs Presented at the 1984 Fall Meeting of Materials Research Society, Boston, 26-30 Nov. 1984  
(NASA-TM-86976; E-2513; NAS 1.15:86976) Avail: NTIS HC  
A02/MF A01 CSCL 11F

The NiAl alloys for potential high temperature applications were studied. Alloys were prepared by powder metallurgy techniques. Flow stress values at slow strain rates and high temperatures were measured. Some ternary alloying additions (Hf, Ta and Nb) were identified. The mechanism of strengthening in alloys containing these additions appears to be a form of particle dislocation interaction. The effects of grain size and stoichiometry in binary alloys are also presented. E.A.K.

**N85-21323\*#** National Aeronautics and Space Administration.  
Lewis Research Center, Cleveland, Ohio.

**EFFECTS OF CHROMIUM AND ALUMINUM ON MECHANICAL  
AND OXIDATION PROPERTIES OF IRON-NICKEL-BASE  
SUPERALLOYS BASED ON CG-27**

S. R. SCHUON Mar. 1985 26 p refs Presented at the  
TMS-AIME Fall Meeting, Detroit, 17-20 Sep. 1984  
(NASA-TP-2443; E-2320; NAS 1.60:2443) Avail: NTIS HC  
A03/MF A01 CSCL 11F

The effects of chromium and aluminum on the mechanical and oxidation properties of a series of gamma-prime-strengthened alloys based on CG-27 were studied. Gamma-prime dispersion and solid-solution strengthening were the principal modes of alloy strengthening. The oxidation attack parameter K sub a decreased with increasing Cr and Al contents for each alloy group based on Al content. As a group, alloys with 3 wt % Al had the lowest attack parameters. Therefore, 3 wt % is the optimum level of Al for parabolic oxidation behavior. Spalling, due to diffusion-induced grain growth, was controlled by the overall Cr and Al levels. The alloy with 4 wt % Cr and 3 wt % Al had stress-rupture properties superior to those of the base alloy, CG-27, and maintained parabolic oxidation behavior while the Cr content was reduced by two-thirds of its value in cast CG-27. E.A.K.

**N85-21324\*#** National Aeronautics and Space Administration.  
Lewis Research Center, Cleveland, Ohio.

**ION-BEAM NITRIDING OF STEELS Patent Application**

J. SALIK and T. E. HUBBELL, JR., inventors (to NASA) 16 Oct. 1984 12 p  
(NASA-CASE-LEW-14104-1; NAS 1.71:LEW-14104-1;  
US-PATENT-APPL-SN-661481) Avail: NTIS HC A02/MF A01  
CSCL 11F

A surface of a steel substrate is nitrided by exposing it to a beam of nitrogen ions under a low pressure. The pressure is much lower than that employed for ion-nitriding, and an ion source is used instead of a glow discharge. Both of these features reduce the introduction of impurities into the substrate surface. NASA

**N85-22660\*#** National Aeronautics and Space Administration. Lewis Research Center, Cleveland, Ohio.

**ORIENTATION AND TEMPERATURE DEPENDENCE OF SOME MECHANICAL PROPERTIES OF THE SINGLE-CRYSTAL NICKEL-BASE SUPERALLOY RENE N4. 3:**

**TENSION-COMPRESSION ANISOTROPY**

R. V. MINER, T. P. GAAB, J. GAYDA, and K. J. HEMKER (Cincinnati Univ.) 1985 21 p refs Presented at the 114th Ann. meeting of the American Inst. of Mining, Metallurgical and Petroleum Engineers, New York, 24-28 Feb. 1985

(NASA-TM-86982; E-2525; NAS 1.15:86982) Avail: NTIS HC A02/MF A01 CSCL 11F

Single crystal superalloy specimens with various crystallographic directions along their axes were tested in compression at room temperature, 650, 760, 870, and 980 deg C. These results are compared with the tensile behavior studied previously. The alloy, Rene N4, was developed for gas turbine engine blades and has the nominal composition 3.7 Al, 4.2 Ti, 4 Ta, 0.5 Nb, 6 W, 1.5 Mo 9 Cr. 7.5 Co, balance Ni, in weight percent. Slip trace analysis showed that primary cube slip occurred even at room temperature for the 111 specimens. With increasing test temperature more orientations exhibited primary cube slip, until at 870 deg C only the 100 and 011 specimens exhibited normal octahedral slip. The yield strength for octahedral slip was numerically analysed using a model proposed by Lall, Chin, and Pope to explain deviations from Schmid's Law in the yielding behavior of a single phase Gamma prime alloy, Ni<sub>3</sub>(Al, Nb). The Schmid's Law deviations in Rene N4 were found to be largely due to a tension-compression anisotropy. A second effect, which increases strength for orientations away from 001, was found to be small in Rene N4. Analysis of recently published data on the single crystal superalloy PWA 1480 yielded the same result. R.J.F.

**N85-22661\*#** Georgia Inst. of Tech., Atlanta. School of Physics.

**STUDY OF THE EFFECTS OF IMPLANTATION ON THE HIGH FE-NI-CR AND NI-CR-AL ALLOYS Final Report**

M. W. RIBARSKY 12 Apr. 1985 36 p refs

(Contract NAG3-255)

(NASA-CR-175625; NAS 1.26:175625) Avail: NTIS HC A03/MF A01 CSCL 11F

A theoretical study of the effects of implantation on the corrosion resistance of Fe-Ni-Cr and Ni-Cr-Al alloys was undertaken. The purpose was to elucidate the process by which corrosion scales form on alloy surfaces. The experiments dealt with Ni implanted with Al, exposed to S at high temperatures, and then analyzed using scanning electron microscopy, scanning Auger spectroscopy and X-ray fluorescence spectroscopy. Pair bonding and tight-binding models were developed to study the compositions of the alloys and as a result, a new surface ordering effect was found which may exist in certain real alloys. With these models, the behavior of alloy constituents in the presence of surface concentrations of O or S was also studied. Improvements of the models to take into account the important effects of long- and short-range ordering were considered. The diffusion kinetics of implant profiles at various temperatures were investigated, and it was found that significant non-equilibrium changes in the profiles can take place which may affect the implants' performance in the presence of surface contaminants. R.J.F.

**N85-26962\*#** Connecticut Univ., Storrs.

**IRON RICH LOW COST SUPERALLOYS Ph.D. Thesis. Final Report**

S. F. WAYNE Cleveland May 1985 169 p refs

(Contract NAG3-271)

(NASA-CR-174900; NAS 1.26:174900) Avail: NTIS HC A08/MF A01 CSCL 11F

An iron-rich low-cost superalloy was developed. The alloy, when processed by conventional chill casting, has physical and mechanical properties that compare favorably with existing nickel and cobalt based superalloys while containing significantly lower amounts of strategic elements. Studies were also made on the properties of Cr(20)-Mn(10)-C(3.4)-Fe(bal.), a eutectic alloy

processed by chill casting and directional solidification which produced an aligned microstructure consisting of M7C<sub>3</sub> fibers in a gamma-Fe matrix. Thermal expansion of the M7C<sub>3</sub> (M = Fe, Cr, Mn) carbide lattice was measured up to 800 C and found to be highly anisotropic, with the a-axis being the predominant mode of expansion. Repetitive impact sliding wear experiments performed with the Fe rich eutectic alloy showed that the directionally solidified microstructure greatly improved the alloy's wear resistance as compared to the chill cast microstructure and conventional nickel base superalloys. Studies on the molybdenum cementite phase prove that the crystal structure of the xi phase is not orthorhombic. The crystal structure of the xi phase is made up of octahedra building elements consisting of four Mo and two Fe atoms and trigonal prisms consisting of four Fe and two Mo atoms. The voids are occupied by carbon atoms. The previous chemical formula for the molybdenum cementite MoFe<sub>2</sub>C is now clearly seen to be Mo<sub>12</sub>Fe<sub>22</sub>C<sub>10</sub>. Author

**N85-26963\*#** National Aeronautics and Space Administration. Lewis Research Center, Cleveland, Ohio.

**PROPERTIES AND MICROSTRUCTURES FOR DUAL ALLOY COMBINATIONS OF THREE SUPERALLOYS WITH ALLOY 901**

F. H. HARF 1985 43 p refs Presented at the 114th Ann. Meeting of the Am. Inst. of Mining, Met. and Petroleum Engr., New York, 24-28 Feb. 1985

(NASA-TM-86987; E-2397; NAS 1.15:86987) Avail: NTIS HC A03/MF A01 CSCL 11F

Dual alloy combinations have potential for use in aircraft engine components such as turbine disks where a wide range of stress and temperature regimes exists during operation. Such alloy combinations may directly result in the conservation of elements which are costly or not available domestically. Preferably, a uniform heat treatment yielding good properties for both alloys should be used. Dual alloy combinations of iron rich Alloy 901 with nickel base superalloys Rene 95, Astroloy, or MERL 76 were not isostatically pressed from prealloyed powders. Individual alloys, alloy mixtures, and layered alloy combinations were given the heat treatments specified for their use in turbine disks or appropriate for Alloy 901. Selected specimens were overaged for 1500 hr at 650 C. Metallographic examinations revealed the absence of phases not originally present in either alloy of a combination. Mechanical tests showed adequate properties in combinations of Rene 95 or Astroloy with Alloy 901 when given the Alloy 901 heat treatment. Combinations with MERL 76 had better properties when given the MERL 76 heat treatment. The results indicate that these combinations are promising candidates for use in turbine disks. Author

**N85-26964\*#** National Aeronautics and Space Administration. Lewis Research Center, Cleveland, Ohio.

**MULTIAXIAL AND THERMOMECHANICAL FATIGUE CONSIDERATIONS IN DAMAGE TOLERANT DESIGN**

G. E. LEESE (TRW, Inc., Cleveland) and R. C. BILL 1985 21 p refs Presented at the 60th Meeting of the Struct. and Mater. Panel, San Antonio, 21-26 Apr. 1985; sponsored by AGARD Prepared in cooperation with Army Research and Technology Labs., Cleveland

(NASA-TM-87022; E-2514; NAS 1.15:87022;

USAAVSCOM-TR-85-C-5; AD-A157112) Avail: NTIS HC A02/MF A01 CSCL 11F

In considering damage tolerant design concepts for gas turbine hot section components, several challenging concerns arise: Complex multiaxial loading situations are encountered; Thermomechanical fatigue loading involving very wide temperature ranges is imposed on components; Some hot section materials are extremely anisotropic; and coatings and environmental interactions play an important role in crack propagation. The effects of multiaxiality and thermomechanical fatigue are considered from the standpoint of their impact on damage tolerant design concepts. Recently obtained research results as well as results from the open literature are examined and their implications for damage tolerant design are discussed. Three important needs required to advance analytical capabilities in support of damage tolerant design



become readily apparent: (1) a theoretical basis to account for the effect of nonproportional loading (mechanical and mechanical/thermal); (2) the development of practical crack growth parameters that are applicable to thermomechanical fatigue situations; and (3) the development of crack growth models that address multiple crack failures. Author

**N85-31283\*#** National Aeronautics and Space Administration. Lewis Research Center, Cleveland, Ohio.

**ADVANCED THERMAL BARRIER SYSTEM BOND COATINGS FOR USE ON NI, CO-, AND FE-BASE ALLOY SUBSTRATES**

S. STECURA Jul. 1985 22 p refs

(NASA-TM-87062; E-2437; NAS 1.15:87062) Avail: NTIS HC A02/MF A01 CSCL 11F

New and improved Ni-, Co-, and Fe-base bond coatings have been identified for the ZrO<sub>2</sub>-Y<sub>2</sub>O<sub>3</sub> thermal barrier coatings to be used on Ni-, Co-, and Fe-base alloy substrates. These bond coatings were evaluated in a cyclic furnace between 1120 and 1175 C. It was found that MCrAlYb (where M = Ni, Co, or Fe) bond coating thermal barrier systems. The longest life was obtained with the FeCrAlYb thermal barrier system followed by NiCrAlYb and CoCrAlYb thermal barrier systems in that order. Author

**N85-31284\*#** National Aeronautics and Space Administration. Lewis Research Center, Cleveland, Ohio.

**A MULTIPLE LINEAR REGRESSION ANALYSIS OF HOT CORROSION ATTACK ON A SERIES OF NICKEL BASE TURBINE ALLOYS**

C. A. BARRETT Jul. 1985 21 p refs

(NASA-TM-87020; E-2491; NAS 1.15:87020) Avail: NTIS HC A02/MF A01 CSCL 11F

Multiple linear regression analysis was used to determine an equation for estimating hot corrosion attack for a series of Ni base cast turbine alloys. The U transform (i.e.,  $1/\sin (\% A/100)$ ) to the  $1/2$  was shown to give the best estimate of the dependent variable,  $y$ . A complete second degree equation is described for the centered weight chemistries for the elements Cr, Al, Ti, Mo, W, Nb, Ta, and Co. In addition linear terms for the minor elements C, B, and Zr were added for a basic 47 term equation. The best reduced equation was determined by the stepwise selection method with essentially 13 terms. The Cr term was found to be the most important accounting for 60 percent of the explained variability hot corrosion attack. Author

**N85-32173\*#** Case Western Reserve Univ., Cleveland, Ohio. Dept. of Chemistry.

**WHY CO BONDS SIDE-ON AT LOW COVERAGE AND BOTH SIDE-ON AND UPRIGHT AT HIGH COVERAGE ON THE CR(110) SURFACE**

S. P. MEHANDRU and A. B. ANDERSON 1985 16 p refs

(Contract NAG3-341)

(NASA-CR-176071; NAS 1.26:176071) Avail: NTIS HC A02/MF A01 CSCL 11F

An atom superposition and electron delocalization molecular orbital study of CO adsorption on the Cr(110) surface shows a high coordinate lying down orientation is favored. This is a result of the large number of empty d-band energy levels in chromium, which allows the antibonding counterparts to sigma and pi donation bonds to the surface to be empty. When lying down, backbonding to CO pi\* orbitals is enhanced. Repulsive interactions cause additional CO to stand upright at  $1/4$  monolayer coverage. The results confirm the recent experimental study of Shinn and Madey. Author

**N85-32174\*#** Case Western Reserve Univ., Cleveland, Ohio. Dept. of Chemistry.

**MOLECULAR ORBITAL STUDIES IN OXIDATION: SULFATE FORMATION AND METAL-METAL OXIDE ADHESION Final Report, 30 Oct. 1982 - 31 Jul. 1985**

A. B. ANDERSON 31 Jul. 1985 5 p refs

(Contract NAG3-341)

(NASA-CR-176070; NAS 1.26:176070) Avail: NTIS HC A02/MF A01 CSCL 11F

The chemical mechanisms for sulfate formation from sodium chloride and sulfur trioxide, which is a product of jet fuel combustion was determined. Molten sodium sulfate leads to hot corrosion of the protective oxide layers on turbine blades. How yttrium dopants in nickel-aluminum alloys used in turbine blades reduce the spalling rate of protective alumina films and enhance their adhesion was also determined. Two other sulfate mechanisms were deduced and structure of carbon monoxide on a clean chromium and clean platinum-titanium alloys surfaces was determined. All studies were by use of the atom superposition and electron delocalization molecular orbital (ASED-MO) theory. Seven studies were completed. Their titles and abstracts are given. Author

**N85-32175\*#** Case Western Reserve Univ., Cleveland, Ohio. Dept. of Chemistry.

**ADSORPTION OF O<sub>2</sub>, SO<sub>2</sub>, AND SO<sub>3</sub> ON NICKEL OXIDE. MECHANISM FOR SULFATE FORMATION**

S. P. MEHANDRU (Delhi Univ., India) and A. B. ANDERSON 1985 28 p refs

(Contract NAG3-341)

(NASA-CR-176072; NAS 1.26:176072) Avail: NTIS HC A03/MF A01 CSCL 11F

Calculations based on the atom superposition and electron delocalization molecular orbital (ASED-MO) technique suggest that O<sub>2</sub> will adsorb preferentially end-on at an angle 45 deg from normal on a nickel cation site on the (100) surface of NiO. SO<sub>2</sub> adsorption is also stronger on the nickel site; SO<sub>2</sub> bonds through the sulfur atom is a plane perpendicular to the surface. Adsorption energies for SO<sub>3</sub> on the nickel and oxygen sites are comparable in the preferred orientation in which the SO<sub>3</sub> plane is parallel to the surface. On activation, SO<sub>3</sub> adsorbed to an O<sub>2</sub>(-) site forms a trigonal pyramidal SO<sub>4</sub> species which yields, with a low barrier, a tetrahedral sulfate anion. Subsequently the anion reorients on the surface. Possibilities for alternative mechanisms which require the formation of Ni<sup>3+</sup> or O<sub>2</sub>(-) are discussed. NiSO<sub>4</sub> thus formed leads to the corrosion of Ni at high temperatures in the SO<sub>2</sub>+O<sub>2</sub>/SO<sub>3</sub> The SO<sub>2</sub>+O<sub>2</sub>/SO<sub>3</sub> atmosphere, as discussed in the experimental literature. Author

**N85-32176\*#** Case Western Reserve Univ., Cleveland, Ohio. Dept. of Chemistry.

**CO ADSORPTION ON (111) AND (100) SURFACES OF THE PT SUB 3 TI ALLOY. EVIDENCE FOR PARALLEL BINDING AND STRONG ACTIVATION OF CO**

S. P. MEHANDRU, A. B. ANDERSON, and P. N. ROSS (California Univ., Lawrence Berkeley Lab.) 1985 25 p refs

(Contract NAG3-341; DE-AC03-76SF-00098)

(NASA-CR-176077; NAS 1.26:176077) Avail: NTIS HC A02/MF A01 CSCL 11F

The CO adsorption on a 40 atom cluster model of the (111) surface and a 36 atom cluster model of the (100) surface of the Pt<sub>3</sub>Ti alloy was studied. Parallel binding to high coordinate sites associated with Ti and low CO bond scission barriers are predicted for both surfaces. The binding of CO to Pt sites occurs in an upright orientation. These orientations are a consequence of the nature of the CO pi donation interactions with the surface. On the Ti sites the orbitals donate to the nearly empty Ti 3d band and the antibonding counterpart orbitals are empty. On the Pt sites, however, they are in the filled Pt 5d region of the alloy band, which causes CO to bond in a vertical orientation by 5 delta donation from the carbon end. E.A.K.



**N85-34265\*#** National Aeronautics and Space Administration. Lewis Research Center, Cleveland, Ohio.

**ALUMINUM WORK FUNCTION: EFFECT OF OXIDATION, MECHANICAL SCRAPING AND ION BOMBARDMENT**

P. VINET, T. LEMOGNE (Ecole Centrale de Lyon), and H. MONTES (Ecole Centrale de Lyon) 1985 17 p refs Presented at Eurotrib 85, 4th Intern. Tribology Symp., Lyon, 9-12 Sep. 1985; sponsored by La Societe Francaise de Tribologie and the International Tribology Council (NASA-TM-87079; E-2657; NAS 1.15:87079) Avail: NTIS HC A02/MF A01 CSCL 11F

Surface studies have been performed on aluminum polycrystalline surfaces which have been mechanically scraped. Such studies were initiated in order to understand surface effects occurring in tribological processes which involve rubbing surfaces and the effects of adsorption of oxygen. To characterize the surfaces, the following three different experimental approaches have been used: (1) X.P.S. (X-ray photoelectron spectroscopy), in order to check the cleanliness of the surfaces and follow the adsorption and oxidation kinetics; (2) Analysis of the work function changes by following the energy spectra of secondary electrons emitted under low energy electron bombardment; and (3) Analysis of photoemission intensities under U.V. excitation. The reference state being chosen to be the surface cleaned by ion bombardment and exposures to oxygen atmospheres have been shown to lower the work function of clean polycrystalline aluminum by 1.2 eV. The oxygen pressure is found to affect only the kinetics of these experiments. Mechanical scraping has been shown to induce a decrease (0.3 eV) in the work function, which could sharply modify the kinetics of adsorption on the surface. Author

**N85-34266\*#** National Aeronautics and Space Administration. Lewis Research Center, Cleveland, Ohio.

**MICROSTRUCTURES IN RAPIDLY SOLIDIFIED NI-MO ALLOYS**

N. JAYARAMAN (Cincinnati Univ.), S. N. TEWARI, K. J. HEMKER, and T. K. GLASGOW 1985 8 p refs Presented at the Intern. Conf. on Rapidly Solidified Mater., San Diego, Calif., 3-5 Feb. 1985; sponsored by the American Society for Metals (NASA-TM-87100; E-2694; NAS 1.15:87100) Avail: NTIS HC A02/MF A01 CSCL 11F

Ni-Mo alloys of compositions ranging from pure Ni to Ni-40 at % Mo were rapidly solidified by Chill Block Melt Spinning in vacuum and were examined by optical metallography, X-ray diffraction and transmission electron microscopy. Rapid solidification resulted in an extension of molybdenum solubility in nickel from 28 to 37.5 at %. A number of different phases and microstructures were seen at different depths (solidification conditions) from the quenched surface of the melt spun ribbons. Author

**N85-34267#** Department of Energy, Washington, D. C. **MANUFACTURING PROCESS TO REDUCE LARGE GRAIN GROWTH IN ZIRCONIUM ALLOYS Patent Application**

P. M. ROSECRANS, inventor (to NASA) (GE, Schenectady, N.Y.) 1 Aug. 1984 11 p (Contract DE-AC12-76SN-00052) (DE85-011649; US-PATENT-APPL-SN-636659) Avail: NTIS HC A02/MF A01

A procedure for desensitizing zirconium based alloys to large grain growth (LGG) during thermal treatment above the recrystallization temperature of the alloy is presented. A method for treating zirconium based alloys which have been cold worked in the range of 2 to 8% strain to reduce large grain growth is devised. A method for fabricating a zirconium alloy clad nuclear fuel element wherein the zirconium clad is resistant to large grain growth is given. DOE

## NONMETALLIC MATERIALS

Includes physical, chemical, and mechanical properties of plastics, elastomers, lubricants, polymers, textiles, adhesives, and ceramic materials.

**A85-10310\*** National Aeronautics and Space Administration. Lewis Research Center, Cleveland, Ohio.

**OXIDATION-BASED MODEL FOR THERMAL BARRIER COATING LIFE**

R. A. MILLER (NASA, Lewis Research Center, Cleveland, OH) American Ceramic Society, Journal (ISSN 0002-7820), vol. 67, Aug. 1984, p. 517-521. refs

A procedure is described for modeling the lives of thermal barrier coatings subjected to high-temperature environments. The model is used to calculate cycles-to-failure as a function of heating cycle duration. It is based on the presumption that oxidation is the single important time-dependent factor which limits the life of these coatings, and that oxidation-induced strains combine with cyclic strains to promote slow crack growth in the ceramic layer. Good agreement is obtained between calculated and experimental lives for specimens tested in a furnace. This shows that an oxidation-based approach is promising. The importance of reproducible specimen preparation is also discussed. Author

**A85-10675\*#** National Aeronautics and Space Administration. Lewis Research Center, Cleveland, Ohio.

**LABORATORY DEGRADATION OF KAPTON IN A LOW ENERGY OXYGEN ION BEAM**

D. C. FERGUSON (NASA, Lewis Research Center, Cleveland, OH) American Institute of Aeronautics and Astronautics, Shuttle Environment and Operations Meeting, Washington, DC, Oct. 31-Nov. 2, 1983. 14 p. Previously announced in STAR as N84-18310. refs (AIAA PAPER 83-2658)

An atomic oxygen ion beam, accelerated from a tunable microwave resonant cavity, was used at Lewis Research Center to bombard samples of the widely used polyimide Kapton. The Kapton experienced degradation and mass loss at high rates, which may be comparable to those found in Space Shuttle operations if the activation energy supplied by the beam enabled surface reactions with the ambient oxygen. The simulation reproduced the directionality (ram-wake dependence) of the degradation, the change in optical properties of the degraded materials, and the structure seen in scanning electron micrographs of samples returned on the Shuttle Trails with a substituted argon ion beam produced no rapid degradation. Energy Dispersive X-ray Analysis (EDAX) showed significant surface composition changes in all bombarded samples. Mass loss rates and surface composition changes are discussed in terms of the possible oxidation chemistry of the interaction. Finally, the question of how the harmful degradation of materials in low earth orbit can be minimized is addressed. Author

**A85-10825\*** National Aeronautics and Space Administration. Lewis Research Center, Cleveland, Ohio.

**DEMONSTRATION OF A SILICON NITRIDE ATTRITION MILL FOR PRODUCTION OF FINE PURE SI AND Si3N4 POWDERS**

T. P. HERBELL, T. K. GLASGOW, and N. W. ORTH (NASA, Lewis Research Center, Cleveland, OH) American Ceramic Society Bulletin (ISSN 0002-7812), vol. 63, Sept. 1984, p. 1176-1178. refs

To avoid metallic impurities normally introduced by milling ceramic powders in conventional steel hardware, an attrition mill (high-energy stirred ball mill) was constructed with the wearing parts (mill body, stirring arms, and media) made from silicon nitride. Commercial silicon and Si3N4 powders were milled to fine uniform particles with only minimal contamination - primarily from wear of the sintered Si3N4 media. Author

**A85-11072\*** National Aeronautics and Space Administration. Lewis Research Center, Cleveland, Ohio.

**SPHERICAL MICROGLASS PARTICLE IMPINGEMENT STUDIES OF THERMOPLASTIC MATERIALS AT NORMAL INCIDENCE**

P. VEERABHADRA RAO and D. H. BUCKLEY (NASA, Lewis Research Center, Cleveland, OH) ASLE Transactions, vol. 27, Oct. 1984, p. 373-379. Previously announced in STAR as N83-25883. refs

Light optical and scanning electron microscope studies were conducted to characterize the erosion resistance of polymethyl methacrylate (PMMA), polycarbonate (PC), polytetrafluoroethylene (PTFE) and ultra-high-molecular-weight-polyethylene (UHMWPE). Erosion was caused by a jet of spherical micro-glass beads at normal impact. During the initial stages of damage, the surfaces of these materials were studied using a profilometer. Material buildup above the original surface was observed on PC and PMMA. As erosion progressed, this buildup disappeared as the pit became deeper. Little or no buildup was observed on PTFE and on UHMWPE. UHMWPE and PTFE are the most resistant materials and PMMA the least. Favorable properties for high erosion resistance seem to be high values of ultimate elongation, and strain energy and a low value of the modulus of elasticity. Erosion-rate-versus-time curves of PC and PTFE exhibit incubation, acceleration and steady state periods. A continuously increasing erosion rate period was observed however for PMMA instead of a steady state period. At early stages of damage and at low impact pressure material removal mechanisms appear to be similar to those for metallic materials. Author

**A85-15195\*** National Aeronautics and Space Administration. Lewis Research Center, Cleveland, Ohio.

**EFFECT OF HOT ISOSTATIC PRESSING ON REACTION-BONDED SILICON NITRIDE**

G. K. WATSON, T. J. MOORE, and M. L. MILLARD (NASA, Lewis Research Center, Cleveland, OH) American Ceramic Society, Communications (ISSN 0002-7820), vol. 67, Oct. 1984, p. C-208 to C-210. refs  
(Contract DE-AI01-77CS-1040)

Specimens of nearly theoretical density have been obtained through the isostatic hot pressing of reaction-bonded silicon nitride under 138 MPa of pressure for two hours at 1850, 1950, and 2050 C. An amorphous phase that is introduced by the hot isostatic pressing partly accounts for the fact that while room temperature flexural strength more than doubles, the 1200 C flexural strength increases significantly only after pressing at 2050 C. O.C.

**A85-19086\*** National Aeronautics and Space Administration. Lewis Research Center, Cleveland, Ohio.

**DEPOSITION STRESS EFFECTS ON THE LIFE OF THERMAL BARRIER COATINGS ON BURNER RIGS**

J. W. WATSON (NASA, Lewis Research Center, Cleveland, OH; Northwestern University, Evanston, IL) and S. R. LEVINE (NASA, Lewis Research Center, Cleveland, OH) Thin Solid Films (ISSN 0040-6090), vol. 119, 1984, p. 185-193. Previously announced in STAR as N84-25830. refs

A study of the effect of plasma spray processing parameters on the life of a two layer thermal barrier coating was conducted. The ceramic layer was plasma sprayed at plasma arc currents of 900 and 600 amps onto uncooled tubes, cooled tubes, and solid bars of Waspalloy in a lathe with 1 or 8 passes of the plasma gun. These processing changes affected the residual stress state of the coating. When the specimens were tested in a Mach 0.3 cyclic burner rig at 1130 deg C, a wide range of coating lives resulted. Processing factors which reduced the residual stress state in the coating, such as reduced plasma temperature and increased heat dissipation, significantly increased coating life. Author

**A85-19087\*** National Aeronautics and Space Administration. Lewis Research Center, Cleveland, Ohio.

**PERFORMANCE OF THERMAL BARRIER COATINGS IN HIGH HEAT FLUX ENVIRONMENTS**

R. A. MILLER and C. C. BERNDT (NASA, Lewis Research Center, Cleveland, OH) Thin Solid Films (ISSN 0040-6090), vol. 119, 1984, p. 195-202. Previously announced in STAR as N84-24772. refs

Thermal barrier coatings were exposed to the high temperature and high heat flux produced by a 30 kW plasma torch. Analysis of the specimen heating rates indicates that the temperature drop across the thickness of the 0.038 cm ceramic layer was about 1100 C after 0.5 sec in the flame. An as-sprayed ZrO<sub>2</sub>-8 percent Y<sub>2</sub>O<sub>3</sub> specimens survived 3000 of the 0.5 sec cycles with falling. Surface spalling was observed when 2.5 sec cycles were employed but this was attributed to uneven heating caused by surface roughness. This surface spalling was prevented by smoothing the surface with silicon carbide paper or by laser glazing. A coated specimen with no surface modification but which was heat treated in argon also did not surface spall. Heat treatment in air led to spalling in as early as 1 cycle from heating stresses. Failures at edges were investigated and shown to be a minor source of concern. Ceramic coatings formed from ZrO<sub>2</sub>-12 percent Y<sub>2</sub>O<sub>3</sub> or ZrO<sub>2</sub>-20 percent Y<sub>2</sub>O<sub>3</sub> were shown to be unsuited for use under the high heat flux conditions of this study. Author

**A85-20938\*** Pennsylvania State Univ., University Park.

**A MORPHOLOGICAL STUDY OF SILICON CARBIDE PREPARED BY CHEMICAL VAPOR DEPOSITION**

P. TSUI and K. E. SPEAR (Pennsylvania State University, University Park, PA) IN: Emergent process methods for high-technology ceramics. New York, Plenum Press, 1984, p. 371-380. refs  
(Contract NAG3-177)

Surface morphologies of SiC deposits obtained via chemical vapor deposition (CVD) were studied as functions of substrate surface temperature and the concentration of the silicon and carbon source material, methyltrichlorosilane. Substrates of graphite and alpha-SiC crystals were used. Explanations of the observed morphologies on graphite substrates and their marked changes with temperature are given in terms of chemical kinetics and mass transport arguments. The results of thermodynamic calculations were used to help explain the observed morphologies of the deposits on alpha-SiC substrates. Author

**A85-21524\*** National Aeronautics and Space Administration. Lewis Research Center, Cleveland, Ohio.

**POLYIMIDES - TRIBOLOGICAL PROPERTIES AND THEIR USE AS LUBRICANTS**

R. L. FUSARO (NASA, Lewis Research Center, Cleveland, OH) IN: Polyimides: Synthesis, characterization, and applications. Volume 2. New York, Plenum Press, 1984, p. 1053-1080. Previously announced in STAR as N83-13257. refs

Friction, wear, and wear mechanisms of several different polyimide films, solid bodies, composites, and bonded solid lubricant films are compared and discussed. In addition, the effect of such parameters as temperatures, type of atmosphere, contact stress, and specimen configuration are investigated. A friction and wear transition occurs in some polyimides at elevated temperatures and this transition is related to molecular relaxations that occur in polyimides. Friction and wear data from an accelerated test (pin-on-disk) are compared to similar data from an end use test device (plain spherical bearing), and to other polymers investigated in a similar geometry. Author

## 27 NONMETALLIC MATERIALS

**A85-21650\*** National Aeronautics and Space Administration. Lewis Research Center, Cleveland, Ohio.

### **MICROSTRUCTURAL DEVELOPMENT OF PROTECTIVE AL<sub>2</sub>O<sub>3</sub> SCALES**

J. L. SMIALEK (NASA, Lewis Research Center, Cleveland, OH) IN: Electron Microscopy Society of America, Annual Meeting, 42nd, Detroit, MI, August 13-17, 1984. San Francisco, San Francisco Press, Inc., 1984, p. 594-597. refs

Microstructural characteristics of Al<sub>2</sub>O<sub>3</sub> scales grown as protective coatings on NiCrAl alloys used in jet engines are described. The alloys were pure or doped with 0.3 percent Zr or Y and oxidized in 1 atm air at 1100 C for 0.1, 1 or 20.0 hr. The scales were then examined under a microscope. Transient epitaxial scales, formed during the 0.1 hr treatment and containing Ni, Cr and Al, consisted of a mosaic of subgrains and precipitates of different phases. The Y and Zr dopants had no effect on the nucleation site locations. The appearance of intergranular porosity at 0.1 hr was exacerbated after the 1 hr treatment. A bimodal void distribution appeared after 20 hr, when no porosity was evident. The detection of local areas of preferred orientation is taken as a spur to further studies of scale growth to gain control of the grain size or even to produce single crystal scales. M.S.K.

**A85-22276\*** National Aeronautics and Space Administration. Lewis Research Center, Cleveland, Ohio.

### **FRICTION, WEAR, TRANSFER, AND WEAR SURFACE MORPHOLOGY OF ULTRAHIGH-MOLECULAR-WEIGHT POLYETHYLENE**

R. L. FUSARO (NASA, Lewis Research Center, Cleveland, OH) ASLE Transactions, vol. 28, Jan. 1985, p. 1-9; Discussion, p. 9; Author's Closure, p. 9, 10. Previously announced in STAR as N83-25882. refs

Tribological studies at 25 C in a 50-percent-relative-humidity air atmosphere were conducted using hemispherically tipped 440 C HT (high temperature) stainless steel pins sliding against ultra-high-molecular-weight polyethylene (UHMWPE) disks. The results indicate that sliding speed, sliding distance, contact stress and specimen geometry can markedly affect friction, UHMWPE wear, UHMWPE transfer and the type of wear mechanisms that occur. Adhesion appears to be the predominant wear mechanism; but after long sliding distances at slow speeds, heavy ridges of transfer result which can induce fatigue-like wear on the UHMWPE disk wear track. In one instance, abrasive wear to the metallic pin was observed. This was caused by a hard particle embedded in the UHMWPE disk wear track. Author

**A85-23833\*** National Aeronautics and Space Administration. Lewis Research Center, Cleveland, Ohio.

### **FRICTION AND WEAR OF CERAMICS**

D. H. BUCKLEY and K. MIYOSHI (NASA, Lewis Research Center, Cleveland, OH) Wear (ISSN 0043-1648), vol. 100, Dec. 1984, p. 333-353. refs

The adhesion, friction, wear and lubricated behaviors of both oxide and non-oxide ceramics are reviewed. Ceramics are examined in contact with themselves, other harder materials and metals. Elastic, plastic and fracture behavior of ceramics in solid state contact is discussed. The contact load necessary to initiate fracture in ceramics is shown to be appreciably reduced with tangential motion. Both friction and wear of ceramics are anisotropic and relate to crystal structure as with metals. Grit size effects in two- and three-body abrasive wear are observed for ceramics. Both free energy of oxide formation and the d valence bond character of metals are related to the friction and wear characteristics for metals in contact with ceramics. Surface contaminants affect friction and adhesive wear. For example, carbon on silicon carbide and chlorine on aluminum oxide reduce friction while oxygen on metal surfaces in contact with ceramics increases friction. Lubrication increases the critical load necessary to initiate fracture of ceramics both in indentation and with sliding or rubbing. Author

**A85-24161\*** Akron Univ., Ohio.

### **PLASTIC FLOW OF PLASMA SPRAYED CERAMICS**

J. PADOVAN, B. T. F. CHUNG, M. J. BRAUN (Akron, University, Akron, OH), G. MCDONALD, R. C. HENDRICKS (NASA, Lewis Research Center, Cleveland, OH), and R. L. MULLEN (Case Western Reserve University, Cleveland, OH) IN: Deformation of ceramic materials II; Proceedings of the International Symposium on Plastic Deformation of Ceramic Materials, University Park, PA, July 20-22, 1983. New York, Plenum Press, 1984, p. 473-485. refs

The plastic flow of plasma-sprayed ZrO<sub>2</sub>-8Y<sub>2</sub>O<sub>3</sub> ceramic has been measured at temperatures up to 1250 C and compared to the plastic flow of pressed and sintered ZrO<sub>2</sub>-8Y<sub>2</sub>O<sub>3</sub>. Plasma spraying of binary oxide ceramics is found to result in a metastable state which is inelastic at high temperature but can also be stabilized or devitrified through heat treating so as to decrease plastic properties. The mechanical properties of the as-plasma sprayed and devitrified ceramic sheet material was measured. An improved algorithm that incorporates the inherently nonlinear thermomechanical field equations was used to determine the influence of inelastic material behavior on the thermomechanical response of ceramic coated seal components. Significant creep was found during the thermal shock and steady heating periods with insufficient time during thermal quench to reverse the process, thereby inducing significant residual stresses into the components. C.D.

**A85-25271\*** National Aeronautics and Space Administration. Lewis Research Center, Cleveland, Ohio.

### **STRENGTH AND MICROSTRUCTURE OF SINTERED Si<sub>3</sub>N<sub>4</sub> WITH RARE-EARTH-OXIDE ADDITIONS**

W. A. SANDERS and D. M. MIESKOWSKI (NASA, Lewis Research Center, Cleveland, OH) American Ceramic Society Bulletin (ISSN 0002-7812), vol. 64, Feb. 1985, p. 304-309. refs (ACS PAPER 130-13-84)

Room temperature, 700-, 1000-, 1200-, and 1370-C examinations of the effect of 1.7-2.6 mol pct rare earth oxide additions to sintered Si<sub>3</sub>N<sub>4</sub> are conducted. While the room temperature-1000 C bend strengths were higher for this material with Y<sub>2</sub>O<sub>3</sub> additions than with CeO<sub>2</sub>, La<sub>2</sub>O<sub>3</sub>, or Sm<sub>2</sub>O<sub>3</sub>, the reverse was true at 1200-1370 C. This phenomenon is explained on the basis of microstructural differences, since quantitative microscopy of SEM replicas showed the Si<sub>3</sub>N<sub>4</sub>-Y<sub>2</sub>O<sub>3</sub> composition to contain both a higher percentage of elongated grains and a coarser microstructure than the other three alternatives. The elongated grains appear to increase this composition's low temperature strength irrespective of microstructural coarseness; this coarseness, however, decreases strength relative to the other compositions at higher temperatures. O.C.

**A85-25963\*** Illinois Univ., Urbana.

### **THE INFLUENCE OF TEMPERATURE ON THE LUBRICATING EFFECTIVENESS OF MoS<sub>2</sub> DISPERSED IN MINERAL OILS**

R. J. ROLEK, C. CUSANO (Illinois, University, Urbana, IL), and H. E. SLINNEY (NASA, Lewis Research Center, Cleveland, OH) American Society of Lubrication Engineers and American Society of Mechanical Engineers, Lubrication Conference, San Diego, CA, Oct. 22-24, 1984. 10 p. refs (Contract NAG3-153) (ASLE PREPRINT 84-LC-2A-2)

The effects of oil viscosity, base oil temperature, and surface-active agents naturally present in mineral oils on the lubricating effectiveness of MoS<sub>2</sub> dispersions under boundary lubrication conditions are investigated. Friction and wear data are obtained from tests conducted under a wide range of oil viscosities and operating temperatures. The dispersion temperature at which the friction dropped below that obtained with the base oils, depended upon the base oil viscosity and the concentration of surface-active agents present in the oil. White oils showed reductions in friction before mineral oils of like viscosity, and lower viscosity oils showed reductions in friction before heavier viscosity oils. The results show that for a given base oil, wear increases as temperature increases, while the wear obtained from a MoS<sub>2</sub>

dispersion made from the base oil remains approximately constant as temperature is increased. Author

**A85-29728\*** National Aeronautics and Space Administration. Lewis Research Center, Cleveland, Ohio.

**LIFE MODELING OF ATMOSPHERIC AND LOW PRESSURE PLASMA-SPRAYED THERMAL-BARRIER COATING**

R. A. MILLER (NASA, Lewis Research Center, Cleveland, OH), P. ARGARWAL (Garrett Turbine Engines, Phoenix, AZ; General Electric Co., Aircraft Engine Group, Cincinnati, OH), and E. C. DUDERSTADT (General Electric Co., Aircraft Engine Group, Cincinnati, OH) Ceramic Engineering and Science Proceedings (ISSN 0196-6219), vol. 5, July-Aug. 1984, p. 470-478. refs

The cycles-to-failure vs cycle duration data for three different thermal barrier coating systems, which consist of atmospheric pressure plasma-sprayed ZrO<sub>2</sub>-8 percent Y<sub>2</sub>O<sub>3</sub> over similarly deposited or low pressure plasma sprayed Ni-base alloys, are presently analyzed by means of the Miller (1980) oxidation-based life model. Specimens were tested at 1100 C for heating cycle lengths of 1, 6, and 20 h, yielding results supporting the model's value. O.C.

**A85-29729\*** National Aeronautics and Space Administration. Lewis Research Center, Cleveland, Ohio.

**MECHANICAL PROPERTY MEASUREMENTS OF PLASMA-SPRAYED THERMAL-BARRIER COATINGS SUBJECTED TO OXIDATION**

C. C. BERNDT and R. A. MILLER (NASA, Lewis Research Center, Surface Protection Section, Cleveland, OH) Ceramic Engineering and Science Proceedings (ISSN 0196-6219), vol. 5, July-Aug. 1984, p. 479-490. refs

Techniques have been developed for measuring the tensile properties of plasma-sprayed coatings which are used in thermal barrier applications. The measurements have included the average Young's modulus, bond strength and elongation at failure. The oxidation behavior of the bond coat plays an important role in the integrity and adhesion of plasma-sprayed thermal barrier coatings. This work studies the nature of the high temperature degradation on the mechanical properties of the coating. Furnace tests have been carried out on U-700 alloy with bond coats of NiCrAlY or NiCrAlZr and an overlay of ZrO<sub>2</sub>-8 percent Y<sub>2</sub>O<sub>3</sub>. Weight gain measurements on the coatings have been examined with relation to the adhesion strength and failure observations. The results from an initial study are reported in this work. Author

**A85-35139\*#** National Aeronautics and Space Administration. Lewis Research Center, Cleveland, Ohio.

**RESIN SELECTION CRITERIA FOR 'TOUGH' COMPOSITE STRUCTURES**

C. C. CHAMIS (NASA, Lewis Research Center, Cleveland, OH) and G. T. SMITH (Structures, Structural Dynamics and Materials Conference, 24th, Lake Tahoe, NV, May 2-4, 1983, Collection of Technical Papers. Part 1, p. 45-60) AIAA Journal (ISSN 0001-1452), vol. 23, June 1985, p. 902-911. Previously cited in issue 12, p. 1717, Accession no. A83-29734. refs

**A85-36229\*** National Aeronautics and Space Administration. Lewis Research Center, Cleveland, Ohio.

**DEPOSITION OF SILICON NITRIDE FROM SiCl<sub>4</sub> AND NH<sub>3</sub> IN A LOW PRESSURE RF PLASMA**

Y. RON, A. RAVEH, U. CARMI, A. INSPEKTOR (Atomic Energy Commission, Negev Nuclear Research Centre, Beersheba, Israel), and R. AVNI (NASA, Lewis Research Center, Cleveland, OH; Atomic Energy Commission, Negev Nuclear Research Centre, Beersheba, Israel) IN: Metallurgical coatings 1983; Proceedings of the Tenth International Conference, San Diego, CA, April 18-22, 1983. Volume 1. Lausanne, Switzerland, Elsevier Sequoia, S.A., 1983, p. 181-189. refs

Silicon nitride coatings were deposited in a low-pressure (1-10 Torr) RF plasma from SiCl<sub>4</sub> and NH<sub>3</sub> in the presence of argon onto stainless martensitic steel grounded and floating substrates at 300 C and 440 C respectively. The heating of the substrates depends mainly on the position and the induced RF power. The

coatings were identified as silicon nitride by X-ray investigation and were found to contain chlorine by energy-dispersive analysis of X-rays. The growth rate, the microhardness and the chlorine concentration of the coatings were determined as a function of the total gas pressure, the RF power input and the NH<sub>3</sub>-to-SiCl<sub>4</sub> ratio. It was observed that the coatings on the floating substrates have higher deposition rates and are of superior quality. Author

**A85-36240\*** Negev Univ., Beersheva (Israel).

**RF-SPUTTERED SILICON AND HAFNIUM NITRIDES - PROPERTIES AND ADHESION TO 440C STAINLESS STEEL**

A. GRILL (Negev, University, Beersheba, Israel) and P. R. ARON (NASA, Lewis Research Center, Cleveland, OH) IN: Metallurgical coatings 1983; Proceedings of the Tenth International Conference, San Diego, CA, April 18-22, 1983. Volume 2. Lausanne, Switzerland, Elsevier Sequoia, S.A., 1983, p. 173-180. Previously announced in STAR as N83-27020. refs

Silicon nitride and hafnium nitride coatings were deposited by reactive RF sputtering on oxidized and unoxidized 440C stainless steel substrates. Sputtering was done in mixtures of argon and nitrogen gases from pressed powder silicon nitride and from hafnium metal targets. Depositions were at two background pressures, 8 and 20 mtorr, and at two different fractions (f) of nitrogen in argon, 0.25 and 0.60, for hafnium nitride and at f = 0.25 for silicon nitride. The coatings and the interface between the coating and substrates were investigated by X-ray diffractometry, scanning electron microscopy, energy dispersive X-ray analysis and Auger electron spectroscopy. A Knoop microhardness of 1650 + or 100 kg/sq mm was measured for hafnium nitride and 3900 + or 500 kg/sq mm for silicon nitride. The friction coefficients between a 440C rider and the coatings were measured under lubricated conditions. Scratch test results demonstrate that the adhesion of hafnium nitride to both oxidized and unoxidized 440C is superior to that of silicon nitride. Oxidized 440C is found to have increased adhesion, to both nitrides, over that of unoxidized 440C. Author

**A85-36246\*** National Aeronautics and Space Administration. Lewis Research Center, Cleveland, Ohio.

**FAILURE DURING THERMAL CYCLING OF PLASMA-SPRAYED THERMAL BARRIER COATINGS**

C. C. BERNDT (NASA, Lewis Research Center, Surface Protection Section, Cleveland, OH; New York, State University, Stony Brook, NY) and H. HERMAN (New York, State University, Stony Brook, NY) IN: Metallurgical coatings 1983; Proceedings of the Tenth International Conference, San Diego, CA, April 18-22, 1983. Volume 2. Lausanne, Switzerland, Elsevier Sequoia, S.A., 1983, p. 427-437. refs  
(Contract NAG3-164)

The thermal cycling behavior of plasma-sprayed ZrO<sub>2</sub>-12 wt pct Y<sub>2</sub>O<sub>3</sub> coatings was studied. Coatings were produced with and without bond coats of Ni-Cr-Al-Zr and in some cases the substrates were heated to above the optimum temperature prior to spraying. The coatings (attached to the substrate) were thermal cycled to 1200 C and their cracking behavior was followed by acoustic emission (AE) techniques. It was possible to examine the failure mechanisms by statistical analysis of the AE data and to evaluate the influence of preheating and bond coating. It is shown that the AE spectrum changes when a bond coat is used because of the presence of microcracks which, in turn, dissipate energy and improve the coating integrity. The preheating effect is reflected by a decrease in the peak count rate and an increase in the temperature at which AE activity is initiated. Author

**A85-39339\*** National Aeronautics and Space Administration. Lewis Research Center, Cleveland, Ohio.

**FEASIBILITY STUDY OF THE WELDING OF SiC**

T. J. MOORE (NASA, Lewis Research Center, Cleveland, OH) American Ceramic Society, Communications (ISSN 0002-7820), vol. 68, June 1985, p. C-151 to C-153. refs

In a brief study of the feasibility of welding sintered alpha-SiC, solid-state welding and brazing were investigated. Joint quality was determined solely by microstructural examination. Hot-pressure

## 27 NONMETALLIC MATERIALS

welding was shown to be feasible at 1950 C. Diffusion welding and brazing were also successful under hot isostatic pressure at 1950 C when boride, carbide, and silicide interlayers were used. Furnace brazing was accomplished at 1750 C when a TiSi2 interlayer was introduced. Author

**A85-39549\*** National Aeronautics and Space Administration. Lewis Research Center, Cleveland, Ohio.

### **CERAMIC WEAR IN INDENTATION AND SLIDING CONTACT**

K. MIYOSHI and D. H. BUCKLEY (NASA, Lewis Research Center, Cleveland, OH) ASLE Transactions, vol. 28, July 1985, p. 296-302. Previously announced in STAR as N84-19566. refs

The various wear mechanisms involved with single-crystal ceramic materials in indentation and in sliding contacts. Experiments simulating interfacial events have been conducted with hemispherical, conical and pyramidal indenters (riders). With spherical riders, under either abrasive or adhesive conditions, two types of fracture pits have been observed. First, spherical-shaped fracture pits and wear particles are found as a result of either indenting or sliding. These are shown to be due to a spherical-shaped fracture along the circular or spherical stress trajectories. Second, polyhedral fracture pits and debris, produced by anisotropic fracture, and also found both during indenting and sliding. These are primarily controlled by surface and subsurface cracking along cleavage planes. Several quantitative results have also been obtained from this work. For example, using a pyramidal diamond, crack length of Mn-Zn ferrite in the indentation process grows linearly with increasing normal load. Moreover, the critical load to fracture both in indentation and sliding is essentially isotropic and is found to be directly proportional to the indenter radius. Author

**A85-39662\*#** National Aeronautics and Space Administration. Lewis Research Center, Cleveland, Ohio.

### **HIGH-TEMPERATURE EROSION OF PLASMA-SPRAYED, YTTRIA-STABILIZED ZIRCONIA IN A SIMULATED TURBINE ENVIRONMENT**

R. F. HANDSCHUH (NASA, Lewis Research Center; U.S. Army Propulsion Laboratory, Cleveland, OH) AIAA, SAE, ASME, and ASSEE, Joint Propulsion Conference, 21st, Monterey, CA, July 8-10, 1985. 13 p. Previously announced in STAR as N85-13045. refs (AIAA PAPER 85-1219)

A series of rig calibration and high temperature tests simulating gas path seal erosion in turbine engines were performed at three impingement angles and at three downstream locations. Plasma sprayed, yttria stabilized zirconia specimens were tested. Steady state erosion curves presented for 19 test specimens indicate a brittle type of material erosion despite scanning electron microscopy evidence of plastic deformation. Steady state erosion results were not sensitive to downstream location but were sensitive to impingement angle. At different downstream locations specimen surface temperature varied from 1250 to 1600 C (2280 to 2900 F) and particle velocity varied from 260 to 320 m/s (850 to 1050 ft/s). The mass ratio of combustion products to erosive grit material was typically 240. Author

**A85-40383\*** Nebraska Univ., Lincoln.

### **'DIAMONDLIKE' CARBON FILMS - OPTICAL ABSORPTION, DIELECTRIC PROPERTIES, AND HARDNESS DEPENDENCE ON DEPOSITION PARAMETERS**

V. NATARAJAN, J. D. LAMB, J. A. WOOLLAM (Nebraska, University, Lincoln), D. C. LIU, and D. A. GULINO (NASA, Lewis Research Center, Cleveland, OH) Journal of Vacuum Science and Technology A (ISSN 0734-2101), vol. 3, May-June 1985, pt. 1, p. 681-685. Research supported by the University of Nebraska, U.S. Army, and NSF. refs (Contract NAG3-95; NAG3-154)

An RF plasma deposition system was used to prepare amorphous 'diamondlike' carbon films. The source gases for the RF system include methane, ethylene, propane, and propylene, and the parameters varied were power, dc substrate bias, and postdeposition anneal temperature. Films were deposited on various substrates. The main diagnostics were optical absorption

in the visible and in the infrared, admittance as a function of frequency, hardness, and Auger and ESCA spectroscopy. Band gap is found to depend strongly on RF power level and band gaps up to 2.7 eV and hardness up to 7 Mohs were found. There appears to be an inverse relationship between hardness and optical band gap. Author

**A85-40384\*** National Aeronautics and Space Administration. Lewis Research Center, Cleveland, Ohio.

### **CERAMIC MICROSTRUCTURE AND ADHESION**

D. H. BUCKLEY (NASA, Lewis Research Center, Cleveland, OH) Journal of Vacuum Science and Technology A (ISSN 0734-2101), vol. 3, May-June 1985, pt. 1, p. 762-771. Previously announced in STAR as N85-10186. refs

When a ceramic is brought into contact with a ceramic, a polymer, or a metal, strong bond forces can develop between the materials. The bonding forces will depend upon the state of the surfaces, cleanliness and the fundamental properties of the two solids, both surface and bulk. Adhesion between a ceramic and another solid are discussed from a theoretical consideration of the nature of the surfaces and experimentally by relating bond forces to interface resulting from solid state contact. Surface properties of ceramics correlated with adhesion include, orientation, reconstruction and diffusion as well as the chemistry of the surface specie. Where a ceramic is in contact with a metal their interactive chemistry and bond strength is considered. Bulk properties examined include elastic and plastic behavior in the surficial regions, cohesive binding energies, crystal structures and crystallographic orientation. Materials examined with respect to interfacial adhesive interactions include silicon carbide, nickel zinc ferrite, manganese zinc ferrite, and aluminum oxide. The surfaces of the contacting solids are studied both in the atomic or molecularly clean state and in the presence of selected surface contaminants. Author

**A85-40973\*** Case Western Reserve Univ., Cleveland, Ohio.

### **DOPANT EFFECT OF YTTRIUM AND THE GROWTH AND ADHERENCE OF ALUMINA ON NICKEL-ALUMINUM ALLOYS**

A. B. ANDERSON, S. P. MEHANDRU (Case Western Reserve University, Cleveland, OH), and J. L. SMIALEK (NASA, Lewis Research Center, Cleveland, OH) Electrochemical Society, Journal (ISSN 0013-4651), vol. 132, July 1985, p. 1695-1701. refs (Contract NAG3-341)

The atom superposition and electron delocalization molecular orbital theory and large cluster models have been employed to study cation vacancy diffusion in alpha-Al2O3 and the bonding of alpha-Al2O3 to nickel, aluminum, and yttrium surfaces. Al(3+) diffusion barriers in alpha-Al2O3 by the vacancy mechanism are in reasonable agreement with experiment. The barrier to Y(3+) diffusion is predicted to be much higher. Since addition of yttrium to transition metal alloys is known to reduce the growth rate and stress convolutions in protective alumina scales, this result suggests the rate-limiting step in scale growth is cation vacancy diffusion. This may partially explain the beneficial effect of yttrium dopants on scale adhesion. The theory also predicts a very strong bonding between alumina and yttrium at the surface of the alloy. This may also be important to the adhesion phenomenon. It is also found that aluminum and yttrium atoms bond very strongly to nickel because of charge transfer from their higher lying valence orbitals to the lower lying nickel s-d band. Author

**A85-42797\*** Ford Motor Co., Dearborn, Mich.

### **FRACTURE OF YTTRIA-DOPED, SINTERED REACTION-BONDED SILICON NITRIDE**

R. K. GOVILA, J. A. MANGELS, and J. R. BAER (Ford Motor Co., Ceramic Material Dept., Dearborn, MI) American Ceramic Society, Journal (ISSN 0002-7820), vol. 68, July 1985, p. 413-418. DOE-supported research. refs (Contract DEN3-167) (ACS PAPER 7-J3-84)

Flexural strength of an yttria-doped, slip-cast, sintered reaction-bonded silicon nitride was evaluated as a function of temperature (20 to 1400 C in air), applied stress, and time. Static oxidation at 700 to 1400 C was investigated in detail; in tests at

1000 C in air, the material showed anomalous weight gain. Flexural stress-rupture testing at 800 to 1200 C in air indicated that the material is susceptible to stress-enhanced oxidation and early failure. Fractographic evidence for time-dependent and -independent failures is presented. Author

**A85-42798\*** National Aeronautics and Space Administration. Lewis Research Center, Cleveland, Ohio.

**OXIDATION OF SILICON NITRIDE SINTERED WITH RARE-EARTH OXIDE ADDITIONS**

D. M. MIESKOWSKI and W. A. SANDERS (NASA, Lewis Research Center, Cleveland, OH). American Ceramic Society, Communications (ISSN 0002-7820), vol. 68, July 1985, p. C-160 to C-163. refs

The effects of rare-earth oxide additions on the oxidation of sintered Si<sub>3</sub>N<sub>4</sub> were examined. Insignificant oxidation occurred at 700 and 1000 C, with no evidence of phase instability. At 1370 C, the oxidation rate was lowest for Y<sub>2</sub>O<sub>3</sub> and increased for additions of La<sub>2</sub>O<sub>3</sub>, Sm<sub>2</sub>O<sub>3</sub>, and CeO<sub>2</sub>, in that order. Data obtained from X-ray diffraction, electron microprobe analysis, and scanning electron microscopy indicate that oxidation occurs via diffusion of cationic species from Si<sub>3</sub>N<sub>4</sub> grain boundaries. Author

**A85-42800\*** National Aeronautics and Space Administration. Lewis Research Center, Cleveland, Ohio.

**EVALUATION OF ALPHA-SiC SINTERING USING STATISTICAL METHODS**

J. B. HURST and M. L. MILLARD (NASA, Lewis Research Center, Cleveland, OH). American Ceramic Society, Communications (ISSN 0002-7820), vol. 68, July 1985, p. C-178 to C-181. refs

The effect of time and temperature on the density and strength of alpha-SiC was studied and mathematically modeled using a central composite experimental design. A sintering temperature of 2150 C for 1.7 h maximized the flexural strength and densification values. However, temperatures above 2200 C promoted abnormal grain growth, with resulting appreciable decreases in strength. Flexural strength increased exponentially with increasing density for specimens with densities less than or equal to 92 percent of theoretical. Author

**A85-43930\*** General Motors Corp., Indianapolis, Ind.  
**PHOTOACOUSTIC MICROSCOPY OF CERAMIC TURBINE BLADES**

P. K. KHANDELWAL, R. R. KINNICK, and P. W. HEITMAN (General Motors Corp., Indianapolis, IN). American Ceramic Society Bulletin (ISSN 0002-7812), vol. 64, Aug. 1985, p. 1112-1115. DOE-supported research. (Contract DEN3-17)

Scanning photoacoustic microscopy (SPAM) is evaluated as a nondestructive technique for the detection of both surface and subsurface flaws in polycrystalline ceramics, such as those currently under consideration for the high temperature components of small vehicular and industrial gas turbine engines; the fracture strength of these brittle materials is controlled by small, 25-200 micron flaws. Attention is given to the correlation of SPAM-detected flaws with actual, fracture-controlling flaws in ceramic turbine blades. O.C.

**A85-45302\*** National Aeronautics and Space Administration. Lewis Research Center, Cleveland, Ohio.

**HOT CORROSION OF SINTERED ALPHA-SiC AT 1000 C**

N. S. JACOBSON and J. L. SMIALEK (NASA, Lewis Research Center, Cleveland, OH). American Ceramic Society, Journal (ISSN 0002-7820), vol. 68, Aug. 1985, p. 432-439. refs (ACS PAPER 19-B-84P)

The hot corrosion of sintered alpha-SiC by thin films of Na<sub>2</sub>SO<sub>4</sub> and Na<sub>2</sub>CO<sub>3</sub> was studied at 1000 C in controlled gas atmospheres. Under all conditions, corrosion led to 10 to 20 times the amount of SiO<sub>2</sub> formed in pure oxidation after a 48-h exposure. In addition, small amounts of sodium silicate formed. Melts of Na<sub>2</sub>SO<sub>4</sub>/SO<sub>3</sub> caused uniform pitting of the SiC substrate; Na<sub>2</sub>CO<sub>3</sub>/CO<sub>2</sub> melts caused localized pitting and grain-boundary attack. In all cases, the protective SiO<sub>2</sub> layer dissolved to form silicate, leading to

corrosion. In the sulfate case, free carbon in the SiC promotes this process. In all cases the presence of liquid films is responsible for rapid transport rates and the subsequent rapid reaction. Author

**A85-45304\*** National Aeronautics and Space Administration. Lewis Research Center, Cleveland, Ohio.

**MICROSTRUCTURE OF REACTION-BONDED SILICON NITRIDE CONSOLIDATED BY ISOSTATIC HOT-PRESSING**

D. M. MIESKOWSKI and W. A. SANDERS (NASA, Lewis Research Center, Cleveland, OH). American Ceramic Society, Communications (ISSN 0002-7820), vol. 68, Aug. 1985, p. C-217, C-218.

A microstructural examination and chemical analysis are conducted for reaction-bonded Si<sub>3</sub>N<sub>4</sub> specimens that were isostatically hot pressed at 1850, 1950, and 2050 C. The present observations indicate that the previously reported increase in the 1200 C bend strength of reaction-bonded Si<sub>3</sub>N<sub>4</sub>, after pressing at 2050 C exclusively, is due to the relative oxygen levels of the isostatically hot pressed specimens; calculations show that an SiO<sub>2</sub> content of less than about 2.2 vol pct is needed to yield the 1200 C strength increase. O.C.

**A85-48757\*** National Aeronautics and Space Administration. Lewis Research Center, Cleveland, Ohio.

**EFFECT OF HOT ISOSTATIC PRESSING ON THE PROPERTIES OF SINTERED ALPHA SILICON CARBIDE**

G. K. WATSON, T. J. MOORE, and M. L. MILLARD (NASA, Lewis Research Center, Cleveland, OH). American Ceramic Society Bulletin (ISSN 0002-7812), vol. 64, Sept. 1985, p. 1253-1256. refs

(Contract DE-AI01-77CS-51040)

Two lots of alpha silicon carbide were isostatically hot-pressed under 138 MPa for 2 h in Ar at temperatures up to 2200 C. Nearly theoretically dense specimens resulted. Hot isostatic pressing increased both room-temperature strength and 1200 C strength, and resulted in improved reliability. One lot of material which was pressed at 2200 C showed increases of about 20 percent in room-temperature strength and about 50 percent in 1200 C flexural strength; the Weibull modulus improved about 100 percent. Author

**N85-10186\*#** National Aeronautics and Space Administration. Lewis Research Center, Cleveland, Ohio.

**CERAMIC MICROSTRUCTURE AND ADHESION**

D. H. BUCKLEY 1984 33 p refs To be presented at the 31st Natl. Am. Vacuum Soc. Symp., Reno, Nevada, 4-7 Dec. 1984

(NASA-TM-83804; E-2311; NAS 1.15:83804) Avail: NTIS HC A03/MF A01 CSCL 11B

When a ceramic is brought into contact with a ceramic, a polymer, or a metal, strong bond forces can develop between the materials. The bonding forces will depend upon the state of the surfaces, cleanliness and the fundamental properties of the two solids, both surface and bulk. Adhesion between a ceramic and another solid are discussed from a theoretical consideration of the nature of the surfaces and experimentally by relating bond forces to interface resulting from solid state contact. Surface properties of ceramics correlated with adhesion include, orientation, reconstruction and diffusion as well as the chemistry of the surface specie. Where a ceramic is in contact with a metal their interactive chemistry and bond strength is considered. Bulk properties examined include elastic and plastic behavior in the surficial regions, cohesive binding energies, crystal structures and crystallographic orientation. Materials examined with respect to interfacial adhesive interactions include silicon carbide, nickel zinc ferrite, manganese zinc ferrite, and aluminum oxide. The surfaces of the contacting solids are studied both in the atomic or molecularly clean state and in the presence of selected surface contaminants. Author



## 27 NONMETALLIC MATERIALS

**N85-10187\*#** National Aeronautics and Space Administration. Lewis Research Center, Cleveland, Ohio.

**STABILITY OF BROMINE INTERCALATED GRAPHITE FIBERS**  
J. R. GAIER 28 Nov. 1984 11 p refs To be presented at the Mater. Res. Soc. Symp., Boston, 28-30 Nov. 1984; sponsored by the Am. Phys. Soc.

(NASA-TM-86859; E-2322; NAS 1.15:86859) Avail: NTIS HC A02/MF A01 CSCL 11D

Previous evidence suggested that bromine intercalation compounds of crystalline graphite spontaneously deintercalate when the bromine atmosphere is removed. However, results show that bromine intercalated P-100 graphite fibers are stable for long periods of time. They are stable under vacuum conditions, high humidity, and current densities up to 24,000 A/sq cm. They are thermally stable to 200 C, and at temperatures as high as 400 C still retain 80 percent of the conductivity gained by intercalation. At temperatures greater than 300 C, there is significant oxidative degradation of the fibers. The environmental stability shown by the bromine compound makes it a promising candidate for practical applications in aerospace technology. R.S.F.

**N85-10191\*#** National Aeronautics and Space Administration. Lewis Research Center, Cleveland, Ohio.

**MILLING OF Si<sub>3</sub>N<sub>4</sub> WITH Si<sub>3</sub>N<sub>4</sub> HARDWARE**

T. P. HERBELL, M. R. FREEDMAN, and J. D. KISER Washington 1984 20 p refs Presented at the 13th Intern. Gas Turbine Conf., Houston, Tex., 17-21 Mar. 1984; sponsored by American Society of Mechanical Engineers

(NASA-TM-86864; E-2328; NAS 1.15:86864) Avail: NTIS HC A02/MF A01 CSCL 11G

The grinding of Si<sub>3</sub>N<sub>4</sub> powder using reaction bonded Si<sub>3</sub>N<sub>4</sub> attrition, vibratory, and ball mills with Si<sub>3</sub>N<sub>4</sub> media was examined. The rate of particle size reduction and the change in the chemical composition of the powder were determined in order to compare the grinding efficiency of each technique and the increase in impurity content resulting from mill and media wear. Attrition and vibratory milling exhibited rates of specific surface area increase that were approximately eight times that observed in ball milling. Ball milling and attrition milling provided the least contamination while vibratory milling introduced the greatest amount of impurity pickup. Author

**N85-12162\*#** Case Western Reserve Univ., Cleveland, Ohio. Dept. of Metallurgy and Materials Science.

**ANALYSIS TECHNIQUES FOR TRACER STUDIES OF OXIDATION** M. S. Thesis Final Report

S. N. BASU Nov. 1984 127 p refs

(Contract NAG3-324)

(NASA-CR-174796; NAS 1.26:174796) Avail: NTIS HC A07/MF A01 CSCL 11G

Analysis techniques to obtain quantitative diffusion data from tracer concentration profiles were developed. Mass balance ideas were applied to determine the mechanism of oxide growth and to separate the fraction of inward and outward growth of oxide scales. The process of inward oxygen diffusion with exchange was theoretically modeled and the effect of lattice diffusivity, grain boundary diffusivity and grain size on the tracer concentration profile was studied. The development of the tracer concentration profile in a growing oxide scale was simulated. The double oxidation technique was applied to a FeCrAl-Zr alloy using O-18 as a tracer. SIMS was used to obtain the tracer concentration profile. The formation of lacy oxide on the alloy was discussed. Careful consideration was given to the quality of data required to obtain quantitative information. Author

**N85-13044\*#** National Aeronautics and Space Administration. Lewis Research Center, Cleveland, Ohio.

**EFFECT OF BARRIER HEIGHT ON FRICTION BEHAVIOR OF THE SEMICONDUCTORS SILICON AND GALLIUM ARSENIDE IN CONTACT WITH PURE METALS**

H. MISHINA (Inst. of Physical and Chemical Research, Saitama, Japan) and D. H. BUCKLEY Dec. 1984 12 p refs

(NASA-TP-2405; E-2219; NAS 1.60:2405) Avail: NTIS HC A02/MF A01 CSCL 11B

Friction experiments were conducted for the semiconductors silicon and gallium arsenide in contact with pure metals. Polycrystalline titanium, tantalum, nickel, palladium, and platinum were made to contact a single crystal silicon (111) surface. Indium, nickel, copper, and silver were made to contact a single crystal gallium arsenide (100) surface. Sliding was conducted both in room air and in a vacuum of 10 to the minus 9th power torr. The friction of semiconductors in contact with metals depended on a Schottky barrier height formed at the metal semiconductor interface. Metals with a higher barrier height on semiconductors gave lower friction. The effect of the barrier height on friction behavior for argon sputtered cleaned surfaces in vacuum was more specific than that for the surfaces containing films in room air. With a silicon surface sliding on titanium, many silicon particles back transferred. In contrast, a large quantity of indium transferred to the gallium arsenide surface. R.J.F.

**N85-13045\*#** National Aeronautics and Space Administration. Lewis Research Center, Cleveland, Ohio.

**HIGH-TEMPERATURE EROSION OF PLASMA-SPRAYED, YTTRIA-STABILIZED ZIRCONIA IN A SIMULATED TURBINE ENVIRONMENT**

R. F. HANSCHUH Dec. 1984 19 p refs Prepared in cooperation with Army Research and Technology Labs., Cleveland

(NASA-TP-2406; E-2271; NAS 1.60:2406; AVSCOM-TR-84-C-17) Avail: NTIS HC A02/MF A01 CSCL 11B

A series of rig calibration and high temperature tests simulating gas path seal erosion in turbine engines were performed at three impingement angles and at three downstream locations. Plasma sprayed, yttria stabilized zirconia specimens were tested. Steady state erosion curves presented for 19 test specimens indicate a brittle type of material erosion despite scanning electron microscopy evidence of plastic deformation. Steady state erosion results were not sensitive to downstream location but were sensitive to impingement angle. At difference downstream locations specimen surface temperature varied from 1250 to 1600 C (2280 to 2900 F) and particle velocity varied from 260 to 320 m/s (850 to 1050 ft/s). The mass ratio of combustion products to erosive grit material was typically 240. Author

**N85-14928\*#** National Aeronautics and Space Administration. Lewis Research Center, Cleveland, Ohio.

**EFFECTS OF SILVER AND GROUP 2 FLUORIDES ADDITION TO PLASMA SPRAYED CHROMIUM CARBIDE HIGH TEMPERATURE SOLID LUBRICANT FOR FOIL GAS BEARING TO 650 DEG C**

R. C. WAGNER (Case Western Reserve Univ.) and H. E. SLINEY 1984 26 p refs Presented at the Ann. Meeting of the American Society of Lubrication Engineers, Las Vegas, Nev., 6-9 May 1985

(Contract DE-AI01-80CS-50194)

(NASA-TM-86895; E-2317; DOE/NASA/50194-40; NAS 1.15:86895) Avail: NTIS HC A03/MF A01 CSCL 11H

A new self-lubricating coating composition of nickel aluminate-bonded chromium carbide formulated with silver and Group II fluorides was developed in a research program on high temperature solid lubricants. One of the proposed applications for this new coating composition is as a wide temperature spectrum solid lubricant for complaint foil gas bearings. Friction and wear properties were obtained using a foil gas bearing start/stop apparatus at temperatures from 25 to 650 C. The journals were Inconel 718. Some were coated with the plasma sprayed experimental coating, others with unmodified nickel



aluminide/chromium carbide as a baseline for comparison. The additional components were provided to assist in achieving low friction over the temperature range of interest. Uncoated, preoxidized Inconel X-750 foil bearings were operated against these surfaces. The foils were subjected to repeated start/stop cycles under a 14-kPa (2-psi) bearing unit loading. Sliding contact occurred during lift-off and coastdown at surface velocities less than 6 m/s (3000 rpm). Testing continued until 9000 start/stop cycles were accumulated or until a rise in starting torque indicated the journal/bearing had failed. Comparison in coating performance as well as discussions of their properties and methods of application are given. Author

**N85-14929\*#** National Aeronautics and Space Administration. Lewis Research Center, Cleveland, Ohio.

**EFFECT OF SUBSTITUTED PHENYLNADIMIDES ON PROCESSING AND PROPERTIES OF PMR POLYIMIDE COMPOSITES**

W. B. ALSTON and R. W. LAUVER 1985 19 p refs Presented at the 30th Natl. SAMPE Symp. and Exhibition, Anaheim, Calif., 19-21 Mar. 1985

(NASA-TM-86902; E-2380; USAAVSCOM-TR-84-C-20; NAS 1.15:86902) Avail: NTIS HC A02/MF A01 CSCL 11B

Three nitrophenylnadimide cure initiators and two phenylnadimides (without nitros) were evaluated as additives to PMR-15 resins and Celion 6000 graphite fiber composites. The results of a resin screening study eliminated all of the additives except 3-nitrophenylnadimide (NO2PN) for use as a low temperature curing additive for PMR-15. Thus, NO2PN and the two control additives were investigated in PMR-15 formulations from which Celion 6000 graphite fiber/PMR-15 composites were processed both with low temperature (274 C) and normal (316 C) cure cycles. Comparisons of the two processing cycles, the resultant glass transition temperatures (T<sub>g</sub>), the ambient, 274 and 316 C composite mechanical properties determined before and after 316 C postcure, the 316 C thermo-oxidative weight losses and the retention of 316 C composite mechanical properties are presented. Empirical correlations of the type and amount of nadimide additives with processing parameters, T<sub>g</sub>, composite mechanical properties, composite thermo-oxidative stability and long term retention of 316 C composite mechanical properties are also presented. Author

**N85-15892\*#** United Technologies Research Center, East Hartford, Conn.

**IMIDE MODIFIED EPOXY MATRIX RESINS Final Report**

D. A. SCOLA Mar. 1984 74 p refs

(Contract NAS3-23528)

(NASA-CR-174695; NAS 1.26:174695; R84-916161-14) Avail: NTIS HC A04/MF A01 CSCL 11G

The results of a program designed to develop tough imide modified epoxy resins cured by bisimide amine (BIA) hardeners are described. State-of-the-art epoxides MY720 and DER383 were used, and four bismide amines were evaluated. These were the BIA's derived from the 6F anhydride (4,4'-(hexafluoroisopropylidene) bis(phthalic anhydride) and the diamines 3,3'-diaminodiphenyl sulfone, 4,4'-oxydianiline, 4,4'-methylene dianiline, and 1,12-dodecane diamine. A key intermediate, designated 6F anhydride, is required for the synthesis of the bisimide amines. Reaction parameters to synthesize a precursor to the 6F anhydride (6FHC) in high yields were investigated. The catalyst trifluoromethane sulfonic acid was studied. Although small scale runs yielded the 6FHC in 50 percent yield, efforts to translate these results to a larger scale synthesis gave the 6FHC in only 9 percent yield. Results show that the concept of using bisimide amine as curing agents to improve the toughness properties of epoxies is valid. R.S.F.

**N85-15893\*#** National Aeronautics and Space Administration. Lewis Research Center, Cleveland, Ohio.

**FUNDAMENTAL TRIBOLOGICAL PROPERTIES OF CERAMICS**  
D. H. BUCKLEY and K. MIYOSHI 1985 25 p refs Presented at the 9th Ann. Conf. on Composites and Advan. Ceram. Mater., Cocoa Beach, Fla., 20-24 Jan. 1985; sponsored by the American Ceramic Society

(NASA-TM-86915; E-2386; NAS 1.15:86915) Avail: NTIS HC A02/MF A01 CSCL 11B

When a ceramic is brought into contact with itself, another ceramic, or a metal, strong bond forces can develop between the materials. Adhesion between a ceramic and itself or another solid are discussed from a theoretical consideration of the nature of the surfaces and experimentally by relating bond forces to the interface resulting from solid state contact. Elastic, plastic, and fracture behavior of ceramics in solid-state contact are discussed as they relate to friction and wear. The contact load necessary to initiate fracture in ceramics is shown to be appreciably reduced with tangential motion. Both friction and wear of ceramics are anisotropic and relate to crystal structure as with metals. Both free energy of oxide formation and the d valence bond character of metals are related to the friction and wear characteristics for metals in contact with ceramics. Lubrication is found to increase the critical load necessary to initiate fracture of ceramics with sliding or rubbing contact. R.S.F.

**N85-15895\*#** Case Western Reserve Univ., Cleveland, Ohio.

**EXPERIMENTAL TEST PROGRAM FOR EVALUATION OF SOLID LUBRICANT COATING AS APPLIED TO COMPLIANT FOIL GAS BEARINGS TO 315 DEG C Final Report**

R. C. WAGNER Jan. 1985 54 p refs

(Contract NCC3-30; DE-AI01-80CS-50194)

(NASA-CR-174837; DOE/NASA/0030-1; E-2416; NAS

1.26:174837) Avail: NTIS HC A04/MF A01 CSCL 11H

An experimental apparatus and test procedure was developed to compare the performance of two solid lubricant coatings for air lubricated compliant foil gas bearings in the temperature range of 25 to 315 C. Polyimide bonded additive (SBGC) were tested extensively for durability and frictional characteristics. A partial arc bearing constructed of Inconel X-750 was coated on the bore with one of these coatings. The foil was subjected to repeated start/stop cycles. Performance comparisons reveal that although both coatings survive thousands of start/stop cycles, only the PBGF coated bearing achieves the specified 9000 start/stops. There is enough wear on the SBGC coated bearing to warrant termination of the test prior to 9000 start/stop cycles due to coating failure. The frictional characteristics of the PBGF are better at the elevated temperatures than at lower temperatures; a marked increase in sliding friction occurs as the temperature decreases. The SBGC maintains relatively constant frictional characteristics independent of operating temperature. R.S.F.

**N85-15896\*#** National Aeronautics and Space Administration. Lewis Research Center, Cleveland, Ohio.

**SURFACE EFFECTS OF CORROSIVE MEDIA ON HARDNESS, FRICTION, AND WEAR OF MATERIALS**

K. MIYOSHI, D. H. BUCKLEY, G. W. P. RENGSTORFF, and H. ISHIGAKI 1985 20 p refs Presented at the Intern. Conf. on Wear of Mater., Vancouver, British Columbia, 14-18 Apr. 1985; sponsored by ASME

(NASA-TM-83711; E-2088; NAS 1.15:83711) Avail: NTIS HC A02/MF A01 CSCL 11G

Hardness, friction, and wear experiments were conducted with magnesium oxide exposed to various corrosive media and also with elemental iron and nickel exposed to water and NaOH. Chlorides such as MgCl<sub>2</sub> and sodium containing films were formed on cleaved magnesium oxide surfaces. The MgCl<sub>2</sub> films softened the magnesium oxide surfaces and caused high friction and great deformation. Hardness was strongly influenced by the pH value of the HCl-containing solution. The lower the pH, the lower the microhardness. Neither the pH value of nor the immersion time in NaOH containing, NaCl containing, and HNO<sub>3</sub> containing solutions influenced the microhardness of magnesium oxide. NaOH formed

## 27 NONMETALLIC MATERIALS

a protective and low friction film on iron surfaces. The coefficient of friction and the wear for iron were low at concentrations of NaOH higher than 0.01 N. An increase in NaOH concentration resulted in a decrease in the concentration of ferric oxide on the iron surface. It took less NaOH to form a protective, low friction film on nickel than on iron. R.S.F.

**N85-15897\*#** National Aeronautics and Space Administration. Lewis Research Center, Cleveland, Ohio.

### **CONTACT ANGLE AND SURFACE TENSION MEASUREMENTS OF A FIVE-RING POLYPHENYL ETHER**

W. R. JONES, JR. 1985 25 p refs Proposed for presentation at the Ann. Meeting of the American Society of Lubrication Engineers, Las Vegas, Nev., 6-9 May 1985 (NASA-TM-86927; E-2313; NAS 1.15:86927) Avail: NTIS HC A02/MF A01 CSCL 11G

Contact angle measurements were performed for a five-ring polyphenyl ether isomeric mixture on M-50 steel in a dry nitrogen atmosphere. Two different techniques were used: (1) a tilting plate apparatus, and (2) a sessile drop apparatus. Measurements were made for the temperature range 25 to 190 C. Surface tension was measured by a differential maximum bubble pressure technique over the range 23 to 220C in room air. The critical surface energy of spreading ( $\gamma_{sc}$ ) was determined for the polyphenyl ether by plotting the cosine of the contact angle ( $\theta$ ) versus the surface tension ( $\gamma_{LV}$ ). The straight line intercept at  $\cos \theta = 1$  is defined as  $\gamma_{sc}$ .  $\gamma_{sc}$  was found to be 30.1 dyn/cm for the tilting plate technique and 31.3 dyn/cm for the sessile drop technique. These results indicate that the polyphenyl ether is inherently autophobic (i.e., it will not spread on its own surface film until its surface tension is less than  $\gamma_{sc}$ ). This phenomenon is discussed in light of the wettability and wear problems encountered with this fluid.

Author

### **N85-15916\*#** Oak Ridge National Lab., Tenn. **DISPERSED METAL-TOUGHENED CERAMICS AND CERAMIC BRAZING**

A. J. MOORHEAD, T. N. TIEGS, and R. J. LAUF 1983 8 p refs Presented at the Automotive Technol. Develop. Contractor Coord. Meeting, Dearborn, Mich., 13 Nov. 1983 (Contract NASA ORDER C-74148-D; NASA ORDER C-72801-D; DE-AC05-84OR-21400; W-7405-ENG-26) (NASA-PR-174284; NAS 1.26:174284; DE85-001552; CONF-831142-3) Avail: NTIS HC A02/MF A01 CSCL 11G

An alumina ( $Al_2O_3$ ) based material that contains approximately 1 vol% finely dispersed platinum or chromium was developed for use in high temperature thermal shock resistant electrical insulators. The work at ORNL is divided into two areas: (1) development of DMT ceramics; and (2) development of brazing filler metals suitable for making ceramic to ceramic and ceramic to metal brazements. The DMT ceramics and brazements are intended for service at elevated temperatures and at high stress levels in the dirty environments of advanced heat engines. The development and characterization of DMT ceramics includes processing (powder preparation, densification and heat treatment) and detailed measurement of mechanical and physical properties (strength, fracture toughness, and thermal conductivity). The brazing work includes: (1) the formulation and melting of small quantities of experimental brazing filler metals; (2) evaluation of the wetting and bonding behavior of these filler metals on  $Al_2O_3$ , partially stabilized zirconia and (ALPHA)-SiC in a sessile drop apparatus; and (3) determine the short term strength and fracture toughness of brazements. DOE

**N85-18153\*#** National Aeronautics and Space Administration. Lewis Research Center, Cleveland, Ohio.

### **TRIBOLOGICAL PROPERTIES OF GRAPHITE-FIBER-REINFORCED, PARTIALLY FLUORINATED POLYIMIDE COMPOSITES**

R. L. FUSARO and W. F. HADY 1985 28 p refs Proposed for presentation at the Ann. Meeting of the American Society of Lubrication Engineers, Las Vegas, Nev., 6-9 May 1985 (NASA-TM-86926; E-2422; NAS 1.15:86926) Avail: NTIS HC A03/MF A01 CSCL 11G

Graphite-fiber-reinforced polyimide (GFRPI) composites were formulated from three new partially fluorinated polyimides and three types of graphite fiber. Nine composites were molded into pins and evaluated in a pin-on-disk tribometer. Friction coefficients, wear rates, pin wear surface morphology, and transfer film formation were assessed at 25 and 300 C. Also assessed was the effect of sliding speed on friction. Wear was up to two orders of magnitude lower at 25 C and up to one order of magnitude lower at 300 C than with previously formulated NASA GFRPI composites.

Author

### **N85-18154\*#** General Motors Corp., Indianapolis, Ind. **AN INVESTIGATION OF ENHANCED CAPABILITY THERMAL BARRIER COATING SYSTEMS FOR DIESEL ENGINE COMPONENTS Final Report**

R. L. HOLTZMAN, J. L. LAYNE, and B. SCHECHTER Aug. 1984 140 p refs (Contract DEN3-326; DE-AI01-80CS-50194) (NASA-CR-174820; DOE/NASA/0326-1; NAS 1.26:174820; EDR-11869) Avail: NTIS HC A07/MF A01 CSCL 11B

Material systems and processes for the development of effective and durable thermal barriers for heavy duty diesel engines were investigated. Seven coating systems were evaluated for thermal conductivity, erosion resistance, corrosion/oxidation resistance, and thermal shock resistance. An advanced coating system based on plasma sprayed particle yttria stabilized zirconia (PS/HYSZ) was judged superior in these tests. The measured thermal conductivity of the selected coating was 0.893 W/m C at 371 C. The PS/HYSZ coating system was applied to the piston crown, fire deck and valves of a single cylinder low heat rejection diesel engine. The coated engine components were tested for 24 hr at power levels from 0.83 MPa to 1.17 MPa brake mean effective pressure. The component coatings survived the engine tests with a minimum of distress. The measured fire deck temperatures decreased 86 C (155 F) on the intake side and 42 C (75 F) on the exhaust side with the coating applied. M.G.

**N85-19136\*#** National Aeronautics and Space Administration. Lewis Research Center, Cleveland, Ohio.

### **FACTORS INFLUENCING THE BALL MILLING OF $Si_3N_4$ IN WATER**

M. R. FREEDMAN, J. D. KISER, and T. P. HERBELL 1985 14 p refs Presented at the 9th Ann. Conf. on Composites and Advanced Ceram. Mater., Cocoa Beach, Fla., 20-23 Jan. 1985; sponsored by American Ceramic Society. (NASA-TM-86932; E-2420; NAS 1.15:86932) Avail: NTIS HC A02/MF A01 CSCL 11G

A statistical study of the ball milling of  $Si_3N_4$  powder in  $Si_3N_4$  hardware was undertaken to understand how the resulting increase in specific surface area is related to solids loading and mill speed. An attempt was made to optimize milling conditions. The degree of comminution was more dependent upon solids loading than mill speed. A practical grinding limit between 0.5 and 0.75 microns was achieved in 144 hr independent of solids loading. Ball mill wear and media wear were independent of both solids loading and mill speed. E.A.K.

**N85-20127\*#** National Aeronautics and Space Administration. Lewis Research Center, Cleveland, Ohio.

**THE ROLE OF SILVER IN SELF-LUBRICATING COATINGS FOR USE AT EXTREME TEMPERATURES**

H. E. SLINNEY 1985 20 p refs To be presented at the Ann. Meeting of the Am. Soc. of Lubrication Engr., Las Vegas, Nev., 6-9 May 1985

(NASA-TM-86943; E-2428; NAS 1.15:86943) Avail: NTIS HC A02/MF A01 CSCL 11H

The advantages and disadvantages of elemental silver as a tribological material are discussed. It is demonstrated that the relatively high melting point of 961 deg C, softness, marked plasticity, and thermochemical stability of silver combine to make this metal useful in thin film solid lubricant coatings over a wide temperature range. Disadvantages of silver during sliding, except when used as a thin film, are shown to be gross ploughing due to plastic deformation under load with associated high friction and excessive transfer to counterface surfaces. This transfer generates an irregular surface topography with consequent undesirable changes in bearing clearance distribution. Research to overcome these disadvantages of element silver is described. A comparison is made of the tribological behavior of pure silver with that of silver formulated with other metals and high-temperature solid lubricants. The composite materials are prepared by co-depositing the powdered components with an airbrush followed by furnace heat treatment or by plasma-spraying. Composite coatings were formulated which are shown to be self-lubricating over repeated, temperature cycles from low temperature to about 900 deg C.

R.J.F.

**N85-21350\*** National Aeronautics and Space Administration. Lewis Research Center, Cleveland, Ohio.

**CHEMICAL APPROACH FOR CONTROLLING NADIMIDE CURE TEMPERATURE AND RATE WITH MALEIMIDE Patent**

R. W. LAUVER, inventor (to NASA) 5 Feb. 1985 9 p Filed 14 Dec. 1983 Supersedes N84-22698 (22 - 13, p 1953) Division of US Patent Appl. SN-516217, filed 22 Jul. 1983

(NASA-CASE-LEW-13770-3; NAS 1.71:LEW-13770-3; US-PATENT-4,497,948; US-PATENT-APPL-SN-561431; US-PATENT-CLASS-528-342; US-PATENT-CLASS-526-217; US-PATENT-CLASS-526-262; US-PATENT-CLASS-528-229; US-PATENT-CLASS-528-315; US-PATENT-CLASS-528-322; US-PATENT-CLASS-528-336; US-PATENT-APPL-SN-516217)

Avail: US Patent and Trademark Office CSCL 07D

Polyimide resins suitable for use as composite matrix materials are formed by copolymerization of maleic and norbornenyl endcapped monomers and oligomers. The copolymers can be cured at temperatures under about 300 C by controlling the available concentration of the maleic end-capped reactant. Control can be achieved by adding sufficient amounts of said maleic reactant, or by chemical modification of either copolymers, so as to either increase Diels-Alder retrogression of the norbornenyl capped reactant and/or holding initiation and polymerization to a rate compatible with the availability of the maleic-capped reactant.

Author

**N85-21351\*** National Aeronautics and Space Administration. Lewis Research Center, Cleveland, Ohio.

**CHEMICAL APPROACH FOR CONTROLLING NADIMIDE CURE TEMPERATURE AND RATE WITH MALEIMIDE Patent**

R. W. LAUVER, inventor (to NASA) 5 Feb. 1985 9 p Filed 14 Dec. 1983 Supersedes N84-22699 (22 - 13, p 1953) Division of US Patent Appl. SN-516217, filed 22 Jul. 1983

(NASA-CASE-LEW-13770-4; NAS 1.71:LEW-13770-4; US-PATENT-4,497,939; US-PATENT-APPL-SN-561429; US-PATENT-CLASS-526-262; US-PATENT-CLASS-528-229; US-PATENT-CLASS-528-322; US-PATENT-CLASS-528-342; US-PATENT-APPL-SN-516217) Avail: US Patent and Trademark Office CSCL 07D

Polyimide resins suitable for use as composite matrix materials are formed by copolymerization of maleic and norbornenyl endcapped monomers and oligomers. The copolymers can be cured at temperatures under about 300 C by controlling the

available concentration of the maleic end-capped reactant. This control can be achieved by adding sufficient amounts of said maleic reactant, or by chemical modification of either copolymer, so as to either increase Diels-Alder retrogression of the norbornenyl capped reactant and/or holding initiation and polymerization to a rate compatible with the available of the maleic-capped reactant.

Author

**N85-21352\*** National Aeronautics and Space Administration. Lewis Research Center, Cleveland, Ohio.

**CHEMICAL APPROACH FOR CONTROLLING NADIMIDE CURE TEMPERATURE AND RATE Patent**

R. W. LAUVER, inventor (to NASA) 5 Feb. 1985 8 p Filed 14 Dec. 1983 Supersedes N84-22700 (22 - 13, p 1953) Division of US Patent Appl. SN-516217, filed 22 Jul. 1983

(NASA-CASE-LEW-13770-5; NAS 1.71:LEW-13770-5; US-PATENT-4,497,940; US-PATENT-APPL-SN-561435; US-PATENT-CLASS-526-262; US-PATENT-CLASS-528-229; US-PATENT-CLASS-528-322; US-PATENT-CLASS-528-342; US-PATENT-APPL-SN-516217) Avail: US Patent and Trademark Office CSCL 07D

Polyimide resins suitable for use as composite matrix materials are formed by copolymerization of maleic and norbornenyl endcapped monomers and oligomers. The copolymers can be cured at temperatures under about 300 C by controlling the available concentration of the maleic endcapped reactant. This control is achieved by adding sufficient amounts of said maleic reactant or by chemical modification of either copolymer, to either increase Diels-Alder retrogression of the norbornenyl capped reactant and/or hold initiation and polymerization to a rate compatible with the availability of the maleic capped reactant.

Official Gazette of the U.S. Patent and Trademark Office

**N85-21355\*#** National Aeronautics and Space Administration. Lewis Research Center, Cleveland, Ohio.

**TRIBOLOGICAL PROPERTIES OF BORON NITRIDE SYNTHESIZED BY ION BEAM DEPOSITION**

K. MIYOSHI, D. H. BUCKLEY, and T. SPALVINS 1985 15 p refs Proposed for presentation at the 12th Intern. Conf. on Met. Coatings, Los Angeles, 15-19 Apr. 1985; sponsored by the American Vacuum Society

(NASA-TM-86962; E-2459; NAS 1.15:86962) Avail: NTIS HC A02/MF A01 CSCL 11G

The adhesion and friction behavior of boron nitride films on 440 C bearing stainless steel substrates was examined. The thin films containing the boron nitride were synthesized using an ion beam extracted from a borazine plasma. Sliding friction experiments were conducted with BN in sliding contact with itself and various transition metals. It is indicated that the surfaces of atomically cleaned BN coating film contain a small amount of oxides and carbides, in addition to boron nitride. The coefficients of friction for the BN in contact with metals are related to the relative chemical activity of the metals. The more active the metal, the higher is the coefficient of friction. The adsorption of oxygen on clean metal and BN increases the shear strength of the metal - BN contact and increases the friction. The friction for BN-BN contact is a function of the shear strength of the elastic contacts. Clean BN surfaces exhibit relatively strong interfacial adhesion and high friction. The presence of adsorbates such as adventitious carbon contaminants on the BN surfaces reduces the shear strength of the contact area. In contrast, chemically adsorbed oxygen enhances the shear strength of the BN-BN contact and increases the friction.

E.A.K.

## 27 NONMETALLIC MATERIALS

**N85-21356\*#** National Aeronautics and Space Administration. Lewis Research Center, Cleveland, Ohio.

### **PARAMETRIC EVALUATION OF BALL MILLING OF SIC IN WATER**

J. D. KISER, T. P. HERBELL, and M. R. FREEDMAN 1985 17 p refs Presented at the 9th Ann. Conf. on Composites and Advanced Ceramic Mater., Cocoa Beach, Fla., 20-23 Jan. 1985 (NASA-TM-86974; E-2399; NAS 1.15:86974) Avail: NTIS HC A02/MF A01 CSCL 11G

A statistically designed experiment was conducted to determine optimum conditions for ball milling alpha-SiC in water. The influence of pH adjustment, volume percent solids loading, and mill rotational speed on grinding effectiveness was examined. An equation defining the effect of those milling variables on specific surface area was obtained. The volume percent solids loading of the slurry had the greatest influence on the grinding effectiveness in terms of increase in specific surface area. As grinding effectiveness improved, mill and media wear also increased. Contamination was minimized by use of sintered alpha-SiC milling hardware. Author

**N85-21357\*#** National Aeronautics and Space Administration. Lewis Research Center, Cleveland, Ohio.

### **CHARACTERIZATION OF LUBRICATED BEARING SURFACES OPERATED UNDER HIGH LOADS**

J. L. LAUER (Rensselaer Polytechnic Inst.), N. MARXER (Rensselaer Polytechnic Inst.), and W. R. JONES, JR. 1985 16 p refs Proposed for presentation at the Intern. Tribology Conf., Tokyo, 8-10 Jul. 1985; sponsored by the Japan Society of Lubrication Engineers (Contract AF-AFOSR-0005-81; DAAG24-83-K-0058) (NASA-TM-86964; E-2462; NAS 1.15:86964) Avail: NTIS HC A02/MF A01 CSCL 11H

The composition and surface profiles of M-50 steel surfaces were measured after operation at high loads in a bearing contact simulator. An ester lubricant (trimethylpropane triheptanoate) was used with and without various additives. Optical profiles were obtained + or - to 30 depth resolution with a phase-locked interference microscope in 10 micron diameter areas within and outside the wear tracks. Optical constants and surface film thickness were measured in the same areas with an electronic scanning ellipsometer. Film composition was measured with a scanning Auger electron spectrometer. It is concluded that metal oxide formation is accelerated within the wear tracks. E.A.K.

**N85-21358\*#** National Aeronautics and Space Administration. Lewis Research Center, Cleveland, Ohio.

### **OXIDATION AND HOT CORROSION OF HOT-PRESSED Si3N4 AT 1000 DEG C**

W. L. FIELDER Apr. 1985 25 p refs (NASA-TM-86977; E-2419; NAS 1.15:86977) Avail: NTIS HC A02/MF A01 CSCL 11G

The oxidation and hot corrosion of a commercial, hot-pressed Si3N4 were investigated at 1000 C under an atmosphere of flowing O2. For the hot corrosion studies, thin films of Na2SO4 were airbrushed on the Si3N4 surface. The hot corrosion attack was monitored by the following techniques: continuous weight measurements, SO2 evolution, film morphology, and chemical analyses. Even though the hot corrosion weight changes after 25 hr were relatively small, the formation of SiO2 from oxidation of Si3N4 was an order of magnitude greater in the presence of molten Na2SO4. The formation of a protective SiO2 phase at the Si3N4 surface is minimized by the fluxing action of the molten Na2SO4 thereby allowing the oxidation of the Si3N4 to proceed more rapidly. A simple process is proposed to account for the hot corrosion process. E.A.K.

**N85-21359\*#** National Aeronautics and Space Administration. Lewis Research Center, Cleveland, Ohio.

### **HUMIDITY EFFECTS ON ADHESION OF NICKEL-ZINC FERRITE IN ELASTIC CONTACT WITH MAGNETIC TAPE AND ITSELF**

K. MIYOSHI, D. H. BUCKLEY, T. KUSAKA (Osaka Inst. of Technology), and C. MAEDA (Osaka Inst. of Technology) Mar. 1985 10 p refs (NASA-TP-2449; E-2361; NAS 1.60:2449) Avail: NTIS HC A02/MF A01 CSCL 11G

The effects of humidity on the adhesion of Ni-Zn ferrite and magnetic tape in elastic contact with a Ni-Zn ferrite hemispherical pin in moist nitrogen were studied. Adhesion was independent of normal load in dry, humid, and saturated nitrogen. Ferrites adhere to ferrites in a saturated atmosphere primarily from the surface tension effects of a thin film of water adsorbed on the ferrite surfaces. The surface tension of the water film calculated from the adhesion results was 48 times 0.00001 to 56 times 0.00001 N/cm; the accepted value for water is 72.7 x 0.00001 N/cm. The adhesion of ferrite-ferrite contacts increased gradually with increases in relative humidity to 80 percent, but rose rapidly above 80 percent. The adhesion at saturation was 30 times or more greater than that below 80 percent relative humidity. Although the adhesion of magnetic tape - ferrite contacts remained low below 40 percent relative humidity and the effect of humidity was small, the adhesion increased considerably with increasing relative humidity above 40 percent. The changes in adhesion of elastic contacts were reversible on humidifying and dehumidifying. Author

**N85-22511\*#** Pennsylvania State Univ., University Park.

### **MASS SPECTRA OF NEUTRAL PARTICLES RELEASED DURING ELECTRICAL BREAKDOWN OF THIN POLYMER FILMS**

B. R. F. KENDALL In NASA. Lewis Research Center Spacecraft Environ. Interactions Technol., 1983 p 525-535 Mar. 1985 refs (Contract NSG-3301)

Avail: NTIS HC A99/MF E03 CSCL 11G

A special type of time-of-flight mass spectrometer triggered from the breakdown event was developed to study the composition of the neutral particle flux released during the electrical breakdown of polymer films problem. Charge is fed onto a metal-backed polymer surface by a movable smooth platinum contact. A slowly increasing potential from a high-impedance source is applied to the contact until breakdown occurs. The breakdown characteristics is made similar to those produced by an electron beam charging system operating at similar potentials. The apparatus showed that intense instantaneous fluxes of neutral particles are released from the sites of breakdown events. For Teflon FEP films of 50 and 75 microns thickness the material released consists almost entirely of fluorocarbon fragments, some of them having masses greater than 350 atomic mass units amu, while the material released from a 50 micron Kapton film consists mainly of light hydrocarbons with masses at or below 44 amu, with additional carbon monoxide and carbon dioxide. The apparatus is modified to allow electron beam charging of the samples. E.A.K.

**N85-22755\*#** National Aeronautics and Space Administration. Lewis Research Center, Cleveland, Ohio.

### **METALLIC AND METALLOCERAMIC COATING BY THERMAL DECOMPOSITION**

R. C. HENDRICKS and G. MCDONALD 1985 7 p refs Presented at the 12th Intern. Conf. on Met. Coatings, Los Angeles, 15-19 Apr. 1985; sponsored by the American Vacuum Society (NASA-TM-86992; E-2538; NAS 1.15:86992) Avail: NTIS HC A02/MF A01 CSCL 11G

Metallic and metalloceramic coatings were prepared by thermal decomposition of a number of inorganic and metallo-organic compounds. The compounds were applied by spraying and by immersion, especially on ceramic fibers and fiber forms, which are easily coated by this procedure. Penetration of low-density ceramics is examined, and procedures are described that were used for converting the deposited materials to metals, oxides, or

metal oxide films. Multiple-component films were also prepared. Photomicrographs illustrate the structure of these films. R.J.F.

**N85-22756\*#** National Aeronautics and Space Administration. Lewis Research Center, Cleveland, Ohio.

**FILM AND INTERSTITIAL FORMATION OF METALS IN PLASMA-SPRAYED CERAMICS**

R. C. HENDRICKS, G. MCDONALD, and R. L. MULLEN (Case Western Reserve Univ., Cleveland) 1985 12 p refs Presented at the 12th Intern. Conf. on Metallurgical Coatings, Los Angeles, 15-19 Apr. 1985

(NASA-TM-86993; NAS 1.15:86993; E-2539) Avail: NTIS HC A02/MF A01 CSCL 11B

A method is described to electrodeposit noble metals such as platinum and ordinary metals such as copper on and within plasma-sprayed ceramic materials and ceramic fiber materials. Low-density ceramic fiber bodies were vacuum impregnated with plating solution and attached to an electrode. Light micrographs illustrating the density and location of deposited materials are presented and discussed. Voids in the plasma-sprayed ceramic were filled with deposits that vary from spherical to lens-shaped circular and have particle size corresponding to the full range of void size. Multiple coatings of ceramic and metal can be sequenced. Author

**N85-22757\*#** Southwest Research Inst., San Antonio, Tex. **SLIDING SEAL MATERIALS FOR ADIABATIC ENGINES Interim Report, Feb. 1984 - Feb. 1985**

J. LANKFORD Apr. 1985 70 p refs

(Contract DEN3-352; DE-AI01-80CS-50194)

(NASA-CR-174893; NAS 1.26:174893; SRI-06-7963;

DOE/NASA/0352-1) Avail: NTIS HC A04/MF A01 CSCL 11B

The sliding friction coefficients and wear rates of promising carbide, oxide, and nitride materials were measured under temperature, environmental, velocity, loading conditions that are representative of the adiabatic engine environment. In order to provide guidance needed to improve materials for this application, the program stressed fundamental understanding of the mechanisms involved in friction and wear. Microhardness tests were performed on the candidate materials at elevated temperatures, and in atmospheres relevant to the piston seal application, and optical and electron microscopy were used to elucidate the micromechanisms of wear following wear testing. X-ray spectroscopy was used to evaluate interface/environment interactions which seemed to be important in the friction and wear process. Electrical effects in the friction and wear processes were explored in order to evaluate the potential usefulness of such effects in modifying the friction and wear rates in service. However, this factor was found to be of negligible significance in controlling friction and wear. R.J.F.

**N85-22758\*#** Oak Ridge National Lab., Tenn. Metal and Ceramics Div.

**DISPERSED-METAL-TOUGHENED ALUMINA**

T. N. TIEGS and A. J. MOORHEAD Feb. 1984 31 p refs

(Contract NASA ORDER C-72801-D; DE-AC05-84OR-21400)

(NASA-CR-174687; DOE/NASA/2801-1; NAS 1.26:174687;

ORNL/TM-9518) Avail: NTIS HC A03/MF A01 CSCL 11B

Hot-pressed alumina with a fine dispersion of Cr metal particles showed good fracture toughness ( $K_{sub I sub c}$  MPa. m  $^{1/2}$ ) and thermal shock resistance. However, the fracture strengths of these materials were relatively low (190 to 240 MPa vs 350 to 580 MPa for pure alumina). The good fracture toughness and thermal shock resistance were found to be related to the relatively large-grain duplex microstructure of the hot-pressed materials. The fracture toughness of alumina with dispersions of Ni and Pt was found to be inferior to that of the  $Al_2O_3$ -Cr materials. Hot-pressed solid solutions of  $Al_2O_3$ - $Cr_2O_3$  also showed good fracture toughness ( $K_{sub I sub c} = 7.3$  to  $7.7$  MPa.m  $^{1/2}$ ), which was again due to the development of a relatively large-grain duplex microstructure. Author

**N85-23781\*#** National Aeronautics and Space Administration. Lewis Research Center, Cleveland, Ohio.

**TRANSMISSION EFFICIENCY MEASUREMENTS AND CORRELATIONS WITH PHYSICAL CHARACTERISTICS OF THE LUBRICANT**

J. J. COY, A. M. MITCHELL, and B. J. HAMROCK In AGARD Gears and Power Transmission Systems for Helicopters and Turboprops 15 p Jan. 1985 refs Previously announced as N84-30293 Prepared in cooperation with Army Research and Technology Labs.

Avail: NTIS HC A17/MF A01 CSCL 11G

Data from helicopter transmission efficiency tests were compared to physical properties of the eleven lubricants used in those tests. The tests were conducted with the OH-58 helicopter main rotor transmission. Efficiencies ranged from 98.3 to 98.8 percent. The data was examined for correlation of physical properties with efficiency. There was a reasonable correlation of efficiency with absolute viscosity if the viscosity was first corrected for temperature and pressure in the lubricated contact. Between lubricants, efficiency did not correlate well with viscosity at atmospheric pressure. Between lubricants, efficiency did not correlate well with calculated lubricant film forming capacity. Bench type sliding friction and wear measurements could not be correlated to transmission efficiency and component wear. Author

**N85-24000\*#** National Aeronautics and Space Administration. Lewis Research Center, Cleveland, Ohio.

**ENVIRONMENTAL EFFECTS ON THE TENSILE STRENGTH OF CHEMICALLY VAPOR DEPOSITED SILICON CARBIDE FIBERS**

R. T. BHATT and M. D. KRAITCHMAN Apr. 1985 33 p refs Presented at 8th Ann. Conf. on Composites and Adv. Ceramic Mater., Cocoa Beach, Fla.; sponsored by American Ceramic Soc. Prepared in cooperation with Army Research and Technology Labs.

(NASA-TM-86981; E-2519; NAS 1.15:86981;

USAAVSCOM-TR-85-C-4; AD-A157111) Avail: NTIS HC

A03/MF A01 CSCL 11G

The room temperature and elevated temperature tensile strengths of commercially available chemically vapor-deposited (CVD) silicon carbide fibers were measured after 15 min heat treatment to 1600 C in various environments. These environments included oxygen, air, argon and nitrogen at one atmosphere and vacuum at 10/9 atmosphere. Two types of fibers were examined which differed in the SiC content of their carbon-rich coatings. Threshold temperature for fiber strength degradation was observed to be dependent on the as-received fiber-flaw structure, on the environment and on the coating. Fractographic analyses and flexural strength measurements indicate that tensile strength losses were caused by surface degradation. Oxidation of the surface coating is suggested as one possible degradation mechanism. The SiC fibers containing the higher percentage of SiC near the surface of the carbon-rich coating show better strength retention and higher elevated temperature strength. E.A.K.

**N85-25521\*#** National Aeronautics and Space Administration. Lewis Research Center, Cleveland, Ohio.

**HOMOGENEITY OF PRISTINE AND BROMINE INTERCALATED GRAPHITE FIBERS**

J. R. GAIER and D. MARINO 1985 16 p refs Presented at the 17th Bien. Conf. on Carbon, Lexington, Ky.; sponsored by the American Carbon Society

(NASA-TM-87016; E-2560; NAS 1.15:87016) Avail: NTIS HC

A02/MF A01 CSCL 11G

Wide variations in the resistivity of intercalated graphite fibers and to use these materials for electrical applications, their bulk properties must be established. The homogeneity of the diameter, the resistivity, and the mass density of 50 graphite fibers, before and after bromine intercalation was measured. Upon intercalation the diameter was found to expand by about 5%, the resistivity to decrease by a factor of five, and the density to increase by about 6%. Each individual fiber was found to have uniform diameter and resistivity over macroscopic regions for lengths as long as 7 cm. The ratio of pristine to intercalated resistivity increases as the

## 27 NONMETALLIC MATERIALS

pristine fiber diameter increases at a rate of 0.16 micron, but decreases with the increasing ratio of intercalated diameter to pristine diameter at a rate of 0.08. E.A.K.

**N85-26867\*#** National Aeronautics and Space Administration. Lewis Research Center, Cleveland, Ohio.

### **ROCKET THRUST CHAMBER THERMAL BARRIER COATINGS**

R. J. QUENTMEYER /in NASA. Marshall Space Flight Center. Advan. High Pressure O2/H2 p 49-58 Apr. 1985

Avail: NTIS HC A99/MF E03; SOD HC CSCL 11B

Subscale rocket thrust chamber tests were conducted to evaluate the effectiveness and durability of thin yttria stabilized zirconium oxide coatings applied to the thrust chamber hot-gas side wall. The fabrication consisted of arc plasma spraying the ceramic coating and bond coat onto a mandrell and then electrodepositing the copper thrust chamber wall around the coating. Chambers were fabricated with coatings .008, and .005 and .003 inches thick. The chambers were thermally cycled at a chamber pressure of 600 psia using oxygen-hydrogen as propellants and liquid hydrogen as the coolant. The thicker coatings tended to delaminate, early in the cyclic testing, down to a uniform sublayer which remained well adhered during the remaining cycles. Two chambers with .003 inch coatings were subjected to 1500 thermal cycles with no coating loss in the throat region, which represents a tenfold increase in life over identical chambers having no coatings. An analysis is presented which shows that the heat lost to the coolant due to the coating, in a rocket thrust chamber design having a coating only in the throat region, can be recovered by adding only one inch to the combustion chamber length.

M.G.

**N85-26991\*#** National Aeronautics and Space Administration. Lewis Research Center, Cleveland, Ohio.

### **EFFECTS OF WEAR ON STRUCTURE-SENSITIVE MAGNETIC PROPERTIES OF CERAMIC FERRITE IN CONTACT WITH MAGNETIC TAPE**

K. MIYOSHI, D. H. BUCKLEY, and K. TANAKA (Kanazawa Univ., Japan) 1985 26 p refs Proposed for presentation at the Tribology Conf., Atlanta, 8-10 Oct. 1985; sponsored in part by Am. Soc. of Lubrication Engr. and ASME

(NASA-TM-87007; E-2483; NAS 1.15:87007) Avail: NTIS HC A03/MF A01 CSCL 11G

Wear experiments and electron microscopy and diffraction studies were conducted to examine the wear and deformed layers in single-crystal Mn-Zn (ceramic) ferrite magnetic head material in contact with magnetic tape and the effects of that contact on magnetic properties. The crystalline state of the single-crystal magnetic head was changed drastically during the sliding process. A nearly amorphous structure was produced on its wear surface. Deformation in the surficial layer of the magnetic head was a critical factor in readback signal loss above 2.5 dB. The signal output level was reduced as applied normal load was increased. Considerable plastic flow occurred on the magnetic tape surface with sliding, and the signal loss due to the tape wear was approximately 1 dB.

Author

**N85-26992\*#** National Aeronautics and Space Administration. Lewis Research Center, Cleveland, Ohio.

### **ENVIRONMENTAL STABILITY OF INTERCALATED GRAPHITE FIBERS**

J. R. GAIER and D. A. JAWORSKE May 1985 16 p refs Presented at the Intern. Symp. in Graphite Intercalation Compounds, Tsukuba, Japan, 27-30 May 1985; sponsored by Physical Society of Japan and the Carbon Society of Japan

(NASA-TM-87025; E-2580; NAS 1.15:87025) Avail: NTIS HC A02/MF A01 CSCL 11G

Graphite fibers intercalated with bromine, iodine monochloride, ferric chloride, and cupric chloride were subjected to stability tests under four environments which are encountered by engineering materials in the aerospace industry: ambient laboratory conditions, as would be experienced during handling operations and terrestrial applications; high vacuum, as would be experienced in space applications; high humidity, as would be experienced in marine

applications; and high temperature, as would be experienced in some processing steps and applications. Monitoring the resistance of the fibers at ambient laboratory conditions revealed that only the ferric chloride intercalated fibers were unstable, due to absorption of water from the air. All four types of intercalated fibers were unstable, due to absorption of water from the air. All four types of intercalated fibers were stable for long periods under high vacuum. Ferric chloride, cupric chloride, and iodine monochloride intercalated fibers were sensitive to high humidity conditions. All intercalated fibers began to degrade above 250 C. The order of their thermal stability, from lowest to highest, was cupric chloride, iodine monochloride, bromine, and ferric chloride. Of the four types of intercalated fibers tested, the bromine intercalated fibers appear to have the most potential for application, based on environmental stability.

Author

**N85-26993\*#** National Aeronautics and Space Administration. Lewis Research Center, Cleveland, Ohio.

### **EFFECT OF COUNTERFACE MATERIAL TYPE AND ITS TOPOGRAPHY ON THE TRIBOLOGICAL PROPERTIES OF POLYIMIDE COMPOSITES**

R. L. FUSARO 1985 33 p refs Proposed for presentation at the Tribology Conf., Atlanta, 8-10 Oct. 1985; sponsored by American Society of Lubrication Engineers and ASME

(NASA-TM-87036; E-2592; NAS 1.15:87036) Avail: NTIS HC A03/MF A01 CSCL 11B

Graphite fiber reinforced polyimide composite pins were slid against seven different counterfaces to determine the effect of material type on the tribological properties of polymer composites. In addition, the effect of sliding a new pin on a pre-established transfer film was investigated. The results indicated that almost a five order of magnitude difference in composite wear rate can occur just by varying the counterface material. An attempt to make all surfaces as smooth as possible was made, but due to differences in material composition this was not possible and a range of surface roughnesses were obtained. The results indicate that the smoother the surface, the lower the composite wear rate; but that small protrusions (not discernible with arithmetic surface roughness measurements) can markedly increase wear rates. A pre-established transfer film improved both run in and steady state wear rates.

M.G.

### **N85-26994\*#** Westinghouse Research Labs., Pittsburgh, Pa. **BREAKWAY FRICTION AND DYNAMIC FRICTION/WEAR MEASUREMENTS OF VARIOUS CERAMIC MATERIALS FROM 25 C (75 F) TO 650 C (1200 F) Final Report**

D. J. BOES Sep. 1984 82 p refs

(Contract DEN3-346; DE-AI01-80CS-50194)

(NASA-CR-174803; DOE/NASA/0346-1; NAS 1.26:174803;

REPT-85-9JDIESL-R1) Avail: NTIS HC A05/MF A01 CSCL 11B

This report describes the results of a program designed to evaluate the breakaway friction and dynamic friction/wear characteristics of materials having potential for use as load bearing components in a high-performance high-temperature heavy duty diesel engine. Ten candidate materials were selected, six of which were evaluated under all possible material combinations as both stationary as well as moving breakaway specimens. The remaining materials were evaluated either in the static mode against themselves and all other materials, or against themselves only. Experiments were performed at five temperatures up to 650 C (1200 F) and unit pressures of 700 kPa (100 lb/sq in.), 3500 kPa (500 lb/sq in.), and 7000 kPa (1000 lb/sq in.). Experimental results indicate that under dynamic conditions, four of the ten materials exhibited good to excellent friction/wear characteristics in various material combinations. These materials were: titanium carbide, silicon nitride, silicon carbide (reaction sintered), and Refel (SiC).

B.W.



**N85-28107\*#** National Aeronautics and Space Administration. Lewis Research Center, Cleveland, Ohio.

**PREPARATION OF SILICON CARBIDE-SILICON NITRIDE FIBERS BY THE PYROLYSIS OF POLYCARBOSILAZANE PRECURSORS Final Report**

B. G. PENN, J. G. DANIELS, F. E. LEDBETTER, III, and J. M. CLEMONS Mar. 1985 12 p refs  
(NASA-TM-86505; NAS 1.15:86505) Avail: NTIS HC A02/MF A01 CSCL 11G

The development of silicon carbide-silicon nitride fibers ( $\text{SiC-Si}_3\text{N}_4$ ) by the pyrolysis of polycarbosilazane precursors is reviewed. Precursor resin, which was prepared by heating tris(N-methylamino)methylsilane or tris(N-methylamino)phenylsilane to about 520 C, was drawn into fibers from the melt and then made unmeltable by humidity conditioning at 100 C and 95 percent relative humidity. The humidity treated precursor fibers were pyrolyzed to ceramic fibers with good mechanical properties and electrical resistivity. For example,  $\text{SiC-Si}_3\text{N}_4$  fibers derived from tris(N-methylamino)methylsilane had a tensile rupture modulus of 29 million psi and electrical resistivity of  $6.9 \times 10^8 \Omega \cdot \text{cm}$ , which is ten to the twelfth power times greater than that obtained for graphite fibers.

R.J.F.

**N85-28109\*#** General Motors Corp., Indianapolis, Ind. Gas Turbine Div.

**CERAMIC APPLICATIONS IN TURBINE ENGINES Final Report**

H. E. HELMS, P. W. HEITMAN, L. C. LINDGREN, and S. R. THRASHER Oct. 1984 268 p refs  
(Contract DEN3-17; DE-AI01-77CS-51040)  
(NASA-CR-174715; DOE/NASA/0017-6; NAS 1.26:174715; EDR-11442) Avail: NTIS HC A12/MF A01 CSCL 11B

The application of ceramic components to demonstrate improved cycle efficiency by raising the operating temperature of the existing Allison IGI 404 vehicular gas turbine engine is discussed. This effort was called the Ceramic Applications in Turbine Engines (CATE) program and has successfully demonstrated ceramic components. Among these components are two design configurations featuring stationary and rotating ceramic components in the IGT 404 engine. A complete discussion of all phases of the program, design, materials development, fabrication of ceramic components, and testing-including rig, engine, and vehicle demonstration test are presented. During the CATE program, a ceramic technology base was established that is now being applied to automotive and other gas turbine engine programs. This technology base is outlined and also provides a description of the CATE program accomplishments.

Author

**N85-28110\*#** National Aeronautics and Space Administration. Lewis Research Center, Cleveland, Ohio.

**A MICROGRAPHIC AND GRAVIMETRIC STUDY OF INTERCALATION AND DEINTERCALATION OF GRAPHITE FIBERS**

C. C. HUNG 1985 13 p refs Presented at 17th Biennial Conf. on Carbon, Lexington, Ky., 16-21 Jun. 1985; sponsored by American Carbon Society  
(NASA-TM-87026; E-2582; NAS 1.15:87026) Avail: NTIS HC A02/MF A01 CSCL 11D

Intercalation and deintercalation of Union Carbide P-100 graphite fibers with liquid and vapor bromine was studied gravimetrically and microscopically. The mass of the bromine intercalated fibers was found to be 17 to 20 percent greater than their pristine counterpart. This variation decreased to 17 to 18 percent after heating in air for 3 days at 200 C and to 14.5 to 18 percent after 6 days of 260 C heating. The fiber length did not change throughout the experiment. The fiber diameter increased during intercalation and decreased slightly upon deintercalation but was not affected by heating to 260 C for 3 days in air. Comparing the mass and volume data to those with highly oriented pyrolytic graphite or natural single crystal graphite suggested the possibility that the intercalated P-100 fibers could be mostly stage 4.

Author

**N85-30135\*#** National Aeronautics and Space Administration. Lewis Research Center, Cleveland, Ohio.

**MECHANISM OF STRENGTH DEGRADATION FOR HOT CORROSION OF ALPHA-SiC**

J. L. SMIALEK and N. S. JACOBSON 1984 40 p refs  
Presented at the Reg. Meeting of the Am. Ceram. Soc., San Francisco, 28-31 Oct. 1984  
(NASA-TM-87052; E-2507; NAS 1.15:87052) Avail: NTIS HC A03/MF A01 CSCL 11G

Sintered alpha SiC was corroded by thin films of  $\text{Na}_2\text{SO}_4$  and  $\text{Na}_2\text{CO}_3$  molten salts at 1000%. This hot corrosion attack reduced room temperature strengths by as much as 50%. Strength degradation was proportional to the degree and uniformity of corrosion pitting attack as controlled by the chemistry of the molten salt. Extensive fractography identified corrosion pits as the most prevalent source of failure. A fracture mechanics treatment of the strength/pit depth relationship produced an average  $K_{\text{sub IC}}$  equal to 2.6 MPa  $\text{sub m}^{1/2}$ , which is consistent with published values.

E.A.K.

**N85-30137\*#** National Aeronautics and Space Administration. Lewis Research Center, Cleveland, Ohio.

**ION BEAM SPUTTER-DEPOSITED THIN FILM COATINGS FOR PROTECTION OF SPACECRAFT POLYMERS IN LOW EARTH ORBIT**

B. A. BANKS, M. J. MIRTICH, S. K. RUTLEDGE, D. M. SWEC, and H. K. NAHRA (Cleveland State Univ.) 1985 24 p refs  
Presented at the 23rd Aerospace Sci. Meeting, Reno, Nev., 14-17 Jan. 1985; sponsored by AIAA  
(NASA-TM-87051; E-2454; NAS 1.15:87051) Avail: NTIS HC A02/MF A01 CSCL 11B

Ion beam sputter-deposited thin films of  $\text{Al}_2\text{O}_3$ ,  $\text{SiO}_2$ , and a codeposited mixture of predominantly  $\text{SiO}_2$  with small amounts of a fluoropolymer were evaluated both in laboratory plasma ashing tests and in space on board shuttle flight STS-8 for effectiveness in preventing oxidation of polyimide Kapton. Measurements of mass loss and optical performance of coated and uncoated polyimide samples exposed to the low Earth orbital environment are presented. Optical techniques were used to measure loss rates of protective films exposed to atomic oxygen. Results of the analysis of the space flight exposed samples indicate that thin film metal oxide coatings are very effective in protecting the polyimide. Metal oxide coatings with a small amount of fluoropolymer codeposited have the additional benefit of great flexibility.

Author

**N85-30138\*#** National Aeronautics and Space Administration. Lewis Research Center, Cleveland, Ohio.

**MECHANICAL PROTECTION OF DLC FILMS ON FUSED SILICA SLIDES**

D. NIR 1985 27 p refs Presented at the 12th Intern. Conf. on Met. Coatings, Los Angeles, 15-19 Apr. 1985; sponsored by American Vacuum Society  
(NASA-TM-87056; E-2423; NAS 1.15:87056) Avail: NTIS HC A03/MF A01 CSCL 11G

Measurements were made with a new test for improved quantitative estimation of the mechanical protection of thin films on optical materials. The mechanical damage was induced by a sand blasting system using spherical glass beads. Development of the surface damage was measured by the changes in the specular transmission and reflection, and by inspection using a surface profilometer and a scanning electron microscope. The changes in the transmittance versus the duration of sand blasting was measured for uncoated fused silica slides and coated ones. It was determined that the diamond like carbon films double the useful optical lifetime of the fused silica. Theoretical expressions were developed to describe the stages in surface deterioration. Conclusions were obtained for the  $\text{SiO}_2$  surface mechanism and for the film removal mechanism.

Author



## 27 NONMETALLIC MATERIALS

**N85-34284\*#** National Aeronautics and Space Administration. Lewis Research Center, Cleveland, Ohio.  
**RELIABILITY OF TWO SINTERED SILICON NITRIDE MATERIALS**

D. M. MIESKOWSKI, W. A. SANDERS, and L. A. PIERCE Aug. 1985 15 p refs  
(NASA-TM-87092; E-2325-1; NAS 1.15:87092) Avail: NTIS HC A02/MF A01 CSCL 11B

Two types of sintered silicon nitride were evaluated in terms of reliability: an experimental high pressure nitrogen sintered material and a commercial material. The results show wide variations in strength for both materials. The Weibull moduli were 5.5, 8.9, and 11 for the experimental material at room temperature, 1200, and 1370 C, respectively. The commercial material showed Weibull moduli of 9.0, 8.6, and 8.9 at these respective temperatures. No correlation between strength and flaw size was noted for the experimental material. The applicability of the Weibull and Griffith theories to processing defects on the order of 100 microns or less in size are discussed. E.A.K.

## 28

### PROPELLANTS AND FUELS

Includes rocket propellants, igniters, and oxidizers; storage and handling; and aircraft fuels.

**N85-10209\*#** SRI International Corp., Menlo Park, Calif.  
**CHEMISTRY OF FUEL DEPOSITS AND SEDIMENTS AND THEIR PRECURSORS Final Report**

F. R. MAYO, B. Y. LAN, S. E. BUTTRILL, JR., and G. A. ST. JOHN Oct. 1984 50 p refs  
(Contract NAS3-22510)  
(NASA-CR-174778; NAS 1.26:174778; YU-2115) Avail: NTIS HC A03/MF A01 CSCL 21D

The mechanism of solid deposit formation on hot engine parts from turbine fuels is investigated. Deposit formation is associated with oxidation of the hydrocarbon fuel. Therefore, oxidation rates and soluble gum formation were measured for several jet turbine fuels and pure hydrocarbon mixtures. Experiments were performed at 130 C using thermal initiation and at 100 C using ditertiary butyl peroxide as a chemical initiator. Correlation of the data shows that the ratio of rate of oxidation to rate of gum formation for a single fuel is not much affected by experimental conditions, even though there are differences in the abilities of different hydrocarbons to initiate and continue the oxidation. This indicates a close association of gum formation with the oxidation process. Oxidations of n-dodecane, tetralin and the more unstable jet fuels are autocatalytic, while those of 2-ethylnaphthalene and a stable jet fuel are self-retarding. However, the ratio of oxidation rate to gum formation rate appear to be nearly constant for each substrate. The effect of oxygen pressure on gum and oxidation formation was also studied. Dependence of gum formation on the concentration of initiator at 100 C is discussed and problems for future study are suggested. Author

**N85-11252\*#** United Technologies Research Center, East Hartford, Conn.  
**EXTERNAL FUEL VAPORIZATION STUDY, PHASE 2 Interim Report**

E. J. SZETELA and L. CHIAPPETTA Jan. 1981 27 p refs  
(Contract NAS3-21971)  
(NASA-CR-174079; NAS 1.26:174079; R81-915326-5) Avail: NTIS HC A03/MF A01 CSCL 21D

An analytical study was conducted to evaluate the effect of variations in fuel properties on the design of an external fuel vaporization system. The fuel properties that were considered included thermal stability, critical temperature, enthalpy a critical conditions, volatility, and viscosity. The design parameters that were evaluated included vaporizer weight and the impact on engine

requirement such as maintenance, transient response, performance, and altitude relight. The baseline fuel properties were those of Jet A. The variation in thermal stability was taken as the thermal stability variation for Experimental Referee Broad Specification (ERBS) fuel. The results of the analysis indicate that a change in thermal stability equivalent to that of ERBS would increase the vaporization system weight by 20 percent, decrease operating time between cleaning by 40 percent and make altitude relight more difficult. An increase in fuel critical temperature of 39 K would require a 40 percent increase in vaporization system weight. The assumed increase in enthalpy and volatility would also increase vaporizer weight by 40 percent and make altitude relight extremely difficult. The variation in fuel viscosity would have a negligible effect on the design parameters. R.S.F.

**N85-12183\*#** National Aeronautics and Space Administration. Lewis Research Center, Cleveland, Ohio.  
**LUBRICITY OF WELL-CHARACTERIZED JET AND BROAD-CUT FUELS BY BALL-ON-CYLINDER MACHINE**

G. M. PROK and W. S. KIM Nov. 1984 15 p refs  
(NASA-TM-83807; E-2308; NAS 1.15:83807) Avail: NTIS HC A02/MF A01 CSCL 21D

A ball-on-cylinder machine (BOCM) was used to measure the lubricity of fuels. The fuels tested were well-characterized fuels available from other programs at the NASA Lewis Research Center plus some in-house mildly hydroprocessed shale fuels from other programs included Jet-A, ERBS fuel, ERBS blends, and blend stock. The BOCM tests were made before and after clay treatment of some of these fuels with both humidified air and dry nitrogen as the preconditioning and cover gas. As expected, clay treatment always reduced fuel lubricity. Using nitrogen preconditioning and cover gas always resulted in a smaller wear scar diameter than when humidified air was used. Also observed was an indication of lower lubricity with lower boiling range fuels and lower aromatic fuels. Gas chromatographic analysis indicated changes in BOCM-stressed fuels. Author

**N85-13066\*#** National Aeronautics and Space Administration. Lewis Research Center, Cleveland, Ohio.

**LIQUID PHASE PRODUCTS AND SOLID DEPOSIT FORMATION FROM THERMALLY STRESSED MODEL JET FUELS**

W. S. KIM and D. A. BITTKER Nov. 1984 30 p refs  
(NASA-TM-86874; E-2334; NAS 1.15:86874) Avail: NTIS HC A03/MF A01 CSCL 21D

The relationship between solid deposit formation and liquid degradation product concentration was studied for the high temperature (400 C) stressing of three hydrocarbon model fuels. A Jet Fuel Thermal Oxidation Tester was used to simulate actual engine fuel system conditions. The effects of fuel type, dissolved oxygen concentration, and hot surface contact time (reaction time) were studied. Effects of reaction time and removal of dissolved oxygen on deposit formation were found to be different for n-dodecane and for 2-ethylnaphthalene. When ten percent tetralin is added to n-dodecane to give a simpler model of an actual jet fuel, the tetralin inhibits both the deposit formation and the degradation of n-dodecane. For 2-ethylnaphthalene primary product analyses indicate a possible self-inhibition at long reaction times of the secondary reactions which form the deposit precursors. The mechanism of the primary breakdown of these fuels is suggested and the primary products which participate in these precursor-forming reactions are identified. Some implications of the results to the thermal degradation of real jet fuels are given. R.S.F.

**N85-19175\*#** General Electric Co., Lynn, Mass. Aircraft Engine Business Group.

**ANALYTICAL FUEL PROPERTY EFFECTS: SMALL COMBUSTORS, PHASE 2 Final Report**

T. G. HILL, J. D. MONTY, and H. L. MORTON Mar. 1985 45 p (Contract NAS3-22829)

(NASA-CR-174848; NAS 1.26:174848; R85AEB014) Avail: NTIS HC A03/MF A01 CSCL 21D

The effects of non-standard aviation fuels on a typical small gas turbine combustor were studied and the effectiveness of design changes intended to counter the effects of these fuels was evaluated. The T700/CT7 turboprop engine family was chosen as being representative of the class of aircraft power plants desired for this study. Fuel properties, as specified by NASA, are characterized by low hydrogen content and high aromatics levels. No. 2 diesel fuel was also evaluated in this program. Results demonstrated the anticipated higher than normal smoke output and flame radiation intensity with resulting increased metal temperatures on the baseline T700 combustor. Three new designs were evaluated using the non standard fuels. The three designs incorporated enhanced cooling features and smoke reduction features. All three designs, when burning the broad specification fuels, exhibited metal temperatures at or below the baseline combustor temperatures on JP-5. Smoke levels were acceptable but higher than predicted. R.S.F.

**N85-19176\*#** Lockheed-California Co., Burbank. Commercial Advanced Design Div.

**STUDY OF ADVANCED FUEL SYSTEM CONCEPTS FOR COMMERCIAL AIRCRAFT AND ENGINES Final Report**

E. F. VERSAW, G. D. BREWER, W. D. BYERS, H. W. FOGG, D. E. HANKS, and J. CHIRIVELLA (Ergo-Tech, Inc.) Jan. 1983 142 p refs

(Contract NAS3-23271)

(NASA-CR-174752; NAS 1.26:174752) Avail: NTIS HC A07/MF A01 CSCL 21D

The impact on a commercial transport aircraft of using fuels which have relaxed property limits relative to current commercial jet fuel was assessed. The methodology of the study is outlined, fuel properties are discussed, and the effect of the relaxation of fuel properties analyzed. Advanced fuel system component designs that permit the satisfactory use of fuel with the candidate relaxed properties in the subject aircraft are described. The two fuel properties considered in detail are freezing point and thermal stability. Three candidate fuel system concepts were selected and evaluated in terms of performance, cost, weight, safety, and maintainability. A fuel system that incorporates insulation and electrical heating elements on fuel tank lower surfaces was found to be most cost effective for the long term. R.S.F.

**N85-19185\*#** California Univ., Berkeley. Lawrence Berkeley Lab. Dept. of Mechanical Engineering.

**KNOCK SYNDROME: ITS CURES AND ITS VICTIMS**

A. K. OPPENHEIM Jul. 1984 11 p refs Presented at the SAE Fuels and Lubricants Meeting, Baltimore, 8 Oct. 1984 (Contract NAG3-133; NAG3-137; DE-AC03-76SF-00098; NSF CPF-81-15163)

(NASA-CR-174395; DE84-016884; LBL-18163; CONF-8410138-1; NAS 1.26:174395) Avail: NTIS HC A02/MF A01 CSCL 21D

The knock phenomenon imposes a major technological constraint upon the automotive and oil industries; its various cures are reviewed. Essential features of combustion instability leading to its onset are exposed, and the methodology is outlined for a rational attack upon the problem it poses. Three different cures for solving the problem are proposed: (1) development of mechanical design for the combustion chamber; (2) alteration of chemical composition of fuel; and (3) mechanical-kinetic development of direct control of the combustion process. DOE

**N85-27012\*#** Exxon Research and Engineering Co., Linden, N.J. Products Research Div.

**JET FUEL PROPERTY CHANGES AND THEIR EFFECT ON PRODUCIBILITY AND COST IN THE U.S., CANADA, AND EUROPE Final Report**

G. M. VARGA, JR., A. J. AVELLA, JR., A. R. CUNNINGHAM, C. D. FEATHERSTON, J. F. GORGOL, A. J. GRAF, M. LIEBERMAN, and G. A. OLIVER Feb. 1985 205 p refs (Contract NAS3-22769)

(NASA-CR-174840; NAS 1.26:174840; RL-1PD-85) Avail: NTIS HC A10/MF A01 CSCL 21D

The effects of changes in properties and blending stocks on the refinery output and cost of jet fuel in the U.S., Canada, and Europe were determined. Computerized refinery models that minimize production costs and incorporated a 1981 cost structure and supply/demand projections to the year 2010 were used. Except in the West U.S., no changes in jet fuel properties were required to meet all projected demands, even allowing for deteriorating crude qualities and changes in competing product demand. In the West U.S., property changes or the use of cracked blendstocks were projected to be required after 1990 to meet expected demand. Generally, relaxation of aromatics and freezing point, or the use of cracked stocks produced similar results, i.e., jet fuel output could be increased by up to a factor of three or its production cost lowered by up to \$10/cu m. High quality hydrocracked stocks are now used on a limited basis to produce jet fuel. The conversion of U.S. and NATO military forces from wide-cut to kerosene-based jet fuel is addressed. This conversion resulted in increased costs of several hundred million dollars annually. These costs can be reduced by relaxing kerosene jet fuel properties, using cracked stocks and/or considering the greater volumetric energy content of kerosene jet fuel. E.A.K.

**N85-28127\*#** Colorado School of Mines, Golden. Dept. of Chemistry and Geochemistry.

**JET FUEL INSTABILITY MECHANISMS Final Technical Report, 1 Aug. 1981 - 31 Mar. 1985**

S. R. DANIEL 31 Mar. 1985 104 p refs

(Contract NAG3-197)

(NASA-CR-175856; NAS 1.26:175856) Avail: NTIS HC A06/MF A01 CSCL 21D

The mechanisms of the formation of fuel-insoluble deposits were studied in several real fuels and in a model fuel consisting of tetralin in dodecane solution. The influence of addition to the fuels of small concentrations of various compounds on the quantities of deposits formed and on the formation and disappearance of oxygenated species in solution was assessed. The effect of temperature on deposit formation was also investigated over the range of 308-453 K. G.L.C.

**N85-31307\*#** National Aeronautics and Space Administration. Lewis Research Center, Cleveland, Ohio.

**RAPID ESTIMATION OF CONCENTRATION OF AROMATIC CLASSES IN MIDDISTILLATE FUELS BY HIGH-PERFORMANCE LIQUID CHROMATOGRAPHY**

D. A. OTTERSON and G. T. SENG Washington Jul. 1985 16 p refs

(NASA-TP-2495; E-2376; NAS 1.60:2495) Avail: NTIS HC A02/MF A01 CSCL 21D

An high performance liquid chromatography (HPLC) method to estimate four aromatic classes in middistillate fuels is presented. Average refractive indices are used in a correlation to obtain the concentrations of each of the aromatic classes from HPLC data. The aromatic class concentrations can be obtained in about 15 min when the concentration of the aromatic group is known. Seven fuels with a wide range of compositions were used to test the method. Relative errors in the concentration of the two major aromatic classes were not over 10 percent. Absolute errors of the minor classes were all less than 0.3 percent. The data show that errors in group-type analyses using sulfuric acid derived standards are greater for fuels containing high concentrations of polycyclic aromatics. Corrections are based on the change in refractive index of the aromatic fraction which can occur when

sulfuric acid and the fuel react. These corrections improved both the precision and the accuracy of the group-type results. Author

**N85-31308\*#** Boeing Commercial Airplane Co., Seattle, Wash.  
**DETAILED STUDIES OF AVIATION FUEL FLOWABILITY Final Report**

H. K. MEHTA and R. S. ARMSTRONG Jun. 1985 95 p refs  
 (Contract NAS3-24081)  
 (NASA-CR-174938; NAS 1.26:174938; D6-52996) Avail: NTIS  
 HC A05/MF A01 CSCL 21D

Six Jet A fuels, with varying compositions, were tested for low temperature flowability in a 190-liter simulator tank that modeled a section of a wing tank of a wide-body commercial airplane. The insulated tank was chilled by circulating coolant through the upper and lower surfaces. Flow-ability was determined as a function of fuel temperature by holdup, the fraction of unflowable fuel remaining in the tank after otherwise complete withdrawal. In static tests with subfreezing tank conditions, hold up varied with temperature and fuel composition. However, a general correlation of two or three classes of fuel type was obtained by plotting holdup as a function of the difference between freezing point and boundary-layer temperature, measured 0.6 cm above the bottom tank surface. Dynamic conditions of vibrations and slosh or rate of fuel withdrawal had very minor effects on holdup. Tests with cooling schedules to represent extreme, cold-day flights showed, at most, slight holdup for any combination of fuel type or dynamic conditions. Tests that superimposed external fuel heating and recirculation during the cooldown period indicates reduced hold up by modification of the low-temperature boundary layer. Fuel heating was just as effective when initiated during the later times of the tests as when applied continuously. Author

**N85-34295\*#** Akron Univ., Ohio. Dept. of Chemical Engineering.

**MEASUREMENT AND CORRELATION OF JET FUEL VISCOSITIES AT LOW TEMPERATURES Final Report**

D. L. SCHRUBEN Aug. 1985 31 p refs  
 (Contract NAG3-488)  
 (NASA-CR-174911; NAS 1.26:174911) Avail: NTIS HC A03/MF A01 CSCL 21D

Apparatus and procedures were developed to measure jet fuel viscosity for eight current and future jet fuels at temperatures from ambient to near -60 C by shear viscometry. Viscosity data showed good reproducibility even at temperatures a few degrees below the measured freezing point. The viscosity-temperature relationship could be correlated by two linear segments when plotted as a standard log-log type representation (ASTM D 341). At high temperatures, the viscosity-temperature slope is low. At low temperatures, where wax precipitation is significant, the slope is higher. The breakpoint between temperature regions is the filter flow temperature, a fuel characteristic approximated by the freezing point. A generalization of the representation for the eight experimental fuels provided a predictive correlation for low-temperature viscosity, considered sufficiently accurate for many design or performance calculations. E.A.K.

## 31

## ENGINEERING (GENERAL)

Includes vacuum technology; control engineering; display engineering; and cryogenics.

**A85-29556\*** National Aeronautics and Space Administration. Lewis Research Center, Cleveland, Ohio.

**A HIGH-SPEED IMPLEMENTATION OF THE RANDOM DECREMENT ALGORITHM**

L. J. KIRALY (NASA, Lewis Research Center, Cleveland, OH) IN: International Instrumentation Symposium, 29th, Albuquerque, NM, May 2-6, 1983, Proceedings. Research Triangle Park, NC, Instrument Society of America, 1983, p. 153-168. Previously announced in STAR as N82-22388.

The algorithm is useful for measuring net system damping levels in stochastic processes and for the development of equivalent linearized system response models. The algorithm works by summing together all subrecords which occur after predefined threshold level is crossed. The random decrement signature is normally developed by scanning stored data and adding subrecords together. The high speed implementation of the random decrement algorithm exploits the digital character of sampled data and uses fixed record lengths of 2(n) samples to greatly speed up the process. The contributions to the random decrement signature of each data point was calculated only once and in the same sequence as the data were taken. A hardware implementation of the algorithm using random logic is diagrammed and the process is shown to be limited only by the record size and the threshold crossing frequency of the sampled data. With a hardware cycle time of 200 ns and 1024 point signature, a threshold crossing frequency of 5000 Hertz can be processed and a stably averaged signature presented in real time. T.M.

**A85-47024\*#** National Aeronautics and Space Administration. Lewis Research Center, Cleveland, Ohio.

**TECHNOLOGY REQUIREMENTS TO BE ADDRESSED BY THE NASA LEWIS RESEARCH CENTER CRYOGENIC FLUID MANAGEMENT FACILITY PROGRAM**

J. C. AYDELOTT (NASA, Lewis Research Center, Cleveland, OH) and R. S. RUDLAND (Martin Marietta Aerospace, Denver, CO) AIAA, SAE, ASME, and ASEE, Joint Propulsion Conference, 21st, Monterey, CA, July 8-10, 1985. 24 p. Previously announced in STAR as N85-29987. refs  
 (AIAA PAPER 85-1229)

The NASA Lewis Research Center is responsible for the planning and execution of a scientific program which will provide advance in space cryogenic fluid management technology. A number of future space missions were identified that require or could benefit from this technology. These fluid management technology needs were prioritized and a shuttle attached reusable test bed, the cryogenic fluid management facility (CFMF), is being designed to provide the experimental data necessary for the technology development effort. Author

**N85-11261\*#** National Aeronautics and Space Administration. Lewis Research Center, Cleveland, Ohio.

**PLASMA VARIABLES AND TRIBOLOGICAL PROPERTIES OF COATINGS IN LOW PRESSURE (0.1 - 10.0 TORR) PLASMA SYSTEMS**

R. AVNI (Ben Gurion Univ. of the Negev) and T. SPALVINS 1984 30 p refs Presented at the 11th Intern. Conf. on Met. Coatings, San Diego, Calif., 9-13 Apr. 1984; sponsored by the American Vacuum Society  
 (NASA-TM-83798; E-2238; NAS 1.15:83798) Avail: NTIS HC A03/MF A01 CSCL 11G

A detailed treatment is presented of the dialog known as plasma surface interactions (PSI) with respect to the coating process and its tribological behavior. Adsorption, morphological changes, defect formation, sputtering, chemical etching, and secondary electron

emission are all discussed as promoting and enhancing the surface chemistry, thus influencing the tribological properties of the deposited flux. Phenomenological correlations of rate of deposition, flux composition, microhardness, and wear with the plasma layer variables give an insight to the formation of chemical bonding between the deposited flux and the substrate surface. B.W.

**N85-20153\*** National Aeronautics and Space Administration. Lewis Research Center, Cleveland, Ohio.

**DEPOSITION OF DIAMONDLIKE CARBON FILMS Patent**

M. J. MIRTICH, J. S. SOVEY, and B. A. BANKS, inventors (to NASA) 25 Dec. 1984 6 p Filed 9 Jul. 1984 Supersedes N84-28986 (22 - 19, p 2996)

(NASA-CASE-LEW-14080-1; NAS 1.71:LEW-14080-1; US-PATENT-4,490,229; US-PATENT-APPL-SN-628866; US-PATENT-CLASS-204-192C; US-PATENT-CLASS-204-192R; US-PATENT-CLASS-204-192SP; US-PATENT-CLASS-423-414; US-PATENT-CLASS-423-445; US-PATENT-CLASS-423-446; US-PATENT-CLASS-423-449; US-PATENT-CLASS-423-DIG.10)

Avail: US Patent and Trademark Office CSCL 13H

A diamondlike carbon film is deposited in the surface of a substrate by exposing the surface to an argon ion beam containing a hydrocarbon. The current density in the ion beam is low during initial deposition of the film. Subsequent to this initial low current condition, the ion beam is increased to full power. At the same time, a second argon ion beam is directed toward the surface of the substrate. The second ion beam has an energy level much greater than that of the ion beam containing the hydrocarbon. This addition of energy to the system increases mobility of the condensing atoms and serves to remove lesser bound atoms.

Official Gazette of the U.S. Patent and Trademark Office

**N85-20155\*#** National Aeronautics and Space Administration. Lewis Research Center, Cleveland, Ohio.

**APPARATUS FOR PRODUCING DIAMOND-LIKE CARBON FLAKES Patent Application**

B. A. BANKS, inventor (to NASA) 5 Nov. 1984 12 p (NASA-CASE-LEW-13837-3; NAS 1.71:LEW-13837-3; US-PATENT-APPL-SN-668433) Avail: NTIS HC A02/MF A01 CSCL 13H

A vacuum arc from a spot at the face of a graphite cathode to a graphite anode produces a beam of carbon ions and atoms. A carbon coating from this beam is deposited on an ion beam sputtered target to produce diamondlike carbon flakes. A graphite tube encloses the cathode, and electrical isolation is provided by an insulating sleeve. The tube forces the vacuum arc spot to be confined to the surface on the outermost end of the cathode. Without the tube the arc spot will wander to the side of the cathode. This spot movement results in low rates of carbon deposition, and the properties of the deposited flakes are more graphite-like than diamond-like. NASA

**N85-20156\*#** National Aeronautics and Space Administration. Lewis Research Center, Cleveland, Ohio.

**TEXTURED CARBON SURFACES ON COPPER Patent Application**

A. N. CURREN, K. A. JENSEN, and R. F. ROMAN, inventors (to NASA) 10 Oct. 1984 12 p (NASA-CASE-LEW-14130-1; NAS 1.71:LEW-14130-1; US-PATENT-APPL-SN-659475) Avail: NTIS HC A02/MF A01 CSCL 13H

A very thin layer of highly textured carbon is applied to a copper surface by a triode sputtering process. A carbon target and a copper substrate are simultaneously exposed to an argon plasma in a vacuum chamber. The resulting carbon surface is

characterized by a dense, random array of needle like spires or peaks which extend perpendicularly from the copper surface. The coated copper is especially useful for electrode plates in multistage depressed collectors. NASA

**N85-29085\*#** National Aeronautics and Space Administration. Lewis Research Center, Cleveland, Ohio.

**THE STRUCTURE OF ION PLATED FILMS IN RELATION TO COATING PROPERTIES**

T. SPALVINS 1985 17 p refs Presented at the Appl. of Ion Plating and Ion Implantation to Mater. Conf., Atlanta, 3-5 Jun. 1985; sponsored in part by American Society for Metals and Georgia Inst. of Technology

(NASA-TM-87055; E-2599; NAS 1.15:87055) Avail: NTIS HC A02/MF A01 CSCL 13H

Ion plating is an ion assisted or glow discharge deposition technique, where ions or energetic atoms transfer energy, momentum and charge to the substrate and the growing film in a manner which can be controlled to favorably modify surface, subsurface chemistry, and microstructure. The glow discharge energizing effects from the initial nucleation stages to the final film growth are discussed. As a result, adherence, coherence, internal stresses, density and morphology of the coatings are significantly improved, over the conventional (nonion-assisted) techniques which in turn favorably affect the surface initiated failures caused by friction, wear, erosion, corrosion and fatigue. Ion plated films because of their graded coating/substrate interface, fine, uniform, densely packed film structure also induce a surface strengthening effect which improved the mechanical properties such as yield, tensile strength and fatigue life. Since a uniform, continuous film can be obtained at lower nominal film thickness, this effect is of great importance in solid film lubrication and in corrosion protection. B.W.

## 32

## COMMUNICATIONS

Includes land and global communications; communications theory; and optical communications.

**A85-14434\*** Motorola, Inc., Scottsdale, Ariz.

**SATELLITE BASEBAND PROCESSOR TEST PERFORMANCE SUMMARY**

J. T. SHANEYFELT, S. W. ATTWOOD, and D. R. CARROLL (Motorola, Inc., Communications Div., Scottsdale, AZ) IN: EASCON '83; Proceedings of the Sixteenth Annual Electronics and Aerospace Conference and Exposition, Washington, DC, September 19-21, 1983. New York, Institute of Electrical and Electronics Engineers, 1983, p. 75-83. refs (Contract NAS3-22502)

A satellite baseband processor (BBP) has been developed for the NASA Lewis 30/20 GHz Satellite Communications Program. The BBP design, reported elsewhere, has been implemented in a proof-of-concept (POC) model. The results of the laboratory system tests of the POC are summarized. Bit error rate test results are presented for the FDM/TDMA communication system operating at 27.5, 110, and 550 Mbps over a variety of operating conditions. The results clearly demonstrate the applicability of baseband processing to future high capacity satellite communication system concepts. A brief description of the system concept, its function, and the role of the baseband processor are presented. The test conditions and means of simulation are also described. The methods of test evaluation and their significance in a system context are given. Author

## 32 COMMUNICATIONS

**A85-14436\*** TRW, Inc., Redondo Beach, Calif.  
**ADVANCED 30/20 GHZ MULTIPLE BEAM ANTENNA FOR FUTURE COMMUNICATIONS SATELLITES**

C. C. CHEN and W. A. MINNIN (TRW, Inc., Space Communications Div., Redondo Beach, CA) IN: EASCON '83; Proceedings of the Sixteenth Annual Electronics and Aerospace Conference and Exposition, Washington, DC, September 19-21, 1983. New York, Institute of Electrical and Electronics Engineers, 1983, p. 95-102. (Contract NAS3-22499)

The technologies which will be implemented in advanced satellite communications systems being studied by NASA and the intended coverage scenarios are described. The systems will function at 30/20 GHz with 2.5 GHz bandwidth for the uplink and downlink. Subfrequencies will have 500 MHz bandwidth and operations will include TDMA modes. Sample scan patterns are presented for the centerminous U.S. The signals will be broadcast from a multibeam offset Cassegrain reflector antenna to obtain a low sidelobe, wide angle scan. Three contiguous low sidelobe beams will be generated with a diplex feed cluster and a 19 element scanning beam-forming network. The same technology will be used to double the capacity of current 14/12 GHz satellites.

M.S.K.

**A85-28233\*#** National Aeronautics and Space Administration. Lewis Research Center, Cleveland, Ohio.  
**TECHNICAL CHARACTERISTICS OF THE BROADCASTING SATELLITE PLAN AT 12 GHZ FOR THE WESTERN HEMISPHERE**

E. F. MILLER (NASA, Lewis Research Center, Cleveland, OH) IN: Globecom '83 - Global Telecommunications Conference, San Diego, CA, November 28-December 1, 1983, Conference Record. Volume 1. New York, Institute of Electrical and Electronics Engineers, Inc., 1983, p. 225-231. Previously announced in STAR as N84-19640.

Technical parameters such as satellite antenna characteristics, earth station requirements, bandwidths, channelization, and allowable carrier-to-interference ratios are discussed. An overview of the downlink plan is given, including a histogram of the transmitter power requirements. The plan includes satellite orbit positions, spacecraft transmitted powers, antennas beam sizes, channel assignments, and polarizations.

Author

**A85-28234\*** National Aeronautics and Space Administration. Lewis Research Center, Cleveland, Ohio.

**THE SUBJECTIVE EFFECT OF MULTIPLE CO-CHANNEL FREQUENCY MODULATED TELEVISION INTERFERENCE**

W. A. WHYTE, M. A. CAULEY (NASA, Lewis Research Center, Cleveland, OH), and P. P. GROUMPOS (Cleveland State University, Cleveland, OH) IN: Globecom '83 - Global Telecommunications Conference, San Diego, CA, November 28-December 1, 1983, Conference Record. Volume 1. New York, Institute of Electrical and Electronics Engineers, Inc., 1983, p. 232-236. Previously announced in STAR as N84-11360. refs (Contract NAG3-156)

As the geostationary orbit/spectrum becomes saturated, there is a need for the ability to reuse frequency assignments. Protection ratios (the ratio of wanted signal power to interfering signal power at the receiver) play a key role in determining efficient frequency reuse plans. A knowledge of the manner in which multiple sources of co-channel interference combine is vital in determining protection ratio requirements such that suitable margin may be allocated for multiple interfering signals. Results of tests examining the subjective assessment of multiple co-channel frequency modulated television signals interfering with another frequency modulated TV system are presented.

Author

**A85-28241\*** Cleveland State Univ., Ohio.  
**ON THE SUBJECTIVE EVALUATION OF THE INTERFERENCE PROTECTION RATIOS' MEASUREMENTS FOR CO-CHANNEL FM-TV SIGNALS**

P. P. GROUMPOS (Cleveland State University, Cleveland, OH) and W. WHYTE (NASA, Lewis Research Center, Space Communications Div., Cleveland, OH) IN: Globecom '83 - Global Telecommunications Conference, San Diego, CA, November 28-December 1, 1983, Conference Record. Volume 1. New York, Institute of Electrical and Electronics Engineers, Inc., 1983, p. 513-518. refs (Contract NAG3-156)

Results of subjective measurements made to determine the relationship between the image impairment grade and the wanted-signal to interference power ratios (C/I) for co-channel FM television signals are presented. The variation of C/I ratio with picture impairment grade is investigated for three different noise levels. The assessment of impairment grade due to thermal noise only and to picture content is also investigated. A statistical analysis for performed experiments is presented. The results presented here may be used by communication system designers to determine the required system characteristics.

Author

**A85-29605\*** Department of Communications, Ottawa (Ontario).  
**DEVELOPMENT AND USE OF THE COMPUTER SOFTWARE PACKAGE FOR PLANNING THE 12 GHZ BROADCASTING-SATELLITE SERVICE AT RARC '83**

R. R. BOWEN, K. E. BROWN, H. S. HOTH (Department of Communications, Ottawa, Canada), and E. F. MILLER (NASA, Lewis Research Center, Cleveland, OH) IEEE Journal on Selected Areas in Communications (ISSN 0733-8716), vol. SAC-3, Jan. 1985, p. 36-43. refs

The 1983 Regional Administrative Radio Conference (RARC '83) had mainly the objective to draw up a plan of detailed frequency assignments and orbital positions for the 12 GHz broadcasting-satellite service (BSS) in ITU Region 2 (the Western Hemisphere) and associated feeder links (earth-to-space) in the 17 GHz band. It was found that for RARC '83 new planning methods and procedures would be needed. The new requirements made it necessary to develop a new generation of planning software. Attention is given to the development of the computer programs to be used at the conference, the package of computer programs, and the use of the computer programs.

G.R.

**A85-29611\*** Department of Communications, Ottawa (Ontario).  
**EXPERIMENTAL RESULTS SUPPORTING THE DETERMINATION OF SERVICE QUALITY OBJECTIVES FOR DBS SYSTEMS**

G. CHOUINARD (Department of Communications, Communications Research Centre, Ottawa, Canada), W. A. WHYTE, JR. (NASA, Lewis Research Center, Cleveland, OH), A. A. GOLDBERG, and B. L. JONES (CBS Technology Center, Stamford, CT) IEEE Journal on Selected Areas in Communications (ISSN 0733-8716), vol. SAC-3, Jan. 1985, p. 87-99. refs

A summary of the results of a joint United States and Canadian program on subjective measurements of the picture degradation caused by noise and interference on an NTSC encoded color television signal is given in this paper. The effects of system noise, cochannel and adjacent channel interference, and both single entry and aggregate as well as a combination of these types of interference were subjectively evaluated by expert and nonexpert viewers under reference conditions. These results were used to develop the rationale used at RARC '83 to establish the service quality objective for planning the DBS service for the American continents.

Author

**A85-32249\*** Illinois Univ., Urbana.

**ON THE CALCULATION OF THE DIRECTIVITY OF PLANAR ARRAY FEEDS FOR SATELLITE REFLECTOR APPLICATIONS**  
P. T. LAM (Illinois, University, Urbana, IL) IEEE Transactions on Antennas and Propagation (ISSN 0018-926X), vol. AP-33, May 1985, p. 570, 571.

(Contract NAG3-419)

The calculation of the directivity of a reflector antenna excited by a planar array feed which is generally polarized, involves a coefficient  $C(mn)$ . A series representation of  $C(mn)$ , which allows efficient numerical evaluation is derived. Numerical results and comments on the behavior of  $C(mn)$  are discussed. M.D.

**A85-34470\*** Mitre Corp., Bedford, Mass.

**A FREQUENCY-ROUTED SATELLITE SYSTEM CONCEPT USING MULTIPLE ORTHOGONALLY-POLARIZED BEAMS FOR FREQUENCY REUSE**

E. ROTHOLZ (Mitre Corp., Bedford, MA) and B. E. WHITE (Signatron, Inc., Lexington, MA) IN: Milcom '83; Proceedings of the Military Communications Conference, Washington, DC, October 31-November 2, 1983. Volume 1. New York, Institute of Electrical and Electronics Engineers, Inc., 1983, p. 140-154.

(Contract NASA ORDER C-49029-D)

The design concepts of a multibeam frequency-division multiplexed satellite system accessed by many moderately sized earth stations are outlined. In the system proposed here, traffic is routed from beam to beam through appropriate apportionment and filtering. Within a beam, the routing to particular users is achieved by conventional FDM. The optimum beam size, beam isolation, orthogonal polarization assignment to beams, the concept of beam groups yielding a simple transponder design, and the establishment of a frequency plan providing interference-free band assignments are discussed. V.L.

**A85-36653\*** Virginia Univ., Charlottesville.

**FOUR-DIMENSIONAL MODULATION AND CODING - AN ALTERNATE TO FREQUENCY-REUSE**

S. G. WILSON, H. A. SLEEPER, and N. K. SRINATH (Virginia, University, Charlottesville, VA) IN: ICC '84 - Links for the future: Science, systems and services for communications; Proceedings of the International Conference on Communications, Amsterdam, Netherlands, May 14-17, 1984. Volume 2. New York/Amsterdam, Institute of Electrical and Electronics Engineers, Inc./North-Holland, 1984, p. 919-923. Previously announced in STAR as N83-36300. refs

(Contract NAG3-141)

Four dimensional modulation as a means of improving communication efficiency on the band-limited Gaussian channel, with the four dimensions of signal space constituted by phase orthogonal carriers ( $\cos \omega_c t$  and  $\sin \omega_c t$ ) simultaneously on space orthogonal electromagnetic waves are discussed. 'Frequency reuse' techniques use such polarization orthogonality to reuse the same frequency slot, but the modulation is not treated as four dimensional, rather a product of two-D modulations, e.g., QPSK. It is well known that, higher dimensionality signalling affords possible improvements in the power bandwidth sense. Four-D modulations based upon subsets of lattice-packings in four-D, which afford simplification of encoding and decoding are described. Sets of up to 1024 signals are constructed in four-D, providing a (Nyquist) spectral efficiency of up to 10 bps/Hz. Energy gains over the reuse technique are in the one to three dB range for equal bandwidth. S.L.

**A85-39356\*** Illinois Univ., Urbana.

**FOCAL SHIFTS IN PARABOLIC REFLECTORS**

H. LING, S.-W. LEE, P. T. C. LAM (Illinois, University, Urbana, IL), and W. V. T. RUSCH (Southern California, University, Los Angeles, CA) IEEE Transactions on Antennas and Propagation (ISSN 0018-926X), vol. AP-33, July 1985, p. 744-748. refs

(Contract NAG3-419; NSF ECS-81-20305)

The case of a parabolic reflector and a point feed is considered, taking into account the question regarding the location in which the feed should be placed for an achievement of maximum

directivity. Based on the tracing of geometrical rays, the obvious answer is obtained that the feed should be placed at the focal point. In the present paper, it is shown that this answer is not always correct. There are situations in which the maximum directivity is achieved when the feed is axially displaced toward the reflector or away from it. This 'focal shift' phenomenon is a result of three competing factors which affect the directivity of a reflector. The factors are related to phase synchronism over the reflector aperture, aperture illumination efficiency, and spillover loss. For achieving the maximum directivity, it is necessary to find the best compromise among the three factors. G.R.

**N85-10234\*#** National Aeronautics and Space Administration. Lewis Research Center, Cleveland, Ohio.

**CASE STUDY OF SAMPLE SPACING IN PLANAR NEAR-FIELD MEASUREMENT OF HIGH GAIN ANTENNAS**

R. J. ACOSTA and R. Q. LEE Washington 1984 10 p refs Presented at the Antenna Appl. Symp., Montecello, Ill., 18-21 Sep. 1984; sponsored by Illinois Univ.

(NASA-TM-86872; E-2301; NAS 1.15:86872) Avail: NTIS HC A02/MF A01 CSCL 20N

Far field antenna patterns can be reconstructed from planar near field measurements acquired at a sample spacing of  $\lambda/2$  or less. For electrically large antennas, sampling at the Nyquist rate may result in errors due to system electronic drift over long acquisition times. The computer capacity may limit the largest size of the near field data set. The requirement to sample at the Nyquist rate is relaxed for high gain antennas which concentrate most of the radiated energy into a small angular region of the far field. The criteria for sample spacing at greater than  $\lambda/e$  through the use of a priori information of the antenna radiation characteristics are presented. Far field patterns of a 30 GHz dual offset reflector system with a 2.7 m parabolic main reflector are computed from near field data obtained at sample spacings ranging from 0.1  $\lambda$  to 10  $\lambda$ . The effects of sampling interval and spectrum cutoff on the far field patterns are discussed. E.A.K.

**N85-11265\*#** Illinois Univ., Urbana-Champaign. Electromagnetics Lab.

**THE STUDY OF MICROSTRIP ANTENNA ARRAYS AND RELATED PROBLEMS** Semiannual Report, 22 May - 21 Nov. 1984

Y. T. LO 19 Nov. 1984 42 p refs Sponsored in part by AF (Contract NAG3-418)

(NASA-CR-174054; NAS 1.26:174054) Avail: NTIS HC A03/MF A01 CSCL 20N

The physical layout of the array elements and the proximity of the microstrip feed network makes the input impedance and radiation pattern values dependent upon the effects of mutual coupling, feedline discontinuities and feed point location. The extent of these dependences was assessed and a number of single patch and module structures were constructed and measured at an operating frequency of approximately 4.0 GHz. The empirical results were compared with the ones which were theoretically predicted by the cavity model of thin microstrip antennas. Each element was modelled as an independent radiating patch and each microstrip feedline as an independent, quasi-TEM transmission line. The effects of the feedline discontinuities are approximated by lumped L-C circuit models. E.A.K.

**N85-15099\*#** National Aeronautics and Space Administration. Lewis Research Center, Cleveland, Ohio.

**DEMAND FOR SATELLITE-PROVIDED DOMESTIC COMMUNICATIONS SERVICES UP TO THE YEAR 2000**

S. STEVENSON, W. POLEY, J. LEKAN, and J. A. SALZMAN Nov. 1984 43 p refs

(NASA-TM-86894; E-2367; NAS 1.15:86894) Avail: NTIS HC A03/MF A01 CSCL 17B

Three fixed service telecommunications demand assessment studies were completed for NASA by The Western Union Telegraph Company and the U.S. Telephone and Telegraph Corporation. They provided forecasts of the total U.S. domestic demand, from 1980

to the year 2000, for voice, data, and video services. That portion that is technically and economically suitable for transmission by satellite systems, both large trunking systems and customer premises services (CPS) systems was also estimated. In order to provide a single set of forecasts a NASA synthesis of the above studies was conducted. The services, associated forecast techniques, and data bases employed by both contractors were examined, those elements of each judged to be the most appropriate were selected, and new forecasts were made. The demand for voice, data, and video services was first forecast in fundamental units of call-seconds, bits/year, and channels, respectively. Transmission technology characteristics and capabilities were then forecast, and the fundamental demand converted to an equivalent transmission capacity. The potential demand for satellite-provided services was found to grow by a factor of 6, from 400 to 2400 equivalent 36 MHz satellite transponders over the 20-year period. About 80 percent of this was found to be more appropriate for trunking systems and 20 percent CPS. M.G.

**N85-15943\*#** Illinois Univ., Urbana. Electromagnetic Communication Lab.

**MMIC DEVICES FOR ACTIVE PHASED ARRAY ANTENNAS**  
**Semiannual Report, 21 May - 20 Dec. 1984**

R. MITTRA Dec. 1984 17 p refs

(Contract NCC3-38)

(NASA-CR-174281; NAS 1.26:174281) Avail: NTIS HC A02/MF A01 CSCL 20N

The study of printed circuit discontinuities is necessary in order to design, for example, transitions between rectangular waveguides and printed circuits. New developments with respect to the analytical approaches to this problem are discussed. A summary of the progress in the experimental approach is presented. The accurate solution for the modes in various millimeter-wave waveguides is essential in the analysis of many integrated circuit components, such as filters and impedance transformers. Problems associated with the numerical computation of these modes in two frequently used waveguide forms, namely, the finline and microstrip, are presented. The spectral domain method of formulation, with a moment method solution, is considered. This approach can be readily extended to analyze an arbitrary configuration of dielectric and metallized regions in a shielded enclosure. Galerkin's method is used, where the testing and basic functions are the same. It is shown that the mode functions, or eigenfunctions, are more sensitive to errors than the phase constants, or eigenvalues. The approximate mode functions do not satisfy the orthogonality relationship well, resulting in difficulties when these modal solutions are used to form an approximate Green's function or are used in a mode matching analysis. B.W.

**N85-15944\*#** Ford Aerospace and Communications Corp., Palo Alto, Calif.

**THE 20 GHZ PROOF-OF-CONCEPT TEST MODEL RESULTS FOR A MULTIPLE SCAN BEAM DUAL REFLECTOR ANTENNA**

T. ROBERTS, A. SMOLL, H. LUH, E. W. MATTHEWS, and W. G. SCOTT 1984 15 p Presented at the IEEE Antenna Propagation Symp., Houston, Tex., 23-27 May 1983

(Contract NAS3-22498)

(NASA-CR-174268; NAS 1.26:174268) Avail: NTIS HC A02/MF A01 CSCL 17B

A full scale 20 GHz antenna model was designed, fabricated and tested. The model is intended to test the low sidelobe beam scanning capability of a new class of an offset dual reflector and feed array configuration. The offset main reflector and subreflector surfaces are custom shaped by a computer synthesis procedure. The derived optics result in beam scan loss under 1 db over the + or - 12.3 beamwidths by + or - 5.8 beamwidths scan volume while maintaining low sidelobes. It is found that the measured and computed patterns are in good agreement. E.A.K.

**N85-17258\*#** Ohio State Univ., Columbus. ElectroScience Lab.  
**ADAPTIVE ANTENNA ARRAYS FOR WEAK INTERFERING SIGNALS**

I. J. GUPTA Jan. 1985 71 p refs

(Contract NAG3-536)

(NASA-CR-174336; NAS 1.26:174336; ESL-716111-2) Avail: NTIS HC A04/MF A01 CSCL 09E

The interference protection provided by adaptive antenna arrays to an Earth station or satellite receive antenna system is studied. The case where the interference is caused by the transmission from adjacent satellites or Earth stations whose signals inadvertently enter the receiving system and interfere with the communication link is considered. Thus, the interfering signals are very weak. To increase the interference suppression, one can either decrease the thermal noise in the feedback loops or increase the gain of the auxiliary antennas in the interfering signal direction. Both methods are examined. It is shown that one may have to reduce the noise correlation to impractically low values and if directive auxiliary antennas are used, the auxiliary antenna size may have to be too large. One can, however, combine the two methods to achieve the specified interference suppression with reasonable requirements of noise decorrelation and auxiliary antenna size. Effects of the errors in the steering vector on the adaptive array performance are studied. R.S.F.

**N85-18238\*#** General Electric Co., Syracuse, N.Y. Electronics Lab.

**CONFIGURATION STUDY FOR A 30 GHZ MONOLITHIC RECEIVE ARRAY: TECHNICAL ASSESSMENT**

W. H. NESTER, B. CLEAVELAND, B. EDWARD, S. GOTKIS, G. HESSERBACKER, J. LOH, and B. MITCHELL 1 Nov. 1984 47 p refs 3 Vol.

(Contract NAS3-23780)

(NASA-CR-174697; NAS 1.26:174697) Avail: NTIS HC A03/MF A01 CSCL 17B

The current status of monolithic microwave integrated circuits (MMICs) in phased array feeds is discussed from the point of view of cost performance, reliability, and design considerations. Transitions to MMICs, compatible antenna radiating elements and reliability considerations are addressed. Hybrid antennas, feed array antenna technology, and offset reflectors versus phased arrays are examined. A.R.H.

**N85-18239\*#** General Electric Co., Syracuse, N.Y. Electronics Lab.

**CONFIGURATION STUDY FOR A 30 GHZ MONOLITHIC RECEIVE ARRAY, VOLUME 1**

W. H. NESTER, B. CLEAVELAND, B. EDWARD, S. GOTKIS, G. HESSERBACKER, J. LOH, and B. MITCHELL 1 Nov. 1984 181 p refs 3 Vol.

(Contract NAS3-23780)

(NASA-CR-174697-VOL-1; NAS 1.26:174697-VOL-1) Avail: NTIS HC A09/MF A01 CSCL 17B

Gregorian, Cassegrain, and single reflector systems were analyzed in configuration studies for communications satellite receive antennas. Parametric design and performance curves were generated. A preliminary design of each reflector/feed system was derived including radiating elements, beam-former network, beamsteering system, and MMIC module architecture. Performance estimates and component requirements were developed for each design. A recommended design was selected for both the scanning beam and the fixed beam case. Detailed design and performance analysis results are presented for the selected Cassegrain configurations. The final design point is characterized in detail and performance measures evaluated in terms of gain, sidelobe level, noise figure, carrier-to-interference ratio, prime power, and beamsteering. The effects of mutual coupling and excitation errors (including phase and amplitude quantization errors) are evaluated. Mechanical assembly drawings are given for the final design point. Thermal design requirements are addressed in the mechanical design. A.R.H.



**N85-18240\*#** General Electric Co., Syracuse, N.Y. Electronics Lab.

**CONFIGURATION STUDY FOR A 30 GHZ MONOLITHIC RECEIVE ARRAY, VOLUME 2**

W. H. NESTER, B. CLEAVELAND, B. EDWARD, S. GOTKIS, G. HESSERBACKER, J. LOH, and B. MITCHELL 1 Nov. 1984 375 p 3 Vol.

(Contract NAS3-23780)

(NASA-CR-174697-VOL-2; NAS 1.26:174697-VOL-2) Avail:

NTIS HC A16/MF A01 CSCL 17B

The formalism of the sidelobe suppression algorithm and the method used to calculate the system noise figure for a 30 GHz monolithic receive array are presented. Results of array element weight determination and performance studies of a Gregorian aperture image system are also given. A.R.H.

**N85-20223\*#** National Aeronautics and Space Administration. Lewis Research Center, Cleveland, Ohio.

**EFFECT OF INTERFACIAL CHARACTERISTICS OF METAL CLAD POLYMERIC SUBSTRATES ON ELECTRICAL HIGH FREQUENCY INTERCONNECTION PERFORMANCE**

K. B. BHASIN, R. R. ROMANOFKY, G. E. PONCHAK, and D. C. LIU 29 Nov. 1984 10 p refs Presented at the Fall Meeting of the Mater. Res. Soc., Boston, 27-29 Nov. 1984

(NASA-TM-86948; E-2469; NAS 1.15:86948) Avail: NTIS HC A02/MF A01 CSCL 20N

Etched metallic conductor lines on metal clad polymeric substrates are used for electronic component interconnections. Significant signal losses are observed for microstrip conductor lines used for interconnecting high frequency devices. At these frequencies, the electronic signal travels closer to the metal-polymer interface due to the skin effect. Copper-teflon interfaces were characterized by scanning electron microscopy (SEM) and Auger electron spectroscopy (AES) to determine the interfacial properties. Data relating roughness of the copper film to signal losses was compared to theory. Films used to enhance adhesion are found, to contribute to these losses. E.A.K.

**N85-20224\*#** National Aeronautics and Space Administration. Lewis Research Center, Cleveland, Ohio.

**AN EXPERIMENTAL INVESTIGATION OF MICROSTRIP PROPERTIES ON SOFT SUBSTRATES FROM 2 TO 40 GHZ**

R. R. ROMANOFKY, K. B. BHASIN, G. E. PONCHAK, A. N. DOWNEY, and D. J. CONNOLLY 1985 10 p refs To be presented at the Intern. Microwave Symp., St. Louis, 4-6 Jun. 1985; sponsored by the IEEE

(NASA-TM-86961; E-2489; NAS 1.15:86961) Avail: NTIS HC A02/MF A01 CSCL 17B

Dispersion and loss characteristics of microstrip lines on 10 mil and 31 mil electrodeposited and electroless copper clad-Teflon substrates were experimentally obtained from 2 to 40 GHz. The roles of surface roughness and radiation in total loss were examined. Author

**N85-21438\*#** Illinois Univ., Urbana. Electromagnetics Lab.

**NUMERICAL METHODS FOR ANALYZING ELECTROMAGNETIC SCATTERING Semiannual Report, 25 Sep. 1984 - 24 Mar. 1985**

S. W. LEE, Y. T. LO, S. L. CHUANG, and C. S. LEE 24 Mar. 1985 66 p refs

(Contract NAG3-475)

(NASA-CR-175507; NAS 1.26:175507) Avail: NTIS HC A04/MF A01 CSCL 20N

Numerical methods to analyze electromagnetic scattering are presented. The dispersions and attenuations of the normal modes in a circular waveguide coated with lossy material were completely analyzed. The radar cross section (RCS) from a circular waveguide coated with lossy material was calculated. The following is observed: (1) the interior irradiation contributes to the RCS much more than does the rim diffraction; (2) at low frequency, the RCS from the circular waveguide terminated by a perfect electric conductor (PEC) can be reduced more than 13 dB down with a coating thickness less than 1% of the radius using the best lossy

material available in a 6 radius-long cylinder; (3) at high frequency, a modal separation between the highly attenuated and the lowly attenuated modes is evident if the coating material is too lossy, however, a large RCS reduction can be achieved for a small incident angle with a thin layer of coating. It is found that the waveguide coated with a lossy magnetic material can be used as a substitute for a corrugated waveguide to produce a circularly polarized radiation yield. E.A.K.

**N85-23815\*#** National Aeronautics and Space Administration. Lewis Research Center, Cleveland, Ohio.

**ALTERNATIVES FOR SATELLITE SOUND BROADCAST SYSTEMS AT HF AND VHF**

B. E. LEROY /n NASA. Langley Research Center Large Space Antenna Systems Technol., 1984 p 27-37 Apr. 1985

Avail: NTIS HC A20/MF A01 CSCL 20N

The National Aeronautics and Space Administration and the United States Information Agency (USIA) are currently engaged in a joint program to assess the technical and economic feasibility of direct sound broadcast satellite systems to meet USIA mission needs. The cooperative effort calls for a series of interrelated studies to provide the respective Agency managements with information on the potential role of direct broadcast satellites. Initial studies focused on HF propagation phenomena and broadcast coverage requirements. These studies served as the basis for parallel systems studies currently in progress. The systems studies are to provide a data base on various satellite configurations and systems concepts capable of supporting potential broadcast requirements ranging from a small fraction to a substantial addition to USIA requirements. Antenna concepts for LEO and GEO orbits are briefly described. M.G.

**N85-25686\*#** Ohio State Univ., Columbus. ElectroScience Lab.

**ANALYSIS OF THE ELECTROMAGNETIC SCATTERING FROM AN INLET GEOMETRY WITH LOSSY WALLS Progress Report**

N. H. MYUNG, P. H. PATHAK, and C. D. CHUNANG Apr. 1985 91 p refs

(Contract NAG3-476)

(NASA-CR-175743; NAS 1.26:175743; PR-715723) Avail: NTIS HC A05/MF A01 CSCL 20N

One of the primary goals is to develop an approximate but sufficiently accurate analysis for the problem of electromagnetic (EM) plane wave scattering by an open ended, perfectly-conducting, semi-infinite hollow circular waveguide (or duct) with a thin, uniform layer of lossy or absorbing material on its inner wall, and with a simple termination inside. The less difficult but useful problem of the EM scattering by a two-dimensional (2-D), semi-infinite parallel plate waveguide with an impedance boundary condition on the inner walls was chosen initially for analysis. The impedance boundary condition in this problem serves to model a thin layer of lossy dielectric/ferrite coating on the otherwise perfectly-conducting interior waveguide walls. An approximate but efficient and accurate ray solution was obtained recently. That solution is presently being extended to the case of a moderately thick dielectric/ferrite coating on the walls so as to be valid for situations where the impedance boundary condition may not remain sufficiently accurate. R.J.F.

**N85-27092\*#** Western Union Telegraph Co., McLean, Va. Government Systems Div.

**SATELLITE PROVIDED CUSTOMER PROMISES SERVICES, A FORECAST OF POTENTIAL DOMESTIC DEMAND THROUGH THE YEAR 2000. VOLUME 4: SENSITIVITY ANALYSIS**

D. KRATOCHVIL, J. BOWYER, C. BHUSHAN, K. STEINNAGEL, D. KAUSHAL, and G. AL-KINANI Mar. 1984 261 p 4 Vol.

(Contract NAS3-23255)

(NASA-CR-174662; NAS 1.26:174662) Avail: NTIS HC A12/MF A01 CSCL 17B

The overall purpose was to forecast the potential United States domestic telecommunications demand for satellite provided customer promises voice, data and video services through the year 2000, so that this information on service demand would be available to aid in NASA program planning. To accomplish this overall purpose the following objectives were achieved: (1)

## 32 COMMUNICATIONS

development of a forecast of the total domestic telecommunications demand; (2) identification of that portion of the telecommunications demand suitable for transmission by satellite systems; (3) identification of that portion of the satellite market addressable by consumer promises service (CPS) systems; (4) identification of that portion of the satellite market addressable by Ka-band CPS system; and (5) postulation of a Ka-band CPS network on a nationwide and local level. The approach employed included the use of a variety of forecasting models, a parametric cost model, a market distribution model and a network optimization model. Forecasts were developed for: 1980, 1990, and 2000; voice, data and video services; terrestrial and satellite delivery modes; and C, Ku and Ka-bands. R.J.F.

**N85-31348\*#** National Aeronautics and Space Administration. Lewis Research Center, Cleveland, Ohio.

### **AUTOMATED TESTING OF DEVELOPMENTAL SATELLITE COMMUNICATIONS SYSTEMS AND SUBSYSTEMS**

K. A. SHALKHAUSER and R. J. KERCZEWSKI 1985 20 p refs Presented at the 25th Conf. of the Automated RF Tech. Group, St. Louis, 6-7 Jun. 1985 (NASA-TM-87070; E-2642; NAS 1.15:87070) Avail: NTIS HC A02/MF A01 CSCL 17B

Lower frequency bands allocated for satellite communications use are becoming saturated due to steadily increasing demand. An ongoing program to develop the new technologies required to meet the demands of future systems is described. Higher frequency components and more efficient system techniques are developed. In order to accurately evaluate the performance of these technologies, an automated test system was designed and built. The automated system's design and capabilities are discussed. E.A.K.

**N85-34329\*#** Ohio State Univ., Columbus. Dept. of Electrical Engineering.

### **ADAPTIVE ANTENNA ARRAYS FOR SATELLITE COMMUNICATIONS: DESIGN AND TESTING**

I. J. GUPTA, W. G. SWARNER, and E. K. WALTON Sep. 1985 116 p refs (Contract NAG3-536) (NASA-CR-176162; NAS 1.26:176162; ESL-716111-3) Avail: NTIS HC A06/MF A01 CSCL 20N

When two separate antennas are used with each feedback loop to decorrelate noise, the antennas should be located such that the phase of the interfering signal in the two antennas is the same while the noise in them is uncorrelated. Thus, the antenna patterns and spatial distribution of the auxiliary antennas are quite important and should be carefully selected. The selection and spatial distribution of auxiliary elements is discussed when the main antenna is a center fed reflector antenna. It is shown that offset feeds of the reflector antenna can be used as auxiliary elements of an adaptive array to suppress weak interfering signals. An experimental system is designed to verify the theoretical analysis. The details of the experimental systems are presented. Author

**N85-35320\*#** Illinois Univ., Urbana. Electromagnetics Lab.

### **NORMAL MODES IN AN OVERMODED CIRCULAR WAVEGUIDE COATED WITH LOSSY MATERIAL**

C. S. LEE, S. W. LEE, and S. L. CHUANG Sep. 1985 55 p refs (Contract NAG3-475) (NASA-CR-176186; NAS 1.26:176186; TR-85-8) Avail: NTIS HC A04/MF A01 CSCL 20N

The normal modes in an overmoded waveguide coated with a lossy material are analyzed, particularly for their attenuation properties as a function of coating material, layer thickness, and frequency. When the coating material is not too lossy, the low-order modes are highly attenuated even with a thin layer of coating. This coated guide serves as a mode suppressor of the low-order modes, which can be particularly useful for reducing the radar cross section (RCS) of a cavity structure such as a jet inlet. When the coating material is very lossy, low-order modes fall into two

distinct groups: highly and lowly attenuated modes. However, as  $a/\lambda$  ( $a$  = radius of the cylinder;  $\lambda$  = the free-space wavelength) increases, the separation between these two groups becomes less distinctive. The attenuation constants of most of the low-order modes become small, and decrease as a function of  $\lambda \sup 2/a \sup 3$ . Author

**N85-35321\*#** Case Western Reserve Univ., Cleveland, Ohio. Dept. of Electrical Engineering and Applied Physics.

### **PERTURBATION-ITERATION THEORY FOR ANALYZING MICROWAVE STRIPLINES**

B. E. KRETCH Sep. 1985 137 p refs (Contract NCC3-29)

(NASA-CR-176189; NAS 1.26:176189; WGR-85-5) Avail: NTIS HC A07/MF A01 CSCL 20N

A perturbation-iteration technique is presented for determining the propagation constant and characteristic impedance of an unshielded microstrip transmission line. The method converges to the correct solution with a few iterations at each frequency and is equivalent to a full wave analysis. The perturbation-iteration method gives a direct solution for the propagation constant without having to find the roots of a transcendental dispersion equation. The theory is presented in detail along with numerical results for the effective dielectric constant and characteristic impedance for a wide range of substrate dielectric constants, stripline dimensions, and frequencies. Author

## 33

## ELECTRONICS AND ELECTRICAL ENGINEERING

Includes test equipment and maintainability; components, e.g., tunnel diodes and transistors; microminiaturization; and integrated circuitry.

**A85-12669\*** Virginia Polytechnic Inst. and State Univ., Blacksburg.

### **BIPOLAR-FET COMBINATIONAL POWER TRANSISTORS FOR POWER CONVERSION APPLICATIONS**

D. Y. CHEN and S. A. CHIN (Virginia Polytechnic Institute and State University, Blacksburg, VA) (International Telecommunication Energy Conference, 5th, Tokyo, Japan, Oct. 1983) IEEE Transactions on Aerospace and Electronic Systems (ISSN 0018-9251), vol. AES-20, Sept. 1984, p. 659-664. refs (Contract NAG3-40)

Four bipolar-FET (field-effect transistor) combinational transistor configurations are compared from the application point of view. The configurations included are FET-Darlington (cascade), emitter-open switch (cascode), parallel configuration, and FET-gated bipolar transistors (FGT). Author

**A85-14432\*#** National Aeronautics and Space Administration, Washington, D.C.

### **STATUS OF NASA'S MULTIBEAM COMMUNICATIONS TECHNOLOGY PROGRAM**

D. E. SANTARPIA (NASA Washington, DC) and J. W. BAGWELL (NASA, Lewis Research Center, Cleveland, OH) IN: EASCON '83; Proceedings of the Sixteenth Annual Electronics and Aerospace Conference and Exposition, Washington, DC, September 19-21, 1983. New York, Institute of Electrical and Electronics Engineers, 1983, p. 53-68.

Progress with prototype components for demonstrating an acceptable performance level for multibeam 30/20 GHz satellite communications scheduled for service in 1988 is summarized. Numerous companies were contracted by NASA for the various components and subsystems, which include 20 GHz transmitters, a traveling wave tube transmitter, an IMPATT amplifier, a GaAs FET amplifier, a 30 GHz low noise receiver, a trunking matrix switch, and a baseband processor. The key system is a 20 GHz offset dual reflector antenna with shaped surfaces for multibeam

transmission. Tests to date have indicated success at meeting the performance objectives. M.S.K.

**A85-14433\*** Hughes Aircraft Co., Torrance, Calif.  
**A 20 GHZ, 75 WATT, HELIX TWT FOR SPACE COMMUNICATIONS**

J. F. HENEY and R. N. TAMASHIRO (Hughes Aircraft Co., Electron Dynamics Div., Torrance, CA) IN: EASCON '83; Proceedings of the Sixteenth Annual Electronics and Aerospace Conference and Exposition, Washington, DC, September 19-21, 1983. New York, Institute of Electrical and Electronics Engineers, 1983, p. 69-74. (Contract NAS3-23351)

A space-qualified, helix-type traveling wave tube is being developed for satellite communication systems in the frequency band of 17.7 to 21.2 GHz. The design approach stresses very high efficiency operation, but with very low distortion. The tube provides multi-mode operation, permitting CW saturated power output levels of 75, 40, and 7.5 W. Operation is also anticipated at 5 dB below these saturation levels to achieve the required low distortion levels. Advanced construction features include a five-stage depressed collector, a diamond supported helix slow-wave circuit, and a type M dispenser cathode. High reliability and long life (10 yr) are objectives of the tube design. Preliminary test results on early developmental models of this tube are very encouraging. An output power of 75 to 90 W has been achieved over the full bandwidth with about 40 dB of saturated gain. More importantly, the basic electronic efficiency of the interaction process has been increased from about 7.5-11 percent by the use of the diamond helix support compared to earlier tubes using BeO support rods. This effort is supported by NASA Lewis Research Center and is aimed toward application in the NASA Advanced Communications Satellite Technology Program. Author

**A85-14435\*#** National Aeronautics and Space Administration. Lewis Research Center, Cleveland, Ohio.  
**THE NASA SATELLITE COMMUNICATION 20 X 20 MATRIX SWITCHES**

A. L. SAUNDERS (NASA, Lewis Research Center, Cleveland, OH) IN: EASCON '83; Proceedings of the Sixteenth Annual Electronics and Aerospace Conference and Exposition, Washington, DC, September 19-21, 1983. New York, Institute of Electrical and Electronics Engineers, 1983, p. 85-94.

The characteristics of two matrix switches designed for high capacity satellite communications systems are described. The switches provide routing between 20 input and 20 output ports at an IF frequency during TDMA operations. Switching speeds of 10 nsec are projected for dual gate GaAs FETs. The two designs differed in the coupling configurations, bandwidth (2.69-1.2 GHz), off-state isolation (-54 to -40 dB), switching speeds (16-37 nsec), and gain ripple (5.3-2.2 dB). Both designs achieved a 2 nsec reconfiguration rate. Further development is required to reduce the ripple effects and attain the potential 2 nsec switching speed offered by the GaAs FETs. M.S.K.

**A85-16424\*#** Tuskegee Inst., Ala.

**FRICTION IN RAIL GUNS**

P. K. KAY (Tuskegee Institute, Tuskegee, AL) IN: International Electric Propulsion Conference, 17th, Tokyo, Japan, May 28-31, 1984, Proceedings. Tokyo, Japan Society for Aeronautical and Space Sciences, 1984, p. 384-389. refs (Contract NAG3-76)

The influence of friction is included in the present equations describing the performance of an inductively driven rail gun. These equations, which have their basis in an empirical formulation, are applied to results from two different experiments. Only an approximate physical description of the problem is attempted, in view of the complexity of details in the interaction among forces of this magnitude over time periods of the order of miliseconds. O.C.

**A85-20170\*** Case Western Reserve Univ., Cleveland, Ohio.  
**CIRCULAR WAVEGUIDE BIFURCATION FOR ASYMMETRIC MODES**

H. W. SCHILLING (LTV Steel Research Center, Independence, OH) and R. E. COLLIN (Case Western Reserve University, Cleveland, OH) IEE Proceedings, Part H - Microwaves, Optics and Antennas (ISSN 0143-7097), vol. 131, pt. H, no. 6, Dec. 1984, p. 397-404. refs (Contract NSF ECS-79-10269; NAS3-22342)

An analytical solution for a circular waveguide bifurcation with incident TE(11)- and TM(11)-modes is presented using the residue calculus method. It is shown how the coupling between the TE(1n)- and TM(1n)-modes can be taken into account by expressing the coupling factor as a contour integral, which is the key step enabling the residue calculus method to be applied. Graphical results for the scattering matrix parameters of the junction are given for a range of waveguide radii of interest in the design of dual-mode coaxial prime focus feeds for paraboloidal antennas. Author

**A85-20171\*** Case Western Reserve Univ., Cleveland, Ohio.  
**DUAL-MODE COAXIAL FEED WITH LOW CROSSPOLARISATION**

R. E. COLLIN (Case Western Reserve University, Cleveland, OH) and H. W. SCHILLING (LTV Steel Research Center, Independence, OH) IEE Proceedings, Part H - Microwaves, Optics and Antennas (ISSN 0143-7097), vol. 131, pt. H, no. 6, Dec. 1984, p. 405-410. refs (Contract NAS3-22342; NSF ECS-79-10269)

Design data for optimized TE(11)-TM(11) dual-mode coaxial prime focus feeds is presented. The optimized feeds have a crosspolarization below -30 dB, an input reflection coefficient below 0.1 and very little phase error in their radiation patterns, over a 5 percent bandwidth. Experimental patterns are also given that show that the theoretically derived design data can be relied upon. The optimized feeds are useful for paraboloidal reflectors with focal-length/diameter ratios in the range 0.3 to 0.5, and will give overall efficiencies as high as 70 percent or more with sidelobes below -30 dB. Author

**A85-20900\*#** Bell Telephone Labs., Inc., Whippany, N. J.  
**A FAST TIME DOMAIN DIGITAL SIMULATION TECHNIQUE FOR POWER CONVERTERS - APPLICATION TO A BUCK CONVERTER WITH FEEDFORWARD COMPENSATION**

S. S. KELKAR (AT & T Electronic Power Systems Laboratory, Whippany, NJ) and F. C. LEE (Virginia Polytechnic Institute and State University, Blacksburg, VA) Institute of Electrical and Electronics Engineers, Power Electronics Specialists Conference, Gaithersburg, MD, June 18-21, 1984, Paper. 12 p. refs (Contract NAG3-220)

Small signal analysis was performed earlier to demonstrate the marked improvement of dynamic properties and stability margins of a switching regulator employing a novel feedforward input filter compensation scheme. A large signal nonlinear recurrent time domain model is presented for the converter to analyse the transient response due to a step input change with and without the presence of the proposed feedforward loop. The results are verified with experimental data. Author

**A85-25170\*** Illinois Univ., Urbana.  
**PLOT OF MODAL FIELD DISTRIBUTION IN RECTANGULAR AND CIRCULAR WAVEGUIDES**

C. S. LEE, S. W. LEE, and S. L. CHUANG (Illinois, University, Urbana, IL) IEEE Transactions on Microwave Theory and Techniques (ISSN 0018-9480), vol. MTT-33, March 1985, p. 271-274. (Contract NAG3-475)

### 33 ELECTRONICS AND ELECTRICAL ENGINEERING

**A85-28230\*** Toledo Univ., Ohio.

**AN ALLPASS FILTER DESIGN FOR LUMINANCE AND CHROMINANCE SEPARATION OF NTSC SIGNALS**

D. A. BORDER and S. C. KWATRA (Toledo, University, Toledo, OH) IN: Globecom '83 - Global Telecommunications Conference, San Diego, CA, November 28-December 1, 1983, Conference Record, Volume 1. New York, Institute of Electrical and Electronics Engineers, Inc., 1983, p. 174-178. refs  
(Contract NAG3-42)

Abstract- Digital techniques for separation of luminance and chrominance components from composite NTSC broadcast television signals are explored. First, comb filters are introduced. Secondly, filters based on linear regression are developed. Finally, a third filtering form, the allpass filter is considered. Techniques are compared based on mean squared error criteria and subjective testing. It is demonstrated that the allpass filtering technique is superior to both the comb filtering as well as the regression filtering. Author

**A85-35306\*** Kansas Univ., Lawrence.

**NUMERICAL SIMULATION OF POSITIVE-POTENTIAL CONDUCTORS IN THE PRESENCE OF A PLASMA AND A SECONDARY-EMITTING DIELECTRIC**

R. L. KESSEL, R. A. MURRAY, R. HETZEL, and T. P. ARMSTRONG (Kansas, University, Lawrence, KS) Journal of Applied Physics (ISSN 0021-8979), vol. 57, June 1, 1985, p. 4991-4995. refs  
(Contract NSG-3290)

A 2 1/2-dimensional, cylindrically symmetric particle in cell program is used to simulate the interaction of a plasma with a positively biased disk covered by a dielectric material (Kapton). Several runs using different combinations of bias voltages and secondary electron yields are discussed. Special attention is paid to the role of the secondaries as the dielectric surface changes from a negative potential to become increasingly positive. This is termed the 'snapover' process. The contribution due to secondaries is examined by plotting the distribution (number versus position) of the particles emitted by the impacting on the dielectric. These plots show that secondaries are drawn back into the dielectric as well as the conductor in the case of snapover. Mechanisms and experimental implications for these particular distributions are discussed. Author

**A85-39453\*** Toledo Univ., Ohio.

**SMALL-SIGNAL MODEL FOR THE SERIES RESONANT CONVERTER**

R. J. KING and T. A. STUART (Toledo, University, Toledo, OH) IEEE Transactions on Aerospace and Electronic Systems (ISSN 0018-9251), vol. AES-21, May 1985, p. 301-319. refs  
(Contract NSG-3281)

The results of a previous discrete-time model of the series resonant dc-dc converter are reviewed and from these a small signal dynamic model is derived. This model is valid for low frequencies and is based on the modulation of the diode conduction angle for control. The basic converter is modeled separately from its output filter to facilitate the use of these results for design purposes. Experimental results are presented. Author

**A85-42156\*** Naval Research Lab., Washington, D. C.

**THE J3 SCR MODEL APPLIED TO RESONANT CONVERTER SIMULATION**

R. L. AVANT (U.S. Navy, Naval Research Laboratory, Washington, DC) and F. C. Y. LEE (Virginia Polytechnic Institute and State University, Blacksburg) IEEE Transactions on Industrial Electronics (ISSN 0278-0046), vol. IE-32, Feb. 1985, p. 1-12. Research supported by the Industry-University Partnership Program in Power Electronics. refs  
(Contract NAG3-425)

The J3 SCR model is a continuous topology computer model for the SCR. Its circuit analog and parameter estimation procedure are uniformly applicable to popular computer-aided design and analysis programs such as SPICE2 and SCEPTRE. The circuit analog is based on the intrinsic three pn junction structure of the SCR. The parameter estimation procedure requires only

manufacturer's specification sheet quantities as a data base.

Author

**A85-45362\*** National Aeronautics and Space Administration. Lewis Research Center, Cleveland, Ohio.

**ADVANCED IN SOLID STATE SWITCHGEAR TECHNOLOGY FOR LARGE SPACE POWER SYSTEMS**

G. R. SUNDBERG (NASA, Lewis Research Center, Cleveland, OH) IN: IECEC '84: Advanced energy systems - Their role in our future; Proceedings of the Nineteenth Intersociety Energy Conversion Engineering Conference, San Francisco, CA, August 19-24, 1984, Volume 1. La Grange Park, IL, American Nuclear Society, 1984, p. 123-132. Previously announced in STAR as N84-22891. refs

High voltage solid state remote power controllers (RPC's) and the required semiconductor power switches to provide baseline technology for large, high power distribution systems in the Space Station, all electric airplane and other advanced aerospace applications were developed. The RPC's were developed for dc voltages from 28 to 1200 V and ac voltages of 115, 230, and 440 V at frequencies of 400 Hz to 20 kHz. The benefits and operation of solid state RPC's and highlights of several developments to bring the RPC to technology readiness for future aerospace needs are examined. The 28 V dc Space Shuttle units, three RPC types at 120 V dc, two at 270/300 V dc, two at 230 V ac and several high power RPC models at voltages up to 1200 V dc with current ratings up to 100 A are reviewed. New technology programs to develop a new family of (DI)2 semiconductor switches and 20 kHz, 440 V ac RPC's are described. E.A.K.

**A85-45373\*** National Aeronautics and Space Administration. Lewis Research Center, Cleveland, Ohio.

**DEVELOPMENT OF HIGH FREQUENCY LOW WEIGHT POWER MAGNETICS FOR AEROSPACE POWER SYSTEMS**

G. E. SCHWARZE (NASA, Lewis Research Center, Cleveland, OH) IN: IECEC '84: Advanced energy systems - Their role in our future; Proceedings of the Nineteenth Intersociety Energy Conversion Engineering Conference, San Francisco, CA, August 19-24, 1984, Volume 1. La Grange Park, IL, American Nuclear Society, 1984, p. 196-204. Previously announced in STAR as N84-22892. refs

A dominant design consideration in the development of space type power magnetic devices is the application of reliable thermal control methods to prevent device failure which is due to excessive temperature rises and hot temperatures in critical areas. The resultant design must also yield low weight, high efficiency, high reliability and maintainability, and long life. The weight savings and high efficiency that results by going to high frequency and unique thermal control techniques is demonstrated by the development of a 25 kVA, 20 kHz space type transformer under the power magnetics technology program. Work in the area of power rotary transformer is also discussed. E.A.K.

**N85-12300\*#** TRW Electronic Systems Group, Redondo Beach, Calif.

**THE 30 GHZ SOLID STATE AMPLIFIER FOR LOW COST LOW DATA RATE GROUND TERMINALS Final Report, Jun. 1982 - Jun. 1984**

Y. C. NGAN and M. A. QUIJIE Sep. 1984 189 p

(Contract NAS3-23266)

(NASA-CR-174795; NAS 1.26:174795; REPT-4-9-T-10-F) Avail: NTIS HC A09/MF A01 CSCL 09C

This report details the development of a 20-W solid state amplifier operating near 30 GHz. The IMPATT amplifier not only met or exceeded all the program objectives, but also possesses the ability to operate in the pulse mode, which was not called for in the original contract requirements. The ability to operate in the pulse mode is essential for TDMA (Time Domain Multiple Access) operation. An output power of 20 W was achieved with a 1-dB instantaneous bandwidth of 260 MHz. The amplifier has also been tested in pulse mode with 50% duty for pulse lengths ranging from 200 ns to 2 micro s with 10 ns rise and fall times and no degradation in output power. This pulse mode operation was made

possible by the development of a stable 12-diode power combiner/amplifier and a single-diode pulsed driver whose RF output power was switched on and off by having its bias current modulated via a fast-switching current pulse modulator. Essential to the overall amplifier development was the successful development of state-of-the-art silicon double-drift IMPATT diodes capable of reproducible 2.5 W CW output power with 12% dc-to-RF conversion efficiency. Output powers of as high as 2.75 W have been observed. Both the device and circuit design are amenable to low cost production. B.W.

**N85-13157\*#** National Aeronautics and Space Administration. Lewis Research Center, Cleveland, Ohio.

**CONTROL ASPECTS OF THE SCHUCHULI VILLAGE STAND-ALONE PHOTOVOLTAIC POWER SYSTEM Final Report**

P. P. GROOMPOS (Cleveland State Univ., Ohio), J. E. CULLER (Cleveland State Univ., Ohio), and R. DELOMBARD Nov. 1984 31 p refs

(Contract DE-AI01-79ET-20485)

(NASA-TM-83790; DOE/NASA/20485-17; E-2286; NAS

1.15:83790) Avail: NTIS HC A03/MF A01 CSCL 09B

A photovoltaic power system in an Arizona Indian village was installed. The control subsystem of this photovoltaic power system was analyzed. The four major functions of the control subsystem are: (1) voltage regulation; (2) load management; (3) water pump control; and (4) system protection. The control subsystem functions flowcharts for the control subsystem operation, and a computer program that models the control subsystem are presented. E.A.K.

**N85-18259\*#** Massachusetts Inst. of Tech., Cambridge. Office of Sponsored Programs.

**METAL VAPOR ARC SWITCH ELECTROMAGNETIC ACCELERATOR TECHNOLOGY Report, 3 Sep. 1983 - 2 Sep. 1984**

P. P. MONGEAU Dec. 1984 60 p refs

(Contract NAG3-283)

(NASA-CR-174380; NAS 1.26:174380) Avail: NTIS HC A04/MF A01 CSCL 09A

A multielectrode device housed in an insulator vacuum vessel, the metal vapor vacuum switch has high power capability and can hold off voltages up to the 100 kilovolt level. Such switches can be electronically triggered and can interrupt or commutate at a zero current crossing. The physics of arc initiation, arc conduction, and interruption are examined, including material considerations; inefficiencies; arc modes; magnetic field effects; passive and forced extinction; and voltage recovery. Heating, electrode lifetime, device configuration, and external circuit configuration are discussed. The metal vapor vacuum switch is compared with SCRs, GTOs, spark gaps, ignitrons, and mechanical breakers. A.R.H.

**N85-19328\*#** Varian Associates, Palo Alto, Calif. Microwave Tube Div.

**DESIGN OF LOW LOSS HELIX CIRCUITS FOR INTERFERENCE FITTED AND BRAZED CIRCUITS Final Report**

A. JACQUEZ Jan. 1983 113 p refs

(Contract NAS3-21509; NAS3-22441)

(NASA-CR-168313; NAS 1.26:168313) Avail: NTIS HC A06/MF A01 CSCL 09C

The RF loss properties and thermal capability of brazed helix circuits and interference fitted circuits were evaluated. The objective was to produce design circuits with minimum RF loss and maximum heat transfer. These circuits were to be designed to operate at 10 kV and at 20 GHz using a gamma a approximately equal to 1.0. This represents a circuit diameter of only 0.75 millimeters. The fabrication of this size circuit and the 0.48 millimeter high support rods required considerable refinements in the assembly techniques and fixtures used on lower frequency circuits. The transition from the helices to the waveguide was designed and the circuits were matched from 20 to 40 GHz since the helix design is a broad band circuit and at a gamma a of 1.0 will operate over this band. The loss measurement was a transmission

measurement and therefore had two such transitions. This resulting double-ended match required tuning elements to achieve the broad band match and external E-H tuners at each end to optimize the match for each frequency where the loss measurement was made. The test method used was a substitution method where the test fixture was replaced by a calibrated attenuator. B.W.

**N85-20246\*#** National Aeronautics and Space Administration. Lewis Research Center, Cleveland, Ohio.

**A NEW VERY HIGH VOLTAGE SEMICONDUCTOR SWITCH**

G. R. SUNDBERG 1985 17 p refs To be presented at the 16th Ann. Power Electron. Spec. Conf. (PESC), Toulouse, 24-28 Jun. 1985; sponsored by Inst. of Electrical and Electronics Engineers

(NASA-TM-86957; E-2480; NAS 1.15:86957) Avail: NTIS HC

A02/MF A01 CSCL 09A

A new family of semiconductor switches using double injection techniques and compensated deep impurities is described. They have the potential to raise switching voltages a factor of 10 higher (up to 100 kV) than p-n junction devices while exhibiting extremely low (or zero) forward voltage. Several potential power switching applications are indicated. E.A.K.

**N85-20248\*#** National Aeronautics and Space Administration. Lewis Research Center, Cleveland, Ohio.

**PRECISION TUNABLE RESONANT MICROWAVE CAVITY Patent Application**

S. NAKANISHI, F. S. CALCO, and A. R. SCARPELLI, inventors (to NASA) 11 Feb. 1985 9 p

(NASA-CASE-LEW-13935-1; NAS 1.71:LEW-13935-1;

US-PATENT-APPL-SN-700255) Avail: NTIS HC A02/MF A01

CSCL 09A

A tunable microwave cavity containing ionizable metallic vapor or gases and an apparatus for precisely positioning a microwave coupling tip in the cavity and for precisely adjusting at least one dimension of the cavity are disclosed. With this combined structure, resonance may be achieved with various types of ionizable gases. A coaxial probe extends into a microwave cavity through a tube. One end of the tube is retained in a spherical joint attached in the cavity wall. This allows the coaxial probe to be pivotally rotated. The coaxial probe is slideable within the tube thus allowing the probe to be extended toward or retracted from the center of the cavity. A tunable wall in the cavity is precisely positioned by a plurality of threaded rods extending through threaded bushings which are geared together. Thus, rotation of one of the bushings caused rotation of the other bushings simultaneously whereby the tuning wall is accurately positioned. Means are provided for moving the tube through which the coaxial probe extends in both a side to side and back and forth motion. NASA

**N85-21492\*** National Aeronautics and Space Administration. Lewis Research Center, Cleveland, Ohio.

**INELASTIC TUNNEL DIODES Patent**

L. M. ANDERSON, inventor (to NASA) 13 Nov. 1984 7 p Filed 19 Apr. 1983 Supersedes N83-25983 (21 - 15, p 2390)

(NASA-CASE-LEW-13833-1; NAS 1.71:LEW-13833-1;

US-PATENT-4,482,779; US-PATENT-APPL-SN-486471;

US-PATENT-CLASS-136-255; US-PATENT-CLASS-357-12;

US-PATENT-CLASS-357-30) Avail: US Patent and Trademark

Office CSCL 09A

Power is extracted from plasmons, photons, or other guided electromagnetic waves at infrared to midultraviolet frequencies by inelastic tunneling in metal-insulator-semiconductor-metal diodes. Inelastic tunneling produces power by absorbing plasmons to pump electrons to higher potential. Specifically, an electron from a semiconductor layer absorbs a plasmon and simultaneously tunnels across an insulator into metal layer which is at higher potential. The diode voltage determines the fraction of energy extracted from the plasmons; any excess is lost to heat.

Official Gazette of the U.S. Patent and Trademark Office

**N85-28222\*#** National Aeronautics and Space Administration. Lewis Research Center, Cleveland, Ohio.

## PERFORMANCE ANALYSIS OF RADIATION COOLED DC TRANSMISSION LINES FOR HIGH POWER SPACE SYSTEMS

G. E. SCHWARZE 1985 32 p refs Prepared for presentation at the 20th Intersoc. Energy Conversion Eng. Conf., Miami Beach, Fla., 18-23 Aug. 1985; sponsored in part by SAE, ANS, ASME, IEEE, AIAA, ACS and AICHE

(NASA-TM-87040; E-2596; NAS 1.15:87040) Avail: NTIS HC A03/MF A01 CSCL 09C

As space power levels increase to meet mission objectives and also as the transmission distance between power source and load increases, the mass, volume, power loss, and operating voltage and temperature become important system design considerations. This analysis develops the dependence of the specific mass and percent power loss on the power and voltage levels, transmission distance, operating temperature and conductor material properties. Only radiation cooling is considered since the transmission line is assumed to operate in a space environment. The results show that the limiting conditions for achieving low specific mass, percent power loss, and volume for a space-type dc transmission line are the permissible transmission voltage and operating temperature. Other means to achieve low specific mass include the judicious choice of conductor materials. The results of this analysis should be immediately applicable to power system trade-off studies including comparisons with ac transmission systems. Author

**N85-29144\*** National Aeronautics and Space Administration. Lewis Research Center, Cleveland, Ohio.

## ALKALINE BATTERY CONTAINING A SEPARATOR OF A CROSS-LINKED COPOLYMER OF VINYL ALCOHOL AND UNSATURATED CARBOXYLIC ACID Patent

L. C. HSU, W. H. PHILIPP, D. W. SHEIBLEY, and O. D. GONZALEZ-SANABRIA, inventors (to NASA) 19 Mar. 1985 6 p Filed 10 Jul. 1981

(NASA-CASE-LEW-13102-1; US-PATENT-4,505,998; US-PATENT-APPL-SN-282298; US-PATENT-CLASS-429-206; US-PATENT-CLASS-429-249) Avail: US Patent and Trademark Office CSCL 10C

A battery separator for an alkaline battery is described. The separator comprises a cross linked copolymer of vinyl alcohol units and unsaturated carboxylic acid units. The cross linked copolymer is insoluble in water, has excellent zincate diffusion and oxygen gas barrier properties and a low electrical resistivity. Cross linking with a polyaldehyde cross linking agent is preferred.

Official Gazette of the U.S. Patent and Trademark Office

**N85-29149\*#** National Aeronautics and Space Administration. Lewis Research Center, Cleveland, Ohio.

## APPARATUS FOR MOUNTING A FIELD EMISSION CATHODE Patent Application

B. T. EBIHARA and R. FORMAN, inventors (to NASA) 9 May 1985 9 p

(NASA-CASE-LEW-14108-1; NAS 1.71:LEW-14108-1; US-PATENT-APPL-SN-732321) Avail: NTIS HC A02/MF A01 CSCL 09A

A field emission cathode is positioned in a pair of intersecting cross grooves, in the end of a ceramic tube by a metal end cap. A spring in electrical contact with the base of the cathode provides the necessary pressure to maintain continuous circumferential electrical contact between the gate film and a raised edge on the end cap. With this structure the cathode chip is self centering and easily replaceable. Also the gate film of the cathode is not abraded or rubbed during installation, and the holder is readily degassed. Author

**N85-31372\*#** National Aeronautics and Space Administration. Lewis Research Center, Cleveland, Ohio.

## REGENERATIVE FUEL CELL SYSTEMS FOR SPACE STATION

M. A. HOBERECHT and D. W. SHEIBLEY /n NASA. Goddard Space Flight Center The 1984 Goddard Space Flight Center Battery Workshop p 21-29 Jul. 1985

Avail: NTIS HC A25/MF A01 CSCL 10A

Regenerative fuel cell (RFC) systems are the leading energy storage candidates for Space Station. Key design features are the advanced state of technology readiness and high degree of system level design flexibility. Technology readiness was demonstrated through testing at the single cell, cell stack, mechanical ancillary component, subsystem, and breadboard levels. Design flexibility characteristics include independent sizing of power and energy storage portions of the system, integration of common reactants with other space station systems, and a wide range of various maintenance approaches. The design features led to selection of a RFC system as the sole electrochemical energy storage technology option for the space station advanced development program. E.A.K.

**N85-31375\*#** National Aeronautics and Space Administration. Lewis Research Center, Cleveland, Ohio.

## SYSTEM LEVEL ELECTROCHEMICAL PRINCIPLES

L. H. THALLER /n NASA. Goddard Space Flight Center The 1984 Goddard Space Flight Center Battery Workshop p 69-76 Jul. 1985 refs

Avail: NTIS HC A25/MF A01 CSCL 10C

The traditional electrochemical storage concepts are difficult to translate into high power, high voltage multikilowatt storage systems. The increased use of electronics, and the use of electrochemical couples that minimize the difficulties associated with the corrective measures to reduce the cell to cell capacity dispersion were adopted by battery technology. Actively cooled bipolar concepts are described which represent some attractive alternative system concepts. They are projected to have higher energy densities lower volumes than current concepts. They should be easier to scale from one capacity to another and have a closer cell to cell capacity balance. These newer storage system concepts are easier to manage since they are designed to be a fully integrated battery. These ideas are referred to as system level electrochemistry. The hydrogen-oxygen regenerative fuel cells (RFC) is probably the best example of the integrated use of these principles. E.A.K.

## N85-31378\*# Rensselaer Polytechnic Inst., Troy, N.Y. DEVELOPMENT OF A LITHIUM SECONDARY BATTERY SEPARATOR

J. A. MOORE and R. WILLIE /n NASA. Goddard Space Flight Center The 1984 Goddard Space Flight Center Battery Workshop p 105-114 Jul. 1985 refs

(Contract NAG3-199)

Avail: NTIS HC A25/MF A01 CSCL 10C

A nonporous membrane based on the polymerization of 2,3-dihydrofuran followed by crosslinking in situ was prepared. The material is compatible with rechargeable Li battery components and, when swollen with an appropriate solvent such as tetrahydrofuran, exhibits separator resistance and Li transport equivalent to Celgard. Author

**N85-31398\*#** National Aeronautics and Space Administration. Lewis Research Center, Cleveland, Ohio.

## DESIGN PRINCIPLES FOR NICKEL HYDROGEN CELLS AND BATTERIES

L. H. THALLER /n NASA. Goddard Space Flight Center The 1984 Goddard Space Flight Center Battery Workshop p 427-436 Jul. 1985 refs

Avail: NTIS HC A25/MF A01 CSCL 10C

Nickel hydrogen cells, and more recently, bipolar batteries have been built by a variety of organizations. The design principles that have been used by the technology group at the Lewis Research Center draw upon their extensive background in separator technology, alkaline fuel cell technology, and several alkaline cell



technology areas. These design principles have been incorporated into both the more contemporary individual pressure vessel (IPV) designs that were pioneered by other groups, as well as the more recent bipolar battery designs using active cooling that are being developed at LeRC and their contractors. These principles are rather straightforward applications of capillary force formalisms, coupled with the slowly developing data base resulting from careful post test analyses. The objective of this overall effort is directed towards the low Earth orbit (LEO) application where the cycle life requirements are much more severe than the geosynchronous orbit (GEO) application. Nickel hydrogen cells have already been successfully flown in an increasing number of GEO missions.

Author

**N85-31404\*** National Aeronautics and Space Administration. Lewis Research Center, Cleveland, Ohio.

**INITIAL PERFORMANCE OF ADVANCED DESIGNS FOR IPV NICKEL-HYDROGEN CELLS**

J. J. SMITHRICK, M. A. MANZO, and O. D. GONZALEZ-SANABRIA /in NASA. Goddard Space Flight Center The 1984 Goddard Space Flight Center Battery Workshop p 513-524 Jul. 1985 refs Previously announced as N85-28444 Avail: NTIS HC A25/MF A01 CSCL 10C

Advanced designs for individual pressure vessel nickel hydrogen cells were conceived which should improve the life cycle at deep depths of discharge and improve thermal management. Features of the designs which are new and not incorporated in either of the contemporary cells (Air Force/Hughes, Comsat) are: (1) the use of alternate methods of oxygen recombination, (2) use of serrated edge separators to facilitate movement of gas within the cell while still maintaining required physical contact with the wall wick, and (3) use of an expandable stack to accommodate some of the nickel electrode expansion. The designs also consider electrolyte volume requirements over the life of the cells, and are fully compatible with the Air Force/Hughes design.

R.J.F.

**N85-31406\*** National Aeronautics and Space Administration. Lewis Research Center, Cleveland, Ohio.

**LIFE CYCLE TEST RESULTS OF A BIPOLAR NICKEL HYDROGEN BATTERY**

R. L. CATALDO /in NASA. Goddard Space Flight Center The 1984 Goddard Space Flight Center Battery Workshop p 537-548 Jul. 1985 refs

Avail: NTIS HC A25/MF A01 CSCL 09C

A history is given of low Earth orbit (LEO) laboratory test data on a 6.5 ampere-hour bipolar nickel hydrogen battery designed and built at the NASA Lewis Research Center. The bipolar concept is a means of achieving the goal of producing an acceptable battery, of higher energy density, able to withstand the demands of low-Earth-orbit regimes. Over 4100 LEO cycles were established on a ten cell battery. It seems that any perturbation on normal cycling effects the cells performance. Explanations and theories of the battery's behavior are varied and widespread among those closely associated with it. Deep discharging does provide a reconditioning effect and further experimentation is planned in this area. The battery watt-hour efficiency is about 75 percent and the time averaged, discharge voltage is about 1.26 volts for all cells at both the C/4 and LEO rate. Since a significant portion of the electrode capacity has degraded, the LEO cycle discharges are approaching depths of 90 to 100 percent of the high rate capacity. Therefore, the low end-of-discharge voltages occur precipitously after the knee of the discharge curve and is more an indication of electrode capacity and is a lesser indicator of overall cell performance.

R.J.F.

**N85-31408\*** Hughes Research Labs., Malibu, Calif.

**THE FAILURE MECHANISM OF A NICKEL ELECTRODE IN A NICKEL-HYDROGEN CELL**

H. S. LIM and S. A. VERZWYVELT /in NASA. Goddard Space Flight Center The 1984 Goddard Space Flight Center Battery Workshop p 565-582 Jul. 1985 refs (Contract NAS3-22238)

Avail: NTIS HC A25/MF A01 CSCL 10C

Studies on a number of types of nickel electrodes after cycle failure in a Ni/H<sub>2</sub> cell showed that the failure is due to the loss of high rate discharge capability rather than an absolute capacity loss. The failure mechanism is speculated to be a combination of migration of the active material away from the current collecting nickel sinter, increased porosity of the active material caused by cycling, and an electrical isolation process of the active material during discharge.

Author

**N85-32251\*** Electrotek Concepts, Inc., Knoxville, Tenn.

**EXPERIMENTAL INVESTIGATION OF A VARIABLE SPEED CONSTANT FREQUENCY ELECTRIC GENERATING SYSTEM FROM A UTILITY PERSPECTIVE**

J. I. HERRERA, T. W. REDDOCH, and J. S. LAWLER May 1985 52 p refs

(Contract NAS3-24105; DE-AI01-76ET-20320)

(NASA-CR-174950; NAS 1.26:174950; DOE/NASA/4105-1)

Avail: NTIS HC A03/MF A01 CSCL 09C

As efforts are accelerated to improve the overall capability and performance of wind electric systems, increased attention to variable speed configurations has developed. A number of potentially viable configurations have emerged. Various attributes of variable speed systems need to be carefully tested to evaluate their performance from the utility points of view. With this purpose, the NASA experimental variable speed constant frequency (VSCF) system has been tested. In order to determine the usefulness of these systems in utility applications, tests are required to resolve issues fundamental to electric utility systems. Legitimate questions exist regarding how variable speed generators will influence the performance of electric utility systems; therefore, tests from a utility perspective, have been performed on the VSCF system and an induction generator at an operating power level of 30 kW on a system rated at 200 kVA and 0.8 power factor.

Author

**N85-33293\*** Hughes Aircraft Co., Torrance, Calif. Microwave Products Div.

**SIXTY GHZ IMPATT DIODE DEVELOPMENT Final Report, Nov. 1981 - Feb. 1985**

Y. E. MA, J. CHEN, E. BENKO, M. J. BARGER, H. NGHIEM, T. Q. TRINH, and J. KUNG May 1985 180 p refs

(Contract NAS3-23253)

(NASA-CR-174969; NAS 1.26:174969; W-45797) Avail: NTIS

HC A09/MF A01 CSCL 09C

The objective of this program is to develop 60 GHz GaAs IMPATT Diodes suitable for communications applications. The performance goal of the 60 GHz IMPATT is 1W CW output power with a conversion efficiency of 15 percent and 10 year life time. During the course of the program, double drift (DD) GaAs IMPATT Diodes have been developed resulting in the state of the art performance at V band frequencies. A CW output power of 1.12 W was demonstrated at 51.9 GHz with 9.7 percent efficiency. The best conversion efficiency achieved was 15.3 percent. V band DD GaAs IMPATTs were developed using both small signal and large signal analyses. GaAs wafers of DD flat, DD hybrid, and DD Read profiles using molecular beam epitaxy (MBE) were developed with excellent doping profile control. Wafer evaluation was routinely made by the capacitance versus voltage (C-V) measurement. Ion mass spectrometry (SIMS) analysis was also used for more detailed profile evaluation.

B.W.



### 33 ELECTRONICS AND ELECTRICAL ENGINEERING

**N85-35342\*#** Illinois Univ., Urbana. Electromagnetic Communication Lab.

#### **CHARACTERIZATION OF MICROSTRIP DISCONTINUITIES IN THE TIME AND FREQUENCY DOMAINS**

U. FELDMAN and R. MITTRA Sep. 1985 49 p refs (Contract NCC3-38)

(NASA-CR-176190; NAS 1.26:176190; UILU-ENG-85-2565; REPT-85-6) Avail: NTIS HC A03/MF A01 CSCL 09C

A number of impedance transitions and interconnections to a microstrip were designed and investigated. The double-step discontinuity on a microstrip was studied in detail, and a procedure was developed to design these structures. Their response was determined by making measurements in both the frequency and time domains in a consistent and repeatable manner. The time-domain presentation of the data was the most useful feature of the measuring system. All undesirable signal components were filtered out through the use of gating functions. Theoretically computed results were verified experimentally. Author

### 34

#### **FLUID MECHANICS AND HEAT TRANSFER**

Includes boundary layers; hydrodynamics; fluidics; mass transfer; and ablation cooling.

**A85-11630\*** National Aeronautics and Space Administration. Lewis Research Center, Cleveland, Ohio.

#### **COMPUTATION OF INTERNAL FLOWS: METHODS AND APPLICATIONS; PROCEEDINGS OF THE ENERGY SOURCES TECHNOLOGY CONFERENCE, NEW ORLEANS, LA, FEBRUARY 12-16, 1984**

P. M. SOCKOL, ED. (NASA, Lewis Research Center, Cleveland, OH) and K. N. GHIA, ED. (Cincinnati, University, Cincinnati, OH) Conference sponsored by the American Society of Mechanical Engineers. New York, American Society of Mechanical Engineers (Fluids Engineering Symposia Series. FED Volume 14), 1983, 182 p. For individual items see A85-11631 to A85-11648.

The present conference covers computational method applications, viscous-inviscid interaction techniques, viscous flow computational methods, and design-related methods. Attention is given to viscous flows in turbomachinery cascades, forbidden signals and apparent Mach numbers in supersonic cascades, the flow field in an engine particle separator, two-dimensional separated channel flows, turbulent separating flows over a rearward-facing step, the semielliptic analysis of two-dimensional internal and compressible viscous flows, spline solutions of the incompressible Navier-Stokes equations in a mildly nonorthogonal coordinate system, the design of highly loaded blades with blockage in cascade, and a finite analytic method for unsteady, three-dimensional Navier-Stokes equations. O.C.

**A85-11631\*#** Pennsylvania State Univ., University Park.

#### **COMPUTATION OF VISCOUS FLOWS IN TURBOMACHINERY CASCADES**

M. POUAGARE, B. LAKSHMINARAYANA, and T. R. GOVINDAN (Pennsylvania State University, University Park, PA) IN: Computation of internal flows: Methods and applications; Proceedings of the Energy Sources Technology Conference, New Orleans, LA, February 12-16, 1984. New York, American Society of Mechanical Engineers, 1983, p. 1-10. refs (Contract NSG-3266)

Analytic and numerical experiments involving the use of the space-marching method for the prediction of the viscous flow field in turbomachinery cascades indicate that the grid lines in the physical domain must be nearly orthogonal in order to arrive at accurate predictions. For staggered cascades, a nonperiodic grid system was used and appropriate approximations were applied in place of the periodicity boundary conditions upstream and downstream of the cascade. Predicted drag coefficient, turning

angle, boundary layer momentum thicknesses, and velocity profiles are compared with experimental data. Good agreement is obtained in most cases. O.C.

**A85-11634\*#** National Aeronautics and Space Administration. Lewis Research Center, Cleveland, Ohio.

#### **COMPARISON OF SECONDARY FLOWS PREDICTED BY A VISCOUS CODE AND AN INVISCID CODE WITH EXPERIMENTAL DATA FOR A TURNING DUCT**

J. R. SCHWAB and L. A. POVINELLI (NASA, Lewis Research Center, Cleveland, OH) IN: Computation of internal flows: Methods and applications; Proceedings of the Energy Sources Technology Conference, New Orleans, LA, February 12-16, 1984. New York, American Society of Mechanical Engineers, 1983, p. 29-36. Previously announced in STAR as N84-17142. refs

A comparison of the secondary flows computed by the viscous Kreskovsky-Briley-McDonald code and the inviscid Denton code with benchmark experimental data for turning duct is presented. The viscous code is a fully parabolized space-marching Navier-Stokes solver while the inviscid code is a time-marching Euler solver. The experimental data were collected by Taylor, Whitelaw, and Yianneskis with a laser Doppler velocimeter system in a 90 deg turning duct of square cross-section. The agreement between the viscous and inviscid computations was generally very good for the streamwise primary velocity and the radial secondary velocity, except at the walls, where slip conditions were specified for the inviscid code. The agreement between both the computations and the experimental data was not as close, especially at the 60.0 deg and 77.5 deg angular positions within the duct. This disagreement was attributed to incomplete modeling of the vortex development near the suction surface. Author

**A85-11640\*#** Cincinnati Univ., Ohio.

#### **TWO-DIMENSIONAL INTERNAL COMPRESSIBLE VISCOUS FLOWS USING SEMI-ELLIPTIC ANALYSIS**

K. N. GHIA, U. GHIA, and R. RAMAMURTI (Cincinnati, University, Cincinnati, OH) IN: Computation of internal flows: Methods and applications; Proceedings of the Energy Sources Technology Conference, New Orleans, LA, February 12-16, 1984. New York, American Society of Mechanical Engineers, 1983, p. 99, 100. refs (Contract NAG3-194)

Subsonic viscous flows through planar cascades are examined by means of a semielliptic form of the Navier-Stokes equations, which is obtained by neglecting the streamwise diffusion of momentum and energy in their respective equations and providing upstream interaction through the pressure field. The influence of downstream conditions is propagated upstream in the subsonic flow, via a streamwise implicit determination of the pressure field, in order to permit departure-free solutions for the overall flow problem. The continuity equation is thereby satisfied directly. Governing equations are written in strong conservation law form, in terms of general, nonorthogonal transformed coordinates and Cartesian velocity components. O.C.

**A85-11647\*#** Iowa Univ., Iowa City.

#### **DEVELOPMENT OF FINITE ANALYTIC METHOD FOR UNSTEADY THREE-DIMENSIONAL NAVIER-STOKES EQUATION**

H.-C. CHEN and C.-J. CHEN (Iowa, University, Iowa City, IA) IN: Computation of internal flows; Methods and applications; Proceedings of the Energy Sources Technology Conference, New Orleans, LA, February 12-16, 1984. New York, American Society of Mechanical Engineers, 1983, p. 159-165. refs (Contract NSG-3305)

A finite analytic (FA) numerical method is described for the numerical study of three-dimensional fluid flow problems. The FA method incorporates a local linearization scheme and a classical analytic solution technique to formulate the algebraic representation of unsteady three-dimensional Navier Stokes Equations. The twenty-eight point FA formula thus obtained gives all positive coefficients and desired upwind shift. Cubic cavity flows are then solved by the FA method for Reynolds numbers of 100 and 400.

A simple variant of SIMPLER algorithm is used to resolve the pressure-velocity coupling problem. The numerical solutions show that the presence of side walls reduce the strength of the primary vortex when compared with the two-dimensional square cavity flows. Author

**A85-11648\*** Purdue Univ. School of Science at Indianapolis, Ind.

**A FINITE ELEMENT SOLUTION OF THREE-DIMENSIONAL INVISCID ROTATIONAL FLOWS THROUGH CURVED DUCTS**

A. ECER, H. U. AKAY, and B. SENER (Purdue University, Indianapolis, IN) IN: Computation of internal flows: Methods and applications; Proceedings of the Energy Sources Technology Conference, New Orleans, LA, February 12-16, 1984. New York, American Society of Mechanical Engineers, 1983, p. 167-176. refs

(Contract NSG-3294)

A previously developed two-dimensional finite element algorithm for the solution of steady Euler equations is extended to three-dimensional problems. Starting with the general three-dimensional problem, the formulation of steady, rotational flows is presented. The boundary conditions for steady flows where the rotationality is introduced through entropy or total enthalpy gradients are introduced. A three-dimensional flow through a curved duct is analyzed as a sample problem, demonstrating the efficiency of the relaxation scheme. The accuracy of the numerical results is investigated by calculating the velocity and vorticity distributions at different sections of the channel, including the exit. C.D.

**A85-14241\*** Arizona Univ., Tucson.

**THE LINEAR TWO-DIMENSIONAL STABILITY OF INVISCID VORTEX STREETS OF FINITE-CORED VORTICES**

D. I. MEIRON (Arizona, University, Tucson, AZ; California Institute of Technology, Pasadena, CA), P. G. SAFFMAN (California Institute of Technology, Pasadena, CA), and J. C. SCHATZMAN (Chevron Oil Field Research Co., La Habra; California Institute of Technology, Pasadena, CA) Journal of Fluid Mechanics (ISSN 0022-1120), vol. 147, Oct. 1984, p. 187-212. Research supported by the U.S. Department of Energy and U.S. Navy. refs

(Contract NAG3-179)

(AD-A153032)

The stability of two-dimensional infinitesimal disturbances of the steady inviscid incompressible flow produced by infinite rows of finite-cored particles is studied. Numerical results are obtained for the growth rate and oscillation frequencies of disturbances of arbitrary subharmonic wavenumber, and the stability boundaries are calculated. The stabilization of the pairing instability by finite area demonstrated by Saffman and Schatzman (1982) is confirmed, as is Kida's (1982) result that this is not the most unstable disturbance when the area is finite. However, the finite area does not stabilize the inviscid Karman vortex street of finite-area vortices to infinitesimal two-dimensional disturbances of arbitrary wavelength. The finite area is always unstable except for one isolated value of the aspect ratio which depends upon the size of the vortices. C.D.

**A85-14349\*** Pennsylvania State Univ., University Park.

**COMPUTATION AND TURBULENCE CLOSURE MODELS FOR SHEAR FLOWS IN ROTATING CURVED BODIES**

M. POUAGARE and B. LAKSHMINARAYANA (Pennsylvania State University, University Park, PA) IN: Symposium on Turbulent Shear Flows, 4th, Karlsruhe, West Germany, September 12-14, 1983, Proceedings. University Park, PA, Pennsylvania State University, 1984, p. 6.6-6.13. refs

(Contract NSG-3266)

This paper is concerned with the effects of rotation and curvature on the turbulence closure model. The k-epsilon model that includes the effects of curvature has been modified to include the anisotropy in turbulence. A space-marching algorithm which solves the parabolized Navier-Stokes equations is coupled with the turbulence closure model to predict the turbulent shear flow over a rotating cylinder and inside a rotating channel. The

agreement between the predictions and available data is good. The rotation and curvature effects are predicted well. Author

**A85-14376\*** California Univ., Irvine.

**A TWO-EQUATION TURBULENCE MODEL FOR TWO-PHASE JETS**

S. ELGHOBASHI, T. ABOU-ARAB, M. RIZK, and A. MOSTAFA (California, University, Irvine, CA) IN: Symposium on Turbulent Shear Flows, 4th, Karlsruhe, West Germany, September 12-14, 1983, Proceedings. University Park, PA, Pennsylvania State University, 1984, p. 12.9-12.14. refs

(Contract DE-FG22-80PC-30303; NAG3-176)

A recently-developed two-equation turbulence model for two-phase flows (Elghobashi and Abou-Arab, 1983) is tested for the flow of a turbulent axisymmetric gaseous jet laden with spherical solid particles of uniform size. The agreement between the predictions of experimental data is good. Author

**A85-14399\*** United Technologies Research Center, East Hartford, Conn.

**MASS AND MOMENTUM TURBULENT TRANSPORT EXPERIMENTS WITH CONFINED COAXIAL JETS**

B. V. JOHNSON (United Technologies Research Center, East Hartford, CT) and J. C. BENNETT (Connecticut, University, Storrs, CT) IN: Symposium on Turbulent Shear Flows, 4th, Karlsruhe, West Germany, September 12-14, 1983, Proceedings. University Park, PA, Pennsylvania State University, 1984, p. 18.14-18.19. refs

(Contract NAS3-22771)

An experimental study of mixing downstream of coaxial jets discharging into an expanded circular duct was conducted to obtain data for the evaluation and improvement of turbulent transport models. A combination of turbulent momentum transport rate and two components of velocity data were obtained from simultaneous measurements with a two-color LV system. A combination of turbulent mass transport rate, concentration and velocity data were obtained from simultaneous measurements with laser velocimeter (LV) and laser induced fluorescence (LIF) systems. Author

**A85-16533\*** Massachusetts Inst. of Tech., Cambridge.

**A NUMERICAL STUDY OF THE STEADY SCALAR CONVECTIVE DIFFUSION EQUATION FOR SMALL VISCOSITY**

M. B. GILES (MIT, Cambridge, MA) and M. E. ROSE (NASA, Langley Research Center, Institute for Computer Applications in Science and Engineering, Hampton, VA) Journal of Computational Physics (ISSN 0021-9991), vol. 56, Dec. 1984, p. 513-529. Previously announced in STAR as N83-35999. refs

(Contract NAG3-9; NAS1-17070; NAS1-17130)

A time-independent convection diffusion equation is studied by means of a compact finite difference scheme and numerical solutions are compared to the analytic inviscid solutions. The correct internal and external boundary layer behavior is observed, due to an inherent feature of the scheme which automatically produces upwind differencing in inviscid regions and the correct viscous behavior in viscous regions. Author

**A85-19377\*** National Aeronautics and Space Administration. Lewis Research Center, Cleveland, Ohio.

**APPROXIMATE ANALYSIS FOR RESONANCE OF AN INCOMPRESSIBLE SHEAR LAYER PLUS EDGES**

P. A. DURBIN (NASA, Lewis Research Center, Cleveland, OH) Physics of Fluids (ISSN 0031-9171), vol. 27, Dec. 1984, p. 2814-2818. refs

A method for approximately analyzing the feedback between downstream and upstream edges in incompressible shear flow is described. The shear flow is modeled by a vortex sheet. Equations for resonance eigenvalues are derived. After the reduction of growth rate by finite shear layer thickness is allowed for, agreement is found between calculated resonances and those that have been observed experimentally. Author

## **A85-19488\*#** United Technologies Corp., East Hartford, Conn. **FINITE DIFFERENCE METHODS FOR REDUCING NUMERICAL DIFFUSION IN TEACH-TYPE CALCULATIONS**

S. A. SYED (United Technologies Corp., Engineering Div., East Hartford, CT) and L. M. CHIAPPETTA (United Technologies Research Center, East Hartford, CT) American Institute of Aeronautics and Astronautics, Aerospace Sciences Meeting, 23rd, Reno, NV, Jan. 14-17, 1985. 17 p. refs

(Contract NAS3-2368)

(AIAA PAPER 85-0057)

A methodological evaluation for two-finite differencing schemes for computer-aided gas turbine design is presented. The two computational schemes include; a Bounded Skewed Finite Differencing Scheme (BSUDS); and a Quadratic Upwind Differencing Scheme (QSDS). In the evaluation, the derivations of the schemes were incorporated into two-dimensional and three-dimensional versions of the Teaching Axisymmetric Characteristics Heuristically (TEACH) computer code. Assessments were made according to performance criteria for the solution of problems of turbulent, laminar, and coannular turbulent flow. The specific performance criteria used in the evaluation were simplicity, accuracy, and computational economy. It is found that the BSUDS scheme performed better with respect to the criteria than the QSDS. Some of the reasons for the more successful performance BSUDS are discussed. I.H.

## **A85-19491\*#** United Technologies Corp., East Hartford, Conn. **CALCULATION OF CONFINED SWIRLING FLOWS**

G. J. STURGESS and S. A. SYED (United Technologies Corp., Engineering Div., East Hartford, CT) American Institute of Aeronautics and Astronautics, Aerospace Sciences Meeting, 23rd, Reno, NV, Jan. 14-17, 1985. 16 p. refs

(Contract NAS3-235924; NAS3-23686)

(AIAA PAPER 85-0060)

Swirling jets are an important constituent flow of many types of combustion equipment. Flame size, shape, stability and combustion intensity are all favorably influenced by swirling some portion of the incoming air with the fuel. Fluid dynamics computer codes are being developed for the mathematical simulation of flows in practical combustors. It is important that these codes have the ability to accurately and reliably calculate swirling flows. Turbulent flow calculations with swirl can be inaccurate due to at least three major reasons: limitations of the turbulence modeling used, incorrect or inadequate specifications of inlet boundary conditions, and, error introduced through the numerics. These sources of error are described, and examples provided of each. The state-of-the-art in such calculations is reviewed. The controlling character of current numerics is demonstrated, and it is concluded that as a first priority, better numerics must be arrived at, and that an improved understanding of the discharge flow from swirl generators is essential as a second priority. When these priorities are satisfied an improved turbulence model is desirable. It is also concluded that an improved understanding of swirl-induced recirculation would be an asset. Author

## **A85-19564\*#** Duke Univ., Durham, N. C.

## **A SPACE-MARCHING METHOD FOR INCOMPRESSIBLE NAVIER-STOKES EQUATIONS**

M. POUAGARE (Duke University, Durham, NC; Pennsylvania State University, University Park, PA) and B. LAKSHMINARAYANA (Pennsylvania State University, University Park, PA) American Institute of Aeronautics and Astronautics, Aerospace Sciences Meeting, 23rd, Reno, NV, Jan. 14-17, 1985. 14 p. refs

(Contract NSG-3266)

(AIAA PAPER 85-0170)

This paper deals with the development of a space-marching method for incompressible flows. The method solves the continuity and momentum equations as a coupled system at each streamwise station. The character of the system of equations has been changed from elliptic to hyperbolic/parabolic in order to enable the equations to be marched in space. The present method has many advantages compared to the existing parabolic or space-marching methods for incompressible flow: (1) it avoids the solution of Poisson

equations, (2) it conserves the mass flow with no additional computation, (3) it does not require the specification of an assumed pressure field when used in the prediction of duct flows. The present method can capture strong secondary velocities and strong transverse pressure gradients. Predictions of the flow through straight and curved ducts are in good agreement with analytical and experimental results. Author

## **A85-19574\*#** Oklahoma State Univ., Stillwater.

## **SWIRLING FLOWS IN TYPICAL COMBUSTOR GEOMETRIES**

D. G. LILLEY (Oklahoma State University, Stillwater, OK) American Institute of Aeronautics and Astronautics, Aerospace Sciences Meeting, 23rd, Reno, NV, Jan. 14-17, 1985. 26 p. refs

(Contract NAG3-74)

(AIAA PAPER 85-0184)

The results of experimental attempts and subsequent computational efforts targeted at improving numerical models for swirling recirculating confined turbulent combustion flows are reported. Attention was focused on the mean flow patterns, scales and shapes of the recirculation zones, mapping the flowfield time-mean velocity, normal and Re shear stresses, and producing a predictive computer code based on the TEACH-T program. The work was performed mainly by graduate students. The studies covered swirl strengths, swirler performance, the effects of downstream contraction nozzle size and placement, expansion ratios, and inlet side-wall angles. The STARPIC program was developed in FORTRAN 4 for computing air flow through expansions and over a wide range of inlet swirl vane angles. M.S.K.

## **A85-19672\*#** Purdue Univ., West Lafayette, Ind.

## **A STAGNATION PRESSURE PROBE FOR DROPLET-LADEN AIR FLOW**

S. N. B. MURTHY, M. LEONARDO, and C. M. EHRESMAN (Purdue University, West Lafayette, IN) American Institute of Aeronautics and Astronautics, Aerospace Sciences Meeting, 23rd, Reno, NV, Jan. 14-17, 1985. 12 p. refs

(Contract F33615-78-C-2401; NAG3-62)

(AIAA PAPER 85-0330)

It is often of interest in a droplet-laden gas flow to obtain the stagnation pressure of both the gas phase and the mixture. A flow-decelerating probe (TPF), with separate, purged ports for the gas phase and the mixture and with a bleed for accumulating liquid at the closed end, has been developed. Measurements obtained utilizing the TPF in a nearly isothermal air-water droplet mixture flow in a smooth circular pipe under various conditions of flow velocity, pressure, liquid concentration and droplet size are presented and compared with data obtained under identical conditions with a conventional, gas phase stagnation pressure probe (CSP). The data obtained with the CSP and TPF probes are analyzed to determine the applicability of the two probes in relation to the multi-phase characteristics of the flow and the geometry of the probe. Author

## **A85-19751\*#** Pratt and Whitney Aircraft Group, East Hartford, Conn.

## **ASSESSMENT OF DISCRETIZATION SCHEMES TO REDUCE NUMERICAL DIFFUSION IN THE CALCULATION OF COMPLEX FLOWS**

S. A. SYED (United Technologies Corp., Pratt and Whitney Group, East Hartford, CT), A. D. GOSMAN, and M. PERIC (Imperial College of Science and Technology, London, England) American Institute of Aeronautics and Astronautics, Aerospace Sciences Meeting, 23rd, Reno, NV, Jan. 14-17, 1985. 14 p. refs

(Contract NAS3-2368)

(AIAA PAPER 85-0441)

Comprehensive criteria for evaluating finite-difference schemes to reduce numerical diffusion in the solution of the Reynolds averaged Navier-Stokes equations have been established in this study. Several candidate schemes have been examined, based on these criteria. Taylor series analyses, model problem studies and examination of the difference equations have been used to assess the schemes. Two schemes, which showed the most

promise, and satisfied a majority of the criteria, are recommended for incorporation into two dimensional and three dimensional computer codes for further evaluation. Author

**A85-24445\*** National Aeronautics and Space Administration. Lewis Research Center, Cleveland, Ohio.

#### **A UNIFIED RELATION FOR CAVITATION EROSION**

P. VEERABHADRA RAO (NASA, Lewis Research Center; Cleveland State University, Cleveland, OH), D. H. BUCKLEY (NASA, Lewis Research Center, Cleveland, OH), and M. MATSUMURA (Hiroshima University, Hiroshima, Japan) International Journal of Mechanical Sciences (ISSN 0020-7403), vol. 26, no. 5, 1984, p. 325-335. refs

A power-law relationship between the average erosion rate and cumulative erosion is presented. Data analyses from Venturi, magnetostriction, and liquid-impingement devices conform to this unified relation. A normalization technique is also suggested for prediction purposes. Author

**A85-25137\*#** Pennsylvania State Univ., University Park.

#### **STRUCTURE OF PARTICLE-LADEN JETS - MEASUREMENTS AND PREDICTIONS**

J.-S. SHUEN, A. S. P. SOLOMON, G. M. FAETH (Pennsylvania State University, University Park, PA), and Q.-F. ZHANG (Nanjing Aeronautical Institute, Nanjing, People's Republic of China; Pennsylvania State University, University Park, PA) AIAA Journal (ISSN 0001-1452), vol. 23, March 1985, p. 396-404. Previously cited in issue 06, p. 762, Accession no. A84-17842. refs (Contract NAG3-190)

**A85-25951\*#** Lockheed-Georgia Co., Marietta.

#### **ACOUSTIC CONTROL OF FREE JET MIXING**

J. LEPICOVSKY, K. K. AHUJA, W. H. BROWN (Lockheed-Georgia Co., Marietta, GA), and P. J. MORRIS (Pennsylvania State University, University Park, PA; Lockheed-Georgia Co., Marietta, GA) American Institute of Aeronautics and Astronautics, Shear Flow Control Conference, Boulder, CO, Mar. 12-14, 1985. 10 p. refs (Contract NAS3-23708) (AIAA PAPER 85-0569)

The paper reports a detailed study on the acoustic control of free jet mixing at realistic Reynolds numbers. The experimental results were obtained at Mach numbers of 0.3 and 0.8 and flow total temperatures up to 800 K. The Reynolds numbers ranged from 350,000 to 1,300,000. Excitation Strouhal numbers were in the range of 0.2 to 0.6. The experimental results are compared with predictions, based on an extension of the analysis by Tam and Morris. The results showed that proper upstream tone excitation enhances mixing of unheated jets for both high-speed, high Reynolds number conditions and for low-speed conditions. The heated jet, however, shows a response to upstream excitation that depends on jet Mach number. The agreement between the predictions and the experiments is very good for unheated jet conditions. However, for jets heated to temperatures above 600 K, the theoretical predictions differ from the experimental results. Author

**A85-26077\*#** Nevada Univ., Reno.

#### **OSCILLATORY CONDUCTIVE HEAT TRANSFER FOR A FIBER IN AN IDEAL GAS**

H. L. KUNTZ (Hoover Keith and Bruce, Inc., Houston, TX) and N. D. PERREIRA (Nevada, University, Reno, NV) ASME, Transactions, Journal of Heat Transfer (ISSN 0022-1481), vol. 107, Feb. 1985, p. 52-56. Navy-supported research. refs (Contract NSG-3198)

A description of the thermal effects created by placing a cylindrical fiber in an inviscid, ideal gas, through which an acoustic wave propagates, is presented. The fibers and the gas have finite heat capacities and thermal conductivities. Expressions for the temperature distribution in the gas and in the material are determined. The temperature distribution is caused by pressure oscillations in the gas which, in turn, are caused by the passage of an acoustic wave. The relative value of a dimensionless

parameter is found to be indicative of whether the exact or approximate equations should be used in the solution. This parameter is a function of the thermal conductivities and heat capacities of the fiber and gas, the acoustic frequency, and the fiber diameter. Author

**A85-26526\*** National Aeronautics and Space Administration. Lewis Research Center, Cleveland, Ohio.

#### **A COMPARISON OF FLOW RATES AND PRESSURE PROFILES FOR N-SEQUENTIAL INLETS AND THREE RELATED SEAL CONFIGURATIONS**

R. C. HENDRICKS (NASA, Lewis Research Center, Cleveland, OH) IN: Advances in cryogenic engineering. Volume 29 - Proceedings of the Cryogenic Engineering Conference, Colorado Springs, CO, August 15-17, 1983. New York, Plenum Press, 1984, p. 837-846. Previously announced in STAR as N83-33103. refs

Experimental and analytical results are presented for choked flows of fluid nitrogen over a range of reduced inlet stagnation temperatures (from 0.67 to ambient) and reduced inlet stagnation pressures to 2. Flow rate and pressure profile comparisons are made between N aligned sequential orifice inlets, a 33-tooth labyrinth seal, a 3-step seal, a cylindrical seal and the classic venturi. Seal effectiveness appears strongly dependent on upstream losses and geometry configuration. Author

**A85-26911\*** Rensselaer Polytechnic Inst., Troy, N.Y.

#### **CONVECTIVE INFLUENCE ON THE STABILITY OF A CYLINDRICAL SOLID-LIQUID INTERFACE**

Q. T. FANG, M. E. GLICKSMAN (Rensselaer Polytechnic Institute, Troy, NY), S. R. CORIELL, G. B. MCFADDEN, and R. F. BOISVERT (National Bureau of Standards, Washington, DC) Journal of Fluid Mechanics (ISSN 0022-1120), vol. 151, Feb. 1985, p. 121-140. refs (Contract NAG3-333)

Experiments in which a long vertical, heated wire is surrounded by concentric annuli of a melt and its crystalline solid show that the convection state changes from a stable unicell surrounded by a stationary cylindrical solid-liquid interface, to a complex time-dependent flow surrounded by a rotating, helical solid-liquid interface. This transition occurs at a Grashof number of approximately 150, which is an order of magnitude less than the critical Grashof number calculated for a liquid annulus surrounded by rigid walls. A linear stability analysis has been carried out for an infinitely tall vertical annulus. When the deformable nature of the crystal-melt interface is taken into account in the boundary conditions, two new modes of instability arise. The most dangerous mode is asymmetrical and corresponds to helical waves travelling vertically upwards. The critical Grashof number and the scaling properties of the eigenstate agree with experiments. The results clearly demonstrate the coupling of convection with crystal-melt interfacial instabilities. Author

**A85-27096\*#** National Aeronautics and Space Administration. Lewis Research Center, Cleveland, Ohio.

#### **AERODYNAMIC EFFECT OF COMBUSTOR INLET AIR PRESSURE ON FUEL JET ATOMIZATION**

R. D. INGEBØ (NASA, Lewis Research Center, Cleveland, OH) Journal of Propulsion and Power (ISSN 0748-4658), vol. 1, Mar.-Apr. 1985, p. 137-142. Previously cited in issue 17, p. 2468, Accession no. A84-36973. refs

**A85-30075\*** National Aeronautics and Space Administration. Lewis Research Center, Cleveland, Ohio.

#### **ANALYSIS OF THREE-DIMENSIONAL SOLIDIFICATION INTERFACE SHAPE**

R. SIEGEL (NASA, Lewis Research Center, Cleveland, OH) International Journal of Heat and Mass Transfer (ISSN 0017-9310), vol. 28, March 1985, p. 701-705. refs

The determination of the shape of the solidification interface in a cooling melt by the thermal boundary conditions is investigated analytically, extending the analysis of Siegel (1982) and Siegel and Sosoka (1982) to the three-dimensional case. The solutions are generated by continuation into the solid region from conditions

## 34 FLUID MECHANICS AND HEAT TRANSFER

at the cooled wall, and some numerical results are presented in tables and graphs. These findings and the analytical approach employed are applicable to crystallization and metal-forming processes. T.K.

**A85-35596\***# National Aeronautics and Space Administration. Lewis Research Center, Cleveland, Ohio.

### **ANALYSIS OF BUOYANCY EFFECT ON FULLY DEVELOPED LAMINAR HEAT TRANSFER IN A ROTATING TUBE**

R. SIEGEL (NASA, Lewis Research Center, Cleveland, OH) ASME, Transactions, Journal of Heat Transfer (ISSN 0022-1481), vol. 107, May 1985, p. 338-344. refs

Laminar heat transfer is analyzed in a tube rotating about an axis perpendicular to the tube axis. The solution applies for flow that is either radially outward from the axis of rotation, or radially inward toward the axis of rotation. The conditions are fully developed, and there is uniform heat addition at the tube wall. The analysis is performed by expanding velocities and temperature in power series using the Taylor number as a perturbation parameter. Coriolis and buoyancy forces caused by tube rotation are included, and the solution is calculated through second-order terms. The secondary flow induced by the Coriolis terms always tends to increase the heat transfer coefficient; this effect can dominate for small wall heating. For radial inflow, buoyancy also tends to improve heat transfer. For radial outflow, however, buoyancy tends to reduce heat transfer; for large wall heating this effect can dominate, and there is a net reduction in heat transfer coefficient. Author

**A85-37047\*** National Aeronautics and Space Administration. Lewis Research Center, Cleveland, Ohio.

### **CONTROL OF SOLIDIFICATION BOUNDARY IN CONTINUOUS CASTING BY ASYMMETRIC COOLING AND MOLD OFFSET**

R. SIEGEL (NASA, Lewis Research Center, Cleveland, OH) International Journal of Heat and Mass Transfer (ISSN 0017-9310), vol. 28, Feb. 1985, p. 500-502.

A solution, developed to obtain solidification-interface shapes for complex situations in which both the ingot cooling and mold geometry are asymmetric, is analyzed. The effect of mold offset and of unequal ingot side temperatures on the interface shapes is illustrated in graphs. The results of the analysis show how the solidification interface in continuous casting can be controlled by asymmetries in both mold geometry and cooling of the ingot sides. M.D.

**A85-38999\***# Nanjing Aeronautical Inst. (China).

### **STRUCTURE OF DUCTED PARTICLE-LADEN TURBULENT JETS**

Q.-F. ZHANG (Nanjing Aeronautical Institute, Nanjing, People's Republic of China; Pennsylvania State University, University Park, PA), J.-S. SHUEN, A. S. P. SOLOMON, and G. M. FAETH (Pennsylvania State University, University Park, PA) AIAA Journal (ISSN 0001-1452), vol. 23, July 1985, p. 1123-1125. refs (Contract NAG3-190)

New and existing measurements have been used to develop and evaluate models of particle-laden jets and sprays, yielding encouraging results for a stochastic separated flow (SSF) model which treats effects of interphase slip and turbulence on the basis of random walk computations of particle or drop motion. An evaluation of the SSF model using the measurements of Modarress et al. (1982, 1983) yielded results comparable to earlier work, suggesting that data from coflowing jets in ducts should be accompanied by static pressure measurements, since even small pressure gradients appreciably influence jet properties. O.C.

**A85-39257\*** National Aeronautics and Space Administration. Lewis Research Center, Cleveland, Ohio.

### **APPLICATION OF VISCOUS AND INVISCID COMPUTATION METHODS FOR ROCKET TURBOPUMP SYSTEMS**

L. A. POVINELLI, J. E. HAAS, K. L. MCLALLIN, J. R. SCHWAB, and R. V. CHIMA (NASA, Lewis Research Center, Cleveland, OH) IN: Space systems technology; Proceedings of the Aerospace Congress and Exposition, Long Beach, CA, October 15-18, 1984. Warrendale, PA, Society of Automotive Engineers, Inc. (SAE SP-593), 1984, p. 39-57. (SAE PAPER 841522)

This paper examines current research efforts underway at Lewis Research Center which have focused on improving the structural durability of the SSME turbopump system through more fully examining the aerothermodynamics of the flow system. This objective was achieved by developing three-dimensional viscous and inviscid computer codes to predict the pressure and temperature distributions in the engine flow passages, particularly within the SSME turbines and turnaround ducts. Author

**A85-39604\***# Texas Technological Univ., Lubbock.

### **TURBULENCE MEASUREMENTS OF LATERAL JET INJECTION INTO CONFINED TUBULAR CROSSFLOW**

G. B. FERRELL (Texas Tech University, Lubbock, TX) and D. G. LILLEY (Oklahoma State University, Stillwater, OK) AIAA, SAE, ASME, and ASEE, Joint Propulsion Conference, 21st, Monterey, CA, July 8-10, 1985. 13 p. refs (Contract NAG3-549) (AIAA PAPER 85-1102)

Experiments have been conducted to characterize the time-mean and turbulent flowfield of a deflected turbulent jet in a confining cylindrical crossflow. Jet-to-crossflow velocity ratios of 2, 4, and 6 were investigated, with no swirl in the crossflow. A six-position single hotwire technique was used to measure the velocities and all turbulent normal and shear stresses. Measurements confirmed that the deflected jet is symmetrical about the vertical plane passing through the crossflow axis, and the jet penetration was found to be reduced from that of comparable velocity-ratio infinite crossflow cases. Author

**A85-39780\***# National Aeronautics and Space Administration. Lewis Research Center, Cleveland, Ohio.

### **NUMERICAL CALCULATION OF SUBSONIC JETS IN CROSSFLOW WITH REDUCED NUMERICAL DIFFUSION**

R. W. CLAUS (NASA, Lewis Research Center, Cleveland, OH) AIAA, SAE, ASME, and ASEE, Joint Propulsion Conference, 21st, Monterey, CA, July 8-10, 1985. 11 p. Previously announced in STAR as N85-25263. refs (AIAA PAPER 85-1441)

A series of calculations are reported for two, subsonic jet in crossflow geometries. The parametric variation examined are the lateral spacing of a row of jets. The first series of calculations corresponds to a widely spaced jet geometry,  $S/D = 4$ , and the second series corresponds to closely spaced jets,  $S/D = 2$ . The calculations are done with alternate differencing schemes to illustrate the impact of numerical diffusion. The calculated jet trajectories agreed well with experimental data in the widely spaced jet geometry, but not in the closely spaced geometry. E.A.K.

**A85-39894\***# Case Western Reserve Univ., Cleveland, Ohio.

### **A NEW INTERPRETATION OF INTERNAL HEAT TRANSFER COEFFICIENTS OF POROUS MEDIA**

A. DYBBS, K. KAR, M. GROENEWEG, J. X. LING, and M. NARAGHI (Case Western Reserve University, Cleveland, OH) American Society of Mechanical Engineers, Winter Annual Meeting, New Orleans, LA, Dec. 9-14, 1984. 7 p. refs (Contract NAG3-97; NSG-3040; NSF CME-79-13389; NSF ENG-78-17782) (ASME PAPER 84-WA/HT-51)

The results of laser anemometer and flow visualization based fluid mechanics studies of porous media are used to obtain heat transfer coefficients for porous materials. Average pore flow  $Re$  ranging from 0.16-700 were examined. Darcy, inertial steady

laminar, unsteady laminar and turbulent flow regimes were detected. A passage length model was devised to derive the heat transfer coefficient. Sample data from flows through porous metals composed of powders and fibers validated the passage length for Darcy and inertial flow regimes. Unsteady laminar and turbulent flow coefficients require the identification of new parameters.

M.S.K.

**A85-39898\*#** Rensselaer Polytechnic Inst., Troy, N.Y.  
**HEAT TRANSFER INVESTIGATION IN THE JUNCTION REGION OF CIRCULAR CYLINDER NORMAL TO A FLAT PLATE AT 90 DEG LOCATION**

H. T. NAGAMATSU (Rensselaer Polytechnic Institute, Troy, NY) and J. N. HINCKEL (Instituto de Estudos Avancados, Sao Jose dos Campos, Sao Paulo, Brazil) American Society of Mechanical Engineers, Winter Annual Meeting, New Orleans, LA, Dec. 9-14, 1984. 7 p. refs

(Contract NSF MEA-80-06806; NAG3-292)

(ASME PAPER 84-WA/HT-70)

External heat-transfer rates were measured on a flat plate in the junction region of a circular cylinder mounted normal to the plate at a location 90 deg from the stagnation point. This configuration simulates the junction of the shroud with gas-turbine vanes. Heat-transfer results are presented for laminar, transition, and turbulent boundary layers for a Mach number of 0.14 with gas temperatures of approximately 750 deg R over a flat plate at room temperature. The measurements were made in air for a unit Reynolds number,  $Re/cm$ , range of 11,000 to 58,000. Heat-transfer measurements were conducted in the 70-ft long, 4-in. diameter shock tube. A shock-wave reflection technique was used to produce a flow Mach number of 0.14. Thin-film platinum heat gages were mounted on the flat plate and along the line of the stagnation point of the cylinder to measure the local heat flux in the junction region. The experimental heat-transfer data were correlated with the laminar and turbulent boundary-layer theories for the flat plate. With the cylinder the heat fluxes on the flat plate were greatly increased in the junction region compared to the heat flux for the plate alone.

Author

**A85-39900\*#** Texas A&M Univ., College Station.  
**HEAT TRANSFER ENHANCEMENT IN CHANNELS WITH TURBULENCE PROMOTERS**

J. C. HAN, J. S. PARK, and C. K. LEI (Texas A&M University, College Station, TX) American Society of Mechanical Engineers, Winter Annual Meeting, New Orleans, LA, Dec. 9-14, 1984. 8 p. Army-supported research. refs

(Contract NAG3-311)

(ASME PAPER 84-WA/HT-72)

Repeated rib-roughness elements have been used in advanced turbine cooling designs to enhance the internal heat transfer. Often the ribs are perpendicular to the main flow direction so that they have an angle-of-attack of 90 degrees. The objective of this investigation was to determine the effect of rib angle-of-attack on the pressure drop and the average heat-transfer coefficients in the fully developed turbulent air flow in a square duct with two opposite rib-roughened walls for Reynolds numbers varied from 7,000 to 90,000. The rib height-to-equivalent diameter ratio was kept at a constant value of 0.063, the rib pitch-to-height ratio was varied from 10 to 20, and the rib angle-of-attack ( $\alpha$ ) was varied from 90 to 60 deg to 45 to 30 deg, respectively. The thermal-performance comparison indicated that the increased heat conductance for the rib with an oblique angle to the flow ( $\alpha = 45 \text{ deg} - 30 \text{ deg}$ ) was about 10-20 percent higher than the rib with a 90 deg angle to the flow, and the pumping power requirement for the angled rib was about 20-50 percent lower than the transverse rib. Semi-empirical correlations for friction factor and heat-transfer coefficients were developed to account for rib spacing and rib angle. The correlations can be used in the design of turbine-blade cooling passages.

Author

**A85-40701\*#** California Univ., Los Angeles.

**VORTEX MODELING OF SINGLE AND MULTIPLE DILUTION JET MIXING IN A CROSSFLOW**

A. R. KARAGOZIAN and C. N. KIM (California, University, Los Angeles) American Institute of Aeronautics and Astronautics, Fluid Dynamics and Plasmadynamics and Lasers Conference, 18th, Cincinnati, OH, July 16-18, 1985. 12 p. refs

(Contract NAG3-543)

(AIAA PAPER 85-1580)

An analytical model for the behavior of normally injected jets in a crossflow is developed and applied to fluids of differing densities. Central to the model are the dynamics of the vortex pair structure associated with the local jet cross-section and the entrainment of crossflow by jet fluid. Two specific cases are modeled: one involving a single dilution jet in a crossflow, in which trajectories are found to scale primarily with jet-to-crossflow momentum ratio, and the other involving a series of spanwise jets injected into a crossflow, which indicates scaling with momentum ratio and with the spacing-to-orifice-diameter ratio. In the case of multiple jet penetration, however, merging of the jets into an approximately two-dimensional jet downstream of injection is observed for low spacing-to-diameter ratios.

Author

**A85-40750\*#** National Aeronautics and Space Administration. Lewis Research Center, Cleveland, Ohio.

**FLOW THROUGH VERY POROUS INCLINED SCREENS**

K. K. MURAMOTO and P. A. DURBIN (NASA, Lewis Research Center, Cleveland, OH) American Institute of Aeronautics and Astronautics, Fluid Dynamics and Plasmadynamics and Lasers Conference, 18th, Cincinnati, OH, July 16-18, 1985. 7 p. Previously announced in STAR as N85-25761. refs

(AIAA PAPER 85-1650)

The steady, inviscid flow through and around a screen inclined at a uniform angle to the incoming flow was investigated. For a screen placed in an infinite flow field, an asymptotic analysis for small resistance coefficients was performed, and the effects of inclination were determined. The velocity at first order in the asymptotic expansion was nonuniform along the screen. This nonuniformity caused the wake behind the screen to contain distributed vorticity at second order. These effects therefore occurred at one order lower than for normal screens.

M.G.

**A85-40752\*#** Pennsylvania State Univ., University Park,  
**TURBULENCE MODELLING FOR COMPLEX SHEAR FLOWS**

B. LAKSHMINARAYANA (Pennsylvania State University, University Park) American Institute of Aeronautics and Astronautics, Fluid Dynamics and Plasmadynamics and Lasers Conference, 18th, Cincinnati, OH, July 16-18, 1985. 38 p. refs

(Contract NSG-3266; NSG-3012; NSG-3212)

(AIAA PAPER 85-1652)

The turbulence models available for the prediction of complex turbulent shear layers are reviewed in this paper, concentrating mainly on three-dimensional flows, flows subjected to curvature and body rotation, separated flows, and vortex flows. A critical review of zero-equation, one-equation, two-equation, algebraic Reynolds stress, and full Reynolds stress models are carried out, with a specific emphasis on their applicability to complex flows. It is concluded that algebraic eddy viscosity models and kappa-epsilon/kappa-omega models, with a constant value of coefficients, are not adequate for complex flows. The models which include a description of stresses, either through an algebraic Reynolds stress model or a full Reynolds stress model, are essential for adequate prediction of these flows. It is recommended that systematic experimental investigations be carried out to isolate various complex interactions in order to understand and model the various effects and to carry out an extension of the present models to include complex flows.

Author



**A85-41326\*** National Aeronautics and Space Administration. Lewis Research Center, Cleveland, Ohio.

## **SOLIDIFICATION INTERFACE SHAPE FOR CONTINUOUS CASTING IN AN OFFSET MOLD - TWO ANALYTICAL METHODS**

R. SIEGEL (NASA, Lewis Research Center, Cleveland, OH) ASME, Transactions, Journal of Heat Transfer (ISSN 0022-1481), vol. 106, Feb. 1984, 4 p.

A solution method for finding the unknown solidification interface in manufacturing slab ingots as a continuous casting is presented, which involves a product solution in the potential plane and the use of conjugate harmonic functions. It is argued that the method may be more direct for some geometries than the Cauchy boundary value method. Moreover, the usefulness of the Cauchy boundary value method is demonstrated through the example of a nonsymmetric horizontal mold where the walls are offset to support the lower ingot boundary. L.T.

**A85-41782\*** Cleveland State Univ., Ohio.

## **COMBINED INFLUENCE OF UNSTEADY FREE STREAM VELOCITY AND FREE STREAM TURBULENCE ON STAGNATION POINT HEAT TRANSFER**

R. S. R. GORLA (Cleveland State University, OH) IN: 1983 Tokyo International Gas Turbine Congress, Tokyo, Japan, October 23-29, 1983, Proceedings. Volume 1. Tokyo, Gas Turbine Society of Japan, 1984, p. 45-49. refs (Contract NCC3-3)

An analysis is presented to study the combined effects of transient free stream velocity and free stream turbulence on heat transfer at a stagnation point over a cylinder situated in a crossflow. An expression for the eddy diffusivity has been formulated and the governing momentum and energy equations are integrated by means of the steepest descent method. The numerical results for the heat transfer rate are correlated by a turbulence parameter. It has been found that the stagnation point heat transfer rate increases with increasing free stream turbulence intensity.

Author

**A85-41787\*** Stanford Univ., Calif.

## **HEAT TRANSFER AND TURBULENCE MEASUREMENTS OF A FILM-COOLED FLOW OVER A CONVEXLY CURVED SURFACE**

K. FURUHAMA, R. J. MOFFAT (Stanford University, CA), and M. N. FROTA (Rio de Janeiro, Pontificia Universidade Catolica, Brazil) IN: 1983 Tokyo International Gas Turbine Congress, Tokyo, Japan, October 23-29, 1983, Proceedings. Volume 1. Tokyo, Gas Turbine Society of Japan, 1984, p. 119-126. refs (Contract NAG3-3)

Heat transfer and hydrodynamic boundary layer measurements were made in a turbulent boundary layer on a convex surface with 13 rows of injection. Both full- and partial-coverage cases were tested for three blowing ratios: 0.2, 0.4, and 0.6. Heat transfer results are discussed in terms of Stanton number with injection air temperature equal to wall temperature. In the blown region, for both  $m$  (blowing ratio) = 0.2 and 0.4, the local response of the boundary layer is dominated by curvature, and  $m = 0.4$  shows higher cooling effects than  $m = 0.2$  or 0.6, as expected, based on flat-plate results. Hydrodynamic measurements with a triple-hot-wire suggest the existence of two streamwise lanes. Lanes containing injection holes are highly affected by injection and show a definite streamwise evolution. Lanes which do not contain holes are not affected much by injection and show little change in the streamwise direction. Author

**A85-45282\*** Arizona State Univ., Tempe.

## **JET CHARACTERISTICS IN CONFINED SWIRLING FLOW**

R. M. C. SO, S. A. AHMED, and H. C. MONGIA (Arizona State University, Tempe) Experiments in fluids (ISSN 0723-4864), vol. 3, no. 4, 1985, p. 221-230. refs (Contract NAG3-260)

Jets in confined swirling flow are investigated in a facility where the swirling flow in the tube is produced by a vane-type swirler. The jet is located centrally in the swirler, and the diameter ratio of the tube to the jet is about 14. Both the jet and the swirling

flow are fully turbulent. Results show that the confined jet is highly dissipative in nature. Consequently, the flow in the tube does not resemble a free jet with axial pressure gradient. The presence of swirl increases the rate of dissipation and the jet decays even faster. A fairly isotropic turbulence field is observed in the confined swirling flow. However, the introduction of the jet does not significantly affect this behavior, and near isotropy of the turbulence field is again observed at about 30 jet diameters downstream.

Author

**A85-45283\*** Arizona State Univ., Tempe.

## **DENSITY EFFECTS ON JET CHARACTERISTICS IN CONFINED SWIRLING FLOW**

S. A. AHMED, R. M. C. SO, and H. C. MONGIA (Arizona State University, Tempe) Experiments in Fluids (ISSN 0723-4864), vol. 3, no. 4, 1985, p. 231-238. refs (Contract NAG3-260)

Density effects on isothermal jet mixing in confined swirling flow are investigated. The experiment is carried out with helium/air as the jet fluid in the same facility as that used by So et al. (1984) and the test conditions are chosen to be the same as before. Contrary to the homogeneous mixing results, the helium jet is preserved up to 40 jet diameters downstream. The behavior of the mean and turbulence field depends highly on the initial jet velocity. Since the jets are fully turbulent and the jet momentum fluxes for inhomogeneous mixing are less than those for homogeneous mixing, the cause of this difference in behavior is directly attributed to the combined action of density difference and swirl. In spite of this, near isotropy of the turbulence field is again observed at about 40 jet diameters downstream. Author

**A85-45856\*** National Aeronautics and Space Administration. Lewis Research Center, Cleveland, Ohio.

## **INTERNAL COMBUSTION ENGINE COMBUSTION CHAMBER PROCESS STUDIES AT NASA LEWIS RESEARCH CENTER**

H. J. SCHOCK (NASA, Lewis Research Center, Cleveland, OH) Journal of Propulsion and Power (ISSN 0748-4658), vol. 1, Sept.-Oct. 1985, p. 351-353. Previously cited in issue 19, p. 2749, Accession no. A84-40242. refs

**A85-46484\*** Pennsylvania State Univ., University Park.

## **MEASUREMENTS AND PREDICTIONS OF THE STRUCTURE OF EVAPORATING SPRAYS**

A. S. P. SOLOMON, J.-S. SHUEN, Q.-F. ZHANG, and G. M. FAETH (Pennsylvania State University, University Park) ASME, Transactions, Journal of Heat Transfer (ISSN 0022-1481), vol. 107, Aug. 1985, p. 679-686. refs (Contract NAG3-190)

In the present experimental and theoretical study of turbulent, evaporating sprays, round, Freon-11 sprays produced by an air-atomizing injector that is directed vertically downward in still air were subjected to structure measurements for mean and fluctuating gas velocities, total Freon-11 concentration, drop size and velocity contributions, mean gas temperature, and liquid flux distributions. An evaluation was then conducted of three spray models: (1) locally homogeneous flow, (2) deterministic separated flow, and (3) stochastic separated flow. The first two of these were found to perform poorly; the stochastic model yielded the best agreement between predictions and measurements. O.C.

**A85-48538\*** Pennsylvania State Univ., University Park.

## **STRUCTURE OF NONEVAPORATING SPRAYS. I - INITIAL CONDITIONS AND MEAN PROPERTIES**

A. S. P. SOLOMON, J.-S. SHUEN, Q.-F. ZHANG, and G. M. FAETH (Pennsylvania State University, University Park) AIAA Journal (ISSN 0001-1452), vol. 23, Oct. 1985, p. 1548-1555. refs (Contract NAG3-190)

Structure measurements were completed within the dilute portion of axisymmetric nonevaporating sprays. Measurements included: mean velocities, velocity fluctuations, and Reynolds stress of the gas phase; and mean velocities, fluctuating velocities, mass flux, and diameter distributions of the drop phase. The measurements were used to evaluate three typical methods of



analyzing sprays: (1) a locally homogeneous flow (LHF) analysis, where slip between the phases is neglected; (2) a deterministic separated flow (DSF) analysis, where slip is considered but effects of drop interactions with turbulence are ignored; and (3) a stochastic separated flow (SSF) analysis, where effects of both slip and turbulence are considered using random-walk computations for drop motion. Measurements of initial conditions of both phases near the injector, mean gas-phase properties, and liquid flux distributions are described herein. Best agreement between predictions and measurements was obtained with the SSF model, which provided a reasonable representation of turbulent dispersion of drops. A companion paper presents additional measurements of drop continuous phase properties. Author

**A85-49354\*** Florida State Univ., Tallahassee.

**A MULTIPLE-SCALES MODEL OF THE SHOCK-CELL STRUCTURE OF IMPERFECTLY EXPANDED SUPERSONIC JETS**

C. K. W. TAM, J. A. JACKSON (Florida State University, Tallahassee), and J. M. SEINER (NASA, Langley Research Center, Hampton, VA) *Journal of Fluid Mechanics* (ISSN 0022-1120), vol. 153, April 1985, p. 123-149. refs  
(Contract NAG3-182)

The present investigation is concerned with the development of an analytical model of the quasi-periodic shock-cell structure of an imperfectly expanded supersonic jet. The investigation represents a part of a program to develop a mathematical theory of broadband shock-associated noise of supersonic jets. Tam and Tanna (1982) have suggested that this type of noise is generated by the weak interaction between the quasi-periodic shock cells and the downstream-propagating large turbulence structures in the mixing layer of the jet. In the model developed in this paper, the effect of turbulence in the mixing layer of the jet is simulated by the addition of turbulent eddy-viscosity terms to the momentum equation. Attention is given to the mean-flow profile and the numerical solution, and a comparison of the numerical results with experimental data. G.R.

**N85-10303\*#** National Aeronautics and Space Administration. Lewis Research Center, Cleveland, Ohio.

**THE EFFECT OF CHANNEL CONVERGENCE ON HEAT TRANSFER IN A PASSAGE WITH SHORT PIN FINS**

B. A. BRIGHAM Oct. 1984 17 p refs  
(NASA-TM-83801; E-2306; NAS 1.15:83801) Avail: NTIS HC A02/MF A01 CSCL 20D

Array averaged heat transfer coefficients were obtained for two configurations of short pin fins in a converging channel and for two flat plate configurations in a converging channel. The effect of flow acceleration due to channel convergence and the effect of varying pin length on the heat transfer was determined. Results are presented in the form of Nusselt number versus Reynolds number for the four geometries tested. Author

**N85-10306\*#** National Aeronautics and Space Administration. Lewis Research Center, Cleveland, Ohio.

**A REVIEW AND ANALYSIS OF BOUNDARY LAYER TRANSITION DATA FOR TURBINE APPLICATION**

R. E. GAUGLER Washington 1984 14 p refs Presented at the 13th Intern. Gas Turbine Conf. and Exhibit, Houston, Tex., 17-21 Mar. 1984; sponsored by the American Society of Mechanical Engineers  
(NASA-TM-86880; E-2341; NAS 1.15:86880) Avail: NTIS HC A02/MF A01 CSCL 20D

A symposium on transition in turbines was held at the NASA Lewis Research Center. One recommendation of the working groups was the collection of existing transition data to provide standard cases against which models could be tested. A number of data sets from the open literature that include heat transfer data in apparently transitional boundary layers, with particular application to the turbine environment, were reviewed and analyzed to extract transition information from the heat transfer data. The data sets reviewed cover a wide range of flow conditions, from low speed, flat plate tests to full scale turbine airfoils operating at

simulated turbine engine conditions. The results indicate that free stream turbulence and pressure gradient have strong, and opposite, effects on the location of the start of transition and on the length of the transition zone. R.S.F.

**N85-11317\*#** National Aeronautics and Space Administration. Lewis Research Center, Cleveland, Ohio.

**PRELIMINARY RESULTS OF A STUDY OF THE RELATIONSHIP BETWEEN FREE STREAM TURBULENCE AND STAGNATION REGION HEAT TRANSFER**

G. J. VAANFOSSSEN, JR. and R. J. SIMONEAU 1984 16 p refs Proposed for presentation at the 30th Intern. Gas Turbine Conf. and Exhibit, Houston, Tex., 17-21 Mar. 1985; sponsored by the American Society of Mechanical Engineers  
(NASA-TM-86884; E-2346; NAS 1.15:86884) Avail: NTIS HC A02/MF A01 CSCL 20D

The mechanism that causes free stream turbulence to increase heat transfer in the stagnation region of turbine vanes and blades was studied. The work is being conducted in a wind tunnel at atmospheric conditions to facilitate measurements of turbulence and heat transfer. The model size is scaled up to simulate Reynolds numbers (based on leading edge diameter) that are to be expected on a turbine blade leading edge. Reynolds numbers from 13,000 to 177,000 were run in the present tests. Spanwise averaged heat transfer measurement with high and low turbulence were made with rough and smooth surface stagnation regions. Results of these measurements show that the boundary layer remains laminar in character even in the presence of free stream turbulence at the Reynolds numbers tested. If roughness is added the boundary layer becomes transitional as evidenced by the heat transfer increase with increasing distance from the stagnation line. Hot wire measurements near the stagnation region downstream of an array of parallel wires has shown that vorticity in the form of mean velocity gradients is amplified as flow approaches the stagnation region. Author

**N85-12314\*#** National Aeronautics and Space Administration. Lewis Research Center, Cleveland, Ohio.

**VORTEX-GENERATING COOLANT-FLOW-PASSAGE DESIGN FOR INCREASED FILM-COOLING EFFECTIVENESS AND SURFACE COVERAGE**

S. S. PAPELL Nov. 1984 24 p refs  
(NASA-TP-2388; E-2147; NAS 1.60:2388) Avail: NTIS HC A02/MF A01 CSCL 20D

The thermal film-cooling footprints observed by infrared imagery for three coolant-passage configurations embedded in adiabatic-test plates are discussed. The configurations included a standard round-hole cross section and two orientations of a vortex-generating flow passage. Both orientations showed up to factors of four increases in both film-cooling effectiveness and surface coverage over that obtained with the round coolant passage. The crossflow data covered a range of tunnel velocities from 15.5 to 45 m/sec with blowing rates from 0.20 to 2.05. A photographic streakline flow visualization technique supported the concept of the counterrotating capability of the flow passage design and gave visual credence to its role in inhibiting flow separation. M.G.

**N85-14078\*#** National Aeronautics and Space Administration. Lewis Research Center, Cleveland, Ohio.

**FLOW RATES AND PRESSURE PROFILES FOR ONE TO FOUR AXIALLY ALIGNED BORDA INLETS**

R. C. HENDRICKS and T. T. STETZ Dec. 1984 32 p refs  
(NASA-TP-2390; E-1979; NAS 1.60:2390) Avail: NTIS HC A03/MF A01:b CSCL 20A

Choked flow rate and pressure profile data were taken on sequential, axially aligned inlets of the Borda type. The configurations consisted of two to four inlets spaced 0.8 and 30 diameters apart. At a spacing of 30 diameters the reduced flow rate appeared to follow the simple empirical relation  $G_{sub\ r}/G_{sub\ r,1} = N(-b)$ , where  $G_{sub\ r,1}$  is the reduced flow rate for a single inlet;  $N$  is the number of inlets; and  $b$ , which is weakly temperature dependent, is approximately 0.4. The relation is in reasonable agreement with

### 34 FLUID MECHANICS AND HEAT TRANSFER

an analysis of the N-inlet configuration. At a spacing of 30 diameters the pressure profiles dropped sharply at the entrance and partially recovered within each inlet somewhat independently of N. Jetting through the last Borda was common at low temperatures. At a spacing of 0.8 diameter fluid jetting was prevalent at low temperatures for each configuration studied and flow rates were the same as that for a single inlet. M.G.

**N85-15133\*#** National Aeronautics and Space Administration. Lewis Research Center, Cleveland, Ohio.

#### **HEAT TRANSFER RESULTS AND OPERATIONAL CHARACTERISTICS OF THE NASA LEWIS RESEARCH CENTER HOT SECTION CASCADE TEST FACILITY**

H. J. GLADDEN, F. C. YEH, and D. L. FRONEK 1985 20 p refs Presented at the 30th Intern. Gas Turbine Conf. and Exhibit, Houston, Tex., 17-21 Mar. 1985; sponsored by ASME

(NASA-TM-86890; E-2357; NAS 1.15:86890) Avail: NTIS HC A02/MF A01 CSCL 20D

The NASA Lewis Research Center gas turbine hot section test facility has been developed to provide a real-engine environment with well known boundary conditions for the aerothermal performance evaluation/verification of computer design codes. The initial aerothermal research data obtained are presented and the operational characteristics of the facility are discussed. This facility is capable of testing at temperatures and pressures up to 1600 K and 18 atm which corresponds to a vane exit Reynolds number range of  $0.5 \times 10^6$  to  $2.5 \times 10^6$  based on vane chord. The component cooling air temperature can be independently modulated between 330 and 700 K providing gas-to-coolant temperature ratios similar to current engine application. Research instrumentation of the test components provide conventional pressure and temperature measurements as well as metal temperatures measured by IR-photography. The primary data acquisition mode is steady state through a 704 channel multiplexer/digitizer. The test facility was configured as an annular cascade of full coverage filmcooled vanes for the initial series of research tests. Author

**N85-17324\*#** Wisconsin Univ., Milwaukee. Dept. of Mechanical Engineering.

#### **A STUDY OF REYNOLDS-STRESS CLOSURE MODEL**

**Semiannual Progress Report, 1 Jun. 1984 - 15 Jan. 1985**

R. S. AMANO and P. GOEL Jan. 1985 50 p refs

(Contract NAG3-546)

(NASA-CR-174342; NAS 1.26:174342) Avail: NTIS HC A03/MF A01 CSCL 20D

A hybrid model of the Reynolds stress closure was developed. This model was tested for various sizes of step flow, and the computed Reynolds stress behavior was compared with experimental data. The third order closure model was reviewed. Transport equations for the triple velocity correlation were developed and implemented in a numerical code to evaluate the behavior of the triple velocity products in various regions of the flow field including recirculating, reattaching, and redeveloping flow domains. B.G.

**N85-18291\*#** Massachusetts Inst. of Tech., Cambridge. Gas Turbine Lab.

#### **RESEARCHED APPLIED TO TRANSONIC COMPRESSORS IN NUMERICAL FLUID MECHANICS OF INVISCID FLOW AND VISCOUS FLOW Final Report**

W. T. THOMPSON, JR. Feb. 1985 83 p refs

(Contract NAG3-9)

(NASA-CR-174353; NAS 1.26:174353) Avail: NTIS HC A05/MF A01 CSCL 20D

A streamline Euler solver which combines high accuracy and good convergence rates with capabilities for inverse or direct mode solution modes and an analysis technique for finite difference models of hyperbolic partial difference equations were developed. B.G.

**N85-18292\*#** Pennsylvania State Univ., State College. Applied Research Lab.

#### **THE BOUNDARY LAYER ON COMPRESSOR CASCADE BLADES**

**Semiannual Progress Report, 1 Jun. - 1 Dec. 1984**

S. DEUTSCH and W. C. ZIERKE 1984 47 p refs

(Contract NSG-3264)

(NASA-CR-174369; NAS 1.26:174369) Avail: NTIS HC A03/MF A01 CSCL 20D

The flow field about an airfoil in a cascade at chord Reynolds number ( $R_{sub C}$ ) near 50,000. The program is experimental and combines laser Doppler anemometry (LDA) with flow visualization techniques in order to obtain detailed flow data (e.g., boundary layer profiles, points of separation and the transition zone) on a cascade of highly-loaded compressor blades. The information provided is to serve as benchmark data for the evaluation of current and future compressor cascade predictive models, in this way aiding in the compressor design process. The completed pressure surface mean velocity profiles, as well as two detailed near wake velocity profiles, all at a single incidence angle are provided. B.G.

**N85-19363\*#** National Aeronautics and Space Administration. Lewis Research Center, Cleveland, Ohio.

#### **EXPERIMENTAL STUDY OF CERAMIC COATED TIP SEALS FOR TURBOJET ENGINES**

T. J. BIESIADNY, G. A. KLANN (Army Research and Technology Labs., Cleveland), E. S. LASSOW (Howmet Corp., Whitehall, Mich.), M. MCHENRY (Army Aviation Logistics School, Fort Eustis, Va.), G. MCDONALD, and R. C. HENDRICKS 1985 22 p refs Presented at the 9th Ann. Conf. on Composites and Advan. Ceram. Mater., Cocoa Beach, Fla., 20-24 Jan. 1985; sponsored by the American Ceramic Society

(NASA-TM-86939; E-2457; NAS 1.15:86939;

USAAVSCOM-TM-84-C-2) Avail: NTIS HC A02/MF A01 CSCL 20D

Ceramic gas-path seals were fabricated and successfully operated over 1000 cycles from flight idle to maximum power in a small turboshaft engine. The seals were fabricated by plasma spraying zirconia over a NiCoCrAlX bond coat on the Haynes 25 substrate. Coolant-side substrate temperatures and related engine parameters were recorded. Post-test inspection revealed mudflat surface cracking with penetration to the ceramic bond-coat interface. Author

**N85-19364\*#** National Aeronautics and Space Administration. Lewis Research Center, Cleveland, Ohio.

#### **RIBBON BURNER SIMULATION OF T-700 TURBINE SHROUD FOR CERAMIC LINED SEALS RESEARCH**

J. K. LITTLE (Arnold Air Force Station, Tullahoma, Tenn.), G. P. ALLEN, G. MCDONALD, and R. C. HENDRICKS 1985 20 p refs Presented at the 9th Ann. Conf. on Composites and Advan. Ceram. Mater., Cocoa Beach, Fla., 20-24 Jan. 1985; sponsored by the American Ceramic Society

(NASA-TM-86940; E-2458; NAS 1.15:86940) Avail: NTIS HC A02/MF A01 CSCL 20D

Experimental and analytical studies were conducted to determine the acceptability of a ribbon-burner simulation of engine conditions for testing ceramic-lined turbine tip shrouds. The calculated values reveal that the ribbon burner establishes at least as harsh a thermal environment as is present at any time within the turbine shroud. Comparisons were made with ceramic components in a turboshaft engine. Author

**N85-20269\*#** National Aeronautics and Space Administration. Lewis Research Center, Cleveland, Ohio.

**FLOW VISUALIZATION STUDY OF THE EFFECT OF INJECTION HOLE GEOMETRY ON AN INCLINED JET IN CROSSFLOW**

F. F. SIMON and M. L. CIANCONE 1985 26 p refs To be presented at the Symp. on Transport Phenomena in Rotating Machinery, held in Honolulu, Hi., 28 Apr. - 3 May 1985; sponsored in part by Michigan Univ., Hawaii Univ., ASME, Gas Turbine Society of Japan, and the Turbomachinery Society of Japan (NASA-TM-86936; E-2450; NAS 1.15:86936) Avail: NTIS HC A03/MF A01 CSCL 20D

A flow visualization was studied by using neutrally buoyant, helium-filled soap bubbles, to determine the effect of injection hole geometry on the trajectory of an air jet in a crossflow and to investigate the mechanisms involved in jet deflection. Experimental variables were the blowing rate, and the injection hole geometry cusp facing upstream (CUS), cusp facing downstream (CDS), round, swirl passage, and oblong. It is indicated that jet deflection is governed by both the pressure drag forces and the entrainment of free-stream fluid into the jet flow. For injection hole geometries with similar cross-sectional areas and similar mass flow rates, the jet configuration with the larger aspect ratio experienced a greater deflection. Entrainment arises from lateral shearing forces on the sides of the jet, which set up a dual vortex motion within the jet and thereby cause some of the main-stream fluid momentum to be swept into the jet flow. This additional momentum forces the jet nearer the surface. Of the jet configurations, the oblong, CDS, and CUS configurations exhibited the largest deflections. The results correlate well with film cooling effectiveness data, which suggests a need to determine the jet exit configuration of optimum aspect ratio to provide maximum film cooling effectiveness. E.A.K.

**N85-21569\*#** National Aeronautics and Space Administration. Lewis Research Center, Cleveland, Ohio.

**ANALYSIS OF EXPERIMENTAL SHAFT SEAL DATA FOR HIGH-PERFORMANCE TURBOMACHINES, AS FOR SPACE SHUTTLE MAIN ENGINES**

R. C. HENDRICKS, M. J. BRAUN (Akron, Univ., Ohio), R. L. MULLEN (Case Western Reserve Univ.), R. E. BURCHAM (Rocketdyne, Canoga Park, Calif.), and W. A. DIAMOND (Rocketdyne, Canoga Park, Calif.) 1985 19 p refs To be presented at the Symp. on Transport Phenomena in Rotating Machinery, Honolulu, Hawaii, 28 Apr. - 3 May 1985; sponsored in part by Michigan Univ., Hawaii Univ., ASME, Gas Turbine Soc. of Japan, and Turbomachinery Society of Japan (NASA-TM-86928; E-2430; NAS 1.15:86928) Avail: NTIS HC A02/MF A01 CSCL 20D

High-pressure, high-temperature seal flow (leakage) data for nonrotating and rotating Raleigh-step and convergent-tapered-bore seals were characterized in terms of a normalized flow coefficient. The data for normalized Rayleigh-step and nonrotating tapered-bore seals were in reasonable agreement with theory, but data for the rotating tapered-bore seals were not. The tapered-bore-seal operational clearances estimated from the flow data were significantly larger than calculated. Although clearances are influenced by wear from conical to cylindrical geometry and errors in clearance corrections, the problem was isolated to the shaft temperature - rotational speed clearance correction. The geometric changes support the use of some conical convergence in any seal. Under these conditions rotation reduced the normalized flow coefficient by nearly 10 percent. Author

**N85-21570\*#** National Aeronautics and Space Administration. Lewis Research Center, Cleveland, Ohio.

**LIQUID FUEL SPRAY PROCESSES IN HIGH-PRESSURE GAS FLOW**

R. D. INGEBO 1985 22 p refs Presented at 3rd Intern. Conf. on Liquid Atomization and Spray Systems, London, 8-10 Jul. 1985 (NASA-TM-86944; E-2463; NAS 1.15:86944) Avail: NTIS HC A02/MF A01 CSCL 20D

Atomization of single liquid jets injected downstream in high pressure and high velocity airflow was investigated to determine

the effect of airstream pressure on mean drop size as measured with a scanning radiometer. For aerodynamic - wave breakup of liquid jets, the ratio of orifice diameter  $D_{sub o}$  to measured mean drop diameter  $D_{sub m}$  which is assumed equal to  $D_{sub 32}$  or Sauter mean diameter, was correlated with the product of the Weber and Reynolds numbers  $WeRe$  and the dimensionless group  $G1/\text{square root of } c$ , where  $G$  is the gravitational acceleration,  $1$  the mean free molecular path, and square root of  $C$  the root mean square velocity, as follows;  $D_{sub o}/D_{sub 32} = 1.2 (WeRe)$  to the  $0.4 (G1/\text{square root of } c)$  to the  $0.15$  for values of  $WeRe$   $1$  million and an airstream pressure range of  $0.10$  to  $2.10$  MPa. G.L.C.

**N85-21574\*#** National Aeronautics and Space Administration. Lewis Research Center, Cleveland, Ohio.

**NESTED SUBCRITICAL FLOWS WITHIN SUPERCRITICAL SYSTEMS**

R. C. HENDRICKS, M. J. BRAUN (Akron Univ.), R. L. WHEELER, III (Akron Univ.), and R. L. MULLEN 1985 12 p refs Proposed for presentation at the 20th Ann. Cavitation and Multiphase Flow Forum, Albuquerque, N. Mex., 24-26 Jun. 1985; sponsored by the American Society of Mechanical Engineers (NASA-TM-86980; E-2518; NAS 1.15:86980) Avail: NTIS HC A02/MF A01 CSCL 20D

In supercritical systems the design inlet and outlet pressures are maintained above the thermodynamic critical pressure  $P_{sub C}$ . Designers rely on this simple rule of thumb to circumvent problems associated with a subcritical pressure regime nested within the supercritical pressure system along with the uncertainties in heat transfer, fluid mechanics, and thermophysical property variations. The simple rule of thumb is adequate in many low-power designs but is inadequate for high-performance turbomachines and linear systems, where nested two-phase regions can exist. Examples for a free-jet expansion with backpressure greater than  $P_{sub C}$  and a rotor (bearing) with ambient pressure greater than  $P_{sub C}$  illustrate the existence of subcritical pressure regimes nested within supercritical systems. Author

**N85-24245\*#** National Aeronautics and Space Administration. Lewis Research Center, Cleveland, Ohio.

**ADVANCED RADIATOR CONCEPTS**

P. S. DIEM-KIRSOP 30 Jun. 1985 13 p refs Proposed for presentation at Soc. of Women Engr. Natl. Convention, Minneapolis, 27-30 Jun. 1985 (NASA-TM-87008; E-2552; NAS 1.15:87008) Avail: NTIS HC A02/MF A01 CSCL 20D

The liquid droplet radiator and the liquid belt radiator currently under study by the NASA LeRC are discussed. These advanced concepts offer benefits in reduced mass, compact stowage, and ease of deployment. Operation and components of the radiators are described, heat transfer characteristics are discussed, and critical technologies are identified. The impact of the radiators on large power systems is also assessed. A.R.H.

**N85-25760\*#** National Aeronautics and Space Administration. Lewis Research Center, Cleveland, Ohio.

**THE INFLUENCE OF JET-GRID TURBULENCE ON HEAT TRANSFER FROM THE STAGNATION REGION OF A CYLINDER IN CROSSFLOW**

J. E. OBRIEN (Pennsylvania State Univ., University Park) and G. J. VANFOSSEN, JR. 1985 13 p refs Proposed for presentation at the Natl. Heat Transfer Conf., Denver, 4-7 Aug. 1985; sponsored by ASME (NASA-TM-87011; E-2555; NAS 1.15:87011) Avail: NTIS HC A02/MF A01 CSCL 20D

The effect of high-intensity turbulence on heat transfer from the stagnation region of a circular cylinder in crossflow was studied. The work was motivated by the desire to be able to more fully understand and predict the heat transfer to the leading edge of a turbine airfoil. In order to achieve high levels of turbulence with a reasonable degree of isotropy and homogeneity, a jet-injection turbulence grid was used. The jet grid provided turbulence intensities of 10 to 12 percent, measured at the test cylinder

## 34 FLUID MECHANICS AND HEAT TRANSFER

location, for downstream blowing with the blowing rate adjusted to an optimal value for flow uniformity. Heat transfer augmentation above the zero-turbulence case ranged from 37 to 53 percent for the test cylinder behind the jet grid for a cylinder Reynolds number range of 48,000 to 180,000, respectively. The level of heat transfer augmentation was found to be fairly uniform with respect to circumferential distance from the stagnation line. Stagnation point heat transfer results (expressed in terms of the Frossling number) were found to be somewhat low with respect to previous studies, when compared on the basis of equal values of the parameter  $Tu Re^{1/2}$ , indicating an additional Reynolds number effect as observed by previous investigators. Consequently, for a specified value of  $Tu Re^{1/2}$ , data obtained with a relatively high turbulence intensity will have a lower value of the Frossling number. M.G.

**N85-25761\*#** National Aeronautics and Space Administration. Lewis Research Center, Cleveland, Ohio.

### FLOW THROUGH VERY POROUS INCLINED SCREENS

K. K. MURAMOTO and P. A. DURBIN 1985 10 p refs Proposed for presentation at the 18th Fluid Dyn. and Plasmasdyn. and Lasers Conf., Cincinnati, 16-18 Jul. 1985; sponsored by AIAA (NASA-TM-86979; E-2517; NAS 1.15:86979) Avail: NTIS HC A02/MF A01 CSCL 20D

The steady, inviscid flow through and around a screen inclined at a uniform angle to the incoming flow was investigated. For a screen placed in an infinite flow field, an asymptotic analysis for small resistance coefficients was performed, and the effects of inclination were determined. The velocity at first order in the asymptotic expansion was nonuniform along the screen. This nonuniformity caused the wake behind the screen to contain distributed vorticity at second order. These effects therefore occurred at one order lower than for normal screens. M.G.

**N85-26902\*#** National Aeronautics and Space Administration. Lewis Research Center, Cleveland, Ohio.

### ANALYTICAL STUDY OF FLOW PHENOMENA IN SSME TURNAROUND DUCT GEOMETRIES

K. L. MCLALLIN In NASA. Marshall Space Flight Center Advan. High Pressure O2/H2 Technol. p 579-598 Apr. 1985 refs Avail: NTIS HC A99/MF E03; SOD HC CSCL 20D

The SSME fuel turbopump hot gas manifold was identified as a source of loss and flow distortion which significantly affects the performance and durability of both the drive turbine and the LOX injector area of the main combustion chamber. Two current SSME geometries were studied, the full power level (FPL) and the first manned orbital flight (FMOF) configuration. The effects of turnaround duct geometry on flow losses and distortions, by varying wall curvature and flow area variation in the 180 deg turnaround region were examined. The effects of the duct inlet flow phenomena such as the radial distortion of the inlet flow and inlet swirl level on turnaround duct performance were also investigated. It is shown that of the two current geometries, the FMOF configuration had lower pressure losses and generated less flow distortion, but had a small flow separation bubble at the 180 deg turnaround exit. It is found that by optimizing wall curvature and flow diffusion in the turnaround, improved duct performance can be achieved. E.A.K.

**N85-27164\*#** Analox Corp., Cleveland, Ohio.

### COMPUTER PROGRAM FOR THE CALCULATION OF MULTICOMPONENT CONVECTIVE DIFFUSION DEPOSITION RATES FROM CHEMICALLY FROZEN BOUNDARY LAYER THEORY Final Report

S. A. GOEKOGLU, B. K. CHEN, and D. E. ROSNER Washington Jan. 1984 35 p refs Prepared in cooperation with Yale Univ., New Haven, Conn. (Contract NAS3-23293; NAG3-201) (NASA-CR-168329; E-1971; NAS 1.26:168329) Avail: NTIS HC A03/MF A01 CSCL 20D

The computer program based on multicomponent chemically frozen boundary layer (CFBL) theory for calculating vapor and/or small particle deposition rates is documented. A specific application to perimeter-averaged  $Na_2SO_4$  deposition rate calculations on a

cylindrical collector is demonstrated. The manual includes a typical program input and output for users. Author

**N85-27165\*#** National Aeronautics and Space Administration. Lewis Research Center, Cleveland, Ohio.

### FLOW RATE AND PRESSURE PROFILES FOR 1 TO 4 AXIALLY ALINED ORIFICE INLETS

R. C. HENDRICKS and T. T. STETZ May 1985 44 p refs (NASA-TP-2460; E-1980; NAS 1.60:2460) Avail: NTIS HC A03/MF A01 CSCL 20D

Choked flow rate and pressure profile data were taken on sequential axially aligned inlets of the orifice type, with an orifice length-to-diameter ratio of 0.5. The configuration consisted of two to four inlets spaced at 0.66 and 32 orifice diameters apart. At a spacing of 32 diameters the reduced flow rate appeared to follow the simple power-law relation  $G(\text{sub } r)/G(\text{sub } r,1) = N(\text{sup } b)$ , where  $G(\text{sub } r,1)$  is the reduced flow rate for a single inlet,  $N$  is the number of inlets, and  $b$ , although temperature dependent, is approximately 0.4. At this spacing the instrumented orifices and spacers gave pressure profiles that dropped sharply at the entrance and partially recovered within each inlet, somewhat independent of  $N$ . At low inlet temperature jetting through the last orifice was common. At a spacing of 0.66 diameter fluid jetting through all  $N$  inlets was prevalent at low temperatures for each configuration studied, as indicated by the flat pressure profiles and flow rates that were nearly identical to those for a single orifice inlet. A simplifying relation was developed between the friction loss parameters for flow through  $N$  sequential tubes and  $N$  sequential inlets. The predicted flow rates for  $N$  tubes were in reasonable agreement with the  $N$  inlet analysis and followed the simple power-law relation. M.G.

**N85-27168\*#** California Inst. of Tech., Pasadena.

### FREE-SURFACE PHENOMENA UNDER LOW- AND ZERO-GRAVITY CONDITIONS Final Technical Report

D. COLES 6 Jun. 1985 16 p refs (Contract NAG3-466) (NASA-CR-175835; NAS 1.26:175835) Avail: NTIS HC A02/MF A01 CSCL 20D

An apparatus to measure contact angle was constructed to exploit the proposed internal-corner criterion. If  $2\alpha$  is the internal angle between two intersecting vertical planes and  $\gamma$  is the contact angle, a meniscus at the corner rises to a finite height if  $\alpha + \gamma < \pi/2$  and to an infinite height if  $\alpha + \gamma \geq \pi/2$ . The apparatus operates by decreasing the angle  $\alpha$  from  $\pi/2$  until the meniscus height changes abruptly. A number of liquids are tested on glass and plexiglas. E.A.K.

**N85-27945\*#** National Aeronautics and Space Administration. Lewis Research Center, Cleveland, Ohio.

### SIMULATION OF MULTISTAGE TURBINE FLOWS

M. L. CELESTINA (Sverdrup Technology, Inc., Middleburg Heights, Ohio), R. A. MULAC (Sverdrup Technology, Inc., Middleburg Heights, Ohio), and J. J. ADAMCZYK In its Struct. Integrity and Durability of Reusable Space Propulsion Systems p 27-36 May 1985

Avail: NTIS HC A09/MF A01 CSCL 20D

The numerical simulation of turbine flows serves to enhance the understanding of the flow phenomena within multistage turbomachinery components. The direct benefit of this activity is improved modeling capability, which can be used to improve component efficiency and durability. A hierarchy of equations was formulated to assess the difficulty in analyzing the flow field within multistage turbomachinery components. The Navier-Stokes equations provides the most complete description. The simplest description is given by a set of equations that govern the quasi-one-dimensional flow. The number of unknowns to be solved for increases monotonically above the number of equations. The development of the additional set of equations needed to mathematically close the system of equations forms the closure problem associated with that level of description. For the Navier-Stokes equation there is no closure problem. For the quasi-one-dimensional equation set random flow fluctuations,

unsteady fluctuations, nonaxisymmetric flow variations, and hub-to-shroud variations on the quasi-one-dimensional flow must be accounted for. E.A.K.

**N85-27947\*#** National Aeronautics and Space Administration. Lewis Research Center, Cleveland, Ohio.

## UNSTEADY HEAT TRANSFER DUE TO TIME-DEPENDENT FREE STREAM VELOCITY Abstract Only

R. S. R. GORLA and A. AMERI /n NASA. Lewis Research Center Struct. Integrity and Durability of Reusable Space Propulsion Systems p 39-40 May 1985 refs  
 Avail: NTIS HC A09/MF A01 CSCL 20D

The present work was undertaken in order to study the unsteady combined convection from a horizontal circular cylinder to a transverse flow. A coordinate perturbation method is used to transform the governing set of partial differential equations into a system of ordinary differential equations. The free stream time-dependent velocity was assumed to be sinusoidal and the boundary layer response due to both low as well as high frequencies of oscillation will be studied. Currently numerical solutions are being obtained for the distribution of the unsteady Nusselt number and the friction factor. Author

**N85-27948\*#** National Aeronautics and Space Administration. Lewis Research Center, Cleveland, Ohio.

## NEW FACILITY TO STUDY UNSTEADY WAKE EFFECTS ON TURBINE AIRFOIL HEAT TRANSFER

R. J. SIMONEAU /n its Struct. Integrity and Durability of Reusable Space Propulsion Systems p 41-47 May 1985  
 Avail: NTIS HC A09/MF A01 CSCL 20D

A significant portion of the SSME aerothermal loads program is directed at the heat transfer effects of the unsteady flows, particularly wakes, that occur naturally in turbomachinery. Although these phenomena occur in all turbomachines, we feel they will be more severe in the SSME turbines because of the high heat transfer associated with the very high Reynolds numbers over the SSME airfoils. G.L.C.

**N85-29179\*** National Aeronautics and Space Administration. Lewis Research Center, Cleveland, Ohio.

## HIGH THERMAL POWER DENSITY HEAT TRANSFER APPARATUS PROVIDING ELECTRICAL ISOLATION AT HIGH TEMPERATURE USING HEAT PIPES Patent

J. F. MORRIS, inventor (to NASA) 19 Mar. 1985 6 p Filed 24 Jun. 1983 Continuation-in-part of abandoned US Patent Appl-SN-202228, filed 30 Nov. 1980  
 (NASA-CASE-LEW-12950-2; US-PATENT-4,506,183;  
 US-PATENT-APPL-SN-507626; US-PATENT-APPL-SN-202228;  
 US-PATENT-CLASS-310-306; US-PATENT-CLASS-165-32;  
 US-PATENT-CLASS-165-104.14) Avail: US Patent and Trademark Office CSCL 20D

This invention is directed to transferring heat from an extremely high temperature source to an electrically isolated lower temperature receiver. The invention is particularly concerned with supplying thermal power to a thermionic converter from a nuclear reactor with electric isolation. Heat from a high temperature heat pipe is transferred through a vacuum or a gap filled with electrically nonconducting gas to a cooler heat pipe. If the receiver requires grater thermal power density, geometries are used with larger heat pipe areas for transmitting and receiving energy than the area for conducting the heat to the thermionic converter. In this way the heat pipe capability for increasing thermal power densities compensates for the comparative low thermal power densities through the electrically nonconducting gap between the two heat pipes. Official Gazette of the U.S. Patent and Trademark Office

**N85-30242\*#** National Aeronautics and Space Administration. Lewis Research Center, Cleveland, Ohio.

## FAST APPROACH FOR CALCULATING FILM THICKNESSES AND PRESSURES IN ELASTOHYDRODYNAMICALLY LUBRICATED CONTACTS AT HIGH LOADS

L. G. HOUPERT (SKF Engineering and Research Center) and B. J. HAMROCK 1985 31 p refs Proposed for presentation at the Joint Lubrication Conf., Atlanta, 8-10 Oct. 1985; sponsored by the American Society of Lubrication Engineers  
 (NASA-TM-87032; E-2581; NAS 1.15:87032) Avail: NTIS HC A03/MF A01 CSCL 20D

The film thicknesses and pressures in elastohydrodynamically lubricated contacts have been calculated for a line contact by using an improved version of Okamura's approach. The new approach allows for lubricant compressibility, the use of Roelands' viscosity, a general mesh (nonconstant step), and accurate calculations of the elastic deformation. The new approach is described, and the effects on film thickness, pressure, and pressure spike of each of the improvements are discussed. Successful runs have been obtained at high pressure (to 4.8 GPa) with low CPU times. Author

**N85-30245\*#** United Technologies Research Center, East Hartford, Conn.

## TURBULENT TRANSPORT AND LENGTH SCALE MEASUREMENT EXPERIMENTS WITH CONFINED COAXIAL JETS Interim Report, 1 Sep. 1983 - 16 Aug. 1984

B. V. JOHNSON and R. ROBACK Nov. 1984 74 p refs  
 (Contract NAS3-2271)  
 (NASA-CR-174831; NAS 1.26:174831; UTRC-R84-915540-34)  
 Avail: NTIS HC A04/MF A01 CSCL 20D

A three phase experimental study of mixing downstream of swirling and nonswirling confined coaxial jets was conducted to obtain data for the evaluation and improvement of turbulent transport models currently employed in a variety of computational procedures. The present effort was directed toward the acquisition of length scale and dissipation rate data that provide more accurate inlet boundary conditions for the computational procedures and a data base to evaluate the turbulent transport models in the near jet region where recirculation does not occur, and the acquisition of mass and momentum turbulent transport data for a nonswirling flow condition with a blunt inner jet inlet configuration rather than the tapered inner jet inlet. A measurement technique, generally used to obtain approximate integral length and microscales of turbulence and dissipation rates, was computerized. Results showed the dissipation rate varied by 2 1/2 orders of magnitude across the inlet plane, by 2 orders of magnitude 51 mm from the inlet plane, and by 1 order of magnitude at 102 mm from the inlet plane for a nonswirling flow test conditions. Author

**N85-30246\*#** National Aeronautics and Space Administration. Lewis Research Center, Cleveland, Ohio.

## GENERATION OF CAPILLARY INSTABILITIES BY EXTERNAL DISTURBANCES IN A LIQUID JET Ph.D. Thesis - State Univ. of N.Y.

S. J. LEIB May 1985 77 p refs  
 (NASA-TM-87041; E-2503; NAS 1.15:87041) Avail: NTIS HC A05/MF A01 CSCL 20D

The receptivity problem in a circular liquid jet is considered. A time harmonic axial pressure gradient is imposed on the steady, parallel flow of a jet of liquid emerging from a circular duct. Using a technique developed in plasma physics a casual solution to the forced problem is obtained over certain ranges of Weber number for a number of mean velocity profiles. This solution contains a term which grows exponentially in the downstream direction and can be identified with a capillary instability wave. Hence, it is found that the externally imposed disturbances can indeed trigger instability waves in a liquid jet. The amplitude of the instability wave generated relative to the amplitude of the forcing is computed numerically for a number of cases. Author

## 34 FLUID MECHANICS AND HEAT TRANSFER

**N85-30247\*#** National Aeronautics and Space Administration. Lewis Research Center, Cleveland, Ohio.  
**APPLICATION OF COMPUTATIONAL FLUID DYNAMICS TO COMPLEX INLET DUCTS**

C. E. TOWNE and E. F. SCHUM (Rockwell International Corp., Columbus, Ohio) 1985 15 p refs Presented at the 21st Joint Propulsion Conf., Monterey, Calif., 8-10 Jul. 1985; sponsored in part by AIAA, SAE, ASME, and ASEE (NASA-TM-87060; E-2629; NAS 1.15:87060; AIAA-85-1213)  
Avail: NTIS HC A02/MF A01 CSCL 20D

A three-dimensional parabolic Navier-Stokes code, PEPSIG, was used to analyze the flow in the subsonic diffuser section of a typical modern inlet design. The effect of curvature of the diffuser centerline and transitioning cross sections was studied to determine the primary cause of flow distortion in the duct. Total pressure values at the engine compressor face are reported. M.G.

**N85-31433\*#** National Aeronautics and Space Administration. Lewis Research Center, Cleveland, Ohio.

### TRANSITION IN TURBINES

Washington Jul. 1985 224 p refs Symp. held in Cleveland, 15-16 May 1984  
(NASA-CP-2386; E-2456; NAS 1.55:2386) Avail: NTIS HC A10/MF A01 CSCL 20D

The concept of a large disturbance bypass mechanism for the initiation of transition is reviewed and studied. This mechanism, or some manifestation thereof, is suspected to be at work in the boundary layers present in a turbine flow passage. Discussion is presented on four relevant subtopics: (1) the effect of upstream disturbances and wakes on transition; (2) transition prediction models, code development, and verification; (3) transition and turbulence measurement techniques; and (4) the hydrodynamic condition of low Reynolds number boundary layers.

**N85-31434\*#** National Aeronautics and Space Administration. Lewis Research Center, Cleveland, Ohio.

### COMBUSTOR TURBULENCE

C. J. MAREK *In its* Transition in Turbines p 5-16 Jul. 1985 refs

Avail: NTIS HC A10/MF A01 CSCL 20D

The turbulence entering the turbine is produced in the combustor. High turbulence levels from the combustor can alter the location of the transition point on the turbine vane. The dynamics of turbulence and the progress being made in computing the flow are discussed. Author

**N85-31435\*#** National Aeronautics and Space Administration. Lewis Research Center, Cleveland, Ohio.

### PRELIMINARY RESULTS OF A STUDY OF THE RELATIONSHIP BETWEEN FREE-STREAM TURBULENCE AND STAGNATION REGION HEAT TRANSFER

G. J. VANFOSSSEN, JR. and R. J. SIMONEAU *In its* Transition in Turbines p 17-34 Jul. 1985 refs Previously announced as N85-11317

Avail: NTIS HC A10/MF A01 CSCL 20D

Preliminary results of a study to investigate the relationship between free stream turbulence and heat transfer augmentation in the stagnation region is presented. The effects of free stream turbulence and surface roughness on spanwise averaged heat transfer were investigated. Turbulence was measured upstream of a cylinder placed in the wake of an array of parallel wires that were perpendicular to the cylinder axis. Finally, flow visualization and thermal visualization techniques were combined to show the relationship between vortices in the stagnation region and spanwise variations in heat transfer. Author

**N85-31438\*#** National Aeronautics and Space Administration. Lewis Research Center, Cleveland, Ohio.

### FLAT-PLATE TRANSITION

B. A. ERCEGOVIC *In its* Transition in Turbines p 61-68 Jul. 1985

Avail: NTIS HC A10/MF A01 CSCL 20D

A new research effort was undertaken to build a boundary-layer transition tunnel. This facility only recently became operational. The data obtained so far are merely qualitative. The main goal is to predict heat transfer given any combination of factors such as pressure gradient, turbulence level, Reynolds number, or intermittency factor. The boundary-layer transition tunnel is a closed-loop tunnel that controls the turbulence level, velocity and temperature of the air within it. Problems associated with the operation of this tunnel are examined. B.W.

**N85-31439\*#** Clemson Univ., S.C.

### HEAT TRANSFER AND FLUID MECHANICS MEASUREMENTS IN TRANSITIONAL BOUNDARY LAYER FLOWS

T. WANG, T. W. SIMON (Minnesota Univ., Minneapolis), and J. BUDDHAVARAPU (TSI, Inc., St. Paul, Minn.) *In* NASA. Lewis Research Center Transition in Turbines p 69-79 Jul. 1985 refs

(Contract NAG3-286)

Avail: NTIS HC A10/MF A01 CSCL 20D

Experimental results are presented to document hydrodynamic and thermal development of flat-plate boundary layers undergoing natural transition. Local heat transfer coefficients, skin friction coefficients and profiles of velocity, temperature and Reynolds normal and shear stresses are presented. A case with no transition and transitional cases with 0.68% and 2.0% free-stream disturbance intensities were investigated. The locations of transition are consistent with earlier data. A late-laminar state with significant levels of turbulence is documented. In late-transitional and early-turbulent flows, turbulent Prandtl number and conduction layer thickness values exceed, and the Reynolds analogy factor is less than, values previously measured in fully turbulent flows. Author

**N85-31440\*#** National Aeronautics and Space Administration. Lewis Research Center, Cleveland, Ohio.

### A REVIEW AND ANALYSIS OF BOUNDARY LAYER TRANSITION DATA FOR TURBINE APPLICATION

R. E. GAUGLER *In its* Transition in Turbines p 81-93 Jul. 1985 refs Previously announced as N85-10306

Avail: NTIS HC A10/MF A01 CSCL 20D

A number of data sets from the open literature that include heat transfer data in apparently transitional boundary layers, with particular application to the turbine environment, were reviewed and analyzed to extract transition information. The data were analyzed by using a version of the STAN5 two-dimensional boundary layer code. The transition starting and ending points were determined by adjusting parameters in STAN5 until the calculations matched the data. The results are presented as a table of the deduced transition location and length as functions of the test parameters. The data sets reviewed cover a wide range of flow conditions, from low-speed, flat-plate tests to full-scale turbine airfoils operating at simulated turbine engine conditions. The results indicate that free-stream turbulence and pressure gradient have strong, and opposite, effects on the location of the start of transition and on the length of the transition zone. Author

**N85-31441\*#** National Aeronautics and Space Administration. Lewis Research Center, Cleveland, Ohio.

### TURBULENT SOLUTIONS OF EQUATIONS OF FLUID MOTION

R. G. DEISSLER *In its* Transition in Turbines p 95-160 Jul. 1985 refs Repr. from Rev. of Modern Phys., v. 56, no. 1, pt. 1, Apr. 1984 Previously announced in IAA as A84-41156

Avail: NTIS HC A10/MF A01 CSCL 20D

Some turbulent solutions of the unaveraged Navier-Stokes equations (equations of fluid motion) are reviewed. Those equations are solved numerically in order to study the nonlinear physics of incompressible turbulent flow. The three components of the



mean-square velocity fluctuations are initially equal for the conditions chosen. The resulting solutions show characteristics of turbulence, such as the linear and nonlinear excitation of small-scale fluctuations. For the stronger fluctuations the initially nonrandom flow develops into an apparently random turbulence. The cases considered include turbulence that is statistically homogeneous or inhomogeneous and isotropic or anisotropic. A statistically steady-state turbulence is obtained by using a spatially periodic body force. Various turbulence processes, including the transfer of energy between eddy sizes and between directional components and the production, dissipation, and spatial diffusion of turbulence, are considered. It is concluded that the physical processes occurring in turbulence can be profitably studied numerically. B.W.

**N85-31443\*** National Aeronautics and Space Administration. Lewis Research Center, Cleveland, Ohio.

**REVERBERATION EFFECTS ON DIRECTIONALITY AND RESPONSE OF STATIONARY MONOPOLE AND DIPOLE SOURCES IN A WIND TUNNEL**

K. J. BAUMEISTER 1985 38 p refs To be presented at the Winter Ann. Meeting of the ASME, Miami Beach, Fla., 17-21 Nov. 1985

(NASA-TM-87063; E-2432; NAS 1.15:87063) Avail: NTIS HC A03/MF A01 CSCL 20D

Analytical solutions for the three dimensional inhomogeneous wave equation with flow in a hardwall rectangular wind tunnel and in the free field are presented for a stationary monopole noise source. Dipole noise sources are calculated by combining two monopoles 180 deg out of phase. Numerical calculations for the modal content, spectral response and directivity for both monopole and dipole sources are presented. In addition, the effect of tunnel alterations, such as the addition of a mounting plate, on the tunnels reverberant response are considered. In the frequency range of practical importance for the turboprop response, important features of the free field directivity can be approximated in a hardwall wind tunnel with flow if the major lobe of the noise source is not directed upstream. However, for an omnidirectional source, such as a monopole, the hardwall wind tunnel and free field response are not comparable. Author

**N85-31444\*** National Aeronautics and Space Administration. Lewis Research Center, Cleveland, Ohio.

**HEAT TRANSFER IN AEROPROPULSION SYSTEMS**

R. J. SIMONEAU 1985 37 p refs To be presented at the 1985 US-Japan Heat Transfer Joint Seminar, San Diego, Calif., 17-20 Sep. 1985; sponsored in part by NSF and Japan Society for the Promotion of Science

(NASA-TM-87066; E-2634; NAS 1.15:87066) Avail: NTIS HC A03/MF A01 CSCL 20D

Aeropropulsion heat transfer is reviewed. A research methodology based on a growing synergism between computations and experiments is examined. The aeropropulsion heat transfer arena is identified as high Reynolds number forced convection in a highly disturbed environment subject to strong gradients, body forces, abrupt geometry changes and high three dimensionality - all in an unsteady flow field. Numerous examples based on heat transfer to the aircraft gas turbine blade are presented to illustrate the types of heat transfer problems which are generic to aeropropulsion systems. The research focus of the near future in aeropropulsion heat transfer is projected. E.A.K.

**N85-31445\*** Stanford Univ., Palo Alto, Calif. Dept. of Mechanical Engineering.

**VELOCITY VISUALIZATION IN GASEOUS FLOWS Final Report**

R. K. HANSON Jul. 1985 17 p refs

(Contract NAS3-285)

(NASA-CR-174954; NAS 1.26:174954) Avail: NTIS HC A02/MF A01 CSCL 20D

Techniques are established for visualizing velocity in gaseous flows. Two approaches are considered, both of which are capable of yielding velocity simultaneously at a large number of flowfield locations, thereby providing images of velocity. The first technique

employs a laser to mark specific fluid elements and a camera to track their subsequent motion. Marking is done by laser-induced phosphorescence of biacetyl, added as a tracer species in a flow of N<sub>2</sub>, or by laser-induced formation of sulfur particulates in SF<sub>6</sub>-H<sub>2</sub>-N<sub>2</sub> mixtures. The second technique is based on the Doppler effect, and uses an intensified photodiode array camera and a planar form of laser-induced fluorescence to detect 2-d velocities of I<sub>2</sub> (in I<sub>2</sub>-N<sub>2</sub> mixtures) via Doppler-shifted absorption of narrow-linewidth laser radiation at 514.5 nm. Author

**N85-33433\*** National Aeronautics and Space Administration. Lewis Research Center, Cleveland, Ohio.

**VORTEX GENERATING FLOW PASSAGE DESIGN FOR INCREASED FILM COOLING EFFECTIVENESS Patent**

S. S. PAPELL, inventor (to NASA) 16 Jul. 1985 8 p Filed 15 Feb. 1984 Supersedes N84-20782 (22 - 11, p 1652)

(NASA-CASE-LEW-14039-1; US-PATENT-4,529,358;

US-PATENT-APPL-SN-580419; US-PATENT-CLASS-416-97A;

US-PATENT-CLASS-415-115) Avail: US Patent and Trademark Office CSCL 20D

It is an object of the invention to provide a film cooling apparatus of increased effectiveness and efficiency. In accordance with the invention, a cooling fluid is injected into a hot flowing gas through a passageway in a wall which contains and is subject to the hot gas. The passageway is slanted in a downstream direction at an acute angle to the wall. A cusp shape is provided in the passageway to generate vortices in the injected cooling fluid thereby reducing the energy extracted from the hot gas for that purpose. The cusp shape increases both film cooling effectiveness and wall area coverage. The cusp may be at either the downstream or upstream side of the passageway, the former substantially eliminating flow separation of the cooling fluid from the wall immediately downstream of the passageway.

Official Gazette of the U.S. Patent and Trademark Office

**N85-33435\*** National Aeronautics and Space Administration. Lewis Research Center, Cleveland, Ohio.

**LOCAL HEAT-TRANSFER MEASUREMENTS ON A LARGE, SCALE-MODEL TURBINE BLADE AIRFOIL USING A COMPOSITE OF A HEATER ELEMENT AND LIQUID CRYSTALS**

S. A. HIPPENSTEELE, L. M. RUSSELL, and F. J. TORRES 1985 21 p refs Presented at the 30th Intern. Gas Turbine Conf. and Exhibit, Houston, Tex., 17-21 Mar. 1985; sponsored by ASME

(NASA-TM-86900; E-2347; NAS 1.15:86900) Avail: NTIS HC A02/MF A01 CSCL 20D

Local heat transfer coefficients were experimentally mapped along the midchord of a five-time-size turbine blade airfoil in a static cascade operated at room temperature over a range of Reynolds numbers. The test surface consisted of a composite of commercially available materials: a mylar sheet with a layer of cholesteric liquid crystals, that change color with temperature, and a heater sheet made of a carbon-impregnated paper, that produces uniform heat flux. After the initial selection and calibration of the composite sheet, accurate, quantitative, and continuous heat transfer coefficients were mapped over the airfoil surface. The local heat transfer coefficients are presented for Reynolds numbers from 2.8 x 10 to the 5th power to 7.6 x 10 to the 5th power. Comparisons are made with analytical values of heat transfer coefficients obtained from the STAN5 boundary layer code. Also, a leading edge separation bubble was revealed by thermal and flow visualization. Author



## 34 FLUID MECHANICS AND HEAT TRANSFER

**N85-33453#** Kentucky Univ., Lexington. Inst. for Mining and Minerals Research.

### **SOLIDS MIXING IN A THREE PHASE FLUIDIZED BED CONTAINING SPHERICALLY SHAPED-POROUS SOLID PARTICLES**

G. J. SNELL and D. ZOPFF May 1984 53 p refs Sponsored by Kentucky Energy Cabinet (PB85-187961; IMMR84-098) Avail: NTIS HC A04/MF A01 CSCI 07A

Solids mixing in a 3 phase fluidized bed containing 1.8 mm nominal diameter porous spherically shaped solids was studied using a batch type tracer technique. High speed photography was used to determine concentration time traces of color code solid tracer in a region near the wall of a 2 in. i.d. fluidization tube, located at a vertical elevation about 7 in. above the distributor. An add mixture of water and gaseous nitrogen at room temperature and essentially ambient pressure was used to fluidize a spherically shaped, nickel molybdate on alumina solid phase throughout this study. An empirical steady state mixing time was defined in order to characterize top to bottom of bed solids mixing. This mixing index was in turn correlated with superficial liquid velocity, superficial gas velocity, and an axial characteristic dimension. GRA

## 35

### **INSTRUMENTATION AND PHOTOGRAPHY**

Includes remote sensors; measuring instruments and gages; detectors; cameras and photographic supplies; and holography.

**A85-10034\*** Aerodyne Research, Inc., Billerica, Mass.

### **AN APPROACH FOR AUTOMATED ANALYSIS OF PARTICLE HOLOGRAMS**

A. C. STANTON, H. J. CAULFIELD, and G. W. STEWART (Aerodyne Research, Inc., Billerica, MA) Optical Engineering (ISSN 0091-3286), vol. 23, Sept.-Oct. 1984, p. 577-582. refs (Contract NAS3-24094)

A simple method for analyzing droplet holograms is proposed that is readily adaptable to automation using modern image digitizers and analyzers for determination of the number, location, and size distributions of spherical or nearly spherical droplets. The method determines these parameters by finding the spatial location of best focus of the droplet images. With this location known, the particle size may be determined by direct measurement of image area in the focal plane. Particle velocity and trajectory may be determined by comparison of image locations at different instants in time. The method is tested by analyzing digitized images from a reconstructed in-line hologram, and the results show that the method is more accurate than a time-consuming plane-by-plane search for sharpest focus. C.D.

**A85-10035\*** Aerometrics, Inc., Mountain View, Calif.

### **PHASE/DOPPLER SPRAY ANALYZER FOR SIMULTANEOUS MEASUREMENTS OF DROP SIZE AND VELOCITY DISTRIBUTIONS**

W. D. BACHALO and M. J. HOUSER (Aerometrics, Inc., Mountain View, CA) Optical Engineering (ISSN 0091-3286), vol. 23, Sept.-Oct. 1984, p. 583-590. refs (Contract NAS3-23684)

Research was conducted on a laser light scatter detection method for measuring the size and velocity of spherical particles. The method is based upon the measurement of the interference fringe pattern produced by spheres passing through the intersection of two laser beams. A theoretical analysis of the method was carried out using the geometrical optics theory. The instrument response function was determined to be linear with drop size. Experimental verification of the theory was obtained by using monodisperse droplet streams. Several optical configurations were tested to identify all of the parametric effects upon the size measurements. Both off-axis forward-scatter and back-scatter light

detection were utilized. Simulated spray environments and fuel spray nozzles were used in the evaluation of the method. The measurements of the monodisperse drops showed complete agreement with the theoretical predictions. The method was demonstrated to be independent of the beam intensity and extinction resulting from the surrounding drops. An instrument based on the concept has been developed. Author

**A85-10036\*** Spectron Development Labs., Inc., Costa Mesa, Calif.

### **SPRAY CHARACTERIZATION WITH A NONINTRUSIVE TECHNIQUE USING ABSOLUTE SCATTERED LIGHT**

C. F. HESS and V. E. ESPINOSA (Spectron Development Laboratories, Inc., Costa Mesa, CA) Optical Engineering (ISSN 0091-3286), vol. 23, Sept.-Oct. 1984, p. 604-609. refs (Contract F49620-83-C-0060; NAS3-23538)

A technique to measure the size and velocity of particles is discussed, and results are presented. In this technique two small laser beams of one color identify the center of a laser beam of a different color. This defines a region of almost uniform intensity where the light scattered by the individual particles can be related to their sizes. A variation of this technique that uses two polarizations of the same color of laser beam is also presented. Results are presented for monodisperse, bimodal, trimodal, and polydisperse sprays produced by the Berglund-Liu droplet generator and a pressure nozzle. Size distributions obtained at three different ranges for the same spray show excellent self-consistency in the overlapping regions. Measurements of a spray of known characteristics exhibit errors in the order of 10 percent. Author

**A85-11100\*#** National Aeronautics and Space Administration. Lewis Research Center, Cleveland, Ohio.

### **EDDY CURRENT JET ENGINE DISK-CRACK MONITOR**

J. P. BARRANGER (NASA, Lewis Research Center, Cleveland, OH) Materials Evaluation (ISSN 0025-5327), vol. 42, Oct. 1984, p. 1374-1378.

A disk-crack monitor is described that is suitable for use on the ground or in flight. The system consists of an engine-mounted eddy current sensor, a series capacitance in each leg of the sensor circuit, and a capacitance-conductance bridge followed by an oscilloscope capable of advanced signal processing. It was applied to the detection of service-induced cracks in the first-stage turbine wheel of a helicopter engine. A 3.5 mm long radial fatigue crack plus smaller cracks, all located in the blade root region of the wheel, were detected during engine test stand operation at ground idle speed and temperature. The calculation of the value of series capacitance is also presented. Author

**A85-16794\*** Spectron Development Labs., Inc., Costa Mesa, Calif.

### **NONINTRUSIVE OPTICAL SINGLE-PARTICLE COUNTER FOR MEASURING THE SIZE AND VELOCITY OF DROPLETS IN A SPRAY**

C. F. HESS (Spectron Development Laboratories, Inc., Costa Mesa, CA) Applied Optics (ISSN 0003-6935), vol. 23, Dec. 1, 1984, p. 4375-4382. refs (Contract NAS3-23538; F49620-83-C-0060)

A technique for measuring nonintrusively, and in real time, the size and velocity of droplets in a spray is presented. A small beam identifies the center of a larger beam, thus defining a region of almost uniform intensity, and only droplets crossing through such a center are measured. The size is obtained from the absolute scattered light and the velocity from the modulated signal produced by the interferometric pattern. A self-calibrating algorithm is also discussed. Results are presented for a spray of predictable characteristics. Author

**A85-21695\*** Stanford Univ., Calif.  
**VELOCITY VISUALIZATION IN GAS FLOWS USING LASER-INDUCED PHOSPHORESCENCE OF BIACETYL**  
 B. HILLER, R. A. BOOMAN, C. HASSA, and R. K. HANSON (Stanford University, Stanford, CA) Review of Scientific Instruments (ISSN 0034-6748), vol. 55, Dec. 1984, p. 1964-1967. refs  
 (Contract F49620-83-K-0004; NAG3-285)

Visualization of a two-dimensional velocity field by means of laser-induced phosphorescence is demonstrated in a nitrogen flow at room temperature. A pulsed dye laser is used to excite seeded biacetyl molecules along a line in the flow. Two successive exposures of the emitted phosphorescence are recorded with an intensified 100 x 100 element photodiode array camera. Velocities are determined from the distance traveled in the time interval between exposures. Important factors in connection with the phosphorescence of biacetyl are discussed. Author

**A85-24464\*** National Aeronautics and Space Administration. Lewis Research Center, Cleveland, Ohio.  
**REMOTE DISPLACEMENT MEASUREMENTS USING A LASER DIODE**

G. BEHEIM (NASA, Lewis Research Center, Cleveland, OH) and K. FRITSCH (John Carroll University, Cleveland, OH) Electronics Letters (ISSN 0013-5194), vol. 21, Jan. 31, 1985, p. 93, 94.

A technique for measuring displacements remotely to minimum distances of 8 mm with a resolution of 2 microns is described. A dynamic interferometer method is employed using a frequency-ramped laser diode. A direct measurement of the period of the resulting beat signal is used to determine the displacement. Author

**A85-28820\*#** National Aeronautics and Space Administration. Lewis Research Center, Cleveland, Ohio.

**RAINBOW SCHLIEREN VS MACH-ZEHNDER INTERFEROMETER - A COMPARISON**

W. L. HOWES (NASA, Lewis Research Center, Cleveland, OH) Applied Optics (ISSN 0003-6935), vol. 24, March 15, 1985, p. 816-822. refs

The rainbow schlieren apparatus is simpler, cheaper, and more easily built to large scale than the interferometer. The accuracies of the two instruments are similar but only if refraction is properly accounted for in interferometry. The measurement thresholds of both instruments are similar. The rainbow schlieren device provides more detailed information because the detection threshold of the rainbow schlieren is an order of magnitude better than that of the interferometer. Author

**A85-29562\*** Michigan State Univ., East Lansing.  
**CLOSED-LOOP STRAIN CONTROLLED TESTING AT ELEVATED TEMPERATURES WITH A NON-CONTACTING GAGE**

J. F. MARTIN and B. E. SCHULTZ (Michigan State University, East Lansing, MI) IN: International Instrumentation Symposium, 29th, Albuquerque, NM, May 2-6, 1983, Proceedings. Research Triangle Park, NC, Instrument Society of America, 1983, p. 237-240.  
 (Contract NAG3-51)

Normal strains were measured over a 100 micron gage length at a distance of 50 microns from the edge of a notch using a non-contacting, laser-based interferometric technique. Tests were performed at 600 C under direct strain control from this interferometric 'micro-gage'. A minicomputer system, that produced a voltage analog of strain as a final output, controlled the strain measuring apparatus. This analog output was used directly as the feedback signal to a closed-loop, electrohydraulic mechanical test system. This allowed both strain rate and strain amplitude to be controlled at the notch root of the specimen. Author

**A85-29563\*** United Technologies Research Center, East Hartford, Conn.

**FIBER OPTIC TEMPERATURE SENSOR**

W. W. MOREY, W. H. GLENN, and E. SNITZER (United Technologies Research Center, East Hartford, CT) IN: International Instrumentation Symposium, 29th, Albuquerque, NM, May 2-6, 1983, Proceedings. Research Triangle Park, NC, Instrument Society of America, 1983, p. 261-274.  
 (Contract NAS3-21841; N00163-81-C-0071)

A temperature sensor has been developed that utilizes the temperature dependent absorption of a rare earth doped optical fiber. The temperature measurement is localized at a remote position by splicing a short section of the rare earth fiber into a loop of commercial data communication fiber that sends and returns an optical probe signal to the temperature sensitive section of fiber. The optical probe signal is generated from two different wavelength filtered LED sources. A four port fiber optic coupler combines the two separate wavelength signals into the fiber sensing loop. Time multiplexing is used so that each signal wavelength is present at a different time. A reference signal level measurement is also made from the LED sources and a ratio taken with the sensor signal to produce a transmission measurement of the fiber loop. The transmission is affected differently at each wavelength by the rare earth temperature sensitive fiber. The temperature is determined from a ratio of the two transmission measurements. This method eliminates any ambiguity with respect to changes in signal level in the fiber loop such as mating and unmating optical connectors. The temperature range of the sensor is limited to about 800 C by the temperature limit to the feed fibers. Author

**A85-31113\*** Stanford Univ., Calif.  
**FAST LASER-INDUCED AEROSOL FORMATION FOR VISUALIZATION OF GAS FLOWS**

C. HASSA and R. K. HANSON (Stanford University, Stanford, CA) Review of Scientific Instruments (ISSN 0034-6748), vol. 56, April 1985, p. 557-559. refs  
 (Contract NAG3-285; F49620-83-K-0004)

A technique for aerosol seeding of gas flows by laser-induced particle formation is demonstrated using a pulsed Nd:YAG laser (1.06 microns) for optical breakdown of a mixture of SF<sub>6</sub> and H<sub>2</sub> in an inert carrier gas. It is noted that, contrary to the smoke-wire approach, the laser-induced particles form first in zones of high turbulence, since mixing enhances coagulation. The method also allows seeding to be performed in locations hardly accessible otherwise and is mechanically nonintrusive. Finally, a study of the mixture and the breakdown effects indicates that for H<sub>2</sub>:SF<sub>6</sub> ratios between 3:1 and 15:1 the particle formation is only limited by the physics of the gas/particle conversion. L.T.

**A85-32294\*** Stanford Univ., Calif.  
**TWO-FREQUENCY LASER-INDUCED FLUORESCENCE TECHNIQUE FOR RAPID VELOCITY-FIELD MEASUREMENTS IN GAS FLOWS**

B. HILLER and R. K. HANSON (Stanford University, Stanford, CA) Optics Letters (ISSN 0146-9592), vol. 10, May 1985, p. 206-208. refs  
 (Contract NAG3-285; F49620-83-K-0004)

A technique is presented for measurements of two-dimensional velocity fields in gas flows. The single-mode frequency of an argon-ion laser is fixed in the wing of an absorption line of iodine molecules that are seeded at low level in the flow of interest. The emitted fluorescence is detected with an image-intensified 100 x 100 photodiode-array camera. two pairs of counterpropagating laser sheets sequentially probe the flow to determine two velocity components. The frequency in one pair is shifted with respect to the other by an acousto-optic modulator. This two-frequency scheme eliminates the need to determine the slope of the line externally and offers the potential for combined pressure and velocity-field measurements. Author

## 35 INSTRUMENTATION AND PHOTOGRAPHY

**A85-36726\*** National Aeronautics and Space Administration. Lewis Research Center, Cleveland, Ohio.  
**ELECTRONIC HETERODYNE READOUT OF FRINGES IN MOIRE DEFLECTOMETRY**

J. STRICKER (NASA, Lewis Research Center, Cleveland, OH; Technion Israel Institute of Technology, Haifa, Israel) *Optics Letters* (ISSN 0146-9592), vol. 10, June 1985, p. 247-249. refs

An electronic heterodyne technique is described for the readout of fringes in moire deflectometry. The technique is based on phase measurements of signals generated by a photodetector observing the light transmitted through a traveling moire fringe pattern. The phase of the signal is proportional to the fringe deviation and thus to the deflection angle of the light ray. The phase is measured on line by a standard phase meter with an accuracy of 1 deg or 1:360 of a fringe. The technique, which is precise and sensitive, is demonstrated by detecting and measuring a fringe shift of 0.15 mm corresponding to 0.029 of a fringe. Author

**A85-37704\*#** National Aeronautics and Space Administration. Lewis Research Center, Cleveland, Ohio.

### THE INFINITE LINE PRESSURE PROBE

D. R. ENGLUND (NASA, Lewis Research Center, Cleveland, OH) and W. B. RICHARDS (Oberlin College, Oberlin, OH) (*Instrument Society of America, International Instrumentation Symposium*, 30th, Denver, CO, May 7-10, 1984) *ISA Transactions* (ISSN 0019-0578), vol. 24, no. 2, 1985, p. 11-19. Previously announced in STAR as N84-19787. refs

The infinite line pressure probe provides a means for measuring high frequency fluctuating pressures in difficult environments. A properly designed infinite line probe does not resonate; thus its frequency response is not limited by acoustic resonance in the probe tubing, as in conventional probes. The characteristics of infinite line pressure probes are reviewed and some applications in turbine engine research are described. A probe with a flat-oval cross section, permitting a constant-impedance pressure transducer installation, is described. Techniques for predicting the frequency response of probes with both circular and flat-oval cross sections are also cited. Author

**A85-39796\*#** National Aeronautics and Space Administration. Lewis Research Center, Cleveland, Ohio.

### TRANSIENT TECHNIQUE FOR MEASURING HEAT TRANSFER COEFFICIENTS ON STATOR AIRFOILS IN A JET ENGINE ENVIRONMENT

H. J. GLADDEN and M. P. PROCTOR (NASA, Lewis Research Center, Cleveland, OH) *AIAA, SAE, ASME, and ASEE, Joint Propulsion Conference*, 21st, Monterey, CA, July 8-10, 1985. 12 p. Previously announced in STAR as N85-25794. refs (AIAA PAPER 85-1471)

A transient technique was used to measure heat transfer coefficients on stator airfoils in a high-temperature annular cascade at real engine conditions. The transient response of thin film thermocouples on the airfoil surface to step changes in the gas stream temperature was used to determine these coefficients. In addition, garden gages and paired thermocouples were also utilized to measure heat flux on the airfoil pressure surface at steady state conditions. The tests were conducted at exit gas stream Reynolds numbers of one-half to 1.9 million based on true chord. The results from the transient technique show good comparison with the steady-state results in both trend and magnitude. In addition, comparison is made with the STAN5 boundary layer code and shows good comparison with the trends. However, the magnitude of the experimental data is consistently higher than the analysis. Author

**A85-39835\*#** Cleveland State Univ., Ohio.

### INCIDENT BEAM POLARIZATION FOR LASER DOPPLER VELOCIMETRY EMPLOYING A SAPPHIRE CYLINDRICAL WINDOW

J. A. LOCK (Cleveland State University, Cleveland, OH) and H. J. SCHOCK (NASA, Lewis Research Center, Cleveland, OH) *Applied Optics* (ISSN 0003-6935), vol. 24, July 1, 1985, p. 1987-1995. refs

For laser Doppler velocimetry studies employing sapphire windows as optical access ports, the birefringency of sapphire produces an extra beam intersection volume which serves to effectively smear the acquired velocity flow field data. It is shown that for a cylindrical window geometry, the extra beam intersection volume may be eliminated with minimal decrease in the fringe visibility of the remaining intersection volume by suitably orienting the polarizations of the initial laser beams. For horizontally incident beams, these polarizations were measured at three intersection locations within the cylinder. It was found that the measured polarization angles agreed with the theoretical predictions. Author

**A85-41634\*** National Aeronautics and Space Administration. Lewis Research Center, Cleveland, Ohio.

### CALIBRATION STABILITY OF SOME HOT-CATHODE ION GAUGES

I. WARSHAWSKY (NASA, Lewis Research Center, Cleveland, OH) *Journal of Vacuum Science and Technology A* (ISSN 0734-2101), vol. 3, Mar.-Apr. 1985, p. 430-432. refs

Data are presented on the stability of calibration of some hot-cathode ion gauges: a conventional triode used in the range of 0.0002-0.2 Pa, and Bayard-Alpert-type gauges used in the range of 0.0002-0.02 Pa. Numerical magnitudes are given of the systematic corrections that must be applied to the gauge indication in order to achieve the highest accuracy of pressure indication. The relative sensitivities of these gauges to Ar, N<sub>2</sub>, Ne, and He are also given. Author

**A85-42854\*#** National Aeronautics and Space Administration. Lewis Research Center, Cleveland, Ohio.

### MOIRE DEFLECTOMETRY WITH DEFERRED ELECTRONIC HETERODYNE READOUT

J. STRICKER (NASA, Lewis Research Center, Cleveland, OH) *Applied Optics* (ISSN 0003-6935), vol. 24, Aug. 1, 1985, p. 2298, 2299. refs

The electronic heterodyne technique is applied to the task of deferred readout of phase objects' moire fringes. In combination with the heterodyne readout technique, moire deflectometry constitutes a powerful tool for the study of phase objects, exhibiting high sensitivity, ease of automation and recording, low cost, use of incoherent illumination, and independence from fringe contrast variations. O.C.

**A85-42857\*#** National Aeronautics and Space Administration. Lewis Research Center, Cleveland, Ohio.

### REMOTE DISPLACEMENT MEASUREMENT USING A PASSIVE INTERFEROMETER WITH A FIBER-OPTIC LINK

G. BEHEIM (NASA, Lewis Research Center, Cleveland, OH) *Applied Optics* (ISSN 0003-6935), vol. 24, Aug. 1, 1985, p. 2335-2340. refs

Remote displacement measurement is demonstrated using a Fabry-Perot cavity with a multimode optical fiber link. The sensing cavity modulates, as a function of its length, the spectrum of a light-emitting diode (LED). The light returns via the fiber and is analyzed by a tunable reference cavity. A closed-loop control causes the reference cavity to track the sensing cavity length within 2 x 10 to the -12th m. Displacement range is 2 x 10 to the -6th m. The reference cavity length is measured interferometrically, using a laser, to obtain the sensing cavity length. Advantages of this sensing technique include compatibility with multimode fiber-optic components, high immunity to optical losses, and large dynamic range. Author

**A85-46607\*** Babcock and Wilcox Co., Alliance, Ohio.  
**HIGH-TEMPERATURE FIBER OPTIC PRESSURE SENSOR**  
 J. W. BERTHOLD (Babcock and Wilcox Co., Research and Development Div., Alliance, OH) IN: International Instrumentation Symposium, 30th, Denver, CO, May 7-10, 1984, Proceedings . Research Triangle Park, NC, ISA, 1984, p. 85-94. refs (Contract NAS3-23712)

Attention is given to a program to develop fiber optic methods to measure diaphragm deflection. The end application is intended for pressure transducers capable of operating to 540 C. In this paper are reported the results of a laboratory study to characterize the performance of the fiber-optic microbend sensor. The data presented include sensitivity and spring constant. The advantages and limitations of the microbend sensor for static pressure measurement applications are described. A proposed design is presented for a 540 C pressure transducer using the fiber optic microbend sensor. Author

**A85-46925\*** Yale Univ., New Haven, Conn.  
**POLARIZATION (ELLIPTIC) MEASUREMENTS OF LIQUID CONDENSATE DEPOSITION AND EVAPORATION RATES AND DEW POINTS IN FLOWING SALT/ASH-CONTAINING COMBUSTION GASES**  
 K. SESHADRI and D. E. ROSNER (Yale University, New Haven, CT) Combustion and Flame (ISSN 0010-2180), vol. 61, Sept. 1985, p. 251-260. refs (Contract NSG-3169; AF-AFOSR-84-0034)

An application of an optical polarization technique in a combustion environment is demonstrated by following, in real-time, growth rates of boric oxide condensate on heated platinum ribbons exposed to seeded propane-air combustion gases. The results obtained agree with the results of earlier interference measurements and also with theoretical chemical vapor deposition predictions. In comparison with the interference method, the polarization technique places less stringent requirements on surface quality, which may justify the added optical components needed for such measurements. V.L.

**A85-48659\*** Minnesota Univ., Minneapolis.  
**HOLOGRAPHIC OPTICAL SYSTEM FOR ABERRATION CORRECTIONS IN LASER DOPPLER VELOCIMETRY**  
 R. C. KIM, S. K. CASE (Minnesota, University, Minneapolis), and H. J. SCHOCK (NASA, Lewis Research Center, Cleveland, OH) Optical Engineering (ISSN 0091-3286), vol. 24, Sept.-Oct. 1985, p. 786-790. refs

An optical system containing multifaceted holographic optical elements (HOEs) has been developed to correct for aberrations introduced by nonflat windows in laser Doppler velocimetry. The multifacet aberration correction approach makes it possible to record on one plate many sets of adjacent HOEs that address different measurement volume locations. By using 5-mm-diameter facets, it is practical to place 10-20 sets of holograms on one 10 x 12.5-cm plate, so that the procedure of moving the entire optical system to examine different locations may not be necessary. The holograms are recorded in dichromated gelatin and therefore are nonabsorptive and suitable for use with high-power argon laser beams. Low f-number optics coupled with a 90-percent efficient distortion-correcting hologram in the collection side of the system yield high optical efficiency. V.L.

**N85-16096\*#** National Aeronautics and Space Administration. Lewis Research Center, Cleveland, Ohio.  
**HIGH TEMPERATURE THERMOCOUPLE AND HEAT FLUX GAUGE USING A UNIQUE THIN FILM-HARDWARE HOT JUNCTION**  
 C. H. LIEBERT, R. HOLANDA, S. A. HIPPENSTEELE, and C. A. ANDRACCHIO Dec. 1984 29 p refs Proposed for presentation at 30th Intern. Gas Turbine Conf. and Exhibition, Houston, Tex., 17-21 Mar. 1985; sponsored by ASME (NASA-TM-86898; E-2365; NAS 1.15:86898) Avail: NTIS HC A03/MF A01 CSCL 14B

A special thin film-hardware material thermocouple (TC) and heat flux gauge concept for a reasonably high temperature and

high flux flat plate heat transfer experiment was fabricated and tested to gauge temperatures of 911 K. This concept was developed for minimal disturbance of boundary layer temperature and flow over the plates and minimal disturbance of heat flux through the plates. Comparison of special heat flux gauge Stanton number output at steady-state conditions with benchmark literature data was good and agreement was within a calculated uncertainty of the measurement system. Also, good agreement of special TC and standard TC outputs was obtained and the results are encouraging. Oxidation of thin film thermoelements was a primary failure mode after about 5 of operation. Author

**N85-16099\*#** National Aeronautics and Space Administration. Lewis Research Center, Cleveland, Ohio.  
**EFFECT OF FIVE LUBRICANTS ON LIFE OF AISI 9310 SPUR GEARS**  
 D. P. TOWNSEND and E. V. ZARETSKY Jan. 1985 15 p refs (NASA-TP-2419; E-2183; NAS 1.60:2419) Avail: NTIS HC A02/MF A01 CSCL 13I

Spur-gear surface fatigue tests were conducted with five lubricants using a single lot of consumable-electrode vacuum melted (CVM) AISI 9310 spur gears. The lot of gears was divided into five groups, each of which was tested with a different lubricant. The test lubricants are classified as either a synthetic hydrocarbon, mineral oil, or ester-based lubricant. All five lubricants have similar viscosity and pressure-viscosity coefficients. A pentaerythritol base stock without sufficient antiwear additives produced a surface fatigue life approximately 22 percent that of the same base stock with chlorine and phosphorus type additives. The presence of sulfur type antiwear additives in the lubricant did not appear to affect the surface fatigue life of the gears tested. No statistical difference in the 10-percent surface fatigue life was produced with four of the five lubricants. Author

**N85-16100\*#** National Aeronautics and Space Administration. Lewis Research Center, Cleveland, Ohio.  
**INTEGRATED EXHAUST GAS ANALYSIS SYSTEM FOR AIRCRAFT TURBINE ENGINE COMPONENT TESTING**  
 R. L. SUMMERS and R. C. ANDERSON Jan. 1985 28 p refs (NASA-TP-2424; E-2302; NAS 1.60:2424) Avail: NTIS HC A03/MF A01 CSCL 14B

An integrated exhaust gas analysis system was designed and installed in the hot-section facility at the Lewis Research Center. The system is designed to operate either manually or automatically and also to be operated from a remote station. The system measures oxygen, water vapor, total hydrocarbons, carbon monoxide, carbon dioxide, and oxides of nitrogen. Two microprocessors control the system and the analyzers, collect data and process them into engineering units, and present the data to the facility computers and the system operator. Within the design of this system there are innovative concepts and procedures that are of general interest and application to other gas analysis tasks. Author

**N85-21604\*#** Spectron Development Labs., Inc., Costa Mesa, Calif.  
**RESEARCH STUDY OF DROPLET SIZING TECHNOLOGY LEADING TO THE DEVELOPMENT OF AN ADVANCED DROPLET SIZING SYSTEM Final Report**  
 C. F. HESS, A. E. SMART, and V. E. ESPINOSA Jan. 1985 88 p refs (Contract NAS3-23538) (NASA-CR-174839; NAS 1.26:174839) Avail: NTIS HC A05/MF A01 CSCL 14B

An instrument to measure the size and velocity of droplets was developed. The instrument uses one of two techniques, as appropriate. In the first technique two small laser beams of one color identify the center of a larger laser beam of a different color. This defines a region of almost uniform intensity where the light scattered by the individual droplets can be related to their size. The first technique uses the visibility of a Doppler burst and validates it against the peak intensity of the signal's pedestal.

## 35 INSTRUMENTATION AND PHOTOGRAPHY

Results are presented for monodisperse, bimodal, trimodal, and polydisperse sprays produced by the Berglund-Liu droplet generator and a pressure nozzle. Size distributions of a given spray obtained using three different size ranges show excellent self-consistency in the overlapping region. Measurements of sprays of known characteristics exhibit errors in the order of 10%. The principles of operation and design criteria of the instrument are discussed in great detail. Author

**N85-21605\*#** National Aeronautics and Space Administration. Lewis Research Center, Cleveland, Ohio.

### EVALUATION RESULTS OF THE 700 DEG C CHINESE STRAIN GAUGES

H. F. HOBART 1985 11 p refs Presented at the High Temperature Measurements for Experimental Mechanics Conf., Knoxville, Tenn., 27-28 Mar. 1985 (NASA-TM-86973; E-2502; NAS 1.15:86973) Avail: NTIS HC A02/MF A01 CSCL 14B

Gauges fabricated from specially developed Fe-Cr-Al-V-Ti-Y alloy wire in the Republic of China were evaluated for use in static strain measurement of hot gas turbine engines. Gauge factor variation with temperature, apparent strain, and drift were included. Results of gauge factor versus temperature tests show gauge factor decreasing with increasing temperature. The average slope is  $-3.1/2$  percent/100 K, with an uncertainty band of  $\pm$  or  $-8$  percent. Values of room temperature gauge factor for the Chinese and Kanthal A-1 gauges averaged 2.73 and 2.12, respectively. The room temperature gauge factor of the Chinese gauges was specified to be 2.62. The apparent strain data for both the Chinese alloy and Kanthal A-1 showed large cycle to cycle nonrepeatability. All apparent strain curves had a similar S-shape, first going negative and then rising to positive value with increasing temperatures. The mean curve for the Chinese gauges between room temperature and 100 K had a total apparent strain of 1500 microstrain. The equivalent value for Kanthal A-1 was about 9000 microstrain. Drift tests at 950 K for 50 hr show an average drift rate of about  $-9$  microstrain/hr. Short-term (1 hr) rates are higher, averaging about  $-40$  microstrain for the first hour. In the temperature range 700 to 870 K, however, short-term drift rates can be as high as 1700 microstrain for the first hour. Therefore, static strain measurements in this temperature range should be avoided. A.R.H.

**N85-21607#** National Bureau of Standards, Gaithersburg, Md.

### ADVANCED THIN FILM THERMOCOUPLES

K. G. KREIDER, S. SEMANCIK, and C. OLSON Oct. 1984 85 p refs

(Contract NASA ORDER C-54715-D)

(NASA-CR-175541; NAS 1.26:175541; PB85-132322;

NBSIR-84-2949) Avail: NTIS HC A05/MF A01 CSCL 14B

The fabrication, materials characterization, and performance of thin film platinum rhodium thermocouples on gas turbine alloys was investigated. The materials chosen for the study were the turbine blade alloy systems MAR M200+Hf with NiCoCrAlY and FeCrAlY coatings, and vane alloy systems MAR M509 with FeCrAlY. Research was focussed on making improvements in the problem areas of coating substrate stability, adhesion, and insulation reliability and durability. Diffusion profiles between the substrate and coating with and without barrier coatings of  $Al_2O_3$  are reported. The relationships between fabrication parameters of thermal oxidation and sputtering of the insulator and its characterization and performance are described. The best thin film thermocouples were fabricated with the NiCoCrAlY coatings which were thermally oxidized and sputter coated with  $Al_2O_3$ . GRA

**N85-25792\*#** General Electric Co., Schenectady, N. Y. Corporate Research and Development.

### ADVANCED SMOKE METER DEVELOPMENT SURVEY AND ANALYSIS Final Report

R. W. PITZ, C. M. PENNEY, C. M. STANFORTH, and W. M. SHAFFERNOCKER Nov. 1984 59 p refs

(Contract NAS3-23532)

(NASA-CR-168287; NAS 1.26:168287) Avail: NTIS HC A04/MF

A01 CSCL 14B

Ideal smoke meter characteristics are determined to provide a basis for evaluation of candidate systems. Five promising techniques are analyzed in detail to evaluate compliance with the practical smoke meter requirements. Four of the smoke measurement concepts are optical methods: Modulated Transmission (MODTRAN), Cross Beam Absorption Counter (CBAC), Laser Induced Incandescence (LIN), and Photoacoustic Spectroscopy (PAS). A rapid response filter instrument called a Taper Element Oscillating Microbalance (TEOM) is also evaluated. For each technique, the theoretical principles are described, the expected performance is determined, and the advantages and disadvantages are discussed. The expected performance is evaluated against each of the smoke meter specifications, and the key questions for further study are given. The most promising smoke meter technique analyzed was MODTRAN, which is a variation on a direct transmission measurement. The soot-laden gas is passed through a transmission cell, and the gas pressure is modulated by a speaker. B.W.

**N85-25794\*#** National Aeronautics and Space Administration. Lewis Research Center, Cleveland, Ohio.

### TRANSIENT TECHNIQUE FOR MEASURING HEAT TRANSFER COEFFICIENTS ON STATOR AIRFOILS IN A JET ENGINE ENVIRONMENT

H. J. GLADDEN and M. P. PROCTOR 1985 17 p refs Proposed for presentation at the 21st Joint Propulsion Conf., Monterey, Calif., 8-10 Jul. 1985; sponsored by AIAA, SAE and ASME

(NASA-TM-87005; E-2501; NAS 1.15:87005) Avail: NTIS HC

A02/MF A01 CSCL 14B

A transient technique was used to measure heat transfer coefficients on stator airfoils in a high-temperature annular cascade at real engine conditions. The transient response of thin film thermocouples on the airfoil surface to step changes in the gas stream temperature was used to determine these coefficients. In addition, gardon gages and paired thermocouples were also utilized to measure heat flux on the airfoil pressure surface at steady state conditions. The tests were conducted at exit gas stream Reynolds numbers of one-half to 1.9 million based on true chord. The results from the transient technique show good comparison with the steady-state results in both trend and magnitude. In addition, comparison is made with the STAN5 boundary layer code and shows good comparison with the trends. However, the magnitude of the experimental data is consistently higher than the analysis. Author

**N85-26903\*#** National Aeronautics and Space Administration. Lewis Research Center, Cleveland, Ohio.

### INSTRUMENTATION TECHNOLOGY OVERVIEW Abstract Only

W. C. NIEBERDING In NASA. Marshall Space Flight Center Advan. High Pressure O2/H2 Technol. p 599-602 Apr. 1985

Avail: NTIS HC A99/MF E03; SOD HC CSCL 14B

The Instrumentation Technology program advances the state of the art of instrumentation associated with the SSME to improve service life and performance by providing increased measurement capability. Two broad categories of instrumentation technology are sought. The first category includes sensors and systems destined to be used in and on the operational engine either during operation or between operations. These measurements supply information necessary for engine control and/or diagnostics throughout the life of the engine. The second category includes measurement systems and techniques whose application will be to engine component test stands and possibly to the test bed engine. The measurements provide the detailed information necessary to verify

computer models of the performance of the various engine subsystems. E.A.K.

**N85-30288\*** National Aeronautics and Space Administration. Lewis Research Center, Cleveland, Ohio.

**FILTER INDUCED ERRORS IN LASER ANEMOMETER MEASUREMENTS USING COUNTER PROCESSORS**

L. G. OBERLE and R. G. SEASHOLTZ 1985 15 p refs To be presented at the Intern. Laser Anemometry Symp., ASME Winter Ann. Meeting, Miami, Fla., 17-21 Nov. 1985 (NASA-TM-87047; E-2609; NAS 1.15:87047) Avail: NTIS HC A02/MF A01 CSCL 14B

Simulations of laser Doppler anemometer (LDA) systems have focused primarily on noise studies or biasing errors. Another possible source of error is the choice of filter types and filter cutoff frequencies. Before it is applied to the counter portion of the signal processor, a Doppler burst is filtered to remove the pedestal and to reduce noise in the frequency bands outside the region in which the signal occurs. Filtering, however, introduces errors into the measurement of the frequency of the input signal which leads to inaccurate results. Errors caused by signal filtering in an LDA counter-processor data acquisition system are evaluated and filters for a specific application which will reduce these errors are chosen. E.A.K.

**N85-32302\*** National Aeronautics and Space Administration. Lewis Research Center, Cleveland, Ohio.

**A COMPARISON OF ELECTRONIC HETERODYNE MOIRE DEFLECTOMETRY AND ELECTRONIC HETERODYNE HOLOGRAPHIC INTERFEROMETRY FOR FLOW MEASUREMENTS**

A. J. DECKER and J. STRICKER (Technion - Israel Inst. of Tech.) 1985 19 p refs Proposed for presentation at the Aerospace Technol. Conf. and Exposition, Long Beach, Calif., 14-17 Oct. 1985; sponsored by Society of Automotive Engineers (NASA-TM-87071; E-2643; NAS 1.15:87071) Avail: NTIS HC A02/MF A01 CSCL 14B

Electronic heterodyne moire deflectometry and electronic heterodyne holographic interferometry are compared as methods for the accurate measurement of refractive index and density change distributions of phase objects. Experimental results are presented to show that the two methods have comparable accuracy for measuring the first derivative of the interferometric fringe shift. The phase object for the measurements is a large crystal of KD\*P, whose refractive index distribution can be changed accurately and repeatably for the comparison. Although the refractive index change causes only about one interferometric fringe shift over the entire crystal, the derivative shows considerable detail for the comparison. As electronic phase measurement methods, both methods are very accurate and are intrinsically compatible with computer controlled readout and data processing. Heterodyne moire is relatively inexpensive and has high variable sensitivity. Heterodyne holographic interferometry is better developed, and can be used with poor quality optical access to the experiment. Author

**N85-33454\*** Department of Energy, Washington, D. C. **APPARATUS AND METHOD FOR IDENTIFICATION OF MATRIX MATERIALS IN WHICH TRANSURANIC ELEMENTS ARE EMBEDDED USING THERMAL NEUTRON CAPTURE GAMMA-RAY EMISSION Patent Application**

D. A. CLOSE (Los Alamos Scientific Lab.), L. A. FRANKS (Los Alamos Scientific Lab.), and S. M. KOCIMSKI, inventor (to DOE) (Los Alamos Scientific Lab.) 16 Aug. 1984 26 p (Contract W-7405-ENG-36) (DE85-011659) Avail: NTIS HC A03/MF A01

An invention is described that enables the quantitative simultaneous identification of the matrix materials in which fertile and fissile nuclides are embedded to be made along with the quantitative assay of the fertile and fissile materials. The invention also enables corrections for any absorption of neutrons by the matrix materials and by the measurement apparatus by the measurement of the prompt and delayed neutron flux emerging from a sample after the sample is interrogated by simultaneously

applied neutrons and gamma radiation. High energy electrons are directed at a first target to produce gamma radiation. A second target receives the resulting pulsed gamma radiation and produces neutrons from the interaction with the gamma radiation. These neutrons are slowed by a moderator surrounding the sample and bathe the sample uniformly, generating second gamma radiation in the interaction. The gamma radiation is then resolved and quantitatively detected, providing a spectroscopic signature of the constituent elements contained in the matrix and in the materials within the vicinity of the sample. DOE

**N85-33456\*** Honeywell, Inc., Lexington, Mass. Aerospace and Defense Group.

**MOSAIC INFRARED SENSOR FOR SPACE ASTRONOMY (MIRSSA) Interim Technical Report**

Dec. 1983 39 p refs (Contract NASW-3688) (NASA-CR-176154; NAS 1.26:176154; H-8407-07) Avail: NTIS HC A03/MF A01 CSCL 14B

The development of mosaic infrared detector/focal plane arrays for space astronomy is reported. The Mosaic IR Sensor for Space Astronomy (MIRSSA) Program is an effort to develop PV HgCdTe detector arrays with the spectral response of up to 5 micron and silicon CCDs for low temperature applications. Desired background-limited performance (BLIP) for space applications requires an extremely high-R sub A product which can be achieved by selecting the detector materials and the operating temperature. The parameters were determined by measurement of HgCdTe PV detector arrays at various temperatures in the SW and MW spectral bands. It is demonstrated that high performance PV HgCdTe detectors can be fabricated for low temperature applications. E.A.K.

**N85-33457\*** Army Armament Research and Development Command, Dover, N. J. Product Assurance Directorate.

**AUTOMATIC SPHERICITY INTERFEROMETER FOR TESTING LENS RADII**

J. SALERNO Jun. 1985 24 p (AD-A155736; AD-E401352; ARPAD-TR-85001) Avail: NTIS HC A02/MF A01 CSCL 20F

The majority of lens radii measurements are made with test plates. This technique has the disadvantage of bringing the lens into direct contact with the test plate which can cause scratching of the surface and subsequent rejection of the test unit. In addition, test plate measurements are subjective because they depend on the experience and skill of the operator. As an alternative, an automated interferometric technique was evaluated for its ability to measure lens radii. This method uses a fizeau interferometer with the following accessories: transmission sphere, lens mount, and digital radius slide. This technique, chosen for its ease of operation and noncontact approach, proved to be a more suitable approach to radius measurement than the use of test plates, because it eliminated both the subjectivity and contact associated with the test plates. GRA

**N85-35389\*** Illinois Univ., Urbana. Dept. of Astronautics and Astronautical Engineering.

**THE USE OF A LASER DOPPLER VELOCIMETER IN A STANDARD FLAMMABILITY TUBE Final Report, Jan. 1981 - May 1982**

R. A. STREHLOW and E. M. FLYNN May 1985 101 p refs (Contract NAS3-2266C) (NASA-CR-174960; NAS 1.26:174960; TR-AAE-85-4; UILU-ENG-85-0504) Avail: NTIS HC A06/MF A01 CSCL 14B

The use of the Laser Doppler Velocimeter, (LDV), to measure the flow associated with the passage of a flame through a standard flammability limit tube (SFLT) was studied. Four major results are presented: (1) it is shown that by using standard ray tracing calculations, the displacement of the LDV volume and the fringe rotation within the experimental error of measurement can be predicted; (2) the flow velocity vector field associated with passage of an upward propagating flame in an SFLT is determined; (3) it is determined that the use of a light interruption technique to

## 35 INSTRUMENTATION AND PHOTOGRAPHY

track particles is not feasible; and (4) it is shown that a 25 mW laser is adequate for LDV measurements in the Shuttle or Spacelab. E.A.K.

**N85-35391\*** Pratt and Whitney Aircraft, East Hartford, Conn. Engineering Div.

### **DEVELOPMENT OF ADVANCED HIGH-TEMPERATURE HEAT FLUX SENSORS. PHASE 2: VERIFICATION TESTING Final Report**

W. H. ATKINSON, M. A. CYR, and R. R. STRANGE Aug. 1985 69 p refs

(Contract NAS3-22133)

(NASA-CR-174973; NAS 1.26:174973; PWA-5914-39) Avail:

NTIS HC A04/MF A01 CSCL 14B

A two-phase program is conducted to develop heat flux sensors capable of making heat flux measurements throughout the hot section of gas turbine engines. In Phase 1, three types of heat flux sensors are selected; embedded thermocouple, laminated, and Gardon gauge sensors. A demonstration of the ability of these sensors to operate in an actual engine environment is reported. A segmented liner of each of two combustors being used in the Broad Specification Fuels Combustor program is instrumented with the three types of heat flux sensors then tested in a high pressure combustor rig. Radiometer probes are also used to measure the radiant heat loads to more fully characterize the combustor environment. Test results show the heat flux sensors to be in good agreement with radiometer probes and the predicted data trends. In general, heat flux sensors have strong potential for use in combustor development programs. Author

## 36

### **LASERS AND MASERS**

Includes parametric amplifiers.

**N85-12341\*** General Electric Co., Schenectady, N. Y. Corporate Research and Development.

### **LASER BALANCING SYSTEM FOR HIGH MATERIAL REMOVAL RATES Final Report**

M. G. JONES, G. GEORGALAS, and A. L. ORTIZ Oct. 1984 28 p refs

(Contract NAS3-22814)

(NASA-CR-174731; NAS 1.26:174731; REPT-84-SRD-042) Avail: NTIS HC A03/MF A01 CSCL 20E

A laser technique to remove material in excess of 10 mg/sec from a spinning rotor is described. This material removal rate is 20 times greater than previously reported for a surface speed of 30 m/sec. Material removal enhancement was achieved by steering a focused laser beam with moving optics to increase the time of laser energy interaction with a particular location on the circumferential surface of a spinning rotor. A neodymium:yttrium aluminum garnet (Nd:YAG) pulse laser was used in this work to evaluate material removal for carbon steel, 347 stainless steel, Inconel 718, and titanium 6-4. This technique is applicable to dynamic laser balancing. Author

## 37

### **MECHANICAL ENGINEERING**

Includes auxiliary systems (non-power); machine elements and processes; and mechanical equipment.

**A85-11069\*** National Aeronautics and Space Administration. Lewis Research Center, Cleveland, Ohio.

### **ELASTOHYDRODYNAMIC LUBRICATION OF LINE CONTACTS**

B. J. HAMROCK (NASA, Lewis Research Center, Cleveland, OH) and B. O. JACOBSON (Lulea, Hogskola, Lulea, Sweden) ASLE Transactions, vol. 27, Oct. 1984, p. 275-286; Discussion, p. 286, 287; Author's Closure, p. 287. Previously announced in STAR as N83-16759. refs

An isothermal elastohydrodynamically lubricated rectangular contact was evaluated numerically. This required the simultaneous solution of the elasticity and Reynolds equations. In the elasticity analysis the contact zone was divided into equal rectangular areas, and it was assumed that a uniform pressure was applied over each area. The elastohydrodynamic lubrication theory thus developed was used to investigate the influence of the dimensionless speed, load, and materials parameters on minimum film thickness. Ten cases were used in obtaining the minimum film thickness formula. Plots are shown that indicate the details of the pressure distribution, film shape, and flow. The characteristic pressure spike is clearly in evidence as is the parallel film shape through the central portion of the contact, with a minimum film thickness occurring near the outlet of the contact. S.L.

**A85-11074\*** Akron Univ., Ohio.

### **AN ANALYSIS OF TEMPERATURE EFFECT IN A FINITE JOURNAL BEARING WITH SPATIAL TILT AND VISCOUS DISSIPATION**

M. J. BRAUN (Akron, University, Akron, OH), R. L. MULLEN (Case Western Reserve University, Cleveland, OH), and R. C. HENDRICKS (NASA, Lewis Research Center, Cleveland, OH) ASLE Transactions, vol. 27, Oct. 1984, p. 405-412; Discussion, p. 412; Authors' Closure, p. 412. refs

The analysis presented herein deals with the evaluation of the pressure, velocity, and temperature profiles in a finite-length plane journal bearing. The geometry of the case under study consists of a spatially tilted shaft. The two-dimensional Reynolds equation accounts for the variation of the clearance gap  $h$  with  $x$  and  $z$  and is used to model the pressure field. The latter is solved for a variety of shaft tilt angles and then used to calculate the two-dimensional flow field. Finally, the flow field is used in the energy equation to solve for the film temperature profile, when the effect of viscous dissipation is taken into account. Author

**A85-15972\*** Garrett Turbine Engine Co., Phoenix, Ariz.

### **CERAMIC COMPONENT DEVELOPMENT FOR THE AGT101 GAS TURBINE ENGINE**

W. D. CARRUTHERS and J. R. SMITH (Garrett Turbine Engine Co., Phoenix, AZ) (University of Michigan, American Ceramic Society, General Motors Corp., et al., Automotive Materials Conference, 12th, Ann Arbor, MI, Mar. 14, 15, 1984) Ceramic Engineering and Science Proceedings (ISSN 0196-6219), vol. 5, May-June 1984, p. 350-368. (Contract DEN3-167)

Under DOE/NASA sponsorship, a team is developing the AGT101, a highly efficient gas turbine engine for automotive application. The regenerated engine will operate at a maximum of 1370 C (2500 F) and 100,000 rpm, and will utilize a variety of Si<sub>3</sub>N<sub>4</sub>, SiC, lithium aluminum silicate and ceramic fiber insulation components. Engine design has been performed to consider the fabrication and material characteristics of these ceramic materials for both the static and rotating hot section components. Component fabrication has been performed, components have been screened in thermal and mechanical tests, and initial engine testing has been performed. Author



**A85-15973\*** General Motors Corp., Indianapolis, Ind.  
**CERAMIC COMPONENTS FOR GAS TURBINE ENGINES**

P. W. HEITMAN (General Motors Corp., Allison Gas Turbine Div., Indianapolis, IN) (University of Michigan, American Ceramic Society, General Motors Corp., et al., Automotive Materials Conference, 12th, Ann Arbor, MI, Mar. 14, 15, 1984) Ceramic Engineering and Science Proceedings (ISSN 0196-6219), vol. 5, May-June 1984, p. 369-378. Research supported by the U.S. Department of Energy.  
 (Contract DEN3-168)

The ceramic component design, manufacturing and inspection technologies under development for the AGT 100 automotive gas turbine promise to meet marketplace cost and performance criteria. Especially consequential developments are noted toward this goal in the case of net and near-net shape component fabrication. Integral turbine rotors, scrolls, combustors, support structures and heat exchangers have been successfully produced and evaluated. Consistency of material properties have yet to be achieved for the processing methods in question, however. O.C.

**A85-19085\*** National Aeronautics and Space Administration.  
 Lewis Research Center, Cleveland, Ohio.

**FRICTIONAL AND MORPHOLOGICAL PROPERTIES OF AU-MOS2 FILMS SPUTTERED FROM A COMPACT TARGET**

T. SPALVINS (NASA, Lewis Research Center, Cleveland, OH) Thin Solid Films (ISSN 0040-6090), vol. 118, 1984, p. 375-384. Previously announced in STAR as N84-20858. refs

Au-MoS<sub>2</sub> films 0.02 to 1.2 microns thick were sputtered from target compacted from 5 wt percent Au + 95 wt percent MoS<sub>2</sub>, to investigate the frictional and morphological film growth characteristics. The gold dispersion effects in MoS<sub>2</sub> films are of interest to increase the densification and strengthening of the film structure. Three microstructural growth stages were identified on the nano-micro-macrostructural level. During sliding both sputtered Au-MoS<sub>2</sub> and MoS<sub>2</sub> films have a tendency to break within the columnar region. The remaining or effective film, about 0.2 microns thick, performs the lubrication. The Au-MoS<sub>2</sub> films displayed a lower friction coefficient with a high degree of frictional stability and less wear debris generation as compared to pure MoS<sub>2</sub> films. The more favorable frictional characteristics of the Au-MoS<sub>2</sub> films are attributed to the effective film thickness and the high density packed columnar zone which has a reduced effect on the fragmentation of the tapered crystallites during fracture. M.G.

**A85-21280\*#** National Aeronautics and Space Administration.  
 Lewis Research Center, Cleveland, Ohio.

**HYDRODYNAMIC LUBRICATION OF RIGID NONCONFORMAL CONTACTS IN COMBINED ROLLING AND NORMAL MOTION**

M. K. GHOSH (NASA, Lewis Research Center, Cleveland, OH; Banaras Hindu University, Varanasi, India), B. J. HAMROCK (NASA, Lewis Research Center, Cleveland, OH), and D. BREWE (U.S. Army, Propulsion Laboratory, Cleveland, OH) ASME, Transactions, Journal of Tribology (ISSN 0742-4787), vol. 107, Jan. 1985, p. 97-103. Previously announced in STAR as N84-17592. refs

(ASME PAPER 84-TRIB-13)

A numerical solution to the problem of hydrodynamic lubrication of rigid point contacts with an isoviscous, incompressible lubricant was obtained. The hydrodynamic load-carrying capacity under unsteady (or dynamic) conditions arising from the combined effects of squeeze motion superposed upon the entraining motion was determined for both normal approach and separation. Superposed normal motion considerably increases net load-carrying capacity during normal approach and substantially reduces net load-carrying capacity during separation. Geometry was also found to have a significant influence on the dynamic load-carrying capacity. The ratio of dynamic to steady state load-carrying capacity increases with increasing geometry parameter for normal approach and decreases during separation. The cavitation (film rupture) boundary is also influenced significantly by the normal motion, moving downstream during approach and upstream during separation. For sufficiently high normal separation velocity the rupture boundary may even move upstream of the minimum-film-thickness position.

Sixty-three cases were used to derive a functional relationship for the ratio of the dynamic to steady state load-carrying capacity in terms of the dimensionless normal velocity parameter (incorporating normal velocity, entraining velocity, and film thickness) and the geometry parameter. M.G.

**A85-21289\*#** National Aeronautics and Space Administration.  
 Lewis Research Center, Cleveland, Ohio.

**FAST NUMERICAL CALCULATIONS OF EHD SLIDING TRACTION FORCES APPLICATION TO ROLLING BEARINGS**

L. HOUPERT (NASA, Lewis Research Center, Cleveland, OH; SKF Nederland, Nieuwegein, Netherlands) American Society of Mechanical Engineers and American Society of Lubrication Engineers, Joint Lubrication Conference, San Diego, CA, Oct. 22-24, 1984. 6 p. refs  
 (ASME PAPER 84-TRIB-26)

Based on analytical calculations assuming isothermal elastohydrodynamic (EHD) lubrication conditions, and on curve-fitting of a thermal correction factor, a new formula is proposed to calculate the sliding traction force developed in a concentrated contact, assuming a nonlinear, viscoelastic lubricant and unidirectional sliding. When sliding occurs in the rolling and transverse directions (bidimensional sliding), a simplified numerical method is outlined by which the components of the local shear stress are quickly calculated. The latter method is applied to the calculation of the shear stress and temperature distribution in the ball-raceway contacts of an angular-contact ball bearing. Because of the viscoelastic behavior of the lubricant, a nonzero lateral traction force is obtained. Author

**A85-22281\*** Washington Univ., Seattle.

**METALLURGICAL AND MECHANICAL PHENOMENA DUE TO RUBBING OF TITANIUM AGAINST SINTERED POWDER NICHROME**

R. ZENAS, T. ARCHBOLD, J. WOLAK, A. F. EMERY, and S. ETEMAD (Washington, University, Seattle, WA) ASLE Transactions, vol. 28, Jan. 1985, p. 97-103. refs  
 (Contract NAG3-7)

Metallurgical and mechanical changes occurring during high-speed rubbing of Ti-6Al-4V blade specimens against an abrasible Nichrome aircraft engine seal material were studied using optical microscopy, electron microscopy, and microhardness techniques. Evidence of temperatures above the beta transus of Ti-6Al-4V (1000 C) and of thermal hardening was found on blade tips that exhibited undesirable abrading characteristics resulting in high forces of interaction, high temperatures, and smearing. The material within the layer of the corresponding seals was found to be work-hardened to a depth of about 0.1 mm and showed evidence of densification extending to a depth of about 0.5 mm below the rubbed surface. Wear particles produced by rub interactions that generated cleanly abraded seal surfaces were found to be several times larger than those produced during interactions which showed evidence of surface smearing and seal densification. Author

**A85-23838\*** Dartmouth Coll., Hanover, N.H.

**THERMAL AND THERMOMECHANICAL EFFECTS IN DRY SLIDING**

F. E. KENNEDY, JR. (Dartmouth College, Hanover, NH) Wear (ISSN 0043-1648), vol. 100, Dec. 1984, p. 453-476. refs  
 (Contract NSG-3253; N00014-81-K-0090)

Developments in the study of interrelated thermal and mechanical phenomena in sliding systems are reviewed. The topics reviewed include mechanisms of frictional heating and the distribution of heat during sliding friction, the experimental measurement and analysis of surface and near-surface temperatures resulting from frictional heating, thermal deformation around sliding contacts and the changes in contact geometry caused by thermal deformation and thermoelastic instability, and the thermomechanical stress distribution around the frictionally heated and thermally deformed contact spots. The influence of the thermal and thermomechanical contact phenomena on friction and wear, surface melting, softening, chemical deterioration, and thermocracking are discussed. The phenomena have important

## 37 MECHANICAL ENGINEERING

implications in the design and application of sliding or sliding-rolling mechanical components such as dynamic seals, brakes, clutches, plastic bearings, solid or boundary-lubricated bearings, and gears.  
M.D.

**A85-24497\*#** California State Univ., Long Beach.  
**INTO MESH LUBRICATION OF SPUR GEARS WITH ARBITRARY OFFSET OIL JET. I - FOR JET VELOCITY LESS THAN OR EQUAL TO GEAR VELOCITY**

L. S. AKIN (California State University, Long Beach, CA) and D. P. TOWNSEND (NASA, Lewis Research Center, Cleveland, OH) ASME, Transactions, Journal of Mechanisms, Transmission, and Automation in Design, vol. 105, Dec. 1983, p. 713-718. refs

An analysis was conducted for into mesh oil jet lubrication with an arbitrary offset and inclination angle from the pitch point for the case where the oil jet velocity is equal to or less than pitch line velocity. The analysis includes the case for the oil jet offset from the pitch point in the direction of the pinion and where the oil jet is inclined to intersect the common pitch point. Equations were developed for the minimum oil jet velocity required to impinge on the pinion or gear and the optimum oil jet velocity to obtain the maximum impingement depth.  
Author

**A85-31202\*** National Aeronautics and Space Administration.  
Lewis Research Center, Cleveland, Ohio.

**THERMAL ELASTOHYDRODYNAMIC LUBRICATION OF LINE CONTACTS**

M. K. GHOSH (NASA, Lewis Research Center, Cleveland, OH; Banaras Hindu University, Varanasi, India) and B. J. HAMROCK (NASA, Lewis Research Center, Cleveland, OH) ASLE Transactions, vol. 28, April 1985, p. 159-169; Discussion, p. 169, 170; Authors' Closure, p. 170, 171. Previously announced in STAR as N83-34326. refs

A numerical solution to the problem of thermal elastohydrodynamic lubrication of line contacts was obtained by using a finite difference formulation. The solution procedure consists of simultaneous solution of the thermal Reynolds equation, the elasticity equation, and the energy equation subject to appropriate boundary conditions. Pressure distribution, film shape, and temperature distribution were obtained for fully flooded conjunctions, a paraffinic lubricant, and various dimensionless speed parameters while the dimensionless load and materials parameters were held constant. Reduction in the minimum film thickness due to thermal effects (as a ratio of thermal to isothermal minimum film thickness) is given by a simple formula as a function of the thermal loading parameter  $Q$ :  $H(\min)/H(\min, I) = 10/10 + Q(0.4)$ . Plots of pressure distribution, film shape, temperature distribution, and flow are shown for some representative cases.

M.G.

**A85-31203\*** National Aeronautics and Space Administration.  
Lewis Research Center, Cleveland, Ohio.

**FIRST-ORDER BALL-BEARING KINEMATICS**

E. KINGSBURY (NASA, Lewis Research Center, Cleveland, OH; Charles Stark Draper Laboratory, Inc., Cambridge, MA) ASLE Transactions, vol. 28, April 1985, p. 239-243; Discussion, p. 243; Author's Closure, p. 243, 244. refs

Two first-order equations are given connecting geometry and internal motions in an angular-contact ball bearing. Total speed, kinematic equivalence, basic speed ratio, and modal speed ratio are defined and discussed; charts are given for the speed ratios covering all bearings and all rotational modes. Instances where specific first-order assumptions might fail are discussed, and the resulting effects on bearing performance reviewed.  
Author

**A85-32960\*#** National Aeronautics and Space Administration.  
Lewis Research Center, Cleveland, Ohio.

**DUAL CLEARANCE SQUEEZE FILM DAMPER FOR HIGH LOAD CONDITIONS**

D. P. FLEMING (NASA, Lewis Research Center, Cleveland, OH) ASME, Transactions, Journal of Tribology (ISSN 0742-4787), vol. 107, April 1985, p. 274-278; Discussion, p. 278; Author's Closure, p. 278, 279. Previously announced in STAR as N84-25064. refs (ASME PAPER 84-TRIB-7)

Squeeze film dampers are widely used to control vibrations in aircraft turbine engines and other rotating machinery. However, if shaft unbalance rises appreciably above the design value (e.g., due to a turbine blade loss), a conventional squeeze film becomes overloaded, and is no longer effective in controlling vibration amplitudes and bearing forces. A damper concept characterized by two oil films is described. Under normal conditions, only one low-clearance film is active, allowing precise location of the shaft centerline. Under high unbalance conditions, both films are active, controlling shaft vibration in a near-optimum manner, and allowing continued operation until a safe shutdown can be made. Author

**A85-33779\*#** Cincinnati Univ., Ohio.

**A COMPUTER AIDED DESIGN PROCEDURE FOR GENERATING GEAR TEETH**

S. H. CHANG, R. L. HUSTON (Cincinnati, University, Cincinnati, OH), and J. J. COY (U.S. Army, Propulsion Laboratory, Cleveland, OH) American Society of Mechanical Engineers, Design Engineering Technical Conference, Cambridge, MA, Oct. 7-10, 1984. 5 p.

(Contract NSG-3188)

(ASME PAPER 84-DET-184)

A procedure for computer aided design (CAD) of gear teeth is presented. It is developed for generated teeth fabricated by a hob cutter or a shaper. It provides a means for analytically and numerically determining the tooth profile, given the cutter profile. An illustrative example with involute tooth profiles is given. Application with non-standard profiles and with bevel, spiral bevel, and hypoid gears is discussed.  
Author

**A85-33780\*#** Cincinnati Univ., Ohio.

**DYNAMIC ANALYSIS OF STRAIGHT AND INVOLUTE TOOTH FORMS**

H. H. LIN, R. L. HUSTON (Cincinnati, University, Cincinnati, OH), and J. J. COY (U.S. Army, Propulsion Laboratory, Cleveland, OH) American Society of Mechanical Engineers, Design Engineering Technical Conference, Cambridge, MA, Oct. 7-10, 1984. 10 p. refs

(Contract NSG-3188)

(ASME PAPER 84-DET-226)

The effect of load speed on straight and involute tooth forms is studied using several finite-element models. It is found that for rapidly rotating gears and sprockets, the load speed along the tooth surface can significantly affect the tooth vibration. Indeed, it is found that for sufficiently high load speeds and for sufficiently slender tooth forms, the tooth deflection can, at times, be directed opposite to the load direction. Comparisons are made of various dynamic models of gear and sprocket teeth. It is shown that for stubby tooth forms there is considerable difference between results obtained with finite element models and results obtained with Timoshenko beam models. Finally, it is shown that gear or sprocket vibrations can be induced by the shape of the tooth form itself. This effect becomes increasingly significant at higher speeds.

Author

**A85-33781\*#** Cleveland State Univ., Ohio.

**GEAR MESH STIFFNESS AND LOAD SHARING IN PLANETARY GEARING**

R. KASUBA (Cleveland State University, Cleveland, OH) and R. AUGUST (Sverdrup Technology, Inc., Tullahoma, TN) American Society of Mechanical Engineers, Design Engineering Technical Conference, Cambridge, MA, Oct. 7-10, 1984. 6 p. refs (Contract NAG3-186) (ASME PAPER 84-DET-229)

An interactive computerized analysis was developed for determining load sharing among planetary gears. The load sharing is established as a function of transmitted torque, degree of sun gear fixity, component flexibility, gear tooth quality, and phasing of individual planet gears. A nonlinear variable gear tooth mesh stiffness model was used to simulate the sun/planet and planet/ring gear meshes. The determined load sharing and gear mesh stiffness parameters then can be used for the subsequent assessment of dynamic load factors. Author

**A85-35049\*#** California State Univ., Long Beach.

**LUBRICANT JET FLOW PHENOMENA IN SPUR AND HELICAL GEARS WITH MODIFIED CENTER DISTANCES AND/OR ADDENDUMS - FOR OUT-OF-MESH CONDITIONS**

L. S. AKIN (California State University, Long Beach, CA) and D. P. TOWNSEND (NASA, Lewis Research Center, Cleveland, OH) ASME, Transactions, Journal of Mechanisms, Transmission, and Automation in Design, vol. 107, March 1985, p. 24-30. Previously announced in STAR as N84-29224. refs (ASME PAPER 84-DET-96)

Out-of-mesh jet lubrication of gears was examined. The pinion impingement cycle was described briefly. An analysis was developed for the lubricant jet flow in the out-of-mesh condition. The analysis provides for the inclusion of modified center distances and modified addendum. Equations were generated for the limit values of variables necessary to remove the severe limitations to facilitate computer analysis. A computer program was designed using these limit formulas to prevent negative impingement (missing) on the pinion. Author

**A85-39938\*** Creare, Inc., Hanover, N.H.

**AN EXPERIMENTAL INVESTIGATION OF RUBBING INTERACTION IN LABYRINTH SEALS AT CRYOGENIC TEMPERATURE**

F. X. DOLAN (Creare, Inc., Hanover, NH), F. E. KENNEDY, and E. M. SCHULSON (Dartmouth College, Hanover, NH) (U.S. Navy, Workshop on Thermomechanical Effects in Sliding Systems, 3rd, Hanover, NH, June 18-20, 1984) Wear (ISSN 0043-1648), vol. 102, March 1985, p. 51-66. refs (Contract NAS3-23276)

An experimental program was carried out to address issues related to the observed cracking of the titanium knife edges on the labyrinth seals of the high pressure fuel pump (HPFP) in the Space Shuttle main engine (SSME). Thermal shock experiments were carried out using a jet specimen with geometry similar to the knife edge geometry. These tests demonstrate that cracking of the titanium alloy is possible in a situation involving repeated thermal cycles over a wide temperature range, as might be realized during a rub in the liquid hydrogen fuel pump. High speed rub interaction tests were conducted using a representative knife edge and seal geometry over a broad range of interaction rates. Alternative materials were also experimentally evaluated. These tests provide information which can be used to design improved labyrinth seals for the HPFP of the SSME. In particular, plasma-sprayed aluminum-graphite was found to be significantly better than aluminum alloy seals used at present from the standpoint of rub performance. Ion nitriding of the titanium alloy knife edges was also found to improve rub performance compared with the untreated baseline knife edge material. Author

**A85-42573\*#** Texas A&M Univ., College Station.

**ROTORDYNAMIC COEFFICIENTS FOR COMPRESSIBLE FLOW IN TAPERED ANNULAR SEALS**

C. C. NELSON (Texas A&M University, College Station) ASME, Transactions, Journal of Tribology (ISSN 0742-4787), vol. 107, July 1985, p. 318-325. refs (Contract NAG3-181)

Derivation of the governing equations for compressible flow in a tapered annular seal is based on Hirs' turbulent bulk-flow model. Zeroth and first-order perturbation equations are developed by an expansion in the eccentricity ratio. These equations are numerically integrated to obtain the leakage, and the direct and cross-coupled stiffness and damping coefficients. Seal parameters similar to the Space Shuttle Main Engine High Pressure Oxidizer Turbopump are used to demonstrate output from the analysis procedure. The effects of preswirl and seal taper are shown for three different length-to-diameter ratios. Generally the results indicate that prerotating the fluid significantly increases the cross-coupled stiffness but has little effect on the other coefficients, and increasing the convergent taper increases the direct stiffness while decreasing the direct damping and cross-coupled stiffness. Author

**A85-45466\*** National Aeronautics and Space Administration, Lewis Research Center, Cleveland, Ohio.

**INITIAL RESULTS OF SENSITIVITY TESTS - PERFORMED ON THE RE-1000 FREE-PISTON STIRLING ENGINE**

J. G. SCHREIBER (NASA, Lewis Research Center, Cleveland, OH) IN: IECEC '84: Advanced energy systems - Their role in our future; Proceedings of the Nineteenth Intersociety Energy Conversion Engineering Conference, San Francisco, CA, August 19-24, 1984. Volume 3. La Grange Park, IL, American Nuclear Society, 1984, p. 1878-1885.

Tests have been performed over several years to investigate the dynamics of a free-piston Stirling engine for the purpose of computer code validation. Tests on the 1 kW (1.33 hp) single cylinder engine have involved the determination of the sensitivity of the engine performance to variations in working space pressure, heater and cooler temperatures, regenerator porosity, power piston mass, and displacer dynamics. Maps of engine performance have been recorded with the use of an 81.2 percent porosity regenerator. Both a high-efficiency displacer and a high-power displacer were tested; efficiencies up to 33 percent were recorded, and power output of approximately 1500 W was obtained. Preliminary results of the sensitivity tests are presented, and descriptions of future tests are given. B.J.

**A85-45473\*** Mechanical Technology, Inc., Latham, N. Y.

**MOD II ENGINE AND TECHNOLOGY DEVELOPMENT**

W. D. ERNST (Mechanical Technology, Inc., Latham, NY) IN: IECEC '84: Advanced energy systems - Their role in our future; Proceedings of the Nineteenth Intersociety Energy Conversion Engineering Conference, San Francisco, CA, August 19-24, 1984. Volume 3. La Grange Park, IL, American Nuclear Society, 1984, p. 1935-1941. DOE-supported research. (Contract DEN3-32)

The second-generation automotive Stirling engine, known as the Mod II, will be used to accomplish the Automotive Stirling Engine (ASE) Program objectives. Preliminary design has advanced to the point of procuring long-lead components to evaluate manufacturability. The heater head castings of the Hot Engine System (working gas cycle) are being procured, while the V-block casting of the Cold Engine/Drive system is being sectioned for evaluation. The technology required for these designs, and their impact on Mod II performance, have progressed to the design substantiation stage, and successful accomplishment of the program objectives is expected. Author

## 37 MECHANICAL ENGINEERING

**A85-45474\*** Mechanical Technology, Inc., Latham, N. Y.

### **AUTOMOTIVE STIRLING ENGINE SYSTEMS DEVELOPMENT**

A. E. RICHEY (Mechanical Technology, Inc., Latham, NY) IN: IECEC '84: Advanced energy systems - Their role in our future; Proceedings of the Nineteenth Intersociety Energy Conversion Engineering Conference, San Francisco, CA, August 19-24, 1984. Volume 3. La Grange Park, IL, American Nuclear Society, 1984, p. 1942-1948. DOE-supported research. (Contract DEN3-32)

The objective of the Automotive Stirling Engine (ASE) program is to develop a Stirling engine for automotive use that provides a 30 percent improvement in fuel economy relative to a comparable internal-combustion engine while meeting emissions goals. This paper traces the engine systems' development efforts focusing on: (1) a summary of engine system performance for all Mod I engines; (2) the development, program conducted for the upgraded Mod I; and (3) vehicle systems work conducted to enhance vehicle fuel economy. Problems encountered during the upgraded Mod I test program are discussed. The importance of the EPA driving cycle cold-start penalty and the measures taken to minimize that penalty with the Mod II are also addressed. Author

**A85-45479\*** National Aeronautics and Space Administration. Lewis Research Center, Cleveland, Ohio.

### **OVERVIEW OF NASA LEWIS RESEARCH CENTER FREE-PISTON STIRLING ENGINE ACTIVITIES**

J. G. SLABY (NASA, Lewis Research Center, Cleveland, OH) IN: IECEC '84: Advanced energy systems - Their role in our future; Proceedings of the Nineteenth Intersociety Energy Conversion Engineering Conference, San Francisco, CA, August 19-24, 1984. Volume 3. La Grange Park, IL, American Nuclear Society, 1984, p. 1994-2008. Previously announced in STAR as N84-22512. refs

A generic free-piston Stirling technology project is being conducted to develop technologies generic to both space power and terrestrial heat pump applications in a cooperative, cost-shared effort. The generic technology effort includes extensive parametric testing of a 1 kW free-piston Stirling engine (RE-1000), development of a free-piston Stirling performance computer code, design and fabrication under contract of a hydraulic output modification for RE-1000 engine tests, and a 1000-hour endurance test, under contract, of a 3 kWe free-piston Stirling/alternator engine. A newly initiated space power technology feasibility demonstration effort addresses the capability of scaling a free-piston Stirling/alternator system to about 25 kWe; developing thermodynamic cycle efficiency or equal to 70 percent of Carnot at temperature ratios in the order of 1.5 to 2.0; achieving a power conversion unit specific weight of 6 kg/kWe; operating with noncontacting gas bearings; and dynamically balancing the system. Planned engine and component design and test efforts are described. A.R.H.

**A85-45488\*** National Aeronautics and Space Administration. Lewis Research Center, Cleveland, Ohio.

### **COMPARISON OF FREE-PISTON STIRLING ENGINE MODEL PREDICTIONS WITH RE1000 ENGINE TEST DATA**

R. C. TEW (NASA, Lewis Research Center, Cleveland, OH) IN: IECEC '84: Advanced energy systems - Their role in our future; Proceedings of the Nineteenth Intersociety Energy Conversion Engineering Conference, San Francisco, CA, August 19-24, 1984. Volume 3. La Grange Park, IL, American Nuclear Society, 1984, p. 2073-2085. Previously announced in STAR as N84-24509. refs

Predictions of a free-piston Stirling engine model are compared with RE1000 engine test data taken at NASA-Lewis Research Center. The model validation and the engine testing are being done under a joint interagency agreement between the Department of Energy's Oak Ridge National Laboratory and NASA-Lewis. A kinematic code developed at Lewis was upgraded to permit simulation of free-piston engine performance; it was further upgraded and modified at Lewis and is currently being validated. The model predicts engine performance by numerical integration of equations for each control volume in the working space. Piston motions are determined by numerical integration of the force

balance on each piston or can be specified as Fourier series. In addition, the model Fourier analyzes the various piston forces to permit the construction of phasor force diagrams. The paper compares predicted and experimental values of power and efficiency and shows phasor force diagrams for the RE1000 engine displacer and piston. Further development plans for the model are also discussed. Author

**N85-13233\*#** National Aeronautics and Space Administration. Lewis Research Center, Cleveland, Ohio.

### **EFFECT OF TWO INNER-RING OIL-FLOW DISTRIBUTION SCHEMES ON THE OPERATING CHARACTERISTICS OF A 35 MILLIMETER BORE BALL BEARING TO 2.5 MILLION DN**

F. T. SCHULLER, S. I. PINEL (Industrial Tectonics, Inc., Rancho Dominguez, Calif.), and H. R. SIGNER (Industrial Tectonics, Inc., Rancho Dominguez, Calif.) Jan. 1985 14 p refs (Contract NAS3-19779)

(NASA-TP-2404; E-2127; NAS 1.60:2404) Avail: NTIS HC A02/MF A01 CSCL 131

Parametric tests were conducted with a 35-mm-bore, split-inner-ring ball bearing with a double-inner-land-guided cage. Provisions were made for through-the-inner-ring lubrication. Test conditions were either a thrust load of 667 N (150 lb) or a combined load of 667 N (150 lb) thrust and 222 N (50 lb) radial, shaft speeds from 32000 to 72000 rpm, and an oil-inlet temperature of 394 K (250 deg F). Outer ring cooling was used in some tests. Tests were run with either 50 or 75 percent of the total oil flow distributed to the inner-ring raceway. Successful operation was experienced with both 50% and 75% flow patterns to 2.5 million DN. Cooling the outer ring had little effect on inner-ring temperature; however, the outer-ring temperature decreased as much as 7% at 2.5 million DN. Maximum recorded power loss was 3.1 kW (4.2 hp), and maximum cage slip was 8.7 percent. Both occurred at a shaft speed of 72000 rpm, a lubricant flow rate of 1900 cu/min (0.50 gal/min), a combined load, and no outer-ring cooling. Author

**N85-13234\*#** National Aeronautics and Space Administration. Lewis Research Center, Cleveland, Ohio.

### **EFFECT OF LUBRICANT EXTREME-PRESSURE ADDITIVES ON SURFACE FATIGUE LIFE OF AISI 9310 SPUR GEARS**

H. W. SCIBBE, D. P. TOWNSEND, and P. R. ARON Dec. 1984 14 p refs

(NASA-TP-2408; E-2042; NAS 1.60:2408) Avail: NTIS HC A02/MF A01 CSCL 131

Surface fatigue tests were conducted with AISI 9310 spur gears using a formulated synthetic tetraester oil (conforming to MIL-L-23699 specifications) as the lubricant containing either sulfur or phosphorus as the EP additive. Four groups of gears were tested. One group of gears tested without an additive in the lubricant acted as the reference oil. In the other three groups either a 0.1 wt % sulfur or phosphorus additive was added to the tetraester oil to enhance gear surface fatigue life. Test conditions included a gear temperature of 334 K (160 F), a maximum Hertz stress of 1.71 GPa (248 000 psi), and a speed of 10,000 rpm. The gears tested with a 0.1 wt % phosphorus additive showed pitting fatigue life 2.6 times the life of gears tested with the reference tetraester based oil. Although fatigue lives of two groups of gears tested with the sulfur additive in the oil showed improvement over the control group gear life, the results, unlike those obtained with the phosphorus oil, were not considered to be statistically significant. R.J.F.

**N85-13235\*#** Cummins Engine Co., Inc., Columbus, Ind.

### **ADVANCED AUTOMOTIVE DIESEL ASSESSMENT PROGRAM Final Report**

R. SEKAR and L. TOZZI Dec. 1983 354 p refs (Contract DEN3-261)

(NASA-CR-168285; DOE/NASA/0261-1; NAS 1.26:168285; CTR-0747-84003) Avail: NTIS HC A16/MF A01 CSCL 131

Cummins Engine Company completed an analytical study to identify an advanced automotive (light duty) diesel (AAD) power plant for a 3,000-pound passenger car. The study resulted in the

definition of a revolutionary diesel engine with several novel features. A 3,000-pound car with this engine is predicted to give 96.3, 72.2, and 78.8 MPG in highway, city, and combined highway-city driving, respectively. This compares with current diesel powered cars yielding 41.7, 35.0, and 37.7 MPG. The time for 0-60 MPH acceleration is 13.9 sec. compared to the baseline of 15.2 sec. Four technology areas were identified as crucial in bringing this concept to fruition. They are: (1) part-load preheating, (2) positive displacement compounding, (3) spark assisted diesel combustion system, and (4) piston development for adiabatic, oilless diesel engine. Marketing and planning studies indicate that an aggressive program with significant commitment could result in a production car in 10 years from the date of commencement.

**N85-14116\*#** National Aeronautics and Space Administration. Lewis Research Center, Cleveland, Ohio.

**ROTORDYNAMIC INSTABILITY PROBLEMS IN HIGH-PERFORMANCE TURBOMACHINERY**

Washington Dec. 1984 507 p refs Workshop held in College Station, Tex., 28-30 May 1984; sponsored by Texas A&M Univ., Army Research Office, and the Air Force Aeropropulsion Lab.

(NASA-CP-2338; E-2214; NAS 1.55:2338) Avail: NTIS HC A22/MF A01 CSCL 131

Rotordynamics and predictions on the stability of characteristics of high performance turbomachinery were discussed. Resolutions of problems on experimental validation of the forces that influence rotordynamics were emphasized. The programs to predict or measure forces and force coefficients in high-performance turbomachinery are illustrated. Data to design new machines with enhanced stability characteristics or upgrading existing machines are presented.

**N85-14122\*#** National Aeronautics and Space Administration. Lewis Research Center, Cleveland, Ohio.

**INTERNAL HYSTERESIS EXPERIENCED ON A HIGH PRESSURE SYN GAS COMPRESSOR**

F. Y. ZEIDAN (Qatar Fertiliser Co., Umm Said) *In its* Rotordynamic Instability Problems in High-Performance Turbomachinery p 97-108 Dec. 1984 refs

Avail: NTIS HC A22/MF A01 CSCL 131

A vibration instability phenomenon experienced in operating high pressure syn gas centrifugal compressors in two ammonia plants is described. The compressors were monitored by orbit and spectrum analysis for changes from baseline readings. It is found that internal hysteresis was the major destabilizing force; however, the problem was further complicated by seal lockup at the suction end of the compressor. A coupling lockup problem and a coupling fit problem, which fretting of the shaft, are also considered as contributors to the self excited vibrations. E.A.K.

**N85-15168\*#** National Aeronautics and Space Administration. Lewis Research Center, Cleveland, Ohio.

**NITRIDING OF TITANIUM AND ITS ALLOYS BY N<sub>2</sub>, NH<sub>3</sub> OR MIXTURES OF N<sub>2</sub> + H<sub>2</sub> IN A DC ARC PLASMA AT LOW PRESSURES (OR = TO TORR)**

R. AVNI Nov. 1984 23 p refs

(NASA-TM-83803; E-2254; NAS 1.15:83803) Avail: NTIS HC A02/MF A01 CSCL 11F

The dc glow discharges in different gas mixtures of Ar + N<sub>2</sub>, Ar + NH<sub>3</sub> or Ar + N<sub>2</sub> + H<sub>2</sub> result in the surface nitriding of Ti metal and its alloy (Ti6Al4V). Various gas mixtures were used in order to establish the main active species governing the nitriding process, i.e., N, N<sub>2</sub>, NH, or NH<sub>2</sub> as excited or ionized particles. The dc discharge was sampled and analyzed by quadrupole mass spectrometry (QPM) and optical emission spectroscopy (OES), and the nitrided samples were analyzed by scanning electron microscopy (SEM) with an EDAX attachment, microhardness, and Fourier transform infrared reflectance spectrometry (FTIR). It was found that the excited and ionized nitrogen and hydrogen atoms are the main species responsible for the nitriding process in a dc glow discharge. Author

**N85-20368\*#** National Aeronautics and Space Administration. Lewis Research Center, Cleveland, Ohio.

**REPORT OF THE CONSTELLATIONS PANEL**

D. J. BENTS, G. VONTIESENHAUSEN (NASA. Marshall Space Flight Center), C. A. LUNDQUIST (Alabama Univ., Huntsville), P. SWAN (California Univ., Los Angeles), H. L. MAYER (Aerospace Corp.), M. J. MANGANO (JPL, California Inst. of Tech., Pasadena), S. BERGAMASUI (Padua Univ.), F. BEVILACQUA (Aeritalia), F. WILLIAMS (Martin Marietta, New Orleans), G. RUM (CNR, Italy) et al. *In* NASA. Marshall Space Flight Center Appl. of Tethers in Space, Vol. 2 16 p Mar. 1985

Avail: NTIS HC A14/MF A01 CSCL 131

The purpose of a constellation is to provide a mode of distributing space systems in a method that could be advantageous and not eliminating the consolidation/aggregation advantages. The applicability of stabilization concepts to various orbital conditions was defined. B.G.

**N85-20377\*#** National Aeronautics and Space Administration. Lewis Research Center, Cleveland, Ohio.

**VARIABLE FRICTION SECONDARY SEAL FOR FACE SEALS Patent Application**

E. DIRUSSO, inventor (to NASA) 16 Nov. 1984 8 p

(NASA-CASE-LEW-14170-1; NAS 1.71:LEW-14170-1;

US-PATENT-APPL-SN-672224) Avail: NTIS HC A02/MF A01 CSCL 11A

Vibration and stability of a primary seal ring are controlled by a secondary seal system. An inflatable bladder which forms a portion of secondary seal varies the damping applied to this seal ring. The amplitude of vibration of the primary seal ring is sensed with a proximity probe that is connected to a microprocessor in a control system. The bladder pressure is changed by the control system to mitigate any sensed instability or vibration. NASA

**N85-21657\*#** National Aeronautics and Space Administration. Lewis Research Center, Cleveland, Ohio.

**TRIBOLOGICAL SYSTEMS AS APPLIED TO AIRCRAFT ENGINES**

D. H. BUCKLEY 26 Apr. 1985 23 p refs To be presented at the 60th AGARD Struct. and Mater. Panel Meeting, San Antonio, 21-26 Apr. 1985

(NASA-TM-86965; E-2478; NAS 1.15:86965) Avail: NTIS HC A02/MF A01 CSCL 131

Tribological systems as applied to aircraft are reviewed. The importance of understanding the fundamental concepts involved in such systems is discussed. Basic properties of materials which can be related to adhesion, friction and wear are presented and correlated with tribology. Surface processes including deposition and treatment are addressed in relation to their present and future application to aircraft components such as bearings, gears and seals. Lubrication of components with both liquids and solids is discussed. Advances in both new liquid molecular structures and additives for those structures are reviewed and related to the needs of advanced engines. Solids and polymer composites are suggested for increasing use and ceramic coatings containing fluoride compounds are offered for the extreme temperatures encountered in such components as advanced bearings and seals. M.G.

**N85-21658\*#** National Aeronautics and Space Administration. Lewis Research Center, Cleveland, Ohio.

**LUBRICATION AND PERFORMANCE OF HIGH-SPEED ROLLING-ELEMENT BEARINGS**

E. V. ZARETSKY, F. T. SCHULLER, and H. H. COE 1985 19 p refs Proposed for presentation at the 1985 Ann. Meeting of the American Society of Lubrications Engineers, Las Vegas, Nev., 6-9 May 1985

(NASA-TM-86958; E-2362; NAS 1.15:86958) Avail: NTIS HC A02/MF A01 CSCL 131

Trends in aircraft engine operating speeds have dictated the need for rolling-element bearings capable of speeds to 3 million DN. A review of high-speed rolling-element bearing state-of-the-art performance and lubrication is presented. Through the use of

## 37 MECHANICAL ENGINEERING

under-race lubrication and bearing thermal management bearing operation can be obtained to speeds of 3 million DN. Jet lubricated ball bearings are limited to 2.5 million DN for large bore sizes and to 3 million DN for small bore sizes. Current computer programs are able to predict bearing thermal performance. Author

**N85-21662\*#** Tuskegee Inst., Ala. Dept. of Mechanical Engineering.

### **ARC-DRIVEN RAIL GUN RESEARCH Annual Report**

P. K. RAY Dec. 1984 69 p refs

(Contract NAG3-76)

(NASA-CR-174816; NAS 1.26:174816) Avail: NTIS HC A04/MF A01 CSCL 14B

The equations describing the performance of an inductively-driven rail gun are analyzed numerically. Friction between the projectile and rails is included through an empirical formulation. The equations are applied to the experiment of Rashleigh and Marshall to obtain an estimate of energy distribution in rail guns as a function of time. The effect of frictional heat dissipation on the bore of the gun is calculated. The mechanism of plasma and projectile acceleration in a dc rail gun is described from a microscopic point of view through the establishment of the Hall field. The plasma conductivity is shown to be a tensor indicating that there is a small component of current parallel to the direction of acceleration. The plasma characteristics are evaluated as a function of plasma mass through a simple fluid mechanical analysis of the plasma. By equating the energy dissipated in the plasma with the radiation heat loss, the properties of the plasma are determined. Author

**N85-23085\*#** National Aeronautics and Space Administration. Lewis Research Center, Cleveland, Ohio.

### **FRICTIONAL AND STRUCTURAL CHARACTERIZATION OF ION-NITRIDED LOW AND HIGH CHROMIUM STEELS**

T. SPALVINS 1985 17 p refs Presented at the 12th Intern. Conf. on Metallurgical Coatings, Los Angeles, 15-19 Apr. 1985 (NASA-TM-86991; E-2487; NAS 1.15:86991) Avail: NTIS HC A02/MF A01 CSCL 13I

Low Cr steels AISI 41410, AISI 4340, and high Cr austenitic stainless steels AISI 304, AISI 316 were ion nitrided in a dc glow discharge plasma consisting of a 75 percent H<sub>2</sub> - 25 percent N<sub>2</sub> mixture. Surface compound layer phases were identified, and compound layer microhardness and diffusion zone microhardness profiles were established. Distinct differences in surface compound layer hardness and diffusion zone profiles were determined between the low and high Cr alloy steels. The high Cr stainless steels after ion nitriding displayed a hard compound layer and an abrupt diffusion zone. The compound layers of the high Cr stainless steels had a columnar structure which accounts for brittleness when layers are exposed to contact stresses. The ion nitrided surfaces of high and low Cr steels displayed a low coefficient of friction with respect to the untreated surfaces when examined in a pin and disk tribotester. Author

**N85-25847\*#** National Aeronautics and Space Administration. Lewis Research Center, Cleveland, Ohio.

### **EXPERIMENTAL STIFFNESS OF TAPERED BORE SEALS**

D. P. FLEMING 1985 20 p refs Presented at the Design Eng. Tech. Conf., Cincinnati, 10-13 Sep. 1985; sponsored by ASME

(NASA-TM-86978; E-2515; NAS 1.15:86978) Avail: NTIS HC A02/MF A01 CSCL 11A

The stiffness of tapered-bore ring seals was measured with air as the sealed fluid. Static stiffness agreed fairly well with results of a previous analysis. Cross-coupled stiffness due to shaft rotation was much less than predicted. It is suggested that part of the disparity may be due to simplifying assumptions in the analysis; however, these do not appear to account for the entire difference observed. E.A.K.

### **N85-25848\*#** Transmission Research, Inc., Cleveland, Ohio. **THERMAL TRACTION CONTACT PERFORMANCE EVALUATION UNDER FULLY FLOODED AND STARVED CONDITIONS Interim Report**

J. L. TEVAARWERK May 1985 132 p refs

(Contract DEN3-35)

(NASA-CR-168173; NAS 1.26:168173; IR-2) Avail: NTIS HC A07/MF A01 CSCL 13I

Ultra high speed traction tests were performed on two traction fluids commonly employed. Traction data on these fluids is required for purposes of traction drive design optimization techniques. To obtain the traction data, an existing twin disc traction test machine was employed. This machine was modified to accommodate the range of test variables. All the data reported was obtained under conditions of side slip, a technique whereby only low power levels are required to simulate real traction drive contacts. Theoretical traction predictions were performed for a representative number of curves that showed the influence of rolling velocity, of contact pressure and of aspect ratio. To establish the accuracy of the thermal model the predictions were performed with increasing levels of independence of experimentally determined parameters. In the final resulting prediction only two non linear thermal parameters were used for the prediction of 15 different traction curves covering the entire range of variables as used in the investigation, with the exception of the influence of asperity traction. Comparison of these theoretical curves and corresponding experimental traces show very good agreement. Author

**N85-26890\*#** National Aeronautics and Space Administration. Lewis Research Center, Cleveland, Ohio.

### **PRELIMINARY RESULTS ON PASSIVE EDDY CURRENT DAMPER TECHNOLOGY FOR SSME TURBOMACHINERY**

R. E. CUNNINGHAM In NASA. Marshall Space Flight Center Advan. High Pressure O<sub>2</sub>/H<sub>2</sub> Technol. p 366-380 Apr. 1985

Avail: NTIS HC A99/MF E03; SOD HC CSCL 13I

Some preliminary results have been obtained for the dynamic response of a rotor operating over a speed range of 800 to 10,000 rpm. Amplitude frequency plots show the lateral vibratory response of an unbalanced rotor with and without external damping. The mode of damping is by means of eddy currents generated with 4 c shaped permanent magnets installed at the lower bearing of a vertically oriented rotor. The lower ball bearing and its damper assembly are totally immersed in liquid nitrogen at a temperature of -197 deg C (-320 deg F). These preliminary results for a referenced or base line passive eddy current damper assembly show that the amplitude of synchronous vibration is reduced at the resonant frequency. Measured damping coefficients were calculated to  $\phi = .086$ ; this compares with a theoretically calculated value of  $\phi = .079$ . Author

**N85-27226\*#** National Aeronautics and Space Administration. Lewis Research Center, Cleveland, Ohio.

### **FATIGUE CRITERION TO SYSTEM DESIGN, LIFE AND RELIABILITY**

E. V. ZARETSKY 10 Jul. 1985 22 p refs Presented at the 21st Joint Propulsion Conf., Monterey, Calif., 8-10 Jul. 1985; sponsored by AIAA, SAE and ASME

(NASA-TM-87017; E-2562; NAS 1.15:87017) Avail: NTIS HC A02/MF A01 CSCL 14D

A generalized methodology to structural life prediction, design, and reliability based upon a fatigue criterion is advanced. The life prediction methodology is based in part on work of W. Weibull and G. Lundberg and A. Palmgren. The approach incorporates the computed life of elemental stress volumes of a complex machine element to predict system life. The results of coupon fatigue testing can be incorporated into the analysis allowing for life prediction and component or structural renewal rates with reasonable statistical certainty. Author



**N85-27227\*#** National Aeronautics and Space Administration. Lewis Research Center, Cleveland, Ohio.

**LIFE AND RELIABILITY MODELING OF BEVEL GEAR REDUCTIONS**

M. SAVAGE (Akron Univ., Ohio), C. K. BRIKMANIS (Akron Univ., Ohio), D. G. LEWICKI (Army Research and Technology Lab., Cleveland), and J. J. COY (Army Research and Technology Lab., Cleveland) 13 Mar. 1985 24 p refs Presented at the Natl. Design Eng. Conf., Chicago, 11-13 Mar. 1985; sponsored by ASME

(NASA-TM-87006; E-2549; NAS 1.15:87006; USAAVSCOM-TR-85-C-3) Avail: NTIS HC A02/MF A01 CSCL 131

A reliability model is presented for bevel gear reductions with either a single input pinion or dual input pinions of equal size. The dual pinions may or may not have the same power applied for the analysis. The gears may be straddle mounted or supported in a bearing quill. The reliability model is based on the Weibull distribution. The reduction's basic dynamic capacity is defined as the output torque which may be applied for one million output rotations of the bevel gear with a 90 percent probability of reduction survival. Author

**N85-27228\*#** National Aeronautics and Space Administration. Lewis Research Center, Cleveland, Ohio.

**FATIGUE LIFE ANALYSIS OF A TURBOPROP REDUCTION GEARBOX**

D. G. LEWICKI (Army Research and Technology Lab., Cleveland, Ohio), J. D. BLACK (Detroit Diesel Allison, Indianapolis, Ind.), M. SAVAGE (Akron Univ.), and J. J. COY (Army Research and Technology Lab., Cleveland, Ohio) 1985 25 p refs Prepared for presentation at the Design Tech. Conf., Cincinnati, 11-13 Sep. 1985; sponsored by ASME

(NASA-TM-87014; E-2559; NAS 1.15:87014; USAAVSCOM-TR-84-C-4) Avail: NTIS HC A02/MF A01 CSCL 131

A fatigue life analysis of the Allison T56/501 turboprop reduction gearbox was developed. The life and reliability of the gearbox was based on the lives and reliabilities of the main power train bearings and gears. The bearing and gear lives were determined using the Lundberg-Palmgren theory and a mission profile. The five planet bearing set had the shortest calculated life among the various gearbox components, which agreed with field experience where the planet bearing had the greatest incidences of failure. The analytical predictions of relative lives among the various bearings were in reasonable agreement with field experience. The predicted gearbox life was in excellent agreement with field data when the material life adjustment factors alone were used. The gearbox had a lower predicted life in comparison with field data when no life adjustment factors were used or when lubrication life adjustment factors were used either alone or in combination with the material factors. Author

**N85-28371\*#** National Aeronautics and Space Administration. Lewis Research Center, Cleveland, Ohio.

**OPERATING CHARACTERISTICS OF A 0.87 KW-HR FLYWHEEL ENERGY STORAGE MODULE**

S. H. LOEWENTHAL, H. W. SCIBBE, R. D. PARKER, and E. V. ZARETSKY 23 Aug. 1985 18 p refs Presented at 20th Intersoc. Energy Conversion Eng. Conf. (IECEC), Miami Beach, Fla., 18-23 Aug. 1985; sponsored by SAE, AIAA, ASME, IEEE, ACS and American Institute of Chemical Engineers (NASA-TM-87038; E-2535; NAS 1.15:87038) Avail: NTIS HC A02/MF A01 CSCL 10C

Discussion is given of the design and loss characteristics of 0.87 kW-hr (peak) flywheel energy storage module suitable for aerospace and automotive applications. The maraging steel flywheel rotor, a 46-cm- (18-in-) diameter, 58-kg (128-lb) tapered disk, delivers 0.65 kW-hr of usable energy between operating speeds of 10,000 and 20,000 rpm. The rotor is supported by 20- and 25-mm bore diameter, deep-groove ball bearings, lubricated by a self-replenishing wick type lubrication system. To reduce aerodynamic losses, the rotor housing was evacuated to vacuum

levels from 40 to 200 millitorr. Dynamic rotor instabilities uncovered during testing necessitated the use of an elastometric-bearing damper to limit shaft excursions. Spindown losses from bearing, seal, and aerodynamic drag at 50 millitorr typically ranged from 64 to 193 W at 10,000 and 20,000 rpm, respectively. Discharge efficiency of the flywheel system exceeded 96 percent at torque levels greater than 21 percent of rated torque. Author

**N85-28372\*#** Hamilton Standard, Windsor Locks, Conn.

**MULTI-MESH GEAR DYNAMICS PROGRAM EVALUATION AND ENHANCEMENTS Final Report**

L. S. BOYD and J. PIKE May 1985 128 p refs (Contract NAS3-23928)

(NASA-CR-174747; NAS 1.26:174747) Avail: NTIS HC A07/MF A01 CSCL 131

A multiple mesh gear dynamics computer program was continually developed and modified during the last four years. The program can handle epicyclic gear systems as well as single mesh systems with internal, buttress, or helical tooth forms. The following modifications were added under the current funding: variable contact friction, planet cage and ring gear rim flexibility options, user friendly options, dynamic side bands, a speed survey option and the combining of the single and multiple mesh options into one general program. The modified program was evaluated by comparing calculated values to published test data and to test data taken on a Hamilton Standard turboprop reduction gear-box. In general, the correlation between the test data and the analytical data is good. R.J.F.

**N85-28373\*#** National Aeronautics and Space Administration. Lewis Research Center, Cleveland, Ohio.

**LUBRICANT AND ADDITIVE EFFECTS ON SPUR GEAR FATIGUE LIFE**

D. P. TOWNSEND, E. V. ZARETSKY, and H. W. SCIBBE 1985 28 p refs To be presented at 1985 Lubrication Conf., Atlanta, 8-10 Oct. 1985, sponsored by ASME and American Society of Lubrication Engineers

(NASA-TM-87044; E-2482; NAS 1.15:87044) Avail: NTIS HC A03/MF A01 CSCL 131

Spur gear endurance tests were conducted with six lubricants using a single lot of consumable-electrode vacuum melted (CVM) AISI 9310 spur gears. The sixth lubricant was divided into four batches each of which had a different additive content. Lubricants tested with a phosphorus-type load carrying additive showed a statistically significant improvement in life over lubricants without this type of additive. The presence of sulfur type antiwear additives in the lubricant did not appear to affect the surface fatigue life of the gears. No statistical difference in life was produced with those lubricants of different base stocks but with similar viscosity, pressure-viscosity coefficients and antiwear additives. Gears tested with a 0.1 wt % sulfur and 0.1 wt % phosphorus EP additives in the lubricant had reactive films that were 200 to 400 (0.8 to 1.6 microns) thick. Author

**N85-29292\*#** National Aeronautics and Space Administration. Lewis Research Center, Cleveland, Ohio.

**VIBRATION CONTROL OF ROTOR SHAFT**

K. NONAMI 1985 19 p refs Proposed for presentation at Design Eng. Tech. Conf., Cincinnati, 10-13 Sep. 1985; sponsored by ASME

(NASA-TM-87053; E-2616; NAS 1.15:87053) Avail: NTIS HC A02/MF A01 CSCL 131

Suppression of flexural forced vibration or the self-excited vibration of a rotating shaft system not by passive elements but by active elements is described. The distinctive feature of this method is not to dissipate the vibration energy but to provide the force cancelling the vibration displacement and the vibration velocity through the bearing housing in rotation. Therefore the bearings of this kind are appropriately named Active Control Bearings. A simple rotor system having one disk at the center of the span on flexible supports is investigated in this paper. The actuators of the electrodynamic transducer are inserted in the sections of the bearing housing. First, applying the optimal regulator



## 37 MECHANICAL ENGINEERING

of optimal control theory, the flexural vibration control of the rotating shaft and the vibration control of support systems are performed by the optimal state feedback system using these actuators. Next, the quasi-modal control based on a modal analysis is applied to this rotor system. This quasi-modal control system is constructed by means of optimal velocity feedback loops. The differences between optimal control and quasi-modal control are discussed and their merits and demerits are made clear. Finally, the experiments are described concerning only the optimal regulator method. Author

**N85-29295\*#** National Aeronautics and Space Administration. Lewis Research Center, Cleveland, Ohio.

**POWDER METALLURGY FORGED GEAR DEVELOPMENT Final Report, Sep. 1980 - Jul. 1984**

D. H. RO, B. L. FERGUSON, S. PILLAY, D. T. OSTBERG (Army Tank-Automotive Command), and D. P. TOWNSEND Mar. 1985 112 p refs

(Contract DAAE07-80-C-9115)

(NASA-TM-87483; NAS 1.15:87483; AD-A153479;

TACOM-TR-13046) Avail: NTIS HC A06/MF A01 CSCL 13I

The purpose of this project is to investigate and develop powder forging methods for producing high-performance gears from sintered performs. Three gears have been forged from grade 4600 steel powder to which sufficient graphite was added to achieve the desired final carbon level. The first gear, referred to as the NASA test gear because it was designed specifically for gear testing at NASA Lewis Research Center, was forged from 4620 and 4640 steel powder preforms. This gear was a straight spur gear with 28 involute teeth, a 0.25 inch-(6.35 mm) thick web, and a top and bottom hub. Both net teeth and oversize teeth (0.004 inches grinding stock per side) were forged, with these gears being carburized after forging. Gears were then tested in a four square gear testing rig at NASA under the guidance of Dennis Townsend. Using a maximum Hertzian stress of 248,000 psi at pitch line and a gear rotational speed of 10,000 rpm, gear lives were obtained for these gears. GRA

**N85-30333\*** National Aeronautics and Space Administration. Lewis Research Center, Cleveland, Ohio.

**VARIABLE FORCE, EDDY-CURRENT OR MAGNETIC DAMPER Patent**

R. E. CUNNINGHAM, inventor (to NASA) 14 May 1985 6 p Filed 3 Feb. 1983

(NASA-CASE-LEW-13717-1; US-PATENT-4,517,505;

US-PATENT-APPL-SN-463456; US-PATENT-CLASS-318-611;

US-PATENT-CLASS-310-77; US-PATENT-CLASS-310-93;

US-PATENT-CLASS-335-100) Avail: US Patent and Trademark Office CSCL 13I

An object of the invention is to provide variable damping for resonant vibrations which may occur at different rotational speeds in the range of rpms in which a rotating machine is operated. A variable force damper in accordance with the invention includes a rotating mass carried on a shaft which is supported by a bearing in a resilient cage. The cage is attached to a support plate whose rim extends into an annular groove in a housing. Variable damping is effected by tabs of electrically conducting nonmagnetic material which extend radially from the cage. The tabs at an index position lie between the pole face of respective C shaped magnets. The magnets are attached by cantilever spring members to the housing. Author

**N85-30342\*#** National Aeronautics and Space Administration. Lewis Research Center, Cleveland, Ohio.

**CORRELATION OF RHEOLOGICAL CHARACTERISTICS OF LUBRICANTS WITH TRANSMISSION EFFICIENCY MEASUREMENTS**

B. O. JACOBSON (Lulea Univ.), B. J. HAMROCK, and E. HOEGLUND (Lulea Univ.) 1985 15 p refs Presented at the Intern. Tribology Conf., Tokyo, 8-10 Jul. 1985; sponsored by Japan Society of Lubrication Engineers

(NASA-TM-86988; E-2531; NAS 1.15:86988) Avail: NTIS HC A02/MF A01 CSCL 11H

The power efficiency of a helicopter transmission has been analyzed for 11 lubricants by looking at the Newtonian and non-Newtonian properties of the lubricants. A non-Newtonian property of the lubricants was the limiting shear strength proportionality constant. The tests were performed on a high-pressure, short-time shear strength analyzer. A power efficiency formula that was obtained by analyzing the Newtonian and non-Newtonian properties of the lubricants is presented in detail. B.W.

**N85-31511\*#** National Aeronautics and Space Administration. Lewis Research Center, Cleveland, Ohio.

**EFFECT OF SPEED AND PRESS FIT ON FATIGUE LIFE OF ROLLER-BEARING INNER-RACE CONTACT**

H. H. COE and E. V. ZARETSKY Jul. 1985 13 p refs

(NASA-TP-2496; E-2476; NAS 1.60:2496) Avail: NTIS HC

A02/MF A01 CSCL 13I

An analysis was performed to determine the effects of inner ring speed and press fit on the rolling element fatigue life of a roller bearing inner race contact. The effects of the resultant hoop and radial stresses on the principal stresses were considered. The maximum shear stresses below the Hertzian contact were determined for different conditions of inner ring speed, load, and geometry and were applied to a conventional ring life analysis. The race contact fatigue life was reduced by more than 90 percent for some conditions when speed and press fit were considered. The depth of the maximum shear stress remained virtually unchanged. Author

**N85-32329\*#** National Aeronautics and Space Administration. Lewis Research Center, Cleveland, Ohio.

**SURFACE ROUGHNESS EFFECTS IN ELASTOHYDRODYNAMIC CONTACTS**

J. H. TRIPP (Case Western Reserve Univ.) and B. J. HAMROCK Jul. 1985 14 p refs Presented at the 11th Leeds-Lyon Symp. on Mixed Lubrication and Lubricated Wear, Leeds, Engl., 4-7 Sep. 1984

(NASA-TP-2488; E-2524; NAS 1.60:2488) Avail: NTIS HC A02/MF A01 CSCL 20K

Surface roughness effects in full-film EHL contacts were studied. A flow factor modification to the Reynolds equation was applied to piezoviscous-elastic line contacts. Results for ensemble-averaged film shape, pressure distribution, and other mechanical quantities were obtained. Asperities elongated in the flow direction by a factor exceeding two decreased both film shape and pressure extrema at constant load; isotropic or transverse asperities increased these extrema. The largest effects are displayed by traction, which increased by over 5% for isotropic or transverse asperities and by slightly less for longitudinal roughness. E.A.K.

**N85-32330\*#** National Aeronautics and Space Administration. Lewis Research Center, Cleveland, Ohio.

**MECHANICS OF A GASEOUS FILM BARRIER TO LUBRICANT WETTING OF ELASTOHYDRODYNAMICALLY LUBRICATED CONJUNCTIONS**

J. M. PRAHL (Case Western Reserve Univ.) and B. J. HAMROCK Aug. 1985 17 p refs Presented at the 11th Leeds-Lyon Symp. on Mixed Lubrication and Lubricated Wear, Leeds, Engl., 4-7 Sep. 1984

(Contract NCC3-30)

(NASA-TP-2500; E-2523; NAS 1.60:2500) Avail: NTIS HC A02/MF A01 CSCL 20K

Two analytical models, one based on simple hydrodynamic lubrication and the other on soft elastohydrodynamic lubrication, are presented and compared to delineate the dominant physical parameters that govern the mechanics of a gaseous film between a small droplet of lubricant and the outer race of a ball bearing. Both models are based on the balance of gravity forces, air drag forces, and air film lubrication forces and incorporate a drag coefficient  $C_{sub D}$  and a lubrication coefficient  $C_{sub L}$  to be determined from experiment. The soft elastohydrodynamic lubrication (EHL) model considers the effects of droplet deformation and solid-surface geometry; the simpler hydrodynamic lubrication (HL) model assumes that the droplet remains essentially spherical. The droplet's angular position depended primarily on the ratio of gas inertia to droplet gravity forces and on the gas Reynolds number and weakly on the ratio of droplet gravity forces to surface tension forces (Bond number) and geometric ratios for the soft EHL. An experimental configuration in which an oil droplet is supported by an air film on the rotating outer race of a ball bearing within a pressure-controlled chamber produced measurements of droplet angular position as a function of outer-race velocity droplet size and type, and chamber pressure. E.A.K.

**N85-32331\*#** National Aeronautics and Space Administration. Lewis Research Center, Cleveland, Ohio.

**HERTZIAN CONTACT IN TWO AND THREE DIMENSIONS**

J. H. TRIPP (Case Western Reserve Univ.) Jul. 1985 27 p refs

(NASA-TP-2473; E-2256; NAS 1.60:2473) Avail: NTIS HC A03/MF A01 CSCL 20K

The basic solution to the problem of mechanical contact between elastically deforming solids was proposed by Hertz over a century ago and has been used by tribologists and others ever since in a steadily increasing number of applications. While the theoretical development is not conceptually difficult and treatments exist to suit all tastes, it is nonetheless interesting to trace the relationships among the solutions in different dimensions. Such an approach is used herein to shed light on the curious and sometimes perplexing behavior of line contacts. A number of the more frequently used contact expressions together as a convenient reference and for comparative purposes. Author

**N85-32333\*#** National Aeronautics and Space Administration. Lewis Research Center, Cleveland, Ohio.

**TAPE CASTING AS AN APPROACH TO AN ALL-CERAMIC TURBINE SHROUD SEAL**

J. D. CAWLEY Jul. 1985 11 p refs

(NASA-TM-87078; E-2607; NAS 1.15:87078) Avail: NTIS HC A02/MF A01 CSCL 11A

Gas path seals have a one-dimensional variation in material requirement. Tape casting is a method which allows the fabrication of thin ceramic sheets, which may be laminated to accommodate these requirements. Using tape casting, thin sheets of zirconia (0.25 mm) were fabricated. These castings were successfully laminated and fired without bloating or delamination, demonstrating the feasibility of this approach. Author

**N85-33489\*** National Aeronautics and Space Administration. Lewis Research Center, Cleveland, Ohio.

**MULTISTAGE SPENT PARTICLE COLLECTOR AND A METHOD FOR MAKING SAME Patent**

B. T. EBIHARA, inventor (to NASA) 2 Jul. 1985 7 p Filed 30 Sep. 1983 Supersedes N84-12447 (22 - 03, p 0376)

(NASA-CASE-LEW-13914-1; US-PATENT-4,527,092;

US-PATENT-APPL-SN-537615; US-PATENT-CLASS-315-5.38;

US-PATENT-CLASS-315-3.5; US-PATENT-CLASS-445-35) Avail:

US Patent and Trademark Office CSCL 13I

A description is given of a spent particle collector which maintains structural integrity when raised to a high temperature although constructed of materials having widely different coefficients of expansion. The collector is comprised of one or more axisymmetric stages, each stage comprising a subassembly. A subassembly includes an inner pyrolytic graphite ring, a transition ring, a ceramic insulator ring and an outer metal ring which forms part of the wall of the collector. Each transition is of a ductile metal having high thermal conductivity and is provided with an annular sputter shield wall extending toward the source of spent particles and, where necessary, a trough in the other surface to enclose the sputter shield of the next adjacent transition ring. A plurality of radial extending slots are provided in a transition ring to form segments which are retained in their position by the sputter shield. Official Gazette of the U.S. Patent and Trademark Office

**N85-33490\*** National Aeronautics and Space Administration. Lewis Research Center, Cleveland, Ohio.

**DUAL CLEARANCE SQUEEZE FILM DAMPER Patent**

D. P. FLEMING, inventor (to NASA) 9 Jul. 1985 8 p Filed 5 Apr. 1984 Supersedes N84-22562 (22 - 13, p 1932)

(NASA-CASE-LEW-13506-1; US-PATENT-4,527,910;

US-PATENT-APPL-SN-596960; US-PATENT-CLASS-384-99;

US-PATENT-CLASS-384-101) Avail: US Patent and Trademark Office CSCL 13I

A dual clearance hydrodynamic liquid squeeze film damper for a gas turbine engine is described. Under normal operating conditions, the device functions as a conventional squeeze film damper, using only one of its oil films. When an unbalance reaches abusive levels, as may occur with a blade loss or foreign object damage, a second, larger clearance film becomes active, controlling vibration amplitudes in a near optimum manner until the engine can be safely shut down and repaired.

Official Gazette of the U.S. Patent and Trademark Office

**N85-33491\*#** Transmission Research, Inc., Cleveland, Ohio.

**ROLLING, SLIP AND TRACTION MEASUREMENTS ON LOW MODULUS MATERIALS Interim Report**

J. L. TEVAARWERK Jul. 1985 122 p refs

(Contract DEN3-35)

(NASA-CR-174909; NAS 1.26:174909; IR-3) Avail: NTIS HC

A06/MF A01 CSCL 13I

Traction and wear tests were performed on six low modulus materials (LMM). Three different traction tests were performed to determine the suitability of the material for use as traction rollers. These were the rolling, slip and endurance traction tests. For each material the combination LMM on LMM and LMM on steel were evaluated. Rolling traction test were conducted to determine the load - velocity limits, the rolling traction coefficient of the materials and to establish the type of failures that would result when loading beyond the limit. It was found that in general a simple constant rolling traction coefficient was enough to describe the results of all the test. The slip traction tests revealed that the peak traction coefficients were considerably higher than for lubricated traction contacts. The endurance traction tests were performed to establish the durability of the LMM under conditions of prolonged traction. Wear measurements were performed during and after the test. Energetic wear rates were determined from the wear measurements conducted in the endurance traction tests. These values show that the roller wear is not severe when reasonable levels of traction are transmitted. Author

## 37 MECHANICAL ENGINEERING

**N85-33524\*#** National Aeronautics and Space Administration. Lewis Research Center, Cleveland, Ohio.

### **ADVANCES IN SPUTTERED AND ION PLATED SOLID FILM LUBRICATION**

T. SPALVINS /In NASA. Ames Research Center 19th Aerospace Mech. Symp. p 209-224 Aug. 1985 refs  
Avail: NTIS HC A17/MF A01 CSCL 13M

The glow discharge or ion assisted vacuum deposition techniques, primarily sputtering and ion plating, have rapidly emerged and offer great potential to deposit solid lubricants. The increased energizing of these deposition processes lead to improved adherence and coherence, favorable morphological growth, higher density, and reduced residual stresses in the film. These techniques are of invaluable importance where high precision machines tribo-components require very thin, uniform lubricating films (0.2 m), which do not interface with component tolerances. The performance of sputtered MoS<sub>2</sub> films and ion plated Au and Pb films are described in terms of film thickness, coefficient of friction, and wear lives. Author

**N85-34402\*** National Aeronautics and Space Administration. Lewis Research Center, Cleveland, Ohio.

### **OXIDIZING SEAL FOR A TURBINE TIP GAS PATH Patent**

J. D. CAWLEY, inventor (to NASA) 10 Sep. 1985 7 p Filed 19 Apr. 1984 Supersedes N84-22935 (22 - 13, p 1993)  
(NASA-CASE-LEW-14053-1; US-PATENT-4,540,336;  
US-PATENT-APPL-SN-602050; US-PATENT-CLASS-415-174;  
US-PATENT-CLASS-415-170-R; US-PATENT-CLASS-415-196;  
US-PATENT-CLASS-415-200; US-PATENT-CLASS-416-174)  
Avail: US Patent and Trademark Office CSCL 11A

The sealing of the gas path in a gas turbine engine at the blade tips is improved by maintaining a minimum clearance between the rotor blade tips and the gas path seal. This is accomplished by taking advantage of an increase in volume during controlled oxidation of certain intermetallic compounds which have high melting points. The increase in volume closes the clearance subsequent to a rub between the blades and the seal. Thus, these compounds re-form the tip seal surface to assure continued engine efficiency.

Official Gazette of the U.S. Patent and Trademark Office

**N85-34404\*#** Ohio State Univ., Columbus. Dept. of Mechanical Engineering.

### **THE DESIGN AND ANALYSIS OF SINGLE FLANK TRANSMISSION ERROR TESTOR FOR LOADED GEARS Final Report, Apr. 1984 - Jul. 1985**

D. R. HOUSER and D. E. BASSETT Sep. 1985 141 p refs  
(Contract NAG3-541)  
(NASA-CR-176163; NAS 1.26:176163; MPN-764038; ESL-716109)  
Avail: NTIS HC A07/MF A01 CSCL 13I

Due to geometrical imperfections in gears and finite tooth stiffnesses, the motion transmitted from an input gear shaft to an output gear shaft will not have conjugate action. In order to strengthen the understanding of transmission error and to verify mathematical models of gear transmission error, a test stand that will measure the transmission error of a gear pair at operating loads, but at reduced speeds would be desirable. This document describes the design and development of a loaded transmission error tester. For a gear box with a gear ratio of one, few tooth meshing combinations will occur during a single test. In order to observe the effects of different tooth mesh combinations and to increase the ability to load test gear pairs with higher gear ratios, the system was designed around a gear box with a gear ratio of two. B.W.

**N85-34405\*#** National Aeronautics and Space Administration. Lewis Research Center, Cleveland, Ohio.

### **GENERATED SPIRAL BEVEL GEARS: OPTIMAL MACHINE-TOOL SETTINGS AND TOOTH CONTACT ANALYSIS**

F. L. LITVIN (Illinois Univ., Chicago), W. J. TSUNG (Illinois Univ., Chicago), J. J. COY, and C. HEINE (Dana Corp.) 1985 14 p refs Presented at the 1985 Off-Highway and Power Plant Congr. and Exposition, Milwaukee, 9-12 Sep. 1985; sponsored by the Society of Automotive Engineers Prepared in cooperation with Army Research and Technology Labs.  
(Contract NSG3-48)

(NASA-TM-87075; E-2648; NAS 1.15:87075;

USAAVSCOM-TR-85-C-9) Avail: NTIS HC A02/MF A01 CSCL 13I

Geometry and kinematic errors were studied for Gleason generated spiral bevel gears. A new method was devised for choosing optimal machine settings. These settings provide zero kinematic errors and an improved bearing contact. The kinematic errors are a major source of noise and vibration in spiral bevel gears. The improved bearing contact gives improved conditions for lubrication. A computer program for tooth contact analysis was developed, and thereby the new generation process was confirmed. The new process is governed by the requirement that during the generation process there is directional constancy of the common normal of the contacting surfaces for generator and generated surfaces of pinion and gear. E.A.K.

**N85-34406\*#** National Aeronautics and Space Administration. Lewis Research Center, Cleveland, Ohio.

### **THERMAL STRESS ANALYSIS OF A NEW TURBINE SHROUD SEAL CONCEPT**

R. F. HANDSCHUH Aug. 1985 16 p refs Prepared in cooperation with Army Aviation Research and Development Command, Cleveland  
(NASA-TM-87082; E-2666; NAS 1.15:87082;  
USAAVSCOM-TR-85-C-16) Avail: NTIS HC A02/MF A01 CSCL 13I

The thermal stress field of a two piece turbine shroud seal concept was analyzed and results compared to one piece designs by finite element analysis. The two piece seal has independently formed structure (substrate) and ceramic components that are assembled at ambient conditions. The boundary conditions used for analysis were hot gas surface temperatures of 1370 and 1650 C (2500 and 3000 F) and cooled surface temperature of 700 C (1285 F). The resulting thermal stress field, of the two piece seal when compared to the one piece seals in the region of all ceramic material, was reduced substantially. Author

**N85-34407\*#** National Aeronautics and Space Administration. Lewis Research Center, Cleveland, Ohio.

### **LUBRICATION AND COOLING FOR HIGH SPEED GEARS**

D. P. TOWNSEND 1985 24 p refs Presented at the Lubrication Session of the Original Equipment Manuf. Design Conf., Philadelphia, 9-11 Sep. 1985  
(NASA-TM-87096; E-2660; NAS 1.15:87096) Avail: NTIS HC A02/MF A01 CSCL 13I

The problems and failures occurring with the operation of high speed gears are discussed. The gearing losses associated with high speed gearing such as tooth mesh friction, bearing friction, churning, and windage are discussed with various ways shown to help reduce these losses and thereby improve efficiency. Several different methods of oil jet lubrication for high speed gearing are given such as into mesh, out of mesh, and radial jet lubrication. The experiments and analytical results for the various methods of oil jet lubrication are shown with the strengths and weaknesses of each method discussed. The analytical and experimental results of gear lubrication and cooling at various test conditions are presented. These results show the very definite need of improved methods of gear cooling at high speed and high load conditions. Author

**N85-34408\*#** National Aeronautics and Space Administration. Lewis Research Center, Cleveland, Ohio.

## ELASTOHYDRODYNAMIC LUBRICATION CALCULATIONS USED AS A TOOL TO STUDY SCUFFING

L. G. HOUPERT and B. J. HAMROCK 1985 20 p refs Presented at the 12th Leeds-Lyon Symp. on Tribology, Lyon, 3-6 Sep. 1985

(NASA-TM-87097; E-2658; NAS 1.15:87097) Avail: NTIS HC A02/MF A01 CSCL 11H

A new Reynolds equation was developed that takes into account the nonlinear viscous behavior of the fluid. The new Reynolds equation considers the nonlinear viscous fluid model of Eyring, the equilibrium equation, the constant mass flow, and the kinematic boundary condition. The new Reynolds equation and the elasticity equation are solved simultaneously by using a system approach and a Newton-Raphson technique. Comparisons are made with results obtained from the classical Reynolds equation. The effects of sliding speed and introducing a bump or a groove within the conjunction are studied. Results are shown for both moderate and heavy loads. E.A.K.

**N85-34409\*#** National Aeronautics and Space Administration. Lewis Research Center, Cleveland, Ohio.

## DESIGN AND LUBRICATION OF HIGH-SPEED ROLLING-ELEMENT BEARINGS

E. V. ZARETSKY 1985 19 p refs Presented at the Original Equipment Manuf. Design Conf., Philadelphia, 9-11 Sep. 1985

(NASA-TM-87107; E-2670; NAS 1.15:87107) Avail: NTIS HC A02/MF A01 CSCL 13I

The speed capability of rolling element bearings has increased from speeds of less than two million DN to speeds of three million DN. The life and reliability of these bearings also increased where they are equal to, or greater than, those of bearings with limited speed capability. Design parameters must be carefully chosen and optimized based upon sophisticated bearing computer programs. Material and lubricant selection must be integrated into the bearing design. Bearing thermal management must be implemented through proper lubrication and cooling. Parameters which can be used to design, specify, and lubricate high speed bearings are discussed. E.A.K.

# 38

## QUALITY ASSURANCE AND RELIABILITY

Includes product sampling procedures and techniques; and quality control.

**A85-42151\*#** National Aeronautics and Space Administration. Lewis Research Center, Cleveland, Ohio.

## THE ROLE OF THE REFLECTION COEFFICIENT IN PRECISION MEASUREMENT OF ULTRASONIC ATTENUATION

E. R. GENERAZIO (NASA, Lewis Research Center, Cleveland, OH) (DARPA, Annual Review of Progress in Quantitative Nondestructive Evaluation, La Jolla, CA, July 8-13, 1984) Materials Evaluation (ISSN 0025-5327), vol. 43, July 1985, p. 995-1004. Previously announced in STAR as N84-32849. refs

Ultrasonic attenuation measurements using contact, pulse-echo techniques are sensitive to surface roughness and couplant thickness variations. This can reduce considerable inaccuracies in the measurement of the attenuation coefficient for broadband pulses. Inaccuracies arise from variations in the reflection coefficient at the buffer-couplant-sample interface. The reflection coefficient is examined as a function of the surface roughness and corresponding couplant thickness variations. Interrelations with ultrasonic frequency are illustrated. Reliable attenuation measurements are obtained only when the frequency dependence of the reflection coefficient is incorporated in signal analysis. Data are given for nickel 200 samples and a silicon nitride ceramic bar

having surface roughness variations in the 0.3 to 3.0 microns range for signal bandwidths in the 50 to 100 MHz range. Author

**N85-10371\*#** National Aeronautics and Space Administration. Lewis Research Center, Cleveland, Ohio.

## ULTRASONIC NONDESTRUCTIVE EVALUATION, MICROSTRUCTURE, AND MECHANICAL PROPERTY INTERRELATIONS

A. VARY Washington Oct. 1984 30 p refs

(NASA-TM-86876; E-2337; NAS 1.15:86876) Avail: NTIS HC A03/MF A01 CSCL 14D

Ultrasonic techniques for mechanical property characterizations are reviewed and conceptual models are advanced for explaining and interpreting the empirically based results. At present, the technology is generally empirically based and is emerging from the research laboratory. Advancement of the technology will require establishment of theoretical foundations for the experimentally observed interrelations among ultrasonic measurements, mechanical properties, and microstructure. Conceptual models are applied to ultrasonic assessment of fracture toughness to illustrate an approach for predicting correlations found among ultrasonic measurements, microstructure, and mechanical properties. R.S.F.

**N85-16195\*#** Ohio State Univ., Columbus.

## FUNDAMENTALS OF MICROCRACK NUCLEATION MECHANICS Final Report

L. S. FU, Y. C. SHEU, C. M. CO, W. F. ZHONG, and H. D. SHEN NASA Washington Jan. 1985 86 p refs

(Contract NAG3-340)

(NASA-CR-3851; E-2296; NAS 1.26:3851; RFP763340/714952)

Avail: NTIS HC A05/MF A01 CSCL 20K

A foundation for ultrasonic evaluation of microcrack nucleation mechanics is identified in order to establish a basis for correlations between plane strain fracture toughness and ultrasonic factors through the interaction of elastic waves with material microstructures. Since microcracking is the origin of (brittle) fracture, it is appropriate to consider the role of stress waves in the dynamics of microcracking. Therefore, the following topics are discussed: (1) microstress distributions with typical microstructural defects located in the stress field; (2) elastic wave scattering from various idealized defects; and (3) dynamic effective-properties of media with randomly distributed inhomogeneities. R.S.F.

**N85-20389\*#** National Aeronautics and Space Administration. Lewis Research Center, Cleveland, Ohio.

## NDE FOR HEAT ENGINE CERAMICS

S. J. KLIMA 1984 13 p refs Presented at 22nd Automotive Technol. Develop. Contractors Coordination Meeting (ATD/CCM), 29 Oct. - 2 Nov. 1984, Dearborn, Mich.; sponsored by Society of Automotive Engineers

(NASA-TM-86949; E-2470; NAS 1.15:86949) Avail: NTIS HC A02/MF A01 CSCL 14B

Radiographic, ultrasonic, and scanning laser acoustic microscopy (SLAM) techniques were used to characterize silicon nitride and silicon carbide MOR bars in various stages of fabrication. Conventional and microfocus x-ray techniques were found capable of detecting minute high density inclusions in as-received powders, green compacts, and fully densified specimens. Significant density gradients in sintered bars were observed by radiography, ultrasonic velocity, and SLAM. Ultrasonic attenuation was found sensitive to microstructural variations due to grain and void morphology and distribution. SLAM was also capable of detecting voids, inclusions, and cracks in finished test bars. It was determined that thermoacoustic microscopy techniques have promise for application to green and densified ceramics. R.J.F.

## 38 QUALITY ASSURANCE AND RELIABILITY

**N85-20390\*** # Massachusetts Inst. of Tech., Cambridge.

### **STRESS WAVES IN AN ISOTROPIC ELASTIC PLATE EXCITED BY A CIRCULAR TRANSDUCER Final Report**

H. KARAGULLE, J. H. WILLIAMS, JR., and S. S. LEE  
Washington NASA Mar. 1985 52 p refs

(Contract NAG3-328)

(NASA-CR-3877; NAS 1.26:3877) Avail: NTIS HC A04/MF A01  
CSCL 14D

Steady state harmonic stress waves in an isotropic elastic plate excited on one face by a circular transducer are analyzed theoretically. The transmitting transducer transforms an electrical voltage into a uniform normal stress at the top of the plate. To solve the boundary value problem, the radiation into a half-space is considered. The receiving transducer produces an electrical voltage proportional to the average spatially integrated normal stress over its face due to an incident wave. A numerical procedure is given to evaluate the frequency response at a receiving point due to a multiply reflected wave in the near field. Its stability and convergence are discussed. Parameterization plots which determine the particular wave whose frequency response has maximum magnitude compared with other multiple reflected waves are given for a range of values of dimensionless parameters. The effects of changes in the values of the parameters are discussed. B.G.

**N85-21673\*** # Massachusetts Inst. of Tech., Cambridge. Dept. of Mechanical Engineering.

### **APPLICATION OF HOMOMORPHIC SIGNAL PROCESSING TO STRESS WAVE FACTOR ANALYSIS**

H. KARAGULLE, J. H. WILLIAMS, JR., and S. S. LEE Feb. 1985 48 p refs

(Contract NSG-3328)

(NAS 1.26:174871; NASA-CR-174871) Avail: NTIS HC A03/MF A01 CSCL 14D

The stress wave factor (SWF) signal, which is the output of an ultrasonic testing system where the transmitting and receiving transducers are coupled to the same face of the test structure, is analyzed in the frequency domain. The SWF signal generated in an isotropic elastic plate is modelled as the superposition of successive reflections. The reflection which is generated by the stress waves which travel  $p$  times as a longitudinal (P) wave and  $s$  times as a shear (S) wave through the plate while reflecting back and forth between the bottom and top faces of the plate is designated as the reflection with  $p, s$ . Short-time portions of the SWF signal are considered for obtaining spectral information on individual reflections. If the significant reflections are not overlapped, the short-time Fourier analysis is used. A summary of the relevant points of homomorphic signal processing, which is also called cepstrum analysis, is given. Homomorphic signal processing is applied to short-time SWF signals to obtain estimates of the log spectra of individual reflections for cases in which the reflections are overlapped. Two typical SWF signals generated in aluminum plates (overlapping and non-overlapping reflections) are analyzed. M.G.

**N85-21674\*** # National Aeronautics and Space Administration. Lewis Research Center, Cleveland, Ohio.

### **RADIOGRAPHIC DETECTABILITY LIMITS FOR SEEDED VOIDS IN SINTERED SILICON CARBIDE AND SILICON NITRIDE**

G. Y. BAAKLINI (Cleveland State Univ.), J. D. KISER, and D. J. ROTH 1984 19 p refs Presented at the Regional Meeting of the American Ceramic Society, San Francisco, 28-31 Oct. 1984

(NASA-TM-86945; E-2464; NAS 1.15:86945) Avail: NTIS HC A02/MF A01 CSCL 14D

Conventional and microfocus X-radiographic techniques were compared to determine relative detectability limits for voids in green and sintered SiC and Si<sub>3</sub>N<sub>4</sub>. The relative sensitivity of the techniques was evaluated by comparing their ability to detect voids that were artificially introduced by a seeding process. For projection microfocus radiography the sensitivity of void detection at a 90/95 probability of detection/confidence level is 1.5% of specimen thickness in sintered SiC and Si<sub>3</sub>N<sub>4</sub>. For conventional contact

radiography the sensitivity is 2.5% of specimen thickness. It appears that microfocus projection radiography is preferable to conventional contact radiography in cases where increased sensitivity is required and where the additional complexity of the technique can be tolerated. E.A.K.

**N85-29307\*** # Massachusetts Inst. of Tech., Cambridge. Dept. of Mechanical Engineering.

### **ULTRASONIC TESTING OF PLATES CONTAINING EDGE CRACKS Final Report**

J. H. WILLIAMS, JR., H. KARAGULLE, and S. S. LEE  
Washington NASA Jun. 1985 37 p refs

(Contract NAG3-328)

(NASA-CR-3904; E-2550; NAS 1.26:3904) Avail: NTIS HC A03/MF A01 CSCL 14D

The stress wave factor (SWF) signal is utilized for the nondestructive evaluation of plates containing perpendicular edge cracks. The effects of the existence lateral location and depth of the crack on the magnitude spectra of individual reflections in the SWF signal are studied. If the reflections in the SWF signal are not overlapped the short time Fourier analysis is applied. If the reflections are overlapped the short time homomorphic analysis (cepstrum analysis) is applied. Several reflections which have average resonant frequencies approximately at 0.9, 1.3, and 1.7 MHz are analyzed. It is observed that the magnitude ratios evaluated at average resonant frequencies decrease more with increasing  $d/h$  if the crack is located between the transducers, where  $h$  is plate thickness and  $d$  is crack depth. Moreover, for the plates, crack geometries, reflections, and frequencies considered, the average decibel drop depends mainly on the dimensionless parameter  $d/h$  and it is approximately -1 dB per 0.07  $d/h$ . Changes in the average resonant frequencies of the magnitude spectra are also observed due to changes in the location of the crack. B.W.

**N85-32337\*** # National Aeronautics and Space Administration. Lewis Research Center, Cleveland, Ohio.

### **RELIABILITY OF VOID DETECTION IN STRUCTURAL CERAMICS USING SCANNING LASER ACOUSTIC MICROSCOPY**

D. J. ROTH, S. J. KLIMA, J. D. KISER, and G. Y. BAAKLINI (Cleveland State Univ.) 1985 54 p refs Presented at the Spring Meeting of the Am. Soc. for Nondestructive Testing, Washington, D.C., 11-14 Mar. 1985

(NASA-TM-87035; E-2591; NAS 1.15:87035) Avail: NTIS HC A04/MF A01 CSCL 14D

The reliability of scanning laser acoustic microscopy (SLAM) for detecting surface voids in structural ceramic test specimens was statistically evaluated. Specimens of sintered silicon nitride and sintered silicon carbide, seeded with surface voids, were examined by SLAM at an ultrasonic frequency of 100 MHz in the as fired condition and after surface polishing. It was observed that polishing substantially increased void detectability. Voids as small as 100 micrometers in diameter were detected in polished specimens with 0.90 probability at a 0.95 confidence level. In addition, inspection times were reduced up to a factor of 10 after polishing. The applicability of the SLAM technique for detection of naturally occurring flaws of similar dimensions to the seeded voids is discussed. A FORTRAN program listing is given for calculating and plotting flaw detection statistics. Author

## STRUCTURAL MECHANICS

Includes structural element design and weight analysis; fatigue; and thermal stress.

**A85-11125\*** Texas Univ., Austin.

**ANALYSIS OF HOURGLASS INSTABILITIES AND CONTROL IN UNDERINTEGRATED FINITE ELEMENT METHODS**

O.-P. JACQUOTTE and J. T. ODEN (Texas, University, Austin, TX) Computer Methods in Applied Mechanics and Engineering (ISSN 0045-7825), vol. 44, Aug. 1984, p. 339-363. refs (Contract NAG3-329)

Belytschko et al. (1981, 1984) has developed stabilization methods for the treatment of underintegrated FEM problems; these methods involve the computation of an underintegrated stiffness matrix, which is rank-deficient, and the addition of a stabilization matrix which effectively eliminates the spurious modes. An attempt is presently made to give this a priori stabilization method a mathematical means of support. Attention is also given to an a posteriori stabilization method for hourglass control, in which an approximate solution of the underintegrated system is obtained and then subjected to a special projection in order to eliminate the hourglass modes. A proof is obtained for the convergence of this stabilized underintegrated approximation to the exact solution of a model problem at almost the same rate (as the mesh is refined) as the fully integrated solutions. O.C.

**A85-12029\*** Massachusetts Inst. of Tech., Cambridge.

**RATIONAL APPROACH FOR ASSUMED STRESS FINITE ELEMENTS**

T. H. H. PIAN (MIT, Cambridge, MA) and K. SUMIHARA International Journal for Numerical Methods in Engineering (ISSN 0029-5981), vol. 20, Sept. 1984, p. 1685-1695. refs (Contract NAG3-33)

A new method for the formulation of hybrid elements by the Hellinger-Reissner principle is established by expanding the essential terms of the assumed stresses as complete polynomials in the natural coordinates of the element. The equilibrium conditions are imposed in a variational sense through the internal displacements which are also expanded in the natural co-ordinates. The resulting element possesses all the ideal qualities, i.e. it is invariant, it is less sensitive to geometric distortion, it contains a minimum number of stress parameters and it provides accurate stress calculations. For the formulation of a 4-node plane stress element, a small perturbation method is used to determine the equilibrium constraint equations. The element has been proved to be always rank sufficient. Author

**A85-12716\*#** National Aeronautics and Space Administration. Lewis Research Center, Cleveland, Ohio.

**FLUTTER OF TURBOFAN ROTORS WITH MISTUNED BLADES**

K. R. V. KAZA and R. E. KIELB (NASA, Lewis Research Center, Cleveland, OH) (Structures, Structural Dynamics and Materials Conference, 23rd, New Orleans, LA, May 10-12, 1982, Collection of Technical Papers. Part 2, p. 446-461) AIAA Journal (ISSN 0001-1452), vol. 22, Nov. 1984, p. 1618-1625. Previously cited in issue 13, p. 2111, Accession no. A82-30175. refs

**A85-12721\*#** Massachusetts Inst. of Tech., Cambridge.

**FLUTTER AND FORCED RESPONSE OF MISTUNED ROTORS USING STANDING WAVE ANALYSIS**

J. DUGUNDJI and D. J. BUNDAS (MIT, Cambridge, MA) (Structures, Structural Dynamics and Materials Conference, 24th, Lake Tahoe, NV, May 2-4, 1983, Collection of Technical Papers. Part 2, p. 149-159) AIAA Journal (ISSN 0001-1452), vol. 22, Nov. 1984, p. 1652-1661. Previously cited in issue 12, p. 1742, Accession no. A83-29823. refs (Contract NAG3-214)

**A85-13942\*** Babcock and Wilcox Co., New York, N.Y.

**EXTENSION OF CONSTRAINED INCREMENTAL NEWTON-RAPHSON SCHEME TO GENERALIZED LOADING FIELDS**

J. PADOVAN (Akron, University, Akron, OH) and S. PAI (Babcock and Wilcox Co., New York, NY; Akron, University, Akron, OH) Franklin Institute, Journal (ISSN 0016-0032), vol. 318, Sept. 1984, p. 165-186. refs (Contract NAG3-54)

This paper develops numerical strategies which enable the constrained incremental Newton-Raphson scheme to handle the static response of structure to loading fields with completely generalized histories. This is made possible through the use of specially warped hyperelliptic constraint surfaces which control successive or clustered load steps in the vicinity of loading events with specific timing schedules. Such an approach enables improved convergence and stability characteristics. Due to the generality of the methodology, pre- and postbuckling behavior caused by both kinematic and material nonlinearity can be handled. To demonstrate the scheme, the results of several bench-mark problems are also presented. These include situations involving nonlinear kinematics as well as highly history-dependent elastic-plastic and thermoelastic-plastic material behavior. Author

**A85-15893\*** Massachusetts Inst. of Tech., Cambridge.

**HYBRID SEMILOOF ELEMENTS FOR PLATES AND SHELLS BASED UPON A MODIFIED HU-WASHIZU PRINCIPLE**

T. H. H. PIAN (MIT, Cambridge, MA) and K. SUMIHARA Computers and Structures (ISSN 0045-7949), vol. 19, no. 1-2, 1984, p. 165-173. refs (Contract NAG3-33)

Hybrid SemiLoof elements for plates and shells are developed based upon modified Hu-Washizu principle. In the new version of the assumed stress hybrid formulation the equilibrium equations are satisfied through the introduction of internal displacement parameters as Lagrange multipliers. The inversion of the resulting H-matrices is simplified particularly when the stresses are expressed in terms of natural coordinates. A 24-DOF triangular element and a 32-DOF quadrilateral element based on shallow shell theory are derived and evaluated. Author

**A85-15894\*** Georgia Inst. of Tech., Atlanta.

**HYBRID STRESS FINITE ELEMENTS FOR LARGE DEFORMATIONS OF INELASTIC SOLIDS**

K. W. REED and S. N. ATLURI (Georgia Institute of Technology, Atlanta, GA) Computers and Structures (ISSN 0045-7949), vol. 19, no. 1-2, 1984, p. 175-182. refs (Contract NAG3-38)

A new hybrid stress finite element algorithm, based on a generalization of Fraeijns de Veubeke's complementary energy principle is presented. Analyses of large quasistatic deformation of inelastic solids (hypoelastic, plastic, viscoplastic) are within its capability. Principle variables in the formulation are the nominal stress rate and spin. A brief account is given of the boundary value problem in these variables, and the 'equivalent' variational principle. The finite element equation, along with initial positions and stresses, comprise an initial value problem. Factors affecting the choice of time integration schemes are discussed. Results found by application of the new algorithm are compared to those obtained by a velocity based finite element algorithm. Author

**A85-16095\*#** National Aeronautics and Space Administration. Lewis Research Center, Cleveland, Ohio.

**VIBRATION AND FLUTTER OF MISTUNED BLADED-DISK ASSEMBLIES**

K. RAO, V. KAZA (NASA, Lewis Research Center, Cleveland, OH), and R. E. KIELB AIAA, ASME, ASCE, and AHS, Structures, Structural Dynamics and Materials Conference, 25th, Palm Springs, CA, May 14-16, 1984. 16 p. Previously announced in STAR as N84-23923. refs (AIAA PAPER 84-0991)

An analytical model for investigating vibration and flutter of mistuned bladed disk assemblies is presented. This model accounts

for elastic, inertial and aerodynamic coupling between bending and torsional motions of each individual blade, elastic and inertial couplings between the blades and the disk, and aerodynamic coupling among the blades. The disk was modeled as a circular plate with constant thickness and each blade was represented by a twisted, slender, straight, nonuniform, elastic beam with a symmetric cross section. The elastic axis, inertia axis, and the tension axis were taken to be noncoincident and the structural warping of the section was explicitly considered. The blade aerodynamic loading in the subsonic and supersonic flow regimes was obtained from two-dimensional unsteady, cascade theories. All the possible standing wave modes of the disk and traveling wave modes of the blades were included. The equations of motion were derived by using the energy method in conjunction with the assumed mode shapes for the disk and the blades. Continuities of displacement and slope at the blade-disk junction were maintained. The equations were solved to investigate the effects of blade-disk coupling and blade frequency mistuning on vibration and flutter. Results showed that the flexibility of practical disks such as those used for current generation turbomachinery did not have a significant influence on either the tuned or mistuned flutter characteristics. However, the disk flexibility may have a strong influence on some of the system frequencies and on forced response. Author

**A85-17039\*** Rice Univ., Houston, Tex.

**OSCILLATOR RESPONSE TO NONSTATIONARY EXCITATION**  
P.-T. D. SPANOS (Rice University, Houston, TX) and G. P. SOLOMOS ASME, Transactions, Journal of Applied Mechanics (ISSN 0021-8936), vol. 51, Dec. 1984, p. 907-912. refs (Contract NAG3-210)  
(ASME PAPER 84-WA/APM-38)

Analytical solutions are presented regarding probability density distributions of various response parameters of a lightly damped oscillator. The oscillator is subjected to a broad-band stochastic excitation which possesses a time-variant power spectrum. The analytical solutions are derived by utilizing appropriate Fokker-Planck equations which govern Markovian approximations of the response parameters considered. The reliability of the approximate analytical solution is tested by using pertinent data generated by a digital Monte Carlo study. Author

**A85-17040\*** National Aeronautics and Space Administration. Lewis Research Center, Cleveland, Ohio.

**EFFECTS OF WARPING AND PRETWIST ON TORSIONAL VIBRATION OF ROTATING BEAMS**

K. R. V. KAZA and R. E. KIELB (NASA, Lewis Research Center, Cleveland, OH) ASME, Transactions, Journal of Applied Mechanics (ISSN 0021-8936), vol. 51, Dec. 1984, p. 913-920. refs  
(ASME PAPER 84-WA/APM-41)

The effect of pretwist and warping on the torsional vibration of short-aspect-ratio rotating beams is examined for application to the modeling of turbofan, turboprop, and compressor blades. The equations of motion and the associated boundary conditions by using both Wagner's hypothesis and Washizu's theory are derived and a few minor limitations of the Wagner's hypothesis, as applied to thick blades, are pointed out and discussed. The equations for several special cases are solved in a closed form. Results are presented indicating the effect of warping, pretwist, and rotation on torsional vibration of beams as aspect ratio is varied. The results show that the structural warping and pretwist terms have a significant effect on torsional frequency and mode shapes of short-aspect-ratio blades whereas the inertial warping terms have negligible effect. Since the torsional frequencies and mode shapes are very important in aeroelastic analyses by using modal methods, the structural warping terms should be included in modeling turbofan, turboprop, compressor, and turbine blades. Author

**A85-18795\*** Battelle Columbus Labs., Ohio.

**A HISTORY DEPENDENT DAMAGE MODEL FOR LOW CYCLE FATIGUE**

B. N. LEIS (Battelle Columbus Laboratories, Columbus, OH) American Society of Mechanical Engineers, Pressure Vessels and Piping Conference and Exhibition, San Antonio, TX, June 17-21, 1984. 10 p. Research supported by the Battelle Columbus Laboratories, and Battelle Memorial Institute. refs  
(Contract NAS3-22825)  
(ASME PAPER 84-PVP-112)

This paper examines damage assessment and accumulation. A nonlinear damage postulate is advanced that embodies the dependence of the damage rate on cycle-dependent changes in the bulk microstructure and the surface topography. The postulate is analytically formulated in terms of the deformation history dependence of the bulk behavior. This formulation is used in conjunction with baseline data in accordance with the damage postulate to predict the low cycle fatigue resistance of OFE copper. Close comparison of the predictions with observed behavior suggests the postulate offers a viable basis for nonlinear damage analysis. Author

**A85-19433\*** Case Western Reserve Univ., Cleveland, Ohio.

**STATISTICS AND THERMODYNAMICS OF FRACTURE**

A. CHUDNOVSKY (Case Western Reserve University, Cleveland, OH) (Michigan Technological University, Workshop on Media with Microstructure and Wave Propagation, Michigan Technological University, Houghton, MI, Jan. 24, 25, 1983) International Journal of Engineering Science (ISSN 0020-7225), vol. 22, no. 8-10, 1984, p. 989-997. refs  
(Contract NAG3-223)

A probabilistic model of the fracture processes unifying the phenomenological study of long term strength of materials, fracture mechanics and statistical approaches to fracture is briefly outlined. The general framework of irreversible thermodynamics is employed to model the deterministic side of the failure phenomenon. The stochastic calculus is used to account for the failure mechanisms controlled by chance; particularly, the random roughness of fracture surfaces. Author

**A85-19899\*** Georgia Inst. of Tech., Atlanta.

**DEVELOPMENT AND TESTING OF STABLE, INVARIANT, ISOPARAMETRIC CURVILINEAR 2- AND 3-D HYBRID-STRESS ELEMENTS**

E. F. PUNCH (Georgia Institute of Technology, Atlanta, GA; GM Research Laboratories, Warren, MI) and S. N. ATLURI (Georgia Institute of Technology, Atlanta, GA) Computer Methods in Applied Mechanics and Engineering (ISSN 0045-7825), vol. 47, Dec. 1984, p. 331-356. refs  
(Contract NAG3-346)

Linear and quadratic Serendipity hybrid-stress elements are examined in respect of stability, coordinate invariance, and optimality. A formulation based upon symmetry group theory successfully addresses these issues in undistorted geometries and is fully detailed for plane elements. The resulting least-order stable invariant stress polynomials can be applied as astute approximations in distorted cases through a variety of tensor components and variational principles. A distortion sensitivity study for two- and three-dimensional elements provides favorable numerical comparisons with the assumed displacement method. Author

**A85-22069\*** Ohio State Univ., Cleveland.

**VIBRATIONS OF TWISTED CANTILEVERED PLATES - SUMMARY OF PREVIOUS AND CURRENT STUDIES**

A. W. LEISSA (Ohio State University, Columbus, OH), J. C. MACBAIN (USAF, Aero Propulsion Laboratory, Wright-Patterson AFB, OH), and R. E. KIELB (NASA, Lewis Research Center, Structural and Mechanical Technology Div., Cleveland, OH) Journal of Sound and Vibration (ISSN 0022-460X), vol. 96, Sept. 22, 1984, p. 159-173. refs

This work summarizes a comprehensive study made of the free vibrations of twisted, cantilevered plates of rectangular



planform. Numerous theoretical and experimental investigations previously made by others have resulted in frequency results which disagree considerably. To clarify the problem a joint industry/government/university research effort was initiated to obtain comprehensive theoretical and experimental results for models having useful ranges of aspect ratios, thickness ratios and twist angles. Theoretical data came from 19 independent computer analyses, including finite element, shell theory and beam theory idealizations. Two independent sets of experimental data were also obtained. The theoretical and experimental results are summarized and compared. Author

**A85-23150\*** National Aeronautics and Space Administration. Lewis Research Center, Cleveland, Ohio.

#### **A SIMPLIFIED METHOD FOR ELASTIC-PLASTIC-CREEP STRUCTURAL ANALYSIS**

A. KAUFMAN (NASA, Lewis Research Center, Cleveland, OH) ASME, Transactions, Journal of Engineering for Gas Turbines and Power (ISSN 0022-0825), vol. 107, Jan. 1985, p. 231-237. refs (ASME PAPER 84-GT-191)

A simplified inelastic analysis computer program (ANSYPM) was developed for predicting the stress-strain history at the critical location of a thermomechanically cycled structure from an elastic solution. The program uses an iterative and incremental procedure to estimate the plastic strains from the material stress-strain properties and a plasticity hardening model. Creep effects are calculated on the basis of stress relaxation at constant strain, creep at constant stress or a combination of stress relaxation and creep accumulation. The simplified method was exercised on a number of problems involving uniaxial and multiaxial loading, isothermal and nonisothermal conditions, dwell times at various points in the cycles, different materials and kinematic hardening. Good agreement was found between these analytical results and nonlinear finite element solutions for these problems. The simplified analysis program used less than 1 percent of the CPU time required for a nonlinear finite element analysis. Author

**A85-24532\*** Northwestern Univ., Evanston, Ill.

#### **ON STRESS FIELD NEAR A STATIONARY CRACK TIP**

S. NEMAT-NASSER and M. OBATA (Northwestern University, Evanston, IL) Mechanics of Materials (ISSN 0167-6636), vol. 3, Sept. 1984, p. 235-243. refs (Contract NAG3-134; DAAG29-82-K-0147) (AD-A152863)

It is well known that the stress and elastic-plastic deformation fields near a crack tip have important roles in the corresponding fracture process. For elastic-perfectly-plastic solids, different solutions are given in the literature. In this work several of these solutions are examined and compared for Mode I (tension), Mode II (shear), and mixed Modes I and II loading conditions in plane strain. By consideration of the dynamic solution, it is shown that the assumption that the material is yielding all around a crack tip may not be reasonable in all cases. By admitting the existence of some elastic sectors, continuous stress fields are obtained even for mixed Modes I and II. Author

**A85-27935\*** Materials Research Lab., Inc., Glenwood, Ill.

#### **FRACTURE OF COMPOSITE-ADHESIVE-COMPOSITE SYSTEMS**

E. J. RIPLING, J. S. SANTNER, and P. B. CROSLLEY (Materials Research Laboratory, Inc., Glenwood, IL) IN: Adhesive joints: Formation, characteristics, and testing. New York, Plenum Press, 1984, p. 755-787. refs (Contract NAS3-21824)

This program was undertaken to initiate the development of a test method for testing adhesive joints in metal-adhesive-composite systems. The uniform double cantilever beam (UDCB) and the width tapered beam (WTB) specimen geometries were evaluated for measuring Mode I fracture toughness in these systems. The WTB specimen is the preferred geometry in spite of the fact that it is more costly to machine than the UDCB specimen. The use of loading tabs attached to thin sheets of composites proved to be experimentally unsatisfactory. Consequently, a new system was

developed to load thin sheets of adherends. This system allows for the direct measurement of displacement along the load line. In well made joints separation occurred between the plies rather than in the adhesive. Author

**A85-30313\*** Pratt and Whitney Aircraft Group, East Hartford, Conn.

#### **FINITE ELEMENT ENGINE BLADE STRUCTURAL OPTIMIZATION**

K. W. BROWN (United Technologies Corp., Pratt and Whitney Group, East Hartford, CT), M. S. HIRSCHBEIN, and C. C. CHAMIS (NASA, Lewis Research Center, Cleveland, OH) IN: Structures, Structural Dynamics, and Materials Conference, 26th, Orlando, FL, April 15-17, 1985, Technical Papers. Part 1. New York, American Institute of Aeronautics and Astronautics, 1985, p. 793-803. refs (Contract NAS3-22525) (AIAA PAPER 85-0645)

The Structural Tailoring of Engine Blades (STAEBL) computer program was developed to perform engine fan blade numerical optimizations. These blade optimizations seek a minimum weight or cost design that satisfies realistic blade design constraints, by tuning one to twenty design variables. The STAEBL system has been generalized to include both fan and compressor blade numerical optimizations. The system analyses have been significantly improved through the inclusion of an efficient plate finite element analysis for blade stress and frequency determinations. Additionally, a finite element based approximate severe foreign object damage (FOD) analysis has been included. The new FOD analysis gives very accurate estimates of the full nonlinear bird ingestion solution. Optimizations of fan and compressor blades have been performed using the system, showing significant cost and weight reductions, while comparing very favorably with refined design validation procedures. Author

**A85-32343\*** Indian Inst. of Tech., Madras.

#### **NATURAL FREQUENCIES OF TWISTED ROTATING PLATES**

V. RAMAMURTI (Indian Institute of Technology, Madras, India) and R. KIELB (NASA, Lewis Research Center, Cleveland, OH) Journal of Sound and Vibration (ISSN 0022-460X), vol. 97, Dec. 8, 1984, p. 429-449. refs

A detailed comparison is presented of the predicted eigenfrequencies of twisted rotating plates as obtained by using two different shape functions. Primarily, rotating twisted plates of two different aspect ratios and two different thickness ratios are considered. The effects of rotation are included by using a 'stress smoothing' technique when calculating the augmented stiffness matrix. In addition, the effects of Coriolis acceleration, contributions from membrane behavior, setting angle and sweep angle are considered. The effects of geometric nonlinearity are briefly discussed. Finally, results of a brief study of cambered plates are presented. Author

**A85-32962\*** National Aeronautics and Space Administration. Lewis Research Center, Cleveland, Ohio.

#### **FLUTTER OF SWEEPED FAN BLADES**

R. E. KIELB and K. R. V. KAZA (NASA, Lewis Research Center, Cleveland, OH) ASME, Transactions, Journal of Engineering for Gas Turbines and Power (ISSN 0022-0825), vol. 107, April 1985, p. 394-398. Previously announced in STAR as N84-16587. refs (ASME PAPER 84-GT-138)

The effect of sweep on fan blade flutter is studied by applying the analytical methods developed for aeroelastic analysis of advance turboprops. Two methods are used. The first method utilizes an approximate structural model in which the blade is represented by a swept, nonuniform beam. The second method utilizes a finite element technique to conduct modal flutter analysis. For both methods the unsteady aerodynamic loads are calculated using two dimensional cascade theories which are modified to account for sweep. An advanced fan stage is analyzed with 0, 15 and 30 degrees of sweep. It is shown that sweep has a beneficial effect on predominantly torsional flutter and a detrimental effect on predominantly bending flutter. This detrimental effect is shown to be significantly destabilizing for 30 degrees of sweep. M.G.

**A85-33847\*** Georgia Inst. of Tech., Atlanta.

## ON THE EXISTENCE AND STABILITY CONDITIONS FOR MIXED-HYBRID FINITE ELEMENT SOLUTIONS BASED ON REISSNER'S VARIATIONAL PRINCIPLE

L. A. KARLOVITZ, S. N. ATLURI (Georgia Institute of Technology, Atlanta, GA), and W.-M. XUE *International Journal of Solids and Structures* (ISSN 0020-7683), vol. 21, no. 1, 1985, p. 97-116. refs

(Contract NAG3-346)

The extensions of Reissner's two-field (stress and displacement) principle to the cases wherein the displacement field is discontinuous and/or the stress field results in unreciprocated tractions, at a finite number of surfaces ('interelement boundaries') in a domain (as, for instance, when the domain is discretized into finite elements), is considered. The conditions for the existence, uniqueness, and stability of mixed-hybrid finite element solutions based on such discontinuous fields, are summarized. The reduction of these global conditions to local ('element') level, and the attendant conditions on the ranks of element matrices, are discussed. Two examples of stable, invariant, least-order elements - a four-node square planar element and an eight-node cubic element - are discussed in detail. Author

**A85-35046\*#** Massachusetts Inst. of Tech., Cambridge.

## EVOLUTION OF ASSUMED STRESS HYBRID FINITE ELEMENT

T. H. H. PIAN (MIT, Cambridge, MA) *World Congress and Exhibition on Finite Element Methods*, 4th, Interlaken, Switzerland, Sept. 17-21, 1984, Preprint. 18 p. refs

(Contract NAG3-33; F33615-83-K-5016)

Early versions of the assumed stress hybrid finite elements were based on the a priori satisfaction of stress equilibrium conditions. In the new version such conditions are relaxed but are introduced through additional internal displacement functions as Lagrange multipliers. A rational procedure is to choose the displacement terms such that the resulting strains are now of complete polynomials up to the same degree as that of the assumed stresses. Several example problems indicate that optimal element properties are resulted by this method. Author

**A85-35048\***

## PLASTICITY, VISCOPLASTICITY, AND CREEP OF SOLIDS BY MECHANICAL SUBELEMENT MODELS

T. H. H. PIAN IN: *Numerical methods in coupled systems*. Chichester, Sussex, England, John Wiley and Sons, Ltd., 1984, p. 119-126. refs

(Contract NAG3-33)

This paper discusses the modelling by mechanical subelements, the general plasticity, the viscoplasticity, and the creep behavior of solids under multiaxial loading conditions. The formulation of a time-independent elastic-plastic analysis is based on the viscoplasticity theory and the assumed stress finite element method. An example of an in-plane stress problem is included. Author

**A85-37440\*** Akron Univ., Ohio.

## PANTOGRAPHING SELF ADAPTIVE GAP ELEMENTS

J. PADOVAN, R. MOSCARELLO (Akron, University, Akron, OH), J. STAFFORD, and F. TABADDOR (B.F. Goodrich Co., Akron, OH) *Computers and Structures* (ISSN 0045-7949), vol. 20, no. 4, 1985, p. 745-758. refs

(Contract NAG3-54)

This paper develops a so-called pantographing self adaptive gap element type contact strategy. Due to the manner of formulation, the scheme has the capability to handle large deformations in the contact zone; contact initiation in structure exhibiting either positive or indefinite stiffness characteristics; kinematic and material nonlinearity as well as; self adaptively adjusts load/time stepping. In this context, contact in pre and postbuckling structure can be treated. To illustrate the scheme, several benchmark problems are presented. These include contacting structure involving large deformation kinematics, inelastic behavior as well as pre and postbuckling stiffness characteristics. Author

**A85-38425\*#** Technion - Israel Inst. of Tech., Haifa.

## THERMODYNAMICALLY CONSISTENT CONSTITUTIVE EQUATIONS FOR NONISOTHERMAL LARGE STRAIN, ELASTO-PLASTIC, CREEP BEHAVIOR

R. RIFF (Technion - Israel Institute of Technology, Haifa, Israel; Georgia Institute of Technology, Atlanta, GA), R. L. CARLSON, and G. J. SIMITSES (Georgia Institute of Technology, Atlanta, GA) *American Institute of Aeronautics and Astronautics, Structures, Structural Dynamics and Materials Conference*, 26th, Orlando, FL, Apr. 15-17, 1985. 11 p.

(Contract NAG3-534)

(AIAA PAPER 85-0621)

The paper is concerned with the development of constitutive relations for large nonisothermal elastic-viscoplastic deformations for metals. The kinematics of elastic-plastic deformation, valid for finite strains and rotations, is presented. The resulting elastic-plastic uncoupled equations for the deformation rate combined with use of the incremental elasticity law permits a precise and purely deductive development of elastic-viscoplastic theory. It is shown that a phenomenological thermodynamic theory in which the elastic deformation and the temperature are state variables, including few internal variables, can be utilized to construct elastic-viscoplastic constitutive equations, which are appropriate for metals. The limiting case of inviscid plasticity is examined. Author

**A85-39769\*#** National Aeronautics and Space Administration. Lewis Research Center, Cleveland, Ohio.

## UNIFIED CONSTITUTIVE MATERIAL MODELS FOR NONLINEAR FINITE-ELEMENT STRUCTURAL ANALYSIS

A. KAUFMAN (NASA, Lewis Research Center, Cleveland, OH), J. H. LAFFLE (General Electric Co., Cincinnati, OH), and U. S. LINDHOLM (Southwest Research Institute, San Antonio, TX) *AIAA, SAE, ASME, and ASCE, Joint Propulsion Conference*, 21st, Monterey, CA, July 8-10, 1985. 10 p. Previously announced in STAR as N85-24338. refs

(AIAA PAPER 85-1418)

Unified constitutive material models were developed for structural analyses of aircraft gas turbine engine components with particular application to isotropic materials used for high-pressure stage turbine blades and vanes. Forms or combinations of models independently proposed by Bodner and Walker were considered. These theories combine time-dependent and time-independent aspects of inelasticity into a continuous spectrum of behavior. This is in sharp contrast to previous classical approaches that partition inelastic strain into uncoupled plastic and creep components. Predicted stress-strain responses from these models were evaluated against monotonic and cyclic test results for uniaxial specimens of two cast nickel-base alloys, B1900+Hf and Rene 80. Previously obtained tension-torsion test results for Hastelloy X alloy were used to evaluate multiaxial stress-strain cycle predictions. The unified models, as well as appropriate algorithms for integrating the constitutive equations, were implemented in finite-element computer codes. Author

**A85-39770\*#** South Carolina State Coll., Orangeburg.

## ON LOCAL TOTAL STRAIN REDISTRIBUTION USING A SIMPLIFIED CYCLIC INELASTIC ANALYSIS BASED ON AN ELASTIC SOLUTION

S. Y. HWANG (South Carolina State College, Orangeburg, SC) and A. KAUFMAN (NASA, Lewis Research Center, Cleveland, OH) *AIAA, SAE, ASME, and ASCE, Joint Propulsion Conference*, 21st, Monterey, CA, July 8-10, 1985. 10 p. Previously announced in STAR as N85-21690. refs

(AIAA PAPER 85-1419)

Strain redistribution corrections were developed for a simplified inelastic analysis procedure to economically calculate material cyclic response at the critical location of a structure for life prediction purposes. The method was based on the assumption that the plastic region in the structure is local and the total strain history required for input can be defined from elastic finite element analyses. Cyclic stress-strain behavior was represented by a bilinear kinematic hardening model. The simplified procedure has been found to predict stress-strain response with reasonable accuracy

for thermally cycled problems but needs improvement for mechanically load cycled problems. This study derived and incorporated Neuber type corrections in the simplified procedure to account for local total strain redistribution under cyclic mechanical loading. The corrected simplified method was exercised on a mechanically load cycled benchmark notched plate problem. Excellent agreement was found between the predicted material response and nonlinear finite element solutions for the problem. The simplified analysis computer program used 0.3 percent of the CPU time required for a nonlinear finite element analysis. Author

**A85-40814\*** # National Aeronautics and Space Administration. Lewis Research Center, Cleveland, Ohio.

**FATIGUE CRITERION TO SYSTEM DESIGN, LIFE AND RELIABILITY**

E. V. ZARETSKY (NASA, Lewis Research Center, Cleveland, OH) AIAA, SAE, ASME, and ASEE, Joint Propulsion Conference, 21st, Monterey, CA, July 8-10, 1985. 9 p. Previously announced in STAR as N85-27226. refs  
(AIAA PAPER 85-1140)

A generalized methodology to structural life prediction, design, and reliability based upon a fatigue criterion is advanced. The life prediction methodology is based in part on work of Weibull and Lundberg and Palmgren. The approach incorporates the computed life of elemental stress volumes of a complex machine element to predict system life. The results of coupon fatigue testing can be incorporated into the analysis allowing for life prediction and component or structural renewal rates with reasonable statistical certainty. Author

**A85-40910\*** Southwest Research Inst., San Antonio, Tex.  
**CONSTITUTIVE MODELING AND COMPUTATIONAL IMPLEMENTATION FOR FINITE STRAIN PLASTICITY**

K. W. REED (Southwest Research Institute, San Antonio, TX) and S. N. ATLURI (Georgia Institute of Technology, Atlanta ) International Journal of Plasticity (ISSN 0749-6419), vol. 1, no. 1, 1985, p. 63-87. refs  
(Contract NAG3-346)

This paper describes a simple alternate approach to the difficult problem of modeling material behavior. Starting from a general representation for a rate-type constitutive equation, it is shown by example how sets of test data may be used to derive restrictions on the scalar functions appearing in the representation. It is not possible to determine these functions from experimental data, but the aforementioned restrictions serve as a guide in their eventual definition. The implications are examined for hypo-elastic, isotropically hardening plastic, and kinematically hardening plastic materials. A simple model for the evolution of the 'back-stress,' in a kinematic-hardening plasticity theory, that is entirely analogous to a hypoelastic stress-strain relation is postulated and examined in detail in modeling finitely plastic tension-torsion test. The implementation of rate-type material models in finite element algorithms is also discussed. Author

**A85-41109\*** Massachusetts Inst. of Tech., Cambridge.  
**AXISYMMETRIC SOLID ELEMENTS BY A RATIONAL HYBRID STRESS METHOD**

Z. TIAN and T. H. H. PIAN (MIT, Cambridge, MA) (George Washington University and NASA, Symposium on Advances and Trends in Structures and Dynamics, Washington, DC, Oct. 22-25, 1984) Computers and Structures (ISSN 0045-7949), vol. 20, no. 1-3, 1985, p. 141-149. refs  
(Contract NAG3-33)

Four-node axisymmetric solid elements are derived by a new version of hybrid method for which the assumed stresses are expressed in complete polynomials in natural coordinates. The stress equilibrium conditions are introduced through the use of additional displacements as Lagrange multipliers. A rational procedure is to choose the displacement terms such that the resulting strains are also of complete polynomials of the same order. Example problems all indicate that elements obtained by this procedure lead to better results in displacements and stresses than that by other finite elements. Author

**A85-41983\*** Akron Univ., Ohio.

**QUASI-STATIC SOLUTION ALGORITHMS FOR KINEMATICALLY/MATERIALLY NONLINEAR THERMOMECHANICAL PROBLEMS**

J. PADOVAN (Akron, University, OH) and S. S. PAI (Babcock and Wilcox Co., Akron, OH) Journal of Thermal Stresses (ISSN 0149-5739), vol. 7, no. 3-4, 1984, p. 227-257. Research supported by Babcock and Wilcox Corp. refs  
(Contract NAG3-54)

This paper develops an algorithmic solution strategy which allows the handling of positive/indefinite stiffness characteristics associated with the pre- and post-buckling of structures subject to complex thermomechanical loading fields. The flexibility of the procedure is such that it can be applied to both finite difference and element-type simulations. Due to the generality of the algorithmic approach developed, both kinematic and thermal/mechanical type material nonlinearity including inelastic effects can be treated. This includes the possibility of handling completely general thermomechanical boundary conditions. To demonstrate the scheme, the results of several benchmark problems is presented. Author

**A85-42047\*** National Aeronautics and Space Administration. Lewis Research Center, Cleveland, Ohio.

**FINITE DIFFERENCE ANALYSIS OF TORSIONAL VIBRATIONS OF PRETWISTED, ROTATING, CANTILEVER BEAMS WITH EFFECTS OF WARPING**

K. B. SUBRAHMANYAM and K. R. V. KAZA (NASA, Lewis Research Center, Cleveland, OH) Journal of Sound and Vibration (ISSN 0022-460X), vol. 99, March 22, 1985, p. 213-224. refs

Theoretical natural frequencies of the first three modes of torsional vibration of pretwisted, rotating cantilever beams are determined for various thickness and aspect ratios. Conclusions concerning individual and collective effects of warping, pretwist, tension-torsion coupling and tennis racket effect (twist-rotational coupling) terms on the natural frequencies are drawn from numerical results obtained by using a finite difference procedure with first order central differences. The relative importance of structural warping, inertial warping, pretwist, tension-torsion and twist-rotational coupling terms is discussed for various rotational speeds. The accuracy of results obtained by using the finite difference approach is verified by a comparison with the exact solution for specialized simple cases of the equation of motion used in this paper. Author

**A85-42566\*** # Garrett Turbine Engine Co., Phoenix, Ariz.

**CREEP-RUPTURE RELIABILITY ANALYSIS**

A. PERALTA-DURAN (Garrett Turbine Engine Co., Phoenix, AZ) and P. H. WIRSCHING (Arizona, University, Phoenix) ASME, Transactions, Journal of Vibration, Acoustics, Stress, and Reliability in Design (ISSN 0739-3717), vol. 107, July 1985, p. 339-346. Previously announced in STAR as N84-19925. refs  
(Contract NAG3-41)

A probabilistic approach to the correlation and extrapolation of creep-rupture data is presented. Time temperature parameters (TTP) are used to correlate the data, and an analytical expression for the master curve is developed. The expression provides a simple model for the statistical distribution of strength and fits neatly into a probabilistic design format. The analysis focuses on the Larson-Miller and on the Manson-Haferd parameters, but it can be applied to any of the TTP's. A method is developed for evaluating material dependent constants for TTP's. It is shown that optimized constants can provide a significant improvement in the correlation of the data, thereby reducing modelling error. Attempts were made to quantify the performance of the proposed method in predicting long term behavior. Uncertainty in predicting long term behavior from short term tests was derived for several sets of data. Examples are presented which illustrate the theory and demonstrate the application of state of the art reliability methods to the design of components under creep. Author

## 39 STRUCTURAL MECHANICS

**A85-47626\*** National Aeronautics and Space Administration. Lewis Research Center, Cleveland, Ohio.

### **VIBRATIONS OF TWISTED CANTILEVER PLATES - A COMPARISON OF THEORETICAL RESULTS**

R. E. KIELB (NASA, Lewis Research Center, Cleveland, OH), A. W. LEISSA (Ohio State University, Columbus), and J. C. MACBAIN (USAF, Aero Propulsion Laboratory, Wright-Patterson AFB, OH) International Journal for Numerical Methods in Engineering (ISSN 0029-5981), vol. 21, Aug. 1985, p. 1365-1380. refs

As a result of significant differences in the published results for various methods of analysis involving the use of finite element techniques, there are now some questions regarding the adequacy of these methods to predict accurately the vibratory characteristics of highly twisted cantilever plates. In an attempt to help in a resolution of the arising problems, a joint government/industry/university research effort was initiated. The primary objective of the present paper is to summarize the theoretical methods used in the study and show samples of the obtained results. The study provided 19 sets of theoretical results which are derived from beam theory, shell theory, and finite element methods. G.R.

**A85-48703\*** Air Force Flight Dynamics Lab., Wright-Patterson AFB, Ohio.

### **STRUCTURAL OPTIMIZATION USING OPTIMALITY CRITERIA METHODS**

N. S. KHOT (USAF, Flight Dynamics Laboratory, Wright-Patterson AFB, OH) and L. BERKE (NASA, Lewis Research Center, Cleveland, OH) IN: New directions in optimum structural design. Chichester, England and New York, Wiley-Interscience, 1984, p. 47-74.

Optimality criteria methods take advantage of some concepts as those of statically determinate or indeterminate structures, and certain variational principles of structural dynamics, to develop efficient algorithms for the sizing of structures that are subjected to stiffness-related constraints. Some of the methods and iterative strategies developed over the last decade for calculations of the Lagrange multipliers in stress and displacement-limited problems, as well as for satisfying the appropriate optimality criterion, are discussed. The application of these methods are illustrated by solving problems with stress and displacement constraints. O.C.

**N85-10384\*#** Stanford Univ., Calif.

### **AUGMENTED WEAK FORMS AND ELEMENT-BY-ELEMENT PRECONDITIONERS: EFFICIENT ITERATIVE STRATEGIES FOR STRUCTURAL FINITE ELEMENTS. A PRELIMINARY STUDY**

A. MULLER and T. J. R. HUGHES / In NASA. Langley Research Center Res. in Struct. and Dyn., 1984 p 95-109 Oct. 1984 refs

(Contract NAG3-319)

Avail: NTIS HC A18/MF A01 CSCL 20K

A weak formulation in structural analysis that provides well conditioned matrices suitable for iterative solutions is presented. A mixed formulation ensures the proper representation of the problem and the constitutive relations are added in a penalized form. The problem is solved by a double conjugate gradient algorithm combined with an element by element approximate factorization procedure. The double conjugate gradient strategy resembles Uzawa's variable-length type algorithms the main difference is the presence of quadratic terms in the mixed variables. In the case of shear deformable beams these terms ensure that the proper finite thickness solution is obtained. E.A.K.

**N85-11380\*#** Arizona Univ., Tucson. Dept. of Aerospace and Mechanical Engineering.

### **RELIABILITY CONSIDERATIONS FOR THE TOTAL STRAIN RANGE VERSION OF STRAINRANGE PARTITIONING Final Report**

P. H. WIRSCHING and Y. T. WU Sep. 1984 85 p refs

(Contract NAG3-41)

(NASA-CR-174757; NAS 1.26:174757) Avail: NTIS HC A05/MF A01 CSCL 20K

A proposed total strainrange version of strainrange partitioning (SRP) to enhance the manner in which SRP is applied to life prediction is considered with emphasis on how advanced reliability technology can be applied to perform risk analysis and to derive safety check expressions. Uncertainties existing in the design factors associated with life prediction of a component which experiences the combined effects of creep and fatigue can be identified. Examples illustrate how reliability analyses of such a component can be performed when all design factors in the SRP model are random variables reflecting these uncertainties. The Rackwitz-Fiessler and Wu algorithms are used and estimates of the safety index and the probability of failure are demonstrated for a SRP problem. Methods of analysis of creep-fatigue data with emphasis on procedures for producing synoptic statistics are presented. An attempt to demonstrate the importance of the contribution of the uncertainties associated with small sample sizes (fatigue data) to risk estimates is discussed. The procedure for deriving a safety check expression for possible use in a design criteria document is presented. A.R.H.

**N85-15184\*#** National Aeronautics and Space Administration. Lewis Research Center, Cleveland, Ohio.

### **THE USE OF AN OPTICAL DATA ACQUISITION SYSTEM FOR BLADED DISK VIBRATION ANALYSIS**

C. LAWRENCE and E. H. MEYN Dec. 1984 23 p refs

(NASA-TM-86891; E-2358; NAS 1.15:86891) Avail: NTIS HC A02/MF A01 CSCL 20K

A new concept in instrumentation was developed by engineers at NASA Lewis Research Center to collect vibration data from multi-bladed rotors. This new concept, known as the optical data acquisition system, uses optical transducers to measure bladed tip deflections by reflection light beams off the tips of the blades as they pass in front of the optical transducer. By using an array of transducers around the perimeter of the rotor, detailed vibration signals can be obtained. In this study, resonant frequencies and mode shapes were determined for a 56 bladed rotor using the optical system. Frequency data from the optical system was also compared to data obtained from strain gauge measurements and finite element analysis and was found to be in good agreement. Author

**N85-16205\*#** National Aeronautics and Space Administration. Lewis Research Center, Cleveland, Ohio.

### **EXPERIMENTAL COMPLIANCE CALIBRATION OF THE NASA LEWIS RESEARCH CENTER MODE 2 FATIGUE SPECIMEN**

R. J. BUZZARD 1985 11 p refs Proposed for presentation at the 18th Natl. Symp. on Fracture Mech., Boulder, Colo., 24-27 Jun. 1985; sponsored by American Society for Testing and Materials

(NASA-TM-86908; E-2398; NAS 1.15:86908) Avail: NTIS HC A02/MF A01 CSCL 20K

Calibration of the mode II aluminum fatigue specimen was performed experimentally to provide displacement and stress intensity coefficients over crack length to specimen width ratios (a/W) of 0.5 to 0.9. Displacements were measured both at the specimen notch mouth and at the intersection of the notch with the centerline of the loading pin holes. R.S.F.

**N85-18375\*#** National Aeronautics and Space Administration. Lewis Research Center, Cleveland, Ohio.

**NASA LEWIS RESEARCH CENTER/UNIVERSITY GRADUATE RESEARCH PROGRAM ON ENGINE STRUCTURES**

C. C. CHAMIS 1985 18 p Presented at the 30th Intern. Gas Turbine Conf. and Exhibit, Houston, Tex., 17-21 Mar. 1985; sponsored by ASME

(NASA-TM-86916; E-2393; NAS 1.15:86916) Avail: NTIS HC A02/MF A01 CSCL 20K

NASA Lewis Research Center established a graduate research program in support of the Engine Structures Research activities. This graduate research program focuses mainly on structural and dynamics analyses, computational mechanics, mechanics of composites and structural optimization. The broad objectives of the program, the specific program, the participating universities and the program status are briefly described. Author

**N85-20396\*#** National Aeronautics and Space Administration. Lewis Research Center, Cleveland, Ohio.

**LOCAL STRAIN REDISTRIBUTION CORRECTIONS FOR A SIMPLIFIED INELASTIC ANALYSIS PROCEDURE BASED ON AN ELASTIC FINITE-ELEMENT ANALYSIS**

A. KAUFMAN and S. Y. HWANG (South Carolina State Coll., Orangeburg) Mar. 1985. 14 p refs To be presented at the 21st AIAA/SAE/ASME Joint Propulsion Conf., Monterey, Calif., 8-11 Jul. 1985

(NASA-TP-2421; E-2373; NAS 1.60:2421) Avail: NTIS HC A02/MF A01 CSCL 20K

Strain redistribution corrections were developed for a simplified inelastic analysis procedure to economically calculate material cyclic response at the critical location of a structure for life prediction purposes. The method was based on the assumption that the plastic region in the structure is local and the total strain history required for input can be defined from elastic finite-element analyses. Cyclic stress-strain behavior was represented by a bilinear kinematic hardening model. The simplified procedure predicts stress-strain response with reasonable accuracy for thermally cycled problems but needs improvement for mechanically load-cycled problems. Neuber-type corrections were derived and incorporated in the simplified procedure to account for local total strain redistribution under cyclic mechanical loading. The corrected simplified method was used on a mechanically load-cycled benchmark notched-plate problem. The predicted material response agrees well with the nonlinear finite-element solutions for the problem. The simplified analysis computer program was 0.3% of the central processor unit time required for a nonlinear finite-element analysis. E.A.K.

**N85-21685\*#** Case Western Reserve Univ., Cleveland, Ohio. Dept. of Civil Engineering.

**TRANSLATIONAL AND EXTENSIONAL ENERGY RELEASE RATES (THE J- AND M-INTEGRALS) FOR A CRACK LAYER IN THERMOELASTICITY Final Report**

A. CHUDNOVSKY and B. GOMMERSTADT Mar. 1985 9 p refs

(Contract NAG3-223)

(NASA-CR-174872; NAS 1.26:174872) Avail: NTIS HC A02/MF A01 CSCL 20K

A number of papers have been presented on the evaluation of energy release rate for thermoelasticity and corresponding J integral. Two main approaches were developed to treat energy release rate in elasticity. The first is based on direct calculation of the potential energy rate with respect to crack length. The second makes use of Lagrangian formalism. The translational and expansional energy release rates in thermoelasticity are studied by employing the formalism of irreversible thermodynamics and the Crack Layer Approach. Author

**N85-21686\*#** Pratt and Whitney Aircraft, East Hartford, Conn. Engineering Div.

**3-D INELASTIC ANALYSIS METHODS FOR HOT SECTION COMPONENTS (BASE PROGRAM) Annual Status Report, 14 Feb. 1983 - 14 Feb. 1984**

R. B. WILSON, M. J. BAK, S. NAKAZAWA, and P. K. BANERJEE Feb. 1984 167 p refs

(Contract NAS3-23697)

(NASA-CR-174700; NAS 1.26:174700; PWA-5940-19; ASR-1)

Avail: NTIS HC A08/MF A01 CSCL 20K

A 3-D inelastic analysis methods program consists of a series of computer codes embodying a progression of mathematical models (mechanics of materials, special finite element, boundary element) for streamlined analysis of combustor liners, turbine blades, and turbine vanes. These models address the effects of high temperatures and thermal/mechanical loadings on the local (stress/strain) and global (dynamics, buckling) structural behavior of the three selected components. These models are used to solve 3-D inelastic problems using linear approximations in the sense that stresses/strains and temperatures in generic modeling regions are linear functions of the spatial coordinates, and solution increments for load, temperature and/or time are extrapolated linearly from previous information. Three linear formulation computer codes, referred to as MOMM (Mechanics of Materials Model), MHOST (MARC-Hot Section Technology), and BEST (Boundary Element Stress Technology), were developed and are described. Author

**N85-21687\*#** Massachusetts Inst. of Tech., Cambridge. Dept. of Aeronautics and Astronautics.

**RECENT ADVANCES IN HYBRID/MIXED FINITE ELEMENTS**

T. H. H. PIAN 1985 8 p refs

(Contract NAG3-33)

(NASA-CR-175574; NAS 1.26:175574) Avail: NTIS HC A02/MF A01 CSCL 20K

In formulations of Hybrid/Mixed finite element methods respectively by the Hellinger-Reissner principle and the Hu-Washizu principle, the stress equilibrium equations are brought in as conditions of constraint through the introduction of additional internal displacement parameters. These two approaches are more flexible and have better computing efficiencies. A procedure for the choice of assumed stress terms for 3-D solids is suggested. Example solutions are given for plates and shells using the present formulations and the idea of semiloof elements. Author

**N85-21690\*#** National Aeronautics and Space Administration. Lewis Research Center, Cleveland, Ohio.

**ON LOCAL TOTAL STRAIN REDISTRIBUTION USING A SIMPLIFIED CYCLIC INELASTIC ANALYSIS BASED ON AN ELASTIC SOLUTION**

S. Y. HWANG (South Carolina State Coll.) and A. KAUFMAN 1985 16 p refs Proposed for presentation at the 21st Joint Propulsion Conf., Monterey, Calif., 9-11 Jul. 1985; sponsored by the AIAA, SAE and ASME

(NASA-TM-86913; E-2406; NAS 1.15:86913) Avail: NTIS HC A02/MF A01 CSCL 20K

Strain redistribution corrections were developed for a simplified inelastic analysis procedure to economically calculate material cyclic response at the critical location of a structure for life prediction purposes. The method was based on the assumption that the plastic region in the structure is local and the total strain history required for input can be defined from elastic finite element analyses. Cyclic stress-strain behavior was represented by a bilinear kinematic hardening model. The simplified procedure has been found to predict stress-strain response with reasonable accuracy for thermally cycled problems but needs improvement for mechanically load cycled problems. This study derived and incorporated Neuber type corrections in the simplified procedure to account for local total strain redistribution under cyclic mechanical loading. The corrected simplified method was exercised on a mechanically load cycled benchmark notched plate problem. Excellent agreement was found between the predicted material response and nonlinear finite element solutions for the problem.

## 39 STRUCTURAL MECHANICS

The simplified analysis computer program used 0.3 percent of the CPU time required for a nonlinear finite element analysis. Author

**N85-21691\*#** Akron Univ., Ohio. Dept. of Civil Engineering.  
**VISCOPLASTIC CONSTITUTIVE RELATIONSHIPS WITH  
DEPENDENCE ON THERMOMECHANICAL HISTORY Final  
Report**

D. N. ROBINSON and P. A. BARTOLOTTA Mar. 1985 42 p  
refs

(Contract NAG3-379)

(NASA-CR-174836; NAS 1.26:174836) Avail: NTIS HC A03/MF  
A01 CSCL 20K

Experimental evidence of thermomechanical history dependence in the cyclic hardening behavior of some common high-temperature structural alloys is presented with special emphasis on dynamic metallurgical changes. The inadequacy of formulating nonisothermal constitutive equations solely on the basis of isothermal testing is discussed. A representation of thermoviscoplasticity is proposed that qualitatively accounts for the observed hereditary behavior. This is achieved by formulating the scalar evolutionary equation in an established viscoplasticity theory to reflect thermomechanical path dependence. To assess the importance of accounting for thermomechanical history dependence in practical structural analyses, two qualitative models are specified: (1) formulated as if based entirely on isothermal information; (2) to reflect thermomechanical path dependence using the proposed thermoviscoplastic representation. Predictions of the two models are compared and the impact the calculated differences in deformation behavior may have on subsequent lifetime predictions is discussed. E.A.K.

**N85-21720\*#** Virginia Polytechnic Inst. and State Univ.,  
Blacksburg. Dept. of Engineering, Science and Mechanics.

**GEOMETRICALLY NONLINEAR ANALYSIS OF LAMINATED  
ELASTIC STRUCTURES Final Report**

J. N. REDDY Nov. 1984 107 p refs

(Contract NAG3-208)

(NASA-CR-175609; NAS 1.26:175609; PB85-127173;

VPI-E-84-36) Avail: NTIS HC A06/MF A01 CSCL 20K

Laminated composite plates and shells that can be used to model automobile bodies, aircraft wings and fuselages, and pressure vessels among many other were analyzed. The finite element method, a numerical technique for engineering analysis of structures, is used to model the geometry and approximate the solution. Various alternative formulations for analyzing laminated plates and shells are developed and their finite element models are tested for accuracy and economy in computation. These include the shear deformation laminate theory and degenerated 3-D elasticity theory for laminates. GRA

**N85-23096\*#** Massachusetts Inst. of Tech., Cambridge.  
**ON HYBRID AND MIXED FINITE ELEMENT METHODS**

T. H. H. PIAN 1981 19 p refs

(Contract NAG3-33)

(NASA-CR-175551; NAS 1.26:175551) Avail: NTIS HC A02/MF  
A01 CSCL 20K

Three versions of the assumed stress hybrid model in finite element methods and the corresponding variational principles for the formulation are presented. Examples of rank deficiency for stiffness matrices by the hybrid stress model are given and their corresponding kinematic deformation modes are identified. A discussion of the derivation of general semi-Loof elements for plates and shells by the hybrid stress method is given. It is shown that the equilibrium model by Fraeijns de Veubeke can be derived by the approach of the hybrid stress model as a special case of semi-Loof elements. Author

**N85-24338\*#** National Aeronautics and Space Administration.  
Lewis Research Center, Cleveland, Ohio.

**UNIFIED CONSTITUTIVE MATERIAL MODELS FOR NONLINEAR  
FINITE-ELEMENT STRUCTURAL ANALYSIS**

A. KAUFMAN, J. H. LAFLEN (General Electric Co., Cincinnati),  
and U. S. LINDHOLM (Southwest Research Inst., San Antonio)  
10 Jul. 1985 16 p refs Proposed for presentation at 21st  
Joint Propulsion Conf., Monterey, Calif., 8-10 Jul. 1985; sponsored  
by AIAA, SAE and ASME

(NASA-TM-86985; E-2529; NAS 1.15:86985) Avail: NTIS HC  
A02/MF A01 CSCL 20K

Unified constitutive material models were developed for structural analyses of aircraft gas turbine engine components with particular application to isotropic materials used for high-pressure stage turbine blades and vanes. Forms or combinations of models independently proposed by Bodner and Walker were considered. These theories combine time-dependent and time-independent aspects of inelasticity into a continuous spectrum of behavior. This is in sharp contrast to previous classical approaches that partition inelastic strain into uncoupled plastic and creep components. Predicted stress-strain responses from these models were evaluated against monotonic and cyclic test results for uniaxial specimens of two cast nickel-base alloys, B1900+Hf and Rene' 80. Previously obtained tension-torsion test results for Hastelloy X alloy were used to evaluate multiaxial stress-strain cycle predictions. The unified models, as well as appropriate algorithms for integrating the constitutive equations, were implemented in finite-element computer codes. Author

**N85-24339\*#** National Aeronautics and Space Administration.  
Lewis Research Center, Cleveland, Ohio.

**CYCLIC STRUCTURAL ANALYSES OF ANISOTROPIC TURBINE  
BLADES FOR REUSABLE SPACE PROPULSION SYSTEMS**

J. M. MANDERSCHIED and A. KAUFMAN 12 Apr. 1985 13 p  
refs Presented at 1985 JANNAF Propulsion Meeting, San Diego,  
Calif., 9-12 Apr. 1985; sponsored by JANNAF

(NASA-TM-86990; E-2534; NAS 1.15:86990) Avail: NTIS HC  
A02/MF A01 CSCL 20K

Turbine blades for reusable space propulsion systems are subject to severe thermomechanical loading cycles that result in large inelastic strains and very short lives. These components require the use of anisotropic high-temperature alloys to meet the safety and durability requirements of such systems. To assess the effects on blade life of material anisotropy, cyclic structural analyses are being performed for the first stage high-pressure fuel turbopump blade of the space shuttle main engine. The blade alloy is directionally solidified MAR-M 246 alloy. The analyses are based on a typical test stand engine cycle. Stress-strain histories at the airfoil critical location are computed using the MARC nonlinear finite-element computer code. The MARC solutions are compared to cyclic response predictions from a simplified structural analysis procedure developed at the NASA Lewis Research Center. Author

**N85-25893\*#** National Aeronautics and Space Administration.  
Lewis Research Center, Cleveland, Ohio.

**VIBRATION AND BUCKLING OF ROTATING, PRETWISTED,  
PRECONED BEAMS INCLUDING COOROLIS EFFECTS**

K. B. SUBRAHMANYAM and K. R. V. KAZA 1985 21 p refs  
Proposed for presentation at the 10th Bien. Design Eng. Conf.  
and Exhibit on Mech. Vibration and Noise, Cincinnati, 10-13 Sep.  
1985; sponsored by ASME

(NASA-TM-87004; E-2310; NAS 1.15:87004) Avail: NTIS HC  
A02/MF A01 CSCL 20K

The effects of pretwist, precone, setting angle and Coriolis forces on the vibration and buckling behavior of rotating, torsionally rigid, cantilevered beams were studied. The beam is considered to be clamped on the axis of rotation in one case, and off the axis of rotation in the other. Two methods are employed for the solution of the vibration problem: (1) one based upon a finite-difference approach using second order central differences for solution of the equations of motion, and (2) based upon the minimum of the total potential energy functional with a Ritz type



of solution procedure making use of complex forms of shape functions for the dependent variables. The individual and collective effects of pretwist, precone, setting angle, thickness ratio and Coriolis forces on the natural frequencies and the buckling boundaries are presented. It is shown that the inclusion of Coriolis effects is necessary for blades of moderate to large thickness ratios while these effects are not so important for small thickness ratio blades. The possibility of buckling due to centrifugal softening terms for large values of precone and rotation is shown. E.A.K.

**N85-25894\*#** Akron Univ., Ohio. Dept. of Civil Engineering.  
**ON THERMOMECHANICAL TESTING IN SUPPORT OF CONSTITUTIVE EQUATION DEVELOPMENT FOR HIGH TEMPERATURE ALLOYS Final Report**

D. N. ROBINSON May 1985 32 p refs

(Contract NAG3-379)

(NASA-CR-174879; NAS 1.26:174879) Avail: NTIS HC A03/MF A01 CSCL 11F

Three major categories of testing are identified that are necessary to provide support for the development of constitutive equations for high temperature alloys. These are exploratory, characterization and verification tests. Each category is addressed and specific examples of each are given. An extensive, but not exhaustive, set of references is provided concerning pertinent experimental results and their relationships to theoretical development. This guide to formulating a meaningful testing effort in support of constitutive equation development can also aid in defining the necessary testing equipment and instrumentation for the establishment of a deformation and structures testing laboratory. Author

**N85-25896\*#** Georgia Inst. of Tech., Atlanta.  
**ANALYSIS OF SHELL TYPE STRUCTURES SUBJECTED TO TIME DEPENDENT MECHANICAL AND THERMAL LOADING Semiannual Status Report, 15 Aug. 1984 - 14 Apr. 1985**

G. J. SIMITSES, R. L. CARLSON, and R. RIFF May 1985 4 p (Contract NAG3-534)

(NASA-CR-175747; NAS 1.26:175747) Avail: NTIS HC A02/MF A01 CSCL 20K

A general mathematical model and solution methodologies for analyzing structural response of thin, metallic shell-type structures under large transient, cyclic or static thermomechanical loads is considered. Among the system responses, which are associated with these load conditions, are thermal buckling, creep buckling and ratcheting. Thus, geometric as well as material-type nonlinearities (of high order) can be anticipated and must be considered in the development of the mathematical model.

G.L.C.

**N85-26885\*#** Wyle Labs., Inc., Huntsville, Ala.  
**FLOW DYNAMIC ENVIRONMENT DATA BASE DEVELOPMENT FOR THE SSME**

C. V. SUNDARAM In NASA. Marshall Space Flight Center Advan. High Pressure O2/H2 Technol. p 277-288 Apr. 1985 refs

Avail: NTIS HC A99/MF E03; SOD HC CSCL 20K

The fluid flow-induced vibration of the Space Shuttle main engine (SSME) components are being studied with a view to correlating the frequency characteristics of the pressure fluctuations in a rocket engine to its operating conditions and geometry. An overview of the data base development for SSME test firing results and the interactive computer software used to access, retrieve, and plot or print the results selectively for given thrust levels, engine numbers, etc., is presented. The various statistical methods available in the computer code for data analysis are discussed. Plots of test data, nondimensionalized using parameters such as fluid flow velocities, densities, and pressures, are presented. Results are compared with those available in the literature. Correlations between the resonant peaks observed at higher frequencies in power spectral density plots with pump geometry and operating conditions are discussed. An overview of the status of the investigation is presented and future directions are discussed. A.R.H.

**N85-26887\*#** National Aeronautics and Space Administration. Lewis Research Center, Cleveland, Ohio.

**NONLINEAR STRUCTURAL ANALYSIS FOR FIBER-REINFORCED SUPERALLOY TURBINE BLADES**

D. A. HOPKINS and C. C. CHAMIS In NASA. Marshall Space Flight Center Advan. High Pressure O2/H2 Technol. p 318-340 Apr. 1985 refs

Avail: NTIS HC A99/MF E03; SOD HC CSCL 20K

A computational capability for predicting the nonlinear thermomechanical structural response of fiber-reinforced superalloy (FRS) turbine blades is described. This capability is embedded in a special purpose computer code (COBSTRAN) developed at the NASA Lewis Research Center. Special features of this computational capability include accounting for: fiber/matrix reaction, nonlinear and anisotropic material behavior, complex stress distribution due to local and global heterogeneity, and residual stresses due to initial fabrication and/or inelastic behavior during subsequent missions. Numerical results are presented from analyses of a hypothetical FRS turbine blade subjected to a fabrication process and subsequent mission cycle. The results demonstrate the capabilities of this computational tool to: predict local stress/strain response and capture trends of local nonlinear and anisotropic material behavior, relate the effects of this local behavior to the global response of a multilayered fiber-composite turbine blade, and trace material history from fabrication through successive missions. Author

**N85-27260\*#** Akron Univ., Ohio. Dept. of Civil Engineering.  
**SOME ADVANCES IN EXPERIMENTATION SUPPORTING DEVELOPMENT OF VISCOPLASTIC CONSTITUTIVE MODELS Final Report**

J. R. ELLIS and D. N. ROBINSON May 1985 62 p refs

(Contract NAG3-379; W-7405-ENG-26)

(NASA-CR-174855; NAS 1.26:174855) Avail: NTIS HC A04/MF A01 CSCL 20K

The development of a biaxial extensometer capable of measuring axial, torsion, and diametral strains to near-microstrain resolution at elevated temperatures is discussed. An instrument with this capability was needed to provide experimental support to the development of viscoplastic constitutive models. The advantages gained when torsional loading is used to investigate inelastic material response at elevated temperatures are highlighted. The development of the biaxial extensometer was conducted in two stages. The first involved a series of bench calibration experiments performed at room temperature. The second stage involved a series of in-place calibration experiments conducted at room and elevated temperature. A review of the calibration data indicated that all performance requirements regarding resolution, range, stability, and crosstalk had been met by the subject instrument over the temperature range of interest, 21 C to 651 C. The scope of the in-place calibration experiments was expanded to investigate the feasibility of generating stress relaxation data under torsional loading. B.W.

**N85-27261\*#** General Electric Co., Cincinnati, Ohio. Aircraft Engine Business Group.

**COMPONENT-SPECIFIC MODELING Annual Status Report**

R. L. MCKNIGHT 1984 115 p

(Contract NAS3-23687)

(NASA-CR-174765; NAS 1.26:174765; ASR-1) Avail: NTIS HC A06/MF A01 CSCL 20K

A series of interdisciplinary modeling and analysis techniques that were specialized to address three specific hot section components are presented. These techniques will incorporate data as well as theoretical methods from many diverse areas including cycle and performance analysis, heat transfer analysis, linear and nonlinear stress analysis, and mission analysis. Building on the proven techniques already available in these fields, the new methods developed will be integrated into computer codes to provide an accurate, efficient and unified approach to analyzing combustor burner liners, hollow air-cooled turbine blades and air-cooled turbine vanes. For these components, the methods



## 39 STRUCTURAL MECHANICS

developed will predict temperature, deformation, stress and strain histories throughout a complete flight mission. Author

**N85-27263\*#** Connecticut Univ., Storrs. Dept. of Mechanical Engineering.

**ELEVATED TEMPERATURE BIAXIAL FATIGUE Final Report, 15 Feb. 1981 - 31 Oct. 1984**

E. H. JORDAN 31 Oct. 1984 167 p refs

(Contract NAG3-160)

(NASA-CR-175795; NAS 1.26:175795) Avail: NTIS HC A09/MF A01 CSCL 20K

A three year experimental program for studying elevated temperature biaxial fatigue of a nickel based alloy Hastelloy-X has been completed. A new high temperature fatigue test facility with unique capabilities has been developed. Effort was directed toward understanding multiaxial fatigue and correlating the experimental data to the existing theories of fatigue failure. The difficult task of predicting fatigue lives for non-proportional loading was used as an ultimate test for various life prediction methods being considered. The primary means of reaching improved understanding were through several critical non-proportional loading experiments. It was discovered that the cracking mode switched from primarily cracking on the maximum shear planes at room temperature to cracking on the maximum normal strain planes at 649 C. Author

**N85-27264\*#** National Aeronautics and Space Administration. Lewis Research Center, Cleveland, Ohio.

**A COMPUTER ANALYSIS PROGRAM FOR INTERFACING THERMAL AND STRUCTURAL CODES**

R. L. THOMPSON and R. J. MAFFEO (GE, Cincinnati) 1985 17 p refs Proposed for presentation at the Intern. Computers in Eng. Conf. and Exhibition, Boston, 4-8 Aug. 1985; sponsored by ASME

(NASA-TM-87021; E-2571; NAS 1.15:87021) Avail: NTIS HC A02/MF A01 CSCL 20K

A software package has been developed to transfer three-dimensional transient thermal information accurately, efficiently, and automatically from a heat transfer analysis code to a structural analysis code. The code is called three-dimensional TRansfer ANalysis Code to Interface Thermal and Structural codes, or 3D TRANCITS. TRANCITS has the capability to couple finite difference and finite element heat transfer analysis codes to linear and nonlinear finite element structural analysis codes. TRANCITS currently supports the output of SINDA and MARC heat transfer codes directly. It will also format the thermal data output directly so that it is compatible with the input requirements of the NASTRAN and MARC structural analysis codes. Other thermal and structural codes can be interfaced using the transfer module with the neutral heat transfer input file and the neutral temperature output file. The transfer module can handle different elemental mesh densities for the heat transfer analysis and the structural analysis. Author

**N85-27952\*#** National Aeronautics and Space Administration. Lewis Research Center, Cleveland, Ohio.

**OVERVIEW OF STRUCTURAL RESPONSE: PROBABILISTIC STRUCTURAL ANALYSIS Abstract Only**

C. C. CHAMIS *In its* Struct. Integrity and Durability of Reusable Space Propulsion Systems p 63-66 May 1985

Avail: NTIS HC A09/MF A01 CSCL 20K

Advanced analysis methods are required to predict accurately the structural response (static, transient, cyclic, etc.) and accompanying local stresses in space propulsion system components operating in a fatigue environment consisting of complex thermal and mechanical load spectra. The probabilistic approach to structural response consists of the following program elements: (1) composite load spectra, (2) probabilistic structural analysis methods development, (3) probabilistic finite element theory, (4) probabilistic structural analysis application, (5) structural tailoring of turbopump blades, (6) unified theory of dynamic creep buckling/ratcheting, (7) creep buckling/ratcheting analyzer, and (8) nonlinear COBSTRAN development. Research activities on all of these program elements (except the creep buckling/ratcheting analyzer) are under way. G.L.C.

**N85-27953\*#** Rockwell International Corp., Canoga Park, Calif. **COMPOSITE LOADS SPECTRA FOR SELECT SPACE PROPULSION STRUCTURAL COMPONENTS Abstract Only**

J. F. NEWELL *In* NASA. Lewis Research Center Struct. Integrity and Durability of Reusable Space Propulsion Systems p 67-75 May 1985

(Contract NAS3-24382)

Avail: NTIS HC A09/MF A01 CSCL 20K

Rocket engine technology continues to demand higher performance with lighter weight components that have man-rated reliability requirements. These requirements have yielded higher operating pressures, temperatures, and transient effects as well as markedly increased mechanical vibration and flow-related loads. The difficulty in installation, cost, and potential for destroying an engine severely limited the required instrumentation and measurements to adequately define loads of key components such as turbine blades. Also, accurate analytical methodologies for defining internal flow-related loads are just emerging for problems typically found in rocket engines. The difficulty of obtaining measured data and verified analysis methodologies has led to the probabilistic load definition approach. G.L.C.

**N85-27954\*#** Battelle Columbus Labs., Ohio.

**COMPOSITE LOADS SPECTRA FOR SELECT SPACE PROPULSION STRUCTURAL COMPONENTS: PROBABILISTIC LOAD MODEL DEVELOPMENT Abstract Only**

R. KURTH *In* NASA. Lewis Research Center Struct. Integrity and Durability of Reusable Space Propulsion Systems p 77-83 May 1985

(Contract NAS3-24382)

Avail: NTIS HC A09/MF A01 CSCL 20K

This effort is in support of the development of the expert system of computer codes to predict the loads on select structural components of a space propulsion engine. The development will be based primarily on the space shuttle main engine (SSME) test data base. Because of random variations of the many different sources of the loadings on the selected structural components and transients, a probabilistic approach to the problems was adopted. The goal of this task is to characterize all of the individual sources of loads at critical structural locations, such as the turbine blades, the transfer ducts, and liquid oxygen posts, using state-of-the-art probabilistic methods with varying levels of sophistication. The second phase of this work is the development of a composite load model based on a probabilistic synthesis of the individual load model previously developed. This model will be based on the stochastic combination of the load variables and not on the physical process for the combination of the individual loads to the composite load seen by the selected structural components. R.J.F.

**N85-27955\*#** Southwest Research Inst., San Antonio, Tex.

**PROBABILISTIC STRUCTURAL ANALYSIS THEORY DEVELOPMENT Abstract Only**

O. H. BURNSIDE *In* NASA. Lewis Research Center Struct. Integrity and Durability of Reusable Space Propulsion Systems p 85-92 May 1985

(Contract NAS3-24389)

Avail: NTIS HC A09/MF A01 CSCL 20K

The objective of the Probabilistic Structural Analysis Methods (PSAM) project is to develop analysis techniques and computer programs for predicting the probabilistic response of critical structural components for current and future space propulsion systems. This technology will play a central role in establishing system performance and durability. The first year's technical activity is concentrating on probabilistic finite element formulation strategy and code development. Work is also in progress to survey critical materials and space shuttle main engine components. The probabilistic finite element computer program NESSUS (Numerical Evaluation of Stochastic Structures Under Stress) is being developed. The final probabilistic code will have, in the general case, the capability of performing nonlinear dynamic of stochastic structures. It is the goal of the approximate methods effort to increase problem solving efficiency relative to finite element

methods by using energy methods to generate trial solutions which satisfy the structural boundary conditions. These approximate methods will be less computer intensive relative to the finite element approach. R.J.F.

**N85-27956\*#** MARC Analysis Research Corp., Palo Alto, Calif.  
**PROBABILISTIC FINITE ELEMENT DEVELOPMENT Abstract Only**

J. NAGTEGAAL /in NASA. Lewis Research Center Struct. Integrity and Durability of Reusable Space Propulsion Systems p 93-98 May 1985  
 (Contract NAS3-24389)  
 Avail: NTIS HC A09/MF A01 CSCL 20K

The probabilistic finite element computer program known as Numerical Evaluation of Stochastic Structures Under Stress (NESSUS) is being developed for the analysis of critical structural components for reusable space propulsion systems. First year efforts involve the formulation of the probabilistic analysis strategy and the development of a probabilistic linear analysis code. The ultimate goal of the 3-year program is the development of a finite element code capable of performing nonlinear dynamic analysis of structures having stochastic material properties, geometry, and boundary conditions and subjected to random loading. Three levels of sophistication are envisioned for the stochastic description of the structural problem, namely: (1) homogeneous random variable for stiffness, mass, damping, and external loading; (2) stochastic characterization of variables at the element level, with specified interelement correlations; and (3) stochastic interpolation of variables within a finite element. Two alternative probabilistic analysis methods will be developed, allowing for all three levels of modeling sophistication. R.J.F.

**N85-27957\*#** Northwestern Univ., Evanston, Ill.  
**PROBABILISTIC FINITE ELEMENT: VARIATIONAL THEORY Abstract Only**

T. BELYTSCHKO and W. K. LIU /in NASA. Lewis Research Center Struct. Integrity and Durability of Reusable Propulsion Systems p 99-107 May 1985  
 (Contract NAG3-535)  
 Avail: NTIS HC A09/MF A01 CSCL 20K

The goal of this research is to provide techniques which are cost-effective and enable the engineer to evaluate the effect of uncertainties in complex finite element models. Embedding the probabilistic aspects in a variational formulation is a natural approach. In addition, a variational approach to probabilistic finite elements enables it to be incorporated within standard finite element methodologies. Therefore, once the procedures are developed, they can easily be adapted to existing general purpose programs. Furthermore, the variational basis for these methods enables them to be adapted to a wide variety of structural elements and to provide a consistent basis for incorporating probabilistic features in many aspects of the structural problem. Tasks concluded include the theoretical development of probabilistic variational equations for structural dynamics, the development of efficient numerical algorithms for probabilistic sensitivity displacement and stress analysis, and integration of methodologies into a pilot computer code. R.J.F.

**N85-27959\*#** Georgia Inst. of Tech., Atlanta.  
**DYNAMIC CREEP BUCKLING: ANALYSIS OF SHELL STRUCTURES SUBJECTED TO TIME-DEPENDENT MECHANICAL AND THERMAL LOADING Abstract Only**

G. J. SIMITSES, R. L. CARLSON, and R. RIFF /in NASA. Lewis Research Center Struct. Integrity and Durability of Reusable Space Propulsion Systems p 117-120 May 1985  
 (Contract NAG3-534)  
 Avail: NTIS HC A09/MF A01 CSCL 20K

The objective of the present research is to develop a general mathematical model and solution methodologies for analyzing the structural response of thin, metallic shell structures under large transient, cyclic, or static thermomechanical loads. Among the system responses associated with these loads and conditions are thermal buckling, creep buckling, and ratcheting. Thus geometric

and material nonlinearities (of high order) can be anticipated and must be considered in developing the mathematical model. A complete, true ab-initio rate theory of kinematics and kinetics for continuum and curved thin structures, without any restriction on the magnitude of the strains or the deformations, was formulated. The time dependence and large strain behavior are incorporated through the introduction of the time rates of metric and curvature in two coordinate systems: fixed (spatial) and convected (material). The relations between the time derivative and the covariant derivative (gradient) were developed for curved space and motion, so the velocity components supply the connection between the equations of motion and the time rates of change of the metric and curvature tensors. R.J.F.

**N85-27961\*#** National Aeronautics and Space Administration. Lewis Research Center, Cleveland, Ohio.

**INTERACTION OF HIGH-CYCLE AND LOW-CYCLE FATIGUE OF HAYNES 188 ALLOY AT 1400 F DEG Abstract Only**

P. T. BIZON, D. J. THOMA, and G. R. HALFORD /in its Struct. Integrity and Durability of Reusable Space Propulsion Systems p 129-138 May 1985  
 Avail: NTIS HC A09/MF A01 CSCL 20K

The interaction of low-cycle fatigue (LCF) and high-cycle fatigue (HCF) was evaluated at the NASA Lewis Research Center on Haynes 188 alloy at 1400 F. Completely reversed, axial-load, strain-controlled fatigue tests were performed to determine the baseline data for this study. Additional specimens for interaction tests were cycled first at a high strain range for various small portions of expected LCF life followed by a step change to a low strain range to failure in HCF. Failure was defined as complete specimen separation. The resultant lives varied between 10 and 5000 cycles for the low-cycle fatigue tests and between 4500 and 3 million for the high-cycle fatigue tests. For the interaction tests the low-cycle-life portion ranged from 30 and 1000 applied cycles while the high-frequency life ranged from 300 and 300,000 cycles to failure. The step change results showed a significant nonlinear interaction in expected life. Application of a small part of the LCF life drastically decreased the available HCF life as compared with what would have been expected by the classical linear damage rule (LDR). B.W.

**N85-27962\*#** National Aeronautics and Space Administration. Lewis Research Center, Cleveland, Ohio.

**REEXAMINATION OF CUMULATIVE FATIGUE DAMAGE LAWS Abstract Only**

G. R. HALFORD and S. S. MANSON (Case Western Reserve Univ.) /in its Struct. Integrity and Durability of Reusable Space Propulsion Systems p 139-145 May 1985 refs  
 Avail: NTIS HC A09/MF A01 CSCL 20K

Treatment of accumulated fatigue damage in materials and structures subjected to a history of nonsimple repetitive loadings has received a large amount of attention in recent years. A method used for the treatment of complex loading is known as linear damage rule. It was recognized that, this method could result in unconservative predictions of material and structural behavior. An intense flurry of activity followed in the pursuit of alternative methods of analysis that would predict behavior more accurately. So many methods were introduced that it became necessary periodically to prepare review papers placing all the new methods into perspective. The current integrated view regarding the state of the art as it applies to this effort is discussed. The more recently proposed cumulative damage life prediction methods are reviewed. The double linear damage rule (DLDR), which has evolved over the past 20 years, is reexamined with the intent of improving its accuracy and applicability to engineering problems. Modifications are introduced to the analytical formulation to achieve greater compatibility between the DLDR and the so-called damage curve approach, which is an alternative continuous representation of the DLDR. B.W.

## 39 STRUCTURAL MECHANICS

**N85-27963\*#** National Aeronautics and Space Administration. Lewis Research Center, Cleveland, Ohio.

### **CYCLIC STRUCTURAL ANALYSES OF SSME TURBINE BLADES**

A. KAUFMAN and J. M. MANDERSCHIED *In its Struct. Integrity and Durability of Reusable Space Propulsion Systems* p 147-154 May 1985 refs

Avail: NTIS HC A09/MF A01 CSCL 20K

The problems of calculating the structural response of high-temperature space propulsion components such as turbine blades for the fuel turbopump are addressed. The first high-pressure-stage fuel turbine blade (HPFTB) in the liquid-hydrogen turbopump of the space shuttle main engine (SSME) was selected for this study. In the past these blades have cracked in the blade shank region and at the airfoil leading edge adjacent to the platform. To achieve the necessary durability, these blades are currently being cast by using directional solidification. Single-crystal alloys are also being investigated for future SSME applications. The study evaluated the utility of advanced structural analysis methods in assessing the low-cycle fatigue lives of these anisotropic components. The turbine blade airfoil of the high-pressure stage of the SSME fuel turbopump was analyzed because it has a history of rapid crack initiation.

B.W.

**N85-30361\*#** National Aeronautics and Space Administration. Lewis Research Center, Cleveland, Ohio.

### **STRUCTURAL ANALYSIS AND COST ESTIMATE OF AN EIGHT-LEG SPACE FRAME AS A SUPPORT STRUCTURE FOR HORIZONTAL AXIS WIND TURBINES Final Report**

R. L. SIZEMORE, J. R. WINEMILLER, S. T. YEE, and G. R. FREDERICK (Toledo Univ.) Oct. 1983 27 p refs

(Contract DE-AI01-76ET-20320)

(NASA-TM-83470; E-1529; DOE/NASA/20320-49; NAS

1.15:83470) Avail: NTIS HC A03/MF A01 CSCL 20K

A structural analysis was performed and a cost estimate was prepared to determine if an eight-leg space frame tower in which the legs lie on the surface of a hyperboloid of revolution was a suitable alternative to the truss-type tower for application to an intermediate size horizontal axis wind turbine. This tower concept had eight straight pipe elements as its main structural members that lie on the surface of a hyperboloid of revolution. The structural analysis included: response to static loads, determination of vibration characteristics, and investigation of overall frame stability. The design was lighter than the four-leg truss-type tower used for the Mod-O and Mod-OA wind turbines. The estimated cost for fabrication and erection of the hyperboloid tower is less than that for any of the four Mod-OA towers constructed to date. It is concluded that the hyperboloid tower concept is a suitable alternative to the truss-type tower for application to horizontal axis wind turbines.

E.A.K.

**N85-31530\*#** National Aeronautics and Space Administration. Lewis Research Center, Cleveland, Ohio.

### **NONLINEAR CONSTITUTIVE RELATIONS FOR HIGH TEMPERATURE APPLICATION, 1984**

Jun. 1985 368 p refs Symp. held in Cleveland, 15-17 Jun. 1984

(NASA-CP-2369; E-2368; NAS 1.55:2369) Avail: NTIS HC A16/MF A01 CSCL 20K

Nonlinear constitutive relations for high temperature applications were discussed. The state of the art in nonlinear constitutive modeling of high temperature materials was reviewed and the need for future research and development efforts in this area was identified. Considerable research efforts are urgently needed in the development of nonlinear constitutive relations for high temperature applications prompted by recent advances in high temperature materials technology and new demands on material and component performance. Topics discussed include: constitutive modeling, numerical methods, material testing, and structural applications.

**N85-31531\*#** Southwest Research Inst., San Antonio, Tex.

### **A SURVEY OF UNIFIED CONSTITUTIVE THEORIES**

K. S. CHAN, U. S. LINDHOLM, S. R. BODNER (Technion - Israel Inst. of Tech., Haifa), and K. P. WALKER (Engineering Scientific Software, Inc., Smithfield, R.I.) *In NASA. Lewis Research Center Nonlinear Constitutive Relations for High Temp. Appl.*, 1984 p 1-23 Jun. 1985 refs

(Contract NAS3-23925)

Avail: NTIS HC A16/MF A01 CSCL 20K

The state of the art of time temperature dependent elastic viscoplastic constitutive theories which are based on the unified approach were assessed. This class of constitutive theories is characterized by the use of kinetic equations and internal variables with appropriate evolutionary equations for treating all aspects of inelastic deformation including plasticity, creep, and stress relaxation. More than 10 such unified theories which are shown to satisfy the uniqueness and stability criteria imposed by Drucker's postulate and Ponter's inequalities are identified. The theories are compared for the types of flow law, kinetic equation, evolutionary equation of the internal variables, and treatment of temperature dependence. The similarities and differences of these theories are outlined in terms of mathematical formulations and illustrated by comparisons of theoretical calculations with experimental results which include monotonic stress-strain curves, cyclic hysteresis loops, creep and stress relaxation rates, and thermomechanical loops. Numerical methods used for integrating these stiff time temperature dependent constitutive equations are reviewed.

E.A.K.

**N85-31533\*#** Akron Univ., Ohio.

### **THERMOMECHANICAL DEFORMATION IN THE PRESENCE OF METALLURGICAL CHANGES**

D. N. ROBINSON *In NASA. Lewis Research Center Nonlinear Constitutive Relations for High Temp. Appl.*, 1984 p 51-54 Jun. 1985 refs

(Contract NAG3-379)

Avail: NTIS HC A16/MF A01 CSCL 20K

Nonisothermal testing that can be used as a basis of a nonisothermal representation is discussed. Related tests regarding metallurgical changes that occur in other high temperature structural alloys are discussed. A viscoplastic constitutive model capable of qualitatively representing the behavioral features was formulated. This model is used to assess the differences in ultimate life prediction in some typical nonisothermal structural problems when the constitutive model does or does not account for metallurgically induced thermomechanical history dependence.

E.A.K.

**N85-31536\*#** Texas A&M Univ., College Station. Aerospace Engineering Dept.

### **ON THE USE OF INTERNAL STATE VARIABLES IN THERMOVISCOPLASTIC CONSTITUTIVE EQUATIONS**

D. H. ALLEN and J. M. BEEK *In NASA. Lewis Research Center Nonlinear Constitutive Relations for High Temp. Appl.*, 1984 p 83-102 Jun. 1985 refs

(Contract NAG3-491)

Avail: NTIS HC A16/MF A01 CSCL 20K

The general theory of internal state variables are reviewed to apply it to inelastic metals in use in high temperature environments. In this process, certain constraints and clarifications will be made regarding internal state variables. It is shown that the Helmholtz free energy can be utilized to construct constitutive equations which are appropriate for metallic superalloys. Internal state variables are shown to represent locally averaged measures of dislocation arrangement, dislocation density, and intergranular fracture. The internal state variable model is demonstrated to be a suitable framework for comparison of several currently proposed models for metals and can therefore be used to exhibit history dependence, nonlinearity, and rate as well as temperature sensitivity.

E.A.K.

**N85-31538\*#** National Aeronautics and Space Administration. Lewis Research Center, Cleveland, Ohio.

**A COMPARISON OF TWO CONTEMPORARY CREEP-FATIGUE LIFE PREDICTION METHODS Abstract Only**

M. A. MCGAW *In its* Nonlinear Constitutive Relations for High Temp. Appl., 1984 p 125 Jun. 1985

Avail: NTIS HC A16/MF A01 CSCL 20K

A comparison of two contemporary approaches to creep fatigue life prediction, the Continuous Damage Mechanics as developed at ONERA, and Strain Range Partitioning, is presented. The general framework of each of these approaches, both being crack initiation life prediction tools, are examined. The basis for, and implications of each predictive method are discussed, relative to the material class(es) for which each was developed, as well as to their general applicability. Evident is a need for critical experiments capable of discriminating among the models; to this end, the question of choice of experiment and material is addressed. Author

**N85-31541\*#** Texas A&M Univ., College Station. Aerospace Engineering Dept.

**NUMERICAL CONSIDERATIONS IN THE DEVELOPMENT AND IMPLEMENTATION OF CONSTITUTIVE MODELS**

W. E. HAISLER and P. K. IMBRIE *In* NASA. Lewis Research Center Nonlinear Constitutive Relations for High Temp. Appl., 1984 p 169-185 Jun. 1985 refs

(Contract NAG3-491)

Avail: NTIS HC A16/MF A01 CSCL 20K

Several unified constitutive models were tested in uniaxial form by specifying input strain histories and comparing output stress histories. The purpose of the tests was to evaluate several time integration methods with regard to accuracy, stability, and computational economy. The sensitivity of the models to slight changes in input constants was also investigated. Results are presented for In100 at 1350 F and Hastelloy-X at 1800 F. Author

**N85-31542\*#** National Aeronautics and Space Administration. Lewis Research Center, Cleveland, Ohio.

**ON NUMERICAL INTEGRATION AND COMPUTER IMPLEMENTATION OF VISCOPLASTIC MODELS**

T. Y. CHANG (Akron Univ., Ohio), J. P. CHANG (Akron Univ., Ohio), and R. L. THOMPSON *In its* Nonlinear Constitutive Relations for High Temp. Appl., 1984 p 187-200 Jun. 1985 refs

Avail: NTIS HC A16/MF A01 CSCL 20K

Due to the stringent design requirement for aerospace or nuclear structural components, considerable research interests have been generated on the development of constitutive models for representing the inelastic behavior of metals at elevated temperatures. In particular, a class of unified theories (or viscoplastic constitutive models) have been proposed to simulate material responses such as cyclic plasticity, rate sensitivity, creep deformations, strain hardening or softening, etc. This approach differs from the conventional creep and plasticity theory in that both the creep and plastic deformations are treated as unified time-dependent quantities. Although most of viscoplastic models give better material behavior representation, the associated constitutive differential equations have stiff regimes which present numerical difficulties in time-dependent analysis. In this connection, appropriate solution algorithm must be developed for viscoplastic analysis via finite element method. G.L.C.

**N85-31543\*#** National Aeronautics and Space Administration. Lewis Research Center, Cleveland, Ohio.

**TWO SIMPLIFIED PROCEDURES FOR PREDICTING CYCLIC MATERIAL RESPONSE FROM A STRAIN HISTORY**

A. KAUFMAN and V. MORENO (Pratt and Whitney Aircraft, East Hartford, Conn.) *In its* Nonlinear Constitutive Relations for High Temp. Appl., 1984 p 201-219 Jun. 1985 refs

Avail: NTIS HC A16/MF A01 CSCL 20K

Simplified inelastic analysis procedures were developed at NASA Lewis and Pratt & Whitney Aircraft for predicting the stress-strain response at the critical location of a

thermomechanically cycled structure. These procedures are intended primarily for use as economical structural analysis tools in the early design stages of aircraft engine hot section components where nonlinear finite-element analyses would be prohibitively expensive. Both simplified methods use as input the total strain history calculated from a linear elastic analysis. The elastic results are modified to approximate the characteristics of the inelastic cycle by incremental solution techniques. A von Mises yield criterion is used to determine the onset of active plasticity. The fundamental assumption of these methods is that the inelastic strain is local and constrained from redistribution by the surrounding elastic material. G.L.C.

**N85-31545\*#** Akron Univ., Ohio. Dept. of Civil Engineering. **SOME ADVANCES IN EXPERIMENTATION SUPPORTING DEVELOPMENT OF VISCOPLASTIC CONSTITUTIVE MODELS**

J. R. ELLIS and D. N. ROBINSON *In* NASA. Lewis Research Center Nonlinear Constitutive Relations for High Temp. Appl., 1984 p 237-271 Jun. 1985 refs Previously announced as N85-27260

(Contract NAG3-379; W-7405-ENG-26)

Avail: NTIS HC A16/MF A01 CSCL 20K

The development of a biaxial extensometer capable of measuring axial, torsion, and diametral strains to near-microstrain resolution at elevated temperatures is discussed. An instrument with this capability was needed to provide experimental support to the development of viscoplastic constitutive models. The advantages gained when torsional loading is used to investigate inelastic material response at elevated temperatures are highlighted. The development of the biaxial extensometer was conducted in two stages. The first involved a series of bench calibration experiments performed at room temperature. The second stage involved a series of in-place calibration experiments performed at room temperature. A review of the calibration data indicated that all performance requirements regarding resolution, range, stability, and crosstalk had been met by the subject instrument over the temperature range of interest, 21 C to 651 C. The scope of the in-placed calibration experiments was expanded to investigate the feasibility of generating stress relaxation data under torsional loading. B.W. (IAA)

**N85-31546\*#** Michigan State Univ., East Lansing. Dept. of Metallurgy, Mechanics, and Materials Science.

**A COMPARISON OF SMOOTH SPECIMEN AND ANALYTICAL SIMULATION TECHNIQUES FOR NOTCHED MEMBERS AT ELEVATED TEMPERATURES**

J. F. MARTIN *In* NASA. Lewis Research Center Nonlinear Constitutive Relations for High Temp. Appl., 1984 p 273-281 Jun. 1985 refs

(Contract NAG3-51)

Avail: NTIS HC A16/MF A01 CSCL 20K

Experimental strain measurements have been made at the highly strained regions on notched plate specimens that were made of Hastelloy X. Tests were performed at temperatures up to 1,600 F. Variable load patterns were chosen so as to produce plastic and creep strains. Where appropriate, notch root stresses were experimentally estimated by subjecting a smooth specimen to the measured notch root strains. The results of three analysis techniques are presented and compared to the experimental data. The most accurate results were obtained from an analysis procedure that used a smooth specimen and the Neuber relation to simulate the notch root stress-strain response. When a generalized constitutive relation was used with the Neuber relation, good results were also obtained, however, these results were not as accurate as those obtained when the smooth specimen was used directly. Finally, a general finite element program, ANYSIS, was used which resulted in acceptable solutions, but, these were the least accurate predictions. Author

**N85-31548\*#** Cincinnati Univ., Ohio. Dept. of Aerospace Engineering and Applied Mechanics.

## FINITE ELEMENT ANALYSIS OF NOTCH BEHAVIOR USING A STATE VARIABLE CONSTITUTIVE EQUATION

L. T. DAME, D. C. STOFFER, and N. ABUELFOUTOUH /*n* NASA. Lewis Research Center Nonlinear Constitutive Relations for High Temp. Appl., 1984 p 297-310 Jun. 1985 refs (Contract NAS3-23698; NAS3-23927; NAG3-511)

Avail: NTIS HC A16/MF A01 CSCL 20K

The state variable constitutive equation of Bodner and Partom was used to calculate the load-strain response of Inconel 718 at 649 C in the root of a notch. The constitutive equation was used with the Bodner-Partom evolution equation and with a second evolution equation that was derived from a potential function of the stress and state variable. Data used in determining constants for the constitutive models was from one-dimensional smooth bar tests. The response was calculated for a plane stress condition at the root of the notch with a finite element code using constant strain triangular elements. Results from both evolution equations compared favorably with the observed experimental response. The accuracy and efficiency of the finite element calculations also compared favorably to existing methods. Author

**N85-32340\*#** Akron Univ., Ohio. Dept. of Civil Engineering. RESULTS OF AN INTERLABORATORY FATIGUE TEST PROGRAM CONDUCTED ON ALLOY 800H AT ROOM AND ELEVATED TEMPERATURES Final Report

J. R. ELLIS Jul. 1985 38 p refs Sponsored in part by General Atomic Co.

(Contract NAG3-379)

(NASA-CR-174940; NAS 1.26:174940) Avail: NTIS HC A03/MF A01 CSCL 20K

The experimental approach adopted for low cycle fatigue tests of alloy 800H involved the use of electrohydraulic test systems, hour glass geometry specimens, diametral extensometers, and axial strain computers. Attempts to identify possible problem areas were complicated by the lack of reliable data for the heat of Alloy 800H under investigation. The method adopted was to generate definitive test data in an Interlaboratory Fatigue Test Program. The laboratories participating in the program were Argonne National Laboratory, Battelle Columbus, Mar-Test, and NASA Lewis. Fatigue tests were conducted on both solid and tubular specimens at temperatures of 20, 593, and 760 C and strain ranges of 2.0, 1.0, and 0.5 percent. The subject test method can, under certain circumstances, produce fatigue data which are serious in error. This approach subsequently was abandoned at General Atomic Company in favor of parallel gage length specimens and axial extensometers. F.M.R.

**N85-32341\*#** Akron Univ., Ohio. Dept. of Civil Engineering. A CONTINUOUS DAMAGE MODEL BASED ON STEPWISE-STRESS CREEP RUPTURE TESTS Final Report

D. N. ROBINSON Cleveland Jul. 1985 24 p refs

(Contract NAG3-379)

(NASA-CR-174941; NAS 1.26:174941) Avail: NTIS HC A02/MF A01 CSCL 20K

A creep damage accumulation model is presented that makes use of the Kachanov damage rate concept with a provision accounting for damage that results from a variable stress history. This is accomplished through the introduction of an additional term in the Kachanov rate equation that is linear in the stress rate. Specification of the material functions and parameters in the model requires two types of constituting a data base: (1) standard constant-stress creep rupture tests, and (2) a sequence of two-step creep rupture tests. Author

**N85-33520\*#** National Aeronautics and Space Administration. Lewis Research Center, Cleveland, Ohio.

## APPLICATION OF TRACTION DRIVES AS SERVO MECHANISMS

S. H. LOEWENTHAL, D. A. ROHN, and B. M. STEINETZ /*n* NASA. Ames Research Center 19th Aerospace Mech. Symp. p 119-139 Aug. 1985 refs

Avail: NTIS HC A17/MF A01 CSCL 20K

The suitability of traction drives for a wide class of aerospace control mechanisms is examined. Potential applications include antenna or solar array drive positioners, robotic joints, control moment gyro (CMG) actuators and propeller pitch change mechanisms. In these and similar applications the zero backlash, high torsional stiffness, low hysteresis and torque ripple characteristics of traction drives are of particular interest, as is the ability to run without liquid lubrication in certain cases. Wear and fatigue considerations for wet and dry operation are examined along with the tribological performance of several promising self lubricating polymers for traction contracts. The speed regulation capabilities of variable ratio traction drives are reviewed. A torsional stiffness analysis described suggests that traction contacts are relatively stiff compared to gears and are significantly stiffer than the other structural elements in the prototype CMG traction drive analyzed. Discussion is also given of an advanced turboprop propeller pitch change mechanism that incorporates a traction drive. Author

**N85-33541\*#** General Electric Co., Cincinnati, Ohio. Advanced Technology Programs Dept.

## A REVIEW OF PATH-INDEPENDENT INTEGRALS IN ELASTIC-PLASTIC FRACTURE MECHANICS, TASK 4 Interim Report

K. S. KIM Aug. 1985 33 p refs

(Contract NAS3-23940)

(NASA-CR-174956; NAS 1.26:174956) Avail: NTIS HC A03/MF A01 CSCL 20K

The path independent (P-I) integrals in elastic plastic fracture mechanics which have been proposed in recent years to overcome the limitations imposed on the J integral are reviewed. The P-I integrals considered herein are the J integral by Rice, the thermoelastic P-I integrals by Wilson and Yu and by Gurtin, the J\* integral by Blackburn, the J sub theta integral by Ainsworth et al., the J integral by Kishimoto et al., and the delta T sub p and delta T\* sub p integrals by Atluri et al. The theoretical foundation of these P-I integrals is examined with emphasis on whether or not path independence is maintained in the presence of nonproportional loading and unloading in the plastic regime, thermal gradients, and material inhomogeneities. The similarities, differences, salient features, and limitations of these P-I integrals are discussed. Comments are also made with regard to the physical meaning, the possibility of experimental measurement, and computational aspects. Author

**N85-34427\*#** National Aeronautics and Space Administration. Lewis Research Center, Cleveland, Ohio.

## NONLINEAR FLAP-LAG-EXTENSIONAL VIBRATIONS OF ROTATING, PRETWISTED, PRECONED BEAMS INCLUDING CORIOLIS EFFECTS

K. B. SUBRAHMANYAM (NBKR Inst. of Science and Tech.) and K. R. V. KAZA 1985 35 p refs Presented at the 19th Midwestern Mech. Conf., Columbus, Ohio, 9-11 Sep. 1985; sponsored by the Ohio State Univ.

(NASA-TM-87102; E-2598; NAS 1.15:87102) Avail: NTIS HC A03/MF A01 CSCL 20K

The effects of pretwist, precone, setting angle, Coriolis forces and second degree geometric nonlinearities on the natural frequencies, steady state deflections and mode shapes of rotating, torsionally rigid, cantilevered beams were studied. The governing coupled equations of flap lag extensional motion are derived including the effects of large precone and retaining geometric nonlinearities up to second degree. The Galerkin method, with nonrotating normal modes, is used for the solution of both steady state nonlinear equations and linear perturbation equations.

Parametric indicating the individual and collective effects of pretwist, precone, Coriolis forces and second degree geometric nonlinearities on the steady state deflection, natural frequencies and mode shapes of rotating blades are presented. It is indicated that the second degree geometric nonlinear terms, which vanish for zero precone, can produce frequency changes of engineering significance. Further confirmation of the validity of including those generated by MSC NASTRAN. It is indicated that the linear and nonlinear Coriolis effects must be included in analyzing thick blades. The Coriolis effects are significant on the first flatwise and the first edgewise modes. E.A.K.

## 43

## EARTH RESOURCES

Includes remote sensing of earth resources by aircraft and spacecraft; photogrammetry; and aerial photography.

**A85-10244\*#** Environmental Research Inst. of Michigan, Ann Arbor.

**COMPARISON OF ATMOSPHERIC CORRECTION ALGORITHMS FOR THE COASTAL ZONE COLOR SCANNER**

F. J. TANIS (Michigan, Environmental Research Institute, Ann Arbor, MI) and S. C. JAIN (MONITEQ Ltd., Concord, Ontario, Canada) IN: International Symposium on Remote Sensing of Environment, 17th, Ann Arbor, MI, May 9-13, 1983, Proceedings. Volume 2. Ann Arbor, MI, Environmental Research Institute of Michigan, 1984, p. 923-935. refs (Contract NAS3-22892)

Before Nimbus-7 Coastal Zone Color Scanner (CZC) data can be used to distinguish between coastal water types, methods must be developed for the removal of spatial variations in aerosol path radiance. These can dominate radiance measurements made by the satellite. An assessment is presently made of the ability of four different algorithms to quantitatively remove haze effects; each was adapted for the extraction of the required scene-dependent parameters during an initial pass through the data set. The CZCS correction algorithms considered are (1) the Gordon (1981, 1983) algorithm; (2) the Smith and Wilson (1981) iterative algorithm; (3) the pseudo-optical depth method; and (4) the residual component algorithm. O.C.

## 44

## ENERGY PRODUCTION AND CONVERSION

Includes specific energy conversion systems, e.g., fuel cells and batteries; global sources of energy; fossil fuels; geophysical conversion; hydroelectric power; and wind power.

**A85-10652\*#** Westinghouse Electric Corp., Pittsburgh, Pa.  
**MEASURED EFFECTS OF WIND TURBINE GENERATION AT THE BLOCK ISLAND POWER COMPANY**

V. F. WILREKER, R. F. SMITH, P. H. STILLER (Westinghouse Electric Corp., Pittsburgh, PA), G. W. SCOT (EnerTech Corp., Norwich, VT), and R. K. SHALTENS (NASA, Lewis Research Center, Cleveland, OH) American Power Conference, Chicago, IL, Apr. 24-26, 1984, Paper. 10 p. Research supported by the U.S. Department of Energy. refs (Contract DEN3-275; DEN3-354)

Data measurements made on the NASA MOD-OA 200-kw wind-turbine generator (WTG) installed on a utility grid form the basis for an overall performance analysis. Fuel displacement/savings, dynamic interactions, and WTG excitation (reactive-power) control effects are studied. Continuous recording of a large number of electrical and mechanical variables on FM

magnetic tape permit evaluation and correlation of phenomena over a bandwidth of at least 20 Hz. Because the wind-power penetration reached peaks of 60 percent, the impact of wind fluctuation and wind-turbine/diesel-utility interaction is evaluated in a worst-case scenario. The speed-governor dynamics of the diesel units exhibited an underdamped response, and the utility operation procedures were not altered to optimize overall WTG/utility performance. Primary findings over the data collection period are: a calculated 6.7-percent reduction in fuel consumption while generating 11 percent of the total electrical energy; acceptable system voltage and frequency fluctuations with WTG connected; and applicability of WTG excitation schemes using voltage, power, or VARS as the controlled variable. Author

**A85-11345\*** Cleveland State Univ., Ohio.

**CONTROL ALGORITHMS AND COMPUTER SIMULATION OF A STAND-ALONE PHOTOVOLTAIC VILLAGE POWER SYSTEM**

P. P. GROOMPOS, J. E. CULLER (Cleveland State University, Cleveland, OH), R. DELOMBARD, A. F. RATAJCZAK (NASA, Lewis Research Center, Cleveland, OH), and R. CULL (NASA, Lewis Research Center; Standard Oil Company of Ohio, Cleveland, OH) IN: Photovoltaic Solar Energy Conference; Proceedings of the Fifth International Conference, Athens, Greece, October 17-21, 1983. Dordrecht, D. Reidel Publishing Co., 1984, p. 353-357. (Contract NCC3-16)

At Stand-Alone Photovoltaic (SAPV) power systems increase in size and load diversity, the design and simulation of control subsystems takes on added importance. These SAPV systems represent 'mini utilities' with commensurate controls requirements, albeit with the added complexity of the energy source (sunlight received) being an uncontrollable variable. This paper briefly describes a stand-alone photovoltaic power/load system computerized simulation model. The model was tested against operational data from the Schuchuli stand-alone village photovoltaic system and has achieved acceptable levels of simulation accuracy. The model can be used to simulate system designs although with probable battery modification. Author

**A85-15800\*** Cleveland State Univ., Ohio.

**NEAR-OPTIMUM DESIGN OF GAAS-BASED CONCENTRATOR SPACE SOLAR CELLS FOR 80 C OPERATION**

C. GORADIA, M. GHALLA-GORADIA (Cleveland State University, Cleveland, OH), and H. CURTIS (NASA, Lewis Research Center, Cleveland, OH) Applied Physics Communications (ISSN 0277-9374), vol. 4, no. 2-3, 1984, p. 97-119. NASA-supported research. refs

Using a detailed computer simulation model and reasonable values of optical, geometrical and material parameters from current published literature, parameter optimization studies were performed on two cell geometries, namely, the circular geometry for a Cassegrainian concentrator with 100 AMO, 80 C operation and the rectangular geometry for a venetian blind concentrator with 20 AMO, 80 C operation. For each cell geometry, three cell configurations were considered: p/n AlGaAs/GaAs; n/p AlGaAs/GaAs; and, n/p GaAs shallow homojunction. The studies show the possibility of designing GaAs-based space solar cells with beginning-of-life efficiencies exceeding 22 percent at 20 to 100 AMO, 80 C and probable efficiency degradation of less than 15 percent after a 70 percent reduction in diffusion length in each cell region. Author



**A85-18608\*** National Aeronautics and Space Administration. Lewis Research Center, Cleveland, Ohio.

## CHARACTERISTICS OF ARC CURRENTS ON A NEGATIVELY BIASED SOLAR CELL ARRAY IN A PLASMA

D. B. SNYDER (NASA, Lewis Research Center, Cleveland, OH) (IEEE, U.S. Defense Nuclear Agency, U.S. Department of Energy, and NASA, Annual Conference on Nuclear and Space Radiation Effects, 21st, Colorado Springs, CO, July 23-25, 1984) IEEE Transactions on Nuclear Science (ISSN 0018-9499), vol. NS-31, Dec. 1984, p. 1584-1587. Previously announced in STAR as N84-27824. refs

The time dependence of the emitted currents during arcing on solar cell arrays is being studied. The arcs are characterized using three parameters: the voltage change of the array during the arc (i.e., the charge lost), the peak current during the arc, and the time constant describing the arc current. This paper reports the dependence of these characteristics on two array parameters, the interconnect bias voltage and the array capacitance to ground. It was found that the voltage change of the array during an arc is nearly equal to the bias voltage. The array capacitance, on the other hand, influences both the peak current and the decay time constant of the arc. Both of these characteristics increase with increasing capacitance. Author

**A85-19948\*** Cleveland State Univ., Ohio.

## APPLICABILITY OF THE MEYER-NELDEL RULE TO SOLAR CELLS

C. GORADIA (Cleveland State University, Cleveland, OH) and V. G. WEIZER (NASA, Lewis Research Center, Cleveland, OH) Applied Physics Letters (ISSN 0003-6951), vol. 45, Dec. 15, 1984, p. 1298-1300.

A comparison of data taken on high quality silicon, GaAs, and GaInAs solar cells with those taken on a variety of homojunction, heterojunction, and metal-insulator-semiconductor devices indicates that while the Meyer-Neldel rule may be applicable to certain types of solar cells it is not applicable to well-behaved, diffusion-controlled homojunction devices. It cannot be used, therefore, as a universal rule to predict maximum achievable solar cell voltages. Author

## A85-21297\*# Westinghouse Electric Corp., Pittsburgh, Pa. FUEL CELL POWER PLANT ECONOMIC AND OPERATIONAL CONSIDERATIONS

J. R. LANCE (Westinghouse Electric Corp., Advanced Energy Systems Div., Pittsburgh, PA) American Society of Mechanical Engineers, Annual Energy Sources Technology Conference and Exhibit, 7th, New Orleans, LA, Feb. 11-17, 1984. 8 p. Research supported by the U.S. Department of Energy. (Contract DEN3-290) (ASME PAPER 84-AES-7)

Fuel cell power plants intended for electric utility and cogeneration applications are now in the design and construction stage. This paper describes economic and operational considerations being used in the development and design of plants utilizing air cooled phosphoric acid fuel cells. Fuel cell power plants have some unique characteristics relative to other types of power plants. As a result it was necessary to develop specific definitions of the fuel cell power plant characteristics in order to perform cost of electricity calculations. This paper describes these characteristics and describes the economic analyses used in the Westinghouse fuel cell power plant program. Author

**A85-24668\*** Cincinnati Univ., Ohio.

## HIGH-VOLTAGE SOLAR-CELL CHIP

V. J. KAPOOR, G. J. VALCO, G. G. SKEBE (Cincinnati University, Cincinnati, OH), and J. C. EVANS, JR. (NASA, Lewis Research Center, Cleveland, OH) Journal of Applied Physics (ISSN 0021-8979), vol. 57, Feb. 15, 1985, p. 1343-1346. refs (Contract NAG3-80)

Integrated circuit technology has been successfully applied to the design and fabrication of 0.5 x 0.5-cm planar multijunction solar-cell chips. Each of these solar cells consisted of six voltage-generating unit cells monolithically connected in series and

fabricated on a 75-micron-thick, p-type, single crystal, silicon substrate. A contact photolithic process employing five photomask levels together with a standard microelectronics batch-processing technique were used to construct the solar-cell chip. The open-circuit voltage increased rapidly with increasing illumination up to 5 AM1 suns where it began to saturate at the sum of the individual unit-cell voltages at a maximum of 3.0 V. A short-circuit current density per unit cell of 240 mA/sq cm was observed at 10 AM1 suns. Author

**A85-28080\*** National Aeronautics and Space Administration. Lewis Research Center, Cleveland, Ohio.

## EFFECT OF SOLAR-CELL JUNCTION GEOMETRY ON OPEN-CIRCUIT VOLTAGE

V. G. WEIZER and M. P. GODLEWSKI (NASA, Lewis Research Center, Cleveland, OH) Journal of Applied Physics (ISSN 0021-8979), vol. 57, March 15, 1985, p. 2292-2294. refs

Simple analytical models have been found that adequately describe the voltage behavior of both the stripe junction and dot junction grating cells as a function of junction area. While the voltage in the former case is found to be insensitive to junction area reduction, significant voltage increases are shown to be possible for the dot junction cell. With regard to cells in which the junction area has been increased in a quest for better performance, it was found that (1) texturation does not affect the average saturation current density  $J_0$ , indicating that the texturation process is equivalent to a simple extension of junction area by a factor of square root of 3 and (2) the vertical junction cell geometry produces a sizable decrease in  $J_0$  that, unfortunately, is more than offset by the effects of attendant areal increases. Author

**A85-32639\*** Cleveland State Univ., Ohio.

## THEORY OF THE HIGH BASE RESISTIVITY N(+)PP(+) SILICON SOLAR CELL AND ITS APPLICATION TO RADIATION DAMAGE EFFECTS

C. GORADIA (Cleveland State University, Cleveland, OH) and I. WEINBERG (NASA, Lewis Research Center, Cleveland, OH) Journal of Applied Physics (ISSN 0021-8979), vol. 57, May 15, 1985, p. 4752-4760. refs

Particulate radiation in space is a principal source of silicon solar cell degradation, and an investigation of cell radiation damage at higher base resistivities appears to have implication toward increasing solar cell and, therefore, useful satellite lifetimes in the space environment. However, contrary to expectations, it has been found that for cells with resistivities of 84 and 1250 ohm cm, the radiation resistance decreases as cell base resistivity increases. An analytical solar-cell computer model was developed with the objective to determine the reasons for this unexpected behavior. The present paper has the aim to describe the analytical model and its use in interpreting the behavior, under irradiation, of high-resistivity solar cells. Attention is given to boundary conditions at the space-charge region edges, cell currents, cell voltages, the generation of the theoretical I-V characteristic, experimental results, and computer calculations. G.R.

**A85-35602\*#** National Aeronautics and Space Administration. Lewis Research Center, Cleveland, Ohio.

## PHOTOVOLTAICS - THE ENDLESS SPRING

H. W. BRANDHORST, JR. (NASA, Lewis Research Center, Cleveland, OH) IN: Photovoltaic Specialists Conference, 17th, Kissimmee, FL, May 1-4, 1984, Conference Record. New York, Institute of Electrical and Electronics Engineers, 1984, p. 1-6. Previously announced in STAR as N84-31782.

An overview of the developments in the photovoltaic field over the past decade or two is presented. Accomplishments in the terrestrial field are reviewed along with projections and challenges toward meeting cost goals. The contrasts and commonality of space and terrestrial photovoltaics are presented. Finally, a strategic philosophy of photovoltaics research highlighting critical factors, appropriate directions, emerging opportunities, and challenges of the future is given. Author



**A85-35604\*#** National Aeronautics and Space Administration, Washington, D.C.

**THE NASA PHOTOVOLTAIC TECHNOLOGY PROGRAM**

J. P. MULLIN, J. C. LORIA (NASA, Washington, DC), and H. W. BRANDHORST, JR. (NASA, Lewis Research Center, Cleveland, OH) IN: Photovoltaic Specialists Conference, 17th, Kissimmee, FL, May 1-4, 1984, Conference Record. New York, Institute of Electrical and Electronics Engineers, 1984, p. 12-16. Previously announced in STAR as N85-32426.

The NASA Office of Aeronautical and Space Technology OAST Program in space photovoltaics is reviewed. From the perspective of national landmark mission requirements and five year and 25-year long range plans, the texture of the program is revealed. Planar silicon and concentrator GaAs array technology advances are discussed. Advances in lightweight (50 micro cell) arrays and radiation tolerance research are presented. Recent progress in cascade cells and ultralightweight GaAs planar cells is noted. Progress in raising silicon cell voltage to its theoretical maximum is detailed. Advanced concepts such as plasmon converters and the Long Duration Exposure Facility LDEF flight experiments pertaining to solar cell and array technology are also shown.

M.A.C.

**A85-35617\*#** National Aeronautics and Space Administration, Lewis Research Center, Cleveland, Ohio.

**VOLTAGE CONTROLLING MECHANISMS IN LOW RESISTIVITY SILICON SOLAR CELLS - A UNIFIED APPROACH**

V. G. WEIZER, C. K. SWARTZ, R. E. HART, and M. P. GODLEWSKI (NASA, Lewis Research Center, Cleveland, OH) IN: Photovoltaic Specialists Conference, 17th, Kissimmee, FL, May 1-4, 1984, Conference Record. New York, Institute of Electrical and Electronics Engineers, 1984, p. 117-122. Previously announced in STAR as N84-20916. refs

An experimental technique capable of resolving the dark saturation current into its base and emitter components is used as the basis of an analysis in which the voltage limiting mechanisms were determined for a variety of high voltage, low resistivity silicon solar cells. The cells studied include the University of Florida hi-low emitter cell, the NASA and the COMSAT multi-step diffused cells, the Spire Corporation ion-implanted emitter cell, and the University of New South Wales MINMIS and MINP cells. The results proved to be, in general, at variance with prior expectations. Most surprising was the finding that the MINP and the MINMIS voltage improvements are due, to a considerable extent, to a previously unrecognized optimization of the base component of the saturation current. This result is substantiated by an independent analysis of the material used to fabricate these devices.

Author

**A85-35707\*#** National Aeronautics and Space Administration, Lewis Research Center, Cleveland, Ohio.

**STATUS OF DOE AND AID STAND-ALONE PHOTOVOLTAIC SYSTEM FIELD TESTS**

W. J. BIFANO, R. DELOMBARD, A. F. RATAJCZAK, and L. R. SCUDDER (NASA, Lewis Research Center, Cleveland, OH) IN: Photovoltaic Specialists Conference, 17th, Kissimmee, FL, May 1-4, 1984, Conference Record. New York, Institute of Electrical and Electronics Engineers, 1984, p. 1159-1167. refs

The NASA Lewis Research Center (LeRC) is managing stand-alone photovoltaic (PV) system projects sponsored by the U.S. Department of Energy (DOE) and the U.S. Agency for International Development (AID). The DOE project includes village PV power demonstration projects in Gabon (four sites) and the Marshall Islands, and PV-powered vaccine refrigerator systems in six countries. The AID project includes a large village power system, a farmhouse system and two water pumping-irrigation systems in Tunisia, a water pumping/grain grinding system in Upper Volta, five medical clinic systems in four countries, PV-powered vaccine refrigerator systems in 18 countries and a PV-powered remote earth station in Indonesia. This paper reviews these PV projects and summarizes significant findings to date.

Author

**A85-36750\*** National Aeronautics and Space Administration, Lewis Research Center, Cleveland, Ohio.

**METHOD FOR EVALUATING WIND TURBINE WAKE EFFECTS ON WIND FARM PERFORMANCE**

H. E. NEUSTADTER and D. A. SPERA (NASA, Lewis Research Center, Cleveland, OH) IN: ASME Wind Energy Symposium, 3rd, Dallas, TX, February 18-20, 1985. New York, American Society of Mechanical Engineering, 1985, p. 61-67.

A method of testing the performance of a cluster of wind turbine units an data analysis equations are presented which together form a simple and direct procedure for determining the reduction in energy output caused by the wake of an upwind turbine. This method appears to solve the problems presented by data scatter and wind variability. Test data from the three-unit Mod-2 wind turbine cluster at Goldendale, Washington, are analyzed to illustrate the application of the proposed method. In this sample case the reduction in energy was found to be about 10 percent when the Mod-2 units were separated a distance equal to seven diameters and winds were below rated.

Author

**A85-45380\*** National Aeronautics and Space Administration, Lewis Research Center, Cleveland, Ohio.

**DESIGN CONSIDERATIONS FOR A 10-KW INTEGRATED HYDROGEN-OXYGEN REGENERATIVE FUEL CELL SYSTEM**

M. A. HOBERECHT, T. B. MILLER, L. L. RIEKER, and O. D. GONZALEZ-SANABRIA (NASA, Lewis Research Center, Cleveland, OH) IN: IECEC '84: Advanced energy systems - Their role in our future; Proceedings of the Nineteenth Intersociety Energy Conversion Engineering Conference, San Francisco, CA, August 19-24, 1984. Volume 1. La Grange Park, IL, American Nuclear Society, 1984, p. 240-246. Previously announced in STAR as N84-23023.

Integration of an alkaline fuel cell subsystem with an alkaline electrolysis subsystem to form a regenerative fuel cell (RFC) system for low earth orbit (LEO) applications characterized by relatively high overall round trip electrical efficiency, long life, and high reliability is possible with present state of the art technology. A hypothetical 10 kW system computer modeled and studied based on data from ongoing contractual efforts in both the alkaline fuel cell and alkaline water electrolysis areas. The alkaline fuel cell technology is under development utilizing advanced cell components and standard Shuttle Orbiter system hardware. The alkaline electrolysis technology uses a static water vapor feed technique and scaled up cell hardware is developed. The computer aided study of the performance, operating, and design parameters of the hypothetical system is addressed.

E.A.K.

**A85-45384\*** National Aeronautics and Space Administration, Lewis Research Center, Cleveland, Ohio.

**DESIGN OF A 1-KWH BIPOLAR NICKEL HYDROGEN BATTERY**

R. L. CATALDO (NASA, Lewis Research Center, Cleveland, OH) IN: IECEC '84: Advanced energy systems - Their role in our future; Proceedings of the Nineteenth Intersociety Energy Conversion Engineering Conference, San Francisco, CA, August 19-24, 1984. Volume 1. La Grange Park, IL, American Nuclear Society, 1984, p. 264-269. Previously announced in STAR as N84-23024. refs

The design of a nickel hydrogen battery utilizing bipolar construction in a common pressure vessel is discussed. Design features are as follows: 40 ampere-hour capacity, 1 kWh stored energy as a 24 cell battery, 1.8 kW delivered in a LEO Cycle and maximum pulse power of 18.0 kW.

Author

## 44 ENERGY PRODUCTION AND CONVERSION

**A85-45385\*** National Aeronautics and Space Administration. Lewis Research Center, Cleveland, Ohio.

### **TEARDOWN ANALYSIS OF A TEN CELL BIPOLAR NICKEL-HYDROGEN BATTERY**

M. A. MANZO, O. D. GONZALEZ-SANABRIA, J. S. HERZAU, and L. J. SCAGLIONE (NASA, Lewis Research Center, Cleveland, OH) IN: IECEC '84: Advanced energy systems - Their role in our future; Proceedings of the Nineteenth Intersociety Energy Conversion Engineering Conference, San Francisco, CA, August 19-24, 1984. Volume 1. La Grange Park, IL, American Nuclear Society, 1984, p. 270-278. Previously announced in STAR as N84-23026. refs

Design studies have identified bipolar nickel-hydrogen batteries as an attractive storage option for high power, high voltage applications. A pre-prototype Ni-H<sub>2</sub> battery was designed, assembled and tested in the early phases of a concept verification program. The initial stack was built with available hardware and components from past programs. The stack performed well. After 2000 low-earth-orbit cycles the stack was dismantled in order to allow evaluation and analysis of the design and components. The results of the teardown analysis and recommended modifications are discussed. Author

**A85-45386\*** National Aeronautics and Space Administration. Lewis Research Center, Cleveland, Ohio.

### **SEPARATOR DEVELOPMENT AND TESTING OF NICKEL-HYDROGEN CELLS**

O. D. GONZALEZ-SANABRIA and M. A. MANZO (NASA, Lewis Research Center, Cleveland, OH) IN: IECEC '84: Advanced energy systems - Their role in our future; Proceedings of the Nineteenth Intersociety Energy Conversion Engineering Conference, San Francisco, CA, August 19-24, 1984. Volume 1. La Grange Park, IL, American Nuclear Society, 1984, p. 279-286. Previously announced in STAR as N84-22712.

The components, design, and operating characteristics of Ni-H<sub>2</sub> cells and batteries were improved. A separator development program was designed to develop a separator that is resistant to penetration by oxygen and loose active material from the nickel electrode, while retaining the required chemical and thermal stability, reservoir capability, and high ionic conductivity. The performance of the separators in terms of cell operating voltage was to at least match that of state-of-the-art separators while eliminating the separator problems. The separators were submitted to initial screening tests and those which successfully completed the tests were built into Ni-H<sub>2</sub> cells for short term testing. The separators with the best performance are tested for long term performance and life. S.L.

**A85-45391\*** Hughes Research Labs., Malibu, Calif.

### **LONG LIFE NICKEL ELECTRODES FOR A NICKEL-HYDROGEN CELL. III - RESULTS OF AN ACCELERATED TEST AND FAILURE ANALYSES**

H. S. LIM and S. A. VERZWYVELT (Hughes Research Laboratories, Malibu, CA) IN: IECEC '84: Advanced energy systems - Their role in our future; Proceedings of the Nineteenth Intersociety Energy Conversion Engineering Conference, San Francisco, CA, August 19-24, 1984. Volume 1. La Grange Park, IL, American Nuclear Society, 1984, p. 312-318. refs (Contract NAS3-22238)

Nineteen different designs of nickel electrodes were tested in Ni/H<sub>2</sub> boiler plate cells in an accelerated low earth orbit cycle regime to the end of their life. The failure analyses of these cells showed that the major performance changes due to the cycling was a severe reduction of their high rate discharge capability rather than an absolute capacity reduction. Many physical changes of the nickel electrodes were observed after the cycling test. These changes include dimensional expansion, sinter rupture, loose black powdering of the active material, morphology changes, active material migration, increase of pore volume, change of pore distribution, and increase of surface area. All of these were caused by active material expansion with cycling. Among these changes, the morphology change which involves migration of active material

away from the current collecting nickel sinter appears to be that most responsible for the reduction of the rate capability. Author

**A85-45408\*** TriSolar Corp., Bedford, Mass.

### **MICROPROCESSOR CONTROL OF PHOTOVOLTALIC SYSTEMS**

A. R. MILLNER and D. L. KAUFMAN (TriSolar Corp., Bedford, MA) IN: IECEC '84: Advanced energy systems - Their role in our future; Proceedings of the Nineteenth Intersociety Energy Conversion Engineering Conference, San Francisco, CA, August 19-24, 1984. Volume 1. La Grange Park, IL, American Nuclear Society, 1984, p. 422-427. (Contract DEN3-310)

The present low power CMOS microprocessor controller for photovoltaic power systems possesses three programs, which are respectively intended for (1) conventional battery-charging systems with state-of-charge estimation and sequential shedding of subarrays and loads, (2) maximum power-controlled battery-charging systems, and (3) variable speed dc motor drives. Attention is presently given to the development of this terrestrial equipment for spacecraft use. O.C.

**A85-45438\*** National Aeronautics and Space Administration. Lewis Research Center, Cleveland, Ohio.

### **ADVANCED DESIGNS FOR IPV NICKEL-HYDROGEN CELLS**

J. J. SMITHRICK, M. A. MANZO, and O. GONZALEZ-SANABRIA (NASA, Lewis Research Center, Cleveland, OH) IN: IECEC '84: Advanced energy systems - Their role in our future; Proceedings of the Nineteenth Intersociety Energy Conversion Engineering Conference, San Francisco, CA, August 19-24, 1984. Volume 1. La Grange Park, IL, American Nuclear Society, 1984, p. 631-635. Previously announced in STAR as N84-23025. refs

Advanced designs for individual pressure vessel nickel-hydrogen cells have been conceived which should improve the cycle life at deep depths-of-discharge. Features of the designs which are new and not incorporated in either of the contemporary cells (Air Force/Hughes, Comsat) are: (1) use of alternate methods of oxygen recombination, (2) use of serrated edge separators to facilitate movement of gas within the cell while still maintaining required physical contact with the wall wick, and (3) use of an expandable stack to accommodate some of the nickel electrode expansion. The designs also consider electrolyte volume requirements over the life of the cells, and are fully compatible with the Air Force/Hughes design. Author

**A85-45443\*** National Aeronautics and Space Administration. Lewis Research Center, Cleveland, Ohio.

### **RESULTS OF ELECTRIC-VEHICLE PROPULSION SYSTEM PERFORMANCE ON THREE LEAD-ACID BATTERY SYSTEMS**

J. G. EWASHINKA (NASA, Lewis Research Center, Cleveland, OH) IN: IECEC '84: Advanced energy systems - Their role in our future; Proceedings of the Nineteenth Intersociety Energy Conversion Engineering Conference, San Francisco, CA, August 19-24, 1984. Volume 2. La Grange Park, IL, American Nuclear Society, 1984, p. 727-735. Previously announced in STAR as N84-25166.

Three types of state of the art 6 V lead acid batteries were tested. The cycle life of lead acid batteries as a function of the electric vehicle propulsion system design was determined. Cycle life, degradation rate and failure modes with different battery types (baseline versus state of the art tubular and thin plate batteries) were compared. The effects of testing strings of three versus six series connected batteries on overall performance were investigated. All three types do not seem to have an economically feasible battery system for the propulsion systems. The tubular plate batteries on the load leveled profile attained 235 cycles with no signs of degradation and minimal capacity loss. E.A.K.

**A85-45512\*** National Aeronautics and Space Administration. Lewis Research Center, Cleveland, Ohio.

**MOD-2 WIND TURBINE FIELD OPERATIONS EXPERIENCE**

L. H. GORDON (NASA, Lewis Research Center, Cleveland, OH) IN: IECEC '84: Advanced energy systems - Their role in our future; Proceedings of the Nineteenth Intersociety Energy Conversion Engineering Conference, San Francisco, CA, August 19-24, 1984. Volume 4. La Grange Park, IL, American Nuclear Society, 1984, p. 2363-2368.

The Mod-2 wind turbine is now in a 2-year research/experimental operations phase which offers a unique opportunity to study the effects of single and multiple wind turbines interacting with each other, the power grid, and the environment. This paper addresses the field operations and research testing experienced at the Mod-2 Cluster Goodnoe Hills Research Test Site near Goldendale, WA. Field operation, both routine and nonroutine, are discussed as well as the role of the participating utility. Technical areas discussed pertain to system performance and loads. Specific research tests relating to acoustics, TV interference, and wake effects are also discussed. Author

**A85-45513\*** National Aeronautics and Space Administration. Lewis Research Center, Cleveland, Ohio.

**AILERON CONTROLS FOR WIND TURBINE APPLICATIONS**

D. R. MILLER and R. L. PUTHOFF (NASA, Lewis Research Center, Cleveland, OH) IN: IECEC '84: Advanced energy systems - Their role in our future; Proceedings of the Nineteenth Intersociety Energy Conversion Engineering Conference, San Francisco, CA, August 19-24, 1984. Volume 4. La Grange Park, IL, American Nuclear Society, 1984, p. 2369-2373. Previously announced in STAR as N85-11458.

Horizontal axis wind turbines which utilize partial or full variable blade pitch to regulate rotor speed were examined. The weight and costs of these systems indicated a need for alternate methods of rotor control. Aileron control is an alternative which has potential to meet this need. Aileron control rotors were tested on the Mod-O wind turbine to determine their power regulation and shutdown characteristics. Test results for a 20 and 38 percent chord aileron control rotor are presented. Test is shown that aileron control is a viable method for safety for safely controlling rotor speed, following a loss of general load. E.A.K.

**A85-45517\*** General Electric Co., Philadelphia, Pa.

**ADVANCED MULTI-MEGAWATT WIND TURBINE DESIGN FOR UTILITY APPLICATION**

W. C. PIJAWKA (General Electric Co., King of Prussia, PA) ANS, SAE, ACS, AIAA, ASME, et al., Intersociety Energy Conversion Engineering Conference on Advanced Energy Systems Their role in our future, 19th, San Francisco, CA, Aug. 19-24, 1984, Paper. 6 p. DOE-sponsored research. (Contract DEN3-153)

A NASA/DOE program to develop a utility class multimegawatt wind turbine, the MOD-5A, is described. The MOD-5A features a 400 foot diameter rotor which is teetered and positioned upwind of the tower; a 7.3 megawatt power rating with a variable speed electric generating system; and a redundant rotor support and torque transmission structure. The rotor blades were fabricated from an epoxy-bonded wood laminate material which was a successful outgrowth of the MOD-OA airfoil design. Preliminary data from operational tests carried out at the NASA Plum Brook test facility are presented. I.H.

**N85-10444\*** Hughes Aircraft Co., El Segundo, Calif.

**ADVANCED NICKEL-HYDROGEN CELL CONFIGURATION STUDY Final Report**

E. ADLER and F. PEREZ Oct. 1984 74 p refs

(Contract NAS3-22249)

(NASA-CR-174775; NAS 1.26:174775; E9787) Avail: NTIS HC A04/MF A01 CSCL 10C

Three nickel hydrogen battery designs, individual pressure vessel (IPV), common pressure vessel (CPV), and a bipolar battery module were studied. Weight, system complexity and cost were compared for a satellite operating in a 6 hour, 5600 nautical mile

orbit. The required energy storage is 52 kWh. A 25% improvement in specific energy is observed by employing a bipolar battery versus a battery comprised of hundreds of IPV's. Further weight benefits are realized by the development of light weight technologies in the bipolar design. E.A.K.

**N85-10445\*** Cleveland State Univ., Ohio.

**MANUAL OF PHOSPHORIC ACID FUEL CELL POWER PLANT OPTIMIZATION MODEL AND COMPUTER PROGRAM Final Report**

C. Y. LU and K. A. ALKASAB May 1984 66 p refs

(Contract NCC3-17; DE-AI21-80ET-17088)

(NASA-CR-174721; DOE/NASA/0017-3; NAS 1.26:174721)

Avail: NTIS HC A04/MF A01 CSCL 10B

An optimized cost and performance model for a phosphoric acid fuel cell power plant system was derived and developed into a modular FORTRAN computer code. Cost, energy, mass, and electrochemical analyses were combined to develop a mathematical model for optimizing the steam to methane ratio in the reformer, hydrogen utilization in the PAFC plates per stack. The nonlinear programming code, COMPUTE, was used to solve this model, in which the method of mixed penalty function combined with Hooke and Jeeves pattern search was chosen to evaluate this specific optimization problem. Author

**N85-10447\*** Cleveland State Univ., Ohio.

**MANUAL OF PHOSPHORIC ACID FUEL CELL STACK THREE-DIMENSIONAL MODEL AND COMPUTER PROGRAM Final Report**

C. Y. LU and K. A. ALKASAB May 1984 66 p refs

(Contract NCC3-17; DE-AI21-80ET-17088)

(NASA-CR-174722; DOE/NASA/0017-4; NAS 1.26:174722)

Avail: NTIS HC A04/MF A01 CSCL 10B

A detailed distributed mathematical model of phosphoric acid fuel cell stack have been developed, with the FORTRAN computer program, for analyzing the temperature distribution in the stack and the associated current density distribution on the cell plates. Energy, mass, and electrochemical analyses in the stack were combined to develop the model. Several reasonable assumptions were made to solve this mathematical model by means of the finite differences numerical method. Author

**N85-11455\*** Clarkson Coll. of Technology, Potsdam, N.Y.

**ELECTROCATALYSIS OF FUEL CELL REACTIONS: INVESTIGATION OF ALTERNATE ELECTROLYTES Final Report**

D. T. CHIN, K. L. HSUEH, and H. H. CHANG Jan. 1984 114 p refs

(Contract NAG3-238; DE-AI21-80ET-17088)

(NASA-CR-174753; DOE/NASA/0238-1; NAS 1.26:174753)

Avail: NTIS HC A06/MF A01 CSCL 10A

Oxygen reduction and transport properties of the electrolyte in the phosphoric acid fuel cell are studied. The areas covered were: (1) development of a theoretical expression for the rotating ring disk electrode technique; (2) determination of the intermediate reaction rate constants for oxygen reduction on platinum in phosphoric acid electrolyte; (3) determination of oxygen reduction mechanism in trifluoromethanesulfonic acid (TFMSA) which was considered as an alternate electrolyte for the acid fuel cells; and (4) the measurement of transport properties of the phosphoric acid electrolyte at high concentrations and temperatures. Author

**N85-11456\*** Cleveland State Univ., Ohio.

**PHOSPHORIC ACID FUEL CELL POWER PLANT SYSTEM PERFORMANCE MODEL AND COMPUTER PROGRAM Final Report**

K. A. ALKASAB and C. Y. LU Jan. 1984 134 p refs

(Contract NCC3-17; DE-AI21-80ET-17088)

(NASA-CR-174638; DOE/NASA/0017-1; NAS 1.26:174638)

Avail: NTIS HC A07/MF A01 CSCL 10A

A FORTRAN computer program was developed for analyzing the performance of phosphoric acid fuel cell power plant systems. Energy mass and electrochemical analysis in the reformer, the

## 44 ENERGY PRODUCTION AND CONVERSION

shaft converters, the heat exchangers, and the fuel cell stack were combined to develop a mathematical model for the power plant for both atmospheric and pressurized conditions, and for several commercial fuels. Author

**N85-11457\*#** Rensselaer Polytechnic Inst., Troy, N.Y. Dept. of Electrical, Computer and Systems Engineering.

### **RESEARCH ON GALLIUM ARSENIDE DIFFUSED JUNCTION SOLAR CELLS Final Report, 1 Oct. 1982 - 30 Jun. 1984**

J. M. BORREGO and S. K. GHANDI Oct. 1984 54 p refs (Contract NAG3-188)

(NASA-CR-174057; NAS 1.26:174057) Avail: NTIS HC A04/MF A01 CSCL 10A

The feasibility of using bulk GaAs for the fabrication of diffused junction solar cells was determined. The effects of thermal processing of GaAs was studied, and the quality of starting bulk GaAs for this purpose was assessed. These cells are to be made by open tube diffusion techniques, and are to be tested for photovoltaic response under AMO conditions. B.G.

**N85-11458\*#** National Aeronautics and Space Administration. Lewis Research Center, Cleveland, Ohio.

### **AILERON CONTROLS FOR WIND TURBINE APPLICATIONS**

D. R. MILLER and R. L. PUTOFF Nov. 1984 14 p refs Presented at the Intersociety Conversion Eng. Conf., San Francisco, 19-24 Aug. 1984

(Contract DE-AI01-76ET-20320)

(NASA-TM-86867; DOE/NASA/20320-60; E-2330; NAS 1.15:86867) Avail: NTIS HC A02/MF A01 CSCL 10A

Horizontal axis wind turbines which utilize partial or full variable blade pitch to regulate rotor speed were examined. The weight and costs of these systems indicated a need for alternate methods of rotor control. Aileron control is an alternative which has potential to meet this need. Aileron control rotors were tested on the Mod-O wind turbine to determine their power regulation and shutdown characteristics. Test results for a 20 and 38% chord aileron control rotor are presented. Test is shown that aileron control is a viable method for safety for safely controlling rotor speed, following a loss of general load. E.A.K.

**N85-12465\*#** National Aeronautics and Space Administration. Lewis Research Center, Cleveland, Ohio.

### **NASA REDOX STORAGE SYSTEM DEVELOPMENT PROJECT Final Report**

N. H. HAGEDORN Oct. 1984 48 p refs

(Contract DE-AI04-80AL-12726)

(NASA-TM-83677; E-2125; NAS 1.15:83677) Avail: NTIS HC A03/MF A01 CSCL 10C

The Redox Storage System Technology Project was jointly supported by the U.S. Department of Energy and NASA. The objectives of the project were to develop the Redox flow battery concept and to probe its technical and economic viability. The iron and chromium redox couples were selected as the reactants. Membranes and electrodes were developed for the original mode of operating at 25 C with the reactants separated by an ion-exchange membrane. Analytical capabilities and system-level operating concepts were developed and verified in a 1-kW, 13-kWh preprototype system. A subsequent change was made in operating mode, going to 65 C and using mixed reactants. New membranes and a new electrode catalyst were developed, resulting in single cell operation as high as 80 mA/sq cm with energy efficiencies greater than 80 percent. Studies indicate a likely system cost of about \$75/kWh. Standard Oil of Ohio (Sohio) has undertaken further development of the Redox system. An exclusive patent license was obtained from NASA by Sohio. Transfer of Redox technology to Sohio is supported by the NASA Technology Utilization Office. Author

**N85-13371\*#** United Technologies Corp., South Windsor, Conn. Power Systems Div.

### **REGENERATIVE FUEL CELL ENERGY STORAGE SYSTEM FOR A LOW EARTH ORBIT SPACE STATION**

R. E. MARTIN, J. GAROW, and K. B. MICHAELS Aug. 1984 146 p refs

(Contract NAS3-22234)

(NASA-CR-174802; NAS 1.26:174802; FCR-6128) Avail: NTIS HC A07/MF A01 CSCL 10B

Results of a study to define the characteristics of a regenerative fuel cell energy storage system for a large space station operating in low earth orbit (LEO) are presented. The regenerative fuel cell system employs an alkaline electrolyte fuel cell with the option of employing either an alkaline or a solid polymer electrolyte electrolyzer. R.S.F.

**N85-13892\*#** National Aeronautics and Space Administration. Lewis Research Center, Cleveland, Ohio.

### **DYNAMIC POWER SYSTEMS FOR POWER GENERATION**

R. E. ENGLISH *In its* Space Power p 137-149 Apr. 1984 refs

Avail: NTIS HC A14/MF A01 CSCL 10B

The characteristics of dynamic power systems have considerable potential value, especially for the space station. The base of technology that makes these dynamic power systems practical is reviewed. The following types of power-generating systems are examined herein: organic Rankine cycle, potassium Rankine cycle, Brayton cycle, and Stirling cycle. R.S.F.

**N85-16291\*#** Westinghouse Electric Corp., Pittsburgh, Pa. Advanced Energy Systems Div.

### **GAS COOLED FUEL CELL SYSTEMS TECHNOLOGY DEVELOPMENT Final Report**

J. M. FERET Aug. 1983 329 p refs

(Contract DEN3-390; DE-AI01-80ET-17088)

(NASA-CR-174732; DOE/NASA/0290-1; NAS 1.26:174732)

Avail: NTIS HC A15/MF A01 CSCL 10B

The first phase of a planned multiphase program to develop a Phosphoric is addressed. This report describes the efforts performed that culminated in the: (1) Establishment of the preliminary design requirements and system conceptual design for the nominally rated 375 kW PAFC module and is interfacing power plant systems; (2) Establishment of PAFC component and stack performance, endurance, and design parameter data needed for design verification for power plant application; (3) Improvement of the existing PAFC materials data base and establishment of materials specifications and process procedures for the cell components; and (4) Testing of 122 subscale cell atmospheric test for 110,000 cumulative test hours, 12 subscale cell pressurized tests for 15,000 cumulative test hours, and 12 pressurized stack test for 10,000 cumulative test hours. B.W.

**N85-16292\*#** Life Systems, Inc., Cleveland, Ohio.

### **ENGINEERING MODEL SYSTEM STUDY FOR A REGENERATIVE FUEL CELL: STUDY REPORT**

B. J. CHANG, F. H. SCHUBERT, A. J. KOVACH, and R. A. WYNVEEN Sep. 1984 91 p refs

(Contract NAS3-21287)

(NASA-CR-174801; NAS 1.26:174801; LSI-TR-376-30) Avail: NTIS HC A05/MF A01 CSCL 10A

Key design issues of the regenerative fuel cell system concept were studied and a design definition of an alkaline electrolyte based engineering model system or low Earth orbit missions was completed. Definition of key design issues for a regenerative fuel cell system include gaseous reactant storage, shared heat exchangers and high pressure pumps. A power flow diagram for the 75 kW initial space station and the impact of different regenerative fuel cell modular sizes on the total 5 year to orbit weight and volume are determined. System characteristics, an isometric drawing, component sizes and mass and energy balances are determined for the 10 kW engineering model system. An open loop regenerative fuel cell concept is considered for integration of the energy storage system with the life support system of the

space station. Technical problems and their solutions, pacing technologies and required developments and demonstrations for the regenerative fuel cell system are defined. E.A.K.

**N85-16293\*#** Georgia Tech Research Inst., Atlanta.  
**INFRARED TECHNOLOGY FOR SATELLITE POWER CONVERSION Semiannual Status Report**  
 D. P. CAMPBELL, M. A. GOUKER, and J. J. GALLAGHER 11 Dec. 1984 26 p refs  
 (Contract NAG3-282)  
 (NASA-CR-174266; NAS 1.26:174266) Avail: NTIS HC A03/MF A01 CSCL 10A

Successful fabrication of bismuth bolometers led to the observation of antenna action from array elements. Fabrication of the best antennas arrays was made more facile with finding that increased argon flow during the dc sputtering produced more uniform bismuth films and bonding to antennas must be done with the substrate temperature below 100 C. Higher temperatures damaged the bolometers. During the testing of the antennas, it was found that the use of a quasi-optical system provided a uniform radiation field. Groups of antennas were bonded in series and in parallel with the parallel configuration showing the greater response. R.S.F.

**N85-16299\*#** National Aeronautics and Space Administration. Lewis Research Center, Cleveland, Ohio.  
**SHUTDOWN CHARACTERISTICS OF THE MOD-O WIND TURBINE WITHAILERON CONTROLS Final Report**  
 D. R. MILLER and R. D. CORRIGAN 1984 23 p refs  
 Presented at the Horizontal-Axis Wind Turbine Technol. Workshop, Cleveland, 8-10 May 1984  
 (Contract DE-AI01-76ET-20320)  
 (NASA-TM-86918; DOE/NASA/20320-61; E-2410; NAS 1.15:86918) Avail: NTIS HC A02/MF A01 CSCL 10B

Horizontal-axis wind turbines utilize partial or full variable blade pitch to regulate rotor speed. The weight and costs of these systems indicated a need for alternate methods of rotor control. Aileron control is an alternative which has potential to meet this need. The NASA Lewis Research Center has been experimentally testing aileron control rotors on the Mod-U wind turbine to determine their power regulation and shutdown characteristics. Experimental and analytical shutdown test results are presented for a 38 percent chord aileron-control rotor. These results indicated that the 38 percent chord ailerons provided overspeed protection over the entire Mod-O operational windspeed range, and had a no-load equilibrium tip speed ratio of 1.9. Thus, the 38 percent chord ailerons had much improved aerodynamic braking capability when compared with the first aileron-control rotor having 20 percent chord ailerons. B.W.

**N85-16300\*#** Garrett Turbine Engine Co., Phoenix, Ariz.  
**ADVANCED TECHNOLOGY COGENERATION SYSTEM CONCEPTUAL DESIGN STUDY: CLOSED CYCLE GAS TURBINES Final Report**  
 E. A. T. MOCK and H. C. DAUDET Oct. 1983 296 p Prepared in cooperation with Gibbs and Hill, Inc., New York, N.Y., Foster-Wheeler Co., Houston, Tex., and Little (Arthur D.) Co., Santa Monica, Calif.  
 (Contract DEN3-215; DE-AI01-77ET-13111)  
 (NASA-CR-168222; DOE/NASA/0215-1; NAS 1.26:168222; GTEC31-4773) Avail: NTIS HC A13/MF A01 CSCL 10B

The results of a three task study performed for the Department of Energy under the direction of the NASA Lewis Research Center are documented. The thermal and electrical energy requirements of three specific industrial plants were surveyed and cost records for the energies consumed were compiled. Preliminary coal fired atmospheric fluidized bed heated closed cycle gas turbine and steam turbine cogeneration system designs were developed for each industrial plant. Preliminary cost and return-on-equity values were calculated and the results compared. The best of the three sites was selected for more detailed design and evaluation of both closed cycle gas turbine and steam turbine cogeneration systems during Task II. Task III involved characterizing the industrial

sector electrical and thermal loads for the 48 contiguous states, applying a family of closed cycle gas turbine and steam turbine cogeneration systems to these loads, and conducting a market penetration analysis of the closed cycle gas turbine cogeneration system. Author

**N85-17421\*#** Toledo Univ., Ohio.  
**THERMAL-STRESS ANALYSIS FOR A WOOD COMPOSITE BLADE Final Report**  
 K. C. FU and A. HARB Jul. 1984 119 p refs  
 (Contract NAG3-373; DE-AI01-79ET-20320)  
 (NASA-CR-174794; DOE/NASA/0373-1; NAS 1.26:174794)  
 Avail: NTIS HC A06/MF A01 CSCL 20K

A thermal-stress analysis of a wind turbine blade made of wood composite material is reported. First, the governing partial differential equation on heat conduction is derived, then, a finite element procedure using variational approach is developed for the solution of the governing equation. Thus, the temperature distribution throughout the blade is determined. Next, based on the temperature distribution, a finite element procedure using potential energy approach is applied to determine the thermal-stress distribution. A set of results is obtained through the use of a computer, which is considered to be satisfactory. All computer programs are contained in the report. B.W.

**N85-17422\*#** United Technologies Corp., South Windsor, Conn. Power Systems Div.  
**ELECTRIC UTILITY ACID FUEL CELL STACK TECHNOLOGY ADVANCEMENT Final Report**  
 J. V. CONGDON, G. J. GOLLER, G. J. GREISING, J. J. OBRIEN, S. A. RANDALL, G. J. SANDELLI, R. D. BREAUULT, G. W. AUSTIN, S. BOPSE, and R. D. COYKENDALL Nov. 1984 158 p refs  
 (Contract DEN3-191; DE-AI21-80ET-17088)  
 (NASA-CR-174804; DOE/NASA/0191-1; NAS 1.26:174804; FCR-4684F) Avail: NTIS HC A08/MF A01 CSCL 10A

The principal effort under this program was directed at the fuel cell stack technology required to accomplish the initial feasibility demonstrations of increased cell stack operating pressures and temperatures, increased cell active area, incorporation of the ribbed substrate cell configuration at the above conditions, and the introduction of higher performance electrocatalysts. The program results were successful with the primary accomplishments being: (1) fabrication of 10 sq ft ribbed substrate, cell components including higher performing electrocatalysts; (2) assembly of a 10 sq ft, 30-cell short stack; and (3) initial test of this stack at 120 psia and 405 F. These accomplishments demonstrate the feasibility of fabricating and handling large area cells using materials and processes that are oriented to low cost manufacture. An additional accomplishment under the program was the testing of two 3.7 sq ft short stacks at 12 psia/405 F to 5400 and 4500 hours respectively. These tests demonstrate the durability of the components and the cell stack configuration to a nominal 5000 hours at the higher pressure and temperature condition planned for the next electric utility power plant. R.S.F.

**N85-18451\*#** Georgia Inst. of Tech., Atlanta.  
**TECHNOLOGY FOR SATELLITE POWER CONVERSION Interim Technical Report**  
 D. P. CAMPBELL, M. A. GOUKER, C. SUMMERS, and J. J. GALLAGHER 5 Oct. 1984 80 p refs  
 (Contract NAG3-282)  
 (NASA-CR-174335; NAS 1.26:174335) Avail: NTIS HC A05/MF A01 CSCL 10A

Techniques for satellite electromagnetic energy transfer and power conversion at millimeter and infrared wavelengths are discussed. The design requirements for rectenna receiving elements are reviewed for both coherent radiation sources and Earth thermal infrared emission. Potential power transmitters including gyrotrons, free electron lasers, and CO2 lasers are assessed along with the rectification properties of metal-oxide metal diode power converters. M.G.

## 44 ENERGY PRODUCTION AND CONVERSION

**N85-19511\*#** Stonehart Associates, Inc., Madison, Conn.  
**PREPARATION AND EVALUATION OF ADVANCED CATALYSTS FOR PHOSPHORIC ACID FUEL CELLS** Final Report

P. STONEHART, J. BARIS, J. HOCKMUTH, and P. PAGLIARO  
Jun. 1984 138 p  
(Contract DEN3-176; DE-AI21-80ET-17088)  
(NASA-CR-168223; NAS 1.26:168223) Avail: NTIS HC A07/MF A01 CSCL 10A

The platinum electrocatalysts were characterized for their crystallite sizes and the degree of dispersion on the carbon supports. One application of these electrocatalysts was for anodic oxidation of hydrogen in hot phosphoric acid fuel cells, coupled with the influence of low concentrations of carbon monoxide in the fuel gas stream. In a similar way, these platinum on carbon electrocatalysts were evaluated for oxygen reduction in hot phosphoric acid. Binary noble metal alloys were prepared for anodic oxidation of hydrogen and noble metal-refractory metal mixtures were prepared for oxygen reduction. An exemplar alloy of platinum and palladium (50/50 atom %) was discovered for anodic oxidation of hydrogen in the presence of carbon monoxide, and patent disclosures were submitted. For the cathode, platinum-vanadium alloys were prepared showing improved performance over pure platinum. Preliminary experiments on electrocatalyst utilization in electrode structures showed low utilization of the noble metal when the electrocatalyst loading exceeded one weight percent on the carbon.

A.R.H.

**N85-20530\*** National Aeronautics and Space Administration.  
Lewis Research Center, Cleveland, Ohio.

**SCREEN PRINTED INTERDIGITATED BACK CONTACT SOLAR CELL Patent**

C. R. BARAONA, G. A. MAZARIS, and A. T. CHAI, inventors (to NASA) 23 Oct. 1984 6 p Filed 10 Feb. 1983 Supersedes N83-20374 (21 - 10, p 1557)  
(NASA-CASE-LEW-13414-1; NAS 1.71:LEW-13414-1;  
US-PATENT-4,478,879; US-PATENT-APPL-SN-465364;  
US-PATENT-CLASS-427-85; US-PATENT-CLASS-136-256)  
Avail: US Patent and Trademark Office CSCL 10A

Interdigitated back contact solar cells are made by screen printing dopant materials onto the back surface of a semiconductor substrate in a pair of interdigitated patterns. These dopant materials are then diffused into the substrate to form junctions having configurations corresponding to these patterns. Contacts having configurations which match the patterns are then applied over the junctions.

Official Gazette of the U.S. Patent and Trademark Office

**N85-20535\*#** National Aeronautics and Space Administration.  
Lewis Research Center, Cleveland, Ohio.

**LITHIUM COUNTERDOPED SILICON SOLAR CELL Patent Application**

I. WEINBERG and H. W. BRANDHORST, JR., inventors (to NASA) 7 Nov. 1984 10 p  
(NASA-CASE-LEW-14177-1; NAS 1.71:LEW-14177-1;  
US-PATENT-APPL-SN-669140) Avail: NTIS HC A02/MF A01 CSCL 10A

The resistance to radiation damage of an n(+)p boron doped silicon solar cell is improved by lithium counterdoping. Even though lithium is an n-dopant in silicon, the lithium is introduced in small enough quantities so that the cell base remains p-type. The lithium is introduced into the solar cell wafer by implantation of lithium ions whose energy is about 50 keV. After this lithium implantation, the wafer is annealed in a nitrogen atmosphere at 375 C for two hours.

NASA

**N85-20545\*#** Michigan State Univ., East Lansing. Div. of Engineering Research.

**IMPROVED MODELS FOR INCREASING WIND PENETRATION, ECONOMICS AND OPERATING RELIABILITY** Final Report

R. A. SCHLUETER, G. L. PARK, G. SIGARI, and T. COSTI Apr. 1984 198 p refs  
(Contract NAG3-399)  
(NASA-CR-175538; NAS 1.26:175538; DE85-000865;  
DOE/NBM-1077) Avail: NTIS HC A09/MF A01 CSCL 10A

The need for wind power prediction in order to enable larger wind power penetrations and improve the economics and reliability of power system operation is discussed. Methods for estimating turbulence and prediction of diurnal wind power prediction are reviewed. A method is presented to predict meteorological event induced wind power variation from measurements of wind speed at reference meteorological towers that encircle all wind turbine clusters and from sites within the wind turbine clusters. The methodology uses a recursive least squares model and requires: (1) detection of even propagation direction; and (2) determination of delays between groups of measurements at reference meteorological towers and those measurements at towers in the array. Proper filtering of the data and methods for switching reference sites and delays for the transition from one frontal system to another are also discussed. The performance of the prediction methodology on data sets from both sites was quite good and indicates one or more hour ahead prediction of wind power for meteorological events is feasible.

DOE

**N85-21768\*** National Aeronautics and Space Administration.  
Lewis Research Center, Cleveland, Ohio.

**SOLAR ENERGY CONVERTER USING SURFACE PLASMA WAVES Patent**

L. M. ANDERSON, inventor (to NASA) 13 Nov. 1984 7 p  
Filed 19 Apr. 1983 Supersedes N83-26258 (21 - 15, p 2430)  
(NASA-CASE-LEW-13827-1; NAS 1.71:LEW-13827-1;  
US-PATENT-4,482,778; US-PATENT-APPL-SN-486470;  
US-PATENT-CLASS-136-246; US-PATENT-CLASS-136-225;  
US-PATENT-CLASS-357-30) Avail: US Patent and Trademark Office CSCL 10A

Sunlight is dispersed over a diffraction grating formed on the surface of a conducting film on a substrate. The angular dispersion controls the effective grating period so that a matching spectrum of surface plasmons is excited for parallel processing on the conducting film. The resulting surface plasmons carry energy to an array of inelastic tunnel diodes. This solar energy converter does not require different materials for each frequency band, and sunlight is directly converted to electricity in an efficient manner by extracting more energy from the more energetic photons.

Official Gazette of the U.S. Patent and Trademark Office

**N85-22499\*#** National Aeronautics and Space Administration.  
Lewis Research Center, Cleveland, Ohio.

**DISCHARGES ON A NEGATIVELY BIASED SOLAR CELL ARRAY IN A CHARGED-PARTICLE ENVIRONMENT**

D. B. SNYDER In its Spacecraft Environ. Interactions Technol. p 379-388 Mar. 1985 refs Previously announced as N84-23690

Avail: NTIS HC A99/MF E03 CSCL 10A

The charging behavior of a negatively biased solar cell array when subjected to a charged particle environment is studied in the ion density range from 200 to 12,000 ions/sq cm with the applied bias range of -500 to -1400 V. The profile of the surface potentials across the array is related to the presence of discharges. At the low end of the ion density range the solar cell cover slides charge to from 0 to +5 volts independent of the applied voltage. No discharges are seen at bias voltages as large as -1400 V. At the higher ion densities the cover slide potential begins to fluctuate, and becomes significantly negative. Under these conditions discharges can occur. The threshold bias voltage for discharges decreases with increasing ion density. A condition for discharges emerging from the experimental observations is that the average coverslide potential must be more negative than -4 V. The observations presented suggest that the plasma potential near



the array becomes negative before a discharge occurs. This suggests that discharges are driven by an instability in the plasma.

Author

**N85-23242\*#** National Aeronautics and Space Administration. Lewis Research Center, Cleveland, Ohio.

## DEVELOPMENT OF LARGE, HORIZONTAL-AXIS WIND TURBINES Final Report

D. H. BALDWIN and J. KENNARD (Sverdrup Technology, Inc., Middleburg Heights, Ohio) Mar. 1985 15 p refs (Contract DE-AI01-76ET-20320) (NASA-TM-86950; E-2471; DOE/NASA/20320-62; NAS 1.15:86950) Avail: NTIS HC A02/MF A01 CSCL 10B

A program to develop large, horizontal-axis wind turbines is discussed. The program is directed toward developing the technology for safe, reliable, environmentally acceptable large wind turbines that can generate a significant amount of electricity at costs competitive with those of conventional electricity-generating systems. In addition, these large wind turbines must be fully compatible with electric utility operations and interface requirements. Several ongoing projects in large-wind-turbine development are directed toward meeting the technology requirements for utility applications. The machines based on first-generation technology (Mod-OA and Mod-1) successfully completed their planned periods of experimental operation in June, 1982. The second-generation machines (Mod-2) are in operation at selected utility sites. A third-generation machine (Mod-5) is under contract. Erection and initial operation of the Mod-5 in Hawaii should take place in 1986. Each successive generation of technology increased reliability and energy capture while reducing the cost of electricity. These advances are being made by gaining a better understanding of the system-design drivers, improving the analytical design tools, verifying design methods with operating field data, and incorporating new technology and innovative designs. Information is given on the results from the first- and second-generation machines (Mod-OA, -1, and -2), the status of the Department of Interior, and the status of the third-generation wind turbine (Mod-5).

R.J.F.

**N85-23243\*#** National Aeronautics and Space Administration. Lewis Research Center, Cleveland, Ohio.

## OPERATIONAL PERFORMANCE OF THE PHOTOVOLTAIC-POWERED GRAIN MILL AND WATER PUMP AT TANGAYE, BURKINA FASO (FORMERLY UPPER VOLTA) Final Report

J. E. MARTZ and A. F. ROBERTS (Michigan Univ., Ann Arbor) Mar. 1985 28 p refs (Contract NASA ORDER DSB-5710-2-79) (NASA-TM-86970; E-2496; NAS 1.15:86970) Avail: NTIS HC A03/MF A01 CSCL 10B

A photovoltaic (PV) system powering a grain mill and water pump was installed in the remote African village of Tangaye, Burkina Faso (formerly Upper Volta) under the sponsorship of the U.S. Agency for International Development (AID) and by the National Aeronautics and Space Administration (NASA) Lewis Research Center (LeRC) in early 1979. The present report covers the second two years of operation from April 1981 through June 1983. During this time, the grain mill and water pump were operational 96 and 88 percent of the time respectively, and the PV system generated sufficient electricity to enable the grinding of about 111 metric tons of finely ground flour and the pumping of over 5000 cm<sup>3</sup> of water from the 10 m deep well. The report includes a description of the current configuration of the system, a review of system performance, a discussion of the socioeconomic impact of the system on the villagers and a summary of results and conclusions covering the entire four-year period.

Author

**N85-25941\*#** Engelhard Industries, Inc., Edison, N.J. Specialty Chemicals Div.

## DEVELOP AND TEST FUEL CELL POWERED ON-SITE INTEGRATED TOTAL ENERGY SYSTEMS. PHASE 3: FULL-SCALE POWER PLANT DEVELOPMENT Quarterly Technical Progress Report, May - Jul. 1984

A. KAUFMAN, S. PUDICK, C. L. WANG, J. WERTH, and J. A. WHELAN 6 Nov. 1984 20 p (Contract DEN3-241; DE-AI01-80ET-17088) (NASA-CR-174887; DOE/NASA/0241-14; NAS 1.26:174887) Avail: NTIS HC A02/MF A01 CSCL 10A

Two 25-cell, 13 inch x 23 inch (4kW) stacks were started up to evaluate the reliability of component and stack technology developed through the end of 1983. Both stacks started up well and are running satisfactorily on hydrogen-air after 1900 hours and 800 hours, respectively. A synthetic-reformat mixing station is nearing completion, and both stacks will be operated on reformat fuel. A stack-protection control system was placed in operation for Stack No. 2, and a similar set-up is in preparation for Stack No. 1. This system serves to change operating conditions or shut the stack down to avoid deleterious effects from nonstack-related upsets. The capability will greatly improve changes of obtaining meaningful long-term test data.

E.A.K.

**N85-27377\*#** General Electric Co., Schenectady, N. Y. Advanced Energy Programs Dept.

## PARAMETRIC STUDY OF POTENTIAL EARLY COMMERCIAL POWER PLANTS TASK 3-A MHD COST ANALYSIS Final Technical Report, Apr. 1983

Apr. 1983 51 p (Contract DEN3-244) (NASA-CR-175839; NAS 1.26:175839) Avail: NTIS HC A04/MF A01 CSCL 10B

The development of costs for an MHD Power Plant and the comparison of these costs to a conventional coal fired power plant are reported. The program is divided into three activities: (1) code of accounts review; (2) MHD pulverized coal power plant cost comparison; (3) operating and maintenance cost estimates. The scope of each NASA code of account item was defined to assure that the recently completed Task 3 capital cost estimates are consistent with the code of account scope. Improvement confidence in MHD plant capital cost estimates by identifying comparability with conventional pulverized coal fired (PCF) power plant systems is undertaken. The basis for estimating the MHD plant operating and maintenance costs of electricity is verified.

E.A.K.

**N85-27385\*#** National Aeronautics and Space Administration. Lewis Research Center, Cleveland, Ohio.

## EFFECT OF PRECIPITATION ON WIND TURBINE PERFORMANCE Final Report

R. D. CORRIGAN and R. D. DEMIGLIO (Sverdrup, Inc.) May 1985 23 p refs (Contract DE-AI01-76ET-20320) (NASA-TM-86986; E-2530; DOE/NASA/20320-64; NAS 1.15:86986) Avail: NTIS HC A02/MF A01 CSCL 10A

The effects of precipitation on wind turbine power output was analyzed. The tests were conducted on the two bladed Mod-0 horizontal axis wind turbine with three different rotor configurations. Experimental data from these tests are presented which clearly indicate that the performance of the Mod-0 wind turbine is affected by rain. Light rainfall degraded performance by as much as 20 percent while heavy rainfall degraded performance by as much as 30 percent. Snow mixed with drizzle degraded performance by as much as 36 percent at low windspeeds. Also presented are the results of an analysis to predict the effect of rain on wind turbine performance. This analysis used a blade element/momentum code with modified airfoil characteristics to account for the effect of rain and predicted a loss in performance of 31 percent in high winds with moderate rainfall rates. These predicted results agreed well with experimental data.

Author



## 44 ENERGY PRODUCTION AND CONVERSION

**N85-27387\*#** National Aeronautics and Space Administration. Lewis Research Center, Cleveland, Ohio.

### **CYCLING PERFORMANCE OF THE IRON-CHROMIUM REDOX ENERGY STORAGE SYSTEM**

R. F. GAHN, N. H. HAGEDORN, and J. A. JOHNSON 1985 19 p refs Proposed for presentation at the 20th Intersoc. Energy Conversion Eng. Conf., Miami Beach, Fla., 18-23 Aug. 1985; sponsored by SAE, ANS, ASME, IEEE, AIAA, ACS, and AICHE (Contract DE-AI04-80AL-12726)

(NASA-TM-87034; E-2590; DOE/NASA/12726-25; NAS 1.15:87034) Avail: NTIS HC A02/MF A01 CSCL 10C

Extended charge-discharge cycling of this electrochemical storage system at 65 C was performed on 14.5 sq cm single cells and a four cell, 867 sq cm bipolar stack. Both the anolyte and catholyte reactant fluids contained 1 molar concentrations of iron and chromium chlorides in hydrochloric acid and were separated by a low-selectivity, cation-exchange membrane. The effect of cycling on the chromium electrode and the cation-exchange membrane was determined. Bismuth and bismuth-lead catalyzed chromium electrodes and a radiation-grafted polyethylene membrane were evaluated by cycling between 5 and 85 percent state-of-charge at 80 mA/sq cm and by periodic charge-discharge polarization measurements to 140 mA/sq cm. Gradual performance losses were observed during cycling but were recoverable by completely discharging the system. Good scale-up to the 867 sq cm stack was achieved. The only difference appeared to be an unexplained resistive-type loss which resulted in a 75 percent W-hr efficiency (at 80 mA/sq cm versus 81 percent for the 14.5 sq cm cell). A new rebalance cell was developed to maintain reactant ionic balance. The cell successfully reduced ferric ions in the iron reactant stream to ferrous ions while chloride ions were oxidized to chlorine gas. Author

**N85-28444\*#** National Aeronautics and Space Administration. Lewis Research Center, Cleveland, Ohio.

### **INITIAL PERFORMANCE OF ADVANCED DESIGNS FOR IPV NICKEL-HYDROGEN CELLS**

J. J. SMITHRICK 23 Aug. 1985 11 p refs Presented at 20th Intersoc. Energy Conversion Eng. Conf. (IECEC), Miami Beach, Fla., 18-23 Aug. 1985; sponsored by SAE, ANS, ASME, IEEE, AIAA, ACS and American Institute of Chemical Engineers (NASA-TM-87029; E-2585; NAS 1.15:87029) Avail: NTIS HC A02/MF A01 CSCL 10C

Advanced designs for individual pressure vessel nickel hydrogen cells were conceived which should improve the life cycle at deep depths of discharge and improve thermal management. Features of the designs which are new and not incorporated in either of the contemporary cells (Air Force/Hughes, Comsat) are: (1) the use of alternate methods of oxygen recombination, (2) use of serrated edge separators to facilitate movement of gas within the cell while still maintaining required physical contact with the wall wick, and (3) use of an expandable stack to accommodate some of the nickel electrode expansion. The designs also consider electrolyte volume requirements over the life of the cells, and are fully compatible with the Air Force/Hughes design. R.J.F.

**N85-29363\*#** Cleveland State Univ., Ohio.

### **CONCEPTUAL DESIGN OF A FIXED-PITCH WIND TURBINE GENERATOR SYSTEM RATED AT 400 KILOWATTS Final Report**

A. PINTZ, R. KASUBA, and J. SPRING Jun. 1984 86 p refs Sponsored in part by DOE

(Contract NCC3-6; DE-AI01-79ET-20320)

(NASA-CR-174877; NAS 1.26:174877; DOE/NASA/0006-1)

Avail: NTIS HC A05/MF A01 CSCL 10B

The design and cost aspects of a fixed pitch, 400 kW Wind Turbine Generator (WTG) concept are presented. Improvements in reliability and cost reductions were achieved with fixed pitch operation and by incorporating recent advances in WTG technology. The specifications for this WTG concept were as follows: (1) A fixed pitch, continuous wooden rotor was to be provided by the Gougeon Bros. Co. (2) An 8 leg hyperboloid tower that showed promise as a low cost structure was to be used. (3) Only

commercially available components and parts that could be easily fabricated were to be considered. (4) Design features deemed desirable based on recent NASA research efforts were to be incorporated. Detailed costs and weight estimates were prepared for the second machine and a wind farm of 12 WTG's. The calculated cost of energy for the fixed pitch, twelve unit windfarm is 11.5 cents/kW hr not including the cost of land and access roads. The study shows feasibility of fixed pitch, intermediate power WTG operation. Author

**N85-29364\*#** Toledo Univ., Ohio.

### **WAKE EFFECTS ON THE AERODYNAMIC PERFORMANCE OF HORIZONTAL AXIS WIND TURBINES**

A. A. AFJEH Aug. 1984 176 p refs

(Contract NCC3-5; DE-AI01-76ET-20320)

(NASA-CR-174920; DOE/NASA/0005-1; NAS 1.26:174920)

Avail: NTIS HC A09/MF A01 CSCL 10A

Success of vortex theories in the performance analysis of horizontal axis wind turbines depends greatly upon accurate specification of the geometry of the vortex wake. Two analysis methods were developed, a new simplified free wake method (SFW) and a prescribed wake method. An earlier wake model of helicopter rotors is extended for wind turbine applications, the fast free wake method (FFW). The FFW was accomplished by partitioning the flow field downstream of the rotor into three regions: (1) the near wake, modeled as a series of straight vortex lines; (2) the intermediate wake, modeled as a number of vortex rings; and (3) the far wake, taken to be a semi-infinite cylindrical wake. In the SFW, a new wake model is proposed. The model assumes that the wake is composed of an intense tip vortex and a diffused inboard wake, consistent with the experimentally observed wake of hovering helicopters. It is assumed that the vortex formation was almost immediate as opposed to the actual gradual rolling-up of the tip vortex. The method is demonstrated by assuming that the wake expansion can be represented by an analytical expression. E.A.K.

**N85-29365\*#** National Aeronautics and Space Administration. Lewis Research Center, Cleveland, Ohio.

### **GOVERNMENT REVIEW OF THE MOD-2 WIND TURBINE (AS-BUILT)**

W. R. JOHNSON, A. G. BIRCHENOUGH, B. S. LINSKOTT, J. R. REAGAN, P. J. SIROCKY, R. L. SIZEMORE, T. L. SULLIVAN, and R. H. HOLEMAN Jun. 1985 76 p refs Prepared in cooperation with Bonneville Power Administration (Contract DE-AI01-76ET-20320)

(NASA-TM-86983; E-2526; DOE/NASA/20320-63; NAS

1.15:86983) Avail: NTIS HC A05/MF A01 CSCL 10B

The findings and recommendations of the Government committee formed to conduct an as-built review of the three Mod-2 wind turbine units at Goldendale, Washington are given. The purpose of the review was to identify any critical deficiencies in machine components that could result in failure, and to recommend any necessary corrective action before resuming safe machine operation. The review concluded that one of the deficiencies identified would preclude planned attended or unattended operation, provided that certain corrective actions were implemented. R.J.F.

**N85-30476\*#** National Aeronautics and Space Administration. Lewis Research Center, Cleveland, Ohio.

### **ANALYTICAL MODEL FOR PREDICTING EMERGENCY SHUTDOWN OF A TWO-BLADED HORIZONTAL AXIS WIND TURBINE**

D. R. MILLER and C. B. F. ENSWORTH 1983 15 p refs Presented at the Wind Workshop 6, Minneapolis, 1-3 Jun. 1983; sponsored by American Solar Energy Society (Contract DE-AI01-76ET-20320)

(NASA-TM-83472; E-1786; DOE/NASA/20320-50; NAS

1.15:83472) Avail: NTIS HC A02/MF A01 CSCL 10A

An analytical model was developed to predict the shutdown characteristics of a large two bladed horizontal-axis wind turbine following a sudden loss of generator load. The analytical model is

described and used to predict rotor speed time histories following a loss of load, for a tip-control rotor and an aileron control rotor. These shutdown predictions are compared with experimental results from full-scale tests conducted on the Mod-O 100 kW wind turbine with both a tip control rotor and an aileron-control rotor. Predicted and measured rotor speed time histories are compared based on peak overspeed rpm, time at which this peak rpm occurs, and the general shape of the time history curve. The results of this comparison indicated there was good agreement between predictions and the full scale test results, thus verifying the analytical shutdown model. In general, the best agreement between predictions and full-scale test results was obtained up to the time where the peak overspeed rpm occurred. Author

**N85-30477\*** # National Aeronautics and Space Administration. Lewis Research Center, Cleveland, Ohio.

**PERFORMANCE COMPARISON BETWEEN NACA 23024 AND NACA 64(3)-618 AIRFOIL CONFIGURATED ROTORS FOR HORIZONTAL-AXIS WIND TURBINES**

R. D. CORRIGAN, C. B. F. ENSWORTH, and T. G. KEITH, JR. (Toledo Univ., Ohio) 1983 22 p refs Presented at the Wind Workshop 6, Minneapolis, 1-3 Jun. 1983; sponsored by American Solar Energy Society

(Contract DE-AI01-76ET-20320)

(NASA-TM-83471; DOE/NASA/20320-51; NAS 1.15:83471)

Avail: NTIS HC A02/MF A01 CSCL 10A

Wind turbine performance tests were conducted on the Mod-O 100-kW horizontal-axis wind turbine to compare a tip-controlled rotor having NACA 23024 airfoil tip sections with a similar rotor having NACA 64 sub 3-618 airfoil tip sections. The inboard portion of the blades had an NACA 23024 airfoil section. The wind turbine configuration consisted of the nacelle-rotor assembly mounted atop a tubular tower with the rotor axis 38 m above ground level. The rotor was 39 m in diameter, coned, and teetered and had 20 deg of pitch and flap coupling delta sub 3. The blades had 23 percent root cutout and the movable tip-control section covered the outer 31 percent of the blade. Testing was conducted at nominal rotor speeds of 20 and 31 rpm with the rotor downwind of the tower. The tests indicate improved performance for the rotor with the NACA 64 sub 3-618 airfoil tip sections over the rotor with the NACA 23024 airfoil tip sections. In addition, performance was predicted for each rotor configuration by using two performance prediction codes. This report presents the test results and compares them with each other and with predicted performance for both rotor configurations. Author

**N85-30478\*** # National Aeronautics and Space Administration. Lewis Research Center, Cleveland, Ohio.

**THE FEDERAL WIND PROGRAM AT NASA LEWIS RESEARCH CENTER**

D. H. BALDWIN and B. S. LINSKOTT 1983 22 p refs Presented at 6th Biennial Wind Energy Conf. and Workshop, Minneapolis, 1-3 Jun. 1983; sponsored by American Solar Energy Society

(Contract DE-AI01-76ET-20320)

(NASA-TM-83480; E-1798; DOE/NASA/20320-52; NAS

1.15:83480) Avail: NTIS HC A02/MF A01 CSCL 10A

There are several ongoing large wind system development projects directed toward meeting the technology requirements for utility applications. The first generation technology machines, Mod-OA and Mod-1, have successfully completed their planned periods of experimental operation. Disposition of these machines is nearly complete. The second generation machines, Mod-2's, continue experimental operation at Goodnoe Hills, WA, and Medicine Bow, WY. Design and engineering development of third generation, Mod-5, machines is underway. Initial experimental operation of Mod-5 is planned for DOE in late 1984 or early 1985. An overview of these project activities is presented. In addition to these projects, NASA also is conducting research on large horizontal axis wind turbines. The four main areas of experimental research are: (1) aerodynamics; (2) structural dynamics and aeroelasticity; (3) composite and hybrid composite materials; and (4) multiple system interaction. Key research

activities and results are described. The continuing need for future wind turbine research and technology development is explored.

Author

**N85-30479\*** # National Aeronautics and Space Administration. Lewis Research Center, Cleveland, Ohio.

**OPERATIONAL RESULTS FOR THE EXPERIMENTAL DOE/NASA MOD-OA WIND TURBINE PROJECT**

R. K. SHALTENS and A. G. BIRCHENOUGH 1983 29 p refs Presented at the 6th Wind Workshop, Minneapolis, 1-3 Jun. 1983; sponsored by American Solar Energy Society

(Contract DE-AI01-76ET-20320)

(NASA-TM-83517; E-1865; DOE/NASA/20320-55; NAS

1.15:83517) Avail: NTIS HC A03/MF A01 CSCL 10A

The Mod-OA wind turbine project which was to gain early experience in the operation of large wind turbines in a utility environment is discussed. The Mod-OA wind turbines were a first generation design, and even though not cost effective, the operating experience and performance characteristics had a significant effect on the design and development of the second and third generation machines. The Mod-OA machines were modified as a result of the operational experience, particularly the blade development and control system strategy. The results of study to investigate the interaction of a Mod-OA wind turbine with an isolated diesel generation system are discussed. The machine configuration, its advantages and disadvantages and the machine performance and availability are discussed. E.A.K.

**N85-30480\*** # National Aeronautics and Space Administration. Lewis Research Center, Cleveland, Ohio.

**LIFE CYCLE TEST RESULTS OF A BIPOLAR NICKEL HYDROGEN BATTERY**

R. L. CATALDO 1985 14 p refs Presented at the 20th Intersociety Energy Conversion Eng. Conf. (IECEC), Miami Beach, Fla., 18-23 Aug. 1985; sponsored by SAE, ANS, ASME, IEEE, AIAA, ACS and AIChE

(NASA-TM-87046; E-2608; NAS 1.15:87056) Avail: NTIS HC

A02/MF A01 CSCL 10C

A history of low Earth orbit laboratory test data on a 6.5 Ah bipolar nickel hydrogen battery designed and built at the NASA Lewis Research Center is presented. During the past several years the Storage and Thermal Branch has been deeply involved in the design, development, and optimization of nickel hydrogen devices. The bipolar concept is a means of achieving the goal of producing an acceptable battery of higher energy density, able to withstand the demands of low Earth orbit regimes. Author

**N85-30481\*** # Mechanical Technology, Inc., Latham, N. Y. **FREE-PISTON STIRLING ENGINE/LINEAR ALTERNATOR 1000-HOUR ENDURANCE TEST Final Report**

J. RAUCH and G. DOCHAT Mar. 1985 98 p

(Contract DEN3-333)

(NASA-CR-174771; DOE/NASA/0333-1; NAS 1.26:174771)

Avail: NTIS HC A05/MF A01 CSCL 10B

The Free Piston Stirling Engine (FPSE) has the potential to be a long lived, highly reliable, power conversion device attractive for many product applications such as space, residential or remote site power. The purpose of endurance testing the FPSE was to demonstrate its potential for long life. The endurance program was directed at obtaining 1000 operational hours under various test conditions: low power, full stroke, duty cycle and stop/start. Critical performance parameters were measured to note any change and/or trend. Inspections were conducted to measure and compare critical seal/bearing clearances. The engine performed well throughout the program, completing more than 1100 hours. Hardware inspection, including the critical clearances, showed no significant change in hardware or clearance dimensions. The performance parameters did not exhibit any increasing or decreasing trends. The test program confirms the potential for long life FPSE applications. Author

## 44 ENERGY PRODUCTION AND CONVERSION

**N85-30483\*#** Engelhard Industries, Inc., Edison, N.J.  
**DEVELOP AND TEST FUEL CELL POWERED ON-SITE INTEGRATED TOTAL ENERGY SYSTEMS. PHASE 3: FULL-SCALE POWER PLANT DEVELOPMENT Quarterly Report, Aug. - Oct. 1983**

A. KAUFMAN, S. PUDICK, C. L. WANG, J. WERTH, and J. A. WHELAN 21 Dec. 1983 30 p  
(Contract DEN3-241; DE-AI-01-80ET-17088)  
(NASA-CR-168338; NAS 1.26:168338; DOE/NASA/0241-11; QR-11) Avail: NTIS HC A03/MF A01 CSCL 10C

On-going test experience with a 5kW methanol-air integrated system is described. Long-term successful operation of a semi-automated electrolyte-replenishment system and non-metallic cooling plates was sustained in a 24-cell, two sq. ft. (4kW) stack. Single-cell test results for two developmental cathode catalysts are reported. Corrosion-protection efforts for metallic current-collecting plates are described. Author

**N85-31374\*#** National Aeronautics and Space Administration. Lewis Research Center, Cleveland, Ohio.

### **SOLAR DYNAMIC SYSTEMS**

M. O. DUSTIN /in NASA. Goddard Space Flight Center The 1984 Goddard Space Flight Center Battery Workshop p 53-68 Jul. 1985

Avail: NTIS HC A25/MF A01 CSCL 10A

The development of the solar dynamic system is discussed. The benefits of the solar dynamic system over pv systems are enumerated. The history of the solar dynamic development is recounted. The purpose and approach of the advanced development are outlined. Critical concentrator technology and critical heat recover technology are examined. E.A.K.

**N85-31624\*#** National Aeronautics and Space Administration. Lewis Research Center, Cleveland, Ohio.

### **HIGH EFFICIENCY SOLAR CELL RESEARCH FOR SPACE APPLICATIONS**

D. J. FLOOD /in JPL Proc. of the Flat-Plate Solar Array Proj. Res. Forum on High-Efficiency Crystalline Silicon Solar Cells p 147-162 15 May 1985 refs

Avail: NTIS HC A21/MF A01 CSCL 10A

A review is given of NASA photovoltaic research with emphasis on the activities of the Lewis Research Center. High efficiency solar cell research is discussed, as well as solar arrays, multi-junction cell bandgaps, and plasmon coupling. R.J.F.

**N85-31646\*#** National Aeronautics and Space Administration. Lewis Research Center, Cleveland, Ohio.

### **DESIGN PRINCIPLES FOR NICKEL-HYDROGEN CELLS AND BATTERIES**

L. H. THALLER, M. A. MANZO, and O. D. GONZALEZ-SANABRIA 1985 13 p refs Presented at the 20th Intersoc. Energy Conversion Eng. Conf., Miami Beach, Fla., 18-23 Aug. 1985; sponsored in part by SAE, ANS, ASME, IEEE, AIAA, ACS and AIChE

(NASA-TM-87037; E-2594; NAS 1.15:87037) Avail: NTIS HC A02/MF A01 CSCL 10C

Nickel-hydrogen cells and, more recently, bipolar batteries have been built by a variety of organizations. The design principles that have been used by the technology group at the NASA Lewis Research Center draw upon their extensive background in separator technology, alkaline fuel cell technology, and several alkaline cell technology areas. These design principles have been incorporated into both the more contemporary individual pressure vessel (IPV) designs that were pioneered by other groups, as well as the more recent bipolar battery designs using active cooling that are being developed at NASA Lewis Research Center and under contract. These principles are rather straightforward applications of capillary force formalisms, coupled with the slowly developing data base resulting from careful post test analyses. The objective of this overall effort is directed towards the low-Earth-orbit (LEO) application where the cycle life requirements are much more severe than the geosynchronous-orbit (GEO) application. A summary of the design principles employed is

presented along with a discussion of the recommendations for component pore sizes and pore size distributions, as well as suggested materials of construction. These will be made based on our experience in these areas to show how these design principles have been translated into operating hardware. Author

**N85-33566\*#** Ohio State Univ., Columbus. Dept. of Welding Engineering.

### **DIFFUSION WELDING OF CASSEGRAINIAN CONCENTRATOR CELL STACK ASSEMBLIES M.S. Thesis Final Report, Jun. 1983 - Sep. 1985**

K. J. GANGL Jul. 1985 137 p refs

(Contract NAG3-448)

(NASA-CR-176104; NAS 1.26:176104) Avail: NTIS HC A07/MF A01 CSCL 10B

Development of a procedure to join the components of the Cassegrainian concentrator photovoltaic cell stack assembly was studied. Diffusion welding was selected as the most promising process, and was concentrated on exclusively. All faying surfaces were coated with silver to promote welding. The first phase of the study consisted of developing the relationship between process parameters and joint strength using silver plated steel samples and an isostatic pressure system. In the second phase, mockups of the cell stack assembly were welded in a hot isostatic press. Excellent joint strength was achieved with parameters of 350 C and 10 ksi, but the delicate GaAs component could not survive the welding cycle without cracking. The tendency towards cracking was found to be affected by both temperature and pressure. Further work will be required in the future to solve this problem. Author

**N85-34441\*** National Aeronautics and Space Administration. Lewis Research Center, Cleveland, Ohio.

### **THERMIONIC PHOTOVOLTAIC ENERGY CONVERTER Patent**

D. L. CHUBB, inventor (to NASA) 9 Jul. 1985 7 p Filed 15 Feb. 1984 Supersedes N84-20918 (22 - 11, p 1673)

(NASA-CASE-LEW-14077-1; US-PATENT-4,528,417; US-PATENT-APPL-SN-580573; US-PATENT-CLASS-136-253)

Avail: US Patent and Trademark Office CSCL 10A

A thermionic photovoltaic energy conversion device comprises a thermionic diode mounted within a hollow tubular photovoltaic converter. The thermionic diode maintains a cesium discharge for producing excited atoms that emit line radiation in the wavelength region of 850 nm to 890 nm. The photovoltaic converter is a silicon or gallium arsenide photovoltaic cell having bandgap energies in this same wavelength region for optimum cell efficiency.

Official Gazette of the U.S. Patent and Trademark Office

**N85-34443\*#** National Aeronautics and Space Administration. Lewis Research Center, Cleveland, Ohio.

### **EVALUATION OF DEVELOPMENTAL MEMBRANES FOR THE MIXED REACTANT IRON-CHROMIUM REDOX SYSTEM**

J. S. LING 1984 13 p refs Presented at the 166th Meeting of the Electrochem. Soc., New Orleans, 7-12 Oct. 1984

(Contract DE-AI04-80AL-12726)

(NASA-TM-87074; E-2646; DOE/NASA/12726-26; NAS 1.15:87074) Avail: NTIS HC A02/MF A01 CSCL 10C

The operation of the redox storage system at 65 C with premixed ion has changed chromium reactant solutions membrane requirements. These new conditions allow the use of low resistivity membranes with relatively poor selectivity compared to membranes developed for system operation with separate reactants at 25 C. The results of in cell evaluations of developmental membranes for the new conditions are presented. Data include diffusion rate, area resistivity, and coulombic and energy efficiencies over a wide range of current densities. Use of these membranes results in peak round trip energy efficiencies greater than 80% at current densities as high as 80 mA/sq cm. E.A.K.

**N85-34444\*#** National Aeronautics and Space Administration. Lewis Research Center, Cleveland, Ohio.

**REFLECTION PLANE TESTS OF A WIND TURBINE BLADE TIP SECTION WITHAILERONS Final Report**

J. M. SAVINO, T. W. NYLAND, A. G. BIRCHENOUGH, F. L. JORDAN (NASA, Langley Research Center), and N. K. CAMPBELL (NASA, Langley Research Center) Aug. 1985 57 p refs (Contract DE-AI01-79ET-20320)

(NASA-TM-87018; E-2564; DOE/NASA/20320-65; NAS 1.15:87018) Avail: NTIS HC A04/MF A01 CSCL 10A

Tests were conducted in the NASA Langley 30 by 60 foot Wind Tunnel on a full scale 7.31 m (24 ft) long tip section of a wind turbine rotor blade. The blade tip section was built with ailerons on the trailing edge. The ailerons, which spanned a length of 6.1 m (20 ft), were designed so that two types could be evaluated: the plain and the balanced. The ailerons were hinged on the suction surface at the 0.62 X chord station behind the leading edge. The purpose of the tests was to measure the aerodynamic characteristics of the blade section for: an angle of attack range from 0 deg to 90 deg aileron deflections from 0 deg to -90 deg, and Reynolds numbers of 0.79 and 1.5 x 10 to the 6th power. These data were then used to determine which aileron configuration had the most desirable rotor control and aerodynamic braking characteristics. Tests were also run to determine the effects of vortex generators, leading edge roughness, and the gaps between the aileron sections on the lift, drag, and chordwise force coefficients of the blade tip section. Author

L. ROSENBLUM Aug. 1985 247 p refs Previously announced as N83-34450

(Contract NAG3-185)

(NASA-CR-174963; NAS 1.26:174963) Avail: NTIS HC A11/MF A01 CSCL 10A

The purpose of this text is to provide the reader with the background, understanding, and computational tools needed to master the practical aspects of photovoltaic (PV) technology, application, and cost. The focus is on stand-alone, silicon solar cell, flat-plate systems in the range of 1 to 25 kWh/day output. Technology topics covered include operation and performance of each of the major system components (e.g., modules, array, battery, regulators, controls, and instrumentation), safety, installation, operation and maintenance, and electrical loads. Application experience and trends are presented. Indices of electrical service performance - reliability, availability, and voltage control - are discussed, and the known service performance of central station electric grid, diesel-generator, and PV stand-alone systems are compared. PV system sizing methods are reviewed and compared, and a procedure for rapid sizing is described and illustrated by the use of several sample cases. The rapid sizing procedure yields an array and battery size that corresponds to a minimum cost system for a given load requirement, insulation condition, and desired level of service performance. PV system capital cost and levelized energy cost are derived as functions of service performance and insulation. Estimates of future trends in PV system costs are made. Author

**N85-35471\*#** Giner, Inc., Waltham, Mass.

**DEVELOPMENT OF ELECTRODES FOR THE NASA IRON/CHROMIUM Final Report**

L. SWETTE and V. JALAN Jun. 1984 285 p refs

(Contract DEN3-262; DE-AI04-80AL-12726)

(NASA-CR-174724; DOE/NASA/O262-1; NAS 1.26:174724)

Avail: NTIS HC A13/MF A01 CSCL 10A

This program was directed primarily to the development of the negative ( $\text{Cr}^{3+}/\text{Cr}^{2+}$ ) electrode for the NASA chromous/ferric Redox battery. The investigation of the effects of substrate processing and gold/lead catalyzation parameters on electrochemical performance were continued. In addition, the effects of reactant cross-mixing, acidity level, and temperature were examined for both Redox couples. Finally, the performance of optimized electrodes was tested in system hardware (1/3 square foot single cell). The major findings are discussed: (1) The recommended processing temperature for the carbon felt, as a substrate for the negative electrode, is 1650 to 1750 C, (2) The recommended gold catalyzation procedure is essentially the published NASA procedure (NASA TM-82724, Nov. 1981) based on deposition from aqueous methanol solution, with the imposition of a few controls such as temperature (25 C) and precatalyzation pH of the felt (7), (3) Experimental observations of the gold catalyzation process and subsequent electron microscopy indicate that the gold is deposited from the colloidal state, induced by contact of the solution with the carbon felt, (4) Electrodeposited lead appears to be present as a thin uniform layer over the entire surface of the carbon fibers, rather than as discrete particles, and (5) Cross-mixing of reactants ( $\text{Fe}^{2+}$  in negative electrode solution or  $\text{Cr}^{3+}$  in the positive electrode solution) did not appear to produce significant interference at either electrode. Author

**N85-35472\*#** Michigan Univ., Ann Arbor.

**PRACTICAL ASPECTS OF PHOTOVOLTAIC TECHNOLOGY, APPLICATIONS AND COST (REVISED) Final Report**

45

## ENVIRONMENT POLLUTION

Includes air, noise, thermal and water pollution; environment monitoring; and contamination control.

**N85-23830\*#** National Aeronautics and Space Administration. Lewis Research Center, Cleveland, Ohio.

**EXTREME PRECISION ANTENNA REFLECTOR STUDY RESULTS**

G. R. SHARP, L. D. GILGER (Harris Corp., Melbourne, Fla.), and K. E. ARD (Harris Corp., Melbourne, Fla.) In NASA. Langley Research Center Large Space Antenna Systems Technol., 1984 p 279-300 Apr. 1985 refs

Avail: NTIS HC A20/MF A01 CSCL 22B

Thermal and mechanical distortion degrade the RF performance of antennas. The complexity of future communications antennas requires accurate, dimensionally stable antenna reflectors and structures built from materials other than those currently used. The advantages and disadvantages of using carbon fibers in an epoxy matrix are reviewed as well as current reflector fabrications technology and adjustment. The manufacturing sequence and coefficient of thermal expansion of carbon fiber/borosilicate glass composites is described. The construction of a parabolic reflector from this material and the assembling of both reflector and antenna are described. A 3M-aperture-diameter carbon/glass reflector that can be used as a subassembly for large reflectors is depicted. The deployment sequence for a 10.5M-aperture-diameter antenna, final reflector adjustment, and the deployment sequence for large reflectors are also illustrated. A.R.H.

## GEOPHYSICS

Includes aeronomy; upper and lower atmosphere studies; ionospheric and magnetospheric physics; and geomagnetism.

**A85-29538\*** Iowa Univ., Iowa City.

**EFFECTS OF CHEMICAL RELEASES BY THE STS 3 ORBITER ON THE IONOSPHERE**

J. S. PICKETT, G. B. MURPHY, W. S. KURTH, C. K. GOERTZ (Iowa, University, Iowa City, IA), and S. D. SHAWHAN (NASA, Washington, DC) *Journal of Geophysical Research* (ISSN 0148-0227), vol. 90, April 1, 1985, p. 3487-3497. Previously announced in STAR as N84-25204. refs (Contract NAS8-32807; NAG3-449)

The Plasma Diagnostics Package, flown aboard STS-3 as part of the first Shuttle payload (OSS-1), recorded the effects of various chemical releases from the Orbiter. Changes in the plasma environment was observed during flash evaporator system releases, water dumps and maneuvering thruster operations. During flash evaporator operations, broadband Orbiter-generated electrostatic noise was enhanced and plasma density irregularities were observed to increase by 3 to 30 times with a spectrum which rose steeply and peaked below 6 Hz. In the case of water dumps, background electrostatic noise was enhanced at frequencies below about 3 kHz and suppressed at frequencies above 2 kHz. Thruster activity also stimulated electrostatic noise with a spectrum which peaked at approximately 0.5 kHz. In addition, ions with energies up to 1 keV were seen during some thruster events.

Author

**A85-37717\*** Iowa Univ., Iowa City.

**DE-1 MEASUREMENTS OF AKR WAVE DIRECTIONS**

W. CALVERT (Iowa, University, Iowa City, IA) *Geophysical Research Letters* (ISSN 0094-8276), vol. 12, June 1985, p. 381-384. refs (Contract NAG3-10)

In addition to its wave rotation sense, the direction of auroral kilometric radiation (AKR) can also be measured with the plasma wave instrument on Dynamics Explorer 1, from the relative phase of the signals received by its orthogonal electric dipole antennas. By this method, which differs in principle from the previous spin-null method for measuring wave directions, it has been found possible to pinpoint the AKR source by triangulation, using measurements from different points along the DE-1 orbit. The resulting apparent source, in one instance, seemed to occupy a well-defined auroral-zone invariant magnetic latitude and showed the expected increase of altitude with decreasing frequency. An analysis of the method also confirmed the validity of the previous rotation sense measurements.

Author

## METEOROLOGY AND CLIMATOLOGY

Includes weather forecasting and modification.

**A85-11979\*#** Control Data Corp., Minneapolis, Minn.

**GASP CLOUD ENCOUNTER STATISTICS - IMPLICATIONS FOR**

**LAMINAR FLOW CONTROL FLIGHT**

W. H. JASPERSON, G. D. NASTROM (Control Data Corp., Minneapolis, MN), R. E. DAVIS (NASA, Langley Research Center, Flight Electronics Div., Hampton, VA), and J. D. HOLDEMAN (NASA, Lewis Research Center, Aerothermodynamics and Fuels Div., Cleveland, OH) *Journal of Aircraft* (ISSN 0021-8669), vol. 21, Nov. 1984, p. 851-857. refs

The cloud observation archive from the NASA Global Atmospheric Sampling Program (GASP) is analyzed in order to derive the probability of cloud encounter at altitudes normally flown by commercial airliners, for application to a determination of the feasibility of Laminar Flow Control (LFC) on long-range routes. The probability of cloud encounter is found to vary significantly with season. Several meteorological circulation features are apparent in the latitudinal distribution of cloud cover. The cloud encounter data are shown to be consistent with the classical midlatitude cyclone model with more clouds encountered in highs than in lows. Aircraft measurements of route-averaged time-in-clouds fit a gamma probability distribution model which is applied to estimate the probability of extended cloud encounter, and the associated loss of LFC effectiveness along seven high-density routes. The probability is demonstrated to be low.

I.H.

**A85-21140\*** Control Data Corp., Minneapolis, Minn.

**A COMPARISON OF NMC AND GWC ANALYSIS FIELD TEMPERATURES WITH AIRCRAFT MEASUREMENTS**

W. H. JASPERSON and G. D. NASTROM (Control Data Corp., Minneapolis, MN) *Journal of Climate and Applied Meteorology* (ISSN 0733-3021), vol. 23, Oct. 1984, p. 1421-1426. refs (Contract NAS3-21249)

Comparison between in situ aircraft observations of temperature and National Meteorological Center and Global Weather Central analysis fields of temperature is presented for a continental and oceanic flight route. The standard deviations of the temperature differences over several hundred flights are found to be 2.5 and 3.5 C for the continental and oceanic route, respectively. A bias towards warm temperatures of about 0.85 C for the analysis fields was found for the oceanic route. Only small differences are found between the NMC and GWC analysis field temperatures.

Author

**A85-31199\*** Control Data Corp., Minneapolis, Minn.

**VARIABILITY OF CLOUDINESS AT AIRLINE CRUISE ALTITUDES FROM GASP MEASUREMENTS**

W. H. JASPERSON, G. D. NASTROM (Control Data Corp., Minneapolis, MN), R. E. DAVIS (NASA, Langley Research Center, Hampton, VA), and J. D. HOLDEMAN (NASA, Lewis Research Center, Cleveland, OH) *Journal of Climate and Applied Meteorology* (ISSN 0733-3021), vol. 24, Jan. 1985, p. 74-82. refs

Additional statistics relating to the climatology of cloud cover at airline cruise altitudes are presented. The data were obtained between 1975 and 1979 from commercial airliners participating in the Global Atmospheric Sampling Program (GASP). The statistics describe the seasonal, latitudinal and altitudinal variation in cloudiness parameters as well as differences in the high-altitude cloud structure attributed to cyclone and convective-cloud generation processes. The latitudinal distribution of cloud cover derived from the GASP data was found to agree with high-altitude satellite observations. The relationships between three different measures of cloudiness and the relative vorticity at high altitudes is also discussed.

I.H.

**N85-10558\*#** National Aeronautics and Space Administration. Lewis Research Center, Cleveland, Ohio.

**MERIT: A MAN/COMPUTER DATA MANAGEMENT AND ENHANCEMENT SYSTEM FOR UPPER AIR NOWCASTING/FORECASTING IN THE UNITED STATES**

R. STEINBERG / In ESA Nowcasting 2. Mesoscale Observations and Very-Short-Range Weather Forecasting p 465-471 Jun. 1984 refs

Avail: NTIS HC A23/MF A01

It is suggested that the very short range forecast problem for aviation is one of data management rather than model development and the possibility of improving the aviation forecast using current technology is underlined. The MERIT concept of modeling technology, and advanced man/computer interactive data management and enhancement techniques to provide a tailored, accurate and timely forecast for aviation is outlined. The MERIT includes utilization of the Lagrangian approach, extensive use of the automated aircraft report to complement the present data base and provide the most current observations; and the concept that a 2 to 12 hour forecast provided every 3 hr. can meet the domestic needs of aviation instead of the present 18 and 24 hr forecast provided every 12 hr.

Author (ESA)

**N85-21872\*#** National Aeronautics and Space Administration. Lewis Research Center, Cleveland, Ohio.

**SIMULTANEOUS CABIN AND AMBIENT OZONE MEASUREMENTS ON TWO BOEING 747 AIRPLANES. VOLUME 3: OCTOBER 1978 - JULY 1979**

J. D. HOLDEMAN and W. H. JASPERSON (Control Data Corp., Minneapolis) Feb. 1985 579 p refs

(Contract DOT-FA78WAI-893)

(NASA-TM-86883; E-2344; NAS 1.15:86883) Avail: NTIS HC A25/MF A01 CSCL 04B

Measurements of ozone concentrations at cruise altitudes both outside and in the cabin of a Boeing 747SP and Boeing 747-100 airliners in routine commercial service are presented. Plotted and tabulated data are identified by route and are arranged chronologically for each airplane. These data were taken at 5- or 10-min intervals by automated instruments used in the NASA Global Atmospheric Sampling Program (GASP). All GASP cabin ozone data obtained from October 1978 to early July 1979 are presented.

R.J.F.

**N85-35534\*#** PRC Planning and Economics, Inc., Lake Success, N.Y.

**COMPARATIVE ANALYSIS OF OPERATIONAL FORECASTS VERSUS ACTUAL WEATHER CONDITIONS IN AIRLINE FLIGHT PLANNING, VOLUME 1**

J. F. KEITZ Apr. 1982 83 p 5 Vol.

(Contract NAS3-22748)

(NASA-CR-167862; NAS 1.26:167862) Avail: NTIS HC A05/MF A01 CSCL 04B

The impact of more timely and accurate weather data on airline flight planning with the emphasis on fuel savings is studied. This volume of the report discusses the results of Task 1 of the four major tasks included in the study. Task 1 compares flight plans based on forecasts with plans based on the verifying analysis from 33 days during the summer and fall of 1979. The comparisons show that: (1) potential fuel savings conservatively estimated to be between 1.2 and 2.5 percent could result from using more timely and accurate weather data in flight planning and route selection; (2) the Suitland forecast generally underestimates wind speeds; and (3) the track selection methodology of many airlines operating on the North Atlantic may not be optimum resulting in their selecting other than the optimum North Atlantic Organized Track about 50 percent of the time.

Author

**N85-35535\*#** PRC Planning and Economics, Inc., Lake Success, N.Y.

**COMPARATIVE ANALYSIS OF OPERATIONAL FORECASTS VERSUS ACTUAL WEATHER CONDITIONS IN AIRLINE FLIGHT PLANNING, VOLUME 2**

J. F. KEITZ Apr. 1982 54 p 5 Vol.

(Contract NAS3-22748)

(NASA-CR-167863; NAS 1.26:167863) Avail: NTIS HC A04/MF A01 CSCL 04B

The impact of more timely and accurate weather data on airline flight planning with the emphasis on fuel savings is studied. This volume of the report discusses the results of Task 2 of the four major tasks included in the study. Task 2 compares various categories of flight plans and flight tracking data produced by a simulation system developed for the Federal Aviation Administrations by SRI International. (Flight tracking data simulate actual flight tracks of all aircraft operating at a given time and provide for rerouting of flights as necessary to resolve traffic conflicts.) The comparisons of flight plans on the forecast to flight plans on the verifying analysis confirm Task 1 findings that wind speeds are generally underestimated. Comparisons involving flight tracking data indicate that actual fuel burn is always higher than planned, in either direction, and even when the same weather data set is used. Since the flight tracking model output results in more diversions than is known to be the case, it was concluded that there is an error in the flight tracking algorithm.

Author

**N85-35536\*#** PRC Planning and Economics, Inc., Lake Success, N.Y.

**COMPARATIVE ANALYSIS OF OPERATIONAL FORECASTS VERSUS ACTUAL WEATHER CONDITIONS IN AIRLINE FLIGHT PLANNING, VOLUME 3**

J. F. KEITZ Apr. 1982 96 p 5 Vol.

(Contract NAS3-22748)

(NASA-CR-167864; NAS 1.26:167864) Avail: NTIS HC A05/MF A01 CSCL 04B

The impact of more timely and accurate weather data on airline flight planning with the emphasis on fuel savings is studied. This volume of the report discusses the results of Task 3 of the four major tasks included in the study. Task 3 compares flight plans developed on the Suitland forecast with actual data observed by the aircraft (and averaged over 10 degree segments). The results show that the average difference between the forecast and observed wind speed is 9 kts. without considering direction, and the average difference in the component of the forecast wind parallel to the direction of the observed wind is 13 kts. - both indicating that the Suitland forecast underestimates the wind speeds. The Root Mean Square (RMS) vector error is 30.1 kts. The average absolute difference in direction between the forecast and observed wind is 26 degrees and the temperature difference is 3 degree Centigrade. These results indicate that the forecast model as well as the verifying analysis used to develop comparison flight plans in Tasks 1 and 2 is a limiting factor and that the average potential fuel savings or penalty are up to 3.6 percent depending on the direction of flight.

Author

**N85-35537\*#** PRC Planning and Economics, Inc., Lake Success, N.Y.

**COMPARATIVE ANALYSIS OF OPERATIONAL FORECASTS VERSUS ACTUAL WEATHER CONDITIONS IN AIRLINE FLIGHT PLANNING, VOLUME 4**

J. F. KEITZ Apr. 1982 93 p 5 Vol.

(Contract NAS3-22748)

(NASA-CR-167865; NAS 1.26:167865) Avail: NTIS HC A05/MF A01 CSCL 04B

The impact of more timely and accurate weather data on airline flight planning with the emphasis on fuel savings is studied. This volume of the report discusses the results of Task 4 of the four major tasks included in the study. Task 4 uses flight plan segment wind and temperature differences as indicators of dates and geographic areas for which significant forecast errors may have occurred. An in-depth analysis is then conducted for the days identified. The analysis show that significant errors occur in the

## 47 METEOROLOGY AND CLIMATOLOGY

operational forecast on 15 of the 33 arbitrarily selected days included in the study. Wind speeds in an area of maximum winds are underestimated by at least 20 to 25 kts. on 14 of these days. The analysis also show that there is a tendency to repeat the same forecast errors from prog to prog. Also, some perceived forecast errors from the flight plan comparisons could not be verified by visual inspection of the corresponding National Meteorological Center forecast and analyses charts, and it is likely that they are the result of weather data interpolation techniques or some other data processing procedure in the airlines' flight planning systems. Author

**N85-35538\*** # PRC Planning and Economics, Inc., Lake Success, N.Y.

### **COMPARATIVE ANALYSIS OF OPERATIONAL FORECASTS VERSUS ACTUAL WEATHER CONDITIONS IN AIRLINE FLIGHT PLANNING: SUMMARY REPORT**

J. F. KEITZ Apr. 1982 47 p 5 Vol.

(Contract NAS3-22748)

(NASA-CR-167866; NAS 1.26:167866) Avail: NTIS HC A03/MF A01 CSDL 04B

The impact of more timely and accurate weather data on airline flight planning with the emphasis on fuel savings is studied. This summary report discusses the results of each of the four major tasks of the study. Task 1 compared airline flight plans based on operational forecasts to plans based on the verifying analyses and found that average fuel savings of 1.2 to 2.5 percent are possible with improved forecasts. Task 2 consisted of similar comparisons but used a model developed for the FAA by SRI International that simulated the impact of ATC diversions on the flight plans. While parts of Task 2 confirm the Task 1 findings, inconsistency with other data and the known impact of ATC suggests that other Task 2 findings are the result of errors in the model. Task 3 compares segment weather data from operational flight plans with the weather actually observed by the aircraft and finds the average error could result in fuel burn penalties (or savings) of up to 3.6 percent for the average 8747 flight. In Task 4 an in-depth analysis of the weather forecast for the 33 days included in the study finds that significant errors exist on 15 days. Wind speeds in the area of maximum winds are underestimated by 20 to 50 kts., a finding confirmed in the other three tasks. Author

51

## **LIFE SCIENCES (GENERAL)**

Includes genetics.

**N85-27508\*** # Applied Medical Technology, Inc., Brecksville, Ohio.

### **PERCUTANEOUS CONNECTORS Annual Report**

G. J. PICHA and S. R. TAYLOR Sep. 1981 49 p refs

(Contract NAS3-22654)

(NASA-CR-175627; NAS 1.26:175627; AR-1) Avail: NTIS HC A03/MF A01 CSDL 06B

A surface possessing a regular array of micro-pillars was evaluated with regard to its ability to control epithelial downgrowth at the percutaneous interface. A range of pillar sizes were applied to the vertical segment of T shaped Biomer (R) implants. These percutaneous tabs were implanted into the dorsum of cats for a period of 6 weeks using a standardized surgical technique. Comments were made post-operatively and at the time of retrieval. A quantitative scoring system was applied to these observations as well as histological results. As observed, the pillar morphology used displayed the ability to control epithelial downgrowth. Collagen ingrowth into the interpillar spaces and possibly direct interactions of the epithelial cells with the morphology may account for the inhibition. The reproducibility of epithelial inhibition is, however, limited by other factors which are currently not well understood.

These factors and potential methods of assessment are discussed. Author

54

## **MAN/SYSTEM TECHNOLOGY AND LIFE SUPPORT**

Includes human engineering; biotechnology; and space suits and protective clothing.

**A85-38444\*** National Aeronautics and Space Administration. Lewis Research Center, Cleveland, Ohio.

### **FRICTION AND WEAR PROPERTIES OF A CHARNLEY ARTIFICIAL HIP JOINT**

W. R. JONES, JR. (NASA, Lewis Research Center, Cleveland, OH) American Society of Lubrication Engineers and American Society of Mechanical Engineers, Lubrication Conference, San Diego, CA, Oct. 22-24, 1984. 10 p. refs  
(ASLE PREPRINT 84-LC-4A-4)

59

## **MATHEMATICAL AND COMPUTER SCIENCES (GENERAL)**

**N85-21990\*** # National Aeronautics and Space Administration. Lewis Research Center, Cleveland, Ohio.

### **A CONVERGENT SERIES EXPANSION FOR HYPERBOLIC SYSTEMS OF CONSERVATION LAWS Final Report**

E. HARABETIAN Feb. 1985 90 p refs

(Contract NAS1-17070)

(NASA-CR-172557; ICASE-85-13; NAS 1.26:172557) Avail: NTIS HC A05/MF A01 CSDL 12A

The discontinuities piecewise analytic initial value problem for a wide class of conservation laws is considered which includes the full three-dimensional Euler equations. The initial interaction at an arbitrary curved surface is resolved in time by a convergent series. Among other features the solution exhibits shock, contact, and expansion waves as well as sound waves propagating on characteristic surfaces. The expansion waves correspond to the one-dimensional rarefactions but have a more complicated structure. The sound waves are generated in place of zero strength shocks, and they are caused by mismatches in derivatives. M.G.

60

## **COMPUTER OPERATIONS AND HARDWARE**

Includes computer graphics and data processing.

**A85-24526\*** Louisiana State Univ., Baton Rouge.

### **TRANSFERRING DATA OSCILLOSCOPE TO AN IBM USING AN APPLE II+**

D. L. MILLER, M. Y. FRENKLACH, P. J. LAUGHLIN, and D. W. CLARY (Louisiana State University, Baton Rouge, LA) Computer Applications in the Laboratory, no. 4, 1984, p. 260-269. (Contract DE-FG22-80PC-30247; NAS3-23542; NAG3-477)

A set of PASCAL programs permitting the use of a laboratory microcomputer to facilitate and control the transfer of data from a digital oscilloscope (used with photomultipliers in experiments on soot formation in hydrocarbon combustion) to a mainframe



computer and the subsequent mainframe processing of these data is presented. Advantages of this approach include the possibility of on-line computations, transmission flexibility, automatic transfer and selection, increased capacity and analysis options (such as smoothing, averaging, Fourier transformation, and high-quality plotting), and more rapid availability of results. The hardware and software are briefly characterized, the programs are discussed, and printouts of the listings are provided. T.K.

**A85-28613\*** Arizona State Univ., Tempe.  
**MULTIBUS-BASED PARALLEL PROCESSOR FOR SIMULATION**

E. P. OGRADY and C.-H. WANG (Arizona State University, Tempe, AZ) IN: Summer Computer Simulation Conference, 15th, Vancouver, Canada, July 11-13, 1983, Proceedings. Volume 1. La Jolla, CA, Society for Computer Simulation, 1983, p. 371-375. refs

(Contract NAG3-112)

A Multibus-based parallel processor simulation system is described. The system is intended to serve as a vehicle for gaining hands-on experience, testing system and application software, and evaluating parallel processor performance during development of a larger system based on the horizontal/vertical-bus interprocessor communication mechanism. The prototype system consists of up to seven Intel iSBC 86/12A single-board computers which serve as processing elements, a multiple transmission controller (MTC) designed to support system operation, and an Intel Model 225 Microcomputer Development System which serves as the user interface and input/output processor. All components are interconnected by a Multibus/IEEE 796 bus. An important characteristic of the system is that it provides a mechanism for a processing element to broadcast data to other selected processing elements. This parallel transfer capability is provided through the design of the MTC and a minor modification to the iSBC 86/12A board. The operation of the MTC, the basic hardware-level operation of the system, and pertinent details about the iSBC 86/12A and the Multibus are described. Author

**A85-28628\*** California Univ., Los Angeles.  
**GENERAL APPROACHES FOR ACHIEVING HIGH SPEED COMPUTATIONS**

T. LANG and M. D. ERCEGOVAC (California, University, Los Angeles, CA) IN: Summer Computer Simulation Conference, 15th, Vancouver, Canada, July 11-13, 1983, Proceedings. Volume 2. La Jolla, CA, Society for Computer Simulation, 1983, p. 992-1006. refs

(Contract NAG3-132)

The basic organizational approach to achieve high speed computations has been to execute several instructions concurrently. Various algorithmic structures and related computer organizations have been identified and used for this purpose. Each of them is better suited for some classes of applications, provides a potential speed-up with respect to the sequential computer, and suffers from degradation factors that reduce the effective speed-up obtained. The basic algorithmic structures are presented, the corresponding computer organizations described and the potential degradation factors identified. Also included are considerations related to the cost of the system and to the corresponding programming methodology. Author

**A85-36727\*** Carnegie-Mellon Univ., Pittsburgh, Pa.  
**OPTICAL LINEAR ALGEBRA PROCESSORS - NOISE AND ERROR-SOURCE MODELING**

D. CASASENT (Carnegie-Mellon University, Pittsburgh, PA) and A. GHOSH (AT&T Bell Laboratories, Allentown; Carnegie-Mellon University, Pittsburgh, PA) Optics Letters (ISSN 0146-9592), vol. 10, June 1985, p. 252-254. Research supported by the Unicorn Systems, Inc. refs

(Contract NAG3-5; AF-AFOSR-79-0091)

The modeling of system and component noise and error sources in optical linear algebra processors (OLAPs) are considered, with attention to the frequency-multiplexed OLAP. General expressions are obtained for the output produced as a function of various

component errors and noise. A digital simulator for this model is discussed. Author

**N85-10659\*#** National Aeronautics and Space Administration.  
Lewis Research Center, Cleveland, Ohio.

**HARDWARE FOR A REAL-TIME MULTIPROCESSOR SIMULATOR**

R. A. BLECH and D. J. ARPASI 1984 11 p refs To be presented at the SCS Multiconf. Distributed Simulation, San Diego, Calif., 24-26 Jan. 1985; sponsored by the Soc. for Computer Simulation (NASA-TM-83805; E-2315; NAS 1.15:83805) Avail: NTIS HC A02/MF A01 CSCL 09B

The hardware for a real time multiprocessor simulator (RTMPS) developed at the NASA Lewis Research Center is described. The RTMPS is a multiple microprocessor system used to investigate the application of parallel processing concepts to real time simulation. It is designed to provide flexible data exchange paths between processors by using off the shelf microcomputer boards and minimal customized interfacing. A dedicated operator interface allows easy setup of the simulator and quick interpreting of simulation data. Simulations for the RTMPS are coded in a NASA designed real time multiprocessor language (RTMPL). This language is high level and geared to the multiprocessor environment. A real time multiprocessor operating system (RTMPOS) has also been developed that provides a user friendly operator interface. The RTMPS and supporting software are currently operational and are being evaluated at Lewis. The results of this evaluation will be used to specify the design of an optimized parallel processing system for real time simulation of dynamic systems. M.G.

## 61

## COMPUTER PROGRAMMING AND SOFTWARE

Includes computer programs, routines, and algorithms.

**A85-28612\*** College of William and Mary, Williamsburg, Va.  
**THE USE OF ADA IN DISTRIBUTED SIMULATIONS**

W. R. COLLINS and S. FEYOCK (College of William and Mary, Williamsburg, VA) IN: Summer Computer Simulation Conference, 15th, Vancouver, Canada, July 11-13, 1983, Proceedings. Volume 1. La Jolla, CA, Society for Computer Simulation, 1983, p. 364-370. refs

(Contract NAG3-232)

The increasing need for detailed information about systems of continually growing complexity enhances steadily the demands regarding the employed models. The present investigation is concerned with work related to the development of high-performance computer hardware intended for the support of the real-time simulation of jet engines. The hardware is structured in the form of a network of communicating microprocessors running in parallel. The need for a higher-order language capability for programming such a network has led to the research considered in this study. Attention is given to the hardware which is being developed, an abstract model, programming language considerations, research considerations, research objectives, Ada tasks, Ada packages, the Ada model, the mapping of the model to the hardware, a precompiler example, and the advantages of Ada. G.R.

**A85-28615\*** California Univ., Los Angeles.

**A FUNCTIONAL LANGUAGE APPROACH IN HIGH-SPEED DIGITAL SIMULATION**

M. D. ERCEGOVAC and S.-L. LU (California, University, Los Angeles, CA) IN: Summer Computer Simulation Conference, 15th, Vancouver, Canada, July 11-13, 1983, Proceedings. Volume 1. La Jolla, CA, Society for Computer Simulation, 1983, p. 383-387. refs

(Contract NAG3-132)

A functional programming approach for a multi-microprocessor architecture is presented. The language, based on Backus FP, its intermediate form and the translation process are discussed and illustrated with an example. The approach allows performance analysis to be performed at a high level as an aid in program partitioning. Author

**A85-34131\*** College of William and Mary, Williamsburg, Va.  
**MOVING TARGET, DISTRIBUTED, REAL-TIME SIMULATION USING ADA**

W. R. COLLINS, S. FEYOCK, L. A. KING, and L. J. MORELL (College of William and Mary, Williamsburg, VA) IN: Simulation in Ada; Proceedings of the Eastern Simulation Conference, Norfolk, VA, March 3-8, 1985. San Diego, CA, Society for Computer Simulation, 1985, p. 27-32. refs

(Contract NAG3-232)

Research on a precompiler solution is described for the moving target compiler problem encountered when trying to run parallel simulation algorithms on several microcomputers. The precompiler is under development at NASA-Lewis for simulating jet engines. Since the behavior of any component of a jet engine, e.g., the fan inlet, rear duct, forward sensor, etc., depends on the previous behaviors and not the current behaviors of other components, the behaviors can be modeled on different processors provided the outputs of the processors reach other processors in appropriate time intervals. The simulator works in compute and transfer modes. The Ada procedure sets for the behaviors of different components are divided up and routed by the precompiler, which essentially receives a multitasking program. The subroutines are synchronized after each computation cycle. M.S.K.

**N85-10683\*** National Aeronautics and Space Administration. Lewis Research Center, Cleveland, Ohio.

**FLOATING-POINT FUNCTION GENERATION ROUTINES FOR 16-BIT MICROCOMPUTERS**

M. A. MACKIN and J. F. SOEDER Oct. 1984 55 p refs (NASA-TM-83783; E-2279; NAS 1.15:83783) Avail: NTIS HC A04/MF A01 CSCL 09B

Several computer subroutines have been developed that interpolate three types of nonanalytic functions: univariate, bivariate, and map. The routines use data in floating-point form. However, because they are written for use on a 16-bit Intel 8086 system with an 8087 mathematical coprocessor, they execute as fast as routines using data in scaled integer form. Although all of the routines are written in assembly language, they have been implemented in a modular fashion so as to facilitate their use with high-level languages. Author

**N85-17576\*** National Aeronautics and Space Administration. Lewis Research Center, Cleveland, Ohio.

**MINDS: A MICROCOMPUTER INTERACTIVE DATA SYSTEM FOR 8086-BASED CONTROLLERS**

J. F. SOEDER Jan. 1985 41 p refs (NASA-TP-2378; E-2172; NAS 1.60:2378) Avail: NTIS HC A03/MF A01 CSCL 09B

A microcomputer interactive data system (MINDS) software package for the 8086 family of microcomputers is described. To enhance program understandability and ease of code maintenance, the software is written in PL/M-86, Intel Corporation's high-level system implementation language. The MINDS software is intended to run in residence with real-time digital control software to provide displays of steady-state and transient data. In addition, the MINDS package provides classic monitor capabilities along with extended provisions for debugging an executing control system. The software

uses the CP/M-86 operating system developed by Digital Research, Inc., to provide program load capabilities along with a uniform file structure for data and table storage. Finally, a library of input and output subroutines to be used with consoles equipped with PL/M-86 and assembly language is described. Author

**N85-28610\*** National Aeronautics and Space Administration. Lewis Research Center, Cleveland, Ohio.

**REAL-TIME MULTIPROCESSOR PROGRAMMING LANGUAGE (RTMPL) USER'S MANUAL**

D. J. ARPASI Jun. 1985 115 p refs (NASA-TP-2422; E-1999; NAS 1.60:2422) Avail: NTIS HC A06/MF A01 CSCL 09B

A real-time multiprocessor programming language (RTMPL) has been developed to provide for high-order programming of real-time simulations on systems of distributed computers. RTMPL is a structured, engineering-oriented language. The RTMPL utility supports a variety of multiprocessor configurations and types by generating assembly language programs according to user-specified targeting information. Many programming functions are assumed by the utility (e.g., data transfer and scaling) to reduce the programming chore. This manual describes RTMPL from a user's viewpoint. Source generation, applications, utility operation, and utility output are detailed. An example simulation is generated to illustrate many RTMPL features. Author

## 62

### COMPUTER SYSTEMS

Includes computer networks.

**A85-28614\*** California Univ., Los Angeles.

**DATA FLOW METHODS FOR DYNAMIC SYSTEM SIMULATION - A CSSL-IV MICROCOMPUTER NETWORK INTERFACE**

A. MAKOUI and W. J. KARPLUS (California, University, Los Angeles, CA) IN: Summer Computer Simulation Conference, 15th, Vancouver, Canada, July 11-13, 1983, Proceedings. Volume 1. La Jolla, CA, Society for Computer Simulation, 1983, p. 376-382. refs

(Contract NAG3-132)

A major problem in employing networks of microcomputers for the real-time simulation of complex systems is to allocate computational tasks to the various microcomputers in such a way that idle time and time lost in interprocess communication is minimized. The research reported in this paper is directed to the development of a software interface between a higher-level simulation language and a network of microcomputers. A CSSL-IV source program is translated to a data flow graph. This graph is then analyzed automatically so as to allocate computing tasks to the various processors. Author

**A85-28629\*** California Univ., Los Angeles.

**FUNCTIONAL LANGUAGE AND DATA FLOW ARCHITECTURES**

M. D. ERCEGOVAC, D. R. PATEL, and T. LANG (California, University, Los Angeles, CA) IN: Summer Computer Simulation Conference, 15th, Vancouver, Canada, July 11-13, 1983, Proceedings. Volume 2. La Jolla, CA, Society for Computer Simulation, 1983, p. 1007-1023. refs

(Contract NAG3-132)

This is a tutorial article about language and architecture approaches for highly concurrent computer systems based on the functional style of programming. The discussion concentrates on the basic aspects of functional languages, and sequencing models such as data-flow, demand-driven and reduction which are essential at the machine organization level. Several examples of highly concurrent machines are described. Author

**N85-17596\*** National Aeronautics and Space Administration. Lewis Research Center, Cleveland, Ohio.

**OPERATING SYSTEM FOR A REAL-TIME MULTIPROCESSOR PROPULSION SYSTEM SIMULATOR. USER'S MANUAL**

G. L. COLE Jan. 1985 42 p refs  
(NASA-TP-2426; D-1998; NAS 1.60:2426) Avail: NTIS HC A03/MF A01 CSCL 09B

The NASA Lewis Research Center is developing and evaluating experimental hardware and software systems to help meet future needs for real-time, high-fidelity simulations of air-breathing propulsion systems. Specifically, the real-time multiprocessor simulator project focuses on the use of multiple microprocessors to achieve the required computing speed and accuracy at relatively low cost. Operating systems for such hardware configurations are generally not available. A real time multiprocessor operating system (RTMPOS) that supports a variety of multiprocessor configurations was developed at Lewis. With some modification, RTMPOS can also support various microprocessors. RTMPOS, by means of menus and prompts, provides the user with a versatile, user-friendly environment for interactively loading, running, and obtaining results from a multiprocessor-based simulator. The menu functions are described and an example simulation session is included to demonstrate the steps required to go from the simulation loading phase to the execution phase. R.S.F.

## 63

## CYBERNETICS

Includes feedback and control theory.

**A85-47704\*** National Aeronautics and Space Administration. Lewis Research Center, Cleveland, Ohio.

**A REAL-TIME FORTRAN IMPLEMENTATION OF A SENSOR FAILURE DETECTION, ISOLATION AND ACCOMMODATION ALGORITHM**

J. C. DELAAT (NASA, Lewis Research Center, Cleveland, OH) IN: 1984 American Control Conference, San Diego, CA, June 6-8, 1984, Proceedings. Volume 1. New York, IEEE, 1984, p. 572, 573. refs

An advanced, sensor failure detection, isolation, and accommodation algorithm has been developed by NASA for the F100 turbofan engine. The algorithm takes advantage of the analytical redundancy of the sensors to improve the reliability of the sensor set. The method requires the controls computer, to determine when a sensor failure has occurred without the help of redundant hardware sensors in the control system. The controls computer provides an estimate of the correct value of the output of the failed sensor. The algorithm has been programmed in FORTRAN using a real-time microprocessor-based controls computer. A detailed description of the algorithm and its implementation on a microprocessor is given. I.H.

**A85-47794\*** ALPHATECH, Inc., Burlington, Mass.

**A DESIGN METHODOLOGY FOR ROBUST FAILURE DETECTION AND ISOLATION**

K. R. PATTIPATI, A. S. WILLSKY, J. C. DECKERT, J. S. ETERNO, and J. S. WEISS (Alphatech, Inc., Burlington, MA) IN: 1984 American Control Conference, San Diego, CA, June 6-8, 1984, Proceedings. Volume 3. New York, IEEE, 1984, p. 1755-1762. refs

(Contract NAS3-24078)

A decentralized failure detection and isolation (FDI) methodology, which is robust with respect to model uncertainties and noise, is presented. Redundancy metrics are developed, and optimization problems are posed for the choices of robust parity relations. Closed-form solutions for some special failure cases are given. Connections are drawn with other disciplines, and the use of the metrics to evaluate alternative FDI schemes is discussed.

Author

## 64

## NUMERICAL ANALYSIS

Includes iteration, difference equations, and numerical approximation.

**A85-21370\*** Concordia Univ., Montreal (Quebec).

**RECENT ADVANCES IN METHODS FOR NUMERICAL SOLUTION OF O.D.E. INITIAL VALUE PROBLEMS**

T. D. BUI (Concordia University, Montreal, Canada), A. K. OPPENHEIM (California, University, Berkeley, CA), and D. T. PRATT (Washington, University, Seattle, WA) Journal of Computational and Applied Mathematics (ISSN 0377-0427), vol. 11, Dec. 1984, p. 283-296. Research supported by the Ministère de l'Éducation du Québec; Natural Sciences and Engineering Research Council of Canada. refs  
(Contract NSERC-A-9265; NSF CPE-81-15163; NAG3-227; DE-AC03-76SF-00098)

In the mathematical modeling of physical systems, it is often necessary to solve an initial value problem (IVP), consisting of a system of ordinary differential equations (ODE). A typical program produces approximate solutions at certain mesh points. Almost all existing codes try to control the local truncation error, while the user is really interested in controlling the true or global error. The present investigation provides a review of recent advances regarding the solution of the IVP, giving particular attention to stiff systems. Stiff phenomena are customarily defined in terms of the eigenvalues of the Jacobian. There are, however, some difficulties connected with this approach. It is pointed out that an estimate of the Lipschitz constant proves to be a very practical way to determine the stiffness of a problem. G.R.

**A85-21979\*** Akron Univ., Ohio.

**ON THE DEVELOPMENT OF HIERARCHICAL SOLUTION STRATEGIES FOR NONLINEAR FINITE ELEMENT FORMULATIONS**

J. PADOVAN and J. LACKNEY (Akron, University, Akron, OH) Computers and Structures (ISSN 0045-7949), vol. 19, no. 4, 1984, p. 535-544. refs  
(Contract NSG-3283)

This paper develops a hierarchical type solution scheme which can handle the field equations associated with nonlinear finite element simulations. The overall procedure possesses various levels of application namely degree of freedom, nodal, elemental, substructural as well as global. In particular iteration, updating, assembly and solution control occurs at the various hierarchical levels. Due to the manner of formulation, the degree of matrix inversion depends on the size of the various hierarchical partitioned groups. In this context, degree of freedom partitioning requires no inversion. To benchmark the overall scheme, the results of several numerical examples are presented. Author

**A85-28006\*** National Aeronautics and Space Administration. Lewis Research Center, Cleveland, Ohio.

**A PROCEDURE FOR OBTAINING EXPLICIT SOLUTIONS TO A CLASS OF FREDHOLM INTEGRAL EQUATIONS**

M. E. GOLDSTEIN (NASA, Lewis Research Center, Cleveland, OH) and M. J. LEITMAN (Case Western Reserve University, Cleveland, OH) Journal of Integral Equations (ISSN 0163-5549), vol. 8, 1985, p. 87-93.

(Contract NSF MCS-83-01844)

A Fredholm integral equation is solved in closed form by reducing it to a standard boundary value problem for a sectionally analytic function. The procedure may be extended to more general classes of functions whose Fourier transforms only exist along certain lines in the complex k-plane. Examples are used to illustrate the results. M.D.

## 64 NUMERICAL ANALYSIS

**A85-28015\*** National Aeronautics and Space Administration. Lewis Research Center, Cleveland, Ohio.

### **CONSTRUCTIVE EXISTENCE AND UNIQUENESS FOR TWO-POINT BOUNDARY-VALUE PROBLEMS WITH A LINEAR GRADIENT TERM**

J. A. PENNLINE (NASA, Lewis Research Center, Computer Services Div., Cleveland, OH) Applied Mathematics and Computation (ISSN 0096-3003), vol. 15, 1984, p. 233-260. refs

**A85-50073\*** Texas Univ., Austin.

### **STABILITY, ACCURACY, AND EFFICIENCY OF SOME UNDERINTEGRATED METHODS IN FINITE ELEMENT COMPUTATIONS**

O.-P. JACQUOTTE (Texas, University, Austin) Computer Methods in Applied Mechanics and Engineering (ISSN 0045-7825), vol. 50, Aug. 1985, p. 275-293. refs  
(Contract NAG3-329)

In an attempt to increase computational efficiency in the numerical solution of highly nonlinear problems in solid and fluid mechanics, underintegrated finite element methods have been employed by many analysts. Underintegration refers to the use of a rule of an order lower than that required to integrate polynomial integrands exactly. The main drawback of this technique is related to the production of rank-deficient stiffness matrices, or equivalently an expanded kernel of the governing linear momentum operators. Such a development can introduce numerical instabilities. In order to overcome this difficulty, artificial stiffness or viscosity methods, or other stabilization methods have been proposed. One approach involves the elimination of spurious modes in a postprocessing operation. The present study is concerned with this a posteriori elimination method, taking into account the results which can be expected from it, and some of its possible extensions. G.R.

**N85-19733\*#** National Aeronautics and Space Administration. Lewis Research Center, Cleveland, Ohio.

### **MODELING THE INTERNAL COMBUSTION ENGINE**

F. J. ZELEZNIK and B. J. MCBRIDE Mar. 1985 309 p refs  
(NASA-RP-1094; E-996; NAS 1.61:1094) Avail: NTIS HC A14/MF A01 CSCL 12A

A flexible and computationally economical model of the internal combustion engine was developed for use on large digital computer systems. It is based on a system of ordinary differential equations for cylinder-averaged properties. The computer program is capable of multicycle calculations, with some parameters varying from cycle to cycle, and has restart capabilities. It can accommodate a broad spectrum of reactants, permits changes in physical properties, and offers a wide selection of alternative modeling functions without any reprogramming. It readily adapts to the amount of information available in a particular case because the model is in fact a hierarchy of five models. The models range from a simple model requiring only thermodynamic properties to a complex model demanding full combustion kinetics, transport properties, and poppet valve flow characteristics. Among its many features the model includes heat transfer, valve timing, supercharging, motoring, finite burning rates, cycle-to-cycle variations in air-fuel ratio, humid air, residual and recirculated exhaust gas, and full combustion kinetics. Author

**N85-27584\*#** Pratt and Whitney Aircraft, East Hartford, Conn. Engineering Div.

### **ERROR REDUCTION PROGRAM Final Report**

S. A. SYED, L. M. CHIAPPETTA, and A. D. GOSMAN 11 Jan. 1985 246 p refs  
(Contract NAS3-23686)

(NASA-CR-174776; NAS 1.26:174776; PWA-5928-25) Avail: NTIS HC A11/MF A01 CSCL 12A

The details of a study to select, incorporate and evaluate the best available finite difference scheme to reduce numerical error in combustor performance evaluation codes are described. The combustor performance computer programs chosen were the two dimensional and three dimensional versions of Pratt & Whitney's TEACH code. The criteria used to select schemes required that the difference equations mirror the properties of the governing

differential equation, be more accurate than the current hybrid difference scheme, be stable and economical, be compatible with TEACH codes, use only modest amounts of additional storage, and be relatively simple. The methods of assessment used in the selection process consisted of examination of the difference equation, evaluation of the properties of the coefficient matrix, Taylor series analysis, and performance on model problems. Five schemes from the literature and three schemes developed during the course of the study were evaluated. This effort resulted in the incorporation of a scheme in 3D-TEACH which is usually more accurate than the hybrid differencing method and never less accurate. M.G.

## 71

## ACOUSTICS

Includes sound generation, transmission, and attenuation.

**A85-10869\*#** Virginia Polytechnic Inst. and State Univ., Blacksburg.

### **THE INFLUENCE OF COMBUSTION LINER HOLES ON NOISE PRODUCTION BY DUCTED BURNERS**

J. R. MAHAN and J. D. JONES (Virginia Polytechnic Institute and State University, Blacksburg, VA) American Institute of Aeronautics and Astronautics and NASA, Aeroacoustics Conference, 9th, Williamsburg, VA, Oct. 15-17, 1984. 7 p. refs  
(Contract NAG3-124)

(AIAA PAPER 84-2322)

The thermoacoustic energy conversion process in a turbulent flame is not yet sufficiently well understood to allow accurate prediction of the sound pressure field of even the simplest of laboratory burners. The present contribution is intended to be a step toward fuller understanding of this process. In particular, the possibility is explored that the source structure, in the form of the thermoacoustic efficiency spectrum, might be influenced by the acoustic response of the burner itself. Experimental results are presented which seem to establish that, at least for the gas-fueled laboratory burner studied, source activity is not affected by the addition of downstream combustion liner holes which otherwise alter the acoustic response of the burner. Author

**A85-10882\*#** Lockheed-Georgia Co., Marietta.

### **AN EXPERIMENTAL STUDY OF TONE EXCITED HEATED JETS**

J. LEPICOVSKY, K. K. AHUJA, and M. SALIKUDDIN (Lockheed-Georgia Co., Marietta, GA) American Institute of Aeronautics and Astronautics and NASA, Aeroacoustics Conference, 9th, Williamsburg, VA, Oct. 15-17, 1984. 11 p. refs  
(Contract NAS3-23708)

(AIAA PAPER 84-2341)

The objective of this investigation was to obtain detailed experimental data on the effects of upstream acoustic excitation on the mixing of heated jets with the surrounding air. Based on the information gathered in the literature survey, a technical approach was developed to carry out a systematic set of mean flowfield measurements for a broad range of jet operating and acoustic excitation conditions. Most of the results were obtained at Mach numbers of 0.3 and 0.8 and total temperatures of up to 800 K. Some measurements were made also for the fully expanded supersonic jet of  $M_j = 1.15$ . The maximum level of excitation was  $Le$  equal to or less than 150 dB and a range of excitation frequencies up to  $f_e = 4$  kHz was used. The important results derived from this study can be summarized as follows: (1) the sensitivity of heated jets to upstream acoustic excitation varies strongly with the jet operating conditions, (2) the threshold excitation level increases with increasing jet temperature, and (3) the preferred Strouhal number does not change significantly with a change of the jet operating conditions. Author

**A85-12301\*** Minnesota Univ., Minneapolis.  
**ACOUSTIC STRUCTURE AND PROPAGATION IN HIGHLY POROUS, LAYERED, FIBROUS MATERIALS**

R. F. LAMBERT and J. S. TESAR (Minnesota, University, Minneapolis, MN) Acoustical Society of America, Journal (ISSN 0001-4966), vol. 76, Oct. 1984, p. 1231-1237. Previously announced in STAR as N84-27546. refs  
 (Contract NSF MEA-80-1136; NAG3-161)

The acoustic structure and propagation of sound in highly porous, layered, fine fiber materials is examined. Of particular interest is the utilization of the Kozeny number for determining the static flow resistance and the static structure factor based on flow permeability measurements. In this formulation the Kozeny number is a numerical constant independent of volume porosity at high porosities. The other essential parameters are then evaluated employing techniques developed earlier for open cell foams. The attenuation and progressive phase characteristics in bulk samples are measured and compared with predicted values. The agreements on the whole are very satisfactory. M.A.C.

**A85-13955\*#** Arizona Univ., Tucson.  
**EFFECT OF AIRFOIL MEAN LOADING ON CONVECTED GUST INTERACTION NOISE**

M. R. MYERS and E. J. KERSCHEN (Arizona, University, Tucson, AZ) American Institute of Aeronautics and Astronautics and NASA, Aeroacoustics Conference, 9th, Williamsburg, VA, Oct. 15-17, 1984. 13 p. refs  
 (Contract NAG3-357)  
 (AIAA PAPER 84-2324)

The present theoretical model for noise generation when a convected vortical or entropic gust encounters an airfoil at a nonzero angle-of-attack is based on a linearization of the Euler equations for the steady, subsonic flow past the airfoil. Noise generation is found to be concentrated at local regions which scale on the gust wavelength and are present at airfoil leading and trailing edges. Steady loading of the airfoil affects noise generation at the leading and trailing edges in significantly different ways. Parametric calculations are presented which illustrate that, at high frequencies, moderate levels of airfoil steady loading can drastically increase the noise level produced by airfoil-convected gust interactions. O.C.

**A85-13956\*#** Arizona Univ., Tucson.  
**NOISE PRODUCED BY THE INTERACTION OF A ROTOR WAKE WITH A SWEEP STATOR BLADE**

E. ENVIA and E. J. KERSCHEN (Arizona, University, Tucson, AZ) American Institute of Aeronautics and Astronautics and NASA, Aeroacoustics Conference, 9th, Williamsburg, VA, Oct. 15-17, 1984. 11 p. refs  
 (Contract NAG3-357)  
 (AIAA PAPER 84-2326)

An analysis is developed for the noise generated by the interaction of rotor viscous wakes and a single swept stator vane. The stator vane spans a channel with infinite parallel walls which contains a uniform subsonic mean flow. High frequency wakes, for which the noise generation is concentrated at the vane leading edge, are considered. The general wake pattern is expanded in spanwise modes and solutions for each mode are derived using the Wiener-Hopf technique applied to the equations in the nonorthogonal coordinates. Closed form expressions for the acoustic farfield are obtained. The results of the analysis are used in parametric calculations of rotor viscous wake-stator vane interactions in order to study the effectiveness of sweep as a noise reduction mechanism. For the cases studied, moderate stator sweep angles produce sizeable reductions in the level of the farfield noise. The presence of rotor wake circumferential lean actually increases the noise reduction produced by moderate stator sweep angles. Author

**A85-16099\*#** National Aeronautics and Space Administration. Lewis Research Center, Cleveland, Ohio.

**SUPERSONIC JET SHOCK NOISE REDUCTION**

J. R. STONE (NASA, Lewis Research Center, Cleveland, OH) American Institute of Aeronautics and Astronautics, Aeroacoustics Conference, 9th, Williamsburg, VA, Oct. 15-17, 1984. 44 p. Previously announced in STAR as N84-35085. refs  
 (AIAA PAPER 84-2278)

Shock-cell noise is identified to be a potentially significant problem for advanced supersonic aircraft at takeoff. Therefore NASA conducted fundamental studies of the phenomena involved and model-scale experiments aimed at developing means of noise reduction. The results of a series of studies conducted to determine means by which supersonic jet shock noise can be reduced to acceptable levels for advanced supersonic cruise aircraft are reviewed. Theoretical studies were conducted on the shock associated noise of supersonic jets from convergent-divergent (C-D) nozzles. Laboratory studies were conducted on the influence of narrowband shock screech on broadband noise and on means of screech reduction. The usefulness of C-D nozzle passages was investigated at model scale for single-stream and dual-stream nozzles. The effect of off-design pressure ratio was determined under static and simulated flight conditions for jet temperatures up to 960 K. Annular and coannular flow passages with center plugs and multi-element suppressor nozzles were evaluated, and the effect of plug tip geometry was established. In addition to the far-field acoustic data, mean and turbulent velocity distributions were measured with a laser velocimeter, and shadowgraph images of the flow field were obtained. Author

**A85-16102\*#** National Aeronautics and Space Administration. Lewis Research Center, Cleveland, Ohio.

**TIME DEPENDENT WAVE ENVELOPE FINITE DIFFERENCE ANALYSIS OF SOUND PROPAGATION**

K. J. BAUMEISTER (NASA, Lewis Research Center, Cleveland, OH) American Institute of Aeronautics and Astronautics and NASA, Aeroacoustics Conference, 9th, Williamsburg, VA, Oct. 15-17, 1984. 9 p. Previously announced in STAR as N84-32118. refs  
 (AIAA PAPER 84-2285)

A transient finite difference wave envelope formulation is presented for sound propagation, without steady flow. Before the finite difference equations are formulated, the governing wave equation is first transformed to a form whose solution tends not to oscillate along the propagation direction. This transformation reduces the required number of grid points by an order of magnitude. Physically, the transformed pressure represents the amplitude of the conventional sound wave. The derivation for the wave envelope transient wave equation and appropriate boundary conditions are presented as well as the difference equations and stability requirements. To illustrate the method, example solutions are presented for sound propagation in a straight hard wall duct and in a two dimensional straight soft wall duct. The numerical results are in good agreement with exact analytical results. Author

**A85-16103\*#** National Aeronautics and Space Administration. Lewis Research Center, Cleveland, Ohio.

**ANALYSIS OF THE EFFECT ON COMBUSTOR NOISE MEASUREMENTS OF ACOUSTIC WAVES REFLECTED BY THE TURBINE AND COMBUSTOR INLET**

R. G. HUFF (NASA, Lewis Research Center, Cleveland, OH) American Institute of Aeronautics and Astronautics and NASA, Aeroacoustics Conference, 9th, Williamsburg, VA, Oct. 15-17, 1984. 11 p. Previously announced in STAR as N84-32122. refs  
 (AIAA PAPER 84-2323)

Spectral analyses of static pressure fluctuations measured in turbine engine combustors at low engine speed show good agreement with theory. At idle speed the high pressure turbine is unchoked. Above idle speed the turbine chokes and a significant change in the shape of the measured combustor pressure spectrum is observed. A simplified theoretical model of the acoustic pressure generated in the combustor due to the turbulence-flame front

interaction did not account for acoustic waves reflected from the turbine. By retaining this simplified combustion noise source model and adding a partial reflecting plane at the turbine and combustor inlet, a simple theoretical model was developed that reproduces the undulations in the combustor fluctuating pressure spectra. Plots of the theoretical combustor fluctuating pressure spectra are compared to the measured pressure spectra obtained from the CF6-50 turbofan engine over a range of engine operating speeds. The simplified combustion noise theory when modified by a simple turbine reflecting plane adequately accounts for the changes in measured combustor pressure spectra. It is further concluded that the shape of the pressure spectra downstream of the turbine, neglecting noise generated by the turbine itself, will be the combustion noise spectra unchanged except for the level reduction due to the energy blocked by the turbine. Author

**A85-16104\*#** Missouri Univ., Rolla.

**MODELLING OF WIND TUNNEL WALL EFFECTS ON THE RADIATION CHARACTERISTICS OF ACOUSTIC SOURCES**

W. EVERSMA (Missouri-Rolla, University, Rolla, MO) and K. J. BAUMEISTER (NASA, Lewis Research Center, Cleveland, OH) American Institute of Aeronautics and Astronautics and NASA, Aeroacoustics Conference, 9th, Williamsburg, VA, Oct. 15-17, 1984. 12 p. refs (AIAA PAPER 84-2364)

It is pointed out that the relatively high fuel economy available from propeller-driven aircraft has renewed interest in high speed, highly loaded multiple blade turboprop propulsion systems. Undesirable features related to community noise and the high intensity cabin noise have stimulated new research on the acoustic characteristics of turboprops. The present investigation has the objective to develop a mathematical model of the essential features of the radiation of acoustic disturbances from propellers in a duct and in free space in order to quantify the success with which duct testing can be expected to approximate free field conditions. In connection with the importance of source directionality, a detailed model is considered which consists of a finite element representation of the Gutin propeller theory valid in both the near and far field. G.R.

**A85-20738\*** National Aeronautics and Space Administration. Lewis Research Center, Cleveland, Ohio.

**SOUND GENERATION AND UPSTREAM INFLUENCE DUE TO INSTABILITY WAVES INTERACTING WITH NON-UNIFORM MEAN FLOWS**

M. E. GOLDSTEIN (NASA, Lewis Research Center, Cleveland, OH) Journal of Fluid Mechanics (ISSN 0022-1120), vol. 149, Dec. 1984, p. 161-177. refs

Attention is given to the sound produced by artificially excited, spatially growing instability waves on subsonic shear layers. Real flows that always diverge in the downstream direction allow sound to be produced by the interaction of the instability waves with the resulting streamwise variations of the flow. The upstream influence, or feedback, can interact with the splitter plate lip to produce a downstream-propagating instability wave that may under certain conditions be the same instability wave that originally generated the upstream influence. The present treatment is restricted to very low Mach number flows, so that compressibility effects can only become important over large distances. O.C.

**A85-25932\*#** Lockheed-Georgia Co., Marietta.

**SOME UNIQUE EXPERIMENTS ON RECEPTIVITY**

K. K. AHUJA (Lockheed-Georgia Co., Advanced Flight Sciences Dept., Marietta, GA) American Institute of Aeronautics and Astronautics, Shear Flow Control Conference, Boulder, CO, Mar. 12-14, 1985. 9 p. refs (Contract NAS3-23286) (AIAA PAPER 85-0533)

The objective of this study is to determine whether or not a solid trailing edge is required to produce efficient coupling between sound and instability waves in a shear layer. Instability waves in the shear layer of a subsonic jet, excited externally by a point sound source, were first visualized by using a phase-locked flow

visualization technique. Various means were adopted to shield the sound reaching the nozzle lip. It was found that the low frequency sound couples more efficiently at distances downstream of the nozzle exit. To substantiate the findings further, a supersonic screeching jet was tested such that it passed through a small opening in a baffle placed parallel to the exit plane. The measured feedback or screech frequencies, and also the excited flow disturbances, were found to change drastically on traversing the baffle axially. Similar conclusions were reached when a second baffle was placed downstream of the first baffle, and the effects of moving the first baffle on the feedback frequency of sound generated by flow impingement on the second baffle were examined. It is argued that sound waves passing through the mixing layer of a jet can excite flow instability without the benefit of assistance and coupling at the trailing edge. Author

**A85-26915\*** California Univ., Los Angeles.

**THE RESPONSE OF HELMHOLTZ RESONATORS TO EXTERNAL EXCITATION. I - SINGLE RESONATORS**

P. A. MONKEWITZ and N.-M. NGUYEN-VO (California, University, Los Angeles, CA) Journal of Fluid Mechanics (ISSN 0022-1120), vol. 151, Feb. 1985, p. 477-497. refs (Contract NSG-3236)

The response of single two- and three-dimensional Helmholtz resonators subject to external excitation by a plane acoustic wave is studied. The inviscid linearized problem is solved by the matched-asymptotic-expansion technique in the low-frequency limit, i.e. when the characteristic neck dimension is small compared with the acoustic wavelength. The scale of the cavity is chosen such as to tune the system to the lowest Helmholtz mode. The results are compared with the classical lumped-element model, and refined expressions are derived for the effective mass (added length) and stiffness (effective cavity volume) of the resonator. Author

**A85-36047\*** National Aeronautics and Space Administration. Lewis Research Center, Cleveland, Ohio.

**THE SCATTERING OF ULTRASONIC THIRD SOUND FROM SUBSTRATE SURFACE DEFECTS**

E. R. GENERAZIO (NASA, Lewis Research Center, Cleveland, OH; Pennsylvania State University, University Park, PA) and R. W. REED (United Technologies Research Center, East Hartford, CT; Pennsylvania State University, University Park, PA) Journal of Low Temperature Physics (ISSN 0022-2291), vol. 56, no. 3-4, 1984, p. 355-377. Navy-supported research. refs

The interaction of third sound with isolated surface defects is examined. Phase-inverted reflections are observed to occur at surface defects even when the wavelength of the third sound is much greater than the dimensions of the defect. The origin of the scattering mechanism is believed to be due to the change in the helium film thickness in the vicinity of the topological variations introduced by the presence of the surface defects. Data are obtained for ultrasonic frequencies in the 20-200 kHz range. Author

**A85-39909\*#** National Aeronautics and Space Administration. Lewis Research Center, Cleveland, Ohio.

**A THEORETICAL PREDICTION OF THE ACOUSTIC PRESSURE GENERATED BY TURBULENCE-FLAME FRONT INTERACTIONS**

R. G. HUFF (NASA, Lewis Research Center, Cleveland, OH) American Society of Mechanical Engineers, Winter Annual Meeting, New Orleans, LA, Dec. 9-14, 1984. 8 p. Previously announced in STAR as N84-26383. refs (ASME PAPER 84-WA/NCA-11)

The equations of momentum and continuity are combined and linearized yielding the one dimensional nonhomogeneous acoustic wave equation. Three terms in the non-homogeneous equation act as acoustic sources and are taken to be forcing functions acting on the homogeneous wave equation. The three source terms are: fluctuating entropy, turbulence gradients, and turbulence-flame interactions. Each source term is discussed. The turbulence-flame interaction source is used as the basis for

computing the source acoustic pressure from the Fourier transformed wave equation. Pressure fluctuations created in turbopump gas generators and turbines may act as a forcing function for turbine and propellant tube vibrations in earth to orbit space propulsion systems and could reduce their life expectancy. A preliminary assessment of the acoustic pressure fluctuations in such systems is presented. Author

**A85-42563\*#** National Aeronautics and Space Administration. Lewis Research Center, Cleveland, Ohio.

**THE PERFORMANCE OF JET NOISE SUPPRESSION DEVICES FOR INDUSTRIAL APPLICATIONS**

M. D. DAHL (NASA, Lewis Research Center, Cleveland, OH) and O. H. MCDANIEL (Pennsylvania State University, University Park) ASME, Transactions, Journal of Vibration, Acoustics, Stress, and Reliability in Design (ISSN 0739-3717), vol. 107, July 1985, p. 303-309. Research supported by the Occupational Safety and Health Administration. refs

**N85-10788\*#** National Aeronautics and Space Administration. Lewis Research Center, Cleveland, Ohio.

**OBSERVATIONS FROM VARYING THE LIFT AND DRAG INPUTS TO A NOISE PREDICTION METHOD FOR SUPERSONIC HELICAL TIP SPEED PROPELLERS**

J. H. DITTMAR Sep. 1984 21 p refs  
(NASA-TM-83797; E-2295; NAS 1.15:83797) Avail: NTIS HC A02/MF A01 CSCL 20A

Previous comparisons between calculated and measured supersonic helical tip speed propeller noise show them to have different trends of peak blade passing tone versus helical tip Mach number. It was postulated that improvements in this comparison could be made first by including the drag force terms in the prediction and then by reducing the blade lift terms at the tip to allow the drag forces to dominate the noise prediction. Propeller hub to tip lift distributions were varied, but they did not yield sufficient change in the predicted lift noise to improve the comparison. This result indicates that some basic changes in the theory may be needed. In addition, the noise predicted by the drag forces did not exhibit the same curve shape as the measured data. So even if the drag force terms were to dominate, the trends with helical tip Mach number for theory and experiment would still not be the same. The effect of the blade shock wave pressure rise was approximated by increasing the drag coefficient at the blade tip. Predictions using this shock wave approximation did have a curve shape similar to the measured data. This result indicates that the shock pressure rise probably controls the noise at supersonic tip speed and that the linear prediction method can give the proper noise trend with Mach number. R.S.F.

**N85-11791\*#** Bolt, Beranek, and Newman, Inc., Cambridge, Mass.

**TURBOFAN NOISE GENERATION. VOLUME 2: COMPUTER PROGRAMS Final Report**

C. S. VENTRES, M. A. THEOBALD, and W. D. MARK Jul. 1982 206 p 2 Vol.

(Contract NAS3-21252)  
(NASA-CR-167952; NAS 1.26:167952; BBN-4770) Avail: NTIS HC A10/MF A01 CSCL 20A

The use of a package of computer programs developed to calculate the in duct acoustic modes excited by a fan/stator stage operating at subsonic tip speed is described. The following three noise source mechanisms are included: (1) sound generated by the rotor blades interacting with turbulence ingested into, or generated within, the inlet duct; (2) sound generated by the stator vanes interacting with the turbulent wakes of the rotor blades; and (3) sound generated by the stator vanes interacting with the velocity deficits in the mean wakes of the rotor blades. The computations for three different noise mechanisms are coded as three separate computer program packages. The computer codes are described by means of block diagrams, tables of data and variables, and example program executions; FORTRAN listings are included. M.G.

**N85-13549\*#** General Electric Co., Cincinnati, Ohio. Aircraft Engine Business Group.

**EXPERIMENTAL INVESTIGATION OF SHOCK-CELL NOISE REDUCTION FOR DUAL-STREAM NOZZLES IN SIMULATED FLIGHT Final Report**

B. A. JANARDAN, K. YAMAMOTO, R. K. MAJJIGI, and J. F. BRAUSCH Washington NASA Nov. 1984 189 p refs  
(Contract NAS3-23166)

(NASA-CR-3846; E-2283; NAS 1.26:3846; R83AEB358) Avail: NTIS HC A09/MF A01 CSCL 20A

Six scale-model nozzles were tested in an anechoic facility to evaluate the effectiveness of convergent-divergent (C-D) terminations in reducing shock-cell noise of unsuppressed and mechanically suppressed coannular plug nozzles. One hundred fifty-three acoustic test points with inverted velocity profiles were conducted under static and simulated flight conditions. Diagnostic flow visualization with a shadowgraph and velocity measurements with a laser velocimeter were performed on selected plumes. Shock-cells were identified on the plug and downstream of the plug of the unsuppressed convergent coannular nozzle with truncated plug. Broadband peak frequencies predicted with the two shock-cell structures were correlated with the observed spectra using the measured shock-cell spacings. Relative to a convergent circular nozzle, the perceived noise level (PNL) data at an observer angle of 60 deg relative to inlet, indicated a reduction of (1) 6.5 dB and 9.2 dB with unsuppressed C-D coannular nozzle with truncated plug and (2) 7.7 dB and 8.3 dB with suppressed C-D coannular nozzle under static and simulated flight conditions, respectively. The unsuppressed C-D coannular nozzle with truncated plug, operating at the C-D design condition, had shock-cells downstream of the plug with no shock-cells on the plug. The downstream shock-cells were eliminated by replacing the truncated plug with a smooth extension to obtain an additional 2.4 dB and 3 dB front quadrant PNL reduction, under static and simulated flight conditions, respectively. Other results are discussed. M.G.

**N85-13550\*#** General Electric Co., Cincinnati, Ohio.

**EXPERIMENTAL INVESTIGATION OF SHOCK-CELL NOISE REDUCTION FOR SINGLE STREAM NOZZLES IN SIMULATED FLIGHT Final Report**

K. YAMAMOTO, J. F. BRAUSCH, T. F. BALSA, B. A. JANARDAN, and P. R. KNOTT Washington NASA Dec. 1984 397 p refs

(Contract NAS3-22514)  
(NASA-CR-3845; E-2282; NAS 1.26:3845; R82AEB492) Avail: NTIS HC A17/MF A01 CSCL 20A

Seven single stream model nozzles were tested in the Anechoic Free-Jet Acoustic Test Facility to evaluate the effectiveness of convergent divergent (C-D) flowpaths in the reduction of shock-cell noise under both static and simulated flight conditions. The test nozzles included a baseline convergent circular nozzle, a C-D circular nozzle, a convergent annular plug nozzle, a C-D annular plug nozzle, a convergent multi-element suppressor plug nozzle, and a C-D multi-element suppressor plug nozzle. Diagnostic flow visualization with a shadowgraph and aerodynamic plume measurements with a laser velocimeter were performed with the test nozzles. A theory of shock-cell noise for annular plug nozzles with shock-cells in the vicinity of the plug was developed. The benefit of these C-D nozzles was observed over a broad range of pressure ratios in the vicinity of their design conditions. At the C-D design condition, the C-D annular nozzle was found to be free of shock-cells on the plug. R.S.F.

**N85-13551\*#** National Aeronautics and Space Administration. Lewis Research Center, Cleveland, Ohio.

**STATIC JET NOISE TEST RESULTS OF FOUR 0.35 SCALE-MODEL QCGAT MIXER NOZZLES**

D. E. GROESBECK and C. A. WASSERBAUER Oct. 1984 47 p refs

(NASA-TM-86871; E-2333; NAS 1.15:86871) Avail: NTIS HC A03/MF A01 CSCL 20A

As part of the NASA Quiet Clean General Aviation Turbofan (QCGAT) engine mixer-nozzle exhaust system program, static jet



## 71 ACOUSTICS

exhaust noise was recorded at microphone angles of 45 to 155 deg relative to the nozzle inlet for a conventional profile coaxial nozzle and three 12-lobed coaxial mixer nozzles. Both flows in all four nozzles are internally mixed before being discharged from a single exhaust nozzle. The conventional profile coaxial nozzle jet noise is compared to the current NASA Lewis coaxial jet noise prediction and after applying an adjustment to the predicted levels based on the ratio of the kinetic energy of the primary and secondary flows, the prediction is within a standard deviation of 0.9 dB of the measured data. The mass average (mixed flow) prediction is also compared to the noise data for the three mixer nozzles with a reasonably good fit after applying another kinetic energy ratio adjustment (standard deviation of 0.7 to 1.5 dB with the measured data). The tests included conditions for the full-scale engine at takeoff (T.O.), cutback (86% T.O.) and approach (67% T.O.). M.G.

**N85-17667\*#** Cleveland State Univ., Ohio.  
**INVESTIGATION ON EXPERIMENTAL TECHNIQUES TO DETECT, LOCATE AND QUANTIFY GEAR NOISE IN HELICOPTER TRANSMISSIONS Final Report**  
P. M. FLANAGAN and W. J. ATHERTON Washington NASA Jan. 1985 101 p refs Original contains color illustrations (Contract NAG3-315)  
(NASA-CR-3847; E-2294; NAS 1.26:3847) Avail: NTIS HC A06/MF A01 CSCL 20A

A robotic system to automate the detection, location, and quantification of gear noise using acoustic intensity measurement techniques has been successfully developed. Major system components fabricated under this grant include an instrumentation robot arm, a robot digital control unit and system software. A commercial, desktop computer, spectrum analyzer and two microphone probe complete the equipment required for the Robotic Acoustic Intensity Measurement System (RAIMS). Large-scale acoustic studies of gear noise in helicopter transmissions cannot be performed accurately and reliably using presently available instrumentation and techniques. Operator safety is a major concern in certain gear noise studies due to the operating environment. The man-hours needed to document a noise field in situ is another shortcoming of present techniques. RAIMS was designed to reduce the labor and hazard in collecting data and to improve the accuracy and repeatability of characterizing the acoustic field by automating the measurement process. Using RAIMS a system operator can remotely control the instrumentation robot to scan surface areas and volumes generating acoustic intensity information using the two microphone technique. Acoustic intensity studies requiring hours of scan time can be performed automatically without operator assistance. During a scan sequence, the acoustic intensity probe is positioned by the robot and acoustic intensity data is collected, processed, and stored.

**N85-19791\*#** General Electric Co., Schenectady, N. Y. Corporate Research and Development.  
**EFFECTS OF VANE/BLADE RATIO AND SPACING ON FAN NOISE, VOLUME 1 Final Technical Report**  
P. R. GLIEBE (GE, Cincinnati) and R. A. KANTOLA Dec. 1983 164 p refs 2 Vol.  
(Contract NAS3-22062)  
(NASA-CR-174664; NAS 1.26:174664; GE-84SRD006-VOL-1) Avail: NTIS HC A08/MF A01 CSCL 20A

The noise characteristics of a high-speed fan were studied. The experimental investigation was carried out on a 50.8 cm (20 in.) diameter scale model fan stage in an anechoic chamber with an inflow turbulence control screen installed. The forty-four blade rotor was tested with forty-eight vane and eighty-six vane stator rows, over a range of axial rotor-stator spacings from 0.5 to 2.3 rotor tip chords. A two-dimensional strip theory model of rotor-stator interaction noise was employed to predict the measured tone power level trends, and good overall agreement with measured trends was obtained. A.R.H.

**N85-19792\*#** General Electric Co., Schenectady, N. Y.  
**EFFECTS OF VANE/BLADE RATIO AND SPACING ON FAN NOISE. VOLUME 2: DATA SUPPLEMENT Final Report**  
P. R. GLIEBE and R. A. KANTOLA Dec. 1983 359 p 2 Vol.  
(Contract NAS3-22062)  
(NASA-CR-174665; NAS 1.26:174665; GE-84SRD006-VOL-2; DS-3-VOL-2) Avail: NTIS HC A16/MF A01 CSCL 20A  
Complete tabulations of 1/3-octave band acoustic measurements are given. Author

**N85-22108\*#** National Aeronautics and Space Administration. Lewis Research Center, Cleveland, Ohio.  
**FURTHER COMPARISON OF WIND TUNNEL AND AIRPLANE ACOUSTIC DATA FOR ADVANCED DESIGN HIGH SPEED PROPELLER MODELS**  
J. H. DITTMAR 1985 23 p refs To be presented at the 109th Meeting of the Acoust. Soc. of Am., Austin, Tex., 8-12 Apr. 1985  
(NASA-TM-86935; E-2448; NAS 1.15:86935) Avail: NTIS HC A02/MF A01 CSCL 20A

Comparisons were made between the SR-2 and SR-3 model propeller noise data taken in the NASA 8-by-6 wind tunnel, in the United Technologies Research Center (UTRC) anechoic tunnel, and with boom and fuselage microphones on the NASA Jetstar airplane. Plots of peak blade passage tone noise versus helical tip Mach number generally showed good agreement. The levels of the airplane fuselage data were somewhat lower than the boom data by an approximately uniform value. The curve shapes were similar except for the UTRC data which was flatter than the other sets. This was attributed to the UTRC data being taken at constant power while the other data were taken at constant advance ratio. General curves of the peak blade passage tone versus helical tip Mach number fit through all the data are also presented. Directivity shape comparisons at the cruise condition were similar for the airplane and 8-by-6 tunnel data. The UTRC data peaked farther forward but, when an angle correction was made for the different axial Mach number used in the UTRC tests, the shape was similar to the others. The general agreement of the data from the four configurations enables the formation of a good consensus of the noise from these propellers. Author

**N85-22109\*#** National Aeronautics and Space Administration. Lewis Research Center, Cleveland, Ohio.  
**NOISE TRANSMISSION LOSS OF A RECTANGULAR PLATE IN AN INFINITE BAFFLE**  
L. A. ROUSSOS Mar. 1985 36 p refs Presented at the 107th Meeting of the Acoustical Society of America, Norfolk, Va., 7-10 May 1984  
(NASA-TP-2398; L-15861; NAS 1.60:2398) Avail: NTIS HC A03/MF A01 CSCL 20A

An improved analytical procedure was developed that allows for the efficient calculation of the noise transmission characteristics of a finite rectangular plate. Both isotropic and symmetrically laminated composite plates are considered. The plate is modeled with classic thin-plate theory and is assumed to be simply supported on all four sides. The incident acoustic pressure is assumed to be a plane wave impinging on the plate at an arbitrary angle. The reradiated pressure is assumed to be negligible compared with the blocked pressure, and the plate vibrations are calculated by a normal-mode approach. A Green's function integral equation is used to link the plate vibrations to be transmitted far-field sound waves, and transmission loss is calculated from the ratio of incident to transmitted acoustic powers. The result is a versatile research and engineering analysis tool that predicts noise transmission loss and enables the determination of the modal behavior of the plate. E.A.K.

**N85-27637\*#** Texas Univ., Austin.  
**INTERACTION OF FINITE-AMPLITUDE SOUND WITH AIR-FILLED POROUS MATERIALS** Final Report, 1 Sep. 1981 - 28 Feb. 1985

D. A. NELSON Mar. 1985 177 p refs  
 (Contract NSG-3198; N00014-75-C-0867; N00014-84-K-0574)  
 (NASA-CR-174885; NAS 1.26:174885; ARL-TR-85-15) Avail:  
 NTIS HC A09/MF A01 CSCL 20A

The propagation of high intensity sound waves through an air-filled porous material was studied. The material is assumed: (1) to be rigid, incompressible, and homogeneous, and (2) to be adequately described by two properties: resistivity  $r$  and porosity. The resulting wave equation is still nonlinear, however, because of the  $u \operatorname{sgn}(u)$  term in the resistivity. The equation is solved in the frequency domain as an infinite set of coupled inhomogeneous Helmholtz equations, one for each harmonic. An approximate but analytical solution leads to predictions of excess attenuation, saturation, and phase speed reduction for the fundamental component. A more general numerical solution is used to calculate the propagation curves for the higher harmonics. The  $u \operatorname{sgn}(u)$  nonlinearity produces a cubic distortion pattern; when the input signal is a pure tone, only odd harmonic distortion products are generated. G.L.C.

**N85-30770\*#** National Aeronautics and Space Administration.  
 Lewis Research Center, Cleveland, Ohio.

**MEASURED ACOUSTIC PROPERTIES OF VARIABLE AND LOW DENSITY BULK ABSORBERS**

M. D. DAHL and E. J. RICE 1985 18 p refs Presented at the Winter Ann. Meeting of the Am. Soc. of Mech. Engr., Miami Beach, Fla., 17-21 Nov. 1985  
 (NASA-TM-87065; E-2633; NAS 1.15:87065) Avail: NTIS HC A02/MF A01 CSCL 20A

Experimental data were taken to determine the acoustic absorbing properties of uniform low density and layered variable density samples using a bulk absorber with a perforated plate facing to hold the material in place. In the layered variable density case, the bulk absorber was packed such that the lowest density layer began at the surface of the sample and progressed to higher density layers deeper inside. The samples were placed in a rectangular duct and measurements were taken using the two microphone method. The data were used to calculate specific acoustic impedances and normal incidence absorption coefficients. Results showed that for uniform density samples the absorption coefficient at low frequencies decreased with increasing density and resonances occurred in the absorption coefficient curve at lower densities. These results were confirmed by a model for uniform density bulk absorbers. Results from layered variable density samples showed that low frequency absorption was the highest when the lowest density possible was packed in the first layer near the exposed surface. The layers of increasing density within the sample had the effect of damping the resonances.

Author

## 72

### ATOMIC AND MOLECULAR PHYSICS

Includes atomic structure and molecular spectra.

**N85-22477\*#** National Aeronautics and Space Administration.  
 Lewis Research Center, Cleveland, Ohio.

### LABORATORY STUDIES OF KAPTON DEGRADATION IN AN OXYGEN ION BEAM

D. C. FERGUSON *In its* Spacecraft Environ. Interactions Technol., 1983 p 81-90 Mar. 1985 refs  
 Avail: NTIS HC A99/MF E03 CSCL 18H

Results are presented from a preliminary laboratory investigation of the degradation of the widely used polyimide Kapton under oxygen ion bombardment. Recent space shuttle flights have shown that Kapton and some other materials exposed to the apparent ram flow of residual atmosphere (at orbital velocity in low Earth orbit) lose mass and change their optical properties. It was hypothesized that these changes are caused by chemical interaction with atomic oxygen, aided by the 5-eV impact energy of atmospheric oxygen atoms in the ram. The reaction rate under  $O(+)$  bombardment seemed to be independent of incident energy over a wide range of energies. Although the flux of thermal ions in this experiment was much greater than the accelerated flux, the observed Kapton degradation was limited to the beam area and ram flow direction. This is consistent with an activation energy above the thermal energies but well below the beam energies. The results reproduce well the material loss, optical changes, SEM surface structure, and ram directionality of the samples returned by the shuttle. These factors, along with the lack of degradation under argon ion bombardment, are convincing evidence for ram flow oxidation as the mechanism of degradation. B.G.

## 73

### NUCLEAR AND HIGH-ENERGY PHYSICS

Includes elementary and nuclear particles; and reactor theory.

**N85-35728\*#** Boeing Aerospace Co., Seattle, Wash. Electrical Power Systems Technology.

**APPLICABILITY OF 100KWE-CLASS OF SPACE REACTOR POWER SYSTEMS TO NASA MANNED SPACE STATION MISSIONS** Final Report

S. W. SILVERMAN, H. J. WILLENBERG, and C. ROBERTSON  
 (General Electric Co., King of Prussia, Pa.) Aug. 1985 184 p refs

(Contract NAS3-23865)  
 (NASA-CR-174696; NAS 1.26:174696; D180-28461-1) Avail:  
 NTIS HC A09/MF A01 CSCL 18I

An assessment is made of a manned space station operating with sufficiently high power demands to require a multihundred kilowatt range electrical power system. The nuclear reactor is a competitor for supplying this power level. Load levels were selected at 150kWe and 300kWe. Interactions among the reactor electrical power system, the manned space station, the space transportation system, and the mission were evaluated. The reactor shield and the conversion equipment were assumed to be in different positions with respect to the station; on board, tethered, and on a free flyer platform. Mission analyses showed that the free flyer concept resulted in unacceptable costs and technical problems. The tethered reactor providing power to an electrolyzer for regenerative fuel cells on the space station, results in a minimum weight shield and can be designed to release the reactor power section so that it moves to a high altitude orbit where the decay period is at least 300 years. Placing the reactor on the station, on a structural boom is an attractive design, but heavier than the long tethered reactor design because of the shield weight for manned activity near the reactor. Author

## OPTICS

Includes light phenomena.

**A85-23134\*** Stanford Univ., Calif.

**OPTICAL COMPUTER SWITCHING NETWORK**

B. CLYMER (Stanford University, Stanford, CA) and S. A. COLLINS, JR. (Ohio State University, Columbus, OH) (IEEE, ICO, and SPIE, International Optical Computing Conference, 10th, Cambridge, MA, Apr. 6-8, 1983) Optical Engineering (ISSN 0091-3286), vol. 24, Jan.-Feb. 1985, p. 74-81. Research supported by the Hughes Aircraft Co. and Ohio State University. refs (Contract NSG-3302)

The design for an optical switching system for minicomputers that uses an optical spatial light modulator such as a Hughes liquid crystal light valve is presented. The switching system is designed to connect 80 minicomputers coupled to the switching system by optical fibers. The system has two major parts: the connection system that connects the data lines by which the computers communicate via a two-dimensional optical matrix array and the control system that controls which computers are connected. The basic system, the matrix-based connecting system, and some of the optical components to be used are described. Finally, the details of the control system are given and illustrated with a discussion of timing.

Author

**N85-13594\*** Opcoa, Inc., Santa Ana, Calif.

**FIBER OPTIC, FABRY-PEROT HIGH TEMPERATURE SENSOR Final Report**

K. JAMES and B. QUICK Nov. 1984 28 p

(Contract NAS3-23522)

(NASA-CR-174712; NAS 1.26:174712) Avail: NTIS HC A03/MF A01 CSCL 20F

A digital, fiber optic temperature sensor using a variable Fabry-Perot cavity as the sensor element was analyzed, designed, fabricated, and tested. The fiber transmitted cavity reflection spectra is dispersed then converted from an optical signal to electrical information by a charged coupled device (CCD). A microprocessor-based color demodulation system converts the wavelength information to temperature. This general sensor concept not only utilizes an all-optical means of parameter sensing and transmitting, but also exploits microprocessor technology for automated control, calibration, and enhanced performance. The complete temperature sensor system was evaluated in the laboratory. Results show that the Fabry-Perot temperature sensor has good resolution (0.5% of full scale), high accuracy, and potential high temperature (1000 C) applications.

Author

**N85-28786\*** National Aeronautics and Space Administration. Lewis Research Center, Cleveland, Ohio.

**INCIDENT BEAM POLARIZATION FOR LASER DOPPLER VELOCIMETRY EMPLOYING A SAPPHIRE CYLINDRICAL WINDOW**

J. A. LOCK (Cleveland State Univ.) and H. J. SCHOCK Jun. 1985 25 p refs

(NASA-TM-87064; E-2316-1; NAS 1.15:87064) Avail: NTIS HC A02/MF A01 CSCL 20F

For laser Doppler velocimetry studies employing sapphire windows as optical access ports, the birefringency of sapphire produces an extra beam intersection volume which serves to effectively smear the acquired velocity flow field data. It is shown that for a cylindrical window geometry, the extra beam intersection volume may be eliminated with minimal decrease in the fringe visibility of the remaining intersection volume by suitably orienting the polarizations of the initial laser beams. For horizontally incident beams, these polarizations were measured at three intersection locations within the cylinder. It was found that the measured polarization angles agreed with the theoretical predictions.

Author

**N85-34631\*** National Aeronautics and Space Administration. Lewis Research Center, Cleveland, Ohio.

**DIAMONDLIKE CARBON PROTECTIVE COATINGS FOR IR MATERIALS**

M. J. MIRTICH, D. NIR, D. M. SWEC, and B. A. BANKS 1985 18 p refs Presented at the 12th Intern. Conf. on Met. Coatings, Los Angeles, 15-19 Apr. 1985; sponsored by the American Vacuum Society

(NASA-TM-87083; E-2506; NAS 1.15:87083) Avail: NTIS HC A02/MF A01 CSCL 20F

Diamondlike carbon (DLC) films have the potential to protect optical windows in applications where it is important to maintain the integrity of the specular transmittance of these films on ZnS and ZnSe infrared transmitting windows. The films must be adherent and durable such that they protect the windows from rain and particle erosion as well as chemical attack. In order to optimize the performance of these films, 0.1 micro m thick diamondlike carbon films were deposited on fused silica and silicon wafers, using three different methods of ion beam deposition. One method was sputter deposition from a carbon target using an 8 cm ion source. The merits of hydrogen addition were experimentally evaluated in conjunction with this method. The second method used a 30 cm hollow cathode ion source with hydrocarbon/Argon gases to deposit diamondlike carbon films from the primary beam at 90 to 250 eV. The third method used a dual beam system employing a hydrocarbon/Argon 30 cm ion source and an 8 cm ion source. Films were evaluated for adherence, intrinsic stress, infrared transmittance between 2.5 and 50 micro m, and protection from particle erosion. An erosion test using a sandblaster was used to give quantitative values of the protection afforded to the fused silica by the diamondlike carbon films. The fused silica surfaces protected by diamondlike carbon films were exposed to 100 micro m diameter SiO particles at 60 mi/hr (26.8/sec) in the sandblaster.

B.W.

## PLASMA PHYSICS

Includes magnetohydrodynamics and plasma fusion.

**A85-12705\*** Colorado State Univ., Fort Collins.

**ION FLOW EXPERIMENTS IN A MULTIPOLE DISCHARGE CHAMBER**

H. R. KAUFMAN, R. S. ROBINSON, and L. E. FRISA (Colorado State University, Fort Collins, CO) AIAA Journal (ISSN 0001-1452), vol. 22, Nov. 1984, p. 1544-1549. Previously cited in issue 03, p. 398, Accession no. A83-14398. refs (Contract NSG-3011)

**A85-16443\*** Michigan State Univ., East Lansing.

**MEASUREMENTS OF ENERGY DISTRIBUTION IN MICROWAVE PLASMAS OF N2 AND HE AND COMPARISONS WITH RESULTS FOR H2**

R. CHAPMAN and M. C. HAWLEY (Michigan State University, East Lansing, MI) IN: International Electric Propulsion Conference, 17th, Tokyo, Japan, May 28-31, 1984, Proceedings. Tokyo, Japan Society for Aeronautical and Space Sciences, 1984, p. 547-550. (Contract NSG-3299)

An electrothermal propulsion concept utilizing a microwave plasma system as the mechanism to convert electromagnetic energy into translational energy of the flowing gas is being investigated. Specifically, this study compares the energy transfer characteristics of three different gases, H2, N2, and He, to gain some insight as to the dominant energy transfer processes present in a microwave plasma. A calorimetric experimental system has been designed and built enclosing the microwave plasma system to accurately determine the net energy transferred to the flowing gas. Results are obtained for N2 and He discharges and compared with previously reported experimental results for H2.

Author

**A85-16444\*** # Michigan State Univ., East Lansing.

**THE ENERGETICS OF HYDROGEN ATOM RECOMBINATION - ANALYSIS, EXPERIMENTS, AND MODELING**

J. W. FILPUS and M. C. HAWLEY (Michigan State University, East Lansing, MI) IN: International Electric Propulsion Conference, 17th, Tokyo, Japan, May 28-31, 1984, Proceedings. Tokyo, Japan Society for Aeronautical and Space Sciences, 1984, p. 551-559. refs

(Contract NSG-3299)

A theoretical investigation of the effect of the microscopic energetics of the recombination reaction on the performance of a microwave-plasma electrothermal propulsion system is described, and the results of the analysis are presented. A series of experiments to test the concept is described and analyzed by comparison with a computer model of the recombination reaction. It is concluded that internal energy considerations are not likely to significantly affect the design of a microwave-plasma electrothermal rocket. The experimental results indicate that the microwave power is far higher than the capacity of the gas to absorb it; the cooling needed to control the energy dominates the experimental results. C.D.

**A85-16455\*** # Michigan State Univ., East Lansing.

**RECENT WORK ON A MICROWAVE ION SOURCE**

J. ASMUSSEN and J. ROOT (Michigan State University, East Lansing, MI) IN: International Electric Propulsion Conference, 17th, Tokyo, Japan, May 28-31, 1984, Proceedings. Tokyo, Japan Society for Aeronautical and Space Sciences, 1984, p. 660-664. refs

(Contract NSG-3299)

The performance of a microwave (2.45 GHz) plasma-disk ion source using a cylindrical microwave cavity is described. The operating characteristics in argon and xenon gases with 50-200 W of input power and gas flow rates from 10-80 sccm are presented. In particular, extracted beam current versus accelerating voltage, and specific energy vs. mass utilization efficiency and extracted beam current are presented. Double Langmuir probe measurements indicate that electron densities in excess of 10 to the 12th per cu cm can be readily achieved in the microwave generated plasma. Author

**A85-17262\*** Kansas Univ., Lawrence.

**NUMERICAL SIMULATIONS OF POSITIVELY-BIASED PROBES AND DIELECTRIC-CONDUCTOR DISKS IN A PLASMA**

S. T. BRANDON, R. L. KESSEL, J. ENOCH, and T. P. ARMSTRONG (Kansas, University, Lawrence, KS) Journal of Applied Physics (ISSN 0021-8979), vol. 56, Dec. 1, 1984, p. 3215-3222. refs

(Contract NSG-3290)

Plasma densities in the low-earth orbit range may be sufficient to cause difficulties for spacecraft operating at high voltages in this environment. The present investigation is concerned with the results of a continuing effort to develop a particle-in-cell (PIC), cylindrically-symmetric, 2-1/2 dimensional, self-consistent numerical simulation code. The simulation has the objective to explore the interactions of an ambient plasma with a conducting disk, which may be partially covered by a dielectric material. The disk and the surrounding dielectric material represent a hole in an insulator covering a conductor. Attention is given to a review of the simulation model, plain disk calculations, the disk and dielectric configuration, and the 'pinhole' effect. G.R.

**A85-43552\*** Michigan State Univ., East Lansing.

**EXPERIMENTAL PERFORMANCE OF A MICROWAVE CAVITY PLASMA DISK ION SOURCE**

J. ROOT and J. ASMUSSEN (Michigan State University, East Lansing) Review of Scientific Instruments (ISSN 0034-6748), vol. 56, Aug. 1985, p. 1511-1519. refs

(Contract NSG-3299)

The detailed description and performance characteristics of a microwave ion source are presented. This ion source utilizes an internally tuned, single-mode (or selective multimode) cylindrical cavity applicator to focus and match microwave energy into a

disk-shaped discharge zone. The combination of mode focus control and variable, internal cavity matching allows the efficient operation and beam extraction over a wide range of pressures, powers and gaseous inputs. Experimental measurements of ion beam current versus accelerating voltage and input microwave power in xenon and oxygen gas are presented. Ion source specific energy and mass utilization versus experimental variables are also determined. The experimental performance demonstrates the ability of this ion source to extract an ion beam with a well matched, stable, and continuous operation over a wide range of input gases, low pressures, and over input gas flow rates in excess of 100 to a few sccm. Double Langmuir probe measurements in xenon gas indicate high degrees of ionization, and electron and ion concentrations in excess of 100 critical densities in the microwave discharge zone. This ion source has many potential uses such as spacecraft electric propulsion, material ion beam processing, and neutral beam ion sources. Author

**N85-22472\*** # National Aeronautics and Space Administration, Washington, D.C.

**SUPRATHERMAL PLASMA OBSERVED ON STS-3 MISSION BY PLASMA DIAGNOSTICS PACKAGE**

W. PATERSON, L. A. FRANK, H. OWENS, J. S. PICKETT, G. B. MURPHY, and S. D. SHAWHAN /in NASA, Lewis Research Center Spacecraft Environ. Interactions Technol., 1983 p 13-17 Mar. 1985 refs Prepared in cooperation with Iowa Univ., Iowa City

(Contract NAG3-449)

Avail: NTIS HC A99/MF E03 CSCL 201

Artificially produced electron beams were used extensively during the past decade as a means of probing the magnetosphere, and more recently as a means of actively controlling spacecraft potential. Experimentation in these areas has proven valuable, yet at times confusing, due to the interaction of the electron beam with the ambient plasma. The OSS-1/STS-3 Mission in March 1982 provided a unique opportunity to study beam-plasma interactions at an altitude of 240 km. On board for this mission was a Fast Pulse Electron Generator (FPEG). Measurements made by the Plasma Diagnostics Package (PDP) while extended on the Orbiter RMS show modifications of the ion and electron energy distributions during electron beam injection. Observations made by charged particle detectors are discussed and related to measurements of Orbiter potential. Several of the PDP instruments, the joint PDP/FPEG experiment, and observations made during electron beam injection are described. B.G.

**N85-22494\*** # National Aeronautics and Space Administration, Lewis Research Center, Cleveland, Ohio.

**THE PIX-2 EXPERIMENT: AN OVERVIEW**

C. K. PURVIS /in its Spacecraft Environ. Interactions Technol. p 321-332 Mar. 1985 refs

Avail: NTIS HC A99/MF E03 CSCL 201

The second Plasma Interactions Experiment (PIX-2) was launched in January 1983 as a piggyback on the second stage of the Delta launch vehicle that carried IRAS into orbit. Placed in a 870 km circular polar orbit, it returned 18 hrs of data on the plasma current collection and arcing behavior of solar arrays biased to +/-1000 V in steps. The four 500 sq cm solar array segments were biased singly and in combinations. In addition to the array segments PIX-2 carried a Sun sensor, a Langmuir probe to measure electron currents, and a hot-wire filament electron emitter to control vehicle potential during positive array bias sequences. The PIX-2 experiment is reviewed from program and operational perspectives. M.G.

## 75 PLASMA PHYSICS

**N85-22495\*#** National Aeronautics and Space Administration. Lewis Research Center, Cleveland, Ohio.

### **PLASMA INTERACTION EXPERIMENT 2 (PIX 2): LABORATORY AND FLIGHT RESULTS**

N. T. GRIER *In its* Spacecraft Environ. Interactions Technol. p 333-347 Mar. 1985

Avail: NTIS HC A99/MF E03 CSCL 201

The Plasma Interaction Experiments 1 and 2 (PIX 1 and 2) were designed as first steps toward understanding interactions between high-voltage solar arrays and the surrounding plasma. The PIX 2 consisted of an approximately 2000-sq cm array divided into four equal segments. Each of the segments could be biased independently and the current measured separately. In addition to the solar array segments, PIX 2 had a hot-wire-filament electron emitter and a spherical Langmuir probe. The emitter was operated when the array segments were biased positively above 125 V. Thermal electrons from the emitter aided in balancing the electron currents collected by the array. Laboratory and flight results of PIX 2 are presented. At high positive voltages on the solar array segments, the flight currents were approximately an order of magnitude larger than the ground test currents. This is attributed to the tank walls in the laboratory interfering with the electron currents to the array segments. From previous tests it is known that the tank walls limit the electron currents at high voltages. This was the first verification of the extent of the laboratory tank effect on the plasma coupling current. M.G.

**N85-22496\*#** National Aeronautics and Space Administration. Lewis Research Center, Cleveland, Ohio.

### **RAM-WAKE EFFECTS ON PLASMA CURRENT COLLECTION OF THE PIX 2 LANGMUIR PROBE**

D. C. FERGUSON *In its* Spacecraft Environ. Interactions Technol. p 349-357 Mar. 1985 refs

Avail: NTIS HC A99/MF E03 CSCL 201

The Plasma Interaction Experiment 2 (PIX 2) Langmuir probe readings of the same polar magnetospheric regions taken on consecutive orbits showed occasional apparent densities as much as 10 times lower than the average, although each pass clearly showed density structures related to the day/night boundary. At other points in the orbit, Langmuir probe currents varied by as much as a factor of 20 on a time scale of minutes. The hypothesis is advanced that these apparent inconsistencies in Langmuir probe current are the results of the probe's orientation relative to the body of the spacecraft and the velocity vector. Theoretical studies predict a possible depletion in collected electron current by a factor of 100 in the wake. Experimental results from other spacecraft indicate that a wake electron depletion by a factor of 10 or so is realistic. This amount of depletion is consistent with the PIX 2 data if the spacecraft was rotating. Both the Sun sensor and temperature sensor data on PIX 2 show a complex variation consistent with rotation of the Langmuir probe into and out of the spacecraft wake on a time scale of minutes. Furthermore, Langmuir probe data taken when the probe was not in the spacecraft wake are consistent from orbit to orbit. This supports the interpretation that ram/wake effects may be the source of apparent discrepancies at other orientations. M.G.

**N85-22497\*#** National Aeronautics and Space Administration. Lewis Research Center, Cleveland, Ohio.

### **NASCAP SIMULATION OF PIX 2 EXPERIMENTS**

J. C. ROCHE and M. J. MANDELL (Systems, Science and Software, San Diego) *In its* Spacecraft Environ. Interactions Technol. p 359-366 Mar. 1985

Avail: NTIS HC A99/MF E03 CSCL 201

The latest version of the NASCAP/LEO digital computer code used to simulate the PIX 2 experiment is discussed. NASCAP is a finite-element code and previous versions were restricted to a single fixed mesh size. As a consequence the resolution was dictated by the largest physical dimension to be modeled. The latest version of NASCAP/LEO can subdivide selected regions. This permitted the modeling of the overall Delta launch vehicle in the primary computational grid at a coarse resolution, with subdivided regions at finer resolution being used to pick up the

details of the experiment module configuration. Langmuir probe data from the flight were used to estimate the space plasma density and temperature and the Delta ground potential relative to the space plasma. This information is needed for input to NASCAP. Because of the uncertainty or variability in the values of these parameters, it was necessary to explore a range around the nominal value in order to determine the variation in current collection. The flight data from PIX 2 were also compared with the results of the NASCAP simulation. R.J.F.

**N85-22498\*#** National Aeronautics and Space Administration. Lewis Research Center, Cleveland, Ohio.

### **AN INVESTIGATION OF ARC DISCHARGING ON NEGATIVELY BIASED DIELECTRIC CONDUCTOR SAMPLES IN A PLASMA**

W. L. MILLER *In its* Spacecraft Environ. Interactions Technol. p 367-377 Mar. 1985 refs

Avail: NTIS HC A99/MF E03 CSCL 201

Proposals are now being developed for the construction of high-power photovoltaic systems for operation in low Earth orbit, where the plasma number density is about 1,000 to 1,000,000 per cubic cm. Existing data indicate that interactions between the plasma and high-voltage surfaces of an orbiting power system will occur. In ground tests, where the applied voltage is increased negatively from ground, the array current collection shows an approximately linear rise until it terminates in arcing at greater than several hundred volts negative. This arcing may reduce the power generation efficiency and could possibly affect the low-level logic circuits of the spacecraft. Therefore it is important that the arcing phenomenon be well understood. This study is a survey of the behavior of different dielectric-conductor samples, including a solar cell module, that were biased negatively in a low-density plasma environment with the intent of defining arc discharge conditions and characteristics. Procedures and results are discussed. Author

## 76

## SOLID-STATE PHYSICS

Includes superconductivity.

### **A85-11466\* Varian Associates, Palo Alto, Calif. MAGNESIUM DOPING OF EFFICIENT GAAS AND GA(0.75)IN(0.25)AS SOLAR CELLS GROWN BY METALORGANIC CHEMICAL VAPOR DEPOSITION**

C. R. LEWIS, C. W. FORD, and J. G. WERTHEN (Varian Associates, Inc., Palo Alto, CA) *Applied Physics Letters* (ISSN 0003-6951), vol. 45, Oct. 15, 1984, p. 895-897. refs (Contract NAS3-22232)

Magnesium has been substituted for zinc in GaAs and Ga(0.75)In(0.25)As solar cells grown by metalorganic chemical vapor deposition (MOCVD). Bis(cyclopentadienyl)magnesium (Cp<sub>2</sub>Mg) is used as the MOCVD transport agent for Mg. Full retention of excellent material quality and efficient cell performance results. The substitution of Mg for Zn would enhance the abruptness and reproducibility of doping profiles, and facilitate high temperature processing and operation, due to the much lower diffusion coefficient of Mg, relative to Zn, in these materials. Author

### **A85-18082\* Michigan Technological Univ., Houghton. THE MECHANISMS OF FORMATION AND PREVENTION OF CHANNEL SEGREGATION DURING ALLOY SOLIDIFICATION**

A. HELLAWELL (Michigan Technological University, Houghton, MI) and A. K. SAMPLE *Metallurgical Transactions A - Physical Metallurgy and Materials Science* (ISSN 0360-2133), vol. 15A, Dec. 1984, p. 2163-2173. refs (Contract NSF DMR-82-12115; NAG3-560; NAS8-33727)

Using a base chilled configuration, conditions for the formation and prevention of segregation channels are studied in the ammonium chloride-water and lead-tin systems. Such channels

develop when the rejected solute is less dense than the solvent and are therefore a result of density inversion, but slow (less than 5 rpm) rates of mold rotation, about axes inclined to the vertical by 20 to 30 deg, throughout the time of solidification, effectively prevent the formation or propagation of these channels. In experiments with artificially created or blocked channels, a simultaneous solute plume in the bulk liquid must be present in order for a channel to develop. The results indicate that channels originate not within the dendritic array, but immediately ahead of the growth front as a result of perturbation from the less dense boundary layer into the bulk liquid. The effect of mold movement is to translate laterally the bulk liquid relative to the growth front so that perturbations are sheared off. The nature of the liquid movement is considered and shown to be a function of the mold dimensions. M.D.

**A85-21425\*** California Univ., Irvine.

**PRISM-COUPLED LIGHT EMISSION FROM TUNNEL JUNCTIONS**

S. USHIOA, J. E. RUTLEDGE, and R. M. PIERCE (California, University, Irvine, CA) Physical Review Letters (ISSN 0031-9007), vol. 54, Jan. 21, 1985, p. 224-226. refs (Contract NAG3-524)

Completely p-polarized light emission has been observed from smooth Al-AIO(x)-Au tunnel junctions placed on a prism coupler. The angle and polarization dependence demonstrate unambiguously that the emitted light is radiated by the fast-mode surface plasmon polariton. The emission spectra suggest that the dominant process for the excitation of the fast mode is through conversion of the slow mode to the fast mode mediated by residual roughness on the junction surface. Author

**A85-24649\*** California Univ., Irvine.

**SUBSTRATE-INDUCED ORIENTATIONAL ORDER IN THE ISOTROPIC PHASE OF LIQUID CRYSTALS**

A. MAUGER, G. ZRIBI, D. L. MILLS (California, University, Irvine, CA), and J. TONER (IBM Thomas J. Watson Research Center, Yorktown Heights, NY) Physical Review Letters (ISSN 0031-9007), vol. 53, Dec. 24, 1984, p. 2485-2488. refs (Contract NAG3-250)

Nematic order induced near a solid boundary in an otherwise isotropic liquid crystal is studied theoretically, at temperatures just above the bulk nematic-isotropic phase transition. Three distinct regimes are found, depending on the strength of orientational torques at the boundary: (1) strong orientational order, (2) strong orientational order followed by a first-order transition to a state of weak orientational order as temperature is raised, and (3) a state of weak orientational order. Author

**A85-32635\*** Perkin-Elmer Corp., Norwalk, Conn.

**ELECTRICAL CHARACTERIZATION OF PLASMA-GROWN OXIDES ON GALLIUM ARSENIDE**

F. I. HSHIEH (Perkin-Elmer Corp., Norwalk, CT; Rensselaer Polytechnic Institute, Troy, NY), K. N. BHAT, S. K. GHANDHI, and J. M. BORREGO (Rensselaer Polytechnic Institute, Troy, NY) Journal of Applied Physics (ISSN 0021-8979), vol. 57, May 15, 1985, p. 4657-4662. refs (Contract NAG3-175)

Plasma-grown GaAs oxides and their interfaces have been characterized by measuring the electrical properties of metal-oxide-semiconductor capacitors and of Schottky junctions. The current transport mechanism in the oxide at high electrical field was found to be Frankel-Poole emission, with an electron trap center at 0.47 eV below the conduction band of the oxide. The interface-state density, evaluated from capacitance and conductance measurements, exhibits a U-shaped interface-state continuum extending over the entire band gap. Two discrete deep states with high concentration are superimposed on this continuum at 0.40 and 0.70 eV below the conduction band. The results obtained from measurements on Schottky junctions have excluded the possibility that these two deep states originate from plasma damage. Possible origins of these states are discussed in this paper. Author

**A85-32636\*** Rensselaer Polytechnic Inst., Troy, N.Y.

**HEAT TREATMENT OF BULK GALLIUM ARSENIDE USING A PHOSPHOSILICATE GLASS CAP**

G. MATHUR, M. L. WHEATON, J. M. BORREGO, and S. K. GHANDHI (Rensselaer Polytechnic Institute, Troy, NY) Journal of Applied Physics (ISSN 0021-8979), vol. 57, May 15, 1985, p. 4711-4714. refs (Contract NAG3-188)

n-type bulk GaAs crystals, capped with chemically vapor-deposited phosphosilicate glass, were heat treated at temperatures in the range of 600 to 950 C. Measurements on Schottky diodes and solar cells fabricated on the heat-treated material, after removal of a damaged surface layer, show an increase in free-carrier concentration, in minority-carrier-diffusion length, and in solar-cell short-circuit current. The observed changes are attributed to a removal of lifetime-reducing acceptorlike impurities, defects, or their complexes. Author

**A85-33645\*** Rensselaer Polytechnic Inst., Troy, N.Y.

**FABRICATION OF P(+)N JUNCTION GAAS SOLAR CELLS BY A NOVEL METHOD**

S. K. GHANDHI, G. MATHUR, H. RODE, and J. M. BORREGO (Rensselaer Polytechnic Institute, Troy, NY) Solid-State Electronics (ISSN 0038-1101), vol. 27, Dec. 1984, p. 1149-1151. (Contract NAG3-188)

A novel method for making p(+)n diffused junction GaAs solar cells, with the formation of a diffusion source, an anti-reflective coating, and a protective cover glass in a single chemical-vapor deposition operation is discussed. Consideration is given to device fabrication and to solar-cell characteristics. The advantages of the technique are that the number of process steps is kept to an absolute minimum, the fabrication procedure is low-cost, and the GaAs surface is protected during the entire operation. M.D.

**A85-35308\*** National Aeronautics and Space Administration. Lewis Research Center, Cleveland, Ohio.

**COMPUTER SIMULATION OF THIN FILM NUCLEATION AND GROWTH**

J. SALIK (NASA, Lewis Research Center, Cleveland, OH) Journal of Applied Physics (ISSN 0021-8979), vol. 57, June 1, 1985, p. 5017-5023. refs

Some of the processes involved in thin film nucleation and growth were simulated by means of a digital computer. The main conclusions drawn from the simulation results are (1) Because of the random nature of the processes involved, a large variation in results is obtained. (2) Upon impingement, clusters are formed up to a coverage of ca. 0.2, and from there on growth of existing clusters, rather than formation of new ones, takes place. (3) Surface migration is responsible for the formation of most of the clusters at coverages smaller than 0.1, whereas at higher coverages most clusters are formed upon impingement. (4) Surface migration accelerates the growth and causes reduction in cluster density. (5) Reevaporation slows the growth and reduces the cluster density dramatically. Author

**A85-35620\*** National Aeronautics and Space Administration. Lewis Research Center, Cleveland, Ohio.

**THE EFFECT OF DIFFUSION INDUCED LATTICE STRESS ON THE OPEN-CIRCUIT VOLTAGE IN SILICON SOLAR CELLS**

V. G. WEIZER and M. P. GODLEWSKI (NASA, Lewis Research Center, Cleveland, OH) IN: Photovoltaic Specialists Conference, 17th, Kissimmee, FL, May 1-4, 1984, Conference Record. New York, Institute of Electrical and Electronics Engineers, 1984, p. 134-137. Previously announced in STAR as N84-23027. refs

It is demonstrated that diffusion induced stresses in low resistivity silicon solar cells can significantly reduce both the open-circuit voltage and collection efficiency. The degradation mechanism involves stress induced changes in both the minority carrier mobility and the diffusion length. Thermal recovery characteristics indicate that the stresses are relieved at higher temperatures by divacancy flow (silicon self diffusion). The level of residual stress in as-fabricated cells was found to be negligible in the cells tested. Author

**A85-35698\*#** National Aeronautics and Space Administration. Lewis Research Center, Cleveland, Ohio.

**RADIATION DAMAGE AND DEFECT BEHAVIOR IN ION-IMPLANTED, LITHIUM COUNTERDOPED SILICON SOLAR CELLS**

I. WEINBERG, S. MEHTA, and C. K. SWARTZ (NASA, Lewis Research Center, Cleveland, OH) IN: Photovoltaic Specialists Conference, 17th, Kissimmee, FL, May 1-4, 1984, Conference Record. New York, Institute of Electrical and Electronics Engineers, 1984, p. 1088-1092. Previously announced in STAR as N84-22890. refs

Boron doped silicon n+p solar cells were counterdoped with lithium by ion implantation and the resultant n+p cells irradiated by 1 MeV electrons. The function of fluence and a Deep Level Transient Spectroscopy (DLTS) was studied to correlate defect behavior with cell performance. It was found that the lithium counterdoped cells exhibited significantly increased radiation resistance when compared to boron doped control cells. It is concluded that the annealing behavior is controlled by dissociation and recombination of defects. The DLTS studies show that counterdoping with lithium eliminates at least three deep level defects and results in three new defects. It is speculated that the increased radiation resistance of the counterdoped cells is due primarily to the interaction of lithium with oxygen, single vacancies and divacancies and that the lithium-oxygen interaction is the most effective in contributing to the increased radiation resistance.

E.A.K.

**A85-35699\*#** National Aeronautics and Space Administration. Lewis Research Center, Cleveland, Ohio.

**EFFECTS OF 1 MEV ELECTRONS AND 10 MEV PROTONS ON THE PERFORMANCE AND REFLECTANCE OF THIN BSR CELLS**

H. B. CURTIS, C. K. SWARTZ (NASA, Lewis Research Center, Cleveland, OH), and R. L. STATLER (U.S. Navy, Naval Research Laboratory, Washington, DC) IN: Photovoltaic Specialists Conference, 17th, Kissimmee, FL, May 1-4, 1984, Conference Record. New York, Institute of Electrical and Electronics Engineers, 1984, p. 1093-1096.

(Contract NAS3-22229)

Thin silicon cells with BSR's were irradiated with 1 MeV electrons on either the front or back side of the cell. There were two types of cells, a 10 ohm-cm with a BSF and a 0.15 ohm-cm without a BSF. Data on the electrical performance and reflectance are given for various fluence levels of 1 MeV electrons for both type cells and 10 MeV protons for the 10 ohm-cm cell. Author

**A85-38019\*** National Aeronautics and Space Administration. Lewis Research Center, Cleveland, Ohio.

**DENDRITIC SOLIDIFICATION. I - ANALYSIS OF CURRENT THEORIES AND MODELS. II - A MODEL FOR DENDRITIC GROWTH UNDER AN IMPOSED THERMAL GRADIENT**

V. LAXMANN (NASA, Lewis Research Center; Case Western Reserve University, Cleveland, OH) Acta Metallurgica (ISSN 0001-6160), vol. 33, June 1985, p. 1023-1049. NASA-supported research. refs

A critical review of the present dendritic growth theories and models is presented. Mathematically rigorous solutions to dendritic growth are found to rely on an ad hoc assumption that dendrites grow at the maximum possible growth rate. This hypothesis is found to be in error and is replaced by stability criteria which consider the conditions under which a dendrite tip advances in a stable fashion in a liquid. The important elements of a satisfactory model for dendritic solidification are summarized and a theoretically consistent model for dendritic growth under an imposed thermal gradient is proposed and described. The model is based on the modification of an analysis due to Burden and Hunt (1974) and predicts correctly in all respects, the transition from a dendritic to a planar interface at both very low and very large growth rates.

M.D.

**A85-38192\*** Nebraska Univ., Lincoln.

**DIELECTRIC PROPERTIES OF 'DIAMONDLIKE' CARBON PREPARED BY RF PLASMA DEPOSITION**

J. D. LAMB and J. A. WOOLLAM (Nebraska, University, Lincoln, NE) Journal of Applied Physics (ISSN 0021-8979), vol. 57, June 15, 1985, p. 5420-5423. Research supported by the University of Nebraska. refs

(Contract NAG3-154)

Metal-carbon-metal structures were fabricated using either gold or aluminum evaporated electrodes and RF plasma (methane) deposited 'diamondlike' carbon films. Alternating-current conductance and capacitance versus voltage and frequency (10 Hz to 13 MHz) data were taken to determine the dielectric properties of these films. Conductance versus frequency data fit a generalized power law, consistent with both dc and hopping conduction components. The capacitance versus frequency data are well matched to the conductance versus frequency data, as predicted by a Kramers-Kronig analysis. The dielectric loss tangent is nearly constant at 0.5 to 1.0 percent over the frequency range from 1 to 100 kHz. The dc resistivity is above 10 to the 13th ohm cm, and the dc breakdown strength is above 8 x 10 to the 6th V/cm is properly prepared samples. Author

**A85-40386\*** National Aeronautics and Space Administration. Lewis Research Center, Cleveland, Ohio.

**PLASMA DEPOSITED HYDROGENATED CARBON ON GAAS AND INP**

J. D. WARNER, J. J. POUCH, S. A. ALTEROVITZ, D. C. LIU (NASA, Lewis Research Center, Cleveland, OH), and W. A. LANFORD (New York, State University, Albany) Journal of Vacuum Science and Technology A (ISSN 0734-2101), vol. 3, May-June 1985, pt. 1, p. 900-903. Army-supported research. Previously announced in STAR as N85-10844. refs

The properties of diamond like carbon films grown by RF flow discharge 30 kHz plasma using methane are reported. The Cis XPS line shape of films showed localized hybrid carbon bonds as low as 40 to as high as 95 percent. Infrared spectroscopy and N(15) nuclear reaction profiling data indicated 35 to 42 percent hydrogen, depending inversely on deposition temperature. The deposition rate of films on Si falls off exponentially with substrate temperature, and nucleation does not occur above 200 C on GaAs and InP. Optical data of the films showed bandgap values of 2.0 to 2.4 eV increasing monotonically with CH4 flow rate. Author

**A85-41635\*** Minnesota Univ., Minneapolis.

**CONE FORMATION AS A RESULT OF WHISKER GROWTH ON ION BOMBARDED METAL SURFACES**

G. K. WEHNER (Minnesota, University, Minneapolis) Journal of Vacuum Science and Technology A (ISSN 0734-2101), vol. 3, July-Aug. 1985, p. 1821-1835. SERC-supported research. refs (Contract NSG-3041)

It is shown experimentally that the seed metals which can cause cone development on ion bombarded metal targets need not to have a lower sputtering yield as widely believed but rather a higher melting point. By lowering the bombarding ion energy to near sputtering threshold values (less than 100 eV) the growth of genuine single crystal whiskers which point in all directions not related to the direction of ion incidence is observed. It is concluded that (intentional or unintentional) seed cones are the result of an interplay among whisker growth, surface movement of atoms, and the effects of sputtering. Author

**A85-48516\*** National Aeronautics and Space Administration. Lewis Research Center, Cleveland, Ohio.

**MONTE CARLO STUDY OF REVERSIBLE GROWTH OF CLUSTERS ON A SURFACE**

J. SALIK (NASA, Lewis Research Center, Cleveland, OH) Physical Review B - Solid State, 3rd Series (ISSN 0556-2805), vol. 32, Aug. 1, 1985, p. 1824-1826. refs

The effect of binding energy on the growth of clusters on a two-dimensional square lattice was studied by a means of a Monte Carlo simulation. The results indicate that for binding energies higher than 0.5kT, clusters grow relative to the initial random



distribution, while for binding energies lower than 0.5 kT, clusters decompose. It was also found that at low binding energies the equilibrium percentage of atoms that are bound in clusters is linearly dependent on the binding energy. The cluster density behaved in a similar manner. This similarity reflects the fact that at low binding energies the growth proceeds mainly by the formation of new clusters rather than by an increase in the size of existing ones.

Author

**N85-10844\*#** National Aeronautics and Space Administration. Lewis Research Center, Cleveland, Ohio.

**PLASMA DEPOSITED DIAMONDLIKE CARBON ON GAAS AND INP**

J. D. WARNER, J. J. POUCH, S. A. ALTEROVITZ, D. C. LIU, and W. A. LANFORD (State Univ. of New York, Albany) 1984 15 p refs Proposed for presentation at the 31st Natl. Symp. of the Am. Vacuum Soc., Reno, Nev., 3-7 Dec. 1984 (NASA-TM-86870; E-2332; NAS 1.15:86870) Avail: NTIS HC A02/MF A01 CSCL 20L

The properties of diamond like carbon films grown by RF low discharge 30 kHz plasma using methane are reported. The C1s XPS line shape of films showed localized hybrid carbon bonds as low as 40 to as high as 95 percent. Infrared spectroscopy and N(15) nuclear reaction profiling data indicated 35 to 42 percent hydrogen, depending inversely on deposition temperature. The deposition rate of films on Si falls off exponentially with substrate temperature, and nucleation does not occur above 200 C on GaAs and InP. Optical data of the films showed bandgap values of 2.0 to 2.4 eV increasing monotonically with CH<sub>4</sub> flow rate. Author

**N85-11862\*#** Connecticut Univ., Storrs. Dept. of Mechanical Engineering.

**BIAXIAL CONSTITUTIVE EQUATION DEVELOPMENT FOR SINGLE CRYSTALS Semiannual Status Report, 6 Jan. - 6 Jul. 1984**

E. H. JORDAN 1984 29 p

(Contract NAG3-512)

(NASA-CR-174056; NAS 1.26:174056) Avail: NTIS HC A03/MF A01 CSCL 20L

Current gas turbine engines utilize large single crystal superalloy components in the hot section. Structural analysis of these components requires a valid stress strain temperature constitutive equation. The goal of the program described is to create one or more models and verify these models. A constitutive equation based on an assumed slip behavior of a single slip system was formulated, programmed, and debugged. Specifically, the basic theory for a model based on aggravating slip behavior on individual slip systems was formulated and programmed and some simulations were run using assumed values of constants. In addition, a formulation allowing strain controlled simulations was completed. An approach to structural analysis of the specimen was developed. This approach uses long tube consistency conditions and finite elements specially formulated to take advantage of the symmetry of 100 oriented specimens. R.S.F.

**N85-23414\*#** Michigan Technological Univ., Houghton. Dept. of Chemistry and Chemical Engineering.

**RAMAN STRUCTURAL STUDIES OF THE NICKEL ELECTRODE Progress Report, 20 Feb. 1984 - 20 Mar. 1985**

B. C. CORNILSEN 1985 39 p refs

(Contract NAG3-519)

(NASA-CR-175619; NAS 1.26:175619) Avail: NTIS HC A03/MF A01 CSCL 20L

Raman spectroscopy is sensitive to empirically controlled nickel electrode structural variations, and has unique potential for structural characterization of these materials. How the structure relates to electrochemical properties is examined so that the latter can be more completely understood, controlled, and optimized. Electrodes were impregnated and cycled, and cyclic voltammetry is being used for electrochemical characterization. Structural variation was observed which has escaped detection using other methods. Structural changes are induced by: (1) cobalt doping, (2) the state of charge or discharge, (3) the preparation conditions and type of buffer used, and (4) the formation process. Charged active mass has an NiOOH-type structure, agreeing with X-ray diffraction results. Discharged active mass, however, is not isostructural with beta-Ni(OH)<sub>2</sub>. Chemically prepared alpha phases are not isostructural either. A disordered structural model, containing point defects, is proposed for the cycled materials. This model explains K(+) incorporation. Band assignments were made and spectra interpreted for beta-Ni(OH)<sub>2</sub>, electrochemical NiOOH and chemically precipitated NiOOH. Author

**N85-24961\*#** National Aeronautics and Space Administration. Lewis Research Center, Cleveland, Ohio.

**MONTE CARLO LATTICE MODELS FOR ADSORBED POLYMER CONFORMATION**

B. S. GOOD May 1985 12 p refs

(NASA-TP-2453; E-2400; NAS 1.60:2453) Avail: NTIS HC A02/MF A01 CSCL 20L

The adhesion between a polymer film and a metal surface is of great technological interest. However, the prediction of adhesion and wear properties of polymer coated metals is quite difficult because a fundamental understanding of the polymer surface interaction does not yet exist. A computer model for the conformation of a polymer molecule adsorbed on a surface is discussed. The chain conformation is assumed to be described by a partially directed random walk on a three dimensional simple cubic lattice. An attractive surface potential is incorporated into the model through the use of a random walk step probability distribution that is anisotropic in the direction normal to the attractive surface. The effects of variations in potential characteristics are qualitatively included by varying both the degree of anisotropy of the step distribution and the range of the anisotropy. Polymer conformation is characterized by the average end to end distance, average radius of gyration, and average number of chain segments adsorbed on the surface. Author

**N85-26406\*#** National Aeronautics and Space Administration. Lewis Research Center, Cleveland, Ohio.

**OPTICAL PROPERTIES OF HYDROGENATED AMORPHOUS CARBON FILMS GROWN FROM METHANE PLASMA**

J. J. POUCH, S. A. ALTEROVITZ, J. D. WARNER, D. C. LIU, and W. A. LANFORD (State Univ. of New York, Albany) 18 Apr. 1985 8 p refs Presented at Spring Meeting of the Mater. Res. Soc., San Francisco, 15-18 Apr. 1985

(NASA-TM-86995; E-2541; NAS 1.15:86995) Avail: NTIS HC A02/MF A01 CSCL 20L

A 30 kHz ac glow discharge formed from methane gas was used to grow carbon films on InP substrates. Both the growth rate, and the relative Ar ion sputtering rate at 3 keV varied monotonically with deposition power. Results from the N-15 nuclear reaction profile experiments indicated a slight drop in the hydrogen concentration as more energy was dissipated in the ac discharge. Values for the index of refraction and extinction coefficient ranged from 1.721 to 1.910 and 0 to -0.188, respectively. Optical bandgaps as high as 2.34 eV were determined. Author

## THERMODYNAMICS AND STATISTICAL PHYSICS

Includes quantum mechanics; and Bose and Fermi statistics.

**N85-16663\*#** National Aeronautics and Space Administration. Lewis Research Center, Cleveland, Ohio.  
**COMPUTER PROGRAM FOR CALCULATION OF COMPLEX CHEMICAL EQUILIBRIUM COMPOSITIONS AND APPLICATIONS. SUPPLEMENT 1: TRANSPORT PROPERTIES**  
 S. GORDON (Gordon (Sanford) and Associates), B. MCBRIDE, and F. J. ZELEZNIK Oct. 1984 26 p refs  
 (NASA-TM-86885; E-2348; NAS 1.15:86885) Avail: NTIS HC A03/MF A01 CSCL 20M

An addition to the computer program of NASA SP-273 is given that permits transport property calculations for the gaseous phase. Approximate mixture formulas are used to obtain viscosity and frozen thermal conductivity. Reaction thermal conductivity is obtained by the same method as in NASA TN D-7056. Transport properties for 154 gaseous species were selected for use with the program. Author

**N85-22204\*#** National Aeronautics and Space Administration. Lewis Research Center, Cleveland, Ohio.  
**IDEAL GAS THERMODYNAMIC PROPERTIES FOR THE PHENYL, PHENOXY, AND O-BIPHENYL RADICALS**  
 A. BURCAT, F. J. ZELEZNIK, and B. J. MCBRIDE Jan. 1985 22 p refs  
 (NASA-TM-83800; E-2303; NAS 1.15:83800) Avail: NTIS HC A02/MF A01 CSCL 20M

Ideal gas thermodynamic properties of the phenyl and o-biphenyl radicals, their deuterated analogs and the phenoxy radical were calculated to 5000 K using estimated vibrational frequencies and structures. The ideal gas thermodynamic properties of benzene, biphenyl, their deuterated analogs and phenyl were also calculated. Author

## DOCUMENTATION AND INFORMATION SCIENCE

Includes information storage and retrieval technology; micrography; and library science.

**N85-22255\*#** National Aeronautics and Space Administration. Lewis Research Center, Cleveland, Ohio.  
**BIBLIOGRAPHY OF LEWIS RESEARCH CENTER TECHNICAL PUBLICATIONS ANNOUNCED IN 1983**  
 Jun. 1984 345 p  
 (NASA-TM-83693; E-2151; NAS 1.15:83693) Avail: NTIS HC A16/MF A01 CSCL 05B

This compilation of abstracts describes and indexes over 800 technical publications that resulted from the scientific and engineering work performed and managed by the Lewis Research Center in 1983. Announced in the 1983 issues of STAR (Scientific and Technical Aerospace Reports) and/or IAA (International Aerospace Abstracts), the documents cited include research reports, journal articles, conference presentations, patents and patent applications, and theses. A.R.H.

**N85-28876\*#** National Aeronautics and Space Administration. Lewis Research Center, Cleveland, Ohio.

## BIBLIOGRAPHY OF LEWIS RESEARCH CENTER TECHNICAL PUBLICATIONS ANNOUNCED IN 1984

May 1985 322 p  
 (NASA-TM-87012; E-2556; NAS 1.15:87012) Avail: NTIS HC A14/MF A01 CSCL 05B

This compilation of abstracts describes and indexes the technical reporting that resulted from the scientific and engineering work performed and managed by the Lewis Research Center in 1984. All the publications were announced in the 1984 issues of STAR (Scientific and Technical Aerospace Reports) and/or IAA (International Aerospace Abstracts). Included are research reports, journal articles, conference presentations, patents and patent applications, and theses. Author

## URBAN TECHNOLOGY AND TRANSPORTATION

Includes applications of space technology to urban problems; technology transfer; technology assessment; and surface and mass transportation.

**N85-12808\*#** Mechanical Technology, Inc., Latham, N. Y.  
**DEVELOPMENT OF GAS-LUBRICATED PISTONS FOR HEAVY DUTY DIESEL ENGINE TECHNOLOGY PROGRAM Final Report**  
 W. SHAPIRO Jul. 1984 192 p refs  
 (Contract DEN3-309; DE-AI01-80CS-50194)  
 (NASA-CR-174746; NAS 1.26:174746; MTI-84TR58) Avail: NTIS HC A09/MF A01 CSCL 13F

Static testing of a segmented, gas-lubricated, piston-ring was accomplished. The ring utilizes high-pressure gas generated during the diesel cycle to energize a hydrostatic gas film between the piston and cylinder liner. The configuration was deficient in overall performance, because all segments of a ring set failed to form a fluid-film simultaneously, when exposed to internal preload. The difficulty was traced to the moment balance required to prevent the segments from overturning and contacting the cylinder walls. Some individual sectors formed a film and performed well in every respect including load capability to 6,000 N. These results produce optimism as to the ultimate feasibility of hydrostatic, gas-lubricated piston rings. In addition to test results, the principles of operation, and theoretical developments are presented. Breathable liner concepts are suggested for future consideration. In these configurations, solid hydrostatic pistons are coupled with flexible liners that elastically deform to form a gas-film under hydrostatic pressurization. Breathable liners afford the mechanical simplicity required for mass produced engines, and initial examination indicates satisfactory operation. Author

**N85-13692\*#** National Aeronautics and Space Administration. Lewis Research Center, Cleveland, Ohio.

## OVERVIEW OF WASTE HEAT UTILIZATION SYSTEMS

M. M. BAILEY 1984 12 p refs Presented at the 22nd Automotive Technol. Development Contractors' Coordination Meeting, Dearborn, Mich., 29 Oct. 1 Nov. 1984; sponsored by DOE  
 (NASA-TM-86901; DOE/NASA/50194-41; NAS 1.15:86901)  
 Avail: NTIS HC A02/MF A01 CSCL 10B

The heavy truck diesel engine rejects a significant fraction of its fuel energy in the form of waste heat. Historically, the Department of Energy has supported technology efforts for utilization of the diesel exhaust heat. Specifically, the Turbocompound and the Organic Rankine Cycle System (ORCS) have demonstrated that meaningful improvements in highway fuel economy can be realized through waste heat utilization. For heat recovery from the high temperature exhaust of future adiabatic diesel engines, the DOE/NASA are investigating a variety of alternatives based on the Rankine, Brayton, and Stirling power

cycles. Initial screening results indicate that systems of this type offer a fuel savings advantage over the turbocompound system. Capital and maintenance cost projections, however, indicate that the alternative power cycles are not competitive on an economic payback basis. Plans call for continued analysis in an attempt to identify a cost effective configuration with adequate fuel savings potential. Author

**N85-16698\*#** General Electric Co., Philadelphia, Pa. Advanced Energy Programs Dept.

**TRANSFORMATION TOUGHENED CERAMICS FOR THE HEAVY DUTY DIESEL ENGINE TECHNOLOGY PROGRAM Final Report** S. MUSIKANT, E. FEINGOLD, H. RAUCH, and S. SAMANTA Oct. 1984 34 p refs

(Contract DEN3-339; DE-AI01-80CS-5019)

(NASA-CR-174689; DOE/NASA/0339-1; NAS 1.26:174689)

Avail: NTIS HC A03/MF A01 CSCL 13F

The objective of this program is to develop an advanced high temperature oxide structural ceramic for application to the heavy duty diesel engine. The approach is to employ transformation toughening by additions of  $ZrO_5HfO_5O_2$  solid solution to the oxide ceramics, mullite ( $2Al_2O_3 \cdot 3SiO_2$ ) and alumina ( $Al_2O_3$ ). The study is planned for three phases, each 12 months in duration. This report covers Phase 1. During this period, processing techniques were developed to incorporate the  $ZrO_5HfO_5O_2$  solid solution in the matrices while retaining the necessary metastable tetragonal phase. Modulus of rupture and of elasticity, coefficient of thermal expansion, fracture toughness by indent technique and thermal diffusivity of representative specimens were measured. In Phase 2, the process will be improved to provide higher mechanical strength and to define the techniques for scale up to component size. In Phase 3, full scale component prototypes will be fabricated. Author

**N85-16699\*#** Integral Technologies, Inc., Westmont, Ill.  
**METHODS FOR HEAT TRANSFER AND TEMPERATURE FIELD ANALYSIS OF THE INSULATED DIESEL Interim Report**

T. MOREL, P. N. BLUMBERG, E. F. FORT, and R. KERIBAR Aug. 1984 274 p refs

(Contract DEN3-342; DE-AI01-80CS-50194)

(NASA-CR-174783; DOE/NASA/0342-1; NAS 1.26:174783)

Avail: NTIS HC A12/MF A01 CSCL 13F

Work done during phase 1 of a three-year program aimed at developing a comprehensive heat transfer and thermal analysis methodology oriented specifically to the design requirements of insulated diesel engines is reported. The technology developed in this program makes possible a quantitative analysis of the low heat rejection concept. The program is comprehensive in that it addresses all the heat transfer issues that are critical to the successful development of the low heat rejection diesel engine: (1) in-cylinder convective and radiative heat transfer; (2) cyclic transient heat transfer in thin solid layers at component surfaces adjacent to the combustion chamber; and (3) steady-state heat conduction in the overall engine structure. The Integral Technologies, Inc. (ITI) program is comprised of a set of integrated analytical and experimental tasks. A detailed review of the ITI program approach is provided, including the technical issues which underlie it and a summary of the methods that were developed. R.S.F.

**N85-18831\*#** Garrett Turbine Engine Co., Phoenix, Ariz. Engineering Staff.

**ADVANCED GAS TURBINE (AGT) POWERTRAIN SYSTEM DEVELOPMENT FOR AUTOMOTIVE APPLICATIONS Semiannual Progress Report, Jul. - Dec. 1983**

Jun. 1984 70 p refs

(Contract DEN3-167)

(NASA-CR-174809; DOE/NASA/0167-8; NAS 1.26:174809;

GARRETT-31-3725(8); SAPR-8) Avail: NTIS HC A04/MF A01

CSCL 13F

Rotor dynamic instability investigations were conducted. Forward ball bearing hydraulic mount configurations were tested with little effect. Trial assembly of S/N 002 ceramic engine was

initiated. Impeller design activities were completed on the straight line element (SLE) blade definition to address near-net-shape powder metal die forging. Performance characteristics of the Baseline Test 2A impeller were closely preserved. The modified blading design has been released for tooling procurement. Developmental testing of the diffusion flame combustor (DFC) for initial use in the S/N 002 2100 F ceramic structures engine was completed. A natural gas slave preheater was designed and fabricated. Preliminary regenerator static seal rig testing showed a significant reduction in leakage and sensitivity to stack height. Ceramic screening tests were completed and two complete sets of ceramic static structures were qualified for engine testing. Efforts on rotor dynamics development to resolve subsynchronous motion were continued. A.S.B.

**N85-19894\*#** Kumm (Emerson L.), Tempe, Ariz.

**FEASIBILITY DEMONSTRATION OF A NOVEL, FLAT-BELT, CONTINUOUSLY VARIABLE TRANSMISSION OR AUTOMOTIVE AND ELECTRIC-HYBRID VEHICLE APPLICATION Final Report**

E. L. KUMM May 1984 138 p Prepared for JPL

(Contract DEN3-272; JPL-956602)

(NASA-CR-174430; JPL-9950-945; NAS 1.26:174430;

DOE/CS-54209/20; KI-P-1008) Avail: NTIS HC A07/MF A01

CSCL 13F

The performance of a flat belt continuously variable transmission (CVT) over its design input speed, output torque, and speed ratio range was determined. The arrangement studied reduces the required width of the pulleys and their actuators as compared to pulleys whose sheaves are moved axially by actuators to vary the belt radius ratio or pulley speed ratio. Topics covered included: (1) flat belt transmission design; (2) variable speed assembly fabrication; (3) critical components; (4) variable speed assembly test stand; (5) test stand control rigs; (6) transmission tests; and (7) improvement assessment of the current design. Results show that the flat belt CVT appears to have significant advantages in reducing the size and weight of the automotive CVT as well as giving high operating efficiencies. A.R.H.

**N85-19895\*#** National Aeronautics and Space Administration. Lewis Research Center, Cleveland, Ohio.

**INITIAL TESTING OF A VARIABLE-STROKE STIRLING ENGINE Final Report**

L. G. THIEME Feb. 1985 28 p refs Presented at the 21st Automotive Technol. Develop. Contractors' Coordination Meeting, Dearborn, Mich., 14-17 Nov. 1983

(Contract DE-AI01-77CS-51040)

(NASA-TM-86875; DOE/NASA/51040-58; E-2336; NAS

1.15:86875) Avail: NTIS HC A03/MF A01 CSCL 13F

In support of the U.S. Department of Energy's Stirling Engine Highway Vehicle Systems Program, NASA Lewis Research Center is evaluating variable-stroke control for Stirling engines. The engine being tested is the Advenco Stirling engine; this engine was manufactured by Philips Research Laboratories of the Netherlands and uses a variable-angle swash-plate drive to achieve variable stroke operation. The engine is described, initial steady-state test data taken at Lewis are presented, a major drive system failure and subsequent modifications are described. Computer simulation results are presented to show potential part-load efficiency gains with variable-stroke control. Author

**N85-27769\*#** National Aeronautics and Space Administration. Lewis Research Center, Cleveland, Ohio.

**OVERVIEW OF THE 1985 NASA LEWIS RESEARCH CENTER SP-100 FREE-PISTON STIRLING ENGINE ACTIVITIES**

J. SLABY 1985 21 p refs Presented at the 20th Intersoc. Energy Conversion Engr. Conf., Miami Beach, Fla., 18-23 Aug. 1985; cosponsored by ASME, ANS, SAE, IEEE, AIAA, ACS, and AICHE

(Contract DE-AI05-82OR-1005)

(NASA-TM-87028; DOE/NASA/1005-5; NAS 1.15:87028; E-2584)

Avail: NTIS HC A02/MF A01 CSCL 10B

This effort is keyed on the design, fabrication, assembly, and testing of a 25 kWe Stirling space-power technology-feasibility

demonstrator engine. Another facet of the SP-100 project covers the status of a 9000-hr endurance test conducted on a 2 kWe free-piston Stirling/linear alternator system employing hydrostatic gas bearings. Dynamic balancing of the RE-1000 engine (a 1 kWe free-piston Stirling engine) using a passive dynamic absorber will be discussed along with the results of a parametric study showing the relationships of Stirling power converter specific weight and efficiency as functions of Stirling engine heater to cooler temperature ratio. Planned tests will be described covering a hydrodynamic gas bearing concept for potential SP-100 application.

Author

**N85-32043\*#** National Aeronautics and Space Administration. Lewis Research Center, Cleveland, Ohio.

### **COMPARATIVE EVALUATION OF THREE ALTERNATIVE POWER CYCLES FOR WASTE HEAT RECOVERY FROM THE EXHAUST OF ADIABATIC DIESEL ENGINES Final Report**

M. M. BAILEY Jul. 1985 27 p refs

(Contract DE-AI01-80CS-50194)

(NASA-TM-86953; E-2196; DOE/NASA/50194-43; NAS 1.15:86953) Avail: NTIS HC A03/MF A01 CSCL 13F

Three alternative power cycles were compared in application as an exhaust-gas heat-recovery system for use with advanced adiabatic diesel engines. The power cycle alternatives considered were steam Rankine, organic Rankine with RC-1 as the working fluid, and variations of an air Brayton cycle. The comparison was made in terms of fuel economy and economic payback potential for heavy-duty trucks operating in line-haul service. The results indicate that, in terms of engine rated specific fuel consumption, a diesel/alternative-power-cycle engine offers a significant improvement over the turbocompound diesel used as the baseline for comparison. The maximum improvement resulted from the use of a Rankine cycle heat-recovery system in series with turbocompounding. The air Brayton cycle alternatives studied, which included both simple-cycle and compression-intercooled configurations, were less effective and provided about half the fuel consumption improvement of the Rankine cycle alternatives under the same conditions. Capital and maintenance cost estimates were also developed for each of the heat-recovery power cycle systems. These costs were integrated with the fuel savings to identify the time required for net annual savings to pay back the initial capital investment. The sensitivity of capital payback time to arbitrary increases in fuel price, not accompanied by corresponding hardware cost inflation, was also examined. The results indicate that a fuel price increase is required for the alternative power cycles to pay back capital within an acceptable time period.

Author

## 99

### **GENERAL**

**N85-17928\*#** National Aeronautics and Space Administration. Lewis Research Center, Cleveland, Ohio.

### **RESEARCH AND TECHNOLOGY HIGHLIGHTS OF THE LEWIS RESEARCH CENTER Annual Report, 1984**

1984 52 p

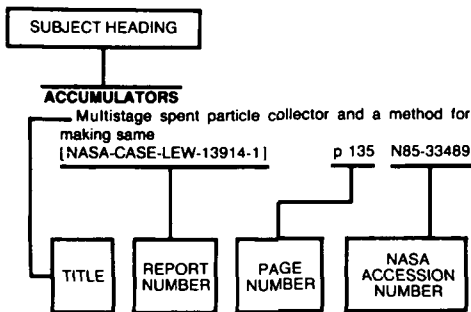
(NASA-TM-86899; NAS 1.15:86899) Avail: NTIS HC A04/MF A01 CSCL 05A

Highlights of research accomplishments of the Lewis Research Center for fiscal year 1984 are presented. The report is divided into four major sections covering aeronautics, space communications, space technology, and materials and structures. Six articles on energy are included in the space technology section.

B.W.

# SUBJECT INDEX

## Typical Subject Index Listing



The subject heading is the key to the subject content of the document. Titles, report numbers, and accession numbers of pertinent documents are provided under each subject heading. When the title is insufficiently descriptive of the document content, a title extension has been added, separated from the title by three hyphens. The report number helps to indicate the type of document cited (e.g., NASA report, NASA translation, NASA contractor report). The NASA accession number is the number by which the document abstracts are arranged in this journal and by which the document is sold or requested. The titles, with title extensions if present, are arranged under each subject heading in ascending accession number order. The subject headings have been selected from the latest revision of the *NASA Thesaurus* (NASA SP-7051).

## A

### ABERRATION

Holographic optical system for aberration corrections in laser Doppler velocimetry p 123 A85-48659

### ABSORBERS (MATERIALS)

Measured acoustic properties of variable and low density bulk absorbers [NASA-TM-87065] p 177 N85-30770

### ABSORPTIVITY

Aluminum work function: Effect of oxidation, mechanical scraping and ion bombardment [NASA-TM-87079] p 78 N85-34265

### ABSTRACTS

Bibliography of Lewis Research Center technical publications announced in 1984 [NASA-TM-87012] p 184 N85-28876

### ACCELERATED LIFE TESTS

Long life nickel electrodes for a nickel-hydrogen cell. III - Results of an accelerated test and failure analyses p 156 A85-45391

### ACCELERATION (PHYSICS)

A unified relation for cavitation erosion p 109 A85-24445

### ACCUMULATORS

Multistage spent particle collector and a method for making same [NASA-CASE-LEW-13914-1] p 135 N85-33489

### ACCURACY

Strainrange partitioning - A total strain range version --- for creep fatigue life prediction by summing inelastic and elastic strain-range-life relations for two Ni base superalloys p 64 A85-11603

Assessment of three-dimensional inviscid codes and loss calculations for turbine aerodynamic computations [ASME PAPER 84-GT-187] p 4 A85-32961

Stability, accuracy, and efficiency of some underintegrated methods in finite element computations p 172 A85-50073

Reducing numerical diffusion for incompressible flow calculations [NASA-TM-83621] p 24 N85-14840

### ACEE PROGRAM

Measurement and prediction of Energy Efficient Engine noise

[AIAA PAPER 84-2284] p 13 A85-13954

Energy efficient engine combustor test hardware detailed design report

[NASA-CR-167945] p 18 N85-10950

Energy efficient engine component development and integration program

[NASA-CR-170034] p 22 N85-10990

Energy efficient engine. Volume 2. Appendix A: Component development and integration program

[NASA-CR-173085] p 22 N85-10991

Energy efficient engine. Volume 1: Component development and integration program

[NASA-CR-173084] p 22 N85-10992

Energy efficient engine. Low pressure turbine test hardware detailed design report

[NASA-CR-167956] p 22 N85-10994

Energy efficient engine high pressure turbine test hardware detailed design report

[NASA-CR-167955] p 23 N85-10995

Energy efficient engine high pressure turbine ceramic shroud support technology report

[NASA-CR-168036] p 23 N85-10996

Energy efficient engine ICLS engine bearings, drives and configuration: Detail design report

[NASA-CR-167871] p 23 N85-10997

Energy efficient engine. High pressure compressor detail design report

[NASA-CR-165558] p 23 N85-10998

Energy efficient engine high-pressure turbine component rig performance test report

[NASA-CR-168189] p 30 N85-29955

Energy efficient engine integrated core/low spool test hardware design report

[NASA-CR-168137] p 31 N85-29956

Energy Efficient Engine (E3) controls and accessories detail design report

[NASA-CR-168017] p 31 N85-29957

Energy efficient engine component development and integration program

[NASA-CR-172846] p 31 N85-29958

Energy efficient engine. Fan and quarter-stage component performance report

[NASA-CR-168070] p 33 N85-34141

Energy efficient engine, high pressure turbine thermal barrier coating. Support technology report

[NASA-CR-168037] p 34 N85-35199

Velocity visualization in gas flows using laser-induced phosphorescence of biacetyl p 121 A85-21695

ACETYL COMPOUNDS

Interaction of finite-amplitude sound with air-filled porous materials

[NASA-CR-174885] p 177 N85-27637

ACOUSTIC EXCITATION

An experimental study of tone excited heated jets

[AIAA PAPER 84-2341] p 172 A85-10882

Some unique experiments on receptivity --- for forced disturbances entering shear flow

[AIAA PAPER 85-0533] p 174 A85-25932

Acoustic control of free jet mixing

[AIAA PAPER 85-0569] p 109 A85-25951

The response of Helmholtz resonators to external excitation. I - Single resonators p 174 A85-26915

Preliminary analysis of tone-excited two-stream jet velocity decay

[NASA-TM-86951] p 8 N85-21114

ACOUSTIC IMPEDANCE

Interaction of finite-amplitude sound with air-filled porous materials

[NASA-CR-174885] p 177 N85-27637

ACOUSTIC MEASUREMENT

Acoustic structure and propagation in highly porous, layered, fibrous materials p 173 A85-12301

Analytical and physical modeling program for the NASA Lewis Research Center's Altitude Wind Tunnel (AWT)

[NASA-TM-86919] p 35 N85-15757

### ACOUSTIC MICROSCOPES

Reliability of void detection in structural ceramics using scanning laser acoustic microscopy

[NASA-TM-87035] p 138 N85-32337

### ACOUSTIC PROPAGATION

Time dependent wave envelope finite difference analysis of sound propagation

[AIAA PAPER 84-2285] p 173 A85-16102

Oscillatory conductive heat transfer for a fiber in an ideal gas p 109 A85-26077

ACOUSTIC PROPERTIES

Acoustic structure and propagation in highly porous, layered, fibrous materials p 173 A85-12301

Measured acoustic properties of variable and low density bulk absorbers

[NASA-TM-87065] p 177 N85-30770

### ACOUSTIC SCATTERING

The scattering of ultrasonic third sound from substrate surface defects p 174 A85-36047

### ACOUSTO-OPTICS

Two-frequency laser-induced fluorescence technique for rapid velocity-field measurements in gas flows p 121 A85-32294

Optical linear algebra processors - Noise and error-source modeling p 169 A85-36727

### ACTIVATION

CO adsorption on (111) and (100) surfaces of the Pt sub 3 Ti alloy. Evidence for parallel binding and strong activation of CO

[NASA-CR-176077] p 77 N85-32176

### ACTIVE CONTROL

Energy efficient engine. Low pressure turbine test hardware detailed design report

[NASA-CR-167956] p 22 N85-10994

Vibration control of rotor shaft

[NASA-TM-87053] p 133 N85-29292

### ADA (PROGRAMMING LANGUAGE)

The use of Ada in distributed simulations p 169 A85-28612

Moving target, distributed, real-time simulation using Ada p 170 A85-34131

### ADDITIVES

Methanol as a soot reducer in a turbulent swirling burner

[ASME PAPER 84-JPGC-GT-2] p 61 A85-23192

Radiation damage and defect behavior in ion-implanted, lithium counterdoped silicon solar cells p 182 A85-35698

Dopant effect of yttrium and the growth and adherence of alumina on nickel-aluminum alloys p 82 A85-40973

Fracture of yttria-doped, sintered reaction-bonded silicon nitride

[ACS PAPER 7-J3-84] p 82 A85-42797

Effect of lubricant extreme-pressure additives on surface fatigue life of AISI 9310 spur gears

[NASA-TP-2408] p 130 N85-13234

Effect of five lubricants on life of AISI 9310 spur gears

[NASA-TP-2419] p 123 N85-16099

Characterization of lubricated bearing surfaces operated under high loads

[NASA-TM-86964] p 88 N85-21357

The effects of lithium counterdoping on radiation damage and annealing in n(+)-p silicon solar cells p 50 N85-22586

Jet fuel instability mechanisms

[NASA-CR-175856] p 93 N85-28127

Lubricant and additive effects on spur gear fatigue life

[NASA-TM-87044] p 133 N85-28373

### ADHESION

Universal binding energy relations in metallic adhesion

[NASA-CR-175856] p 72 N85-12132

Fundamental tribological properties of ceramics

[NASA-TM-86915] p 85 N85-15893

Humidity effects on adhesion of nickel-zinc ferrite in elastic contact with magnetic tape and itself

[NASA-TP-2449] p 88 N85-21359

Monte Carlo lattice models for adsorbed polymer conformation

[NASA-TP-2453] p 183 N85-24961

SUBJECT

## ADHESION TESTS

Mechanical property measurements of plasma-sprayed thermal-barrier coatings subjected to oxidation  
p 81 A85-29729

## ADHESIVE BONDING

Fracture of composite-adhesive-composite systems  
p 141 A85-27935

Ceramic microstructure and adhesion  
p 82 A85-40384

Ceramic microstructure and adhesion  
[NASA-TM-83804]  
p 83 N85-10186

Molecular orbital studies in oxidation: Sulfate formation and metal-metal oxide adhesion  
[NASA-CR-176070]  
p 77 N85-32174

## ADIABATIC EQUATIONS

An interactive computer code for calculation of gas-phase chemical equilibrium (EQLBRM)  
[NASA-CR-168337]  
p 18 N85-10948

## ADSORPTION

Adsorption of O<sub>2</sub>, SO<sub>2</sub>, and SO<sub>3</sub> on nickel oxide. Mechanism for sulfate formation  
[NASA-CR-176072]  
p 77 N85-32175

CO adsorption on (111) and (100) surfaces of the Pt sub 3 Ti alloy. Evidence for parallel binding and strong activation of CO  
[NASA-CR-176077]  
p 77 N85-32176

## AEROACOUSTICS

Acoustic pressures emanating from a turbomachine stage  
[AIAA PAPER 84-2325]  
p 2 A85-10870

Effect of airfoil mean loading on convected gust interaction noise  
[AIAA PAPER 84-2324]  
p 173 A85-13955

Modelling of wind tunnel wall effects on the radiation characteristics of acoustic sources  
[AIAA PAPER 84-2364]  
p 174 A85-16104

A theoretical prediction of the acoustic pressure generated by turbulence-flame front interactions  
[ASME PAPER 84-WA/NCA-11]  
p 174 A85-39909

Turbofan noise generation. Volume 2: Computer programs  
[NASA-CR-176952]  
p 175 N85-11791

## AEROASSIST

OTV Propulsion Issues  
[NASA-CP-2347]  
p 37 N85-16989

## AERODYNAMIC CHARACTERISTICS

Progress in development of a Navier-Stokes solver for evaluation of iced airfoil performance  
[AIAA PAPER 85-0410]  
p 3 A85-19731

Analytical modeling of circuit aerodynamics in the new NASA Lewis Altitude Wind Tunnel  
[AIAA PAPER 85-0380]  
p 3 A85-26389

Icing flight research - Aerodynamic effects of ice and ice shape documentation with stereo photography  
[AIAA PAPER 85-0468]  
p 11 A85-30192

Low-speed aerodynamic test of an axisymmetric supersonic inlet with variable cowl slot  
[AIAA PAPER 85-1210]  
p 5 A85-40819

Noise constraints effecting optimal propeller designs  
[SAE PAPER 850871]  
p 7 A85-50106

Design and wind tunnel evaluation of a symmetric airfoil series for large wind turbine applications  
[NASA-CR-174764]  
p 7 N85-10919

Energy efficient engine ICLS Nacelle detail design report  
[NASA-CR-167870]  
p 22 N85-10993

Analytical modeling of circuit aerodynamics in the new NASA Lewis wind tunnel  
[NASA-TM-86912]  
p 8 N85-15688

Icing flight research: Aerodynamic effects of ice and ice shape documentation with stereo photography  
[NASA-TM-86906]  
p 12 N85-18049

The Altitude Wind Tunnel (AWT): A unique facility for propulsion system and adverse weather testing  
[NASA-TM-86921]  
p 35 N85-18067

Noise constraints effecting optimal propeller designs  
[NASA-TM-86967]  
p 8 N85-19923

Large-scale Advanced Propfan (LAP) performance, acoustic and weight estimation, January, 1984  
[NASA-CR-174782]  
p 9 N85-22368

Low-speed aerodynamic test of an axisymmetric supersonic inlet with variable cowl slot  
[NASA-TM-87039]  
p 28 N85-26710

Wake effects on the aerodynamic performance of horizontal axis wind turbines  
[NASA-CR-174920]  
p 162 N85-29364

Heat transfer in aeropropulsion systems  
[NASA-TM-87066]  
p 119 N85-31444

**AERODYNAMIC COEFFICIENTS**

Analytical determination of propeller performance degradation due to ice accretion  
[AIAA PAPER 85-0339]  
p 14 A85-20867

Optimization of cascade blade mistuning. I - Equations of motion and basic inherent properties  
p 16 A85-42365

## AERODYNAMIC CONFIGURATIONS

Energy efficient engine ICLS Nacelle detail design report  
[NASA-CR-167870]  
p 22 N85-10993

Performance comparison between NACA 23024 and NACA 64(3)-618 airfoil configured rotors for horizontal-axis wind turbines  
[NASA-TM-83471]  
p 163 N85-30477

## AERODYNAMIC DRAG

Preliminary assessment of power-generating tethers in space and of propulsion for their orbit maintenance  
p 37 N85-22520

Ice shapes and the resulting drag increase for a NACA 0012 airfoil  
[NASA-TM-83556]  
p 11 N85-27839

## AERODYNAMIC HEATING

Unsteady heat transfer due to time-dependent free stream velocity  
p 117 N85-27947

## AERODYNAMIC LOADS

Effect of airfoil mean loading on convected gust interaction noise  
[AIAA PAPER 84-2324]  
p 173 A85-13955

A linearized unsteady aerodynamic analysis for transonic cascades  
p 3 A85-20744

Overview of aerothermodynamic loads definition study  
p 51 N85-27942

## AERODYNAMIC NOISE

Effect of airfoil mean loading on convected gust interaction noise  
[AIAA PAPER 84-2324]  
p 173 A85-13955

Noise constraints effecting optimal propeller designs  
[SAE PAPER 850871]  
p 7 A85-50106

Noise constraints effecting optimal propeller designs  
[NASA-TM-86967]  
p 8 N85-19923

Noise transmission loss of a rectangular plate in an infinite baffle  
[NASA-TP-2398]  
p 176 N85-22109

Large-scale Advanced Propfan (LAP) performance, acoustic and weight estimation, January, 1984  
[NASA-CR-174782]  
p 9 N85-22368

## AERODYNAMIC STABILITY

Effects of friction dampers on aerodynamically unstable rotor stages  
p 14 A85-21866

Optimization of cascade blade mistuning. II - Global optimum and numerical optimization  
p 16 A85-45715

Aerodynamic detuning analysis of an unstalled supersonic turbofan cascade  
[NASA-TM-87001]  
p 9 N85-26670

## AERODYNAMIC STALLING

Stall recovery control strategy methodology and results  
[AIAA PAPER 85-1433]  
p 16 A85-40841

## AERODYNAMICS

Energy efficient engine combustor test hardware detailed design report  
[NASA-CR-167945]  
p 18 N85-10950

Inverse design technique for cascades  
[NASA-CR-3836]  
p 7 N85-12008

Aerodynamic analysis of a horizontal axis wind turbine by use of helical vortex theory. Volume 1: Theory  
[NASA-CR-168054]  
p 9 N85-29916

## AEROELASTICITY

Flutter of turbopump rotors with mistuned blades  
p 139 A85-12716

Flutter and forced response of mistuned rotors using standing wave analysis  
p 139 A85-12721

Flutter of swept fan blades  
[ASME PAPER 84-GT-138]  
p 141 A85-32962

Vibration and flutter of mistuned bladed-disk assemblies  
p 16 A85-45854

Structural response of a rotating bladed disk to rotor whirl  
[NASA-CR-175605]  
p 27 N85-22391

## AERONAUTICAL ENGINEERING

Bibliography of Lewis Research Center technical publications announced in 1983  
[NASA-TM-83693]  
p 184 N85-22255

Future directions in aeropropulsion technology  
[NASA-TM-87010]  
p 1 N85-23685

Alternatives for jet engine control  
[NASA-CR-175832]  
p 29 N85-26714

Alternatives for jet engine control  
[NASA-CR-175833]  
p 29 N85-26715

## AERONAUTICS

Research and technology highlights of the Lewis Research Center  
[NASA-TM-86899]  
p 186 N85-17928

## AEROSOLS

Fast laser-induced aerosol formation for visualization of gas flows  
p 121 A85-31113

## AEROSPACE ENGINEERING

PMR polyimide composites for aerospace applications --- Polymerization of Monomer Reactants  
p 55 A85-21520

Bibliography of Lewis Research Center technical publications announced in 1983  
[NASA-TM-83693]  
p 184 N85-22255

## AEROSPACE ENVIRONMENTS

Ion beam sputter-deposited thin film coatings for protection of spacecraft polymers in low Earth orbit  
[NASA-TM-87051]  
p 91 N85-30137

## AEROSPACE SYSTEMS

High temperature metal and ceramic composites  
p 55 A85-37483

## AEROTHERMODYNAMICS

Application of viscous and inviscid computation methods for rocket turbopump systems  
[SAE PAPER 841522]  
p 110 A85-39257

Future fundamental combustion research for aeropropulsion systems  
[AIAA PAPER 85-1398]  
p 16 A85-42671

Heat transfer results and operational characteristics of the NASA Lewis Research Center Hot Section Cascade Test Facility  
[NASA-TM-86890]  
p 114 N85-15133

Analytical and physical modeling program for the NASA Lewis Research Center's Altitude Wind Tunnel (AWT)  
[NASA-TM-86919]  
p 35 N85-15757

Combustion research for gas turbine engines  
[NASA-TM-86963]  
p 26 N85-21164

Future fundamental combustion research for aeropropulsion systems  
[NASA-TM-87049]  
p 30 N85-27870

Structural Integrity and Durability of Reusable Space Propulsion Systems  
[NASA-CP-2381]  
p 51 N85-27941

Overview of aerothermodynamic loads definition study  
p 51 N85-27942

## AGING (MATERIALS)

Ten year environmental test of glass fiber/epoxy pressure vessels  
[AIAA PAPER 85-1198]  
p 56 A85-47022

Ten year environmental test of glass fiber/epoxy pressure vessels  
[NASA-TM-87058]  
p 58 N85-30034

Thermomechanical deformation in the presence of metallurgical changes  
p 150 N85-31533

## AILERONS

Aileron controls for wind turbine applications  
p 157 A85-45513

Aileron controls for wind turbine applications  
[NASA-TM-86867]  
p 158 N85-11458

Shutdown characteristics of the Mod-O wind turbine with aileron controls  
[NASA-TM-86918]  
p 159 N85-16299

Reflection plane tests of a wind turbine blade tip section with ailerons  
[NASA-TM-87018]  
p 165 N85-34444

## AIR FLOW

Swirling flows in typical combustor geometries  
[AIAA PAPER 85-0184]  
p 108 A85-19574

A stagnation pressure probe for droplet-laden air flow  
[AIAA PAPER 85-0330]  
p 108 A85-19672

Contingency power concepts for helicopter turboshaft engine  
p 15 A85-32005

Heat transfer enhancement in channels with turbulence promoters  
[ASME PAPER 84-WA/HT-72]  
p 111 A85-39900

Internal combustion engine combustion chamber process studies at NASA Lewis Research Center  
p 112 A85-45856

Turbine heat transfer  
p 19 N85-10964

Energy efficient engine. High pressure compressor detail design report  
[NASA-CR-165558]  
p 23 N85-10998

Liquid fuel spray processes in high-pressure gas flow  
[NASA-TM-86944]  
p 115 N85-21570

## AIR INTAKES

Low-speed aerodynamic test of an axisymmetric supersonic inlet with variable cowl slot  
[AIAA PAPER 85-1210]  
p 5 A85-40819

Low-speed aerodynamic test of an axisymmetric supersonic inlet with variable cowl slot  
[NASA-TM-87039]  
p 28 N85-26710

## AIR JETS

The performance of jet noise suppression devices for industrial applications  
p 175 A85-42563

Density effects on jet characteristics in confined swirling flow  
p 112 A85-45283

Flow visualization study of the effect of injection hole geometry on an inclined jet in crossflow  
[NASA-TM-86936]  
p 115 N85-20269

## AIR TRAFFIC

MERIT: A man/computer data management and enhancement system for upper air nowcasting/forecasting in the United States --- Minimum Energy Routes using Interactive Techniques (MERIT)  
p 167 N85-10558

## AIRBORNE/SPACEBORNE COMPUTERS

Satellite baseband processor test performance summary  
p 95 A85-14434

## AIRCRAFT COMPARTMENTS

- Simultaneous cabin and ambient ozone measurements on two Boeing 747 airplanes. Volume 3: October 1978 - July 1979  
[NASA-TM-86883] p 167 N85-21872

## AIRCRAFT CONTROL

- High-temperature optically activated GaAs power switching for aircraft digital electronic control  
[NASA-CR-174711] p 34 N85-12901

## AIRCRAFT DESIGN

- Noise constraints effecting optimal propeller designs [SAE PAPER 850871] p 7 A85-50106  
Observations from varying the lift and drag inputs to a noise prediction method for supersonic helical tip speed propellers  
[NASA-TM-83797] p 175 N85-10788  
Energy efficient engine component development and integration program  
[NASA-CR-169496] p 22 N85-10989  
Energy efficient engine component development and integration program  
[NASA-CR-170034] p 22 N85-10990  
Energy efficient engine. Volume 2. Appendix A: Component development and integration program  
[NASA-CR-173085] p 22 N85-10991  
Study of advanced fuel system concepts for commercial aircraft and engines  
[NASA-CR-174752] p 93 N85-19176  
Noise constraints effecting optimal propeller designs  
[NASA-TM-86967] p 8 N85-19923  
Lubrication and performance of high-speed rolling-element bearings  
[NASA-TM-86958] p 131 N85-21658

## AIRCRAFT ENGINES

- The role of modern control theory in the design of controls for aircraft turbine engines p 13 A85-13627  
Comparison of scaled model data to full size energy efficient engine test results  
[AIAA PAPER 84-2281] p 13 A85-13953  
Vibration and flutter of mistuned bladed-disk assemblies p 16 A85-45854  
A real-time FORTRAN implementation of a sensor failure detection, isolation and accommodation algorithm  
p 171 A85-47704  
Turbine Engine Hot Section Technology (HOST)  
[NASA-TM-83022] p 18 N85-10951  
Nonlinear structural and life analyses of a turbine blade p 19 N85-10954  
Nonlinear structural and life analyses of a combustor liner p 19 N85-10955  
Pre-HOST high temperature crack propagation  
p 19 N85-10956  
Structural analysis p 20 N85-10969  
Component-specific modeling p 20 N85-10971  
The 3-D inelastic analysis methods for hot section components: Brief description p 20 N85-10972  
Constitutive model development for isotropic materials p 20 N85-10975  
Airfoil deposition model p 21 N85-10979  
Effects of surface chemistry on hot corrosion life: Overview p 21 N85-10980  
Combustion system for radiation investigations  
p 21 N85-10986  
Energy efficient engine component development and integration program  
[NASA-CR-170034] p 22 N85-10990  
Energy efficient engine. Low pressure turbine test hardware detailed design report  
[NASA-CR-167956] p 22 N85-10994  
Energy efficient engine high pressure turbine test hardware detailed design report  
[NASA-CR-167955] p 23 N85-10995  
Energy efficient engine. High pressure compressor detail design report  
[NASA-CR-165558] p 23 N85-10998  
Static jet noise test results of four 0.35 scale-model QCGAT mixer nozzles  
[NASA-TM-86871] p 175 N85-13551  
Design description of a microprocessor based Engine Monitoring and Control unit (EMAC) for small turboshaft  
[NASA-TM-86860] p 1 N85-17935  
NASA Lewis Research Center/University Graduate Research Program on Engine Structures  
[NASA-TM-86916] p 145 N85-18375  
Analytical fuel property effects: Small combustors, phase 2  
[NASA-CR-174848] p 93 N85-19175  
Study of advanced fuel system concepts for commercial aircraft and engines  
[NASA-CR-174752] p 93 N85-19176  
Study of advanced fuel system concepts for commercial aircraft  
[NASA-CR-174751] p 12 N85-19978  
A theory of post-stall transients in multistage axial compression systems  
[NASA-CR-3878] p 8 N85-21117

- Stratified charge rotary aircraft engine technology enablement program  
[NASA-CR-174812] p 25 N85-21163  
Tribological systems as applied to aircraft engines  
[NASA-TM-86965] p 131 N85-21657  
Advanced smoke meter development survey and analysis  
[NASA-CR-168287] p 124 N85-25792  
Component-specific modeling  
[NASA-CR-174925] p 32 N85-32119
- AIRCRAFT EQUIPMENT**  
Icing tunnel tests of Electro-Impulse De-icing of an engine inlet and high-speed wings  
[AIAA PAPER 85-0466] p 10 A85-20872  
Electro-impulse de-icing of a turbofan engine inlet  
[AIAA PAPER 85-1118] p 12 A85-40811
- AIRCRAFT FUEL SYSTEMS**  
Study of advanced fuel system concepts for commercial aircraft and engines  
[NASA-CR-174752] p 93 N85-19176  
Study of advanced fuel system concepts for commercial aircraft  
[NASA-CR-174751] p 12 N85-19978
- AIRCRAFT FUELS**  
Study of advanced fuel system concepts for commercial aircraft  
[NASA-CR-174751] p 12 N85-19978  
Applications of high pressure differential scanning calorimetry to aviation fuel thermal stability research  
[NASA-TM-87002] p 83 N85-23941  
Jet fuel property changes and their effect on producibility and cost in the U.S., Canada, and Europe  
[NASA-CR-174840] p 93 N85-27012  
Detailed studies of aviation fuel flowability  
[NASA-CR-174938] p 94 N85-31308  
Comparative analysis of operational forecasts versus actual weather conditions in airline flight planning, volume 1  
[NASA-CR-167862] p 167 N85-35534  
Comparative analysis of operational forecasts versus actual weather conditions in airline flight planning, volume 4  
[NASA-CR-167865] p 167 N85-35537  
Comparative analysis of operational forecasts versus actual weather conditions in airline flight planning: Summary report  
[NASA-CR-167866] p 168 N85-35538
- AIRCRAFT NOISE**  
Analysis of the effect on combustor noise measurements of acoustic waves reflected by the turbine and combustor inlet  
[AIAA PAPER 84-2323] p 173 A85-16103  
Static jet noise test results of four 0.35 scale-model QCGAT mixer nozzles  
[NASA-TM-86871] p 175 N85-13551
- AIRCRAFT PERFORMANCE**  
Comparative analysis of operational forecasts versus actual weather conditions in airline flight planning, volume 1  
[NASA-CR-167862] p 167 N85-35534
- AIRCRAFT POWER SUPPLIES**  
Advanced secondary power system for transport aircraft  
[NASA-TP-2463] p 30 N85-28944
- AIRCRAFT STRUCTURES**  
Icing flight research - Aerodynamic effects of ice and ice shape documentation with stereo photography  
[AIAA PAPER 85-0468] p 11 A85-30192  
Icing flight research: Aerodynamic effects of ice and ice shape documentation with stereo photography  
[NASA-TM-86906] p 12 N85-18049
- AIRCRAFT WAKES**  
Noise produced by the interaction of a rotor wake with a swept stator blade  
[AIAA PAPER 84-2326] p 173 A85-13956
- AIRFOIL PROFILES**  
Progress in development of a Navier-Stokes solver for evaluation of iced airfoil performance  
[AIAA PAPER 85-0410] p 3 A85-19731
- AIRFOILS**  
Effect of airfoil mean loading on convected gust interaction noise  
[AIAA PAPER 84-2324] p 173 A85-13955  
Predicting rim ice accretion on airfoils  
p 3 A85-25135  
Feedback in separated flows over symmetric airfoils  
[AIAA PAPER 84-2297] p 3 A85-28899  
Transient technique for measuring heat transfer coefficients on stator airfoils in a jet engine environment  
[AIAA PAPER 85-1471] p 122 A85-39796  
The computation of viscous/inviscid interaction on airfoils with separated flow  
p 6 A85-42954  
Design and wind tunnel evaluation of a symmetric airfoil series for large wind turbine applications  
[NASA-CR-174764] p 7 N85-10919  
Turbine heat transfer  
p 19 N85-10964

- Unsteady pressure measurements on a biconvex airfoil in a transonic oscillating cascade  
[NASA-TM-86914] p 8 N85-15689  
High temperature thermocouple and heat flux gauge using a unique thin film hardware hot junction  
[NASA-TM-86898] p 123 N85-16096  
Study of controlled diffusion stator blading  
[NASA-CR-167995] p 25 N85-18058  
The boundary layer on compressor cascade blades  
[NASA-CR-174369] p 114 N85-18292  
Transient technique for measuring heat transfer coefficients on stator airfoils in a jet engine environment  
[NASA-TM-87005] p 124 N85-25794  
Ice shapes and the resulting drag increase for a NACA 0012 airfoil  
[NASA-TM-83556] p 11 N85-27839  
New facility to study unsteady wake effects on turbine airfoil heat transfer  
p 117 N85-27948  
Performance comparison between NACA 23024 and NACA 64(3)-618 airfoil configured rotors for horizontal-axis wind turbines  
[NASA-TM-83471] p 163 N85-30477  
Heat transfer in aeropropulsion systems  
[NASA-TM-87066] p 119 N85-31444  
Local heat-transfer measurements on a large, scale-model turbine blade airfoil using a composite of a heater element and liquid crystals  
[NASA-TM-86900] p 119 N85-33435
- ALCOHOLS**  
Alkaline battery containing a separator of a cross-linked copolymer of vinyl alcohol and unsaturated carboxylic acid  
[NASA-CASE-LEW-13102-1] p 104 N85-29144
- ALGEBRA**  
Alternatives for jet engine control  
[NASA-CR-175831] p 29 N85-26713
- ALGORITHMS**  
Hybrid stress finite elements for large deformations of inelastic solids p 139 A85-15894  
Efficient solution of the Euler and Navier-Stokes equations with a vectorized multiple-grid algorithm  
p 2 A85-18679  
Accelerated convergence for incompressible flow calculations  
[AIAA PAPER 85-0058] p 2 A85-19489  
Inviscid and viscous flows in cascades with an explicit multiple-grid algorithm p 7 A85-48539  
Comparison of numerical techniques for integration of stiff ordinary differential equations arising in combustion chemistry  
[NASA-TP-2372] p 17 N85-10065  
CREKID: A computer code for transient, gas-phase combustion of kinetics  
[NASA-TM-83806] p 17 N85-10068  
Augmented weak forms and element-by-element preconditioners: Efficient iterative strategies for structural finite elements. A preliminary study p 144 N85-10384  
Accelerated convergence for incompressible flow calculations  
[NASA-TM-86863] p 18 N85-10949  
A comparison of the efficiency of numerical methods for integrating chemical kinetic rate equations  
[NASA-TM-83590] p 25 N85-21162  
Linearization of digital derived rate algorithm for use in linear stability analysis  
[NASA-TM-87000] p 41 N85-23904  
Comparative analysis of operational forecasts versus actual weather conditions in airline flight planning, volume 2  
[NASA-CR-167863] p 167 N85-35535
- ALKALINE BATTERIES**  
Alkaline battery containing a separator of a cross-linked copolymer of vinyl alcohol and unsaturated carboxylic acid  
[NASA-CASE-LEW-13102-1] p 104 N85-29144
- ALKANES**  
Liquid phase products and solid deposit formation from thermally stressed model jet fuels  
[NASA-TM-86874] p 92 N85-13066
- ALLOYS**  
Effects of cobalt, boron, and zirconium on the microstructure of Udimet 738  
[NASA-CR-174762] p 70 N85-10166  
Characterization of erosion of metallic materials under cavitation attack in a mineral oil  
[NASA-TM-86934] p 74 N85-19075  
Alloys based on NiAl for high temperature applications  
[NASA-TM-86976] p 75 N85-21322  
Advanced thin film thermocouples  
[NASA-CR-175541] p 124 N85-21607  
Viscoplastic constitutive relationships with dependence on thermomechanical history  
[NASA-CR-174836] p 146 N85-21691  
Effects of surface chemistry on hot corrosion life  
[NASA-CR-174915] p 28 N85-26711



Properties and microstructures for dual alloy combinations of three superalloys with alloy 901 [NASA-TM-86987] p 76 N85-26963  
Thermomechanical deformation in the presence of metallurgical changes p 150 N85-31533  
Results of an interlaboratory fatigue test program conducted on alloy 800H at room and elevated temperatures [NASA-CR-174940] p 152 N85-32340

# ALTITUDE

Analytical and physical modeling program for the NASA Lewis Research Center's Altitude Wind Tunnel (AWT) [NASA-TM-86919] p 35 N85-15757

## ALTITUDE SIMULATION

The Altitude Wind Tunnel (AWT) - A unique facility for propulsion system and adverse weather testing [AIAA PAPER 85-0314] p 34 A85-19861  
Analytical and physical modeling program for the NASA Lewis Research Center's Altitude Wind Tunnel (AWT) [AIAA PAPER 85-0379] p 34 A85-19709  
The NASA altitude wind tunnel - Its role in advanced icing research and development [AIAA PAPER 85-0090] p 35 A85-26381  
Analytical modeling of circuit aerodynamics in the new NASA Lewis Altitude Wind Tunnel [AIAA PAPER 85-0380] p 3 A85-26389  
Analytical modeling of circuit aerodynamics in the new NASA Lewis wind tunnel [NASA-TM-86912] p 8 N85-15688  
The NASA Altitude Wind Tunnel (AWT): Its role in advanced icing research and development [NASA-TM-86920] p 35 N85-15758

## ALTITUDE TESTS

Altitude testing of a flight weight, self-cooled, 2D thrust vectoring exhaust nozzle [SAE PAPER 841557] p 14 A85-25984

## ALUMINATES

Alloys based on NiAl for high temperature applications [NASA-TM-86976] p 75 N85-21322

## ALUMINUM

Universal binding energy relations in metallic adhesion [NASA-TM-86889] p 72 N85-12132  
Optimization of the NiCrAl-Y/ZrO-Y2O3 thermal barrier system [NASA-TM-86905] p 72 N85-15878  
Experimental compliance calibration of the NASA Lewis Research Center Mode 2 fatigue specimen [NASA-TM-86908] p 144 N85-16205  
High temperature properties of equiatomic FeAl with ternary additions [NASA-TM-86938] p 73 N85-19072  
Effects of chromium and aluminum on mechanical and oxidation properties of iron-nickel-base superalloys based on CG-27 [NASA-TP-2443] p 75 N85-21323  
Aluminum work function: Effect of oxidation, mechanical scraping and ion bombardment [NASA-TM-87079] p 78 N85-34265

## ALUMINUM ALLOYS

Deformation and erosion of f.c.c. metals and alloys under cavitation attack p 65 A85-12789  
Modeling of gamma/gamma-prime phase equilibrium in the nickel-aluminum system p 65 A85-14959  
Ductility in rapidly solidified NiAl p 66 A85-26158  
The transient oxidation of single crystal NiAl+Zr [NASA-CR-174756] p 70 N85-11221  
A study of spectrum fatigue crack propagation in two aluminum alloys. 1: Spectrum simplification [NASA-TM-86929] p 72 N85-18124  
A study of spectrum fatigue crack propagation in two aluminum alloys. 2: Influence of microstructures [NASA-TM-86930] p 73 N85-18125  
Rapidly solidified NiAl and FeAl [NASA-TM-86941] p 74 N85-20042

## ALUMINUM COATINGS

Microstructural development of protective Al2O3 scales p 80 A85-21650

## ALUMINUM COMPOUNDS

The B2 aluminides as alternative materials [NASA-TM-86937] p 74 N85-19076

## ALUMINUM GRAPHITE COMPOSITES

Select fiber composites for space applications - A mechanistic assessment p 54 A85-16040

## ALUMINUM OXIDES

Microstructural development of protective Al2O3 scales p 80 A85-21650  
Dopant effect of yttrium and the growth and adherence of alumina on nickel-aluminum alloys p 82 A85-40973  
The transient oxidation of single crystal NiAl+Zr [NASA-CR-174756] p 70 N85-11221  
Fundamental tribological properties of ceramics [NASA-TM-86915] p 85 N85-15893  
Dispersed metal-toughened ceramics and ceramic brazing [NASA-CR-174284] p 86 N85-15916

Transformation toughened ceramics for the heavy duty diesel engine technology program [NASA-CR-174689] p 185 N85-16698

Dispersed-metal-toughened alumina [NASA-CR-174687] p 89 N85-22758

## AMBIENT TEMPERATURE

Results of an interlaboratory fatigue test program conducted on alloy 800H at room and elevated temperatures [NASA-CR-174940] p 152 N85-32340

## AMMONIA

Performance characterization tests of a 1-kW resistojet using hydrogen, nitrogen and ammonia as propellants [AIAA PAPER 85-1159] p 44 A85-39628

## AMORPHOUS MATERIALS

Mechanical-contact-induced transformation from the amorphous to the partially crystalline state in metallic glass p 65 A85-19084  
'Diamondlike' carbon films - Optical absorption, dielectric properties, and hardness dependence on deposition parameters p 82 A85-40383  
Optical properties of hydrogenated amorphous carbon films grown from methane plasma [NASA-TM-86995] p 183 N85-26406

## AMPLIFICATION

Adaptive antenna arrays for weak interfering signals [NASA-CR-174336] p 98 N85-17258

## AMPLIFIER DESIGN

A 20 GHz, 75 watt, helix TWT for space communications p 101 A85-14433

## AMPLIFIERS

The 30 GHz solid state amplifier for low cost low data rate ground terminals [NASA-CR-174795] p 102 N85-12300

## AMPLITUDES

The use of an optical data acquisition system for bladed disk vibration analysis [NASA-TM-86891] p 144 N85-15184

## ANEMOMETERS

Hot section laser anemometry p 19 N85-10962

## ANGLE OF ATTACK

Performance and surge limits of a TF30-P-3 turbofan engine/axisymmetric mixed-compression inlet propulsion system at Mach 2.5 [NASA-TP-2461] p 27 N85-25261

## ANGLES (GEOMETRY)

Free-surface phenomena under low- and zero-gravity conditions [NASA-CR-175835] p 116 N85-27168

## ANISOTROPY

Low cycle fatigue of MAR-M 200 single crystals at 760 and 870 deg C [NASA-TM-86933] p 74 N85-19074  
Orientation and temperature dependence of some mechanical properties of the single-crystal nickel-base superalloy Rene N4. 3: Tension-compression anisotropy [NASA-TM-86982] p 76 N85-22660

## ANNEALING

Heat treatment of bulk gallium arsenide using a phosphosilicate glass cap p 181 A85-32636  
The effects of lithium counterdoping on radiation damage and annealing in n(+)-p silicon solar cells p 50 N85-22586

## ANNULAR DUCTS

Rotordynamic coefficients for compressible flow in tapered annular seals p 129 A85-42573

## ANNULAR FLOW

Supersonic jet shock noise reduction [AIAA PAPER 84-2278] p 173 A85-16099  
An improved computer model for prediction of axial gas turbine performance losses [NASA-CR-174246] p 24 N85-15724

## ANNULAR NOZZLES

Experimental investigation of shock-cell noise reduction for single stream nozzles in simulated flight [NASA-CR-3845] p 175 N85-13550

## ANTENNA ARRAYS

On the calculation of the directivity of planar array feeds for satellite reflector applications p 97 A85-32249  
The study of microstrip antenna arrays and related problems [NASA-CR-174054] p 97 N85-11265  
Characterization of MMIC devices for active array antennas [NASA-TM-86907] p 38 N85-15779  
Infrared technology for satellite power conversion ... antenna arrays and bolometers p 159 N85-16293  
Adaptive antenna arrays for weak interfering signals [NASA-CR-174336] p 98 N85-17258  
Adaptive antenna arrays for satellite communications: Design and testing [NASA-CR-176162] p 100 N85-34329

## ANTENNA COMPONENTS

Characterization of MMIC devices for active array antennas [NASA-TM-86907] p 38 N85-15779

## ANTENNA DESIGN

Advanced 30/20 GHz multiple beam antenna for future communications satellites p 96 A85-14436  
The 20 GHz proof-of-concept test model results for a multiple scan beam dual reflector antenna [NASA-CR-174268] p 98 N85-15944  
Configuration study for a 30 GHz monolithic receive array: Technical assessment [NASA-CR-174697] p 98 N85-18238  
Configuration study for a 30 GHz monolithic receive array, volume 1 [NASA-CR-174697-VOL-1] p 98 N85-18239  
Configuration study for a 30 GHz monolithic receive array, volume 2 [NASA-CR-174697-VOL-2] p 99 N85-18240  
Extreme precision antenna reflector study results p 165 N85-23830

## ANTENNA FEEDS

Dual-mode coaxial feed with low crosspolarisation p 101 A85-20171  
On the calculation of the directivity of planar array feeds for satellite reflector applications p 97 A85-32249

## ANTENNA RADIATION PATTERNS

Dual-mode coaxial feed with low crosspolarisation p 101 A85-20171  
Case study of sample spacing in planar near-field measurement of high gain antennas [NASA-TM-86872] p 97 N85-10234  
The 20 GHz proof-of-concept test model results for a multiple scan beam dual reflector antenna [NASA-CR-174268] p 98 N85-15944  
Adaptive antenna arrays for satellite communications: Design and testing [NASA-CR-176162] p 100 N85-34329

## ANTENNAS

Case study of sample spacing in planar near-field measurement of high gain antennas [NASA-TM-86872] p 97 N85-10234  
MMIC devices for active phased array antennas [NASA-CR-174281] p 98 N85-15943

## ANTIKNOCK ADDITIVES

Knock syndrome: Its cures and its victims [NASA-CR-174395] p 93 N85-19185

## APERTURES

Focal shifts in parabolic reflectors p 97 A85-39356  
Characterization of MMIC devices for active array antennas [NASA-TM-86907] p 38 N85-15779

## ARC DISCHARGES

Cathode degradation and erosion in high pressure arc discharges p 43 A85-16445  
Characteristics of arc currents on a negatively biased solar cell array in a plasma p 154 A85-18608  
An investigation of arc discharging on negatively biased dielectric conductor samples in a plasma p 180 N85-22498  
Hollow cathodes in high pressure arc discharges [NASA-TM-87098] p 52 N85-34179

## ARC JET ENGINES

Cathode degradation and erosion in high pressure arc discharges p 43 A85-16445  
Electrode erosion in arc discharges at atmospheric pressure [NASA-TM-87087] p 52 N85-34178  
Hollow cathodes in high pressure arc discharges [NASA-TM-87098] p 52 N85-34179

## ARC SPRAYING

Arc spray fabrication of metal matrix composite monolayer [NASA-CASE-LEW-13828-1] p 58 N85-30027

## ARCHITECTURE (COMPUTERS)

A functional language approach in high-speed digital simulation p 170 A85-28615  
General approaches for achieving high speed computations p 169 A85-28628  
Functional language and data flow architectures p 170 A85-28629

## ARIZONA

Control aspects of the Schuchuli Village stand-alone photovoltaic power system [NASA-TM-83790] p 103 N85-13157

## AROMATIC COMPOUNDS

Liquid phase products and solid deposit formation from thermally stressed model jet fuels [NASA-TM-86874] p 92 N85-13066

## ARRAYS

Mosaic Infrared Sensor for Space Astronomy (MIRSSA) [NASA-CR-176154] p 125 N85-33456

## ASBESTOS

Separator development and testing of nickel-hydrogen cells p 156 A85-45386

**ASSEMBLING**

- Extreme precision antenna reflector study results  
p 165 N85-23830

**ATMOSPHERIC CORRECTION**

- Comparison of atmospheric correction algorithms for the  
Coastal Zone Color Scanner p 153 A85-10244

**ATMOSPHERIC PRESSURE**

- Electrode erosion in arc discharges at atmospheric  
pressure p 52 N85-34178  
[NASA-TM-87087]

**ATMOSPHERIC TEMPERATURE**

- A comparison of NMC and GWC analysis field  
temperatures with aircraft measurements p 166 A85-21140

**ATOMIC RECOMBINATION**

- Molecular orbital studies in oxidation: Sulfate formation  
and metal-metal oxide adhesion p 77 N85-32174  
[NASA-CR-176070]

**ATOMIC STRUCTURE**

- AES and LEED study of the zinc blende SiC(100)  
surface p 61 A85-41633  
Mechanism for chelated sulfate formation from SO<sub>2</sub> and  
bis (triphenylphosphine) platinum p 62 A85-48493

**ATOMIZING**

- Liquid fuel spray processes in high-pressure gas flow  
[NASA-TM-86944] p 115 N85-21570

**ATTENUATION**

- Normal modes in an overmoded circular waveguide  
coated with lossy material p 100 N85-35320  
[NASA-CR-176186]

**ATTENUATORS**

- Design of low loss helix circuits for interference fitted  
and brazed circuits p 103 N85-19328  
[NASA-CR-168313]

**ATTITUDE CONTROL**

- Report of the Constellations Panel p 131 N85-20368  
Operating characteristics of a 0.87 kW-hr flywheel  
energy storage module p 133 N85-28371  
[NASA-TM-87038]

**AURORAL ARCS**

- Circuit transients due to negative bias arcs on a  
high-voltage solar array in low Earth orbit p 39 N85-14858  
[NASA-TP-2407]

**AURORAL ELECTROJETS**

- Polar orbit electrostatic charging of objects in shuttle  
wake p 40 N85-22487

**AURORAS**

- DE-1 measurements of AKR wave directions --- auroral  
kilometric radiation p 166 A85-37717

**AUTOMATIC CONTROL**

- Fiber optic, Fabry-Perot high temperature sensor  
[NASA-CR-174712] p 178 N85-13594  
Automated testing of developmental satellite  
communications systems and subsystems p 100 N85-31348  
[NASA-TM-87070]

**AUTOMATIC TEST EQUIPMENT**

- An approach for automated analysis of particle  
holograms p 120 A85-10034  
Satellite baseband processor test performance  
summary p 95 A85-14434  
Closed-loop strain controlled testing at elevated  
temperatures with a non-contacting gage p 121 A85-29562

- Automated testing of developmental satellite  
communications systems and subsystems p 100 N85-31348  
[NASA-TM-87070]

**AUTOMOBILE ENGINES**

- Ceramic component development for the AGT101 gas  
turbine engine p 126 A85-15972  
Ceramic components for gas turbine engines p 127 A85-15973  
Mod II engine and technology development p 129 A85-45473

- Automotive Stirling engine systems development  
p 130 A85-45474

- Advanced automotive diesel assessment program  
[NASA-CR-168285] p 130 N85-13235

- Advanced Gas Turbine (AGT) powertrain system  
development for automotive applications p 185 N85-18831  
[NASA-CR-174809]

- Knock syndrome: Its cures and its victims p 93 N85-19185  
[NASA-CR-174395]

- Advanced Gas Turbine (AGT) technology project  
[NASA-CR-174798] p 31 N85-29961

**AUTOMOBILES**

- Advanced automotive diesel assessment program  
[NASA-CR-168285] p 130 N85-13235  
Knock syndrome: Its cures and its victims p 93 N85-19185  
[NASA-CR-174395]  
Feasibility demonstration of a novel, flat-belt,  
continuously variable transmission or automotive and  
electric-hybrid vehicle application p 185 N85-19894  
[NASA-CR-174430]

**AUXILIARY POWER SOURCES**

- Ion thruster system (8-cm) cyclic endurance test  
[NASA-CR-174745] p 47 N85-12937  
Regenerative fuel cell systems for space station  
p 104 N85-31372

**AUXILIARY PROPULSION**

- Ion thruster system (8-cm) cyclic endurance test  
[NASA-CR-174745] p 47 N85-12937

**AVALANCHE DIODES**

- The 30 GHz solid state amplifier for low cost low data  
rate ground terminals p 102 N85-12300  
[NASA-CR-174795]  
Sixty GHz IMPATT diode development p 105 N85-33293  
[NASA-CR-174969]

**AVERAGE**

- Model equation for simulating flows in multistage  
turbomachinery p 7 N85-12036  
[NASA-TM-86869]

**AXES OF ROTATION**

- Wake effects on the aerodynamic performance of  
horizontal axis wind turbines p 162 N85-29364  
[NASA-CR-174920]

**AXIAL FLOW**

- Rotor wake characteristics of a transonic axial flow  
fan p 6 A85-43974  
[AIAA PAPER 85-1133]

**AXIAL FLOW TURBINES**

- Predicted turbine stage performance using  
quasi-three-dimensional and boundary-layer analyses p 15 A85-34013

**AXIAL LOADS**

- Plasticity, viscoplasticity, and creep of solids by  
mechanical subelement models p 142 A85-35048

**AXIAL STRAIN**

- Results of an interlaboratory fatigue test program  
conducted on alloy 800H at room and elevated  
temperatures p 152 N85-32340  
[NASA-CR-174940]

**AXISYMMETRIC FLOW**

- Prediction of an axisymmetric combustor flow p 59 A85-12713  
Analytical modeling of circuit aerodynamics in the new  
NASA Lewis Altitude Wind Tunnel p 3 A85-26389  
[AIAA PAPER 85-0380]  
A three-dimensional axisymmetric calculation procedure  
for turbulent flows in a radial vaneless diffuser p 7 N85-14798  
[NASA-TM-86903]  
Analytical modeling of circuit aerodynamics in the new  
NASA Lewis wind tunnel p 8 N85-15688  
[NASA-TM-86912]

**B****BALANCING**

- Laser balancing system for high material removal  
rates p 126 N85-12341  
[NASA-CR-174731]  
Development of a multiplane multispeed balancing  
system for turbine systems p 35 N85-22400  
[NASA-CR-174750]

**BALL BEARINGS**

- Topological reaction rate measurements related to  
scuffing p 64 A85-11070  
First-order ball-bearing kinematics p 128 A85-31203

- Effect of two inner-ring oil-flow distribution schemes on  
the operating characteristics of a 35 millimeter bore ball  
bearing to 2.5 million DN p 130 N85-13233  
[NASA-TP-2404]

- Operating characteristics of a 0.87 kW-hr flywheel  
energy storage module p 133 N85-28371  
[NASA-TM-87038]

- Mechanics of a gaseous film barrier to lubricant wetting  
of elastohydrodynamically lubricated conjunctions p 135 N85-32330  
[NASA-TP-2500]

**BARRIER LAYERS**

- Advanced thermal barrier system bond coatings for use  
on Ni, Co-, and Fe-base alloy substrates p 77 N85-31283  
[NASA-TM-87062]

**BARS**

- Thermal-mechanical fatigue crack growth in Inconel  
X-750 p 72 N85-15877  
[NASA-CR-174740]  
NDE for heat engine ceramics p 137 N85-20389  
[NASA-TM-86949]

**BATCH PROCESSING**

- High-voltage solar-cell chip p 154 A85-24668

**BEADS**

- Spherical microglass particle impingement studies of  
thermoplastic materials at normal incidence p 79 A85-11072

**BEAMS (SUPPORTS)**

- Effects of warping and pretwist on torsional vibration  
of rotating beams p 140 A85-17040  
[ASME PAPER 84-WA/APM-41]

**BEARINGS**

- Characterization of lubricated bearing surfaces operated  
under high loads p 88 N85-21357  
[NASA-TM-86964]

- Reusable rocket engine turbopump condition  
monitoring p 51 N85-26907

- Fatigue life analysis of a turboprop reduction gearbox  
[NASA-TM-87014] p 133 N85-27228

**BENDING MOMENTS**

- Nonlinear flap-lag-extensional vibrations of rotating,  
pretwisted, precone beams including Coriolis effects p 152 N85-34427  
[NASA-TM-87102]

**BENZENE**

- Formation of high molecular weight products from  
benzene during boundary lubrication p 62 N85-22644  
[NASA-TM-86966]  
Fuel-rich catalytic combustion: A soot-free technique  
for in situ hydrogen-like enrichment p 63 N85-31244  
[NASA-TP-2498]

**BERYLLIUM**

- Fracture toughness of hot-pressed beryllium p 66 A85-25835

**BIAS**

- Circuit transients due to negative bias arcs on a  
high-voltage solar array in low Earth orbit p 39 N85-14858  
[NASA-TP-2407]

**BIBLIOGRAPHIES**

- Bibliography of Lewis Research Center technical  
publications announced in 1983 p 184 N85-22255  
[NASA-TM-83693]

**BINARY ALLOYS**

- Dendritic solidification. III - Some further refinements  
to the model for dendritic growth under an imposed thermal  
gradient p 69 A85-44703

**BINARY SYSTEMS (MATERIALS)**

- Ultrasonic wave propagation in two-phase media -  
Spherical inclusions p 54 A85-11926

**BINDING**

- Universal binding energy relations in metallic adhesion  
[NASA-TM-86889] p 72 N85-12132  
CO adsorption on (111) and (100) surfaces of the Pt  
sub 3 Ti alloy. Evidence for parallel binding and strong  
activation of CO p 77 N85-32176  
[NASA-CR-176077]

**BIPOLAR TRANSISTORS**

- Bipolar-FET combinational power transistors for power  
conversion applications p 100 A85-12669  
High voltage-high power components for large space  
power distribution systems p 45 A85-45370

**BIPOLARITY**

- Teardown analysis of a ten cell bipolar nickel-hydrogen  
battery p 156 A85-45385  
Advanced nickel-hydrogen cell configuration study p 157 N85-10444  
[NASA-CR-174775]  
Life cycle test results of a bipolar nickel hydrogen  
battery p 163 N85-30480  
[NASA-TM-87046]

**BIREFRINGENCE**

- Incident beam polarization for laser Doppler velocimetry  
employing a sapphire cylindrical window p 122 A85-39835

- Incident beam polarization for laser Doppler velocimetry  
employing a sapphire cylindrical window p 178 N85-28786  
[NASA-TM-87064]

**BIT ERROR RATE**

- Satellite baseband processor test performance  
summary p 95 A85-14434

**BITS**

- Floating-point function generation routines for 16-bit  
microcomputers p 170 N85-10683  
[NASA-TM-83783]

**BLADE TIPS**

- Metallurgical and mechanical phenomena due to rubbing  
of titanium against sintered powder Nichrome p 127 A85-22281

- An experimental investigation and numerical prediction  
of thermomechanical phenomena in high speed rotor tip  
rubbing p 14 A85-25442

- Observations from varying the lift and drag inputs to a  
noise prediction method for supersonic helical tip speed  
propellers p 175 N85-10788  
[NASA-TM-83797]

- Oxidizing seal for a turbine tip gas path p 136 N85-34402  
[NASA-CASE-LEW-14053-1]

**BLOWING**

- Analytical study of blowing boundary layer control for  
subsonic V-STOL inlets p 2 A85-11646

**BLUFF BODIES**

- The mechanisms of flame holding in the wake of a bluff  
body p 26 N85-21166  
[NASA-CR-3866]

**BOEING 747 AIRCRAFT**

- Simultaneous cabin and ambient ozone measurements  
on two Boeing 747 airplanes. Volume 3: October 1978  
- July 1979 p 167 N85-21872  
[NASA-TM-86883]

## BOLOMETERS

### BOLOMETERS

Infrared technology for satellite power conversion --- antenna arrays and bolometers  
[NASA-CR-174266] p 159 N85-16293

### BORHOLES

Experimental stiffness of tapered bore seals  
[NASA-TM-86978] p 132 N85-25847

### BORIDES

Surface hardening of steel by boriding in a cold rf plasma p 68 A85-40275

### BORON

Effects of cobalt, boron, and zirconium on the microstructure of Udimet 738  
[NASA-CR-174762] p 70 N85-10166

### BORON FIBERS

Fibers for structurally reliable metal and ceramic composites p 55 A85-37484

### BORON NITRIDES

Tribological properties of boron nitride synthesized by ion beam deposition  
[NASA-TM-86962] p 87 N85-21355

### BOTTLES

Ten year environmental test of glass fiber/epoxy pressure vessels  
[AIAA PAPER 85-1198] p 56 A85-47022  
Ten year environmental test of glass fiber/epoxy pressure vessels  
[NASA-TM-87058] p 58 N85-30034

### BOUNDARY LAYER CONTROL

Analytical study of blowing boundary layer control for subsonic V-STOL inlets p 2 A85-11646

### BOUNDARY LAYER EQUATIONS

A three-dimensional boundary-layer analysis including heat-transfer and blade-rotation effects p 6 A85-42988

### BOUNDARY LAYER FLOW

A note on blade wake interaction influence on compressor stator row aerodynamic performance p 4 A85-32965

Design and wind tunnel evaluation of a symmetric airfoil series for large wind turbine applications  
[NASA-CR-174764] p 7 N85-10919

### BOUNDARY LAYER SEPARATION

Low-speed aerodynamic test of an axisymmetric supersonic inlet with variable cowl slot  
[AIAA PAPER 85-1210] p 5 A85-40819  
Low-speed aerodynamic test of an axisymmetric supersonic inlet with variable cowl slot  
[NASA-TM-87039] p 28 N85-26710

### BOUNDARY LAYER TRANSITION

A review and analysis of boundary layer transition data for turbine application  
[NASA-TM-86880] p 113 N85-10306  
Transition in Turbines  
[NASA-CP-2386] p 118 N85-31433  
Flat-plate transition p 118 N85-31438  
Heat transfer and fluid mechanics measurements in transitional boundary layer flows p 118 N85-31439  
A review and analysis of boundary layer transition data for turbine application p 118 N85-31440

### BOUNDARY LAYERS

Free-surface phenomena under low- and zero-gravity conditions  
[NASA-CR-175885] p 36 N85-27922  
Unsteady flow in a supersonic cascade with two in-passage shocks  
[NASA-CR-3925] p 10 N85-35158

### BOUNDARY LUBRICATION

Hydrodynamic lubrication of rigid nonconformal contacts in combined rolling and normal motion  
[ASME PAPER 84-TRIB-13] p 127 A85-21280  
The influence of temperature on the lubricating effectiveness of MoS<sub>2</sub> dispersed in mineral oils  
[ASLE PREPRINT 84-LC-2A-2] p 80 A85-25963  
Thermal elastohydrodynamic lubrication of line contacts p 128 A85-31202  
Formation of high molecular weight products from benzene during boundary lubrication  
[NASA-TM-86966] p 62 N85-22644

### BOUNDARY VALUE PROBLEMS

Recent advances in methods for numerical solution of O.D.E. initial value problems p 171 A85-21370  
A procedure for obtaining explicit solutions to a class of Fredholm integral equations p 171 A85-28006  
Constructive existence and uniqueness for two-point boundary-value problems with a linear gradient term p 172 A85-28015  
Analysis of three-dimensional solidification interface shape p 109 A85-30075  
Solidification interface shape for continuous casting in an offset mold - Two analytical methods p 112 A85-41326  
A convergent series expansion for hyperbolic systems of conservation laws  
[NASA-CR-172557] p 168 N85-21990

### BRANCHING (MATHEMATICS)

Nonlinear global stability analysis of compressor stall phenomena  
[NASA-CR-174908] p 31 N85-29960

### BRANCHING (PHYSICS)

Circular waveguide bifurcation for asymmetric modes p 101 A85-20170

### BRAYTON CYCLE

Dynamic power systems for power generation p 158 N85-13892

Comparative evaluation of three alternative power cycles for waste heat recovery from the exhaust of adiabatic diesel engines  
[NASA-TM-86953] p 186 N85-32043

### BRAZING

Dispersed metal-toughened ceramics and ceramic brazing  
[NASA-CR-174284] p 86 N85-15916  
Design of low loss helix circuits for interference fitted and brazed circuits  
[NASA-CR-168313] p 103 N85-19328

### BREADBOARD MODELS

Design and analysis report for the RL10-2B breadboard low thrust engine  
[NASA-CR-174857] p 48 N85-19020

### BREATHING APPARATUS

Ten year environmental test of glass fiber/epoxy pressure vessels  
[AIAA PAPER 85-1198] p 56 A85-47022  
Ten year environmental test of glass fiber/epoxy pressure vessels  
[NASA-TM-87058] p 58 N85-30034

### BROADCASTING

Technical characteristics of the broadcasting satellite plan at 12 GHz for the Western Hemisphere p 96 A85-28233

Development and use of the computer software package for planning the 12 GHz broadcasting-satellite service at RARC '83 p 96 A85-29605

Experimental results supporting the determination of service quality objectives for DBS systems p 96 A85-29611

Alternatives for satellite sound broadcast systems at HF and VHF p 99 N85-23815

### BROMIDES

Graphite fiber intercalation: Dynamics of the bromine intercalation process  
[NASA-TM-87015] p 53 N85-26921

### BROMINE

Stability of bromine intercalated graphite fibers  
[NASA-TM-86859] p 84 N85-10187  
Homogeneity of pristine and bromine intercalated graphite fibers  
[NASA-TM-87016] p 89 N85-25521  
Environmental stability of intercalated graphite fibers  
[NASA-TM-87025] p 90 N85-26992  
A micrographic and gravimetric study of intercalation and deintercalation of graphite fibers  
[NASA-TM-87026] p 91 N85-28110

### BUOYANCY

Analysis of buoyancy effect on fully developed laminar heat transfer in a rotating tube p 110 A85-35596

### BURNERS

Ribbon burner simulation of T-700 turbine shroud for ceramic lined seals research  
[NASA-TM-86940] p 114 N85-19364  
Digital temperature and velocity control of mach 0.3 atmospheric pressure durability testing burner rigs in long time, unattended cyclic testing  
[NASA-TM-86959] p 75 N85-21321

### BUTT JOINTS

Diffusion welding of MA 6000 and a conventional nickel-base superalloy p 69 A85-43551

### BYPASS RATIO

Effect of combined pressure and temperature distortion orientation on high-bypass-ratio turbofan engine stability  
[NASA-TM-83771] p 17 N85-10067  
Effect of steady-state temperature distortion on inlet flow to a high-bypass-ratio turbofan engine  
[NASA-TM-86896] p 24 N85-15725  
Energy efficient engine. Fan and quarter-stage component performance report  
[NASA-CR-168070] p 33 N85-34141  
Energy Efficient Engine Program technology benefit/cost study, volume 1  
[NASA-CR-174766-VOL-1] p 33 N85-35197  
Energy Efficient Engine Program technology benefit/cost study, volume 2  
[NASA-CR-174766-VOL-2] p 33 N85-35198

## C

## SUBJECT INDEX

### CABIN ATMOSPHERES

Simultaneous cabin and ambient ozone measurements on two Boeing 747 airplanes. Volume 3: October 1978 - July 1979  
[NASA-TM-86883] p 167 N85-21872

### CALIBRATING

Calibration stability of some hot-cathode ion gauges p 122 A85-41634  
Heat flux sensor calibrator p 41 N85-27970

### CALORIMETERS

Applications of high pressure differential scanning calorimetry to aviation fuel thermal stability research  
[NASA-TM-87002] p 63 N85-23941

### CAMERA SHUTTERS

Initial feasibility ground test of a proposed photogrammetric system for measuring the shapes of ice accretions on helicopter rotor blades during forward flight  
[NASA-TM-87391] p 12 N85-12887

### CANS

Flame radiation and linear heat transfer in a tubular-can combustor p 15 A85-39580

### CANTILEVER BEAMS

Finite difference analysis of torsional vibrations of pretwisted, rotating, cantilever beams with effects of warping p 143 A85-42047  
Nonlinear flap-lag-extensional vibrations of rotating, pretwisted, precone beams including Coriolis effects  
[NASA-TM-87102] p 152 N85-34427

### CANTILEVER PLATES

Vibrations of twisted cantilevered plates - Summary of previous and current studies p 140 A85-22069  
Vibrations of twisted cantilever plates - A comparison of theoretical results p 144 A85-47626

### CAPACITANCE

Characteristics of arc currents on a negatively biased solar cell array in a plasma p 154 A85-18608  
Sixty GHz IMPATT diode development  
[NASA-CR-174969] p 105 N85-33293

### CAPACITORS

High voltage-high power components for large space power distribution systems p 45 A85-45370

### CAPILLARY FLOW

Generation of capillary instabilities by external disturbances in a liquid jet  
[NASA-TM-87041] p 117 N85-30246

### CARBIDES

The effect of tantalum on the structure/properties of two polycrystalline nickel-base superalloys: B-1900 + Hf MAR-M247  
[NASA-CR-174847] p 73 N85-18127

### CARBON

Dielectric properties of 'diamondlike' carbon prepared by RF plasma deposition p 182 A85-38192  
'Diamondlike' carbon films - Optical absorption, dielectric properties, and hardness dependence on deposition parameters p 82 A85-40383  
Plasma deposited hydrogenated carbon on GaAs and InP p 182 A85-40386  
Plasma deposited diamondlike carbon on GaAs and InP  
[NASA-TM-86870] p 183 N85-10844  
The effect of tantalum and carbon on the structure/properties of a single crystal nickel-base superalloy  
[NASA-CR-174779] p 71 N85-11223  
Deposition of diamondlike carbon films  
[NASA-CASE-LEW-14080-1] p 95 N85-20153  
Apparatus for producing diamond-like carbon flakes  
[NASA-CASE-LEW-13837-3] p 95 N85-20155  
Textured carbon surfaces on copper  
[NASA-CASE-LEW-14130-1] p 95 N85-20156  
Optical properties of hydrogenated amorphous carbon films grown from methane plasma  
[NASA-TM-86995] p 183 N85-26406  
Mechanical protection of DLC films on fused silica slides  
[NASA-TM-87056] p 91 N85-30138  
Diamondlike carbon protective coatings for IR materials  
[NASA-TM-87083] p 178 N85-34631

### CARBON ARCS

Diamondlike flakes  
[NASA-CASE-LEW-13837-2] p 57 N85-21267

### CARBON COMPOUNDS

Gas cooled fuel cell systems technology development  
[NASA-CR-174732] p 158 N85-16291

### CARBON DIOXIDE LASERS

Technology for satellite power conversion  
[NASA-CR-174335] p 159 N85-18451

### CARBON FIBERS

Environmental effects on the tensile strength of chemically vapor deposited silicon carbide fibers  
[NASA-TM-86981] p 89 N85-24000

- Graphite fiber intercalation: Dynamics of the bromine intercalation process  
[NASA-TM-87015] p 53 N85-26921
- Environmental stability of intercalated graphite fibers [NASA-TM-87025] p 90 N85-26992
- CARBON MONOXIDE**
- Shock tube measurements of growth constants in the branched-chain ethane-carbon monoxide-oxygen system [NASA-TM-87068] p 64 N85-32156
- Why CO bonds side-on at low coverage and both side-on and upright at high coverage on the Cr(110) surface [NASA-CR-176071] p 77 N85-32173
- CO adsorption on (111) and (100) surfaces of the Pt sub 3 Ti alloy. Evidence for parallel binding and strong activation of CO [NASA-CR-176077] p 77 N85-32176
- CARBON STEELS**
- Powder metallurgy forged gear development [NASA-TM-87483] p 134 N85-29295
- CARBOXYLIC ACIDS**
- Alkaline battery containing a separator of a cross-linked copolymer of vinyl alcohol and unsaturated carboxylic acid [NASA-CASE-LEW-13102-1] p 104 N85-29144
- CARRIER DENSITY (SOLID STATE)**
- Heat treatment of bulk gallium arsenide using a phosphosilicate glass cap p 181 A85-32636
- CARRIER TO NOISE RATIOS**
- On the subjective evaluation of the interference protection ratios' measurements for co-channel FM-TV signals p 96 A85-28241
- CASCADE FLOW**
- Computation of internal flows: Methods and applications; Proceedings of the Energy Sources Technology Conference, New Orleans, LA, February 12-16, 1984 p 106 A85-11630
- Computation of viscous flows in turbomachinery cascades p 106 A85-11631
- Two-dimensional internal compressible viscous flows using semi-elliptical analysis p 106 A85-11640
- Flutter of turbfan rotors with mistuned blades p 139 A85-12716
- A linearized unsteady aerodynamic analysis for transonic cascades p 3 A85-20744
- Design and performance of a fixed, nonaccelerating guide vane cascade that operates over an inlet flow angle range of 60 deg [ASME PAPER 84-GT-75] p 4 A85-32964
- Application of Runge Kutta time marching scheme for the computation of transonic flows in turbomachines [AIAA PAPER 85-1332] p 5 A85-39728
- Time dependent computation of the Euler equations for designing 2-D cascades, including the case of transonic shock free design p 5 A85-41814
- Optimization of cascade blade mistuning. II - Global optimum and numerical optimization p 16 A85-45715
- Inviscid and viscous flows in cascades with an explicit multiple-grid algorithm p 7 A85-48539
- Inverse design technique for cascades [NASA-CR-3836] p 7 N85-12008
- Incompressible lifting-surface aerodynamics for a rotor-stator combination [NASA-TM-83767] p 7 N85-12039
- Unsteady pressure measurements on a biconvex airfoil in a transonic oscillating cascade [NASA-TM-86914] p 8 N85-15689
- Unsteady flow in a supersonic cascade with two in-passage shocks [NASA-CR-3925] p 10 N85-35158
- CASCADE WIND TUNNELS**
- Inverse design technique for cascades [NASA-CR-3836] p 7 N85-12008
- CASSEGRAIN ANTENNAS**
- Configuration study for a 30 GHz monolithic receive array: Technical assessment p 98 N85-18238
- Configuration study for a 30 GHz monolithic receive array, volume 1 [NASA-CR-174697-VOL-1] p 98 N85-18239
- CASTING**
- Control of solidification boundary in continuous casting by asymmetric cooling and mold offset p 110 A85-37047
- Solidification interface shape for continuous casting in an offset mold - Two analytical methods p 112 A85-41326
- The effect of tantalum on the structure/properties of two polycrystalline nickel-base superalloys: B-1900 + Hf MAR-M247 [NASA-CR-174847] p 73 N85-18127
- Tape casting as an approach to an all-ceramic turbine shroud seal [NASA-TM-87078] p 135 N85-32333
- CATALYSIS**
- Fuel-rich catalytic combustion: A soot-free technique for in situ hydrogen-like enrichment [NASA-TP-2498] p 63 N85-31244
- CATALYSTS**
- Imide modified epoxy matrix resins [NASA-CR-174695] p 85 N85-15892
- Electric utility acid fuel cell stack technology advancement [NASA-CR-174804] p 159 N85-17422
- Solids mixing in a three phase fluidized bed containing spherically shaped-porous solid particles [PB85-187961] p 120 N85-33453
- CATALYTIC ACTIVITY**
- The role of surface generated radicals in catalytic combustion p 30 N85-27869
- Fuel rich catalytic combustion: The first stage of a two-stage combustor [NASA-TM-87042] p 63 N85-28983
- CATASTROPHE THEORY**
- Nonlinear global stability analysis of compressor stall phenomena [NASA-CR-174908] p 31 N85-29960
- CATHODES**
- Cathode degradation and erosion in high pressure arc discharges p 43 A85-16445
- Electric utility acid fuel cell stack technology advancement [NASA-CR-174804] p 159 N85-17422
- Apparatus for mounting a field emission cathode [NASA-CASE-LEW-14108-1] p 104 N85-29149
- Electrode erosion in arc discharges at atmospheric pressure [NASA-TM-87087] p 52 N85-34178
- CATHODIC COATINGS**
- Cathode degradation and erosion in high pressure arc discharges p 43 A85-16445
- CATS**
- Percutaneous connectors [NASA-CR-175627] p 168 N85-27508
- CAVITATION CORROSION**
- Cavitation erosion size scale effects p 65 A85-11935
- Deformation and erosion of f.c.c. metals and alloys under cavitation attack p 65 A85-12789
- A unified relation for cavitation erosion p 109 A85-24445
- Characterization of erosion of metallic materials under cavitation attack in a mineral oil [NASA-TM-86934] p 74 N85-19075
- CELL ANODES**
- Moderate temperature sodium cells. V - Discharge reactions and rechargeability of NiS and NiS<sub>2</sub> positive electrodes in molten NaAlCl<sub>4</sub> p 59 A85-11892
- CENTAUR LAUNCH VEHICLE**
- A high energy stage for the National Space Transportation System [IAF PAPER 84-15] p 36 A85-23200
- Shuttle/Centaur project perspective p 37 N85-16991
- Linearization of digital derived rate algorithm for use in linear stability analysis [NASA-TM-87000] p 41 N85-23904
- CENTRIFUGAL COMPRESSORS**
- Internal hysteresis experienced on a high pressure syn gas compressor p 131 N85-14122
- CENTRIFUGAL PUMPS**
- Small centrifugal pumps for low thrust rockets [AIAA PAPER 85-1302] p 45 A85-43978
- CERAMIC COATINGS**
- Oxidation-based model for thermal barrier coating life p 78 A85-10310
- Performance of thermal barrier coatings in high heat flux environments p 79 A85-19087
- A morphological study of silicon carbide prepared by chemical vapor deposition p 79 A85-20938
- Plastic flow of plasma sprayed ceramics p 80 A85-24161
- Life modeling of atmospheric and low pressure plasma-sprayed thermal-barrier coating p 81 A85-29728
- Mechanical property measurements of plasma-sprayed thermal-barrier coatings subjected to oxidation p 81 A85-29729
- Deposition of silicon nitride from SiCl<sub>4</sub> and NH<sub>3</sub> in a low pressure RF plasma p 81 A85-36229
- Failure during thermal cycling of plasma-sprayed thermal barrier coatings p 81 A85-36246
- An investigation of enhanced capability thermal barrier coating systems for diesel engine components [NASA-CR-174820] p 86 N85-18154
- Thermal barrier coating system [NASA-CASE-LEW-13324-2] p 57 N85-21266
- Tribological properties of boron nitride synthesized by ion beam deposition [NASA-TM-86962] p 87 N85-21355
- Metallic and metal/ceramic coating by thermal decomposition [NASA-TM-86992] p 88 N85-22755
- Rocket thrust chamber thermal barrier coatings p 90 N85-26867
- CERAMIC MATRIX COMPOSITES**
- High temperature metal and ceramic composites p 55 A85-37483
- Fibers for structurally reliable metal and ceramic composites p 55 A85-37484
- Factors influencing the ball milling of Si<sub>3</sub>N<sub>4</sub> in water [NASA-TM-86932] p 86 N85-19136
- Film and interstitial formation of metals in plasma-sprayed ceramics [NASA-TM-86993] p 89 N85-22756
- CERAMICS**
- Ceramic component development for the AGT101 gas turbine engine p 126 A85-15972
- Ceramic components for gas turbine engines p 127 A85-15973
- Deposition stress effects on the life of thermal barrier coatings on burner rigs p 79 A85-19086
- Friction and wear of ceramics p 80 A85-23833
- Feasibility study of the welding of SiC p 81 A85-39339
- Ceramic wear in indentation and sliding contact p 82 A85-39549
- Ceramic microstructure and adhesion p 82 A85-40384
- Photoacoustic microscopy of ceramic turbine blades p 83 A85-43930
- Ceramic microstructure and adhesion [NASA-TM-83804] p 83 N85-10186
- Milling of Si<sub>3</sub>N<sub>4</sub> with Si<sub>3</sub>N<sub>4</sub> hardware [NASA-TM-86864] p 84 N85-10191
- Surface protection overview p 21 N85-10978
- Energy efficient engine high pressure turbine ceramic shroud support technology report [NASA-CR-168036] p 23 N85-10996
- High performance fibers for structurally reliable metal and ceramic composites --- advanced gas turbine engine materials [NASA-TM-86878] p 56 N85-12095
- Fundamental tribological properties of ceramics [NASA-TM-86915] p 85 N85-15893
- Dispersed metal-toughened ceramics and ceramic brazing [NASA-CR-174284] p 86 N85-15916
- Transformation toughened ceramics for the heavy duty diesel engine technology program [NASA-CR-174689] p 185 N85-16698
- Experimental and analytical study of ceramic-coated turbine-tip shroud seals for small turbine engines [NASA-TM-86881] p 25 N85-18057
- Advanced Gas Turbine (AGT) powertrain system development for automotive applications [NASA-CR-174809] p 185 N85-18831
- Experimental study of ceramic coated tip seals for turbojet engines [NASA-TM-86939] p 114 N85-19363
- Ribbon burner simulation of T-700 turbine shroud for ceramic lined seals research [NASA-TM-86940] p 114 N85-19364
- NDE for heat engine ceramics [NASA-TM-86949] p 137 N85-20389
- Oxidation and hot corrosion of hot-pressed Si<sub>3</sub>N<sub>4</sub> at 1000 deg C [NASA-TM-86977] p 88 N85-21358
- Fabrication of ceramic substrate-reinforced and free forms [NASA-TM-86994] p 50 N85-23926
- Effects of wear on structure-sensitive magnetic properties of ceramic ferrite in contact with magnetic tape [NASA-TM-87007] p 90 N85-26991
- Breakaway friction and dynamic friction/wear measurements of various ceramic materials from 25 C (75 F) to 650 C (1200 F) [NASA-CR-174803] p 90 N85-26994
- Preparation of silicon carbide-silicon nitride fibers by the pyrolysis of polycarbosilazane precursors [NASA-TM-86505] p 91 N85-28107
- Ceramic applications in turbine engines [NASA-CR-174715] p 91 N85-28109
- Burner rig corrosion of SiC at 1000 deg C [NASA-TM-87061] p 53 N85-30011
- Tape casting as an approach to an all-ceramic turbine shroud seal [NASA-TM-87078] p 135 N85-32333
- Reliability of void detection in structural ceramics using scanning laser acoustic microscopy [NASA-TM-87035] p 138 N85-32337
- CH-47 HELICOPTER**
- Performance degradation of helicopter rotor in forward flight due to ice p 11 A85-42937

## CHANNEL FLOW

Computation of internal flows: Methods and applications; Proceedings of the Energy Sources Technology Conference, New Orleans, LA, February 12-16, 1984

p 106 A85-11630

Heat transfer enhancement in channels with turbulence promoters

[ASME PAPER 84-WA/HT-72] p 111 A85-39900

The effect of channel convergence on heat transfer in a passage with short pin fins

[NASA-TM-83801] p 113 N85-10303

A study of Reynolds-stress closure model

[NASA-CR-174342] p 114 N85-17324

## CHANNELS (DATA TRANSMISSION)

Multibus-based parallel processor for simulation

p 169 A85-28613

## CHARGED PARTICLES

Suprathermal plasma observed on STS-3 Mission by plasma diagnostics package

p 179 N85-22472

Discharges on a negatively biased solar cell array in a charged-particle environment

p 160 N85-22499

Spacecraft environmental interactions: A joint Air Force and NASA research and technology program

p 40 N85-22517

Multistage spent particle collector and a method for making same

[NASA-CASE-LEW-13914-1] p 135 N85-33489

## CHELATES

Mechanism for chelated sulfate formation from SO<sub>2</sub> and bis (triphenylphosphine) platinum

p 62 A85-48493

## CHEMICAL ATTACK

Study of Kapton under simulated shuttle environment

[NASA-CR-176003] p 41 N85-29997

Burner rig corrosion of SiC at 1000 deg C

[NASA-TM-87061] p 53 N85-30011

## CHEMICAL BONDS

Why CO bonds side-on at low coverage and both side-on and upright at high coverage on the Cr(110) surface

[NASA-CR-176071] p 77 N85-32173

## CHEMICAL CLOUDS

Effects of chemical releases by the STS 3 orbiter on the ionosphere

p 166 A85-29538

## CHEMICAL COMPOSITION

Milling of Si<sub>3</sub>N<sub>4</sub> with Si<sub>3</sub>N<sub>4</sub> hardware

[NASA-TM-86864] p 84 N85-10191

Optimization of the NiCrAl-Y/ZrO<sub>2</sub>-Y<sub>2</sub>O<sub>3</sub> thermal barrier system

[NASA-TM-86905] p 72 N85-15878

## CHEMICAL EQUILIBRIUM

Effect of water on hydrogen permeability --- Stirling engines

[NASA-TM-86904] p 53 N85-14864

Computer program for calculation of complex chemical equilibrium compositions and applications. Supplement 1: Transport properties

[NASA-TM-86885] p 184 N85-16663

Combustion gas properties. Part 3: Hydrogen gas fuel and dry air

[NASA-TP-2477] p 32 N85-31058

## CHEMICAL PROPULSION

Preliminary assessment of power-generating tethers in space and of propulsion for their orbit maintenance

p 37 N85-22520

Primary propulsion of electrothermal, ion and chemical systems for space-based radar orbit transfer

[NASA-TM-87043] p 51 N85-27972

## CHEMICAL REACTIONS

Reactions of NaCl with gaseous SO<sub>3</sub>, SO<sub>2</sub>, and O<sub>2</sub>

p 59 A85-11897

Direct numerical simulations of a reacting mixing layer with chemical heat release

[AIAA PAPER 85-0143] p 60 A85-19548

Direct simulations of chemically reacting turbulent mixing layers

[AIAA PAPER 85-0321] p 60 A85-19666

Chemical reactions involved in the initiation of hot corrosion of IN-738

p 66 A85-31688

Mechanism for forming hydrogen chloride and sodium sulfate from sulfur trioxide, water, and sodium chloride

p 62 A85-48513

The reactions of cobalt, iron and nickel in SO<sub>2</sub> atmospheres: Similarities and differences

[NASA-TM-86868] p 70 N85-11217

Integrating chemical kinetic rate equations by selective use of stiff and nonstiff methods

[NASA-TM-86923] p 24 N85-15726

Imide modified epoxy matrix resins

[NASA-CR-174695] p 85 N85-15892

Chemical approach for controlling nadimide cure temperature and rate

[NASA-CASE-LEW-13770-5] p 87 N85-21352

Shock tube study of the fuel structure effects on the chemical kinetic mechanisms responsible for soot formation, part 2

[NASA-CR-174880] p 63 N85-25444

## CHEMICAL TESTS

Chemical approach for controlling nadimide cure temperature and rate

[NASA-CASE-LEW-13770-6] p 63 N85-30039

## CHEMISORPTION

Why CO bonds side-on at low coverage and both side-on and upright at high coverage on the Cr(110) surface

[NASA-CR-176071] p 77 N85-32173

## CHIPS (ELECTRONICS)

High-voltage solar-cell chip

p 154 A85-24668

## CHLORIDES

Dynamics of graphite fiber intercalation: In situ resistivity measurements with a four point probe

[NASA-TM-86858] p 53 N85-10105

## CHROMIUM

Optimization of the NiCrAl-Y/ZrO<sub>2</sub>-Y<sub>2</sub>O<sub>3</sub> thermal barrier system

[NASA-TM-86905] p 72 N85-15878

Effects of chromium and aluminum on mechanical and oxidation properties of iron-nickel-base superalloys based on CG-27

[NASA-TP-2443] p 75 N85-21323

Dispersed-metal-toughened alumina

[NASA-CR-174687] p 89 N85-22758

Why CO bonds side-on at low coverage and both side-on and upright at high coverage on the Cr(110) surface

[NASA-CR-176071] p 77 N85-32173

Development of electrodes for the NASA iron/chromium

[NASA-CR-174724] p 165 N85-35471

## CHROMIUM ALLOYS

Orientation and temperature dependence of some mechanical properties of the single-crystal nickel-base superalloy Rene N4. 3: Tension-compression anisotropy

[NASA-TM-86982] p 76 N85-22660

Study of the effects of implantation on the high Fe-Ni-Cr and Ni-Cr-Al alloys

[NASA-CR-175625] p 76 N85-22661

## CHROMIUM CARBIDES

Effects of silver and group 2 fluorides addition to plasma sprayed chromium carbide high temperature solid lubricant for foil gas bearing to 650 deg C

[NASA-TM-86895] p 84 N85-14928

## CHROMIUM COMPOUNDS

Chemical and electrochemical behavior of the Cr(III)/Cr(II) half-cell in the iron-chromium redox energy storage system

p 61 A85-33785

## CHROMIUM STEELS

Frictional and structural characterization of ion-nitrided low and high chromium steels

[NASA-TM-86991] p 132 N85-23085

## CIRCUIT BREAKERS

High-voltage, high-power, solid-state remote power controllers for aerospace applications

[NASA-TP-2437] p 49 N85-21263

## CIRCUIT PROTECTION

Circuit transients due to negative bias arcs on a high-voltage solar array in low Earth orbit

[NASA-TP-2407] p 39 N85-14858

## CIRCUITS

Design of low loss helix circuits for interference fitted and brazed circuits

[NASA-CR-168313] p 103 N85-19328

## CIRCULAR CYLINDERS

Heat transfer investigation in the junction region of circular cylinder normal to a flat plate at 90 deg location

[ASME PAPER 84-WA/HT-70] p 111 A85-39898

The influence of jet-grid turbulence on heat transfer from the stagnation region of a cylinder in crossflow

[NASA-TM-87011] p 115 N85-25760

## CIRCULAR PLATES

Vibration and flutter of mistuned bladed-disk assemblies

[AIAA PAPER 84-0991] p 139 A85-16095

Vibration and flutter of mistuned bladed-disk assemblies

p 16 A85-45854

## CIRCULAR WAVEGUIDES

Circular waveguide bifurcation for asymmetric modes

p 101 A85-20170

Plot of modal field distribution in rectangular and circular waveguides

p 101 A85-25170

## CIVIL AVIATION

Energy efficient engine. Volume 2. Appendix A: Component development and integration program

[NASA-CR-173085] p 22 N85-10991

## CLADDING

Manufacturing process to reduce large grain growth in zirconium alloys

[DE85-011649] p 78 N85-34267

## CLEAN ENERGY

Measured effects of wind turbine generation at the Block Island Power Company

p 153 A85-10652

## CLEARANCES

Dual clearance squeeze film damper for high load conditions

[ASME PAPER 84-TRIB-7] p 128 A85-32960

## CLIMATOLOGY

Variability of cloudiness at airline cruise altitudes from GASP measurements

p 166 A85-31199

## CLIMBING FLIGHT

Wind tunnel results of advanced high speed propellers in the takeoff, climb, and landing operating regimes

[AIAA PAPER 85-1259] p 6 A85-47025

Wind tunnel results of advanced high speed propellers in the takeoff, climb and landing operating regimes

[NASA-TM-87054] p 9 N85-29925

## CLOSE PACKED LATTICES

Effect of hot isostatic pressing on the properties of sintered alpha silicon carbide

p 83 A85-48757

## CLOSED CYCLES

Advanced technology cogeneration system conceptual design study: Closed cycle gas turbines

[NASA-CR-168222] p 159 N85-16300

## CLOSURE LAW

A study of Reynolds-stress closure model

[NASA-CR-174342] p 114 N85-17324

## CLOUD COVER

Variability of cloudiness at airline cruise altitudes from GASP measurements

p 166 A85-31199

## CLOUDS (METEOROLOGY)

GASP cloud encounter statistics - Implications for laminar flow control flight

p 166 A85-11979

Comparison of icing cloud instruments for 1982-1983 icing season flight program

[AIAA PAPER 84-0020] p 13 A85-16098

## COASTAL ZONE COLOR SCANNER

Comparison of atmospheric correction algorithms for the Coastal Zone Color Scanner

p 153 A85-10244

## COATING

Textured carbon surfaces on copper

[NASA-CASE-LEW-14130-1] p 95 N85-20156

## COATINGS

RF-sputtered silicon and hafnium nitrides - Properties and adhesion to 440C stainless steel

p 81 A85-36240

Turbine Engine Hot Section Technology (HOST)

[NASA-TM-83022] p 18 N85-10951

Plasma variables and tribological properties of coatings in low pressure (0.1 - 10.0 torr) plasma systems

[NASA-TM-83798] p 94 N85-11261

Effect of water on hydrogen permeability --- Stirling engines

[NASA-TM-86904] p 53 N85-14864

Experimental test program for evaluation of solid lubricant coating as applied to compliant foil gas bearings to 315 deg C

[NASA-CR-174837] p 85 N85-15895

Diamondlike flakes

[NASA-CASE-LEW-13837-2] p 57 N85-21267

Numerical methods for analyzing electromagnetic scattering

[NASA-CR-175507] p 99 N85-21438

Advanced thin film thermocouples

[NASA-CR-175541] p 124 N85-21607

## COAXIAL CABLES

Dual-mode coaxial feed with low crosspolarisation

p 101 A85-20171

## COAXIAL FLOW

Mass and momentum turbulent transport experiments with confined coaxial jets

p 107 A85-14399

Turbulent transport and length scale measurement experiments with confined coaxial jets

[NASA-CR-174831] p 117 N85-30245

## COBALT

Effects of cobalt, boron, and zirconium on the microstructure of Udimet 738

[NASA-CR-174762] p 70 N85-10166

The reactions of cobalt, iron and nickel in SO<sub>2</sub> atmospheres: Similarities and differences

[NASA-TM-86868] p 70 N85-11217

The response of cobalt-free Udimet 700 type alloy to modified heat treatments

[NASA-TM-86942] p 75 N85-20043

## COBALT ALLOYS

Effects of cobalt on the hot workability of nickel-base superalloys

p 67 A85-32412

Quasi-static solution algorithms for kinematically/materially nonlinear thermomechanical problems

p 143 A85-41983

Creep-rupture behavior of iron superalloys in high-pressure hydrogen

[NASA-CR-174411] p 74 N85-19078

## COGENERATION

Advanced technology cogeneration system conceptual design study: Closed cycle gas turbines

[NASA-CR-168222] p 159 N85-16300

## COLLIMATION

Electronic heterodyne readout of fringes in moire deflectometry

p 122 A85-36726

**COLOR CODING**

An allpass filter design for luminance and chrominance separation of NTSC signals p 102 A85-28230

**COLOR PHOTOGRAPHY**

Rainbow schlieren vs Mach-Zehnder interferometer - A comparison p 121 A85-28820

**COLOR TELEVISION**

An allpass filter design for luminance and chrominance separation of NTSC signals p 102 A85-28230  
Experimental results supporting the determination of service quality objectives for DBS systems p 96 A85-29611

**COMBINED STRESS**

On stress field near a stationary crack tip [AD-A152863] p 141 A85-24532

**COMBUSTIBLE FLOW**

Prediction of an axisymmetric combustor flow p 59 A85-12713  
Direct simulations of chemically reacting turbulent mixing layers [AIAA PAPER 85-0321] p 60 A85-19666  
Growth of a diffusion flame in the field of a vortex p 61 A85-47320  
Dilution zone mixing studies p 21 N85-10984  
The mechanisms of flame holding in the wake of a bluff body [NASA-CR-3866] p 26 N85-21166  
Investigation of flowfields found in typical combustor geometries [NASA-CR-3869] p 26 N85-21167  
Error reduction program --- combustor performance evaluation codes [NASA-CR-174776] p 172 N85-27584

**COMBUSTION**

Integrating chemical kinetic rate equations by selective use of stiff and nonstiff methods [AIAA PAPER 85-0237] p 60 A85-19607  
CREKID: A computer code for transient, gas-phase combustion of kinetics [NASA-TM-83806] p 17 N85-10068  
Turbine Engine Hot Section Technology (HOST) [NASA-TM-83022] p 18 N85-10951  
New integration techniques for chemical kinetic rate equations. 2: Accuracy comparison [NASA-TM-86893] p 23 N85-13798  
Integrating chemical kinetic rate equations by selective use of stiff and nonstiff methods [NASA-TM-86923] p 24 N85-15726  
The structure of dilute combustor sprays [NASA-CR-174838] p 24 N85-15728  
Combustion gas properties. 2: Natural gas fuel and dry air [NASA-TP-2435] p 26 N85-21168  
Fuel rich catalytic combustion: The first stage of a two-stage combustor [NASA-TM-87042] p 63 N85-28983  
Combustion gas properties. Part 3: Hydrogen gas fuel and dry air [NASA-TP-2477] p 32 N85-31058

**COMBUSTION CHAMBERS**

The influence of combustion liner holes on noise production by ducted burners [AIAA PAPER 84-2322] p 172 A85-10869  
Analysis of the effect on combustor noise measurements of acoustic waves reflected by the turbine and combustor inlet [AIAA PAPER 84-2323] p 173 A85-16103  
Calculation of confined swirling flows [AIAA PAPER 85-0060] p 108 A85-19491  
Flame flashback in a premixed dump combustor [AIAA PAPER 85-0145] p 60 A85-19550  
Swirling flows in typical combustor geometries [AIAA PAPER 85-0184] p 108 A85-19574  
Direct simulations of chemically reacting turbulent mixing layers [AIAA PAPER 85-0321] p 60 A85-19666  
Aerodynamic effect of combustor inlet air pressure on fuel jet atomization p 109 A85-27096  
Flame radiation and linear heat transfer in a tubular-can combustor p 15 A85-39580  
Turbulence measurements of lateral jet injection into confined tubular crossflow [AIAA PAPER 85-1102] p 110 A85-39604  
Experiments in dilution jet mixing - Effects of multiple rows and non-circular orifices [AIAA PAPER 85-1104] p 15 A85-39606  
Advanced liner-cooling techniques for gas turbine combustors [AIAA PAPER 85-1290] p 15 A85-39703  
Small gas turbine combustor study - Fuel injector performance in a transpiration-cooled liner [AIAA PAPER 85-1312] p 16 A85-39717  
Progress report - Advanced cryogenic OTV engine technology [AIAA PAPER 85-1341] p 44 A85-39735

Combustion efficiency of a premixed continuous flow combustor p 61 A85-42571  
Future fundamental combustion research for aeropropulsion systems [AIAA PAPER 85-1398] p 16 A85-42671  
Internal combustion engine combustion chamber process studies at NASA Lewis Research Center p 112 A85-45856  
Turbine Engine Hot Section Technology (HOST) [NASA-TM-83022] p 18 N85-10951  
Nonlinear structural and life analyses of a combustor liner p 19 N85-10955  
Effects of surface chemistry on hot corrosion life: Overview p 21 N85-10980  
Dilution zone mixing studies p 21 N85-10984  
Combustion system for radiation investigations p 21 N85-10986  
Validation of structural analysis methods using the in-house liner cyclic rigs p 21 N85-10987  
Energy efficient engine component development and integration program [NASA-CR-170034] p 22 N85-10990  
The structure of dilute combustor sprays [NASA-CR-174838] p 24 N85-15728  
Analytical fuel property effects: Small combustors, phase 2 [NASA-CR-174848] p 93 N85-19175  
Advanced liner-cooling techniques for gas turbine combustors [NASA-TM-86952] p 8 N85-21115  
Combustion research for gas turbine engines [NASA-TM-86963] p 26 N85-21164  
Investigation of flowfields found in typical combustor geometries [NASA-CR-3869] p 26 N85-21167  
Deflected jet experiments in a turbulent combustor flowfield [NASA-CR-174863] p 26 N85-22390  
Dilution jet configurations in a reverse flow combustor [NASA-CR-174888] p 27 N85-22392  
Small gas turbine combustor study: Fuel injector performance in a transpiration-cooled liner [NASA-TM-86989] p 27 N85-25264  
Experiments in dilution jet mixing effects of multiple rows and non-circular orifices [NASA-TM-86996] p 28 N85-25266  
Analytical fuel property effects-small combustors [NASA-CR-174738] p 28 N85-26709  
Turbulence characteristics of swirling flowfields [NASA-CR-174918] p 29 N85-26717  
Rocket thrust chamber thermal barrier coatings p 90 N85-26867  
Error reduction program --- combustor performance evaluation codes [NASA-CR-174776] p 172 N85-27584  
Predictions and measurements of isothermal flowfields in axisymmetric combustor geometries [NASA-CR-174916] p 29 N85-27867  
The role of surface generated radicals in catalytic combustion p 30 N85-27869  
Future fundamental combustion research for aeropropulsion systems [NASA-TM-87049] p 30 N85-27870  
Fuel rich catalytic combustion: The first stage of a two-stage combustor [NASA-TM-87042] p 63 N85-28983  
Combustor turbulence p 118 N85-31434  
Flow modifying device [NASA-CASE-LEW-13562-2] p 33 N85-35195  
Development of advanced high-temperature heat flux sensors. Phase 2: Verification testing [NASA-CR-174973] p 126 N85-35391

**COMBUSTION CHEMISTRY**

Comparison of numerical techniques for integration of stiff ordinary differential equations arising in combustion chemistry [NASA-TP-2372] p 17 N85-10065

**COMBUSTION CONTROL**

Energy efficient engine combustor test hardware detailed design report [NASA-CR-167945] p 18 N85-10950  
The mechanisms of flame holding in the wake of a bluff body [NASA-CR-174058] p 62 N85-11149

**COMBUSTION EFFICIENCY**

Flame flashback in a premixed dump combustor [AIAA PAPER 85-0145] p 60 A85-19550  
Aerodynamic effect of combustor inlet air pressure on fuel jet atomization p 109 A85-27096  
Combustion efficiency of a premixed continuous flow combustor p 61 A85-42571  
Comparison of numerical techniques for integration of stiff ordinary differential equations arising in combustion chemistry [NASA-TP-2372] p 17 N85-10065

An interactive computer code for calculation of gas-phase chemical equilibrium (EQLBRM) [NASA-CR-168337] p 18 N85-10948  
The mechanisms of flame holding in the wake of a bluff body [NASA-CR-174058] p 62 N85-11149  
Shock tube study of the fuel structure effects on the chemical kinetic mechanisms responsible for soot formation, part 2 [NASA-CR-174880] p 63 N85-25444  
The role of surface generated radicals in catalytic combustion p 30 N85-27869  
SSME fuel preburner two-dimensional analysis p 51 N85-27943

**COMBUSTION PHYSICS**

The mechanisms of flame holding in the wake of a bluff body [NASA-CR-174058] p 62 N85-11149  
A comparison of the efficiency of numerical methods for integrating chemical kinetic rate equations [NASA-TM-83590] p 25 N85-21162

**COMBUSTION PRODUCTS**

Polarization (ellipsometric) measurements of liquid condensate deposition and evaporation rates and dew points in flowing salt/ash-containing combustion gases p 123 A85-46925  
Combustion gas properties I-ASTM jet A fuel and dry air [NASA-TP-2359] p 17 N85-10064  
Combustion gas properties. 2: Natural gas fuel and dry air [NASA-TP-2435] p 26 N85-21168  
Digital temperature and velocity control of mach 0.3 atmospheric pressure durability testing burner rigs in long time, unattended cyclic testing [NASA-TM-86959] p 75 N85-21321  
Jet fuel instability mechanisms [NASA-CR-175856] p 93 N85-28127  
Fuel-rich catalytic combustion: A soot-free technique for in situ hydrogen-like enrichment [NASA-TP-2498] p 63 N85-31244

**COMBUSTION STABILITY**

A theoretical prediction of the acoustic pressure generated by turbulence-flame front interactions [ASME PAPER 84-WA/NCA-11] p 174 A85-39909  
Chemistry of fuel deposits and sediments and their precursors [NASA-CR-174778] p 92 N85-10209  
Combustor turbulence p 118 N85-31434

**COMMERCIAL AIRCRAFT**

Variability of cloudiness at airline cruise altitudes from GASP measurements p 166 A85-31199  
Energy efficient engine component development and integration program [NASA-CR-170034] p 22 N85-10990  
Study of advanced fuel system concepts for commercial aircraft and engines [NASA-CR-174752] p 93 N85-19176  
Study of advanced fuel system concepts for commercial aircraft [NASA-CR-174751] p 12 N85-19978

**COMMUNICATION SATELLITES**

Status of NASA's multibeam communications technology program p 100 A85-14432  
A 20 GHz, 75 watt, helix TWT for space communications p 101 A85-14433  
Satellite baseband processor test performance summary p 95 A85-14434  
The NASA satellite communication 20 x 20 matrix switches p 101 A85-14435  
Advanced 30/20 GHz multiple beam antenna for future communications satellites p 96 A85-14436  
Ion propulsion for communications satellites p 42 A85-16412  
Technical characteristics of the broadcasting satellite plan at 12 GHz for the Western Hemisphere p 96 A85-28233  
On the subjective evaluation of the interference protection ratios' measurements for co-channel FM-TV signals p 96 A85-28241  
Development and use of the computer software package for planning the 12 GHz broadcasting-satellite service at RARC '83 p 96 A85-29605  
Four-dimensional modulation and coding - An alternate to frequency-reuse p 97 A85-36653  
Modeling of NASA's 30/20 GHz satellite communications system p 38 A85-36683  
Demand for satellite-provided domestic communications services up to the year 2000 p 97 N85-15099  
Engineering calculations for communications satellite systems planning [NASA-CR-175552] p 37 N85-21233  
Alternatives for satellite sound broadcast systems at HF and VHF p 99 N85-23815



- Satellite provided customer promises services, a forecast of potential domestic demand through the year 2000. Volume 4: Sensitivity analysis [NASA-CR-174662] p 99 N85-27092  
Telecommunications forecast for ITU Region 2 to the year 1995 [NASA-TM-87077] p 38 N85-34150
- COMPARISON**  
Predicted turbine stage performance using quasi-three-dimensional and boundary-layer analyses p 15 A85-34013
- COMPENSATORS**  
A fast time domain digital simulation technique for power converters - Application to a buck converter with feedforward compensation p 101 A85-20900
- COMPONENT RELIABILITY**  
Creep-rupture reliability analysis p 143 A85-42566  
Engine cyclic durability by analysis and material testing p 25 N85-15744  
Component-specific modeling [NASA-CR-174765] p 147 N85-27261  
Composite loads spectra for select space propulsion structural components p 148 N85-27953  
High pressure compressor component performance report [NASA-CR-168245] p 33 N85-34138
- COMPOSITE MATERIALS**  
Advanced blade tip seal system, volume 2 [NASA-CR-167851] p 23 N85-10999  
Chemical approach for controlling nadimide cure temperature and rate with maleimide [NASA-CASE-LEW-13770-3] p 87 N85-21350  
Chemical approach for controlling nadimide cure temperature and rate with maleimide [NASA-CASE-LEW-13770-4] p 87 N85-21351  
A study of the stress wave factor technique for the characterization of composite materials [NASA-CR-174870] p 58 N85-30035
- COMPOSITE STRUCTURES**  
Design procedures for fiber composite structural components - Rods, beams, and beam columns p 54 A85-15636  
Fracture of composite-adhesive-composite systems p 141 A85-27935
- COMPOSITION (PROPERTY)**  
The effects of Cr, Co, Al, Mo and Ta on the cyclic oxidation behavior of a prototype cast Ni-base superalloy based on a 2(5) composite statistically designed experiment [NASA-TM-83784] p 71 N85-12131
- COMPOUNDING**  
Milling of Si3N4 with Si3N4 hardware [NASA-TM-86864] p 84 N85-10191
- COMPRESSED GAS**  
Internal hysteresis experienced on a high pressure syn gas compressor p 131 N85-14122
- COMPRESSIBLE FLOW**  
Acoustic pressures emanating from a turbomachine stage [AIAA PAPER 84-2325] p 2 A85-10870  
Two-dimensional internal compressible viscous flows using semi-elliptic analysis p 106 A85-11640  
Calculation of compressible flow about three-dimensional inlets with auxiliary inlets, slats and vanes by means of a panel method [AIAA PAPER 85-1196] p 5 A85-40817  
The three-dimensional compressible flow in a radial inflow turbine scroll p 6 A85-41826  
Rotordynamic coefficients for compressible flow in tapered annular seals p 129 A85-42573  
Application of computational fluid dynamics to complex inlet ducts [AIAA PAPER 85-1213] p 6 A85-47023  
Application of computational fluid dynamics to complex inlet ducts [NASA-TM-87060] p 118 N85-30247  
Calculation of compressible flow about three-dimensional inlets with auxiliary inlets, slats and vanes by means of a panel method [NASA-CR-174975] p 10 N85-35162
- COMPRESSION LOADS**  
Design procedures for fiber composite structural components - Rods, beams, and beam columns p 54 A85-15636  
Orientation and temperature dependence of some mechanical properties of the single-crystal nickel-base superalloy Rene N4. 3: Tension-compression anisotropy [NASA-TM-86982] p 76 N85-22660
- COMPRESSOR BLADES**  
Optimization of cascade blade mistuning. I - Equations of motion and basic inherent properties p 16 A85-42365  
Rotor wake characteristics of a transonic axial flow fan [AIAA PAPER 85-1133] p 6 A85-43974

- Optimization of cascade blade mistuning. II - Global optimum and numerical optimization p 16 A85-45715  
Unsteady flow in a supersonic cascade with two in-passage shocks [NASA-CR-3925] p 10 N85-35158
- COMPRESSOR ROTORS**  
Energy efficient engine component development and integration program [NASA-CR-170034] p 22 N85-10990
- COMPRESSORS**  
Energy efficient engine. High pressure compressor detail design report [NASA-CR-165558] p 23 N85-10998  
Nonlinear global stability analysis of compressor stall phenomena [NASA-CR-174908] p 31 N85-29960  
High pressure compressor component performance report [NASA-CR-168245] p 33 N85-34138
- COMPUTATION**  
Error reduction program --- combustor performance evaluation codes [NASA-CR-174776] p 172 N85-27584
- COMPUTATIONAL CHEMISTRY**  
Integrating chemical kinetic rate equations by selective use of stiff and nonstiff methods [NASA-TM-86923] p 24 N85-15726
- COMPUTATIONAL FLUID DYNAMICS**  
Computation of internal flows: Methods and applications; Proceedings of the Energy Sources Technology Conference, New Orleans, LA, February 12-16, 1984 p 106 A85-11630  
Computation of viscous flows in turbomachinery cascades p 106 A85-11631  
Two-dimensional internal compressible viscous flows using semi-elliptic analysis p 106 A85-11640  
Analytical study of blowing boundary layer control for subsonic V/STOL inlets p 2 A85-11646  
Development of finite analytic method for unsteady three-dimensional Navier-Stokes equation p 106 A85-11647  
Prediction of an axisymmetric combustor flow p 59 A85-12713  
Computation and turbulence closure models for shear flows in rotating curved bodies p 107 A85-14349  
Efficient solution of the Euler and Navier-Stokes equations with a vectorized multiple-grid algorithm p 2 A85-18679  
Finite difference methods for reducing numerical diffusion in TEACH-type calculations --- Teaching Elliptic Axisymmetric Characteristics Heuristically [AIAA PAPER 85-0057] p 108 A85-19488  
Calculation of confined swirling flows [AIAA PAPER 85-0060] p 108 A85-19491  
Computational thermo-fluid dynamics contributions to advanced gas turbine engine design [AIAA PAPER 85-0083] p 14 A85-19509  
Direct numerical simulations of a reacting mixing layer with chemical heat release [AIAA PAPER 85-0143] p 60 A85-19548  
A space-marching method for incompressible Navier-Stokes equations [AIAA PAPER 85-0170] p 108 A85-19564  
Swirling flows in typical combustor geometries [AIAA PAPER 85-0184] p 108 A85-19574  
Progress in development of a Navier-Stokes solver for evaluation of iced airfoil performance [AIAA PAPER 85-0410] p 3 A85-19731  
Assessment of discretization schemes to reduce numerical diffusion in the calculation of complex flows [AIAA PAPER 85-0441] p 108 A85-19751  
Computation of three-dimensional viscous flows using a space-marching method p 4 A85-29259  
Lubricant jet flow phenomena in spur and helical gears with modified center distances and/or addendums - For out-of-mesh conditions [ASME PAPER 84-DET-96] p 129 A85-35049  
Application of viscous and inviscid computation methods for rocket turbopump systems [SAE PAPER 841522] p 110 A85-39257  
Application of Runge Kutta time marching scheme for the computation of transonic flows in turbomachines [AIAA PAPER 85-1332] p 5 A85-39728  
Turbulence modelling for complex shear flows [AIAA PAPER 85-1652] p 111 A85-40752  
Calculation of compressible flow about three-dimensional inlets with auxiliary inlets, slats and vanes by means of a panel method [AIAA PAPER 85-1196] p 5 A85-40817  
Time dependent computation of the Euler equations for designing 2-D cascades, including the case of transonic shock free design p 5 A85-41814  
Future fundamental combustion research for aer propulsion systems [AIAA PAPER 85-1398] p 16 A85-42671

- The computation of viscous/inviscid interaction on airfoils with separated flow p 6 A85-42954  
A three-dimensional boundary-layer analysis including heat-transfer and blade-rotation effects p 6 A85-42988  
Inviscid analysis of advanced turboprop propeller flow fields [AIAA PAPER 85-1263] p 6 A85-43977  
Application of computational fluid dynamics to complex inlet ducts [AIAA PAPER 85-1213] p 6 A85-47023  
A multiple-scales model of the shock-cell structure of imperfectly expanded supersonic jets p 113 A85-49354  
Computational thermo-fluid dynamics contributions to advanced gas turbine engine design [NASA-TM-86865] p 18 N85-10069  
Inverse design technique for cascades [NASA-CR-3836] p 7 N85-12008  
Model equation for simulating flows in multistage turbomachinery [NASA-TM-86869] p 7 N85-12036  
Researched applied to transonic compressors in numerical fluid mechanics of inviscid flow and viscous flow [NASA-CR-174353] p 114 N85-18291  
NASA Lewis Research Center/University Graduate Research Program on Engine Structures [NASA-TM-86916] p 145 N85-18375  
Combustion research for gas turbine engines [NASA-TM-86963] p 26 N85-21164  
Future fundamental combustion research for aer propulsion systems [NASA-TM-87049] p 30 N85-27870  
Application of computational fluid dynamics to complex inlet ducts [NASA-TM-87060] p 118 N85-30247
- COMPUTATIONAL GRIDS**  
Rational approach for assumed stress finite elements p 139 A85-12029  
Efficient solution of the Euler and Navier-Stokes equations with a vectorized multiple-grid algorithm p 2 A85-18679  
Finite difference methods for reducing numerical diffusion in TEACH-type calculations --- Teaching Elliptic Axisymmetric Characteristics Heuristically [AIAA PAPER 85-0057] p 108 A85-19488  
Inviscid and viscous flows in cascades with an explicit multiple-grid algorithm p 7 A85-48539
- COMPUTER AIDED DESIGN**  
Interdisciplinary design analysis of a precision spacecraft antenna [AIAA PAPER 85-0804] p 38 A85-30303  
Finite element engine blade structural optimization [AIAA PAPER 85-0645] p 141 A85-30313  
A computer aided design procedure for generating gear teeth [ASME PAPER 84-DET-184] p 128 A85-33779  
Design considerations for a 10-kW integrated hydrogen-oxygen regenerative fuel cell system p 155 A85-45380  
Advanced secondary power system for transport aircraft [NASA-TP-2463] p 30 N85-28944  
Design and lubrication of high-speed rolling-element bearings [NASA-TM-87107] p 137 N85-34409
- COMPUTER GRAPHICS**  
A computer aided design procedure for generating gear teeth [ASME PAPER 84-DET-184] p 128 A85-33779
- COMPUTER NETWORKS**  
Optical computer switching network p 178 A85-23134  
Data flow methods for dynamic system simulation - A CSSL-IV microcomputer network interface p 170 A85-28614
- COMPUTER PROGRAMS**  
Progress toward the development of an aircraft icing analysis capability [AIAA PAPER 84-0105] p 10 A85-10653  
ICAN - Integrated composites analyzer [AIAA PAPER 84-0974] p 54 A85-16094  
Analytical determination of propeller performance degradation due to ice accretion [AIAA PAPER 85-0339] p 14 A85-20867  
A simplified method for elastic-plastic-creep structural analysis [ASME PAPER 84-GT-191] p 141 A85-23150  
Assessment of three-dimensional inviscid codes and loss calculations for turbine aerodynamic computations [ASME PAPER 84-GT-187] p 4 A85-32961  
Design and performance of a fixed, nonaccelerating guide vane cascade that operates over an inlet flow angle range of 60 deg [ASME PAPER 84-GT-75] p 4 A85-32964



Predicted turbine stage performance using quasi-three-dimensional and boundary-layer analyses p 15 A85-34013

A study of interply layer effects on the free edge stress field of angle-ply laminates p 55 A85-41127

A generalized computer code for developing dynamic gas turbine engine models (DIGTEM) p 17 A85-49021

CREKID: A computer code for transient, gas-phase combustion of kinetics p 17 N85-10068

[NASA-TM-83806] Manual of phosphoric acid fuel cell stack three-dimensional model and computer program [NASA-CR-174722] p 157 N85-10447

Floating-point function generation routines for 16-bit microcomputers [NASA-TM-83783] p 170 N85-10683

An interactive computer code for calculation of gas-phase chemical equilibrium (EQLBRM) [NASA-CR-168337] p 18 N85-10948

Phosphoric acid fuel cell power plant system performance model and computer program [NASA-CR-174638] p 157 N85-11456

Turbofan noise generation. Volume 2: Computer programs [NASA-CR-167952] p 175 N85-11791

Development of gas-lubricated pistons for heavy duty diesel engine technology program [NASA-CR-174746] p 184 N85-12808

Integrating chemical kinetic rate equations by selective use of stiff and nonstiff methods [NASA-TM-86923] p 24 N85-15726

A study of interply layer effects on the free-edge stress field of angle-ply laminates [NASA-TM-86924] p 57 N85-15822

Computer program for calculation of complex chemical equilibrium compositions and applications. Supplement 1: Transport properties [NASA-TM-86885] p 184 N85-16663

Modeling the internal combustion engine [NASA-RP-1094] p 172 N85-19733

3-D inelastic analysis methods for hot section components (base program) --- turbine blades, turbine vanes, and combustor liners [NASA-CR-174700] p 145 N85-21686

Three-dimensional calculation of shuttle charging in polar orbit p 40 N85-22486

NASCAP simulation of PIX 2 experiments p 180 N85-22497

Confined turbulent swirling recirculating flow predictions [NASA-CR-174917] p 29 N85-26716

Computer program for the calculation of multicomponent convective diffusion deposition rates from chemically frozen boundary layer theory [NASA-CR-168329] p 116 N85-27164

Component-specific modeling [NASA-CR-174765] p 147 N85-27261

Error reduction program --- combustor performance evaluation codes p 172 N85-27584

[NASA-CR-174776] Predictions and measurements of isothermal flowfields in axisymmetric combustor geometries [NASA-CR-174916] p 29 N85-27867

Composite loads spectra for select space propulsion structural components: Probabilistic load model development p 148 N85-27954

Probabilistic finite element development p 149 N85-27956

Multi-mesh gear dynamics program evaluation and enhancements [NASA-CR-174747] p 133 N85-28372

DEAN: A program for dynamic engine analysis [NASA-TM-87033] p 30 N85-28945

Fast approach for calculating film thicknesses and pressures in elastohydrodynamically lubricated contacts at high loads p 117 N85-30242

[NASA-TM-87032] Combustion gas properties. Part 3: Hydrogen gas fuel and dry air p 32 N85-31058

[NASA-TP-2477] A comparison of smooth specimen and analytical simulation techniques for notched members at elevated temperatures p 151 N85-31546

Component-specific modeling p 32 N85-32119

[NASA-CR-174925] Component-specific modeling p 33 N85-34140

[NASA-CR-174765] General design method for 3-dimensional, potential flow fields. Part 2: Computer program DIN3D1 for simple, unbranched ducts [NASA-CR-3926] p 10 N85-35159

**COMPUTER SYSTEMS DESIGN**

General approaches for achieving high speed computations p 169 A85-28628

# COMPUTER SYSTEMS PERFORMANCE

General approaches for achieving high speed computations p 169 A85-28628

# COMPUTER SYSTEMS PROGRAMS

Development and use of the computer software package for planning the 12 GHz broadcasting-satellite service at RARC '83 p 96 A85-29605

MINDS: A microcomputer interactive data system for 8086-based controllers [NASA-TP-2378] p 170 N85-17576

# COMPUTER SYSTEMS SIMULATION

Hardware for a real-time multiprocessor simulator [NASA-TM-83805] p 169 N85-10659

# COMPUTER TECHNIQUES

Recent advances in methods for numerical solution of O.D.E. initial value problems p 171 A85-21370

Closed-loop strain controlled testing at elevated temperatures with a non-contacting gage p 121 A85-29562

# COMPUTERIZED SIMULATION

Control algorithms and computer simulation of a stand-alone photovoltaic village power system p 153 A85-11345

Numerical simulations of positively-biased probes and dielectric-conductor disks in a plasma --- for low earth orbit plasma densities p 179 A85-17262

Direct simulations of chemically reacting turbulent mixing layers [AIAA PAPER 85-0321] p 60 A85-19666

Computer simulation of plasma electron collection by PIX-II --- solar array-space plasma interaction [AIAA PAPER 85-0386] p 43 A85-19715

Circular waveguide bifurcation for asymmetric modes p 101 A85-20170

On the development of hierarchical solution strategies for nonlinear finite element formulations p 171 A85-21979

Moving target, distributed, real-time simulation using Ada p 170 A85-34131

Numerical simulation of positive-potential conductors in the presence of a plasma and a secondary-emitting dielectric p 102 A85-35306

Computer simulation of thin film nucleation and growth p 181 A85-35308

On local total strain redistribution using a simplified cyclic inelastic analysis based on an elastic solution [AIAA PAPER 85-1419] p 142 A85-39770

The J3 SCR model applied to resonant converter simulation p 102 A85-42156

Comparison of free-piston Stirling engine model predictions with RE1000 engine test data p 130 A85-45488

A computer simulation of thin film nucleation and growth: The Volmer-Weber case [NASA-TM-86968] p 53 N85-21264

On local total strain redistribution using a simplified cyclic inelastic analysis based on an elastic solution [NASA-TM-86913] p 145 N85-21690

Three-dimensional calculation of shuttle charging in polar orbit p 40 N85-22486

NASCAP simulation of PIX 2 experiments p 180 N85-22497

Simulation of multistage turbine flows p 116 N85-27945

DEAN: A program for dynamic engine analysis [NASA-TM-87033] p 30 N85-28945

**CONCENTRATION (COMPOSITION)**

Simultaneous cabin and ambient ozone measurements on two Boeing 747 airplanes. Volume 3: October 1978 - July 1979 [NASA-TM-86883] p 167 N85-21872

# CONCENTRATORS

Near-optimum design of GaAs-based concentrator space solar cells for 80 C operation p 153 A85-15800

# CONCURRENT PROCESSING

Functional language and data flow architectures p 170 A85-28629

# CONDUCTIVE HEAT TRANSFER

Oscillatory conductive heat transfer for a fiber in an ideal gas p 109 A85-26077

# CONFERENCES

Computation of internal flows: Methods and applications; Proceedings of the Energy Sources Technology Conference, New Orleans, LA, February 12-16, 1984 p 106 A85-11630

Turbine Engine Hot Section Technology (HOST) [NASA-TM-83022] p 18 N85-10951

Space Power [NASA-CP-2352] p 47 N85-13880

Rotordynamic Instability Problems in High-Performance Turbomachinery [NASA-CR-2338] p 131 N85-14116

OTV Propulsion Issues [NASA-CP-2347] p 37 N85-16989

# CONVECTIVE HEAT TRANSFER

Spacecraft Environmental Interactions Technology, 1983 [NASA-CP-2359] p 39 N85-22470

Structural Integrity and Durability of Reusable Space Propulsion Systems [NASA-CP-2381] p 51 N85-27941

Nonlinear Constitutive Relations for High Temperature Application, 1984 [NASA-CP-2369] p 150 N85-31530

# CONFINEMENT

Behavior of turbulent gas jets in an axisymmetric confinement [NASA-CR-174829] p 28 N85-25265

# CONSERVATION LAWS

A convergent series expansion for hyperbolic systems of conservation laws [NASA-CR-172557] p 168 N85-21990

# CONSTITUTIVE EQUATIONS

Thermodynamically consistent constitutive equations for nonisothermal large strain, elasto-plastic, creep behavior [AIAA PAPER 85-0621] p 142 A85-38425

Unified constitutive material models for nonlinear finite-element structural analysis --- gas turbine engine blades and vanes [AIAA PAPER 85-1418] p 142 A85-39769

Constitutive modeling and computational implementation for finite strain plasticity p 143 A85-40910

Biaxial constitutive equation development for single crystals [NASA-CR-174056] p 183 N85-11862

Viscoplastic constitutive relationships with dependence on thermomechanical history [NASA-CR-174836] p 146 N85-21691

Unified constitutive material models for nonlinear finite-element structural analysis --- gas turbine engine blades and vanes [NASA-TM-86985] p 146 N85-24338

On thermomechanical testing in support of constitutive equation development for high temperature alloys [NASA-CR-174879] p 147 N85-25894

Nonlinear Constitutive Relations for High Temperature Application, 1984 [NASA-CP-2369] p 150 N85-31530

A survey of unified constitutive theories p 150 N85-31531

Numerical considerations in the development and implementation of constitutive models p 151 N85-31541

On numerical integration and computer implementation of viscoplastic models p 151 N85-31542

Finite element analysis of notch behavior using a state variable constitutive equation p 152 N85-31548

# CONTACTORS

Free-surface phenomena under low- and zero-gravity conditions [NASA-CR-175835] p 116 N85-27168

# CONTAINERS

Flame radiation and linear heat transfer in a tubular-can combustor p 15 A85-39580

# CONTROL MOMENT GYROSCOPES

Application of traction drives as servo mechanisms p 152 N85-33520

# CONTROL SIMULATION

The use of Ada in distributed simulations p 169 A85-28612

Multibus-based parallel processor for simulation p 169 A85-28613

A functional language approach in high-speed digital simulation p 170 A85-28615

Control aspects of the Schuchuli Village stand-alone photovoltaic power system [NASA-TM-83790] p 103 N85-13157

# CONTROL THEORY

The role of modern control theory in the design of controls for aircraft turbine engines p 13 A85-13627

Nonlinear global stability analysis of compressor stall phenomena [NASA-CR-174908] p 31 N85-29960

# CONVECTIVE FLOW

Effect of airfoil mean loading on convected gust interaction noise [AIAA PAPER 84-2324] p 173 A85-13955

A numerical study of the steady scalar convective diffusion equation for small viscosity p 107 A85-16533

Convective influence on the stability of a cylindrical solid-liquid interface p 109 A85-26911

# CONVECTIVE HEAT TRANSFER

Methods for heat transfer and temperature field analysis of the insulated diesel [NASA-CR-174783] p 185 N85-16699

Unsteady heat transfer due to time-dependent free stream velocity p 117 N85-27947

**CONVERGENCE**

Accelerated convergence for incompressible flow calculations

[AIAA PAPER 85-0058] p 2 A85-19489

The effect of channel convergence on heat transfer in a passage with short pin fins

[NASA-TM-83801] p 113 N85-10303

Accelerated convergence for incompressible flow calculations

[NASA-TM-86863] p 18 N85-10949

**CONVERGENT NOZZLES**

Experimental investigation of shock-cell noise reduction for dual-stream nozzles in simulated flight

[NASA-CR-3846] p 175 N85-13549

Experimental investigation of shock-cell noise reduction for single stream nozzles in simulated flight

[NASA-CR-3845] p 175 N85-13550

**CONVERGENT-DIVERGENT NOZZLES**

Supersonic jet shock noise reduction

[AIAA PAPER 84-2278] p 173 A85-16099

Experimental investigation of shock-cell noise reduction for dual-stream nozzles in simulated flight

[NASA-CR-3846] p 175 N85-13549

Experimental investigation of shock-cell noise reduction for single stream nozzles in simulated flight

[NASA-CR-3845] p 175 N85-13550

Vacuum chamber pressure effects on thrust measurements of low Reynolds number nozzles

[NASA-TM-86955] p 49 N85-21259

**CONVEXITY**

Heat transfer and turbulence measurements of a film-cooled flow over a convexly curved surface

p 112 A85-41787

**CONVOLUTION INTEGRALS**

Convolute nozzle design for the RL10 derivative 2B engine

[NASA-CR-174953] p 32 N85-29965

**COOLANTS**

Coolant passage heat transfer with rotation

p 20 N85-10968

**COOLING**

Small gas turbine combustor study - Fuel injector performance in a transpiration-cooled liner

[AIAA PAPER 85-1312] p 16 A85-39717

The effect of channel convergence on heat transfer in a passage with short pin fins

[NASA-TM-83801] p 113 N85-10303

Fabrication of ceramic substrate-reinforced and free forms

[NASA-TM-86994] p 50 N85-23926

Small gas turbine combustor study: Fuel injector performance in a transpiration-cooled liner

[NASA-TM-86989] p 27 N85-25264

Performance analysis of radiation cooled dc transmission lines for high power space systems

[NASA-TM-87040] p 104 N85-28222

Design principles for nickel-hydrogen cells and batteries

[NASA-TM-87037] p 164 N85-31646

Design and lubrication of high-speed rolling-element bearings

[NASA-TM-87107] p 137 N85-34409

**COOLING SYSTEMS**

High thermal power density heat transfer apparatus providing electrical isolation at high temperature using heat pipes

[NASA-CASE-LEW-12950-2] p 117 N85-29179

Vortex generating flow passage design for increased film cooling effectiveness

[NASA-CASE-LEW-14039-1] p 119 N85-33433

**COPOLYMERIZATION**

Chemical control of nadimide cure temperature and rate

[NASA-CASE-LEW-13770-2] p 63 N85-28982

**COPOLYMERS**

Chemical approach for controlling nadimide cure temperature and rate with maleimide

[NASA-CASE-LEW-13770-3] p 87 N85-21350

Chemical approach for controlling nadimide cure temperature and rate with maleimide

[NASA-CASE-LEW-13770-4] p 87 N85-21351

Alkaline battery containing a separator of a cross-linked copolymer of vinyl alcohol and unsaturated carboxylic acid

[NASA-CASE-LEW-13102-1] p 104 N85-29144

**COPPER**

Effect of interfacial characteristics of metal clad polymeric substrates on electrical high frequency interconnection performance

[NASA-TM-86948] p 99 N85-20223

**COPPER ALLOYS**

Deformation and erosion of f.c.c. metals and alloys under cavitation attack

p 65 A85-12789

**COPPER CHLORIDES**

Environmental stability of intercalated graphite fibers

[NASA-TM-87025] p 90 N85-26992

**COPPER OXIDES**

Textured carbon surfaces on copper

[NASA-CASE-LEW-14130-1] p 95 N85-20156

**CORIOLIS EFFECT**

Vibration and buckling of rotating, pretwisted, preconed beams including Coriolis effects

[NASA-TM-87004] p 146 N85-25893

Nonlinear flap-lag-extensional vibrations of rotating, pretwisted, preconed beams including Coriolis effects

[NASA-TM-87102] p 152 N85-34427

**CORNERS**

Free-surface phenomena under low- and zero-gravity conditions

[NASA-CR-175835] p 116 N85-27168

**CORRELATION**

Ground correlation investigation of thruster/spacecraft interactions to be measured on the IAPS flight test

p 59 A85-11897

Elevated temperature biaxial fatigue

[NASA-CR-175795] p 148 N85-27263

**CORROSION**

Reactions of NaCl with gaseous SO<sub>3</sub>, SO<sub>2</sub>, and O<sub>2</sub>

p 59 A85-11897

The reactions of cobalt, iron and nickel in SO<sub>2</sub> atmospheres: Similarities and differences

[NASA-TM-86868] p 70 N85-11217

Surface effects of corrosive media on hardness, friction, and wear of materials

[NASA-TM-83711] p 85 N85-15896

Replaceable blade turbine and stationary specimen corrosion testing facility

[NASA-TM-86931] p 73 N85-18126

**CORROSION RESISTANCE**

The transient oxidation of single crystal NiAl + Zr

[NASA-CR-174756] p 70 N85-11221

Study of the effects of implantation on the high Fe-Ni-Cr and Ni-Cr-Al alloys

[NASA-CR-175625] p 76 N85-22661

Mechanism of strength degradation for hot corrosion of alpha-SiC

[NASA-TM-87052] p 91 N85-30135

**CORROSION TESTS**

Replaceable blade turbine and stationary specimen corrosion testing facility

[NASA-TM-86931] p 73 N85-18126

Compatibility experiments of facilities, materials, and propellants for electrothermal thrusters

[NASA-TM-86956] p 49 N85-21260

Burner rig corrosion of SiC at 1000 deg C

[NASA-TM-87061] p 53 N85-30011

**COST ANALYSIS**

Space Station propulsion - The Advanced Development Program at Lewis

[AIAA PAPER 85-1154] p 44 A85-39626

Space station propulsion: The advanced development program at Lewis

[NASA-TM-86999] p 50 N85-25386

Conceptual design of a fixed-pitch wind turbine generator system rated at 400 kilowatts

[NASA-CR-174877] p 162 N85-29363

Energy Efficient Engine Program technology benefit/cost study, volume 1

[NASA-CR-174766-VOL-1] p 33 N85-35197

Energy Efficient Engine Program technology benefit/cost study, volume 2

[NASA-CR-174766-VOL-2] p 33 N85-35198

**COST EFFECTIVENESS**

Parametric study of potential early commercial power plants Task 3-A MHD cost analysis

[NASA-CR-175839] p 161 N85-27377

Energy efficient engine component development and integration program

[NASA-CR-172846] p 31 N85-29958

Operational results for the experimental DOE/NASA Mod-OA wind turbine project

[NASA-TM-83517] p 163 N85-30479

**COST ESTIMATES**

Structural analysis and cost estimate of an eight-leg space frame as a support structure for horizontal axis wind turbines

[NASA-TM-83470] p 150 N85-30361

**COST REDUCTION**

Energy efficient engine. Volume 1: Component development and integration program

[NASA-CR-173084] p 22 N85-10992

**COSTS**

Jet fuel property changes and their effect on producibility and cost in the U.S., Canada, and Europe

[NASA-CR-174840] p 93 N85-27012

**COUPLED MODES**

Vibration and flutter of mistuned bladed-disk assemblies

[AIAA PAPER 84-0991] p 139 A85-16095

Circular waveguide bifurcation for asymmetric modes

p 101 A85-20170

Nonlinear flap-lag-extensional vibrations of rotating, pretwisted, preconed beams including Coriolis effects

[NASA-TM-87102] p 152 N85-34427

**COUPLING**

Dilute plasma coupling currents to a high voltage solar array in weak magnetic fields

p 46 A85-45388

**COWLINGS**

Low-speed aerodynamic test of an axisymmetric supersonic inlet with variable cowl slot

[AIAA PAPER 85-1210] p 5 A85-40819

Low-speed aerodynamic test of an axisymmetric supersonic inlet with variable cowl slot

[NASA-TM-87039] p 28 N85-26710

**CRACK GEOMETRY**

Eddy current jet engine disk-crack monitor

p 120 A85-11100

**CRACK INITIATION**

Development of coated single-crystal superalloy systems for gas turbine applications

p 68 A85-32440

Application of two creep fatigue life models for the prediction of elevated temperature crack initiation of a nickel base alloy

[AIAA PAPER 85-1420] p 69 A85-43979

Nonlinear structural and life analyses of a combustor liner

p 19 N85-10955

Life prediction and constitutive behavior: Overview

p 20 N85-10973

Constitutive model development for isotropic materials

p 20 N85-10975

Creep fatigue life prediction for engine hot section materials (isotropic)

[NASA-CR-168228] p 32 N85-31057

**CRACK PROPAGATION**

Fracture toughness of hot-pressed beryllium

p 66 A85-25835

On the fatigue crack propagation behavior of superalloys at intermediate temperatures

p 68 A85-32434

Pre-HOST high temperature crack propagation

p 19 N85-10956

HOST high temperature crack propagation

p 21 N85-10977

Thermal-mechanical fatigue crack growth in Inconel X-750

[NASA-CR-174740] p 72 N85-15877

A study of spectrum fatigue crack propagation in two aluminum alloys. 1: Spectrum simplification

[NASA-TM-86929] p 72 N85-18124

A study of spectrum fatigue crack propagation in two aluminum alloys. 2: Influence of microstructures

[NASA-TM-86930] p 73 N85-18125

Translational and extensional energy release rates (the J- and M-integrals) for a crack layer in thermoelasticity

[NASA-CR-174872] p 145 N85-21685

Ultrasonic testing of plates containing edge cracks

[NASA-CR-3904] p 138 N85-29307

**CRACK TIPS**

On stress field near a stationary crack tip

[AD-A152863] p 141 A85-24532

**CRACKING (CHEMICAL ENGINEERING)**

Jet fuel property changes and their effect on producibility and cost in the U.S., Canada, and Europe

[NASA-CR-174840] p 93 N85-27012

**CRACKS**

Ultrasonic testing of plates containing edge cracks

[NASA-CR-3904] p 138 N85-29307

**CREEP ANALYSIS**

Strainrange partitioning - A total strain range version --- for creep fatigue life prediction by summing inelastic and elastic strain-range-life relations for two Ni base superalloys

p 64 A85-11603

Thermodynamically consistent constitutive equations for nonisothermal large strain, elasto-plastic, creep behavior

[AIAA PAPER 85-0621] p 142 A85-38425

**CREEP BUCKLING**

Dynamic creep buckling: Analysis of shell structures subjected to time-dependent mechanical and thermal loading

p 149 N85-27959

**CREEP PROPERTIES**

Influence of composition on the microstructure and mechanical properties of a nickel-base superalloy single crystal

p 66 A85-32387

Factors which influence directional coarsening of gamma-prime during creep in nickel-base superalloy single crystals

p 67 A85-32388

The influence of hold times on LCF and FCG behavior in a P/M Ni-base superalloy --- Low Cycle Fatigue/Fatigue Crack Growth

p 67 A85-32400

Plasticity, viscoplasticity, and creep of solids by mechanical subelement models

p 142 A85-35048

Nonlinear structural and life analyses of a combustor liner

p 19 N85-10955

Reliability considerations for the total strain range version of strainrange partitioning

[NASA-CR-174757] p 144 N85-11380

- Creep fatigue life prediction for engine hot section materials (isotropic)  
[NASA-CR-168228] p 32 N85-31057
- A comparison of two contemporary creep-fatigue life prediction methods p 151 N85-31538
- CREEP RUPTURE STRENGTH**  
Elevated temperature creep-rupture behavior of the single crystal nickel-base superalloy NASAIR 100 p 66 A85-27812
- Development of coated single-crystal superalloy systems for gas turbine applications p 68 A85-32440
- Creep-rupture reliability analysis p 143 A85-42566
- Fracture of yttria-doped, sintered reaction-bonded silicon nitride p 82 A85-42797
- [ACS PAPER 7-J3-84] p 82 A85-42797
- The effects of seven alloying elements on the microstructure and stress-rupture behavior of nickel-base superalloys p 70 N85-10168
- [NASA-TM-83791] p 70 N85-10168
- Effects of tin on microstructure and mechanical behavior of Inconel 718 p 71 N85-12129
- [NASA-TM-86866] p 71 N85-12129
- Stirling material technology p 72 N85-13007
- [NASA-TM-86888] p 72 N85-13007
- Creep-rupture behavior of iron superalloys in high-pressure hydrogen p 74 N85-19078
- [NASA-CR-174411] p 74 N85-19078
- CREEP STRENGTH**  
Advanced stress analysis methods applicable to turbine engine structures p 26 N85-21165
- [NASA-CR-175573] p 26 N85-21165
- Alloys based on NiAl for high temperature applications p 75 N85-21322
- [NASA-TM-86976] p 75 N85-21322
- CREEP TESTS**  
A continuous damage model based on stepwise-stress creep rupture tests p 152 N85-32341
- [NASA-CR-174941] p 152 N85-32341
- CRITICAL TEMPERATURE**  
External fuel vaporization study, phase 2 p 92 N85-11252
- [NASA-CR-174079] p 92 N85-11252
- CROSS FLOW**  
Flow visualization of lateral jet injection into swirling crossflow p 2 A85-19490
- [AIAA PAPER 85-0059] p 2 A85-19490
- Turbulence measurements of lateral jet injection into confined tubular crossflow p 110 A85-39604
- [AIAA PAPER 85-1102] p 110 A85-39604
- Numerical calculation of subsonic jets in crossflow with reduced numerical diffusion p 110 A85-39780
- [AIAA PAPER 85-1441] p 110 A85-39780
- Vortex modeling of single and multiple dilution jet mixing in a crossflow p 111 A85-40701
- [AIAA PAPER 85-1580] p 111 A85-40701
- Dilution zone mixing studies p 21 N85-10984
- Flow visualization study of the effect of injection hole geometry on an inclined jet in crossflow p 115 N85-20269
- [NASA-TM-86936] p 115 N85-20269
- Development of a temperature measurement system with application to a jet in a cross flow experiment p 27 A85-25262
- [NASA-CR-174896] p 27 A85-25262
- Numerical calculation of subsonic jets in crossflow with reduced numerical diffusion p 27 N85-25263
- [NASA-TM-87003] p 27 N85-25263
- The influence of jet-grid turbulence on heat transfer from the stagnation region of a cylinder in crossflow p 115 N85-25760
- [NASA-TM-87011] p 115 N85-25760
- CROSS POLARIZATION**  
Dual-mode coaxial feed with low crosspolarisation p 101 A85-20171
- CROSSLINKING**  
Chemical approach for controlling nadimide cure temperature and rate p 87 N85-21352
- [NASA-CASE-LEW-13770-5] p 87 N85-21352
- Chemical control of nadimide cure temperature and rate p 63 N85-28982
- [NASA-CASE-LEW-13770-2] p 63 N85-28982
- Development of a lithium secondary battery separator p 104 N85-31378
- CRYOGENIC EQUIPMENT**  
Cryogenic upper stage test bed engine p 44 A85-39733
- [AIAA PAPER 85-1339] p 44 A85-39733
- CRYOGENIC FLUID STORAGE**  
Technology requirements to be addressed by the NASA Lewis Research Center Cryogenic Fluid Management Facility program p 94 A85-47024
- [AIAA PAPER 85-1229] p 94 A85-47024
- Technology requirements to be addressed by the NASA Lewis Research Center Cryogenic Fluid Management Facility program p 38 N85-29987
- [NASA-TM-87048] p 38 N85-29987
- CRYOGENIC FLUIDS**  
Technology requirements to be addressed by the NASA Lewis Research Center Cryogenic Fluid Management Facility program p 94 A85-47024
- [AIAA PAPER 85-1229] p 94 A85-47024
- OTV Propulsion Issues p 37 N85-16989
- [NASA-CP-2347] p 37 N85-16989
- Technology requirements to be addressed by the NASA Lewis Research Center Cryogenic Fluid Management Facility program p 38 N85-29987
- [NASA-TM-87048] p 38 N85-29987
- CRYOGENIC ROCKET PROPELLANTS**  
Progress report - Advanced cryogenic OTV engine technology p 44 A85-39735
- [AIAA PAPER 85-1341] p 44 A85-39735
- CRYOGENICS**  
Select fiber composites for space applications - A mechanistic assessment p 54 A85-16040
- An experimental investigation of rubbing interaction in labyrinth seals at cryogenic temperature p 129 A85-39938
- Manrating orbital transfer vehicle propulsion p 50 N85-25385
- [NASA-TM-87019] p 50 N85-25385
- CRYSTAL GROWTH**  
Analysis of three-dimensional solidification interface shape p 109 A85-30075
- Electrical characterization of plasma-grown oxides on gallium arsenide p 181 A85-32635
- Dendritic solidification. I - Analysis of current theories and models. II - A model for dendritic growth under an imposed thermal gradient p 182 A85-38019
- Cone formation as a result of whisker growth on ion bombarded metal surfaces p 182 A85-41635
- Dendritic solidification. III - Some further refinements to the model for dendritic growth under an imposed thermal gradient p 69 A85-44703
- Monte Carlo study of reversible growth of clusters on a surface p 182 A85-48516
- A computer simulation of thin film nucleation and growth: The Volmer-Weber case p 53 N85-21264
- [NASA-TM-86968] p 53 N85-21264
- Manufacturing process to reduce large grain growth in zirconium alloys p 78 N85-34267
- [DE85-011649] p 78 N85-34267
- CRYSTAL LATTICES**  
Monte Carlo study of reversible growth of clusters on a surface p 182 A85-48516
- Monte Carlo lattice models for adsorbed polymer conformation p 183 N85-24961
- [NASA-TP-2453] p 183 N85-24961
- CRYSTAL STRUCTURE**  
Frictional and morphological properties of Au-MoS<sub>2</sub> films sputtered from a compact target p 127 A85-19085
- Substrate-induced orientational order in the isotropic phase of liquid crystals p 181 A85-24649
- Characterization of erosion of metallic materials under cavitation attack in a mineral oil p 74 N85-19075
- [NASA-TM-86934] p 74 N85-19075
- CRYSTAL SURFACES**  
AES and LEED study of the zinc blende SiC(100) surface p 61 A85-41633
- CRYSTALLIZATION**  
Mechanical-contact-induced transformation from the amorphous to the partially crystalline state in metallic glass p 65 A85-19084
- CUMULATIVE DAMAGE**  
Considerations for damage analysis of gas turbine hot section components p 14 A85-18792
- [ASME PAPER 84-PVP-77] p 14 A85-18792
- A history dependent damage model for low cycle fatigue p 140 A85-18795
- [ASME PAPER 84-PVP-112] p 140 A85-18795
- A unified relation for cavitation erosion p 109 A85-24445
- CURING**  
Chemical approach for controlling nadimide cure temperature and rate with maleimide p 87 N85-21350
- [NASA-CASE-LEW-13770-3] p 87 N85-21350
- Chemical approach for controlling nadimide cure temperature and rate with maleimide p 87 N85-21351
- [NASA-CASE-LEW-13770-4] p 87 N85-21351
- Chemical control of nadimide cure temperature and rate p 63 N85-28982
- [NASA-CASE-LEW-13770-2] p 63 N85-28982
- CURRENT DENSITY**  
Manual of phosphoric acid fuel cell stack three-dimensional model and computer program p 157 N85-10447
- [NASA-CR-174722] p 157 N85-10447
- CYCLIC LOADS**  
Hygrothermomechanical evaluation of transverse filament tape epoxy/polyester fiberglass composites p 54 A85-15632
- A history dependent damage model for low cycle fatigue p 140 A85-18795
- [ASME PAPER 84-PVP-112] p 140 A85-18795
- On local total strain redistribution using a simplified cyclic inelastic analysis based on an elastic solution p 142 A85-39770
- [AIAA PAPER 85-1419] p 142 A85-39770
- Application of two creep fatigue life models for the prediction of elevated temperature crack initiation of a nickel base alloy p 69 A85-43979
- [AIAA PAPER 85-1420] p 69 A85-43979
- Nonlinear structural and life analyses of a combustor liner p 19 N85-10955
- Design procedures for fiber composite structural components: Panels subjected to combined in-plane loads p 57 N85-15823
- [NASA-TM-86909] p 57 N85-15823
- Low cycle fatigue of MAR-M 200 single crystals at 760 and 870 deg C p 74 N85-19074
- [NASA-TM-86933] p 74 N85-19074
- Local strain redistribution corrections for a simplified inelastic analysis procedure based on an elastic finite-element analysis p 145 N85-20396
- [NASA-TP-2421] p 145 N85-20396
- On local total strain redistribution using a simplified cyclic inelastic analysis based on an elastic solution p 145 N85-21690
- [NASA-TM-86913] p 145 N85-21690
- Cyclic structural analyses of anisotropic turbine blades for reusable space propulsion systems --- ssme fuel turbopump p 146 N85-24339
- [NASA-TM-86990] p 146 N85-24339
- Long-life high performance fuel cell program p 50 N85-25384
- [NASA-CR-174874] p 50 N85-25384
- Analysis of shell type structures subjected to time dependent mechanical and thermal loading p 147 N85-25896
- [NASA-CR-175747] p 147 N85-25896
- Interaction of high-cycle and low-cycle fatigue of Haynes 188 alloy at 1400 F deg p 149 N85-27961
- Thermomechanical deformation in the presence of metallurgical changes p 150 N85-31533
- Results of an interlaboratory fatigue test program conducted on alloy 800H at room and elevated temperatures p 152 N85-32340
- [NASA-CR-174940] p 152 N85-32340
- CYLINDRICAL BODIES**  
Combined influence of unsteady free stream velocity and free stream turbulence on stagnation point heat transfer p 112 A85-41782
- CZOCHEWSKI METHOD**  
Research on gallium arsenide diffused junction solar cells p 158 N85-11457
- [NASA-CR-174057] p 158 N85-11457

## D

### DAMAGE

- Reexamination of cumulative fatigue damage laws p 149 N85-27962
- A continuous damage model based on stepwise-stress creep rupture tests p 152 N85-32341
- [NASA-CR-174941] p 152 N85-32341

- DAMPERS (VALVES)**  
Dual clearance squeeze film damper p 135 N85-33490
- [NASA-CASE-LEW-13506-1] p 135 N85-33490

- DAMAGE ASSESSMENT**  
Spherical microglass particle impingement studies of thermoplastic materials at normal incidence p 79 A85-11072

- A history dependent damage model for low cycle fatigue p 140 A85-18795
- [ASME PAPER 84-PVP-112] p 140 A85-18795

- DAMPERS (VALVES)**  
Dual clearance squeeze film damper p 135 N85-33490
- [NASA-CASE-LEW-13506-1] p 135 N85-33490

- DATA ACQUISITION**  
Development of a multiplane multispeed balancing system for turbine systems p 35 N85-22400
- [NASA-CR-174750] p 35 N85-22400

- DATA BASE MANAGEMENT SYSTEMS**  
Flow dynamic environment data base development for the SSME p 147 N85-26885

- DATA BASES**  
Flow dynamic environment data base development for the SSME p 147 N85-26885

- DATA CORRELATION**  
Creep-rupture reliability analysis p 143 A85-42566

- DATA FLOW ANALYSIS**  
Data flow methods for dynamic system simulation - A CSSL-IV microcomputer network interface p 170 A85-28614

- Functional language and data flow architectures p 170 A85-28629

- DATA MANAGEMENT**  
MERIT: A man/computer data management and enhancement system for upper air nowcasting/forecasting in the United States --- Minimum Energy Routes using Interactive Techniques (MERIT) p 167 N85-10558

- DATA STORAGE**  
Transferring data oscilloscope to an IBM using an Apple II+ p 168 A85-24526

- DATA TRANSMISSION**  
Transferring data oscilloscope to an IBM using an Apple II+ p 168 A85-24526

**DECELERATION**

A unified relation for cavitation erosion  
p 109 A85-24445

**DEFECTS**

Radiation damage and defect behavior in ion-implanted, lithium counterdoped silicon solar cells  
p 182 A85-35698  
Reliability of void detection in structural ceramics using scanning laser acoustic microscopy  
[NASA-TM-87035] p 138 N85-32337

**DEFLECTION**

A comparison of electronic heterodyne moire deflectometry and electronic heterodyne holographic interferometry for flow measurements  
[NASA-TM-87071] p 125 N85-32302

**DEFORMATION**

Pantographing self adaptive gap elements  
p 142 A85-37440  
Creep of chemically vapor deposited SiC fibers  
[NASA-TM-86897] p 56 N85-14878  
Advanced stress analysis methods applicable to turbine engine structures  
[NASA-CR-175573] p 26 N85-21165  
On Hybrid and mixed finite element methods  
[NASA-CR-175551] p 146 N85-23096  
A comparison of electronic heterodyne moire deflectometry and electronic heterodyne holographic interferometry for flow measurements  
[NASA-TM-87071] p 125 N85-32302

**DEGRADATION**

Laboratory degradation of Kapton in a low energy oxygen ion beam  
[AIAA PAPER 83-2658] p 78 A85-10675  
Interply layer degradation effects on composite structural response  
[AIAA PAPER 84-0849] p 54 A85-16096  
Cathode degradation and erosion in high pressure arc discharges  
p 43 A85-16445  
Interply layer degradation effects on composite structural response  
p 55 A85-39215  
Performance degradation of helicopter rotor in forward flight due to ice  
p 11 A85-42937  
Study of Kapton under simulated shuttle environment  
[NASA-CR-176003] p 41 N85-29997

**DEICERS**

Icing tunnel tests of Electro-Impulse De-icing of an engine inlet and high-speed wings  
[AIAA PAPER 85-0466] p 10 A85-20872

**DEICING**

Electro-impulse de-icing of a turbofan engine inlet  
[AIAA PAPER 85-1118] p 12 A85-40811  
Analytical and physical modeling program for the NASA Lewis Research Center's Altitude Wind Tunnel (AWT)  
[NASA-TM-86919] p 35 N85-15757

**DELAMINATING**

Interply layer degradation effects on composite structural response  
[AIAA PAPER 84-0849] p 54 A85-16096  
Interply layer degradation effects on composite structural response  
p 55 A85-39215

**DEMAND (ECONOMICS)**

Demand for satellite-provided domestic communications services up to the year 2000  
[NASA-TM-86894] p 97 N85-15099  
Satellite provided customer promises services, a forecast of potential domestic demand through the year 2000. Volume 4: Sensitivity analysis  
[NASA-CR-174662] p 99 N85-27092

**DENDRITIC CRYSTALS**

The mechanisms of formation and prevention of channel segregation during alloy solidification  
p 180 A85-18082  
Dendritic solidification. I - Analysis of current theories and models. II - A model for dendritic growth under an imposed thermal gradient  
p 182 A85-38019  
Dendritic solidification. III - Some further refinements to the model for dendritic growth under an imposed thermal gradient  
p 69 A85-44703

**DENSIFICATION**

Evaluation of alpha-SiC sintering using statistical methods  
p 83 A85-42800

**DENSITY DISTRIBUTION**

Vortex modeling of single and multiple dilution jet mixing in a crossflow  
[AIAA PAPER 85-1580] p 111 A85-40701

**DEPOSITION**

Plasma deposited hydrogenated carbon on GaAs and InP  
p 182 A85-40386  
Analysis of glow discharges for understanding the process of film formation  
[NASA-TM-83750] p 62 N85-10138  
Plasma deposited diamondlike carbon on GaAs and InP  
[NASA-TM-86870] p 183 N85-10844

Initial feasibility ground test of a proposed photogrammetric system for measuring the shapes of ice accretions on helicopter rotor blades during forward flight  
[NASA-TM-87391] p 12 N85-12887

Liquid phase products and solid deposit formation from thermally stressed model jet fuels  
[NASA-TM-86874] p 92 N85-13066

Deposition of diamondlike carbon films  
[NASA-CASE-LEW-14080-1] p 95 N85-20153

Optical properties of hydrogenated amorphous carbon films grown from methane plasma  
[NASA-TM-86995] p 183 N85-26406

Jet fuel instability mechanisms  
[NASA-CR-175856] p 93 N85-28127

The structure of ion plated films in relation to coating properties  
[NASA-TM-87055] p 95 N85-29085

Diamondlike carbon protective coatings for IR materials  
[NASA-TM-87083] p 178 N85-34631

**DESENSITIZING**

Manufacturing process to reduce large grain growth in zirconium alloys  
[DE85-011649] p 78 N85-34267

**DESIGN ANALYSIS**

Near-optimum design of GaAs-based concentrator space solar cells for 80 C operation  
p 153 A85-15800  
A high energy stage for the National Space Transportation System  
[IAF PAPER 84-15] p 36 A85-23200  
Interdisciplinary design analysis of a precision spacecraft antenna  
[AIAA PAPER 85-0804] p 38 A85-30303  
Contingency power concepts for helicopter turboshaft engine  
p 15 A85-32005  
Design and performance of a fixed, nonaccelerating guide vane cascade that operates over an inlet flow angle range of 60 deg  
[ASME PAPER 84-GT-75] p 4 A85-32964  
Preliminary design of a 10 kW thermophotovoltaic system for space applications  
p 45 A85-45371  
A 37.5-kW point design comparison of the nickel-cadmium battery, bipolar nickel-hydrogen battery, and regenerative hydrogen-oxygen fuel cell energy storage subsystems for low earth orbit  
p 46 A85-45387  
Advanced designs for IPV nickel-hydrogen cells  
p 156 A85-45438  
Advanced multi-megawatt wind turbine design for utility application  
p 157 A85-45517  
Energy efficient engine flight propulsion system preliminary analysis and design report  
[NASA-CR-174701] p 18 N85-10947  
Energy efficient engine high pressure turbine test hardware detailed design report  
[NASA-CR-167955] p 23 N85-10995  
Inverse design technique for cascades  
[NASA-CR-3836] p 7 N85-12008  
Fuel and oxidizer turbine loss analysis  
p 50 N85-26900

**DETECTION**

Sensor failure detection for jet engines using analytical redundancy  
[AIAA PAPER 84-1452] p 13 A85-16097  
Radiographic detectability limits for seeded voids in sintered silicon carbide and silicon nitride  
[NASA-TM-86945] p 138 N85-21674

**DIAMONDS**

Apparatus for producing diamond-like carbon flakes  
[NASA-CASE-LEW-13837-3] p 95 N85-20155

Diamondlike flakes  
[NASA-CASE-LEW-13837-2] p 57 N85-21267

**DIAPHRAGMS (MECHANICS)**

Variable friction secondary seal for face seals  
[NASA-CASE-LEW-14170-1] p 131 N85-20377

**DIELECTRIC PROPERTIES**

Dielectric properties of 'diamondlike' carbon prepared by RF plasma deposition  
p 182 A85-38192

**DIELECTRICS**

Numerical simulation of positive-potential conductors in the presence of a plasma and a secondary-emitting dielectric  
p 102 A85-35306  
An investigation of arc discharging on negatively biased dielectric conductor samples in a plasma  
p 180 N85-22498

**DIELS-ALDER REACTIONS**

Chemical approach for controlling nadimide cure temperature and rate  
[NASA-CASE-LEW-13770-6] p 63 N85-30039

**DIESEL ENGINES**

Development of gas-lubricated pistons for heavy duty diesel engine technology program  
[NASA-CR-174746] p 184 N85-12808  
Advanced automotive diesel assessment program  
[NASA-CR-168285] p 130 N85-13235

Overview of waste heat utilization systems  
[NASA-TM-86901] p 184 N85-13692  
Transformation toughened ceramics for the heavy duty diesel engine technology program  
[NASA-CR-174689] p 185 N85-16698  
Methods for heat transfer and temperature field analysis of the insulated diesel  
[NASA-CR-174783] p 185 N85-16699  
An investigation of enhanced capability thermal barrier coating systems for diesel engine components  
[NASA-CR-174820] p 86 N85-18154  
Sliding seal materials for adiabatic engines  
[NASA-CR-174893] p 89 N85-22757  
Breakway friction and dynamic friction/wear measurements of various ceramic materials from 25 C (75 F) to 650 C (1200 F)  
[NASA-CR-174803] p 90 N85-26994

**DIFFERENTIAL EQUATIONS**

Integrating chemical kinetic rate equations by selective use of stiff and nonstiff methods  
[AIAA PAPER 85-0237] p 60 A85-19607  
Recent advances in methods for numerical solution of O.D.E. initial value problems  
p 171 A85-21370  
New integration techniques for chemical kinetic rate equations. 2: Accuracy comparison  
[NASA-TM-86893] p 23 N85-13798  
Integrating chemical kinetic rate equations by selective use of stiff and nonstiff methods  
[NASA-TM-86923] p 24 N85-15726  
Modeling the internal combustion engine  
[NASA-RP-1094] p 172 N85-19733  
A comparison of the efficiency of numerical methods for integrating chemical kinetic rate equations  
[NASA-TM-83590] p 25 N85-21162  
Nonlinear flap-lag-extensional vibrations of rotating, pretwisted, precone beams including Coriolis effects  
[NASA-TM-87102] p 152 N85-34427

**DIFFRACTION PATTERNS**

Ion-beam nitriding of steels  
p 66 A85-24667  
Electronic heterodyne readout of fringes in moire deflectometry  
p 122 A85-36726

**DIFFUSION**

A numerical study of the steady scalar convective diffusion equation for small viscosity  
p 107 A85-16533  
The effect of diffusion induced lattice stress on the open-circuit voltage in silicon solar cells  
p 181 A85-35620  
Analysis techniques for tracer studies of oxidation  
[NASA-CR-174796] p 84 N85-12162  
Reducing numerical diffusion for incompressible flow calculations  
[NASA-TM-83621] p 24 N85-14840  
The structure of dilute combustor sprays  
[NASA-CR-174838] p 24 N85-15728  
Study of controlled diffusion stator blading  
[NASA-CR-167995] p 25 N85-18058  
A study of interdiffusion in beta + gamma/gamma + gamma prime Ni-Cr-Al  
[NASA-CR-174852] p 74 N85-20041

**DIFFUSION FLAMES**

Drop-turbulence interactions in a diffusion flame  
[AIAA PAPER 85-0319] p 60 A85-19665  
Growth of a diffusion flame in the field of a vortex  
p 61 A85-47320

**DIFFUSION WELDING**

Diffusion welding of MA 6000 and a conventional nickel-base superalloy  
p 69 A85-43551  
Diffusion welding of Cassegrainian concentrator cell stack assemblies  
[NASA-CR-176104] p 164 N85-33566

**DIFFUSIVITY**

The reactions of cobalt, iron and nickel in SO-2 atmospheres: Similarities and differences  
[NASA-TM-86868] p 70 N85-11217

**DIGITAL FILTERS**

An allpass filter design for luminance and chrominance separation of NTSC signals  
p 102 A85-28230  
Linearization of digital derived rate algorithm for use in linear stability analysis  
[NASA-TM-87000] p 41 N85-23904

**DIGITAL SIMULATION**

A fast time domain digital simulation technique for power converters - Application to a buck converter with feedforward compensation  
p 101 A85-20900  
The use of Ada in distributed simulations  
p 169 A85-28612  
Multibus-based parallel processor for simulation  
p 169 A85-28613  
A functional language approach in high-speed digital simulation  
p 170 A85-28615  
Optical linear algebra processors - Noise and error-source modeling  
p 169 A85-36727

**DIGITAL SYSTEMS**

- High-temperature optically activated GaAs power switching for aircraft digital electronic control [NASA-CR-174711] p 34 N85-12901  
Energy Efficient Engine (E3) controls and accessories detail design report [NASA-CR-168017] p 31 N85-29957

**DILUTION**

- Dilution zone mixing studies p 21 N85-10984  
Development of a temperature measurement system with application to a jet in a cross flow experiment [NASA-CR-174896] p 27 N85-25262

**DIODES**

- Remote displacement measurements using a laser diode p 121 A85-24464  
High voltage-high power components for large space power distribution systems p 45 A85-45370

**DIPOLE ANTENNAS**

- DE-1 measurements of AKR wave directions --- auroral kilometer radiation p 166 A85-37717  
Infrared technology for satellite power conversion --- antenna arrays and bolometers [NASA-CR-174266] p 159 N85-16293

**DIRECT CURRENT**

- Nitriding of titanium and its alloys by N<sub>2</sub>, NH<sub>3</sub> or mixtures of N<sub>2</sub> + H<sub>2</sub> in a dc arc plasma at low pressures (or = to torr) [NASA-TM-83803] p 131 N85-15168  
Performance analysis of radiation cooled dc transmission lines for high power space systems [NASA-TM-87040] p 104 N85-28222

**DIRECT POWER GENERATORS**

- Operational performance of the photovoltaic-powered grain mill and water pump at Tangaye, Burkina Faso (formerly Upper Volta) [NASA-TM-86970] p 161 N85-23243

**DIRECTIONAL SOLIDIFICATION (CRYSTALS)**

- Materials for advanced turbine engines. Project 2: Rene 150 directionally solidified superalloy turbine blades, volume 2 [NASA-CR-167993] p 23 N85-12059

**DIRECTIVITY**

- On the calculation of the directivity of planar array feeds for satellite reflector applications p 97 A85-32249

**DISCHARGERS**

- Extended performance technology study 30-cm thruster [NASA-CR-168259] p 48 N85-15806

**DISCONTINUITY**

- MMIC devices for active phased array antennas [NASA-CR-174281] p 98 N85-15943  
Characterization of microstrip discontinuities in the time and frequency domains [NASA-CR-176190] p 106 N85-35342

**DISCRETE FUNCTIONS**

- Assessment of discretization schemes to reduce numerical diffusion in the calculation of complex flows [AIAA PAPER 85-0441] p 108 A85-19751

**DISKS (SHAPES)**

- Hot isostatically pressed manufacture of high strength MERL 76 disk and seal shapes [NASA-CR-165550] p 71 N85-11225

**DISPERSION**

- An experimental investigation of microstrip properties on soft substrates from 2 to 40 GHz [NASA-TM-86961] p 99 N85-20224

**DISPLACEMENT**

- Experimental compliance calibration of the NASA Lewis Research Center Mode 2 fatigue specimen [NASA-TM-86908] p 144 N85-16205  
Recent advances in hybrid/mixed finite elements [NASA-CR-175574] p 145 N85-21687

**DISPLACEMENT MEASUREMENT**

- Remote displacement measurements using a laser diode p 121 A85-24464  
Remote displacement measurement using a passive interferometer with a fiber-optic link p 122 A85-42857

**DISTORTION**

- Temperature distortion generator for turboshaft engine testing [SAE PAPER 841541] p 15 A85-39065  
Effect of combined pressure and temperature distortion orientation on high-bypass-ratio turbofan engine stability [NASA-TM-83771] p 17 N85-10067  
Temperature distortion generator for turboshaft engine testing [NASA-TM-83748] p 1 N85-15658  
Effect of steady-state temperature distortion on inlet flow to a high-bypass-ratio turbofan engine [NASA-TM-86896] p 24 N85-15725

**DISTRIBUTED PROCESSING**

- The use of Ada in distributed simulations p 169 A85-28612  
Real-Time Multiprocessor Programming Language (RTMPL) user's manual [NASA-TP-2422] p 170 N85-28610

**DOCUMENTATION**

- Bibliography of Lewis Research Center technical publications announced in 1984 [NASA-TM-87012] p 184 N85-28876

**DOMESTIC ENERGY**

- Operational results for the experimental DOE/NASA Mod-OA wind turbine project [NASA-TM-83517] p 163 N85-30479

**DOMESTIC SATELLITE COMMUNICATIONS SYSTEMS**

- Experimental results supporting the determination of service quality objectives for DBS systems p 96 A85-29611

**DOPED CRYSTALS**

- Magnesium doping of efficient GaAs and Ga(0.75)In(0.25)As solar cells grown by metalorganic chemical vapor deposition p 180 A85-11466  
The transient oxidation of single crystal NiAl + Zr [NASA-CR-174756] p 70 N85-11221

**DOPES**

- Lithium counterdoped silicon solar cell [NASA-CASE-LEW-14177-1] p 160 N85-20535  
Molecular orbital studies in oxidation: Sulfate formation and metal-metal oxide adhesion [NASA-CR-176070] p 77 N85-32174

**DOPPLER EFFECT**

- Filter induced errors in laser anemometer measurements using counter processors [NASA-TM-87047] p 125 N85-30288  
Velocity visualization in gaseous flows [NASA-CR-174954] p 119 N85-31445

**DRAG**

- Icing flight research - Aerodynamic effects of ice and ice shape documentation with stereo photography [AIAA PAPER 85-0468] p 11 A85-30192  
Observations from varying the lift and drag inputs to a noise prediction method for supersonic helical tip speed propellers [NASA-TM-83797] p 175 N85-10788  
Icing flight research: Aerodynamic effects of ice and ice shape documentation with stereo photography [NASA-TM-86906] p 12 N85-18049  
Report of the Constellations Panel p 131 N85-20368

**DROP SIZE**

- An approach for automated analysis of particle holograms p 120 A85-10034  
Phase/doppler spray analyzer for simultaneous measurements of drop size and velocity distributions p 120 A85-10035  
Spray characterization with a nonintrusive technique using absolute scattered light p 120 A85-10036  
Nonintrusive optical single-particle counter for measuring the size and velocity of droplets in a spray p 120 A85-16794  
Aerodynamic effect of combustor inlet air pressure on fuel jet atomization p 109 A85-27096  
Structure of nonevaporating sprays. I - Initial conditions and mean properties p 112 A85-48538  
Liquid fuel spray processes in high-pressure gas flow [NASA-TM-86944] p 115 N85-21570  
Research study of droplet sizing technology leading to the development of an advanced droplet sizing system [NASA-CR-174839] p 123 N85-21604

**DROP TESTS**

- Graphite/PMR polyimide composites with improved toughness [NASA-TM-87081] p 58 N85-32148

**DROPS (LIQUIDS)**

- Comparison of icing cloud instruments for 1982-1983 icing season flight program [AIAA PAPER 84-0020] p 13 A85-16098  
Drop-turbulence interactions in a diffusion flame [AIAA PAPER 85-0319] p 60 A85-19665  
Experimental study of the spray characteristics of a research aircraft atomizer [NASA-TM-86911] p 24 N85-15727  
The structure of dilute combustor sprays [NASA-CR-174838] p 24 N85-15728  
Advanced radiator concepts [NASA-TM-87008] p 115 N85-24245

**DRY FRICTION**

- Effects of friction dampers on aerodynamically unstable rotor stages p 14 A85-21866  
Metallurgical and mechanical phenomena due to rubbing of titanium against sintered powder Nichrome p 127 A85-22281  
Thermal and thermomechanical effects in dry sliding p 127 A85-23838

**DUCT GEOMETRY**

- Analytical study of flow phenomena in SSME turnaround duct geometries p 116 N85-26902

**DUCTED FLOW**

- The influence of combustion liner holes on noise production by ducted burners [AIAA PAPER 84-2322] p 172 A85-10869

- A finite element solution of three-dimensional inviscid rotational flows through curved ducts p 107 A85-11648

- Mass and momentum turbulent transport experiments with confined coaxial jets p 107 A85-14399

- Flow control in a diffusing S-Duct [AIAA PAPER 85-0524] p 3 A85-25928

- Review - Computational methods for internal flows with emphasis on turbomachinery p 4 A85-29126

- Structure of ducted particle-laden turbulent jets p 110 A85-38999

- Application of viscous and inviscid computation methods for rocket turbopump systems [SAE PAPER 841522] p 110 A85-39257

- Heat transfer enhancement in channels with turbulence promoters [ASME PAPER 84-WA/HT-72] p 111 A85-39900

- Application of computational fluid dynamics to complex inlet ducts [AIAA PAPER 85-1213] p 6 A85-47023

- Application of computational fluid dynamics to complex inlet ducts [NASA-TM-87060] p 118 N85-30247

- Application of computational fluid dynamics to complex inlet ducts [NASA-TM-87060] p 118 N85-30247

- Application of computational fluid dynamics to complex inlet ducts [NASA-TM-87060] p 118 N85-30247

- Application of computational fluid dynamics to complex inlet ducts [NASA-TM-87060] p 118 N85-30247

- Application of computational fluid dynamics to complex inlet ducts [NASA-TM-87060] p 118 N85-30247

- Application of computational fluid dynamics to complex inlet ducts [NASA-TM-87060] p 118 N85-30247

- Application of computational fluid dynamics to complex inlet ducts [NASA-TM-87060] p 118 N85-30247

- Application of computational fluid dynamics to complex inlet ducts [NASA-TM-87060] p 118 N85-30247

- Application of computational fluid dynamics to complex inlet ducts [NASA-TM-87060] p 118 N85-30247

- Application of computational fluid dynamics to complex inlet ducts [NASA-TM-87060] p 118 N85-30247

- Application of computational fluid dynamics to complex inlet ducts [NASA-TM-87060] p 118 N85-30247

- Application of computational fluid dynamics to complex inlet ducts [NASA-TM-87060] p 118 N85-30247

- Application of computational fluid dynamics to complex inlet ducts [NASA-TM-87060] p 118 N85-30247

- Application of computational fluid dynamics to complex inlet ducts [NASA-TM-87060] p 118 N85-30247

- Application of computational fluid dynamics to complex inlet ducts [NASA-TM-87060] p 118 N85-30247

- Application of computational fluid dynamics to complex inlet ducts [NASA-TM-87060] p 118 N85-30247

- Application of computational fluid dynamics to complex inlet ducts [NASA-TM-87060] p 118 N85-30247

- Application of computational fluid dynamics to complex inlet ducts [NASA-TM-87060] p 118 N85-30247

- Application of computational fluid dynamics to complex inlet ducts [NASA-TM-87060] p 118 N85-30247

- Application of computational fluid dynamics to complex inlet ducts [NASA-TM-87060] p 118 N85-30247

- Application of computational fluid dynamics to complex inlet ducts [NASA-TM-87060] p 118 N85-30247

- Application of computational fluid dynamics to complex inlet ducts [NASA-TM-87060] p 118 N85-30247

- Application of computational fluid dynamics to complex inlet ducts [NASA-TM-87060] p 118 N85-30247

- Application of computational fluid dynamics to complex inlet ducts [NASA-TM-87060] p 118 N85-30247

- Application of computational fluid dynamics to complex inlet ducts [NASA-TM-87060] p 118 N85-30247

- Application of computational fluid dynamics to complex inlet ducts [NASA-TM-87060] p 118 N85-30247

- Application of computational fluid dynamics to complex inlet ducts [NASA-TM-87060] p 118 N85-30247

- Application of computational fluid dynamics to complex inlet ducts [NASA-TM-87060] p 118 N85-30247

- Application of computational fluid dynamics to complex inlet ducts [NASA-TM-87060] p 118 N85-30247

- Application of computational fluid dynamics to complex inlet ducts [NASA-TM-87060] p 118 N85-30247

- Application of computational fluid dynamics to complex inlet ducts [NASA-TM-87060] p 118 N85-30247

- Application of computational fluid dynamics to complex inlet ducts [NASA-TM-87060] p 118 N85-30247

- Application of computational fluid dynamics to complex inlet ducts [NASA-TM-87060] p 118 N85-30247

- Application of computational fluid dynamics to complex inlet ducts [NASA-TM-87060] p 118 N85-30247

- Application of computational fluid dynamics to complex inlet ducts [NASA-TM-87060] p 118 N85-30247

- Application of computational fluid dynamics to complex inlet ducts [NASA-TM-87060] p 118 N85-30247

## E

## EARTH ATMOSPHERE

Study of Kapton under simulated shuttle environment  
[NASA-CR-176003] p 41 N85-29997

## EARTH ORBITS

Laboratory degradation of Kapton in a low energy oxygen ion beam  
[AIAA PAPER 83-2658] p 78 A85-10675

Teardown analysis of a ten cell bipolar nickel-hydrogen battery p 156 A85-45385

A 37.5-kW point design comparison of the nickel-cadmium battery, bipolar nickel-hydrogen battery, and regenerative hydrogen-oxygen fuel cell energy storage subsystems for low earth orbit p 46 A85-45387

Advanced designs for IPV nickel-hydrogen cells p 156 A85-45438

OTV propulsion technology programmatic overview p 37 N85-16997

Report of the Constellations Panel p 131 N85-20368

Radiation exposure and performance of multiple burn LEO-GEO orbit transfer trajectories p 36 N85-21228

Spacecraft Environmental Interactions Technology, 1983 p 39 N85-22470

Study of Kapton under simulated shuttle environment [NASA-CR-176003] p 41 N85-29997

Design principles for nickel hydrogen cells and batteries p 104 N85-31398

Life cycle test results of a bipolar nickel hydrogen battery p 105 N85-31406

## ECONOMIC ANALYSIS

Fuel cell power plant economic and operational considerations [ASME PAPER 84-AES-7] p 154 A85-21297

PM superalloys - A troubled adolescent? p 69 A85-44772

## EDDY CURRENTS

Eddy current jet engine disk-crack monitor p 120 A85-11100

Preliminary results on passive eddy current damper technology for SSME turbomachinery p 132 N85-26890

## EDDY VISCOSITY

SSME fuel preburner two-dimensional analysis p 51 N85-27943

## EDGES

A study of interply layer effects on the free edge stress field of angle-ply laminates p 55 A85-41127

A study of interply layer effects on the free-edge stress field of angle-ply laminates p 57 N85-15822

Ultrasonic testing of plates containing edge cracks [NASA-CR-3904] p 138 N85-29307

## EDUCATION

NASA Lewis Research Center/University Graduate Research Program on Engine Structures [NASA-TM-86916] p 145 N85-18375

## EFFICIENCY

Component-specific modeling p 20 N85-10971

Energy efficient engine. High pressure compressor detail design report [NASA-CR-165558] p 23 N85-10998

Sixty GHz IMPATT diode development [NASA-CR-174969] p 105 N85-33293

Lubrication and cooling for high speed gears [NASA-TM-87096] p 136 N85-34407

## ELASTIC BODIES

Development and testing of stable, invariant, isoparametric curvilinear 2- and 3-D hybrid-stress elements p 140 A85-19899

## ELASTIC DEFORMATION

Deformation and fracture behavior of Ni-Mo-Al(gamma/gamma prime-alpha) in situ composite p 64 A85-11058

On the existence and stability conditions for mixed-hybrid finite element solutions based on Reissner's variational principle p 142 A85-33847

Thermodynamically consistent constitutive equations for nonisothermal large strain, elasto-plastic, creep behavior [AIAA PAPER 85-0621] p 142 A85-38425

On local total strain redistribution using a simplified cyclic inelastic analysis based on an elastic solution [AIAA PAPER 85-1419] p 142 A85-39770

Fundamental tribological properties of ceramics [NASA-TM-86915] p 85 N85-15893

On local total strain redistribution using a simplified cyclic inelastic analysis based on an elastic solution [NASA-TM-86913] p 145 N85-21690

Hertzian contact in two and three dimensions [NASA-TP-2473] p 135 N85-32331

## ELASTIC MEDIA

Ultrasonic wave propagation in two-phase media - Spherical inclusions p 54 A85-11926

## ELASTIC PROPERTIES

A survey of unified constitutive theories p 150 N85-31531

On the use of internal state variables in thermoviscoplastic constitutive equations p 150 N85-31536

## ELASTIC SCATTERING

Fundamentals of microcrack nucleation mechanics [NASA-CR-3851] p 137 N85-16195

## ELASTIC WAVES

Fundamentals of microcrack nucleation mechanics [NASA-CR-3851] p 137 N85-16195

## ELASTOHYDRODYNAMICS

Elastohydrodynamic lubrication of line contacts p 126 A85-11069

Topological reaction rate measurements related to scuffing p 64 A85-11070

Fast numerical calculations of EHD sliding traction forces Application to rolling bearings [ASME PAPER 84-TRIB-26] p 127 A85-21289

Thermal elastohydrodynamic lubrication of line contacts p 128 A85-31202

Fast approach for calculating film thicknesses and pressures in elastohydrodynamically lubricated contacts at high loads p 117 N85-30242

Surface roughness effects in elastohydrodynamic contacts [NASA-TP-2488] p 134 N85-32329

Mechanics of a gaseous film barrier to lubricant wetting of elastohydrodynamically lubricated conjunctions [NASA-TP-2500] p 135 N85-32330

## ELASTOPLASTICITY

On stress field near a stationary crack tip [AD-A152863] p 141 A85-24532

Plasticity, viscoplasticity, and creep of solids by mechanical subelement models p 142 A85-35048

Thermodynamically consistent constitutive equations for nonisothermal large strain, elasto-plastic, creep behavior [AIAA PAPER 85-0621] p 142 A85-38425

Constitutive modeling and computational implementation for finite strain plasticity p 143 A85-40910

## HOST high temperature crack propagation

A review of path-independent integrals in elastic-plastic fracture mechanics, task 4 [NASA-CR-174956] p 152 N85-33541

## ELECTRIC ARCS

Metal vapor arc switch electromagnetic accelerator technology [NASA-CR-174380] p 103 N85-18259

Apparatus for producing diamond-like carbon flakes [NASA-CASE-LEW-13837-3] p 95 N85-20155

## ELECTRIC CONDUCTORS

Numerical simulation of positive-potential conductors in the presence of a plasma and a secondary-emitting dielectric p 102 A85-35306

An investigation of arc discharging on negatively biased dielectric conductor samples in a plasma p 180 N85-22498

## ELECTRIC CONTACTS

Screen printed interdigitated back contact solar cell [NASA-CASE-LEW-13414-1] p 160 N85-20530

## ELECTRIC DISCHARGES

Mass spectra of neutral particles released during electrical breakdown of thin polymer films p 88 N85-22511

## ELECTRIC ENERGY STORAGE

Cycling performance of the iron-chromium redox energy storage system [NASA-TM-87034] p 162 N85-27387

## ELECTRIC FILTERS

A fast time domain digital simulation technique for power converters - Application to a buck converter with feedforward compensation p 101 A85-20900

## ELECTRIC GENERATORS

Preliminary assessment of power-generating tethers in space and of propulsion for their orbit maintenance p 37 N85-22520

Free-piston Stirling engine/linear alternator 1000-hour endurance test [NASA-CR-174771] p 163 N85-30481

Experimental investigation of a variable speed constant frequency electric generating system from a utility perspective [NASA-CR-174950] p 105 N85-32251

## ELECTRIC HYBRID VEHICLES

Feasibility demonstration of a novel, flat-belt, continuously variable transmission or automotive and electric-hybrid vehicle application [NASA-CR-174430] p 185 N85-19894

## ELECTRIC MOTOR VEHICLES

Results of electric-vehicle propulsion system performance on three lead-acid battery systems p 156 A85-45443

## ELECTRIC POTENTIAL

Voltage controlling mechanisms in low resistivity silicon solar cells - A unified approach p 155 A85-35617

The effect of diffusion induced lattice stress on the open-circuit voltage in silicon solar cells p 181 A85-35620

Teardown analysis of a ten cell bipolar nickel-hydrogen battery p 156 A85-45385

Discharges on a negatively biased solar cell array in a charged-particle environment p 160 N85-22499

## ELECTRIC POWER

Measured effects of wind turbine generation at the Block Island Power Company p 153 A85-10652

## ELECTRIC POWER PLANTS

Fuel cell power plant economic and operational considerations [ASME PAPER 84-AES-7] p 154 A85-21297

Advanced multi-megawatt wind turbine design for utility application p 157 A85-45517

Manual of phosphoric acid fuel cell power plant optimization model and computer program [NASA-CR-174721] p 157 N85-10445

Phosphoric acid fuel cell power plant system performance model and computer program [NASA-CR-174638] p 157 N85-11456

## ELECTRIC POWER SUPPLIES

High voltage-high power components for large space power distribution systems p 45 A85-45370

High voltage requirements and issues for the 1990's -- for spacecraft power supplies p 46 A85-45429

Electric power - Photovoltaic or solar dynamic? p 46 A85-47042

A historical overview of the electrical power systems in the US manned and some US unmanned spacecraft [NASA-CR-174806] p 47 N85-13910

Experimental investigation of a variable speed constant frequency electric generating system from a utility perspective [NASA-CR-174950] p 105 N85-32251

Applicability of 100kWe-class of space reactor power systems to NASA manned space station missions [NASA-CR-174696] p 177 N85-35728

## ELECTRIC PROPULSION

Performance capabilities of the 12-centimeter Xenon ion thruster p 42 A85-16439

Extended performance technology study 30-cm thruster [NASA-CR-168259] p 48 N85-15806

High frequency plasma generator for ion thrusters [NASA-CR-174772] p 48 N85-17023

Preliminary assessment of power-generating tethers in space and of propulsion for their orbit maintenance p 37 N85-22520

Primary propulsion of electrothermal, ion and chemical systems for space-based radar orbit transfer [NASA-TM-87043] p 51 N85-27972

## ELECTRIC SWITCHES

Metal vapor arc switch electromagnetic accelerator technology [NASA-CR-174380] p 103 N85-18259

High-voltage, high-power, solid-state remote power controllers for aerospace applications [NASA-TP-2437] p 49 N85-21263

## ELECTRICAL FAULTS

Mass analysis of neutral particles and ions released during electrical breakdowns on spacecraft surfaces [NASA-CR-175585] p 39 N85-21250

Mass spectra of neutral particles released during electrical breakdown of thin polymer films p 88 N85-22511

## ELECTRICAL MEASUREMENT

Electrical characterization of plasma-grown oxides on gallium arsenide p 181 A85-32635

The high voltage silicon cell: A comparative analysis p 49 N85-22569

## ELECTRICAL RESISTIVITY

Theory of the high base resistivity n(+)/pp(+) silicon solar cell and its application to radiation damage effects p 154 A85-32639

Voltage controlling mechanisms in low resistivity silicon solar cells - A unified approach p 155 A85-35617

The effect of diffusion induced lattice stress on the open-circuit voltage in silicon solar cells p 181 A85-35620

Dynamics of graphite fiber intercalation: In situ resistivity measurements with a four point probe [NASA-TM-86858] p 53 N85-10105

Graphite fiber intercalation: Dynamics of the bromine intercalation process [NASA-TM-87015] p 53 N85-26921

## ELECTROCATALYSTS

Electrocatalyst advances for hydrogen oxidation in phosphoric acid fuel cells p 60 A85-15614

Preparation and evaluation of advanced catalysts for phosphoric acid fuel cells [NASA-CR-168223] p 160 N85-19511



- Regenerative fuel cell systems for space station  
p 104 N85-31372
- ELECTROCHEMICAL CELLS**  
Advanced nickel-hydrogen cell configuration study  
[NASA-CR-174775] p 157 N85-10444  
Cycling performance of the iron-chromium redox energy storage system  
[NASA-TM-87034] p 162 N85-27387
- ELECTROCHEMISTRY**  
Chemical and electrochemical behavior of the Cr(III)/Cr(II) half-cell in the iron-chromium redox energy storage system p 61 A85-33785  
NASA Redox Storage System Development Project  
[NASA-TM-83677] p 158 N85-12465  
Electrochemistry and storage p 62 N85-13889  
Raman structural studies of the nickel electrode  
[NASA-CR-175619] p 183 N85-23414  
Regenerative fuel cell systems for space station p 104 N85-31372  
System level electrochemical principles p 104 N85-31375
- ELECTRODE MATERIALS**  
Chemical and electrochemical behavior of the Cr(III)/Cr(II) half-cell in the iron-chromium redox energy storage system p 61 A85-33785  
Long life nickel electrodes for a nickel-hydrogen cell. III - Results of an accelerated test and failure analyses p 156 A85-45391  
Preparation and evaluation of advanced catalysts for phosphoric acid fuel cells  
[NASA-CR-168223] p 160 N85-19511
- ELECTRODEPOSITION**  
Film and interstitial formation of metals in plasma-sprayed ceramics  
[NASA-TM-86993] p 89 N85-22756
- ELECTRODES**  
Advanced designs for IPV nickel-hydrogen cells p 156 A85-45438  
Electric utility acid fuel cell stack technology advancement  
[NASA-CR-174804] p 159 N85-17422  
Raman structural studies of the nickel electrode  
[NASA-CR-175619] p 183 N85-23414  
The failure mechanism of a nickel electrode in a nickel-hydrogen cell p 105 N85-31408  
Electrode erosion in arc discharges at atmospheric pressure  
[NASA-TM-87087] p 52 N85-34178  
Development of electrodes for the NASA iron/chromium  
[NASA-CR-174724] p 165 N85-35471
- ELECTRODYNAMICS**  
Spacecraft Environmental Interactions Technology, 1983  
[NASA-CP-2359] p 39 N85-22470
- ELECTROHYDRAULIC FORMING**  
Results of an interlaboratory fatigue test program conducted on alloy 800H at room and elevated temperatures  
[NASA-CR-174940] p 152 N85-32340
- ELECTROHYDRODYNAMICS**  
Elastohydrodynamic lubrication calculations used as a tool to study scuffing  
[NASA-TM-87097] p 137 N85-34408
- ELECTROLYSIS**  
Engineering model system study for a regenerative fuel cell: Study report  
[NASA-CR-174801] p 158 N85-16292
- ELECTROLYTES**  
Develop and test fuel cell powered on-site integrated total energy systems. Phase 3: Full-scale power plant development  
[NASA-CR-168338] p 164 N85-30483
- ELECTROLYTIC CELLS**  
Engineering model system study for a regenerative fuel cell: Study report  
[NASA-CR-174801] p 158 N85-16292
- ELECTROMAGNETIC COMPATIBILITY**  
Design guidelines for assessing and controlling spacecraft charging effects p 40 N85-22500
- ELECTROMAGNETIC INTERFERENCE**  
On the subjective evaluation of the interference protection ratios' measurements for co-channel FM-TV signals p 96 A85-28241  
Adaptive antenna arrays for weak interfering signals  
[NASA-CR-174336] p 98 N85-17258
- ELECTROMAGNETIC NOISE MEASUREMENT**  
On the subjective evaluation of the interference protection ratios' measurements for co-channel FM-TV signals p 96 A85-28241
- ELECTROMAGNETIC PROPULSION**  
Preliminary analysis of space mission applications for electromagnetic launchers  
[NASA-CR-174067] p 35 N85-12071

- ELECTROMAGNETIC PULSES**  
Electro-impulse de-icing of a turbofan engine inlet  
[AIAA PAPER 85-1118] p 12 A85-40811  
Design guidelines for assessing and controlling spacecraft charging effects p 40 N85-22500
- ELECTROMAGNETIC SCATTERING**  
Numerical methods for analyzing electromagnetic scattering  
[NASA-CR-175507] p 99 N85-21438  
Analysis of the electromagnetic scattering from an inlet geometry with lossy walls  
[NASA-CR-175743] p 99 N85-25686
- ELECTRON BEAMS**  
Electron beam charging of Space Shuttle thermal protection system tiles p 39 N85-22478  
Electron yields from spacecraft materials p 40 N85-22512
- ELECTRON BOMBARDMENT**  
Ground correlation investigation of thruster/spacecraft interactions to be measured on the IAPS flight test p 42 A85-16408  
Performance capabilities of the 12-centimeter Xenon ion thruster p 42 A85-16439  
Aluminum work function: Effect of oxidation, mechanical scraping and ion bombardment  
[NASA-TM-87079] p 78 N85-34265
- ELECTRON CYCLOTRON HEATING**  
High frequency plasma generator for ion thrusters  
[NASA-CR-174772] p 48 N85-17023
- ELECTRON EMISSION**  
Plasma variables and tribological properties of coatings in low pressure (0.1 - 10.0 torr) plasma systems  
[NASA-TM-83798] p 94 N85-11261  
Textured carbon surfaces on copper  
[NASA-CASE-LEW-14130-1] p 95 N85-20156  
Electron yields from spacecraft materials p 40 N85-22512  
Hollow cathodes in high pressure arc discharges  
[NASA-TM-87098] p 52 N85-34179
- ELECTRON FLUX DENSITY**  
Three-dimensional calculation of shuttle charging in polar orbit p 40 N85-22486  
Polar orbit electrostatic charging of objects in shuttle wake p 40 N85-22487
- ELECTRON IRRADIATION**  
Effects of 1 MeV electrons and 10 MeV protons on the performance and reflectance of thin BSR cells --- back surface reflector p 182 A85-35699  
The effects of lithium counterdoping on radiation damage and annealing in n(+)-p silicon solar cells p 50 N85-22586
- ELECTRON MICROSCOPY**  
Friction and wear of some ferrous-base metallic glasses p 64 A85-11071  
Microstructures in rapidly solidified Ni-Mo alloys  
[NASA-TM-87100] p 78 N85-34266
- ELECTRON TRAJECTORIES**  
Theory of ion acceleration with closed electron drift --- in spacecraft plasma propulsion p 41 A85-15512
- ELECTRON TUNNELING**  
Inelastic tunnel diodes  
[NASA-CASE-LEW-13833-1] p 103 N85-21492
- ELECTRONIC CONTROL**  
A real-time FORTRAN implementation of a sensor failure detection, isolation and accommodation algorithm p 171 A85-47704
- ELECTRONIC MODULES**  
The study of microstrip antenna arrays and related problems  
[NASA-CR-174054] p 97 N85-11265
- ELECTRONIC RECORDING SYSTEMS**  
Moire deflectometry with deferred electronic heterodyne readout p 122 A85-42854
- ELECTROSTATIC ENGINES**  
Precision tunable resonant microwave cavity  
[NASA-CASE-LEW-13935-1] p 103 N85-20248
- ELECTROSTATIC PROBES**  
Numerical simulations of positively-biased probes and dielectric-conductor disks in a plasma --- for low earth orbit plasma densities p 179 A85-17262  
Ram-wake effects on plasma current collection of the PIX 2 Langmuir probe p 180 N85-22496
- ELECTROTHERMAL ENGINES**  
Electrothermal thruster diagnostics p 42 A85-16440  
Experiments with a microwave electrothermal thruster concept p 42 A85-16441  
The energetics of hydrogen atom recombination - Analysis, experiments, and modeling --- in electrothermal propulsion system p 179 A85-16444  
Investigation of a pulsed electrothermal thruster system  
[NASA-CR-174768] p 46 N85-11132  
Compatibility experiments of facilities, materials, and propellants for electrothermal thrusters  
[NASA-TM-86956] p 49 N85-21260

- ELLIPTIC FUNCTIONS**  
Two-dimensional internal compressible viscous flows using semi-elliptic analysis p 106 A85-11640
- ELLIPTICAL POLARIZATION**  
Polarization (ellipsometric) measurements of liquid condensate deposition and evaporation rates and dew points in flowing salt/ash-containing combustion gases p 123 A85-46925
- ELOGATION**  
Spherical microglass particle impingement studies of thermoplastic materials at normal incidence p 79 A85-11072
- EMISSION SPECTRA**  
Prism-coupled light emission from tunnel junctions p 181 A85-21425
- EMITTERS**  
Voltage controlling mechanisms in low resistivity silicon solar cells - A unified approach p 155 A85-35617  
Preliminary design of a 10 kW thermophotovoltaic system for space applications p 45 A85-45371
- ENDURANCE**  
IAPS (8-cm) ion thruster cyclic endurance test --- Ion Auxiliary Propulsion System p 42 A85-16406
- ENERGY ABSORPTION**  
Impact resistance of fiber composites  
Energy-absorbing mechanisms and environmental effects p 56 A85-46543
- ENERGY CONSERVATION**  
Energy efficient engine flight propulsion system preliminary analysis and design report  
[NASA-CR-174701] p 18 N85-10947  
Energy Efficient Engine Program technology benefit/cost study, volume 2 p 33 N85-35198  
[NASA-CR-174766-VOL-2] p 33 N85-35198  
Comparative analysis of operational forecasts versus actual weather conditions in airline flight planning, volume 1 p 167 N85-35534  
[NASA-CR-167862] p 167 N85-35534  
Comparative analysis of operational forecasts versus actual weather conditions in airline flight planning, volume 2 p 167 N85-35535  
[NASA-CR-167863] p 167 N85-35535  
Comparative analysis of operational forecasts versus actual weather conditions in airline flight planning, volume 3 p 167 N85-35536  
[NASA-CR-167864] p 167 N85-35536  
Comparative analysis of operational forecasts versus actual weather conditions in airline flight planning, volume 4 p 167 N85-35537  
[NASA-CR-167865] p 167 N85-35537  
Comparative analysis of operational forecasts versus actual weather conditions in airline flight planning: Summary report  
[NASA-CR-167866] p 168 N85-35538
- ENERGY CONSUMPTION**  
Wind tunnel results of advanced high speed propellers in the takeoff, climb, and landing operating regimes  
[AIAA PAPER 85-1259] p 6 A85-47025  
Wind tunnel results of advanced high speed propellers in the takeoff, climb and landing operating regimes  
[NASA-TM-87054] p 9 N85-29925
- ENERGY CONVERSION EFFICIENCY**  
Magnesium doping of efficient GaAs and Ga(0.75)In(0.25)As solar cells grown by metalorganic chemical vapor deposition p 180 A85-11466  
Measurements of energy distribution in microwave plasmas of N<sub>2</sub> and He and comparisons with results for H<sub>2</sub> p 178 A85-16443  
Effect of solar-cell junction geometry on open-circuit voltage p 154 A85-28080  
Fabrication of p(+)-n junction GaAs solar cells by a novel method p 181 A85-33645  
The NASA photovoltaic technology program p 155 A85-35604  
Method for evaluating wind turbine wake effects on wind farm performance p 155 A85-36750  
Energy efficient engine high pressure turbine test hardware detailed design report  
[NASA-CR-167955] p 23 N85-10995  
NASA Redox Storage System Development Project  
[NASA-TM-83677] p 158 N85-12465  
Overview of the 1985 NASA Lewis Research Center SP-100 free-piston Stirling engine activities  
[NASA-TM-87028] p 185 N85-27769  
Develop and test fuel cell powered on-site integrated total energy systems. Phase 3: Full-scale power plant development  
[NASA-CR-168338] p 164 N85-30483  
Energy Efficient Engine Program technology benefit/cost study, volume 1 p 33 N85-35197  
[NASA-CR-174766-VOL-1] p 33 N85-35197
- ENERGY DISTRIBUTION**  
Measurements of energy distribution in microwave plasmas of N<sub>2</sub> and He and comparisons with results for H<sub>2</sub> p 178 A85-16443



## ENERGY STORAGE

- A rotating superconducting solenoid for 100 kWh energy storage --- in space p 44 A85-33144
- Chemical and electrochemical behavior of the Cr(III)/Cr(II) half-cell in the iron-chromium redox energy storage system p 61 A85-33785
- Design considerations for a 10-kW integrated hydrogen-oxygen regenerative fuel cell system p 155 A85-45380
- Design of a 1-kWh bipolar nickel hydrogen battery p 155 A85-45384
- NASA Redox Storage System Development Project [NASA-TM-83677] p 158 A85-12465
- Regenerative fuel cell energy storage system for a low Earth orbit space station [NASA-CR-174802] p 158 A85-13371
- Engineering model system study for a regenerative fuel cell: Study report [NASA-CR-174801] p 158 A85-16292
- Operating characteristics of a 0.87 kW-hr flywheel energy storage module [NASA-TM-87038] p 133 A85-28371
- Regenerative fuel cell systems for space station p 104 A85-31372
- System level electrochemical principles p 104 A85-31375
- Evaluation of developmental membranes for the mixed reactant iron-chromium redox system [NASA-TM-87074] p 164 A85-34443

## ENERGY TECHNOLOGY

- Measured effects of wind turbine generation at the Block Island Power Company p 153 A85-10652
- Fuel cell power plant economic and operational considerations [ASME PAPER 84-AES-7] p 154 A85-21297
- Status of DOE and AID stand-alone photovoltaic system field tests p 155 A85-35707
- Parametric study of potential early commercial power plants Task 3-A MHD cost analysis [NASA-TM-175839] p 161 A85-27377

## ENGINE AIRFRAME INTEGRATION

- The Altitude Wind Tunnel (AWT) - A unique facility for propulsion system and adverse weather testing [AIAA PAPER 85-0314] p 34 A85-19661
- Energy efficient engine component development and integration program [NASA-CR-172846] p 31 A85-29958

## ENGINE ANALYZERS

- DEAN: A program for dynamic engine analysis [NASA-TM-87033] p 30 A85-28945

## ENGINE CONTROL

- The role of modern control theory in the design of controls for aircraft turbine engines p 13 A85-13627
- The use of Ada in distributed simulations p 169 A85-28612
- Multibus-based parallel processor for simulation p 169 A85-28613
- TF34 convertible engine control system design p 15 A85-32006
- A real-time FORTRAN implementation of a sensor failure detection, isolation and accommodation algorithm p 171 A85-47704
- Energy Efficient Engine (E3) controls and accessories detail design report [NASA-CR-168017] p 31 A85-29957

## ENGINE COOLANTS

- Vortex-generating coolant-flow-passage design for increased film-cooling effectiveness and surface coverage [NASA-TP-2388] p 113 A85-12314

## ENGINE DESIGN

- The role of modern control theory in the design of controls for aircraft turbine engines p 13 A85-13627
- Ceramic component development for the AGT101 gas turbine engine p 126 A85-15972
- Ceramic components for gas turbine engines p 127 A85-15973
- Computational thermo-fluid dynamics contributions to advanced gas turbine engine design [AIAA PAPER 85-0083] p 14 A85-19509
- Three-dimensional inviscid flow analysis of turbofan forced mixers [AIAA PAPER 85-0086] p 2 A85-19510
- Predicted turbine stage performance using quasi-three-dimensional and boundary-layer analyses p 15 A85-34013
- Main propulsion system design recommendations for an advanced Orbit Transfer Vehicle [AIAA PAPER 85-1336] p 36 A85-39730
- Stall recovery control strategy methodology and results [AIAA PAPER 85-1433] p 16 A85-40841
- Inviscid analysis of advanced turboprop propeller flow fields [AIAA PAPER 85-1263] p 6 A85-43977

## Mod II engine and technology development

- p 129 A85-45473
- Automotive Stirling engine systems development p 130 A85-45474
- Overview of NASA Lewis Research Center free-piston Stirling engine activities p 130 A85-45479
- Computational thermo-fluid dynamics contributions to advanced gas turbine engine design [NASA-TM-86865] p 18 A85-10069
- Energy efficient engine flight propulsion system preliminary analysis and design report [NASA-CR-174701] p 18 A85-10947
- Energy efficient engine component development and integration program [NASA-CR-170034] p 22 A85-10990
- Energy efficient engine ICLS Nacelle detail design report [NASA-CR-167870] p 22 A85-10993
- Energy efficient engine. Low pressure turbine test hardware detailed design report [NASA-CR-167956] p 22 A85-10994
- Energy efficient engine ICLS engine bearings, drives and configuration: Detail design report [NASA-CR-167871] p 23 A85-10997
- External fuel vaporization study, phase 2 [NASA-CR-174079] p 92 A85-11252
- Stirling material technology [NASA-TM-86888] p 72 A85-13007
- Advanced automotive diesel assessment program [NASA-CR-168285] p 130 A85-13235
- Fabrication and quality assurance processes for superhybrid composite fan blades [NASA-TM-83354] p 57 A85-14882
- Vehicle/engine integration --- orbit transfer vehicles p 37 A85-17008
- Advanced Gas Turbine (AGT) powertrain system development for automotive applications [NASA-CR-174809] p 185 A85-18831
- Creep-rupture behavior of iron superalloys in high-pressure hydrogen [NASA-CR-174411] p 74 A85-19078
- Analytical fuel property effects: Small combustors, phase 2 [NASA-CR-174848] p 93 A85-19175
- Initial testing of a variable-stroke Stirling engine [NASA-TM-86875] p 185 A85-19895
- Lubrication and performance of high-speed rolling-element bearings [NASA-TM-86958] p 131 A85-21658
- Ceramic applications in turbine engines [NASA-CR-174715] p 91 A85-28109
- Energy efficient engine. Fan and quarter-stage component performance report [NASA-CR-168070] p 33 A85-34141

## ENGINE FAILURE

- Contingency power concepts for helicopter turboshaft engine p 15 A85-32005
- Reusable rocket engine turbopump condition monitoring [SAE PAPER 841619] p 44 A85-39267
- A theory of post-stall transients in multistage axial compression systems [NASA-CR-3878] p 8 A85-21117
- Nonlinear global stability analysis of compressor stall phenomena [NASA-CR-174908] p 31 A85-29960

## ENGINE INLETS

- Icing tunnel tests of Electro-Impulse De-Icing of an engine inlet and high-speed wings [AIAA PAPER 85-0466] p 10 A85-20872
- Electro-impulse de-icing of a turbofan engine inlet [AIAA PAPER 85-1118] p 12 A85-40811
- Stall recovery control strategy methodology and results [AIAA PAPER 85-1433] p 16 A85-40841
- Effect of steady-state temperature distortion on inlet flow to a high-bypass-ratio turbofan engine [NASA-TM-86896] p 24 A85-15725
- Calculation of compressible flow about three-dimensional inlets with auxiliary inlets, slats and vanes by means of a panel method [NASA-CR-174975] p 10 A85-35162

## ENGINE MONITORING INSTRUMENTS

- Eddy current jet engine disk-crack monitor p 120 A85-11100
- Reusable rocket engine turbopump condition monitoring [SAE PAPER 841619] p 44 A85-39267
- ENGINE NOISE
- Comparison of scaled model data to full size energy efficient engine test results [AIAA PAPER 84-2281] p 13 A85-13953
- Measurement and prediction of Energy Efficient Engine noise [AIAA PAPER 84-2284] p 13 A85-13954

- Analysis of the effect on combustor noise measurements of acoustic waves reflected by the turbine and combustor inlet [AIAA PAPER 84-2323] p 173 A85-16103
- Energy efficient engine component development and integration program [NASA-CR-169496] p 22 A85-10989
- Turbofan noise generation. Volume 2: Computer programs [NASA-CR-167952] p 175 A85-11791
- Experimental investigation of shock-cell noise reduction for dual-stream nozzles in simulated flight [NASA-CR-3846] p 175 A85-13549
- Static jet noise test results of four 0.35 scale-model QCGAT mixer nozzles [NASA-TM-86871] p 175 A85-13551

## ENGINE PARTS

- Ceramic component development for the AGT101 gas turbine engine p 126 A85-15972
- Ceramic components for gas turbine engines p 127 A85-15973
- Considerations for damage analysis of gas turbine hot section components [ASME PAPER 84-PVP-77] p 14 A85-18792
- Finite element engine blade structural optimization [AIAA PAPER 85-0645] p 141 A85-30313
- Effect of low temperature on fatigue and fracture properties of Ti-5Al-2.5Sn(ELI) for use in engine components p 70 A85-47972
- Component-specific modeling p 20 A85-10971
- Constitutive model development for isotropic materials p 20 A85-10975
- Energy efficient engine ICLS engine bearings, drives and configuration: Detail design report [NASA-CR-167871] p 23 A85-10997
- An investigation of enhanced capability thermal barrier coating systems for diesel engine components [NASA-CR-174820] p 86 A85-18154
- Advanced Gas Turbine (AGT) powertrain system development for automotive applications [NASA-CR-174809] p 185 A85-18831
- Tribological systems as applied to aircraft engines [NASA-TM-86965] p 131 A85-21657
- Properties and microstructures for dual alloy combinations of three superalloys with alloy 901 [NASA-TM-86987] p 76 A85-26963
- Ceramic applications in turbine engines [NASA-CR-174715] p 91 A85-28109
- Energy efficient engine component development and integration program [NASA-CR-172846] p 31 A85-29958
- Creep fatigue life prediction for engine hot section materials (isotropic) [NASA-CR-168228] p 32 A85-31057
- Component-specific modeling [NASA-CR-174925] p 32 A85-32119

## ENGINE TESTING LABORATORIES

- The Altitude Wind Tunnel (AWT) - A unique facility for propulsion system and adverse weather testing [AIAA PAPER 85-0314] p 34 A85-19661

## ENGINE TESTS

- Eddy current jet engine disk-crack monitor p 120 A85-11100
- Comparison of scaled model data to full size energy efficient engine test results [AIAA PAPER 84-2281] p 13 A85-13953
- IAPS (8-cm) ion thruster cyclic endurance test --- Ion Auxiliary Propulsion System p 42 A85-16406
- Electrothermal thruster diagnostics p 42 A85-16440
- Altitude testing of a flight weight, self-cooled, 2D thrust vectoring exhaust nozzle [SAE PAPER 841557] p 14 A85-25984
- Inert gas test of two 12-cm magnetostatic thrusters p 43 A85-29310
- Temperature distortion generator for turboshaft engine testing [SAE PAPER 841541] p 15 A85-39065
- Performance characterization tests of a 1-kW resistojel using hydrogen, nitrogen and ammonia as propellants [AIAA PAPER 85-1159] p 44 A85-39628
- Initial results of sensitivity tests - Performed on the RE-1000 free-piston Stirling engine p 129 A85-45466
- Combustion system for radiation investigations p 21 A85-10986
- HOST liner cyclic facilities: Facility description p 22 A85-10988
- Energy efficient engine component development and integration program [NASA-CR-170034] p 22 A85-10990
- Advanced blade tip seal system, volume 2 [NASA-CR-167851] p 23 A85-10999
- Temperature distortion generator for turboshaft engine testing [NASA-TM-83748] p 1 A85-15658

- Integrated exhaust gas analysis system for aircraft turbine engine component testing [NASA-TP-2424] p 123 N85-16100
- Study of advanced fuel system concepts for commercial aircraft [NASA-CR-174751] p 12 N85-19978
- Ceramic applications in turbine engines [NASA-CR-174715] p 91 N85-28109
- Energy efficient engine high-pressure turbine component rig performance test report [NASA-CR-168189] p 30 N85-29955
- Free-piston Stirling engine/linear alternator 1000-hour endurance test [NASA-CR-174771] p 163 N85-30481
- Energy efficient engine. Fan and quarter-stage component performance report [NASA-CR-168070] p 33 N85-34141
- ENGINES**
- Effect of water on hydrogen permeability --- Stirling engines [NASA-TM-86904] p 53 N85-14864
- ENTHALPY**
- External fuel vaporization study, phase 2 [NASA-CR-174079] p 92 N85-11252
- ENVIRONMENT EFFECTS**
- High voltage requirements and issues for the 1990's --- for spacecraft power supplies p 46 A85-45429
- Impact resistance of fiber composites - Energy-absorbing mechanisms and environmental effects p 56 A85-46543
- ENVIRONMENT SIMULATION**
- The Altitude Wind Tunnel (AWT) - A unique facility for propulsion system and adverse weather testing [AIAA PAPER 85-0314] p 34 A85-19661
- Ribbon burner simulation of T-700 turbine shroud for ceramic lined seals research [NASA-TM-86940] p 114 N85-19364
- ENVIRONMENTAL TESTS**
- Ten year environmental test of glass fiber/epoxy pressure vessels [AIAA PAPER 85-1198] p 56 A85-47022
- Ten year environmental test of glass fiber/epoxy pressure vessels [NASA-TM-87058] p 58 N85-30034
- EPOXY COMPOUNDS**
- Ten year environmental test of glass fiber/epoxy pressure vessels [AIAA PAPER 85-1198] p 56 A85-47022
- Ten year environmental test of glass fiber/epoxy pressure vessels [NASA-TM-87058] p 58 N85-30034
- EPOXY MATRIX COMPOSITES**
- Imide modified epoxy matrix resins [NASA-CR-174695] p 85 N85-15892
- EPOXY RESINS**
- Fiberglass epoxy laminate fatigue properties at 300 and 20 K p 56 A85-47970
- Imide modified epoxy matrix resins [NASA-CR-174695] p 85 N85-15892
- EQUATIONS OF MOTION**
- Flutter of turbfan rotors with mistuned blades p 139 A85-12716
- Optimization of cascade blade mistuning. I - Equations of motion and basic inherent properties p 16 A85-42365
- Transition in Turbines [NASA-CP-2386] p 118 N85-31433
- EQUATIONS OF STATE**
- Universal binding energy relations in metallic adhesion [NASA-TM-86889] p 72 N85-12132
- EQUILIBRIUM FLOW**
- Reducing numerical diffusion for incompressible flow calculations [NASA-TM-83621] p 24 N85-14840
- Elastohydrodynamic lubrication calculations used as a tool to study scuffing [NASA-TM-87097] p 137 N85-34408
- EROSION**
- Spherical microglass particle impingement studies of thermoplastic materials at normal incidence p 79 A85-11072
- Deformation and erosion of f.c.c. metals and alloys under cavitation attack p 65 A85-12789
- Cathode degradation and erosion in high pressure arc discharges p 43 A85-16445
- A unified relation for cavitation erosion p 109 A85-24445
- High-temperature erosion of plasma-sprayed, yttria-stabilized zirconia in a simulated turbine environment [AIAA PAPER 85-1219] p 82 A85-39662
- Effect of surface configuration during solid particle impingement erosion p 69 A85-42568
- Characterization of solid particle erosion resistance of ductile metals based on their properties p 69 A85-42569
- High-temperature erosion of plasma-sprayed, yttria-stabilized zirconia in a simulated turbine environment [NASA-TP-2406] p 84 N85-13045
- Characterization of erosion of metallic materials under cavitation attack in a mineral oil [NASA-TM-86934] p 74 N85-19075
- Mechanical protection of DLC films on fused silica slides [NASA-TM-87056] p 91 N85-30138
- Electrode erosion in arc discharges at atmospheric pressure [NASA-TM-87087] p 52 N85-34178
- ERROR ANALYSIS**
- Finite difference methods for reducing numerical diffusion in TEACH-type calculations --- Teaching Elliptic Axisymmetric Characteristics Heuristically [AIAA PAPER 85-0057] p 108 A85-19488
- Calculation of confined swirling flows [AIAA PAPER 85-0060] p 108 A85-19491
- ERRORS**
- Optical linear algebra processors - Noise and error-source modeling p 169 A85-36727
- Error reduction program --- combustor performance evaluation codes [NASA-CR-174776] p 172 N85-27584
- Filter induced errors in laser anemometer measurements using counter processors [NASA-TM-87047] p 125 N85-30288
- Comparative analysis of operational forecasts versus actual weather conditions in airline flight planning, volume 4 [NASA-CR-167865] p 167 N85-35537
- Comparative analysis of operational forecasts versus actual weather conditions in airline flight planning: Summary report [NASA-CR-167866] p 168 N85-35538
- ETHANE**
- Shock tube measurements of growth constants in the branched-chain ethane-carbon monoxide-oxygen system [NASA-TM-87068] p 64 N85-32156
- EULER EQUATIONS OF MOTION**
- Efficient solution of the Euler and Navier-Stokes equations with a vectorized multiple-grid algorithm p 2 A85-18679
- Time dependent computation of the Euler equations for designing 2-D cascades, including the case of transonic shock free design p 5 A85-41814
- Researched applied to transonic compressors in numerical fluid mechanics of inviscid flow and viscous flow [NASA-CR-174353] p 114 N85-18291
- A convergent series expansion for hyperbolic systems of conservation laws [NASA-CR-172557] p 168 N85-21990
- Redistribution of the inlet temperature profile through the SSME fuel turbine p 50 N85-26901
- EUTECTIC ALLOYS**
- New eutectic alloys and their heats of transformation p 66 A85-27808
- EUTECTIC COMPOSITES**
- Deformation and fracture behavior of Ni-Mo-Al( $\gamma/\gamma'$ ) in situ composite p 64 A85-11058
- EVALUATION**
- Operational performance of the photovoltaic-powered grain mill and water pump at Tangaye, Burkina Faso (formerly Upper Volta) [NASA-TM-86970] p 161 N85-23243
- EVAPORATION**
- Measurements and predictions of the structure of evaporating sprays p 112 A85-46484
- EXHAUST DIFFUSERS**
- Energy efficient engine combustor test hardware detailed design report [NASA-CR-167945] p 18 N85-10950
- EXHAUST EMISSION**
- Energy efficient engine component development and integration program [NASA-CR-169496] p 22 N85-10989
- EXHAUST GASES**
- Overview of waste heat utilization systems [NASA-TM-86901] p 184 N85-13692
- Integrated exhaust gas analysis system for aircraft turbine engine component testing [NASA-TP-2424] p 123 N85-16100
- Comparative evaluation of three alternative power cycles for waste heat recovery from the exhaust of adiabatic diesel engines [NASA-TM-86953] p 186 N85-32043
- EXHAUST NOZZLES**
- Altitude testing of a flight weight, self-cooled, 2D thrust vectoring exhaust nozzle [SAE PAPER 841557] p 14 A85-25984
- The performance of jet noise suppression devices for industrial applications p 175 A85-42563
- A multiple-scales model of the shock-cell structure of imperfectly expanded supersonic jets p 113 A85-49354
- Static jet noise test results of four 0.35 scale-model OGCAT mixer nozzles [NASA-TM-86871] p 175 N85-13551
- EXISTENCE THEOREMS**
- Constructive existence and uniqueness for two-point boundary-value problems with a linear gradient term p 172 A85-28015
- EXPERIMENTATION**
- On thermomechanical testing in support of constitutive equation development for high temperature alloys [NASA-CR-174879] p 147 N85-25894
- EXPERT SYSTEMS**
- Composite loads spectra for select space propulsion structural components: Probabilistic load model development p 148 N85-27954
- EXTENSOMETERS**
- Some advances in experimentation supporting development of viscoplastic constitutive models [NASA-CR-174855] p 147 N85-27260
- Some advances in experimentation supporting development of viscoplastic constitutive models p 151 N85-31545
- Results of an interlaboratory fatigue test program conducted on alloy 800H at room and elevated temperatures [NASA-CR-174940] p 152 N85-32340
- EXTERNAL COMBUSTION ENGINES**
- Stirling material technology [NASA-TM-86888] p 72 N85-13007
- EXTERNAL SURFACE CURRENTS**
- Surface interactions and high-voltage current collection p 40 N85-22493
- EXTRUDING**
- High temperature properties of equiatomic FeAl with ternary additions [NASA-TM-86938] p 73 N85-19072
- F**
- FABRICATION**
- Ceramic components for gas turbine engines p 127 A85-15973
- Fabrication and quality assurance processes for superhybrid composite fan blades [NASA-TM-83354] p 57 N85-14882
- Effect of substituted phenylindimides on processing and properties of PMR polyimide composites [NASA-TM-86902] p 85 N85-14929
- Infrared technology for satellite power conversion --- antenna arrays and bolometers [NASA-CR-174266] p 159 N85-16293
- Investigation on experimental techniques to detect, locate and quantify gear noise in helicopter transmissions [NASA-CR-3847] p 176 N85-17667
- Extreme precision antenna reflector study results p 165 N85-23830
- Tape casting as an approach to an all-ceramic turbine shroud seal [NASA-TM-87078] p 135 N85-32333
- FABRY-PEROT INTERFEROMETERS**
- Remote displacement measurement using a passive interferometer with a fiber-optic link p 122 A85-42857
- FACE CENTERED CUBIC LATTICES**
- Deformation and erosion of f.c.c. metals and alloys under cavitation attack p 65 A85-12789
- Modeling of gamma/gamma-prime phase equilibrium in the nickel-aluminum system p 65 A85-14959
- FACTORIZATION**
- Augmented weak forms and element-by-element preconditioners: Efficient iterative strategies for structural finite elements. A preliminary study p 144 N85-10384
- FAILURE ANALYSIS**
- Sensor failure detection for jet engines using analytical redundancy [AIAA PAPER 84-1452] p 13 A85-16097
- Deposition stress effects on the life of thermal barrier coatings on burner rigs p 79 A85-19086
- Contingency power concepts for helicopter turboshaft engine p 15 A85-32005
- Tear-down analysis of a ten cell bipolar nickel-hydrogen battery p 156 A85-45385
- Long life nickel electrodes for a nickel-hydrogen cell. III - Results of an accelerated test and failure analyses p 156 A85-45391
- A design methodology for robust failure detection and isolation p 171 A85-47794
- Airfoil deposition model p 21 N85-10979
- Reusable rocket engine turbopump condition monitoring p 51 N85-26907
- The failure mechanism of a nickel electrode in a nickel-hydrogen cell p 105 N85-31408

- A comparison of two contemporary creep-fatigue life prediction methods p 151 N85-31538
- FAILURE MODES**
- Failure during thermal cycling of plasma-sprayed thermal barrier coatings p 81 A85-36246
- A design methodology for robust failure detection and isolation p 171 A85-47794
- A continuous damage model based on stepwise-stress creep rupture tests [NASA-CR-174941] p 152 N85-32341
- FAN BLADES**
- Finite element engine blade structural optimization [AIAA PAPER 85-0645] p 141 A85-30313
- Flutter of swept fan blades [ASME PAPER 84-GT-138] p 141 A85-32962
- Rotor wake characteristics of a transonic axial flow fan [AIAA PAPER 85-1133] p 6 A85-43974
- Energy efficient engine. Volume 2. Appendix A: Component development and integration program [NASA-CR-173085] p 22 N85-10991
- Fabrication and quality assurance processes for superhybrid composite fan blades [NASA-TM-83354] p 57 N85-14882
- Effects of vane/blade ratio and spacing on fan noise, volume 1 [NASA-CR-174664] p 176 N85-19791
- Effects of vane/blade ratio and spacing on fan noise. Volume 2: Data supplement [NASA-CR-174665] p 176 N85-19792
- Energy Efficient Engine Program technology benefit/cost study, volume 1 [NASA-CR-174766-VOL-1] p 33 N85-35197
- FAN FIELDS**
- Case study of sample spacing in planar near-field measurement of high gain antennas [NASA-TM-86872] p 97 N85-10234
- FATIGUE (MATERIALS)**
- Spherical microglass particle impingement studies of thermoplastic materials at normal incidence p 79 A85-11072
- Fatigue criterion to system design, life and reliability [AIAA PAPER 85-1140] p 143 A85-40814
- Turbine Engine Hot Section Technology (HOST) [NASA-TM-83022] p 18 N85-10951
- Experimental compliance calibration of the NASA Lewis Research Center Mode 2 fatigue specimen [NASA-TM-86908] p 144 N85-16205
- Fatigue criterion to system design, life and reliability [NASA-TM-87017] p 132 N85-27226
- Elevated temperature biaxial fatigue [NASA-CR-175795] p 148 N85-27263
- Structural Integrity and Durability of Reusable Space Propulsion Systems [NASA-CP-2381] p 51 N85-27941
- Interaction of high-cycle and low-cycle fatigue of Haynes 188 alloy at 1400 F deg p 149 N85-27961
- Reexamination of cumulative fatigue damage laws p 149 N85-27962
- Two simplified procedures for predicting cyclic material response from a strain history p 151 N85-31543
- Application of traction drives as servo mechanisms p 152 N85-33520
- FATIGUE LIFE**
- Strainrange partitioning - A total strain range version --- for creep fatigue life prediction by summing inelastic and elastic strain-range-life relations for two Ni base superalloys p 64 A85-11603
- A study of fatigue damage mechanisms in Waspaloy from 25 to 800 C p 65 A85-12098
- Considerations for damage analysis of gas turbine hot section components [ASME PAPER 84-PVP-77] p 14 A85-18792
- A history dependent damage model for low cycle fatigue [ASME PAPER 84-PVP-112] p 140 A85-18795
- Fracture toughness of hot-pressed beryllium p 66 A85-25835
- Simplified design and life prediction of rocket thrust chambers p 44 A85-29314
- On the fatigue crack propagation behavior of superalloys at intermediate temperatures p 68 A85-32434
- Application of two creep fatigue life models for the prediction of elevated temperature crack initiation of a nickel base alloy [AIAA PAPER 85-1420] p 69 A85-43979
- Fiberglass epoxy laminate fatigue properties at 300 and 20 K p 56 A85-47970
- Life prediction and constitutive behavior: Overview p 20 N85-10973
- Effect of lubricant extreme-pressure additives on surface fatigue life of AISI 9310 spur gears [NASA-TP-2408] p 130 N85-13234
- Thermal-mechanical fatigue crack growth in Inconel X-750 [NASA-CR-174740] p 72 N85-15877

- Fundamentals of microcrack nucleation mechanics [NASA-CR-3851] p 137 N85-16195
- Fatigue life analysis of a turboprop reduction gearbox [NASA-TM-87014] p 133 N85-27228
- Creep fatigue life prediction for engine hot section materials (isotropic) [NASA-CR-168228] p 32 N85-31057
- Effect of speed and press fit on fatigue life of roller-bearing inner-race contact [NASA-TP-2496] p 134 N85-31511
- A comparison of two contemporary creep-fatigue life prediction methods p 151 N85-31538
- FATIGUE TESTS**
- Hygrothermomechanical evaluation of transverse filament tape epoxy/polyester fiberglass composites p 54 A85-15632
- Engine cyclic durability by analysis and material testing p 25 N85-15744
- Effect of five lubricants on life of AISI 9310 spur gears [NASA-TP-2419] p 123 N85-16099
- Low cycle fatigue of MAR-M 200 single crystals at 760 and 870 deg C [NASA-TM-86933] p 74 N85-19074
- Lubricant and additive effects on spur gear fatigue life [NASA-TM-87044] p 133 N85-28373
- Results of an interlaboratory fatigue test program conducted on alloy 800H at room and elevated temperatures [NASA-CR-174940] p 152 N85-32340
- FEASIBILITY**
- Initial feasibility ground test of a proposed photogrammetric system for measuring the shapes of ice accretions on helicopter rotor blades during forward flight [NASA-TM-87391] p 12 N85-12887
- FEASIBILITY ANALYSIS**
- Feasibility study of the welding of SiC p 81 A85-39339
- Research on gallium arsenide diffused junction solar cells [NASA-CR-174057] p 158 N85-11457
- Diffusion welding of Cassegrainian concentrator cell stack assemblies [NASA-CR-176104] p 164 N85-33566
- FEEDBACK**
- Feedback in separated flows over symmetric airfoils [AIAA PAPER 84-2297] p 3 A85-28899
- FEEDBACK CONTROL**
- Identification of multivariable high-performance turbofan engine dynamics from closed-loop data p 13 A85-13630
- Closed-loop strain controlled testing at elevated temperatures with a non-contacting gage p 121 A85-29562
- Small-signal model for the series resonant converter p 102 A85-39453
- FEEDFORWARD CONTROL**
- A fast time domain digital simulation technique for power converters - Application to a buck converter with feedforward compensation p 101 A85-20900
- FERRIC IONS**
- Dynamics of graphite fiber intercalation: In situ resistivity measurements with a four point probe [NASA-TM-86858] p 53 N85-10105
- FERRITES**
- Fundamental tribological properties of ceramics [NASA-TM-86915] p 85 N85-15893
- Humidity effects on adhesion of nickel-zinc ferrite in elastic contact with magnetic tape and itself [NASA-TP-2449] p 88 N85-21359
- Effects of wear on structure-sensitive magnetic properties of ceramic ferrite in contact with magnetic tape [NASA-TM-87007] p 90 N85-26991
- FERROUS METALS**
- Friction and wear of some ferrous-base metallic glasses p 64 A85-11071
- FIBER COMPOSITES**
- Acoustic structure and propagation in highly porous, layered, fibrous materials p 173 A85-12301
- Select fiber composites for space applications - A mechanistic assessment p 54 A85-16040
- ICAN - Integrated composites analyzer [AIAA PAPER 84-0974] p 54 A85-16094
- Interply layer degradation effects on composite structural response [AIAA PAPER 84-0849] p 54 A85-16096
- Interply layer degradation effects on composite structural response p 55 A85-39215
- Impact resistance of fiber composites - Energy-absorbing mechanisms and environmental effects p 56 A85-46543
- Fundamental studies of composite toughness p 56 N85-12948

- Design procedures for fiber composite structural components: Panels subjected to combined in-plane loads [NASA-TM-86909] p 57 N85-15823
- Tribological properties of graphite-fiber-reinforced, partially fluorinated polyimide composites [NASA-TM-86926] p 86 N85-18153
- Homogeneity of pristine and bromine intercalated graphite fibers [NASA-TM-87016] p 89 N85-25521
- Designing for fiber composite structural durability in hygrothermomechanical environment [NASA-TM-87045] p 58 N85-27978
- Arc spray fabrication of metal matrix composite monolayer [NASA-CASE-LEW-13828-1] p 58 N85-30027
- Structural characteristics of high temperature composites [NASA-CR-175998] p 58 N85-30037
- FIBER OPTICS**
- Fiber optic temperature sensor p 121 A85-29563
- Remote displacement measurement using a passive interferometer with a fiber-optic link p 122 A85-42857
- High-temperature fiber optic pressure sensor p 123 A85-46607
- High-temperature optically activated GaAs power switching for aircraft digital electronic control [NASA-CR-174711] p 34 N85-12901
- Fiber optic, Fabry-Perot high temperature sensor [NASA-CR-174712] p 178 N85-13594
- Reusable rocket engine turbopump condition monitoring p 51 N85-26907
- FIBER REINFORCED COMPOSITES**
- Use of static indentation laws in the impact analysis of laminated composite plates p 55 A85-29133
- Ten year environmental test of glass fiber/epoxy pressure vessels [AIAA PAPER 85-1198] p 56 A85-47022
- Nonlinear analysis for high-temperature multilayered fiber composite structures --- turbine blades [NASA-TM-83754] p 57 N85-21273
- Nonlinear structural analysis for fiber-reinforced superalloy turbine blades p 147 N85-26887
- Ten year environmental test of glass fiber/epoxy pressure vessels [NASA-TM-87058] p 58 N85-30034
- Mechanical properties of SiC fiber-reinforced reaction-bonded Si3N4 composites [NASA-TM-87085] p 59 N85-34223
- FIBER STRENGTH**
- Fibers for structurally reliable metal and ceramic composites p 55 A85-37484
- High performance fibers for structurally reliable metal and ceramic composites --- advanced gas turbine engine materials [NASA-TM-86878] p 56 N85-12095
- FIBERS**
- Oscillatory conductive heat transfer for a fiber in an ideal gas p 109 A85-26077
- Dynamics of graphite fiber intercalation: In situ resistivity measurements with a four point probe [NASA-TM-86858] p 53 N85-10105
- Stability of bromine intercalated graphite fibers [NASA-TM-86859] p 84 N85-10187
- Creep of chemically vapor deposited SiC fibers [NASA-TM-86897] p 56 N85-14878
- A micrographic and gravimetric study of intercalation and deintercalation of graphite fibers [NASA-TM-87026] p 91 N85-28110
- FIELD EFFECT TRANSISTORS**
- Bipolar-FET combinational power transistors for power conversion applications p 100 A85-12669
- High-temperature optically activated GaAs power switching for aircraft digital electronic control [NASA-CR-174711] p 34 N85-12901
- High-voltage, high-power, solid-state remote power controllers for aerospace applications [NASA-TP-2437] p 49 N85-21263
- FIELD EMISSION**
- Apparatus for mounting a field emission cathode [NASA-CASE-LEW-14108-1] p 104 N85-29149
- FILM COOLING**
- Advanced liner-cooling techniques for gas turbine combustors [AIAA PAPER 85-1290] p 15 A85-39703
- Heat transfer and turbulence measurements of a film-cooled flow over a convexly curved surface p 112 A85-41787
- Vortex-generating coolant-flow-passage design for increased film-cooling effectiveness and surface coverage [NASA-TP-2388] p 113 N85-12314
- Heat transfer results and operational characteristics of the NASA Lewis Research Center Hot Section Cascade Test Facility [NASA-TM-86890] p 114 N85-15133

- Flow visualization study of the effect of injection hole geometry on an inclined jet in crossflow  
[NASA-TM-86936] p 115 N85-20269
- Advanced liner-cooling techniques for gas turbine combustors  
[NASA-TM-86952] p 8 N85-21115
- Vortex generating flow passage design for increased film cooling effectiveness  
[NASA-CASE-LEW-14039-1] p 119 N85-33433
- FILM THICKNESS**
- Thermal elastohydrodynamic lubrication of line contacts  
p 128 A85-31202
- The scattering of ultrasonic third sound from substrate surface defects  
p 174 A85-36047
- Fast approach for calculating film thicknesses and pressures in elastohydrodynamically lubricated contacts at high loads  
[NASA-TM-87032] p 117 N85-30242
- FINITE DIFFERENCE THEORY**
- Time dependent wave envelope finite difference analysis of sound propagation  
[AIAA PAPER 84-2285] p 173 A85-16102
- Finite difference methods for reducing numerical diffusion in TEACH-type calculations --- Teaching Elliptic Axisymmetric Characteristics Heuristically  
[AIAA PAPER 85-0057] p 108 A85-19488
- Finite difference analysis of torsional vibrations of pretwisted, rotating, cantilever beams with effects of warping  
p 143 A85-42047
- Researched applied to transonic compressors in numerical fluid mechanics of inviscid flow and viscous flow  
[NASA-CR-174353] p 114 N85-18291
- Vibration and buckling of rotating, pretwisted, precone beams including Coriolis effects  
[NASA-TM-87004] p 146 N85-25893
- A computer analysis program for interfacing thermal and structural codes  
[NASA-TM-87021] p 148 N85-27264
- Error reduction program --- combustor performance evaluation codes  
[NASA-CR-174776] p 172 N85-27584
- FINITE ELEMENT METHOD**
- Analysis of hourglass instabilities and control in underintegrated finite element methods  
p 139 A85-11125
- A finite element solution of three-dimensional inviscid rotational flows through curved ducts  
p 107 A85-11648
- Rational approach for assumed stress finite elements  
p 139 A85-12029
- Hybrid Semiloof elements for plates and shells based upon a modified Hu-Washizu principle  
p 139 A85-15893
- Hybrid stress finite elements for large deformations of inelastic solids  
p 139 A85-15894
- Development and testing of stable, invariant, isoparametric curvilinear 2- and 3-D hybrid-stress elements  
p 140 A85-19899
- On the development of hierarchical solution strategies for nonlinear finite element formulations  
p 171 A85-21979
- A simplified method for elastic-plastic-creep structural analysis  
[ASME PAPER 84-GT-191] p 141 A85-23150
- Finite element engine blade structural optimization  
[AIAA PAPER 85-0645] p 141 A85-30313
- Natural frequencies of twisted rotating plates  
p 141 A85-32343
- On the existence and stability conditions for mixed-hybrid finite element solutions based on Reissner's variational principle  
p 142 A85-33847
- Evolution of assumed stress hybrid finite element  
p 142 A85-35046
- Plasticity, viscoplasticity, and creep of solids by mechanical subelement models  
p 142 A85-35048
- Pantographing self adaptive gap elements  
p 142 A85-37440
- Unified constitutive material models for nonlinear finite-element structural analysis --- gas turbine engine blades and vanes  
[AIAA PAPER 85-1418] p 142 A85-39769
- Axisymmetric solid elements by a rational hybrid stress method  
p 143 A85-41109
- A study of interply layer effects on the free edge stress field of angle-ply laminates  
p 55 A85-41127
- Impact resistance of fiber composites  
p 56 A85-46543
- Energy-absorbing mechanisms and environmental effects  
p 56 A85-46543
- Stability, accuracy, and efficiency of some underintegrated methods in finite element computations  
p 172 A85-50073
- Augmented weak forms and element-by-element preconditioners: Efficient iterative strategies for structural finite elements. A preliminary study  
p 144 N85-10384
- Constitutive model development for isotropic materials  
p 20 N85-10975
- A study of interply layer effects on the free-edge stress field of angle-ply laminates  
[NASA-TM-86924] p 57 N85-15822
- Analytical and experimental investigation of rubbing interaction in labyrinth seals for a liquid hydrogen fuel pump --- space shuttle main engine  
[NASA-CR-174657] p 48 N85-18084
- Local strain redistribution corrections for a simplified inelastic analysis procedure based on an elastic finite-element analysis  
[NASA-TP-2421] p 145 N85-20396
- Advanced stress analysis methods applicable to turbine engine structures  
[NASA-CR-175573] p 26 N85-21165
- Nonlinear analysis for high-temperature multilayered fiber composite structures --- turbine blades  
[NASA-TM-83754] p 57 N85-21273
- 3-D inelastic analysis methods for hot section components (base program) --- turbine blades, turbine vanes, and combustor liners  
[NASA-CR-174700] p 145 N85-21686
- Recent advances in hybrid/mixed finite elements  
[NASA-CR-175574] p 145 N85-21687
- Geometrically nonlinear analysis of laminated elastic structures  
[NASA-CR-175609] p 146 N85-21720
- On Hybrid and mixed finite element methods  
[NASA-CR-175551] p 146 N85-23096
- Unified constitutive material models for nonlinear finite-element structural analysis --- gas turbine engine blades and vanes  
[NASA-TM-86985] p 146 N85-24338
- A computer analysis program for interfacing thermal and structural codes  
[NASA-TM-87021] p 148 N85-27264
- Probabilistic finite element development  
p 149 N85-27956
- Probabilistic finite element: Variational theory  
p 149 N85-27957
- Designing for fiber composite structural durability in hygrothermomechanical environment  
[NASA-TM-87045] p 58 N85-27978
- A review of path-independent integrals in elastic-plastic fracture mechanics, task 4  
[NASA-CR-174956] p 152 N85-33541
- Thermal stress analysis of a new turbine shroud seal concept  
[NASA-TM-87082] p 136 N85-34406
- FINITE VOLUME METHOD**
- Thermodynamic evaluation of transonic compressor rotors using the finite volume approach  
[NASA-CR-175811] p 29 N85-26712
- FINS**
- The effect of channel convergence on heat transfer in a passage with short pin fins  
[NASA-TM-83801] p 113 N85-10303
- FLAME HOLDERS**
- The mechanisms of flame holding in the wake of a bluff body  
[NASA-CR-3866] p 26 N85-21166
- FLAME PROPAGATION**
- The influence of combustion liner holes on noise production by ducted burners  
[AIAA PAPER 84-2322] p 172 A85-10869
- Gravitational effects on flames spreading over thick solid surfaces  
[IAF PAPER 84-154] p 59 A85-13092
- Flame flashback in a premixed dump combustor  
[AIAA PAPER 85-0145] p 60 A85-19550
- Drop-turbulence interactions in a diffusion flame  
[AIAA PAPER 85-0319] p 60 A85-19665
- Growth of a diffusion flame in the field of a vortex  
p 61 A85-47320
- Behavior of the lean methane-air flame at zero-gravity  
[NASA-CR-175586] p 62 N85-21283
- FLAME SPECTROSCOPY**
- Flame radiation and linear heat transfer in a tubular-can combustor  
p 15 A85-39580
- Polarization (ellipsometric) measurements of liquid condensate deposition and evaporation rates and dew points in flowing salt/ash-containing combustion gases  
p 123 A85-46925
- Shock tube measurements of growth constants in the branched-chain ethane-carbon monoxide-oxygen system  
[NASA-TM-87068] p 64 N85-32156
- FLAME SPRAYING**
- Drop-turbulence interactions in a diffusion flame  
[AIAA PAPER 85-0319] p 60 A85-19665
- Thermal barrier coating system  
[NASA-CASE-LEW-14057-1] p 59 N85-35233
- FLAME STABILITY**
- The mechanisms of flame holding in the wake of a bluff body  
[NASA-CR-3866] p 26 N85-21166
- FLAMEOUT**
- The mechanisms of flame holding in the wake of a bluff body  
[NASA-CR-174058] p 62 N85-11149
- FLAMES**
- A theoretical prediction of the acoustic pressure generated by turbulence-flame front interactions  
[ASME PAPER 84-WA/NCA-11] p 174 A85-39909
- The structure of dilute combustor sprays  
[NASA-CR-174838] p 24 N85-15728
- Behavior of the lean methane-air flame at zero-gravity  
[NASA-CR-175586] p 62 N85-21283
- FLAMMABILITY**
- Effect of gravity on halogenated hydrocarbon flame retardant effectiveness  
[IAF PAPER 84-156] p 61 A85-23199
- The use of a laser Doppler velocimeter in a standard flammability tube  
[NASA-CR-174960] p 125 N85-35389
- FLASHBACK**
- Flame flashback in a premixed dump combustor  
[AIAA PAPER 85-0145] p 60 A85-19550
- FLAT PLATES**
- Resonance in flows with vortex sheets and edges  
p 1 A85-10357
- Vortex induced lift on a flat plate with a curved forward-facing flap  
p 4 A85-30175
- Heat transfer investigation in the junction region of circular cylinder normal to a flat plate at 90 deg location  
[ASME PAPER 84-WA/HT-70] p 111 A85-39898
- FLEXIBILITY**
- Vibration and flutter of mistuned bladed-disk assemblies  
[AIAA PAPER 84-0991] p 139 A85-16095
- FLEXING**
- Graphite/PMR polyimide composites with improved toughness  
[NASA-TM-87081] p 58 N85-32148
- Reliability of two sintered silicon nitride materials  
[NASA-TM-87092] p 92 N85-34284
- FLIGHT CHARACTERISTICS**
- Performance degradation of helicopter rotor in forward flight due to ice  
p 11 A85-42937
- FLIGHT CONDITIONS**
- GASP cloud encounter statistics - Implications for laminar flow control flight  
p 166 A85-11979
- The Altitude Wind Tunnel (AWT): A unique facility for propulsion system and adverse weather testing  
[NASA-TM-86921] p 35 N85-18067
- FLIGHT CONTROL**
- Advanced secondary power system for transport aircraft  
[NASA-TP-2463] p 30 N85-28944
- FLIGHT HAZARDS**
- Experimental aerodynamic characteristics of an NACA 0012 airfoil with simulated ice  
p 12 A85-21844
- FLIGHT PATHS**
- Comparative analysis of operational forecasts versus actual weather conditions in airline flight planning, volume 2  
[NASA-CR-167863] p 167 N85-35535
- Comparative analysis of operational forecasts versus actual weather conditions in airline flight planning, volume 3  
[NASA-CR-167864] p 167 N85-35536
- Comparative analysis of operational forecasts versus actual weather conditions in airline flight planning, volume 4  
[NASA-CR-167865] p 167 N85-35537
- Comparative analysis of operational forecasts versus actual weather conditions in airline flight planning: Summary report  
[NASA-CR-167866] p 168 N85-35538
- FLIGHT PLANS**
- Comparative analysis of operational forecasts versus actual weather conditions in airline flight planning, volume 1  
[NASA-CR-167862] p 167 N85-35534
- Comparative analysis of operational forecasts versus actual weather conditions in airline flight planning, volume 2  
[NASA-CR-167863] p 167 N85-35535
- Comparative analysis of operational forecasts versus actual weather conditions in airline flight planning: Summary report  
[NASA-CR-167866] p 168 N85-35538
- FLIGHT SIMULATION**
- Comparative analysis of operational forecasts versus actual weather conditions in airline flight planning, volume 2  
[NASA-CR-167863] p 167 N85-35535
- FLIGHT TESTS**
- Ground correlation investigation of thruster/spacecraft interactions to be measured on the IAPS flight test  
p 42 A85-16408

The UH-1H helicopter icing flight test program - An overview  
[AIAA PAPER 85-0338] p 11 A85-28898

The UH-1H helicopter icing flight test program: An overview  
[NASA-TM-86925] p 11 N85-15702

**FLOATING POINT ARITHMETIC**  
Floating-point function generation routines for 16-bit microcomputers  
[NASA-TM-83783] p 170 N85-10683

**FLOW CHARACTERISTICS**  
Acoustic structure and propagation in highly porous, layered, fibrous materials p 173 A85-12301  
Analytical modeling of circuit aerodynamics in the new NASA Lewis Altitude Wind Tunnel  
[AIAA PAPER 85-0380] p 3 A85-26389  
Flow through very porous inclined screens  
[AIAA PAPER 85-1650] p 111 A85-40750  
Coolant passage heat transfer with rotation p 20 N85-10968  
Vortex-generating coolant-flow-passage design for increased film-cooling effectiveness and surface coverage  
[NASA-TP-2388] p 113 N85-12314  
Analytical modeling of circuit aerodynamics in the new NASA Lewis wind tunnel  
[NASA-TM-86912] p 8 N85-15688  
Flow through very porous inclined screens  
[NASA-TM-86979] p 116 N85-25761  
Fuel and oxidizer turbine loss analysis p 50 N85-26900  
Detailed studies of aviation fuel flowability  
[NASA-CR-174938] p 94 N85-31308  
Transition in Turbines  
[NASA-CP-2386] p 118 N85-31433

**FLOW COEFFICIENTS**  
Generation of instability waves in flows separating from smooth surfaces p 1 A85-10352  
Analysis of experimental shaft seal data for high-performance turbomachines, as for Space Shuttle main engines  
[NASA-TM-86928] p 115 N85-21569

**FLOW DISTRIBUTION**  
An experimental study of tone excited heated jets  
[AIAA PAPER 84-2341] p 172 A85-10882  
Assessment of three-dimensional inviscid codes and loss calculations for turbine aerodynamic computations  
[ASME PAPER 84-GT-187] p 4 A85-32961  
Turbulence measurements of lateral jet injection into confined tubular crossflow  
[AIAA PAPER 85-1102] p 110 A85-39604  
Inviscid analysis of advanced turboprop propeller flow fields  
[AIAA PAPER 85-1263] p 6 A85-43977  
Inviscid and viscous flows in cascades with an explicit multiple-grid algorithm p 7 A85-48539  
Hot section laser anemometry p 19 N85-10962  
Energy efficient engine high pressure turbine test hardware detailed design report  
[NASA-CR-167955] p 23 N85-10995  
Effect of two inner-ring oil-flow distribution schemes on the operating characteristics of a 35 millimeter bore ball bearing to 2.5 million DN  
[NASA-TP-2404] p 130 N85-13233  
A three-dimensional axisymmetric calculation procedure for turbulent flows in a radial vaneless diffuser  
[NASA-TM-86903] p 7 N85-14798  
The boundary layer on compressor cascade blades  
[NASA-CR-174369] p 114 N85-18292  
Investigation of flowfields found in typical combustor geometries  
[NASA-CR-3869] p 26 N85-21167  
The influence of jet-grid turbulence on heat transfer from the stagnation region of a cylinder in crossflow  
[NASA-TM-87011] p 115 N85-25760  
Turbulence characteristics of swirling flowfields  
[NASA-CR-174918] p 29 N85-26717  
Predictions and measurements of isothermal flowfields in axisymmetric combustor geometries  
[NASA-CR-174916] p 29 N85-27867  
Simulation of multistage turbine flows p 116 N85-27945  
Feasibility of mapping velocity flow fields in SSME powerhead by laser anemometry techniques p 41 N85-27971  
General design method for 3-dimensional, potential flow fields. Part 2: Computer program DIN3D1 for simple, unbranched ducts  
[NASA-CR-3926] p 10 N85-35159  
Calculation of compressible flow about three-dimensional inlets with auxiliary inlets, slats and vanes by means of a panel method  
[NASA-CR-174975] p 10 N85-35162

**FLOW EQUATIONS**  
A two-equation turbulence model for two-phase jets p 107 A85-14376

**FLOW GEOMETRY**  
Computation and turbulence closure models for shear flows in rotating curved bodies p 107 A85-14349  
Flow control in a diffusing S-Duct  
[AIAA PAPER 85-0524] p 3 A85-25928  
Structure of ducted particle-laden turbulent jets p 110 A85-38999  
Numerical calculation of subsonic jets in crossflow with reduced numerical diffusion  
[AIAA PAPER 85-1441] p 110 A85-39780  
Turbulence modelling for complex shear flows  
[AIAA PAPER 85-1652] p 111 A85-40752  
An improved computer model for prediction of axial gas turbine performance losses  
[NASA-CR-174246] p 24 N85-15724  
Numerical calculation of subsonic jets in crossflow with reduced numerical diffusion  
[NASA-TM-87003] p 27 N85-25263

**FLOW MEASUREMENT**  
An experimental study of tone excited heated jets  
[AIAA PAPER 84-2341] p 172 A85-10882  
Flow control in a diffusing S-Duct  
[AIAA PAPER 85-0524] p 3 A85-25928  
An experimental study of three-dimensional shock wave/turbulent boundary layer interactions in a supersonic flow  
[AIAA PAPER 85-1566] p 5 A85-40691  
Measurements and predictions of the structure of evaporating sprays p 112 A85-46484  
Holographic optical system for aberration corrections in laser Doppler velocimetry p 123 A85-48659  
Velocity visualization in gaseous flows  
[NASA-CR-174954] p 119 N85-31445

**FLOW REGULATORS**  
Flow through very porous inclined screens  
[AIAA PAPER 85-1650] p 111 A85-40750  
Flow through very porous inclined screens  
[NASA-TM-86979] p 116 N85-25761

**FLOW STABILITY**  
Generation of instability waves in flows separating from smooth surfaces p 1 A85-10352  
The linear two-dimensional stability of inviscid vortex streets of finite-cored vortices  
[AD-A153032] p 107 A85-14241  
Some unique experiments on receptivity --- for forced disturbances entering shear flow  
[AIAA PAPER 85-0533] p 174 A85-25932  
Generation of capillary instabilities by external disturbances in a liquid jet  
[NASA-TM-87041] p 117 N85-30246

**FLOW VELOCITY**  
Velocity visualization in gas flows using laser-induced phosphorescence of biacetyl p 121 A85-21695  
Into mesh lubrication of spur gears with arbitrary offset oil jet. I - For jet velocity less than or equal to gear velocity p 128 A85-24497  
Structure of particle-laden jets - Measurements and predictions p 109 A85-25137  
A comparison of flow rates and pressure profiles for N-sequential inlets and three related seal configurations p 109 A85-26526  
Combined influence of unsteady free stream velocity and free stream turbulence on stagnation point heat transfer p 112 A85-41782  
Structure of nonevaporating sprays. I - Initial conditions and mean properties p 112 A85-48538  
Flow rates and pressure profiles for one to four axially aligned Borda inlets  
[NASA-TP-2390] p 113 N85-14078  
Preliminary analysis of tone-excited two-stream jet velocity decay p 8 N85-21114  
Fuel and oxidizer turbine loss analysis p 50 N85-26900  
Flow rate and pressure profiles for 1 to 4 axially aligned orifice inlets  
[NASA-TP-2460] p 116 N85-27165  
Burner rig corrosion of SiC at 1000 deg C  
[NASA-TM-87061] p 53 N85-30011  
Combustor turbulence p 118 N85-31434  
Preliminary results of a study of the relationship between free-stream turbulence and stagnation region heat transfer p 118 N85-31435  
Velocity visualization in gaseous flows  
[NASA-CR-174954] p 119 N85-31445  
Flow modifying device  
[NASA-CASE-LEW-13562-2] p 33 N85-35195  
The use of a laser Doppler velocimeter in a standard flammability tube  
[NASA-CR-174960] p 125 N85-35389

**FLOW VISUALIZATION**  
Flow visualization of lateral jet injection into swirling crossflow  
[AIAA PAPER 85-0059] p 2 A85-19490  
Velocity visualization in gas flows using laser-induced phosphorescence of biacetyl p 121 A85-21695

Some unique experiments on receptivity --- for forced disturbances entering shear flow  
[AIAA PAPER 85-0533] p 174 A85-25932  
Rainbow schlieren vs Mach-Zehnder interferometer - A comparison p 121 A85-28820  
Fast laser-induced aerosol formation for visualization of gas flows p 121 A85-31113  
Unsteady pressure measurements on a biconvex airfoil in a transonic oscillating cascade  
[NASA-TM-86914] p 8 N85-15689  
Flow visualization study of the effect of injection hole geometry on an inclined jet in crossflow  
[NASA-TM-86936] p 115 N85-20269  
Deflected jet experiments in a turbulent combustor flowfield  
[NASA-CR-174863] p 26 N85-22390  
Preliminary results of a study of the relationship between free-stream turbulence and stagnation region heat transfer p 118 N85-31435  
Velocity visualization in gaseous flows  
[NASA-CR-174954] p 119 N85-31445

**FLUID DYNAMICS**  
Design and performance of a fixed, nonaccelerating guide vane cascade that operates over an inlet flow angle range of 60 deg  
[ASME PAPER 84-GT-75] p 4 A85-32964  
Researched applied to transonic compressors in numerical fluid mechanics of inviscid flow and viscous flow  
[NASA-CR-174353] p 114 N85-18291  
Advanced research and technology programs for advanced high-pressure oxygen-hydrogen rocket propulsion  
[NASA-TM-86969] p 37 N85-21231  
Flow dynamic environment data base development for the SSME p 147 N85-26885  
Analytical study of flow phenomena in SSME turnaround duct geometries p 116 N85-26902

**FLUID FILMS**  
Fast numerical calculations of EHD sliding traction forces  
Application to rolling bearings  
[ASME PAPER 84-TRIB-26] p 127 A85-21289

**FLUID FLOW**  
Thermal traction contact performance evaluation under fully flooded and starved conditions  
[NASA-CR-168173] p 132 N85-25848  
Flow modifying device  
[NASA-CASE-LEW-13562-2] p 33 N85-35195

**FLUID INJECTION**  
Vortex modeling of single and multiple dilution jet mixing in a crossflow  
[AIAA PAPER 85-1580] p 111 A85-40701

**FLUID JETS**  
Generation of capillary instabilities by external disturbances in a liquid jet  
[NASA-TM-87041] p 117 N85-30246

**FLUID MANAGEMENT**  
Technology requirements to be addressed by the NASA Lewis Research Center Cryogenic Fluid Management Facility program  
[AIAA PAPER 85-1229] p 94 A85-47024  
Technology requirements to be addressed by the NASA Lewis Research Center Cryogenic Fluid Management Facility program  
[NASA-TM-87048] p 38 N85-29987

**FLUID MECHANICS**  
A new interpretation of internal heat transfer coefficients of porous media  
[ASME PAPER 84-WA/HT-51] p 110 A85-39894  
Advanced research and technology programs for advanced high-pressure oxygen-hydrogen rocket propulsion  
[NASA-TM-86969] p 37 N85-21231  
Nested subcritical flows within supercritical systems  
[NASA-TM-86980] p 115 N85-21574  
Arc-driven rail gun research  
[NASA-CR-174816] p 132 N85-21662  
Transition in Turbines  
[NASA-CP-2386] p 118 N85-31433  
Heat transfer and fluid mechanics measurements in transitional boundary layer flows p 118 N85-31439

**FLUID POWER**  
Rotordynamic Instability Problems in High-Performance Turbomachinery  
[NASA-CP-2338] p 131 N85-14116

**FLUIDIZED BED PROCESSORS**  
Advanced technology cogeneration system conceptual design study: Closed cycle gas turbines  
[NASA-CR-168222] p 159 N85-16300  
Solids mixing in a three phase fluidized bed containing spherically shaped-porous solid particles  
[PB85-187961] p 120 N85-33453

**FLUORESCENCE**  
Two-frequency laser-induced fluorescence technique for rapid velocity-field measurements in gas flows p 121 A85-32294

Velocity visualization in gaseous flows  
[NASA-CR-174954] p 119 N85-31445

**FLUORIDES**  
Effects of silver and group 2 fluorides addition to plasma sprayed chromium carbide high temperature solid lubricant for foil gas bearing to 650 deg C  
[NASA-TM-86895] p 84 N85-14928

**FLUTTER**  
Vibration and flutter of mistuned bladed-disk assemblies  
[AIAA PAPER 84-0991] p 139 A85-16095  
Flutter of swept fan blades  
[ASME PAPER 84-GT-138] p 141 A85-32962  
Vibration and flutter of mistuned bladed-disk assemblies p 16 A85-45854  
Aerodynamic detuning analysis of an unstalled supersonic turbofan cascade  
[NASA-TM-87001] p 9 N85-26670  
Unsteady flow in a supersonic cascade with two in-passage shocks  
[NASA-CR-3925] p 10 N85-35158

**FLUTTER ANALYSIS**  
Flutter and forced response of mistuned rotors using standing wave analysis p 139 A85-12721  
Flutter of swept fan blades  
[ASME PAPER 84-GT-138] p 141 A85-32962

**FLUX DENSITY**  
Mass analysis of neutral particles and ions released during electrical breakdowns on spacecraft surfaces  
[NASA-CR-175585] p 39 N85-21250

**FLYWHEELS**  
A rotating superconducting solenoid for 100 kWh energy storage --- in space p 44 A85-33144  
Operating characteristics of a 0.87 kw-hr flywheel energy storage module  
[NASA-TM-87038] p 133 N85-28371

**FOCI**  
Focal shifts in parabolic reflectors p 97 A85-39356

**FOIL BEARINGS**  
Effects of silver and group 2 fluorides addition to plasma sprayed chromium carbide high temperature solid lubricant for foil gas bearing to 650 deg C  
[NASA-TM-86895] p 84 N85-14928

**FORCED CONVECTION**  
Heat transfer in aeropropulsion systems  
[NASA-TM-87066] p 119 N85-31444

**FORCED VIBRATION**  
Flutter and forced response of mistuned rotors using standing wave analysis p 139 A85-12721  
Vibration and flutter of mistuned bladed-disk assemblies  
[AIAA PAPER 84-0991] p 139 A85-16095  
A study of internal and distributed damping for vibrating turbomachinery blades  
[NASA-CR-175901] p 30 N85-27868

**FORECASTING**  
Satellite provided customer promises services, a forecast of potential domestic demand through the year 2000. Volume 4: Sensitivity analysis  
[NASA-CR-174662] p 99 N85-27092

**FORGING**  
Powder metallurgy forged gear development  
[NASA-TM-87483] p 134 N85-29295

**FORMING TECHNIQUES**  
Factors influencing the ball milling of Si3N4 in water  
[NASA-TM-86932] p 86 N85-19136

**FORTRAN**  
A generalized computer code for developing dynamic gas turbine engine models (DIGTEM) p 17 A85-49021  
Manual of phosphoric acid fuel cell stack three-dimensional model and computer program  
[NASA-CR-174722] p 157 N85-10447  
Phosphoric acid fuel cell power plant system performance model and computer program  
[NASA-CR-174638] p 157 N85-11456  
Reliability of void detection in structural ceramics using scanning laser acoustic microscopy  
[NASA-TM-87035] p 138 N85-32337

**FRACTURE MECHANICS**  
Deformation and fracture behavior of Ni-Mo-Al(gamma/gamma prime-alpha) in situ composite p 64 A85-11058  
A study of fatigue damage mechanisms in Waspaloy from 25 to 800 C p 65 A85-12098  
Statistics and thermodynamics of fracture p 140 A85-19433  
On stress field near a stationary crack tip  
[AD-A152863] p 141 A85-24532  
HOST high temperature crack propagation p 21 N85-10977  
Rapidly solidified NiAl and FeAl  
[NASA-TM-86941] p 74 N85-20042  
Translational and extensional energy release rates (the J- and M-integrals) for a crack layer in thermoelasticity  
[NASA-CR-174872] p 145 N85-21685

Multiaxial and thermomechanical fatigue considerations in damage tolerant design  
[NASA-TM-87022] p 76 N85-26964  
Interaction of high-cycle and low-cycle fatigue of Haynes 188 alloy at 1400 F deg p 149 N85-27961  
A review of path-independent integrals in elastic-plastic fracture mechanics, task 4  
[NASA-CR-174956] p 152 N85-33541

**FRACTURE STRENGTH**  
Fracture toughness of hot-pressed beryllium p 66 A85-25835  
Fracture of composite-adhesive-composite systems p 141 A85-27935  
Effect of low temperature on fatigue and fracture properties of Ti-5Al-2.5Sn(ELI) for use in engine components p 70 A85-47972  
Fundamental studies of composite toughness p 56 N85-12948  
Dispersed metal-toughened ceramics and ceramic brazing  
[NASA-CR-174284] p 86 N85-15916  
Dispersed-metal-toughened alumina  
[NASA-CR-174687] p 89 N85-22758  
Mechanism of strength degradation for hot corrosion of alpha-SiC  
[NASA-TM-87052] p 91 N85-30135

**FRACTURES (MATERIALS)**  
Turbine Engine Hot Section Technology (HOST)  
[NASA-TM-83022] p 18 N85-10951  
Fundamental tribological properties of ceramics  
[NASA-TM-86915] p 85 N85-15893

**FRACTURING**  
Structural Integrity and Durability of Reusable Space Propulsion Systems  
[NASA-CP-2381] p 51 N85-27941  
Designing for fiber composite structural durability in hydrothermomechanical environment  
[NASA-TM-87045] p 58 N85-27978

**FREDHOLM EQUATIONS**  
A procedure for obtaining explicit solutions to a class of Fredholm integral equations p 171 A85-28006

**FREE BOUNDARIES**  
Control of solidification boundary in continuous casting by asymmetric cooling and mold offset p 110 A85-37047

**FREE ELECTRON LASERS**  
Technology for satellite power conversion  
[NASA-CR-174335] p 159 N85-18451

**FREE FLOW**  
Combined influence of unsteady free stream velocity and free stream turbulence on stagnation point heat transfer p 112 A85-41782  
Preliminary results of a study of the relationship between free stream turbulence and stagnation region heat transfer  
[NASA-TM-86884] p 113 N85-11317  
Preliminary results of a study of the relationship between free-stream turbulence and stagnation region heat transfer p 118 N85-31435

**FREE JETS**  
Acoustic control of free jet mixing  
[AIAA PAPER 85-0569] p 109 A85-25951

**FREE RADICALS**  
Analysis of glow discharges for understanding the process of film formation  
[NASA-TM-83750] p 62 N85-10138  
Shock tube measurements of growth constants in the branched-chain ethane-carbon monoxide-oxygen system  
[NASA-TM-87068] p 64 N85-32156

**FREE VIBRATION**  
Vibrations of twisted cantilevered plates - Summary of previous and current studies p 140 A85-22069  
Vibrations of twisted cantilever plates - A comparison of theoretical results p 144 A85-47626  
A study of internal and distributed damping for vibrating turbomachinery blades  
[NASA-CR-175901] p 30 N85-27868

**FREEZING**  
Jet fuel property changes and their effect on producibility and cost in the U.S., Canada, and Europe  
[NASA-CR-174840] p 93 N85-27012

**FREQUENCIES**  
Vibration and flutter of mistuned bladed-disk assemblies  
[AIAA PAPER 84-0991] p 139 A85-16095

**FREQUENCY ASSIGNMENT**  
The subjective effect of multiple co-channel frequency modulated television interference p 96 A85-28234  
Development and use of the computer software package for planning the 12 GHz broadcasting-satellite service at RARC '83 p 96 A85-29605  
Engineering calculations for communications satellite systems planning  
[NASA-CR-175552] p 37 N85-21233

**FREQUENCY DIVISION MULTIPLE ACCESS**  
A frequency-routed satellite system concept using multiple orthogonally-polarized beams for frequency reuse p 97 A85-34470

**FREQUENCY MEASUREMENT**  
Characterization of microstrip discontinuities in the time and frequency domains  
[NASA-CR-176190] p 106 N85-35342

**FREQUENCY MODULATION**  
On the subjective evaluation of the interference protection ratios' measurements for co-channel FM-TV signals p 96 A85-28241  
Four-dimensional modulation and coding - An alternate to frequency-reuse p 97 A85-36653

**FREQUENCY RESPONSE**  
Experimental results supporting the determination of service quality objectives for DBS systems p 96 A85-29611

**FREQUENCY REUSE**  
A frequency-routed satellite system concept using multiple orthogonally-polarized beams for frequency reuse p 97 A85-34470  
Four-dimensional modulation and coding - An alternate to frequency-reuse p 97 A85-36653

**FRESH WATER**  
Operational performance of the photovoltaic-powered grain mill and water pump at Tangaye, Burkina Faso (formerly Upper Volta)  
[NASA-TM-86970] p 161 N85-23243

**FRESNEL REFLECTORS**  
Focal shifts in parabolic reflectors p 97 A85-39356

**FRETTING**  
Effect of humidity on fretting wear of several pure metals  
[NASA-TP-2403] p 72 N85-13006

**FRICTION**  
Friction in rail guns p 101 A85-16424  
Frictional and morphological properties of Au-MoS2 films sputtered from a compact target p 127 A85-19085  
Polyimides - Tribological properties and their use as lubricants p 79 A85-21524  
Friction, wear, transfer, and wear surface morphology of ultrahigh-molecular-weight polyethylene p 80 A85-22276  
Friction and wear of ceramics p 80 A85-23833  
Effects of silver and group 2 fluorides addition to plasma sprayed chromium carbide high temperature solid lubricant for foil gas bearing to 650 deg C  
[NASA-TM-86895] p 84 N85-14928  
Fundamental tribological properties of ceramics  
[NASA-TM-86915] p 85 N85-15893  
Experimental test program for evaluation of solid lubricant coating as applied to compliant foil gas bearings to 315 deg C  
[NASA-CR-174837] p 85 N85-15895  
Surface effects of corrosive media on hardness, friction, and wear of materials  
[NASA-TM-83711] p 85 N85-15896  
Tribological properties of boron nitride synthesized by ion beam deposition  
[NASA-TM-86962] p 87 N85-21355  
Tribological systems as applied to aircraft engines  
[NASA-TM-86965] p 131 N85-21657  
Breakway friction and dynamic friction/wear measurements of various ceramic materials from 25 C (75 F) to 650 C (1200 F)  
[NASA-CR-174803] p 90 N85-26994  
Surface roughness effects in elastohydrodynamic contacts  
[NASA-TP-2488] p 134 N85-32329  
Lubrication and cooling for high speed gears  
[NASA-TM-87096] p 136 N85-34407

**FRICTION REDUCTION**  
Effects of friction dampers on aerodynamically unstable rotor stages p 14 A85-21866  
Lubricant and additive effects on spur gear fatigue life  
[NASA-TM-87044] p 133 N85-28373

**FUEL CELL POWER PLANTS**  
Electric utility acid fuel cell stack technology advancement  
[NASA-CR-174804] p 159 N85-17422

**FUEL CELLS**  
Long-life high performance fuel cell program  
[NASA-CR-174874] p 50 N85-25384  
Evaluation of developmental membranes for the mixed reactant iron-chromium redox system  
[NASA-TM-87074] p 164 N85-34443

**FUEL COMBUSTION**  
Methanol as a soot reducer in a turbulent swirling burner  
[ASME PAPER 84-JPGC-GT-2] p 61 A85-23192  
Internal combustion engine combustion chamber process studies at NASA Lewis Research Center p 112 A85-45856  
Growth of a diffusion flame in the field of a vortex p 61 A85-47320



- Combustion gas properties I-ASTM jet A fuel and dry air  
[NASA-TP-2359] p 17 N85-10064  
The mechanisms of flame holding in the wake of a bluff body  
[NASA-CR-174058] p 62 N85-11149  
The mechanisms of flame holding in the wake of a bluff body  
[NASA-CR-3866] p 26 N85-21166  
Shock tube study of the fuel structure effects on the chemical kinetic mechanisms responsible for soot formation, part 2  
[NASA-CR-174880] p 63 N85-25444  
Analytical fuel property effects—small combustors  
[NASA-CR-174738] p 28 N85-26709  
Fuel-rich catalytic combustion: A soot-free technique for in situ hydrogen-like enrichment  
[NASA-TP-2498] p 63 N85-31244
- FUEL CONSUMPTION**  
Energy efficient engine flight propulsion system preliminary analysis and design report  
[NASA-CR-174701] p 18 N85-10947  
Energy efficient engine. Volume 1: Component development and integration program  
[NASA-CR-173084] p 22 N85-10992  
Energy efficient engine high-pressure turbine component rig performance test report  
[NASA-CR-168189] p 30 N85-29955  
Energy efficient engine integrated core/low spool test hardware design report  
[NASA-CR-168137] p 31 N85-29956  
Energy Efficient Engine (E3) controls and accessories detail design report  
[NASA-CR-168017] p 31 N85-29957  
Comparative analysis of operational forecasts versus actual weather conditions in airline flight planning, volume 1  
[NASA-CR-167862] p 167 N85-35534  
Comparative analysis of operational forecasts versus actual weather conditions in airline flight planning, volume 2  
[NASA-CR-167863] p 167 N85-35535  
Comparative analysis of operational forecasts versus actual weather conditions in airline flight planning, volume 3  
[NASA-CR-167864] p 167 N85-35536  
Comparative analysis of operational forecasts versus actual weather conditions in airline flight planning, volume 4  
[NASA-CR-167865] p 167 N85-35537
- FUEL CONTROL**  
Energy Efficient Engine (E3) controls and accessories detail design report  
[NASA-CR-168017] p 31 N85-29957
- FUEL FLOW**  
Energy efficient engine high-pressure turbine component rig performance test report  
[NASA-CR-168189] p 30 N85-29955  
Detailed studies of aviation fuel flowability  
[NASA-CR-174938] p 94 N85-31308
- FUEL INJECTION**  
Aerodynamic effect of combustor inlet air pressure on fuel jet atomization  
p 109 A85-27096  
Turbulence measurements of lateral jet injection into confined tubular crossflow  
[AIAA PAPER 85-1102] p 110 A85-39604  
Small gas turbine combustor study - Fuel injector performance in a transpiration-cooled liner  
[AIAA PAPER 85-1312] p 16 A85-39717  
Experimental study of the spray characteristics of a research airblast atomizer  
[NASA-TM-86911] p 24 N85-15727  
Small gas turbine combustor study: Fuel injector performance in a transpiration-cooled liner  
[NASA-TM-86989] p 27 N85-25264
- FUEL PRODUCTION**  
Jet fuel property changes and their effect on producibility and cost in the U.S., Canada, and Europe  
[NASA-CR-174840] p 93 N85-27012
- FUEL PUMPS**  
An experimental investigation of rubbing interaction in labyrinth seals at cryogenic temperature  
p 129 A85-39938  
Effect of low temperature on fatigue and fracture properties of Ti-5Al-2.5Sn(ELI) for use in engine components  
p 70 A85-47972  
Analytical and experimental investigation of rubbing interaction in labyrinth seals for a liquid hydrogen fuel pump - space shuttle main engine  
[NASA-CR-174657] p 48 N85-18084
- FUEL SPRAYS**  
Liquid fuel spray processes in high-pressure gas flow  
[NASA-TM-86944] p 115 N85-21570

**FUEL SYSTEMS**

- Energy Efficient Engine (E3) controls and accessories detail design report  
[NASA-CR-168017] p 31 N85-29957

**FUEL TESTS**

- Rapid estimation of concentration of aromatic classes in middistillate fuels by high-performance liquid chromatography  
[NASA-TP-2495] p 93 N85-31307

**FUEL-AIR RATIO**

- Combustion gas properties. 2: Natural gas fuel and dry air  
[NASA-TP-2435] p 26 N85-21168  
Behavior of the lean methane-air flame at zero-gravity  
[NASA-CR-175586] p 62 N85-21283  
Flow modifying device  
[NASA-CASE-LEW-13562-2] p 33 N85-35195

**FUELS**

- External fuel vaporization study, phase 2  
[NASA-CR-174079] p 92 N85-11252

**FULL SCALE TESTS**

- Comparison of scaled model data to full size energy efficient engine test results  
[AIAA PAPER 84-2281] p 13 A85-13953

**FUSION (MELTING)**

- New eutectic alloys and their heats of transformation  
p 66 A85-27808

**G****GALERKIN METHOD**

- A study of internal and distributed damping for vibrating turbomachinery blades  
[NASA-CR-175901] p 30 N85-27868

**GALILEO PROJECT**

- A high energy stage for the National Space Transportation System  
[IAF PAPER 84-15] p 36 A85-23200

**GALLIUM ARSENIDES**

- Magnesium doping of efficient GaAs and Ga(0.75)In(0.25)As solar cells grown by metalorganic chemical vapor deposition  
p 180 A85-11466  
Near-optimum design of GaAs-based concentrator space solar cells for 80 C operation  
p 153 A85-15800  
Electrical characterization of plasma-grown oxides on gallium arsenide  
p 181 A85-32635  
Heat treatment of bulk gallium arsenide using a phosphosilicate glass cap  
p 181 A85-32636  
Fabrication of p(+)-n junction GaAs solar cells by a novel method  
p 181 A85-33645  
Plasma deposited hydrogenated carbon on GaAs and InP  
p 182 A85-40386  
Plasma deposited diamondlike carbon on GaAs and InP  
[NASA-TM-86870] p 183 N85-10844  
High-temperature optically activated GaAs power switching for aircraft digital electronic control  
[NASA-CR-174711] p 34 N85-12901  
Effect of barrier height on friction behavior of the semiconductors silicon and gallium arsenide in contact with pure metals  
[NASA-TP-2405] p 84 N85-13044  
GaAs and 3-5 compound solar cells status and prospects for use in space  
[NASA-TM-86960] p 49 N85-21261  
GaAs and 3-5 compound solar cells status and prospects for use in space  
p 49 N85-22580  
Sixty GHz IMPATT diode development  
[NASA-CR-174969] p 105 N85-33293  
Diffusion welding of Cassegrainian concentrator cell stack assemblies  
[NASA-CR-176104] p 164 N85-33566

**GAMMA RAYS**

- Apparatus and method for identification of matrix materials in which transuranic elements are embedded using thermal neutron capture gamma-ray emission  
[DE85-011659] p 125 N85-33454

**GAS ANALYSIS**

- Integrated exhaust gas analysis system for aircraft turbine engine component testing  
[NASA-TP-2424] p 123 N85-16100

**GAS BEARINGS**

- Development of gas-lubricated pistons for heavy duty diesel engine technology program  
[NASA-CR-174746] p 184 N85-12808  
Experimental test program for evaluation of solid lubricant coating as applied to compliant foil gas bearings to 315 deg C  
[NASA-CR-174837] p 85 N85-15895

**GAS COMPOSITION**

- Combustion gas properties I-ASTM jet A fuel and dry air  
[NASA-TP-2359] p 17 N85-10064

- Combustion gas properties. Part 3: Hydrogen gas fuel and dry air  
[NASA-TP-2477] p 32 N85-31058

**GAS COOLING**

- Gas cooled fuel cell systems technology development  
[NASA-CR-174732] p 158 N85-16291

**GAS DENSITY**

- Density effects on jet characteristics in confined swirling flow  
p 112 A85-45283

**GAS DYNAMICS**

- Time dependent wave envelope finite difference analysis of sound propagation  
[AIAA PAPER 84-2285] p 173 A85-16102  
Advanced research and technology programs for advanced high-pressure oxygen-hydrogen rocket propulsion  
[NASA-TM-86969] p 37 N85-21231  
Ideal gas thermodynamic properties for the phenyl, phenoxy, and o-biphenyl radicals  
[NASA-TM-83800] p 184 N85-22204  
Velocity visualization in gaseous flows  
[NASA-CR-174954] p 119 N85-31445  
Mechanics of a gaseous film barrier to lubricant wetting of elastohydrodynamically lubricated conjunctions  
[NASA-TP-2500] p 135 N85-32330

**GAS FLOW**

- Velocity visualization in gas flows using laser-induced phosphorescence of biacetyl  
p 121 A85-21695  
Fast laser-induced aerosol formation for visualization of gas flows  
p 121 A85-31113  
Two-frequency laser-induced fluorescence technique for rapid velocity-field measurements in gas flows  
p 121 A85-32294

- Replaceable blade turbine and stationary specimen corrosion testing facility  
[NASA-TM-86931] p 73 N85-18126

- Vortex generating flow passage design for increased film cooling effectiveness  
[NASA-CASE-LEW-14039-1] p 119 N85-33433

**GAS IONIZATION**

- Frictional and structural characterization of ion-nitrided low and high chromium steels  
[NASA-TM-86991] p 132 N85-23085

**GAS LUBRICANTS**

- Dual clearance squeeze film damper  
[NASA-CASE-LEW-13506-1] p 135 N85-33490

**GAS MIXTURES**

- Combustion gas properties. Part 3: Hydrogen gas fuel and dry air  
[NASA-TP-2477] p 32 N85-31058

**GAS TEMPERATURE**

- HOST instrumentation R and D program overview  
p 19 N85-10957

**GAS TURBINE ENGINES**

- Reactions of NaCl with gaseous SO<sub>3</sub>, SO<sub>2</sub>, and O<sub>2</sub>  
p 59 A85-11897  
Ceramic component development for the AGT101 gas turbine engine  
p 126 A85-15972  
Ceramic components for gas turbine engines  
p 127 A85-15973

- Sensor failure detection for jet engines using analytical redundancy  
[AIAA PAPER 84-1452] p 13 A85-16097

- Considerations for damage analysis of gas turbine hot section components  
[ASME PAPER 84-PVP-77] p 14 A85-18792

- Computational thermo-fluid dynamics contributions to advanced gas turbine engine design  
[AIAA PAPER 85-0083] p 14 A85-19509

- Effects of friction dampers on aerodynamically unstable rotor stages  
p 14 A85-21866

- The effect of aerodynamic and structural detuning on turbomachine supersonic unstalled torsional flutter  
[AIAA PAPER 85-0761] p 14 A85-30378

- Progress in the utilization of an oxide-dispersion-strengthened alloy for small engine turbine blades  
[SAE PAPER 841512] p 68 A85-39284

- Experiments in dilution jet mixing - Effects of multiple rows and non-circular orifices  
[AIAA PAPER 85-1104] p 15 A85-39606

- High-temperature erosion of plasma-sprayed, yttria-stabilized zirconia in a simulated turbine environment  
[AIAA PAPER 85-1219] p 82 A85-39662

- Advanced liner-cooling techniques for gas turbine combustors  
[AIAA PAPER 85-1290] p 15 A85-39703

- Computational thermo-fluid dynamics contributions to advanced gas turbine engine design  
[NASA-TM-86865] p 18 N85-10069

- A review and analysis of boundary layer transition data for turbine application  
[NASA-TM-86880] p 113 N85-10306



Energy efficient engine flight propulsion system preliminary analysis and design report [NASA-CR-174701] p 18 N85-10947

Turbine Engine Hot Section Technology (HOST) [NASA-TM-83022] p 18 N85-10951

Nonlinear structural and life analyses of a turbine blade p 19 N85-10954

Nonlinear structural and life analyses of a combustor liner p 19 N85-10955

Pre-HOST high temperature crack propagation p 19 N85-10956

High temperature static strain sensor development program p 19 N85-10959

Component-specific modeling p 20 N85-10971

The 3-D inelastic analysis methods for hot section components: Brief description p 20 N85-10972

Constitutive model development for isotropic materials p 20 N85-10975

Surface protection overview p 21 N85-10978

Airfoil deposition model p 21 N85-10979

Effects of surface chemistry on hot corrosion life: Overview p 21 N85-10980

Dilution zone mixing studies p 21 N85-10984

Studies on the hot corrosion of a nickel-base superalloy, Udimet 700 [NASA-TM-86882] p 71 N85-11224

Hot isostatically pressed manufacture of high strength MERL 76 disk and seal shapes [NASA-CR-165550] p 71 N85-11225

External fuel vaporization study, phase 2 [NASA-CR-174079] p 92 N85-11252

Biaxial constitutive equation development for single crystals [NASA-CR-174056] p 183 N85-11862

High performance fibers for structurally reliable metal and ceramic composites --- advanced gas turbine engine materials [NASA-TM-86878] p 56 N85-12095

High-temperature erosion of plasma-sprayed, yttria-stabilized zirconia in a simulated turbine environment [NASA-TP-2406] p 84 N85-13045

Fabrication and quality assurance processes for superhybrid composite fan blades [NASA-TM-83354] p 57 N85-14882

Engine cyclic durability by analysis and material testing p 25 N85-15744

Integrated exhaust gas analysis system for aircraft turbine engine component testing [NASA-TP-2424] p 123 N85-16100

Advanced Gas Turbine (AGT) powertrain system development for automotive applications [NASA-CR-174809] p 185 N85-18831

Advanced liner-cooling techniques for gas turbine combustors [NASA-TM-86952] p 8 N85-21115

Combustion research for gas turbine engines [NASA-TM-86963] p 26 N85-21164

Evaluation results of the 700 deg C Chinese strain gauges --- for gas turbine engine [NASA-TM-86973] p 124 N85-21605

Advanced thin film thermocouples [NASA-CR-175541] p 124 N85-21607

Development of a multiplane multispeed balancing system for turbine systems [NASA-CR-174750] p 35 N85-22400

Experiments in dilution jet mixing effects of multiple rows and non-circular orifices [NASA-TM-86996] p 28 N85-25266

Analytical fuel property effects--small combustors [NASA-CR-174738] p 28 N85-26709

Multiaxial and thermomechanical fatigue considerations in damage tolerant design [NASA-TM-87022] p 76 N85-26964

Ceramic applications in turbine engines [NASA-CR-174715] p 91 N85-28109

Energy efficient engine high-pressure turbine component rig performance test report [NASA-CR-168189] p 30 N85-29955

Energy efficient engine integrated core/low spool test hardware design report [NASA-CR-168137] p 31 N85-29956

Advanced Gas Turbine (AGT) technology project [NASA-CR-174798] p 31 N85-29961

Creep fatigue life prediction for engine hot section materials (isotropic) [NASA-CR-168228] p 32 N85-31057

Flat-plate transition p 118 N85-31438

A review and analysis of boundary layer transition data for turbine application p 118 N85-31440

Tape casting as an approach to an all-ceramic turbine shroud seal [NASA-TM-87078] p 135 N85-32333

Dual clearance squeeze film damper [NASA-CASE-LEW-13506-1] p 135 N85-33490

Oxidizing seal for a turbine tip gas path [NASA-CASE-LEW-14053-1] p 136 N85-34402

Energy Efficient Engine Program technology benefit/cost study, volume 2 [NASA-CR-174766-VOL-2] p 33 N85-35198

Energy efficient engine, high pressure turbine thermal barrier coating. Support technology report [NASA-CR-168037] p 34 N85-35199

Development of advanced high-temperature heat flux sensors. Phase 2: Verification testing [NASA-CR-174973] p 126 N85-35391

**GAS TURBINES**

Predicted turbine stage performance using quasi-three-dimensional and boundary-layer analyses p 15 A85-34013

Small gas turbine combustor study - Fuel injector performance in a transpiration-cooled liner [AIAA PAPER 85-1312] p 16 A85-39717

Effect of surface configuration during solid particle impingement erosion p 69 A85-42568

Future fundamental combustion research for aer propulsion systems [AIAA PAPER 85-1398] p 16 A85-42671

The effect of channel convergence on heat transfer in a passage with short pin fins [NASA-TM-83801] p 113 N85-10303

Coolant passage heat transfer with rotation p 20 N85-10968

Structural analysis p 20 N85-10969

Heat transfer results and operational characteristics of the NASA Lewis Research Center Hot Section Cascade Test Facility [NASA-TM-86890] p 114 N85-15133

An improved computer model for prediction of axial gas turbine performance losses [NASA-CR-174246] p 24 N85-15724

Advanced technology cogeneration system conceptual design study: Closed cycle gas turbines [NASA-CR-168222] p 159 N85-16300

NASA Lewis Research Center/University Graduate Research Program on Engine Structures [NASA-TM-86916] p 145 N85-18375

Small gas turbine combustor study: Fuel injector performance in a transpiration-cooled liner [NASA-TM-86989] p 27 N85-25264

Future fundamental combustion research for aer propulsion systems [NASA-TM-87049] p 30 N85-27870

**GAS-LIQUID INTERACTIONS**

Mechanics of a gaseous film barrier to lubricant wetting of elastohydrodynamically lubricated conjunctions [NASA-TP-2500] p 135 N85-32330

**GAS-METAL INTERACTIONS**

Effects of SO<sub>2</sub> and SO<sub>3</sub> on the Na<sub>2</sub>SO<sub>4</sub> induced corrosion of nickel. p 65 A85-15603

Effects of MAR-M247 substrate (modified) composition on coating oxidation coating/substrate interdiffusion --- protective coatings for hot section components of gas turbine engines [NASA-CR-174851] p 73 N85-19073

Oxidation and hot corrosion of hot-pressed Si<sub>3</sub>N<sub>4</sub> at 1000 deg C [NASA-TM-86977] p 88 N85-21358

**GAS-SOLID INTERFACES**

Gravitational effects on flames spreading over thick solid surfaces [IAF PAPER 84-154] p 59 A85-13092

**GASES**

Combustion gas properties I-ASTM jet A fuel and dry air [NASA-TP-2359] p 17 N85-10064

**GATES (CIRCUITS)**

A new very high voltage semiconductor switch [NASA-TM-86957] p 103 N85-20246

**GEAR TEETH**

A computer aided design procedure for generating gear teeth [ASME PAPER 84-DET-184] p 128 A85-33779

Dynamic analysis of straight and involute tooth forms [ASME PAPER 84-DET-226] p 128 A85-33780

Gear mesh stiffness and load sharing in planetary gearing [ASME PAPER 84-DET-229] p 129 A85-33781

Lubricant jet flow phenomena in spur and helical gears with modified center distances and/or addendums - For out-of-mesh conditions [ASME PAPER 84-DET-96] p 129 A85-35049

Planetary-gear-support bearing test rig design [NASA-CR-174927] p 12 N85-35185

**GEARS**

Into mesh lubrication of spur gears with arbitrary offset oil jet. I - For jet velocity less than or equal to gear velocity p 128 A85-24497

Lubricant jet flow phenomena in spur and helical gears with modified center distances and/or addendums - For out-of-mesh conditions [ASME PAPER 84-DET-96] p 129 A85-35049

Energy efficient engine ICLS engine bearings, drives and configuration: Detail design report [NASA-CR-167871] p 23 N85-10997

Effect of lubricant extreme-pressure additives on surface fatigue life of AISI 9310 spur gears [NASA-TP-2408] p 130 N85-13234

Effect of five lubricants on life of AISI 9310 spur gears [NASA-TP-2419] p 123 N85-16099

Life and reliability modeling of bevel gear reductions [NASA-TM-87006] p 133 N85-27227

Fatigue life analysis of a turboprop reduction gearbox [NASA-TM-87014] p 133 N85-27228

Multi-mesh gear dynamics program evaluation and enhancements [NASA-CR-174747] p 133 N85-28372

Lubricant and additive effects on spur gear fatigue life [NASA-TM-87044] p 133 N85-28373

Powder metallurgy forged gear development [NASA-TM-87483] p 134 N85-29295

Spiral bevel and circular arc helical gears: Tooth contact analysis and the effect of misalignment on circular arc helical gears [NASA-TM-87013] p 32 N85-31060

The design and analysis of single flank transmission error test for loaded gears [NASA-CR-176163] p 136 N85-34404

Generated spiral bevel gears: Optimal machine-tool settings and tooth contact analysis [NASA-TM-87075] p 136 N85-34405

Lubrication and cooling for high speed gears [NASA-TM-87096] p 136 N85-34407

Elastohydrodynamic lubrication calculations used as a tool to study scuffing [NASA-TM-87097] p 137 N85-34408

Planetary-gear-support bearing test rig design [NASA-CR-174927] p 12 N85-35185

**GEOMAGNETISM**

DE-1 measurements of AKR wave directions --- auroral kilometeric radiation p 166 A85-37717

**GEOMETRY**

A comparison of flow rates and pressure profiles for N-sequal inlets and three related seal configurations p 109 A85-26526

**GEOSYNCHRONOUS ORBITS**

Experiments in charge control at geosynchronous orbit - ATS-5 and ATS-6 p 39 A85-35379

OTV propulsion technology programmatic overview p 37 N85-16997

Radiation exposure and performance of multiple burn LEO-GEO orbit transfer trajectories [NASA-TM-86946] p 36 N85-21228

Design guidelines for assessing and controlling spacecraft charging effects p 40 N85-22500

**GLASS**

Spherical microglass particle impingement studies of thermoplastic materials at normal incidence p 79 A85-11072

Structural characteristics of high temperature composites [NASA-CR-175998] p 58 N85-30037

**GLASS FIBER REINFORCED PLASTICS**

Hygrothermomechanical evaluation of transverse filament tape epoxy/polyester fiberglass composites p 54 A85-15632

Fiberglass epoxy laminate fatigue properties at 300 and 20 K p 56 A85-47970

**GLASS FIBERS**

Ten year environmental test of glass fiber/epoxy pressure vessels [AIAA PAPER 85-1198] p 56 A85-47022

Ten year environmental test of glass fiber/epoxy pressure vessels [NASA-TM-87058] p 58 N85-30034

**GLOBAL AIR SAMPLING PROGRAM**

GASP cloud encounter statistics - Implications for laminar flow control flight p 166 A85-11979

Variability of cloudiness at airline cruise altitudes from GASP measurements p 166 A85-31199

**GLOW DISCHARGES**

Analysis of glow discharges for understanding the process of film formation [NASA-TM-83750] p 62 N85-10138

Nitriding of titanium and its alloys by N<sub>2</sub>, NH<sub>3</sub> or mixtures of N<sub>2</sub> + H<sub>2</sub> in a dc arc plasma at low pressures (or = to torr) [NASA-TM-83803] p 131 N85-15168

Frictional and structural characterization of ion-nitrided low and high chromium steels [NASA-TM-86991] p 132 N85-23085

The structure of ion plated films in relation to coating properties [NASA-TM-87055] p 95 N85-29085

## GOLD COATINGS

Frictional and morphological properties of Au-MoS<sub>2</sub> films sputtered from a compact target p 127 A85-19085

## GRAIN BOUNDARIES

Oxidation of silicon nitride sintered with rare-earth oxide additions p 83 A85-42798

Analysis techniques for tracer studies of oxidation [NASA-CR-174796] p 84 N85-12162

High temperature properties of equiatomic FeAl with ternary additions [NASA-TM-86938] p 73 N85-19072

## GRAIN SIZE

On the fatigue crack propagation behavior of superalloys at intermediate temperatures p 68 A85-32434

Evaluation of alpha-SiC sintering using statistical methods p 83 A85-42800

## GRAINS (FOOD)

Operational performance of the photovoltaic-powered grain mill and water pump at Tangaye, Burkina Faso (formerly Upper Volta) [NASA-TM-86970] p 161 N85-23243

## GRAPHITE

Dynamics of graphite fiber intercalation: In situ resistivity measurements with a four point probe [NASA-TM-86858] p 53 N85-10105

Stability of bromine intercalated graphite fibers [NASA-TM-86859] p 84 N85-10187

Experimental test program for evaluation of solid lubricant coating as applied to compliant foil gas bearings to 315 deg C [NASA-CR-174837] p 85 N85-15895

Tribological properties of graphite-fiber-reinforced, partially fluorinated polyimide composites [NASA-TM-86926] p 86 N85-18153

Homogeneity of pristine and bromine intercalated graphite fibers [NASA-TM-87016] p 89 N85-25521

Graphite fiber intercalation: Dynamics of the bromine intercalation process [NASA-TM-87015] p 53 N85-26921

Environmental stability of intercalated graphite fibers [NASA-TM-87025] p 90 N85-26992

A micrographic and gravimetric study of intercalation and deintercalation of graphite fibers [NASA-TM-87026] p 91 N85-28110

Multistage spent particle collector and a method for making same [NASA-CASE-LEW-13914-1] p 135 N85-33489

Graphite-EPOXY COMPOSITES

Select fiber composites for space applications - A mechanistic assessment p 54 A85-16040

Graphite-POLYIMIDE COMPOSITES

PMR polyimide composites for aerospace applications --- Polymerization of Monomer Reactants p 55 A85-21520

Effect of counterface material type and its topography on the tribological properties of polyimide composites [NASA-TM-87036] p 90 N85-26993

Graphite/PMR polyimide composites with improved toughness [NASA-TM-87081] p 58 N85-32148

GRASHOF NUMBER

Convective influence on the stability of a cylindrical solid-liquid interface p 109 A85-26911

GRATINGS (SPECTRA)

Solar energy converter using surface plasma waves [NASA-CASE-LEW-13827-1] p 160 N85-21768

GRAVIMETRY

A micrographic and gravimetric study of intercalation and deintercalation of graphite fibers [NASA-TM-87026] p 91 N85-28110

GRAVITATIONAL EFFECTS

Gravitational effects on flames spreading over thick solid surfaces [IAF PAPER 84-154] p 59 A85-13092

Effect of gravity on halogenated hydrocarbon flame retardant effectiveness [IAF PAPER 84-156] p 61 A85-23199

GREAT LAKES (NORTH AMERICA)

Comparison of atmospheric correction algorithms for the Coastal Zone Color Scanner p 153 A85-10244

GREEN'S FUNCTIONS

Noise transmission loss of a rectangular plate in an infinite baffle [NASA-TP-2398] p 176 N85-22109

GRINDING (COMMUNION)

Milling of Si<sub>3</sub>N<sub>4</sub> with Si<sub>3</sub>N<sub>4</sub> hardware [NASA-TM-86864] p 84 N85-10191

GRINDING (MATERIAL REMOVAL)

Factors influencing the ball milling of Si<sub>3</sub>N<sub>4</sub> in water [NASA-TM-86932] p 86 N85-19136

Parametric evaluation of ball milling of SiC in water [NASA-TM-86974] p 88 N85-21356

GRINDING MILLS

Milling of Si<sub>3</sub>N<sub>4</sub> with Si<sub>3</sub>N<sub>4</sub> hardware [NASA-TM-86864] p 84 N85-10191

Operational performance of the photovoltaic-powered grain mill and water pump at Tangaye, Burkina Faso (formerly Upper Volta) [NASA-TM-86970] p 161 N85-23243

## GROUND TESTS

Spacecraft environmental interactions: A joint Air Force and NASA research and technology program p 40 N85-22517

## GUIDE VANES

Design and performance of a fixed, nonaccelerating guide vane cascade that operates over an inlet flow angle range of 60 deg [ASME PAPER 84-GT-75] p 4 A85-32964

## GUST LOADS

Effect of airfoil mean loading on convected gust interaction noise [AIAA PAPER 84-2324] p 173 A85-13955

## H

## HAFNIUM ALLOYS

RF-sputtered silicon and hafnium nitrides - Properties and adhesion to 440C stainless steel p 81 A85-36240

## HALL ACCELERATORS

Theory of ion acceleration with closed electron drift --- in spacecraft plasma propulsion p 41 A85-15512

## HARDENING (MATERIALS)

Metallurgical and mechanical phenomena due to rubbing of titanium against sintered powder Nichrome p 127 A85-22281

Surface hardening of steel by boriding in a cold rf plasma p 68 A85-40275

## HARDNESS

Creep-rupture behavior of iron superalloys in high-pressure hydrogen [NASA-CR-174411] p 74 N85-19078

Deposition of diamondlike carbon films [NASA-CASE-LEW-14080-1] p 95 N85-20153

## HARDWARE

Energy efficient engine integrated core/low spool test hardware design report [NASA-CR-168137] p 31 N85-29956

## HARMONIC ANALYSIS

Effects of vane/blade ratio and spacing on fan noise, volume 1 [NASA-CR-174664] p 176 N85-19791

## HASTELLOY (TRADEMARK)

Elevated temperature biaxial fatigue [NASA-CR-175795] p 148 N85-27263

A comparison of smooth specimen and analytical simulation techniques for notched members at elevated temperatures p 151 N85-31546

HEAT EXCHANGERS

Advanced radiator concepts [NASA-TM-87008] p 115 N85-24245

## HEAT FLUX

Performance of thermal barrier coatings in high heat flux environments p 79 A85-19087

Heat transfer investigation in the junction region of circular cylinder normal to a flat plate at 90 deg location [ASME PAPER 84-WA/HT-70] p 111 A85-39898

High temperature thermocouple and heat flux gauge using a unique thin film hardware hot junction [NASA-TM-86898] p 123 N85-16096

Heat flux sensor calibrator p 41 N85-27970

Development of advanced high-temperature heat flux sensors. Phase 2: Verification testing [NASA-CR-174973] p 126 N85-35391

HEAT GENERATION

An experimental investigation and numerical prediction of thermomechanical phenomena in high speed rotor tip rubbing p 14 A85-25442

Generated spiral bevel gears: Optimal machine-tool settings and tooth contact analysis [NASA-TM-87075] p 136 N85-34405

HEAT MEASUREMENT

Transient technique for measuring heat transfer coefficients on stator airfoils in a jet engine environment [AIAA PAPER 85-1471] p 122 A85-39796

Transient technique for measuring heat transfer coefficients on stator airfoils in a jet engine environment [NASA-TM-87005] p 124 N85-25794

Heat flux sensor calibrator p 41 N85-27970

HEAT OF FORMATION

Direct numerical simulations of a reacting mixing layer with chemical heat release [AIAA PAPER 85-0143] p 60 A85-19548

HEAT OF FUSION

New eutectic alloys and their heats of transformation p 66 A85-27808

HEAT PIPES

High thermal power density heat transfer apparatus providing electrical isolation at high temperature using heat pipes [NASA-CASE-LEW-12950-2] p 117 N85-29179

## HEAT PUMPS

Overview of NASA Lewis Research Center free-piston Stirling engine activities p 130 A85-45479

## HEAT RADIATORS

Methods for heat transfer and temperature field analysis of the insulated diesel [NASA-CR-174783] p 185 N85-16699

## HEAT RESISTANT ALLOYS

Microstructural development of protective Al<sub>2</sub>O<sub>3</sub> scales p 80 A85-21650

Elevated temperature creep-rupture behavior of the single crystal nickel-base superalloy NASAIR 100 p 66 A85-27812

Chemical reactions involved in the initiation of hot corrosion of IN-738 p 66 A85-31688

Influence of composition on the microstructure and mechanical properties of a nickel-base superalloy single crystal p 66 A85-32387

Factors which influence directional coarsening of gamma-prime during creep in nickel-base superalloy single crystals p 67 A85-32388

The influence of hold times on LCF and FCG behavior in a P/M Ni-base superalloy --- Low Cycle Fatigue/Fatigue Crack Growth p 67 A85-32400

Effects of cobalt on the hot workability of nickel-base superalloys p 67 A85-32412

Rapid solidification and dynamic compaction of Ni-base superalloy powders p 67 A85-32414

On the fatigue crack propagation behavior of superalloys at intermediate temperatures p 68 A85-32434

Development of coated single-crystal superalloy systems for gas turbine applications p 68 A85-32440

Dopant effect of yttrium and the growth and adherence of alumina on nickel-aluminum alloys p 82 A85-40973

Diffusion welding of MA 6000 and a conventional nickel-base superalloy p 69 A85-43551

PM superalloys - A troubled adolescent? p 69 A85-44772

Morphological changes of gamma prime precipitates in nickel-base superalloy single crystals [NASA-TM-83698] p 70 N85-10165

The effects of seven alloying elements on the microstructure and stress-rupture behavior of nickel-base superalloys [NASA-TM-83791] p 70 N85-10168

High temperature static strain sensor development program p 19 N85-10959

The transient oxidation of single crystal NiAl-Zr [NASA-CR-174756] p 70 N85-11221

The effect of tantalum and carbon on the structure/properties of a single crystal nickel-base superalloy [NASA-CR-174779] p 71 N85-11223

Studies on the hot corrosion of a nickel-base superalloy, Udmet 700 [NASA-TM-86882] p 71 N85-11224

Materials for advanced turbine engines. Project 2: Rene 150 directionally solidified superalloy turbine blades, volume 2 [NASA-CR-167993] p 23 N85-12059

Effects of tin on microstructure and mechanical behavior of Inconel 718 [NASA-TM-86866] p 71 N85-12129

The effects of Cr, Co, Al, Mo and Ta on the cyclic oxidation behavior of a prototype cast Ni-base superalloy based on a 2(5) composite statistically designed experiment. [NASA-TM-83784] p 71 N85-12131

Analysis techniques for tracer studies of oxidation [NASA-CR-174796] p 84 N85-12162

The effect of tantalum on the structure/properties of two polycrystalline nickel-base superalloys: B-1900 + Hf MAR-M247 [NASA-CR-174847] p 73 N85-18127

Effects of MAR-M247 substrate (modified) composition on coating oxidation coating/substrate interdiffusion --- protective coatings for hot section components of gas turbine engines [NASA-CR-174851] p 73 N85-19073

Low cycle fatigue of MAR-M 200 single crystals at 760 and 870 deg C [NASA-TM-86933] p 74 N85-19074

Creep-rupture behavior of iron superalloys in high-pressure hydrogen [NASA-CR-174411] p 74 N85-19078

Effect of reduction of strategic Columbian addition in 718 Alloy on the structure and properties [NASA-CR-174841] p 75 N85-21320

Orientation and temperature dependence of some mechanical properties of the single-crystal nickel-base superalloy Rene N4. 3: Tension-compression anisotropy [NASA-TM-86982] p 76 N85-22660

On thermomechanical testing in support of constitutive equation development for high temperature alloys [NASA-CR-174879] p 147 N85-25894

Nonlinear structural analysis for fiber-reinforced  
superalloy turbine blades p 147 N85-26887

Iron rich low cost superalloys p 76 N85-26962

[NASA-CR-174900] p 76 N85-26962

On the use of internal state variables in  
thermoviscoplastic constitutive equations p 150 N85-31536

**HEAT TRANSFER**

Flame radiation and linear heat transfer in a tubular-can  
combustor p 15 A85-39580

Advanced liner-cooling techniques for gas turbine  
combustors p 15 A85-39703

[AIAA PAPER 85-1290] p 15 A85-39703

Transient technique for measuring heat transfer  
coefficients on stator airfoils in a jet engine environment  
[AIAA PAPER 85-1471] p 122 A85-39796

Heat transfer investigation in the junction region of  
circular cylinder normal to a flat plate at 90 deg location  
[ASME PAPER 84-WA/HT-70] p 111 A85-39898

Solidification interface shape for continuous casting in  
an offset mold - Two analytical methods p 112 A85-41326

Future fundamental combustion research for  
aeropropulsion systems p 16 A85-42671

[AIAA PAPER 85-1398] p 16 A85-42671

The effect of channel convergence on heat transfer in  
a passage with short pin fins p 113 N85-10303

[NASA-TM-83801] p 113 N85-10303

A review and analysis of boundary layer transition data  
for turbine application p 113 N85-10306

[NASA-TM-86880] p 113 N85-10306

Turbine Engine Hot Section Technology (HOST)  
[NASA-TM-83022] p 18 N85-10951

Turbine heat transfer p 19 N85-10964

Coolant passage heat transfer with rotation p 20 N85-10968

Preliminary results of a study of the relationship between  
free stream turbulence and stagnation region heat  
transfer p 113 N85-11317

[NASA-TM-86884] p 113 N85-11317

Heat transfer results and operational characteristics of  
the NASA Lewis Research Center Hot Section Cascade  
Test Facility p 114 N85-15133

[NASA-TM-86890] p 114 N85-15133

High temperature thermocouple and heat flux gauge  
using a unique thin film-hardware hot junction  
[NASA-TM-86898] p 123 N85-16096

Design of low loss helix circuits for interference fitted  
and brazed circuits p 103 N85-19328

[NASA-CR-168313] p 103 N85-19328

Experimental study of ceramic coated tip seals for  
turbojet engines p 114 N85-19363

[NASA-TM-86939] p 114 N85-19363

Ribbon burner simulation of T-700 turbine shroud for  
ceramic lined seals research p 114 N85-19364

[NASA-TM-86940] p 114 N85-19364

Advanced liner-cooling techniques for gas turbine  
combustors p 8 N85-21115

[NASA-TM-86952] p 8 N85-21115

Nested subcritical flows within supercritical systems  
[NASA-TM-86980] p 115 N85-21574

Manrating orbital transfer vehicle propulsion p 50 N85-25385

[NASA-TM-87019] p 50 N85-25385

The influence of jet-grid turbulence on heat transfer from  
the stagnation region of a cylinder in crossflow p 115 N85-25760

[NASA-TM-87011] p 115 N85-25760

Transient technique for measuring heat transfer  
coefficients on stator airfoils in a jet engine environment  
[NASA-TM-87005] p 124 N85-25794

Component-specific modeling p 147 N85-27261

[NASA-CR-174765] p 147 N85-27261

A computer analysis program for interfacing thermal and  
structural codes p 148 N85-27264

[NASA-TM-87021] p 148 N85-27264

Future fundamental combustion research for  
aeropropulsion systems p 30 N85-27870

[NASA-TM-87049] p 30 N85-27870

Overview of aerothermodynamic loads definition study p 51 N85-27942

High thermal power density heat transfer apparatus  
providing electrical isolation at high temperature using heat  
pipes p 117 N85-29179

[NASA-CASE-LEW-12950-2] p 117 N85-29179

Turbulent transport and length scale measurement  
experiments with confined coaxial jets p 117 N85-30245

[NASA-CR-174831] p 117 N85-30245

Transition in Turbines p 118 N85-31433

[NASA-CP-2386] p 118 N85-31433

Preliminary results of a study of the relationship between  
free-stream turbulence and stagnation region heat  
transfer p 118 N85-31435

Flat-plate transition p 118 N85-31438

Heat transfer and fluid mechanics measurements in  
transitional boundary layer flows p 118 N85-31439

A review and analysis of boundary layer transition data  
for turbine application p 118 N85-31440

Heat transfer in aeropropulsion systems p 119 N85-31444

[NASA-TM-87066] p 119 N85-31444

Local heat-transfer measurements on a large,  
scale-model turbine blade airfoil using a composite of a  
heater element and liquid crystals p 119 N85-33435

[NASA-TM-86900] p 119 N85-33435

Component-specific modeling p 33 N85-34140

[NASA-CR-174765] p 33 N85-34140

**HEAT TRANSFER COEFFICIENTS**

A new interpretation of internal heat transfer coefficients  
of porous media p 110 A85-39894

[ASME PAPER 84-WA/HT-51] p 110 A85-39894

Combined influence of unsteady free stream velocity  
and free stream turbulence on stagnation point heat  
transfer p 112 A85-41782

Heat transfer and turbulence measurements of a  
film-cooled flow over a convexly curved surface p 112 A85-41787

Local heat-transfer measurements on a large,  
scale-model turbine blade airfoil using a composite of a  
heater element and liquid crystals p 119 N85-33435

[NASA-TM-86900] p 119 N85-33435

**HEAT TREATMENT**

Heat treatment of bulk gallium arsenide using a  
phosphosilicate glass cap p 181 A85-32636

Creep of chemically vapor deposited SiC fibers p 56 N85-14878

[NASA-TM-86897] p 56 N85-14878

The response of cobalt-free Udmet 700 type alloy to  
modified heat treatments p 75 N85-20043

[NASA-TM-86942] p 75 N85-20043

Properties and microstructures for dual alloy  
combinations of three superalloys with alloy 901 p 76 N85-26963

[NASA-TM-86987] p 76 N85-26963

**HELICAL WINDINGS**

A 20 GHz, 75 watt, helix TWT for space  
communications p 101 A85-14433

**HELICOPTER DESIGN**

Transmission efficiency measurements and correlations  
with physical characteristics of the lubricant p 89 N85-23781

**HELICOPTER PERFORMANCE**

Experimental aerodynamic characteristics of an NACA  
0012 airfoil with simulated ice p 12 A85-21844

**HELICOPTERS**

The UH-1H helicopter icing flight test program - An  
overview p 11 A85-28898

[AIAA PAPER 85-0338] p 11 A85-28898

Contingency power concepts for helicopter turboshaft  
engine p 15 A85-32005

Initial feasibility ground test of a proposed  
photogrammetric system for measuring the shapes of ice  
accretions on helicopter rotor blades during forward  
flight p 12 N85-12887

[NASA-TM-87391] p 12 N85-12887

The UH-1H helicopter icing flight test program: An  
overview p 11 N85-15702

[NASA-TM-86925] p 11 N85-15702

Investigation on experimental techniques to detect,  
locate and quantify gear noise in helicopter  
transmissions p 176 N85-17667

[NASA-CR-3847] p 176 N85-17667

Correlation of rheological characteristics of lubricants  
with transmission efficiency measurements p 134 N85-30342

[NASA-TM-86988] p 134 N85-30342

**HELIUM**

Density effects on jet characteristics in confined swirling  
flow p 112 A85-45283

**HELIUM PLASMA**

Measurements of energy distribution in microwave  
plasmas of N2 and He and comparisons with results for  
H2 p 178 A85-16443

**HELMHOLTZ RESONATORS**

The response of Helmholtz resonators to external  
excitation. I - Single resonators p 174 A85-26915

**HELMHOLTZ VORTICITY EQUATION**

On the use of internal state variables in  
thermoviscoplastic constitutive equations p 150 N85-31536

**HERMETIC SEALS**

Experimental stiffness of tapered bore seals  
[NASA-TM-86978] p 132 N85-25847

**HETERODYNING**

A comparison of electronic heterodyne moire  
deflectometry and electronic heterodyne holographic  
interferometry for flow measurements p 125 N85-32302

[NASA-TM-87071] p 125 N85-32302

**HETEROJUNCTION DEVICES**

GaAs and 3-5 compound solar cells status and prospects  
for use in space p 49 N85-22580

**HIERARCHIES**

On the development of hierarchical solution strategies  
for nonlinear finite element formulations p 171 A85-21979

**HIGH ALTITUDE**

Variability of cloudiness at airline cruise altitudes from  
GASP measurements p 166 A85-31199

**HIGH CURRENT**

Surface interactions and high-voltage current  
collection p 40 N85-22493

**HIGH FREQUENCIES**

Development of high frequency low weight power  
magnetics for aerospace power systems p 102 A85-45373

Effect of Interfacial characteristics of metal clad  
polymeric substrates on electrical high frequency  
interconnection performance p 99 N85-20223

[NASA-TM-86948] p 99 N85-20223

Alternatives for satellite sound broadcast systems at HF  
and VHF p 99 N85-23815

**HIGH GAIN**

Case study of sample spacing in planar near-field  
measurement of high gain antennas p 97 N85-10234

[NASA-TM-86872] p 97 N85-10234

**HIGH LEVEL LANGUAGES**

Data flow methods for dynamic system simulation - A  
CSSL-IV microcomputer network interface p 170 A85-28614

A functional language approach in high-speed digital  
simulation p 170 A85-28615

Functional language and data flow architectures p 170 A85-28629

Floating-point function generation routines for 16-bit  
microcomputers p 170 N85-10683

[NASA-TM-83783] p 170 N85-10683

**HIGH PRESSURE**

Cathode degradation and erosion in high pressure arc  
discharges p 43 A85-16445

Energy efficient engine high pressure turbine ceramic  
shroud support technology report p 23 N85-10996

[NASA-CR-168036] p 23 N85-10996

Energy efficient engine. High pressure compressor  
detail design report p 23 N85-10998

[NASA-CR-165558] p 23 N85-10998

Liquid fuel spray processes in high-pressure gas flow  
[NASA-TM-86944] p 115 N85-21570

Applications of high pressure differential scanning  
calorimetry to aviation fuel thermal stability research p 63 N85-23941

[NASA-TM-87002] p 63 N85-23941

Graphite fiber intercalation: Dynamics of the bromine  
intercalation process p 53 N85-26921

[NASA-TM-87015] p 53 N85-26921

Energy efficient engine high-pressure turbine component  
rig performance test report p 30 N85-29955

[NASA-CR-168189] p 30 N85-29955

High pressure compressor component performance  
report p 33 N85-34138

[NASA-CR-168245] p 33 N85-34138

Hollow cathodes in high pressure arc discharges  
[NASA-TM-87098] p 52 N85-34179

**HIGH SPEED**

Wind tunnel results of advanced high speed propellers  
in the takeoff, climb, and landing operating regimes p 6 A85-47025

[AIAA PAPER 85-1259] p 6 A85-47025

Effect of two inner-ring oil-flow distribution schemes on  
the operating characteristics of a 35 millimeter bore ball  
bearing to 2.5 million DN p 130 N85-13233

[NASA-TP-2404] p 130 N85-13233

Lubrication and performance of high-speed  
rolling-element bearings p 131 N85-21658

[NASA-TM-86958] p 131 N85-21658

Development of a multiplane multispeed balancing  
system for turbine systems p 35 N85-22400

[NASA-CR-174750] p 35 N85-22400

Wind tunnel results of advanced high speed propellers  
in the takeoff, climb and landing operating regimes p 9 N85-29925

[NASA-TM-87054] p 9 N85-29925

**HIGH SPEED PHOTOGRAPHY**

Solids mixing in a three phase fluidized bed containing  
spherically shaped-porous solid particles p 120 N85-33453

[PB85-187961] p 120 N85-33453

**HIGH STRENGTH ALLOYS**

Hot isostatically pressed manufacture of high strength  
MERL 76 disk and seal shapes p 71 N85-11225

[NASA-CR-165550] p 71 N85-11225

**HIGH TEMPERATURE**

High temperature oxidation of propene p 61 A85-33570

High-temperature fiber optic pressure sensor p 123 A85-46607

Stability of bromine intercalated graphite fibers p 84 N85-10187

[NASA-TM-86859] p 84 N85-10187

Pre-HOST high temperature crack propagation p 19 N85-10956

Effects of tin on microstructure and mechanical behavior  
of Inconel 718 p 71 N85-12129

[NASA-TM-86866] p 71 N85-12129

High-temperature optically activated GaAs power  
switching for aircraft digital electronic control p 34 N85-12901

[NASA-CR-174711] p 34 N85-12901

- Effects of silver and group 2 fluorides addition to plasma sprayed chromium carbide high temperature solid lubricant for foil gas bearing to 650 deg C  
[NASA-TM-86895] p 84 N85-14928
- Dispersed metal-toughened ceramics and ceramic brazing  
[NASA-CR-174284] p 86 N85-15916
- Transformation toughened ceramics for the heavy duty diesel engine technology program  
[NASA-CR-174689] p 185 N85-16698
- High temperature properties of equiatomic FeAl with ternary additions  
[NASA-TM-86938] p 73 N85-19072
- Chemical approach for controlling nadimide cure temperature and rate  
[NASA-CASE-LEW-13770-5] p 87 N85-21352
- 3-D inelastic analysis methods for hot section components (base program) — turbine blades, turbine vanes, and combustor liners  
[NASA-CR-174700] p 145 N85-21686
- Multiaxial and thermomechanical fatigue considerations in damage tolerant design  
[NASA-TM-87022] p 76 N85-26964
- Structural characteristics of high temperature composites  
[NASA-CR-175998] p 58 N85-30037
- Creep fatigue life prediction for engine hot section materials (isotropic)  
[NASA-CR-168228] p 32 N85-31057
- On numerical integration and computer implementation of viscoplastic models p 151 N85-31542
- A comparison of smooth specimen and analytical simulation techniques for notched members at elevated temperatures p 151 N85-31546
- Shock tube measurements of growth constants in the branched-chain ethane-carbon monoxide-oxygen system  
[NASA-TM-87068] p 64 N85-32156
- Results of an interlaboratory fatigue test program conducted on alloy 800H at room and elevated temperatures  
[NASA-CR-174940] p 152 N85-32340
- Multistage spent particle collector and a method for making same  
[NASA-CASE-LEW-13914-1] p 135 N85-33489
- HIGH TEMPERATURE ENVIRONMENTS**
- Performance of thermal barrier coatings in high heat flux environments p 79 A85-19087
- Component-specific modeling p 20 N85-10971
- The 3-D inelastic analysis methods for hot section components: Brief description p 20 N85-10972
- Life prediction and constitutive behavior: Overview p 20 N85-10973
- HOST high temperature crack propagation p 21 N85-10977
- Surface protection overview p 21 N85-10978
- Airfoil deposition model p 21 N85-10979
- Evaluation results of the 700 deg C Chinese strain gauges — for gas turbine engine  
[NASA-TM-86973] p 124 N85-21605
- Thermal barrier coating system  
[NASA-CASE-LEW-14057-1] p 59 N85-35233
- HIGH TEMPERATURE TESTS**
- Ceramic component development for the AGT101 gas turbine engine p 126 A85-15972
- Plastic flow of plasma sprayed ceramics p 80 A85-24161
- Strength and microstructure of sintered Si3N4 with rare-earth-oxide additions  
[ACS PAPER 130-13-84] p 80 A85-25271
- Closed-loop strain controlled testing at elevated temperatures with a non-contacting gage p 121 A85-29562
- On the fatigue crack propagation behavior of superalloys at intermediate temperatures p 68 A85-32434
- Analysis of stress-strain, fracture, and ductility behavior of aluminum matrix composites containing discontinuous silicon carbide reinforcement p 55 A85-37421
- Fracture of yttria-doped, sintered reaction-bonded silicon nitride  
[ACS PAPER 7-J3-84] p 82 A85-42797
- Compatibility experiments of facilities, materials, and propellants for electrothermal thrusters  
[NASA-TM-86956] p 49 N85-21260
- Analysis of experimental shaft seal data for high-performance turbomachines, as for Space Shuttle main engines  
[NASA-TM-86928] p 115 N85-21569
- Burner rig corrosion of SiC at 1000 deg C  
[NASA-TM-87061] p 53 N85-30011
- Nonlinear Constitutive Relations for High Temperature Application, 1984  
[NASA-CP-2369] p 150 N85-31530
- HIGH VACUUM**
- Vacuum chamber pressure effects on thrust measurements of low Reynolds number nozzles  
[NASA-TM-86955] p 49 N85-21259
- HIGH VOLTAGES**
- High-voltage solar-cell chip p 154 A85-24668
- Dilute plasma coupling currents to a high voltage solar array in weak magnetic fields p 46 A85-45388
- High voltage requirements and issues for the 1990's — for spacecraft power supplies p 46 A85-45429
- Circuit transients due to negative bias arcs on a high-voltage solar array in low Earth orbit  
[NASA-TP-2407] p 39 N85-14858
- A new very high voltage semiconductor switch  
[NASA-TM-86957] p 103 N85-20246
- Spacecraft Environmental Interactions Technology, 1983  
[NASA-CP-2359] p 39 N85-22470
- HISTORIES**
- A historical overview of the electrical power systems in the US manned and some US unmanned spacecraft  
[NASA-CR-174806] p 47 N85-13910
- HOLDERS**
- Apparatus for mounting a field emission cathode  
[NASA-CASE-LEW-14108-1] p 104 N85-29149
- HOLE GEOMETRY (MECHANICS)**
- Flow visualization study of the effect of injection hole geometry on an inclined jet in crossflow  
[NASA-TM-86936] p 115 N85-20269
- HOLLOW CATHODES**
- Extended performance technology study 30-cm thruster  
[NASA-CR-168259] p 48 N85-15806
- Heaterless ignition of inert gas ion thruster hollow cathodes  
[NASA-TM-87086] p 52 N85-34177
- Hollow cathodes in high pressure arc discharges  
[NASA-TM-87098] p 52 N85-34179
- HOLOGRAPHIC INTERFEROMETRY**
- A comparison of electronic heterodyne moire deflectometry and electronic heterodyne holographic interferometry for flow measurements  
[NASA-TM-87071] p 125 N85-32302
- HOLOGRAPHY**
- An approach for automated analysis of particle holograms p 120 A85-10034
- HOMOGENEITY**
- Homogeneity of pristine and bromine intercalated graphite fibers  
[NASA-TM-87016] p 89 N85-25521
- HOMOJUNCTIONS**
- GaAs and 3-5 compound solar cells status and prospects for use in space p 49 N85-22580
- HORIZONTAL ORIENTATION**
- Wake effects on the aerodynamic performance of horizontal axis wind turbines  
[NASA-CR-174920] p 162 N85-29364
- HOT CATHODES**
- Calibration stability of some hot-cathode ion gauges p 122 A85-41634
- HOT CORROSION**
- Effects of SO2 and SO3 on the Na2SO4 induced corrosion of nickel p 65 A85-15603
- Chemical reactions involved in the initiation of hot corrosion of IN-738 p 66 A85-31688
- Hot corrosion of sintered alpha-SiC at 1000 C  
[ACS PAPER 19-B-84P] p 83 A85-45302
- Effects of surface chemistry on hot corrosion life: Overview p 21 N85-10980
- Studies on the hot corrosion of a nickel-base superalloy, Udimet 700  
[NASA-TM-86882] p 71 N85-11224
- Digital temperature and velocity control of mach 0.3 atmospheric pressure durability testing burner rigs in long time, unattended cyclic testing  
[NASA-TM-86959] p 75 N85-21321
- Oxidation and hot corrosion of hot-pressed Si3N4 at 1000 deg C  
[NASA-TM-86977] p 88 N85-21358
- Effects of surface chemistry on hot corrosion life  
[NASA-CR-174915] p 28 N85-26711
- Burner rig corrosion of SiC at 1000 deg C  
[NASA-TM-87061] p 53 N85-30011
- Mechanism of strength degradation for hot corrosion of alpha-SiC  
[NASA-TM-87052] p 91 N85-30135
- A multiple linear regression analysis of hot corrosion attack on a series of nickel base turbine alloys  
[NASA-TM-87020] p 77 N85-31284
- HOT PRESSING**
- Effect of hot isostatic pressing on reaction-bonded silicon nitride p 79 A85-15195
- Fracture toughness of hot-pressed beryllium p 66 A85-25835
- The effect of microstructure, temperature, and hold-time on low-cycle fatigue of As HIP P/M Rene 95 p 67 A85-32399
- The substitution of nickel for cobalt in hot isostatically pressed powder metallurgy UDIMET 700 alloys p 68 A85-37415
- Microstructure of reaction-bonded silicon nitride consolidated by isostatic hot-pressing p 83 A85-45304
- Effect of hot isostatic pressing on the properties of sintered alpha silicon carbide p 83 A85-48757
- Hot isostatically pressed manufacture of high strength MERL 76 disk and seal shapes  
[NASA-CR-165550] p 71 N85-11225
- Oxidation and hot corrosion of hot-pressed Si3N4 at 1000 deg C  
[NASA-TM-86977] p 88 N85-21358
- Dispersed metal-toughened alumina  
[NASA-CR-174687] p 89 N85-22758
- HOT SURFACES**
- Component-specific modeling  
[NASA-CR-174765] p 33 N85-34140
- HOT WORKING**
- Effects of cobalt on the hot workability of nickel-base superalloys p 67 A85-32412
- HUMIDITY**
- Effect of humidity on fretting wear of several pure metals  
[NASA-TP-2403] p 72 N85-13006
- Humidity effects on adhesion of nickel-zinc ferrite in elastic contact with magnetic tape and itself  
[NASA-TP-2449] p 88 N85-21359
- HYBRID STRUCTURES**
- Evolution of assumed stress hybrid finite element p 142 A85-35046
- Axisymmetric solid elements by a rational hybrid stress method p 143 A85-41109
- HYDROCARBON COMBUSTION**
- Transferring data oscilloscope to an IBM using an Apple II+ p 168 A85-24526
- HYDROCARBON FUELS**
- Chemistry of fuel deposits and sediments and their precursors  
[NASA-CR-174778] p 92 N85-10209
- Combustion gas properties. 2: Natural gas fuel and dry air  
[NASA-TP-2435] p 26 N85-21168
- Fuel-rich catalytic combustion: A soot-free technique for in situ hydrogen-like enrichment  
[NASA-TP-2498] p 63 N85-31244
- Rapid estimation of concentration of aromatic classes in middlestage fuels by high-performance liquid chromatography  
[NASA-TP-2495] p 93 N85-31307
- HYDROCARBONS**
- Effect of gravity on halogenated hydrocarbon flame retardant effectiveness  
[IAF PAPER 84-156] p 61 A85-23199
- Plasma deposited hydrogenated carbon on GaAs and InP p 182 A85-40386
- Plasma deposited diamondlike carbon on GaAs and InP  
[NASA-TM-86870] p 183 N85-10844
- Applications of high pressure differential scanning calorimetry to aviation fuel thermal stability research  
[NASA-TM-87002] p 63 N85-23941
- Fuel rich catalytic combustion: The first stage of a two-stage combustor  
[NASA-TM-87042] p 63 N85-28983
- HYDRODYNAMICS**
- Hydrodynamic lubrication of rigid nonconformal contacts in combined rolling and normal motion  
[ASME PAPER 84-TRIB-13] p 127 A85-21280
- Rotordynamic Instability Problems in High-Performance Turbomachinery  
[NASA-CP-2338] p 131 N85-14116
- Mechanics of a gaseous film barrier to lubricant wetting of elastohydrodynamically lubricated conjunctions  
[NASA-TP-2500] p 135 N85-32330
- Dual clearance squeeze film damper  
[NASA-CASE-LEW-13506-1] p 135 N85-33490
- HYDROGEN**
- Effect of water on hydrogen permeability — Stirling engines  
[NASA-TM-86904] p 53 N85-14864
- HYDROGEN CHLORIDES**
- Mechanism for forming hydrogen chloride and sodium sulfate from sulfur trioxide, water, and sodium chloride p 62 A85-48513
- HYDROGEN FUELS**
- Electrocatalyst advances for hydrogen oxidation in phosphoric acid fuel cells p 60 A85-15614
- Performance characterization tests of a 1-kW resistojel using hydrogen, nitrogen and ammonia as propellants  
[AIAA PAPER 85-1159] p 44 A85-39628
- Combustion gas properties. Part 3: Hydrogen gas fuel and dry air  
[NASA-TP-2477] p 32 N85-31058
- HYDROGEN IONS**
- Three-dimensional calculation of shuttle charging in polar orbit p 40 N85-22486

**HYDROGEN OXYGEN ENGINES**

An evaluation of oxygen/hydrogen propulsion systems for the Space Station  
[AIAA PAPER 85-1156] p 45 A85-43976

Advanced research and technology programs for advanced high-pressure oxygen-hydrogen rocket propulsion  
[NASA-TM-86969] p 37 N85-21231

An evaluation of oxygen-hydrogen propulsion systems for the Space Station  
[NASA-TM-87059] p 52 N85-28971

Status of advanced orbital transfer propulsion  
[NASA-TM-87069] p 52 N85-35225

**HYDROGEN OXYGEN FUEL CELLS**

Design considerations for a 10-kW integrated hydrogen-oxygen regenerative fuel cell system  
p 155 A85-45380

**HYDROGEN PLASMA**

Frictional and structural characterization of ion-nitrided low and high chromium steels  
[NASA-TM-86991] p 132 N85-23085

**HYDROGEN RECOMBINATIONS**

The energetics of hydrogen atom recombination - Analysis, experiments, and modeling --- in electrothermal propulsion system  
p 179 A85-16444

**HYDROGEN-BASED ENERGY**

Design principles for nickel hydrogen cells and batteries  
p 104 N85-31398

**HYDROGENATION**

Optical properties of hydrogenated amorphous carbon films grown from methane plasma  
[NASA-TM-86995] p 183 N85-26406

**HYDROSTATICS**

Development of gas-lubricated pistons for heavy duty diesel engine technology program  
[NASA-CR-174746] p 184 N85-12808

**HYDROTHERMAL STRESS ANALYSIS**

Designing for fiber composite structural durability in hydrothermomechanical environment  
[NASA-TM-87045] p 58 N85-27978

**HYGRAL PROPERTIES**

Hygrothermomechanical evaluation of transverse filament tape epoxy/polyester fiberglass composites  
p 54 A85-15632

ICAN - Integrated composites analyzer  
[AIAA PAPER 84-0974] p 54 A85-16094

Designing for fiber composite structural durability in hydrothermomechanical environment  
[NASA-TM-87045] p 58 N85-27978

**HYPERBOLIC DIFFERENTIAL EQUATIONS**

A convergent series expansion for hyperbolic systems of conservation laws  
[NASA-CR-172557] p 168 N85-21990

**HYPERVELOCITY LAUNCHERS**

Preliminary analysis of space mission applications for electromagnetic launchers  
[NASA-CR-174067] p 35 N85-12071

**HYPERVELOCITY PROJECTILES**

Rail accelerator technology and applications  
[NASA-TM-86947] p 48 N85-21258

Arc-driven rail gun research  
[NASA-CR-174816] p 132 N85-21662

**HYSTERESIS**

Internal hysteresis experienced on a high pressure syn gas compressor  
p 131 N85-14122  
Application of traction drives as servo mechanisms  
p 152 N85-33520

**IBM 370 COMPUTER**

Transferring data oscilloscope to an IBM using an Apple II+  
p 168 A85-24526

**ICE**

Comparison of icing cloud instruments for 1982-1983 icing season flight program  
[AIAA PAPER 84-0020] p 13 A85-16098

Initial feasibility ground test of a proposed photogrammetric system for measuring the shapes of ice accretions on helicopter rotor blades during forward flight  
[NASA-TM-87391] p 12 N85-12887

**ICE FORMATION**

Progress toward the development of an aircraft icing analysis capability  
[AIAA PAPER 84-0105] p 10 A85-10653

Progress in development of a Navier-Stokes solver for evaluation of iced airfoil performance  
[AIAA PAPER 85-0410] p 3 A85-19731

Analytical determination of propeller performance degradation due to ice accretion  
[AIAA PAPER 85-0339] p 14 A85-20867

Icing tunnel tests of Electro-Impulse De-Icing of an engine inlet and high-speed wings  
[AIAA PAPER 85-0466] p 10 A85-20872

Experimental aerodynamic characteristics of an NACA 0012 airfoil with simulated ice  
p 12 A85-21844  
Predicting rime ice accretion on airfoils  
p 3 A85-25135

The NASA altitude wind tunnel - Its role in advanced icing research and development  
[AIAA PAPER 85-0090] p 35 A85-26381

The UH-1H helicopter icing flight test program - An overview  
[AIAA PAPER 85-0338] p 11 A85-28898

Icing flight research - Aerodynamic effects of ice and ice shape documentation with stereo photography  
[AIAA PAPER 85-0468] p 11 A85-30192

Performance degradation of helicopter rotor in forward flight due to ice  
p 11 A85-42937  
The UH-1H helicopter icing flight test program: An overview  
[NASA-TM-86925] p 11 N85-15702

The NASA Altitude Wind Tunnel (AWT): Its role in advanced icing research and development  
[NASA-TM-86920] p 35 N85-15758

Icing flight research: Aerodynamic effects of ice and ice shape documentation with stereo photography  
[NASA-TM-86906] p 12 N85-18049

Ice shapes and the resulting drag increase for a NACA 0012 airfoil  
[NASA-TM-83556] p 11 N85-27839

**ICE PREVENTION**  
Progress toward the development of an aircraft icing analysis capability  
[AIAA PAPER 84-0105] p 10 A85-10653

Analytical and physical modeling program for the NASA Lewis Research Center's Altitude Wind Tunnel (AWT)  
[NASA-TM-86919] p 35 N85-15757

**IDEAL GAS**

Oscillatory conductive heat transfer for a fiber in an ideal gas  
p 109 A85-26077

Ideal gas thermodynamic properties for the phenyl, phenoxy, and o-phenyl radicals  
[NASA-TM-83800] p 184 N85-22204

**IGNITION LIMITS**

Systematic optimization of a detailed kinetic model using a methane ignition example  
p 59 A85-12890

Effect of gravity on halogenated hydrocarbon flame retardant effectiveness  
[IAF PAPER 84-156] p 61 A85-23199

High temperature oxidation of propene  
p 61 A85-33570

Behavior of the lean methane-air flame at zero-gravity  
[NASA-CR-175586] p 62 N85-21283

The use of a laser Doppler velocimeter in a standard flammability tube  
[NASA-CR-174960] p 125 N85-35389

**ILLUMINATION**

Focal shifts in parabolic reflectors  
p 97 A85-39356

**IMAGE ANALYSIS**

An approach for automated analysis of particle holograms  
p 120 A85-10034

**IMAGE PROCESSING**

An allpass filter design for luminance and chrominance separation of NTSC signals  
p 102 A85-28230

Free-surface phenomena under low- and zero-gravity conditions  
[NASA-CR-175885] p 36 N85-27922

**IMIDES**

Imide modified epoxy matrix resins  
[NASA-CR-174695] p 85 N85-15892

**IMPACT RESISTANCE**

Impact resistance of fiber composites - Energy-absorbing mechanisms and environmental effects  
p 56 A85-46543

Fundamental studies of composite toughness  
p 56 N85-12948

**IMPACT TESTS**

Characterization of solid particle erosion resistance of ductile metals based on their properties  
p 69 A85-42569

**IMPEDANCE**

Characterization of microstrip discontinuities in the time and frequency domains  
[NASA-CR-176190] p 106 N85-35342

**IMPINGEMENT**

Into mesh lubrication of spur gears with arbitrary offset oil jet. I - For jet velocity less than or equal to gear velocity  
p 128 A85-24497

Lubricant jet flow phenomena in spur and helical gears with modified center distances and/or addendums - For out-of-mesh conditions  
[ASME PAPER 84-DET-96] p 129 A85-35049

Effect of surface configuration during solid particle impingement erosion  
p 69 A85-42568

Characterization of solid particle erosion resistance of ductile metals based on their properties  
p 69 A85-42569

**IMPLANTATION**

Percutaneous connectors  
[NASA-CR-175627] p 168 N85-27508

**IMPURITIES**

Milling of Si3N4 with Si3N4 hardware  
[NASA-TM-86864] p 84 N85-10191

**INCIDENT RADIATION**

Incident beam polarization for laser Doppler velocimetry employing a sapphire cylindrical window  
p 122 A85-39835

**INCLUSIONS**

Ultrasonic wave propagation in two-phase media - Spherical inclusions  
p 54 A85-11926

**INCOMPRESSIBLE FLOW**

Approximate analysis for resonance of an incompressible shear layer plus edges  
p 107 A85-19377

Accelerated convergence for incompressible flow calculations  
[AIAA PAPER 85-0058] p 2 A85-19489

A space-marching method for incompressible Navier-Stokes equations  
[AIAA PAPER 85-0170] p 108 A85-19564

Vortex induced lift on a flat plate with a curved forward-facing flap  
p 4 A85-30175

Accelerated convergence for incompressible flow calculations  
[NASA-TM-86863] p 18 N85-10949

Incompressible lifting-surface aerodynamics for a rotor-stator combination  
[NASA-TM-83767] p 7 N85-12039

Reducing numerical diffusion for incompressible flow calculations  
[NASA-TM-83621] p 24 N85-14840

Turbulent solutions of equations of fluid motion  
p 118 N85-31441

General design method for 3-dimensional, potential flow fields. Part 2: Computer program DIN3D1 for simple, unbranched ducts  
[NASA-CR-3926] p 10 N85-35159

**INCONEL (TRADEMARK)**

Effects of tin on microstructure and mechanical behavior of Inconel 718  
[NASA-TM-86866] p 71 N85-12129

Thermal-mechanical fatigue crack growth in Inconel X-750  
[NASA-CR-174740] p 72 N85-15877

Effect of reduction of strategic Columbium addition in 718 Alloy on the structure and properties  
[NASA-CR-174841] p 75 N85-21320

Finite element analysis of notch behavior using a state variable constitutive equation  
p 152 N85-31548

**INDENTATION**

Use of static indentation laws in the impact analysis of laminated composite plates  
p 55 A85-29133

Ceramic wear in indentation and sliding contact  
p 82 A85-39549

**INDEXES (DOCUMENTATION)**

Bibliography of Lewis Research Center technical publications announced in 1984  
[NASA-TM-87012] p 184 N85-28876

**INDIUM PHOSPHIDES**

Plasma deposited hydrogenated carbon on GaAs and InP  
p 182 A85-40386

Plasma deposited diamondlike carbon on GaAs and InP  
[NASA-TM-86870] p 183 N85-10844

**INDUCTION HEATING**

High frequency plasma generator for ion thrusters  
[NASA-CR-174772] p 48 N85-17023

**INDUSTRIAL ENERGY**

Advanced technology cogeneration system conceptual design study: Closed cycle gas turbines  
[NASA-CR-168222] p 159 N85-16300

**INDUSTRIAL PLANTS**

Advanced technology cogeneration system conceptual design study: Closed cycle gas turbines  
[NASA-CR-168222] p 159 N85-16300

**INELASTIC STRESS**

Strainrange partitioning - A total strain range version --- for creep fatigue life prediction by summing inelastic and elastic strain-range-life relations for two Ni base superalloys  
p 64 A85-11603

A history dependent damage model for low cycle fatigue  
[ASME PAPER 84-PVP-112] p 140 A85-18795

Unified constitutive material models for nonlinear finite-element structural analysis --- gas turbine engine blades and vanes  
[AIAA PAPER 85-1418] p 142 A85-39769

The 3-D inelastic analysis methods for hot section components: Brief description  
p 20 N85-10972

Local strain redistribution corrections for a simplified inelastic analysis procedure based on an elastic finite-element analysis  
[NASA-TP-2421] p 145 N85-20396

- 3-D inelastic analysis methods for hot section components (base program) --- turbine blades, turbine vanes, and combustor liners  
[NASA-CR-174700] p 145 N85-21686
- Unified constitutive material models for nonlinear finite-element structural analysis --- gas turbine engine blades and vanes  
[NASA-TM-86985] p 146 N85-24338
- A survey of unified constitutive theories p 150 N85-31531
- INFRARED ASTRONOMY**  
Mosaic Infrared Sensor for Space Astronomy (MIRSSA)  
[NASA-CR-176154] p 125 N85-33456
- INFRARED DETECTORS**  
Mosaic Infrared Sensor for Space Astronomy (MIRSSA)  
[NASA-CR-176154] p 125 N85-33456
- INFRARED SPECTRA**  
Nitriding of titanium and its alloys by N<sub>2</sub>, NH<sub>3</sub> or mixtures of N<sub>2</sub> + H<sub>2</sub> in a dc arc plasma at low pressures (or = to torr)  
[NASA-TM-83803] p 131 N85-15168
- INGESTION (ENGINES)**  
Temperature distortion generator for turboshaft engine testing  
[SAE PAPER 841541] p 15 A85-39065
- Temperature distortion generator for turboshaft engine testing  
[NASA-TM-83748] p 1 N85-15658
- INGOTS**  
Control of solidification boundary in continuous casting by asymmetric cooling and mold offset  
p 110 A85-37047
- INJECTION**  
A new very high voltage semiconductor switch  
[NASA-TM-86957] p 103 N85-20246
- INLET AIRFRAME CONFIGURATIONS**  
Performance and surge limits of a TF30-P-3 turbofan engine/axisymmetric mixed-compression inlet propulsion system at Mach 2.5  
[NASA-TP-2461] p 27 N85-25261
- INLET FLOW**  
Analytical study of blowing boundary layer control for subsonic V/STOL inlets p 2 A85-11646
- Calculation of compressible flow about three-dimensional inlets with auxiliary inlets, slats and vanes by means of a panel method  
[AIAA PAPER 85-1196] p 5 A85-40817
- The three-dimensional compressible flow in a radial inflow turbine scroll p 6 A85-41826
- Application of computational fluid dynamics to complex inlet ducts  
[AIAA PAPER 85-1213] p 6 A85-47023
- Flow rates and pressure profiles for one to four axially aligned Borda inlets  
[NASA-TP-2390] p 113 N85-14078
- Effect of steady-state temperature distortion on inlet flow to a high-bypass-ratio turbofan engine  
[NASA-TM-86896] p 24 N85-15725
- Aerodynamic detuning analysis of an unstalled supersonic turbofan cascade  
[NASA-TM-87001] p 9 N85-26670
- Flow rate and pressure profiles for 1 to 4 axially aligned orifice inlets  
[NASA-TP-2460] p 116 N85-27165
- Application of computational fluid dynamics to complex inlet ducts  
[NASA-TM-87060] p 118 N85-30247
- INLET PRESSURE**  
A comparison of flow rates and pressure profiles for N-sequential inlets and three related seal configurations  
p 109 A85-26526
- Flow rates and pressure profiles for one to four axially aligned Borda inlets  
[NASA-TP-2390] p 113 N85-14078
- INLET TEMPERATURE**  
Redistribution of the inlet temperature profile through the SSME fuel turbine p 50 N85-26901
- SSME fuel preburner two-dimensional analysis p 51 N85-27943
- INSPECTION**  
Advanced blade tip seal system, volume 2  
[NASA-CR-167851] p 23 N85-10999
- INSTRUMENT ERRORS**  
Fiber optic temperature sensor p 121 A85-29563
- INSTRUMENTS**  
HOST instrumentation R and D program overview  
p 19 N85-10957
- Instrumentation technology overview p 124 N85-26903
- INSULATORS**  
Dispersed metal-toughened ceramics and ceramic brazing  
[NASA-CR-174284] p 86 N85-15916
- INTAKE SYSTEMS**  
A comparison of flow rates and pressure profiles for N-sequential inlets and three related seal configurations  
p 109 A85-26526
- Flow rates and pressure profiles for one to four axially aligned Borda inlets  
[NASA-TP-2390] p 113 N85-14078
- Performance and surge limits of a TF30-P-3 turbofan engine/axisymmetric mixed-compression inlet propulsion system at Mach 2.5  
[NASA-TP-2461] p 27 N85-25261
- Calculation of compressible flow about three-dimensional inlets with auxiliary inlets, slats and vanes by means of a panel method  
[NASA-CR-174975] p 10 N85-35162
- INTEGRAL EQUATIONS**  
Noise transmission loss of a rectangular plate in an infinite baffle  
[NASA-TP-2398] p 176 N85-22109
- INTEGRALS**  
Translational and extensional energy release rates (the J- and M-integrals) for a crack layer in thermoelasticity  
[NASA-CR-174872] p 145 N85-21685
- INTEGRATED CIRCUITS**  
High-voltage solar-cell chip p 154 A85-24668
- Characterization of MMIC devices for active array antennas  
[NASA-TM-86907] p 38 N85-15779
- Configuration study for a 30 GHz monolithic receive array: Technical assessment  
[NASA-CR-174697] p 98 N85-18238
- INTEGRATED ENERGY SYSTEMS**  
Develop and test fuel cell powered on-site integrated total energy systems. Phase 3: Full-scale power plant development  
[NASA-CR-174887] p 161 N85-25941
- INTERACTIONAL AERODYNAMICS**  
Noise produced by the interaction of a rotor wake with a swept stator blade  
[AIAA PAPER 84-2326] p 173 A85-13956
- A linearized unsteady aerodynamic analysis for transonic cascades p 3 A85-20744
- A note on blade wake interaction influence on compressor stator row aerodynamic performance p 4 A85-32965
- The computation of viscous/inviscid interaction on airfoils with separated flow p 6 A85-42954
- INTERACTIVE CONTROL**  
MINDS: A microcomputer interactive data system for 8086-based controllers  
[NASA-TP-2378] p 170 N85-17576
- INTERCALATION**  
Dynamics of graphite fiber intercalation: In situ resistivity measurements with a four point probe  
[NASA-TM-86858] p 53 N85-10105
- Stability of bromine intercalated graphite fibers  
[NASA-TM-86859] p 84 N85-10187
- Homogeneity of pristine and bromine intercalated graphite fibers  
[NASA-TM-87016] p 89 N85-25521
- Graphite fiber intercalation: Dynamics of the bromine intercalation process p 53 N85-26921
- Environmental stability of intercalated graphite fibers  
[NASA-TM-87025] p 90 N85-26992
- A micrographic and gravimetric study of intercalation and deintercalation of graphite fibers  
[NASA-TM-87026] p 91 N85-28110
- INTERFACE STABILITY**  
Convective influence on the stability of a cylindrical solid-liquid interface p 109 A85-26911
- INTERFACES**  
Effect of Interfacial characteristics of metal clad polymeric substrates on electrical high frequency interconnection performance  
[NASA-TM-86948] p 99 N85-20223
- INTERFACIAL TENSION**  
Contact angle and surface tension measurements of a five-ring polyphenyl ether p 86 N85-15897
- Tribological properties of boron nitride synthesized by ion beam deposition  
[NASA-TM-86962] p 87 N85-21355
- Hertzian contact in two and three dimensions  
[NASA-TP-2473] p 135 N85-32331
- INTERFEROMETERS**  
Automatic sphericity interferometer for testing lens radii  
[AD-A155736] p 125 N85-33457
- INTERLAYERS**  
Graphite fiber intercalation: Dynamics of the bromine intercalation process  
[NASA-TM-87015] p 53 N85-26921
- INTERMETALLICS**  
Ductility in rapidly solidified NiAl p 66 A85-26158
- New eutectic alloys and their heats of transformation p 66 A85-27808
- High temperature properties of equiatomic FeAl with ternary additions  
[NASA-TM-86938] p 73 N85-19072
- The B2 aluminides as alternative materials p 74 N85-19076
- Alloys based on NiAl for high temperature applications  
[NASA-TM-86976] p 75 N85-21322
- Oxidizing seal for a turbine tip gas path  
[NASA-CASE-LEW-14053-1] p 136 N85-34402
- INTERNAL COMBUSTION ENGINES**  
Internal combustion engine combustion chamber process studies at NASA Lewis Research Center  
p 112 A85-45856
- Knock syndrome: Its cures and its victims  
[NASA-CR-174395] p 93 N85-19185
- Modeling the internal combustion engine  
[NASA-RP-1094] p 172 N85-19733
- NDE for heat engine ceramics  
[NASA-TM-86949] p 137 N85-20389
- Stratified charge rotary aircraft engine technology enablement program  
[NASA-CR-174812] p 25 N85-21163
- INTERNAL ENERGY**  
On the use of internal state variables in thermoviscoplastic constitutive equations  
p 150 N85-31536
- INTERNATIONAL COOPERATION**  
Development and use of the computer software package for planning the 12 GHz broadcasting-satellite service at RARC '83 p 96 A85-29605
- INTERORBITAL TRAJECTORIES**  
Radiation exposure and performance of multiple burn LEO-GEO orbit transfer trajectories  
[NASA-TM-86946] p 36 N85-21228
- INTERPOLATION**  
Floating-point function generation routines for 16-bit microcomputers  
[NASA-TM-83783] p 170 N85-10683
- INTERSTELLAR RADIATION**  
Radiation exposure and performance of multiple burn LEO-GEO orbit transfer trajectories  
[NASA-TM-86946] p 36 N85-21228
- INVERTERS**  
The J3 SCR model applied to resonant converter simulation p 102 A85-42156
- INVISID FLOW**  
Progress toward the development of an aircraft icing analysis capability  
[AIAA PAPER 84-0105] p 10 A85-10653
- Comparison of secondary flows predicted by a viscous code and an inviscid code with experimental data for a turning duct p 106 A85-11634
- A finite element solution of three-dimensional inviscid rotational flows through curved ducts p 107 A85-11648
- The linear two-dimensional stability of inviscid vortex streets of finite-cored vortices  
[AD-A153032] p 107 A85-14241
- Three-dimensional inviscid flow analysis of turbofan forced mixers  
[AIAA PAPER 85-0086] p 2 A85-19510
- Vortex induced lift on a flat plate with a curved forward-facing flap p 4 A85-30175
- Assessment of three-dimensional inviscid codes and loss calculations for turbine aerodynamic computations  
[ASME PAPER 84-GT-187] p 4 A85-32961
- Application of viscous and inviscid computation methods for rocket turbopump systems  
[SAE PAPER 841522] p 110 A85-39257
- Flow through very porous inclined screens  
[AIAA PAPER 85-1650] p 111 A85-40750
- Inviscid analysis of advanced turboprop propeller flow fields  
[AIAA PAPER 85-1263] p 6 A85-43977
- Inviscid and viscous flows in cascades with an explicit multiple-grid algorithm p 7 A85-48539
- Flow through very porous inclined screens  
[NASA-TM-86979] p 116 N85-25761
- IODINE COMPOUNDS**  
Environmental stability of intercalated graphite fibers  
[NASA-TM-87025] p 90 N85-26992
- ION ACCELERATORS**  
Theory of ion acceleration with closed electron drift --- in spacecraft plasma propulsion p 41 A85-15512
- ION BEAMS**  
Laboratory degradation of Kapton in a low energy oxygen ion beam  
[AIAA PAPER 83-2658] p 78 A85-10675
- Ion-beam nitriding of steels p 66 A85-24667
- Properties of coated and modified surfaces p 53 A85-36694
- Experimental performance of a microwave cavity plasma disk ion source p 179 A85-43552



Extended performance technology study 30-cm thruster  
[NASA-CR-168259] p 48 N85-15806

Deposition of diamondlike carbon films  
[NASA-CASE-LEW-14080-1] p 95 N85-20153

Diamondlike flakes  
[NASA-CASE-LEW-13837-2] p 57 N85-21267

Ion-beam nitriding of steels  
[NASA-CASE-LEW-14104-1] p 75 N85-21324

Ion beam sputter-deposited thin film coatings for protection of spacecraft polymers in low Earth orbit  
[NASA-TM-87051] p 91 N85-30137

Diamondlike carbon protective coatings for IR materials  
[NASA-TM-87083] p 178 N85-34631

**ION ENGINES**

Ion flow experiments in a multipole discharge chamber  
p 178 N85-12705

Performance capabilities of the 12-centimeter Xenon ion thruster  
p 42 N85-16439

Cathode degradation and erosion in high pressure arc discharges  
p 43 N85-16445

Inert gas test of two 12-cm magnetostatic thrusters  
p 43 N85-29310

Development of a large insert gas ion thruster  
p 45 N85-42922

Investigation of a pulsed electrothermal thruster system  
[NASA-CR-174768] p 46 N85-11132

Precision tunable resonant microwave cavity  
[NASA-CASE-LEW-13935-1] p 103 N85-20248

Heaterless ignition of inert gas ion thruster hollow cathodes  
[NASA-TM-87086] p 52 N85-34177

**ION EXCHANGE MEMBRANE ELECTROLYTES**

Development of a lithium secondary battery separator  
p 104 N85-31378

Evaluation of developmental membranes for the mixed reactant iron-chromium redox system  
[NASA-TM-87074] p 164 N85-34443

**ION EXTRACTION**

Extended performance technology study 30-cm thruster  
[NASA-CR-168259] p 48 N85-15806

**ION IMPLANTATION**

Radiation damage and defect behavior in ion-implanted, lithium counterdoped silicon solar cells  
p 182 N85-35698

Study of the effects of implantation on the high Fe-Ni-Cr and Ni-Cr-Al alloys  
[NASA-CR-175625] p 76 N85-22661

**ION IRRADIATION**

Cone formation as a result of whisker growth on ion bombarded metal surfaces  
p 182 N85-41635

**ION MOTION**

Ion flow experiments in a multipole discharge chamber  
p 178 N85-12705

**ION PLATING**

Tribological properties of boron nitride synthesized by ion beam deposition  
[NASA-TM-86962] p 87 N85-21355

The structure of ion plated films in relation to coating properties  
[NASA-TM-87055] p 95 N85-29085

Advances in sputtered and ion plated solid film lubrication  
p 136 N85-33524

**ION PROPULSION**

Theory of ion acceleration with closed electron drift --- in spacecraft plasma propulsion  
p 41 N85-15512

Ground correlation investigation of thruster/spacecraft interactions to be measured on the IAPS flight test  
p 42 N85-16408

Ion propulsion for communications satellites  
p 42 N85-16412

Characterization of 8-cm engineering model thruster  
[NASA-CR-174673] p 46 N85-11131

Ring-cusp ion thruster with shell anode  
[NASA-CASE-LEW-13881-1] p 48 N85-21256

**ION SOURCES**

Recent work on a microwave ion source  
p 179 N85-16455

Plasma deposited hydrogenated carbon on GaAs and InP  
p 182 N85-40386

Experimental performance of a microwave cavity plasma disk ion source  
p 179 N85-43552

Plasma deposited diamondlike carbon on GaAs and InP  
[NASA-TM-86870] p 183 N85-10844

**IONIZATION GAGES**

Calibration stability of some hot-cathode ion gauges  
p 122 N85-41634

**IONOSPHERIC CURRENTS**

Three-dimensional calculation of shuttle charging in polar orbit  
p 40 N85-22486

**IRON**

The reactions of cobalt, iron and nickel in SO-2 atmospheres: Similarities and differences  
[NASA-TM-86868] p 70 N85-11217

Surface effects of corrosive media on hardness, friction, and wear of materials  
[NASA-TM-83711] p 85 N85-15896

High temperature properties of equiatomic FeAl with ternary additions  
[NASA-TM-86938] p 73 N85-19072

Development of electrodes for the NASA iron/chromium  
[NASA-CR-174724] p 165 N85-35471

**IRON ALLOYS**

Stirling material technology  
[NASA-TM-86888] p 72 N85-13007

Creep-rupture behavior of iron superalloys in high-pressure hydrogen  
[NASA-CR-174411] p 74 N85-19078

Effects of chromium and aluminum on mechanical and oxidation properties of iron-nickel-base superalloys based on CG-27  
[NASA-TP-2443] p 75 N85-21323

Study of the effects of implantation on the high Fe-Ni-Cr and Ni-Cr-Al alloys  
[NASA-CR-175625] p 76 N85-22661

Iron rich low cost superalloys  
[NASA-CR-174900] p 76 N85-26962

Thermal barrier coating system  
[NASA-CASE-LEW-14057-1] p 59 N85-35233

**IRON CHLORIDES**

Environmental stability of intercalated graphite fibers  
[NASA-TM-87025] p 90 N85-26992

**ISOPARAMETRIC FINITE ELEMENTS**

Development and testing of stable, invariant, isoparametric curvilinear 2- and 3-D hybrid-stress elements  
p 140 N85-19899

Use of static indentation laws in the impact analysis of laminated composite plates  
p 55 N85-29133

**ISOSTATIC PRESSURE**

Effect of hot isostatic pressing on reaction-bonded silicon nitride  
p 79 N85-15195

The substitution of nickel for cobalt in hot isostatically pressed powder metallurgy UDIMET 700 alloys  
p 68 N85-37415

Microstructure of reaction-bonded silicon nitride consolidated by isostatic hot-pressing  
p 83 N85-45304

Effect of hot isostatic pressing on the properties of sintered alpha silicon carbide  
p 83 N85-48757

**ISOTHERMAL FLOW**

Predictions and measurements of isothermal flowfields in axisymmetric combustor geometries  
[NASA-CR-174916] p 29 N85-27867

**ISOTHERMAL PROCESSES**

Elastohydrodynamic lubrication of line contacts  
p 126 N85-11069

**ISOTROPIC MEDIA**

Unified constitutive material models for nonlinear finite-element structural analysis --- gas turbine engine blades and vanes  
[AIAA PAPER 85-1418] p 142 N85-39769

Unified constitutive material models for nonlinear finite-element structural analysis --- gas turbine engine blades and vanes  
[NASA-TM-86985] p 146 N85-24338

**ISOTROPY**

Substrate-induced orientational order in the isotropic phase of liquid crystals  
p 181 N85-24649

Constitutive model development for isotropic materials  
p 20 N85-10975

**ITERATION**

Perturbation-iteration theory for analyzing microwave striplines  
[NASA-CR-176189] p 100 N85-35321

**ITERATIVE SOLUTION**

Augmented weak forms and element-by-element preconditioners: Efficient iterative strategies for structural finite elements. A preliminary study  
p 144 N85-10384

**J**

**J INTEGRAL**

Translational and extensional energy release rates (the J- and M-integrals) for a crack layer in thermoelasticity  
[NASA-CR-174872] p 145 N85-21685

A review of path-independent integrals in elastic-plastic fracture mechanics, task 4  
[NASA-CR-174956] p 152 N85-33541

**JET AIRCRAFT**

Observations from varying the lift and drag inputs to a noise prediction method for supersonic helical tip speed propellers  
[NASA-TM-83797] p 175 N85-10788

**JET AIRCRAFT NOISE**

Supersonic jet shock noise reduction  
[AIAA PAPER 84-2278] p 173 N85-16099

Experimental investigation of shock-cell noise reduction for dual-stream nozzles in simulated flight  
[NASA-CR-3846] p 175 N85-13549

**JET ENGINE FUELS**

Combustion gas properties I-ASTM jet A fuel and dry air  
[NASA-TP-2359] p 17 N85-10064

Lubricity of well-characterized jet and broad-cut fuels by ball-on-cylinder machine  
[NASA-TM-83807] p 92 N85-12183

Liquid phase products and solid deposit formation from thermally stressed model jet fuels  
[NASA-TM-86874] p 92 N85-13066

Study of advanced fuel system concepts for commercial aircraft and engines  
[NASA-CR-174752] p 93 N85-19176

Jet fuel property changes and their effect on producibility and cost in the U.S., Canada, and Europe  
[NASA-CR-174840] p 93 N85-27012

Jet fuel instability mechanisms  
[NASA-CR-175856] p 93 N85-28127

Measurement and correlation of jet fuel viscosities at low temperatures  
[NASA-CR-174911] p 94 N85-34295

**JET ENGINES**

Eddy current jet engine disk-crack monitor  
p 120 N85-11100

The use of Ada in distributed simulations  
p 169 N85-28612

Multibus-based parallel processor for simulation  
p 169 N85-28613

Fabrication of ceramic substrate-reinforced and free forms  
[NASA-TM-86994] p 50 N85-23926

Advanced smoke meter development survey and analysis  
[NASA-CR-168287] p 124 N85-25792

Alternatives for jet engine control  
[NASA-CR-175831] p 29 N85-26713

Alternatives for jet engine control  
[NASA-CR-175832] p 29 N85-26714

Alternatives for jet engine control  
[NASA-CR-175833] p 29 N85-26715

Component-specific modeling  
[NASA-CR-174765] p 33 N85-34140

**JET FLOW**

Into mesh lubrication of spur gears with arbitrary offset oil jet. I - For jet velocity less than or equal to gear velocity  
p 128 N85-24497

Some unique experiments on receptivity --- for forced disturbances entering shear flow  
[AIAA PAPER 85-0533] p 174 N85-25932

Lubricant jet flow phenomena in spur and helical gears with modified center distances and/or addendums - For out-of-mesh conditions  
[ASME PAPER 84-DET-96] p 129 N85-35049

Experiments in dilution jet mixing - Effects of multiple rows and non-circular orifices  
[AIAA PAPER 85-1104] p 15 N85-39606

Numerical calculation of subsonic jets in crossflow with reduced numerical diffusion  
[AIAA PAPER 85-1441] p 110 N85-39780

Flow visualization study of the effect of injection hole geometry on an inclined jet in crossflow  
[NASA-TM-86936] p 115 N85-20269

Preliminary analysis of tone-excited two-stream jet velocity decay  
[NASA-TM-86951] p 8 N85-21114

Liquid fuel spray processes in high-pressure gas flow  
[NASA-TM-86944] p 115 N85-21570

Numerical calculation of subsonic jets in crossflow with reduced numerical diffusion  
[NASA-TM-87003] p 27 N85-25263

Experiments in dilution jet mixing effects of multiple rows and non-circular orifices  
[NASA-TM-86996] p 28 N85-25266

The influence of jet-grid turbulence on heat transfer from the stagnation region of a cylinder in crossflow  
[NASA-TM-87011] p 115 N85-25760

Turbulent transport and length scale measurement experiments with confined coaxial jets  
[NASA-CR-174831] p 117 N85-30245

**JET IMPINGEMENT**

Spherical microglass particle impingement studies of thermoplastic materials at normal incidence  
p 79 N85-11072

**JET MIXING FLOW**

An experimental study of tone excited heated jets  
[AIAA PAPER 84-2341] p 172 N85-10882

Mass and momentum turbulent transport experiments with confined coaxial jets  
p 107 N85-14399

Acoustic control of free jet mixing  
[AIAA PAPER 85-0569] p 109 N85-25951



- Experiments in dilution jet mixing - Effects of multiple rows and non-circular orifices  
[AIAA PAPER 85-1104] p 15 A85-39606
- Vortex modeling of single and multiple dilution jet mixing in a crossflow  
[AIAA PAPER 85-1580] p 111 A85-40701
- Jet characteristics in confined swirling flow  
p 112 A85-45282
- Density effects on jet characteristics in confined swirling flow  
p 112 A85-45283
- Dilution zone mixing studies  
p 21 N85-10984
- Development of a temperature measurement system with application to a jet in a cross flow experiment  
[NASA-CR-174896] p 27 N85-25262
- Experiments in dilution jet mixing effects of multiple rows and non-circular orifices  
[NASA-TM-86996] p 28 N85-25266
- JET NOZZLES**
- Lubricant jet flow phenomena in spur and helical gears with modified center distances and/or addendums - For out-of-mesh conditions  
[ASME PAPER 84-DET-96] p 129 A85-35049
- JOINING**
- Effect of Interfacial characteristics of metal clad polymeric substrates on electrical high frequency interconnection performance  
[NASA-TM-86948] p 99 N85-20223
- JOINTS (ANATOMY)**
- Friction and wear properties of a Charnley artificial hip joint  
[ASLE PREPRINT 84-LC-4A-4] p 168 A85-38444
- JOINTS (JUNCTIONS)**
- Fracture of composite-adhesive-composite systems  
p 141 A85-27935
- JOURNAL BEARINGS**
- An analysis of temperature effect in a finite journal bearing with spatial tilt and viscous dissipation  
p 126 A85-11074
- Vibration control of rotor shaft  
[NASA-TM-87053] p 133 N85-29292
- JUNCTION TRANSISTORS**
- The study of microstrip antenna arrays and related problems  
[NASA-CR-174054] p 97 N85-11265

## K

- KALMAN FILTERS**
- A design methodology for robust failure detection and isolation  
p 171 A85-47794
- KAPTON (TRADEMARK)**
- Laboratory studies of Kapton degradation in an oxygen ion beam  
p 177 N85-22477
- Study of Kapton under simulated shuttle environment  
[NASA-CR-176003] p 41 N85-29997
- KARMAN VORTEX STREET**
- The linear two-dimensional stability of inviscid vortex streets of finite-cored vortices  
[AD-A153032] p 107 A85-14241
- KELVIN-HELMHOLTZ INSTABILITY**
- Feedback in separated flows over symmetric airfoils  
[AIAA PAPER 84-2297] p 3 A85-28899
- KILOMETRIC WAVES**
- DE-1 measurements of AKR wave directions --- auroral kilometric radiation  
p 166 A85-37717
- KINEMATIC EQUATIONS**
- First-order ball-bearing kinematics  
p 128 A85-31203
- KINEMATICS**
- Advanced stress analysis methods applicable to turbine engine structures  
[NASA-CR-175573] p 26 N85-21165
- On Hybrid and mixed finite element methods  
[NASA-CR-175551] p 146 N85-23096
- Dynamic creep buckling: Analysis of shell structures subjected to time-dependent mechanical and thermal loading  
p 149 N85-27959
- Spiral bevel and circular arc helical gears: Tooth contact analysis and the effect of misalignment on circular arc helical gears  
[NASA-TM-87013] p 32 N85-31060
- Generated spiral bevel gears: Optimal machine-tool settings and tooth contact analysis  
[NASA-TM-87075] p 136 N85-34405
- KINETIC FRICTION**
- Friction and wear properties of a Charnley artificial hip joint  
[ASLE PREPRINT 84-LC-4A-4] p 168 A85-38444
- KINETICS**
- Future fundamental combustion research for aeropropulsion systems  
[AIAA PAPER 85-1398] p 16 A85-42671

- Nitriding of titanium and its alloys by N<sub>2</sub>, NH<sub>3</sub> or mixtures of N<sub>2</sub> + H<sub>2</sub> in a dc arc plasma at low pressures (or = to torr)  
[NASA-TM-83803] p 131 N85-15168
- Shock tube study of the fuel structure effects on the chemical kinetic mechanisms responsible for soot formation, part 2  
[NASA-CR-174880] p 63 N85-25444
- Future fundamental combustion research for aeropropulsion systems  
[NASA-TM-87049] p 30 N85-27870
- Dynamic creep buckling: Analysis of shell structures subjected to time-dependent mechanical and thermal loading  
p 149 N85-27959

## L

## LABYRINTH SEALS

- An experimental investigation of rubbing interaction in labyrinth seals at cryogenic temperature  
p 129 A85-39938
- Analytical and experimental investigation of rubbing interaction in labyrinth seals for a liquid hydrogen fuel pump - space shuttle main engine  
[NASA-CR-174657] p 48 N85-18084

## LAGRANGE MULTIPLIERS

- Recent advances in hybrid/mixed finite elements  
[NASA-CR-175574] p 145 N85-21687

## LAMINAR FLOW

- GASP cloud encounter statistics - Implications for laminar flow control flight  
p 166 A85-11979
- A review and analysis of boundary layer transition data for turbine application  
[NASA-TM-86680] p 113 N85-10306
- Thermodynamic evaluation of transonic compressor rotors using the finite volume approach  
[NASA-CR-175811] p 29 N85-26712

## LAMINAR HEAT TRANSFER

- Analysis of buoyancy effect on fully developed laminar heat transfer in a rotating tube  
p 110 A85-35596

## LAMINAR WAKES

- The mechanisms of flame holding in the wake of a bluff body  
[NASA-CR-3886] p 26 N85-21166

## LAMINATES

- Interply layer degradation effects on composite structural response  
[AIAA PAPER 84-0849] p 54 A85-16096
- Use of static indentation laws in the impact analysis of laminated composite plates  
p 55 A85-29133
- Interply layer degradation effects on composite structural response  
p 55 A85-39215
- A study of interply layer effects on the free edge stress field of angle-ply laminates  
p 55 A85-41127
- Fiberglass epoxy laminate fatigue properties at 300 and 20 K  
p 56 A85-47970
- Energy efficient engine. Volume 2. Appendix A: Component development and integration program  
[NASA-CR-173085] p 22 N85-10991
- A study of interply layer effects on the free-edge stress field of angle-ply laminates  
[NASA-TM-86924] p 57 N85-15822
- Design procedures for fiber composite structural components: Panels subjected to combined in-plane loads  
[NASA-TM-86909] p 57 N85-15823

## LANDING

- Wind tunnel results of advanced high speed propellers in the takeoff, climb, and landing operating regimes  
[AIAA PAPER 85-1259] p 6 A85-47025
- Wind tunnel results of advanced high speed propellers in the takeoff, climb and landing operating regimes  
[NASA-TM-87054] p 9 N85-29925

## LARGE SPACE STRUCTURES

- Environmentally-induced voltage limitations in large space power systems  
p 43 A85-18584
- Research and technology highlights of the Lewis Research Center  
[NASA-TM-86899] p 186 N85-17928
- Spacecraft environmental interactions: A joint Air Force and NASA research and technology program  
p 40 N85-22517
- Alternatives for satellite sound broadcast systems at HF and VHF  
p 99 N85-23815
- Extreme precision antenna reflector study results  
p 165 N85-23830

## LASER ANEMOMETERS

- Two-frequency laser-induced fluorescence technique for rapid velocity-field measurements in gas flows  
p 121 A85-32294
- Investigation of flow phenomena in a transonic fan rotor using laser anemometry  
[ASME PAPER 84-GT-199] p 4 A85-32963

- Feasibility of mapping velocity flow fields in SSME powerhead by laser anemometry techniques  
p 41 N85-27971

- Filter induced errors in laser anemometer measurements using counter processors  
[NASA-TM-87047] p 125 N85-30288

## LASER APPLICATIONS

- Velocity visualization in gas flows using laser-induced phosphorescence of biacetyl  
p 121 A85-21695
- Fast laser-induced aerosol formation for visualization of gas flows  
p 121 A85-31113
- Laser balancing system for high material removal rates  
[NASA-CR-174731] p 126 N85-12341
- Velocity visualization in gaseous flows  
[NASA-CR-174954] p 119 N85-31445

## LASER DOPPLER VELOCIMETERS

- Phase/doppler spray analyzer for simultaneous measurements of drop size and velocity distributions  
p 120 A85-10035
- Incident beam polarization for laser Doppler velocimetry employing a sapphire cylindrical window  
p 122 A85-39835
- Jet characteristics in confined swirling flow  
p 112 A85-45282
- Internal combustion engine combustion chamber process studies at NASA Lewis Research Center  
p 112 A85-45856
- Holographic optical system for aberration corrections in laser Doppler velocimetry  
p 123 A85-48659
- Hot section laser anemometry  
p 19 N85-10962
- The boundary layer on compressor cascade blades  
[NASA-CR-174369] p 114 N85-18292
- Incident beam polarization for laser Doppler velocimetry employing a sapphire cylindrical window  
[NASA-TM-87064] p 178 N85-28786
- Velocity visualization in gaseous flows  
[NASA-CR-174954] p 119 N85-31445
- The use of a laser Doppler velocimeter in a standard flammability tube  
[NASA-CR-174960] p 125 N85-35389
- LASER INDUCED FLUORESCENCE**
- Two-frequency laser-induced fluorescence technique for rapid velocity-field measurements in gas flows  
p 121 A85-32294

## LASER INTERFEROMETRY

- Phase/doppler spray analyzer for simultaneous measurements of drop size and velocity distributions  
p 120 A85-10035
- Spray characterization with a nonintrusive technique using absolute scattered light  
p 120 A85-10036
- Remote displacement measurements using a laser diode  
p 121 A85-24464

## LASER OUTPUTS

- Research study of droplet sizing technology leading to the development of an advanced droplet sizing system  
[NASA-CR-174839] p 123 N85-21604

## LASER WINDOWS

- Incident beam polarization for laser Doppler velocimetry employing a sapphire cylindrical window  
p 122 A85-39835
- Incident beam polarization for laser Doppler velocimetry employing a sapphire cylindrical window  
[NASA-TM-87064] p 178 N85-28786

## LASERS

- Hot section laser anemometry  
p 19 N85-10962

## LATERAL CONTROL

- Aileron controls for wind turbine applications  
p 157 A85-45513
- Aileron controls for wind turbine applications  
[NASA-TM-86867] p 158 N85-11458

## LEAD ACID BATTERIES

- Results of electric-vehicle propulsion system performance on three lead-acid battery systems  
p 156 A85-45443

## LEADING EDGE SLATS

- Calculation of compressible flow about three-dimensional inlets with auxiliary inlets, slats and vanes by means of a panel method  
[AIAA PAPER 85-1196] p 5 A85-40817

## LEADING EDGES

- Progress in development of a Navier-Stokes solver for evaluation of iced airfoil performance  
[AIAA PAPER 85-0410] p 3 A85-19731

## LEAKAGE

- A comparison of flow rates and pressure profiles for N-sequential inlets and three related seal configurations  
p 109 A85-26526
- Analysis of experimental shaft seal data for high-performance turbomachines, as for Space Shuttle main engines  
[NASA-TM-86928] p 115 N85-21569

## LEAST SQUARES METHOD

- Improved models for increasing wind penetration, economics and operating reliability  
[NASA-CR-175538] p 160 N85-20545

# LENSES

- Automatic sphericity interferometer for testing lens radii [AD-A155736] p 125 N85-33457

# LIFE (DURABILITY)

- Turbine Engine Hot Section Technology (HOST) [NASA-TM-83022] p 18 N85-10951
- Nonlinear structural and life analyses of a turbine blade p 19 N85-10954
- Nonlinear structural and life analyses of a combustor liner p 19 N85-10955
- Constitutive model development for isotropic materials p 20 N85-10975
- Surface protection overview p 21 N85-10978
- Effects of surface chemistry on hot corrosion life: Overview p 21 N85-10980
- Reliability considerations for the total strain range version of strainrange partitioning [NASA-CR-174757] p 144 N85-11380
- Engine cyclic durability by analysis and material testing p 25 N85-15744
- A study of interdiffusion in beta + gamma/gamma + gamma prime Ni-Cr-Al [NASA-CR-174852] p 74 N85-20041
- Fabrication of ceramic substrate-reinforced and free forms [NASA-TM-86994] p 50 N85-23926
- Effects of surface chemistry on hot corrosion life [NASA-CR-174915] p 28 N85-26711
- Life and reliability modeling of bevel gear reductions [NASA-TM-87006] p 133 N85-27227
- Fatigue life analysis of a turboprop reduction gearbox [NASA-TM-87014] p 133 N85-27228
- Reexamination of cumulative fatigue damage laws p 149 N85-27962
- Heat flux sensor calibrator p 41 N85-27970
- Feasibility of mapping velocity flow fields in SSME powerhead by laser anemometry techniques p 41 N85-27971

# LIFE CYCLE COSTS

- Main propulsion system design recommendations for an advanced Orbit Transfer Vehicle [AIAA PAPER 85-1336] p 36 A85-39730

# LIFT

- Vortex induced lift on a flat plate with a curved forward-facing flap p 4 A85-30175
- Icing flight research - Aerodynamic effects of ice and ice shape documentation with stereo photography [AIAA PAPER 85-0468] p 11 A85-30192
- Observations from varying the lift and drag inputs to a noise prediction method for supersonic helical tip speed propellers [NASA-TM-83797] p 175 N85-10788
- Icing flight research: Aerodynamic effects of ice and ice shape documentation with stereo photography [NASA-TM-86906] p 12 N85-18049

# LIFT DEVICES

- Incompressible lifting-surface aerodynamics for a rotor-stator combination [NASA-TM-83767] p 7 N85-12039

# LIGHT EMISSION

- Prism-coupled light emission from tunnel junctions p 181 A85-21425

# LIGHT SCATTERING

- Spray characterization with a nonintrusive technique using absolute scattered light p 120 A85-10036
- Research study of droplet sizing technology leading to the development of an advanced droplet sizing system [NASA-CR-174839] p 123 N85-21604

# LIGHT VALVES

- Optical computer switching network p 178 A85-23134

# LIMNOLOGY

- Comparison of atmospheric correction algorithms for the Coastal Zone Color Scanner p 153 A85-10244

# LINEAR EQUATIONS

- A multiple linear regression analysis of hot corrosion attack on a series of nickel base turbine alloys [NASA-TM-87020] p 77 N85-31284

# LINEAR FILTERS

- Linearization of digital derived rate algorithm for use in linear stability analysis [NASA-TM-87000] p 41 N85-23904

# LINEAR TRANSFORMATIONS

- Optical linear algebra processors - Noise and error-source modeling p 169 A85-36727

# LINEAR VIBRATION

- Oscillator response to nonstationary excitation [ASME PAPER 84-WA/APM-38] p 140 A85-17039

# LININGS

- Advanced liner-cooling techniques for gas turbine combustors [AIAA PAPER 85-1290] p 15 A85-39703
- Nonlinear structural and life analyses of a combustor liner p 19 N85-10955

- Validation of structural analysis methods using the in-house liner cyclic rigs p 21 N85-10987
- HOST liner cyclic facilities: Facility description p 22 N85-10988

- Advanced liner-cooling techniques for gas turbine combustors [NASA-TM-86952] p 8 N85-21115

- Development of advanced high-temperature heat flux sensors. Phase 2: Verification testing [NASA-CR-174973] p 126 N85-35391

# LIQUID CHROMATOGRAPHY

- Rapid estimation of concentration of aromatic classes in middle distillate fuels by high-performance liquid chromatography [NASA-TP-2495] p 93 N85-31307

# LIQUID CRYSTALS

- Substrate-induced orientational order in the isotropic phase of liquid crystals p 181 A85-24649

# LIQUID INJECTION

- Vortex generating flow passage design for increased film cooling effectiveness [NASA-CASE-LEW-14039-1] p 119 N85-33433

# LIQUID METALS

- Arc spray fabrication of metal matrix composite monolayer [NASA-CASE-LEW-13828-1] p 58 N85-30027

# LIQUID PROPELLANT ROCKET ENGINES

- Cryogenic upper stage test bed engine [AIAA PAPER 85-1339] p 44 A85-39733

# LIQUID-LIQUID INTERFACES

- Free-surface phenomena under low- and zero-gravity conditions [NASA-CR-175885] p 36 N85-27922

# LIQUID-SOLID INTERFACES

- The mechanisms of formation and prevention of channel segregation during alloy solidification p 180 A85-18082
- Convective influence on the stability of a cylindrical solid-liquid interface p 109 A85-26911
- Analysis of three-dimensional solidification interface shape p 109 A85-30075
- Control of solidification boundary in continuous casting by asymmetric cooling and mold offset p 110 A85-37047
- Dendritic solidification. I - Analysis of current theories and models. II - A model for dendritic growth under an imposed thermal gradient p 182 A85-38019

# LITHIUM

- Radiation damage and defect behavior in ion-implanted, lithium counterdoped silicon solar cells p 182 A85-35698
- Lithium counterdoped silicon solar cell [NASA-CASE-LEW-14177-1] p 160 N85-20535
- The effects of lithium counterdoping on radiation damage and annealing in n(+)-p silicon solar cells p 50 N85-22586

# LITHIUM SULFUR BATTERIES

- Development of a lithium secondary battery separator p 104 N85-31378

# LOAD DISTRIBUTION (FORCES)

- Extension of constrained incremental Newton-Raphson scheme to generalized loading fields p 139 A85-13942
- Gear mesh stiffness and load sharing in planetary gearing [ASME PAPER 84-DET-229] p 129 A85-33781

# LOAD TESTS

- Use of static indentation laws in the impact analysis of laminated composite plates p 55 A85-29133
- A study of spectrum fatigue crack propagation in two aluminum alloys. 1: Spectrum simplification [NASA-TM-86929] p 72 N85-18124
- A study of spectrum fatigue crack propagation in two aluminum alloys. 2: Influence of microstructures [NASA-TM-86930] p 73 N85-18125
- Composite loads spectra for select space propulsion structural components p 148 N85-27953

# LOADS (FORCES)

- Dual clearance squeeze film damper for high load conditions [ASME PAPER 84-TRIB-7] p 128 A85-32960
- Structural analysis p 20 N85-10969
- Characterization of lubricated bearing surfaces operated under high loads [NASA-TM-86964] p 88 N85-21357
- Breakaway friction and dynamic friction/wear measurements of various ceramic materials from 25 C (75 F) to 650 C (1200 F) [NASA-CR-174803] p 90 N85-26994
- Some advances in experimentation supporting development of viscoplastic constitutive models [NASA-CR-174855] p 147 N85-27260
- Structural Integrity and Durability of Reusable Space Propulsion Systems [NASA-CP-2381] p 51 N85-27941

- Composite loads spectra for select space propulsion structural components: Probabilistic load model development p 148 N85-27954

- Dynamic creep buckling: Analysis of shell structures subjected to time-dependent mechanical and thermal loading p 149 N85-27959

- A study of the stress wave factor technique for the characterization of composite materials [NASA-CR-174870] p 58 N85-30035

- Some advances in experimentation supporting development of viscoplastic constitutive models p 151 N85-31545

- A comparison of smooth specimen and analytical simulation techniques for notched members at elevated temperatures p 151 N85-31546

- The design and analysis of single flank transmission error test for loaded gears [NASA-CR-176163] p 136 N85-34404

# LOSSES

- An improved computer model for prediction of axial gas turbine performance losses [NASA-CR-174246] p 24 N85-15724
- Fuel and oxidizer turbine loss analysis p 50 N85-26900

- Study of Kapton under simulated shuttle environment [NASA-CR-176003] p 41 N85-29997

# LOSSY MEDIA

- Numerical methods for analyzing electromagnetic scattering [NASA-CR-175507] p 99 N85-21438
- Normal modes in an overmoded circular waveguide coated with lossy material [NASA-CR-176166] p 100 N85-35320

# LOUVERS

- Pre-HOST high temperature crack propagation p 19 N85-10956

# LOW ASPECT RATIO

- Study of controlled diffusion stator blading [NASA-CR-167995] p 25 N85-18058

# LOW COST

- Replaceable blade turbine and stationary specimen corrosion testing facility [NASA-TM-86931] p 73 N85-18126
- Iron rich low cost superalloys [NASA-CR-174900] p 76 N85-26962

# LOW FREQUENCIES

- Design of low loss helix circuits for interference fitted and brazed circuits [NASA-CR-168313] p 103 N85-19328
- Automated testing of developmental satellite communications systems and subsystems [NASA-TM-87070] p 100 N85-31348

# LOW PRESSURE

- Energy efficient engine. Low pressure turbine test hardware detailed design report [NASA-CR-167956] p 22 N85-10994
- Nitriding of titanium and its alloys by N<sub>2</sub>, NH<sub>3</sub> or mixtures of N<sub>2</sub> + H<sub>2</sub> in a dc arc plasma at low pressures (or = to torr) [NASA-TM-83803] p 131 N85-15168

# LOW TEMPERATURE

- Detailed studies of aviation fuel flowability [NASA-CR-174938] p 94 N85-31308
- Measurement and correlation of jet fuel viscosities at low temperatures [NASA-CR-174911] p 94 N85-34295

# LOW TEMPERATURE TESTS

- Fiberglass epoxy laminate fatigue properties at 300 and 20 K p 56 A85-47970
- Effect of low temperature on fatigue and fracture properties of Ti-5Al-2.5Sn(ELI) for use in engine components p 70 A85-47972

# LOW THRUST

- Small centrifugal pumps for low thrust rockets [AIAA PAPER 85-1302] p 45 A85-43978

# LOW THRUST PROPULSION

- Design and analysis report for the RL10-2B breadboard low thrust engine [NASA-CR-174857] p 48 N85-19020

# LOW WEIGHT

- Free-surface phenomena under low- and zero-gravity conditions [NASA-CR-175835] p 118 N85-27168

# LUBRICANTS

- Fast numerical calculations of EHD sliding traction forces Application to rolling bearings [ASME PAPER 84-TRIB-26] p 127 A85-21289
- Effect of lubricant extreme-pressure additives on surface fatigue life of AISI 9310 spur gears [NASA-TP-2408] p 130 N85-13234
- Effects of silver and group 2 fluorides addition to plasma sprayed chromium carbide high temperature solid lubricant for foil gas bearing to 650 deg C [NASA-TM-86895] p 84 N85-14928

## M

- Contact angle and surface tension measurements of a five-ring polyphenyl ether  
[NASA-TM-86927] p 86 N85-15897
- Effect of five lubricants on life of AISI 9310 spur gears  
[NASA-TM-2419] p 123 N85-16099
- Tribological properties of graphite-fiber-reinforced, partially fluorinated polyimide composites  
[NASA-TM-86926] p 86 N85-18153
- Characterization of lubricated bearing surfaces operated under high loads  
[NASA-TM-86964] p 88 N85-21357
- Formation of high molecular weight products from benzene during boundary lubrication  
[NASA-TM-86966] p 62 N85-22644
- Transmission efficiency measurements and correlations with physical characteristics of the lubricant  
p 89 N85-23781
- Thermal traction contact performance evaluation under fully flooded and starved conditions  
[NASA-CR-168173] p 132 N85-25848
- Lubricant and additive effects on spur gear fatigue life  
[NASA-TM-87044] p 133 N85-28373
- Correlation of rheological characteristics of lubricants with transmission efficiency measurements  
[NASA-TM-86988] p 134 N85-30342
- LUBRICATING OILS**
- Into mesh lubrication of spur gears with arbitrary offset oil jet. I - For jet velocity less than or equal to gear velocity  
p 128 A85-24497
- The influence of temperature on the lubricating effectiveness of MoS<sub>2</sub> dispersed in mineral oils  
[ASLE PREPRINT 84-LC-2A-2] p 80 A85-25963
- Effect of two inner-ring oil-flow distribution schemes on the operating characteristics of a 35 millimeter bore ball bearing to 2.5 million DN  
[NASA-TP-2404] p 130 N85-13233
- LUBRICATION**
- Elastohydrodynamic lubrication of line contacts  
p 126 A85-11069
- An analysis of temperature effect in a finite journal bearing with spatial tilt and viscous dissipation  
p 126 A85-11074
- Lubricant jet flow phenomena in spur and helical gears with modified center distances and/or addendums - For out-of-mesh conditions  
[ASME PAPER 84-DET-96] p 129 A85-35049
- Lubricity of well-characterized jet and broad-cut fuels by ball-on-cylinder machine  
[NASA-TM-83807] p 92 N85-12183
- Development of gas-lubricated pistons for heavy duty diesel engine technology program  
[NASA-CR-174746] p 184 N85-12808
- Fundamental tribological properties of ceramics  
[NASA-TM-86915] p 85 N85-15893
- Study of advanced fuel system concepts for commercial aircraft  
[NASA-CR-174751] p 12 N85-19978
- Tribological systems as applied to aircraft engines  
[NASA-TM-86965] p 131 N85-21657
- Lubrication and performance of high-speed rolling-element bearings  
[NASA-TM-86958] p 131 N85-21658
- Development of a multiplane multispeed balancing system for turbine systems  
[NASA-CR-174750] p 35 N85-22400
- Fast approach for calculating film thicknesses and pressures in elastohydrodynamically lubricated contacts at high loads  
[NASA-TM-87032] p 117 N85-30242
- Surface roughness effects in elastohydrodynamic contacts  
[NASA-TP-2488] p 134 N85-32329
- Mechanics of a gaseous film barrier to lubricant wetting of elastohydrodynamically lubricated conjunctions  
[NASA-TP-2500] p 135 N85-32330
- Lubrication and cooling for high speed gears  
[NASA-TM-87096] p 136 N85-34407
- Elastohydrodynamic lubrication calculations used as a tool to study scuffing  
[NASA-TM-87097] p 137 N85-34408
- Design and lubrication of high-speed rolling-element bearings  
[NASA-TM-87107] p 137 N85-34409
- LUMINANCE**
- An allpass filter design for luminance and chrominance separation of NTSC signals  
p 102 A85-28230
- LUMINOUS INTENSITY**
- Research study of droplet sizing technology leading to the development of an advanced droplet sizing system  
[NASA-CR-174839] p 123 N85-21604

## MACH NUMBER

- Unsteady flow in a supersonic cascade with two in-passage-shocks  
[NASA-CR-3925] p 10 N85-35158

## MACH-ZEHNDER INTERFEROMETERS

- Rainbow schlieren vs Mach-Zehnder interferometer - A comparison  
p 121 A85-28820

## MACHINE TOOLS

- Spiral bevel and circular arc helical gears: Tooth contact analysis and the effect of misalignment on circular arc helical gears  
[NASA-TM-87013] p 32 N85-31060
- Generated spiral bevel gears: Optimal machine-tool settings and tooth contact analysis  
[NASA-TM-87075] p 136 N85-34405

## MAGNESIUM

- Magnesium doping of efficient GaAs and Ga(0.75)In(0.25)As solar cells grown by metalorganic chemical vapor deposition  
p 180 A85-11466
- Select fiber composites for space applications - A mechanistic assessment  
p 54 A85-16040
- Universal binding energy relations in metallic adhesion  
[NASA-TM-86889] p 72 N85-12132

## MAGNESIUM OXIDES

- Surface effects of corrosive media on hardness, friction, and wear of materials  
[NASA-TM-83711] p 85 N85-15896

## MAGNETIC FIELD CONFIGURATIONS

- High frequency plasma generator for ion thrusters  
[NASA-CR-174772] p 48 N85-17023

## MAGNETIC FLUX

- Dilute plasma coupling currents to a high voltage solar array in weak magnetic fields  
p 46 A85-45388

## MAGNETIC PROPERTIES

- Effects of wear on structure-sensitive magnetic properties of ceramic ferrite in contact with magnetic tape  
[NASA-TM-87007] p 90 N85-26991

## MAGNETIC RESONANCE

- Analysis of glow discharges for understanding the process of film formation  
[NASA-TM-83750] p 62 N85-10138

## MAGNETIC TAPES

- Humidity effects on adhesion of nickel-zinc ferrite in elastic contact with magnetic tape and itself  
[NASA-TP-2449] p 88 N85-21359
- Effects of wear on structure-sensitive magnetic properties of ceramic ferrite in contact with magnetic tape  
[NASA-TM-87007] p 90 N85-26991

## MAGNETIZATION

- Development of high frequency low weight power magnetics for aerospace power systems  
p 102 A85-45373

## MAGNETOHYDRODYNAMIC GENERATORS

- Parametric study of potential early commercial power plants Task 3-A MHD cost analysis  
[NASA-TP-175839] p 161 N85-27377

## MAGNETOHYDRODYNAMIC STABILITY

- Discharges on a negatively biased solar cell array in a charged-particle environment  
p 160 N85-22499

## MAN MACHINE SYSTEMS

- MERIT: A man/computer data management and enhancement system for upper air nowcasting/forecasting in the United States - Minimum Energy Routes using Interactive Techniques (MERIT)  
p 167 N85-10558

## MANNED SPACECRAFT

- A historical overview of the electrical power systems in the US manned and some US unmanned spacecraft  
[NASA-CR-174806] p 47 N85-13910

## MANUFACTURING

- Manufacturing process to reduce large grain growth in zirconium alloys  
[DE85-011649] p 78 N85-34267

## MARTENSITIC STAINLESS STEELS

- Deposition of silicon nitride from SiCl<sub>4</sub> and NH<sub>3</sub> in a low pressure RF plasma  
p 81 A85-36229

## MASERS

- Technology for satellite power conversion  
[NASA-CR-174335] p 159 N85-18451

## MASS SPECTRA

- Nitriding of titanium and its alloys by N<sub>2</sub>, NH<sub>3</sub> or mixtures of N<sub>2</sub> + H<sub>2</sub> in a dc arc plasma at low pressures (or = to torr)  
[NASA-TM-83803] p 131 N85-15168
- Mass analysis of neutral particles and ions released during electrical breakdowns on spacecraft surfaces  
[NASA-CR-175585] p 39 N85-21250

## MASS SPECTROMETERS

- Mass spectra of neutral particles released during electrical breakdown of thin polymer films  
p 88 N85-22511

## MASS TRANSFER

- Density effects on jet characteristics in confined swirling flow  
p 112 A85-45283
- Turbulent transport and length scale measurement experiments with confined coaxial jets  
[NASA-CR-174831] p 117 N85-30245

## MATERIALS SCIENCE

- Research and technology highlights of the Lewis Research Center  
[NASA-TM-86899] p 186 N85-17928

## MATHEMATICAL MODELS

- Identification of multivariable high-performance turbofan engine dynamics from closed-loop data  
p 13 A85-13630
- Modeling of gamma/gamma-prime phase equilibrium in the nickel-aluminum system  
p 65 A85-14959
- Vortex modeling of single and multiple dilution jet mixing in a crossflow  
[AIAA PAPER 85-1580] p 111 A85-40701
- Constitutive modeling and computational implementation for finite strain plasticity  
p 143 A85-40910
- Comparison of free-piston Stirling engine model predictions with RE1000 engine test data  
p 130 A85-45488

- A study of Reynolds-stress closure model*  
[NASA-CR-174342] p 114 N85-17324
- Analysis of shell type structures subjected to time dependent mechanical and thermal loading  
[NASA-CR-175747] p 147 N85-25896
- Composite loads spectra for select space propulsion structural components: Probabilistic load model development  
p 148 N85-27954
- Turbulent transport and length scale measurement experiments with confined coaxial jets  
[NASA-CR-174831] p 117 N85-30245
- Numerical considerations in the development and implementation of constitutive models  
p 151 N85-31541

- On numerical integration and computer implementation of viscoplastic models  
p 151 N85-31542
- A continuous damage model based on stepwise-stress creep rupture tests  
[NASA-CR-174941] p 152 N85-32341
- Component-specific modeling  
[NASA-CR-174765] p 33 N85-34140

## MATHEMATICAL PROGRAMMING

- Structural optimization using optimality criteria methods  
p 144 A85-48703

## MATRIX MATERIALS

- Resin selection criteria for 'tough' composite structures  
p 81 A85-35139
- High performance fibers for structurally reliable metal and ceramic composites - advanced gas turbine engine materials  
[NASA-TM-86878] p 56 N85-12095
- Chemical approach for controlling nadimide cure temperature and rate with maleimide  
[NASA-CASE-LEW-13770-3] p 87 N85-21350
- Chemical approach for controlling nadimide cure temperature and rate with maleimide  
[NASA-CASE-LEW-13770-4] p 87 N85-21351
- Chemical approach for controlling nadimide cure temperature and rate  
[NASA-CASE-LEW-13770-6] p 63 N85-30039
- Apparatus and method for identification of matrix materials in which transuranic elements are embedded using thermal neutron capture gamma-ray emission  
[DE85-011659] p 125 N85-33454
- Mechanical properties of SiC fiber-reinforced reaction-bonded Si<sub>3</sub>N<sub>4</sub> composites  
[NASA-TM-87085] p 59 N85-34223

## MATRIX METHODS

- Analysis of hourglass instabilities and control in underintegrated finite element methods  
p 139 A85-11125

## MEASURING INSTRUMENTS

- Comparison of icing cloud instruments for 1982-1983 icing season flight program  
[AIAA PAPER 84-0020] p 13 A85-16098
- High temperature thermocouple and heat flux gauge using a unique thin film-hardware hot junction  
[NASA-TM-86898] p 123 N85-16096
- Advanced smoke meter development survey and analysis  
[NASA-CR-168287] p 124 N85-25792
- Free-surface phenomena under low- and zero-gravity conditions  
[NASA-CR-175835] p 116 N85-27168
- Development of advanced high-temperature heat flux sensors. Phase 2: Verification testing  
[NASA-CR-174973] p 126 N85-35391

## MECHANICAL DEVICES

- Apparatus for mounting a field emission cathode  
[NASA-CASE-LEW-14108-1] p 104 N85-29149

**MECHANICAL DRIVES**

- Thermal traction contact performance evaluation under fully flooded and starved conditions  
[NASA-CR-168173] p 132 N85-25848  
Application of traction drives as servo mechanisms p 152 N85-33520

**MECHANICAL OSCILLATORS**

- Oscillator response to nonstationary excitation  
[ASME PAPER 84-WA/APM-38] p 140 A85-17039

**MECHANICAL PROPERTIES**

- ICAN - Integrated composites analyzer  
[AIAA PAPER 84-0974] p 54 A85-16094  
Effects of cobalt on the hot workability of nickel-base superalloys p 67 A85-32412  
Analysis of stress-strain, fracture, and ductility behavior of aluminum matrix composites containing discontinuous silicon carbide reinforcement p 55 A85-37421  
Quasi-static solution algorithms for kinematically/materially nonlinear thermomechanical problems p 143 A85-41983  
Evaluation of alpha-SiC sintering using statistical methods p 83 A85-42800  
Diffusion welding of MA 6000 and a conventional nickel-base superalloy p 69 A85-43551  
Microstructure of reaction-bonded silicon nitride consolidated by isostatic hot-pressing p 83 A85-45304  
Effect of hot isostatic pressing on the properties of sintered alpha silicon carbide p 83 A85-48757  
Ultrasonic nondestructive evaluation, microstructure, and mechanical property interrelations  
[NASA-TM-86876] p 137 N85-10371  
Effect of substituted phenylindimides on processing and properties of PMR polyimide composites  
[NASA-TM-86902] p 85 N85-14929  
Effect of reduction of strategic Columbium addition in 718 Alloy on the structure and properties  
[NASA-CR-174841] p 75 N85-21320  
Effects of chromium and aluminum on mechanical and oxidation properties of iron-nickel-base superalloys based on CG-27 p 75 N85-21323  
Extreme precision antenna reflector study results p 165 N85-23830  
Mechanical protection of DLC films on fused silica slides  
[NASA-TM-87056] p 91 N85-30138  
Mechanical properties of SiC fiber-reinforced reaction-bonded Si3N4 composites  
[NASA-TM-87085] p 59 N85-34223  
Generated spiral bevel gears: Optimal machine-tool settings and tooth contact analysis  
[NASA-TM-87075] p 136 N85-34405

**MELT SPINNING**

- Rapidly solidified NiAl and FeAl  
[NASA-TM-86941] p 74 N85-20042  
Microstructures in rapidly solidified Ni-Mo alloys  
[NASA-TM-87100] p 78 N85-34266

**MELTING POINTS**

- Study of advanced fuel system concepts for commercial aircraft and engines  
[NASA-CR-174752] p 93 N85-19176  
Jet fuel property changes and their effect on producibility and cost in the U.S., Canada, and Europe  
[NASA-CR-174840] p 93 N85-27012  
Measurement and correlation of jet fuel viscosities at low temperatures  
[NASA-CR-174911] p 94 N85-34295

**MELTS (CRYSTAL GROWTH)**

- The mechanisms of formation and prevention of channel segregation during alloy solidification p 180 A85-18082

**MEMBRANE STRUCTURES**

- Evaluation of developmental membranes for the mixed reactant iron-chromium redox system  
[NASA-TM-87074] p 164 N85-34443

**MENISCI**

- Advanced radiator concepts  
[NASA-TM-87008] p 115 N85-24245

**MERCURY CADMIUM TELLURIDES**

- Mosaic Infrared Sensor for Space Astronomy (MIRSSA)  
[NASA-CR-176154] p 125 N85-33456

**MERCURY ION ENGINES**

- IAPS (8-cm) ion thruster cyclic endurance test --- Ion Auxiliary Propulsion System p 42 A85-16406  
Ring-cusp ion thrusters p 42 A85-16438  
Ion thruster system (8-cm) cyclic endurance test  
[NASA-CR-174745] p 47 N85-12937

**MESH**

- Into mesh lubrication of spur gears with arbitrary offset oil jet. I - For jet velocity less than or equal to gear velocity p 128 A85-24497  
Flow through very porous inclined screens  
[AIAA PAPER 85-1650] p 111 A85-40750

- Flow through very porous inclined screens  
[NASA-TM-86979] p 116 N85-25761

**METAL BONDING**

- Advanced thermal barrier system bond coatings for use on Ni, Co-, and Fe-base alloy substrates  
[NASA-TM-87062] p 77 N85-31283

**METAL COATINGS**

- Effects of MAR-M247 substrate (modified) composition on coating oxidation coating/substrate interdiffusion --- protective coatings for hot section components of gas turbine engines  
[NASA-CR-174851] p 73 N85-19073  
The role of silver in self-lubricating coatings for use at extreme temperatures  
[NASA-TM-86943] p 87 N85-20127  
Metallic and metal/ceramic coating by thermal decomposition  
[NASA-TM-86992] p 88 N85-22755  
Film and interstitial formation of metals in plasma-sprayed ceramics  
[NASA-TM-86993] p 89 N85-22756  
Effects of surface chemistry on hot corrosion life  
[NASA-CR-174915] p 28 N85-26711

**METAL CRYSTALS**

- Deformation and erosion of f.c.c. metals and alloys under cavitation attack p 65 A85-12789  
Dendritic solidification. III - Some further refinements to the model for dendritic growth under an imposed thermal gradient p 69 A85-44703

**METAL FATIGUE**

- Strainrange partitioning - A total strain range version --- for creep fatigue life prediction by summing inelastic and elastic strain-range-life relations for two Ni base superalloys p 64 A85-11603  
A history dependent damage model for low cycle fatigue  
[ASME PAPER 84-PVP-112] p 140 A85-18795  
The effect of microstructure, temperature, and hold-time on low-cycle fatigue of As HIP P/M Rene 95 p 67 A85-32399  
The influence of hold times on LCF and FCG behavior in a P/M Ni-base superalloy --- Low Cycle Fatigue/Fatigue Crack Growth p 67 A85-32400  
Effect of low temperature on fatigue and fracture properties of Ti-5Al-2.5Sn(ELI) for use in engine components p 70 A85-47972  
Reliability considerations for the total strain range version of strainrange partitioning  
[NASA-CR-174757] p 144 N85-11380  
Thermal-mechanical fatigue crack growth in Inconel X-750 p 72 N85-15877  
A study of spectrum fatigue crack propagation in two aluminum alloys. 1: Spectrum simplification  
[NASA-TM-86929] p 72 N85-18124  
A study of spectrum fatigue crack propagation in two aluminum alloys. 2: Influence of microstructures  
[NASA-TM-86930] p 73 N85-18125

**METAL FILMS**

- Effect of Interfacial characteristics of metal clad polymeric substrates on electrical high frequency interconnection performance  
[NASA-TM-86948] p 99 N85-20223

**METAL MATRIX COMPOSITES**

- Analysis of stress-strain, fracture, and ductility behavior of aluminum matrix composites containing discontinuous silicon carbide reinforcement p 55 A85-37421  
High temperature metal and ceramic composites p 55 A85-37483  
Fibers for structurally reliable metal and ceramic composites p 55 A85-37484  
High performance fibers for structurally reliable metal and ceramic composites --- advanced gas turbine engine materials  
[NASA-TM-86878] p 56 N85-12095  
Nonlinear structural analysis for fiber-reinforced superalloy turbine blades p 147 N85-26887  
Arc spray fabrication of metal matrix composite monotype  
[NASA-CASE-LEW-13828-1] p 58 N85-30027

**METAL OXIDES**

- Thermal barrier coating system  
[NASA-CASE-LEW-13324-2] p 57 N85-21266  
Molecular orbital studies in oxidation: Sulfate formation and metal-metal oxide adhesion  
[NASA-CR-176070] p 77 N85-32174

**METAL POWDER**

- Rapid solidification and dynamic compaction of Ni-base superalloy powders p 67 A85-32414  
A new interpretation of internal heat transfer coefficients of porous media  
[ASME PAPER 84-WA/HT-51] p 110 A85-39894  
Powder metallurgy forged gear development  
[NASA-TM-87483] p 134 N85-29295

**METAL SHELLS**

- Dynamic creep buckling: Analysis of shell structures subjected to time-dependent mechanical and thermal loading p 149 N85-27959

**METAL SURFACES**

- Surface hardening of steel by boriding in a cold rf plasma p 68 A85-40275  
Cone formation as a result of whisker growth on ion bombarded metal surfaces p 182 A85-41635  
Effect of surface configuration during solid particle impingement erosion p 69 A85-42568  
Characterization of solid particle erosion resistance of ductile metals based on their properties p 69 A85-42569

- Surface effects of corrosive media on hardness, friction, and wear of materials  
[NASA-TM-83711] p 85 N85-15896

- Characterization of erosion of metallic materials under cavitation attack in a mineral oil  
[NASA-TM-86934] p 74 N85-19075

- Mass analysis of neutral particles and ions released during electrical breakdowns on spacecraft surfaces  
[NASA-CR-175585] p 39 N85-21250

- Ion-beam nitriding of steels  
[NASA-CASE-LEW-14104-1] p 75 N85-21324

- Study of the effects of implantation on the high Fe-Ni-Cr and Ni-Cr-Al alloys  
[NASA-CR-175625] p 76 N85-22661

- Why CO bonds side-on at low coverage and both side-on and upright at high coverage on the Cr(110) surface  
[NASA-CR-176071] p 77 N85-32173

**METAL VAPORS**

- Metal vapor arc switch electromagnetic accelerator technology  
[NASA-CR-174380] p 103 N85-18259

**METAL WORKING**

- Thermomechanical deformation in the presence of metallurgical changes p 150 N85-31533

**METAL-METAL BONDING**

- Molecular orbital studies in oxidation: Sulfate formation and metal-metal oxide adhesion  
[NASA-CR-176070] p 77 N85-32174

**METALLIC GLASSES**

- Friction and wear of some ferrous-base metallic glasses p 64 A85-11071  
Mechanical-contact-induced transformation from the amorphous to the partially crystalline state in metallic glass p 65 A85-19084

**METALLOGRAPHY**

- Properties and microstructures for dual alloy combinations of three superalloys with alloy 901  
[NASA-TM-86987] p 76 N85-26963

**METALS**

- Universal binding energy relations in metallic adhesion  
[NASA-TM-86889] p 72 N85-12132  
Effect of humidity on fretting wear of several pure metals  
[NASA-TP-2403] p 72 N85-13006  
Effect of barrier height on friction behavior of the semiconductors silicon and gallium arsenide in contact with pure metals  
[NASA-TP-2405] p 84 N85-13044

- Characterization of erosion of metallic materials under cavitation attack in a mineral oil  
[NASA-TM-86934] p 74 N85-19075

- Monte Carlo lattice models for adsorbed polymer conformation  
[NASA-TP-2453] p 183 N85-24961

- On the use of internal state variables in thermoviscoplastic constitutive equations p 150 N85-31536

- On numerical integration and computer implementation of viscoplastic models p 151 N85-31542

**METEOROLOGICAL FLIGHT**

- A comparison of NMC and GWC analysis field temperatures with aircraft measurements p 166 A85-21140

**METEOROLOGICAL SERVICES**

- GASP cloud encounter statistics - Implications for laminar flow control flight p 166 A85-11979

**METHANE**

- Systematic optimization of a detailed kinetic model using a methane ignition example p 59 A85-12890  
Effect of gravity on halogenated hydrocarbon flame retardant effectiveness  
[IAF PAPER 84-156] p 61 A85-23199

- Plasma deposited hydrogenated carbon on GaAs and InP p 182 A85-40386

- Plasma deposited diamondlike carbon on GaAs and InP  
[NASA-TM-86870] p 183 N85-10844

- The structure of dilute combusting sprays  
[NASA-CR-174838] p 24 N85-15728

- Optical properties of hydrogenated amorphous carbon films grown from methane plasma  
[NASA-TM-86995] p 183 N85-26406

## METHYL ALCOHOLS

Methanol as a soot reducer in a turbulent swirling burner  
[ASME PAPER 84-JPGG-GT-2] p 61 A85-23192

## METHYL CHLOROSILANES

A morphological study of silicon carbide prepared by chemical vapor deposition p 79 A85-20938

## MICROCOMPUTERS

Data flow methods for dynamic system simulation - A CSSL-IV microcomputer network interface p 170 A85-28614

Floating-point function generation routines for 16-bit microcomputers  
[NASA-TM-83783] p 170 A85-10683

MINDS: A microcomputer interactive data system for 8086-based controllers  
[NASA-TP-2378] p 170 A85-17576

## MICROCRACKS

Fundamentals of microcrack nucleation mechanics  
[NASA-CR-3851] p 137 A85-16195

Experimental and analytical study of ceramic-coated turbine-tip shroud seals for small turbine engines  
[NASA-TM-86881] p 25 A85-18057

## MICROHARDNESS

Nitriding of titanium and its alloys by N<sub>2</sub>, NH<sub>3</sub> or mixtures of N<sub>2</sub> + H<sub>2</sub> in a dc arc plasma at low pressures (or = to torr)

[NASA-TM-83803] p 131 A85-15168

Surface effects of corrosive media on hardness, friction, and wear of materials  
[NASA-TM-83711] p 85 A85-15896

Ion-beam nitriding of steels  
[NASA-CASE-LEW-14104-1] p 75 A85-21324

Frictional and structural characterization of ion-nitrided low and high chromium steels  
[NASA-TM-86991] p 132 A85-23085

## MICROPROCESSORS

A functional language approach in high-speed digital simulation p 170 A85-28615

Microprocessor control of photovoltaic systems p 156 A85-45408

A generalized computer code for developing dynamic gas turbine engine models (DIGTEM) p 17 A85-49021

Fiber optic, Fabry-Perot high temperature sensor  
[NASA-CR-174712] p 178 A85-13594

Design description of a microprocessor based Engine Monitoring and Control unit (EMAC) for small turboshaft  
[NASA-TM-86860] p 1 A85-17935

## MICROSCOPY

A micrographic and gravimetric study of intercalation and deintercalation of graphite fibers  
[NASA-TM-87026] p 91 A85-28110

## MICROSTRIP TRANSMISSION LINES

The study of microstrip antenna arrays and related problems

[NASA-CR-174054] p 97 A85-11265

Effect of interfacial characteristics of metal clad polymeric substrates on electrical high frequency interconnection performance

[NASA-TM-86948] p 99 A85-20223

An experimental investigation of microstrip properties on soft substrates from 2 to 40 GHz

[NASA-TM-86961] p 99 A85-20224

Perturbation-iteration theory for analyzing microwave striplines

[NASA-CR-176189] p 100 A85-35321

Characterization of microstrip discontinuities in the time and frequency domains

[NASA-CR-176190] p 106 A85-35342

## MICROSTRUCTURE

Frictional and morphological properties of Au-MoS<sub>2</sub> films sputtered from a compact target p 127 A85-19085

Strength and microstructure of sintered Si<sub>3</sub>N<sub>4</sub> with rare-earth-oxide additions

[ACS PAPER 130-13-84] p 80 A85-25271

Ductility in rapidly solidified NiAl p 66 A85-26158

Influence of composition on the microstructure and mechanical properties of a nickel-base superalloy single crystal p 66 A85-32387

Feasibility study of the welding of SiC p 81 A85-39339

Ceramic microstructure and adhesion p 82 A85-40384

The role of the reflection coefficient in precision measurement of ultrasonic attenuation p 137 A85-42151

Microstructure of reaction-bonded silicon nitride consolidated by isostatic hot-pressing p 83 A85-45304

Effects of cobalt, boron, and zirconium on the microstructure of Udimet 738  
[NASA-CR-174762] p 70 A85-10166

The effects of seven alloying elements on the microstructure and stress-rupture behavior of nickel-base superalloys

[NASA-TM-83791] p 70 A85-10168

## Ceramic microstructure and adhesion

[NASA-TM-83804] p 83 A85-10186

Ultrasonic nondestructive evaluation, microstructure, and mechanical property interrelations

[NASA-TM-86876] p 137 A85-10371

Effects of tin on microstructure and mechanical behavior of Inconel 718

[NASA-TM-86866] p 71 A85-12129

Fundamentals of microcrack nucleation mechanics  
[NASA-CR-3851] p 137 A85-16195

A study of spectrum fatigue crack propagation in two aluminum alloys. 2: Influence of microstructures  
[NASA-TM-86930] p 73 A85-18125

The effect of tantalum on the structure/properties of two polycrystalline nickel-base superalloys: B-1900 + Hf MAR-M247

[NASA-CR-174847] p 73 A85-18127

Creep-rupture behavior of iron superalloys in high-pressure hydrogen  
[NASA-CR-174411] p 74 A85-19078

Effect of reduction of strategic Columbium addition in 718 Alloy on the structure and properties

[NASA-CR-174841] p 75 A85-21320

Properties and microstructures for dual alloy combinations of three superalloys with alloy 901

[NASA-TM-86987] p 76 A85-26963

Manufacturing process to reduce large grain growth in zirconium alloys  
[DE85-011649] p 78 A85-34267

## MICROWAVE AMPLIFIERS

A 20 GHz, 75 watt, helix TWT for space communications p 101 A85-14433

## MICROWAVE ANTENNAS

Advanced 30/20 GHz multiple beam antenna for future communications satellites p 96 A85-14436

Characterization of MMIC devices for active array antennas

[NASA-TM-86907] p 38 A85-15779

The 20 GHz proof-of-concept test model results for a multiple scan beam dual reflector antenna

[NASA-CR-174268] p 98 A85-15944

## MICROWAVE CIRCUITS

Characterization of MMIC devices for active array antennas

[NASA-TM-86907] p 38 A85-15779

Configuration study for a 30 GHz monolithic receive array, volume 1

[NASA-CR-174697-VOL-1] p 98 A85-18239

## MICROWAVE EQUIPMENT

Status of NASA's multibeam communications technology program p 100 A85-14432

Experiments with a microwave electrothermal thruster concept p 42 A85-16441

Measurements of energy distribution in microwave plasmas of N<sub>2</sub> and He and comparisons with results for H<sub>2</sub> p 178 A85-16443

## MICROWAVE OSCILLATORS

The energetics of hydrogen atom recombination - Analysis, experiments, and modeling --- in electrothermal propulsion system p 179 A85-16444

## MICROWAVE PLASMA PROBES

Recent work on a microwave ion source p 179 A85-16455

Experimental performance of a microwave cavity plasma disk ion source p 179 A85-43552

## MICROWAVE SWITCHING

The NASA satellite communication 20 x 20 matrix switches p 101 A85-14435

## MICROWAVE TRANSMISSION

Plot of modal field distribution in rectangular and circular waveguides p 101 A85-25170

Modeling of NASA's 30/20 GHz satellite communications system p 38 A85-36663

Perturbation-iteration theory for analyzing microwave striplines

[NASA-CR-176189] p 100 A85-35321

## MICROWAVES

Laboratory degradation of Kapton in a low energy oxygen ion beam

[AIAA PAPER 83-2658] p 78 A85-10675

Effect of interfacial characteristics of metal clad polymeric substrates on electrical high frequency interconnection performance

[NASA-TM-86948] p 99 A85-20223

Precision tunable resonant microwave cavity  
[NASA-CASE-LEW-13935-1] p 103 A85-20248

## MIE SCATTERING

Fast laser-induced aerosol formation for visualization of gas flows p 121 A85-31113

## MILLIMETER WAVES

MMIC devices for active phased array antennas  
[NASA-CR-174281] p 98 A85-15943

## MILLING (MACHINING)

Factors influencing the ball milling of Si<sub>3</sub>N<sub>4</sub> in water  
[NASA-TM-86932] p 86 A85-19136

Parametric evaluation of ball milling of SiC in water  
[NASA-TM-86974] p 88 A85-21356

## MILLING MACHINES

Demonstration of a silicon nitride attrition mill for production of fine pure Si and Si<sub>3</sub>N<sub>4</sub> powders p 78 A85-10825

## MIM (SEMICONDUCTORS)

Dielectric properties of 'diamondlike' carbon prepared by RF plasma deposition p 182 A85-38192

## MINERAL OILS

The influence of temperature on the lubricating effectiveness of MoS<sub>2</sub> dispersed in mineral oils  
[ASLE PREPRINT 84-LC-2A-2] p 80 A85-25963

Characterization of erosion of metallic materials under cavitation attack in a mineral oil

[NASA-TM-86934] p 74 A85-19075

## MISSION PLANNING

Missions/planning panel p 36 A85-13886

Tethered nuclear power for the Space Station  
[NASA-TM-87023] p 51 A85-26912

Component-specific modeling  
[NASA-CR-174765] p 147 A85-27261

## MIXED OXIDES

Plastic flow of plasma sprayed ceramics p 80 A85-24161

## MIXERS

Three-dimensional inviscid flow analysis of turbofan forced mixers

[AIAA PAPER 85-0086] p 2 A85-19510

## MODELS

Effects of surface chemistry on hot corrosion life: Overview p 21 A85-10980

Three-dimensional calculation of shuttle charging in polar orbit p 40 A85-22486

Composite loads spectra for select space propulsion structural components p 148 A85-27953

Comparative analysis of operational forecasts versus actual weather conditions in airline flight planning, volume 2

[NASA-CR-167863] p 167 A85-35535

Comparative analysis of operational forecasts versus actual weather conditions in airline flight planning: Summary report

[NASA-CR-167866] p 168 A85-35538

## MODULES

Operating characteristics of a 0.87 kW-hr flywheel energy storage module

[NASA-TM-87036] p 133 A85-28371

## MODULUS OF ELASTICITY

Spherulic microglass particle impingement studies of thermoplastic materials at normal incidence p 79 A85-11072

Transformation toughened ceramics for the heavy duty diesel engine technology program

[NASA-CR-174689] p 185 A85-16698

Rolling, slip and traction measurements on low modulus materials

[NASA-CR-174909] p 135 A85-33491

## MOIRE EFFECTS

A comparison of electronic heterodyne moire deflectometry and electronic heterodyne holographic interferometry for flow measurements

[NASA-TM-87071] p 125 A85-32302

## MOIRE FRINGES

Electronic heterodyne readout of fringes in moire deflectometry p 122 A85-36726

Moire deflectometry with deferred electronic heterodyne readout p 122 A85-42854

## MOLECULAR BEAM EPITAXY

Sixty GHz IMPATT diode development  
[NASA-CR-174969] p 105 A85-33293

## MOLECULAR ORBITALS

Mechanism for chelated sulfate formation from SO<sub>2</sub> and bis (triphenylphosphine) platinum p 62 A85-48493

Mechanism for forming hydrogen chloride and sodium sulfate from sulfur trioxide, water, and sodium chloride

p 62 A85-48513

Why CO bonds side-on at low coverage and both side-on and upright at high coverage on the Cr(110) surface  
[NASA-CR-176071] p 77 A85-32173

Molecular orbital studies in oxidation: Sulfate formation and metal-metal oxide adhesion

[NASA-CR-176070] p 77 A85-32174

## MOLECULAR SPECTRA

Mass analysis of neutral particles and ions released during electrical breakdowns on spacecraft surfaces

[NASA-CR-175585] p 39 A85-21250

## MOLTEN SALT ELECTROLYTES

Moderate temperature sodium cells. V - Discharge reactions and rechargeability of NiS and NiS<sub>2</sub> positive electrodes in molten NaAlCl<sub>4</sub> p 59 A85-11892

## MOLTEN SALTS

Mechanism of strength degradation for hot corrosion of alpha-SiC

[NASA-TM-87052] p 91 A85-30135

## N

## MOLYBDENUM ALLOYS

Deformation and fracture behavior of  
Ni-Mo-Al(gamma/gamma prime-alpha) in situ composite  
p 64 A85-11058

Microstructures in rapidly solidified Ni-Mo alloys  
[NASA-TM-87100] p 78 N85-34266

## MOLYBDENUM DISULFIDES

Frictional and morphological properties of Au-MoS<sub>2</sub> films  
sputtered from a compact target p 127 A85-19085  
The influence of temperature on the lubricating  
effectiveness of MoS<sub>2</sub> dispersed in mineral oils  
[ASLE PREPRINT 84-LC-2A-2] p 80 A85-25963

## MOM (SEMICONDUCTORS)

Prism-coupled light emission from tunnel junctions  
p 181 A85-21425

## MONITORS

Design description of a microprocessor based Engine  
Monitoring and Control unit (EMAC) for small turboshaft  
[NASA-TM-86860] p 1 N85-17935  
Reusable rocket engine turbopump condition  
monitoring p 51 N85-26907

## MONOMERS

PMR polyimide composites for aerospace applications  
— Polymerization of Monomer Reactants  
p 55 A85-21520  
Graphite/PMR polyimide composites with improved  
toughness  
[NASA-TM-87081] p 58 N85-32148

## MONTE CARLO METHOD

Monte Carlo study of reversible growth of clusters on  
a surface p 182 A85-48516  
Monte Carlo lattice models for adsorbed polymer  
conformation  
[NASA-TP-2453] p 183 N85-24961

## MORPHOLOGY

Frictional and morphological properties of Au-MoS<sub>2</sub> films  
sputtered from a compact target p 127 A85-19085  
Morphological changes of gamma prime precipitates in  
nickel-base superalloy single crystals  
[NASA-TM-83698] p 70 N85-10165  
Tribological properties of graphite-fiber-reinforced,  
partially fluorinated polyimide composites  
[NASA-TM-86926] p 86 N85-18153  
Percutaneous connectors  
[NASA-CR-175627] p 168 N85-27508  
The structure of ion plated films in relation to coating  
properties  
[NASA-TM-87055] p 95 N85-29085

## MOSAICS

Mosaic Infrared Sensor for Space Astronomy  
(MIRSA)  
[NASA-CR-176154] p 125 N85-33456

## MOTION STABILITY

Linearization of digital derived rate algorithm for use in  
linear stability analysis  
[NASA-TM-87000] p 41 N85-23904

## MOVING TARGET INDICATORS

Moving target, distributed, real-time simulation using  
Ada p 170 A85-34131

## MULLITES

Transformation toughened ceramics for the heavy duty  
diesel engine technology program  
[NASA-CR-174689] p 185 N85-16698

## MULTIBEAM ANTENNAS

Status of NASA's multibeam communications  
technology program p 100 A85-14432  
Advanced 30/20 GHz multiple beam antenna for future  
communications satellites p 96 A85-14436  
A frequency-routed satellite system concept using  
multiple orthogonally-polarized beams for frequency  
reuse p 97 A85-34470

Configuration study for a 30 GHz monolithic receive  
array: Technical assessment  
[NASA-CR-174697] p 98 N85-18238

Configuration study for a 30 GHz monolithic receive  
array, volume 1  
[NASA-CR-174697-VOL-1] p 98 N85-18239

## MULTIPLE BEAM INTERVAL SCANNERS

The 20 GHz proof-of-concept test model results for a  
multiple scan beam dual reflector antenna  
[NASA-CR-174268] p 98 N85-15944

## MULTIPROCESSING (COMPUTERS)

A functional language approach in high-speed digital  
simulation p 170 A85-28615  
Hardware for a real-time multiprocessor simulator  
[NASA-TM-83805] p 169 N85-10659  
Operating system for a real-time multiprocessor  
propulsion system simulator. User's manual  
[NASA-TP-2426] p 171 N85-17596  
Real-Time Multiprocessor Programming Language  
(RTMPL) user's manual  
[NASA-TP-2422] p 170 N85-28610

## MULTIVARIATE STATISTICAL ANALYSIS

Identification of multivariable high-performance turbofan  
engine dynamics from closed-loop data  
p 13 A85-13630

## N-TYPE SEMICONDUCTORS

Heat treatment of bulk gallium arsenide using a  
phosphosilicate glass cap p 181 A85-32636  
Fabrication of p(+)-n junction GaAs solar cells by a  
novel method p 181 A85-33645

## NACELLES

Electro-impulse de-icing of a turbofan engine inlet  
[AIAA PAPER 85-1118] p 12 A85-40811  
Energy efficient engine ICLS Nacelle detail design  
report  
[NASA-CR-167870] p 22 N85-10993

## NASA PROGRAMS

Status of NASA's multibeam communications  
technology program p 100 A85-14432  
Analytical and physical modeling program for the NASA  
Lewis Research Center's Altitude Wind Tunnel (AWT)  
[AIAA PAPER 85-0379] p 34 A85-19709  
Overview of NASA Lewis Research Center free-piston  
Stirling engine activities p 130 A85-45479  
Bibliography of Lewis Research Center technical  
publications announced in 1983  
[NASA-TM-83693] p 184 N85-22255

## NATURAL GAS

Combustion gas properties. 2: Natural gas fuel and  
dry air  
[NASA-TP-2435] p 26 N85-21168

## NAVIER-STOKES EQUATION

Development of finite analytic method for unsteady  
three-dimensional Navier-Stokes equation  
p 106 A85-11647

Efficient solution of the Euler and Navier-Stokes  
equations with a vectorized multiple-grid algorithm  
p 2 A85-18679

Accelerated convergence for incompressible flow  
calculations  
[AIAA PAPER 85-0058] p 2 A85-19489

A space-marching method for incompressible  
Navier-Stokes equations  
[AIAA PAPER 85-0170] p 108 A85-19564

Progress in development of a Navier-Stokes solver for  
evaluation of iced airfoil performance  
[AIAA PAPER 85-0410] p 3 A85-19731

Assessment of discretization schemes to reduce  
numerical diffusion in the calculation of complex flows  
[AIAA PAPER 85-0441] p 108 A85-19751

Application of computational fluid dynamics to complex  
inlet ducts  
[AIAA PAPER 85-1213] p 6 A85-47023

Accelerated convergence for incompressible flow  
calculations  
[NASA-TM-86863] p 18 N85-10949

Model equation for simulating flows in multistage  
turbomachinery  
[NASA-TM-86869] p 7 N85-12036

Reducing numerical diffusion for incompressible flow  
calculations  
[NASA-TM-83621] p 24 N85-14840

Research applied to transonic compressors in  
numerical fluid mechanics of inviscid flow and viscous  
flow  
[NASA-CR-174353] p 114 N85-18291

Application of computational fluid dynamics to complex  
inlet ducts  
[NASA-TM-87060] p 118 N85-30247

Turbulent solutions of equations of fluid motion  
p 118 N85-31441

## NEAR FIELDS

On stress field near a stationary crack tip  
[AD-A152863] p 141 A85-24532

Case study of sample spacing in planar near-field  
measurement of high gain antennas  
[NASA-TM-86872] p 97 N85-10234

## NEGATIVE CONDUCTANCE

Circuit transients due to negative bias arcs on a  
high-voltage solar array in low Earth orbit  
[NASA-TP-2407] p 39 N85-14858

## NEODYMIUM LASERS

Laser balancing system for high material removal  
rates  
[NASA-CR-174731] p 126 N85-12341

## NETWORK ANALYSIS

Small-signal model for the series resonant converter  
p 102 A85-39453  
The J3 SCR model applied to resonant converter  
simulation p 102 A85-42156

## NETWORK CONTROL

Optical computer switching network  
p 178 A85-23134

A frequency-routed satellite system concept using  
multiple orthogonally-polarized beams for frequency  
reuse p 97 A85-34470

## NETWORK SYNTHESIS

Bipolar-FET combinational power transistors for power  
conversion applications p 100 A85-12669

The NASA satellite communication 20 x 20 matrix  
switches p 101 A85-14435

## NEUTRAL PARTICLES

Mass analysis of neutral particles and ions released  
during electrical breakdowns on spacecraft surfaces  
[NASA-CR-175585] p 39 N85-21250  
Mass spectra of neutral particles released during  
electrical breakdown of thin polymer films  
p 88 N85-22511

## NEUTRON EMISSION

Apparatus and method for identification of matrix  
materials in which transuranic elements are embedded  
using thermal neutron capture gamma-ray emission  
[DE85-011659] p 125 N85-33454

## NEWTON-RAPHSON METHOD

Extension of constrained incremental Newton-Raphson  
scheme to generalized loading fields  
p 139 A85-13942

On the development of hierarchical solution strategies  
for nonlinear finite element formulations  
p 171 A85-21979

## NICHROME (TRADEMARK)

Metallurgical and mechanical phenomena due to rubbing  
of titanium against sintered powder, Nichrome  
p 127 A85-22281

## NICKEL

Effects of SO<sub>2</sub> and SO<sub>3</sub> on the Na<sub>2</sub>SO<sub>4</sub> induced  
corrosion of nickel p 65 A85-15603

The substitution of nickel for cobalt in hot isostatically  
pressed powder metallurgy UDIMET 700 alloys  
p 68 A85-37415

The effects of seven alloying elements on the  
microstructure and stress-rupture behavior of nickel-base  
superalloys  
[NASA-TM-83791] p 70 N85-10168

The reactions of cobalt, iron and nickel in SO<sub>2</sub>  
atmospheres: Similarities and differences  
[NASA-TM-86868] p 70 N85-11217

Optimization of the NiCrAlY/ZrO<sub>2</sub> thermal barrier  
system  
[NASA-TM-86905] p 72 N85-15878

Surface effects of corrosive media on hardness, friction,  
and wear of materials  
[NASA-TM-83711] p 85 N85-15896

Humidity effects on adhesion of nickel-zinc ferrite in  
elastic contact with magnetic tape and itself  
[NASA-TP-2449] p 88 N85-21359

## NICKEL ALLOYS

Deformation and fracture behavior of  
Ni-Mo-Al(gamma/gamma prime-alpha) in situ composite  
p 64 A85-11058

Modeling of gamma/gamma prime phase equilibrium in  
the nickel-aluminum system p 65 A85-14959

Ductility in rapidly solidified NiAl p 66 A85-26158  
Elevated temperature creep-rupture behavior of the  
single crystal nickel-base superalloy NISAIR 100  
p 66 A85-27812

Chemical reactions involved in the initiation of hot  
corrosion of IN-738 p 66 A85-31688

Factors which influence directional coarsening of  
gamma prime during creep in nickel-base superalloy single  
crystals p 67 A85-32388

The influence of hold times on LCF and FCG behavior  
in a P/M Ni-base superalloy — Low Cycle Fatigue/Fatigue  
Crack Growth p 67 A85-32400

Effects of cobalt on the hot workability of nickel-base  
superalloys p 67 A85-32412

Rapid solidification and dynamic compaction of Ni-base  
superalloy powders p 67 A85-32414

Cyclic oxidation behavior of beta + gamma overlay  
coatings on gamma and gamma + gamma prime alloys  
p 68 A85-32431

On the fatigue crack propagation behavior of superalloys  
at intermediate temperatures p 68 A85-32434

Progress in the utilization of an  
oxide-dispersion-strengthened alloy for small engine  
turbine blades  
[SAE PAPER 841512] p 68 A85-39284

Dopant effect of yttrium and the growth and adherence  
of alumina on nickel-aluminum alloys p 82 A85-40973

Diffusion welding of MA 6000 and a conventional  
nickel-base superalloy p 69 A85-43551

Application of two creep fatigue life models for the  
prediction of elevated temperature crack initiation of a  
nickel base alloy  
[AIAA PAPER 85-1420] p 69 A85-43979

Morphological changes of gamma prime precipitates in  
nickel-base superalloy single crystals  
[NASA-TM-83698] p 70 N85-10165

The transient oxidation of single crystal NiAl+Zr  
[NASA-CR-174756] p 70 N85-11221

The effect of tantalum and carbon on the  
structure/properties of a single crystal nickel-base  
superalloy  
[NASA-CR-174779] p 71 N85-11223



- Studies on the hot corrosion of a nickel-base superalloy, Udmet 700  
[NASA-TM-86882] p 71 N85-11224
- The effects of Cr, Co, Al, Mo and Ta on the cyclic oxidation behavior of a prototype cast Ni-base superalloy based on a 2(5) composite statistically designed experiment  
[NASA-TM-83784] p 71 N85-12131
- The effect of tantalum on the structure/properties of two polycrystalline nickel-base superalloys: B-1900 + Hf MAR-M247  
[NASA-CR-174847] p 73 N85-18127
- Low cycle fatigue of MAR-M 200 single crystals at 760 and 870 deg C  
[NASA-TM-86933] p 74 N85-19074
- Study of the effects of implantation on the high Fe-Ni-Cr and Ni-Cr-Al alloys  
[NASA-CR-175625] p 76 N85-22661
- A multiple linear regression analysis of hot corrosion attack on a series of nickel base turbine alloys  
[NASA-TM-87020] p 77 N85-31284
- Microstructures in rapidly solidified Ni-Mo alloys  
[NASA-TM-87100] p 78 N85-34266
- NICKEL CADMIUM BATTERIES**
- A 37.5-kW point design comparison of the nickel-cadmium battery, bipolar nickel-hydrogen battery, and regenerative hydrogen-oxygen fuel cell energy storage subsystems for low earth orbit p 46 A85-45387
- NICKEL COMPOUNDS**
- Moderate temperature sodium cells. V - Discharge reactions and rechargeability of NiS and NiS<sub>2</sub> positive electrodes in molten NaAlCl<sub>4</sub> p 59 A85-11892
- Alloys based on NiAl for high temperature applications  
[NASA-TM-86976] p 75 N85-21322
- Raman structural studies of the nickel electrode  
[NASA-CR-175619] p 183 N85-23414
- NICKEL HYDROGEN BATTERIES**
- Design of a 1-kWh bipolar nickel hydrogen battery p 155 A85-45384
- Teardown analysis of a ten cell bipolar nickel-hydrogen battery p 156 A85-45385
- Separator development and testing of nickel-hydrogen cells p 156 A85-45386
- A 37.5-kW point design comparison of the nickel-cadmium battery, bipolar nickel-hydrogen battery, and regenerative hydrogen-oxygen fuel cell energy storage subsystems for low earth orbit p 46 A85-45387
- Long life nickel electrodes for a nickel-hydrogen cell. III - Results of an accelerated test and failure analyses p 156 A85-45391
- Advanced designs for IPV nickel-hydrogen cells p 156 A85-45438
- Advanced nickel-hydrogen cell configuration study  
[NASA-CR-174775] p 157 N85-10444
- Initial performance of advanced designs for IPV nickel-hydrogen cells  
[NASA-TM-87029] p 162 N85-28444
- Life cycle test results of a bipolar nickel hydrogen battery  
[NASA-TM-87046] p 163 N85-30480
- Design principles for nickel hydrogen cells and batteries p 104 N85-31398
- Initial performance of advanced designs for IPV nickel-hydrogen cells p 105 N85-31404
- Life cycle test results of a bipolar nickel hydrogen battery p 105 N85-31406
- The failure mechanism of a nickel electrode in a nickel-hydrogen cell p 105 N85-31408
- Design principles for nickel-hydrogen cells and batteries  
[NASA-TM-87037] p 164 N85-31646
- NICKEL OXIDES**
- Adsorption of O<sub>2</sub>, SO<sub>2</sub>, and SO<sub>3</sub> on nickel oxide. Mechanism for sulfate formation  
[NASA-CR-176072] p 77 N85-32175
- NIOBIUM ALLOYS**
- Effect of reduction of strategic Columbium addition in 718 Alloy on the structure and properties  
[NASA-CR-174841] p 75 N85-21320
- NITRIDING**
- Ion-beam nitriding of steels p 66 A85-24667
- Nitriding of titanium and its alloys by N<sub>2</sub>, NH<sub>3</sub> or mixtures of N<sub>2</sub> + H<sub>2</sub> in a dc arc plasma at low pressures (or = to torr)  
[NASA-TM-83803] p 131 N85-15168
- Ion-beam nitriding of steels  
[NASA-CASE-LEW-14104-1] p 75 N85-21324
- NITROGEN**
- Performance characterization tests of a 1-kW resistojet using hydrogen, nitrogen and ammonia as propellants  
[AIAA PAPER 85-1159] p 44 A85-39628
- Lubricity of well-characterized jet and broad-cut fuels by ball-on-cylinder machine  
[NASA-TM-83807] p 92 N85-12183
- Electrode erosion in arc discharges at atmospheric pressure  
[NASA-TM-87087] p 52 N85-34178
- NITROGEN PLASMA**
- Measurements of energy distribution in microwave plasmas of N<sub>2</sub> and He and comparisons with results for H<sub>2</sub> p 178 A85-16443
- Frictional and structural characterization of ion-nitrided low and high chromium steels  
[NASA-TM-86991] p 132 N85-23085
- NOBLE METALS**
- Electrocatalyst advances for hydrogen oxidation in phosphoric acid fuel cells p 60 A85-15614
- NOISE (SOUND)**
- Further comparison of wind tunnel and airplane acoustic data for advanced design high speed propeller models  
[NASA-TM-86935] p 176 N85-22108
- Generated spiral bevel gears: Optimal machine-tool settings and tooth contact analysis  
[NASA-TM-87075] p 136 N85-34405
- NOISE INTENSITY**
- Acoustic pressures emanating from a turbomachine stage  
[AIAA PAPER 84-2325] p 2 A85-10870
- Investigation on experimental techniques to detect, locate and quantify gear noise in helicopter transmissions  
[NASA-CR-3847] p 176 N85-17667
- NOISE MEASUREMENT**
- Comparison of scaled model data to full size energy efficient engine test results  
[AIAA PAPER 84-2281] p 13 A85-13953
- Measurement and prediction of Energy Efficient Engine noise  
[AIAA PAPER 84-2284] p 13 A85-13954
- Analysis of the effect on combustor noise measurements of acoustic waves reflected by the turbine and combustor inlet  
[AIAA PAPER 84-2323] p 173 A85-16103
- NOISE PREDICTION**
- A theoretical prediction of the acoustic pressure generated by turbulence-flame front interactions  
[ASME PAPER 84-WA/NCA-11] p 174 A85-39909
- NOISE PREDICTION (AIRCRAFT)**
- Measurement and prediction of Energy Efficient Engine noise  
[AIAA PAPER 84-2284] p 13 A85-13954
- Noise produced by the interaction of a rotor wake with a swept stator blade  
[AIAA PAPER 84-2326] p 173 A85-13956
- Modelling of wind tunnel wall effects on the radiation characteristics of acoustic sources  
[AIAA PAPER 84-2364] p 174 A85-16104
- Observations from varying the lift and drag inputs to a noise prediction method for supersonic helical tip speed propellers  
[NASA-TM-83797] p 175 N85-10788
- NOISE PROPAGATION**
- Noise transmission loss of a rectangular plate in an infinite baffle  
[NASA-TP-2398] p 176 N85-22109
- Interaction of finite-amplitude sound with air-filled porous materials  
[NASA-CR-174885] p 177 N85-27637
- NOISE REDUCTION**
- Supersonic jet shock noise reduction  
[AIAA PAPER 84-2278] p 173 A85-16099
- A high-speed implementation of the random decrement algorithm p 94 A85-29556
- The performance of jet noise suppression devices for industrial applications p 175 A85-42563
- Noise constraints effecting optimal propeller designs  
[SAE PAPER 850871] p 7 A85-50106
- Experimental investigation of shock-cell noise reduction for dual-stream nozzles in simulated flight  
[NASA-CR-3846] p 175 N85-13549
- Experimental investigation of shock-cell noise reduction for single stream nozzles in simulated flight  
[NASA-CR-3845] p 175 N85-13550
- Noise constraints effecting optimal propeller designs  
[NASA-TM-86967] p 8 N85-19923
- Interaction of finite-amplitude sound with air-filled porous materials  
[NASA-CR-174885] p 177 N85-27637
- NOISE SPECTRA**
- Effects of vane/blade ratio and spacing on fan noise, volume 1  
[NASA-CR-174664] p 176 N85-19791
- Effects of vane/blade ratio and spacing on fan noise. Volume 2: Data supplement  
[NASA-CR-174665] p 176 N85-19792
- NONDESTRUCTIVE TESTS**
- Eddy current jet engine disk-crack monitor p 120 A85-11100
- Ultrasonic nondestructive evaluation, microstructure, and mechanical property interrelations  
[NASA-TM-86876] p 137 N85-10371
- NDE for heat engine ceramics  
[NASA-TM-86949] p 137 N85-20389
- Stress waves in an isotropic elastic plate excited by a circular transducer  
[NASA-CR-3877] p 138 N85-20390
- Structural Integrity and Durability of Reusable Space Propulsion Systems  
[NASA-CP-2381] p 51 N85-27941
- Ultrasonic testing of plates containing edge cracks  
[NASA-CR-3904] p 138 N85-29307
- A study of the stress wave factor technique for the characterization of composite materials  
[NASA-CR-174870] p 58 N85-30035
- Reliability of void detection in structural ceramics using scanning laser acoustic microscopy  
[NASA-TM-87035] p 138 N85-32337
- NONISOTHERMAL PROCESSES**
- Thermodynamically consistent constitutive equations for nonisothermal large strain, elasto-plastic, creep behavior  
[AIAA PAPER 85-0621] p 142 A85-38425
- Thermomechanical deformation in the presence of metallurgical changes p 150 N85-31533
- NONLINEAR EQUATIONS**
- On the development of hierarchical solution strategies for nonlinear finite element formulations p 171 A85-21979
- Local strain redistribution corrections for a simplified inelastic analysis procedure based on an elastic finite-element analysis  
[NASA-TP-2421] p 145 N85-20396
- Nonlinear flap-lag-extensional vibrations of rotating, pretwisted, precone beams including Coriolis effects  
[NASA-TM-87102] p 152 N85-34427
- NONLINEAR SYSTEMS**
- Alternatives for jet engine control  
[NASA-CR-175831] p 29 N85-26713
- Alternatives for jet engine control  
[NASA-CR-175832] p 29 N85-26714
- Alternatives for jet engine control  
[NASA-CR-175833] p 29 N85-26715
- NONLINEARITY**
- A simplified method for elastic-plastic-creep structural analysis  
[ASME PAPER 84-GT-191] p 141 A85-23150
- On local total strain redistribution using a simplified cyclic inelastic analysis based on an elastic solution  
[AIAA PAPER 85-1419] p 142 A85-39770
- Nonlinear analysis for high-temperature multilayered fiber composite structures --- turbine blades  
[NASA-TM-83754] p 57 N85-21273
- On local total strain redistribution using a simplified cyclic inelastic analysis based on an elastic solution  
[NASA-TM-86913] p 145 N85-21690
- Nonlinear Constitutive Relations for High Temperature Application, 1984 p 150 N85-31530
- Elastohydrodynamic lubrication calculations used as a tool to study scuffing  
[NASA-TM-87097] p 137 N85-34408
- NONSTABILIZED OSCILLATION**
- Oscillator response to nonstationary excitation  
[ASME PAPER 84-WA/APM-38] p 140 A85-17039
- NONUNIFORM FLOW**
- Sound generation and upstream influence due to instability waves interacting with non-uniform mean flows p 174 A85-20738
- NOTCH STRENGTH**
- Finite element analysis of notch behavior using a state variable constitutive equation p 152 N85-31548
- NOTCH TESTS**
- Finite element analysis of notch behavior using a state variable constitutive equation p 152 N85-31548
- NOWCASTING**
- MERIT: A man/computer data management and enhancement system for upper air nowcasting/forecasting in the United States --- Minimum Energy Routes using Interactive Techniques (MERIT) p 167 N85-10558
- NOZZLE DESIGN**
- Supersonic jet shock noise reduction  
[AIAA PAPER 84-2278] p 173 A85-16099
- Experimental investigation of shock-cell noise reduction for single stream nozzles in simulated flight  
[NASA-CR-3845] p 175 N85-13550
- Convolute nozzle design for the RL10 derivative 2B engine  
[NASA-CR-174953] p 32 N85-29965
- NOZZLE EFFICIENCY**
- Altitude testing of a flight weight, self-cooled, 2D thrust vectoring exhaust nozzle  
[SAE PAPER 841557] p 14 A85-25984
- NOZZLE FLOW**
- The three-dimensional compressible flow in a radial inflow turbine scroll p 6 A85-41826



## O

- A multiple-scales model of the shock-cell structure of imperfectly expanded supersonic jets p 113 A85-49354
- Experimental investigation of shock-cell noise reduction for single stream nozzles in simulated flight [NASA-CR-3845] p 175 N85-13550
- NOZZLE GEOMETRY**
- Supersonic jet shock noise reduction [AIAA PAPER 84-2278] p 173 A85-16099
- Preliminary analysis of tone-excited two-stream jet velocity decay [NASA-TM-86951] p 8 N85-21114
- NUCLEAR BINDING ENERGY**
- Monte Carlo study of reversible growth of clusters on a surface p 182 A85-48516
- NUCLEAR ELECTRIC PROPULSION**
- An evaluation of oxygen/hydrogen propulsion systems for the Space Station [AIAA PAPER 85-1156] p 45 A85-43976
- Tethered nuclear power for the Space Station [NASA-TM-87023] p 51 N85-26912
- An evaluation of oxygen-hydrogen propulsion systems for the Space Station [NASA-TM-87059] p 52 N85-28971
- NUCLEAR POWER REACTORS**
- Applicability of 100kWe-class of space reactor power systems to NASA manned space station missions [NASA-CR-174696] p 177 N85-35728
- NUCLEAR REACTORS**
- High thermal power density heat transfer apparatus providing electrical isolation at high temperature using heat pipes [NASA-CASE-LEW-12950-2] p 117 N85-29179
- NUCLEATION**
- Computer simulation of thin film nucleation and growth p 181 A85-35308
- Fundamentals of microcrack nucleation mechanics [NASA-CR-3851] p 137 N85-16195
- A computer simulation of thin film nucleation and growth: The Volmer-Weber case [NASA-TM-86968] p 53 N85-21264
- NUMERICAL ANALYSIS**
- Comparison of numerical techniques for integration of stiff ordinary differential equations arising in combustion chemistry [NASA-TP-2372] p 17 N85-10065
- Nonlinear structural analysis for fiber-reinforced superalloy turbine blades p 147 N85-26887
- NUMERICAL CONTROL**
- Microprocessor control of photovoltaic systems p 156 A85-45408
- Design description of a microprocessor based Engine Monitoring and Control unit (EMAC) for small turbohaft [NASA-TM-86860] p 1 N85-17935
- Digital temperature and velocity control of mach 0.3 atmospheric pressure durability testing burner rigs in long time, unattended cyclic testing [NASA-TM-86959] p 75 N85-21321
- NUMERICAL INTEGRATION**
- Analysis of hourglass instabilities and control in underintegrated finite element methods p 139 A85-11125
- Integrating chemical kinetic rate equations by selective use of stiff and nonstiff methods [AIAA PAPER 85-0237] p 60 A85-19607
- Recent advances in methods for numerical solution of O.D.E. initial value problems p 171 A85-21370
- A comparison of the efficiency of numerical methods for integrating chemical kinetic rate equations [NASA-TM-83590] p 25 N85-21162
- NUMERICAL STABILITY**
- Analysis of hourglass instabilities and control in underintegrated finite element methods p 139 A85-11125
- Extension of constrained incremental Newton-Raphson scheme to generalized loading fields p 139 A85-13942
- Assessment of discretization schemes to reduce numerical diffusion in the calculation of complex flows [AIAA PAPER 85-0441] p 108 A85-19751
- Development and testing of stable, invariant, isoparametric curvilinear 2- and 3-D hybrid-stress elements p 140 A85-19899
- Recent advances in methods for numerical solution of O.D.E. initial value problems p 171 A85-21370
- Stability, accuracy, and efficiency of some underintegrated methods in finite element computations p 172 A85-50073

## O RING SEALS

- Analysis of experimental shaft seal data for high-performance turbomachines, as for Space Shuttle main engines [NASA-TM-86928] p 115 N85-21569
- Experimental stiffness of tapered bore seals [NASA-TM-86978] p 132 N85-25847

## ONBOARD DATA PROCESSING

- Satellite baseband processor test performance summary p 95 A85-14434

## ONE DIMENSIONAL FLOW

- Unsteady flow in a supersonic cascade with two in-passage shocks [NASA-CR-3925] p 10 N85-35158

## OPEN CHANNEL FLOW

- Behavior of turbulent gas jets in an axisymmetric confinement [NASA-CR-174829] p 28 N85-25265

## OPEN CIRCUIT VOLTAGE

- High-voltage solar-cell chip p 154 A85-24668
- Effect of solar-cell junction geometry on open-circuit voltage p 154 A85-28080

## OPERATING COSTS

- Energy efficient engine flight propulsion system preliminary analysis and design report [NASA-CR-174701] p 18 N85-10947
- Energy efficient engine component development and integration program [NASA-CR-169496] p 22 N85-10989
- Energy efficient engine. Volume 1: Component development and integration program [NASA-CR-173084] p 22 N85-10992

## OPERATORS (MATHEMATICS)

- Model equation for simulating flows in multistage turbomachinery [NASA-TM-86869] p 7 N85-12036

## OPTICAL COMPUTERS

- Optical computer switching network p 178 A85-23134
- Optical linear algebra processors - Noise and error-source modeling p 169 A85-36727

## OPTICAL CORRECTION PROCEDURE

- Holographic optical system for aberration corrections in laser Doppler velocimetry p 123 A85-48659

## OPTICAL DATA PROCESSING

- Optical computer switching network p 178 A85-23134
- Optical linear algebra processors - Noise and error-source modeling p 169 A85-36727

## OPTICAL FILTERS

- Filter induced errors in laser anemometer measurements using counter processors [NASA-TM-87047] p 125 N85-30288

## OPTICAL HETERODYNYING

- Electronic heterodyne readout of fringes in moire deflectometry p 122 A85-36726
- Moire deflectometry with deferred electronic heterodyne readout p 122 A85-42854

## OPTICAL MEASURING INSTRUMENTS

- An approach for automated analysis of particle holograms p 120 A85-10034
- Nonintrusive optical single-particle counter for measuring the size and velocity of droplets in a spray p 120 A85-16794
- Remote displacement measurements using a laser diode p 121 A85-24464
- Fiber optic temperature sensor p 121 A85-29563

## OPTICAL POLARIZATION

- Incident beam polarization for laser Doppler velocimetry employing a sapphire cylindrical window p 122 A85-39835

## OPTICAL PROPERTIES

- Laboratory degradation of Kapton in a low energy oxygen ion beam [AIAA PAPER 83-2658] p 78 A85-10675
- Optical properties of hydrogenated amorphous carbon films grown from methane plasma [NASA-TM-86995] p 183 N85-26406

## OPTICS

- The use of an optical data acquisition system for bladed disk vibration analysis [NASA-TM-86891] p 144 N85-15184

## OPTIMIZATION

- Optimization of cascade blade mistuning. I - Equations of motion and basic inherent properties p 16 A85-42365
- Optimization of cascade blade mistuning. II - Global optimum and numerical optimization p 16 A85-45715
- Structural optimization using optimality criteria methods p 144 A85-48703
- Noise constraints effecting optimal propeller designs [SAE PAPER 850871] p 7 A85-50106

- Manual of phosphoric acid fuel cell power plant optimization model and computer program [NASA-CR-174721] p 157 N85-10445
- Energy efficient engine. High pressure compressor detail design report [NASA-CR-165558] p 23 N85-10998
- An improved computer model for prediction of axial gas turbine performance losses [NASA-CR-174246] p 24 N85-15724
- Optimization of the NiCrAl-Y/ZrO<sub>2</sub> thermal barrier system [NASA-TM-86905] p 72 N85-15878
- Noise constraints effecting optimal propeller designs [NASA-TM-86967] p 8 N85-19923
- Alternatives for jet engine control [NASA-CR-175831] p 29 N85-26713
- Alternatives for jet engine control [NASA-CR-175833] p 29 N85-26715
- High pressure compressor component performance report [NASA-CR-168245] p 33 N85-34138
- OPTIONS**
- Space station propulsion options [AIAA PAPER 85-1155] p 45 A85-43975
- ORBIT SPECTRUM UTILIZATION**
- Engineering calculations for communications satellite systems planning [NASA-CR-175552] p 37 N85-21233
- ORBIT TRANSFER VEHICLES**
- Main propulsion system design recommendations for an advanced Orbit Transfer Vehicle [AIAA PAPER 85-1336] p 36 A85-39730
- Cryogenic upper stage test bed engine [AIAA PAPER 85-1339] p 44 A85-39733
- Progress report - Advanced cryogenic OTV engine technology [AIAA PAPER 85-1341] p 44 A85-39735
- OTV Propulsion Issues [NASA-CP-2347] p 37 N85-16989
- OTV propulsion technology programmatic overview p 37 N85-16997
- Vehicle/engine integration --- orbit transfer vehicles p 37 N85-17008
- Design and analysis report for the RL10-2B breadboard low thrust engine [NASA-CR-174857] p 48 N85-19020
- Convolute nozzle design for the RL10 derivative 2B engine [NASA-CR-174953] p 32 N85-29965
- Status of advanced orbital transfer propulsion [NASA-TM-87069] p 52 N85-35225
- ORBITAL MANEUVERING VEHICLES**
- Status of advanced orbital transfer propulsion [NASA-TM-87069] p 52 N85-35225
- ORBITAL SERVICING**
- OTV propulsion technology programmatic overview p 37 N85-16997
- ORBITAL SPACE STATIONS**
- Engineering model system study for a regenerative fuel cell: Study report [NASA-CR-174801] p 158 N85-16292
- Manrating orbital transfer vehicle propulsion [NASA-TM-87019] p 50 N85-25385
- Applicability of 100kWe-class of space reactor power systems to NASA manned space station missions [NASA-CR-174696] p 177 N85-35728
- ORGANIC SILICON COMPOUNDS**
- Preparation of silicon carbide-silicon nitride fibers by the pyrolysis of polycarbosilazane precursors [NASA-TM-86505] p 91 N85-28107
- ORGANOMETALLIC COMPOUNDS**
- Magnesium doping of efficient GaAs and Ga(0.75)In(0.25)As solar cells grown by metalorganic chemical vapor deposition p 180 A85-11466
- ORIFICE FLOW**
- Experiments in dilution jet mixing - Effects of multiple rows and non-circular orifices [AIAA PAPER 85-1104] p 15 A85-39606
- Experiments in dilution jet mixing effects of multiple rows and non-circular orifices [NASA-TM-86996] p 28 N85-25266
- Flow rate and pressure profiles for 1 to 4 axially aligned orifice inlets [NASA-TP-2460] p 116 N85-27165
- ORIFICES**
- Flow rate and pressure profiles for 1 to 4 axially aligned orifice inlets [NASA-TP-2460] p 116 N85-27165
- OSCILLATING FLOW**
- Resonance in flows with vortex sheets and edges p 1 A85-10357
- Approximate analysis for resonance of an incompressible shear layer plus edges p 107 A85-19377

**OSCILLATION DAMPERS**

Variable force, eddy-current or magnetic damper  
[NASA-CASE-LEW-13717-1] p 134 N85-30333

**OSCILLOSCOPES**

Transferring data oscilloscope to an IBM using an Apple II+ p 168 A85-24526

**OXIDATION**

Systematic optimization of a detailed kinetic model using a methane ignition example p 59 A85-12890  
Electrocatalyst advances for hydrogen oxidation in phosphoric acid fuel cells p 60 A85-15614  
Performance of thermal barrier coatings in high heat flux environments p 79 A85-19087  
Cyclic oxidation behavior of beta+gamma overlay coatings on gamma and gamma+gamma-prime alloys p 68 A85-32431  
High temperature oxidation of propene p 61 A85-33570

The transient oxidation of single crystal NiAl+Zr [NASA-CR-174756] p 70 N85-11221  
Analysis techniques for tracer studies of oxidation [NASA-CR-174796] p 84 N85-12162  
Optimization of the NiCrAl-Y/ZrO<sub>2</sub>Y<sub>2</sub>O<sub>3</sub> thermal barrier system [NASA-TM-86905] p 72 N85-15878  
Effects of chromium and aluminum on mechanical and oxidation properties of iron-nickel-base superalloys based on CG-27 [NASA-TP-2443] p 75 N85-21323

Oxidation and hot corrosion of hot-pressed Si<sub>3</sub>N<sub>4</sub> at 1000 deg C [NASA-TM-86977] p 88 N85-21358  
Shock tube study of the fuel structure effects on the chemical kinetic mechanisms responsible for soot formation, part 2 [NASA-CR-174880] p 63 N85-25444

Effects of surface chemistry on hot corrosion life [NASA-CR-174915] p 28 N85-26711  
Burner rig corrosion of SiC at 1000 deg C [NASA-TM-87061] p 53 N85-30011  
Ion beam sputter-deposited thin film coatings for protection of spacecraft polymers in low Earth orbit [NASA-TM-87051] p 91 N85-30137

Fuel-rich catalytic combustion: A soot-free technique for in situ hydrogen-like enrichment [NASA-TP-2498] p 63 N85-31244  
Shock tube measurements of growth constants in the branched-chain ethane-carbon monoxide-oxygen system [NASA-TM-87068] p 64 N85-32156  
Molecular orbital studies in oxidation: Sulfate formation and metal-metal oxide adhesion [NASA-CR-176070] p 77 N85-32174  
Aluminum work function: Effect of oxidation, mechanical scraping and ion bombardment [NASA-TM-87079] p 78 N85-34265

**OXIDATION RESISTANCE**

Oxidation-based model for thermal barrier coating life p 78 A85-10310  
Oxidation of silicon nitride sintered with rare-earth oxide additions p 83 A85-42798

The effects of Cr, Co, Al, Mo and Ta on the cyclic oxidation behavior of a prototype cast Ni-base superalloy based on a 2(5) composite statistically designed experiment [NASA-TM-83784] p 71 N85-12131

Effects of MAR-M247 substrate (modified) composition on coating oxidation coating/substrate interdiffusion --- protective coatings for hot section components of gas turbine engines [NASA-CR-174851] p 73 N85-19073  
Thermal barrier coating system [NASA-CASE-LEW-14057-1] p 59 N85-35233

**OXIDATION-REDUCTION REACTIONS**

NASA Redox Storage System Development Project [NASA-TM-83677] p 158 N85-12465  
Cycling performance of the iron-chromium redox energy storage system [NASA-TM-87034] p 162 N85-27387

**OXIDE FILMS**

Cyclic oxidation behavior of beta+gamma overlay coatings on gamma and gamma+gamma-prime alloys p 68 A85-32431

Electrical characterization of plasma-grown oxides on gallium arsenide p 181 A85-32635  
Ion beam sputter-deposited thin film coatings for protection of spacecraft polymers in low Earth orbit [NASA-TM-87051] p 91 N85-30137  
Thermal barrier coating system [NASA-CASE-LEW-14057-1] p 59 N85-35233

**OXYGEN**

Separator development and testing of nickel-hydrogen cells p 156 A85-45386  
Electrocatalysis of fuel cell reactions: Investigation of alternate electrolytes [NASA-CR-174753] p 157 N85-11455

Study of Kapton under simulated shuttle environment [NASA-CR-176003] p 41 N85-29997  
Shock tube measurements of growth constants in the branched-chain ethane-carbon monoxide-oxygen system [NASA-TM-87068] p 64 N85-32156

**OXYGEN ATOMS**

Adsorption of O<sub>2</sub>, SO<sub>2</sub>, and SO<sub>3</sub> on nickel oxide. Mechanism for sulfate formation [NASA-CR-176072] p 77 N85-32175

**OXYGEN IONS**

Three-dimensional calculation of shuttle charging in polar orbit p 40 N85-22486

**OXYGENATION**

Jet fuel instability mechanisms [NASA-CR-175856] p 93 N85-28127

**OXYNITRIDES**

Strength and microstructure of sintered Si<sub>3</sub>N<sub>4</sub> with rare-earth-oxide additions [ACS PAPER 130-13-84] p 80 A85-25271  
Oxidation of silicon nitride sintered with rare-earth oxide additions p 83 A85-42798

**OZONE**

Simultaneous cabin and ambient ozone measurements on two Boeing 747 airplanes. Volume 3: October 1978 - July 1979 [NASA-TM-86883] p 167 N85-21872

**P**

**P-N JUNCTIONS**

Theory of the high base resistivity n(+)/pp(+) silicon solar cell and its application to radiation damage effects p 154 A85-32639  
Fabrication of p(+)-n junction GaAs solar cells by a novel method p 181 A85-33645

**PANEL METHOD (FLUID DYNAMICS)**

Calculation of compressible flow about three-dimensional inlets with auxiliary inlets, slats and vanes by means of a panel method [AIAA PAPER 85-1196] p 5 A85-40817  
Calculation of compressible flow about three-dimensional inlets with auxiliary inlets, slats and vanes by means of a panel method [NASA-CR-174975] p 10 N85-35162

**PANELS**

Design procedures for fiber composite structural components: Panels subjected to combined in-plane loads [NASA-TM-86909] p 57 N85-15823

**PARABOLIC REFLECTORS**

Focal shifts in parabolic reflectors p 97 A85-39356  
Optical analysis of parabolic dish concentrators for solar dynamic power systems in space [NASA-TM-87080] p 52 N85-34176

**PARALLEL PLATES**

Analysis of the electromagnetic scattering from an inlet geometry with lossy walls [NASA-CR-175743] p 99 N85-25686

**PARALLEL PROCESSING (COMPUTERS)**

Multibus-based parallel processor for simulation p 169 A85-28613  
General approaches for achieving high speed computations p 169 A85-28628  
Hardware for a real-time multiprocessor simulator [NASA-TM-83805] p 169 N85-10659

**PARAMETER IDENTIFICATION**

Identification of multivariable high-performance turbofan engine dynamics from closed-loop data p 13 A85-13630

**PARAMETERIZATION**

Stress waves in an isotropic elastic plate excited by a circular transducer [NASA-CR-3877] p 138 N85-20390

**PARTIAL DIFFERENTIAL EQUATIONS**

Thermal-stress analysis for a wood composite blade [NASA-CR-174794] p 159 N85-17421

**PARTICLE IN CELL TECHNIQUE**

Numerical simulations of positively-biased probes and dielectric-conductor disks in a plasma --- for low earth orbit plasma densities p 179 A85-17262

**PARTICLE LADEN JETS**

A two-equation turbulence model for two-phase jets p 107 A85-14376  
Structure of particle-laden jets - Measurements and predictions p 109 A85-25137  
Structure of ducted particle-laden turbulent jets p 110 A85-38999  
Effect of surface configuration during solid particle impingement erosion p 69 A85-42568  
Characterization of solid particle erosion resistance of ductile metals based on their properties p 69 A85-42569

**PARTICLE SIZE DISTRIBUTION**

An approach for automated analysis of particle holograms p 120 A85-10034

Phase/doppler spray analyzer for simultaneous measurements of drop size and velocity distributions p 120 A85-10035

Spray characterization with a noninvasive technique using absolute scattered light p 120 A85-10036  
Predicting rime ice accretion on airfoils p 3 A85-25135

Milling of Si<sub>3</sub>N<sub>4</sub> with Si<sub>3</sub>N<sub>4</sub> hardware [NASA-TM-86864] p 84 N85-10191  
Research study of droplet sizing technology leading to the development of an advanced droplet sizing system [NASA-CR-174839] p 123 N85-21604

**PARTICULATE SAMPLING**

Fuel-rich catalytic combustion: A soot-free technique for in situ hydrogen-like enrichment [NASA-TP-2498] p 63 N85-31244

**PASCAL (PROGRAMMING LANGUAGE)**

Transferring data oscilloscope to an IBM using an Apple II+ p 168 A85-24526

**PASSAGEWAYS**

Vortex-generating coolant-flow-passage design for increased film-cooling effectiveness and surface coverage [NASA-TP-2388] p 113 N85-12314

**PAYLOADS**

Rail accelerator technology and applications [NASA-TM-86947] p 48 N85-21258

**PELVIS**

Friction and wear properties of a Chamley artificial hip joint [ASLE PREPRINT 84-LC-4A-4] p 168 A85-38444

**PERFORMANCE**

Life cycle test results of a bipolar nickel hydrogen battery [NASA-TM-87046] p 163 N85-30480

**PERFORMANCE PREDICTION**

Progress toward the development of an aircraft icing analysis capability [AIAA PAPER 84-0105] p 10 A85-10653  
Predicted turbine stage performance using quasi-three-dimensional and boundary-layer analyses p 15 A85-34013  
Comparison of free-piston Stirling engine model predictions with RE1000 engine test data p 130 A85-45488

Phosphoric acid fuel cell power plant system performance model and computer program [NASA-CR-174638] p 157 N85-11456

Analytical fuel property effects--small combustors [NASA-CR-174738] p 28 N85-26709  
Aerodynamic analysis of a horizontal axis wind turbine by use of helical vortex theory. Volume 1: Theory [NASA-CR-168054] p 9 N85-29916

Analytical model for predicting emergency shutdown of a two-bladed horizontal axis wind turbine [NASA-TM-83472] p 162 N85-30476

Performance comparison between NACA 23024 and NACA 64(3)-618 airfoil configured rotors for horizontal-axis wind turbines [NASA-TM-83471] p 163 N85-30477

**PERFORMANCE TESTS**

Satellite baseband processor test performance summary p 95 A85-14434  
IAPS (8-cm) ion thruster cyclic endurance test --- Ion Auxiliary Propulsion System p 42 A85-16406  
Performance capabilities of the 12-centimeter Xenon ion thruster p 42 A85-16439  
Recent work on a microwave ion source p 179 A85-16455

Altitude testing of a flight weight, self-cooled, 2D thrust vectoring exhaust nozzle [SAE PAPER 841557] p 14 A85-25984

Status of DOE and AID stand-alone photovoltaic system field tests p 155 A85-35707  
Method for evaluating wind turbine wake effects on wind farm performance p 155 A85-36750

Space Station propulsion - The Advanced Development Program at Lewis [AIAA PAPER 85-1154] p 44 A85-39626

Performance characterization tests of a 1-kW resistojet using hydrogen, nitrogen and ammonia as propellants [AIAA PAPER 85-1159] p 44 A85-39628

Small centrifugal pumps for low thrust rockets [AIAA PAPER 85-1302] p 45 A85-43978  
Advanced blade tip seal system, volume 2 [NASA-CR-167851] p 23 N85-10999

Space station propulsion: The advanced development program at Lewis [NASA-TM-86999] p 50 N85-25386

Instrumentation technology overview p 124 N85-26903

Effect of precipitation on wind turbine performance [NASA-TM-86986] p 161 N85-27385

Free-piston Stirling engine/linear alternator 1000-hour endurance test [NASA-CR-174771] p 163 N85-30481

Develop and test fuel cell powered on-site integrated total energy systems. Phase 3: Full-scale power plant development  
[NASA-CR-168338] p 164 N85-30483

Rolling, slip and traction measurements on low modulus materials  
[NASA-CR-174909] p 135 N85-33491

Planetary-gear-support bearing test rig design  
[NASA-CR-174927] p 12 N85-35185

**PERMEABILITY**  
Acoustic structure and propagation in highly porous, layered, fibrous materials p 173 A85-12301  
Effect of water on hydrogen permeability --- Stirling engines  
[NASA-TM-86904] p 53 N85-14864

**PERMITTIVITY**  
An experimental investigation of microstrip properties on soft substrates from 2 to 40 GHz  
[NASA-TM-86961] p 99 N85-20224

**PERTURBATION THEORY**  
Perturbation-iteration theory for analyzing microwave striplines  
[NASA-CR-176189] p 100 N85-35321

**PHASE DIAGRAMS**  
Modeling of gamma/gamma-prime phase equilibrium in the nickel-aluminum system p 65 A85-14959

**PHASE ERROR**  
Dual-mode coaxial feed with low crosspolarisation p 101 A85-20171

**PHASE TRANSFORMATIONS**  
Rapid solidification and dynamic compaction of Ni-base superalloy powders p 67 A85-32414  
A study of interdiffusion in beta + gamma/gamma + gamma prime Ni-Cr-Al  
[NASA-CR-174852] p 74 N85-20041

**PHASED ARRAYS**  
MMIC devices for active phased array antennas  
[NASA-CR-174281] p 98 N85-15943  
Configuration study for a 30 GHz monolithic receive array: Technical assessment  
[NASA-CR-174697] p 98 N85-18238  
Configuration study for a 30 GHz monolithic receive array, volume 1  
[NASA-CR-174697-VOL-1] p 98 N85-18239

**PHENYLS**  
Effect of substituted phenylindimides on processing and properties of PMR polyimide composites  
[NASA-TM-86902] p 85 N85-14929  
Ideal gas thermodynamic properties for the phenyl, phenoxy, and o-biphenyl radicals  
[NASA-TM-83800] p 184 N85-22204

**PHOSPHORESCENCE**  
Velocity visualization in gas flows using laser-induced phosphorescence of biacetyl p 121 A85-21695

**PHOSPHORIC ACID FUEL CELLS**  
Electrocatalyst advances for hydrogen oxidation in phosphoric acid fuel cells p 60 A85-15614  
Fuel cell power plant economic and operational considerations  
[ASME PAPER 84-AES-7] p 154 A85-21297  
Manual of phosphoric acid fuel cell power plant optimization model and computer program  
[NASA-CR-174721] p 157 N85-10445  
Manual of phosphoric acid fuel cell stack three-dimensional model and computer program  
[NASA-CR-174722] p 157 N85-10447  
Electrocatalysis of fuel cell reactions: Investigation of alternate electrolytes  
[NASA-CR-174753] p 157 N85-11455  
Phosphoric acid fuel cell power plant system performance model and computer program  
[NASA-CR-174638] p 157 N85-11456  
Gas cooled fuel cell systems technology development  
[NASA-CR-174732] p 158 N85-16291  
Electric utility acid fuel cell stack technology advancement  
[NASA-CR-174804] p 159 N85-17422  
Preparation and evaluation of advanced catalysts for phosphoric acid fuel cells  
[NASA-CR-168223] p 160 N85-19511  
Develop and test fuel cell powered on-site integrated total energy systems. Phase 3: Full-scale power plant development  
[NASA-CR-174887] p 161 N85-25941

**PHOTOACOUSTIC MICROSCOPY**  
Photoacoustic microscopy of ceramic turbine blades p 83 A85-43930

**PHOTOELECTRIC MATERIALS**  
Practical aspects of photovoltaic technology, applications and cost (revised)  
[NASA-CR-174963] p 165 N85-35472

**PHOTOGRAMMETRY**  
Initial feasibility ground test of a proposed photogrammetric system for measuring the shapes of ice accretions on helicopter rotor blades during forward flight  
[NASA-TM-87391] p 12 N85-12887

**PHOTOGRAPHS**  
Initial feasibility ground test of a proposed photogrammetric system for measuring the shapes of ice accretions on helicopter rotor blades during forward flight  
[NASA-TM-87391] p 12 N85-12887

**PHOTONS**  
Preliminary design of a 10 kW thermophotovoltaic system for space applications p 45 A85-45371

**PHOTOTRANSISTORS**  
High-temperature optically activated GaAs power switching for aircraft digital electronic control  
[NASA-CR-174711] p 34 N85-12901

**PHOTOVOLTAIC CELLS**  
Photovoltaics - The endless spring p 154 A85-35602  
The NASA photovoltaic technology program p 155 A85-35604  
Preliminary design of a 10 kW thermophotovoltaic system for space applications p 45 A85-45371  
Microprocessor control of photovoltaic systems p 156 A85-45408  
Control aspects of the Schuchuli Village stand-alone photovoltaic power system  
[NASA-TM-83790] p 103 N85-13157  
GaAs and 3-5 compound solar cells status and prospects for use in space p 49 N85-21261  
[NASA-TM-86960] p 49 N85-22569  
The high voltage silicon cell: A comparative analysis p 49 N85-22580  
GaAs and 3-5 compound solar cells status and prospects for use in space p 49 N85-22580  
Operational performance of the photovoltaic-powered grain mill and water pump at Tangaye, Burkina Faso (formerly Upper Volta)  
[NASA-TM-86970] p 161 N85-23243  
Thermionic photovoltaic energy converter  
[NASA-CASE-LEW-14077-1] p 164 N85-34441  
Practical aspects of photovoltaic technology, applications and cost (revised)  
[NASA-CR-174963] p 165 N85-35472

**PHOTOVOLTAIC CONVERSION**  
Control algorithms and computer simulation of a stand-alone photovoltaic village power system p 153 A85-11345  
Status of DOE and AID stand-alone photovoltaic system field tests p 155 A85-35707

**PHOTOVOLTAIC EFFECT**  
Preliminary design of a 10 kW thermophotovoltaic system for space applications p 45 A85-45371  
Research on gallium arsenide diffused junction solar cells  
[NASA-CR-174057] p 158 N85-11457  
High efficiency solar cell research for space applications p 164 N85-31624  
Thermionic photovoltaic energy converter  
[NASA-CASE-LEW-14077-1] p 164 N85-34441

**PHYSIOLOGICAL EFFECTS**  
Percutaneous connectors  
[NASA-CR-175627] p 168 N85-27508

**PIPE FLOW**  
Analysis of buoyancy effect on fully developed laminar heat transfer in a rotating tube p 110 A85-35596  
Behavior of turbulent gas jets in an axisymmetric confinement  
[NASA-CR-174829] p 28 N85-25265

**PISTON ENGINES**  
Initial results of sensitivity tests - Performed on the RE-1000 free-piston Stirling engine p 129 A85-45466  
Mod II engine and technology development p 129 A85-45473  
Overview of NASA Lewis Research Center free-piston Stirling engine activities p 130 A85-45479  
Overview of the 1985 NASA Lewis Research Center SP-100 free-piston Stirling engine activities  
[NASA-TM-87028] p 185 N85-27769

**PISTONS**  
Comparison of free-piston Stirling engine model predictions with RE1000 engine test data p 130 A85-45488  
Development of gas-lubricated pistons for heavy duty diesel engine technology program  
[NASA-CR-174746] p 184 N85-12808  
Sliding seal materials for adiabatic engines  
[NASA-CR-174893] p 89 N85-22757

**PITCH (INCLINATION)**  
Conceptual design of a fixed-pitch wind turbine generator system rated at 400 kilowatts  
[NASA-CR-174877] p 162 N85-29363

**PITTING**  
Mechanism of strength degradation for hot corrosion of alpha-SiC  
[NASA-TM-87052] p 91 N85-30135

**PLANE STRAIN**  
Fundamentals of microcrack nucleation mechanics  
[NASA-CR-3851] p 137 N85-16195

**PLANE WAVES**  
The response of Helmholtz resonators to external excitation. I - Single resonators p 174 A85-26915  
Analysis of the electromagnetic scattering from an inlet geometry with lossy walls  
[NASA-CR-175743] p 99 N85-25686

**PLASMA CURRENTS**  
Ion flow experiments in a multipole discharge chamber p 178 A85-12705  
Dilute plasma coupling currents to a high voltage solar array in weak magnetic fields p 46 A85-45388  
Ram-wake effects on plasma current collection of the PIX 2 Langmuir probe p 180 N85-22496

**PLASMA DENSITY**  
Ram-wake effects on plasma current collection of the PIX 2 Langmuir probe p 180 N85-22496  
NASCAP simulation of PIX 2 experiments p 180 N85-22497

**PLASMA DIAGNOSTICS**  
Effects of chemical releases by the STS 3 orbiter on the ionosphere p 166 A85-29538  
Analysis of glow discharges for understanding the process of film formation  
[NASA-TM-83750] p 62 N85-10138  
Nitriding of titanium and its alloys by N<sub>2</sub>, NH<sub>3</sub> or mixtures of N<sub>2</sub> + H<sub>2</sub> in a dc arc plasma at low pressures (or = to torr)  
[NASA-TM-83803] p 131 N85-15168  
Arc-driven rail gun research p 132 N85-21662  
Suprathermal plasma observed on STS-3 Mission by plasma diagnostics package p 179 N85-22472  
Electron and ion density depletions measured in the STS-3 orbiter wake p 39 N85-22474  
Ram-wake effects on plasma current collection of the PIX 2 Langmuir probe p 180 N85-22496

**PLASMA DISPLAY DEVICES**  
Frictional and structural characterization of ion-nitrided low and high chromium steels  
[NASA-TM-86991] p 132 N85-23085

**PLASMA DYNAMICS**  
Ion flow experiments in a multipole discharge chamber p 178 A85-12705  
Rail accelerator technology and applications  
[NASA-TM-86947] p 48 N85-21258

**PLASMA ENGINES**  
Ring-cusp ion thrusters p 42 A85-16438

**PLASMA GENERATORS**  
Recent work on a microwave ion source p 179 A85-16455  
High frequency plasma generator for ion thrusters  
[NASA-CR-174772] p 48 N85-17023

**PLASMA HEATING**  
High frequency plasma generator for ion thrusters  
[NASA-CR-174772] p 48 N85-17023

**PLASMA INTERACTION EXPERIMENT**  
Computer simulation of plasma electron collection by PIX-II --- solar array-space plasma interaction  
[AIAA PAPER 85-0386] p 43 A85-19715  
The PIX-2 experiment: An overview p 179 N85-22494  
Plasma interaction experiment 2 (PIX 2): Laboratory and flight results p 180 N85-22495  
Ram-wake effects on plasma current collection of the PIX 2 Langmuir probe p 180 N85-22496

**PLASMA INTERACTIONS**  
Characteristics of arc currents on a negatively biased solar cell array in a plasma p 154 A85-18608  
The effect of plasma on solar cell array arc characteristics  
[AIAA PAPER 85-0384] p 43 A85-19713  
Numerical simulation of positive-potential conductors in the presence of a plasma and a secondary-emitting dielectric p 102 A85-35306  
The effect of plasma on solar cell array arc characteristics  
[NASA-TM-86887] p 47 N85-11133  
Spacecraft Environmental Interactions Technology, 1983 p 39 N85-22470  
Surface interactions and high-voltage current collection p 40 N85-22493  
The PIX-2 experiment: An overview p 179 N85-22494  
Plasma interaction experiment 2 (PIX 2): Laboratory and flight results p 180 N85-22495  
Discharges on a negatively biased solar cell array in a charged-particle environment p 160 N85-22499

Spacecraft environmental interactions: A joint Air Force and NASA research and technology program p 40 N85-22517

**PLASMA JETS**

Ion flow experiments in a multipole discharge chamber p 178 A85-12705

Deposition stress effects on the life of thermal barrier coatings on burner rigs p 79 A85-19086

The effect of plasma on solar cell array arc characteristics [AIAA PAPER 85-0384] p 43 A85-19713

Properties of coated and modified surfaces p 53 A85-36694

Experimental performance of a microwave cavity plasma disk ion source p 179 A85-43552

The effect of plasma on solar cell array arc characteristics [NASA-TM-86887] p 47 N85-11133

**PLASMA LAYERS**

Plasma variables and tribological properties of coatings in low pressure (0.1 - 10.0 torr) plasma systems [NASA-TM-83798] p 94 N85-11261

**PLASMA PHYSICS**

Plasma deposited hydrogenated carbon on GaAs and InP p 182 A85-40386

Plasma deposited diamondlike carbon on GaAs and InP [NASA-TM-86870] p 183 N85-10844

**PLASMA PROPULSION**

The energetics of hydrogen atom recombination - Analysis, experiments, and modeling --- in electrothermal propulsion system p 179 A85-16444

Ring-cusp ion thruster with shell anode [NASA-CASE-LEW-13881-1] p 48 N85-21256

**PLASMA SPRAYING**

Deposition stress effects on the life of thermal barrier coatings on burner rigs p 79 A85-19086

Plastic flow of plasma sprayed ceramics p 80 A85-24161

Cyclic oxidation behavior of beta + gamma overlay coatings on gamma and gamma + gamma-prime alloys p 68 A85-32431

Electrical characterization of plasma-grown oxides on gallium arsenide p 181 A85-32635

Deposition of silicon nitride from SiCl<sub>4</sub> and NH<sub>3</sub> in a low pressure RF plasma p 81 A85-36229

Failure during thermal cycling of plasma-sprayed thermal barrier coatings p 81 A85-36246

Dielectric properties of 'diamondlike' carbon prepared by RF plasma deposition p 182 A85-38192

High-temperature erosion of plasma-sprayed, yttria-stabilized zirconia in a simulated turbine environment [AIAA PAPER 85-1219] p 82 A85-39662

Surface hardening of steel by boriding in a cold rf plasma p 68 A85-40275

'Diamondlike' carbon films - Optical absorption, dielectric properties, and hardness dependence on deposition parameters p 82 A85-40383

Energy efficient engine high pressure turbine ceramic shroud support technology report [NASA-CR-168036] p 23 N85-10996

High-temperature erosion of plasma-sprayed, yttria-stabilized zirconia in a simulated turbine environment [NASA-TP-2406] p 84 N85-13045

Film and interstitial formation of metals in plasma-sprayed ceramics [NASA-TM-86993] p 89 N85-22756

Thermal barrier coating system [NASA-CASE-LEW-14057-1] p 59 N85-35233

**PLASMAS (PHYSICS)**

Plasma variables and tribological properties of coatings in low pressure (0.1 - 10.0 torr) plasma systems [NASA-TM-83798] p 94 N85-11261

**PLASMONS**

Inelastic tunnel diodes [NASA-CASE-LEW-13833-1] p 103 N85-21492

Solar energy converter using surface plasma waves [NASA-CASE-LEW-13827-1] p 160 N85-21768

**PLASTIC DEFORMATION**

Deformation and erosion of f.c.c. metals and alloys under cavitation attack p 65 A85-12789

Hybrid stress finite elements for large deformations of inelastic solids p 139 A85-15894

Simplified design and life prediction of rocket thrust chambers p 44 A85-29314

**PLASTIC FLOW**

Plastic flow of plasma sprayed ceramics p 80 A85-24161

**PLATE THEORY**

Hybrid Semiloof elements for plates and shells based upon a modified Hu-Washizu principle p 139 A85-15893

Vibrations of twisted cantilevered plates - Summary of previous and current studies p 140 A85-22069

**PLATES (STRUCTURAL MEMBERS)**

Stress waves in an isotropic elastic plate excited by a circular transducer [NASA-CR-3877] p 138 N85-20390

Geometrically nonlinear analysis of laminated elastic structures [NASA-CR-175609] p 146 N85-21720

Ultrasonic testing of plates containing edge cracks [NASA-CR-3904] p 138 N85-29307

**PLATINUM**

Mechanism for chelated sulfate formation from SO<sub>2</sub> and bis (triphenylphosphine) platinum p 62 A85-48493

Dispersed metal-toughened ceramics and ceramic brazing [NASA-CR-174284] p 86 N85-15916

Advanced thin film thermocouples [NASA-CR-175541] p 124 N85-21607

**PLATINUM ALLOYS**

Compatibility experiments of facilities, materials, and propellants for electrothermal thrusters [NASA-TM-86956] p 49 N85-21260

CO adsorption on (111) and (100) surfaces of the Pt sub 3 Ti alloy. Evidence for parallel binding and strong activation of CO [NASA-CR-176077] p 77 N85-32176

**PLOTTING**

Plot of modal field distribution in rectangular and circular waveguides p 101 A85-25170

**PLUG NOZZLES**

Experimental investigation of shock-cell noise reduction for dual-stream nozzles in simulated flight [NASA-CR-3846] p 175 N85-13549

Experimental investigation of shock-cell noise reduction for single stream nozzles in simulated flight [NASA-CR-3845] p 175 N85-13550

**PLUMES**

Preliminary analysis of tone-excited two-stream jet velocity decay [NASA-TM-86951] p 8 N85-21114

**POLAR ORBITS**

Three-dimensional calculation of shuttle charging in polar orbit p 40 N85-22486

Polar orbit electrostatic charging of objects in shuttle wake p 40 N85-22487

**POLARIZATION (WAVES)**

Incident beam polarization for laser Doppler velocimetry employing a sapphire cylindrical window [NASA-TM-87064] p 178 N85-28786

POLARIZED ELECTROMAGNETIC RADIATION

A frequency-routed satellite system concept using multiple orthogonally-polarized beams for frequency reuse p 97 A85-34470

**POLARIZED LIGHT**

Prism-coupled light emission from tunnel junctions p 181 A85-21425

**POLLUTION CONTROL**

Methanol as a soot reducer in a turbulent swirling burner [ASME PAPER 84-JPGC-GT-2] p 61 A85-23192

**POLYCRYSTALS**

The effect of tantalum on the structure/properties of two polycrystalline nickel-base superalloys: B-1900 + Hf MAR-M247 [NASA-CR-174847] p 73 N85-18127

Aluminum work function: Effect of oxidation, mechanical scraping and ion bombardment [NASA-TM-87079] p 78 N85-34265

**POLYETHYLENES**

Friction, wear, transfer, and wear surface morphology of ultrahigh-molecular-weight polyethylene p 80 A85-22276

**POLYIMIDE RESINS**

Polyimides - Tribological properties and their use as lubricants p 79 A85-21524

Chemical approach for controlling nadimide cure temperature and rate with maleimide [NASA-CASE-LEW-13770-3] p 87 N85-21350

Chemical approach for controlling nadimide cure temperature and rate with maleimide [NASA-CASE-LEW-13770-4] p 87 N85-21351

Chemical approach for controlling nadimide cure temperature and rate [NASA-CASE-LEW-13770-5] p 87 N85-21352

Chemical control of nadimide cure temperature and rate [NASA-CASE-LEW-13770-2] p 63 N85-28982

Chemical approach for controlling nadimide cure temperature and rate [NASA-CASE-LEW-13770-6] p 63 N85-30039

Graphite/PMR polyimide composites with improved toughness [NASA-TM-87081] p 58 N85-32148

**POLYIMIDES**

Effect of substituted phenylnadimides on processing and properties of PMR polyimide composites [NASA-TM-86902] p 85 N85-14929

Tribological properties of graphite-fiber-reinforced, partially fluorinated polyimide composites [NASA-TM-86926] p 86 N85-18153

Ion beam sputter-deposited thin film coatings for protection of spacecraft polymers in low Earth orbit [NASA-TM-87051] p 91 N85-30137

Graphite/PMR polyimide composites with improved toughness [NASA-TM-87081] p 58 N85-32148

**POLYMER CHEMISTRY**

PMR polyimide composites for aerospace applications --- Polymerization of Monomer Reactants p 55 A85-21520

Chemical approach for controlling nadimide cure temperature and rate [NASA-CASE-LEW-13770-6] p 63 N85-30039

**POLYMER MATRIX COMPOSITES**

PMR polyimide composites for aerospace applications --- Polymerization of Monomer Reactants p 55 A85-21520

Effect of counterface material type and its topography on the tribological properties of polyimide composites [NASA-TM-87036] p 90 N85-26993

**POLYMERIC FILMS**

Effect of Interfacial characteristics of metal clad polymeric substrates on electrical high frequency interconnection performance [NASA-TM-86948] p 99 N85-20223

Mass analysis of neutral particles and ions released during electrical breakdowns on spacecraft surfaces [NASA-CR-175585] p 39 N85-21250

Mass spectra of neutral particles released during electrical breakdown of thin polymer films p 88 N85-22511

Monte Carlo lattice models for adsorbed polymer conformation [NASA-TP-2453] p 183 N85-24961

**POLYMERIZATION**

PMR polyimide composites for aerospace applications --- Polymerization of Monomer Reactants p 55 A85-21520

Development of a lithium secondary battery separator p 104 N85-31378

Graphite/PMR polyimide composites with improved toughness [NASA-TM-87081] p 58 N85-32148

**POLYMERS**

Tribological properties of graphite-fiber-reinforced, partially fluorinated polyimide composites [NASA-TM-86926] p 86 N85-18153

**POLYPHENYL ETHER**

Contact angle and surface tension measurements of a five-ring polyphenyl ether [NASA-TM-86927] p 86 N85-15897

Formation of high molecular weight products from benzene during boundary lubrication [NASA-TM-86956] p 62 N85-22644

**POROUS MATERIALS**

Acoustic structure and propagation in highly porous, layered, fibrous materials p 173 A85-12301

A new interpretation of internal heat transfer coefficients of porous media [ASME PAPER 84-WA/HT-51] p 110 A85-39894

Flow through very porous inclined screens [AIAA PAPER 85-1650] p 111 A85-40750

Flow through very porous inclined screens [NASA-TM-86979] p 116 N85-25761

Interaction of finite-amplitude sound with air-filled porous materials [NASA-CR-174885] p 177 N85-27637

**POTENTIAL ENERGY**

Translational and extensional energy release rates (the J- and M-integrals) for a crack layer in thermoelasticity [NASA-CR-174872] p 145 N85-21685

**POTENTIAL FLOW**

A linearized unsteady aerodynamic analysis for transonic cascades p 3 A85-20744

Calculation of compressible flow about three-dimensional inlets with auxiliary inlets, slats and vanes by means of a panel method [NASA-CR-174975] p 10 N85-35162

**POWDER (PARTICLES)**

Milling of Si<sub>3</sub>N<sub>4</sub> with Si<sub>3</sub>N<sub>4</sub> hardware [NASA-TM-86864] p 84 N85-10191

Factors influencing the ball milling of Si<sub>3</sub>N<sub>4</sub> in water [NASA-TM-86932] p 86 N85-19136

**POWDER METALLURGY**

Demonstration of a silicon nitride attrition mill for production of fine pure Si and Si<sub>3</sub>N<sub>4</sub> powders p 78 A85-10825

- The effect of microstructure, temperature, and hold-time on low-cycle fatigue of As HIP P/M Rene 95 p 67 A85-32399
- The influence of hold times on LCF and FCG behavior in a P/M Ni-base superalloy --- Low Cycle Fatigue/Fatigue Crack Growth p 67 A85-32400
- The substitution of nickel for cobalt in hot isostatically pressed powder metallurgy UDIMET 700 alloys p 68 A85-37415
- PM superalloys - A troubled adolescent? p 69 A85-44772
- Hot isostatically pressed manufacture of high strength MERL 76 disk and seal shapes [NASA-CR-165550] p 71 N85-11225
- Alloys based on NiAl for high temperature applications [NASA-TM-86976] p 75 N85-21322
- Fabrication of ceramic substrate-reinforced and free forms [NASA-TM-86994] p 50 N85-23926
- Powder metallurgy forged gear development [NASA-TM-87483] p 134 N85-29295
- POWER**
- Development of high frequency low weight power magnetics for aerospace power systems p 102 A85-45373
- POWER CONDITIONING**
- Control algorithms and computer simulation of a stand-alone photovoltaic village power system p 153 A85-11345
- A 20 GHz, 75 watt, helix TWT for space communications p 101 A85-14433
- Inelastic tunnel diodes [NASA-CASE-LEW-13833-1] p 103 N85-21492
- POWER CONVERTERS**
- Bipolar-FET combinational power transistors for power conversion applications p 100 A85-12669
- A fast time domain digital simulation technique for power converters - Application to a buck converter with feedforward compensation p 101 A85-20900
- POWER EFFICIENCY**
- Development of high frequency low weight power magnetics for aerospace power systems p 102 A85-45373
- Automotive Stirling engine systems development p 130 A85-45474
- Wind tunnel results of advanced high speed propellers in the takeoff, climb, and landing operating regimes [AIAA PAPER 85-1259] p 6 A85-47025
- Effect of precipitation on wind turbine performance [NASA-TM-86986] p 161 N85-27385
- Wind tunnel results of advanced high speed propellers in the takeoff, climb and landing operating regimes [NASA-TM-87054] p 9 N85-29925
- Free-piston Stirling engine/linear alternator 1000-hour endurance test [NASA-CR-174771] p 163 N85-30481
- POWER FACTOR CONTROLLERS**
- Advanced in solid state switchgear technology for large space power systems p 102 A85-45362
- Microprocessor control of photovoltaic systems p 156 A85-45408
- POWER REACTORS**
- Applicability of 100kW-class of space reactor power systems to NASA manned space station missions [NASA-CR-174696] p 177 N85-35728
- POWER SUPPLIES**
- Development of high frequency low weight power magnetics for aerospace power systems p 102 A85-45373
- POWER SUPPLY CIRCUITS**
- Small-signal model for the series resonant converter p 102 A85-39453
- Development of high frequency low weight power magnetics for aerospace power systems p 102 A85-45373
- Control aspects of the Schuchuli Village stand-alone photovoltaic power system [NASA-TM-83790] p 103 N85-13157
- Developments in space power components for power management and distribution p 47 N85-13877
- High-voltage, high-power, solid-state remote power controllers for aerospace applications [NASA-TM-2437] p 49 N85-21263
- POWER TRANSMISSION (LASERS)**
- Technology for satellite power conversion [NASA-CR-174335] p 159 N85-18451
- PREBURNERS**
- SSME fuel preburner two-dimensional analysis p 51 N85-27943
- PRECIPITATION (METEOROLOGY)**
- Effect of precipitation on wind turbine performance [NASA-TM-86986] p 161 N85-27385

**PRECIPITATION HARDENING**

- Progress in the utilization of an oxide-dispersion-strengthened alloy for small engine turbine blades [SAE PAPER 841512] p 68 A85-39284
- Diffusion welding of MA 6000 and a conventional nickel-base superalloy p 69 A85-43551
- Thermomechanical deformation in the presence of metallurgical changes p 150 N85-31533
- PREDICTION ANALYSIS TECHNIQUES**
- Computation of viscous flows in turbomachinery cascades p 106 A85-11631
- Predicting rime ice accretion on airfoils p 3 A85-25135
- A theoretical prediction of the acoustic pressure generated by turbulence-flame front interactions [ASME PAPER 84-WA/NCA-11] p 174 A85-39909
- Nonlinear structural and life analyses of a turbine blade p 19 N85-10954
- Nonlinear structural and life analyses of a combustor liner p 19 N85-10955
- Life prediction and constitutive behavior: Overview p 20 N85-10973
- Validation of structural analysis methods using the in-house liner cyclic rigs p 21 N85-10987
- Reliability considerations for the total strain range version of strainrange partitioning [NASA-CR-174757] p 144 N85-11380
- Confined turbulent swirling recirculating flow predictions [NASA-CR-174917] p 29 N85-26716
- Elevated temperature biaxial fatigue [NASA-CR-175795] p 148 N85-27263
- Predictions and measurements of isothermal flowfields in axisymmetric combustor geometries [NASA-CR-174916] p 29 N85-27867
- Reexamination of cumulative fatigue damage laws p 149 N85-27962
- Analytical model for predicting emergency shutdown of a two-bladed horizontal axis wind turbine [NASA-TM-83472] p 162 N85-30476
- Heat transfer and fluid mechanics measurements in transitional boundary layer flows p 118 N85-31439
- A review and analysis of boundary layer transition data for turbine application p 118 N85-31440
- A comparison of two contemporary creep-fatigue life prediction methods p 151 N85-31538
- Two simplified procedures for predicting cyclic material response from a strain history p 151 N85-31543
- Lubrication and cooling for high speed gears [NASA-TM-87096] p 136 N85-34407
- PREDICTIONS**
- Effects of surface chemistry on hot corrosion life: Overview p 21 N85-10980
- PREMIXED FLAMES**
- Flame flashback in a premixed dump combustor [AIAA PAPER 85-0145] p 60 A85-19550
- Combustion efficiency of a premixed continuous flow combustor p 61 A85-42571
- PRESSURE DISTRIBUTION**
- Effect of combined pressure and temperature distortion orientation on high-bypass-ratio turbofan engine stability [NASA-TM-83771] p 17 N85-10067
- Flow rate and pressure profiles for 1 to 4 axially aligned orifice inlets [NASA-TP-2460] p 116 N85-27165
- PRESSURE EFFECTS**
- Fast approach for calculating film thicknesses and pressures in elastohydrodynamically lubricated contacts at high loads [NASA-TM-87032] p 117 N85-30242
- PRESSURE GRADIENTS**
- Nested subcritical flows within supercritical systems [NASA-TM-86980] p 115 N85-21574
- PRESSURE MEASUREMENT**
- A stagnation pressure probe for droplet-laden air flow [AIAA PAPER 85-0330] p 108 A85-19672
- The infinite line pressure probe p 122 A85-37704
- Unsteady pressure measurements on a biconvex airfoil in a transonic oscillating cascade [NASA-TM-86914] p 8 N85-15689
- PRESSURE OSCILLATIONS**
- Approximate analysis for resonance of an incompressible shear layer plus edges p 107 A85-19377
- Oscillatory conductive heat transfer for a fiber in an ideal gas p 109 A85-26077
- PRESSURE PULSES**
- Flow dynamic environment data base development for the SSME p 147 N85-26885
- PRESSURE RATIO**
- High pressure compressor component performance report [NASA-CR-168245] p 33 N85-34138

**PRESSURE SENSORS**

- A stagnation pressure probe for droplet-laden air flow [AIAA PAPER 85-0330] p 108 A85-19672
- The infinite line pressure probe p 122 A85-37704
- High-temperature fiber optic pressure sensor p 123 A85-46607
- PRESSURE VESSEL DESIGN**
- Advanced nickel-hydrogen cell configuration study [NASA-CR-174775] p 157 N85-10444
- PRESSURE VESSELS**
- Ten year environmental test of glass fiber/epoxy pressure vessels [AIAA PAPER 85-1198] p 56 A85-47022
- Initial performance of advanced designs for IPV nickel-hydrogen cells [NASA-TM-87029] p 162 N85-28444
- Ten year environmental test of glass fiber/epoxy pressure vessels [NASA-TM-87058] p 58 N85-30034
- Initial performance of advanced designs for IPV nickel-hydrogen cells p 105 N85-31404
- PRESTRESSING**
- Effects of warping and pretwist on torsional vibration of rotating beams [ASME PAPER 84-WA/APM-41] p 140 A85-17040
- Vibration and buckling of rotating, pretwisted, precone beams including Coriolis effects [NASA-TM-87004] p 146 N85-25893
- PRIMARY BATTERIES**
- Electrochemistry and storage p 62 N85-13889
- PRINTED CIRCUITS**
- MMIC devices for active phased array antennas [NASA-CR-174281] p 98 N85-15943
- PRINTING**
- Screen printed interdigitated back contact solar cell [NASA-CASE-LEW-13414-1] p 160 N85-20530
- PROBABILITY THEORY**
- Creep-rupture reliability analysis p 143 A85-42566
- Probabilistic structural analysis theory development p 148 N85-27955
- Probabilistic finite element development p 149 N85-27956
- Reliability of void detection in structural ceramics using scanning laser acoustic microscopy [NASA-TM-87035] p 138 N85-32337
- PROBES**
- Precision tunable resonant microwave cavity [NASA-CASE-LEW-13935-1] p 103 N85-20248
- PROBLEM SOLVING**
- New integration techniques for chemical kinetic rate equations. 2: Accuracy comparison [NASA-TM-86893] p 23 N85-13798
- PROCESS CONTROL (INDUSTRY)**
- Chemical approach for controlling nadimide cure temperature and rate with maleimide [NASA-CASE-LEW-13770-3] p 87 N85-21350
- Chemical approach for controlling nadimide cure temperature and rate with maleimide [NASA-CASE-LEW-13770-4] p 87 N85-21351
- PRODUCT DEVELOPMENT**
- Conceptual design of a fixed-pitch wind turbine generator system rated at 400 kilowatts [NASA-CR-174877] p 162 N85-29363
- PROFILOMETERS**
- Characterization of lubricated bearing surfaces operated under high loads [NASA-TM-86964] p 88 N85-21357
- PROGRAM VERIFICATION (COMPUTERS)**
- Comparison of free-piston Stirling engine model predictions with RE1000 engine test data p 130 A85-45488
- PROGRAMMING LANGUAGES**
- Functional language and data flow architectures p 170 A85-28629
- PROJECT MANAGEMENT**
- Life prediction and constitutive behavior: Overview p 20 N85-10973
- PROP-FAN TECHNOLOGY**
- Large-scale advanced propfan (LAP) program progress report [AIAA PAPER 85-1187] p 17 A85-47021
- Large-scale Advanced Propfan (LAP) performance, acoustic and weight estimation, January, 1984 [NASA-CR-174782] p 9 N85-22368
- Large-scale Advanced Propfan (LAP) program [NASA-TM-87067] p 32 N85-29964
- PROPAGATION MODES**
- Circular waveguide bifurcation for asymmetric modes p 101 A85-20170
- Dual-mode coaxial feed with low crosspolarisation p 101 A85-20171
- Plot of modal field distribution in rectangular and circular waveguides p 101 A85-25170
- Turbulent noise generation. Volume 2: Computer programs [NASA-CR-167952] p 175 N85-11791

**PROPELLANT TANKS**

Ion thruster system (8-cm) cyclic endurance test  
[NASA-CR-174745] p 47 N85-12937

**PROPELLANT TESTS**

Electrothermal thruster diagnostics p 42 A85-16440  
Compatibility experiments of facilities, materials, and  
propellants for electrothermal thrusters  
[NASA-TM-86956] p 49 N85-21260

**PROPELLER BLADES**

Large-scale advanced propfan (LAP) program progress  
report  
[AIAA PAPER 85-1187] p 17 A85-47021  
Noise constraints effecting optimal propeller designs  
[SAE PAPER 850871] p 7 A85-50106  
Noise constraints effecting optimal propeller designs  
[NASA-TM-86967] p 8 N85-19923  
Large-scale Advanced Propfan (LAP) program  
[NASA-TM-87067] p 32 N85-29964

**PROPELLER EFFICIENCY**

Analytical determination of propeller performance  
degradation due to ice accretion  
[AIAA PAPER 85-0339] p 14 A85-20867  
Large-scale advanced propfan (LAP) program progress  
report  
[AIAA PAPER 85-1187] p 17 A85-47021  
Large-scale Advanced Propfan (LAP) program  
[NASA-TM-87067] p 32 N85-29964

**PROPELLER FANS**

Wind tunnel results of advanced high speed propellers  
in the takeoff, climb, and landing operating regimes  
[AIAA PAPER 85-1259] p 6 A85-47025  
Large-scale Advanced Propfan (LAP) performance,  
acoustic and weight estimation, January, 1984  
[NASA-CR-174782] p 9 N85-22368  
Wind tunnel results of advanced high speed propellers  
in the takeoff, climb and landing operating regimes  
[NASA-TM-87054] p 9 N85-29925

**PROPELLERS**

Modelling of wind tunnel wall effects on the radiation  
characteristics of acoustic sources  
[AIAA PAPER 84-2364] p 174 A85-16104  
Inviscid analysis of advanced turboprop propeller flow  
fields  
[AIAA PAPER 85-1263] p 6 A85-43977  
Wind tunnel results of advanced high speed propellers  
in the takeoff, climb, and landing operating regimes  
[AIAA PAPER 85-1259] p 6 A85-47025  
Further comparison of wind tunnel and airplane acoustic  
data for advanced design high speed propeller models  
[NASA-TM-86935] p 176 N85-22108  
Wind tunnel results of advanced high speed propellers  
in the takeoff, climb and landing operating regimes  
[NASA-TM-87054] p 9 N85-29925

**PROPULSION**

Energy efficient engine. Volume 1: Component  
development and integration program  
[NASA-CR-173084] p 22 N85-10992  
Future directions in aeropropulsion technology  
[NASA-TM-87010] p 1 N85-23685  
Heat transfer in aeropropulsion systems  
[NASA-TM-87066] p 119 N85-31444  
Status of advanced orbital transfer propulsion  
[NASA-TM-87069] p 52 N85-35225

**PROPULSION SYSTEM CONFIGURATIONS**

The energetics of hydrogen atom recombination -  
Analysis, experiments, and modeling --- in electrothermal  
propulsion system p 179 A85-16444  
Aerodynamic effect of combustor inlet air pressure on  
fuel jet atomization p 109 A85-27096  
Review - Computational methods for internal flows with  
emphasis on turbomachinery p 4 A85-29126  
Main propulsion system design recommendations for an  
advanced Orbit Transfer Vehicle  
[AIAA PAPER 85-1336] p 36 A85-39730  
Future fundamental combustion research for  
aeropropulsion systems  
[AIAA PAPER 85-1398] p 16 A85-42671  
Space station propulsion options  
[AIAA PAPER 85-1155] p 45 A85-43975  
Investigation of a pulsed electrothermal thruster  
system  
[NASA-CR-174768] p 46 N85-11132  
OTV Propulsion Issues  
[NASA-CP-2347] p 37 N85-16989  
Manrating orbital transfer vehicle propulsion  
[NASA-TM-87019] p 50 N85-25385  
Future fundamental combustion research for  
aeropropulsion systems  
[NASA-TM-87049] p 30 N85-27870

**PROPULSION SYSTEM PERFORMANCE**

IAPS (8-cm) ion thruster cyclic endurance test --- Ion  
Auxiliary Propulsion System p 42 A85-16406  
Ion propulsion for communications satellites  
p 42 A85-16412  
Ring-cusp ion thrusters p 42 A85-16438

Experiments with a microwave electrothermal thruster  
concept p 42 A85-16441  
Aerodynamic effect of combustor inlet air pressure on  
fuel jet atomization p 109 A85-27096  
Development of a large insert gas ion thruster  
p 45 A85-42922

An evaluation of oxygen/hydrogen propulsion systems  
for the Space Station  
[AIAA PAPER 85-1156] p 45 A85-43976  
Results of electric-vehicle propulsion system  
performance on three lead-acid battery systems  
p 156 A85-45443

Energy efficient engine component development and  
integration program  
[NASA-CR-169496] p 22 N85-10989  
Investigation of a pulsed electrothermal thruster  
system  
[NASA-CR-174768] p 46 N85-11132

The Altitude Wind Tunnel (AWT): A unique facility for  
propulsion system and adverse weather testing  
[NASA-TM-86921] p 35 N85-18067  
Performance and surge limits of a TF30-P-3 turbofan  
engine/axisymmetric mixed-compression inlet propulsion  
system at Mach 2.5  
[NASA-TP-2461] p 27 N85-25261  
Error reduction program --- combustor performance  
evaluation codes  
[NASA-CR-174776] p 172 N85-27584

An evaluation of oxygen-hydrogen propulsion systems  
for the Space Station  
[NASA-TM-87059] p 52 N85-28971  
Energy efficient engine integrated core/low spool test  
hardware design report  
[NASA-CR-168137] p 31 N85-29956

**PROPULSIVE EFFICIENCY**

Inert gas test of two 12-cm magnetostatic thrusters  
p 43 A85-29310  
Manrating orbital transfer vehicle propulsion  
[NASA-TM-87019] p 50 N85-25385

**PROPYLENE**

High temperature oxidation of propene  
p 61 A85-33570

**PROSTHETIC DEVICES**

Friction and wear properties of a Charnley artificial hip  
joint  
[ASLE PREPRINT 84-LC-4A-4] p 168 A85-38444

**PROTECTIVE COATINGS**

Oxidation-based model for thermal barrier coating life  
p 78 A85-10310  
Performance of thermal barrier coatings in high heat  
flux environments p 79 A85-19087  
Microstructural development of protective Al<sub>2</sub>O<sub>3</sub>  
scales p 80 A85-21650  
Cyclic oxidation behavior of beta+gamma overlay  
coatings on gamma and gamma+gamma-prime alloys  
p 68 A85-32431  
Development of coated single-crystal superalloy  
systems for gas turbine applications p 68 A85-32440  
Properties of coated and modified surfaces  
p 53 A85-36694  
Dopant effect of yttrium and the growth and adherence  
of alumina on nickel-aluminum alloys p 82 A85-40973  
Surface protection overview p 21 N85-10978  
Energy efficient engine high pressure turbine ceramic  
shroud support technology report  
[NASA-CR-168036] p 23 N85-10996  
Experimental and analytical study of ceramic-coated  
turbine-tip shroud seals for small turbine engines  
[NASA-TM-86881] p 25 N85-18057  
Effects of MAR-M247 substrate (modified) composition  
on coating oxidation coating/substrate interdiffusion ---  
protective coatings for hot section components of gas  
turbine engines  
[NASA-CR-174851] p 73 N85-19073  
Effects of surface chemistry on hot corrosion life  
[NASA-CR-174915] p 28 N85-26711  
Ion beam sputter-deposited thin film coatings for  
protection of spacecraft polymers in low Earth orbit  
[NASA-TM-87051] p 91 N85-30137  
Mechanical protection of DLC films on fused silica  
slides  
[NASA-TM-87056] p 91 N85-30138  
Diamondlike carbon protective coatings for IR  
materials  
[NASA-TM-87083] p 178 N85-34631

**PROTON IRRADIATION**

Effects of 1 MeV electrons and 10 MeV protons on the  
performance and reflectance of thin BSR cells --- back  
surface reflector p 182 A85-35699

**PULLEYS**

Feasibility demonstration of a novel, flat-belt,  
continuously variable transmission or automotive and  
electric-hybrid vehicle application  
[NASA-CR-174430] p 185 N85-19894

**PULSED JET ENGINES**

Investigation of a pulsed electrothermal thruster  
system  
[NASA-CR-174768] p 46 N85-11132

**PULSED LASERS**

Laser balancing system for high material removal  
rates  
[NASA-CR-174731] p 126 N85-12341

**PUMPS**

Operational performance of the photovoltaic-powered  
grain mill and water pump at Tangaye, Burkina Faso  
(formerly Upper Volta)  
[NASA-TM-86970] p 161 N85-23243

**PYROELECTRICITY**

Pyroelectric conversion in space p 45 A85-45377

**PYROLYSIS**

Shock tube study of the fuel structure effects on the  
chemical kinetic mechanisms responsible for soot  
formation, part 2  
[NASA-CR-174880] p 63 N85-25444  
Preparation of silicon carbide-silicon nitride fibers by the  
pyrolysis of polycarbosilazane precursors  
[NASA-TM-86505] p 91 N85-28107  
Fuel-rich catalytic combustion: A soot-free technique  
for in situ hydrogen-like enrichment  
[NASA-TP-2498] p 63 N85-31244

**Q**

**QUALITY CONTROL**

Fabrication and quality assurance processes for  
superhybrid composite fan blades  
[NASA-TM-83354] p 57 N85-14882

**QUANTITATIVE ANALYSIS**

Rapid estimation of concentration of aromatic classes  
in middistillate fuels by high-performance liquid  
chromatography  
[NASA-TP-2495] p 93 N85-31307

**R**

**RADAR CROSS SECTIONS**

Numerical methods for analyzing electromagnetic  
scattering  
[NASA-CR-175507] p 99 N85-21438  
Normal modes in an overmoded circular waveguide  
coated with lossy material  
[NASA-CR-176186] p 100 N85-35320

**RADIAL FLOW**

Analysis of buoyancy effect on fully developed laminar  
heat transfer in a rotating tube p 110 A85-35596  
The three-dimensional compressible flow in a radial  
inflow turbine scroll p 6 A85-41826

**RADIANT HEATING**

Development of advanced high-temperature heat flux  
sensors. Phase 2: Verification testing  
[NASA-CR-174973] p 126 N85-35391

**RADIATION CHEMISTRY**

Fast laser-induced aerosol formation for visualization of  
gas flows p 121 A85-31113

**RADIATION DAMAGE**

Theory of the high base resistivity n(+)-pp(+) silicon  
solar cell and its application to radiation damage effects  
p 154 A85-32639  
Radiation damage and defect behavior in ion-implanted,  
lithium counterdoped silicon solar cells  
p 182 A85-35698  
Lithium counterdoped silicon solar cell  
[NASA-CASE-LEW-14177-1] p 160 N85-20535  
The effects of lithium counterdoping on radiation damage  
and annealing in n(+)-p silicon solar cells  
p 50 N85-22586

**RADIATION DISTRIBUTION**

Numerical methods for analyzing electromagnetic  
scattering  
[NASA-CR-175507] p 99 N85-21438

**RADIATION DOSAGE**

Radiation exposure and performance of multiple burn  
LEO-GEO orbit transfer trajectories  
[NASA-TM-86946] p 36 N85-21228

**RADIATION EFFECTS**

Effects of 1 MeV electrons and 10 MeV protons on the  
performance and reflectance of thin BSR cells --- back  
surface reflector p 182 A85-35699

**RADIATION MEASUREMENT**

Flame radiation and linear heat transfer in a tubular-can  
combustor p 15 A85-39580  
Combustion system for radiation investigations  
p 21 N85-10986

**RADIATION SHIELDING**

Applicability of 100kWe-class of space reactor power  
systems to NASA manned space station missions  
[NASA-CR-174696] p 177 N85-35728



- RADIATION TOLERANCE**  
Lithium counterdoped silicon solar cell  
[NASA-CASE-LEW-14177-1] p 160 N85-20535
- RADIATIVE HEAT TRANSFER**  
Methods for heat transfer and temperature field analysis of the insulated diesel  
[NASA-CR-174783] p 185 N85-16699  
Performance analysis of radiation cooled dc transmission lines for high power space systems  
[NASA-TM-87040] p 104 N85-28222
- RADICALS**  
Ideal gas thermodynamic properties for the phenyl, phenoxy, and o-biphenyl radicals  
[NASA-TM-83800] p 184 N85-22204
- RADII**  
Automatic sphericity interferometer for testing lens radii  
[AD-A155736] p 125 N85-33457
- RADIO FREQUENCIES**  
Precision tunable resonant microwave cavity  
[NASA-CASE-LEW-13935-1] p 103 N85-20248  
Automated testing of developmental satellite communications systems and subsystems  
[NASA-TM-87070] p 100 N85-31348
- RADIO FREQUENCY DISCHARGE**  
Deposition of silicon nitride from SiCl<sub>4</sub> and NH<sub>3</sub> in a low pressure RF plasma  
p 81 A85-36229  
Dielectric properties of 'diamondlike' carbon prepared by RF plasma deposition  
p 182 A85-38192  
Experimental performance of a microwave cavity plasma disk ion source  
p 179 A85-43552
- RADIO FREQUENCY HEATING**  
High frequency plasma generator for ion thrusters  
[NASA-CR-174772] p 48 N85-17023
- RADIO FREQUENCY INTERFERENCE**  
Adaptive antenna arrays for satellite communications: Design and testing  
[NASA-CR-176162] p 100 N85-34329
- RADIOGRAPHY**  
Radiographic detectability limits for seeded voids in sintered silicon carbide and silicon nitride  
[NASA-TM-86945] p 138 N85-21674
- RADIOMETERS**  
Liquid fuel spray processes in high-pressure gas flow  
[NASA-TM-86944] p 115 N85-21570  
Development of advanced high-temperature heat flux sensors. Phase 2: Verification testing  
[NASA-CR-174973] p 126 N85-35391
- RAILGUN ACCELERATORS**  
Friction in rail guns  
p 101 A85-16424  
Preliminary analysis of space mission applications for electromagnetic launchers  
[NASA-CR-174067] p 35 N85-12071  
Rail accelerator technology and applications  
[NASA-TM-86947] p 48 N85-21258  
Arc-driven rail gun research  
[NASA-CR-174816] p 132 N85-21662
- RAMAN SPECTROSCOPY**  
Raman structural studies of the nickel electrode  
[NASA-CR-175619] p 183 N85-23414
- RANDOM NOISE**  
A high-speed implementation of the random decrement algorithm  
p 94 A85-29556
- RANDOM VIBRATION**  
Oscillator response to nonstationary excitation  
[ASME PAPER 84-WA/APM-38] p 140 A85-17039
- RANDOM WALK**  
Monte Carlo lattice models for adsorbed polymer conformation  
[NASA-TP-2453] p 183 N85-24961
- RANKINE CYCLE**  
Overview of waste heat utilization systems  
[NASA-TM-86901] p 184 N85-13692  
Dynamic power systems for power generation  
p 158 N85-13892  
Comparative evaluation of three alternative power cycles for waste heat recovery from the exhaust of adiabatic diesel engines  
[NASA-TM-86953] p 186 N85-32043
- RAPID QUENCHING (METALLURGY)**  
Rapid solidification and dynamic compaction of Ni-base superalloy powders  
p 67 A85-32414  
Rapidly solidified NiAl and FeAl  
[NASA-TM-86941] p 74 N85-20042
- RARE EARTH COMPOUNDS**  
Strength and microstructure of sintered Si<sub>3</sub>N<sub>4</sub> with rare-earth-oxide additions  
[ACS PAPER 130-13-84] p 80 A85-25271  
Oxidation of silicon nitride sintered with rare-earth oxide additions  
p 83 A85-42798
- RARE GASES**  
Inert gas test of two 12-cm magnetostatic thrusters  
p 43 A85-29310  
Development of a large insert gas ion thruster  
p 45 A85-42922
- Heaterless ignition of inert gas ion thruster hollow cathodes  
[NASA-TM-87086] p 52 N85-34177
- RATIONAL FUNCTIONS**  
Axisymmetric solid elements by a rational hybrid stress method  
p 143 A85-41109
- REACTION BONDING**  
Effect of hot isostatic pressing on reaction-bonded silicon nitride  
p 79 A85-15195  
Microstructure of reaction-bonded silicon nitride consolidated by isostatic hot-pressing  
p 83 A85-45304  
Radiographic detectability limits for seeded voids in sintered silicon carbide and silicon nitride  
[NASA-TM-86945] p 138 N85-21674
- REACTION KINETICS**  
Moderate temperature sodium cells. V - Discharge reactions and rechargeability of NiS and NiS<sub>2</sub> positive electrodes in molten NaAlCl<sub>4</sub>  
p 59 A85-11892  
Systematic optimization of a detailed kinetic model using a methane ignition example  
p 59 A85-12890  
Integrating chemical kinetic rate equations by selective use of stiff and nonstiff methods  
[AIAA PAPER 85-0237] p 60 A85-19607  
Chemical reactions involved in the initiation of hot corrosion of IN-738  
p 66 A85-31688  
Polarization (ellipsometric) measurements of liquid condensate deposition and evaporation rates and dew points in flowing salt/ash-containing combustion gases  
p 123 A85-46925  
Comparison of numerical techniques for integration of stiff ordinary differential equations arising in combustion chemistry  
[NASA-TP-2372] p 17 N85-10065  
CREKID: A computer code for transient, gas-phase combustion of kinetics  
[NASA-TM-83806] p 17 N85-10068  
New integration techniques for chemical kinetic rate equations. 2: Accuracy comparison  
[NASA-TM-86893] p 23 N85-13798  
Integrating chemical kinetic rate equations by selective use of stiff and nonstiff methods  
[NASA-TM-86923] p 24 N85-15726  
A study of interdiffusion in beta + gamma/gamma + gamma prime Ni-Cr-Al  
[NASA-CR-174852] p 74 N85-20041  
A comparison of the efficiency of numerical methods for integrating chemical kinetic rate equations  
[NASA-TM-83590] p 25 N85-21162
- READOUT**  
Electronic heterodyne readout of fringes in moire deflectometry  
p 122 A85-36726
- REAL TIME OPERATION**  
Moving target, distributed, real-time simulation using Ada  
p 170 A85-34131  
A generalized computer code for developing dynamic gas turbine engine models (DIGTEM)  
p 17 A85-49021  
Hardware for a real-time multiprocessor simulator  
[NASA-TM-83805] p 169 N85-10659  
Operating system for a real-time multiprocessor propulsion system simulator. User's manual  
[NASA-TP-2426] p 171 N85-17596  
Real-Time Multiprocessor Programming Language (RTMPL) user's manual  
[NASA-TP-2422] p 170 N85-28610
- RECIRCULATIVE FLUID FLOW**  
Calculation of confined swirling flows  
[AIAA PAPER 85-0060] p 108 A85-19491  
Confined turbulent swirling recirculating flow predictions  
[NASA-CR-174917] p 29 N85-26716
- RECRYSTALLIZATION**  
Rapid solidification and dynamic compaction of Ni-base superalloy powders  
p 67 A85-32414
- RECTANGLES**  
Elastohydrodynamic lubrication of line contacts  
p 126 A85-11069
- RECTANGULAR PANELS**  
Noise transmission loss of a rectangular plate in an infinite baffle  
[NASA-TP-2398] p 176 N85-22109
- RECTANGULAR PLATES**  
Vibrations of twisted cantilevered plates - Summary of previous and current studies  
p 140 A85-22069
- RECTANGULAR WAVEGUIDES**  
Plot of modal field distribution in rectangular and circular waveguides  
p 101 A85-25170
- RECTENNAS**  
Technology for satellite power conversion  
[NASA-CR-174335] p 159 N85-18451
- REDOX CELLS**  
Chemical and electrochemical behavior of the Cr(III)/Cr(II) half-cell in the iron-chromium redox energy storage system  
p 61 A85-33785
- Cycling performance of the iron-chromium redox energy storage system  
[NASA-TM-87034] p 162 N85-27387  
Evaluation of developmental membranes for the mixed reactant iron-chromium redox system  
[NASA-TM-87074] p 164 N85-34443  
Development of electrodes for the NASA iron/chromium  
[NASA-CR-174724] p 165 N85-35471
- REDUCED GRAVITY**  
Free-surface phenomena under low- and zero-gravity conditions  
[NASA-CR-175885] p 36 N85-27922
- REDUCTION**  
Life and reliability modeling of bevel gear reductions  
[NASA-TM-87006] p 133 N85-27227
- REDUCTION (CHEMISTRY)**  
Electrocatalysis of fuel cell reactions: Investigation of alternate electrolytes  
[NASA-CR-174753] p 157 N85-11455  
Effect of water on hydrogen permeability --- Stirling engines  
[NASA-TM-86904] p 53 N85-14864
- REDUNDANCY**  
Sensor failure detection for jet engines using analytical redundancy  
[AIAA PAPER 84-1452] p 13 A85-16097
- REFINING**  
Jet fuel property changes and their effect on producibility and cost in the U.S., Canada, and Europe  
[NASA-CR-174840] p 93 N85-27012
- REFLECTANCE**  
Nitriding of titanium and its alloys by N<sub>2</sub>, NH<sub>3</sub> or mixtures of N<sub>2</sub> + H<sub>2</sub> in a dc arc plasma at low pressures (or = to torr)  
[NASA-TM-83803] p 131 N85-15168
- REFLECTION**  
Preliminary design of a 10 kW thermophotovoltaic system for space applications  
p 45 A85-45371
- REFRACTIVITY**  
A comparison of electronic heterodyne moire deflectometry and electronic heterodyne holographic interferometry for flow measurements  
[NASA-TM-87071] p 125 N85-32302  
The use of a laser Doppler velocimeter in a standard flammability tube  
[NASA-CR-174960] p 125 N85-35389
- REFRACTORY COATINGS**  
Thermal barrier coating system  
[NASA-CASE-LEW-13324-2] p 57 N85-21266
- REFRACTORY MATERIALS**  
Milling of Si<sub>3</sub>N<sub>4</sub> with Si<sub>3</sub>N<sub>4</sub> hardware  
[NASA-TM-86864] p 84 N85-10191  
Nonlinear analysis for high-temperature multilayered fiber composite structures --- turbine blades  
[NASA-TM-83754] p 57 N85-21273  
Viscoplastic constitutive relationships with dependence on thermomechanical history.  
[NASA-CR-174836] p 146 N85-21691  
Convolute nozzle design for the RL10 derivative 2B engine  
[NASA-CR-174953] p 32 N85-29965
- REFRACTORY METAL ALLOYS**  
Application of two creep fatigue life models for the prediction of elevated temperature crack initiation of a nickel base alloy  
[AIAA PAPER 85-1420] p 69 A85-43979
- REFRACTORY METALS**  
High temperature metal and ceramic composites  
p 55 A85-37483
- REGENERATION (ENGINEERING)**  
Initial results of sensitivity tests - Performed on the RE-1000 free-piston Stirling engine  
p 129 A85-45466
- REGENERATIVE FUEL CELLS**  
Design considerations for a 10-kW integrated hydrogen-oxygen regenerative fuel cell system  
p 155 A85-45380  
Regenerative fuel cell energy storage system for a low Earth orbit space station  
[NASA-CR-174802] p 158 N85-13371  
Engineering model system study for a regenerative fuel cell: Study report  
[NASA-CR-174801] p 158 N85-16292  
Develop and test fuel cell powered on-site integrated total energy systems. Phase 3: Full-scale power plant development  
[NASA-CR-168338] p 164 N85-30483  
Regenerative fuel cell systems for space station  
p 104 N85-31372  
System level electrochemical principles  
p 104 N85-31375
- REGIONAL PLANNING**  
Development and use of the computer software package for planning the 12 GHz broadcasting-satellite service at RARC '83  
p 96 A85-29605

**REGRESSION ANALYSIS**

The effects of seven alloying elements on the microstructure and stress-rupture behavior of nickel-base superalloys  
[NASA-TM-83791] p 70 N85-10168

Thermal traction contact performance evaluation under fully flooded and starved conditions  
[NASA-CR-168173] p 132 N85-25848

A multiple linear regression analysis of hot corrosion attack on a series of nickel base turbine alloys  
[NASA-TM-87020] p 77 N85-31284

**REINFORCING FIBERS**

Fibers for structurally reliable metal and ceramic composites p 55 A85-37484

High performance fibers for structurally reliable metal and ceramic composites --- advanced gas turbine engine materials

[NASA-TM-86878] p 56 N85-12095

Preparation of silicon carbide-silicon nitride fibers by the pyrolysis of polycarbosilazane precursors

[NASA-TM-86505] p 91 N85-28107

**REISSNER THEORY**

Rational approach for assumed stress finite elements  
p 139 A85-12029

On the existence and stability conditions for mixed-hybrid finite element solutions based on Reissner's variational principle p 142 A85-33847

**RELIABILITY**

The 30 GHz solid state amplifier for low cost low data rate ground terminals  
[NASA-CR-174795] p 102 N85-12300

Life and reliability modeling of bevel gear reductions  
[NASA-TM-87006] p 133 N85-27227

**RELIABILITY ANALYSIS**

Fatigue criterion to system design, life and reliability  
[AIAA PAPER 85-1140] p 143 A85-40814

Reliability considerations for the total strain range version of strainrange partitioning

[NASA-CR-174757] p 144 N85-11380

Improved models for increasing wind penetration, economics and operating reliability

[NASA-CR-175538] p 160 N85-20545

Fatigue criterion to system design, life and reliability  
[NASA-TM-87017] p 132 N85-27226

**REMOTE CONTROL**

Advanced in solid state switchgear technology for large space power systems p 102 A85-45362

**REMOTE SENSORS**

Fiber optic temperature sensor p 121 A85-29563

Remote displacement measurement using a passive interferometer with a fiber-optic link p 122 A85-42857

**RENE 95**

The effect of microstructure, temperature, and hold-time on low-cycle fatigue of As HIP P/M Rene 95 p 67 A85-32399

The influence of hold times on LCF and FCG behavior in a P/M Ni-base superalloy --- Low Cycle Fatigue/Fatigue Crack Growth p 67 A85-32400

**REPORTS**

Research and technology highlights of the Lewis Research Center  
[NASA-TM-86899] p 186 N85-17928

**RESEARCH**

Bibliography of Lewis Research Center technical publications announced in 1983  
[NASA-TM-83693] p 184 N85-22255

**RESEARCH AND DEVELOPMENT**

The role of modern control theory in the design of controls for aircraft turbine engines p 13 A85-13627

Recent work on a microwave ion source p 179 A85-16455

Environmentally-induced voltage limitations in large space power systems p 43 A85-18584

High temperature metal and ceramic composites p 55 A85-37483

The trend of future gas turbine technology p 16 A85-41778

Development of a large insert gas ion thruster p 45 A85-42922

Research and technology highlights of the Lewis Research Center  
[NASA-TM-86899] p 186 N85-17928

Bibliography of Lewis Research Center technical publications announced in 1984  
[NASA-TM-87012] p 184 N85-28876

**RESEARCH FACILITIES**

Research and technology highlights of the Lewis Research Center  
[NASA-TM-86899] p 186 N85-17928

High efficiency solar cell research for space applications p 164 N85-31624

**RESEARCH MANAGEMENT**

The NASA photovoltaic technology program p 155 A85-35604

**RESIN MATRIX COMPOSITES**

Resin selection criteria for 'tough' composite structures p 81 A85-35139

Fundamental studies of composite toughness p 56 N85-12948

**RESINS**

Resin selection criteria for 'tough' composite structures p 81 A85-35139

**RESISTANCE THERMOMETERS**

High temperature static strain sensor development program p 19 N85-10959

**RESISTOJET ENGINES**

Space Station propulsion - The Advanced Development Program at Lewis

[AIAA PAPER 85-1154] p 44 A85-39626

Performance characterization tests of a 1-kW resistojet using hydrogen, nitrogen and ammonia as propellants

[AIAA PAPER 85-1159] p 44 A85-39628

An evaluation of oxygen/hydrogen propulsion systems for the Space Station

[AIAA PAPER 85-1156] p 45 A85-43976

Compatibility experiments of facilities, materials, and propellants for electrothermal thrusters

[NASA-TM-86956] p 49 N85-21260

Space station propulsion: The advanced development program at Lewis

[NASA-TM-86999] p 50 N85-25386

An evaluation of oxygen-hydrogen propulsion systems for the Space Station

[NASA-TM-87059] p 52 N85-28971

**RESONANCE**

Precision tunable resonant microwave cavity

[NASA-CASE-LEW-13935-1] p 103 N85-20248

**RESONANT FREQUENCIES**

The response of Helmholtz resonators to external excitation. I - Single resonators p 174 A85-26915

Natural frequencies of twisted rotating plates p 141 A85-32343

The use of an optical data acquisition system for bladed disk vibration analysis

[NASA-TM-86891] p 144 N85-15184

**REUSABLE HEAT SHIELDING**

Electron beam charging of Space Shuttle thermal protection system tiles p 39 N85-22478

**REUSABLE ROCKET ENGINES**

Reusable rocket engine turbopump condition monitoring

[SAE PAPER 841619] p 44 A85-39267

Structural Integrity and Durability of Reusable Space Propulsion Systems

[NASA-CP-2381] p 51 N85-27941

**REUSABLE SPACECRAFT**

Advanced research and technology programs for advanced high-pressure oxygen-hydrogen rocket propulsion

[NASA-TM-86969] p 37 N85-21231

**REVERBERATION**

Reverberation effects on directionality and response of stationary monopole and dipole sources in a wind tunnel

[NASA-TM-87063] p 119 N85-31443

**REVERSED FLOW**

Small gas turbine combustor study - Fuel injector performance in a transpiration-cooled liner

[AIAA PAPER 85-1312] p 16 A85-39717

Dilution jet configurations in a reverse flow combustor

[NASA-CR-174888] p 27 N85-22392

Small gas turbine combustor study: Fuel injector performance in a transpiration-cooled liner

[NASA-TM-86989] p 27 N85-25264

**REYNOLDS NUMBER**

A review and analysis of boundary layer transition data for turbine application

[NASA-TM-86880] p 113 N85-10306

Heat transfer in aeropropulsion systems

[NASA-TM-87066] p 119 N85-31444

**REYNOLDS STRESS**

A study of Reynolds-stress closure model

[NASA-CR-174342] p 114 N85-17324

**RHENIUM**

Compatibility experiments of facilities, materials, and propellants for electrothermal thrusters

[NASA-TM-86956] p 49 N85-21260

**RHODIUM**

Advanced thin film thermocouples

[NASA-CR-175541] p 124 N85-21607

**RIGGING**

Behavior of the lean methane-air flame at zero-gravity

[NASA-CR-175586] p 62 N85-21283

**RITZ AVERAGING METHOD**

A study of internal and distributed damping for vibrating turbomachine blades

[NASA-CR-175901] p 30 N85-27868

**RL-10 ENGINES**

Convolute nozzle design for the RL10 derivative 2B engine

[NASA-CR-174953] p 32 N85-29965

**ROBOTICS**

Investigation on experimental techniques to detect, locate and quantify gear noise in helicopter transmissions

[NASA-CR-38471] p 176 N85-17667

**ROBUSTNESS (MATHEMATICS)**

A design methodology for robust failure detection and isolation p 171 A85-47794

**ROCKET ENGINE DESIGN**

Electrothermal thruster diagnostics p 42 A85-16440

The energetics of hydrogen atom recombination - Analysis, experiments, and modeling --- in electrothermal propulsion system p 179 A85-16444

Simplified design and life prediction of rocket thrust chambers p 44 A85-29314

Reusable rocket engine turbopump condition monitoring

[SAE PAPER 841619] p 44 A85-39267

Progress report - Advanced cryogenic OTV engine technology

[AIAA PAPER 85-1341] p 44 A85-39735

Development of a large insert gas ion thruster p 45 A85-42922

Design and analysis report for the RL10-2B breadboard low thrust engine

[NASA-CR-174857] p 48 N85-19020

**ROCKET ENGINES**

Electrothermal thruster diagnostics p 42 A85-16440

Small centrifugal pumps for low thrust rockets

[AIAA PAPER 85-1302] p 45 A85-43978

Characterization of 8-cm engineering model thruster

[NASA-CR-174673] p 46 N85-11131

Design and analysis report for the RL10-2B breadboard low thrust engine

[NASA-CR-174857] p 48 N85-19020

Ring-cusp ion thruster with shell anode

[NASA-CASE-LEW-13881-1] p 48 N85-21256

**ROCKET EXHAUST**

Effects of chemical releases by the STS 3 orbiter on the ionosphere p 166 A85-29538

**ROCKET THRUST**

Heaterless ignition of inert gas ion thruster hollow cathodes

[NASA-TM-87086] p 52 N85-34177

**ROLLER BEARINGS**

Fast numerical calculations of EHD sliding traction forces

Application to rolling bearings

[ASME PAPER 84-TRIB-26] p 127 A85-21289

Effect of two inner-ring oil-flow distribution schemes on the operating characteristics of a 35 millimeter bore ball bearing to 2.5 million DN

[NASA-TP-2404] p 130 N85-13233

Lubrication and performance of high-speed rolling-element bearings

[NASA-TM-86958] p 131 N85-21658

Effect of speed and press fit on fatigue life of roller-bearing inner-race contact

[NASA-TP-2496] p 134 N85-31511

Elastohydrodynamic lubrication calculations used as a tool to study scuffing

[NASA-TM-87097] p 137 N85-34408

Design and lubrication of high-speed rolling-element bearings

[NASA-TM-87107] p 137 N85-34409

Planetary-gear-support bearing test rig design

[NASA-CR-174927] p 12 N85-35185

**ROLLING**

Hydrodynamic lubrication of rigid nonconformal contacts in combined rolling and normal motion

[ASME PAPER 84-TRIB-13] p 127 A85-21280

**ROLLING CONTACT LOADS**

Hydrodynamic lubrication of rigid nonconformal contacts in combined rolling and normal motion

[ASME PAPER 84-TRIB-13] p 127 A85-21280

Fast numerical calculations of EHD sliding traction forces

Application to rolling bearings

[ASME PAPER 84-TRIB-26] p 127 A85-21289

Pantographing self adaptive gap elements

p 142 A85-37440

Effect of speed and press fit on fatigue life of roller-bearing inner-race contact

[NASA-TP-2496] p 134 N85-31511

Rolling, slip and traction measurements on low modulus materials

[NASA-CR-174909] p 135 N85-33491

**ROOT-MEAN-SQUARE ERRORS**

Comparative analysis of operational forecasts versus actual weather conditions in airline flight planning, volume 3

[NASA-CR-167864] p 167 N85-35536

**ROTARY ENGINES**

Stratified charge rotary aircraft engine technology enablement program

[NASA-CR-174812] p 25 N85-21163

**ROTARY STABILITY**

- The effect of aerodynamic and structural detuning on turbomachine supersonic unstalled torsional flutter  
[AIAA PAPER 85-0761] p 14 A85-30378  
Dynamic analysis of straight and involute tooth forms  
[ASME PAPER 84-DET-226] p 128 A85-33780  
Structural response of a rotating bladed disk to rotor whirl  
[NASA-CR-175605] p 27 N85-22391

**ROTARY WINGS**

- Experimental aerodynamic characteristics of an NACA 0012 airfoil with simulated ice p 12 A85-21844  
Performance degradation of helicopter rotor in forward flight due to ice p 11 A85-42937  
Initial feasibility ground test of a proposed photogrammetric system for measuring the shapes of ice accretions on helicopter rotor blades during forward flight  
[NASA-TM-87391] p 12 N85-12887

**ROTATING BODIES**

- Effects of warping and pretwist on torsional vibration of rotating beams  
[ASME PAPER 84-WA/APM-41] p 140 A85-17040  
Finite difference analysis of torsional vibrations of pretwisted, rotating, cantilever beams with effects of warping p 143 A85-42047

**ROTATING CYLINDERS**

- Computation and turbulence closure models for shear flows in rotating curved bodies p 107 A85-14349  
Convective influence on the stability of a cylindrical solid-liquid interface p 109 A85-26911  
Analysis of buoyancy effect on fully developed laminar heat transfer in a rotating tube p 110 A85-35596

**ROTATING DISKS**

- Vibration and flutter of mistuned bladed-disk assemblies  
[AIAA PAPER 84-0991] p 139 A85-16095

**ROTATING FLUIDS**

- Computation and turbulence closure models for shear flows in rotating curved bodies p 107 A85-14349

**ROTATING SHAFTS**

- Rotordynamic coefficients for compressible flow in tapered annular seals p 129 A85-42573  
Analysis of experimental shaft seal data for high-performance turbomachines, as for Space Shuttle main engines  
[NASA-TM-86928] p 115 N85-21569  
Variable force, eddy-current or magnetic damper  
[NASA-CASE-LEW-13717-1] p 134 N85-30333

**ROTATING STALLS**

- Stall recovery control strategy methodology and results  
[AIAA PAPER 85-1433] p 16 A85-40841  
A theory of post-stall transients in multistage axial compression systems  
[NASA-CR-3878] p 8 N85-21117

**ROTATION**

- Linearization of digital derived rate algorithm for use in linear stability analysis  
[NASA-TM-87000] p 41 N85-23904

**ROTOR AERODYNAMICS**

- Flutter and forced response of mistuned rotors using standing wave analysis p 139 A85-12721  
Effects of friction dampers on aerodynamically unstable rotor stages p 14 A85-21866  
The UH-1H helicopter icing flight test program - An overview  
[AIAA PAPER 85-0338] p 11 A85-28898  
Investigation of flow phenomena in a transonic fan rotor using laser anemometry  
[ASME PAPER 84-GT-199] p 4 A85-32963  
Rotordynamic Instability Problems in High-Performance Turbomachinery  
[NASA-CP-2338] p 131 N85-14116  
The UH-1H helicopter icing flight test program: An overview  
[NASA-TM-86925] p 11 N85-15702  
Operating characteristics of a 0.87 kW-hr flywheel energy storage module  
[NASA-TM-87038] p 133 N85-28371  
Vibration control of rotor shaft  
[NASA-TM-87053] p 133 N85-29292

**ROTOR BLADES**

- Noise produced by the interaction of a rotor wake with a swept stator blade  
[AIAA PAPER 84-2326] p 173 A85-13956  
An experimental investigation and numerical prediction of thermomechanical phenomena in high speed rotor tip rubbing p 14 A85-25442  
Turbofan noise generation. Volume 2: Computer programs  
[NASA-CR-167952] p 175 N85-11791

**ROTOR BLADES (TURBOMACHINERY)**

- Acoustic pressures emanating from a turbomachine stage  
[AIAA PAPER 84-2325] p 2 A85-10870

- Review - Computational methods for internal flows with emphasis on turbomachinery p 4 A85-29126  
Natural frequencies of twisted rotating plates p 141 A85-32343  
Calculation of three-dimensional, viscous flow through turbomachinery blade passages by parabolic marching  
[AIAA PAPER 85-1408] p 5 A85-39767  
A three-dimensional boundary-layer analysis including heat-transfer and blade-rotation effects p 6 A85-42988

- Coolant passage heat transfer with rotation p 20 N85-10968  
Structural analysis p 20 N85-10969  
Incompressible lifting-surface aerodynamics for a rotor-stator combination p 7 N85-12039  
[NASA-TM-83767]  
Structural response of a rotating bladed disk to rotor whirl  
[NASA-CR-175605] p 27 N85-22391

- Calculation of three-dimensional, viscous flow through turbomachinery blade passages by parabolic marching  
[NASA-TM-86984] p 9 N85-23711  
Vibration and buckling of rotating, pretwisted, preonced beams including Coriolis effects p 146 N85-25893  
[NASA-TM-87004]  
Development of a rotor wake-vortex model, volume 1  
[NASA-CR-174849] p 9 N85-26668  
Aerodynamic detuning analysis of an unstalled supersonic turbofan cascade p 9 N85-26670  
[NASA-TM-87001]  
Ice shapes and the resulting drag increase for a NACA 0012 airfoil p 11 N85-27839  
[NASA-TM-83556]  
Reflection plane tests of a wind turbine blade tip section with ailerons p 165 N85-34444  
[NASA-TM-87018]

**ROTOR SPEED**

- Shutdown characteristics of the Mod-O wind turbine with aileron controls  
[NASA-TM-86918] p 159 N85-16299  
Development of a rotor wake-vortex model, volume 1  
[NASA-CR-174849] p 9 N85-26668

**ROTORS**

- Aileron controls for wind turbine applications p 157 A85-45513  
Aileron controls for wind turbine applications  
[NASA-TM-86867] p 158 N85-11458  
Laser balancing system for high material removal rates  
[NASA-CR-174731] p 126 N85-12341  
The use of an optical data acquisition system for bladed disk vibration analysis  
[NASA-TM-86891] p 144 N85-15184  
Reusable rocket engine turbopump condition monitoring p 51 N85-26907

**RUNGE-KUTTA METHOD**

- Recent advances in methods for numerical solution of O.D.E. initial value problems p 171 A85-21370  
Application of Runge Kutta time marching scheme for the computation of transonic flows in turbomachines  
[AIAA PAPER 85-1332] p 5 A85-39728

**RUPTURING**

- A continuous damage model based on stepwise-stress creep rupture tests  
[NASA-CR-174941] p 152 N85-32341

**S**

**S MATRIX THEORY**

- Circular waveguide bifurcation for asymmetric modes p 101 A85-20170

**SALTS**

- Airfoil deposition model p 21 N85-10979

**SAPPHIRE**

- Incident beam polarization for laser Doppler velocimetry employing a sapphire cylindrical window p 122 A85-39835  
Incident beam polarization for laser Doppler velocimetry employing a sapphire cylindrical window  
[NASA-TM-87064] p 178 N85-28786

**SATELLITE ANTENNAS**

- Status of NASA's multibeam communications technology program p 100 A85-14432  
Advanced 30/20 GHz multiple beam antenna for future communications satellites p 96 A85-14436  
Technical characteristics of the broadcasting satellite plan at 12 GHz for the Western Hemisphere p 96 A85-28233  
On the calculation of the directivity of planar array feeds for satellite reflector applications p 97 A85-32249  
Configuration study for a 30 GHz monolithic receive array, volume 2  
[NASA-CR-174697-VOL-2] p 99 N85-18240  
Alternatives for satellite sound broadcast systems at HF and VHF p 99 N85-23815

**SATELLITE NETWORKS**

- A frequency-routed satellite system concept using multiple orthogonally-polarized beams for frequency reuse p 97 A85-34470  
Modeling of NASA's 30/20 GHz satellite communications system p 38 A85-36663  
Demand for satellite-provided domestic communications services up to the year 2000  
[NASA-TM-86894] p 97 N85-15099

**SATELLITE ORBITS**

- Engineering calculations for communications satellite systems planning  
[NASA-CR-175552] p 37 N85-21233

**SATELLITE TELEVISION**

- On the subjective evaluation of the interference protection ratios' measurements for co-channel FM-TV signals p 96 A85-28241  
Experimental results supporting the determination of service quality objectives for DBS systems p 96 A85-29611

**SATELLITE TEMPERATURE**

- Interdisciplinary design analysis of a precision spacecraft antenna  
[AIAA PAPER 85-0804] p 38 A85-30303

**SATELLITE TRANSMISSION**

- Adaptive antenna arrays for satellite communications: Design and testing  
[NASA-CR-176162] p 100 N85-34329

**SCALE (CORROSION)**

- Cavitation erosion size scale effects p 65 A85-11935  
Microstructural development of protective Al<sub>2</sub>O<sub>3</sub> scales p 80 A85-21650

**SCALE MODELS**

- Comparison of scaled model data to full size energy efficient engine test results  
[AIAA PAPER 84-2281] p 13 A85-13953

**SCALING**

- Universal binding energy relations in metallic adhesion  
[NASA-TM-86889] p 72 N85-12132

**SCHLIEREN PHOTOGRAPHY**

- Rainbow schlieren vs Mach-Zehnder interferometer - A comparison p 121 A85-28820

**SCHOTTKY DIODES**

- Effect of barrier height on friction behavior of the semiconductors silicon and gallium arsenide in contact with pure metals  
[NASA-TP-2405] p 84 N85-13044

**SCINTILLATION**

- Unsteady pressure measurements on a biconvex airfoil in a transonic oscillating cascade  
[NASA-TM-86914] p 8 N85-15689

**SCREENS**

- Flow through very porous inclined screens  
[AIAA PAPER 85-1650] p 111 A85-40750  
Flow through very porous inclined screens  
[NASA-TM-86979] p 116 N85-25761

**SEALS (STOPPERS)**

- Metallurgical and mechanical phenomena due to rubbing of titanium against sintered powder Nichrome p 127 A85-22281  
An experimental investigation and numerical prediction of thermomechanical phenomena in high speed rotor tip rubbing p 14 A85-25442  
A comparison of flow rates and pressure profiles for N-sequential inlets and three related seal configurations p 109 A85-26526  
High-temperature erosion of plasma-sprayed, yttria-stabilized zirconia in a simulated turbine environment  
[AIAA PAPER 85-1219] p 82 A85-39662  
Rotordynamic coefficients for compressible flow in tapered annular seals p 129 A85-42573  
High-temperature erosion of plasma-sprayed, yttria-stabilized zirconia in a simulated turbine environment  
[NASA-TP-2406] p 84 N85-13045  
Experimental study of ceramic coated tip seals for turbojet engines  
[NASA-TM-86939] p 114 N85-19363  
Ribbon burner simulation of T-700 turbine shroud for ceramic lined seals research  
[NASA-TM-86940] p 114 N85-19364  
Variable friction secondary seal for face seals  
[NASA-CASE-LEW-14170-1] p 131 N85-20377  
Sliding seal materials for adiabatic engines  
[NASA-CR-174893] p 89 N85-22757  
Experimental stiffness of tapered bore seals  
[NASA-TM-86978] p 132 N85-25847  
Tape casting as an approach to an all-ceramic turbine shroud seal  
[NASA-TM-87078] p 135 N85-32333  
Oxidizing seal for a turbine tip gas path  
[NASA-CASE-LEW-14053-1] p 136 N85-34402

- Thermal stress analysis of a new turbine shroud seal concept  
[NASA-TM-87082] p 136 N85-34406
- SECONDARY EMISSION**  
Numerical simulation of positive-potential conductors in the presence of a plasma and a secondary-emitting dielectric p 102 A85-35306  
Textured carbon surfaces on copper  
[NASA-CASE-LEW-14130-1] p 95 N85-20156  
Electron yields from spacecraft materials p 40 N85-22512
- SECONDARY FLOW**  
Comparison of secondary flows predicted by a viscous code and an inviscid code with experimental data for a turning duct p 106 A85-11634  
Flow control in a diffusing S-Duct  
[AIAA PAPER 85-0524] p 3 A85-25928
- SEDIMENTS**  
Chemistry of fuel deposits and sediments and their precursors  
[NASA-CR-174778] p 92 N85-10209
- SELECTION**  
Resin selection criteria for 'tough' composite structures p 81 A85-35139
- SELF EXCITATION**  
Internal hysteresis experienced on a high pressure syn gas compressor p 131 N85-14122
- SELF SEALING**  
Experimental stiffness of tapered bore seals  
[NASA-TM-86978] p 132 N85-25847
- SEMICONDUCTING FILMS**  
Dielectric properties of 'diamondlike' carbon prepared by RF plasma deposition p 182 A85-38192
- SEMICONDUCTOR DEVICES**  
A new very high voltage semiconductor switch  
[NASA-TM-86957] p 103 N85-20246  
Inelastic tunnel diodes  
[NASA-CASE-LEW-13833-1] p 103 N85-21492
- SEMICONDUCTOR JUNCTIONS**  
Prism-coupled light emission from tunnel junctions p 181 A85-21425  
Effect of solar-cell junction geometry on open-circuit voltage p 154 A85-28080  
Screen printed interdigitated back contact solar cell  
[NASA-CASE-LEW-13414-1] p 160 N85-20530
- SEMICONDUCTOR LASERS**  
Remote displacement measurements using a laser diode p 121 A85-24464
- SEMICONDUCTORS (MATERIALS)**  
AES and LEED study of the zinc blende SiC(100) surface p 61 A85-41633  
Advanced in solid state switchgear technology for large space power systems p 102 A85-45362  
Effect of barrier height on friction behavior of the semiconductors silicon and gallium arsenide in contact with pure metals p 84 N85-13044  
GaAs and 3-5 compound solar cells status and prospects for use in space p 49 N85-21261
- SENSITIVITY**  
Radiographic detectability limits for seeded voids in sintered silicon carbide and silicon nitride  
[NASA-TM-86945] p 138 N85-21674
- SENSORS**  
Sensor failure detection for jet engines using analytical redundancy  
[AIAA PAPER 84-1452] p 13 A85-16097  
A real-time FORTRAN implementation of a sensor failure detection, isolation and accommodation algorithm p 171 A85-47704
- SEPARATED FLOW**  
Generation of instability waves in flows separating from smooth surfaces p 1 A85-10352  
Feedback in separated flows over symmetric airfoils  
[AIAA PAPER 84-2297] p 3 A85-28899  
Structure of ducted particle-laden turbulent jets p 110 A85-38999  
The computation of viscous/inviscid interaction on airfoils with separated flow p 6 A85-42954  
The structure of dilute combustor sprays  
[NASA-CR-174838] p 24 N85-15728  
Vacuum chamber pressure effects on thrust measurements of low Reynolds number nozzles  
[NASA-TM-86955] p 49 N85-21259
- SEPARATION**  
The mechanisms of formation and prevention of channel segregation during alloy solidification p 180 A85-18082
- SEPARATORS**  
Separator development and testing of nickel-hydrogen cells p 156 A85-45386  
Electric utility acid fuel cell stack technology advancement  
[NASA-CR-174804] p 159 N85-17422
- Alkaline battery containing a separator of a cross-linked copolymer of vinyl alcohol and unsaturated carboxylic acid  
[NASA-CASE-LEW-13102-1] p 104 N85-29144  
Development of a lithium secondary battery separator p 104 N85-31378
- SERIES EXPANSION**  
A convergent series expansion for hyperbolic systems of conservation laws  
[NASA-CR-172557] p 168 N85-21990
- SERVICE LIFE**  
Life modeling of atmospheric and low pressure plasma-sprayed thermal-barrier coating p 81 A85-29728  
Fatigue criterion to system design, life and reliability  
[AIAA PAPER 85-1140] p 143 A85-40814  
Long-life high performance fuel cell program  
[NASA-CR-174874] p 50 N85-25384  
Fatigue criterion to system design, life and reliability  
[NASA-TM-87017] p 132 N85-27226  
Life cycle test results of a bipolar nickel hydrogen battery  
[NASA-TM-87046] p 163 N85-30480  
Free-piston Stirling engine/linear alternator 1000-hour endurance test  
[NASA-CR-174771] p 163 N85-30481  
Design principles for nickel-hydrogen cells and batteries  
[NASA-TM-87037] p 164 N85-31646
- SERVICES**  
Demand for satellite-provided domestic communications services up to the year 2000  
[NASA-TM-86894] p 97 N85-15099
- SERVO MECHANISMS**  
Application of traction drives as servo mechanisms p 152 N85-33520
- SHAFTS (MACHINE ELEMENTS)**  
An analysis of temperature effect in a finite journal bearing with spatial tilt and viscous dissipation p 126 A85-11074  
Vibration control of rotor shaft  
[NASA-TM-87053] p 133 N85-29292
- SHALE OIL**  
Lubricity of well-characterized jet and broad-cut fuels by ball-on-cylinder machine  
[NASA-TM-83807] p 92 N85-12183
- SHEAR FLOW**  
Computation and turbulence closure models for shear flows in rotating curved bodies p 107 A85-14349  
Approximate analysis for resonance of an incompressible shear layer plus edges p 107 A85-19377  
Some unique experiments on receptivity --- for forced disturbances entering shear flow p 174 A85-25932  
Turbulence modelling for complex shear flows  
[AIAA PAPER 85-1652] p 111 A85-40752
- SHEAR LAYERS**  
Generation of instability waves in flows separating from smooth surfaces p 1 A85-10352  
Approximate analysis for resonance of an incompressible shear layer plus edges p 107 A85-19377  
Sound generation and upstream influence due to instability waves interacting with non-uniform mean flows p 174 A85-20738  
Turbulent solutions of equations of fluid motion p 118 N85-31441
- SHEAR PROPERTIES**  
Structural characteristics of high temperature composites  
[NASA-CR-175998] p 58 N85-30037
- SHEAR STRENGTH**  
Imide modified epoxy matrix resins  
[NASA-CR-174695] p 85 N85-15892  
Graphite/PMR polyimide composites with improved toughness  
[NASA-TM-87081] p 58 N85-32148
- SHEAR STRESS**  
A study of Reynolds-stress closure model  
[NASA-CR-174342] p 114 N85-17324
- SHELL ANODES**  
Ring-cusp ion thruster with shell anode  
[NASA-CASE-LEW-13881-1] p 48 N85-21256
- SHELL STABILITY**  
Analysis of shell type structures subjected to time dependent mechanical and thermal loading  
[NASA-CR-175747] p 147 N85-25896  
Dynamic creep buckling: Analysis of shell structures subjected to time-dependent mechanical and thermal loading p 149 N85-27959
- SHELL THEORY**  
Hybrid Semiloof elements for plates and shells based upon a modified Hu-Washizu principle p 139 A85-15893
- Dynamic creep buckling: Analysis of shell structures subjected to time-dependent mechanical and thermal loading p 149 N85-27959
- SHELLS (STRUCTURAL FORMS)**  
Geometrically nonlinear analysis of laminated elastic structures  
[NASA-CR-175609] p 146 N85-21720
- SHOCK RESISTANCE**  
Dispersed-metal-toughened alumina  
[NASA-CR-174687] p 89 N85-22758
- SHOCK TUBES**  
Shock tube measurements of growth constants in the branched-chain ethane-carbon monoxide-oxygen system  
[NASA-TM-87068] p 64 N85-32156
- SHOCK WAVE ATTENUATION**  
Time dependent computation of the Euler equations for designing 2-D cascades, including the case of transonic shock free design p 5 A85-41814
- SHOCK WAVE INTERACTION**  
Heat transfer investigation in the junction region of circular cylinder normal to a flat plate at 90 deg location  
[ASME PAPER 84-WA/HT-70] p 111 A85-39898  
An experimental study of three-dimensional shock wave/turbulent boundary layer interactions in a supersonic flow  
[AIAA PAPER 85-1566] p 5 A85-40691
- SHOCK WAVES**  
A multiple-scales model of the shock-cell structure of imperfectly expanded supersonic jets p 113 A85-49354  
Observations from varying the lift and drag inputs to a noise prediction method for supersonic helical tip speed propellers  
[NASA-TM-83797] p 175 N85-10788  
Experimental investigation of shock-cell noise reduction for dual-stream nozzles in simulated flight  
[NASA-CR-3846] p 175 N85-13549  
Unsteady flow in a supersonic cascade with two in-passage shocks  
[NASA-CR-3925] p 10 N85-35158
- SHROUDED TURBINES**  
Ribron burner simulation of T-700 turbine shroud for ceramic lined seals research  
[NASA-TM-86940] p 114 N85-19364  
Thermal stress analysis of a new turbine shroud seal concept  
[NASA-TM-87082] p 136 N85-34406
- SHROUDS**  
Energy efficient engine high pressure turbine ceramic shroud support technology report  
[NASA-CR-168036] p 23 N85-10996  
Experimental and analytical study of ceramic-coated turbine-tip shroud seals for small turbine engines  
[NASA-TM-86881] p 25 N85-18057
- SHUTDOWNS**  
Shutdown characteristics of the Mod-O wind turbine with aileron controls  
[NASA-TM-86918] p 159 N85-18299  
Analytical model for predicting emergency shutdown of a two-bladed horizontal axis wind turbine  
[NASA-TM-83472] p 162 N85-30476
- SIDELobe REDUCTION**  
Configuration study for a 30 GHz monolithic receive array, volume 2  
[NASA-CR-174697-VOL-2] p 99 N85-18240
- SIDELOBES**  
The 20 GHz proof-of-concept test model results for a multiple scan beam dual reflector antenna  
[NASA-CR-174268] p 98 N85-15944
- SIGNAL ANALYSIS**  
The role of the reflection coefficient in precision measurement of ultrasonic attenuation p 137 A85-42151
- SIGNAL PROCESSING**  
A high-speed implementation of the random decrement algorithm p 94 A85-29556  
Application of homomorphic signal processing to stress wave factor analysis  
[NAS 1.26:174871] p 138 N85-21673
- SIGNAL TO NOISE RATIOS**  
Experimental results supporting the determination of service quality objectives for DBS systems p 96 A85-29611  
Configuration study for a 30 GHz monolithic receive array, volume 2  
[NASA-CR-174697-VOL-2] p 99 N85-18240
- SIGNAL TRANSMISSION**  
Four-dimensional modulation and coding - An alternate to frequency-reuse p 97 A85-36653  
Effect of interfacial characteristics of metal clad polymeric substrates on electrical high frequency interconnection performance  
[NASA-TM-86948] p 99 N85-20223
- SILENCERS**  
The performance of jet noise suppression devices for industrial applications p 175 A85-42563

**SILICON**

Voltage controlling mechanisms in low resistivity silicon solar cells - A unified approach p 155 A85-35617

The effect of diffusion induced lattice stress on the open-circuit voltage in silicon solar cells p 181 A85-35620

Effect of barrier height on friction behavior of the semiconductors silicon and gallium arsenide in contact with pure metals [NASA-TP-2405] p 84 N85-13044

The effects of lithium counterdoping on radiation damage and annealing in n(+)-p silicon solar cells p 50 N85-22586

**SILICON CARBIDES**

A morphological study of silicon carbide prepared by chemical vapor deposition p 79 A85-20938

Fibers for structurally reliable metal and ceramic composites p 55 A85-37484

Feasibility study of the welding of SiC p 81 A85-39339

AES and LEED study of the zinc blende SiC(100) surface p 61 A85-41633

Evaluation of alpha-SiC sintering using statistical methods p 83 A85-42800

Hot corrosion of sintered alpha-SiC at 1000 C [ACS PAPER 19-B-84P] p 83 A85-45302

Effect of hot isostatic pressing on the properties of sintered alpha silicon carbide p 83 A85-48757

Creep of chemically vapor deposited SiC fibers [NASA-TM-86897] p 56 N85-14878

Fundamental tribological properties of ceramics [NASA-TM-86915] p 85 N85-15893

Gas cooled fuel cell systems technology development [NASA-CR-174732] p 158 N85-16291

NDE for heat engine ceramics [NASA-TM-86949] p 137 N85-20389

Parametric evaluation of ball milling of SiC in water [NASA-TM-86974] p 88 N85-21356

Radiographic detectability limits for seeded voids in sintered silicon carbide and silicon nitride [NASA-TM-86945] p 138 N85-21674

Environmental effects on the tensile strength of chemically vapor deposited silicon carbide fibers [NASA-TM-86981] p 89 N85-24000

Preparation of silicon carbide-silicon nitride fibers by the pyrolysis of polycarbosilazane precursors [NASA-TM-86505] p 91 N85-28107

Burner rig corrosion of SiC at 1000 deg C [NASA-TM-87061] p 53 N85-30011

Mechanism of strength degradation for hot corrosion of alpha-SiC [NASA-TM-87052] p 91 N85-30135

Reliability of void detection in structural ceramics using scanning laser acoustic microscopy [NASA-TM-87035] p 138 N85-32337

Mechanical properties of SiC fiber-reinforced reaction-bonded Si3N4 composites [NASA-TM-87085] p 59 N85-34223

**SILICON CONTROLLED RECTIFIERS**

The J3 SCR model applied to resonant converter simulation p 102 A85-42156

**SILICON DIOXIDE**

Mechanical protection of DLC films on fused silica slides [NASA-TM-87056] p 91 N85-30138

**SILICON JUNCTIONS**

Theory of the high base resistivity n(+)-pp(+) silicon solar cell and its application to radiation damage effects p 154 A85-32639

Effects of 1 MeV electrons and 10 MeV protons on the performance and reflectance of thin BSR cells --- back surface reflector p 182 A85-35699

**SILICON NITRIDES**

Demonstration of a silicon nitride attrition mill for production of fine pure Si and Si3N4 powders p 78 A85-10825

Effect of hot isostatic pressing on reaction-bonded silicon nitride p 79 A85-15195

Strength and microstructure of sintered Si3N4 with rare-earth-oxide additions [ACS PAPER 130-13-84] p 80 A85-25271

Deposition of silicon nitride from SiCl4 and NH3 in a low pressure RF plasma p 81 A85-36229

RF-sputtered silicon and hafnium nitrides - Properties and adhesion to 440C stainless steel p 81 A85-36240

Fracture of yttria-doped, sintered reaction-bonded silicon nitride [ACS PAPER 7-J3-84] p 82 A85-42797

Oxidation of silicon nitride sintered with rare-earth oxide additions p 83 A85-42798

Microstructure of reaction-bonded silicon nitride consolidated by isostatic hot-pressing p 83 A85-45304

Milling of Si3N4 with Si3N4 hardware [NASA-TM-86864] p 84 N85-10191

Factors influencing the ball milling of Si3N4 in water [NASA-TM-86932] p 86 N85-19136

NDE for heat engine ceramics [NASA-TM-86949] p 137 N85-20389

Oxidation and hot corrosion of hot-pressed Si3N4 at 1000 deg C [NASA-TM-86977] p 88 N85-21358

Radiographic detectability limits for seeded voids in sintered silicon carbide and silicon nitride [NASA-TM-86945] p 138 N85-21674

Preparation of silicon carbide-silicon nitride fibers by the pyrolysis of polycarbosilazane precursors [NASA-TM-86505] p 91 N85-28107

Reliability of void detection in structural ceramics using scanning laser acoustic microscopy [NASA-TM-87035] p 138 N85-32337

Mechanical properties of SiC fiber-reinforced reaction-bonded Si3N4 composites [NASA-TM-87085] p 59 N85-34223

Reliability of two sintered silicon nitride materials [NASA-TM-87092] p 92 N85-34284

**SILICON POLYMERS**

Preparation of silicon carbide-silicon nitride fibers by the pyrolysis of polycarbosilazane precursors [NASA-TM-86505] p 91 N85-28107

**SILVER**

Effects of silver and group 2 fluorides addition to plasma sprayed chromium carbide high temperature solid lubricant for foil gas bearing to 650 deg C [NASA-TM-86895] p 84 N85-14928

The role of silver in self-lubricating coatings for use at extreme temperatures [NASA-TM-86943] p 87 N85-20127

**SIMULATORS**

Hardware for a real-time multiprocessor simulator [NASA-TM-83805] p 169 N85-10659

Operating system for a real-time multiprocessor propulsion system simulator. User's manual [NASA-TP-2426] p 171 N85-17596

**SINGLE CRYSTALS**

Elevated temperature creep-rupture behavior of the single crystal nickel-base superalloy NASAIR 100 p 66 A85-27812

Influence of composition on the microstructure and mechanical properties of a nickel-base superalloy single crystal p 66 A85-32387

Factors which influence directional coarsening of gamma-prime during creep in nickel-base superalloy single crystals p 67 A85-32388

Development of coated single-crystal superalloy systems for gas turbine applications p 68 A85-32440

Morphological changes of gamma prime precipitates in nickel-base superalloy single crystals [NASA-TM-83698] p 70 N85-10165

The transient oxidation of single crystal NiAl+Zr [NASA-CR-174756] p 70 N85-11221

The effect of tantalum and carbon on the structure/properties of a single crystal nickel-base superalloy [NASA-CR-174779] p 71 N85-11223

Biaxial constitutive equation development for single crystals [NASA-CR-174056] p 183 N85-11862

Low cycle fatigue of MAR-M 200 single crystals at 760 and 870 deg C [NASA-TM-86933] p 74 N85-19074

Diamondlike flakes [NASA-CASE-LEW-13837-2] p 57 N85-21267

Orientation and temperature dependence of some mechanical properties of the single-crystal nickel-base superalloy Rene N4. 3: Tension-compression anisotropy [NASA-TM-86982] p 76 N85-22660

Effects of wear on structure-sensitive magnetic properties of ceramic ferrite in contact with magnetic tape [NASA-TM-87007] p 90 N85-26991

**SINTERING**

Strength and microstructure of sintered Si3N4 with rare-earth-oxide additions [ACS PAPER 130-13-84] p 80 A85-25271

Fracture of yttria-doped, sintered reaction-bonded silicon nitride [ACS PAPER 7-J3-84] p 82 A85-42797

Oxidation of silicon nitride sintered with rare-earth oxide additions p 83 A85-42798

Evaluation of alpha-SiC sintering using statistical methods p 83 A85-42800

Hot corrosion of sintered alpha-SiC at 1000 C [ACS PAPER 19-B-84P] p 83 A85-45302

Effect of hot isostatic pressing on the properties of sintered alpha silicon carbide p 83 A85-48757

Powder metallurgy forged gear development [NASA-TM-87483] p 134 N85-29295

Reliability of void detection in structural ceramics using scanning laser acoustic microscopy [NASA-TM-87035] p 138 N85-32337

Reliability of two sintered silicon nitride materials [NASA-TM-87092] p 92 N85-34284

**SIZE (DIMENSIONS)**

Cavitation erosion size scale effects p 65 A85-11935

Effect of solar-cell junction geometry on open-circuit voltage p 154 A85-28080

**SIZE DETERMINATION**

Spray characterization with a nonintrusive technique using absolute scattered light p 120 A85-10036

Nonintrusive optical single-particle counter for measuring the size and velocity of droplets in a spray p 120 A85-16794

Research study of droplet sizing technology leading to the development of an advanced droplet sizing system [NASA-CR-174839] p 123 N85-21604

**SIZE DISTRIBUTION**

Experimental study of the spray characteristics of a research airblast atomizer [NASA-TM-86911] p 24 N85-15727

**SKIN TEMPERATURE (NON-BIOLOGICAL)**

Turbine heat transfer p 19 N85-10964

**SLIDING**

Hydrodynamic lubrication of rigid nonconformal contacts in combined rolling and normal motion [ASME PAPER 84-TRIB-13] p 127 A85-21280

**SLIDING CONTACT**

Hydrodynamic lubrication of rigid nonconformal contacts in combined rolling and normal motion [ASME PAPER 84-TRIB-13] p 127 A85-21280

Fast numerical calculations of EHD sliding traction forces [ASME PAPER 84-TRIB-26] p 127 A85-21289

Application to rolling bearings [ASME PAPER 84-TRIB-26] p 127 A85-21289

Friction and wear of ceramics p 80 A85-23833

**SLIDING FRICTION**

Elastohydrodynamic lubrication of line contacts p 126 A85-11069

Friction and wear of some ferrous-base metallic glasses p 64 A85-11071

Mechanical-contact-induced transformation from the amorphous to the partially crystalline state in metallic glass p 65 A85-19084

Thermal and thermomechanical effects in dry sliding p 127 A85-23838

Ceramic wear in indentation and sliding contact p 82 A85-39549

An experimental investigation of rubbing interaction in labyrinth seals at cryogenic temperature p 129 A85-39938

Effect of barrier height on friction behavior of the semiconductors silicon and gallium arsenide in contact with pure metals [NASA-TP-2405] p 84 N85-13044

Analytical and experimental investigation of rubbing interaction in labyrinth seals for a liquid hydrogen fuel pump --- space shuttle main engine [NASA-CR-174657] p 48 N85-18084

Sliding seal materials for adiabatic engines [NASA-CR-174893] p 89 N85-22757

Rolling, slip and traction measurements on low modulus materials [NASA-CR-174909] p 135 N85-33491

**SMOKE**

Analytical fuel property effects: Small combustors, phase 2 [NASA-CR-174848] p 93 N85-19175

Advanced smoke meter development survey and analysis [NASA-CR-168287] p 124 N85-25792

**SODIUM CARBONATES**

Hot corrosion of sintered alpha-SiC at 1000 C [ACS PAPER 19-B-84P] p 83 A85-45302

**SODIUM CHLORIDES**

Reactions of NaCl with gaseous SO3, SO2, and O2 p 59 A85-11897

Mechanism for forming hydrogen chloride and sodium sulfate from sulfur trioxide, water, and sodium chloride p 62 A85-48513

**SODIUM SULFATES**

Reactions of NaCl with gaseous SO3, SO2, and O2 p 59 A85-11897

Effects of SO2 and SO3 on the Na2SO4 induced corrosion of nickel p 65 A85-15603

Hot corrosion of sintered alpha-SiC at 1000 C [ACS PAPER 19-B-84P] p 83 A85-45302

Mechanism for forming hydrogen chloride and sodium sulfate from sulfur trioxide, water, and sodium chloride p 62 A85-48513

**SODIUM SULFUR BATTERIES**

Moderate temperature sodium cells. V - Discharge reactions and rechargeability of NiS and NiS2 positive electrodes in molten NaAlCl4 p 59 A85-11892

## SOLAR ARRAYS

- Control algorithms and computer simulation of a stand-alone photovoltaic village power system p 153 A85-11345
- Characteristics of arc currents on a negatively biased solar cell array in a plasma p 154 A85-18608
- Computer simulation of plasma electron collection by PIX-II — solar array-space plasma interaction [AIAA PAPER 85-0386] p 43 A85-19715
- The NASA photovoltaic technology program p 155 A85-35604
- A 37.5-kW point design comparison of the nickel-cadmium battery, bipolar nickel-hydrogen battery, and regenerative hydrogen-oxygen fuel cell energy storage subsystems for low earth orbit p 46 A85-45387
- Dilute plasma coupling currents to a high voltage solar array in weak magnetic fields p 46 A85-45388
- Electric power - Photovoltaic or solar dynamic? p 46 A85-47042
- A historical overview of the electrical power systems in the US manned and some US unmanned spacecraft [NASA-CR-174806] p 47 A85-13910
- Circuit transients due to negative bias arcs on a high-voltage solar array in low Earth orbit [NASA-TP-2407] p 39 A85-14858
- The PIX-2 experiment: An overview p 179 A85-22494
- Plasma interaction experiment 2 (PIX 2): Laboratory and flight results p 180 A85-22495
- Discharges on a negatively biased solar cell array in a charged-particle environment p 160 A85-22499
- GaAs and 3-5 compound solar cells status and prospects for use in space p 49 A85-22580
- SOLAR CELLS**
- Magnesium doping of efficient GaAs and Ga(0.75)In(0.25)As solar cells grown by metalorganic chemical vapor deposition p 180 A85-11466
- Near-optimum design of GaAs-based concentrator space solar cells for 80 C operation p 153 A85-15800
- Characteristics of arc currents on a negatively biased solar cell array in a plasma p 154 A85-18608
- The effect of plasma on solar cell array arc characteristics [AIAA PAPER 85-0384] p 43 A85-19713
- Applicability of the Meyer-Neldel rule to solar cells p 154 A85-19948
- High-voltage solar-cell chip p 154 A85-24668
- Effect of solar-cell junction geometry on open-circuit voltage p 154 A85-28080
- Theory of the high base resistivity  $n(+)/pp(+)$  silicon solar cell and its application to radiation damage effects p 154 A85-32639
- Fabrication of  $p(+)-n$  junction GaAs solar cells by a novel method p 181 A85-33645
- Voltage controlling mechanisms in low resistivity silicon solar cells - A unified approach p 155 A85-35617
- The effect of diffusion induced lattice stress on the open-circuit voltage in silicon solar cells p 181 A85-35620
- Radiation damage and defect behavior in ion-implanted, lithium counterdoped silicon solar cells p 182 A85-35698
- Effects of 1 MeV electrons and 10 MeV protons on the performance and reflectance of thin BSR cells — back surface reflector p 182 A85-35699
- Microprocessor control of photovoltaic systems p 156 A85-45408
- The effect of plasma on solar cell array arc characteristics [NASA-TM-86887] p 47 A85-11133
- Research on gallium arsenide diffused junction solar cells [NASA-CR-174057] p 158 A85-11457
- Screen printed interdigitated back contact solar cell [NASA-CASE-LEW-13414-1] p 160 A85-20530
- Lithium counterdoped silicon solar cell [NASA-CASE-LEW-14177-1] p 160 A85-20535
- GaAs and 3-5 compound solar cells status and prospects for use in space p 49 A85-21261
- An investigation of arc discharging on negatively biased dielectric conductor samples in a plasma p 180 A85-22498
- Discharges on a negatively biased solar cell array in a charged-particle environment p 160 A85-22499
- The high voltage silicon cell: A comparative analysis p 49 A85-22569
- The effects of lithium counterdoping on radiation damage and annealing in  $n(+)/p$  silicon solar cells p 50 A85-22586
- High efficiency solar cell research for space applications p 164 A85-31624
- Diffusion welding of Cassegrainian concentrator cell stack assemblies [NASA-CR-176104] p 164 A85-33566

- Practical aspects of photovoltaic technology, applications and cost (revised) [NASA-CR-174963] p 165 A85-35472
- SOLAR COLLECTORS**
- Solar dynamic systems p 164 A85-31374
- Optical analysis of parabolic dish concentrators for solar dynamic power systems in space [NASA-TM-87080] p 52 A85-34176
- SOLAR ENERGY**
- Optical analysis of parabolic dish concentrators for solar dynamic power systems in space [NASA-TM-87080] p 52 A85-34176
- SOLAR ENERGY ABSORBERS**
- Solar dynamic systems p 164 A85-31374
- SOLAR ENERGY CONVERSION**
- The NASA photovoltaic technology program p 155 A85-35604
- Pyroelectric conversion in space p 45 A85-45377
- Electric power - Photovoltaic or solar dynamic? p 46 A85-47042
- Solar energy converter using surface plasma waves [NASA-CASE-LEW-13827-1] p 160 A85-21768
- Practical aspects of photovoltaic technology, applications and cost (revised) [NASA-CR-174963] p 165 A85-35472
- SOLAR GENERATORS**
- Environmentally-induced voltage limitations in large space power systems p 43 A85-18584
- SOLAR THERMAL PROPULSION**
- Measurements of energy distribution in microwave plasmas of N<sub>2</sub> and He and comparisons with results for H<sub>2</sub> p 178 A85-16443
- SOLENOIDS**
- A rotating superconducting solenoid for 100 kWh energy storage — in space p 44 A85-33144
- SOLID LUBRICANTS**
- Polyimides - Tribological properties and their use as lubricants p 79 A85-21524
- Experimental test program for evaluation of solid lubricant coating as applied to compliant foil gas bearings to 315 deg C [NASA-CR-174837] p 85 A85-15895
- The role of silver in self-lubricating coatings for use at extreme temperatures [NASA-TM-86943] p 87 A85-20127
- Effect of counterface material type and its topography on the tribological properties of polyimide composites [NASA-TM-87036] p 90 A85-26993
- Advances in sputtered and ion plated solid film lubrication p 136 A85-33524
- SOLID SOLUTIONS**
- Solids mixing in a three phase fluidized bed containing spherically shaped-porous solid particles [PB85-187961] p 120 A85-33453
- SOLID STATE DEVICES**
- Advanced in solid state switchgear technology for large space power systems p 102 A85-45382
- The 30 GHz solid state amplifier for low cost low data rate ground terminals [NASA-CR-174795] p 102 A85-12300
- A new very high voltage semiconductor switch [NASA-TM-86957] p 103 A85-20246
- Solar energy converter using surface plasma waves [NASA-CASE-LEW-13827-1] p 160 A85-21768
- SOLID SURFACES**
- Gravitational effects on flames spreading over thick solid surfaces [IAF PAPER 84-154] p 59 A85-13092
- SOLID-SOLID INTERFACES**
- On the existence and stability conditions for mixed-hybrid finite element solutions based on Reissner's variational principle p 142 A85-33847
- Solidification interface shape for continuous casting in an offset mold - Two analytical methods p 112 A85-41326
- SOLIDIFICATION**
- The mechanisms of formation and prevention of channel segregation during alloy solidification p 180 A85-18082
- Analysis of three-dimensional solidification interface shape p 109 A85-30075
- Control of solidification boundary in continuous casting by asymmetric cooling and mold offset p 110 A85-37047
- Dendritic solidification. I - Analysis of current theories and models. II - A model for dendritic growth under an imposed thermal gradient p 182 A85-38019
- Solidification interface shape for continuous casting in an offset mold - Two analytical methods p 112 A85-41326
- Dendritic solidification. III - Some further refinements to the model for dendritic growth under an imposed thermal gradient p 69 A85-44703
- Microstructures in rapidly solidified Ni-Mo alloys [NASA-TM-87100] p 78 A85-34266

## SOLIDS

- Hybrid stress finite elements for large deformations of inelastic solids p 139 A85-15894
- SOOT**
- Methanol as a soot reducer in a turbulent swirling burner [ASME PAPER 84-JPGC-GT-2] p 61 A85-23192
- Ideal gas thermodynamic properties for the phenyl, phenoxy, and *o*-biphenyl radicals [NASA-TM-83800] p 184 A85-22204
- Shock tube study of the fuel structure effects on the chemical kinetic mechanisms responsible for soot formation, part 2 [NASA-CR-174880] p 63 A85-25444
- Fuel-rich catalytic combustion: A soot-free technique for in situ hydrogen-like enrichment [NASA-TP-2498] p 63 A85-31244
- SOUND GENERATORS**
- Sound generation and upstream influence due to instability waves interacting with non-uniform mean flows p 174 A85-20738
- A theoretical prediction of the acoustic pressure generated by turbulence-flame front interactions [ASME PAPER 84-WA/NCA-11] p 174 A85-39909
- SOUND PRESSURE**
- The influence of combustion liner holes on noise production by ducted burners [AIAA PAPER 84-2322] p 172 A85-10869
- Effects of vane/blade ratio and spacing on fan noise, volume 1 [NASA-CR-174664] p 176 A85-19791
- SOUND PROPAGATION**
- Acoustic structure and propagation in highly porous, layered, fibrous materials p 173 A85-12301
- Analysis of the effect on combustor noise measurements of acoustic waves reflected by the turbine and combustor inlet [AIAA PAPER 84-2323] p 173 A85-16103
- SOUND TRANSMISSION**
- Measured acoustic properties of variable and low density bulk absorbers [NASA-TM-87065] p 177 A85-30770
- SOUND WAVES**
- Analysis of the effect on combustor noise measurements of acoustic waves reflected by the turbine and combustor inlet [AIAA PAPER 84-2323] p 173 A85-16103
- The response of Helmholtz resonators to external excitation. I - Single resonators p 174 A85-26915
- SPACE BASED RADAR**
- Primary propulsion of electrothermal, ion and chemical systems for space-based radar orbit transfer [NASA-TM-87043] p 51 A85-27972
- SPACE ENVIRONMENT SIMULATION**
- Numerical simulations of positively-biased probes and dielectric-conductor disks in a plasma — for low earth orbit plasma densities p 179 A85-17262
- SPACE MISSIONS**
- Preliminary analysis of space mission applications for electromagnetic launchers [NASA-CR-174067] p 35 A85-12071
- SPACE PLASMAS**
- Numerical simulations of positively-biased probes and dielectric-conductor disks in a plasma — for low earth orbit plasma densities p 179 A85-17262
- Computer simulation of plasma electron collection by PIX-II — solar array-space plasma interaction [AIAA PAPER 85-0386] p 43 A85-19715
- Dilute plasma coupling currents to a high voltage solar array in weak magnetic fields p 46 A85-45388
- Three-dimensional calculation of shuttle charging in polar orbit p 40 A85-22486
- Surface interactions and high-voltage current collection p 40 A85-22493
- The PIX-2 experiment: An overview p 179 A85-22494
- Plasma interaction experiment 2 (PIX 2): Laboratory and flight results p 180 A85-22495
- Ram-wake effects on plasma current collection of the PIX 2 Langmuir probe p 180 A85-22496
- NASCAP simulation of PIX 2 experiments p 180 A85-22497
- An investigation of arc discharging on negatively biased dielectric conductor samples in a plasma p 180 A85-22498
- SPACE POWER REACTORS**
- Design of a 1-kWh bipolar nickel hydrogen battery p 155 A85-45384
- SPACE POWER UNIT REACTORS**
- Overview of the 1985 NASA Lewis Research Center SP-100 free-piston Stirling engine activities [NASA-TM-87028] p 185 A85-27769
- SPACE SHUTTLE MAIN ENGINE**
- Application of viscous and inviscid computation methods for rocket turbopump systems [SAE PAPER 841522] p 110 A85-39257



An experimental investigation of rubbing interaction in labyrinth seals at cryogenic temperature p 129 A85-39938

Analytical and experimental investigation of rubbing interaction in labyrinth seals for a liquid hydrogen fuel pump --- space shuttle main engine [NASA-CR-174657] p 48 N85-18084

Cyclic structural analyses of anisotropic turbine blades for reusable space propulsion systems --- ssme fuel turbopump [NASA-TM-86990] p 146 N85-24339

Flow dynamic environment data base development for the SSME p 147 N85-26885

Preliminary results on passive eddy current damper technology for SSME turbomachinery p 132 N85-26890

Redistribution of the inlet temperature profile through the SSME fuel turbine p 50 N85-26901

Analytical study of flow phenomena in SSME turnaround duct geometries p 116 N85-26902

Instrumentation technology overview p 124 N85-26903

Structural Integrity and Durability of Reusable Space Propulsion Systems [NASA-CP-2381] p 51 N85-27941

Overview of aerothermodynamic loads definition study p 51 N85-27942

SSME fuel preburner two-dimensional analysis p 51 N85-27943

Simulation of multistage turbine flows p 116 N85-27945

New facility to study unsteady wake effects on turbine airfoil heat transfer p 117 N85-27948

Overview of structural response: Probabilistic structural analysis p 148 N85-27952

Composite loads spectra for select space propulsion structural components p 148 N85-27953

Cyclic structural analyses of SSME turbine blades p 150 N85-27963

Thin-film sensors for space propulsion technology p 41 N85-27968

Heat flux sensor calibrator p 41 N85-27970

Feasibility of mapping velocity flow fields in SSME powerhead by laser anemometry techniques p 41 N85-27971

**SPACE SHUTTLE PAYLOADS**

Effects of chemical releases by the STS 3 orbiter on the ionosphere p 166 A85-29538

Shuttle/Centaur project perspective p 37 N85-16991

Suprathermal plasma observed on STS-3 Mission by plasma diagnostics package p 179 N85-22472

Electron and ion density depletions measured in the STS-3 orbiter wake p 39 N85-22474

**SPACE SHUTTLES**

Laboratory degradation of Kapton in a low energy oxygen ion beam [AIAA PAPER 83-2658] p 78 A85-10675

A high energy stage for the National Space Transportation System [IAF PAPER 84-15] p 36 A85-23200

Advanced research and technology programs for advanced high-pressure oxygen-hydrogen rocket propulsion [NASA-TM-86969] p 37 N85-21231

Spacecraft Environmental Interactions Technology, 1983 [NASA-CP-2359] p 39 N85-22470

Laboratory studies of Kapton degradation in an oxygen ion beam p 177 N85-22477

Electron beam charging of Space Shuttle thermal protection system tiles p 39 N85-22478

Study of Kapton under simulated shuttle environment [NASA-CR-176003] p 41 N85-29997

**SPACE STATIONS**

Space Station propulsion - The Advanced Development Program at Lewis [AIAA PAPER 85-1154] p 44 A85-39626

Space station propulsion options [AIAA PAPER 85-1155] p 45 A85-43975

An evaluation of oxygen/hydrogen propulsion systems for the Space Station [AIAA PAPER 85-1156] p 45 A85-43976

Electric power - Photovoltaic or solar dynamic? p 46 A85-47042

Regenerative fuel cell energy storage system for a low Earth orbit space station [NASA-CR-174802] p 158 N85-13371

Space Power [NASA-CP-2352] p 47 N85-13880

Advanced research and technology programs for advanced high-pressure oxygen-hydrogen rocket propulsion [NASA-TM-86969] p 37 N85-21231

Long-life high performance fuel cell program [NASA-CR-174874] p 50 N85-25384

Space station propulsion: The advanced development program at Lewis [NASA-TM-86999] p 50 N85-25386

Tethered nuclear power for the Space Station [NASA-TM-87023] p 51 N85-26912

Performance analysis of radiation cooled dc transmission lines for high power space systems [NASA-TM-87040] p 104 N85-28222

An evaluation of oxygen-hydrogen propulsion systems for the Space Station [NASA-TM-87059] p 52 N85-28971

Regenerative fuel cell systems for space station p 104 N85-31372

Optical analysis of parabolic dish concentrators for solar dynamic power systems in space [NASA-TM-87080] p 52 N85-34176

**SPACE TRANSPORTATION SYSTEM**

A high energy stage for the National Space Transportation System [IAF PAPER 84-15] p 36 A85-23200

Progress report - Advanced cryogenic OTV engine technology [AIAA PAPER 85-1341] p 44 A85-39735

**SPACEBORNE ASTRONOMY**

Mosaic Infrared Sensor for Space Astronomy (MIRSSA) [NASA-CR-176154] p 125 N85-33456

**SPACEBORNE EXPERIMENTS**

Experiments in charge control at geosynchronous orbit - ATS-5 and ATS-6 p 39 A85-35379

**SPACECRAFT ANTENNAS**

Interdisciplinary design analysis of a precision spacecraft antenna [AIAA PAPER 85-0804] p 38 A85-30303

**SPACECRAFT CHARGING**

Experiments in charge control at geosynchronous orbit - ATS-5 and ATS-6 p 39 A85-35379

Spacecraft Environmental Interactions Technology, 1983 [NASA-CP-2359] p 39 N85-22470

Electron and ion density depletions measured in the STS-3 orbiter wake p 39 N85-22474

Laboratory studies of Kapton degradation in an oxygen ion beam p 177 N85-22477

Electron beam charging of Space Shuttle thermal protection system tiles p 39 N85-22478

Three-dimensional calculation of shuttle charging in polar orbit p 40 N85-22486

Polar orbit electrostatic charging of objects in shuttle wake p 40 N85-22487

Surface interactions and high-voltage current collection p 40 N85-22493

The PIX-2 experiment: An overview p 179 N85-22494

Plasma interaction experiment 2 (PIX 2): Laboratory and flight results p 180 N85-22495

Design guidelines for assessing and controlling spacecraft charging effects p 40 N85-22500

Electron yields from spacecraft materials p 40 N85-22512

Spacecraft environmental interactions: A joint Air Force and NASA research and technology program p 40 N85-22517

**SPACECRAFT COMMUNICATION**

Demand for satellite-provided domestic communications services up to the year 2000 [NASA-TM-86894] p 97 N85-15099

Research and technology highlights of the Lewis Research Center [NASA-TM-86899] p 186 N85-17928

Automated testing of developmental satellite communications systems and subsystems [NASA-TM-87070] p 100 N85-31348

**SPACECRAFT COMPONENTS**

High voltage-high power components for large space power distribution systems p 45 A85-45370

**SPACECRAFT CONFIGURATIONS**

Vehicle/engine integration --- orbit transfer vehicles p 37 N85-17008

Report of the Constellations Panel p 131 N85-20368

**SPACECRAFT CONSTRUCTION MATERIALS**

Ion beam sputter-deposited thin film coatings for protection of spacecraft polymers in low Earth orbit [NASA-TM-87051] p 91 N85-30137

**SPACECRAFT DESIGN**

Main propulsion system design recommendations for an advanced Orbit Transfer Vehicle [AIAA PAPER 85-1336] p 36 A85-39730

Design guidelines for assessing and controlling spacecraft charging effects p 40 N85-22500

**SPACECRAFT ENVIRONMENTS**

High voltage requirements and issues for the 1990's --- for spacecraft power supplies p 46 A85-45429

**SPACECRAFT EQUIPMENT**

Developments in space power components for power management and distribution p 47 N85-13877

High-voltage, high-power, solid-state remote power controllers for aerospace applications [NASA-TP-2437] p 49 N85-21263

**SPACECRAFT MAINTENANCE**

Technology requirements to be addressed by the NASA Lewis Research Center Cryogenic Fluid Management Facility program [AIAA PAPER 85-1229] p 94 A85-47024

Technology requirements to be addressed by the NASA Lewis Research Center Cryogenic Fluid Management Facility program [NASA-TM-87048] p 38 N85-29987

**SPACECRAFT MODULES**

Mass analysis of neutral particles and ions released during electrical breakdowns on spacecraft surfaces [NASA-CR-175585] p 39 N85-21250

**SPACECRAFT ORBITS**

Life cycle test results of a bipolar nickel hydrogen battery p 105 N85-31406

**SPACECRAFT POWER SUPPLIES**

Environmentally-induced voltage limitations in large space power systems p 43 A85-18584

A rotating superconducting solenoid for 100 kWh energy storage --- in space p 44 A85-33144

Advanced in solid state switchgear technology for large space power systems p 102 A85-45362

Pyroelectric conversion in space p 45 A85-45377

Microprocessor control of photovoltaic systems p 156 A85-45408

High voltage requirements and issues for the 1990's --- for spacecraft power supplies p 46 A85-45429

Overview of NASA Lewis Research Center free-piston Stirling engine activities p 130 A85-45479

Electric power - Photovoltaic or solar dynamic? p 46 A85-47042

Space Power [NASA-CP-2352] p 47 N85-13880

Missions/planning panel p 36 N85-13886

Electrochemistry and storage p 62 N85-13889

Dynamic power systems for power generation p 158 N85-13892

Engineering model system study for a regenerative fuel cell: Study report [NASA-CR-174801] p 158 N85-16292

Technology for satellite power conversion [NASA-CR-174335] p 159 N85-18451

GaAs and 3-5 compound solar cells status and prospects for use in space p 49 N85-21261

GaAs and 3-5 compound solar cells status and prospects for use in space p 49 N85-22580

Long-life high performance fuel cell program [NASA-CR-174874] p 50 N85-25384

Tethered nuclear power for the Space Station [NASA-TM-87023] p 51 N85-26912

Performance analysis of radiation cooled dc transmission lines for high power space systems [NASA-TM-87040] p 104 N85-28222

Solar dynamic systems p 164 N85-31374

System level electrochemical principles p 104 N85-31375

Design principles for nickel hydrogen cells and batteries p 104 N85-31398

Life cycle test results of a bipolar nickel hydrogen battery p 105 N85-31406

The failure mechanism of a nickel electrode in a nickel-hydrogen cell p 105 N85-31408

High efficiency solar cell research for space applications p 164 N85-31624

Design principles for nickel-hydrogen cells and batteries [NASA-TM-87037] p 164 N85-31646

Optical analysis of parabolic dish concentrators for solar dynamic power systems in space [NASA-TM-87080] p 52 N85-34176

**SPACECRAFT PROPULSION**

Ground correlation investigation of thruster/spacecraft interactions to be measured on the IAPS flight test p 42 A85-16408

Ion propulsion for communications satellites p 42 A85-16412

Friction in rail guns p 101 A85-16424

Electrothermal thruster diagnostics p 42 A85-16440

Inert gas test of two 12-cm magnetostatic thrusters p 43 A85-29310

Space Station propulsion - The Advanced Development Program at Lewis [AIAA PAPER 85-1154] p 44 A85-39626

Progress report - Advanced cryogenic OTV engine technology [AIAA PAPER 85-1341] p 44 A85-39735

Space station propulsion options [AIAA PAPER 85-1155] p 45 A85-43975

- A historical overview of the electrical power systems in the US manned and some US unmanned spacecraft [NASA-CR-174806] p 47 N85-13910
- OTV propulsion technology programmatic overview p 37 N85-16997
- Vehicle/engine integration --- orbit transfer vehicles p 37 N85-17008
- Space station propulsion: The advanced development program at Lewis p 50 N85-25386
- Structural Integrity and Durability of Reusable Space Propulsion Systems [NASA-CP-2381] p 51 N85-27941
- Composite loads spectra for select space propulsion structural components: Probabilistic load model development p 148 N85-27954
- Probabilistic structural analysis theory development p 148 N85-27955
- Probabilistic finite element development p 149 N85-27956
- Thin-film sensors for space propulsion technology p 41 N85-27968
- SPACECRAFT RADIATORS**
- Preliminary evaluation of a liquid belt radiator for space applications [NASA-CR-174807] p 47 N85-15804
- Advanced radiator concepts [NASA-TM-87008] p 115 N85-24245
- SPACING**
- Effects of vane/blade ratio and spacing on fan noise, volume 1 [NASA-CR-174664] p 176 N85-19791
- Effects of vane/blade ratio and spacing on fan noise, Volume 2: Data supplement [NASA-CR-174665] p 176 N85-19792
- SPATIAL DISTRIBUTION**
- Plot of modal field distribution in rectangular and circular waveguides p 101 N85-25170
- SPATIAL MARCHING**
- Computation of viscous flows in turbomachinery cascades p 106 N85-11631
- A space-marching method for incompressible Navier-Stokes equations [AIAA PAPER 85-0170] p 108 N85-19564
- Computation of three-dimensional viscous flows using a space-marching method p 4 N85-29259
- SPECIFICATIONS**
- Spacecraft environmental interactions: A joint Air Force and NASA research and technology program p 40 N85-22517
- SPECIMEN GEOMETRY**
- Results of an interlaboratory fatigue test program conducted on alloy 800H at room and elevated temperatures [NASA-CR-174940] p 152 N85-32340
- SPEED CONTROL**
- Feasibility demonstration of a novel, flat-belt, continuously variable transmission or automotive and electric-hybrid vehicle application [NASA-CR-174430] p 185 N85-19894
- Experimental investigation of a variable speed constant frequency electric generating system from a utility perspective [NASA-CR-174950] p 105 N85-32251
- SPHERES**
- Ultrasonic wave propagation in two-phase media - Spherical inclusions p 54 N85-11926
- SPIN**
- Thermal traction contact performance evaluation under fully flooded and starved conditions [NASA-CR-168173] p 132 N85-25848
- SPIRAL WRAPPING**
- Generated spiral bevel gears: Optimal machine-tool settings and tooth contact analysis [NASA-TM-87075] p 136 N85-34405
- SPRAY CHARACTERISTICS**
- Phase/doppler spray analyzer for simultaneous measurements of drop size and velocity distributions p 120 N85-10035
- Spray characterization with a nonintrusive technique using absolute scattered light p 120 N85-10036
- Structure of nonevaporating sprays. I - Initial conditions and mean properties p 112 N85-48538
- SPRAY NOZZLES**
- Experimental study of the spray characteristics of a research airblast atomizer [NASA-TM-86911] p 24 N85-15727
- SPRAYED COATINGS**
- Plastic flow of plasma sprayed ceramics p 80 N85-24161
- Life modeling of atmospheric and low pressure plasma-sprayed thermal-barrier coating p 81 N85-29728
- Mechanical property measurements of plasma-sprayed thermal-barrier coatings subjected to oxidation p 81 N85-29729

- Cyclic oxidation behavior of beta+gamma overlay coatings on gamma and gamma+gamma-prime alloys p 68 N85-32431
- An investigation of enhanced capability thermal barrier coating systems for diesel engine components [NASA-CR-174820] p 86 N85-18154
- Rocket thrust chamber thermal barrier coatings p 90 N85-26867
- SPRAYERS**
- Nonintrusive optical single-particle counter for measuring the size and velocity of droplets in a spray p 120 N85-16794
- Measurements and predictions of the structure of evaporating sprays p 112 N85-46484
- The structure of dilute combustor sprays [NASA-CR-174838] p 24 N85-15728
- Research study of droplet sizing technology leading to the development of an advanced droplet sizing system [NASA-CR-174839] p 123 N85-21604
- SPUTTERING**
- Frictional and morphological properties of Au-MoS2 films sputtered from a compact target p 127 N85-19085
- RF-sputtered silicon and hafnium nitrides - Properties and adhesion to 440C stainless steel p 81 N85-36240
- Properties of coated and modified surfaces p 53 N85-36694
- Textured carbon surfaces on copper [NASA-CASE-LEW-14130-1] p 95 N85-20156
- Diamondlike flakes [NASA-CASE-LEW-13837-2] p 57 N85-21267
- Ion beam sputter-deposited thin film coatings for protection of spacecraft polymers in low Earth orbit [NASA-TM-87051] p 91 N85-30137
- Advances in sputtered and ion plated solid film lubrication p 136 N85-33524
- SPUTTERING GAGES**
- Thin-film sensors for space propulsion technology p 41 N85-27968
- SQUEEZE FILMS**
- Dual clearance squeeze film damper for high load conditions [ASME PAPER 84-TRIB-7] p 128 N85-32960
- Dual clearance squeeze film damper [NASA-CASE-LEW-13506-1] p 135 N85-33490
- STABILITY**
- Effect of combined pressure and temperature distortion orientation on high-bypass-ratio turbofan engine stability [NASA-TM-83771] p 17 N85-10067
- Rotordynamic Instability Problems in High-Performance Turbomachinery [NASA-CP-2338] p 131 N85-14116
- Internal hysteresis experienced on a high pressure syn gas compressor p 131 N85-14122
- STABILITY TESTS**
- Environmental stability of intercalated graphite fibers [NASA-TM-87025] p 90 N85-26992
- STACKS**
- Gas cooled fuel cell systems technology development [NASA-CR-174732] p 158 N85-16291
- Develop and test fuel cell powered on-site integrated total energy systems. Phase 3: Full-scale power plant development [NASA-CR-174887] p 161 N85-25941
- STAGNATION POINT**
- Combined influence of unsteady free stream velocity and free stream turbulence on stagnation point heat transfer p 112 N85-41782
- Preliminary results of a study of the relationship between free stream turbulence and stagnation region heat transfer [NASA-TM-86884] p 113 N85-11317
- The influence of jet-grid turbulence on heat transfer from the stagnation region of a cylinder in crossflow [NASA-TM-87011] p 115 N85-25760
- Preliminary results of a study of the relationship between free-stream turbulence and stagnation region heat transfer p 118 N85-31435
- STAGNATION PRESSURE**
- A stagnation pressure probe for droplet-laden air flow [AIAA PAPER 85-0330] p 108 N85-19672
- A comparison of flow rates and pressure profiles for N-sequential inlets and three related seal configurations p 109 N85-26526
- STAINLESS STEELS**
- Topological reaction rate measurements related to scuffing p 64 N85-11070
- RF-sputtered silicon and hafnium nitrides - Properties and adhesion to 440C stainless steel p 81 N85-36240
- STANDING WAVES**
- Flutter and forced response of mistuned rotors using standing wave analysis p 139 N85-12721
- Vibration and flutter of mistuned bladed-disk assemblies [AIAA PAPER 84-0991] p 139 N85-16095

- STATIC LOADS**
- Hygrothermomechanical evaluation of transverse filament tape epoxy/polyester fiberglass composites p 54 N85-15632
- Design procedures for fiber composite structural components - Rods, beams, and beam columns p 54 N85-15636
- STATIC PRESSURE**
- Effect of combined pressure and temperature distortion orientation on high-bypass-ratio turbofan engine stability [NASA-TM-83771] p 17 N85-10067
- High temperature static strain sensor development program p 19 N85-10959
- STATIC TESTS**
- Static jet noise test results of four 0.35 scale-model OCGAT mixer nozzles [NASA-TM-86871] p 175 N85-13551
- STATISTICAL ANALYSIS**
- Evaluation of alpha-SiC sintering using statistical methods p 83 N85-42800
- Factors influencing the ball milling of Si3N4 in water [NASA-TM-86932] p 86 N85-19136
- Reliability of void detection in structural ceramics using scanning laser acoustic microscopy [NASA-TM-87035] p 138 N85-32337
- STATISTICAL DISTRIBUTIONS**
- Creep-rupture reliability analysis p 143 N85-42566
- STATISTICAL MECHANICS**
- Statistics and thermodynamics of fracture p 140 N85-19433
- STATISTICAL WEATHER FORECASTING**
- GASP cloud encounter statistics - Implications for laminar flow control flight p 166 N85-11979
- STATOR BLADES**
- Noise produced by the interaction of a rotor wake with a swept stator blade [AIAA PAPER 84-2326] p 173 N85-13956
- A note on blade wake interaction influence on compressor stator row aerodynamic performance p 4 N85-32965
- Study of controlled diffusion stator blading [NASA-CR-167995] p 25 N85-18058
- Development of a rotor wake-vortex model, volume 1 [NASA-CR-174849] p 9 N85-26668
- STATORS**
- Transient technique for measuring heat transfer coefficients on stator airfoils in a jet engine environment [AIAA PAPER 85-1471] p 122 N85-39796
- Energy efficient engine component development and integration program [NASA-CR-170034] p 22 N85-10990
- Transient technique for measuring heat transfer coefficients on stator airfoils in a jet engine environment [NASA-TM-87005] p 124 N85-25794
- STEADY STATE**
- Effect of steady-state temperature distortion on inlet flow to a high-bypass-ratio turbofan engine [NASA-TM-86896] p 24 N85-15725
- Initial testing of a variable-stroke Stirling engine [NASA-TM-86875] p 185 N85-19895
- STEAM TURBINES**
- Advanced technology cogeneration system conceptual design study: Closed cycle gas turbines [NASA-CR-168222] p 159 N85-16300
- STEELS**
- Ion-beam nitriding of steels p 66 N85-24667
- Surface hardening of steel by boriding in a cold rf plasma p 68 N85-40275
- Effect of lubricant extreme-pressure additives on surface fatigue life of AISI 9310 spur gears [NASA-TP-2408] p 130 N85-13234
- Ion-beam nitriding of steels [NASA-CASE-LEW-14104-1] p 75 N85-21324
- Characterization of lubricated bearing surfaces operated under high loads [NASA-TM-86964] p 88 N85-21357
- STELLITE (TRADEMARK)**
- Interaction of high-cycle and low-cycle fatigue of Haynes 188 alloy at 1400 F deg p 149 N85-27961
- STIFFNESS**
- Gear mesh stiffness and load sharing in planetary gearing [ASME PAPER 84-DET-229] p 129 N85-33781
- Comparison of numerical techniques for integration of stiff ordinary differential equations arising in combustion chemistry [NASA-TP-2372] p 17 N85-10065
- Experimental stiffness of tapered bore seals [NASA-TM-86978] p 132 N85-25847
- Application of traction drives as servo mechanisms p 152 N85-33520
- STIFFNESS MATRIX**
- Analysis of hourglass instabilities and control in underintegrated finite element methods p 139 N85-11125

- Stability, accuracy, and efficiency of some underintegrated methods in finite element computations p 172 A85-50073
- STIRLING CYCLE**  
Initial results of sensitivity tests - Performed on the RE-1000 free-piston Stirling engine p 129 A85-45466  
Mod II engine and technology development p 129 A85-45473  
Automotive Stirling engine systems development p 130 A85-45474  
Overview of NASA Lewis Research Center free-piston Stirling engine activities p 130 A85-45479  
Comparison of free-piston Stirling engine model predictions with RE1000 engine test data p 130 A85-45488  
Stirling material technology [NASA-TM-86888] p 72 N85-13007  
Overview of waste heat utilization systems [NASA-TM-86901] p 184 N85-13692  
Dynamic power systems for power generation p 158 N85-13892  
Effect of water on hydrogen permeability --- Stirling engines [NASA-TM-86904] p 53 N85-14864  
Initial testing of a variable-stroke Stirling engine [NASA-TM-86875] p 185 N85-19895  
Overview of the 1985 NASA Lewis Research Center SP-100 free-piston Stirling engine activities [NASA-TM-87028] p 185 N85-27769  
Free-piston Stirling engine/linear alternator 1000-hour endurance test [NASA-CR-174771] p 163 N85-30481
- STOCHASTIC PROCESSES**  
A design methodology for robust failure detection and isolation p 171 A85-47794  
Probabilistic finite element development p 149 N85-27956
- STORAGE BATTERIES**  
Electrochemistry and storage p 62 N85-13889  
Regenerative fuel cell systems for space station p 104 N85-31372  
System level electrochemical principles p 104 N85-31375
- STRAIN GAGES**  
Closed-loop strain controlled testing at elevated temperatures with a non-contacting gage p 121 A85-29562  
High temperature static strain sensor development program p 19 N85-10959  
Evaluation results of the 700 deg C Chinese strain gauges --- for gas turbine engine [NASA-TM-86973] p 124 N85-21605
- STRAIN MEASUREMENT**  
Some advances in experimentation supporting development of viscoplastic constitutive models [NASA-CR-174855] p 147 N85-27260  
Some advances in experimentation supporting development of viscoplastic constitutive models p 151 N85-31545
- STRAIN RATE**  
Reliability considerations for the total strain range version of strainrange partitioning [NASA-CR-174757] p 144 N85-11380
- STRATEGIC MATERIALS**  
The B2 aluminides as alternative materials [NASA-TM-86937] p 74 N85-19076
- STRATIFICATION**  
Stratified charge rotary aircraft engine technology enablement program [NASA-CR-174812] p 25 N85-21163
- STRATIFIED FLOW**  
Direct simulations of chemically reacting turbulent mixing layers [AIAA PAPER 85-0321] p 60 A85-19666
- STREAM FUNCTIONS (FLUIDS)**  
Review - Computational methods for internal flows with emphasis on turbomachinery p 4 A85-29126
- STRENGTH**  
Fundamentals of microcrack nucleation mechanics [NASA-CR-3851] p 137 N85-16195
- STRESS ANALYSIS**  
Rational approach for assumed stress finite elements p 139 A85-12029  
Hybrid stress finite elements for large deformations of inelastic solids p 139 A85-15894  
Interply layer degradation effects on composite structural response [AIAA PAPER 84-0849] p 54 A85-16096  
Development and testing of stable, invariant, isoparametric curvilinear 2- and 3-D hybrid-stress elements p 140 A85-19899  
Simplified design and life prediction of rocket thrust chambers p 44 A85-29314  
Evolution of assumed stress hybrid finite element p 142 A85-35046
- Interply layer degradation effects on composite structural response p 55 A85-39215  
Axisymmetric solid elements by a rational hybrid stress method p 143 A85-41109  
A study of interply layer effects on the free edge stress field of angleplyed laminates p 55 A85-41127  
The 3-D inelastic analysis methods for hot section components: Brief description p 20 N85-10972  
A study of interply layer effects on the free-edge stress field of angleplyed laminates [NASA-TM-86924] p 57 N85-15822  
Thermal-stress analysis for a wood composite blade [NASA-CR-174794] p 159 N85-17421  
Advanced stress analysis methods applicable to turbine engine structures [NASA-CR-175573] p 26 N85-21165  
3-D inelastic analysis methods for hot section components (base program) --- turbine blades, turbine vanes, and combustor liners [NASA-CR-174700] p 145 N85-21686  
Component-specific modeling [NASA-CR-174765] p 147 N85-27261  
Effect of speed and press fit on fatigue life of roller-bearing inner-race contact [NASA-TP-2496] p 134 N85-31511  
Thermal stress analysis of a new turbine shroud seal concept [NASA-CR-87082] p 136 N85-34406
- STRESS CONCENTRATION**  
Development and testing of stable, invariant, isoparametric curvilinear 2- and 3-D hybrid-stress elements p 140 A85-19899  
On stress field near a stationary crack tip [AD-A152863] p 141 A85-24532  
On local total strain redistribution using a simplified cyclic inelastic analysis based on an elastic solution [AIAA PAPER 85-1419] p 142 A85-39770  
Fundamentals of microcrack nucleation mechanics [NASA-CR-3851] p 137 N85-16195  
Local strain redistribution corrections for a simplified inelastic analysis procedure based on an elastic finite-element analysis [NASA-TP-2421] p 145 N85-20396  
On local total strain redistribution using a simplified cyclic inelastic analysis based on an elastic solution [NASA-TM-86913] p 145 N85-21690  
On Hybrid and mixed finite element methods [NASA-CR-175551] p 146 N85-23096  
Two simplified procedures for predicting cyclic material response from a strain history p 151 N85-31543
- STRESS CYCLES**  
Two simplified procedures for predicting cyclic material response from a strain history p 151 N85-31543
- STRESS FUNCTIONS**  
Recent advances in hybrid/mixed finite elements [NASA-CR-175574] p 145 N85-21687
- STRESS INTENSITY FACTORS**  
Experimental compliance calibration of the NASA Lewis Research Center Mode 2 fatigue specimen [NASA-TM-86908] p 144 N85-16205
- STRESS MEASUREMENT**  
Deposition stress effects on the life of thermal barrier coatings on burner rigs p 79 A85-19086
- STRESS WAVES**  
Stress waves in an isotropic elastic plate excited by a circular transducer [NASA-CR-3877] p 138 N85-20390  
Application of homomorphic signal processing to stress wave factor analysis [NAS 1.26:174871] p 138 N85-21673  
A study of the stress wave factor technique for the characterization of composite materials [NASA-CR-174870] p 58 N85-30035
- STRESS-STRAIN DIAGRAMS**  
Analysis of stress-strain, fracture, and ductility behavior of aluminum matrix composites containing discontinuous silicon carbide reinforcement p 55 A85-37421  
Constitutive modeling and computational implementation for finite strain plasticity p 143 A85-40910
- STRESS-STRAIN RELATIONSHIPS**  
A simplified method for elastic-plastic-creep structural analysis [ASME PAPER 84-GT-191] p 141 A85-23150  
Plasticity, viscoplasticity, and creep of solids by mechanical subelement models p 142 A85-35048  
Application of two creep fatigue life models for the prediction of elevated temperature crack initiation of a nickel base alloy [AIAA PAPER 85-1420] p 69 A85-43979  
A study of Reynolds-stress closure model [NASA-CR-174342] p 114 N85-17324  
Local strain redistribution corrections for a simplified inelastic analysis procedure based on an elastic finite-element analysis [NASA-TP-2421] p 145 N85-20396
- On thermomechanical testing in support of constitutive equation development for high temperature alloys [NASA-CR-174879] p 147 N85-25894  
Cyclic structural analyses of SSME turbine blades p 150 N85-27963  
Finite element analysis of notch behavior using a state variable constitutive equation p 152 N85-31548  
Component-specific modeling [NASA-CR-174925] p 32 N85-32119  
Hertzian contact in two and three dimensions [NASA-TP-2473] p 135 N85-32331
- STRUCTURAL ANALYSIS**  
Extension of constrained incremental Newton-Raphson scheme to generalized loading fields p 139 A85-13942  
Hybrid Semiloof elements for plates and shells based upon a modified Hu-Washizu principle p 139 A85-15893  
ICAN - Integrated composites analyzer [AIAA PAPER 84-0974] p 54 A85-16094  
Interply layer degradation effects on composite structural response [AIAA PAPER 84-0849] p 54 A85-16096  
Considerations for damage analysis of gas turbine hot section components [ASME PAPER 84-PVP-77] p 14 A85-18792  
On the development of hierarchical solution strategies for nonlinear finite element formulations p 171 A85-21979  
Evolution of assumed stress hybrid finite element p 142 A85-35046  
Interply layer degradation effects on composite structural response p 55 A85-39215  
Unified constitutive material models for nonlinear finite-element structural analysis --- gas turbine engine blades and vanes [AIAA PAPER 85-1418] p 142 A85-39769  
On local total strain redistribution using a simplified cyclic inelastic analysis based on an elastic solution [AIAA PAPER 85-1419] p 142 A85-39770  
Turbine Engine Hot Section Technology (HOST) [NASA-TM-83022] p 18 N85-10951  
Nonlinear structural and life analyses of a turbine blade p 19 N85-10954  
Nonlinear structural and life analyses of a combustor liner p 19 N85-10955  
Component-specific modeling p 20 N85-10971  
The 3-D inelastic analysis methods for hot section components: Brief description p 20 N85-10972  
Constitutive model development for isotropic materials p 20 N85-10975  
Validation of structural analysis methods using the in-house liner cyclic rigs p 21 N85-10987  
Biaxial constitutive equation development for single crystals [NASA-CR-174056] p 183 N85-11862  
Engine cyclic durability by analysis and material testing p 25 N85-15744  
NASA Lewis Research Center/University Graduate Research Program on Engine Structures [NASA-TM-86916] p 145 N85-18375  
Nonlinear analysis for high-temperature multilayered fiber composite structures --- turbine blades [NASA-TM-83754] p 57 N85-21273  
3-D inelastic analysis methods for hot section components (base program) --- turbine blades, turbine vanes, and combustor liners [NASA-CR-174700] p 145 N85-21686  
On local total strain redistribution using a simplified cyclic inelastic analysis based on an elastic solution [NASA-TM-86913] p 145 N85-21690  
Geometrically nonlinear analysis of laminated elastic structures [NASA-CR-175609] p 146 N85-21720  
Raman structural studies of the nickel electrode [NASA-CR-175619] p 183 N85-23414  
Unified constitutive material models for nonlinear finite-element structural analysis --- gas turbine engine blades and vanes [NASA-TM-86985] p 146 N85-24338  
Cyclic structural analyses of anisotropic turbine blades for reusable space propulsion systems --- ssme fuel turbopump [NASA-TM-86990] p 146 N85-24339  
Vibration and buckling of rotating, pretwisted, precone beams including Coriolis effects [NASA-TM-87004] p 146 N85-25893  
Nonlinear structural analysis for fiber-reinforced superalloy turbine blades p 147 N85-26887  
A computer analysis program for interfacing thermal and structural codes [NASA-TM-87021] p 148 N85-27264  
Probabilistic structural analysis theory development p 148 N85-27955  
Probabilistic finite element: Variational theory p 149 N85-27957

- Cyclic structural analyses of SSME turbine blades  
p 150 N85-27963
- Structural analysis and cost estimate of an eight-leg space frame as a support structure for horizontal axis wind turbines  
[NASA-TM-83470] p 150 N85-30361
- Two simplified procedures for predicting cyclic material response from a strain history  
p 151 N85-31543
- STRUCTURAL DESIGN**
- Finite element engine blade structural optimization  
[AIAA PAPER 85-0645] p 141 A85-30313
- Design procedures for fiber composite structural components: Panels subjected to combined in-plane loads  
[NASA-TM-86909] p 57 N85-15823
- Operational results for the experimental DOE/NASA Mod-OA wind turbine project  
[NASA-TM-83517] p 163 N85-30479
- STRUCTURAL DESIGN CRITERIA**
- Design procedures for fiber composite structural components - Rods, beams, and beam columns  
p 54 A85-15636
- Structural optimization using optimality criteria methods  
p 144 A85-48703
- Energy efficient engine combustor test hardware detailed design report  
[NASA-CR-167945] p 18 N85-10950
- Structural analysis  
p 20 N85-10969
- Overview of structural response: Probabilistic structural analysis  
p 148 N85-27952
- STRUCTURAL MEMBERS**
- Viscoplastic constitutive relationships with dependence on thermomechanical history  
[NASA-CR-174836] p 146 N85-21691
- A comparison of smooth specimen and analytical simulation techniques for notched members at elevated temperatures  
p 151 N85-31546
- STRUCTURAL RELIABILITY**
- Overview of structural response: Probabilistic structural analysis  
p 148 N85-27952
- STRUCTURAL STABILITY**
- On the existence and stability conditions for mixed-hybrid finite element solutions based on Reissner's variational principle  
p 142 A85-33847
- Effects of cobalt, boron, and zirconium on the microstructure of Udimet 738  
[NASA-CR-174762] p 70 N85-10166
- STRUCTURAL VIBRATION**
- Vibration and flutter of mistuned bladed-disk assemblies  
[AIAA PAPER 84-0991] p 139 A85-16095
- Natural frequencies of twisted rotating plates  
p 141 A85-32343
- Vibration and flutter of mistuned bladed-disk assemblies  
p 16 A85-45854
- Vibrations of twisted cantilever plates - A comparison of theoretical results  
p 144 A85-47626
- SUBASSEMBLIES**
- Multistage spent particle collector and a method for making same  
[NASA-CASE-LEW-13914-1] p 135 N85-33489
- SUBSONIC AIRCRAFT**
- Energy efficient engine component development and integration program  
[NASA-CR-170034] p 22 N85-10990
- SUBSONIC FLOW**
- Analytical study of blowing boundary layer control for subsonic V/STOL inlets  
p 2 A85-11646
- Sound generation and upstream influence due to instability waves interacting with non-uniform mean flows  
p 174 A85-20738
- SUBSONIC FLUTTER**
- Flutter of turbfan rotors with mistuned blades  
p 139 A85-12716
- SUBSONIC WIND TUNNELS**
- The Altitude Wind Tunnel (AWT) - A unique facility for propulsion system and adverse weather testing  
[AIAA PAPER 85-0314] p 34 A85-19661
- Analytical modeling of circuit aerodynamics in the new NASA Lewis Altitude Wind Tunnel  
[AIAA PAPER 85-0380] p 3 A85-26389
- Analytical modeling of circuit aerodynamics in the new NASA Lewis wind tunnel  
[NASA-TM-86912] p 8 N85-15688
- SUBSTITUTES**
- The B2 aluminides as alternative materials  
[NASA-TM-86937] p 74 N85-19076
- SUBSTRATES**
- Laboratory degradation of Kapton in a low energy oxygen ion beam  
[AIAA PAPER 83-2658] p 78 A85-10675
- Deposition stress effects on the life of thermal barrier coatings on burner rigs  
p 79 A85-19086
- The scattering of ultrasonic third sound from substrate surface defects  
p 174 A85-36047
- Effects of MAR-M247 substrate (modified) composition on coating oxidation coating/substrate interdiffusion --- protective coatings for hot section components of gas turbine engines  
[NASA-CR-174851] p 73 N85-19073
- The structure of ion plated films in relation to coating properties  
[NASA-TM-87055] p 95 N85-29085
- Thermal barrier coating system  
[NASA-CASE-LEW-14057-1] p 59 N85-35233
- SULFATION**
- Molecular orbital studies in oxidation: Sulfate formation and metal-metal oxide adhesion  
[NASA-CR-176070] p 77 N85-32174
- Adsorption of O<sub>2</sub>, SO<sub>2</sub>, and SO<sub>3</sub> on nickel oxide. Mechanism for sulfate formation  
[NASA-CR-176072] p 77 N85-32175
- SULFUR DIOXIDES**
- Mechanism for chelated sulfate formation from SO<sub>2</sub> and bis (triphenylphosphine) platinum  
p 62 A85-48493
- SULFUR OXIDES**
- Effects of SO<sub>2</sub> and SO<sub>3</sub> on the Na<sub>2</sub>SO<sub>4</sub> induced corrosion of nickel  
p 65 A85-15603
- Mechanism for forming hydrogen chloride and sodium sulfate from sulfur trioxide, water, and sodium chloride  
p 62 A85-48513
- Adsorption of O<sub>2</sub>, SO<sub>2</sub>, and SO<sub>3</sub> on nickel oxide. Mechanism for sulfate formation  
[NASA-CR-176072] p 77 N85-32175
- SULFURIC ACID**
- Rapid estimation of concentration of aromatic classes in middistillate fuels by high-performance liquid chromatography  
[NASA-TP-2495] p 93 N85-31307
- SUPERCOMPUTERS**
- General approaches for achieving high speed computations  
p 169 A85-28628
- Functional language and data flow architectures  
p 170 A85-28629
- SUPERCONDUCTORS**
- A rotating superconducting solenoid for 100 kWh energy storage --- in space  
p 44 A85-33144
- SUPERCOOLING**
- Dendritic solidification. I - Analysis of current theories and models. II - A model for dendritic growth under an imposed thermal gradient  
p 182 A85-38019
- SUPERCritical FLOW**
- Nested subcritical flows within supercritical systems  
[NASA-TM-86980] p 115 N85-21574
- SUPERHYBRID MATERIALS**
- Fabrication and quality assurance processes for superhybrid composite fan blades  
[NASA-TM-83354] p 57 N85-14882
- SUPERSONIC AIRCRAFT**
- Supersonic jet shock noise reduction  
[AIAA PAPER 84-2278] p 173 A85-16099
- SUPERSONIC BOUNDARY LAYERS**
- An experimental study of three-dimensional shock wave/turbulent boundary layer interactions in a supersonic flow  
[AIAA PAPER 85-1566] p 5 A85-40691
- SUPERSONIC FLOW**
- Numerical calculation of subsonic jets in crossflow with reduced numerical diffusion  
[AIAA PAPER 85-1441] p 110 A85-39780
- Numerical calculation of subsonic jets in crossflow with reduced numerical diffusion  
[NASA-TM-87003] p 27 N85-25263
- Unsteady flow in a supersonic cascade with two in-passage shocks  
[NASA-CR-3925] p 10 N85-35158
- SUPERSONIC FLUTTER**
- The effect of aerodynamic and structural detuning on turbomachine supersonic unstalled torsional flutter  
[AIAA PAPER 85-0761] p 14 A85-30378
- SUPERSONIC JET FLOW**
- A multiple-scales model of the shock-cell structure of imperfectly expanded supersonic jets  
p 113 A85-49354
- SUPERSONIC SPEEDS**
- Observations from varying the lift and drag inputs to a noise prediction method for supersonic helical tip speed propellers  
[NASA-TM-83797] p 175 N85-10788
- SURFACE COOLING**
- Heat transfer and turbulence measurements of a film-cooled flow over a convexly curved surface  
p 112 A85-41787
- Unsteady heat transfer due to time-dependent free stream velocity  
p 117 N85-27947
- SURFACE DEFECTS**
- The scattering of ultrasonic third sound from substrate surface defects  
p 174 A85-36047
- SURFACE ENERGY**
- Mechanism for chelated sulfate formation from SO<sub>2</sub> and bis (triphenylphosphine) platinum  
p 62 A85-48493
- SURFACE FINISHING**
- Laser balancing system for high material removal rates  
[NASA-CR-174731] p 126 N85-12341
- Textured carbon surfaces on copper  
[NASA-CASE-LEW-14130-1] p 95 N85-20156
- Diamondlike flakes  
[NASA-CASE-LEW-13837-2] p 57 N85-21267
- Ion-beam nitriding of steels  
[NASA-CASE-LEW-14104-1] p 75 N85-21324
- Reliability of void detection in structural ceramics using scanning laser acoustic microscopy  
[NASA-TM-87035] p 138 N85-32337
- SURFACE GEOMETRY**
- Effect of surface configuration during solid particle impingement erosion  
p 69 A85-42568
- SURFACE PROPERTIES**
- Topological reaction rate measurements related to scuffing  
p 64 A85-11070
- Surface hardening of steel by boriding in a cold rf plasma  
p 68 A85-40275
- Effect of five lubricants on life of AISI 9310 spur gears  
[NASA-TP-2419] p 123 N85-16099
- Tribological properties of boron nitride synthesized by ion beam deposition  
[NASA-TM-86962] p 87 N85-21355
- Monte Carlo lattice models for adsorbed polymer conformation  
[NASA-TP-2453] p 183 N85-24961
- Free-surface phenomena under low- and zero-gravity conditions  
[NASA-CR-175835] p 116 N85-27168
- Interaction of high-cycle and low-cycle fatigue of Haynes 188 alloy at 1400 F deg  
p 149 N85-27961
- SURFACE REACTIONS**
- Cathode degradation and erosion in high pressure arc discharges  
p 43 A85-16445
- Mechanical-contact-induced transformation from the amorphous to the partially crystalline state in metallic glass  
p 65 A85-19084
- A morphological study of silicon carbide prepared by chemical vapor deposition  
p 79 A85-20938
- Characterization of erosion of metallic materials under cavitation attack in a mineral oil  
[NASA-TM-86934] p 74 N85-19075
- Three-dimensional calculation of shuttle charging in polar orbit  
p 40 N85-22486
- Effects of surface chemistry on hot corrosion life  
[NASA-CR-174915] p 28 N85-26711
- The role of surface generated radicals in catalytic combustion  
p 30 N85-27869
- SURFACE ROUGHNESS**
- The role of the reflection coefficient in precision measurement of ultrasonic attenuation  
p 137 A85-42151
- An experimental investigation of microstrip properties on soft substrates from 2 to 40 GHz  
[NASA-TM-86961] p 99 N85-20224
- Surface roughness effects in elastohydrodynamic contacts  
[NASA-TP-2488] p 134 N85-32329
- SURFACE TEMPERATURE**
- Analytical fuel property effects: Small combustors, phase 2  
[NASA-CR-174848] p 93 N85-19175
- Fabrication of ceramic substrate-reinforced and free forms  
[NASA-TM-86994] p 50 N85-23926
- SURFACE WAVES**
- Solar energy converter using surface plasma waves  
[NASA-CASE-LEW-13827-1] p 160 N85-21768
- SURFACES**
- Incompressible lifting-surface aerodynamics for a rotor-stator combination  
[NASA-TM-83767] p 7 N85-12039
- SURGES**
- Circuit transients due to negative bias arcs on a high-voltage solar array in low Earth orbit  
[NASA-TP-2407] p 39 N85-14858
- A theory of post-stall transients in multistage axial compression systems  
[NASA-CR-3878] p 8 N85-21117
- SWEEP EFFECT**
- Flutter of swept fan blades  
[ASME PAPER 84-GT-138] p 141 A85-32962
- SWEEP WINGS**
- Computation of three-dimensional viscous flows using a space-marching method  
p 4 A85-29259

**SWIRLING**

- Flow visualization of lateral jet injection into swirling crossflow p 2 A85-19490
- [AIAA PAPER 85-0059]
- Calculation of confined swirling flows p 108 A85-19491
- [AIAA PAPER 85-0060]
- Swirling flows in typical combustor geometries p 108 A85-19574
- [AIAA PAPER 85-0184]
- Jet characteristics in confined swirling flow p 112 A85-45282
- Density effects on jet characteristics in confined swirling flow p 112 A85-45283
- Turbulence characteristics of swirling flowfields [NASA-CR-174918] p 29 N85-26717
- Flow modifying device [NASA-CASE-LEW-13562-2] p 33 N85-35195

**SWITCHES**

- Advanced in solid state switchgear technology for large space power systems p 102 A85-45362
- High-temperature optically activated GaAs power switching for aircraft digital electronic control [NASA-CR-174711] p 34 N85-12901
- A new very high voltage semiconductor switch [NASA-TM-86957] p 103 N85-20246

**SWITCHING**

- High voltage-high power components for large space power distribution systems p 45 A85-45370

**SWITCHING CIRCUITS**

- The NASA satellite communication 20 x 20 matrix switches p 101 A85-14435
- A fast time domain digital simulation technique for power converters - Application to a buck converter with feedforward compensation p 101 A85-20900
- Optical computer switching network p 178 A85-23134
- The J3 SCR model applied to resonant converter simulation p 102 A85-42156

**SYNTHESIS (CHEMISTRY)**

- Ideal gas thermodynamic properties for the phenyl, phenoxy, and o-biphenyl radicals p 184 N85-22204
- [NASA-TM-83800]
- Preparation of silicon carbide-silicon nitride fibers by the pyrolysis of polycarbosilazane precursors [NASA-TM-86505] p 91 N85-28107

**SYNTHETIC RESINS**

- Fundamental studies of composite toughness p 56 N85-12948

**SYSTEM EFFECTIVENESS**

- Mod-2 wind turbine field operations experience p 157 A85-45512
- NASA Redox Storage System Development Project [NASA-TM-83677] p 158 N85-12465
- Transmission efficiency measurements and correlations with physical characteristics of the lubricant p 89 N85-23781

**SYSTEM FAILURES**

- A real-time FORTRAN implementation of a sensor failure detection, isolation and accommodation algorithm p 171 A85-47704

**SYSTEM GENERATED ELECTROMAGNETIC PULSES**

- Electron yields from spacecraft materials p 40 N85-22512

**SYSTEMS ANALYSIS**

- Energy efficient engine. Volume 1: Component development and integration program [NASA-CR-173084] p 22 N85-10992
- Preliminary analysis of space mission applications for electromagnetic launchers [NASA-CR-174067] p 35 N85-12071

**SYSTEMS ENGINEERING**

- The role of modern control theory in the design of controls for aircraft turbine engines p 13 A85-13627
- Status of DOE and AID stand-alone photovoltaic system field tests p 155 A85-35707
- Fatigue criterion to system design, life and reliability [AIAA PAPER 85-1140] p 143 A85-40814
- Combustion system for radiation investigations p 21 N85-10986
- Fatigue criterion to system design, life and reliability [NASA-TM-87017] p 132 N85-27226

**SYSTEMS INTEGRATION**

- An evaluation of oxygen/hydrogen propulsion systems for the Space Station [AIAA PAPER 85-1156] p 45 A85-43976
- An evaluation of oxygen-hydrogen propulsion systems for the Space Station [NASA-TM-87059] p 52 N85-28971

**SYSTEMS SIMULATION**

- Data flow methods for dynamic system simulation - A CSSL-IV microcomputer network interface p 170 A85-28614
- Moving target, distributed, real-time simulation using Ada p 170 A85-34131

**T**

**TAKEOFF**

- Wind tunnel results of advanced high speed propellers in the takeoff, climb, and landing operating regimes [AIAA PAPER 85-1259] p 6 A85-47025
- Wind tunnel results of advanced high speed propellers in the takeoff, climb and landing operating regimes [NASA-TM-87054] p 9 N85-29925

**TANTALUM**

- The effect of tantalum on the structure/properties of two polycrystalline nickel-base superalloys: B-1900 + Hf MAR-M247 [NASA-CR-174847] p 73 N85-18127

**TANTALUM ALLOYS**

- Effects of MAR-M247 substrate (modified) composition on coating oxidation coating/substrate interdiffusion --- protective coatings for hot section components of gas turbine engines [NASA-CR-174851] p 73 N85-19073

**TAPERING**

- Rotordynamic coefficients for compressible flow in tapered annular seals p 129 A85-42573

**TARGET SIMULATORS**

- Moving target, distributed, real-time simulation using Ada p 170 A85-34131

**TECHNOLOGICAL FORECASTING**

- The trend of future gas turbine technology p 16 A85-41778
- PM superalloys - A troubled adolescent? p 69 A85-44772
- Telecommunications forecast for ITU Region 2 to the year 1995 [NASA-TM-87077] p 38 N85-34150

**TECHNOLOGY ASSESSMENT**

- Status of NASA's multibeam communications technology program p 100 A85-14432
- The NASA photovoltaic technology program p 155 A85-35604
- PM superalloys - A troubled adolescent? p 69 A85-44772
- Mod II engine and technology development p 129 A85-45473

- Preliminary analysis of space mission applications for electromagnetic launchers [NASA-CR-174067] p 35 N85-12071
- Missions/planning panel p 36 N85-13886
- Configuration study for a 30 GHz monolithic receive array: Technical assessment [NASA-CR-174697] p 98 N85-18238
- The high voltage silicon cell: A comparative analysis p 49 N85-22569

**Instrumentation technology overview**

- p 124 N85-26903
- The Federal Wind Program at NASA Lewis Research Center [NASA-TM-83480] p 163 N85-30478
- A survey of unified constitutive theories p 150 N85-31531

- Energy Efficient Engine Program technology benefit/cost study, volume 2 [NASA-CR-174766-VOL-2] p 33 N85-35198
- Practical aspects of photovoltaic technology, applications and cost (revised) [NASA-CR-174963] p 165 N85-35472

**TECHNOLOGY TRANSFER**

- Energy efficient engine. Volume 2. Appendix A: Component development and integration program [NASA-CR-173085] p 22 N85-10991

**TECHNOLOGY UTILIZATION**

- Status of DOE and AID stand-alone photovoltaic system field tests p 155 A85-35707
- Progress in the utilization of an oxide-dispersion-strengthened alloy for small engine turbine blades [SAE PAPER 841512] p 68 A85-39284
- Solar dynamic systems p 164 N85-31374
- Energy Efficient Engine Program technology benefit/cost study, volume 1 [NASA-CR-174766-VOL-1] p 33 N85-35197

**TEETH**

- Spiral bevel and circular arc helical gears: Tooth contact analysis and the effect of misalignment on circular arc helical gears [NASA-TM-87013] p 32 N85-31060

**TEFLON (TRADEMARK)**

- An experimental investigation of microstrip properties on soft substrates from 2 to 40 GHz [NASA-TM-86961] p 99 N85-20224

**TELECOMMUNICATION**

- The subjective effect of multiple co-channel frequency modulated television interference p 96 A85-28234
- Satellite provided customer promises services, a forecast of potential domestic demand through the year 2000. Volume 4: Sensitivity analysis [NASA-CR-174662] p 99 N85-27092

**TELEVISION TRANSMISSION**

- An allpass filter design for luminance and chrominance separation of NTSC signals p 102 A85-28230
- The subjective effect of multiple co-channel frequency modulated television interference p 96 A85-28234

**TEMPERATURE**

- Digital temperature and velocity control of mach 0.3 atmospheric pressure durability testing burner rigs in long time, unattended cyclic testing [NASA-TM-86959] p 75 N85-21321

**TEMPERATURE CONTROL**

- Advanced thermal barrier system bond coatings for use on Ni, Co-, and Fe-base alloy substrates [NASA-TM-87062] p 77 N85-31283

**TEMPERATURE DEPENDENCE**

- Heat treatment of bulk gallium arsenide using a phosphosilicate glass cap p 181 A85-32636
- A 37.5-kW point design comparison of the nickel-cadmium battery, bipolar nickel-hydrogen battery, and regenerative hydrogen-oxygen fuel cell energy storage subsystems for low earth orbit p 46 A85-45387
- Orientations and temperature dependence of some mechanical properties of the single-crystal nickel-base superalloy Rene N4. 3: Tension-compression anisotropy [NASA-TM-86982] p 76 N85-22660
- A survey of unified constitutive theories p 150 N85-31531

**TEMPERATURE DISTRIBUTION**

- A comparison of NMC and GWC analysis field temperatures with aircraft measurements p 166 A85-21140
- Manual of phosphoric acid fuel cell stack three-dimensional model and computer program [NASA-CR-174722] p 157 N85-10447
- Dilution jet configurations in a reverse flow combustor [NASA-CR-174888] p 27 N85-22392
- Development of a temperature measurement system with application to a jet in a cross flow experiment [NASA-CR-174896] p 27 N85-25262

**TEMPERATURE EFFECTS**

- An experimental study of tone excited heated jets [AIAA PAPER 84-2341] p 172 A85-10882
- Design procedures for fiber composite structural components - Rods, beams, and beam columns p 54 A85-15636
- The influence of temperature on the lubricating effectiveness of MoS<sub>2</sub> dispersed in mineral oils [ASLE PREPRINT 84-LC-2A-2] p 80 A85-25963
- Oscillatory conductive heat transfer for a fiber in an ideal gas p 109 A85-26077
- Thermal elastohydrodynamic lubrication of line contacts p 128 A85-31202
- Stability of bromine intercalated graphite fibers [NASA-TM-86859] p 84 N85-10187
- Burner rig corrosion of SiC at 1000 deg C [NASA-TM-87061] p 53 N85-30011
- Nonlinear Constitutive Relations for High Temperature Application, 1984 [NASA-CP-2369] p 150 N85-31530
- On the use of internal state variables in thermoviscoplastic constitutive equations p 150 N85-31536

**TEMPERATURE GRADIENTS**

- Temperature distortion generator for turboshaft engine testing [SAE PAPER 841541] p 15 A85-39065
- Dendritic solidification. III - Some further refinements to the model for dendritic growth under an imposed thermal gradient p 69 A85-44703
- Temperature distortion generator for turboshaft engine testing [NASA-TM-83748] p 1 N85-15658
- Comparative analysis of operational forecasts versus actual weather conditions in airline flight planning, volume 4 [NASA-CR-167865] p 167 N85-35537

**TEMPERATURE INVERSIONS**

- Effect of steady-state temperature distortion on inlet flow to a high-bypass-ratio turbofan engine [NASA-TM-86986] p 24 N85-15725

**TEMPERATURE MEASUREMENT**

- Effect of combined pressure and temperature distortion orientation on high-bypass-ratio turbofan engine stability [NASA-TM-83771] p 17 N85-10067
- An interactive computer code for calculation of gas-phase chemical equilibrium (EQLBRM) [NASA-CR-168337] p 18 N85-10948
- Dilution jet configurations in a reverse flow combustor [NASA-CR-174888] p 27 N85-22392
- Development of a temperature measurement system with application to a jet in a cross flow experiment [NASA-CR-174896] p 27 N85-25262
- Measurement and correlation of jet fuel viscosities at low temperatures [NASA-CR-174911] p 94 N85-34295

## TEMPERATURE SENSORS

- Fiber optic temperature sensor p 121 A85-29563  
Fiber optic, Fabry-Perot high temperature sensor  
[NASA-CR-174712] p 178 N85-13594

## TENSILE CREEP

- Morphological changes of gamma prime precipitates in nickel-base superalloy single crystals  
[NASA-TM-83698] p 70 N85-10165

## TENSILE STRENGTH

- Design procedures for fiber composite structural components - Rods, beams, and beam columns p 54 A85-15636  
Effects of tin on microstructure and mechanical behavior of Inconel 718  
[NASA-TM-86866] p 71 N85-12129  
Imide modified epoxy matrix resins  
[NASA-CR-174695] p 85 N85-15892  
Effects of chromium and aluminum on mechanical and oxidation properties of iron-nickel-base superalloys based on CG-27  
[NASA-TP-2443] p 75 N85-21323  
Environmental effects on the tensile strength of chemically vapor deposited silicon carbide fibers  
[NASA-TM-86981] p 89 N85-24000

## TENSILE STRESS

- Orientation and temperature dependence of some mechanical properties of the single-crystal nickel-base superalloy Rene N4. 3: Tension-compression anisotropy  
[NASA-TM-86982] p 76 N85-22660  
A continuous damage model based on stepwise-stress creep rupture tests  
[NASA-CR-174941] p 152 N85-32341

## TENSILE TESTS

- Deformation and fracture behavior of Ni-Mo-Al(gamma/gamma prime-alpha) in situ composite p 64 A85-11058  
Fracture toughness of hot-pressed beryllium p 66 A85-25835  
Mechanical property measurements of plasma-sprayed thermal-barrier coatings subjected to oxidation p 81 A85-29729  
Constitutive modeling and computational implementation for finite strain plasticity p 143 A85-40910

- Graphite/PMR polyimide composites with improved toughness  
[NASA-TM-87081] p 58 N85-32148

## TENSOR ANALYSIS

- Alternatives for jet engine control  
[NASA-CR-175831] p 29 N85-26713  
Alternatives for jet engine control  
[NASA-CR-175832] p 29 N85-26714  
Alternatives for jet engine control  
[NASA-CR-175833] p 29 N85-26715

## TERNARY ALLOYS

- High temperature properties of equiatomic FeAl with ternary additions  
[NASA-TM-86938] p 73 N85-19072

## TERNARY SYSTEMS

- High temperature properties of equiatomic FeAl with ternary additions  
[NASA-TM-86938] p 73 N85-19072  
A study of interdiffusion in beta + gamma/gamma + gamma prime Ni-Cr-Al  
[NASA-CR-174852] p 74 N85-20041

## TEST EQUIPMENT

- Flame flashback in a premixed dump combustor  
[AIAA PAPER 85-0145] p 60 A85-19550  
Cryogenic upper stage test bed engine  
[AIAA PAPER 85-1339] p 44 A85-39733  
The design and analysis of single flank transmission error test for loaded gears  
[NASA-CR-176163] p 136 N85-34404

## TEST FACILITIES

- HOST liner cyclic facilities: Facility description p 22 N85-10988  
Heat transfer results and operational characteristics of the NASA Lewis Research Center Hot Section Cascade Test Facility  
[NASA-TM-86890] p 114 N85-15133

## TEST STANDS

- HOST liner cyclic facilities: Facility description p 22 N85-10988  
The design and analysis of single flank transmission error test for loaded gears  
[NASA-CR-176163] p 136 N85-34404

## TEST VEHICLES

- Energy efficient engine ICLS Nacelle detail design report  
[NASA-CR-167870] p 22 N85-10993

## TETHERING

- Report of the Constellations Panel p 131 N85-20368

- Preliminary assessment of power-generating tethers in space and of propulsion for their orbit maintenance p 37 N85-22520

## TETRAHYDROFURAN

- Development of a lithium secondary battery separator p 104 N85-31378

## TF-34 ENGINE

- TF34 convertible engine control system design p 15 A85-32006  
Nonlinear global stability analysis of compressor stall phenomena  
[NASA-CR-174908] p 31 N85-29960

## THERMAL ANALYSIS

- Energy efficient engine combustor test hardware detailed design report  
[NASA-CR-167945] p 18 N85-10950  
Applications of high pressure differential scanning calorimetry to aviation fuel thermal stability research  
[NASA-TM-87002] p 63 N85-23941

## THERMAL BUCKLING

- Quasi-static solution algorithms for kinematically/materially nonlinear thermomechanical problems p 143 A85-41983

## THERMAL CONTROL COATINGS

- Oxidation-based model for thermal barrier coating life p 78 A85-10310  
Life modeling of atmospheric and low pressure plasma-sprayed thermal-barrier coating p 81 A85-29728  
Mechanical property measurements of plasma-sprayed thermal-barrier coatings subjected to oxidation p 81 A85-29729  
Failure during thermal cycling of plasma-sprayed thermal barrier coatings p 81 A85-36246  
Optimization of the NiCrAl-Y/ZrO<sub>2</sub>-Y<sub>2</sub>O<sub>3</sub> thermal barrier system  
[NASA-TM-86905] p 72 N85-15878  
An investigation of enhanced capability thermal barrier coating systems for diesel engine components  
[NASA-CR-174820] p 86 N85-18154  
Rocket thrust chamber thermal barrier coatings p 90 N85-26867  
Advanced thermal barrier system bond coatings for use on Ni, Co, and Fe-base alloy substrates  
[NASA-TM-87062] p 77 N85-31283  
Energy efficient engine, high pressure turbine thermal barrier coating. Support technology report  
[NASA-CR-168037] p 34 N85-35199

## THERMAL CYCLING TESTS

- Simplified design and life prediction of rocket thrust chambers p 44 A85-29314  
Failure during thermal cycling of plasma-sprayed thermal barrier coatings p 81 A85-36246  
HOST instrumentation R and D program overview p 19 N85-10957  
Validation of structural analysis methods using the in-house liner cyclic rigs p 21 N85-10987  
HOST liner cyclic facilities: Facility description p 22 N85-10988  
Rocket thrust chamber thermal barrier coatings p 90 N85-26867

## THERMAL DECOMPOSITION

- Metallic and metal/ceramic coating by thermal decomposition  
[NASA-TM-86992] p 88 N85-22755

## THERMAL DEGRADATION

- Liquid phase products and solid deposit formation from thermally stressed model jet fuels  
[NASA-TM-86874] p 92 N85-13066  
Laboratory studies of Kapton degradation in an oxygen ion beam p 177 N85-22477

## THERMAL DISSOCIATION

- Jet fuel property changes and their effect on producibility and cost in the U.S., Canada, and Europe  
[NASA-CR-174840] p 93 N85-27012

## THERMAL EXPANSION

- Extreme precision antenna reflector study results p 165 N85-23830

## THERMAL FATIGUE

- A study of fatigue damage mechanisms in Waspaloy from 25 to 800 C p 65 A85-12098  
Considerations for damage analysis of gas turbine hot section components  
[ASME PAPER 84-PVP-77] p 14 A85-18792  
Engine cyclic durability by analysis and material testing p 25 N85-15744  
Thermal-mechanical fatigue crack growth in Inconel X-750 p 72 N85-15877  
Analytical and experimental investigation of rubbing interaction in labyrinth seals for a liquid hydrogen fuel pump - space shuttle main engine  
[NASA-CR-174657] p 48 N85-18084

## THERMAL NEUTRONS

- Apparatus and method for identification of matrix materials in which transuranic elements are embedded using thermal neutron capture gamma-ray emission  
[DE85-011659] p 125 N85-33454

## THERMAL NOISE

- The influence of combustion liner holes on noise production by ducted burners  
[AIAA PAPER 84-2322] p 172 A85-10869  
Adaptive antenna arrays for weak interfering signals  
[NASA-CR-174336] p 98 N85-17258

## THERMAL PROTECTION

- Electron beam charging of Space Shuttle thermal protection system tiles p 39 N85-22478

## THERMAL RESISTANCE

- Performance of thermal barrier coatings in high heat flux environments p 79 A85-19087  
An experimental investigation and numerical prediction of thermomechanical phenomena in high speed rotor tip rubbing p 14 A85-25442

## Thermal barrier coating system

- [NASA-CASE-LEW-13324-2] p 57 N85-21266

## THERMAL SHOCK

- Dispersed-metal-toughened alumina  
[NASA-CR-174687] p 89 N85-22758

## THERMAL STABILITY

- Stability of bromine intercalated graphite fibers  
[NASA-TM-86859] p 84 N85-10187  
External fuel vaporization study, phase 2  
[NASA-CR-174079] p 92 N85-11252  
Study of advanced fuel system concepts for commercial aircraft and engines  
[NASA-CR-174752] p 93 N85-19176  
Applications of high pressure differential scanning calorimetry to aviation fuel thermal stability research  
[NASA-TM-87002] p 63 N85-23941  
Graphite/PMR polyimide composites with improved toughness  
[NASA-TM-87081] p 58 N85-32148

## THERMAL STRESSES

- Liquid phase products and solid deposit formation from thermally stressed model jet fuels  
[NASA-TM-86874] p 92 N85-13066  
Thermal-stress analysis for a wood composite blade  
[NASA-CR-174794] p 159 N85-17421  
Thermal stress analysis of a new turbine shroud seal concept  
[NASA-TM-87082] p 136 N85-34406

## THERMIONIC POWER GENERATION

- High thermal power density heat transfer apparatus providing electrical isolation at high temperature using heat pipes  
[NASA-CASE-LEW-12950-2] p 117 N85-29179  
Thermionic photovoltaic energy converter  
[NASA-CASE-LEW-14077-1] p 164 N85-34441

## THERMOCOUPLE PYROMETERS

- Thin-film sensors for space propulsion technology p 41 N85-27968

## THERMOCOUPLES

- High temperature thermocouple and heat flux gauge using a unique thin film-hardware hot junction  
[NASA-TM-86898] p 123 N85-16096  
Advanced thin film thermocouples  
[NASA-CR-175541] p 124 N85-21607  
Development of a temperature measurement system with application to a jet in a cross flow experiment  
[NASA-CR-174896] p 27 N85-25262

## THERMODYNAMIC CYCLES

- Initial testing of a variable-stroke Stirling engine  
[NASA-TM-86875] p 185 N85-19895

## THERMODYNAMIC EFFICIENCY

- Overview of NASA Lewis Research Center free-piston Stirling engine activities p 130 A85-45479

## THERMODYNAMIC EQUILIBRIUM

- An interactive computer code for calculation of gas-phase chemical equilibrium (EQLBRM)  
[NASA-CR-168337] p 18 N85-10948

## THERMODYNAMIC PROPERTIES

- ICAN - Integrated composites analyzer  
[AIAA PAPER 84-0974] p 54 A85-16094  
Combustion gas properties I-ASTM jet A fuel and dry air  
[NASA-TP-2359] p 17 N85-10064  
Computer program for calculation of complex chemical equilibrium compositions and applications. Supplement 1: Transport properties  
[NASA-TM-86885] p 184 N85-16663  
Chemical approach for controlling nadimide cure temperature and rate  
[NASA-CASE-LEW-13770-5] p 87 N85-21352  
Ideal gas thermodynamic properties for the phenyl, phenoxy, and o-biphenyl radicals  
[NASA-TM-83800] p 184 N85-22204  
On thermomechanical testing in support of constitutive equation development for high temperature alloys  
[NASA-CR-174879] p 147 N85-25894



- Computer program for the calculation of multicomponent convective diffusion deposition rates from chemically frozen boundary layer theory  
[NASA-CR-168329] p 116 N85-27164
- Design and lubrication of high-speed rolling-element bearings  
[NASA-TM-87107] p 137 N85-34409
- THERMODYNAMICS**  
Statistics and thermodynamics of fracture  
p 140 A85-19433
- Review - Computational methods for internal flows with emphasis on turbomachinery  
p 4 A85-29126
- Thermodynamically consistent constitutive equations for nonisothermal large strain, elasto-plastic, creep behavior  
[AIAA PAPER 85-0621] p 142 A85-38425
- Viscoplastic constitutive relationships with dependence on thermomechanical history  
[NASA-CR-174836] p 146 N85-21691
- Analytical fuel property effects--small combustors  
[NASA-CR-174738] p 28 N85-26709
- Dynamic creep buckling: Analysis of shell structures subjected to time-dependent mechanical and thermal loading  
p 149 N85-27959
- Designing for fiber composite structural durability in hydrothermomechanical environment  
[NASA-TM-87045] p 58 N85-27978
- THERMOELASTICITY**  
Quasi-static solution algorithms for kinematically/materially nonlinear thermomechanical problems  
p 143 A85-41983
- Translational and extensional energy release rates (the J- and M-integrals) for a crack layer in thermoelasticity  
[NASA-CR-174872] p 145 N85-21685
- A review of path-independent integrals in elastic-plastic fracture mechanics, task 4  
[NASA-CR-174956] p 152 N85-33541
- THERMOGRAVIMETRY**  
Applications of high pressure differential scanning calorimetry to aviation fuel thermal stability research  
[NASA-TM-87002] p 63 N85-23941
- THERMOMECHANICAL TREATMENT**  
Select fiber composites for space applications - A mechanistic assessment  
p 54 A85-16040
- Quasi-static solution algorithms for kinematically/materially nonlinear thermomechanical problems  
p 143 A85-41983
- Analysis of shell type structures subjected to time dependent mechanical and thermal loading  
[NASA-CR-175747] p 147 N85-25896
- Multiaxial and thermomechanical fatigue considerations in damage tolerant design  
[NASA-TM-87022] p 76 N85-26964
- Thermomechanical deformation in the presence of metallurgical changes  
p 150 N85-31533
- THERMOPHYSICAL PROPERTIES**  
Thermal and thermomechanical effects in dry sliding  
p 127 A85-23838
- Nested subcritical flows within supercritical systems  
[NASA-TM-86980] p 115 N85-21574
- THERMOPLASTICITY**  
Spherical microglass particle impingement studies of thermoplastic materials at normal incidence  
p 79 A85-11072
- Nonlinear structural and life analyses of a combustor liner  
p 19 N85-10955
- THIN FILMS**  
Frictional and morphological properties of Au-MoS<sub>2</sub> films sputtered from a compact target  
p 127 A85-19085
- Computer simulation of thin film nucleation and growth  
p 181 A85-35308
- Properties of coated and modified surfaces  
p 53 A85-36694
- 'Diamondlike' carbon films - Optical absorption, dielectric properties, and hardness dependence on deposition parameters  
p 82 A85-40383
- Hot corrosion of sintered alpha-SiC at 1000 C  
[ACS PAPER 19-B-84P] p 83 A85-45302
- Monte Carlo study of reversible growth of clusters on a surface  
p 182 A85-48516
- Analysis of glow discharges for understanding the process of film formation  
[NASA-TM-83750] p 62 N85-10138
- High temperature thermocouple and heat flux gauge using a unique thin film hardware hot junction  
[NASA-TM-86898] p 123 N85-16096
- Deposition of diamondlike carbon films  
[NASA-CASE-LEW-14080-1] p 95 N85-20153
- A computer simulation of thin film nucleation and growth: The Volmer-Weber case  
[NASA-TM-86968] p 53 N85-21264
- Advanced thin film thermocouples  
[NASA-CR-175541] p 124 N85-21607
- Mass spectra of neutral particles released during electrical breakdown of thin polymer films  
p 88 N85-22511
- Thin-film sensors for space propulsion technology  
p 41 N85-27968
- The structure of ion plated films in relation to coating properties  
[NASA-TM-87055] p 95 N85-29085
- Ion beam sputter-deposited thin film coatings for protection of spacecraft polymers in low Earth orbit  
[NASA-TM-87051] p 91 N85-30137
- Mechanical protection of DLC films on fused silica slides  
[NASA-TM-87056] p 91 N85-30138
- Advances in sputtered and ion plated solid film lubrication  
p 136 N85-33524
- THIN WALLED SHELLS**  
Fabrication of ceramic substrate-reinforced and free forms  
[NASA-TM-86994] p 50 N85-23926
- Dynamic creep buckling: Analysis of shell structures subjected to time-dependent mechanical and thermal loading  
p 149 N85-27959
- THIOLS**  
Formation of high molecular weight products from benzene during boundary lubrication  
[NASA-TM-86966] p 62 N85-22644
- THREE DIMENSIONAL BODIES**  
Recent advances in hybrid/mixed finite elements  
[NASA-CR-175574] p 145 N85-21687
- THREE DIMENSIONAL BOUNDARY LAYER**  
A three-dimensional boundary-layer analysis including heat-transfer and blade-rotation effects  
p 6 A85-42988
- THREE DIMENSIONAL FLOW**  
Development of finite analysis method for unsteady three-dimensional Navier-Stokes equation  
p 106 A85-11647
- A finite element solution of three-dimensional inviscid rotational flows through curved ducts  
p 107 A85-11648
- Three-dimensional inviscid flow analysis of turbofan forced mixers  
[AIAA PAPER 85-0086] p 2 A85-19510
- Computation of three-dimensional viscous flows using a space-marching method  
p 4 A85-29259
- Calculation of three-dimensional, viscous flow through turbomachinery blade passages by parabolic marching  
[AIAA PAPER 85-1408] p 5 A85-39767
- An experimental study of three-dimensional shock wave/turbulent boundary layer interactions in a supersonic flow  
[AIAA PAPER 85-1566] p 5 A85-40691
- Calculation of compressible flow about three-dimensional inlets with auxiliary inlets, slats and vanes by means of a panel method  
[AIAA PAPER 85-1196] p 5 A85-40817
- The three-dimensional compressible flow in a radial inflow turbine scroll  
p 6 A85-41826
- Inviscid analysis of advanced turboprop propeller flow fields  
[AIAA PAPER 85-1263] p 6 A85-43977
- Calculation of three-dimensional, viscous flow through turbomachinery blade passages by parabolic marching  
[NASA-TM-86984] p 9 N85-23711
- Turbulence characteristics of swirling flowfields  
[NASA-CR-174918] p 29 N85-26717
- Fuel and oxidizer turbine loss analysis  
p 50 N85-26900
- Redistribution of the inlet temperature profile through the SSME fuel turbine  
p 50 N85-26901
- Unsteady flow in a supersonic cascade with two in-passage shocks  
[NASA-CR-3925] p 10 N85-35158
- General design method for 3-dimensional, potential flow fields. Part 2: Computer program DIN3D1 for simple, unbranched ducts  
[NASA-CR-3926] p 10 N85-35159
- THRUST**  
Energy efficient engine ICLS engine bearings, drives and configuration: Detail design report  
[NASA-CR-167871] p 23 N85-10997
- THRUST CHAMBERS**  
Simplified design and life prediction of rocket thrust chambers  
p 44 A85-29314
- Extended performance technology study 30-cm thruster  
[NASA-CR-168259] p 48 N85-15806
- THRUST MEASUREMENT**  
Vacuum chamber pressure effects on thrust measurements of low Reynolds number nozzles  
[NASA-TM-86955] p 49 N85-21259
- THRUST VECTOR CONTROL**  
Altitude testing of a flight weight, self-cooled, 2D thrust vectoring exhaust nozzle  
[SAE PAPER 841557] p 14 A85-25984
- THRUSTORS**  
IAPS (8-cm) ion thruster cyclic endurance test -- Ion Auxiliary Propulsion System  
p 42 A85-16406
- Ring-cusp ion thrusters  
p 42 A85-16438
- Experiments with a microwave electrothermal thruster concept  
p 42 A85-16441
- THYRISTORS**  
High-voltage, high-power, solid-state remote power controllers for aerospace applications  
[NASA-TP-2437] p 49 N85-21263
- TILES**  
Electron beam charging of Space Shuttle thermal protection system tiles  
p 39 N85-22478
- TIME CONSTANT**  
Development of a temperature measurement system with application to a jet in a cross flow experiment  
[NASA-CR-174896] p 27 N85-25262
- TIME DEPENDENCE**  
Time dependent wave envelope finite difference analysis of sound propagation  
[AIAA PAPER 84-2285] p 173 A85-16102
- Some advances in experimentation supporting development of viscoplastic constitutive models  
[NASA-CR-174855] p 147 N85-27260
- Some advances in experimentation supporting development of viscoplastic constitutive models  
p 151 N85-31545
- TIME DIVISION MULTIPLE ACCESS**  
The NASA satellite communication 20 x 20 matrix switches  
p 101 A85-14435
- Advanced 30/20 GHz multiple beam antenna for future communications satellites  
p 96 A85-14436
- Modeling of NASA's 30/20 GHz satellite communications system  
p 38 A85-36663
- TIME MARCHING**  
Application of Runge Kutta time marching scheme for the computation of transonic flows in turbomachines  
[AIAA PAPER 85-1332] p 5 A85-39728
- Thermodynamic evaluation of transonic compressor rotors using the finite volume approach  
[NASA-CR-175811] p 29 N85-26712
- TIME MEASUREMENT**  
Characterization of microstrip discontinuities in the time and frequency domains  
[NASA-CR-176190] p 106 N85-35342
- TIME SERIES ANALYSIS**  
Identification of multivariable high-performance turbofan engine dynamics from closed-loop data  
p 13 A85-13630
- Numerical considerations in the development and implementation of constitutive models  
p 151 N85-31541
- TIN**  
Effects of tin on microstructure and mechanical behavior of Inconel 718  
[NASA-TM-86866] p 71 N85-12129
- TIP DRIVEN ROTORS**  
Performance comparison between NACA 23024 and NACA 64(3)-618 airfoil configured rotors for horizontal-axis wind turbines  
[NASA-TM-83471] p 163 N85-30477
- TIP SPEED**  
Shutdown characteristics of the Mod-O wind turbine with aileron controls  
[NASA-TM-86918] p 159 N85-16289
- Study of controlled diffusion stator blading  
[NASA-CR-167895] p 25 N85-18058
- Further comparison of wind tunnel and airplane acoustic data for advanced design high speed propeller models  
[NASA-TM-86935] p 176 N85-22108
- Energy efficient engine. Fan and quarter-stage component performance report  
[NASA-CR-168070] p 33 N85-34141
- TITANIUM**  
Nitriding of titanium and its alloys by N<sub>2</sub>, NH<sub>3</sub> or mixtures of N<sub>2</sub> + H<sub>2</sub> in a dc arc plasma at low pressures ( or = to torr)  
[NASA-TM-83803] p 131 N85-15168
- TITANIUM ALLOYS**  
Metallurgical and mechanical phenomena due to rubbing of titanium against sintered powder Nichrome  
p 127 A85-22281
- An experimental investigation of rubbing interaction in labyrinth seals at cryogenic temperature  
p 129 A85-39938
- Effect of low temperature on fatigue and fracture properties of Ti-5Al-2.5Sn(ELI) for use in engine components  
p 70 A85-47972
- Nitriding of titanium and its alloys by N<sub>2</sub>, NH<sub>3</sub> or mixtures of N<sub>2</sub> + H<sub>2</sub> in a dc arc plasma at low pressures ( or = to torr)  
[NASA-TM-83803] p 131 N85-15168
- CO adsorption on (111) and (100) surfaces of the Pt sub 3 Ti alloy. Evidence for parallel binding and strong activation of CO  
[NASA-CR-176077] p 77 N85-32176

**TOLERANCES (MECHANICS)**

Multiaxial and thermomechanical fatigue considerations in damage tolerant design  
[NASA-TM-87022] p 76 N85-26964

**TORQUE**

Application of traction drives as servo mechanisms  
p 152 N85-33520

**TORSION**

Application of traction drives as servo mechanisms  
p 152 N85-33520

**TORSIONAL STRESS**

Constitutive modeling and computational implementation for finite strain plasticity  
p 143 A85-40910

**TORSIONAL VIBRATION**

Flutter of turbofan rotors with mistuned blades  
p 139 A85-12716

Effects of warping and pretwist on torsional vibration of rotating beams  
[ASME PAPER 84-WA/APM-41] p 140 A85-17040

The effect of aerodynamic and structural detuning on turbomachine supersonic unstalled torsional flutter  
[AIAA PAPER 85-0761] p 14 A85-30378

Finite difference analysis of torsional vibrations of pretwisted, rotating, cantilever beams with effects of warping  
p 143 A85-42047

Optimization of cascade blade mistuning. I - Equations of motion and basic inherent properties  
p 16 A85-42365

Optimization of cascade blade mistuning. II - Global optimum and numerical optimization  
p 16 A85-45715

Precision tunable resonant microwave cavity  
[NASA-CASE-LEW-13935-1] p 103 N85-20248

Hygrothermomechanical evaluation of transverse filament tape epoxy/polyester fiberglass composites  
p 54 A85-15632

Plasma variables and tribological properties of coatings in low pressure (0.1 - 10.0 torr) plasma systems  
[NASA-TM-83798] p 94 N85-11261

Tribological properties of graphite-fiber-reinforced, partially fluorinated polyimide composites  
[NASA-TM-86926] p 86 N85-18153

The role of silver in self-lubricating coatings for use at extreme temperatures  
[NASA-TM-86943] p 87 N85-20127

Tribological properties of boron nitride synthesized by ion beam deposition  
[NASA-TM-86962] p 87 N85-21355

Tribological systems as applied to aircraft engines  
[NASA-TM-86965] p 131 N85-21657

Effect of counterface material type and its topography on the tribological properties of polyimide composites  
[NASA-TM-87036] p 90 N85-26993

Hertzian contact in two and three dimensions  
[NASA-TP-2473] p 135 N85-32331

Aluminum work function: Effect of oxidation, mechanical scraping and ion bombardment  
[NASA-TM-87079] p 78 N85-34265

Textured carbon surfaces on copper  
[NASA-CASE-LEW-14130-1] p 95 N85-20156

Flame radiation and linear heat transfer in a tubular-can combustor  
p 15 A85-39580

Apparatus for producing diamond-like carbon flakes  
[NASA-CASE-LEW-13837-3] p 95 N85-20155

Vibration and flutter of mistuned bladed-disk assemblies  
[AIAA PAPER 84-0991] p 139 A85-16095

The effect of aerodynamic and structural detuning on turbomachine supersonic unstalled torsional flutter  
[AIAA PAPER 85-0761] p 14 A85-30378

Optimization of cascade blade mistuning. I - Equations of motion and basic inherent properties  
p 16 A85-42365

Optimization of cascade blade mistuning. II - Global optimum and numerical optimization  
p 16 A85-45715

Precision tunable resonant microwave cavity  
[NASA-CASE-LEW-13935-1] p 103 N85-20248

Hygrothermomechanical evaluation of transverse filament tape epoxy/polyester fiberglass composites  
p 54 A85-15632

Plasma variables and tribological properties of coatings in low pressure (0.1 - 10.0 torr) plasma systems  
[NASA-TM-83798] p 94 N85-11261

Tribological properties of graphite-fiber-reinforced, partially fluorinated polyimide composites  
[NASA-TM-86926] p 86 N85-18153

The role of silver in self-lubricating coatings for use at extreme temperatures  
[NASA-TM-86943] p 87 N85-20127

Tribological properties of boron nitride synthesized by ion beam deposition  
[NASA-TM-86962] p 87 N85-21355

Tribological systems as applied to aircraft engines  
[NASA-TM-86965] p 131 N85-21657

Effect of counterface material type and its topography on the tribological properties of polyimide composites  
[NASA-TM-87036] p 90 N85-26993

Hertzian contact in two and three dimensions  
[NASA-TP-2473] p 135 N85-32331

Aluminum work function: Effect of oxidation, mechanical scraping and ion bombardment  
[NASA-TM-87079] p 78 N85-34265

Textured carbon surfaces on copper  
[NASA-CASE-LEW-14130-1] p 95 N85-20156

Flame radiation and linear heat transfer in a tubular-can combustor  
p 15 A85-39580

Apparatus for producing diamond-like carbon flakes  
[NASA-CASE-LEW-13837-3] p 95 N85-20155

Vibration and flutter of mistuned bladed-disk assemblies  
[AIAA PAPER 84-0991] p 139 A85-16095

The effect of aerodynamic and structural detuning on turbomachine supersonic unstalled torsional flutter  
[AIAA PAPER 85-0761] p 14 A85-30378

Optimization of cascade blade mistuning. I - Equations of motion and basic inherent properties  
p 16 A85-42365

Optimization of cascade blade mistuning. II - Global optimum and numerical optimization  
p 16 A85-45715

Precision tunable resonant microwave cavity  
[NASA-CASE-LEW-13935-1] p 103 N85-20248

Hygrothermomechanical evaluation of transverse filament tape epoxy/polyester fiberglass composites  
p 54 A85-15632

Plasma variables and tribological properties of coatings in low pressure (0.1 - 10.0 torr) plasma systems  
[NASA-TM-83798] p 94 N85-11261

Tribological properties of graphite-fiber-reinforced, partially fluorinated polyimide composites  
[NASA-TM-86926] p 86 N85-18153

The role of silver in self-lubricating coatings for use at extreme temperatures  
[NASA-TM-86943] p 87 N85-20127

Tribological properties of boron nitride synthesized by ion beam deposition  
[NASA-TM-86962] p 87 N85-21355

Tribological systems as applied to aircraft engines  
[NASA-TM-86965] p 131 N85-21657

**TRANSFER ORBITS**

Radiation exposure and performance of multiple burn LEO-GEO orbit transfer trajectories  
[NASA-TM-86946] p 36 N85-21228

Manrating orbital transfer vehicle propulsion  
[NASA-TM-87019] p 50 N85-25385

Primary propulsion of electrothermal, ion and chemical systems for space-based radar orbit transfer  
[NASA-TM-87043] p 51 N85-27972

**TRANSFORMERS**

Development of high frequency low weight power magnetics for aerospace power systems  
p 102 A85-45373

Developments in space power components for power management and distribution  
p 47 N85-13877

Analysis of shell type structures subjected to time dependent mechanical and thermal loading  
[NASA-CR-175747] p 147 N85-25896

Analysis of shell type structures subjected to time dependent mechanical and thermal loading  
[NASA-CR-175747] p 147 N85-25896

Analysis of shell type structures subjected to time dependent mechanical and thermal loading  
[NASA-CR-175747] p 147 N85-25896

Analysis of shell type structures subjected to time dependent mechanical and thermal loading  
[NASA-CR-175747] p 147 N85-25896

Analysis of shell type structures subjected to time dependent mechanical and thermal loading  
[NASA-CR-175747] p 147 N85-25896

Analysis of shell type structures subjected to time dependent mechanical and thermal loading  
[NASA-CR-175747] p 147 N85-25896

Analysis of shell type structures subjected to time dependent mechanical and thermal loading  
[NASA-CR-175747] p 147 N85-25896

Analysis of shell type structures subjected to time dependent mechanical and thermal loading  
[NASA-CR-175747] p 147 N85-25896

Analysis of shell type structures subjected to time dependent mechanical and thermal loading  
[NASA-CR-175747] p 147 N85-25896

Analysis of shell type structures subjected to time dependent mechanical and thermal loading  
[NASA-CR-175747] p 147 N85-25896

Analysis of shell type structures subjected to time dependent mechanical and thermal loading  
[NASA-CR-175747] p 147 N85-25896

Analysis of shell type structures subjected to time dependent mechanical and thermal loading  
[NASA-CR-175747] p 147 N85-25896

Analysis of shell type structures subjected to time dependent mechanical and thermal loading  
[NASA-CR-175747] p 147 N85-25896

Analysis of shell type structures subjected to time dependent mechanical and thermal loading  
[NASA-CR-175747] p 147 N85-25896

Analysis of shell type structures subjected to time dependent mechanical and thermal loading  
[NASA-CR-175747] p 147 N85-25896

Analysis of shell type structures subjected to time dependent mechanical and thermal loading  
[NASA-CR-175747] p 147 N85-25896

Analysis of shell type structures subjected to time dependent mechanical and thermal loading  
[NASA-CR-175747] p 147 N85-25896

Analysis of shell type structures subjected to time dependent mechanical and thermal loading  
[NASA-CR-175747] p 147 N85-25896

Analysis of shell type structures subjected to time dependent mechanical and thermal loading  
[NASA-CR-175747] p 147 N85-25896

Analysis of shell type structures subjected to time dependent mechanical and thermal loading  
[NASA-CR-175747] p 147 N85-25896

Analysis of shell type structures subjected to time dependent mechanical and thermal loading  
[NASA-CR-175747] p 147 N85-25896

Analysis of shell type structures subjected to time dependent mechanical and thermal loading  
[NASA-CR-175747] p 147 N85-25896

Analysis of shell type structures subjected to time dependent mechanical and thermal loading  
[NASA-CR-175747] p 147 N85-25896

Analysis of shell type structures subjected to time dependent mechanical and thermal loading  
[NASA-CR-175747] p 147 N85-25896

Analysis of shell type structures subjected to time dependent mechanical and thermal loading  
[NASA-CR-175747] p 147 N85-25896

Analysis of shell type structures subjected to time dependent mechanical and thermal loading  
[NASA-CR-175747] p 147 N85-25896

Analysis of shell type structures subjected to time dependent mechanical and thermal loading  
[NASA-CR-175747] p 147 N85-25896

Analysis of shell type structures subjected to time dependent mechanical and thermal loading  
[NASA-CR-175747] p 147 N85-25896

Analysis of shell type structures subjected to time dependent mechanical and thermal loading  
[NASA-CR-175747] p 147 N85-25896

Analysis of shell type structures subjected to time dependent mechanical and thermal loading  
[NASA-CR-175747] p 147 N85-25896

Analysis of shell type structures subjected to time dependent mechanical and thermal loading  
[NASA-CR-175747] p 147 N85-25896

Analysis of shell type structures subjected to time dependent mechanical and thermal loading  
[NASA-CR-175747] p 147 N85-25896

Analysis of shell type structures subjected to time dependent mechanical and thermal loading  
[NASA-CR-175747] p 147 N85-25896

Analysis of shell type structures subjected to time dependent mechanical and thermal loading  
[NASA-CR-175747] p 147 N85-25896

Analysis of shell type structures subjected to time dependent mechanical and thermal loading  
[NASA-CR-175747] p 147 N85-25896

Analysis of shell type structures subjected to time dependent mechanical and thermal loading  
[NASA-CR-175747] p 147 N85-25896

Analysis of shell type structures subjected to time dependent mechanical and thermal loading  
[NASA-CR-175747] p 147 N85-25896

Analysis of shell type structures subjected to time dependent mechanical and thermal loading  
[NASA-CR-175747] p 147 N85-25896

Analysis of shell type structures subjected to time dependent mechanical and thermal loading  
[NASA-CR-175747] p 147 N85-25896

Analysis of shell type structures subjected to time dependent mechanical and thermal loading  
[NASA-CR-175747] p 147 N85-25896

Analysis of shell type structures subjected to time dependent mechanical and thermal loading  
[NASA-CR-175747] p 147 N85-25896

Analysis of shell type structures subjected to time dependent mechanical and thermal loading  
[NASA-CR-175747] p 147 N85-25896

Analysis of shell type structures subjected to time dependent mechanical and thermal loading  
[NASA-CR-175747] p 147 N85-25896

Analysis of shell type structures subjected to time dependent mechanical and thermal loading  
[NASA-CR-175747] p 147 N85-25896

Analysis of shell type structures subjected to time dependent mechanical and thermal loading  
[NASA-CR-175747] p 147 N85-25896

Analysis of shell type structures subjected to time dependent mechanical and thermal loading  
[NASA-CR-175747] p 147 N85-25896

Analysis of shell type structures subjected to time dependent mechanical and thermal loading  
[NASA-CR-175747] p 147 N85-25896

Analysis of shell type structures subjected to time dependent mechanical and thermal loading  
[NASA-CR-175747] p 147 N85-25896

- The effect of aerodynamic and structural detuning on turbomachine supersonic unstalled torsional flutter [AIAA PAPER 85-0761] p 14 A85-30378
- Development of coated single-crystal superalloy systems for gas turbine applications p 68 A85-32440
- A note on blade wake interaction influence on compressor stator row aerodynamic performance p 4 A85-32965
- Progress in the utilization of an oxide-dispersion-strengthened alloy for small engine turbine blades [SAE PAPER 841512] p 68 A85-39284
- Unified constitutive material models for nonlinear finite-element structural analysis --- gas turbine engine blades and vanes [AIAA PAPER 85-1418] p 142 A85-39769
- Heat transfer investigation in the junction region of circular cylinder normal to a flat plate at 90 deg location [ASME PAPER 84-WA/HT-70] p 111 A85-39898
- Effect of surface configuration during solid particle impingement erosion p 69 A85-42568
- Photoacoustic microscopy of ceramic turbine blades p 83 A85-43930
- The effect of channel convergence on heat transfer in a passage with short pin fins [NASA-TM-83801] p 113 N85-10303
- Nonlinear structural and life analyses of a turbine blade p 19 N85-10954
- Studies on the hot corrosion of a nickel-base superalloy, Udimet 700 [NASA-TM-86882] p 71 N85-11224
- Preliminary results of a study of the relationship between free stream turbulence and stagnation region heat transfer [NASA-TM-86884] p 113 N85-11317
- Materials for advanced turbine engines. Project 2: Rene 150 directionally solidified superalloy turbine blades, volume 2 [NASA-CR-167993] p 23 N85-12059
- Thermal-stress analysis for a wood composite blade [NASA-CR-174794] p 159 N85-17421
- Replaceable blade turbine and stationary specimen corrosion testing facility [NASA-TM-86931] p 73 N85-18126
- Nonlinear analysis for high-temperature multilayered fiber composite structures --- turbine blades [NASA-TM-83754] p 57 N85-21273
- Unified constitutive material models for nonlinear finite-element structural analysis --- gas turbine engine blades and vanes [NASA-TM-86985] p 146 N85-24338
- Cyclic structural analyses of anisotropic turbine blades for reusable space propulsion systems --- ssme fuel turbopump [NASA-TM-86990] p 146 N85-24339
- Nonlinear structural analysis for fiber-reinforced superalloy turbine blades p 147 N85-26887
- Redistribution of the inlet temperature profile through the SSME fuel turbine p 50 N85-26901
- Reusable rocket engine turbopump condition monitoring p 51 N85-26907
- Cyclic structural analyses of SSME turbine blades p 150 N85-27963
- Preliminary results of a study of the relationship between free-stream turbulence and stagnation region heat transfer p 118 N85-31435
- Component-specific modeling [NASA-CR-174925] p 32 N85-32119
- Local heat-transfer measurements on a large, scale-model turbine blade airfoil using a composite of a heater element and liquid crystals [NASA-TM-86900] p 119 N85-33435
- TURBINE ENGINES**
- The role of modern control theory in the design of controls for aircraft turbine engines p 13 A85-13627
- A generalized computer code for developing dynamic gas turbine engine models (DIGTEM) p 17 A85-49021
- Chemistry of fuel deposits and sediments and their precursors [NASA-CR-174778] p 92 N85-10209
- HOST instrumentation R and D program overview p 19 N85-10957
- Hot section laser anemometry p 19 N85-10962
- Turbine heat transfer p 19 N85-10964
- Life prediction and constitutive behavior: Overview p 20 N85-10973
- Combustion system for radiation investigations p 21 N85-10986
- Validation of structural analysis methods using the in-house liner cyclic rigs p 21 N85-10987
- HOST liner cyclic facilities: Facility description p 22 N85-10988
- Energy efficient engine. Low pressure turbine test hardware detailed design report [NASA-CR-167956] p 22 N85-10994
- Materials for advanced turbine engines. Project 2: Rene 150 directionally solidified superalloy turbine blades, volume 2 [NASA-CR-167993] p 23 N85-12059
- Design description of a microprocessor based Engine Monitoring and Control unit (EMAC) for small turboshaft [NASA-TM-86860] p 1 N85-17935
- Experimental and analytical study of ceramic-coated turbine-tip shroud seals for small turbine engines [NASA-TM-86881] p 25 N85-18057
- Advanced stress analysis methods applicable to turbine engine structures [NASA-CR-175573] p 26 N85-21165
- New facility to study unsteady wake effects on turbine airfoil heat transfer p 117 N85-27948
- Component-specific modeling [NASA-CR-174925] p 32 N85-32119
- Energy efficient engine, high pressure turbine thermal barrier coating. Support technology report [NASA-CR-168037] p 34 N85-35199
- TURBINE INSTRUMENTS**
- A real-time FORTRAN implementation of a sensor failure detection, isolation and accommodation algorithm p 171 A85-47704
- TURBINE PUMPS**
- Application of viscous and inviscid computation methods for rocket turbopump systems [SAE PAPER 841522] p 110 A85-39257
- Reusable rocket engine turbopump condition monitoring [SAE PAPER 841619] p 44 A85-39267
- Cyclic structural analyses of anisotropic turbine blades for reusable space propulsion systems --- ssme fuel turbopump [NASA-TM-86990] p 146 N85-24339
- Preliminary results on passive eddy current damper technology for SSME turbomachinery p 132 N85-26890
- Analytical study of flow phenomena in SSME turnaround duct geometries p 116 N85-26902
- Reusable rocket engine turbopump condition monitoring p 51 N85-26907
- SSME fuel preburner two-dimensional analysis p 51 N85-27943
- Cyclic structural analyses of SSME turbine blades p 150 N85-27963
- TURBINE WHEELS**
- Properties and microstructures for dual alloy combinations of three superalloys with alloy 901 [NASA-TM-86987] p 76 N85-26963
- Unsteady heat transfer due to time-dependent free stream velocity p 117 N85-27947
- TURBINES**
- Assessment of three-dimensional inviscid codes and loss calculations for turbine aerodynamic computations [ASME PAPER 84-GT-187] p 4 A85-32961
- The three-dimensional compressible flow in a radial inflow turbine scroll p 6 A85-41826
- Energy efficient engine high pressure turbine ceramic shroud support technology report [NASA-CR-168036] p 23 N85-10996
- Fuel and oxidizer turbine loss analysis p 50 N85-26900
- Combustor turbulence p 118 N85-31434
- Heat transfer in aeropropulsion systems [NASA-TM-87066] p 119 N85-31444
- TURBOCOMPRESSORS**
- Energy efficient engine component development and integration program [NASA-CR-170034] p 22 N85-10990
- A theory of post-stall transients in multistage axial compression systems [NASA-CR-3878] p 8 N85-21117
- Simulation of multistage turbine flows p 116 N85-27945
- TURBOFAN AIRCRAFT**
- Aerodynamic detuning analysis of an unstalled supersonic turbofan cascade [NASA-TM-87001] p 9 N85-26670
- TURBOFAN ENGINES**
- Identification of multivariable high-performance turbofan engine dynamics from closed-loop data p 13 A85-13630
- Three-dimensional inviscid flow analysis of turbofan forced mixers [AIAA PAPER 85-0086] p 2 A85-19510
- TF34 convertible engine control system design p 15 A85-32006
- Transient technique for measuring heat transfer coefficients on stator airfoils in a jet engine environment [AIAA PAPER 85-1471] p 122 A85-39796
- Stall recovery control strategy methodology and results [AIAA PAPER 85-1433] p 16 A85-40841
- The trend of future gas turbine technology p 16 A85-41778
- Effect of combined pressure and temperature distortion orientation on high-bypass-ratio turbofan engine stability [NASA-TM-83771] p 17 N85-10067
- Energy efficient engine. Volume 1: Component development and integration program [NASA-CR-173084] p 22 N85-10992
- Energy efficient engine ICLS engine bearings, drives and configuration: Detail design report [NASA-CR-167871] p 23 N85-10997
- Turbofan noise generation. Volume 2: Computer programs [NASA-CR-167952] p 175 N85-11791
- Static jet noise test results of four 0.35 scale-model QCGAT mixer nozzles [NASA-TM-86871] p 175 N85-13551
- Effect of steady-state temperature distortion on inlet flow to a high-bypass-ratio turbofan engine [NASA-TM-86896] p 24 N85-15725
- Performance and surge limits of a TF30-P-3 turbofan engine/axisymmetric mixed-compression inlet propulsion system at Mach 2.5 [NASA-TP-2461] p 27 N85-25261
- Transient technique for measuring heat transfer coefficients on stator airfoils in a jet engine environment [NASA-TM-87005] p 124 N85-25794
- DEAN: A program for dynamic engine analysis [NASA-TM-87033] p 30 N85-28945
- Energy efficient engine component development and integration program [NASA-CR-172846] p 31 N85-29958
- Energy Efficient Engine Program technology benefit/cost study, volume 1 [NASA-CR-174766-VOL-1] p 33 N85-35197
- Energy Efficient Engine Program technology benefit/cost study, volume 2 [NASA-CR-174766-VOL-2] p 33 N85-35198
- TURBOFANS**
- Vibration and flutter of mistuned bladed-disk assemblies [AIAA PAPER 84-0991] p 139 A85-16095
- Electro-impulse de-icing of a turbofan engine inlet [AIAA PAPER 85-1118] p 12 A85-40811
- Energy efficient engine component development and integration program [NASA-CR-170034] p 22 N85-10990
- Turbofan noise generation. Volume 2: Computer programs [NASA-CR-167952] p 175 N85-11791
- Structural response of a rotating bladed disk to rotor whirl [NASA-CR-175605] p 27 N85-22391
- Energy efficient engine. Fan and quarter-stage component performance report [NASA-CR-168070] p 33 N85-34141
- TURBOGENERATORS**
- Conceptual design of a fixed-pitch wind turbine generator system rated at 400 kilowatts [NASA-CR-174877] p 162 N85-29363
- TURBOJET ENGINE CONTROL**
- Stall recovery control strategy methodology and results [AIAA PAPER 85-1433] p 16 A85-40841
- TURBOJET ENGINES**
- Transient technique for measuring heat transfer coefficients on stator airfoils in a jet engine environment [AIAA PAPER 85-1471] p 122 A85-39796
- The trend of future gas turbine technology p 16 A85-41778
- Experimental study of ceramic coated tip seals for turbojet engines [NASA-TM-86939] p 114 N85-19363
- Transient technique for measuring heat transfer coefficients on stator airfoils in a jet engine environment [NASA-TM-87005] p 124 N85-25794
- TURBOMACHINE BLADES**
- Flutter of turbofan rotors with mistuned blades p 139 A85-12716
- Vibration and flutter of mistuned bladed-disk assemblies [AIAA PAPER 84-0991] p 139 A85-16095
- Vibration and flutter of mistuned bladed-disk assemblies p 16 A85-45854
- Vibrations of twisted cantilever plates - A comparison of theoretical results p 144 A85-47626
- Model equation for simulating flows in multistage turbomachinery [NASA-TM-86869] p 7 N85-12036
- An improved computer model for prediction of axial gas turbine performance losses [NASA-CR-174246] p 24 N85-15724
- A study of internal and distributed damping for vibrating turbomachinery blades [NASA-CR-175901] p 30 N85-27868
- Unsteady heat transfer due to time-dependent free stream velocity p 117 N85-27947

- Composite loads spectra for select space propulsion structural components p 148 N85-27953
- TURBOMACHINERY**
- Computation of viscous flows in turbomachinery cascades p 106 A85-11631
- Application of Runge Kutta time marching scheme for the computation of transonic flows in turbomachines [AIAA PAPER 85-1332] p 5 A85-39728
- Inviscid and viscous flows in cascades with an explicit multiple-grid algorithm p 7 A85-48539
- Advanced blade tip seal system, volume 2 [NASA-CR-167851] p 23 N85-10999
- Model equation for simulating flows in multistage turbomachinery [NASA-TM-86869] p 7 N85-12036
- Rotordynamic Instability Problems in High-Performance Turbomachinery [NASA-CP-2338] p 131 N85-14116
- The use of an optical data acquisition system for bladed disk vibration analysis [NASA-TM-86891] p 144 N85-15184
- Analysis of experimental shaft seal data for high-performance turbomachines, as for Space Shuttle main engines [NASA-TM-86928] p 115 N85-21569
- Future directions in aeropropulsion technology [NASA-TM-87010] p 1 N85-23685
- Simulation of multistage turbine flows p 116 N85-27945
- TURBOPROP AIRCRAFT**
- Inviscid analysis of advanced turboprop propeller flow fields [AIAA PAPER 85-1263] p 6 A85-43977
- Observations from varying the lift and drag inputs to a noise prediction method for supersonic helical tip speed propellers [NASA-TM-83797] p 175 N85-10788
- TURBOPROP ENGINES**
- Large-scale advanced propfan (LAP) program progress report [AIAA PAPER 85-1187] p 17 A85-47021
- Wind tunnel results of advanced high speed propellers in the takeoff, climb, and landing operating regimes [AIAA PAPER 85-1259] p 6 A85-47025
- Analytical fuel property effects: Small combustors, phase 2 [NASA-CR-174848] p 93 N85-19175
- Fatigue life analysis of a turboprop reduction gearbox [NASA-TM-87014] p 133 N85-27228
- Wind tunnel results of advanced high speed propellers in the takeoff, climb and landing operating regimes [NASA-TM-87054] p 9 N85-29925
- Large-scale Advanced Propfan (LAP) program [NASA-TM-87067] p 32 N85-29964
- TURBOSHAFTS**
- TF34 convertible engine control system design p 15 A85-32006
- Dual clearance squeeze film damper for high load conditions [ASME PAPER 84-TRIB-7] p 128 A85-32960
- Temperature distortion generator for turboshaft engine testing [SAE PAPER 841541] p 15 A85-39065
- Temperature distortion generator for turboshaft engine testing [NASA-TM-83748] p 1 N85-15658
- TURBULENCE**
- The structure of dilute combusting sprays [NASA-CR-174838] p 24 N85-15728
- Transition in Turbines [NASA-CP-2386] p 118 N85-31433
- Preliminary results of a study of the relationship between free-stream turbulence and stagnation region heat transfer p 118 N85-31435
- Flat-plate transition p 118 N85-31438
- TURBULENCE METERS**
- Heat transfer and turbulence measurements of a film-cooled flow over a convexly curved surface p 112 A85-41787
- TURBULENCE BOUNDARY LAYER**
- An experimental study of three-dimensional shock wave/turbulent boundary layer interactions in a supersonic flow [AIAA PAPER 85-1566] p 5 A85-40691
- Heat transfer and turbulence measurements of a film-cooled flow over a convexly curved surface p 112 A85-41787
- Thermodynamic evaluation of transonic compressor rotors using the finite volume approach [NASA-CR-175811] p 29 N85-26712
- Transition in Turbines [NASA-CP-2386] p 118 N85-31433
- TURBULENCE FLOW**
- The influence of combustion liner holes on noise production by ducted burners [AIAA PAPER 84-2322] p 172 A85-10869

- Prediction of an axisymmetric combustor flow p 59 A85-12713
- Computation and turbulence closure models for shear flows in rotating curved bodies p 107 A85-14349
- Mass and momentum turbulent transport experiments with confined coaxial jets p 107 A85-14399
- Accelerated convergence for incompressible flow calculations [AIAA PAPER 85-0058] p 2 A85-19489
- Swirling flows in typical combustor geometries [AIAA PAPER 85-0184] p 108 A85-19574
- Drop-turbulence interactions in a diffusion flame [AIAA PAPER 85-0319] p 60 A85-19665
- Turbulence modelling for complex shear flows [AIAA PAPER 85-1652] p 111 A85-40752
- Combustion efficiency of a premixed continuous flow combustor p 61 A85-42571
- Jet characteristics in confined swirling flow p 112 A85-45282
- Internal combustion engine combustion chamber process studies at NASA Lewis Research Center p 112 A85-45856
- Measurements and predictions of the structure of evaporating sprays p 112 A85-46484
- A review and analysis of boundary layer transition data for turbine application [NASA-TM-86880] p 113 N85-10306
- Accelerated convergence for incompressible flow calculations [NASA-TM-86863] p 18 N85-10949
- Preliminary results of a study of the relationship between free stream turbulence and stagnation region heat transfer [NASA-TM-86884] p 113 N85-11317
- A three-dimensional axisymmetric calculation procedure for turbulent flows in a radial vaneless diffuser [NASA-TM-86903] p 7 N85-14798
- Investigation of flowfields found in typical combustor geometries [NASA-CR-3869] p 26 N85-21167
- The influence of jet-grid turbulence on heat transfer from the stagnation region of a cylinder in crossflow [NASA-TM-87011] p 115 N85-25760
- Thermodynamic evaluation of transonic compressor rotors using the finite volume approach [NASA-CR-175811] p 29 N85-26712
- Confined turbulent swirling recirculating flow predictions [NASA-CR-174917] p 29 N85-26716
- Turbulence characteristics of swirling flowfields [NASA-CR-174918] p 29 N85-26717
- Turbulent transport and length scale measurement experiments with confined coaxial jets [NASA-CR-174831] p 117 N85-30245
- Combustor turbulence p 118 N85-31434
- Heat transfer and fluid mechanics measurements in transitional boundary layer flows p 118 N85-31439
- A review and analysis of boundary layer transition data for turbine application p 118 N85-31440
- Turbulent solutions of equations of fluid motion p 118 N85-31441
- TURBULENCE HEAT TRANSFER**
- Heat transfer enhancement in channels with turbulence promoters [ASME PAPER 84-WA/HT-72] p 111 A85-39900
- TURBULENCE JETS**
- A two-equation turbulence model for two-phase jets p 107 A85-14376
- Flow visualization of lateral jet injection into swirling crossflow [AIAA PAPER 85-0059] p 2 A85-19490
- Calculation of confined swirling flows [AIAA PAPER 85-0060] p 108 A85-19491
- Structure of particle-laden jets - Measurements and predictions p 109 A85-25137
- Structure of ducted particle-laden turbulent jets p 110 A85-38999
- Turbulence measurements of lateral jet injection into confined tubular crossflow [AIAA PAPER 85-1102] p 110 A85-39604
- Jet characteristics in confined swirling flow p 112 A85-45282
- Deflected jet experiments in a turbulent combustor flowfield [NASA-CR-174863] p 26 N85-22390
- Behavior of turbulent gas jets in an axisymmetric confinement [NASA-CR-174829] p 28 N85-25265
- TURBULENCE MIXING**
- Direct simulations of chemically reacting turbulent mixing layers [AIAA PAPER 85-0321] p 60 A85-19666
- A theoretical prediction of the acoustic pressure generated by turbulence-flame front interactions [ASME PAPER 84-WA/NCA-11] p 174 A85-39909

- The performance of jet noise suppression devices for industrial applications p 175 A85-42563
- Behavior of turbulent gas jets in an axisymmetric confinement [NASA-CR-174829] p 28 N85-25265
- TURBULENCE WAKES**
- Development of a rotor wake-vortex model, volume 1 [NASA-CR-174849] p 9 N85-26668
- New facility to study unsteady wake effects on turbine airfoil heat transfer p 117 N85-27948
- TWISTING**
- Vibrations of twisted cantilevered plates - Summary of previous and current studies p 140 A85-22069
- Natural frequencies of twisted rotating plates p 141 A85-32343
- Finite difference analysis of torsional vibrations of pretwisted, rotating, cantilever beams with effects of warping p 143 A85-42047
- Vibrations of twisted cantilever plates - A comparison of theoretical results p 144 A85-47626
- TWO DIMENSIONAL FLOW**
- Resonance in flows with vortex sheets and edges p 1 A85-10357
- Two-dimensional internal compressible viscous flows using semi-elliptic analysis p 106 A85-11640
- The linear two-dimensional stability of inviscid vortex streets of finite-cored vortices [AD-A153032] p 107 A85-14241
- Assessment of discretization schemes to reduce numerical diffusion in the calculation of complex flows [AIAA PAPER 85-0441] p 108 A85-19751
- Vortex induced lift on a flat plate with a curved forward-facing flap p 4 A85-30175
- Time dependent computation of the Euler equations for designing 2-D cascades, including the case of transonic shock free design p 5 A85-41814
- Unsteady flow in a supersonic cascade with two in-passage shocks [NASA-CR-3925] p 10 N85-35158
- TWO PHASE FLOW**
- A two-equation turbulence model for two-phase jets p 107 A85-14376
- A stagnation pressure probe for droplet-laden air flow [AIAA PAPER 85-0330] p 108 A85-19672
- Structure of particle-laden jets - Measurements and predictions p 109 A85-25137
- Structure of ducted particle-laden turbulent jets p 110 A85-38999
- Structure of nonevaporating sprays. I - Initial conditions and mean properties p 112 A85-48538
- TWO REFLECTOR ANTENNAS**
- The 20 GHz proof-of-concept test model results for a multiple scan beam dual reflector antenna [NASA-CR-174268] p 98 N85-15944
- TWO-WAVELENGTH LASERS**
- Two-frequency laser-induced fluorescence technique for rapid velocity-field measurements in gas flows p 121 A85-32294

## U

- UDIMET ALLOYS**
- The substitution of nickel for cobalt in hot isostatically pressed powder metallurgy UDIMET 700 alloys p 68 A85-37415
- The response of cobalt-free Udimet 700 type alloy to modified heat treatments [NASA-TM-86942] p 75 N85-20043
- ULTRASONIC RADIATION**
- Ultrasonic wave propagation in two-phase media - Spherical inclusions p 54 A85-11926
- The scattering of ultrasonic third sound from substrate surface defects p 174 A85-36047
- ULTRASONIC TESTS**
- Ultrasonic nondestructive evaluation, microstructure, and mechanical property interrelations [NASA-TM-86876] p 137 N85-10371
- Application of homomorphic signal processing to stress wave factor analysis [NAS 1.26:174871] p 138 N85-21673
- ULTRASONICS**
- The role of the reflection coefficient in precision measurement of ultrasonic attenuation p 137 A85-42151
- Stress waves in an isotropic elastic plate excited by a circular transducer [NASA-CR-3877] p 138 N85-20390
- Ultrasonic testing of plates containing edge cracks [NASA-CR-3904] p 138 N85-29307
- Reliability of void detection in structural ceramics using scanning laser acoustic microscopy [NASA-TM-87035] p 138 N85-32337

## UNIQUENESS THEOREM

- Constructive existence and uniqueness for two-point boundary-value problems with a linear gradient term p 172 A85-28015

## UNIVERSITIES

- NASA Lewis Research Center/University Graduate Research Program on Engine Structures [NASA-TM-86916] p 145 N85-18375

## UNSTEADY FLOW

- Development of finite analytic method for unsteady three-dimensional Navier-Stokes equation p 106 A85-11647
- A linearized unsteady aerodynamic analysis for transonic cascades p 3 A85-20744
- Combined influence of unsteady free stream velocity and free stream turbulence on stagnation point heat transfer p 112 A85-41782
- New facility to study unsteady wake effects on turbine airfoil heat transfer p 117 N85-27948
- Unsteady flow in a supersonic cascade with two in-passage shocks [NASA-CR-3925] p 10 N85-35158

## UPPER ATMOSPHERE

- MERIT: A man/computer data management and enhancement system for upper air nowcasting/forecasting in the United States -- Minimum Energy Routes using Interactive Techniques (MERIT) p 167 N85-10558

## UPPER STAGE ROCKET ENGINES

- Cryogenic upper stage test bed engine [AIAA PAPER 85-1339] p 44 A85-39733
- Shuttle/Centaur project perspective p 37 N85-16991

## USER MANUALS (COMPUTER PROGRAMS)

- Manual of phosphoric acid fuel cell power plant optimization model and computer program [NASA-CR-174721] p 157 N85-10445
- Operating system for a real-time multiprocessor propulsion system simulator. User's manual [NASA-TP-2426] p 171 N85-17596
- Real-Time Multiprocessor Programming Language (RTMPL) user's manual [NASA-TP-2422] p 170 N85-28610

## USER REQUIREMENTS

- Shuttle/Centaur project perspective p 37 N85-16991

## UTILITIES

- Experimental investigation of a variable speed constant frequency electric generating system from a utility perspective [NASA-CR-174950] p 105 N85-32251

## UTILIZATION

- Space Station propulsion - The Advanced Development Program at Lewis [AIAA PAPER 85-1154] p 44 A85-39626
- Space station propulsion: The advanced development program at Lewis [NASA-TM-86999] p 50 N85-25386

## V

## V/STOL AIRCRAFT

- Analytical study of blowing boundary layer control for subsonic V/STOL inlets p 2 A85-11646

## VACUUM APPARATUS

- Metal vapor arc switch electromagnetic accelerator technology [NASA-CR-174380] p 103 N85-18259

## VACUUM DEPOSITION

- Apparatus for producing diamond-like carbon flakes [NASA-CASE-LEW-13837-3] p 95 N85-20155
- Diamondlike flakes [NASA-CASE-LEW-13837-2] p 57 N85-21267
- Advances in sputtered and ion plated solid film lubrication p 136 N85-33524

## VANELESS DIFFUSERS

- A three-dimensional axisymmetric calculation procedure for turbulent flows in a radial vaneless diffuser [NASA-TM-86903] p 7 N85-14798

## VANES

- Studies on the hot corrosion of a nickel-base superalloy, Udmet 700 [NASA-TM-86882] p 71 N85-11224
- Preliminary results of a study of the relationship between free stream turbulence and stagnation region heat transfer [NASA-TM-86884] p 113 N85-11317
- Replaceable blade turbine and stationary specimen corrosion testing facility [NASA-TM-86931] p 73 N85-18126
- Effects of vane/blade ratio and spacing on fan noise, volume 1 [NASA-CR-174664] p 176 N85-19791
- Effects of vane/blade ratio and spacing on fan noise, Volume 2: Data supplement [NASA-CR-174665] p 176 N85-19792

- Preliminary results of a study of the relationship between free-stream turbulence and stagnation region heat transfer p 118 N85-31435

## VAPOR DEPOSITION

- Magnesium doping of efficient GaAs and Ga(0.75)In(0.25)As solar cells grown by metalorganic chemical vapor deposition p 180 A85-11466
- A morphological study of silicon carbide prepared by chemical vapor deposition p 79 A85-20938
- Fabrication of p(+)-n junction GaAs solar cells by a novel method p 181 A85-33645
- 'Diamondlike' carbon films - Optical absorption, dielectric properties, and hardness dependence on deposition parameters p 82 A85-40383
- Polarization (ellipsometric) measurements of liquid condensate deposition and evaporation rates and dew points in flowing salt/ash-containing combustion gases p 123 A85-46925
- Creep of chemically vapor deposited SiC fibers [NASA-TM-86897] p 56 N85-14878
- Environmental effects on the tensile strength of chemically vapor deposited silicon carbide fibers [NASA-TM-86981] p 89 N85-24000
- Computer program for the calculation of multicomponent convective diffusion deposition rates from chemically frozen boundary layer theory [NASA-CR-168329] p 116 N85-27164

## VAPOR PHASES

- CREKID: A computer code for transient, gas-phase combustion of kinetics [NASA-TM-83806] p 17 N85-10068

## VAPOR PRESSURE

- Metal vapor arc switch electromagnetic accelerator technology [NASA-CR-174380] p 103 N85-18259

## VARIATIONAL PRINCIPLES

- Rational approach for assumed stress finite elements p 139 A85-12029
- On Hybrid and mixed finite element methods [NASA-CR-175551] p 146 N85-23096

## VARIATIONS

- Probabilistic finite element: Variational theory p 149 N85-27957

## VELOCITY

- Digital temperature and velocity control of mach 0.3 atmospheric pressure durability testing burner rigs in long time, unattended cyclic testing [NASA-TM-86959] p 75 N85-21321
- Design and lubrication of high-speed rolling-element bearings [NASA-TM-87107] p 137 N85-34409

## VELOCITY DISTRIBUTION

- Phase/doppler spray analyzer for simultaneous measurements of drop size and velocity distributions p 120 A85-10035
- Dilution jet configurations in a reverse flow combustor [NASA-CR-174888] p 27 N85-22392
- Feasibility of mapping velocity flow fields in SSME powerhead by laser anemometry techniques p 41 N85-27971
- Generation of capillary instabilities by external disturbances in a liquid jet [NASA-TM-87041] p 117 N85-30246

## VELOCITY MEASUREMENT

- Nonintrusive optical single-particle counter for measuring the size and velocity of droplets in a spray p 120 A85-16794
- Structure of particle-laden jets - Measurements and predictions p 109 A85-25137
- Two-frequency laser-induced fluorescence technique for rapid velocity-field measurements in gas flows p 121 A85-32294
- Hot section laser anemometry p 19 N85-10962
- Dilution jet configurations in a reverse flow combustor [NASA-CR-174888] p 27 N85-22392
- Velocity visualization in gaseous flows [NASA-CR-174954] p 119 N85-31445

## VENTURI TUBES

- A unified relation for cavitation erosion p 109 A85-24445

## VERTICAL TAKEOFF AIRCRAFT

- TF34 convertible engine control system design p 15 A85-32006

## VERY HIGH FREQUENCIES

- Alternatives for satellite sound broadcast systems at HF and VHF p 99 N85-23815

## VIBRATION

- Internal hysteresis experienced on a high pressure syn gas compressor p 131 N85-14122
- Flow dynamic environment data base development for the SSME p 147 N85-26885
- Generated spiral bevel gears: Optimal machine-tool settings and tooth contact analysis [NASA-TM-87075] p 136 N85-34405

- Nonlinear flap-lag-extensional vibrations of rotating, pretwisted, precone beams including Coriolis effects [NASA-TM-87102] p 152 N85-34427

## VIBRATION DAMPING

- Dual clearance squeeze film damper for high load conditions [ASME PAPER 84-TRIB-7] p 128 A85-32960
- Variable friction secondary seal for face seals [NASA-CASE-LEW-14170-1] p 131 N85-20377
- Preliminary results on passive eddy current damper technology for SSME turbomachinery p 132 N85-26890
- A study of internal and distributed damping for vibrating turbomachinery blades [NASA-CR-175901] p 30 N85-27868
- Vibration control of rotor shaft [NASA-TM-87053] p 133 N85-29292
- Variable force, eddy-current or magnetic damper [NASA-CASE-LEW-13717-1] p 134 N85-30333

## VIBRATION ISOLATORS

- Preliminary results on passive eddy current damper technology for SSME turbomachinery p 132 N85-26890

- Variable force, eddy-current or magnetic damper [NASA-CASE-LEW-13717-1] p 134 N85-30333

## VIBRATION MODE

- The use of an optical data acquisition system for bladed disk vibration analysis [NASA-TM-86891] p 144 N85-15184

## VIBRATIONAL SPECTRA

- Investigation on experimental techniques to detect, locate and quantify gear noise in helicopter transmissions [NASA-CR-3847] p 176 N85-17667

## VISCOPLASTICITY

- Plasticity, viscoplasticity, and creep of solids by mechanical subelement models p 142 A85-35048
- Thermodynamically consistent constitutive equations for nonisothermal large strain, elasto-plastic, creep behavior [AIAA PAPER 85-0621] p 142 A85-38425
- Viscoplastic constitutive relationships with dependence on thermomechanical history [NASA-CR-174836] p 146 N85-21691
- On thermomechanical testing in support of constitutive equation development for high temperature alloys [NASA-CR-174879] p 147 N85-25894
- Some advances in experimentation supporting development of viscoplastic constitutive models [NASA-CR-174855] p 147 N85-27260
- Nonlinear Constitutive Relations for High Temperature Application, 1984 [NASA-CP-2369] p 150 N85-31530
- On the use of internal state variables in thermoviscoplastic constitutive equations p 150 N85-31536
- Some advances in experimentation supporting development of viscoplastic constitutive models p 151 N85-31545

## VISCOSITY

- A numerical study of the steady scalar convective diffusion equation for small viscosity p 107 A85-16533
- External fuel vaporization study, phase 2 [NASA-CR-174079] p 92 N85-11252
- Measurement and correlation of jet fuel viscosities at low temperatures [NASA-CR-174911] p 94 N85-34295

## VISCOUS DAMPING

- An analysis of temperature effect in a finite journal bearing with spatial tilt and viscous dissipation p 126 A85-11074
- Effects of friction dampers on aerodynamically unstable rotor stages p 14 A85-21866

## VISCOUS FLOW

- Computation of viscous flows in turbomachinery cascades p 106 A85-11631
- Comparison of secondary flows predicted by a viscous code and an inviscid code with experimental data for a turning duct p 106 A85-11634
- Two-dimensional internal compressible viscous flows using semi-elliptical analysis p 106 A85-11640
- Analytical modeling of circuit aerodynamics in the new NASA Lewis Altitude Wind Tunnel [AIAA PAPER 85-0380] p 3 A85-26389
- Review - Computational methods for internal flows with emphasis on turbomachinery p 4 A85-29126
- Computation of three-dimensional viscous flows using a space-marching method p 4 A85-29259
- A note on blade wake interaction influence on compressor stator row aerodynamic performance p 4 A85-32965
- Application of viscous and inviscid computation methods for rocket turbopump systems [SAE PAPER 841522] p 110 A85-39257

## W

## WAVE REFLECTION

- Application of homomorphic signal processing to stress wave factor analysis  
[NAS 1.26:174871] p 138 N85-21673

## WAVEGUIDES

- MMIC devices for active phased array antennas  
[NASA-CR-174281] p 98 N85-15943  
Design of low loss helix circuits for interference fitted and brazed circuits  
[NASA-CR-168313] p 103 N85-19328  
Numerical methods for analyzing electromagnetic scattering  
[NASA-CR-175507] p 99 N85-21438  
Analysis of the electromagnetic scattering from an inlet geometry with lossy walls  
[NASA-CR-175743] p 99 N85-25686  
Normal modes in an overmoded circular waveguide coated with lossy material  
[NASA-CR-176186] p 100 N85-35320

## WEAR

- Friction and wear of some ferrous-base metallic glasses  
p 64 A85-11071  
Mechanical-contact-induced transformation from the amorphous to the partially crystalline state in metallic glass  
p 65 A85-19084  
Frictional and morphological properties of Au-MoS<sub>2</sub> films sputtered from a compact target  
p 127 A85-19085  
Polyimides - Tribological properties and their use as lubricants  
p 79 A85-21524  
Friction, wear, transfer, and wear surface morphology of ultrahigh-molecular-weight polyethylene  
p 80 A85-22276

- Friction and wear of ceramics  
p 80 A85-23833  
Ceramic wear in indentation and sliding contact  
p 82 A85-39549

- Lubricity of well-characterized jet and broad-cut fuels by ball-on-cylinder machine  
[NASA-TM-83807] p 92 N85-12183

- Effect of humidity on fretting wear of several pure metals  
[NASA-TP-2403] p 72 N85-13006

- Effects of silver and group 2 fluorides addition to plasma sprayed chromium carbide high temperature solid lubricant for foil gas bearing to 650 deg C  
[NASA-TM-86895] p 84 N85-14928

- Fundamental tribological properties of ceramics  
[NASA-TM-86915] p 85 N85-15893

- Surface effects of corrosive media on hardness, friction, and wear of materials  
[NASA-TM-83711] p 85 N85-15896

- Effect of five lubricants on life of AISI 9310 spur gears  
[NASA-TP-2419] p 123 N85-16099

- Ion-beam nitriding of steels  
[NASA-CASE-LEW-14104-1] p 75 N85-21324

- Tribological systems as applied to aircraft engines  
[NASA-TM-86965] p 131 N85-21657

- Sliding seal materials for adiabatic engines  
[NASA-CR-174893] p 89 N85-22757

- Reusable rocket engine turbopump condition monitoring  
p 51 N85-26907

- Effects of wear on structure-sensitive magnetic properties of ceramic ferrite in contact with magnetic tape  
[NASA-TM-87007] p 90 N85-26991

- Effect of counterface material type and its topography on the tribological properties of polyimide composites  
[NASA-TM-87036] p 90 N85-26993

- Breakaway friction and dynamic friction/wear measurements of various ceramic materials from 25 C (75 F) to 650 C (1200 F)  
[NASA-CR-174803] p 90 N85-26994

- Rolling, slip and traction measurements on low modulus materials  
[NASA-CR-174909] p 135 N85-33491

- Application of traction drives as servo mechanisms  
p 152 N85-33520

## WEAR INHIBITORS

- Lubricant and additive effects on spur gear fatigue life  
[NASA-TM-87044] p 133 N85-28373

## WEAR TESTS

- Friction and wear properties of a Charnley artificial hip joint  
[ASLE PREPRINT 84-LC-4A-4] p 168 A85-38444

- Lubricant and additive effects on spur gear fatigue life  
[NASA-TM-87044] p 133 N85-28373

- Mechanical protection of DLC films on fused silica slides  
[NASA-TM-87056] p 91 N85-30138

## WEATHER

- Effect of precipitation on wind turbine performance  
[NASA-TM-86986] p 161 N85-27385

## WEATHER FORECASTING

- Improved models for increasing wind penetration, economics and operating reliability  
[NASA-CR-175538] p 160 N85-20545

## WAFERS

- Lithium counterdoped silicon solar cell  
[NASA-CASE-LEW-14177-1] p 160 N85-20535

- Sixty GHz IMPATT diode development  
[NASA-CR-174969] p 105 N85-33293

## WAKES

- A note on blade wake interaction influence on compressor stator row aerodynamic performance  
p 4 A85-32965

- Method for evaluating wind turbine wake effects on wind farm performance  
p 155 A85-36750

- Rotor wake characteristics of a transonic axial flow fan  
[AIAA PAPER 85-1133] p 6 A85-43974

- Turbofan noise generation. Volume 2: Computer programs  
[NASA-CR-167952] p 175 N85-11791

- Electron and ion density depletions measured in the STS-3 orbiter wake  
p 39 N85-22474

- Polar orbit electrostatic charging of objects in shuttle wake  
p 40 N85-22487

- Ram-wake effects on plasma current collection of the PIX 2 Langmuir probe  
p 180 N85-22496

- Wake effects on the aerodynamic performance of horizontal axis wind turbines  
[NASA-CR-174920] p 162 N85-29364

## WALL FLOW

- A three-dimensional boundary-layer analysis including heat-transfer and blade-rotation effects  
p 6 A85-42988

## WALL TEMPERATURE

- High temperature thermocouple and heat flux gauge using a unique thin film hardware hot junction  
[NASA-TM-86898] p 123 N85-16096

## WARNING SYSTEMS

- Reusable rocket engine turbopump condition monitoring  
p 51 N85-26907

## WARPAGE

- Finite difference analysis of torsional vibrations of pretwisted, rotating, cantilever beams with effects of warping  
p 143 A85-42047

## WASPALOY

- A study of fatigue damage mechanisms in Waspaloy from 25 to 800 C  
p 65 A85-12098

## WASTE ENERGY UTILIZATION

- Overview of waste heat utilization systems  
[NASA-TM-86901] p 184 N85-13692

- Comparative evaluation of three alternative power cycles for waste heat recovery from the exhaust of adiabatic diesel engines  
[NASA-TM-86953] p 186 N85-32043

- Comparative evaluation of three alternative power cycles for waste heat recovery from the exhaust of adiabatic diesel engines  
[NASA-TM-86953] p 186 N85-32043

## WATER

- Mechanism for forming hydrogen chloride and sodium sulfate from sulfur trioxide, water, and sodium chloride  
p 62 A85-48513

- Effect of water on hydrogen permeability --- Stirling engines  
[NASA-TM-86904] p 53 N85-14864

- Factors influencing the ball milling of Si<sub>3</sub>N<sub>4</sub> in water  
[NASA-TM-86932] p 86 N85-19136

- Parametric evaluation of ball milling of SiC in water  
[NASA-TM-86974] p 88 N85-21356

## WAVE ATTENUATION

- The role of the reflection coefficient in precision measurement of ultrasonic attenuation  
p 174 A85-42151

## WAVE EQUATIONS

- Reverberation effects on directionality and response of stationary monopole and dipole sources in a wind tunnel  
[NASA-TM-87063] p 119 N85-31443

## WAVE EXCITATION

- The response of Helmholtz resonators to external excitation. I - Single resonators  
p 174 A85-26915

## WAVE INTERACTION

- Sound generation and upstream influence due to instability waves interacting with non-uniform mean flows  
p 174 A85-20738

## WAVE PROPAGATION

- Generation of instability waves in flows separating from smooth surfaces  
p 1 A85-10352

- Ultrasonic wave propagation in two-phase media - Spherical inclusions  
p 54 A85-11926

- Feedback in separated flows over symmetric airfoils  
[AIAA PAPER 84-2297] p 3 A85-28899

- Perturbation-iteration theory for analyzing microwave striplines  
[NASA-CR-176189] p 100 N85-35321

- Calculation of three-dimensional, viscous flow through turbomachinery blade passages by parabolic marching  
[AIAA PAPER 85-1408] p 5 A85-39767

- Numerical calculation of subsonic jets in crossflow with reduced numerical diffusion  
[AIAA PAPER 85-1441] p 110 A85-39780

- A three-dimensional boundary-layer analysis including heat-transfer and blade-rotation effects  
p 6 A85-42988

- Application of computational fluid dynamics to complex inlet ducts  
[AIAA PAPER 85-1213] p 6 A85-47023

- Inviscid and viscous flows in cascades with an explicit multiple-grid algorithm  
p 7 A85-48539

- Model equation for simulating flows in multistage turbomachinery  
[NASA-TM-86869] p 7 N85-12036

- Analytical modeling of circuit aerodynamics in the new NASA Lewis wind tunnel  
[NASA-TM-86912] p 8 N85-15688

- Calculation of three-dimensional, viscous flow through turbomachinery blade passages by parabolic marching  
[NASA-TM-86984] p 9 N85-23711

- Numerical calculation of subsonic jets in crossflow with reduced numerical diffusion  
[NASA-TM-87003] p 27 N85-25263

- Application of computational fluid dynamics to complex inlet ducts  
[NASA-TM-87060] p 118 N85-30247

- Elastohydrodynamic lubrication calculations used as a tool to study scuffing  
[NASA-TM-87097] p 137 N85-34408

## VOIDS

- Reliability of void detection in structural ceramics using scanning laser acoustic microscopy  
[NASA-TM-87035] p 138 N85-32337

## VOLT-AMPERE CHARACTERISTICS

- Environmentally-induced voltage limitations in large space power systems  
p 43 A85-18584

- Applicability of the Meyer-Neldel rule to solar cells  
p 154 A85-19948

- Electrical characterization of plasma-grown oxides on gallium arsenide  
p 181 A85-32635

- Theory of the high base resistivity n(+)/pp(+) silicon solar cell and its application to radiation damage effects  
p 154 A85-32639

## VOLTAGE CONVERTERS (DC TO DC)

- Small-signal model for the series resonant converter  
p 102 A85-39453

- The J3 SCR model applied to resonant converter simulation  
p 102 A85-42156

## VOLTAGE REGULATORS

- Small-signal model for the series resonant converter  
p 102 A85-39453

## VORTEX ALLEVIATION

- Wake effects on the aerodynamic performance of horizontal axis wind turbines  
[NASA-CR-174920] p 162 N85-29364

## VORTEX GENERATORS

- Flow control in a diffusing S-Duct  
[AIAA PAPER 85-0524] p 3 A85-25928

- Vortex generating flow passage design for increased film cooling effectiveness  
[NASA-CASE-LEW-14039-1] p 119 N85-33433

## VORTEX SHEDDING

- Rotor wake characteristics of a transonic axial flow fan  
[AIAA PAPER 85-1133] p 6 A85-43974

## VORTEX SHEETS

- Resonance in flows with vortex sheets and edges  
p 1 A85-10357

## VORTICES

- A finite element solution of three-dimensional inviscid rotational flows through curved ducts  
p 107 A85-11648

- Vortex induced lift on a flat plate with a curved forward-facing flap  
p 4 A85-30175

- Vortex modeling of single and multiple dilution jet mixing in a crossflow  
[AIAA PAPER 85-1580] p 111 A85-40701

- Growth of a diffusion flame in the field of a vortex  
p 61 A85-47320

- Vortex-generating coolant-flow-passage design for increased film-cooling effectiveness and surface coverage  
[NASA-TP-2388] p 113 N85-12314

- Deflected jet experiments in a turbulent combustor flowfield  
[NASA-CR-174863] p 26 N85-22390

- Development of a rotor wake-vortex model, volume 1  
[NASA-CR-174849] p 9 N85-26668

- Aerodynamic analysis of a horizontal axis wind turbine by use of helical vortex theory. Volume 1: Theory  
[NASA-CR-168054] p 9 N85-29916



- Comparative analysis of operational forecasts versus actual weather conditions in airline flight planning, volume 1  
[NASA-CR-167862] p 167 N85-35534
- Comparative analysis of operational forecasts versus actual weather conditions in airline flight planning, volume 2  
[NASA-CR-167863] p 167 N85-35535
- Comparative analysis of operational forecasts versus actual weather conditions in airline flight planning, volume 3  
[NASA-CR-167864] p 167 N85-35536
- Comparative analysis of operational forecasts versus actual weather conditions in airline flight planning, volume 4  
[NASA-CR-167865] p 167 N85-35537
- Comparative analysis of operational forecasts versus actual weather conditions in airline flight planning: Summary report  
[NASA-CR-167866] p 168 N85-35538
- WEIBULL DENSITY FUNCTIONS**  
Reliability of two sintered silicon nitride materials  
[NASA-TM-87092] p 92 N85-34284
- WEIGHT (MASS)**  
Study of Kapton under simulated shuttle environment  
[NASA-CR-176003] p 41 N85-29997
- WEIGHTLESSNESS**  
Free-surface phenomena under low- and zero-gravity conditions  
[NASA-CR-175835] p 116 N85-27168
- Free-surface phenomena under low- and zero-gravity conditions  
[NASA-CR-175885] p 36 N85-27922
- The use of a laser Doppler velocimeter in a standard flammability tube  
[NASA-CR-174960] p 125 N85-35389
- WELD STRENGTH**  
Diffusion welding of Cassegrainian concentrator cell stack assemblies  
[NASA-CR-176104] p 164 N85-33566
- WELDED JOINTS**  
Feasibility study of the welding of SiC  
[NASA-CR-176104] p 81 N85-39339
- WETTABILITY**  
Preliminary evaluation of a liquid belt radiator for space applications  
[NASA-CR-174807] p 47 N85-15804
- Contact angle and surface tension measurements of a five-ring polyphenyl ether  
[NASA-TM-86927] p 86 N85-15897
- WETTING**  
Factors influencing the ball milling of Si<sub>3</sub>N<sub>4</sub> in water  
[NASA-TM-86932] p 86 N85-19136
- Mechanics of a gaseous film barrier to lubricant wetting of elastohydrodynamically lubricated conjunctions  
[NASA-TP-2500] p 135 N85-32330
- WHISKER COMPOSITES**  
Analysis of stress-strain, fracture, and ductility behavior of aluminum matrix composites containing discontinuous silicon carbide reinforcement  
[NASA-CR-176104] p 55 N85-37421
- WHISKERS (CRYSTALS)**  
Cone formation as a result of whisker growth on ion bombarded metal surfaces  
[NASA-CR-176104] p 182 N85-41635
- WIND EFFECTS**  
Comparative analysis of operational forecasts versus actual weather conditions in airline flight planning, volume 4  
[NASA-CR-167865] p 167 N85-35537
- WIND MEASUREMENT**  
Improved models for increasing wind penetration, economics and operating reliability  
[NASA-CR-175538] p 160 N85-20545
- WIND TUNNEL APPARATUS**  
The NASA altitude wind tunnel - Its role in advanced icing research and development  
[AIAA PAPER 85-0090] p 35 A85-26381
- Analytical and physical modeling program for the NASA Lewis Research Center's Altitude Wind Tunnel (AWT)  
[NASA-TM-86919] p 35 N85-15757
- The NASA Altitude Wind Tunnel (AWT): Its role in advanced icing research and development  
[NASA-TM-86920] p 35 N85-15758
- WIND TUNNEL MODELS**  
Analytical and physical modeling program for the NASA Lewis Research Center's Altitude Wind Tunnel (AWT)  
[AIAA PAPER 85-0379] p 34 A85-19709
- WIND TUNNEL TESTS**  
Modelling of wind tunnel wall effects on the radiation characteristics of acoustic sources  
[AIAA PAPER 84-2364] p 174 A85-16104
- The Altitude Wind Tunnel (AWT) - A unique facility for propulsion system and adverse weather testing  
[AIAA PAPER 85-0314] p 34 A85-19661
- The NASA altitude wind tunnel - Its role in advanced icing research and development  
[AIAA PAPER 85-0090] p 35 A85-26381
- Analytical modeling of circuit aerodynamics in the new NASA Lewis Altitude Wind Tunnel  
[AIAA PAPER 85-0380] p 3 A85-26389
- The UH-1H helicopter icing flight test program - An overview  
[AIAA PAPER 85-0338] p 11 A85-28898
- Design and performance of a fixed, nonaccelerating guide vane cascade that operates over an inlet flow angle range of 60 deg  
[ASME PAPER 84-GT-75] p 4 A85-32964
- Experiments in dilution jet mixing - Effects of multiple rows and non-circular orifices  
[AIAA PAPER 85-1104] p 15 A85-39606
- Design and wind tunnel evaluation of a symmetric airfoil series for large wind turbine applications  
[NASA-CR-174764] p 7 N85-10919
- Analytical modeling of circuit aerodynamics in the new NASA Lewis wind tunnel  
[NASA-TM-86912] p 8 N85-15688
- The UH-1H helicopter icing flight test program: An overview  
[NASA-TM-86925] p 11 N85-15702
- Analytical and physical modeling program for the NASA Lewis Research Center's Altitude Wind Tunnel (AWT)  
[NASA-TM-86919] p 35 N85-15757
- The NASA Altitude Wind Tunnel (AWT): Its role in advanced icing research and development  
[NASA-TM-86920] p 35 N85-15758
- The Altitude Wind Tunnel (AWT): A unique facility for propulsion system and adverse weather testing  
[NASA-TM-86921] p 35 N85-18067
- Further comparison of wind tunnel and airplane acoustic data for advanced design high speed propeller models  
[NASA-TM-86935] p 176 N85-22108
- Deflected jet experiments in a turbulent combustor flowfield  
[NASA-CR-174863] p 26 N85-22390
- Behavior of turbulent gas jets in an axisymmetric confinement  
[NASA-CR-174829] p 28 N85-25265
- Experiments in dilution jet mixing effects of multiple rows and non-circular orifices  
[NASA-TM-86996] p 28 N85-25266
- Reverberation effects on directionality and response of stationary monopole and dipole sources in a wind tunnel  
[NASA-TM-87063] p 119 N85-31443
- Reflection plane tests of a wind turbine blade tip section with ailerons  
[NASA-TM-87018] p 165 N85-34444
- WIND TUNNEL WALLS**  
Modelling of wind tunnel wall effects on the radiation characteristics of acoustic sources  
[AIAA PAPER 84-2364] p 174 A85-16104
- Reverberation effects on directionality and response of stationary monopole and dipole sources in a wind tunnel  
[NASA-TM-87063] p 119 N85-31443
- WIND TURBINES**  
Analytical and physical modeling program for the NASA Lewis Research Center's Altitude Wind Tunnel (AWT)  
[AIAA PAPER 85-0379] p 34 A85-19709
- WIND TURBINES**  
Measured effects of wind turbine generation at the Block Island Power Company  
[NASA-TM-86867] p 153 A85-10652
- Method for evaluating wind turbine wake effects on wind farm performance  
[NASA-TM-86867] p 155 A85-36750
- Mod-2 wind turbine field operations experience  
[NASA-TM-86867] p 157 A85-45512
- Aileron controls for wind turbine applications  
[NASA-TM-86867] p 157 A85-45513
- Advanced multi-megawatt wind turbine design for utility application  
[NASA-TM-86867] p 157 A85-45517
- Design and wind tunnel evaluation of a symmetric airfoil series for large wind turbine applications  
[NASA-CR-174764] p 7 N85-10919
- Aileron controls for wind turbine applications  
[NASA-TM-86867] p 158 N85-11458
- Shutdown characteristics of the Mod-O wind turbine with aileron controls  
[NASA-TM-86918] p 159 N85-16299
- Improved models for increasing wind penetration, economics and operating reliability  
[NASA-CR-175538] p 160 N85-20545
- Development of large, horizontal-axis wind turbines  
[NASA-TM-86950] p 161 N85-23242
- Effect of precipitation on wind turbine performance  
[NASA-TM-86986] p 161 N85-27385
- Conceptual design of a fixed-pitch wind turbine generator system rated at 400 kilowatts  
[NASA-CR-174877] p 162 N85-29363
- Wake effects on the aerodynamic performance of horizontal axis wind turbines  
[NASA-CR-174920] p 162 N85-29364
- Government review of the Mod-2 wind turbine (as-built)  
[NASA-TM-86983] p 162 N85-29365
- Aerodynamic analysis of a horizontal axis wind turbine by use of helical vortex theory. Volume 1: Theory  
[NASA-CR-168054] p 9 N85-29916
- Structural analysis and cost estimate of an eight-leg space frame as a support structure for horizontal axis wind turbines  
[NASA-TM-83470] p 150 N85-30361
- Analytical model for predicting emergency shutdown of a two-bladed horizontal axis wind turbine  
[NASA-TM-83472] p 162 N85-30476
- Performance comparison between NACA 23024 and NACA 64(3)-618 airfoil configured rotors for horizontal-axis wind turbines  
[NASA-TM-83471] p 163 N85-30477
- The Federal Wind Program at NASA Lewis Research Center  
[NASA-TM-83480] p 163 N85-30478
- Operational results for the experimental DOE/NASA Mod-OA wind turbine project  
[NASA-TM-83517] p 163 N85-30479
- Experimental investigation of a variable speed constant frequency electric generating system from a utility perspective  
[NASA-CR-174950] p 105 N85-32251
- Reflection plane tests of a wind turbine blade tip section with ailerons  
[NASA-TM-87018] p 165 N85-34444
- WIND VELOCITY**  
Comparative analysis of operational forecasts versus actual weather conditions in airline flight planning, volume 1  
[NASA-CR-167862] p 167 N85-35534
- Comparative analysis of operational forecasts versus actual weather conditions in airline flight planning, volume 2  
[NASA-CR-167863] p 167 N85-35535
- Comparative analysis of operational forecasts versus actual weather conditions in airline flight planning, volume 3  
[NASA-CR-167864] p 167 N85-35536
- Comparative analysis of operational forecasts versus actual weather conditions in airline flight planning, volume 4  
[NASA-CR-167865] p 167 N85-35537
- Comparative analysis of operational forecasts versus actual weather conditions in airline flight planning: Summary report  
[NASA-CR-167866] p 168 N85-35538
- WINDMILLS (WINDPOWERED MACHINES)**  
Government review of the Mod-2 wind turbine (as-built)  
[NASA-TM-86983] p 162 N85-29365
- Aerodynamic analysis of a horizontal axis wind turbine by use of helical vortex theory. Volume 1: Theory  
[NASA-CR-168054] p 9 N85-29916
- WINDOWS (APERTURES)**  
Diamondlike carbon protective coatings for IR materials  
[NASA-TM-87083] p 178 N85-34631
- WINDPOWER UTILIZATION**  
Mod-2 wind turbine field operations experience  
[NASA-TM-86867] p 157 A85-45512
- Aileron controls for wind turbine applications  
[NASA-TM-86867] p 157 A85-45513
- Aileron controls for wind turbine applications  
[NASA-TM-86867] p 158 N85-11458
- Improved models for increasing wind penetration, economics and operating reliability  
[NASA-CR-175538] p 160 N85-20545
- Government review of the Mod-2 wind turbine (as-built)  
[NASA-TM-86983] p 162 N85-29365
- Aerodynamic analysis of a horizontal axis wind turbine by use of helical vortex theory. Volume 1: Theory  
[NASA-CR-168054] p 9 N85-29916
- The Federal Wind Program at NASA Lewis Research Center  
[NASA-TM-83480] p 163 N85-30478
- WINDPOWERED GENERATORS**  
Development of large, horizontal-axis wind turbines  
[NASA-TM-86950] p 161 N85-23242
- Government review of the Mod-2 wind turbine (as-built)  
[NASA-TM-86983] p 162 N85-29365
- Structural analysis and cost estimate of an eight-leg space frame as a support structure for horizontal axis wind turbines  
[NASA-TM-83470] p 150 N85-30361
- The Federal Wind Program at NASA Lewis Research Center  
[NASA-TM-83480] p 163 N85-30478
- Operational results for the experimental DOE/NASA Mod-OA wind turbine project  
[NASA-TM-83517] p 163 N85-30479

**WINGS****WINGS**

Icing tunnel tests of Electro-Impulse De-Icing of an engine inlet and high-speed wings  
[AIAA PAPER 85-0466] p 10 A85-20872

**WOOD**

Thermal-stress analysis for a wood composite blade  
[NASA-CR-174794] p 159 N85-17421

**WORKING FLUIDS**

Preliminary evaluation of a liquid belt radiator for space applications  
[NASA-CR-174807] p 47 N85-15804  
Advanced radiator concepts  
[NASA-TM-87008] p 115 N85-24245

**X****X RAY ANALYSIS**

Laboratory degradation of Kapton in a low energy oxygen ion beam  
[AIAA PAPER 83-2658] p 78 A85-10675

**XENON**

Performance capabilities of the 12-centimeter Xenon ion thruster p 42 A85-16439

**Y****YAG LASERS**

Laser balancing system for high material removal rates  
[NASA-CR-174731] p 126 N85-12341

**YIELD**

Electron yields from spacecraft materials p 40 N85-22512

**YTTERBIUM**

Optimization of the NiCrAl-Y/ZrO-Y2O3 thermal barrier system  
[NASA-TM-86905] p 72 N85-15878  
Thermal barrier coating system  
[NASA-CASE-LEW-14057-1] p 59 N85-35233

**YTTRIUM**

High-temperature erosion of plasma-sprayed, yttria-stabilized zirconia in a simulated turbine environment  
[AIAA PAPER 85-1219] p 82 A85-39662  
Dopant effect of yttrium and the growth and adherence of alumina on nickel-aluminum alloys p 82 A85-40973  
High-temperature erosion of plasma-sprayed, yttria-stabilized zirconia in a simulated turbine environment  
[NASA-TP-2406] p 84 N85-13045  
Compatibility experiments of facilities, materials, and propellants for electrothermal thrusters  
[NASA-TM-86956] p 49 N85-21260

**YTTRIUM OXIDES**

Progress in the utilization of an oxide-dispersion-strengthened alloy for small engine turbine blades  
[SAE PAPER 841512] p 68 A85-39284  
Fracture of yttria-doped, sintered reaction-bonded silicon nitride  
[ACS PAPER 7-J3-84] p 82 A85-42797

**Z****ZINC**

AES and LEED study of the zinc blende SiC(100) surface p 61 A85-41633  
Universal binding energy relations in metallic adhesion  
[NASA-TM-86889] p 72 N85-12132  
Humidity effects on adhesion of nickel-zinc ferrite in elastic contact with magnetic tape and itself  
[NASA-TP-2449] p 88 N85-21359

**ZIRCONIUM**

High-temperature erosion of plasma-sprayed, yttria-stabilized zirconia in a simulated turbine environment  
[AIAA PAPER 85-1219] p 82 A85-39662  
Effects of cobalt, boron, and zirconium on the microstructure of Udimet 738  
[NASA-CR-174762] p 70 N85-10166  
High-temperature erosion of plasma-sprayed, yttria-stabilized zirconia in a simulated turbine environment  
[NASA-TP-2406] p 84 N85-13045  
Thermal barrier coating system  
[NASA-CASE-LEW-14057-1] p 59 N85-35233

**ZIRCONIUM ALLOYS**

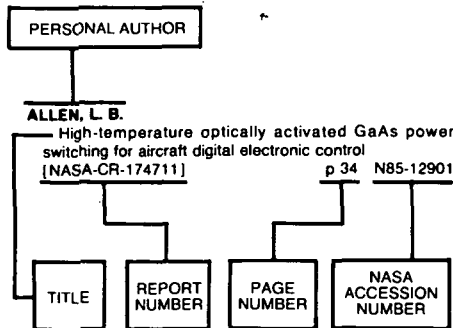
Manufacturing process to reduce large grain growth in zirconium alloys  
[DE85-011649] p 78 N85-34267

**ZIRCONIUM OXIDES**

Separator development and testing of nickel-hydrogen cells p 156 A85-45386

An investigation of enhanced capability thermal barrier coating systems for diesel engine components  
[NASA-CR-174820] p 86 N85-18154  
Rocket thrust chamber thermal barrier coatings p 90 N85-26867

## Typical Personal Author Index Listing



Listings in this index are arranged alphabetically by personal author. The NASA accession number denotes the number by which the citation is identified.

## A

- ABBOTT, J. M.**  
Analytical and physical modeling program for the NASA Lewis Research Center's Altitude Wind Tunnel (AWT) [AIAA PAPER 85-0379] p 34 N85-19709  
Analytical and physical modeling program for the NASA Lewis Research Center's Altitude Wind Tunnel (AWT) [NASA-TM-86919] p 35 N85-15757
- ABOU-ARAB, T.**  
A two-equation turbulence model for two-phase jets p 107 N85-14376
- ABRAHAM, K. M.**  
Moderate temperature sodium cells. V - Discharge reactions and rechargeability of NiS and NiS<sub>2</sub> positive electrodes in molten NaAlCl<sub>4</sub> p 59 N85-11892
- ABUELFOUOUH, N.**  
Finite element analysis of notch behavior using a state variable constitutive equation p 152 N85-31548
- ABUJELALA, M. T.**  
Confined turbulent swirling recirculating flow predictions [NASA-CR-174917] p 29 N85-26716
- ACOSTA, R. J.**  
Case study of sample spacing in planar near-field measurement of high gain antennas [NASA-TM-86872] p 97 N85-10234
- ACOSTA, W. A.**  
Experimental study of the spray characteristics of a research airblast atomizer [NASA-TM-86911] p 24 N85-15727
- ADAMCZYK, J. J.**  
Computational thermo-fluid dynamics contributions to advanced gas turbine engine design [AIAA PAPER 85-0083] p 14 N85-19509  
Computational thermo-fluid dynamics contributions to advanced gas turbine engine design [NASA-TM-86865] p 18 N85-10069  
Model equation for simulating flows in multistage turbomachinery [NASA-TM-86869] p 7 N85-12036  
Simulation of multistage turbine flows p 116 N85-27945
- ADLER, E.**  
Advanced nickel-hydrogen cell configuration study [NASA-CR-174775] p 157 N85-10444

- AFJEH, A. A.**  
Wake effects on the aerodynamic performance of horizontal axis wind turbines [NASA-CR-174920] p 162 N85-29364
- AGARWAL, P.**  
Energy efficient engine, high pressure turbine thermal barrier coating. Support technology report [NASA-CR-168037] p 34 N85-35199
- AHMED, S. A.**  
Jet characteristics in confined swirling flow p 112 N85-45282  
Density effects on jet characteristics in confined swirling flow p 112 N85-45283  
Behavior of turbulent gas jets in an axisymmetric confinement [NASA-CR-174829] p 28 N85-25265
- AHUJA, K. K.**  
An experimental study of tone excited heated jets [AIAA PAPER 84-2341] p 172 N85-10882  
Some unique experiments on receptivity [AIAA PAPER 85-0533] p 174 N85-25932  
Acoustic control of free jet mixing [AIAA PAPER 85-0569] p 109 N85-25951
- AKAY, H. U.**  
A finite element solution of three-dimensional inviscid rotational flows through curved ducts p 107 N85-11648
- AKIN, L. S.**  
Into mesh lubrication of spur gears with arbitrary offset oil jet. I - For jet velocity less than or equal to gear velocity p 128 N85-24497  
Lubricant jet flow phenomena in spur and helical gears with modified center distances and/or addendums - For out-of-mesh conditions [ASME PAPER 84-DET-96] p 129 N85-35049
- AL-KINANI, G.**  
Satellite provided customer promises services, a forecast of potential domestic demand through the year 2000. Volume 4: Sensitivity analysis [NASA-CR-174662] p 99 N85-27092
- ALIAKBARKHANAFJEH, A.**  
Aerodynamic analysis of a horizontal axis wind turbine by use of helical vortex theory. Volume 1: Theory [NASA-CR-168054] p 9 N85-29916
- ALKASAB, K. A.**  
Manual of phosphoric acid fuel cell power plant optimization model and computer program [NASA-CR-174721] p 157 N85-10445  
Manual of phosphoric acid fuel cell stack three-dimensional model and computer program [NASA-CR-174722] p 157 N85-10447  
Phosphoric acid fuel cell power plant system performance model and computer program [NASA-CR-174638] p 157 N85-11456
- ALLEN, D. H.**  
On the use of internal state variables in thermoviscoplastic constitutive equations p 150 N85-31536
- ALLEN, G. P.**  
Ribbon burner simulation of T-700 turbine shroud for ceramic lined seals research [NASA-TM-86940] p 114 N85-19364
- ALLEN, L. B.**  
High-temperature optically activated GaAs power switching for aircraft digital electronic control [NASA-CR-174711] p 34 N85-12901
- ALSTON, W. B.**  
Effect of substituted phenylhydrazines on processing and properties of PMR polyimide composites [NASA-TM-86902] p 85 N85-14929
- ALTENKIRCH, R. A.**  
Gravitational effects on flames spreading over thick solid surfaces [IAF PAPER 84-154] p 59 N85-13092
- ALTEROVITZ, S. A.**  
Plasma deposited hydrogenated carbon on GaAs and InP p 182 N85-40386  
Plasma deposited diamondlike carbon on GaAs and InP [NASA-TM-86870] p 183 N85-10844
- Optical properties of hydrogenated amorphous carbon films grown from methane plasma [NASA-TM-86995] p 183 N85-26406**
- AMANO, R. S.**  
A study of Reynolds-stress closure model [NASA-CR-174342] p 114 N85-17324
- AMERI, A.**  
Unsteady heat transfer due to time-dependent free stream velocity p 117 N85-27947
- ANAND, M. S.**  
Combustion efficiency of a premixed continuous flow combustor p 61 N85-42571
- ANDERSON, A. B.**  
Dopant effect of yttrium and the growth and adherence of alumina on nickel-aluminum alloys p 82 N85-40973  
Mechanism for chelated sulfate formation from SO<sub>2</sub> and bis (triphenylphosphine) platinum p 62 N85-48493  
Mechanism for forming hydrogen chloride and sodium sulfate from sulfur trioxide, water, and sodium chloride p 62 N85-48513  
Why CO bonds side-on at low coverage and both side-on and upright at high coverage on the Cr(110) surface [NASA-CR-176071] p 77 N85-32173  
Molecular orbital studies in oxidation: Sulfate formation and metal-metal oxide adhesion [NASA-CR-176070] p 77 N85-32174  
Adsorption of O<sub>2</sub>, SO<sub>2</sub>, and SO<sub>3</sub> on nickel oxide. Mechanism for sulfate formation [NASA-CR-176072] p 77 N85-32175  
CO adsorption on (111) and (100) surfaces of the Pt sub 3 Ti alloy. Evidence for parallel binding and strong activation of CO [NASA-CR-176077] p 77 N85-32176
- ANDERSON, D. N.**  
Flame flashback in a premixed dump combustor [AIAA PAPER 85-0145] p 60 N85-19550
- ANDERSON, G. G.**  
High temperature properties of equiatomic FeAl with ternary additions [NASA-TM-86938] p 73 N85-19072
- ANDERSON, L. M.**  
Inelastic tunnel diodes [NASA-CASE-LEW-13833-1] p 103 N85-21492  
Solar energy converter using surface plasma waves [NASA-CASE-LEW-13827-1] p 160 N85-21768
- ANDERSON, R. C.**  
Integrated exhaust gas analysis system for aircraft turbine engine component testing [NASA-TP-2424] p 123 N85-16100
- ANDRACCHIO, C. A.**  
High temperature thermocouple and heat flux gauge using a unique thin film-hardware hot junction [NASA-TM-86898] p 123 N85-16096
- ANTOLOVICH, S. D.**  
A study of fatigue damage mechanisms in Waspaloy from 25 to 800 C p 65 N85-12098  
The effect of microstructure, temperature, and hold-time on low-cycle fatigue of As HIP P/M Rene 95 p 67 N85-32399  
A study of spectrum fatigue crack propagation in two aluminum alloys. 1: Spectrum simplification [NASA-TM-86929] p 72 N85-18124  
A study of spectrum fatigue crack propagation in two aluminum alloys. 2: Influence of microstructures [NASA-TM-86930] p 73 N85-18125
- AOKI, K.**  
Flow visualization of lateral jet injection into swirling crossflow [AIAA PAPER 85-0059] p 2 N85-19490
- ARCHBOLD, T.**  
Metallurgical and mechanical phenomena due to rubbing of titanium against sintered powder Nichrome p 127 N85-22281
- ARD, K. E.**  
Extreme precision antenna reflector study results p 165 N85-23830
- ARGARWAL, P.**  
Life modeling of atmospheric and low pressure plasma-sprayed thermal-barrier coating p 81 N85-29728

**ARMSTRONG, R. S.**

Detailed studies of aviation fuel flowability  
[NASA-CR-174938] p 94 N85-31308

**ARMSTRONG, T. P.**

Numerical simulations of positively-biased probes and dielectric-conductor disks in a plasma p 179 A85-17262

Numerical simulation of positive-potential conductors in the presence of a plasma and a secondary-emitting dielectric p 102 A85-35306

**ARON, P. R.**

RF-sputtered silicon and hafnium nitrides - Properties and adhesion to 440C stainless steel p 81 A85-36240  
Effect of lubricant extreme-pressure additives on surface fatigue life of AISI 9310 spur gears  
[NASA-TP-2408] p 130 N85-13234

**ARPASI, D. J.**

Hardware for a real-time multiprocessor simulator  
[NASA-TM-83805] p 169 N85-10659  
Real-Time Multiprocessor Programming Language (RTMPL) user's manual  
[NASA-TP-2422] p 170 N85-28610

**ASLANIDIS, I.**

Alloys based on NiAl for high temperature applications  
[NASA-TM-86976] p 75 N85-21322

**ASMUSSEN, J.**

Experiments with a microwave electrothermal thruster concept p 42 A85-16441  
Recent work on a microwave ion source p 179 A85-16455  
Experimental performance of a microwave cavity plasma disk ion source p 179 A85-43552

**ATASSI, H. M.**

Feedback in separated flows over symmetric airfoils  
[AIAA PAPER 84-2297] p 3 A85-28899

**ATHERTON, W. J.**

Investigation on experimental techniques to detect, locate and quantify gear noise in helicopter transmissions  
[NASA-CR-3847] p 176 N85-17667

**ATKINSON, W. H.**

Development of advanced high-temperature heat flux sensors. Phase 2: Verification testing  
[NASA-CR-174973] p 126 N85-35391

**ATLURI, S. N.**

Hybrid stress finite elements for large deformations of inelastic solids p 139 A85-15894  
Development and testing of stable, invariant, isoparametric curvilinear 2- and 3-D hybrid-stress elements p 140 A85-19899  
On the existence and stability conditions for mixed-hybrid finite element solutions based on Reissner's variational principle p 142 A85-33847  
Constitutive modeling and computational implementation for finite strain plasticity p 143 A85-40910

**ATTWOOD, S. W.**

Satellite baseband processor test performance summary p 95 A85-14434

**AUGUST, R.**

Gear mesh stiffness and load sharing in planetary gearing  
[ASME PAPER 84-DET-229] p 129 A85-33781

**AUSTIN, G. W.**

Electric utility acid fuel cell stack technology advancement  
[NASA-CR-174804] p 159 N85-17422

**AVANT, R. L.**

The J3 SCR model applied to resonant converter simulation p 102 A85-42156

**AVELLA, A. J., JR.**

Jet fuel property changes and their effect on producibility and cost in the U.S., Canada, and Europe  
[NASA-CR-174840] p 93 N85-27012

**AVNI, R.**

Deposition of silicon nitride from SiCl<sub>4</sub> and NH<sub>3</sub> in a low pressure RF plasma p 81 A85-36229  
Surface hardening of steel by boriding in a cold rf plasma p 68 A85-40275  
Analysis of glow discharges for understanding the process of film formation  
[NASA-TM-83750] p 62 N85-10138  
Plasma variables and tribological properties of coatings in low pressure (0.1 - 10.0 torr) plasma systems  
[NASA-TM-83798] p 94 N85-11261  
Nitriding of titanium and its alloys by N<sub>2</sub>, NH<sub>3</sub> or mixtures of N<sub>2</sub> + H<sub>2</sub> in a dc arc plasma at low pressures (or = to torr)  
[NASA-TM-83803] p 131 N85-15168

**AYDELOTT, J. C.**

Technology requirements to be addressed by the NASA Lewis Research Center Cryogenic Fluid Management Facility program  
[AIAA PAPER 85-1229] p 94 A85-47024

Technology requirements to be addressed by the NASA Lewis Research Center Cryogenic Fluid Management Facility program  
[NASA-TM-87048] p 38 N85-29987

**B****BAKLINI, G. Y.**

Radiographic detectability limits for seeded voids in sintered silicon carbide and silicon nitride  
[NASA-TM-86945] p 138 N85-21674

Reliability of void detection in structural ceramics using scanning laser acoustic microscopy  
[NASA-TM-87035] p 138 N85-32337

**BACHALO, W. D.**

Phase/doppler spray analyzer for simultaneous measurements of drop size and velocity distributions p 120 A85-10035

**BADGLEY, P. R.**

Stratified charge rotary aircraft engine technology enablement program  
[NASA-CR-174812] p 25 N85-21163

**BADLANI, M. L.**

Simplified design and life prediction of rocket thrust chambers p 44 A85-29314

**BAER, J. R.**

Fracture of yttria-doped, sintered reaction-bonded silicon nitride  
[ACS PAPER 7-J3-84] p 82 A85-42797

**BAEZ, A. N.**

Design description of a microprocessor based Engine Monitoring and Control unit (EMAC) for small turboshaft  
[NASA-TM-86860] p 1 N85-17935

**BAGWELL, J. W.**

Status of NASA's multibeam communications technology program p 100 A85-14432

**BAILEY, M. M.**

Overview of waste heat utilization systems  
[NASA-TM-86901] p 184 N85-13692

Comparative evaluation of three alternative power cycles for waste heat recovery from the exhaust of adiabatic diesel engines  
[NASA-TM-86953] p 186 N85-32043

**BAILEY, R.**

High temperature static strain sensor development program p 19 N85-10959

**BAILEY, W. J.**

Fiberglass epoxy laminate fatigue properties at 300 and 20 K p 56 A85-47970

**BAK, M. J.**

3-D inelastic analysis methods for hot section components (base program)  
[NASA-CR-174700] p 145 N85-21686

**BALDWIN, D. H.**

Development of large, horizontal-axis wind turbines  
[NASA-TM-86950] p 161 N85-23242  
The Federal Wind Program at NASA Lewis Research Center  
[NASA-TM-83480] p 163 N85-30478

**BALSA, T. F.**

Experimental investigation of shock-cell noise reduction for single stream nozzles in simulated flight  
[NASA-CR-3845] p 175 N85-13550

**BANERJEE, P. K.**

3-D inelastic analysis methods for hot section components (base program)  
[NASA-CR-174700] p 145 N85-21686

**BANKS, B. A.**

Deposition of diamondlike carbon films  
[NASA-CASE-LEW-14080-1] p 95 N85-20153  
Apparatus for producing diamond-like carbon flakes  
[NASA-CASE-LEW-13837-3] p 95 N85-20155  
Diamondlike flakes  
[NASA-CASE-LEW-13837-2] p 57 N85-21267  
Ion beam sputter-deposited thin film coatings for protection of spacecraft polymers in low Earth orbit  
[NASA-TM-87051] p 91 N85-30137  
Diamondlike carbon protective coatings for IR materials  
[NASA-TM-87083] p 178 N85-34631

**BARAONA, C. R.**

Screen printed interdigitated back contact solar cell  
[NASA-CASE-LEW-13414-1] p 160 N85-20530

**BARBER, T. J.**

Three-dimensional inviscid flow analysis of turbofan forced mixers  
[AIAA PAPER 85-0086] p 2 A85-19510

**BARFOOT, J. R.**

Modeling of gamma/gamma-prime phase equilibrium in the nickel-aluminum system p 65 A85-14959

**BARGER, M. J.**

Sixty GHz IMPATT diode development  
[NASA-CR-174969] p 105 N85-33293

**BARIS, J.**

Preparation and evaluation of advanced catalysts for phosphoric acid fuel cells  
[NASA-CR-168223] p 160 N85-19511

**BARKHOUDARIAN, S.**

Reusable rocket engine turbopump condition monitoring p 51 N85-26907

**BARRANGER, J. P.**

Eddy current jet engine disk-crack monitor p 120 A85-11100

**BARRETT, C. A.**

The effects of seven alloying elements on the microstructure and stress-rupture behavior of nickel-base superalloys  
[NASA-TM-83791] p 70 N85-10168  
The effects of Cr, Co, Al, Mo and Ta on the cyclic oxidation behavior of a prototype cast Ni-base superalloy based on a 2(5) composite statistically designed experiment  
[NASA-TM-83784] p 71 N85-12131  
A multiple linear regression analysis of hot corrosion attack on a series of nickel base turbine alloys  
[NASA-TM-87020] p 77 N85-31284

**BARTH, R. L.**

Temperature distortion generator for turboshaft engine testing  
[SAE PAPER 841541] p 15 A85-39065

Temperature distortion generator for turboshaft engine testing  
[NASA-TM-83748] p 1 N85-15658

**BARTOLOTTA, P. A.**

Viscoplastic constitutive relationships with dependence on thermomechanical history  
[NASA-CR-174836] p 146 N85-21691

**BARTON, J. M.**

Inviscid analysis of advanced turboprop propeller flow fields  
[AIAA PAPER 85-1263] p 6 A85-43977

**BASHIR, S.**

The effect of microstructure, temperature, and hold-time on low-cycle fatigue of As HIP P/M Rene 95 p 67 A85-32399

**BASSETT, D. E.**

The design and analysis of single flank transmission error testor for loaded gears  
[NASA-CR-176163] p 136 N85-34404

**BASU, S. N.**

Analysis techniques for tracer studies of oxidation  
[NASA-CR-174796] p 84 N85-12162

**BAUMEISTER, K. J.**

Time dependent wave envelope finite difference analysis of sound propagation  
[AIAA PAPER 84-2285] p 173 A85-16102  
Modelling of wind tunnel wall effects on the radiation characteristics of acoustic sources  
[AIAA PAPER 84-2364] p 174 A85-16104  
Reverberation effects on directionality and response of stationary monopole and dipole sources in a wind tunnel  
[NASA-TM-87063] p 119 N85-31443

**BEACH, R. F.**

Advanced secondary power system for transport aircraft  
[NASA-TP-2463] p 30 N85-28944

**BEATTIE, J. R.**

IAPS (8-cm) ion thruster cyclic endurance test  
Ring-cusp ion thrusters p 42 A85-16406  
Ion thruster system (8-cm) cyclic endurance test  
[NASA-CR-174745] p 47 N85-12937  
Extended performance technology study 30-cm thruster  
[NASA-CR-168259] p 48 N85-15806

**BEATTY, T. G.**

Progress in the utilization of an oxide-dispersion-strengthened alloy for small engine turbine blades  
[SAE PAPER 841512] p 68 A85-39284

**BEEK, J. M.**

On the use of internal state variables in thermoviscoplastic constitutive equations p 150 N85-31536

**BEHEIM, G.**

Remote displacement measurements using a laser diode p 121 A85-24464  
Remote displacement measurement using a passive interferometer with a fiber-optic link p 122 A85-42857

**BEHLKE, R. F.**

Study of controlled diffusion stator blading  
[NASA-CR-167995] p 25 N85-18058

**BEITLER, R. S.**

Energy Efficient Engine (E3) controls and accessories detail design report  
[NASA-CR-168017] p 31 N85-29957

**BELYTSCHKO, T.**

Probabilistic finite element: Variational theory p 149 N85-27957

- BENKO, E.**  
Sixty GHz IMPATT diode development  
[NASA-CR-174969] p 105 N85-33293
- BENNETT, J. C.**  
Mass and momentum turbulent transport experiments with confined coaxial jets p 107 A85-14399
- BENTS, D. J.**  
Report of the Constellations Panel p 131 N85-20368  
Tethered nuclear power for the Space Station  
[NASA-TM-87023] p 51 N85-26912
- BERAK, J. M.**  
High-temperature optically activated GaAs power switching for aircraft digital electronic control  
[NASA-CR-174711] p 34 N85-12901
- BERGAMASU, S.**  
Report of the Constellations Panel p 131 N85-20368
- BERGERON, R. P.**  
Vehicle/engine integration p 37 N85-17008
- BERKE, L.**  
Structural optimization using optimality criteria methods p 144 A85-48703
- BERNDT, C. C.**  
Performance of thermal barrier coatings in high heat flux environments p 79 A85-19087  
Mechanical property measurements of plasma-sprayed thermal-barrier coatings subjected to oxidation p 81 A85-29729  
Failure during thermal cycling of plasma-sprayed thermal barrier coatings p 81 A85-36246
- BERTHOLD, J. W.**  
High-temperature fiber optic pressure sensor p 123 A85-46607
- BEVILACQUA, F.**  
Report of the Constellations Panel p 131 N85-20368
- BEYERLE, R. A.**  
Combustion gas properties. Part 3: Hydrogen gas fuel and dry air  
[NASA-TP-2477] p 32 N85-31058
- BHASIN, K. B.**  
Effect of interfacial characteristics of metal clad polymeric substrates on electrical high frequency interconnection performance  
[NASA-TM-86948] p 99 N85-20223  
An experimental investigation of microstrip properties on soft substrates from 2 to 40 GHz  
[NASA-TM-86961] p 99 N85-20224
- BHAT, K. N.**  
Electrical characterization of plasma-grown oxides on gallium arsenide p 181 A85-32635
- BHAT, M. K.**  
Flow control in a diffusing S-Duct  
[AIAA PAPER 85-0524] p 3 A85-25928
- BHATT, R. T.**  
Environmental effects on the tensile strength of chemically vapor deposited silicon carbide fibers  
[NASA-TM-86981] p 89 N85-24000  
Mechanical properties of SiC fiber-reinforced reaction-bonded Si<sub>3</sub>N<sub>4</sub> composites  
[NASA-TM-87085] p 59 N85-34223
- BHATTACHARYA, S.**  
Creep-rupture behavior of iron superalloys in high-pressure hydrogen  
[NASA-CR-174411] p 74 N85-19078
- BHUSHAN, C.**  
Satellite provided customer promises services, a forecast of potential domestic demand through the year 2000. Volume 4: Sensitivity analysis  
[NASA-CR-174662] p 99 N85-27092
- BIESIADNY, T. J.**  
Temperature distortion generator for turboshaft engine testing  
[SAE PAPER 841541] p 15 A85-39065  
Temperature distortion generator for turboshaft engine testing  
[NASA-TM-83748] p 1 N85-15658  
Experimental and analytical study of ceramic-coated turbine-tip shroud seals for small turbine engines  
[NASA-TM-86881] p 25 N85-18057  
Experimental study of ceramic coated tip seals for turbojet engines  
[NASA-TM-86939] p 114 N85-19363
- BIFANO, W. J.**  
Status of DOE and AID stand-alone photovoltaic system field tests p 155 A85-35707
- BILL, R. C.**  
Low cycle fatigue of MAR-M 200 single crystals at 760 and 870 deg C  
[NASA-TM-86933] p 74 N85-19074  
Multiaxial and thermomechanical fatigue considerations in damage tolerant design  
[NASA-TM-87022] p 76 N85-26964
- BIRCHENALL, C. E.**  
New eutectic alloys and their heats of transformation p 66 A85-27808
- BIRCHENROUGH, A. G.**  
Government review of the Mod-2 wind turbine (as-built)  
[NASA-TM-86983] p 162 N85-29365  
Operational results for the experimental DOE/NASA Mod-OA wind turbine project  
[NASA-TM-83517] p 163 N85-30479  
Reflection plane tests of a wind turbine blade tip section with ailerons  
[NASA-TM-87018] p 165 N85-34444
- BISSET, J. W.**  
Energy efficient engine flight propulsion system preliminary analysis and design report  
[NASA-CR-174701] p 18 N85-10947  
Energy efficient engine integrated core/low spool test hardware design report  
[NASA-CR-168137] p 31 N85-29956
- BITTKER, D. A.**  
Liquid phase products and solid deposit formation from thermally stressed model jet fuels  
[NASA-TM-86874] p 92 N85-13066
- BIZON, P. T.**  
Interaction of high-cycle and low-cycle fatigue of Haynes 188 alloy at 1400 F deg p 149 N85-27961
- BLACK, J. D.**  
Fatigue life analysis of a turboprop reduction gearbox  
[NASA-TM-87014] p 133 N85-27228
- BLACK, J. F.**  
High-temperature optically activated GaAs power switching for aircraft digital electronic control  
[NASA-CR-174711] p 34 N85-12901
- BLAHA, B. J.**  
The NASA altitude wind tunnel - Its role in advanced icing research and development  
[AIAA PAPER 85-0090] p 35 A85-26381  
The NASA Altitude Wind Tunnel (AWT): Its role in advanced icing research and development  
[NASA-TM-86920] p 35 N85-15758
- BLECH, R. A.**  
Hardware for a real-time multiprocessor simulator  
[NASA-TM-83805] p 169 N85-10659
- BLOZY, J. T.**  
Altitude testing of a flight weight, self-cooled, 2D thrust vectoring exhaust nozzle  
[SAE PAPER 841557] p 14 A85-25984
- BLUMBERG, P. N.**  
Methods for heat transfer and temperature field analysis of the insulated diesel  
[NASA-CR-174783] p 185 N85-16699
- BOBER, L. J.**  
Inviscid analysis of advanced turboprop propeller flow fields  
[AIAA PAPER 85-1263] p 6 A85-43977
- BODNER, S. R.**  
A survey of unified constitutive theories p 150 N85-31531
- BOES, D. J.**  
Breakaway friction and dynamic friction/wear measurements of various ceramic materials from 25 C (75 F) to 650 C (1200 F)  
[NASA-CR-174803] p 90 N85-26994
- BOISVERT, R. F.**  
Convective influence on the stability of a cylindrical solid-liquid interface p 109 A85-26911
- BOLDMAN, D. R.**  
Unsteady pressure measurements on a biconvex airfoil in a transonic oscillating cascade  
[NASA-TM-86914] p 8 N85-15689
- BOOMAN, R. A.**  
Velocity visualization in gas flows using laser-induced phosphorescence of biacetyl p 121 A85-21695
- BOPSE, S.**  
Electric utility acid fuel cell stack technology advancement  
[NASA-CR-174804] p 159 N85-17422
- BORDER, D. A.**  
An allpass filter design for luminance and chrominance separation of NTSC signals p 102 A85-28230
- BORREGO, J. M.**  
Electrical characterization of plasma-grown oxides on gallium arsenide p 181 A85-32635  
Heat treatment of bulk gallium arsenide using a phosphosilicate glass cap p 181 A85-32636  
Fabrication of p(+)-n junction GaAs solar cells by a novel method p 181 A85-33645  
Research on gallium arsenide diffused junction solar cells  
[NASA-CR-174057] p 158 N85-11457
- BOWEN, R. R.**  
Development and use of the computer software package for planning the 12 GHz broadcasting-satellite service at RARC '83 p 96 A85-29605
- BOWLES, K. J.**  
Fundamental studies of composite toughness p 56 N85-12948  
Graphite/PMR polyimide composites with improved toughness  
[NASA-TM-87081] p 58 N85-32148
- BOWYER, J.**  
Satellite provided customer promises services, a forecast of potential domestic demand through the year 2000. Volume 4: Sensitivity analysis  
[NASA-CR-174662] p 99 N85-27092
- BOYCE, D. A.**  
Fiberglass epoxy laminate fatigue properties at 300 and 20 K p 56 A85-47970
- BOYD, L. S.**  
Multi-mesh gear dynamics program evaluation and enhancements  
[NASA-CR-174747] p 133 N85-28372
- BOYLE, R. J.**  
Predicted turbine stage performance using quasi-three-dimensional and boundary-layer analyses p 15 A85-34013
- BOZZOLA, R.**  
Application of Runge Kutta time marching scheme for the computation of transonic flows in turbomachines  
[AIAA PAPER 85-1332] p 5 A85-39728
- BRABBS, T. A.**  
Fuel rich catalytic combustion: The first stage of a two-stage combustor p 63 N85-28983  
Fuel-rich catalytic combustion: A soot-free technique for in situ hydrogen-like enrichment  
[NASA-TP-2498] p 63 N85-31244  
Shock tube measurements of growth constants in the branched-chain ethane-carbon monoxide-oxygen system  
[NASA-TM-87068] p 64 N85-32156
- BRAGG, M. B.**  
Predicting rime ice accretion on airfoils p 3 A85-25135
- BRANDHORST, H. W., JR.**  
Photovoltaics - The endless spring p 154 A85-35602  
The NASA photovoltaic technology program p 155 A85-35604  
Lithium counterdoped silicon solar cell  
[NASA-CASE-LEW-14177-1] p 160 N85-20535  
The effects of lithium counterdoping on radiation damage and annealing in n(+)-p silicon solar cells p 50 N85-22586
- BRANDON, S. T.**  
Numerical simulations of positively-biased probes and dielectric-conductor disks in a plasma p 179 A85-17262
- BRAUN, M. J.**  
An analysis of temperature effect in a finite journal bearing with spatial tilt and viscous dissipation p 126 A85-11074  
Plastic flow of plasma sprayed ceramics p 80 A85-24161  
Analysis of experimental shaft seal data for high-performance turbomachines, as for Space Shuttle main engines  
[NASA-TM-86928] p 115 N85-21569  
Nested subcritical flows within supercritical systems  
[NASA-TM-86980] p 115 N85-21574
- BRAUN, W. H.**  
Unsteady flow in a supersonic cascade with two in-passage shocks  
[NASA-CR-3925] p 10 N85-35158
- BRAUSCH, J. F.**  
Experimental investigation of shock-cell noise reduction for dual-stream nozzles in simulated flight  
[NASA-CR-3846] p 175 N85-13549  
Experimental investigation of shock-cell noise reduction for single stream nozzles in simulated flight  
[NASA-CR-3845] p 175 N85-13550
- BREAULT, R. D.**  
Electric utility acid fuel cell stack technology advancement  
[NASA-CR-174804] p 159 N85-17422
- BRENNAN, S. M.**  
Space station propulsion options  
[AIAA PAPER 85-1155] p 45 A85-43975
- BREWE, D.**  
Hydrodynamic lubrication of rigid nonconformal contacts in combined rolling and normal motion  
[ASME PAPER 84-TRIB-13] p 127 A85-21280
- BREWER, G. D.**  
Study of advanced fuel system concepts for commercial aircraft and engines  
[NASA-CR-174752] p 93 N85-19176
- BRIGHAM, B. A.**  
The effect of channel convergence on heat transfer in a passage with short pin fins  
[NASA-TM-83801] p 113 N85-10303

**BRIKMANIS, C. K.**

Life and reliability modeling of bevel gear reductions  
[NASA-TM-87006] p 133 N85-27227

**BRINKER, D. J.**

GaAs and 3-5 compound solar cells status and prospects for use in space  
[NASA-TM-86960] p 49 N85-21261  
GaAs and 3-5 compound solar cells status and prospects for use in space p 49 N85-22580

**BROKAW, R. S.**

Shock tube measurements of growth constants in the branched-chain ethane-carbon monoxide-oxygen system  
[NASA-TM-87068] p 64 N85-32156

**BROMAN, C. L.**

Energy efficient engine ICLS engine bearings, drives and configuration: Detail design report  
[NASA-CR-167871] p 23 N85-10997

**BROOK, J. W.**

The computation of viscid/inviscid interaction on airfoils with separated flow p 6 A85-42954

**BROOKY, J. D.**

Study of controlled diffusion stator blading  
[NASA-CR-167995] p 25 N85-18058

**BROWN, J. R.**

Vehicle/engine integration p 37 N85-17008  
Design and analysis report for the RL10-2B breadboard low thrust engine  
[NASA-CR-174857] p 48 N85-19020

**BROWN, K. E.**

Development and use of the computer software package for planning the 12 GHz broadcasting-satellite service at RARC '83 p 96 A85-29605

**BROWN, K. W.**

Finite element engine blade structural optimization  
[AIAA PAPER 85-0645] p 141 A85-30313

**BROWN, W. F., JR.**

Fracture toughness of hot-pressed beryllium p 66 A85-25835

**BROWN, W. H.**

Acoustic control of free jet mixing  
[AIAA PAPER 85-0569] p 109 A85-25951

**BUCKLEY, D. H.**

Friction and wear of some ferrous-base metallic glasses p 64 A85-11071  
Spherical microglass particle impingement studies of thermoplastic materials at normal incidence p 79 A85-11072  
Cavitation erosion size scale effects p 65 A85-11935

Deformation and erosion of f.c.c. metals and alloys under cavitation attack p 65 A85-12789  
Mechanical-contact-induced transformation from the amorphous to the partially crystalline state in metallic glass p 65 A85-19084  
Friction and wear of ceramics p 80 A85-23833  
A unified relation for cavitation erosion p 109 A85-24445

Properties of coated and modified-surfaces p 53 A85-36694  
Ceramic wear in indentation and sliding contact p 82 A85-39549

Surface hardening of steel by boriding in a cold rf plasma p 68 A85-40275  
Ceramic microstructure and adhesion p 82 A85-40384

Effect of surface configuration during solid particle impingement erosion p 69 A85-42568  
Characterization of solid particle erosion resistance of ductile metals based on their properties p 69 A85-42569

Ceramic microstructure and adhesion  
[NASA-TM-83804] p 83 N85-10186

Effect of humidity on fretting wear of several pure metals  
[NASA-TP-2403] p 72 N85-13006

Effect of barrier height on friction behavior of the semiconductors silicon and gallium arsenide in contact with pure metals p 84 N85-13044

Fundamental tribological properties of ceramics  
[NASA-TM-86915] p 85 N85-15893

Surface effects of corrosive media on hardness, friction, and wear of materials p 85 N85-15896

Characterization of erosion of metallic materials under cavitation attack in a mineral oil  
[NASA-TM-86934] p 74 N85-19075

Tribological properties of boron nitride synthesized by ion beam deposition  
[NASA-TM-86962] p 87 N85-21355

Humidity effects on adhesion of nickel-zinc ferrite in elastic contact with magnetic tape and itself  
[NASA-TP-2449] p 88 N85-21359

Tribological systems as applied to aircraft engines  
[NASA-TM-86965] p 131 N85-21657

Effects of wear on structure-sensitive magnetic properties of ceramic ferrite in contact with magnetic tape  
[NASA-TM-87007] p 90 N85-26991

**BUDDHAVARAPU, J.**

Heat transfer and fluid mechanics measurements in transitional boundary layer flows p 118 N85-31439

**BUFFUM, D. H.**

Unsteady pressure measurements on a biconvex airfoil in a transonic oscillating cascade  
[NASA-TM-86914] p 8 N85-15689

**BUGGELE, A. E.**

Unsteady pressure measurements on a biconvex airfoil in a transonic oscillating cascade  
[NASA-TM-86914] p 8 N85-15689

**BUI, T. D.**

Recent advances in methods for numerical solution of O.D.E. initial value problems p 171 A85-21370

**BUNDAS, D. J.**

Flutter and forced response of mistuned rotors using standing wave analysis p 139 A85-12721

**BURCAT, A.**

High temperature oxidation of propene p 61 A85-33570

Ideal gas thermodynamic properties for the phenyl, phenoxy, and o-biphenyl radicals  
[NASA-TM-83800] p 184 N85-22204

**BURCHAM, R. E.**

Analysis of experimental shaft seal data for high-performance turbomachines, as for Space Shuttle main engines  
[NASA-TM-86928] p 115 N85-21569

**BURGESS, R. M.**

Small centrifugal pumps for low thrust rockets  
[AIAA PAPER 85-1302] p 45 A85-43978

**BURNSIDE, O. H.**

Probabilistic structural analysis theory development p 148 N85-27955

**BURTON, R. L.**

Investigation of a pulsed electrothermal thruster system  
[NASA-CR-174768] p 46 N85-11132

**BUTTRILL, S. E., JR.**

Chemistry of fuel deposits and sediments and their precursors  
[NASA-CR-174778] p 92 N85-10209

**BUZZARD, R. J.**

Experimental compliance calibration of the NASA Lewis Research Center Mode 2 fatigue specimen  
[NASA-TM-86908] p 144 N85-16205

**BYERS, W. D.**

Study of advanced fuel system concepts for commercial aircraft and engines  
[NASA-CR-174752] p 93 N85-19176

**C****CALCO, F. S.**

Precision tunable resonant microwave cavity  
[NASA-CASE-LEW-13935-1] p 103 N85-20248

**CALFO, F. D.**

Replaceable blade turbine and stationary specimen corrosion testing facility  
[NASA-TM-86931] p 73 N85-18126

**CALVERT, W.**

DE-1 measurements of AKR wave directions p 166 A85-37717

**CAMPBELL, D. P.**

Infrared technology for satellite power conversion  
[NASA-CR-174266] p 159 N85-16293

Technology for satellite power conversion  
[NASA-CR-174335] p 159 N85-18451

**CAMPBELL, N. K.**

Reflection plane tests of a wind turbine blade tip section with ailerons  
[NASA-TM-87018] p 165 N85-34444

**CANAL, E.**

Study of controlled diffusion stator blading  
[NASA-CR-167995] p 25 N85-18058

**CARLSON, R. G.**

Energy efficient engine high pressure turbine ceramic shroud support technology report  
[NASA-CR-168036] p 23 N85-10996

**CARLSON, R. L.**

Thermodynamically consistent constitutive equations for nonisothermal large strain, elasto-plastic, creep behavior  
[AIAA PAPER 85-0621] p 142 A85-38425

Analysis of shell type structures subjected to time dependent mechanical and thermal loading  
[NASA-CR-175747] p 147 N85-25896

Dynamic creep buckling: Analysis of shell structures subjected to time-dependent mechanical and thermal loading p 149 N85-27959

**CARM, U.**

Deposition of silicon nitride from SiCl<sub>4</sub> and NH<sub>3</sub> in a low pressure RF plasma p 81 A85-36229

**CAROL, L. A.**

Cyclic oxidation behavior of beta + gamma overlay coatings on gamma and gamma + gamma-prime alloys p 68 A85-32431

A study of interdiffusion in beta + gamma/gamma + gamma prime Ni-Cr-Al  
[NASA-CR-174852] p 74 N85-20041

**CARROLL, D. R.**

Satellite baseband processor test performance summary p 95 A85-14434

**CARRUTHERS, W. D.**

Ceramic component development for the AGT101 gas turbine engine p 126 A85-15972

**CASENT, D.**

Optical linear algebra processors - Noise and error-source modeling p 169 A85-36727

**CASE, S. K.**

Holographic optical system for aberration corrections in laser Doppler velocimetry p 123 A85-48659

**CASPAR, J. R.**

A linearized unsteady aerodynamic analysis for transonic cascades p 3 A85-20744

**CASSADY, P. L.**

Initial feasibility ground test of a proposed photogrammetric system for measuring the shapes of ice accretions on helicopter rotor blades during forward flight  
[NASA-TM-87391] p 12 N85-12887

**CATALDO, R. L.**

Design of a 1-kWh bipolar nickel hydrogen battery p 155 A85-45384

Life cycle test results of a bipolar nickel hydrogen battery  
[NASA-TM-87046] p 163 N85-30480

Life cycle test results of a bipolar nickel hydrogen battery p 105 N85-31406

**CAULEY, M. A.**

The subjective effect of multiple co-channel frequency modulated television interference p 96 A85-28234

**CAULFIELD, H. J.**

An approach for automated analysis of particle holograms p 120 A85-10034

**CAVICCHI, R. H.**

Design and performance of a fixed, nonaccelerating guide vane cascade that operates over an inlet flow angle range of 60 deg  
[ASME PAPER 84-GT-75] p 4 A85-32964

**CRAWLEY, J. D.**

Tape casting as an approach to an all-ceramic turbine shroud seal  
[NASA-TM-87078] p 135 N85-32333

Oxidizing seal for a turbine tip gas path  
[NASA-CASE-LEW-14053-1] p 136 N85-34402

**CELESTINA, M. L.**

Simulation of multistage turbine flows p 116 N85-27945

**CHAI, A. T.**

Screen printed interdigitated back contact solar cell  
[NASA-CASE-LEW-13414-1] p 160 N85-20530

**CHAMBERLIN, R.**

Comparison of scaled model data to full size energy efficient engine test results p 13 A85-13953

Measurement and prediction of Energy Efficient Engine noise  
[AIAA PAPER 84-2284] p 13 A85-13954

The Altitude Wind Tunnel (AWT) - A unique facility for propulsion system and adverse weather testing  
[AIAA PAPER 85-0314] p 34 A85-19661

The Altitude Wind Tunnel (AWT): A unique facility for propulsion system and adverse weather testing  
[NASA-TM-86921] p 35 N85-18067

**CHAMIS, C. C.**

Hygrothermomechanical evaluation of transverse filament tape epoxy/polyester fiberglass composites p 54 A85-15632

Design procedures for fiber composite structural components - Rods, beams, and beam columns p 54 A85-15636

Select fiber composites for space applications - A mechanistic assessment p 54 A85-16040

ICAN - Integrated composites analyzer  
[AIAA PAPER 84-0974] p 54 A85-16094

Interply layer degradation effects on composite structural response p 54 A85-16096

Finite element engine blade structural optimization  
[AIAA PAPER 85-0645] p 141 A85-30313

Resin selection criteria for 'tough' composite structures p 81 A85-35139

Interply layer degradation effects on composite structural response p 55 A85-39215



- A study of interply layer effects on the free edge stress field of angleplied laminates p 55 A85-41127
- Impact resistance of fiber composites
- Energy-absorbing mechanisms and environmental effects p 56 A85-46543
- The 3-D inelastic analysis methods for hot section components: Brief description p 20 N85-10972
- Fabrication and quality assurance processes for superhybrid composite fan blades [NASA-TM-83354] p 57 N85-14882
- A study of interply layer effects on the free-edge stress field of angleplied laminates [NASA-TM-86924] p 57 N85-15822
- Design procedures for fiber composite structural components: Panels subjected to combined in-plane loads [NASA-TM-86909] p 57 N85-15823
- NASA Lewis Research Center/University Graduate Research Program on Engine Structures [NASA-TM-86916] p 145 N85-18375
- Nonlinear structural analysis for fiber-reinforced superalloy turbine blades p 147 N85-26887
- Overview of structural response: Probabilistic structural analysis p 148 N85-27952
- Designing for fiber composite structural durability in hydrothermomechanical environment [NASA-TM-87045] p 58 N85-27978
- CHAN, K. S.**
- A survey of unified constitutive theories p 150 N85-31531
- CHANG, B. J.**
- Engineering model system study for a regenerative fuel cell: Study report [NASA-CR-174801] p 158 N85-16292
- CHANG, H. H.**
- Electrocatalysis of fuel cell reactions: Investigation of alternate electrolytes [NASA-CR-174753] p 157 N85-11455
- CHANG, J. P.**
- On numerical integration and computer implementation of viscoplastic models p 151 N85-31542
- CHANG, S. H.**
- A computer aided design procedure for generating gear teeth [ASME PAPER 84-DET-184] p 128 A85-33779
- CHANG, T. Y.**
- On numerical integration and computer implementation of viscoplastic models p 151 N85-31542
- CHAPMAN, R.**
- Measurements of energy distribution in microwave plasmas of N<sub>2</sub> and He and comparisons with results for H<sub>2</sub> p 178 A85-16443
- CHEN, B. K.**
- Computer program for the calculation of multicomponent convective diffusion deposition rates from chemically frozen boundary layer theory [NASA-CR-168329] p 116 N85-27164
- CHEN, C. C.**
- Advanced 30/20 GHz multiple beam antenna for future communications satellites p 96 A85-14436
- CHEN, C.-J.**
- Development of finite analytic method for unsteady three-dimensional Navier-Stokes equation p 106 A85-11647
- CHEN, D. Y.**
- Bipolar-FET combinational power transistors for power conversion applications p 100 A85-12669
- CHEN, H.-C.**
- Development of finite analytic method for unsteady three-dimensional Navier-Stokes equation p 106 A85-11647
- CHEN, J.**
- Sixty GHz IMPATT diode development [NASA-CR-174969] p 105 N85-33293
- CHERRY, D. G.**
- Energy efficient engine. Low pressure turbine test hardware detailed design report [NASA-CR-167956] p 22 N85-10994
- CHIAPPETTA, L.**
- External fuel vaporization study, phase 2 [NASA-CR-174079] p 92 N85-11252
- CHIAPPETTA, L. M.**
- Finite difference methods for reducing numerical diffusion in TEACH-type calculations [AIAA PAPER 85-0057] p 108 A85-19488
- Error reduction program [NASA-CR-174776] p 172 N85-27584
- CHILDS, M. E.**
- An experimental study of three-dimensional shock wave/turbulent boundary layer interactions in a supersonic flow [AIAA PAPER 85-1566] p 5 A85-40691
- CHIMA, R. C.**
- Efficient solution of the Euler and Navier-Stokes equations with a vectorized multiple-grid algorithm p 2 A85-18679
- CHIMA, R. V.**
- Application of viscous and inviscid computation methods for rocket turbopump systems [SAE PAPER 841522] p 110 A85-39257
- Inviscid and viscous flows in cascades with an explicit multiple-grid algorithm p 7 A85-48539
- CHIN, D. T.**
- Electrocatalysis of fuel cell reactions: Investigation of alternate electrolytes [NASA-CR-174753] p 157 N85-11455
- CHIN, S. A.**
- Bipolar-FET combinational power transistors for power conversion applications p 100 A85-12669
- CHIRIVELLA, J.**
- Study of advanced fuel system concepts for commercial aircraft and engines [NASA-CR-174752] p 93 N85-19176
- CHOE, S. J.**
- The influence of hold times on LCF and FCG behavior in a P/M Ni-base superalloy p 67 A85-32400
- CHOI, S. R.**
- An experimental investigation and numerical prediction of thermomechanical phenomena in high speed rotor tip rubbing p 14 A85-25442
- CHOU, J. H.**
- An experimental study of three-dimensional shock wave/turbulent boundary layer interactions in a supersonic flow [AIAA PAPER 85-1566] p 5 A85-40691
- CHOUINARD, G.**
- Experimental results supporting the determination of service quality objectives for DBS systems p 96 A85-29611
- CHUANG, S. L.**
- Plot of modal field distribution in rectangular and circular waveguides p 101 A85-25170
- Numerical methods for analyzing electromagnetic scattering [NASA-CR-175507] p 99 N85-21438
- Normal modes in an overmoded circular waveguide coated with lossy material p 100 N85-35320
- CHUBB, D. L.**
- Thermionic photovoltaic energy converter [NASA-CASE-LEW-14077-1] p 164 N85-34441
- CHUDNOVSKY, A.**
- Statistics and thermodynamics of fracture p 140 A85-19433
- Translational and extensional energy release rates (the J- and M-integrals) for a crack layer in thermoelasticity [NASA-CR-174872] p 145 N85-21685
- CHUNANG, C. D.**
- Analysis of the electromagnetic scattering from an inlet geometry with lossy walls [NASA-CR-175743] p 99 N85-25686
- CHUNG, B. T. F.**
- Plastic flow of plasma sprayed ceramics p 80 A85-24161
- CIANCONE, M. L.**
- Flow visualization study of the effect of injection hole geometry on an inclined jet in crossflow [NASA-TM-86936] p 115 N85-20269
- CLARK, R. W.**
- Calculation of compressible flow about three-dimensional inlets with auxiliary inlets, slats and vanes by means of a panel method [AIAA PAPER 85-1196] p 5 A85-40817
- Calculation of compressible flow about three-dimensional inlets with auxiliary inlets, slats and vanes by means of a panel method [NASA-CR-174975] p 10 N85-35162
- CLARY, D. W.**
- Transferring data oscilloscope to an IBM using an Apple II+ p 168 A85-24526
- Shock tube study of the fuel structure effects on the chemical kinetic mechanisms responsible for soot formation, part 2 [NASA-CR-174880] p 63 N85-25444
- CLAUS, R. W.**
- Accelerated convergence for incompressible flow calculations [AIAA PAPER 85-0058] p 2 A85-19489
- Flame radiation and linear heat transfer in a tubular-can combustor p 15 A85-39580
- Numerical calculation of subsonic jets in crossflow with reduced numerical diffusion [AIAA PAPER 85-1441] p 110 A85-39780
- Accelerated convergence for incompressible flow calculations [NASA-TM-86863] p 18 N85-10949
- Reducing numerical diffusion for incompressible flow calculations [NASA-TM-83621] p 24 N85-14840
- Combustion research for gas turbine engines [NASA-TM-86963] p 26 N85-21164
- Numerical calculation of subsonic jets in crossflow with reduced numerical diffusion [NASA-TM-87003] p 27 N85-25263
- CLEAVELAND, B.**
- Configuration study for a 30 GHz monolithic receive array: Technical assessment [NASA-CR-174697] p 98 N85-18238
- Configuration study for a 30 GHz monolithic receive array, volume 1 [NASA-CR-174697-VOL-1] p 98 N85-18239
- Configuration study for a 30 GHz monolithic receive array, volume 2 [NASA-CR-174697-VOL-2] p 99 N85-18240
- CLEMONS, J. M.**
- Preparation of silicon carbide-silicon nitride fibers by the pyrolysis of polycarbosilazane precursors [NASA-TM-86505] p 91 N85-28107
- CLINE, S. J.**
- High pressure compressor component performance report [NASA-CR-168245] p 33 N85-34138
- Energy efficient engine. Fan and quarter-stage component performance report [NASA-CR-168070] p 33 N85-34141
- CLOSE, D. A.**
- Apparatus and method for identification of matrix materials in which transuranic elements are embedded using thermal neutron capture gamma-ray emission [DE85-011659] p 125 N85-33454
- CLYMER, B.**
- Optical computer switching network p 178 A85-23134
- CO, C. M.**
- Fundamentals of microcrack nucleation mechanics [NASA-CR-3851] p 137 N85-16195
- COE, H. H.**
- Lubrication and performance of high-speed rolling-element bearings [NASA-TM-86958] p 131 N85-21658
- Effect of speed and press fit on fatigue life of roller-bearing inner-race contact [NASA-TP-2496] p 134 N85-31511
- COFFINBERRY, G. A.**
- Study of advanced fuel system concepts for commercial aircraft [NASA-CR-174751] p 12 N85-19978
- COHEN, S.**
- Large-scale Advanced Propfan (LAP) performance, acoustic and weight estimation, January, 1984 [NASA-CR-174782] p 9 N85-22368
- COLE, G. L.**
- Operating system for a real-time multiprocessor propulsion system simulator. User's manual [NASA-TP-2426] p 171 N85-17596
- COLEMAN, E. B.**
- Experiments in dilution jet mixing - Effects of multiple rows and non-circular orifices [AIAA PAPER 85-1104] p 15 A85-39606
- Experiments in dilution jet mixing effects of multiple rows and non-circular orifices [NASA-TM-86996] p 28 N85-25266
- COLES, D.**
- Free-surface phenomena under low- and zero-gravity conditions [NASA-CR-175835] p 116 N85-27168
- COLLIER, J. P.**
- Effects of cobalt on the hot workability of nickel-base superalloys p 67 A85-32412
- COLLIN, R. E.**
- Circular waveguide bifurcation for asymmetric modes p 101 A85-20170
- Dual-mode coaxial feed with low crosspolarisation p 101 A85-20171
- COLLINS, S. A., JR.**
- Optical computer switching network p 178 A85-23134
- COLLINS, W. R.**
- The use of Ada in distributed simulations p 169 A85-28612
- Moving target, distributed, real-time simulation using Ada p 170 A85-34131
- CONGDON, J. V.**
- Electric utility acid fuel cell stack technology advancement [NASA-CR-174804] p 159 N85-17422
- CONLON, R. J.**
- Preliminary analysis of space mission applications for electromagnetic launchers [NASA-CR-174067] p 35 N85-12071
- CONNOLLY, D. J.**
- An experimental investigation of microstrip properties on soft substrates from 2 to 40 GHz [NASA-TM-86961] p 99 N85-20224

## COOK, C. R.

Energy efficient engine. Volume 2. Appendix A: Component development and integration program [NASA-CR-173085] p 22 N85-10991

## COOK, T. S.

Considerations for damage analysis of gas turbine hot section components [ASME PAPER 84-PVP-77] p 14 A85-18792

## COOKE, D. L.

Three-dimensional calculation of shuttle charging in polar orbit p 40 N85-22486  
Polar orbit electrostatic charging of objects in shuttle wake p 40 N85-22487

## COOPER, L. P.

OTV propulsion technology programmatic overview p 37 N85-16997  
Vehicle/engine integration p 37 N85-17008  
Manrating orbital transfer vehicle propulsion [NASA-TM-87019] p 50 N85-25385  
Status of advanced orbital transfer propulsion [NASA-TM-87069] p 52 N85-35225

## CORIELL, S. R.

Convective influence on the stability of a cylindrical solid-liquid interface p 109 A85-26911

## CORNELL, C. C.

Experimental aerodynamic characteristics of an NACA 0012 airfoil with simulated ice p 12 A85-21844

## CORNILSEN, B. C.

Raman structural studies of the nickel electrode [NASA-CR-175619] p 183 N85-23414

## CORREA, S. M.

Prediction of an axisymmetric combustor flow p 59 A85-12713

## CORRIGAN, R. D.

Shutdown characteristics of the Mod-O wind turbine with aileron controls [NASA-TM-86918] p 159 N85-16299  
Effect of precipitation on wind turbine performance [NASA-TM-86986] p 161 N85-27385  
Performance comparison between NACA 23024 and NACA 64(3)-618 airfoil configured rotors for horizontal-axis wind turbines [NASA-TM-83471] p 163 N85-30477

## COSTI, T.

Improved models for increasing wind penetration, economics and operating reliability [NASA-CR-175538] p 160 N85-20545

## COY, J. J.

A computer aided design procedure for generating gear teeth [ASME PAPER 84-DET-184] p 128 A85-33779  
Dynamic analysis of straight and involute tooth forms [ASME PAPER 84-DET-226] p 128 A85-33780  
Transmission efficiency measurements and correlations with physical characteristics of the lubricant p 89 N85-23781

Life and reliability modeling of bevel gear reductions [NASA-TM-87006] p 133 N85-27227  
Fatigue life analysis of a turboprop reduction gearbox [NASA-TM-87014] p 133 N85-27228  
Spiral bevel and circular arc helical gears: Tooth contact analysis and the effect of misalignment on circular arc helical gears [NASA-TM-87013] p 32 N85-31060  
Generated spiral bevel gears: Optimal machine-tool settings and tooth contact analysis [NASA-TM-87075] p 136 N85-34405

## COYKENDALL, R. D.

Electric utility acid fuel cell stack technology advancement [NASA-CR-174804] p 159 N85-17422

## CRAWLEY, E. F.

Structural response of a rotating bladed disk to rotor whirl [NASA-CR-175605] p 27 N85-22391

## CRIMP, M. A.

Rapidly solidified NiAl and FeAl [NASA-TM-86941] p 74 N85-20042

## CROSLEY, P. B.

Fracture of composite-adhesive-composite systems p 141 A85-27935

## CROSS, E. J., JR.

Experimental aerodynamic characteristics of an NACA 0012 airfoil with simulated ice p 12 A85-21844

## CULL, R.

Control algorithms and computer simulation of a stand-alone photovoltaic village power system p 153 A85-11345

## CULLER, J. E.

Control algorithms and computer simulation of a stand-alone photovoltaic village power system p 153 A85-11345  
Control aspects of the Schuchuli Village stand-alone photovoltaic power system [NASA-TM-83790] p 103 N85-13157

## CUNNINGHAM, A. R.

Jet fuel property changes and their effect on producibility and cost in the U.S., Canada, and Europe [NASA-CR-174840] p 93 N85-27012

## CUNNINGHAM, R. E.

Preliminary results on passive eddy current damper technology for SSME turbomachinery p 132 N85-26890

Variable force, eddy-current or magnetic damper [NASA-CASE-LEW-13717-1] p 134 N85-30333

## CURRAN, F. M.

Hollow cathodes in high pressure arc discharges [NASA-TM-87098] p 52 N85-34179

## CURREN, A. N.

Textured carbon surfaces on copper [NASA-CASE-LEW-14130-1] p 95 N85-20156

## CURTIS, H.

Near-optimum design of GaAs-based concentrator space solar cells for 80 C operation p 153 A85-15800

## CURTIS, H. B.

Effects of 1 MeV electrons and 10 MeV protons on the performance and reflectance of thin BSR cells p 182 A85-35699

## CUSANO, C.

The influence of temperature on the lubricating effectiveness of MoS<sub>2</sub> dispersed in mineral oils [ASLE PREPRINT 84-LC-2A-2] p 80 A85-25963

## CYR, M. A.

Development of advanced high-temperature heat flux sensors. Phase 2: Verification testing [NASA-CR-174973] p 126 N85-35391

## D

## DADONE, L.

Performance degradation of helicopter rotor in forward flight due to ice p 11 A85-42937

## DAHL, M. D.

The performance of jet noise suppression devices for industrial applications p 175 A85-42563  
Measured acoustic properties of variable and low density bulk absorbers [NASA-TM-87065] p 177 N85-30770

## DAME, L. T.

Finite element analysis of notch behavior using a state variable constitutive equation p 152 N85-31548

## DANIEL, S. R.

Jet fuel instability mechanisms [NASA-CR-175856] p 93 N85-28127

## DANIELE, C. J.

A generalized computer code for developing dynamic gas turbine engine models (DIGTEM) p 17 A85-49021

## DANIELS, J. G.

Preparation of silicon carbide-silicon nitride fibers by the pyrolysis of polycarbosilazane precursors [NASA-TM-86505] p 91 N85-28107

## DAUDET, H. C.

Advanced technology cogeneration system conceptual design study: Closed cycle gas turbines [NASA-CR-168222] p 159 N85-16300

## DAVIS, R. E.

GASP cloud encounter statistics - Implications for laminar flow control flight p 166 A85-11979  
Variability of cloudiness at airline cruise altitudes from GASP measurements p 166 A85-31199

## DAVIS, R. H.

Contingency power concepts for helicopter turboshaft engine p 15 A85-32005

## DAYAN, M.

AES and LEED study of the zinc blende SiC(100) surface p 61 A85-41633

## DEADMORE, D. L.

Digital temperature and velocity control of mach 0.3 atmospheric pressure durability testing burner rigs in long time, unattended cyclic testing [NASA-TM-86959] p 75 N85-21321

## DEBOER, G. J.

Materials for advanced turbine engines. Project 2: Rene 150 directionally solidified superalloy turbine blades, volume 2 [NASA-CR-167993] p 23 N85-12059

## DECKER, A. J.

A comparison of electronic heterodyne moire deflectometry and electronic heterodyne holographic interferometry for flow measurements [NASA-TM-87071] p 125 N85-32302

## DECKERT, J. C.

A design methodology for robust failure detection and isolation p 171 A85-47794

## DEGAETANO, E.

Cryogenic upper stage test bed engine [AIAA PAPER 85-1339] p 44 A85-39733

## DEIDRICH, J. H.

Analytical and physical modeling program for the NASA Lewis Research Center's Altitude Wind Tunnel (AWT) [NASA-TM-86919] p 35 N85-15757

## DEISSLER, R. G.

Turbulent solutions of equations of fluid motion p 118 N85-31441

## DELAAT, J. C.

A real-time FORTRAN implementation of a sensor failure detection, isolation and accommodation algorithm p 171 A85-47704

## DELOMBARD, R.

Control algorithms and computer simulation of a stand-alone photovoltaic village power system p 153 A85-11345  
Status of DOE and AID stand-alone photovoltaic system field tests p 155 A85-35707  
Control aspects of the Schuchuli Village stand-alone photovoltaic power system [NASA-TM-83790] p 103 N85-13157

## DEMIGLIO, R. D.

Effect of precipitation on wind turbine performance [NASA-TM-86986] p 161 N85-27385

## DENGLER, R. P.

Advanced secondary power system for transport aircraft [NASA-TP-2463] p 30 N85-28944

## DEUTSCH, S.

The boundary layer on compressor cascade blades [NASA-CR-174369] p 114 N85-18292

## DIAMOND, W. A.

Analysis of experimental shaft seal data for high-performance turbomachines, as for Space Shuttle main engines [NASA-TM-86928] p 115 N85-21569

## DICARLO, J. A.

High temperature metal and ceramic composites p 55 A85-37483  
Fibers for structurally reliable metal and ceramic composites p 55 A85-37484  
High performance fibers for structurally reliable metal and ceramic composites [NASA-TM-86878] p 56 N85-12095  
Creep of chemically vapor deposited SiC fibers [NASA-TM-86897] p 56 N85-14878

## DIEDRICH, J. H.

Analytical and physical modeling program for the NASA Lewis Research Center's Altitude Wind Tunnel (AWT) [AIAA PAPER 85-0379] p 34 A85-19709

## DIEM-KIRSOP, P. S.

Advanced radiator concepts [NASA-TM-87008] p 115 N85-24245

## DIRUSSO, E.

Variable friction secondary seal for face seals [NASA-CASE-LEW-14170-1] p 131 N85-20377

## DITTMAR, J. H.

Observations from varying the lift and drag inputs to a noise prediction method for supersonic helical tip speed propellers [NASA-TM-83797] p 175 N85-10788  
Further comparison of wind tunnel and airplane acoustic data for advanced design high speed propeller models [NASA-TM-86935] p 176 N85-22108

## DIVERGILIO, W. F.

High frequency plasma generator for ion thrusters [NASA-CR-174772] p 48 N85-17023

## DOCHAT, G.

Free-piston Stirling engine/linear alternator 1000-hour endurance test [NASA-CR-174771] p 163 N85-30481

## DOLAN, F. X.

An experimental investigation of rubbing interaction in labyrinth seals at cryogenic temperature p 129 A85-39938

Analytical and experimental investigation of rubbing interaction in labyrinth seals for a liquid hydrogen fuel pump [NASA-CR-174657] p 48 N85-18084

## DOWNEY, A. N.

An experimental investigation of microstrip properties on soft substrates from 2 to 40 GHz [NASA-TM-86961] p 99 N85-20224

## DOYCHAK, J. K.

The transient oxidation of single crystal NiAl + Zr [NASA-CR-174756] p 70 N85-11221

## DRESFIELD, R. L.

PM superalloys - A troubled adolescent? p 69 A85-44772

Effects of tin on microstructure and mechanical behavior of Inconel 718 [NASA-TM-86866] p 71 N85-12129

## DUBIEL, D. J.

Energy efficient engine combustor test hardware detailed design report [NASA-CR-167945] p 18 N85-10950

**DUDERSTADT, E. C.**

Life modeling of atmospheric and low pressure plasma-sprayed thermal-barrier coating

p 81 A85-29728

Energy efficient engine, high pressure turbine thermal barrier coating. Support technology report [NASA-CR-168037] p 34 N85-35199

**DUGUNDJI, J.**

Flutter and forced response of mistuned rotors using standing wave analysis p 139 A85-12721

**DUKE, J. C., JR.**

A study of the stress wave factor technique for the characterization of composite materials [NASA-CR-174870] p 58 N85-30035

**DULGEROFF, C. R.**

IAPS (8-cm) ion thruster cyclic endurance test p 42 A85-16406

Ion thruster system (8-cm) cyclic endurance test [NASA-CR-174745] p 47 N85-12937

**DUNBAR, W. G.**

High voltage requirements and issues for the 1990's p 46 A85-45429

**DUQUETTE, D. J.**

The influence of hold times on LCF and FCG behavior in a P/M Ni-base superalloy p 67 A85-32400

**DURBIN, P. A.**

Resonance in flows with vortex sheets and edges p 1 A85-10357

Approximate analysis for resonance of an incompressible shear layer plus edges p 107 A85-19377

Flow through very porous inclined screens [AIAA PAPER 85-1650] p 111 A85-40750

Flow through very porous inclined screens [NASA-TM-86979] p 116 N85-25761

**DUSTIN, M. O.**

Solar dynamic systems p 164 N85-31374

**DYBBS, A.**

A new interpretation of internal heat transfer coefficients of porous media [ASME PAPER 84-WA/HT-51] p 110 A85-39894

**E****EARHART, R. W.**

Preliminary analysis of space mission applications for electromagnetic launchers [NASA-CR-174067] p 35 N85-12071

**EBERT, L. J.**

Elevated temperature creep-rupture behavior of the single crystal nickel-base superalloy NASAIR 100 p 66 A85-27812

Influence of composition on the microstructure and mechanical properties of a nickel-base superalloy single crystal p 66 A85-32387

Factors which influence directional coarsening of gamma-prime during creep in nickel-base superalloy single crystals p 67 A85-32388

**EBIHARA, B. T.**

Apparatus for mounting a field emission cathode [NASA-CASE-LEW-14108-1] p 104 N85-29149

Multistage spent particle collector and a method for making same [NASA-CASE-LEW-13914-1] p 135 N85-33489

**ECER, A.**

A finite element solution of three-dimensional inviscid rotational flows through curved ducts p 107 A85-11648

**ECK, T. G.**

Study of Kapton under simulated shuttle environment [NASA-CR-176003] p 41 N85-29997

**EDWARD, B.**

Configuration study for a 30 GHz monolithic receive array: Technical assessment [NASA-CR-174697] p 98 N85-18238

Configuration study for a 30 GHz monolithic receive array, volume 1 [NASA-CR-174697-VOL-1] p 98 N85-18239

Configuration study for a 30 GHz monolithic receive array, volume 2 [NASA-CR-174697-VOL-2] p 99 N85-18240

**EHRESMAN, C. M.**

A stagnation pressure probe for droplet-laden air flow [AIAA PAPER 85-0330] p 108 A85-19672

**ELGHOBASHI, S.**

A two-equation turbulence model for two-phase jets p 107 A85-14376

**ELLIOT, J. E.**

Moderate temperature sodium cells. V - Discharge reactions and rechargeability of NiS and NiS<sub>2</sub> positive electrodes in molten NaAlCl<sub>4</sub> p 59 A85-11892

**ELLIS, J. R.**

Some advances in experimentation supporting development of viscoplastic constitutive models [NASA-CR-174855] p 147 N85-27260

Some advances in experimentation supporting development of viscoplastic constitutive models p 151 N85-31545

Results of an interlaboratory fatigue test program conducted on alloy 800H at room and elevated temperatures [NASA-CR-174940] p 152 N85-32340

**EMERY, A. F.**

Metallurgical and mechanical phenomena due to rubbing of titanium against sintered powder Nichrome p 127 A85-22281

An experimental investigation and numerical prediction of thermomechanical phenomena in high speed rotor tip rubbing p 14 A85-25442

**ENGLISH, R. E.**

Dynamic power systems for power generation p 158 N85-13892

Preliminary assessment of power-generating tethers in space and of propulsion for their orbit maintenance p 37 N85-22520

**ENGLUND, D. R.**

The infinite line pressure probe p 122 A85-37704

Thin-film sensors for space propulsion technology p 41 N85-27968

**ENOCH, J.**

Numerical simulations of positively-biased probes and dielectric-conductor disks in a plasma p 179 A85-17262

**ENSWORTH, C. B. F.**

Analytical model for predicting emergency shutdown of a two-bladed horizontal axis wind turbine [NASA-TM-83472] p 162 N85-30476

Performance comparison between NACA 23024 and NACA 64(3)-618 airfoil configured rotors for horizontal-axis wind turbines [NASA-TM-83471] p 163 N85-30477

**ENVIA, E.**

Noise produced by the interaction of a rotor wake with a swept stator blade [AIAA PAPER 84-2326] p 173 A85-13956

**EPSTEIN, A.**

Rotor wake characteristics of a transonic axial flow fan [AIAA PAPER 85-1133] p 6 A85-43974

**ERCEGOVAC, M. D.**

A functional language approach in high-speed digital simulation p 170 A85-28615

General approaches for achieving high speed computations p 169 A85-28628

Functional language and data flow architectures p 170 A85-28629

**ERCEGOVIC, B. A.**

Flat-plate transition p 118 N85-31438

**ERNST, W. D.**

Mod II engine and technology development p 129 A85-45473

**ESKRIDGE, R. R.**

Energy efficient engine ICLS Nacelle detail design report [NASA-CR-167870] p 22 N85-10993

**ESPINOSA, V. E.**

Spray characterization with a nonintrusive technique using absolute scattered light p 120 A85-10036

Research study of droplet sizing technology leading to the development of an advanced droplet sizing system [NASA-CR-174839] p 123 N85-21604

**ETEMAD, S.**

Metallurgical and mechanical phenomena due to rubbing of titanium against sintered powder Nichrome p 127 A85-22281

An experimental investigation and numerical prediction of thermomechanical phenomena in high speed rotor tip rubbing p 14 A85-25442

**ETERNO, J. S.**

A design methodology for robust failure detection and isolation p 171 A85-47794

**EVANS, D. J.**

Hot isostatically pressed manufacture of high strength MERL 76 disk and seal shapes [NASA-CR-165550] p 71 N85-11225

**EVANS, J. C., JR.**

High-voltage solar-cell chip p 154 A85-24668

**EVERSMAN, W.**

Modelling of wind tunnel wall effects on the radiation characteristics of acoustic sources [AIAA PAPER 84-2364] p 174 A85-16104

**EWASHINKA, J. G.**

Results of electric-vehicle propulsion system performance on three lead-acid battery systems p 156 A85-45443

**EYSSA, Y. M.**

A rotating superconducting solenoid for 100 kWh energy storage p 44 A85-33144

**F****FADDOUL, J. R.**

Ten year environmental test of glass fiber/epoxy pressure vessels [AIAA PAPER 85-1198] p 56 A85-47022

Ten year environmental test of glass fiber/epoxy pressure vessels [NASA-TM-87058] p 58 N85-30034

**FAETH, F. M.**

The structure of dilute combustive sprays [NASA-CR-174838] p 24 N85-15728

**FAETH, G. M.**

Drop-turbulence interactions in a diffusion flame [AIAA PAPER 85-0319] p 60 A85-19665

Structure of particle-laden jets - Measurements and predictions p 109 A85-25137

Structure of ducted particle-laden turbulent jets p 110 A85-38999

Measurements and predictions of the structure of evaporating sprays p 112 A85-46484

Structure of nonevaporating sprays. I - Initial conditions and mean properties p 112 A85-48538

**FAIRBANKS, N. P.**

Advanced blade tip seal system, volume 2 [NASA-CR-167851] p 23 N85-10999

**FANG, Q. T.**

Convective influence on the stability of a cylindrical solid-liquid interface p 109 A85-26911

**FARKAS, D.**

New eutectic alloys and their heats of transformation p 66 A85-27808

**FARR, E.**

Characterization of MMIC devices for active array antennas [NASA-TM-86907] p 38 N85-15779

**FAYMON, K. A.**

High voltage requirements and issues for the 1990's p 46 A85-45429

**FEATHERSTON, C. D.**

Jet fuel property changes and their effect on producibility and cost in the U.S., Canada, and Europe [NASA-CR-174840] p 93 N85-27012

**FEINGOLD, E.**

Transformation toughened ceramics for the heavy duty diesel engine technology program [NASA-CR-174689] p 185 N85-16698

**FELDMAN, U.**

Characterization of microstrip discontinuities in the time and frequency domains [NASA-CR-176190] p 106 N85-35342

**FENG, Z.**

A rotating superconducting solenoid for 100 kWh energy storage p 44 A85-33144

**FERET, J. M.**

Gas cooled fuel cell systems technology development [NASA-CR-174732] p 158 N85-16291

**FERGUSON, B. L.**

Powder metallurgy forged gear development. [NASA-TM-87483] p 134 N85-29295

**FERGUSON, D. C.**

Laboratory degradation of Kapton in a low energy oxygen ion beam [AIAA PAPER 83-2658] p 78 A85-10675

Laboratory studies of Kapton degradation in an oxygen ion beam p 177 N85-22477

Ram-wake effects on plasma current collection of the PIX 2 Langmuir probe p 180 N85-22496

**FERGUSON, T. V.**

Feasibility of mapping velocity flow fields in SSME powerhead by laser anemometry techniques p 41 N85-27971

**FERRANTE, J.**

Universal binding energy relations in metallic adhesion [NASA-TM-86869] p 72 N85-12132

**FERRELL, G. B.**

Flow visualization of lateral jet injection into swirling crossflow [AIAA PAPER 85-0059] p 2 A85-19490

Turbulence measurements of lateral jet injection into confined tubular crossflow [AIAA PAPER 85-1102] p 110 A85-39604

Deflected jet experiments in a turbulent combustor flowfield [NASA-CR-174863] p 26 N85-22390

**FESLER, W.**

High pressure compressor component performance report [NASA-CR-168245] p 33 N85-34138

**FEYOCK, S.**

The use of Ada in distributed simulations p 169 A85-28612

Moving target, distributed, real-time simulation using Ada p 170 A85-34131

- FIELD, R. D.**  
Rapid solidification and dynamic compaction of Ni-base superalloy powders p 67 A85-32414
- FIEDLER, W. L.**  
Reactions of NaCl with gaseous SO<sub>3</sub>, SO<sub>2</sub>, and O<sub>2</sub> p 59 A85-11897  
Oxidation and hot corrosion of hot-pressed Si<sub>3</sub>N<sub>4</sub> at 1000 deg C [NASA-TM-86977] p 88 N85-21358
- FILPUS, J. W.**  
The energetics of hydrogen atom recombination - Analysis, experiments, and modeling p 179 A85-16444
- FINBERG, I.**  
Surface hardening of steel by boriding in a cold rf plasma p 68 A85-40275
- FINNEGAN, P. M.**  
Preliminary assessment of power-generating tethers in space and of propulsion for their orbit maintenance p 37 N85-22520
- FITZGERALD, K.**  
Preliminary evaluation of a liquid belt radiator for space applications [NASA-CR-174807] p 47 N85-15804
- FLANAGAN, P. M.**  
Investigation on experimental techniques to detect, locate and quantify gear noise in helicopter transmissions [NASA-CR-3847] p 176 N85-17667
- FLEETER, S.**  
The effect of aerodynamic and structural detuning on turbomachine supersonic unstalled torsional flutter [AIAA PAPER 85-0761] p 14 A85-30378  
Aerodynamic detuning analysis of an unstalled supersonic turbofan cascade [NASA-TM-87001] p 9 N85-26670
- FLEMING, D. P.**  
Dual clearance squeeze film damper for high load conditions [ASME PAPER 84-TRIB-7] p 128 A85-32960  
Experimental stiffness of tapered bore seals [NASA-TM-86978] p 132 N85-25847  
Dual clearance squeeze film damper [NASA-CASE-LEW-13506-1] p 135 N85-33490
- FLOOD, D. J.**  
GaAs and 3-5 compound solar cells status and prospects for use in space [NASA-TM-86960] p 49 N85-21261  
GaAs and 3-5 compound solar cells status and prospects for use in space p 49 N85-22580  
High efficiency solar cell research for space applications p 164 N85-31624
- FLORENCE, D. E.**  
Vehicle/engine integration p 37 N85-17008
- FLYNN, E. M.**  
The use of a laser Doppler velocimeter in a standard flammability tube [NASA-CR-174960] p 125 N85-35389
- FOGG, H. W.**  
Study of advanced fuel system concepts for commercial aircraft and engines [NASA-CR-174752] p 93 N85-19176
- FORD, C. W.**  
Magnesium doping of efficient GaAs and Ga(0.75)In(0.25)As solar cells grown by metalorganic chemical vapor deposition p 180 A85-11466
- FORDYCE, J. S.**  
Missions/planning panel p 36 N85-13886
- FORMAN, R.**  
Apparatus for mounting a field emission cathode [NASA-CASE-LEW-14108-1] p 104 N85-29149
- FORT, E. F.**  
Methods for heat transfer and temperature field analysis of the insulated diesel [NASA-CR-174783] p 185 N85-16699
- FOSNIGHT, V. V.**  
High frequency plasma generator for ion thrusters [NASA-CR-174772] p 48 N85-17023
- FOSS, J. F.**  
Development of a temperature measurement system with application to a jet in a cross flow experiment [NASA-CR-174896] p 27 N85-25262
- FOUST, R. R.**  
Design and analysis report for the RL10-2B breadboard low thrust engine [NASA-CR-174857] p 48 N85-19020
- FRANK, L. A.**  
Suprathermal plasma observed on STS-3 Mission by plasma diagnostics package p 179 N85-22472
- FRANKS, L. A.**  
Apparatus and method for identification of matrix materials in which transuranic elements are embedded using thermal neutron capture gamma-ray emission [DE85-011659] p 125 N85-33454
- FRASER, H. L.**  
Rapid solidification and dynamic compaction of Ni-base superalloy powders p 67 A85-32414
- FREDERICK, G. R.**  
Structural analysis and cost estimate of an eight-leg space frame as a support structure for horizontal axis wind turbines [NASA-TM-83470] p 150 N85-30361
- FREEDMAN, M. R.**  
Milling of Si<sub>3</sub>N<sub>4</sub> with Si<sub>3</sub>N<sub>4</sub> hardware [NASA-TM-86864] p 84 N85-10191  
Factors influencing the ball milling of Si<sub>3</sub>N<sub>4</sub> in water [NASA-TM-86932] p 86 N85-19136  
Parametric evaluation of ball milling of SiC in water [NASA-TM-86974] p 88 N85-21356
- FREEDMAN, R. J.**  
Initial feasibility ground test of a proposed photogrammetric system for measuring the shapes of ice accretions on helicopter rotor blades during forward flight [NASA-TM-87391] p 12 N85-12887
- FRENKLACH, M.**  
Systematic optimization of a detailed kinetic model using a methane ignition example p 59 A85-12890  
Shock tube study of the fuel structure effects on the chemical kinetic mechanisms responsible for soot formation, part 2 [NASA-CR-174880] p 63 N85-25444
- FRENKLACH, M. Y.**  
Transferring data oscilloscope to an IBM using an Apple II+ p 168 A85-24526
- FRIEDMAN, D. M.**  
Calculation of compressible flow about three-dimensional inlets with auxiliary inlets, slats and vanes by means of a panel method [AIAA PAPER 85-1196] p 5 A85-40817  
Calculation of compressible flow about three-dimensional inlets with auxiliary inlets, slats and vanes by means of a panel method [NASA-CR-174975] p 10 N85-35162
- FRISA, L. E.**  
Ion flow experiments in a multipole discharge chamber p 178 A85-12705
- FRITSCH, K.**  
Remote displacement measurements using a laser diode p 121 A85-24464
- FRONEK, D. L.**  
Heat transfer results and operational characteristics of the NASA Lewis Research Center Hot Section Cascade Test Facility [NASA-TM-86890] p 114 N85-15133
- FROTA, M. N.**  
Heat transfer and turbulence measurements of a film-cooled flow over a convexly curved surface p 112 A85-41787
- FRYBURG, G. C.**  
Chemical reactions involved in the initiation of hot corrosion of IN-738 p 66 A85-31688
- FRYE, R. J.**  
Advanced secondary power system for transport aircraft [NASA-TP-2463] p 30 N85-28944
- FRYXELL, R. E.**  
Effects of surface chemistry on hot corrosion life [NASA-CR-174915] p 28 N85-26711
- FU, K. C.**  
Thermal-stress analysis for a wood composite blade [NASA-CR-174794] p 159 N85-17421
- FU, L. S.**  
Ultrasonic wave propagation in two-phase media - Spherical inclusions p 54 A85-11926  
Fundamentals of microcrack nucleation mechanics [NASA-CR-3851] p 137 N85-16195
- FUJII, M.**  
Development of coated single-crystal superalloy systems for gas turbine applications p 68 A85-32440
- FUNG, S. S.**  
Topological reaction rate measurements related to scuffing p 64 A85-11070
- FURST, R. B.**  
Small centrifugal pumps for low thrust rockets [AIAA PAPER 85-1302] p 45 A85-43978
- FURUHAMA, K.**  
Heat transfer and turbulence measurements of a film-cooled flow over a convexly curved surface p 112 A85-41787
- FUSARO, R. L.**  
Polyimides - Tribological properties and their use as lubricants p 79 A85-21524  
Friction, wear, transfer, and wear surface morphology of ultrahigh-molecular-weight polyethylene p 80 A85-22276  
Tribological properties of graphite-fiber-reinforced, partially fluorinated polyimide composites [NASA-TM-86926] p 86 N85-18153
- Effect of counterface material type and its topography on the tribological properties of polyimide composites [NASA-TM-87036] p 90 N85-26993

## G

- GAAB, T. P.**  
Orientation and temperature dependence of some mechanical properties of the single-crystal nickel-base superalloy Rene N4. 3: Tension-compression anisotropy [NASA-TM-86982] p 76 N85-22660
- GABB, T. P.**  
On the fatigue crack propagation behavior of superalloys at intermediate temperatures p 68 A85-32434
- GAHN, R. F.**  
Cycling performance of the iron-chromium redox energy storage system [NASA-TM-87034] p 162 N85-27387
- GAIER, J. R.**  
Stability of bromine intercalated graphite fibers [NASA-TM-86859] p 84 N85-10187  
Homogeneity of pristine and bromine intercalated graphite fibers [NASA-TM-87016] p 89 N85-25521  
Environmental stability of intercalated graphite fibers [NASA-TM-87025] p 90 N85-26992
- GALLAGHER, J. J.**  
Infrared technology for satellite power conversion [NASA-CR-174266] p 159 N85-16293  
Technology for satellite power conversion [NASA-CR-174335] p 159 N85-18451
- GALLER, D. E.**  
Design and analysis report for the RL10-2B breadboard low thrust engine [NASA-CR-174857] p 48 N85-19020
- GANGL, K. J.**  
Diffusion welding of Cassegrainian concentrator cell stack assemblies [NASA-CR-176104] p 164 N85-33566
- GARDNER, W. B.**  
Energy Efficient Engine Program technology benefit/cost study, volume 1 [NASA-CR-174766-VOL-1] p 33 N85-35197  
Energy Efficient Engine Program technology benefit/cost study, volume 2 [NASA-CR-174766-VOL-2] p 33 N85-35198
- GAROW, J.**  
Regenerative fuel cell energy storage system for a low Earth orbit space station [NASA-CR-174802] p 158 N85-13371
- GARRETT, H. B.**  
Design guidelines for assessing and controlling spacecraft charging effects p 40 N85-22500
- GARRISON, P. W.**  
An evaluation of oxygen/hydrogen propulsion systems for the Space Station [AIAA PAPER 85-1156] p 45 A85-43976  
An evaluation of oxygen-hydrogen propulsion systems for the Space Station [NASA-TM-87059] p 52 N85-28971
- GAUGLER, R. E.**  
A review and analysis of boundary layer transition data for turbine application [NASA-TM-86880] p 113 N85-10306  
A review and analysis of boundary layer transition data for turbine application p 118 N85-31440
- GAUNTNER, J. W.**  
Contingency power concepts for helicopter turboshaft engine p 15 A85-32005
- GAY, C. H.**  
Energy efficient engine. Low pressure turbine test hardware detailed design report [NASA-CR-167956] p 22 N85-10994
- GAYDA, J.**  
On the fatigue crack propagation behavior of superalloys at intermediate temperatures p 68 A85-32434  
Orientation and temperature dependence of some mechanical properties of the single-crystal nickel-base superalloy Rene N4. 3: Tension-compression anisotropy [NASA-TM-86982] p 76 N85-22660
- GAYDOSH, D. J.**  
Ductility in rapidly solidified NiAl p 66 A85-26158  
Rapidly solidified NiAl and FeAl [NASA-TM-86941] p 74 N85-20042
- GELDER, T. F.**  
Design and performance of a fixed, nonaccelerating guide vane cascade that operates over an inlet flow angle range of 60 deg [ASME PAPER 84-GT-75] p 4 A85-32964
- GENERAZIO, E. R.**  
The scattering of ultrasonic third sound from substrate surface defects p 174 A85-36047

- The role of the reflection coefficient in precision measurement of ultrasonic attenuation p 137 A85-42151
- GEORGALAS, G.**  
Laser balancing system for high material removal rates [NASA-CR-174731] p 126 N85-12341
- GERHART, P. M.**  
Progress in development of a Navier-Stokes solver for evaluation of iced airfoil performance [AIAA PAPER 85-0410] p 3 A85-19731
- GERTZ, J.**  
Rotor wake characteristics of a transonic axial flow fan [AIAA PAPER 85-1133] p 6 A85-43974
- GHALLA-GORADIA, M.**  
Near-optimum design of GaAs-based concentrator space solar cells for 80 C operation p 153 A85-15800  
Preliminary design of a 10 kW thermophotovoltaic system for space applications p 45 A85-45371
- GHANDHI, S. K.**  
Electrical characterization of plasma-grown oxides on gallium arsenide p 181 A85-32635  
Heat treatment of bulk gallium arsenide using a phosphosilicate glass cap p 181 A85-32636  
Fabrication of p(+)-n junction GaAs solar cells by a novel method p 181 A85-33645
- GHANDI, S. K.**  
Research on gallium arsenide diffused junction solar cells [NASA-CR-174057] p 158 N85-11457
- GHIA, K. N.**  
Computation of internal flows: Methods and applications; Proceedings of the Energy Sources Technology Conference, New Orleans, LA, February 12-16, 1984 p 106 A85-11630  
Two-dimensional internal compressible viscous flows using semi-elliptic analysis p 106 A85-11640
- GHIA, U.**  
Two-dimensional internal compressible viscous flows using semi-elliptic analysis p 106 A85-11640
- GHOSE, H. M.**  
A computer simulation of thin film nucleation and growth: The Volmer-Weber case [NASA-TM-86968] p 53 N85-21264
- GHOSH, A.**  
Optical linear algebra processors - Noise and error-source modeling p 169 A85-36727
- GHOSH, M. K.**  
Hydrodynamic lubrication of rigid nonconformal contacts in combined rolling and normal motion [ASME PAPER 84-TRIB-13] p 127 A85-21280  
Thermal elastohydrodynamic lubrication of line contacts p 128 A85-31202
- GILES, M. B.**  
A numerical study of the steady scalar convective diffusion equation for small viscosity p 107 A85-16533
- GILGER, L. D.**  
Extreme precision antenna reflector study results p 165 N85-23830
- GILMORE, D. R., JR.**  
TF34 convertible engine control system design p 15 A85-32006
- GINTY, C. A.**  
Select fiber composites for space applications - A mechanistic assessment p 54 A85-16040
- GLADDEN, H. J.**  
Transient technique for measuring heat transfer coefficients on stator airfoils in a jet engine environment [AIAA PAPER 85-1471] p 122 A85-39796  
Heat transfer results and operational characteristics of the NASA Lewis Research Center Hot Section Cascade Test Facility [NASA-TM-86890] p 114 N85-15133  
Transient technique for measuring heat transfer coefficients on stator airfoils in a jet engine environment [NASA-TM-87005] p 124 N85-25794
- GLASGOW, T. K.**  
Demonstration of a silicon nitride attrition mill for production of fine pure Si and Si<sub>3</sub>N<sub>4</sub> powders p 78 A85-10825  
Diffusion welding of MA 6000 and a conventional nickel-base superalloy p 69 A85-43551  
Microstructures in rapidly solidified Ni-Mo alloys [NASA-TM-87100] p 78 N85-34266
- GLASSMAN, A. J.**  
Future directions in aeropropulsion technology [NASA-TM-87010] p 1 N85-23685
- GLENN, W. H.**  
Fiber optic temperature sensor p 121 A85-29563
- GLICKSMAN, M. E.**  
Convective influence on the stability of a cylindrical solid-liquid interface p 109 A85-26911
- GLIEBE, P. R.**  
Effects of vane/blade ratio and spacing on fan noise, volume 1 p 176 N85-19791 [NASA-CR-174664]  
Effects of vane/blade ratio and spacing on fan noise. Volume 2: Data supplement p 176 N85-19792 [NASA-CR-174665]  
Development of a rotor wake-vortex model, volume 1 [NASA-CR-174849] p 9 N85-26668
- GODLEWSKI, M. P.**  
Effect of solar-cell junction geometry on open-circuit voltage p 154 A85-28080  
Voltage controlling mechanisms in low resistivity silicon solar cells - A unified approach p 155 A85-35617  
The effect of diffusion induced lattice stress on the open-circuit voltage in silicon solar cells p 181 A85-35620  
The high voltage silicon cell: A comparative analysis p 49 N85-22569
- GOEDE, H.**  
High frequency plasma generator for ion thrusters [NASA-CR-174772] p 48 N85-17023
- GOEKOGLU, S. A.**  
Computer program for the calculation of multicomponent convective diffusion deposition rates from chemically frozen boundary layer theory [NASA-CR-168329] p 116 N85-27164
- GOEL, P.**  
A study of Reynolds-stress closure model [NASA-CR-174342] p 114 N85-17324
- GOERTZ, C. K.**  
Effects of chemical releases by the STS 3 orbiter on the ionosphere p 166 A85-29538
- GOLDBERG, A. A.**  
Experimental results supporting the determination of service quality objectives for DBS systems p 96 A85-29611
- GOLDSTEIN, D. N.**  
Contingency power concepts for helicopter turboshaft engine p 15 A85-32005
- GOLDSTEIN, M. E.**  
Generation of instability waves in flows separating from smooth surfaces p 1 A85-10352  
Sound generation and upstream influence due to instability waves interacting with non-uniform mean flows p 174 A85-20738  
A procedure for obtaining explicit solutions to a class of Fredholm integral equations p 171 A85-28006
- GOLDSTEIN, S. A.**  
Investigation of a pulsed electrothermal thruster system [NASA-CR-174768] p 46 N85-11132
- GOLLER, G. J.**  
Electric utility acid fuel cell stack technology advancement [NASA-CR-174804] p 159 N85-17422
- GOLWALKER, S. V.**  
The influence of hold times on LCF and FCG behavior in a P/M Ni-base superalloy p 67 A85-32400
- GOMMERSTADT, B.**  
Translational and extensional energy release rates (the J- and M-integrals) for a crack layer in thermoelasticity [NASA-CR-174872] p 145 N85-21685
- GONSALVEZ, D. J.**  
Engineering calculations for communications satellite systems planning [NASA-CR-175552] p 37 N85-21233
- GONZALEZ-SANABRIA, O.**  
Advanced designs for IPV nickel-hydrogen cells p 156 A85-45438
- GONZALEZ-SANABRIA, O. D.**  
Design considerations for a 10-kW integrated hydrogen-oxygen regenerative fuel cell system p 155 A85-45380  
Tear-down analysis of a ten cell bipolar nickel-hydrogen battery p 156 A85-45385  
Separator development and testing of nickel-hydrogen cells p 156 A85-45386  
Alkaline battery containing a separator of a cross-linked copolymer of vinyl alcohol and unsaturated carboxylic acid [NASA-CASE-LEW-13102-1] p 104 N85-29144  
Initial performance of advanced designs for IPV nickel-hydrogen cells p 105 N85-31404  
Design principles for nickel-hydrogen cells and batteries [NASA-TM-87037] p 164 N85-31646
- GOOD, B. S.**  
Monte Carlo lattice models for adsorbed polymer conformation [NASA-TP-2453] p 183 N85-24961
- GORADIA, C.**  
Near-optimum design of GaAs-based concentrator space solar cells for 80 C operation p 153 A85-15800  
Applicability of the Meyer-Neldel rule to solar cells p 154 A85-19948
- Theory of the high base resistivity n(+)-pp(+) silicon solar cell and its application to radiation damage effects p 154 A85-32639
- GORDON, L. H.**  
Mod-2 wind turbine field operations experience p 157 A85-45512
- GORDON, S.**  
Computer program for calculation of complex chemical equilibrium compositions and applications. Supplement 1: Transport properties [NASA-TM-86885] p 184 N85-16663
- GORDON, W. L.**  
Electron yields from spacecraft materials p 40 N85-22512
- GORGOL, J. F.**  
Jet fuel property changes and their effect on producibility and cost in the U.S., Canada, and Europe [NASA-CR-174840] p 93 N85-27012
- GORLA, R. S. R.**  
Combined influence of unsteady free stream velocity and free stream turbulence on stagnation point heat transfer p 112 A85-41782  
Unsteady heat transfer due to time-dependent free stream velocity p 117 N85-27947
- GORLAND, S. H.**  
Radiation exposure and performance of multiple burn LEO-GEO orbit transfer trajectories [NASA-TM-86946] p 36 N85-21228
- GOSMAN, A. D.**  
Assessment of discretization schemes to reduce numerical diffusion in the calculation of complex flows [AIAA PAPER 85-0441] p 108 A85-19751  
Error reduction program [NASA-CR-174776] p 172 N85-27584
- GOTKIS, S.**  
Configuration study for a 30 GHz monolithic receive array: Technical assessment [NASA-CR-174697] p 98 N85-18238  
Configuration study for a 30 GHz monolithic receive array, volume 1 [NASA-CR-174697-VOL-1] p 98 N85-18239  
Configuration study for a 30 GHz monolithic receive array, volume 2 [NASA-CR-174697-VOL-2] p 99 N85-18240
- GOTO, H.**  
Effect of humidity on fretting wear of several pure metals [NASA-TP-2403] p 72 N85-13006
- GOUKER, M. A.**  
Infrared technology for satellite power conversion [NASA-CR-174266] p 159 N85-16293  
Technology for satellite power conversion [NASA-CR-174335] p 159 N85-18451
- GOULDIN, F. C.**  
Combustion efficiency of a premixed continuous flow combustor p 61 A85-42571
- GOVADA, A. K.**  
A study of the stress wave factor technique for the characterization of composite materials [NASA-CR-174870] p 58 N85-30035
- GOVILA, R. K.**  
Fracture of yttria-doped, sintered reaction-bonded silicon nitride [ACS PAPER 7-J3-84] p 82 A85-42797
- GOVINDAN, T. R.**  
Computation of viscous flows in turbomachinery cascades p 106 A85-11631
- GRAF, A. J.**  
Jet fuel property changes and their effect on producibility and cost in the U.S., Canada, and Europe [NASA-CR-174840] p 93 N85-27012
- GRAHAM, R. E.**  
Linearization of digital derived rate algorithm for use in linear stability analysis [NASA-TM-87000] p 41 N85-23904
- GRAHAM, R. W.**  
Computational thermo-fluid dynamics contributions to advanced gas turbine engine design [AIAA PAPER 85-0083] p 14 A85-19509  
Computational thermo-fluid dynamics contributions to advanced gas turbine engine design [NASA-TM-86865] p 18 N85-10069
- GRANT, H.**  
High temperature static strain sensor development program p 19 N85-10959
- GRANTHAM, D. H.**  
High-temperature optically activated GaAs power switching for aircraft digital electronic control [NASA-CR-174711] p 34 N85-12901
- GRAY, D. E.**  
Energy Efficient Engine Program technology benefit/cost study, volume 1 [NASA-CR-174766-VOL-1] p 33 N85-35197  
Energy Efficient Engine Program technology benefit/cost study, volume 2 [NASA-CR-174766-VOL-2] p 33 N85-35198

- GRAY, H. R.**  
PM superalloys - A troubled adolescent?  
p 69 A85-44772
- GREENE, J. E.**  
Properties of coated and modified surfaces  
p 53 A85-36694
- GREENE, W.**  
Energy efficient engine combustor test hardware  
detailed design report  
[NASA-TM-167945] p 18 N85-10950
- GREGOREK, G. M.**  
Design and wind tunnel evaluation of a symmetric airfoil  
series for large wind turbine applications  
[NASA-CR-174764] p 7 N85-10919
- GREISING, G. J.**  
Electric utility acid fuel cell stack technology  
advancement  
[NASA-CR-174804] p 159 N85-17422
- GREITZER, E. M.**  
A theory of post-stall transients in multistage axial  
compression systems  
[NASA-CR-3878] p 8 N85-21117
- GRIER, N. T.**  
Dilute plasma coupling currents to a high voltage solar  
array in weak magnetic fields p 46 A85-45388  
Plasma interaction experiment 2 (PIX 2): Laboratory  
and flight results p 180 N85-22495
- GRIFFIN, J. H.**  
Effects of friction dampers on aerodynamically unstable  
rotor stages p 14 A85-21866
- GRILL, A.**  
RF-sputtered silicon and hafnium nitrides - Properties  
and adhesion to 440C stainless steel p 81 A85-36240  
Surface hardening of steel by boriding in a cold rf  
plasma p 68 A85-40275
- GRISNIK, S. P.**  
Vacuum chamber pressure effects on thrust  
measurements of low Reynolds number nozzles  
[NASA-TM-86955] p 49 N85-21259  
Compatibility experiments of facilities, materials, and  
propellants for electrothermal thrusters  
[NASA-TM-86956] p 49 N85-21260
- GROENEWEG, J. F.**  
Analytical and physical modeling program for the NASA  
Lewis Research Center's Altitude Wind Tunnel (AWT)  
[AIAA PAPER 85-0379] p 34 A85-19709  
Analytical and physical modeling program for the NASA  
Lewis Research Center's Altitude Wind Tunnel (AWT)  
[NASA-TM-86919] p 35 N85-15757
- GROENEWEG, M.**  
A new interpretation of internal heat transfer coefficients  
of porous media  
[ASME PAPER 84-WA/HT-51] p 110 A85-39894
- GROESBECK, D. E.**  
Static jet noise test results of four 0.35 scale-model  
QCGAT mixer nozzles  
[NASA-TM-86871] p 175 N85-13551
- GROUMPOS, P. P.**  
Control algorithms and computer simulation of a  
stand-alone photovoltaic village power system  
p 153 A85-11345  
The subjective effect of multiple co-channel frequency  
modulated television interference p 96 A85-28234  
On the subjective evaluation of the interference  
protection ratios' measurements for co-channel FM-TV  
signals p 96 A85-28241  
Control aspects of the Schuchuli Village stand-alone  
photovoltaic power system  
[NASA-TM-83790] p 103 N85-13157
- GULBRANDSEN, N. C.**  
Small centrifugal pumps for low thrust rockets  
[AIAA PAPER 85-1302] p 45 A85-43978
- GULINO, D. A.**  
'Diamondlike' carbon films - Optical absorption, dielectric  
properties, and hardness dependence on deposition  
parameters p 82 A85-40383
- GUPTA, I. J.**  
Adaptive antenna arrays for weak interfering signals  
[NASA-CR-174336] p 98 N85-17258  
Adaptive antenna arrays for satellite communications:  
Design and testing  
[NASA-CR-176162] p 100 N85-34329
- H**
- HAAS, J. E.**  
Predicted turbine stage performance using  
quasi-three-dimensional and boundary-layer analyses  
p 15 A85-34013  
Application of viscous and inviscid computation methods  
for rocket turbopump systems  
[SAE PAPER 841522] p 110 A85-39257  
Fuel and oxidizer turbine loss analysis  
p 50 N85-26900
- HADY, W. F.**  
Tribological properties of graphite-fiber-reinforced,  
partially fluorinated polyimide composites  
[NASA-TM-86926] p 86 N85-18153
- HAFTKA, R. T.**  
Optimization of cascade blade mistuning. II - Global  
optimum and numerical optimization p 16 A85-45715
- HAGEDORN, N. H.**  
NASA Redox Storage System Development Project  
[NASA-TM-83677] p 158 N85-12465  
Cycling performance of the iron-chromium redox energy  
storage system  
[NASA-TM-87034] p 162 N85-27387
- HAISLER, W. E.**  
Numerical considerations in the development and  
implementation of constitutive models  
p 151 N85-31541
- HALES, S. J.**  
Rapid solidification and dynamic compaction of Ni-base  
superalloy powders p 67 A85-32414
- HALFORD, G. R.**  
Strainrange partitioning - A total strain range version  
p 64 A85-11603  
Application of two creep fatigue life models for the  
prediction of elevated temperature crack initiation of a  
nickel base alloy  
[AIAA PAPER 85-1420] p 69 A85-43979  
Life prediction and constitutive behavior: Overview  
p 20 N85-10973  
Engine cyclic durability by analysis and material  
testing p 25 N85-15744  
Interaction of high-cycle and low-cycle fatigue of Haynes  
188 alloy at 1400 F deg p 149 N85-27961  
Reexamination of cumulative fatigue damage laws  
p 149 N85-27962
- HALLA, E. E.**  
Energy efficient engine high pressure turbine test  
hardware detailed design report  
[NASA-CR-167955] p 23 N85-10995
- HALLINAN, G. J.**  
Electric power - Photovoltaic or solar dynamic?  
p 46 A85-47042
- HALTER, P. H.**  
Energy efficient engine. Fan and quarter-stage  
component performance report  
[NASA-CR-168070] p 33 N85-34141
- HAMED, A.**  
The three-dimensional compressible flow in a radial  
inflow turbine scroll p 6 A85-41826
- HAMPSON, M. E.**  
Reusable rocket engine turbopump condition  
monitoring  
[SAE PAPER 841619] p 44 A85-39267  
Reusable rocket engine turbopump condition  
monitoring p 51 N85-26907
- HAMROCK, B. J.**  
Elastohydrodynamic lubrication of line contacts  
p 126 A85-11069  
Hydrodynamic lubrication of rigid nonconformal contacts  
in combined rolling and normal motion  
[ASME PAPER 84-TRIB-13] p 127 A85-21280  
Thermal elastohydrodynamic lubrication of line  
contacts p 128 A85-31202  
Transmission efficiency measurements and correlations  
with physical characteristics of the lubricant  
p 89 N85-23781  
Fast approach for calculating film thicknesses and  
pressures in elastohydrodynamically lubricated contacts  
at high loads  
[NASA-TM-87032] p 117 N85-30242  
Correlation of rheological characteristics of lubricants  
with transmission efficiency measurements  
[NASA-TM-86988] p 134 N85-30342  
Surface roughness effects in elastohydrodynamic  
contacts  
[NASA-TP-2488] p 134 N85-32329  
Mechanics of a gaseous film barrier to lubricant wetting  
of elastohydrodynamically lubricated conjunctions  
[NASA-TP-2500] p 135 N85-32330  
Elastohydrodynamic lubrication calculations used as a  
tool to study scuffing  
[NASA-TM-87097] p 137 N85-34408
- HAN, J. C.**  
Heat transfer enhancement in channels with turbulence  
promoters  
[ASME PAPER 84-WA/HT-72] p 111 A85-39900
- HANDSCHUH, R. F.**  
High-temperature erosion of plasma-sprayed,  
yttria-stabilized zirconia in a simulated turbine  
environment  
[AIAA PAPER 85-1219] p 82 A85-39662  
Spiral bevel and circular arc helical gears: Tooth contact  
analysis and the effect of misalignment on circular arc  
helical gears  
[NASA-TM-87013] p 32 N85-31060
- Thermal stress analysis of a new turbine shroud seal  
concept  
[NASA-TM-87082] p 136 N85-34406
- HANKS, D. E.**  
Study of advanced fuel system concepts for commercial  
aircraft and engines  
[NASA-CR-174752] p 93 N85-19176
- HANNUM, N. P.**  
An evaluation of oxygen/hydrogen propulsion systems  
for the Space Station  
[AIAA PAPER 85-1156] p 45 A85-43976  
An evaluation of oxygen-hydrogen propulsion systems  
for the Space Station  
[NASA-TM-87059] p 52 N85-28971
- HANSCHUH, R. F.**  
High-temperature erosion of plasma-sprayed,  
yttria-stabilized zirconia in a simulated turbine  
environment  
[NASA-TP-2406] p 84 N85-13045
- HANSEN, I. G.**  
Advanced secondary power system for transport  
aircraft  
[NASA-TP-2463] p 30 N85-28944
- HANSEN, J. L.**  
A note on blade wake interaction influence on  
compressor stator row aerodynamic performance  
p 4 A85-32965
- HANSON, R. K.**  
Velocity visualization in gas flows using laser-induced  
phosphorescence of biacetyl p 121 A85-21695  
Fast laser-induced aerosol formation for visualization of  
gas flows p 121 A85-31113  
Two-frequency laser-induced fluorescence technique for  
rapid velocity-field measurements in gas flows  
p 121 A85-32294  
Velocity visualization in gaseous flows  
[NASA-CR-174954] p 119 N85-31445
- HARABETIAN, E.**  
A convergent series expansion for hyperbolic systems  
of conservation laws  
[NASA-CR-172557] p 168 N85-21990
- HARB, A.**  
Thermal-stress analysis for a wood composite blade  
[NASA-CR-174794] p 159 N85-17421
- HARDY, T. L.**  
Cathode degradation and erosion in high pressure arc  
discharges p 43 A85-16445  
Electrode erosion in arc discharges at atmospheric  
pressure  
[NASA-TM-87087] p 52 N85-34178  
Hollow cathodes in high pressure arc discharges  
[NASA-TM-87098] p 52 N85-34179
- HARF, F. H.**  
The substitution of nickel for cobalt in hot isostatically  
pressed powder metallurgy UDIMET 700 alloys  
p 68 A85-37415  
The response of cobalt-free Udimet 700 type alloy to  
modified heat treatments  
[NASA-TM-86942] p 75 N85-20043  
Properties and microstructures for dual alloy  
combinations of three superalloys with alloy 901  
[NASA-TM-86987] p 76 N85-26963
- HART, R. E.**  
Voltage controlling mechanisms in low resistivity silicon  
solar cells - A unified approach p 155 A85-35617  
The high voltage silicon cell: A comparative analysis  
p 49 N85-22569
- HARTMANN, M. J.**  
The trend of future gas turbine technology  
p 16 A85-41778
- HASSA, C.**  
Velocity visualization in gas flows using laser-induced  
phosphorescence of biacetyl p 121 A85-21695  
Fast laser-induced aerosol formation for visualization of  
gas flows p 121 A85-31113
- HATHAWAY, M. D.**  
A note on blade wake interaction influence on  
compressor stator row aerodynamic performance  
p 4 A85-32965  
Rotor wake characteristics of a transonic axial flow  
fan  
[AIAA PAPER 85-1133] p 6 A85-43974
- HAWLEY, M. C.**  
Measurements of energy distribution in microwave  
plasmas of N<sub>2</sub> and He and comparisons with results for  
H<sub>2</sub> p 178 A85-16443  
The energetics of hydrogen atom recombination -  
Analysis, experiments, and modeling  
p 179 A85-16444
- HAYNES, J. F.**  
Contingency power concepts for helicopter turboshaft  
engine p 15 A85-32005
- HECKEL, R. W.**  
Cyclic oxidation behavior of beta+gamma overlay  
coatings on gamma and gamma+gamma-prime alloys  
p 68 A85-32431



- HEINE, C.**  
Generated spiral bevel gears: Optimal machine-tool settings and tooth contact analysis  
[NASA-TM-87075] p 136 N85-34405
- HEITMAN, P. W.**  
Ceramic components for gas turbine engines  
p 127 A85-15973  
Photoacoustic microscopy of ceramic turbine blades  
p 83 A85-43930  
Ceramic applications in turbine engines  
[NASA-CR-174715] p 91 N85-28109
- HELLAWELL, A.**  
The mechanisms of formation and prevention of channel segregation during alloy solidification  
p 180 A85-18082
- HELMS, H. E.**  
Ceramic applications in turbine engines  
[NASA-CR-174715] p 91 N85-28109
- HEMKER, K. J.**  
Orientation and temperature dependence of some mechanical properties of the single-crystal nickel-base superalloy Rene N4. 3: Tension-compression anisotropy  
[NASA-TM-86982] p 76 N85-22660  
Microstructures in rapidly solidified Ni-Mo alloys  
[NASA-TM-87100] p 78 N85-34266
- HENDRICKS, R. C.**  
An analysis of temperature effect in a finite journal bearing with spatial tilt and viscous dissipation  
p 126 A85-11074  
Plastic flow of plasma sprayed ceramics  
p 80 A85-24161  
A comparison of flow rates and pressure profiles for N-sequential inlets and three related seal configurations  
p 109 A85-26526  
Flow rates and pressure profiles for one to four axially aligned Borda inlets  
[NASA-TP-2390] p 113 N85-14078  
Experimental and analytical study of ceramic-coated turbine-tip shroud seals for small turbine engines  
[NASA-TM-86881] p 25 N85-18057  
Experimental study of ceramic coated tip seals for turbojet engines  
[NASA-TM-86939] p 114 N85-19363  
Ribbon burner simulation of T-700 turbine shroud for ceramic lined seals research  
[NASA-TM-86940] p 114 N85-19364  
Analysis of experimental shaft seal data for high-performance turbomachines, as for Space Shuttle main engines  
[NASA-TM-86928] p 115 N85-21569  
Nested subcritical flows within supercritical systems  
[NASA-TM-86980] p 115 N85-21574  
Metallic and metal/ceramic coating by thermal decomposition  
[NASA-TM-86992] p 88 N85-22755  
Film and interstitial formation of metals in plasma-sprayed ceramics  
[NASA-TM-86993] p 89 N85-22756  
Fabrication of ceramic substrate-reinforced and free forms  
[NASA-TM-86994] p 50 N85-23926  
Flow rate and pressure profiles for 1 to 4 axially aligned orifice inlets  
[NASA-TP-2460] p 116 N85-27165
- HENEY, J. F.**  
A 20 GHz, 75 watt, helix TWT for space communications  
p 101 A85-14433
- HENNEKE, E. G., II**  
A study of the stress wave factor technique for the characterization of composite materials  
[NASA-CR-174870] p 58 N85-30035
- HERBELL, T. P.**  
Demonstration of a silicon nitride attrition mill for production of fine pure Si and Si<sub>3</sub>N<sub>4</sub> powders  
p 78 A85-10825  
Milling of Si<sub>3</sub>N<sub>4</sub> with Si<sub>3</sub>N<sub>4</sub> hardware  
[NASA-TM-86864] p 84 N85-10191  
Factors influencing the ball milling of Si<sub>3</sub>N<sub>4</sub> in water  
[NASA-TM-86932] p 86 N85-19136  
Parametric evaluation of ball milling of SiC in water  
[NASA-TM-86974] p 88 N85-21356
- HERMAN, H.**  
Failure during thermal cycling of plasma-sprayed thermal barrier coatings  
p 81 A85-36246
- HERRERA, J. I.**  
Experimental investigation of a variable speed constant frequency electric generating system from a utility perspective  
[NASA-CR-174950] p 105 N85-32251
- HERZAU, J. S.**  
Teardown analysis of a ten cell bipolar nickel-hydrogen battery  
p 156 A85-45385
- HESS, C. F.**  
Spray characterization with a nonintrusive technique using absolute scattered light  
p 120 A85-10036
- Nonintrusive optical single-particle counter for measuring the size and velocity of droplets in a spray  
p 120 A85-16794
- Research study of droplet sizing technology leading to the development of an advanced droplet sizing system  
[NASA-CR-174839] p 123 N85-21604
- HESS, J. L.**  
Calculation of compressible flow about three-dimensional inlets with auxiliary inlets, slats and vanes by means of a panel method  
[AIAA PAPER 85-1196] p 5 A85-40817  
Calculation of compressible flow about three-dimensional inlets with auxiliary inlets, slats and vanes by means of a panel method  
[NASA-CR-174975] p 10 N85-35162
- HESSLEINK, L.**  
Free-surface phenomena under low- and zero-gravity conditions  
[NASA-CR-175885] p 36 N85-27922
- HESSERBACKER, G.**  
Configuration study for a 30 GHz monolithic receive array: Technical assessment  
[NASA-CR-174697] p 98 N85-18238  
Configuration study for a 30 GHz monolithic receive array, volume 1  
[NASA-CR-174697-VOL-1] p 98 N85-18239  
Configuration study for a 30 GHz monolithic receive array, volume 2  
[NASA-CR-174697-VOL-2] p 99 N85-18240
- HETZEL, R.**  
Numerical simulation of positive-potential conductors in the presence of a plasma and a secondary-emitting dielectric  
p 102 A85-35306
- HIEATT, J. L.**  
Electric power - Photovoltaic or solar dynamic?  
p 46 A85-47042
- HILKO, B. K.**  
Investigation of a pulsed electrothermal thruster system  
[NASA-CR-174768] p 46 N85-11132
- HILL, T. G.**  
Analytical fuel property effects: Small combustors, phase 2  
[NASA-CR-174848] p 93 N85-19175
- HILLER, B.**  
Velocity visualization in gas flows using laser-induced phosphorescence of biacetyl  
p 121 A85-21695  
Two-frequency laser-induced fluorescence technique for rapid velocity-field measurements in gas flows  
p 121 A85-32294
- HINCKEL, J. N.**  
Heat transfer investigation in the junction region of circular cylinder normal to a flat plate at 90 deg location  
[ASME PAPER 84-WA/HT-70] p 111 A85-39898
- HIPPENSTEELE, S. A.**  
High temperature thermocouple and heat flux gauge using a unique thin film-hardware hot junction  
[NASA-TM-86898] p 123 N85-16096  
Local heat-transfer measurements on a large, scale-model turbine blade airfoil using a composite of a heater element and liquid crystals  
[NASA-TM-86900] p 119 N85-33435
- HIRSCHBEIN, M. S.**  
Finite element engine blade structural optimization  
[AIAA PAPER 85-0645] p 141 A85-30313  
Component-specific modeling  
p 20 N85-10971
- HIRSCHKRON, R.**  
Contingency power concepts for helicopter turboshaft engine  
p 15 A85-32005
- HO, P. Y.**  
Comparison of scaled model data to full size energy efficient engine test results  
[AIAA PAPER 84-2281] p 13 A85-13953  
Measurement and prediction of Energy Efficient Engine noise  
[AIAA PAPER 84-2284] p 13 A85-13954
- HOBART, H. F.**  
Evaluation results of the 700 deg C Chinese strain gauges  
[NASA-TM-86973] p 124 N85-21605
- HOBERECHT, M. A.**  
Design considerations for a 10-kW integrated hydrogen-oxygen regenerative fuel cell system  
p 155 A85-45380  
A 37.5-kW point design comparison of the nickel-cadmium battery, bipolar nickel-hydrogen battery, and regenerative hydrogen-oxygen fuel cell energy storage subsystems for low earth orbit  
p 46 A85-45387  
Regenerative fuel cell systems for space station  
p 104 N85-31372
- HOCKMUTH, J.**  
Preparation and evaluation of advanced catalysts for phosphoric acid fuel cells  
[NASA-CR-168223] p 160 N85-19511
- HOEGLUND, E.**  
Correlation of rheological characteristics of lubricants with transmission efficiency measurements  
[NASA-TM-86988] p 134 N85-30342
- HOFFMAN, A. C.**  
Advanced secondary power system for transport aircraft  
[NASA-TP-2463] p 30 N85-28944
- HOFFMAN, R. W.**  
Electron yields from spacecraft materials  
p 40 N85-22512  
Study of Kapton under simulated shuttle environment  
[NASA-CR-176003] p 41 N85-29997
- HOLANDA, R.**  
High temperature thermocouple and heat flux gauge using a unique thin film-hardware hot junction  
[NASA-TM-86898] p 123 N85-16096
- HOLDEMAN, J. D.**  
GASP cloud encounter statistics - Implications for laminar flow control flight  
p 166 A85-11979  
Variability of cloudiness at airline cruise altitudes from GASP measurements  
p 166 A85-31199  
Experiments in dilution jet mixing - Effects of multiple rows and non-circular orifices  
[AIAA PAPER 85-1104] p 15 A85-39606  
Dilution zone mixing studies  
p 21 N85-10984  
Simultaneous cabin and ambient ozone measurements on two Boeing 747 airplanes. Volume 3: October 1978 - July 1979  
[NASA-TM-86883] p 167 N85-21872  
Experiments in dilution jet mixing effects of multiple rows and non-circular orifices  
[NASA-TM-86896] p 28 N85-25266
- HOLEMAN, R. H.**  
Government review of the Mod-2 wind turbine (as-built)  
[NASA-TM-86983] p 162 N85-29365
- HOLLANSWORTH, J. E.**  
Telecommunications forecast for ITU Region 2 to the year 1995  
[NASA-TM-87077] p 38 N85-34150
- HOLLOWAY, P. R.**  
Energy efficient engine. High pressure compressor detail design report  
[NASA-CR-165558] p 23 N85-10998
- HOLTZMAN, R. L.**  
An investigation of enhanced capability thermal barrier coating systems for diesel engine components  
[NASA-CR-174820] p 86 N85-18154
- HOPF, W. R.**  
Stall recovery control strategy methodology and results  
[AIAA PAPER 85-1433] p 16 A85-40841
- HOPKINS, D. A.**  
Nonlinear analysis for high-temperature multilayered fiber composite structures  
[NASA-TM-83754] p 57 N85-21273  
Nonlinear structural analysis for fiber-reinforced superalloy turbine blades  
p 147 N85-26887
- HOTHI, H. S.**  
Development and use of the computer software package for planning the 12 GHz broadcasting-satellite service at RARC '83  
p 96 A85-29605
- HOULT, D. P.**  
Methanol as a soot reducer in a turbulent swirling burner  
[ASME PAPER 84-JPGC-GT-2] p 61 A85-23192
- HOUPERT, L.**  
Fast numerical calculations of EHD sliding traction forces  
Application to rolling bearings  
[ASME PAPER 84-TRIB-26] p 127 A85-21289
- HOUPERT, L. G.**  
Fast approach for calculating film thicknesses and pressures in elastohydrodynamically lubricated contacts at high loads  
[NASA-TM-87032] p 117 N85-30242  
Elastohydrodynamic lubrication calculations used as a tool to study scuffing  
[NASA-TM-87097] p 137 N85-34408
- HOUSER, D. R.**  
The design and analysis of single flank transmission error test for loaded gears  
[NASA-CR-176163] p 136 N85-34404
- HOUSER, M. J.**  
Phase/doppler spray analyzer for simultaneous measurements of drop size and velocity distributions  
p 120 A85-10035
- HOWE, D. C.**  
Energy efficient engine flight propulsion system preliminary analysis and design report  
[NASA-CR-174701] p 18 N85-10947  
Energy efficient engine integrated core/low spool test hardware design report  
[NASA-CR-168137] p 31 N85-29956

- HOWES, W. L.**  
Rainbow schlieren vs Mach-Zehnder interferometer - A comparison p 121 A85-28820
- HOYNIK, D.**  
The effect of aerodynamic and structural detuning on turbomachine supersonic unstalled torsional flutter [AIAA PAPER 85-0761] p 14 A85-30378  
Aerodynamic detuning analysis of an unstalled supersonic turbofan cascade [NASA-TM-87001] p 9 N85-26670
- HSIEH, F. I.**  
Electrical characterization of plasma-grown oxides on gallium arsenide p 181 A85-32635
- HSU, L. C.**  
Alkaline battery containing a separator of a cross-linked copolymer of vinyl alcohol and unsaturated carboxylic acid [NASA-CASE-LEW-13102-1] p 104 N85-29144
- HSUEH, K. L.**  
Electrocatalysis of fuel cell reactions: Investigation of alternate electrolytes [NASA-CR-174753] p 157 N85-11455
- HUBBELL, T. E., JR.**  
Ion-beam nitriding of steels [NASA-CASE-LEW-14104-1] p 75 N85-21324
- HUDSON, W. R.**  
Spacecraft environmental interactions: A joint Air Force and NASA research and technology program p 40 N85-22517
- HUFF, R. G.**  
Analysis of the effect on combustor noise measurements of acoustic waves reflected by the turbine and combustor inlet [AIAA PAPER 84-2323] p 173 A85-16103  
A theoretical prediction of the acoustic pressure generated by turbulence-flame front interactions [ASME PAPER 84-WA/NCA-11] p 174 A85-39909
- HUGHES, C. E.**  
Analytical modeling of circuit aerodynamics in the new NASA Lewis Altitude Wind Tunnel [AIAA PAPER 85-0380] p 3 A85-26389  
Analytical modeling of circuit aerodynamics in the new NASA Lewis wind tunnel [NASA-TM-86912] p 8 N85-15688
- HUGHES, T. J. R.**  
Augmented weak forms and element-by-element preconditioners: Efficient iterative strategies for structural finite elements. A preliminary study p 144 N85-10384
- HULL, D. R.**  
The effects of seven alloying elements on the microstructure and stress-rupture behavior of nickel-base superalloys [NASA-TM-83791] p 70 N85-10168
- HULLIGAN, D. D.**  
Effect of water on hydrogen permeability [NASA-TM-86904] p 53 N85-14864
- HULSE, C.**  
High temperature static strain sensor development program p 19 N85-10959
- HUMENIK, F. M.**  
Flame radiation and linear heat transfer in a tubular-can combustor p 15 A85-39580
- HUNG, C. C.**  
A micrographic and gravimetric study of intercalation and deintercalation of graphite fibers [NASA-TM-87026] p 91 N85-28110
- HURST, J. B.**  
Evaluation of alpha-SiC sintering using statistical methods p 83 A85-42800
- HUSTON, R. L.**  
A computer aided design procedure for generating gear teeth [ASME PAPER 84-DET-184] p 128 A85-33779  
Dynamic analysis of straight and involute tooth forms [ASME PAPER 84-DET-226] p 128 A85-33780
- HWANG, D. P.**  
Analytical study of blowing boundary layer control for subsonic V-STOL inlets p 2 A85-11646
- HWANG, S. Y.**  
On local total strain redistribution using a simplified cyclic inelastic analysis based on an elastic solution [AIAA PAPER 85-1419] p 142 A85-39770  
Local strain redistribution corrections for a simplified inelastic analysis procedure based on an elastic finite-element analysis [NASA-TP-2421] p 145 N85-20396  
On local total strain redistribution using a simplified cyclic inelastic analysis based on an elastic solution [NASA-TM-86913] p 145 N85-21690
- HYMAN, J. JR.**  
IAPS (8-cm) ion thruster cyclic endurance test p 42 A85-16406  
Ion thruster system (8-cm) cyclic endurance test [NASA-CR-174745] p 47 N85-12937
- IDE, R. F.**  
Comparison of icing cloud instruments for 1982-1983 icing season flight program [AIAA PAPER 84-0020] p 13 A85-16098
- IMBRIE, P. K.**  
Numerical considerations in the development and implementation of constitutive models p 151 N85-31541
- INGEBO, R. D.**  
Aerodynamic effect of combustor inlet air pressure on fuel jet atomization p 109 A85-27096  
Liquid fuel spray processes in high-pressure gas flow [NASA-TM-86944] p 115 N85-21570
- INSPEKTOR, A.**  
Deposition of silicon nitride from SiCl<sub>4</sub> and NH<sub>3</sub> in a low pressure RF plasma p 81 A85-36229
- IRION, C. E.**  
Stratified charge rotary aircraft engine technology enablement program [NASA-CR-174812] p 25 N85-21163
- ISHIGAKI, H.**  
Surface effects of corrosive media on hardness, friction, and wear of materials [NASA-TM-83711] p 85 N85-15896
- IZQUIERDO, A. J.**  
Methanol as a soot reducer in a turbulent swirling burner [ASME PAPER 84-JPGC-GT-2] p 61 A85-23192
- JACKSON, J. A.**  
A multiple-scales model of the shock-cell structure of imperfectly expanded supersonic jets p 113 A85-49354
- JACKSON, T. W.**  
Turbulence characteristics of swirling flowfields [NASA-CR-174918] p 29 N85-26717
- JACOBSON, B. O.**  
Elastohydrodynamic lubrication of line contacts p 126 A85-11069  
Correlation of rheological characteristics of lubricants with transmission efficiency measurements [NASA-TM-86988] p 134 N85-30342
- JACOBSON, N. S.**  
Hot corrosion of sintered alpha-SiC at 1000 C [ACS PAPER 19-B-84P] p 83 A85-45302  
The reactions of cobalt, iron and nickel in SO<sub>2</sub> atmospheres: Similarities and differences [NASA-TM-86868] p 70 N85-11217  
Burner rig corrosion of SiC at 1000 deg C [NASA-TM-87061] p 53 N85-30011  
Mechanism of strength degradation for hot corrosion of alpha-SiC [NASA-TM-87052] p 91 N85-30135
- JACQUEZ, A.**  
Design of low loss helix circuits for interference fitted and brazed circuits [NASA-CR-168313] p 103 N85-19328
- JACQUOTTE, O.-P.**  
Analysis of hourglass instabilities and control in underintegrated finite element methods p 139 A85-11125  
Stability, accuracy, and efficiency of some underintegrated methods in finite element computations p 172 A85-50073
- JAIN, S. C.**  
Comparison of atmospheric correction algorithms for the Coastal Zone Color Scanner p 153 A85-10244
- JALAN, V.**  
Development of electrodes for the NASA iron/chromium [NASA-CR-174724] p 165 N85-35471
- JAMES, K.**  
Fiber optic, Fabry-Perot high temperature sensor [NASA-CR-174712] p 178 N85-13594
- JANARDAN, B. A.**  
Experimental investigation of shock-cell noise reduction for dual-stream nozzles in simulated flight [NASA-CR-3846] p 175 N85-13549  
Experimental investigation of shock-cell noise reduction for single stream nozzles in simulated flight [NASA-CR-3845] p 175 N85-13550
- JANOWSKI, G. M.**  
The effect of tantalum on the structure/properties of two polycrystalline nickel-base superalloys: B-1900 + Hf MAR-M247 [NASA-CR-174847] p 73 N85-18127
- JARRETT, R. N.**  
Modeling of gamma/gamma-prime phase equilibrium in the nickel-aluminum system p 65 A85-14959  
Effects of cobalt on the hot workability of nickel-base superalloys p 67 A85-32412
- JASPERSON, W. H.**  
GASP cloud encounter statistics - Implications for laminar flow control flight p 166 A85-11979  
A comparison of NMC and GWC analysis field temperatures with aircraft measurements p 166 A85-21140  
Variability of cloudiness at airline cruise altitudes from GASP measurements p 166 A85-31199  
Simultaneous cabin and ambient ozone measurements on two Boeing 747 airplanes. Volume 3: October 1978 - July 1979 [NASA-TM-86883] p 167 N85-21872
- JAWORSKE, D. A.**  
Dynamics of graphite fiber intercalation: In situ resistivity measurements with a four point probe [NASA-TM-86858] p 53 N85-10105  
Graphite fiber intercalation: Dynamics of the bromine intercalation process [NASA-TM-87015] p 53 N85-26921  
Environmental stability of intercalated graphite fibers [NASA-TM-87025] p 90 N85-26992
- JAYARAMAN, N.**  
A study of fatigue damage mechanisms in Waspaloy from 25 to 800 C p 65 A85-12098  
Low cycle fatigue of MAR-M 200 single crystals at 760 and 870 deg C [NASA-TM-86933] p 74 N85-19074  
Microstructures in rapidly solidified Ni-Mo alloys [NASA-TM-87100] p 78 N85-34266
- JECH, R. W.**  
Ductility in rapidly solidified NiAl p 66 A85-26158
- JEFFERIES, K. S.**  
Advanced secondary power system for transport aircraft [NASA-TP-2463] p 30 N85-28944  
Optical analysis of parabolic dish concentrators for solar dynamic power systems in space [NASA-TM-87080] p 52 N85-34176
- JENG, D. R.**  
Aerodynamic analysis of a horizontal axis wind turbine by use of helical vortex theory. Volume 1: Theory [NASA-CR-168054] p 9 N85-29916
- JENKINS, R. M.**  
An improved computer model for prediction of axial gas turbine performance losses [NASA-CR-174246] p 24 N85-15724
- JENSEN, K. A.**  
Textured carbon surfaces on copper [NASA-CASE-LEW-14130-1] p 95 N85-20156
- JERACKI, R. J.**  
Wind tunnel results of advanced high speed propellers in the takeoff, climb, and landing operating regimes [AIAA PAPER 85-1259] p 6 A85-47025  
Wind tunnel results of advanced high speed propellers in the takeoff, climb and landing operating regimes [NASA-TM-87054] p 9 N85-29925
- JOHNS, R. H.**  
Structural analysis p 20 N85-10969
- JOHNSON, B. V.**  
Mass and momentum turbulent transport experiments with confined coaxial jets p 107 A85-14399  
Turbulent transport and length scale measurement experiments with confined coaxial jets [NASA-CR-174831] p 117 N85-30245
- JOHNSON, D. A.**  
Chemical and electrochemical behavior of the Cr(III)/Cr(II) half-cell in the iron-chromium redox energy storage system p 61 A85-33785
- JOHNSON, G. M.**  
Efficient solution of the Euler and Navier-Stokes equations with a vectorized multiple-grid algorithm p 2 A85-18679
- JOHNSON, J. A.**  
Cycling performance of the iron-chromium redox energy storage system [NASA-TM-87034] p 162 N85-27387
- JOHNSON, W. A.**  
Effects of tin on microstructure and mechanical behavior of Inconel 718 [NASA-TM-86866] p 71 N85-12129
- JOHNSON, W. R.**  
Government review of the Mod-2 wind turbine (as-built) [NASA-TM-86983] p 162 N85-29365
- JONES, B. L.**  
Experimental results supporting the determination of service quality objectives for DBS systems p 96 A85-29611
- JONES, J. D.**  
The influence of combustion liner holes on noise production by ducted burners [AIAA PAPER 84-2322] p 172 A85-10869
- JONES, M. G.**  
Laser balancing system for high material removal rates [NASA-CR-174731] p 126 N85-12341

- JONES, R. E.**  
Space Station propulsion - The Advanced Development Program at Lewis  
[AIAA PAPER 85-1154] p 44 A85-39626  
Combustion gas properties I-ASTM jet A fuel and dry air  
[NASA-TP-2359] p 17 N85-10064  
Combustion gas properties. 2: Natural gas fuel and dry air  
[NASA-TP-2435] p 26 N85-21168  
Space station propulsion: The advanced development program at Lewis  
[NASA-TM-86999] p 50 N85-25386  
Combustion gas properties. Part 3: Hydrogen gas fuel and dry air  
[NASA-TP-2477] p 32 N85-31058
- JONES, W. R., JR.**  
Topological reaction rate measurements related to scuffing p 64 A85-11070  
Friction and wear properties of a Charnley artificial hip joint  
[ASLE PREPRINT 84-LC-4A-4] p 168 A85-38444  
Contact angle and surface tension measurements of a five-ring polyphenyl ether  
[NASA-TM-86927] p 86 N85-15897  
Characterization of lubricated bearing surfaces operated under high loads  
[NASA-TM-86964] p 88 N85-21357
- JONGEWARD, G. A.**  
Computer simulation of plasma electron collection by PIX-II  
[AIAA PAPER 85-0386] p 43 A85-19715
- JORDAN, E. H.**  
Biaxial constitutive equation development for single crystals  
[NASA-CR-174056] p 183 N85-11862  
Elevated temperature biaxial fatigue  
[NASA-CR-175795] p 148 N85-27263
- JORDAN, F. L.**  
Reflection plane tests of a wind turbine blade tip section with ailerons  
[NASA-TM-87018] p 165 N85-34444
- JOU, W.-H.**  
Direct numerical simulations of a reacting mixing layer with chemical heat release  
[AIAA PAPER 85-0143] p 60 A85-19548

## K

- KANIC, P. G.**  
Design and analysis report for the RL10-2B breadboard low thrust engine  
[NASA-CR-174857] p 48 N85-19020
- KANTOLA, R. A.**  
Effects of vane/blade ratio and spacing on fan noise, volume 1  
[NASA-CR-174664] p 176 N85-19791  
Effects of vane/blade ratio and spacing on fan noise, Volume 2: Data supplement  
[NASA-CR-174665] p 176 N85-19792
- KAPOOR, V. J.**  
High-voltage solar-cell chip p 154 A85-24668
- KAR, K.**  
A new interpretation of internal heat transfer coefficients of porous media  
[ASME PAPER 84-WA/HT-51] p 110 A85-39894
- KARAGOZIAN, A. R.**  
Vortex modeling of single and multiple dilution jet mixing in a crossflow  
[AIAA PAPER 85-1580] p 111 A85-40701
- KARAGULLE, H.**  
Stress waves in an isotropic elastic plate excited by a circular transducer  
[NASA-CR-3877] p 138 N85-20390  
Application of homomorphic signal processing to stress wave factor analysis  
[NAS 1.26:174871] p 138 N85-21673  
Ultrasonic testing of plates containing edge cracks  
[NASA-CR-3904] p 138 N85-29307
- KARLOVITZ, L. A.**  
On the existence and stability conditions for mixed-hybrid finite element solutions based on Reissner's variational principle p 142 A85-33847
- KARPLUS, W. J.**  
Data flow methods for dynamic system simulation - A CSSL-IV microcomputer network interface p 170 A85-28614
- KASPER, H. J.**  
Simplified design and life prediction of rocket thrust chambers p 44 A85-29314
- KASRAIE, B.**  
Simplified design and life prediction of rocket thrust chambers p 44 A85-29314

- KASUBA, R.**  
Gear mesh stiffness and load sharing in planetary gearing  
[ASME PAPER 84-DET-229] p 129 A85-33781  
Conceptual design of a fixed-pitch wind turbine generator system rated at 400 kilowatts  
[NASA-CR-174877] p 162 N85-29363
- KATSANIS, T.**  
Predicted turbine stage performance using quasi-three-dimensional and boundary-layer analyses p 15 A85-34013  
Calculation of three-dimensional, viscous flow through turbomachinery blade passages by parabolic marching  
[AIAA PAPER 85-1408] p 5 A85-39767  
Calculation of three-dimensional, viscous flow through turbomachinery blade passages by parabolic marching  
[NASA-TM-86984] p 9 N85-23711
- KATZ, I.**  
Computer simulation of plasma electron collection by PIX-II  
[AIAA PAPER 85-0386] p 43 A85-19715  
Three-dimensional calculation of shuttle charging in polar orbit p 40 N85-22486  
Polar orbit electrostatic charging of objects in shuttle wake p 40 N85-22487  
Surface interactions and high-voltage current collection p 40 N85-22493
- KAUFMAN, A.**  
A simplified method for elastic-plastic-creep structural analysis  
[ASME PAPER 84-GT-191] p 141 A85-23150  
Unified constitutive material models for nonlinear finite-element structural analysis p 142 A85-39769  
On local total strain redistribution using a simplified cyclic inelastic analysis based on an elastic solution p 142 A85-39770  
Nonlinear structural and life analyses of a turbine blade p 19 N85-10954  
Nonlinear structural and life analyses of a combustor liner p 19 N85-10955  
Constitutive model development for isotropic materials p 20 N85-10975  
Engine cyclic durability by analysis and material testing p 25 N85-15744  
Local strain redistribution corrections for a simplified inelastic analysis procedure based on an elastic finite-element analysis p 145 N85-20396  
[NASA-TP-2421] p 145 N85-20396  
On local total strain redistribution using a simplified cyclic inelastic analysis based on an elastic solution p 145 N85-21690  
[NASA-TM-86913] p 145 N85-21690  
Unified constitutive material models for nonlinear finite-element structural analysis p 146 N85-24338  
[NASA-TM-86985] p 146 N85-24338  
Cyclic structural analyses of anisotropic turbine blades for reusable space propulsion systems p 146 N85-24339  
[NASA-TM-86990] p 146 N85-24339  
Develop and test fuel cell powered on-site integrated total energy systems. Phase 3: Full-scale power plant development p 161 N85-25941  
[NASA-CR-174887] p 161 N85-25941  
Cyclic structural analyses of SSME turbine blades p 150 N85-27963  
Develop and test fuel cell powered on-site integrated total energy systems. Phase 3: Full-scale power plant development p 164 N85-30483  
[NASA-CR-168338] p 164 N85-30483  
Two simplified procedures for predicting cyclic material response from a strain history p 151 N85-31543
- KAUFMAN, D. L.**  
Microprocessor control of photovoltaic systems p 156 A85-45408
- KAUFMAN, H. R.**  
Ion flow experiments in a multipole discharge chamber p 178 A85-12705  
Theory of ion acceleration with closed electron drift p 41 A85-15512
- KAUSHAL, D.**  
Satellite provided customer promises services, a forecast of potential domestic demand through the year 2000. Volume 4: Sensitivity analysis  
[NASA-CR-174662] p 99 N85-27092
- KAY, P. K.**  
Friction in rail guns p 101 A85-16424
- KAZA, K. R. V.**  
Flutter of turbofan rotors with mistuned blades p 139 A85-12716  
Effects of warping and pretwist on torsional vibration of rotating beams  
[ASME PAPER 84-WA/APM-41] p 140 A85-17040  
Flutter of swept fan blades  
[ASME PAPER 84-GT-138] p 141 A85-32962  
Finite difference analysis of torsional vibrations of pretwisted, rotating, cantilever beams with effects of warping p 143 A85-42047

- Vibration and flutter of mistuned bladed-disk assemblies p 16 A85-45854  
Vibration and buckling of rotating, pretwisted, precone beams including Coriolis effects  
[NASA-TM-87004] p 146 N85-25893  
Nonlinear flap-lag-extensional vibrations of rotating, pretwisted, precone beams including Coriolis effects  
[NASA-TM-87102] p 152 N85-34427
- KAZA, V.**  
Vibration and flutter of mistuned bladed-disk assemblies  
[AIAA PAPER 84-0991] p 139 A85-16095
- KEITH, T. G., JR.**  
Aerodynamic analysis of a horizontal axis wind turbine by use of helical vortex theory. Volume 1: Theory  
[NASA-CR-168054] p 9 N85-29916  
Performance comparison between NACA 23024 and NACA 64(3)-618 airfoil configured rotors for horizontal-axis wind turbines  
[NASA-TM-83471] p 163 N85-30477
- KEITZ, J. F.**  
Comparative analysis of operational forecasts versus actual weather conditions in airline flight planning, volume 1  
[NASA-CR-167862] p 167 N85-35534  
Comparative analysis of operational forecasts versus actual weather conditions in airline flight planning, volume 2  
[NASA-CR-167863] p 167 N85-35535  
Comparative analysis of operational forecasts versus actual weather conditions in airline flight planning, volume 3  
[NASA-CR-167864] p 167 N85-35536  
Comparative analysis of operational forecasts versus actual weather conditions in airline flight planning, volume 4  
[NASA-CR-167865] p 167 N85-35537  
Comparative analysis of operational forecasts versus actual weather conditions in airline flight planning: Summary report  
[NASA-CR-167866] p 168 N85-35538
- KELKAR, S. S.**  
A fast time domain digital simulation technique for power converters - Application to a buck converter with feedforward compensation p 101 A85-20900
- KELM, J. S.**  
Flow modifying device  
[NASA-CASE-LEW-13562-2] p 33 N85-35195
- KENDALL, B. R. F.**  
Mass analysis of neutral particles and ions released during electrical breakdowns on spacecraft surfaces  
[NASA-CR-175585] p 39 N85-21250  
Mass spectra of neutral particles released during electrical breakdown of thin polymer films p 88 N85-22511
- KENNARD, J.**  
Development of large, horizontal-axis wind turbines  
[NASA-TM-86950] p 161 N85-23242
- KENNEDY, F. E.**  
An experimental investigation of rubbing interaction in labyrinth seals at cryogenic temperature p 129 A85-39938  
Analytical and experimental investigation of rubbing interaction in labyrinth seals for a liquid hydrogen fuel pump  
[NASA-CR-174657] p 48 N85-18084
- KENNEDY, F. E., JR.**  
Thermal and thermomechanical effects in dry sliding p 127 A85-23838
- KERCZEWSKI, R. J.**  
Automated testing of developmental satellite communications systems and subsystems  
[NASA-TM-867070] p 100 N85-31348
- KERIBAR, R.**  
Methods for heat transfer and temperature field analysis of the insulated diesel  
[NASA-CR-174783] p 185 N85-16699
- KERSCHEN, E. J.**  
Effect of airfoil mean loading on convected gust interaction noise  
[AIAA PAPER 84-2324] p 173 A85-13955  
Noise produced by the interaction of a rotor wake with a swept stator blade  
[AIAA PAPER 84-2326] p 173 A85-13956
- KERSLAKE, W. R.**  
Rail accelerator technology and applications  
[NASA-TM-86947] p 48 N85-21258
- KESSEL, R. L.**  
Numerical simulations of positively-biased probes and dielectric-conductor disks in a plasma p 179 A85-17262  
Numerical simulation of positive-potential conductors in the presence of a plasma and a secondary-emitting dielectric p 102 A85-35306

**KHANDELWAL, P. K.**

Photoacoustic microscopy of ceramic turbine blades  
p 83 A85-43930

**KHOT, N. S.**

Structural optimization using optimality criteria  
methods p 144 A85-48703

**KIELB, R.**

Natural frequencies of twisted rotating plates  
p 141 A85-32343

**KIELB, R. E.**

Flutter of turbofan rotors with mistuned blades  
p 139 A85-12716

Vibration and flutter of mistuned bladed-disk  
assemblies [AIAA PAPER 84-0991] p 139 A85-16095

Effects of warping and pretwist on torsional vibration  
of rotating beams [ASME PAPER 84-WA/APM-41] p 140 A85-17040

Vibrations of twisted cantilevered plates - Summary of  
previous and current studies p 140 A85-22069

Flutter of swept fan blades  
[ASME PAPER 84-GT-138] p 141 A85-32962

Vibration and flutter of mistuned bladed-disk  
assemblies p 16 A85-45854

Vibrations of twisted cantilever plates - A comparison  
of theoretical results p 144 A85-47626

**KIM, C. N.**

Vortex modeling of single and multiple dilution jet mixing  
in a crossflow [AIAA PAPER 85-1580] p 111 A85-40701

**KIM, K. S.**

A review of path-independent integrals in elastic-plastic  
fracture mechanics, task 4 [NASA-CR-174956] p 152 A85-33541

**KIM, R. C.**

Holographic optical system for aberration corrections  
in laser Doppler velocimetry p 123 A85-48659

**KIM, W. S.**

Lubricity of well-characterized jet and broad-cut fuels  
by ball-on-cylinder machine [NASA-TM-83807] p 92 A85-12183

Liquid phase products and solid deposit formation from  
thermally stressed model jet fuels [NASA-TM-86874] p 92 A85-13066

Thin-film sensors for space propulsion technology  
p 41 A85-27968

**KING, L. A.**

Moving target, distributed, real-time simulation using  
Ada p 170 A85-34131

**KING, R. J.**

Small-signal model for the series resonant converter  
p 102 A85-39453

**KINGSBURY, E.**

First-order ball-bearing kinematics  
p 128 A85-31203

**KINNICK, R. R.**

Photoacoustic microscopy of ceramic turbine blades  
p 83 A85-43930

**KIRALY, L. J.**

A high-speed implementation of the random decrement  
algorithm p 94 A85-29556

**KISER, J. D.**

Milling of Si3N4 with Si3N4 hardware  
[NASA-TM-86864] p 84 A85-10191

Factors influencing the ball milling of Si3N4 in water  
[NASA-TM-86932] p 86 A85-19136

Parametric evaluation of ball milling of SiC in water  
[NASA-TM-86974] p 88 A85-21356

Radiographic detectability limits for seeded voids in  
sintered silicon carbide and silicon nitride  
[NASA-TM-86945] p 138 A85-21674

Reliability of void detection in structural ceramics using  
scanning laser acoustic microscopy [NASA-TM-87035] p 138 A85-32337

**KLANN, G. A.**

Temperature distortion generator for turboshaft engine  
testing [SAE PAPER 84-1541] p 15 A85-39065

Temperature distortion generator for turboshaft engine  
testing [NASA-TM-83748] p 1 A85-15658

Experimental and analytical study of ceramic-coated  
turbine-tip shroud seals for small turbine engines  
[NASA-TM-86881] p 25 A85-18057

Experimental study of ceramic coated tip seals for  
turbojet engines [NASA-TM-86939] p 114 A85-19363

**KLEMETSON, R. W.**

An evaluation of oxygen/hydrogen propulsion systems  
for the Space Station [AIAA PAPER 85-1156] p 45 A85-43976

An evaluation of oxygen-hydrogen propulsion systems  
for the Space Station [NASA-TM-87059] p 52 A85-28971

**KLIMA, S. J.**

NDE for heat engine ceramics  
[NASA-TM-86949] p 137 A85-20389

Reliability of void detection in structural ceramics using  
scanning laser acoustic microscopy [NASA-TM-87035] p 138 A85-32337

**KMIEC, T. D.**

Design and analysis report for the RL10-2B breadboard  
low thrust engine [NASA-CR-174857] p 48 A85-19020

**KNIGHT, G. L.**

Energy efficient engine. High pressure compressor  
detail design report [NASA-CR-165558] p 23 A85-10998

**KNOTT, P. R.**

Experimental investigation of shock-cell noise reduction  
for single stream nozzles in simulated flight  
[NASA-CR-3845] p 175 A85-13550

**KOCH, C. C.**

Energy efficient engine. High pressure compressor  
detail design report [NASA-CR-165558] p 23 A85-10998

**KOCIMSKI, S. M.**

Apparatus and method for identification of matrix  
materials in which transuranic elements are embedded  
using thermal neutron capture gamma-ray emission  
[DE85-011659] p 125 A85-33454

**KOHL, F. J.**

Reactions of NaCl with gaseous SO3, SO2, and O2  
p 59 A85-11897

Chemical reactions involved in the initiation of hot  
corrosion of IN-738 p 66 A85-31688

Airfoil deposition model p 21 A85-10979

**KOMATSU, G.**

High frequency plasma generator for ion thrusters  
[NASA-CR-174772] p 48 A85-17023

**KORKAN, K. D.**

Analytical determination of propeller performance  
degradation due to ice accretion [AIAA PAPER 85-0339] p 14 A85-20867

Experimental aerodynamic characteristics of an NACA  
0012 airfoil with simulated ice p 12 A85-21844

Performance degradation of helicopter rotor in forward  
flight due to ice p 11 A85-42937

**KOVACH, A. J.**

Engineering model system study for a regenerative fuel  
cell: Study report [NASA-CR-174801] p 158 A85-16292

**KRAITCHMAN, M. D.**

Environmental effects on the tensile strength of  
chemically vapor deposited silicon carbide fibers  
[NASA-TM-86981] p 89 A85-24000

**KRATOCHVIL, D.**

Satellite provided customer promises services, a  
forecast of potential domestic demand through the year  
2000. Volume 4: Sensitivity analysis [NASA-CR-174662] p 99 A85-27092

**KREIDER, K. G.**

Advanced thin film thermocouples  
[NASA-CR-175541] p 124 A85-21607

**KRETCH, B. E.**

Perturbation-iteration theory for analyzing microwave  
striplines [NASA-CR-176189] p 100 A85-35321

**KUCHAR, A. P.**

Energy efficient engine ICLS Nacelle detail design  
report [NASA-CR-167870] p 22 A85-10993

**KUMM, E. L.**

Feasibility demonstration of a novel, flat-belt,  
continuously variable transmission or automotive and  
electric-hybrid vehicle application [NASA-CR-174430] p 185 A85-19894

**KUNG, J.**

Sixty GHz IMPATT diode development  
[NASA-CR-174969] p 105 A85-33293

**KUNIK, W. G.**

Analytical modeling of circuit aerodynamics in the new  
NASA Lewis Altitude Wind Tunnel [AIAA PAPER 85-0380] p 3 A85-26389

Analytical modeling of circuit aerodynamics in the new  
NASA Lewis wind tunnel [NASA-TM-86912] p 8 A85-15688

**KUNTZ, H. L.**

Oscillatory conductive heat transfer for a fiber in an ideal  
gas p 109 A85-26077

**KURTH, R.**

Composite loads spectra for select space propulsion  
structural components: Probabilistic load model  
development p 148 A85-27954

**KURTH, W. S.**

Effects of chemical releases by the STS 3 orbiter on  
the ionosphere p 166 A85-29538

**KUSAKA, T.**

Humidity effects on adhesion of nickel-zinc ferrite in  
elastic contact with magnetic tape and itself  
[NASA-TP-2449] p 88 A85-21359

**KUTNEY, J. T., JR.**

Energy efficient engine. Fan and quarter-stage  
component performance report [NASA-CR-168070] p 33 A85-34141

**KWATRA, S. C.**

An allpass filter design for luminance and chrominance  
separation of NTSC signals p 102 A85-28230

Modeling of NASA's 30/20 GHz satellite  
communications system p 38 A85-36663

**L****LACKNEY, J.**

On the development of hierarchical solution strategies  
for nonlinear finite element formulations p 171 A85-21979

**LAFLIN, J. H.**

Considerations for damage analysis of gas turbine hot  
section components [ASME PAPER 84-PVP-77] p 14 A85-18792

Unified constitutive material models for nonlinear  
finite-element structural analysis [AIAA PAPER 85-1418] p 142 A85-39769

Unified constitutive material models for nonlinear  
finite-element structural analysis [NASA-TM-86985] p 146 A85-24338

**LAKSHMINARAYANA, B.**

Computation of viscous flows in turbomachinery  
cascades p 106 A85-11631

Computation and turbulence closure models for shear  
flows in rotating curved bodies p 107 A85-14349

A space-marching method for incompressible  
Navier-Stokes equations [AIAA PAPER 85-0170] p 108 A85-19564

Computation of three-dimensional viscous flows using  
a space-marching method p 4 A85-29259

Turbulence modelling for complex shear flows  
[AIAA PAPER 85-1652] p 111 A85-40752

**LAM, P. T.**

On the calculation of the directivity of planar array feeds  
for satellite reflector applications p 97 A85-32249

**LAM, P. T. C.**

Focal shifts in parabolic reflectors p 97 A85-39356

**LAMB, J. D.**

Dielectric properties of 'diamondlike' carbon prepared  
by RF plasma deposition p 182 A85-38192

'Diamondlike' carbon films - Optical absorption, dielectric  
properties, and hardness dependence on deposition  
parameters p 82 A85-40383

**LAMBERT, R. F.**

Acoustic structure and propagation in highly porous,  
layered, fibrous materials p 173 A85-12301

**LAN, B. Y.**

Chemistry of fuel deposits and sediments and their  
precursors [NASA-CR-174778] p 92 A85-10209

**LANCE, J. R.**

Fuel cell power plant economic and operational  
considerations [ASME PAPER 84-AES-7] p 154 A85-21297

**LANFORD, W. A.**

Plasma deposited hydrogenated carbon on GaAs and  
InP p 182 A85-40386

Plasma deposited diamondlike carbon on GaAs and  
InP [NASA-TM-86870] p 183 A85-10844

Optical properties of hydrogenated amorphous carbon  
films grown from methane plasma [NASA-TM-86995] p 183 A85-26406

**LANG, T.**

General approaches for achieving high speed  
computations p 169 A85-28628

Functional language and data flow architectures  
p 170 A85-28629

**LANKFORD, J.**

Sliding seal materials for adiabatic engines  
[NASA-CR-174893] p 89 A85-22757

**LARK, R. F.**

Hygrothermomechanical evaluation of transverse  
filament tape epoxy/polyester fiberglass composites  
p 54 A85-15632

Fabrication and quality assurance processes for  
superhybrid composite fan blades  
[NASA-TM-83354] p 57 A85-14882

**LASSOW, E. S.**

Experimental and analytical study of ceramic-coated  
turbine-tip shroud seals for small turbine engines  
[NASA-TM-86881] p 25 A85-18057

Experimental study of ceramic coated tip seals for  
turbojet engines [NASA-TM-86939] p 114 A85-19363

- LAUER, J. L.**  
Topological reaction rate measurements related to scuffing p 64 A85-11070  
Characterization of lubricated bearing surfaces operated under high loads [NASA-TM-86964] p 88 N85-21357
- LAUF, R. J.**  
Dispersed metal-toughened ceramics and ceramic brazing [NASA-CR-174284] p 86 N85-15916
- LAUGHLIN, P. J.**  
Transferring data oscilloscope to an IBM using an Apple II+ p 168 A85-24526
- LAUVER, R. W.**  
Effect of substituted phenylindimides on processing and properties of PMR polyimide composites [NASA-TM-86902] p 85 N85-14929  
Chemical approach for controlling nadimide cure temperature and rate with maleimide [NASA-CASE-LEW-13770-3] p 87 N85-21350  
Chemical approach for controlling nadimide cure temperature and rate with maleimide [NASA-CASE-LEW-13770-4] p 87 N85-21351  
Chemical approach for controlling nadimide cure temperature and rate [NASA-CASE-LEW-13770-5] p 87 N85-21352  
Chemical control of nadimide cure temperature and rate [NASA-CASE-LEW-13770-2] p 63 N85-28982  
Chemical approach for controlling nadimide cure temperature and rate [NASA-CASE-LEW-13770-6] p 63 N85-30039
- LAVASH, J. P.**  
Energy Efficient Engine (E3) controls and accessories detail design report [NASA-CR-168017] p 31 N85-29957
- LAVIN, S. P.**  
Comparison of scaled model data to full size energy efficient engine test results [AIAA PAPER 84-2281] p 13 A85-13953  
Measurement and prediction of Energy Efficient Engine noise [AIAA PAPER 84-2284] p 13 A85-13954
- LAWLER, J. S.**  
Experimental investigation of a variable speed constant frequency electric generating system from a utility perspective [NASA-CR-174950] p 105 N85-32251
- LAWRENCE, C.**  
The use of an optical data acquisition system for bladed disk vibration analysis [NASA-TM-86891] p 144 N85-15184
- LAXMANAN, V.**  
Dendritic solidification. III - Some further refinements to the model for dendritic growth under an imposed thermal gradient p 69 A85-44703
- LAXMANN, V.**  
Dendritic solidification. I - Analysis of current theories and models. II - A model for dendritic growth under an imposed thermal gradient p 182 A85-38019
- LAYNE, J. L.**  
An investigation of enhanced capability thermal barrier coating systems for diesel engine components [NASA-CR-174820] p 86 N85-18154
- LEACH, K. P.**  
Energy efficient engine high-pressure turbine component rig performance test report [NASA-CR-168189] p 30 N85-29955
- LEDBETTER, F. E., III**  
Preparation of silicon carbide-silicon nitride fibers by the pyrolysis of polycarbosilazane precursors [NASA-TM-86505] p 91 N85-28107
- LEE, C. S.**  
Plot of modal field distribution in rectangular and circular waveguides p 101 A85-25170  
Numerical methods for analyzing electromagnetic scattering [NASA-CR-175507] p 99 N85-21438  
Normal modes in an overmoded circular waveguide coated with lossy material [NASA-CR-176186] p 100 N85-35320
- LEE, F. C.**  
A fast time domain digital simulation technique for power converters - Application to a buck converter with feedforward compensation p 101 A85-20900
- LEE, F. C. Y.**  
The J3 SCR model applied to resonant converter simulation p 102 A85-42156
- LEE, R. Q.**  
Case study of sample spacing in planar near-field measurement of high gain antennas [NASA-TM-86872] p 97 N85-10234
- LEE, S. S.**  
Stress waves in an isotropic elastic plate excited by a circular transducer [NASA-CR-3877] p 138 N85-20390
- Application of homomorphic signal processing to stress wave factor analysis [NAS 1.26:174871] p 138 N85-21673  
Ultrasonic testing of plates containing edge cracks [NASA-CR-3904] p 138 N85-29307
- LEE, S. W.**  
Plot of modal field distribution in rectangular and circular waveguides p 101 A85-25170  
Numerical methods for analyzing electromagnetic scattering [NASA-CR-175507] p 99 N85-21438  
Normal modes in an overmoded circular waveguide coated with lossy material [NASA-CR-176186] p 100 N85-35320
- LEE, S.-W.**  
Focal shifts in parabolic reflectors p 97 A85-39356
- LEESE, G. E.**  
Multiaxial and thermomechanical fatigue considerations in damage tolerant design [NASA-TM-87022] p 76 N85-26964
- LEHTINEN, B.**  
The role of modern control theory in the design of controls for aircraft turbine engines p 13 A85-13627
- LEI, C. K.**  
Heat transfer enhancement in channels with turbulence promoters [ASME PAPER 84-WA/HT-72] p 111 A85-39900
- LEIB, S. J.**  
Generation of capillary instabilities by external disturbances in a liquid jet [NASA-TM-87041] p 117 N85-30246
- LEIS, B. N.**  
A history dependent damage model for low cycle fatigue [ASME PAPER 84-PVP-112] p 140 A85-18795
- LEISSA, A. W.**  
Vibrations of twisted cantilevered plates - Summary of previous and current studies p 140 A85-22069  
Vibrations of twisted cantilever plates - A comparison of theoretical results p 144 A85-47626  
A study of internal and distributed damping for vibrating turbomachiner blades [NASA-CR-175901] p 30 N85-27868
- LEITMAN, M. J.**  
A procedure for obtaining explicit solutions to a class of Fredholm integral equations p 171 A85-28006
- LEKAN, J.**  
Demand for satellite-provided domestic communications services up to the year 2000 [NASA-TM-86894] p 97 N85-15099
- LEMKEY, F.**  
High temperature static strain sensor development program p 19 N85-10959
- LEMOGNE, T.**  
Aluminum work function: Effect of oxidation, mechanical scraping and ion bombardment [NASA-TM-87079] p 78 N85-34265
- LEMON, D. D.**  
Fracture toughness of hot-pressed beryllium p 66 A85-25835
- LENAHAN, D. T.**  
Energy efficient engine. Low pressure turbine test hardware detailed design report [NASA-CR-167958] p 22 N85-10994  
Energy efficient engine high pressure turbine test hardware detailed design report [NASA-CR-167955] p 23 N85-10995
- LEONARDO, M.**  
A stagnation pressure probe for droplet-laden air flow [AIAA PAPER 85-0330] p 108 A85-19672
- LEPICOVSKY, J.**  
An experimental study of tone excited heated jets [AIAA PAPER 84-2341] p 172 A85-10882  
Acoustic control of free jet mixing [AIAA PAPER 85-0569] p 109 A85-25951
- LERCH, B. A.**  
A study of fatigue damage mechanisms in Waspaloy from 25 to 800 C p 65 A85-12098
- LEROY, B. E.**  
Alternatives for satellite sound broadcast systems at HF and VHF p 99 N85-23815
- LEVINE, S. R.**  
Deposition stress effects on the life of thermal barrier coatings on burner rigs p 79 A85-19086  
Surface protection overview p 21 N85-10978
- LEVIS, C. A.**  
Engineering calculations for communications satellite systems planning [NASA-CR-175552] p 37 N85-21233
- LEVY, R.**  
Analytical modeling of circuit aerodynamics in the new NASA Lewis Altitude Wind Tunnel [AIAA PAPER 85-0380] p 3 A85-26389  
Analytical modeling of circuit aerodynamics in the new NASA Lewis wind tunnel [NASA-TM-86912] p 8 N85-15688
- LEWICKI, D. G.**  
Life and reliability modeling of bevel gear reductions [NASA-TM-87006] p 133 N85-27227  
Fatigue life analysis of a turboprop reduction gearbox [NASA-TM-87014] p 133 N85-27228
- LEWIS, C. R.**  
Magnesium doping of efficient GaAs and Ga(0.75)In(0.25)As solar cells grown by metalorganic chemical vapor deposition p 180 A85-11466
- LIEBERMAN, M.**  
Jet fuel property changes and their effect on producibility and cost in the U.S., Canada, and Europe [NASA-CR-174840] p 93 N85-27012
- LIEBERT, C. H.**  
High temperature thermocouple and heat flux gauge using a unique thin film-hardware hot junction [NASA-TM-86898] p 123 N85-16096  
Heat flux sensor calibrator p 41 N85-27970
- LILLEY, D. G.**  
Flow visualization of lateral jet injection into swirling crossflow [AIAA PAPER 85-0059] p 2 A85-19490  
Swirling flows in typical combustor geometries [AIAA PAPER 85-0184] p 108 A85-19574  
Turbulence measurements of lateral jet injection into confined tubular crossflow [AIAA PAPER 85-1102] p 110 A85-39604  
Investigation of flowfields found in typical combustor geometries [NASA-CR-3869] p 26 N85-21167  
Deflected jet experiments in a turbulent combustor flowfield [NASA-CR-174863] p 26 N85-22390  
Confined turbulent swirling recirculating flow predictions [NASA-CR-174917] p 29 N85-26716  
Turbulence characteristics of swirling flowfields [NASA-CR-174918] p 29 N85-26717  
Predictions and measurements of isothermal flowfields in axisymmetric combustor geometries [NASA-CR-174916] p 29 N85-27867
- LILLEY, J. R., JR.**  
Three-dimensional calculation of shuttle charging in polar orbit p 40 N85-22486
- LIM, H. S.**  
Long life nickel electrodes for a nickel-hydrogen cell. III - Results of an accelerated test and failure analyses p 156 A85-45391  
The failure mechanism of a nickel electrode in a nickel-hydrogen cell p 105 N85-31408
- LIMERICK, C. D.**  
Design and analysis report for the RL10-2B breadboard low thrust engine [NASA-CR-174857] p 48 N85-19020
- LIN, H. H.**  
Dynamic analysis of straight and involute tooth forms [ASME PAPER 84-DET-226] p 128 A85-33780
- LINDGREN, L. C.**  
Ceramic applications in turbine engines [NASA-CR-174715] p 91 N85-28109
- LINDHOLM, U. S.**  
Unified constitutive material models for nonlinear finite-element structural analysis [AIAA PAPER 85-1418] p 142 A85-39769  
Unified constitutive material models for nonlinear finite-element structural analysis [NASA-TM-86985] p 146 N85-24338  
A survey of unified constitutive theories p 150 N85-31531
- LING, H.**  
Focal shifts in parabolic reflectors p 97 A85-39356
- LING, J. S.**  
Evaluation of developmental membranes for the mixed reactant iron-chromium redox system [NASA-TM-87074] p 164 N85-34443
- LING, J. X.**  
A new interpretation of internal heat transfer coefficients of porous media [ASME PAPER 84-WA/HT-51] p 110 A85-39894
- LINSCOTT, B. S.**  
Government review of the Mod-2 wind turbine (as-built) [NASA-TM-86983] p 162 N85-29365  
The Federal Wind Program at NASA Lewis Research Center [NASA-TM-83480] p 163 N85-30478
- LITTLE, J. K.**  
Experimental and analytical study of ceramic-coated turbine-tip shroud seals for small turbine engines [NASA-TM-86881] p 25 N85-18057  
Ribbon burner simulation of T-700 turbine shroud for ceramic lined seals research [NASA-TM-86940] p 114 N85-19364

- LITVIN, F. L.**  
Spiral bevel and circular arc helical gears: Tooth contact analysis and the effect of misalignment on circular arc helical gears  
[NASA-TM-87013] p 32 N85-31060  
Generated spiral bevel gears: Optimal machine-tool settings and tooth contact analysis  
[NASA-TM-87075] p 136 N85-34405
- LIU, D. C.**  
"Diamondlike" carbon films - Optical absorption, dielectric properties, and hardness dependence on deposition parameters p 82 A85-40383  
Plasma deposited hydrogenated carbon on GaAs and InP p 182 A85-40386  
Plasma deposited diamondlike carbon on GaAs and InP  
[NASA-TM-86870] p 183 N85-10844  
Effect of interfacial characteristics of metal clad polymeric substrates on electrical high frequency interconnection performance p 99 N85-20223  
Optical properties of hydrogenated amorphous carbon films grown from methane plasma  
[NASA-TM-86995] p 183 N85-26406
- LIU, H. S.**  
High pressure compressor component performance report  
[NASA-CR-168245] p 33 N85-34138
- LIU, W. K.**  
Probabilistic finite element: Variational theory p 149 N85-27957
- LIVER, P.**  
Flow control in a diffusing S-Duct  
[AIAA PAPER 85-0524] p 3 A85-25928
- LO, Y. T.**  
The study of microstrip antenna arrays and related problems  
[NASA-CR-174054] p 97 N85-11265  
Numerical methods for analyzing electromagnetic scattering  
[NASA-CR-175507] p 99 N85-21438
- LOCK, J. A.**  
Incident beam polarization for laser Doppler velocimetry employing a sapphire cylindrical window p 122 A85-39835  
Incident beam polarization for laser Doppler velocimetry employing a sapphire cylindrical window  
[NASA-TM-87064] p 178 N85-28786
- LOEWENTHAL, S. H.**  
Operating characteristics of a 0.87 kW-hr flywheel energy storage module p 133 N85-28371  
Application of traction drives as servo mechanisms p 152 N85-33520
- LOH, J.**  
Configuration study for a 30 GHz monolithic receive array: Technical assessment  
[NASA-CR-174697] p 98 N85-18238  
Configuration study for a 30 GHz monolithic receive array, volume 1  
[NASA-CR-174697-VOL-1] p 98 N85-18239  
Configuration study for a 30 GHz monolithic receive array, volume 2  
[NASA-CR-174697-VOL-2] p 99 N85-18240
- LORIA, J. C.**  
The NASA photovoltaic technology program p 155 A85-35604
- LOTTIG, R. A.**  
Altitude testing of a flight weight, self-cooled, 2D thrust vectoring exhaust nozzle  
[SAE PAPER 841557] p 14 A85-25984
- LOVELL, R. C.**  
High pressure compressor component performance report  
[NASA-CR-168245] p 33 N85-34138
- LU, C. Y.**  
Manual of phosphoric acid fuel cell power plant optimization model and computer program  
[NASA-CR-174721] p 157 N85-10445  
Manual of phosphoric acid fuel cell stack three-dimensional model and computer program  
[NASA-CR-174722] p 157 N85-10447  
Phosphoric acid fuel cell power plant system performance model and computer program  
[NASA-CR-174638] p 157 N85-11456
- LU, S.-L.**  
A functional language approach in high-speed digital simulation p 170 A85-28615
- LUDEMANN, S. G.**  
Large-scale advanced propan (LAP) program progress report  
[AIAA PAPER 85-1187] p 17 A85-47021  
Large-scale Advanced Propan (LAP) program  
[NASA-TM-87067] p 32 N85-29964
- LUH, H.**  
The 20 GHz proof-of-concept test model results for a multiple scan beam dual reflector antenna  
[NASA-CR-174268] p 98 N85-15944
- LUNDQUIST, C. A.**  
Report of the Constellations Panel p 131 N85-20368
- M**
- MA, Y. E.**  
Sixty GHz IMPATT diode development  
[NASA-CR-174969] p 105 N85-33293
- MACBAIN, J. C.**  
Vibrations of twisted cantilevered plates - Summary of previous and current studies p 140 A85-22069  
Vibrations of twisted cantilever plates - A comparison of theoretical results p 144 A85-47626
- MACKEY, R. A.**  
Factors which influence directional coarsening of gamma-prime during creep in nickel-base superalloy single crystals p 67 A85-32388  
Morphological changes of gamma prime precipitates in nickel-base superalloy single crystals  
[NASA-TM-83698] p 70 N85-10165
- MACKIN, M. A.**  
Floating-point function generation routines for 16-bit microcomputers  
[NASA-TM-83783] p 170 N85-10683
- MAEDA, C.**  
Humidity effects on adhesion of nickel-zinc ferrite in elastic contact with magnetic tape and itself  
[NASA-TP-2449] p 88 N85-21359
- MAFFEO, R. J.**  
A computer analysis program for interfacing thermal and structural codes  
[NASA-TM-87021] p 148 N85-27264
- MAHAN, J. R.**  
The influence of combustion liner holes on noise production by ducted burners  
[AIAA PAPER 84-2322] p 172 A85-10869
- MAISEL, J. E.**  
A historical overview of the electrical power systems in the US manned and some US unmanned spacecraft  
[NASA-CR-174806] p 47 N85-13910
- MAJJIGI, R. K.**  
Experimental investigation of shock-cell noise reduction for dual-stream nozzles in simulated flight  
[NASA-CR-3846] p 175 N85-13549  
Development of a rotor wake-vortex model, volume 1  
[NASA-CR-174849] p 9 N85-26668
- MAKOU, A.**  
Data flow methods for dynamic system simulation - A CSSL-IV microcomputer network interface p 170 A85-28614
- MALAK, M.**  
The three-dimensional compressible flow in a radial inflow turbine scroll p 6 A85-41826
- MALIK, S.**  
The mechanisms of flame holding in the wake of a bluff body  
[NASA-CR-174058] p 62 N85-11149  
The mechanisms of flame holding in the wake of a bluff body  
[NASA-CR-3866] p 26 N85-21166
- MANDELL, J. F.**  
Structural characteristics of high temperature composites  
[NASA-CR-175998] p 58 N85-30037
- MANDELL, M. J.**  
Computer simulation of plasma electron collection by PIX-II  
[AIAA PAPER 85-0386] p 43 A85-19715  
Three-dimensional calculation of shuttle charging in polar orbit p 40 N85-22486  
Polar orbit electrostatic charging of objects in shuttle wake p 40 N85-22487  
Surface interactions and high-voltage current collection p 40 N85-22493  
NASCAP simulation of PIX 2 experiments p 180 N85-22497
- MANDERSCHIED, J. M.**  
Cyclic structural analyses of anisotropic turbine blades for reusable space propulsion systems  
[NASA-TM-86990] p 146 N85-24339  
Cyclic structural analyses of SSME turbine blades p 150 N85-27963
- MANGANO, M. J.**  
Report of the Constellations Panel p 131 N85-20368
- MANGELS, J. A.**  
Fracture of yttria-doped, sintered reaction-bonded silicon nitride  
[ACS PAPER 7-J3-84] p 82 A85-42797
- MANSON, S. S.**  
Reexamination of cumulative fatigue damage laws p 149 N85-27962
- MANTENIEKS, M.**  
Performance capabilities of the 12-centimeter Xenon ion thruster p 42 A85-16439
- MANZO, M. A.**  
Teardown analysis of a ten cell bipolar nickel-hydrogen battery p 156 A85-45385  
Separator development and testing of nickel-hydrogen cells p 156 A85-45386  
A 37.5-kW point design comparison of the nickel-cadmium battery, bipolar nickel-hydrogen battery, and regenerative hydrogen-oxygen fuel cell energy storage subsystems for low earth orbit p 46 A85-45387  
Advanced designs for IPV nickel-hydrogen cells p 156 A85-45388  
Initial performance of advanced designs for IPV nickel-hydrogen cells p 105 N85-31404  
Design principles for nickel-hydrogen cells and batteries  
[NASA-TM-87037] p 164 N85-31646
- MAPLES, B. W.**  
Modeling of NASA's 30/20 GHz satellite communications system p 38 A85-36663
- MARAM, J. M.**  
Feasibility of mapping velocity flow fields in SSME powerhead by laser anemometry techniques p 41 N85-27971
- MARBLE, F. E.**  
Growth of a diffusion flame in the field of a vortex p 61 A85-47320
- MARCHAND, N.**  
Thermal-mechanical fatigue crack growth in Inconel X-750  
[NASA-CR-174740] p 72 N85-15877
- MAREK, C. J.**  
Combustor turbulence p 118 N85-31434
- MARINO, D.**  
Homogeneity of pristine and bromine intercalated graphite fibers  
[NASA-TM-87016] p 89 N85-25521
- MARK, W. D.**  
Turbofan noise generation. Volume 2: Computer programs  
[NASA-CR-167952] p 175 N85-11791
- MARSIK, S. J.**  
Advanced research and technology programs for advanced high-pressure oxygen-hydrogen rocket propulsion  
[NASA-TM-86969] p 37 N85-21231
- MARTIN, C. H.**  
Engineering calculations for communications satellite systems planning  
[NASA-CR-175552] p 37 N85-21233
- MARTIN, J. F.**  
Closed-loop strain controlled testing at elevated temperatures with a non-contacting gage p 121 A85-29562  
A comparison of smooth specimen and analytical simulation techniques for notched members at elevated temperatures p 151 N85-31546
- MARTIN, M. R.**  
Development of a multiplane multispeed balancing system for turbine systems  
[NASA-CR-174750] p 35 N85-22400
- MARTIN, R. E.**  
Regenerative fuel cell energy storage system for a low Earth orbit space station  
[NASA-CR-174802] p 158 N85-13371  
Long-life high performance fuel cell program  
[NASA-CR-174874] p 50 N85-25384
- MARTZ, J. E.**  
Operational performance of the photovoltaic-powered grain mill and water pump at Tangaye, Burkina Faso (formerly Upper Volta)  
[NASA-TM-86970] p 161 N85-23243
- MARXER, N.**  
Characterization of lubricated bearing surfaces operated under high loads  
[NASA-TM-86964] p 88 N85-21357
- MATHUR, G.**  
Heat treatment of bulk gallium arsenide using a phosphosilicate glass cap p 181 A85-32636  
Fabrication of p(+)-n junction GaAs solar cells by a novel method p 181 A85-33645
- MATSUMURA, M.**  
A unified relation for cavitation erosion p 109 A85-24445
- MATTHEWS, E. W.**  
The 20 GHz proof-of-concept test model results for a multiple scan beam dual reflector antenna  
[NASA-CR-174268] p 98 N85-15944
- MATTOX, D. M.**  
Properties of coated and modified surfaces p 53 A85-36694



- MAUGER, A.**  
Substrate-induced orientational order in the isotropic phase of liquid crystals p 181 A85-24649
- MAURER, G. A.**  
Effects of tin on microstructure and mechanical behavior of Inconel 718 [NASA-TM-86866] p 71 N85-12129
- MAYER, H. L.**  
Report of the Constellations Panel p 131 N85-20368
- MAYO, F. R.**  
Chemistry of fuel deposits and sediments and their precursors [NASA-CR-174778] p 92 N85-10209
- MAZARIS, G. A.**  
Screen printed interdigitated back contact solar cell [NASA-Case-LEW-13414-1] p 160 N85-20530
- MCBRIDE, B. S.**  
Computer program for calculation of complex chemical equilibrium compositions and applications. Supplement 1: Transport properties [NASA-TM-86885] p 184 N85-16663
- MCBRIDE, B. J.**  
Combustion gas properties I-ASTM jet A fuel and dry air [NASA-TP-2359] p 17 N85-10064  
Modeling the internal combustion engine [NASA-RP-1094] p 172 N85-19733  
Combustion gas properties. 2: Natural gas fuel and dry air [NASA-TP-2435] p 26 N85-21168  
Ideal gas thermodynamic properties for the phenyl, phenoxy, and o-biphenyl radicals [NASA-TM-83800] p 184 N85-22204  
Combustion gas properties. Part 3: Hydrogen gas fuel and dry air [NASA-TP-2477] p 32 N85-31058
- MCDANIELS, D. L.**  
Analysis of stress-strain, fracture, and ductility behavior of aluminum matrix composites containing discontinuous silicon carbide reinforcement p 55 A85-37421
- MCDANIEL, O. H.**  
The performance of jet noise suppression devices for industrial applications p 175 A85-42563
- MCDONALD, G.**  
Plastic flow of plasma sprayed ceramics p 80 A85-24161  
Experimental study of ceramic coated tip seals for turbojet engines [NASA-TM-86939] p 114 N85-19363  
Ribbon burner simulation of T-700 turbine shroud for ceramic lined seals research [NASA-TM-86940] p 114 N85-19364  
Metallic and metalloceramic coating by thermal decomposition [NASA-TM-86992] p 88 N85-22755  
Film and interstitial formation of metals in plasma-sprayed ceramics [NASA-TM-86993] p 89 N85-22756  
Fabrication of ceramic substrate-reinforced and free forms [NASA-TM-86994] p 50 N85-23926
- MCDONALD, G. E.**  
Experimental and analytical study of ceramic-coated turbine-tip shroud seals for small turbine engines [NASA-TM-86881] p 25 N85-18057
- MCFADDEN, G. B.**  
Convective influence on the stability of a cylindrical solid-liquid interface p 109 A85-26911
- MC FARLAND, E. R.**  
Design and performance of a fixed, nonaccelerating guide vane cascade that operates over an inlet flow angle range of 60 deg [ASME PAPER 84-GT-75] p 4 A85-32964
- MCGAW, M. A.**  
A comparison of two contemporary creep-fatigue life prediction methods p 151 N85-31538
- MCHENRY, M.**  
Experimental study of ceramic coated tip seals for turbojet engines [NASA-TM-86939] p 114 N85-19363
- MCINTOSH, G. E.**  
A rotating superconducting solenoid for 100 kWh energy storage p 44 A85-33144
- MCKEVITT, F. X.**  
Performance characterization tests of a 1-kW resistojet using hydrogen, nitrogen and ammonia as propellants [AIAA PAPER 85-1159] p 44 A85-39628
- MCKNIGHT, R. C.**  
Icing flight research - Aerodynamic effects of ice and ice shape documentation with stereo photography [AIAA PAPER 85-0468] p 11 A85-30192
- Initial feasibility ground test of a proposed photogrammetric system for measuring the shapes of ice accretions on helicopter rotor blades during forward flight [NASA-TM-87391] p 12 N85-12887  
Icing flight research: Aerodynamic effects of ice and ice shape documentation with stereo photography [NASA-TM-86906] p 12 N85-18049
- MCKNIGHT, R. L.**  
Component-specific modeling [NASA-CR-174765] p 147 N85-27261  
Component-specific modeling [NASA-CR-174925] p 32 N85-32119  
Component-specific modeling [NASA-CR-174765] p 33 N85-34140
- MCLALLIN, K. L.**  
Application of viscous and inviscid computation methods for rocket turbopump systems [SAE PAPER 841522] p 110 A85-39257  
Analytical study of flow phenomena in SSME turnaround duct geometries p 116 N85-26902
- MC MURTRY, P. A.**  
Direct numerical simulations of a reacting mixing layer with chemical heat release [AIAA PAPER 85-0143] p 60 A85-19548
- MCNALLY, W. O.**  
Review - Computational methods for internal flows with emphasis on turbomachinery p 4 A85-29126
- MEHALIC, C. M.**  
Effect of combined pressure and temperature distortion orientation on high-bypass-ratio turbofan engine stability [NASA-TM-83771] p 17 N85-10067  
Effect of steady-state temperature distortion on inlet flow to a high-bypass-ratio turbofan engine [NASA-TM-86896] p 24 N85-15725
- MEHANDRU, S. P.**  
Dopant effect of yttrium and the growth and adherence of alumina on nickel-aluminum alloys p 82 A85-40973  
Mechanism for chelated sulfate formation from SO<sub>2</sub> and bis (triphenylphosphine) platinum p 62 A85-48493  
Why CO bonds side-on at low coverage and both side-on and upright at high coverage on the Cr(110) surface [NASA-CR-176071] p 77 N85-32173  
Adsorption of O<sub>2</sub>, SO<sub>2</sub>, and SO<sub>3</sub> on nickel oxide. Mechanism for sulfate formation [NASA-CR-176072] p 77 N85-32175  
CO adsorption on (111) and (100) surfaces of the Pt sub 3 Ti alloy. Evidence for parallel binding and strong activation of CO [NASA-CR-176077] p 77 N85-32176
- MEHTA, H. K.**  
Detailed studies of aviation fuel flowability [NASA-CR-174938] p 94 N85-31308
- MEHTA, S.**  
Radiation damage and defect behavior in ion-implanted, lithium counterdoped silicon solar cells p 182 A85-35698  
The effects of lithium counterdoping on radiation damage and annealing in n(+)-p silicon solar cells p 50 N85-22586
- MEIRON, D. I.**  
The linear two-dimensional stability of inviscid vortex streets of finite-cored vortices [AD-A153032] p 107 A85-14241
- MELCHER, K. J.**  
DEAN: A program for dynamic engine analysis [NASA-TM-87033] p 30 N85-28945
- MELNIK, R. E.**  
The computation of viscous/inviscid interaction on airfoils with separated flow p 6 A85-42954
- MERRILL, W.**  
The role of modern control theory in the design of controls for aircraft turbine engines p 13 A85-13627  
Identification of multivariable high-performance turbofan engine dynamics from closed-loop data p 13, A85-13630
- MERRILL, W. C.**  
Sensor failure detection for jet engines using analytical redundancy [AIAA PAPER 84-1452] p 13 A85-16097
- MERUTKA, J.**  
Effects of surface chemistry on hot corrosion life: Overview p 21 N85-10980
- METCALFE, R. W.**  
Direct numerical simulations of a reacting mixing layer with chemical heat release [AIAA PAPER 85-0143] p 60 A85-19548  
Direct simulations of chemically reacting turbulent mixing layers [AIAA PAPER 85-0321] p 60 A85-19666
- METZ, R. N.**  
Circuit transients due to negative bias arcs on a high-voltage solar array in low Earth orbit [NASA-TP-2407] p 39 N85-14858
- MEYERS, G. D.**  
Experiments in dilution jet mixing - Effects of multiple rows and non-circular orifices [AIAA PAPER 85-1104] p 15 A85-39606  
Experiments in dilution jet mixing effects of multiple rows and non-circular orifices [NASA-TM-86996] p 28 N85-25266
- MEYN, E. H.**  
The use of an optical data acquisition system for bladed disk vibration analysis [NASA-TM-86891] p 144 N85-15184
- MICHAELS, K. B.**  
Regenerative fuel cell energy storage system for a low Earth orbit space station [NASA-CR-174802] p 158 N85-13371
- MICHEL, R. W.**  
Vehicle/engine integration p 37 N85-17008
- MIESKOWSKI, D. M.**  
Strength and microstructure of sintered Si<sub>3</sub>N<sub>4</sub> with rare-earth-oxide additions [ACS PAPER 130-13-84] p 80 A85-25271  
Oxidation of silicon nitride sintered with rare-earth oxide additions p 83 A85-42798  
Microstructure of reaction-bonded silicon nitride consolidated by isostatic hot-pressing p 83 A85-45304  
Reliability of two sintered silicon nitride materials [NASA-TM-87092] p 92 N85-34284
- MIKKELSEN, K. L.**  
Icing flight research - Aerodynamic effects of ice and ice shape documentation with stereo photography [AIAA PAPER 85-0468] p 11 A85-30192  
Icing flight research: Aerodynamic effects of ice and ice shape documentation with stereo photography [NASA-TM-86906] p 12 N85-18049
- MILES, G. A.**  
Analytical fuel property effects-small combustors [NASA-CR-174738] p 28 N85-26709
- MILLAN, P. P.**  
Progress in the utilization of an oxide-dispersion-strengthened alloy for small engine turbine blades [SAE PAPER 841512] p 68 A85-39284
- MILLARD, M. L.**  
Effect of hot isostatic pressing on reaction-bonded silicon nitride p 79 A85-15195  
Evaluation of alpha-SiC sintering using statistical methods p 83 A85-42800  
Effect of hot isostatic pressing on the properties of sintered alpha silicon carbide p 83 A85-48757
- MILLER, C. J.**  
Noise constraints effecting optimal propeller designs [SAE PAPER 850871] p 7 A85-50106  
Noise constraints effecting optimal propeller designs [NASA-TM-86967] p 8 N85-19923
- MILLER, D. L.**  
Transferring data oscilloscope to an IBM using an Apple II+ p 168 A85-24526
- MILLER, D. R.**  
Aileron controls for wind turbine applications p 157 A85-45513  
Aileron controls for wind turbine applications [NASA-TM-86867] p 158 N85-11458  
Shutdown characteristics of the Mod-O wind turbine with aileron controls [NASA-TM-86918] p 159 N85-16299  
Analytical model for predicting emergency shutdown of a two-bladed horizontal axis wind turbine [NASA-TM-83472] p 162 N85-30476
- MILLER, E. F.**  
Technical characteristics of the broadcasting satellite plan at 12 GHz for the Western Hemisphere p 96 A85-28233  
Development and use of the computer software package for planning the 12 GHz broadcasting-satellite service at RARC '83 p 96 A85-29605
- MILLER, L. A.**  
Preliminary analysis of space mission applications for electromagnetic launchers [NASA-CR-174067] p 35 N85-12071
- MILLER, R. A.**  
Oxidation-based model for thermal barrier coating life p 78 A85-10310  
Performance of thermal barrier coatings in high heat flux environments p 79 A85-19087  
Life modeling of atmospheric and low pressure plasma-sprayed thermal-barrier coating p 81 A85-29728  
Mechanical property measurements of plasma-sprayed thermal-barrier coatings subjected to oxidation p 81 A85-29729
- MILLER, T. B.**  
Design considerations for a 10-kW integrated hydrogen-oxygen regenerative fuel cell system p 155 A85-45380

- MILLER, T. L.**  
Analytical determination of propeller performance degradation due to ice accretion  
[AIAA PAPER 85-0339] p 14 A85-20867
- MILLER, W. L.**  
An investigation of arc discharging on negatively biased dielectric conductor samples in a plasma  
p 180 N85-22498
- MILLIGAN, W. W.**  
Low cycle fatigue of MAR-M 200 single crystals at 760 and 870 deg C  
[NASA-TM-86933] p 74 N85-19074
- MILLNER, A. R.**  
Microprocessor control of photovoltaic systems  
p 156 A85-45408
- MILLS, D. L.**  
Substrate-induced orientational order in the isotropic phase of liquid crystals  
p 181 A85-24649
- MINER, R. V.**  
On the fatigue crack propagation behavior of superalloys at intermediate temperatures p 68 A85-32434  
The effects of seven alloying elements on the microstructure and stress-rupture behavior of nickel-base superalloys  
[NASA-TM-83791] p 70 N85-10168  
Orientation and temperature dependence of some mechanical properties of the single-crystal nickel-base superalloy Rene N4. 3: Tension-compression anisotropy  
[NASA-TM-86982] p 76 N85-22660
- MINNIN, W. A.**  
Advanced 30/20 GHz multiple beam antenna for future communications satellites p 96 A85-14436
- MIRITCH, M. J.**  
Deposition of diamondlike carbon films  
[NASA-CASE-LEW-14080-1] p 95 N85-20153  
Ion beam sputter-deposited thin film coatings for protection of spacecraft polymers in low Earth orbit  
[NASA-TM-87051] p 91 N85-30137  
Diamondlike carbon protective coatings for IR materials  
[NASA-TM-87083] p 178 N85-34631
- MISHINA, H.**  
Effect of barrier height on friction behavior of the semiconductors silicon and gallium arsenide in contact with pure metals  
[NASA-TP-2405] p 84 N85-13044
- MISRA, A. K.**  
Effects of SO<sub>2</sub> and SO<sub>3</sub> on the Na<sub>2</sub>SO<sub>4</sub> induced corrosion of nickel p 65 A85-15603  
Studies on the hot corrosion of a nickel-base superalloy, Udimet 700  
[NASA-TM-86882] p 71 N85-11224
- MITCHELL, A. M.**  
Transmission efficiency measurements and correlations with physical characteristics of the lubricant  
p 89 N85-23781
- MITCHELL, B.**  
Configuration study for a 30 GHz monolithic receive array: Technical assessment  
[NASA-CR-174697] p 98 N85-18238  
Configuration study for a 30 GHz monolithic receive array, volume 1  
[NASA-CR-174697-VOL-1] p 98 N85-18239  
Configuration study for a 30 GHz monolithic receive array, volume 2  
[NASA-CR-174697-VOL-2] p 99 N85-18240
- MITTRA, R.**  
Characterization of MMIC devices for active array antennas  
[NASA-TM-86907] p 38 N85-15779  
MMIC devices for active phased array antennas  
[NASA-CR-174281] p 98 N85-15943  
Characterization of microstrip discontinuities in the time and frequency domains  
[NASA-CR-176190] p 106 N85-35342
- MIYAKE, C. I.**  
Performance characterization tests of a 1-kW resistojet using hydrogen, nitrogen and ammonia as propellants  
[AIAA PAPER 85-1159] p 44 A85-39628
- MIYOSHI, K.**  
Friction and wear of some ferrous-base metallic glasses p 64 A85-11071  
Mechanical-contact-induced transformation from the amorphous to the partially crystalline state in metallic glass  
p 65 A85-19084  
Friction and wear of ceramics p 80 A85-23833  
Ceramic wear in indentation and sliding contact  
p 82 A85-39549  
Fundamental tribological properties of ceramics  
[NASA-TM-86915] p 85 N85-15893  
Surface effects of corrosive media on hardness, friction, and wear of materials  
[NASA-TM-83711] p 85 N85-15896
- Tribological properties of boron nitride synthesized by ion beam deposition  
[NASA-TM-86962] p 87 N85-21355  
Humidity effects on adhesion of nickel-zinc ferrite in elastic contact with magnetic tape and itself  
[NASA-TP-2449] p 88 N85-21359  
Effects of wear on structure-sensitive magnetic properties of ceramic ferrite in contact with magnetic tape  
[NASA-TM-87007] p 90 N85-26991
- MOCK, E. A. T.**  
Advanced technology cogeneration system conceptual design study: Closed cycle gas turbines  
[NASA-CR-168222] p 159 N85-16300
- MOFFAT, R. J.**  
Heat transfer and turbulence measurements of a film-cooled flow over a convexly curved surface  
p 112 A85-41787
- MONGEAU, P. P.**  
Metal vapor arc switch electromagnetic accelerator technology  
[NASA-CR-174380] p 103 N85-18259
- MONGIA, H. C.**  
Jet characteristics in confined swirling flow  
p 112 A85-45282  
Density effects on jet characteristics in confined swirling flow  
p 112 A85-45283
- MONKEWITZ, P. A.**  
The response of Helmholtz resonators to external excitation. I - Single resonators p 174 A85-26915
- MONTE, H.**  
Aluminum work function: Effect of oxidation, mechanical scraping and ion bombardment  
[NASA-TM-87079] p 78 N85-34265
- MONTY, J. D.**  
Analytical fuel property effects: Small combustors, phase 2  
[NASA-CR-174848] p 93 N85-19175
- MOORE, F. K.**  
A theory of post-stall transients in multistage axial compression systems  
[NASA-CR-3878] p 8 N85-21117
- MOORE, J.**  
Thermodynamic evaluation of transonic compressor rotors using the finite volume approach  
[NASA-CR-175811] p 29 N85-26712
- MOORE, J. A.**  
Development of a lithium secondary battery separator  
p 104 N85-31378
- MOORE, T. J.**  
Effect of hot isostatic pressing on reaction-bonded silicon nitride p 79 A85-15195  
Feasibility study of the welding of SiC  
p 81 A85-39339  
Diffusion welding of MA 6000 and a conventional nickel-base superalloy p 69 A85-43551  
Effect of hot isostatic pressing on the properties of sintered alpha silicon carbide p 83 A85-48757
- MOORHEAD, A. J.**  
Dispersed metal-toughened ceramics and ceramic brazing  
[NASA-CR-174284] p 86 N85-15916  
Dispersed-metal-toughened alumina  
[NASA-CR-174687] p 89 N85-22758
- MORACZ, D. J.**  
Energy efficient engine. Volume 2. Appendix A: Component development and integration program  
[NASA-CR-173085] p 22 N85-10991
- MORALES, W.**  
Formation of high molecular weight products from benzene during boundary lubrication  
[NASA-TM-86966] p 62 N85-22644
- MOREA, S. F.**  
Advanced research and technology programs for advanced high-pressure oxygen-hydrogen rocket propulsion  
[NASA-TM-86969] p 37 N85-21231
- MOREL, T.**  
Methods for heat transfer and temperature field analysis of the insulated diesel  
[NASA-CR-174783] p 185 N85-16699
- MORELL, L. J.**  
Moving target, distributed, real-time simulation using Ada  
p 170 A85-34131
- MORENO, V.**  
Application of two creep fatigue life models for the prediction of elevated temperature crack initiation of a nickel base alloy  
[AIAA PAPER 85-1420] p 69 A85-43979  
Creep fatigue life prediction for engine hot section materials (isotropic)  
[NASA-CR-168228] p 32 N85-31057  
Two simplified procedures for predicting cyclic material response from a strain history p 151 N85-31543
- MOREY, W. W.**  
Fiber optic temperature sensor p 121 A85-29563
- MORRIS, J. F.**  
High thermal power density heat transfer apparatus providing electrical isolation at high temperature using heat pipes  
[NASA-CASE-LEW-12950-2] p 117 N85-29179
- MORRIS, P. J.**  
Acoustic control of free jet mixing  
[AIAA PAPER 85-0569] p 109 A85-25951
- MORTON, H. L.**  
Analytical fuel property effects: Small combustors, phase 2  
[NASA-CR-174848] p 93 N85-19175
- MOSCARELLO, R.**  
Pantographing self adaptive gap elements  
p 142 A85-37440
- MOSTAFA, A.**  
A two-equation turbulence model for two-phase jets  
p 107 A85-14376
- MUCKLEY, E. T.**  
Shuttle/Centaur project perspective  
p 37 N85-16991
- MULAC, R. A.**  
Simulation of multistage turbine flows  
p 116 N85-27945
- MULARZ, E. J.**  
Future fundamental combustion research for aeropropulsion systems  
[AIAA PAPER 85-1398] p 16 A85-42671  
Combustion research for gas turbine engines  
[NASA-TM-86963] p 26 N85-21164  
Future fundamental combustion research for aeropropulsion systems  
[NASA-TM-87049] p 30 N85-27870
- MULLEN, R. L.**  
An analysis of temperature effect in a finite journal bearing with spatial tilt and viscous dissipation  
p 126 A85-11074  
Plastic flow of plasma sprayed ceramics  
p 80 A85-24161  
Analysis of experimental shaft seal data for high-performance turbomachines, as for Space Shuttle main engines  
[NASA-TM-86928] p 115 N85-21569  
Nested subcritical flows within supercritical systems  
[NASA-TM-86980] p 115 N85-21574  
Film and interstitial formation of metals in plasma-sprayed ceramics  
[NASA-TM-86993] p 89 N85-22756
- MULLER, A.**  
Augmented weak forms and element-by-element preconditioners: Efficient iterative strategies for structural finite elements. A preliminary study p 144 N85-10384
- MULLER, G. L.**  
Three-dimensional inviscid flow analysis of turbofan forced mixers  
[AIAA PAPER 85-0086] p 2 A85-19510
- MULLIN, J. P.**  
The NASA photovoltaic technology program  
p 155 A85-35604
- MURAMOTI, K. K.**  
Analytical modeling of circuit aerodynamics in the new NASA Lewis Altitude Wind Tunnel  
[AIAA PAPER 85-0380] p 3 A85-26389
- MURAMOTO, K. K.**  
Flow through very porous inclined screens  
[AIAA PAPER 85-1650] p 111 A85-40750  
Analytical modeling of circuit aerodynamics in the new NASA Lewis wind tunnel  
[NASA-TM-86912] p 8 N85-15688  
Flow through very porous inclined screens  
[NASA-TM-86979] p 116 N85-25761
- MURMAN, E. M.**  
Three-dimensional inviscid flow analysis of turbofan forced mixers  
[AIAA PAPER 85-0086] p 2 A85-19510
- MURPHY, G. B.**  
Effects of chemical releases by the STS 3 orbiter on the ionosphere p 166 A85-29538  
Suprathermal plasma observed on STS-3 Mission by plasma diagnostics package p 179 N85-22472  
Electron and ion density depletions measured in the STS-3 orbiter wake p 39 N85-22474
- MURRAY, R. A.**  
Numerical simulation of positive-potential conductors in the presence of a plasma and a secondary-emitting dielectric  
p 102 A85-35306
- MURTHY, K. N. S.**  
Computation of three-dimensional viscous flows using a space-marching method p 4 A85-29259
- MURTHY, P. L. N.**  
ICAN - Integrated composites analyzer  
[AIAA PAPER 84-0974] p 54 A85-16094  
A study of interply layer effects on the free edge stress field of angleply laminates p 55 A85-41127

- A study of interply layer effects on the free-edge stress field of angleplyed laminates  
[NASA-TM-86924] p 57 N85-15822
- MURTHY, S. N. B.**  
A stagnation pressure probe for droplet-laden air flow  
[AIAA PAPER 85-0330] p 108 A85-19672
- MUSIKANT, S.**  
Transformation toughened ceramics for the heavy duty diesel engine technology program  
[NASA-CR-174689] p 185 N85-16698
- MYERS, D. M.**  
Stratified charge rotary aircraft engine technology enablement program  
[NASA-CR-174812] p 25 N85-21163
- MYERS, M. R.**  
Effect of airfoil mean loading on convected gust interaction noise  
[AIAA PAPER 84-2324] p 173 A85-13955
- MYUNG, N. H.**  
Analysis of the electromagnetic scattering from an inlet geometry with lossy walls  
[NASA-CR-175743] p 99 N85-25686

## N

- NAGAMATSU, H. T.**  
Heat transfer investigation in the junction region of circular cylinder normal to a flat plate at 90 deg location  
[ASME PAPER 84-WA/HT-70] p 111 A85-39898
- NAGTEGAAL, J.**  
Probabilistic finite element development  
p 149 N85-27956
- NAHRA, H. K.**  
Ion beam sputter-deposited thin film coatings for protection of spacecraft polymers in low Earth orbit  
[NASA-TM-87051] p 91 N85-30137
- NAKANISHI, S.**  
Experiments with a microwave electrothermal thruster concept  
p 42 A85-16441  
Cathode degradation and erosion in high pressure arc discharges  
p 43 A85-16445  
Precision tunable resonant microwave cavity  
[NASA-CASE-LEW-13935-1] p 103 N85-20248
- NAKANISHI, T. G.**  
Effects of cobalt, boron, and zirconium on the microstructure of Udimet 738  
[NASA-CR-174762] p 70 N85-10166
- NAKAZAWA, S.**  
3-D inelastic analysis methods for hot section components (base program)  
[NASA-CR-174700] p 145 N85-21686
- NARAGHI, M.**  
A new interpretation of internal heat transfer coefficients of porous media  
[ASME PAPER 84-WA/HT-51] p 110 A85-39894
- NASTROM, G. D.**  
GASP cloud encounter statistics - Implications for laminar flow control flight  
p 166 A85-11979  
A comparison of NMC and GWC analysis field temperatures with aircraft measurements  
p 166 A85-21140  
Variability of cloudiness at airline cruise altitudes from GASP measurements  
p 166 A85-31199
- NATARAJAN, V.**  
"Diamondlike" carbon films - Optical absorption, dielectric properties, and hardness dependence on deposition parameters  
p 82 A85-40383
- NATHAL, M. V.**  
Elevated temperature creep-rupture behavior of the single crystal nickel-base superalloy NASAIR 100  
p 66 A85-27812  
Influence of composition on the microstructure and mechanical properties of a nickel-base superalloy single crystal  
p 66 A85-32387
- NEELY, G. M.**  
Accelerated convergence for incompressible flow calculations  
[AIAA PAPER 85-0058] p 2 A85-19489  
Flame radiation and linear heat transfer in a tubular-can combustor  
p 15 A85-39580  
Accelerated convergence for incompressible flow calculations  
[NASA-TM-86863] p 18 N85-10949  
Reducing numerical diffusion for incompressible flow calculations  
[NASA-TM-83621] p 24 N85-14840
- NELSON, C. C.**  
Rotordynamic coefficients for compressible flow in tapered annular seals  
p 129 A85-42573
- NELSON, D. A.**  
Interaction of finite-amplitude sound with air-filled porous materials  
[NASA-CR-174885] p 177 N85-27637

- NELSON, W. A.**  
Energy efficient engine high pressure turbine ceramic shroud support technology report  
[NASA-CR-168036] p 23 N85-10996
- NEMAT-NASSER, S.**  
On stress field near a stationary crack tip  
[AD-A152863] p 141 A85-24532
- NESBITT, J. A.**  
Cyclic oxidation behavior of beta+gamma overlay coatings on gamma and gamma+gamma-prime alloys  
p 68 A85-32431
- NESTER, W. H.**  
Configuration study for a 30 GHz monolithic receive array: Technical assessment  
[NASA-CR-174697] p 98 N85-18238  
Configuration study for a 30 GHz monolithic receive array, volume 1  
[NASA-CR-174697-VOL-1] p 98 N85-18239  
Configuration study for a 30 GHz monolithic receive array, volume 2  
[NASA-CR-174697-VOL-2] p 99 N85-18240
- NEUMANN, H. E.**  
Performance and surge limits of a TF30-P-3 turbofan engine/axisymmetric mixed-compression inlet propulsion system at Mach 2.5  
[NASA-TP-2461] p 27 N85-25261
- NEUSTADTER, H. E.**  
Method for evaluating wind turbine wake effects on wind farm performance  
p 155 A85-36750
- NEVEU, M. C.**  
Applications of high pressure differential scanning calorimetry to aviation fuel thermal stability research  
[NASA-TM-87002] p 63 N85-23941
- NEWELL, J. F.**  
Composite loads spectra for select space propulsion structural components  
p 148 N85-27953
- NEWTON, J.**  
Ice shapes and the resulting drag increase for a NACA 0012 airfoil  
[NASA-TM-83556] p 11 N85-27839
- NGAN, Y. C.**  
The 30 GHz solid state amplifier for low cost low data rate ground terminals  
[NASA-CR-174795] p 102 N85-12300
- NGHIEM, H.**  
Sixty GHz IMPATT diode development  
[NASA-CR-174969] p 105 N85-33293
- NGUYEN-DINH, X.**  
Development of coated single-crystal superalloy systems for gas turbine applications  
p 68 A85-32440
- NGUYEN-VO, N.-M.**  
The response of Helmholtz resonators to external excitation. I - Single resonators  
p 174 A85-26915
- NGUYEN, H. C.**  
The effect of tantalum and carbon on the structure/properties of a single crystal nickel-base superalloy  
[NASA-CR-174779] p 71 N85-11223
- NICHOLSON, S.**  
Thermodynamic evaluation of transonic compressor rotors using the finite volume approach  
[NASA-CR-175811] p 29 N85-26712
- NIEBERDING, W. C.**  
Hot section laser anemometry  
p 19 N85-10962  
Instrumentation technology overview  
p 124 N85-26903
- NIR, D.**  
Mechanical protection of DLC films on fused silica slides  
[NASA-TM-87056] p 91 N85-30138  
Diamondlike carbon protective coatings for IR materials  
[NASA-CR-170883] p 178 N85-34631
- NISSIM, E.**  
Optimization of cascade blade mistuning. I - Equations of motion and basic inherent properties  
p 16 A85-42365  
Optimization of cascade blade mistuning. II - Global optimum and numerical optimization  
p 16 A85-45715
- NISSLEY, D. M.**  
Application of two creep fatigue life models for the prediction of elevated temperature crack initiation of a nickel base alloy  
[AIAA PAPER 85-1420] p 69 A85-43979
- NOE, K. A.**  
Behavior of the lean methane-air flame at zero-gravity  
[NASA-CR-175586] p 62 N85-21283
- NONAMI, K.**  
Vibration control of rotor shaft  
[NASA-TM-87053] p 133 N85-29292
- NORGREN, C. T.**  
Advanced liner-cooling techniques for gas turbine combustors  
[AIAA PAPER 85-1290] p 15 A85-39703

- Small gas turbine combustor study - Fuel injector performance in a transpiration-cooled liner  
[AIAA PAPER 85-1312] p 16 A85-39717  
Advanced liner-cooling techniques for gas turbine combustors  
p 8 N85-21115  
Small gas turbine combustor study: Fuel injector performance in a transpiration-cooled liner  
[NASA-TM-86989] p 27 N85-25264
- NYLAND, T. W.**  
Reflection plane tests of a wind turbine blade tip section with ailerons  
[NASA-TM-87018] p 165 N85-34444

## O

- OBATA, M.**  
On stress field near a stationary crack tip  
[AD-A152863] p 141 A85-24532
- OBERLE, L. G.**  
Filter induced errors in laser anemometer measurements using counter processors  
[NASA-TM-87047] p 125 N85-30288
- O'BRIEN, J. E.**  
The influence of jet-grid turbulence on heat transfer from the stagnation region of a cylinder in crossflow  
[NASA-TM-87011] p 115 N85-25760
- O'BRIEN, J. J.**  
Electric utility acid fuel cell stack technology advancement  
[NASA-CR-174804] p 159 N85-17422
- ODEN, J. T.**  
Analysis of hourglass instabilities and control in underintegrated finite element methods  
p 139 A85-11125
- ODONNELL, W. J.**  
Simplified design and life prediction of rocket thrust chambers  
p 44 A85-29314
- OGRADY, E. P.**  
Multibus-based parallel processor for simulation  
p 169 A85-28613
- OKIISHI, T. H.**  
A note on blade wake interaction influence on compressor stator row aerodynamic performance  
p 4 A85-32965
- OLIVER, G. A.**  
Jet fuel property changes and their effect on producibility and cost in the U.S., Canada, and Europe  
[NASA-CR-174840] p 93 N85-27012
- OLSEN, R. B.**  
Pyroelectric conversion in space  
p 45 A85-45377
- OLSEN, R. C.**  
Experiments in charge control at geosynchronous orbit - ATS-5 and ATS-6  
p 39 A85-35379
- OLSEN, W.**  
Ice shapes and the resulting drag increase for a NACA 0012 airfoil  
[NASA-TM-83556] p 11 N85-27839
- OLSON, C.**  
Advanced thin film thermocouples  
[NASA-CR-175541] p 124 N85-21607
- OLSON, S. L.**  
Fuel rich catalytic combustion: The first stage of a two-stage combustor  
[NASA-TM-87042] p 63 N85-28983  
Fuel-rich catalytic combustion: A soot-free technique for in situ hydrogen-like enrichment  
[NASA-TP-2498] p 63 N85-31244
- OPPENHEIM, A. K.**  
Recent advances in methods for numerical solution of O.D.E. initial value problems  
p 171 A85-21370  
Knock syndrome: Its cures and its victims  
[NASA-CR-174395] p 93 N85-19185
- ORANGE, T. W.**  
Pre-HOST high temperature crack propagation  
p 19 N85-10956  
HOST high temperature crack propagation  
p 21 N85-10977
- ORTH, N. W.**  
Demonstration of a silicon nitride attrition mill for production of fine pure Si and Si<sub>3</sub>N<sub>4</sub> powders  
p 78 A85-10825
- ORTIZ, A. L.**  
Laser balancing system for high material removal rates  
[NASA-CR-174731] p 126 N85-12341
- OSTBERG, D. T.**  
Powder metallurgy forged gear development  
[NASA-TM-87483] p 134 N85-29295
- OTTERSON, D. A.**  
Rapid estimation of concentration of aromatic classes in middistillate fuels by high-performance liquid chromatography  
[NASA-TP-2495] p 93 N85-31307

## OWENS, H.

Suprathermal plasma observed on STS-3 Mission by plasma diagnostics package p 179 N85-22472

## P

## PADOVAN, J.

Extension of constrained incremental Newton-Raphson scheme to generalized loading fields p 139 A85-13942

On the development of hierarchical solution strategies for nonlinear finite element formulations p 171 A85-21979

Plastic flow of plasma sprayed ceramics p 80 A85-24161

Pantographing self adaptive gap elements p 142 A85-37440

Quasi-static solution algorithms for kinematically/materially nonlinear thermomechanical problems p 143 A85-41983

## PAGLIARO, P.

Preparation and evaluation of advanced catalysts for phosphoric acid fuel cells [NASA-CR-168223] p 160 N85-19511

## PAI, S.

Extension of constrained incremental Newton-Raphson scheme to generalized loading fields p 139 A85-13942

## PAI, S. S.

Quasi-static solution algorithms for kinematically/materially nonlinear thermomechanical problems p 143 A85-41983

## PALKO, R. L.

Initial feasibility ground test of a proposed photogrammetric system for measuring the shapes of ice accretions on helicopter rotor blades during forward flight [NASA-TM-87391] p 12 N85-12887

## PANDOLFI, M.

Inverse design technique for cascades [NASA-CR-3836] p 7 N85-12008

## PAPELL, S. S.

Vortex-generating coolant-flow-passage design for increased film-cooling effectiveness and surface coverage [NASA-TP-2388] p 113 N85-12314

Vortex generating flow passage design for increased film cooling effectiveness [NASA-CASE-LEW-14039-1] p 119 N85-33433

## PARK, G. L.

Improved models for increasing wind penetration, economics and operating reliability [NASA-CR-175538] p 160 N85-20545

## PARK, J. S.

Heat transfer enhancement in channels with turbulence promoters [ASME PAPER 84-WA/HT-72] p 111 A85-39900

## PARKER, R. D.

Operating characteristics of a 0.87 kw-hr flywheel energy storage module [NASA-TM-87038] p 133 N85-28371

## PARKS, D. E.

Polar orbit electrostatic charging of objects in shuttle wake p 40 N85-22487

## PARZYCH, D.

Large-scale Advanced Proptan (LAP) performance, acoustic and weight estimation, January, 1984 [NASA-CR-174782] p 9 N85-22368

## PATEL, D. R.

Functional language and data flow architectures p 170 A85-28629

## PATERSON, W.

Suprathermal plasma observed on STS-3 Mission by plasma diagnostics package p 179 N85-22472

## PATHAK, P. H.

Analysis of the electromagnetic scattering from an inlet geometry with lossy walls [NASA-CR-175743] p 99 N85-25686

## PATHARE, V.

Alloys based on NiAl for high temperature applications [NASA-TM-86976] p 75 N85-21322

## PATTIPATI, K. R.

A design methodology for robust failure detection and isolation p 171 A85-47794

## PAUCKERT, R.

Cryogenic upper stage test bed engine [AIAA PAPER 85-1339] p 44 A85-39733

## PECKHAM, R. J.

Design and analysis report for the RL10-2B breadboard low thrust engine [NASA-CR-174857] p 48 N85-19020

## PELACCIO, D. G.

Feasibility of mapping velocity flow fields in SSME powerhead by laser anemometry techniques p 41 N85-27971

## PELLOUX, R. M.

Thermal-mechanical fatigue crack growth in Inconel X-750 [NASA-CR-174740] p 72 N85-15877

## PENKO, P. F.

Vacuum chamber pressure effects on thrust measurements of low Reynolds number nozzles [NASA-TM-86955] p 49 N85-21259

## PENN, B. G.

Preparation of silicon carbide-silicon nitride fibers by the pyrolysis of polycarbosilazane precursors [NASA-TM-86505] p 91 N85-28107

## PENNEY, C. M.

Advanced smoke meter development survey and analysis [NASA-CR-168287] p 124 N85-25792

## PENNLIN, J. A.

Constructive existence and uniqueness for two-point boundary-value problems with a linear gradient term p 172 A85-28015

## PERALTA-DURAN, A.

Creep-rupture reliability analysis p 143 A85-42566

## PEREZ, F.

Advanced nickel-hydrogen cell configuration study [NASA-CR-174775] p 157 N85-10444

## PERIC, M.

Assessment of discretization schemes to reduce numerical diffusion in the calculation of complex flows [AIAA PAPER 85-0441] p 108 A85-19751

## PERKINS, P. J., JR.

Icing flight research - Aerodynamic effects of ice and ice shape documentation with stereo photography [AIAA PAPER 85-0468] p 11 A85-30192

Icing flight research: Aerodynamic effects of ice and ice shape documentation with stereo photography [NASA-TM-86906] p 12 N85-18049

## PERREIRA, N. D.

Oscillatory conductive heat transfer for a fiber in an ideal gas p 109 A85-26077

## PETERMAN, W.

Creep-rupture behavior of iron superalloys in high-pressure hydrogen [NASA-CR-174411] p 74 N85-19078

## PHILIPP, W. H.

Alkaline battery containing a separator of a cross-linked copolymer of vinyl alcohol and unsaturated carboxylic acid [NASA-CASE-LEW-13102-1] p 104 N85-29144

## PIAN, T. H. H.

Rational approach for assumed stress finite elements p 139 A85-12029

Hybrid Semiloof elements for plates and shells based upon a modified Hu-Washizu principle p 139 A85-15893

Evolution of assumed stress hybrid finite element p 142 A85-35046

Plasticity, viscoplasticity, and creep of solids by mechanical subelement models p 142 A85-35048

Axisymmetric solid elements by a rational hybrid stress method p 143 A85-41109

Advanced stress analysis methods applicable to turbine engine structures [NASA-CR-175573] p 26 N85-21165

Recent advances in hybrid/mixed finite elements [NASA-CR-175574] p 145 N85-21687

On Hybrid and mixed finite element methods [NASA-CR-175551] p 146 N85-23096

## PICH, G. J.

Percutaneous connectors [NASA-CR-175627] p 168 N85-27508

## PICKETT, J. S.

Effects of chemical releases by the STS 3 orbiter on the ionosphere p 166 A85-29538

Suprathermal plasma observed on STS-3 Mission by plasma diagnostics package p 179 N85-22472

Electron and ion density depletions measured in the STS-3 orbiter wake p 39 N85-22474

## PIERCE, L. A.

Reliability of two sintered silicon nitride materials [NASA-TM-87092] p 92 N85-34284

## PIERCE, R. M.

Prism-coupled light emission from tunnel junctions p 181 A85-21425

## PIAWKA, W. C.

Advanced multi-megawatt wind turbine design for utility application p 157 A85-45517

## PIKE, C. P.

Spacecraft environmental interactions: A joint Air Force and NASA research and technology program p 40 N85-22517

## PIKE, J.

Multi-mesh gear dynamics program evaluation and enhancements [NASA-CR-174747] p 133 N85-28372

## PILLAY, S.

Powder metallurgy forged gear development [NASA-TM-87483] p 134 N85-29295

## PILSNER, B. H.

Cyclic oxidation behavior of beta+gamma overlay coatings on gamma and gamma+gamma-prime alloys p 68 A85-32431

Effects of MAR-M247 substrate (modified) composition on coating oxidation coating/substrate interdiffusion [NASA-CR-174851] p 73 N85-19073

## PINEL, S. I.

Effect of two inner-ring oil-flow distribution schemes on the operating characteristics of a 35 millimeter bore ball bearing to 2.5 million DN [NASA-TP-2404] p 130 N85-13233

## PINKOWSKI, S.

Feasibility of mapping velocity flow fields in SSME powerhead by laser anemometry techniques p 41 N85-27971

## PINTZ, A.

Conceptual design of a fixed-pitch wind turbine generator system rated at 400 kilowatts [NASA-CR-174877] p 162 N85-29363

## PISZCZOR, M. F., JR.

Preliminary design of a 10 kW thermophotovoltaic system for space applications p 45 A85-45371

## PITZ, R. W.

Advanced smoke meter development survey and analysis [NASA-CR-168287] p 124 N85-25792

## PLENCNER, R. M.

Advanced secondary power system for transport aircraft [NASA-TP-2463] p 30 N85-28944

## POESCHEL, R. L.

IAPS (8-cm) ion thruster cyclic endurance test p 42 A85-16406

Ion propulsion for communications satellites p 42 A85-16412

Ring-cusp ion thrusters p 42 A85-16438

Ion thruster system (8-cm) cyclic endurance test [NASA-CR-174745] p 47 N85-12937

## POLEY, W.

Demand for satellite-provided domestic communications services up to the year 2000 [NASA-TM-86894] p 97 N85-15099

## PONCHAK, G. E.

Effect of Interfacial characteristics of metal clad polymeric substrates on electrical high frequency interconnection performance p 99 N85-20223

An experimental investigation of microstrip properties on soft substrates from 2 to 40 GHz [NASA-TM-86961] p 99 N85-20224

## PORADA, T. W.

Linearization of digital derived rate algorithm for use in linear stability analysis [NASA-TM-87000] p 41 N85-23904

## POROWSKI, J. S.

Simplified design and life prediction of rocket thrust chambers p 44 A85-29314

## POTAPCZUK, M. G.

Progress in development of a Navier-Stokes solver for evaluation of iced airfoil performance [AIAA PAPER 85-0410] p 3 A85-19731

## POUGARE, M.

Computation of viscous flows in turbomachinery cascades p 106 A85-11631

Computation and turbulence closure models for shear flows in rotating curved bodies p 107 A85-14349

A space-marching method for incompressible Navier-Stokes equations [AIAA PAPER 85-0170] p 108 A85-19564

## POUCH, J. J.

Plasma deposited hydrogenated carbon on GaAs and InP p 182 A85-40386

Plasma deposited diamondlike carbon on GaAs and InP [NASA-TM-86870] p 183 N85-10844

Optical properties of hydrogenated amorphous carbon films grown from methane plasma [NASA-TM-86995] p 183 N85-26406

## POVINELLI, L. A.

Comparison of secondary flows predicted by a viscous code and an inviscid code with experimental data for a turning duct p 106 A85-11634

Analytical and physical modeling program for the NASA Lewis Research Center's Altitude Wind Tunnel (AWT) [AIAA PAPER 85-0379] p 34 A85-19709

Analytical modeling of circuit aerodynamics in the new NASA Lewis Altitude Wind Tunnel [AIAA PAPER 85-0380] p 3 A85-26389

Assessment of three-dimensional inviscid codes and loss calculations for turbine aerodynamic computations [ASME PAPER 84-GT-187] p 4 A85-32961

- Application of viscous and inviscid computation methods for rocket turbopump systems  
[SAE PAPER 841522] p 110 A85-39257
- Analytical modeling of circuit aerodynamics in the new NASA Lewis wind tunnel  
[NASA-TM-86912] p 8 N85-15688
- Analytical and physical modeling program for the NASA Lewis Research Center's Altitude Wind Tunnel (AWT)  
[NASA-TM-86919] p 35 N85-15757
- Overview of aerothermodynamic loads definition study  
p 51 N85-27942

**POWELL, A. G.**

- Low-speed aerodynamic test of an axisymmetric supersonic inlet with variable cowl slot  
[AIAA PAPER 85-1210] p 5 A85-40819
- Low-speed aerodynamic test of an axisymmetric supersonic inlet with variable cowl slot  
[NASA-TM-87039] p 28 N85-26710

**POWER, J. L.**

- Ground correlation investigation of thruster/spacecraft interactions to be measured on the IAPS flight test  
p 42 A85-16408

**POWERS, W. O.**

- Rapid solidification and dynamic compaction of Ni-base superalloy powders  
p 67 A85-32414

**PRAHL, J. M.**

- Mechanics of a gaseous film barrier to lubricant wetting of elastohydrodynamically lubricated conjunctions  
[NASA-TP-2500] p 135 N85-32330

**PRATT, B. S.**

- An interactive computer code for calculation of gas-phase chemical equilibrium (EQLBRM)  
[NASA-CR-168337] p 18 N85-10948

**PRATT, D. T.**

- Recent advances in methods for numerical solution of O.D.E. initial value problems  
p 171 A85-21370
- CREKID: A computer code for transient, gas-phase combustion of kinetics  
[NASA-TM-83806] p 17 N85-10068
- An interactive computer code for calculation of gas-phase chemical equilibrium (EQLBRM)  
[NASA-CR-168337] p 18 N85-10948

**PROCTOR, M. P.**

- Flame flashback in a premixed dump combustor  
[AIAA PAPER 85-0145] p 60 A85-19550
- Transient technique for measuring heat transfer coefficients on stator airfoils in a jet engine environment  
[AIAA PAPER 85-1471] p 122 A85-39796
- Transient technique for measuring heat transfer coefficients on stator airfoils in a jet engine environment  
[NASA-TM-87005] p 124 N85-25794

**PROK, G. M.**

- Lubricity of well-characterized jet and broad-cut fuels by ball-on-cylinder machine  
[NASA-TM-83807] p 92 N85-12183

**PUDICK, S.**

- Develop and test fuel cell powered on-site integrated total energy systems. Phase 3: Full-scale power plant development  
[NASA-CR-174887] p 161 N85-25941
- Develop and test fuel cell powered on-site integrated total energy systems. Phase 3: Full-scale power plant development  
[NASA-CR-168338] p 164 N85-30483

**PUNCH, E. F.**

- Development and testing of stable, invariant, isoparametric curvilinear 2- and 3-D hybrid-stress elements  
p 140 A85-19899

**PURVIS, C. K.**

- The PIX-2 experiment: An overview  
p 179 N85-22494
- Design guidelines for assessing and controlling spacecraft charging effects  
p 40 N85-22500
- Spacecraft environmental interactions: A joint Air Force and NASA research and technology program  
p 40 N85-22517

**PUTHOFF, R. L.**

- Aileron controls for wind turbine applications  
p 157 A85-45513

**PUTOFF, R. L.**

- Aileron controls for wind turbine applications  
[NASA-TM-86867] p 158 N85-11458

**Q****QUENTMEYER, R. J.**

- Fabrication of ceramic substrate-reinforced and free forms  
[NASA-TM-86994] p 50 N85-23926
- Rocket thrust chamber thermal barrier coatings  
p 90 N85-26867

**QUICK, B.**

- Fiber optic, Fabry-Perot high temperature sensor  
[NASA-CR-174712] p 178 N85-13594

**QUIJJE, M. A.**

- The 30 GHz solid state amplifier for low cost low data rate ground terminals  
[NASA-CR-174795] p 102 N85-12300

**R****RADHAKRISHNAN, K.**

- Integrating chemical kinetic rate equations by selective use of stiff and nonstiff methods  
[AIAA PAPER 85-0237] p 60 A85-19607
- High temperature oxidation of propene  
p 61 A85-33570

- Comparison of numerical techniques for integration of stiff ordinary differential equations arising in combustion chemistry  
[NASA-TP-2372] p 17 N85-10065

**CREKID: A computer code for transient, gas-phase combustion of kinetics**

- [NASA-TM-83806] p 17 N85-10068
- New integration techniques for chemical kinetic rate equations. 2: Accuracy comparison  
[NASA-TM-86893] p 23 N85-13798

- Integrating chemical kinetic rate equations by selective use of stiff and nonstiff methods  
[NASA-TM-86923] p 24 N85-15726

- A comparison of the efficiency of numerical methods for integrating chemical kinetic rate equations  
[NASA-TM-83590] p 25 N85-21162

**RAITT, W. S.**

- Electron and ion density depletions measured in the STS-3 orbiter wake  
p 39 N85-22474

**RAMACHANDRA, M. K.**

- Shock tube study of the fuel structure effects on the chemical kinetic mechanisms responsible for soot formation, part 2  
[NASA-CR-174880] p 63 N85-25444

**RAMACHANDRA, S. M.**

- Acoustic pressures emanating from a turbomachine stage  
[AIAA PAPER 84-2325] p 2 A85-10870
- Incompressible lifting-surface aerodynamics for a rotor-stator combination  
[NASA-TM-83767] p 7 N85-12039

**RAMAMURTI, R.**

- Two-dimensional internal compressible viscous flows using semi-elliptic analysis  
p 106 A85-11640

**RAMAMURTI, V.**

- Natural frequencies of twisted rotating plates  
p 141 A85-32343

**RAMLER, J. R.**

- Telecommunications forecast for ITU Region 2 to the year 1995  
[NASA-TM-87077] p 38 N85-34150

**RAMSAY, S. M.**

- Three-dimensional inviscid flow analysis of turbofan forced mixers  
[AIAA PAPER 85-0086] p 2 A85-19510

**RAMSEY, W. D.**

- Inert gas test of two 12-cm magnetostatic thrusters  
p 43 A85-29310

**RANAUDO, R. J.**

- Icing flight research - Aerodynamic effects of ice and ice shape documentation with stereo photography  
[AIAA PAPER 85-0468] p 11 A85-30192
- Icing flight research: Aerodynamic effects of ice and ice shape documentation with stereo photography  
[NASA-TM-86906] p 12 N85-18049

**RANDALL, S. A.**

- Electric utility acid fuel cell stack technology advancement  
[NASA-CR-174804] p 159 N85-17422

**RAO, B. C. S.**

- Deformation and erosion of f.c.c. metals and alloys under cavitation attack  
p 65 A85-12789
- Characterization of erosion of metallic materials under cavitation attack in a mineral oil  
[NASA-TM-86934] p 74 N85-19075

**RAO, K.**

- Vibration and flutter of mistuned bladed-disk assemblies  
[AIAA PAPER 84-0991] p 139 A85-16095

**RAO, P. V.**

- Cavitation erosion size scale effects  
p 65 A85-11935
- Effect of surface configuration during solid particle impingement erosion  
p 69 A85-42568
- Characterization of solid particle erosion resistance of ductile metals based on their properties  
p 69 A85-42569

**RATAJCZAK, A. F.**

- Control algorithms and computer simulation of a stand-alone photovoltaic village power system  
p 153 A85-11345

- Status of DOE and AID stand-alone photovoltaic system field tests  
p 155 A85-35707

**RAUCH, H.**

- Transformation toughened ceramics for the heavy duty diesel engine technology program  
[NASA-CR-174689] p 185 N85-16698

**RAUCH, J.**

- Free-piston Stirling engine/linear alternator 1000-hour endurance test  
[NASA-CR-174771] p 163 N85-30481

**RAVEH, A.**

- Deposition of silicon nitride from SiCl<sub>4</sub> and NH<sub>3</sub> in a low pressure RF plasma  
p 81 A85-36229

**RAWLIN, V. K.**

- Ring-cusp ion thruster with shell anode  
[NASA-CASE-LEW-13881-1] p 48 N85-21256

**RAY, P. K.**

- Arc-driven rail gun research  
[NASA-CR-174816] p 132 N85-21662

**RAZAVI, H.**

- Nonlinear global stability analysis of compressor stall phenomena  
[NASA-CR-174908] p 31 N85-29960

**REAGAN, J. R.**

- Government review of the Mod-2 wind turbine (as-built)  
[NASA-TM-86983] p 162 N85-29365

**REDD, L.**

- Main propulsion system design recommendations for an advanced Orbit Transfer Vehicle  
[AIAA PAPER 85-1336] p 36 A85-39730

**REDDOCH, T. W.**

- Experimental investigation of a variable speed constant frequency electric generating system from a utility perspective  
[NASA-CR-174950] p 105 N85-32251

**REDDY, J. N.**

- Geometrically nonlinear analysis of laminated elastic structures  
[NASA-CR-175609] p 146 N85-21720

**REED, K. W.**

- Hybrid stress finite elements for large deformations of inelastic solids  
p 139 A85-15894
- Constitutive modeling and computational implementation for finite strain plasticity  
p 143 A85-40910

**REED, R. W.**

- The scattering of ultrasonic third sound from substrate surface defects  
p 174 A85-36047

**REID, L.**

- Analytical and physical modeling program for the NASA Lewis Research Center's Altitude Wind Tunnel (AWT)  
[AIAA PAPER 85-0379] p 34 A85-19709
- Analytical and physical modeling program for the NASA Lewis Research Center's Altitude Wind Tunnel (AWT)  
[NASA-TM-86919] p 35 N85-15757

**REID, M. A.**

- Chemical and electrochemical behavior of the Cr(III)/Cr(II) half-cell in the iron-chromium redox energy storage system  
p 61 A85-33785

**REILLY, C. H.**

- Engineering calculations for communications satellite systems planning  
[NASA-CR-175552] p 37 N85-21233

**REINMANN, J. J.**

- Analytical and physical modeling program for the NASA Lewis Research Center's Altitude Wind Tunnel (AWT)  
[AIAA PAPER 85-0379] p 34 A85-19709

- Analytical and physical modeling program for the NASA Lewis Research Center's Altitude Wind Tunnel (AWT)  
[NASA-TM-86919] p 35 N85-15757

**RENGSTORFF, G. W. P.**

- Surface effects of corrosive media on hardness, friction, and wear of materials  
[NASA-TM-83711] p 85 N85-15896

**RENZ, D. D.**

- High voltage-high power components for large space power distribution systems  
p 45 A85-45370
- Developments in space power components for power management and distribution  
p 47 N85-13877

**RHODES, D. L.**

- Predictions and measurements of isothermal flowfields in axisymmetric combustor geometries  
[NASA-CR-174916] p 29 N85-27867

**RIBARSKY, M. W.**

- Study of the effects of implantation on the high Fe-Ni-Cr and Ni-Cr-Al alloys  
[NASA-CR-175625] p 76 N85-22661

**RICE, E. E.**

- Preliminary analysis of space mission applications for electromagnetic launchers  
[NASA-CR-174067] p 35 N85-12071

**RICE, E. J.**

- Measured acoustic properties of variable and low density bulk absorbers  
[NASA-TM-87065] p 177 N85-30770

- RICHARDS, W. B.**  
The infinite line pressure probe p 122 A85-37704
- RICHIE, A. E.**  
Automotive Stirling engine systems development p 130 A85-45474
- RICHTER, G. P.**  
Comparison of icing cloud instruments for 1982-1983 icing season flight program [AIAA PAPER 84-0020] p 13 A85-16098  
The UH-1H helicopter icing flight test program - An overview [AIAA PAPER 85-0338] p 11 A85-28898  
The UH-1H helicopter icing flight test program: An overview [NASA-TM-86925] p 11 N85-15702
- RIDDLEBAUGH, S. M.**  
Advanced liner-cooling techniques for gas turbine combustors [AIAA PAPER 85-1290] p 15 A85-39703  
Small gas turbine combustor study - Fuel injector performance in a transpiration-cooled liner [AIAA PAPER 85-1312] p 16 A85-39717  
Advanced liner-cooling techniques for gas turbine combustors [NASA-TM-86952] p 8 N85-21115  
Small gas turbine combustor study: Fuel injector performance in a transpiration-cooled liner [NASA-TM-86989] p 27 N85-25264
- RIEKER, L. L.**  
Design considerations for a 10-kW integrated hydrogen-oxygen regenerative fuel cell system p 155 A85-45380
- RIFF, R.**  
Thermodynamically consistent constitutive equations for nonisothermal large strain, elasto-plastic, creep behavior [AIAA PAPER 85-0621] p 142 A85-38425  
Analysis of shell type structures subjected to time dependent mechanical and thermal loading [NASA-CR-175747] p 147 N85-25896  
Dynamic creep buckling: Analysis of shell structures subjected to time-dependent mechanical and thermal loading p 149 N85-27959
- RILEY, J. J.**  
Direct numerical simulations of a reacting mixing layer with chemical heat release [AIAA PAPER 85-0143] p 60 A85-19548  
Direct simulations of chemically reacting turbulent mixing layers [AIAA PAPER 85-0321] p 60 A85-19666
- RIPLING, E. J.**  
Fracture of composite-adhesive-composite systems p 141 A85-27935
- RIZK, M.**  
A two-equation turbulence model for two-phase jets p 107 A85-14376
- RO, D. H.**  
Powder metallurgy forged gear development [NASA-TM-87483] p 134 N85-29295
- ROBACK, R.**  
Turbulent transport and length scale measurement experiments with confined coaxial jets [NASA-CR-174831] p 117 N85-30245
- ROBERTS, A. F.**  
Operational performance of the photovoltaic-powered grain mill and water pump at Tangaye, Burkina Faso (formerly Upper Volta) [NASA-TM-86970] p 161 N85-23243
- ROBERTS, T.**  
The 20 GHz proof-of-concept test model results for a multiple scan beam dual reflector antenna [NASA-CR-174268] p 98 N85-15944
- ROBERTSON, C.**  
Applicability of 100kWe-class of space reactor power systems to NASA manned space station missions [NASA-CR-174696] p 177 N85-35728
- ROBINSON, D. N.**  
Viscoplastic constitutive relationships with dependence on the thermomechanical history [NASA-CR-174836] p 146 N85-21691  
On thermomechanical testing in support of constitutive equation development for high temperature alloys [NASA-CR-174879] p 147 N85-25894  
Some advances in experimentation supporting development of viscoplastic constitutive models [NASA-CR-174855] p 147 N85-27260  
Thermomechanical deformation in the presence of metallurgical changes p 150 N85-31533  
Some advances in experimentation supporting development of viscoplastic constitutive models p 151 N85-31545  
A continuous damage model based on stepwise-stress creep rupture tests [NASA-CR-174941] p 152 N85-32341

- ROBINSON, R. A.**  
Experimental and analytical study of ceramic-coated turbine-tip shroud seals for small turbine engines [NASA-TM-86881] p 25 N85-18057
- ROBINSON, R. S.**  
Ion flow experiments in a multipole discharge chamber p 178 A85-12705
- ROCHE, J. C.**  
Computer simulation of plasma electron collection by PIX-II [AIAA PAPER 85-0386] p 43 A85-19715  
NASCAP simulation of PIX 2 experiments p 180 N85-22497
- RODE, H.**  
Fabrication of p(+) - n junction GaAs solar cells by a novel method p 181 A85-33645
- ROHDE, J. E.**  
Turbine heat transfer p 19 N85-10964  
Coolant passage heat transfer with rotation p 20 N85-10968
- ROHLIK, H. E.**  
Computational thermo-fluid dynamics contributions to advanced gas turbine engine design [AIAA PAPER 85-0083] p 14 A85-19509  
Computational thermo-fluid dynamics contributions to advanced gas turbine engine design [NASA-TM-86865] p 18 N85-10069
- ROHN, D. A.**  
Application of traction drives as servo mechanisms p 152 N85-33520
- ROLEK, R. J.**  
The influence of temperature on the lubricating effectiveness of MoS<sub>2</sub> dispersed in mineral oils [ASLE PREPRINT 84-LC-2A-2] p 80 A85-25963
- ROMAN, R. F.**  
Textured carbon surfaces on copper [NASA-CASE-LEW-14130-1] p 95 N85-20156  
Ring-cusp ion thruster with shell anode [NASA-CASE-LEW-13881-1] p 48 N85-21256
- ROMANOFSKY, R. R.**  
Effect of interfacial characteristics of metal clad polymeric substrates on electrical high frequency interconnection performance [NASA-TM-86948] p 99 N85-20223  
An experimental investigation of microstrip properties on soft substrates from 2 to 40 GHz [NASA-TM-86961] p 99 N85-20224
- RON, Y.**  
Deposition of silicon nitride from SiCl<sub>4</sub> and NH<sub>3</sub> in a low pressure RF plasma p 81 A85-36229
- RONNEY, P. D.**  
Effect of gravity on halogenated hydrocarbon flame retardant effectiveness [IAF PAPER 84-156] p 61 A85-23199
- ROOT, J.**  
Recent work on a microwave ion source p 179 A85-16455  
Experimental performance of a microwave cavity plasma disk ion source p 179 A85-43552
- ROSE, J. J.**  
Universal binding energy relations in metallic adhesion [NASA-TM-86889] p 72 N85-12132
- ROSE, M. E.**  
A numerical study of the steady scalar convective diffusion equation for small viscosity p 107 A85-16533
- ROSECRANS, P. M.**  
Manufacturing process to reduce large grain growth in zirconium alloys [DE85-011649] p 78 N85-34267
- ROSENBLUM, L.**  
Practical aspects of photovoltaic technology, applications and cost (revised) [NASA-CR-174963] p 165 N85-35472
- ROSENBLIEB, J. W.**  
Planetary-gear-support bearing test rig design [NASA-CR-174927] p 12 N85-35185
- ROSNER, D. E.**  
Polarization (ellipsometric) measurements of liquid condensate deposition and evaporation rates and dew points in flowing salt/ash-containing combustion gases p 123 A85-46925  
Computer program for the calculation of multicomponent convective diffusion deposition rates from chemically frozen boundary layer theory [NASA-CR-168329] p 116 N85-27164
- ROSS, P. N.**  
CO adsorption on (111) and (100) surfaces of the Pt sub 3 Ti alloy. Evidence for parallel binding and strong activation of CO [NASA-CR-176077] p 77 N85-32176
- ROTH, D. J.**  
Radiographic detectability limits for seeded voids in sintered silicon carbide and silicon nitride [NASA-TM-86945] p 138 N85-21674

- Reliability of void detection in structural ceramics using scanning laser acoustic microscopy [NASA-TM-87035] p 138 N85-32337
- ROTHOLZ, E.**  
A frequency-routed satellite system concept using multiple orthogonally-polarized beams for frequency reuse p 97 A85-34470
- ROUSSOS, L. A.**  
Noise transmission loss of a rectangular plate in an infinite baffle [NASA-TP-2398] p 176 N85-22109
- ROYCE, B. S. H.**  
The role of surface generated radicals in catalytic combustion p 30 N85-27869
- RUBIN, A. J.**  
Three-dimensional calculation of shuttle charging in polar orbit p 40 N85-22486  
Polar orbit electrostatic charging of objects in shuttle wake p 40 N85-22487
- RUDLAND, R. S.**  
Technology requirements to be addressed by the NASA Lewis Research Center Cryogenic Fluid Management Facility program [AIAA PAPER 85-1229] p 94 A85-47024  
Technology requirements to be addressed by the NASA Lewis Research Center Cryogenic Fluid Management Facility program [NASA-TM-87048] p 38 N85-29987
- RUM, G.**  
Report of the Constellations Panel p 131 N85-20368
- RUSCH, W. V. T.**  
Focal shifts in parabolic reflectors p 97 A85-39356
- RUSSELL, L. M.**  
Local heat-transfer measurements on a large, scale-model turbine blade airfoil using a composite of a heater element and liquid crystals [NASA-TM-86900] p 119 N85-33435
- RUTLEDGE, J. E.**  
Prism-coupled light emission from tunnel junctions p 181 A85-21425
- RUTLEDGE, S. K.**  
Ion beam sputter-deposited thin film coatings for protection of spacecraft polymers in low Earth orbit [NASA-TM-87051] p 91 N85-30137
- RYDER, J. T.**  
Effect of low temperature on fatigue and fracture properties of Ti-5Al-2.5Sn(ELI) for use in engine components p 70 A85-47972

**S**

- SADLER, G. G.**  
DEAN: A program for dynamic engine analysis [NASA-TM-87033] p 30 N85-28945
- SAFFMAN, P. G.**  
The linear two-dimensional stability of inviscid vortex streets of finite-cored vortices [AD-A153032] p 107 A85-14241
- SAGERSE, D. A.**  
Large-scale advanced propfan (LAP) program progress report [AIAA PAPER 85-1187] p 17 A85-47021  
Large-scale Advanced Propfan (LAP) program [NASA-TM-87067] p 32 N85-29964
- SAIN, M. K.**  
Alternatives for jet engine control [NASA-CR-175831] p 29 N85-26713  
Alternatives for jet engine control [NASA-CR-175832] p 29 N85-26714  
Alternatives for jet engine control [NASA-CR-175833] p 29 N85-26715
- SALERNO, J.**  
Automatic sphericity interferometer for testing lens radii [AD-A155736] p 125 N85-33457
- SALIK, J.**  
Ion-beam nitriding of steels p 66 A85-24667  
Computer simulation of thin film nucleation and growth p 181 A85-35308  
Monte Carlo study of reversible growth of clusters on a surface p 182 A85-48516  
A computer simulation of thin film nucleation and growth: The Volmer-Weber case [NASA-TM-86968] p 53 N85-21264  
Ion-beam nitriding of steels [NASA-CASE-LEW-14104-1] p 75 N85-21324
- SALIKUDDIN, M.**  
An experimental study of tone excited heated jets [AIAA PAPER 84-2341] p 172 A85-10882
- SALTSMAN, J. F.**  
Strainrange partitioning - A total strain range version p 64 A85-11603



- Application of two creep fatigue life models for the prediction of elevated temperature crack initiation of a nickel base alloy  
[AIAA PAPER 85-1420] p 69 A85-43979
- SALZMAN, J. A.**  
Demand for satellite-provided domestic communications services up to the year 2000  
[NASA-TM-86894] p 97 N85-15099  
Telecommunications forecast for ITU Region 2 to the year 1995  
[NASA-TM-87077] p 38 N85-34150
- SAMANTA, S.**  
Transformation toughened ceramics for the heavy duty diesel engine technology program  
[NASA-CR-174689] p 185 N85-16698
- SAMPLE, A. K.**  
The mechanisms of formation and prevention of channel segregation during alloy solidification  
p 180 A85-18082
- SANCHEZ, J. M.**  
Modeling of gamma/gamma-prime phase equilibrium in the nickel-aluminum system p 65 A85-14959
- SANDELLI, G. J.**  
Electric utility acid fuel cell stack technology advancement  
[NASA-CR-174804] p 159 N85-17422
- SANDERS, W. A.**  
Strength and microstructure of sintered Si<sub>3</sub>N<sub>4</sub> with rare-earth-oxide additions  
[ACS PAPER 130-13-84] p 80 A85-25271  
Oxidation of silicon nitride sintered with rare-earth oxide additions p 83 A85-42798  
Microstructure of reaction-bonded silicon nitride consolidated by isostatic hot-pressing p 83 A85-45304  
Reliability of two sintered silicon nitride materials  
[NASA-TM-87092] p 92 N85-34284
- SANGER, N. L.**  
Design and performance of a fixed, nonaccelerating guide vane cascade that operates over an inlet flow angle range of 60 deg  
[ASME PAPER 84-GT-75] p 4 A85-32964
- SANTARPIA, D. E.**  
Status of NASA's multibeam communications technology program p 100 A85-14432
- SANTAVICCA, D. A.**  
The role of surface generated radicals in catalytic combustion p 30 N85-27869
- SANTNER, J. S.**  
Fracture of composite-adhesive-composite systems p 141 A85-27935
- SANTORO, G. J.**  
Replaceable blade turbine and stationary specimen corrosion testing facility  
[NASA-TM-86931] p 73 N85-18126
- SANZ, J. M.**  
Design and performance of a fixed, nonaccelerating guide vane cascade that operates over an inlet flow angle range of 60 deg  
[ASME PAPER 84-GT-75] p 4 A85-32964
- SAUNDERS, A. L.**  
The NASA satellite communication 20 x 20 matrix switches p 101 A85-14435
- SAUNDERS, N. T.**  
Future directions in aeropropulsion technology  
[NASA-TM-87010] p 1 N85-23685
- SAVAGE, M.**  
Life and reliability modeling of bevel gear reductions  
[NASA-TM-87006] p 133 N85-27227  
Fatigue life analysis of a turboprop reduction gearbox  
[NASA-TM-87014] p 133 N85-27228
- SAVINO, J. M.**  
Reflection plane tests of a wind turbine blade tip section with ailerons  
[NASA-TM-87018] p 165 N85-34444
- SCAGLIONE, L. J.**  
Teardown analysis of a ten cell bipolar nickel-hydrogen battery p 156 A85-45385
- SCARPELLI, A. R.**  
Precision tunable resonant microwave cavity  
[NASA-CASE-LEW-13935-1] p 103 N85-20248
- SCHATZ, M.**  
Performance capabilities of the 12-centimeter Xenon ion thruster p 42 A85-16439
- SCHATZ, M. F.**  
Heaterless ignition of inert gas ion thruster hollow cathodes  
[NASA-TM-87086] p 52 N85-34177
- SCHATZMAN, J. C.**  
The linear two-dimensional stability of inviscid vortex streets of finite-cored vortices  
[AD-A153032] p 107 A85-14241
- SCHECHTER, B.**  
An investigation of enhanced capability thermal barrier coating systems for diesel engine components  
[NASA-CR-174820] p 86 N85-18154
- SCHERER, D. D.**  
Small centrifugal pumps for low thrust rockets  
[AIAA PAPER 85-1302] p 45 A85-43978
- SCHUEERMANN, C. M.**  
Stirling material technology  
[NASA-TM-86888] p 72 N85-13007
- SCHILLING, H. W.**  
Circular waveguide bifurcation for asymmetric modes p 101 A85-20170  
Dual-mode coaxial feed with low crosspolarisation p 101 A85-20171
- SCHLUETER, R. A.**  
Improved models for increasing wind penetration, economics and operating reliability  
[NASA-CR-175538] p 160 N85-20545
- SCHOCK, H. J.**  
Incident beam polarization for laser Doppler velocimetry employing a sapphire cylindrical window p 122 A85-39835  
Internal combustion engine combustion chamber process studies at NASA Lewis Research Center p 112 A85-45856  
Holographic optical system for aberration corrections in laser Doppler velocimetry p 123 A85-48659  
Incident beam polarization for laser Doppler velocimetry employing a sapphire cylindrical window  
[NASA-TM-87064] p 178 N85-28786
- SCHOENMAN, L.**  
Progress report - Advanced cryogenic OTV engine technology  
[AIAA PAPER 85-1341] p 44 A85-39735
- SCHREIBER, J. G.**  
Initial results of sensitivity tests - Performed on the RE-1000 free-piston Stirling engine p 129 A85-45466
- SCHRUBEN, D. L.**  
Measurement and correlation of jet fuel viscosities at low temperatures  
[NASA-CR-174911] p 94 N85-34295
- SCHUBERT, F. H.**  
Engineering model system study for a regenerative fuel cell: Study report  
[NASA-CR-174801] p 158 N85-16292
- SCHULLER, F. T.**  
Effect of two inner-ring oil-flow distribution schemes on the operating characteristics of a 35 millimeter bore ball bearing to 2.5 million DN  
[NASA-TP-2404] p 130 N85-13233  
Lubrication and performance of high-speed rolling-element bearings  
[NASA-TM-86958] p 131 N85-21658
- SCHULSON, E. M.**  
An experimental investigation of rubbing interaction in labyrinth seals at cryogenic temperature p 129 A85-39938  
Analytical and experimental investigation of rubbing interaction in labyrinth seals for a liquid hydrogen fuel pump  
[NASA-CR-174657] p 48 N85-18084
- SCHULTZ, B. E.**  
Closed-loop strain controlled testing at elevated temperatures with a non-contacting gage p 121 A85-29562
- SCHULTZ, D.**  
HOST liner cyclic facilities: Facility description p 22 N85-10988
- SCHUM, E. F.**  
Application of computational fluid dynamics to complex inlet ducts  
[AIAA PAPER 85-1213] p 6 A85-47023  
Application of computational fluid dynamics to complex inlet ducts  
[NASA-TM-87060] p 118 N85-30247
- SCHUMANN, L. F.**  
A three-dimensional axisymmetric calculation procedure for turbulent flows in a radial vaneless diffuser  
[NASA-TM-86903] p 7 N85-14798
- SCHUON, S. R.**  
Effects of chromium and aluminum on mechanical and oxidation properties of iron-nickel-base superalloys based on CG-27  
[NASA-TP-2443] p 75 N85-21323
- SCHWAB, J. R.**  
Comparison of secondary flows predicted by a viscous code and an inviscid code with experimental data for a turning duct p 106 A85-11634  
Application of viscous and inviscid computation methods for rocket turbopump systems  
[SAE PAPER 841522] p 110 A85-39257  
Redistribution of the inlet temperature profile through the SSME fuel turbine p 50 N85-26901
- SCHWARZE, G. E.**  
Development of high frequency low weight power magnetics for aerospace power systems p 102 A85-45373
- Performance analysis of radiation cooled dc transmission lines for high power space systems  
[NASA-TM-87040] p 104 N85-28222
- SCIBBE, H. W.**  
Effect of lubricant extreme-pressure additives on surface fatigue life of AISI 9310 spur gears  
[NASA-TP-2408] p 130 N85-13234  
Operating characteristics of a 0.87 kW-hr flywheel energy storage module p 133 N85-28371  
Lubricant and additive effects on spur gear fatigue life  
[NASA-TM-87044] p 133 N85-28373
- SCOLA, D. A.**  
Imide modified epoxy matrix resins  
[NASA-CR-174695] p 85 N85-15892
- SCOT, G. W.**  
Measured effects of wind turbine generation at the Block Island Power Company p 153 A85-10652
- SCOTT, W. G.**  
The 20 GHz proof-of-concept test model results for a multiple scan beam dual reflector antenna  
[NASA-CR-174268] p 98 N85-15944
- SCUDDER, L. R.**  
Status of DOE and AID stand-alone photovoltaic system field tests p 155 A85-35707
- SEASHOLTZ, R. G.**  
Filter induced errors in laser anemometer measurements using counter processors  
[NASA-TM-87047] p 125 N85-30288
- SEINER, J. M.**  
A multiple-scales model of the shock-cell structure of imperfectly expanded supersonic jets p 113 A85-49354
- SEKAR, R.**  
Advanced automotive diesel assessment program  
[NASA-CR-168285] p 130 N85-13235
- SEMANKIC, S.**  
Advanced thin film thermocouples  
[NASA-CR-175541] p 124 N85-21607
- SENER, B.**  
A finite element solution of three-dimensional inviscid rotational flows through curved ducts p 107 A85-11648
- SENG, G. T.**  
Rapid estimation of concentration of aromatic classes in middistillate fuels by high-performance liquid chromatography  
[NASA-TP-2495] p 93 N85-31307
- SERAFINI, T. T.**  
PMR polyimide composites for aerospace applications p 55 A85-21520
- SESHADRI, K.**  
Polarization (ellipsometric) measurements of liquid condensate deposition and evaporation rates and dew points in flowing salt/ash-containing combustion gases p 123 A85-46925
- SHAFFER, S. J.**  
High pressure compressor component performance report  
[NASA-CR-168245] p 33 N85-34138
- SHAFFER, S. L.**  
Energy efficient engine. High pressure compressor detail design report  
[NASA-CR-165558] p 23 N85-10998
- SHAFFERNOCKER, W. M.**  
Advanced smoke meter development survey and analysis  
[NASA-CR-168287] p 124 N85-25792
- SHALKHAUSER, K. A.**  
Automated testing of developmental satellite communications systems and subsystems  
[NASA-TM-87070] p 100 N85-31348
- SHALTENS, R. K.**  
Measured effects of wind turbine generation at the Block Island Power Company p 153 A85-10652  
Operational results for the experimental DOE/NASA Mod-OA wind turbine project  
[NASA-TM-83517] p 163 N85-30479
- SHANEYFELT, J. T.**  
Satellite baseband processor test performance summary p 95 A85-14434
- SHAPIRO, W.**  
Development of gas-lubricated pistons for heavy duty diesel engine technology program  
[NASA-CR-174746] p 184 N85-12808
- SHARMA, L. K.**  
Feasibility of mapping velocity flow fields in SSME powerhead by laser anemometry techniques p 41 N85-27971
- SHARP, G. R.**  
Extreme precision antenna reflector study results p 165 N85-23830
- SHAW, L. M.**  
Unsteady pressure measurements on a biconvex airfoil in a transonic oscillating cascade  
[NASA-TM-86914] p 8 N85-15689

## SHAW, R. J.

- Progress toward the development of an aircraft icing analysis capability  
[AIAA PAPER 84-0105] p 10 A85-10653
- Analytical determination of propeller performance degradation due to ice accretion  
[AIAA PAPER 85-0339] p 14 A85-20867
- The NASA altitude wind tunnel - Its role in advanced icing research and development  
[AIAA PAPER 85-0090] p 35 A85-26381
- The UH-1H helicopter icing flight test program - An overview  
[AIAA PAPER 85-0338] p 11 A85-26898
- Performance degradation of helicopter rotor in forward flight due to ice  
p 11 A85-42937
- The UH-1H helicopter icing flight test program: An overview  
[NASA-TM-86925] p 11 N85-15702
- The NASA Altitude Wind Tunnel (AWT): Its role in advanced icing research and development  
[NASA-TM-86920] p 35 N85-15758
- Performance and surge limits of a TF30-P-3 turbofan engine/axisymmetric mixed-compression inlet propulsion system at Mach 2.5  
[NASA-TP-2461] p 27 N85-25261
- Ice shapes and the resulting drag increase for a NACA 0012 airfoil  
[NASA-TM-83556] p 11 N85-27839
- SHAWHAN, S. D.**
- Effects of chemical releases by the STS 3 orbiter on the ionosphere  
p 166 A85-29538
- Suprathermal plasma observed on STS-3 Mission by plasma diagnostics package  
p 179 N85-22472
- Electron and ion density depletions measured in the STS-3 orbiter wake  
p 39 N85-22474
- SHEIBLEY, D. W.**
- Alkaline battery containing a separator of a cross-linked copolymer of vinyl alcohol and unsaturated carboxylic acid  
[NASA-CASE-LEW-13102-1] p 104 N85-29144
- Regenerative fuel cell systems for space station  
p 104 N85-31372
- SHEN, H. D.**
- Fundamentals of microcrack nucleation mechanics  
[NASA-CR-3851] p 137 N85-16195
- SHENKMAN, A.**
- Large-scale Advanced Propfan (LAP) performance, acoustic and weight estimation, January, 1984  
[NASA-CR-174782] p 9 N85-22368
- SHEU, Y. C.**
- Ultrasonic wave propagation in two-phase media - Spherical inclusions  
p 54 A85-11926
- Fundamentals of microcrack nucleation mechanics  
[NASA-CR-3851] p 137 N85-16195
- SHUEN, J. S.**
- The structure of dilute combustng sprays  
[NASA-CR-174838] p 24 N85-15728
- SHUEN, J.-S.**
- Drop-turbulence interactions in a diffusion flame  
[AIAA PAPER 85-0319] p 60 A85-19665
- Structure of particle-laden jets - Measurements and predictions  
p 109 A85-25137
- Structure of ducted particle-laden turbulent jets  
p 110 A85-38999
- Measurements and predictions of the structure of evaporating sprays  
p 112 A85-46484
- Structure of nonevaporating sprays. I - Initial conditions and mean properties  
p 112 A85-48538
- SIEGEL, R.**
- Analysis of three-dimensional solidification interface shape  
p 109 A85-30075
- Analysis of buoyancy effect on fully developed laminar heat transfer in a rotating tube  
p 110 A85-35596
- Control of solidification boundary in continuous casting by asymmetric cooling and mold offset  
p 110 A85-37047
- Solidification interface shape for continuous casting in an offset mold - Two analytical methods  
p 112 A85-41326
- SIGARI, G.**
- Improved models for increasing wind penetration, economics and operating reliability  
[NASA-CR-175538] p 160 N85-20545
- SIGNER, H. R.**
- Effect of two inner-ring oil-flow distribution schemes on the operating characteristics of a 35 millimeter bore ball bearing to 2.5 million DN  
[NASA-TP-2404] p 130 N85-13233
- SIGNORELLI, R. A.**
- High temperature metal and ceramic composites  
p 55 A85-37483
- SILVERMAN, S. W.**
- Applicability of 100kWe-class of space reactor power systems to NASA manned space station missions  
[NASA-CR-174696] p 177 N85-35728

## SIMITSSES, G. J.

- Thermodynamically consistent constitutive equations for nonisothermal large strain, elasto-plastic, creep behavior  
[AIAA PAPER 85-0621] p 142 A85-38425
- Analysis of shell type structures subjected to time dependent mechanical and thermal loading  
[NASA-CR-175747] p 147 N85-25896
- Dynamic creep buckling: Analysis of shell structures subjected to time-dependent mechanical and thermal loading  
p 149 N85-27959
- SIMON, F. F.**
- Flow visualization study of the effect of injection hole geometry on an inclined jet in crossflow  
[NASA-TM-86936] p 115 N85-20269
- SIMON, T. W.**
- Heat transfer and fluid mechanics measurements in transitional boundary layer flows  
p 118 N85-31439
- SIMONEAU, R. J.**
- Preliminary results of a study of the relationship between free stream turbulence and stagnation region heat transfer  
[NASA-TM-86884] p 113 N85-11317
- New facility to study unsteady wake effects on turbine airfoil heat transfer  
p 117 N85-27948
- Preliminary results of a study of the relationship between free-stream turbulence and stagnation region heat transfer  
p 118 N85-31435
- Heat transfer in aeropropulsion systems  
[NASA-TM-87066] p 119 N85-31444
- SINCLAIR, J. H.**
- Impact resistance of fiber composites - Energy-absorbing mechanisms and environmental effects  
p 56 A85-46543
- SINHA, A.**
- Effects of friction dampers on aerodynamically unstable rotor stages  
p 14 A85-21866
- SIROCKY, P. J.**
- Government review of the Mod-2 wind turbine (as-built)  
[NASA-TM-86983] p 162 N85-29365
- SIZEMORE, R. L.**
- Government review of the Mod-2 wind turbine (as-built)  
[NASA-TM-86983] p 162 N85-29365
- Structural analysis and cost estimate of an eight-leg space frame as a support structure for horizontal axis wind turbines  
[NASA-TM-83470] p 150 N85-30361
- SKEBE, G. G.**
- High-voltage solar-cell chip  
p 154 A85-24668
- SLABY, J.**
- Overview of the 1985 NASA Lewis Research Center SP-100 free-piston Stirling engine activities  
[NASA-TM-87028] p 185 N85-27769
- SLABY, J. G.**
- Overview of NASA Lewis Research Center free-piston Stirling engine activities  
p 130 A85-45479
- SLEEPER, H. A.**
- Four-dimensional modulation and coding - An alternate to frequency-reuse  
p 97 A85-36653
- SLINEY, H. E.**
- The influence of temperature on the lubricating effectiveness of MoS<sub>2</sub> dispersed in mineral oils  
[ASLE PREPRINT 84-LC-2A-2] p 80 A85-25963
- Effects of silver and group 2 fluorides addition to plasma sprayed chromium carbide high temperature solid lubricant for foil gas bearing to 650 deg C  
[NASA-TM-86895] p 84 N85-14928
- The role of silver in self-lubricating coatings for use at extreme temperatures  
[NASA-TM-86943] p 87 N85-20127
- SMART, A. E.**
- Research study of droplet sizing technology leading to the development of an advanced droplet sizing system  
[NASA-CR-174839] p 123 N85-21604
- SMETANA, J.**
- Characterization of MMIC devices for active array antennas  
[NASA-TM-86907] p 38 N85-15779
- SMIALEK, J. L.**
- Microstructural development of protective Al<sub>2</sub>O<sub>3</sub> scales  
p 80 A85-21650
- Dopant effect of yttrium and the growth and adherence of alumina on nickel-aluminum alloys  
p 82 A85-40973
- Hot corrosion of sintered alpha-SiC at 1000 C  
[ACS PAPER 19-B-84P] p 83 A85-45302
- Burner rig corrosion of SiC at 1000 deg C  
[NASA-TM-87061] p 53 N85-30011
- Mechanism of strength degradation for hot corrosion of alpha-SiC  
[NASA-TM-87052] p 91 N85-30135
- SMITH, G. T.**
- Resin selection criteria for 'tough' composite structures  
p 81 A85-35139

## SMITH, J. R.

- Ceramic component development for the AGT101 gas turbine engine  
p 126 A85-15972
- Universal binding energy relations in metallic adhesion  
[NASA-TM-86889] p 72 N85-12132
- SMITH, R. F.**
- Measured effects of wind turbine generation at the Block Island Power Company  
p 153 A85-10652
- SMITHRICK, J. J.**
- Advanced designs for IPV nickel-hydrogen cells  
p 156 A85-45438
- Initial performance of advanced designs for IPV nickel-hydrogen cells  
[NASA-TM-87029] p 162 N85-28444
- Initial performance of advanced designs for IPV nickel-hydrogen cells  
p 105 N85-31404
- SMOLL, A.**
- The 20 GHz proof-of-concept test model results for a multiple scan beam dual reflector antenna  
[NASA-CR-174268] p 98 N85-15944
- SNELL, G. J.**
- Solids mixing in a three phase fluidized bed containing spherically shaped-porous solid particles  
[PB85-187961] p 120 N85-33453
- SNITZER, E.**
- Fiber optic temperature sensor  
p 121 A85-29563
- SNYDER, C. A.**
- Shock tube measurements of growth constants in the branched-chain ethane-carbon monoxide-oxygen system  
[NASA-TM-87068] p 64 N85-32156
- SNYDER, D. B.**
- Characteristics of arc currents on a negatively biased solar cell array in a plasma  
p 154 A85-18608
- The effect of plasma on solar cell array arc characteristics  
[AIAA PAPER 85-0384] p 43 A85-19713
- The effect of plasma on solar cell array arc characteristics  
[NASA-TM-86887] p 47 N85-11133
- Discharges on a negatively biased solar cell array in a charged-particle environment  
p 160 N85-22499
- SO, R. M. C.**
- Jet characteristics in confined swirling flow  
p 112 A85-45282
- Density effects on jet characteristics in confined swirling flow  
p 112 A85-45283
- Behavior of turbulent gas jets in an axisymmetric confinement  
[NASA-CR-174829] p 28 N85-25265
- SOCKOL, P. M.**
- Computation of internal flows: Methods and applications; Proceedings of the Energy Sources Technology Conference, New Orleans, LA, February 12-16, 1984  
p 106 A85-11630
- Review - Computational methods for internal flows with emphasis on turbomachinery  
p 4 A85-29126
- SOEDER, J. F.**
- Floating-point function generation routines for 16-bit microcomputers  
[NASA-TM-83783] p 170 N85-10683
- MINDS: A microcomputer interactive data system for 8086-based controllers  
[NASA-TP-2378] p 170 N85-17576
- SOEDER, R. H.**
- Effect of combined pressure and temperature distortion orientation on high-bypass-ratio turbofan engine stability  
[NASA-TM-83771] p 17 N85-10067
- Effect of steady-state temperature distortion on inlet flow to a high-bypass-ratio turbofan engine  
[NASA-TM-86896] p 24 N85-15725
- SOLOMON, A. S. P.**
- Drop-turbulence interactions in a diffusion flame  
[AIAA PAPER 85-0319] p 60 A85-19665
- Structure of particle-laden jets - Measurements and predictions  
p 109 A85-25137
- Structure of ducted particle-laden turbulent jets  
p 110 A85-38999
- Measurements and predictions of the structure of evaporating sprays  
p 112 A85-46484
- Structure of nonevaporating sprays. I - Initial conditions and mean properties  
p 112 A85-48538
- The structure of dilute combustng sprays  
[NASA-CR-174838] p 24 N85-15728
- SOLOMONS, G. P.**
- Oscillator response to nonstationary excitation  
[ASME PAPER 84-WA/APM-38] p 140 A85-17039
- SOMORJAI, G. A.**
- Properties of coated and modified surfaces  
p 53 A85-36694
- SOVEY, J. S.**
- Deposition of diamondlike carbon films  
[NASA-CASE-LEW-14080-1] p 95 N85-20153
- Ring-cusp ion thruster with shell anode  
[NASA-CASE-LEW-13881-1] p 48 N85-21256

- Vacuum chamber pressure effects on thrust measurements of low Reynolds number nozzles [NASA-TM-86955] p 49 N85-21259
- Compatibility experiments of facilities, materials, and propellants for electrothermal thrusters [NASA-TM-86956] p 49 N85-21260
- SPALVINS, T.**
- Frictional and morphological properties of Au-MoS<sub>2</sub> films sputtered from a compact target p 127 A85-19085
- Surface hardening of steel by boriding in a cold rf plasma p 68 A85-40275
- Plasma variables and tribological properties of coatings in low pressure (0.1 - 10.0 torr) plasma systems [NASA-TM-83798] p 94 N85-11261
- Tribological properties of boron nitride synthesized by ion beam deposition [NASA-TM-86962] p 87 N85-21355
- Frictional and structural characterization of ion-nitrided low and high chromium steels p 132 N85-23085
- The structure of ion plated films in relation to coating properties [NASA-TM-87055] p 95 N85-29085
- Advances in sputtered and ion plated solid film lubrication p 136 N85-33524
- SPANOS, P.-T. D.**
- Oscillator response to nonstationary excitation [ASME PAPER 84-WA/APM-38] p 140 A85-17039
- SPEAR, K. E.**
- A morphological study of silicon carbide prepared by chemical vapor deposition p 79 A85-20938
- SPEIR, D. W.**
- Altitude testing of a flight weight, self-cooled, 2D thrust vectoring exhaust nozzle [SAE PAPER 841557] p 14 A85-25984
- SPERA, D. A.**
- Method for evaluating wind turbine wake effects on wind farm performance p 155 A85-36750
- SPRING, J.**
- Conceptual design of a fixed-pitch wind turbine generator system rated at 400 kilowatts [NASA-CR-174877] p 162 N85-29363
- SRINATH, N. K.**
- Four-dimensional modulation and coding - An alternate to frequency-reuse p 97 A85-36653
- SRINIVASAN, R.**
- Experiments in dilution jet mixing - Effects of multiple rows and non-circular orifices [AIAA PAPER 85-1104] p 15 A85-39606
- Experiments in dilution jet mixing effects of multiple rows and non-circular orifices [NASA-TM-86996] p 28 N85-25266
- SRIRAMAMURTHY, A. M.**
- Deformation and fracture behavior of Ni-Mo-Al(gamma/gamma prime-alpha) in situ composite p 64 A85-11058
- ST. JOHN, G. A.**
- Chemistry of fuel deposits and sediments and their precursors [NASA-CR-174778] p 92 N85-10209
- STAFFORD, J.**
- Pantographing self adaptive gap elements p 142 A85-37440
- STAIGER, P. J.**
- Primary propulsion of electrothermal, ion and chemical systems for space-based radar orbit transfer [NASA-TM-87043] p 51 N85-27972
- STANCIK, K.**
- Effect of steady-state temperature distortion on inlet flow to a high-bypass-ratio turbofan engine [NASA-TM-86896] p 24 N85-15725
- STANFORTH, C. M.**
- Advanced smoke meter development survey and analysis [NASA-CR-168287] p 124 N85-25792
- STANITZ, J. D.**
- General design method for 3-dimensional, potential flow fields. Part 2: Computer program DIN3D1 for simple, unbranched ducts [NASA-CR-3926] p 10 N85-35159
- STANTON, A. C.**
- An approach for automated analysis of particle holograms p 120 A85-10034
- STASKUS, J. V.**
- Electron beam charging of Space Shuttle thermal protection system tiles p 39 N85-22478
- STATLER, R. L.**
- Effects of 1 MeV electrons and 10 MeV protons on the performance and reflectance of thin BSR cells p 182 A85-35699
- STEARNS, C. A.**
- Reactions of NaCl with gaseous SO<sub>3</sub>, SO<sub>2</sub>, and O<sub>2</sub> p 59 A85-11897
- Chemical reactions involved in the initiation of hot corrosion of IN-738 p 66 A85-31688
- Burner rig corrosion of SiC at 1000 deg C [NASA-TM-87061] p 53 N85-30011
- STECURA, S.**
- Optimization of the NiCrAl-Y/ZrO<sub>2</sub>-Y<sub>2</sub>O<sub>3</sub> thermal barrier system [NASA-TM-86905] p 72 N85-15878
- Thermal barrier coating system [NASA-CASE-LEW-13324-2] p 57 N85-21266
- Advanced thermal barrier system bond coatings for use on Ni, Co-, and Fe-base alloy substrates [NASA-TM-87062] p 77 N85-31283
- Thermal barrier coating system [NASA-CASE-LEW-14057-1] p 59 N85-35233
- STEENKEN, W. G.**
- Stall recovery control strategy methodology and results [AIAA PAPER 85-1433] p 16 A85-40841
- STEFKO, G. L.**
- Wind tunnel results of advanced high speed propellers in the takeoff, climb, and landing operating regimes [AIAA PAPER 85-1259] p 6 A85-47025
- Wind tunnel results of advanced high speed propellers in the takeoff, climb and landing operating regimes [NASA-TM-87054] p 9 N85-29925
- STEIN, Y.**
- The role of surface generated radicals in catalytic combustion p 30 N85-27869
- STEINBACH, R. E.**
- Interdisciplinary design analysis of a precision spacecraft antenna [AIAA PAPER 85-0804] p 38 A85-30303
- STEINBERG, R.**
- MERIT: A man/computer data management and enhancement system for upper air nowcasting/forecasting in the United States p 167 N85-10558
- STEINER, G.**
- Development of a large insert gas ion thruster p 45 A85-42922
- STEINETZ, B. M.**
- Application of traction drives as servo mechanisms p 152 N85-33520
- STEINNAGEL, K.**
- Satellite provided customer promises services, a forecast of potential domestic demand through the year 2000. Volume 4: Sensitivity analysis [NASA-CR-174662] p 99 N85-27092
- STEPHENS, J. R.**
- Stirling material technology [NASA-TM-86888] p 72 N85-13007
- The B2 aluminides as alternative materials [NASA-CR-186937] p 74 N85-19076
- STETZ, T. T.**
- Flow rates and pressure profiles for one to four axially aligned Borda inlets [NASA-TP-2390] p 113 N85-14078
- Flow rate and pressure profiles for 1 to 4 axially aligned orifice inlets [NASA-TP-2460] p 116 N85-27165
- STEVENS, G. A.**
- Modeling of NASA's 30/20 GHz satellite communications system p 38 A85-36663
- STEVENS, N. J.**
- Environmentally-induced voltage limitations in large space power systems p 43 A85-18584
- Design guidelines for assessing and controlling spacecraft charging effects p 40 N85-22500
- STEVENSON, S.**
- Demand for satellite-provided domestic communications services up to the year 2000 [NASA-TM-86894] p 97 N85-15099
- STEWART, G. W.**
- An approach for automated analysis of particle holograms p 120 A85-10034
- STILLER, P. H.**
- Measured effects of wind turbine generation at the Block Island Power Company p 153 A85-10652
- STINCHCOMB, W. W.**
- A study of the stress wave factor technique for the characterization of composite materials [NASA-CR-174870] p 58 N85-30035
- STOCKER, D. P.**
- Applications of high pressure differential scanning calorimetry to aviation fuel thermal stability research [NASA-TM-87002] p 63 N85-23941
- STOFAN, A. J.**
- A high energy stage for the National Space Transportation System [IAF PAPER 84-15] p 36 A85-23200
- STOLOFF, N. S.**
- The influence of hold times on LCF and FCG behavior in a P/M Ni-base superalloy p 67 A85-32400
- STONE, J. R.**
- Supersonic jet shock noise reduction [AIAA PAPER 84-2278] p 173 A85-18099
- STONEHART, P.**
- Electrocatalyst advances for hydrogen oxidation in phosphoric acid fuel cells p 60 A85-15614
- Preparation and evaluation of advanced catalysts for phosphoric acid fuel cells [NASA-CR-168223] p 160 N85-19511
- STOTLER, C. L.**
- Energy efficient engine ICLS Nacelle detail design report [NASA-CR-167870] p 22 N85-10993
- STOUFFER, D. C.**
- Finite element analysis of notch behavior using a state variable constitutive equation p 152 N85-31548
- STRANGE, R. R.**
- Development of advanced high-temperature heat flux sensors. Phase 2: Verification testing [NASA-CR-174973] p 126 N85-35391
- STRANGMAN, T. E.**
- Development of coated single-crystal superalloy systems for gas turbine applications p 68 A85-32440
- STRAZISAR, A. J.**
- Investigation of flow phenomena in a transonic fan rotor using laser anemometry [ASME PAPER 84-GT-199] p 4 A85-32963
- Rotor wake characteristics of a transonic axial flow fan [AIAA PAPER 85-1133] p 6 A85-43974
- STREHLOW, R. A.**
- The mechanisms of flame holding in the wake of a bluff body [NASA-CR-174058] p 62 N85-11149
- The mechanisms of flame holding in the wake of a bluff body [NASA-CR-3866] p 26 N85-21166
- Behavior of the lean methane-air flame at zero-gravity [NASA-CR-175586] p 62 N85-21283
- The use of a laser Doppler velocimeter in a standard flammability tube [NASA-CR-174960] p 125 N85-35389
- STRICKER, J.**
- Electronic heterodyne readout of fringes in moire deflectometry p 122 A85-36726
- Moire deflectometry with deferred electronic heterodyne readout p 122 A85-42854
- A comparison of electronic heterodyne moire deflectometry and electronic heterodyne holographic interferometry for flow measurements [NASA-TM-87071] p 125 N85-32302
- STUART, T. A.**
- Small-signal model for the series resonant converter p 102 A85-39453
- STURGESS, G. J.**
- Calculation of confined swirling flows [AIAA PAPER 85-0060] p 108 A85-19491
- STURMAN, J. C.**
- High-voltage, high-power, solid-state remote power controllers for aerospace applications [NASA-TP-2437] p 49 N85-21263
- SUBRAHMANYAM, K. B.**
- Finite difference analysis of torsional vibrations of pretwisted, rotating, cantilever beams with effects of warping p 143 A85-42047
- Vibration and buckling of rotating, pretwisted, precone beams including Coriolis effects [NASA-TM-87004] p 146 N85-25893
- Nonlinear flap-lag-extensional vibrations of rotating, pretwisted, precone beams including Coriolis effects [NASA-TM-87102] p 152 N85-34427
- SUBRAMANIAN, S. V.**
- Application of Runge Kutta time marching scheme for the computation of transonic flows in turbomachines [AIAA PAPER 85-1332] p 5 A85-39728
- SULLIVAN, J. P.**
- Noise constraints effecting optimal propeller designs [SAE PAPER 850871] p 7 A85-50106
- Noise constraints effecting optimal propeller designs [NASA-TM-86967] p 8 N85-19923
- SULLIVAN, T. J.**
- Energy efficient engine. Fan and quarter-stage component performance report [NASA-CR-168070] p 33 N85-34141
- SULLIVAN, T. L.**
- Government review of the Mod-2 wind turbine (as-built) [NASA-TM-86983] p 162 N85-29365
- SUMIHARA, K.**
- Rational approach for assumed stress finite elements p 139 A85-12029
- Hybrid Semiloof elements for plates and shells based upon a modified Hu-Washizu principle p 139 A85-15893
- SUMMERS, C.**
- Technology for satellite power conversion [NASA-CR-174335] p 159 N85-18451

**SUMMERS, R. L.**

Integrated exhaust gas analysis system for aircraft turbine engine component testing  
[NASA-TP-2424] p 123 N85-16100

**SUN, C. T.**

Use of static indentation laws in the impact analysis of laminated composite plates p 55 A85-29133

**SUNDARAM, C. V.**

Flow dynamic environment data base development for the SSME p 147 N85-26885

**SUNDBERG, G. R.**

Advanced in solid state switchgear technology for large space power systems p 102 A85-45362  
A new very high voltage semiconductor switch  
[NASA-TM-86957] p 103 N85-20246

**SUTTON, R.**

Cryogenic upper stage test bed engine  
[AIAA PAPER 85-1339] p 44 A85-39733

**SUTTON, R. D.**

Analytical fuel property effects--small combustors  
[NASA-CR-174738] p 28 N85-26709

**SWAN, P.**

Report of the Constellations Panel p 131 N85-20368

**SWARNER, W. G.**

Adaptive antenna arrays for satellite communications: Design and testing  
[NASA-CR-176162] p 100 N85-34329

**SWARTWOUT, T.**

Design and analysis report for the RL10-2B breadboard low thrust engine  
[NASA-CR-174857] p 48 N85-19020

**SWARTZ, C. K.**

Voltage controlling mechanisms in low resistivity silicon solar cells - A unified approach p 155 A85-35617  
Radiation damage and defect behavior in ion-implanted, lithium counterdoped silicon solar cells p 182 A85-35698

Effects of 1 MeV electrons and 10 MeV protons on the performance and reflectance of thin BSR cells p 182 A85-35699

The high voltage silicon cell: A comparative analysis p 49 N85-22569

The effects of lithium counterdoping on radiation damage and annealing in n(+)-p silicon solar cells p 50 N85-22586

**SWEC, D. M.**

Ion beam sputter-deposited thin film coatings for protection of spacecraft polymers in low Earth orbit  
[NASA-TM-87051] p 91 N85-30137  
Diamondlike carbon protective coatings for IR materials  
[NASA-TM-87083] p 178 N85-34631

**SWETTE, L.**

Development of electrodes for the NASA iron/chromium  
[NASA-CR-174724] p 165 N85-35471

**SWINDAL, J. L.**

High-temperature optically activated GaAs power switching for aircraft digital electronic control  
[NASA-CR-174711] p 34 N85-12901

**SYED, S. A.**

Finite difference methods for reducing numerical diffusion in TEACH-type calculations  
[AIAA PAPER 85-0057] p 108 A85-19488  
Calculation of confined swirling flows  
[AIAA PAPER 85-0060] p 108 A85-19491  
Assessment of discretization schemes to reduce numerical diffusion in the calculation of complex flows  
[AIAA PAPER 85-0441] p 108 A85-19751

Reducing numerical diffusion for incompressible flow calculations  
[NASA-TM-83621] p 24 N85-14840

Error reduction program  
[NASA-CR-174776] p 172 N85-27584

**SZETELA, E. J.**

External fuel vaporization study, phase 2  
[NASA-CR-174079] p 92 N85-11252

**SZUCH, J. R.**

Analytical and physical modeling program for the NASA Lewis Research Center's Altitude Wind Tunnel (AWT)  
[AIAA PAPER 85-0379] p 34 A85-19709

Analytical and physical modeling program for the NASA Lewis Research Center's Altitude Wind Tunnel (AWT)  
[NASA-TM-86919] p 35 N85-15757

**T****TABADDOR, F.**

Pantographing self adaptive gap elements p 142 A85-37440

**TABAKOFF, W.**

The three-dimensional compressible flow in a radial inflow turbine scroll p 6 A85-41826

**TAM, C. K. W.**

A multiple-scales model of the shock-cell structure of imperfectly expanded supersonic jets p 113 A85-49354

**TAMASHIRO, R. N.**

A 20 GHz, 75 watt, helix TWT for space communications p 101 A85-14433

**TAN, T. M.**

Use of static indentation laws in the impact analysis of laminated composite plates p 55 A85-29133

**TANAKA, K.**

Effects of wear on structure-sensitive magnetic properties of ceramic ferrite in contact with magnetic tape  
[NASA-TM-87007] p 90 N85-26991

**TANIS, F. J.**

Comparison of atmospheric correction algorithms for the Coastal Zone Color Scanner p 153 A85-10244

**TANVEER, S.**

Vortex induced lift on a flat plate with a curved forward-facing flap p 4 A85-30175

**TAYLOR, J. R.**

Flow modifying device  
[NASA-CASE-LEW-13562-2] p 33 N85-35195

**TAYLOR, S. R.**

Percutaneous connectors  
[NASA-CR-175627] p 168 N85-27508

**TEAGAN, W. P.**

Preliminary evaluation of a liquid belt radiator for space applications  
[NASA-CR-174807] p 47 N85-15804

**TELESMA, J.**

A study of spectrum fatigue crack propagation in two aluminum alloys. 1: Spectrum simplification  
[NASA-TM-86929] p 72 N85-18124  
A study of spectrum fatigue crack propagation in two aluminum alloys. 2: Influence of microstructures  
[NASA-TM-86930] p 73 N85-18125

**TESAR, J. S.**

Acoustic structure and propagation in highly porous, layered, fibrous materials p 173 A85-12301

**TEVAARWERK, J. L.**

Thermal traction contact performance evaluation under fully flooded and starved conditions  
[NASA-CR-168173] p 132 N85-25848  
Rolling, slip and traction measurements on low modulus materials  
[NASA-CR-174909] p 135 N85-33491

**TEW, R. C.**

Comparison of free-piston Stirling engine model predictions with RE1000 engine test data p 130 A85-45488

**TEWARI, S. N.**

Deformation and fracture behavior of Ni-Mo-Al(gamma/gamma prime-alpha) in situ composite p 64 A85-11058

Microstructures in rapidly solidified Ni-Mo alloys  
[NASA-TM-87100] p 78 N85-34266

**THALLER, L. H.**

Electrochemistry and storage p 62 N85-13889

System level electrochemical principles p 104 N85-31375

Design principles for nickel hydrogen cells and batteries p 104 N85-31398

Design principles for nickel-hydrogen cells and batteries  
[NASA-TM-87037] p 164 N85-31646

**THEOBALD, M. A.**

Turbobal noise generation. Volume 2: Computer programs  
[NASA-CR-167952] p 175 N85-11791

**THIEME, L. G.**

Initial testing of a variable-stroke Stirling engine  
[NASA-TM-86875] p 185 N85-19895

**THOMA, D. J.**

Interaction of high-cycle and low-cycle fatigue of Haynes 188 alloy at 1400 F deg p 149 N85-27961

**THOMAS, R. L.**

Electric power - Photovoltaic or solar dynamic? p 46 A85-47042

**THOMAS, T. T.**

Energy efficient engine high pressure turbine test hardware detailed design report  
[NASA-CR-167955] p 23 N85-10995

**THOMPSON, W. T., JR.**

Researched applied to transonic compressors in numerical fluid mechanics of inviscid flow and viscous flow  
[NASA-CR-174353] p 114 N85-18291

**THOMPSON, R. L.**

Validation of structural analysis methods using the in-house liner cyclic rigs p 21 N85-10987

A computer analysis program for interfacing thermal and structural codes  
[NASA-TM-87021] p 148 N85-27264

On numerical integration and computer implementation of viscoplastic models p 151 N85-31542

**THRASHER, S. R.**

Ceramic applications in turbine engines  
[NASA-CR-174715] p 91 N85-28109

**TIAN, Z.**

Axisymmetric solid elements by a rational hybrid stress method p 143 A85-41109

**TIDMAN, D. A.**

Investigation of a pulsed electrothermal thruster system  
[NASA-CR-174768] p 46 N85-11132

**TIEGS, T. N.**

Dispersed metal-toughened ceramics and ceramic brazing  
[NASA-CR-174284] p 86 N85-15916

Dispersed-metal-toughened alumina  
[NASA-CR-174687] p 89 N85-22758

**TIEN, J. K.**

Modeling of gamma/gamma-prime phase equilibrium in the nickel-aluminum system p 65 A85-14959

Effects of cobalt on the hot workability of nickel-base superalloys p 67 A85-32412

**TIEN, J. S.**

Flame flashback in a premixed dump combustor  
[AIAA PAPER 85-0145] p 60 A85-19550

**TITMAN, R. H.**

Ductility in rapidly solidified NiAl p 66 A85-26158

Stirling material technology  
[NASA-TM-86888] p 72 N85-13007

High temperature properties of equiatomic FeAl with ternary additions  
[NASA-TM-86938] p 73 N85-19072

Alloys based on NiAl for high temperature applications  
[NASA-TM-86976] p 75 N85-21322

**TOMAZIC, W. A.**

Effect of water on hydrogen permeability  
[NASA-TM-86904] p 53 N85-14864

**TONER, J.**

Substrate-induced orientational order in the isotropic phase of liquid crystals p 181 A85-24649

**TORRES, F. J.**

Local heat-transfer measurements on a large, scale-model turbine blade airfoil using a composite of a heater element and liquid crystals  
[NASA-TM-86900] p 119 N85-33435

**TOTH, J. M., JR.**

Fiberglass epoxy laminate fatigue properties at 300 and 20 K p 56 A85-47970

**TOWNE, C. E.**

Analytical modeling of circuit aerodynamics in the new NASA Lewis Altitude Wind Tunnel  
[AIAA PAPER 85-0380] p 3 A85-26389

Application of computational fluid dynamics to complex inlet ducts  
[AIAA PAPER 85-1213] p 6 A85-47023

Analytical modeling of circuit aerodynamics in the new NASA Lewis wind tunnel  
[NASA-TM-86912] p 8 N85-15688

Application of computational fluid dynamics to complex inlet ducts  
[NASA-TM-87060] p 118 N85-30247

**TOWNSEND, D. P.**

Into mesh lubrication of spur gears with arbitrary offset oil jet. I - For jet velocity less than or equal to gear velocity p 128 A85-24497

Lubricant jet flow phenomena in spur and helical gears with modified center distances and/or addendums - For out-of-mesh conditions  
[ASME PAPER 84-DET-96] p 129 A85-35049

Effect of lubricant extreme-pressure additives on surface fatigue life of AISI 9310 spur gears  
[NASA-TP-2408] p 130 N85-13234

Effect of five lubricants on life of AISI 9310 spur gears  
[NASA-TP-2419] p 123 N85-16099

Lubricant and additive effects on spur gear fatigue life  
[NASA-TM-87044] p 133 N85-28373

Powder metallurgy forged gear development  
[NASA-TM-87483] p 134 N85-29295

Lubrication and cooling for high speed gears  
[NASA-TM-87096] p 136 N85-34407

**TOZZI, L.**

Advanced automotive diesel assessment program  
[NASA-CR-168285] p 130 N85-13235

**TREFNY, C. J.**

Low-speed aerodynamic test of an axisymmetric supersonic inlet with variable cowl slot  
[AIAA PAPER 85-1210] p 5 A85-40819

Low-speed aerodynamic test of an axisymmetric supersonic inlet with variable cowl slot  
[NASA-TM-87039] p 28 N85-26710

**TRINH, T. Q.**

Sixty GHz IMPATT diode development  
[NASA-CR-174969] p 105 N85-33293

## TRIPP, J. H.

- Surface roughness effects in elastohydrodynamic contacts  
[NASA-TP-2488] p 134 N85-32329  
Hertzian contact in two and three dimensions  
[NASA-TP-2473] p 135 N85-32331

## TROTTH, D. L.

- Analytical fuel property effects—small combustors  
[NASA-CR-174738] p 28 N85-26709

## TROUT, A. M.

- Combustion gas properties I-ASTM jet A fuel and dry air  
[NASA-TP-2359] p 17 N85-10064  
Combustion gas properties. 2: Natural gas fuel and dry air  
[NASA-TP-2435] p 26 N85-21168

## TSAY, C. B.

- Spiral bevel and circular arc helical gears: Tooth contact analysis and the effect of misalignment on circular arc helical gears  
[NASA-TM-87013] p 32 N85-31060

## TSUI, P.

- A morphological study of silicon carbide prepared by chemical vapor deposition p 79 A85-20938

## TSUNG, W. J.

- Generated spiral bevel gears: Optimal machine-tool settings and tooth contact analysis  
[NASA-TM-87075] p 136 N85-34405

## TSUNG, W. T.

- Spiral bevel and circular arc helical gears: Tooth contact analysis and the effect of misalignment on circular arc helical gears  
[NASA-TM-87013] p 32 N85-31060

## TYREE, E.

- The effect of plasma on solar cell array arc characteristics  
[AIAA PAPER 85-0384] p 43 A85-19713  
The effect of plasma on solar cell array arc characteristics  
[NASA-TM-86887] p 47 N85-11133

## U

## USHIODA, S.

- Prism-coupled light emission from tunnel junctions p 181 A85-21425

## V

## VAANFOSSEN, G. J., JR.

- Preliminary results of a study of the relationship between free stream turbulence and stagnation region heat transfer  
[NASA-TM-86884] p 113 N85-11317

## VAKILI, A. D.

- Flow control in a diffusing S-Duct  
[AIAA PAPER 85-0524] p 3 A85-25928

## VALCO, G. J.

- High-voltage solar-cell chip p 154 A85-24668

## VALGORA, M. E.

- Space station propulsion options  
[AIAA PAPER 85-1155] p 45 A85-43975

## VANFOSSEN, G. J., JR.

- The influence of jet-grid turbulence on heat transfer from the stagnation region of a cylinder in crossflow  
[NASA-TM-87011] p 115 N85-25760  
Preliminary results of a study of the relationship between free-stream turbulence and stagnation region heat transfer p 118 N85-31435

## VANNUCCI, R. D.

- Graphite/PMR polyimide composites with improved toughness  
[NASA-TM-87081] p 58 N85-32148

## VANOVERBEKE, T. J.

- SSME fuel preburner two-dimensional analysis p 51 N85-27943

## VARGA, G. M., JR.

- Jet fuel property changes and their effect on producibility and cost in the U.S., Canada, and Europe  
[NASA-CR-174840] p 93 N85-27012

## VARY, A.

- Ultrasonic nondestructive evaluation, microstructure, and mechanical property interrelations  
[NASA-TM-86876] p 137 N85-10371

## VATSA, V. N.

- A three-dimensional boundary-layer analysis including heat-transfer and blade-rotation effects p 6 A85-42988

## VEDHA-NAYAGAM, M.

- Gravitational effects on flames spreading over thick solid surfaces  
[IAF PAPER 84-154] p 59 A85-13092

## VEDULA, K. M.

- High temperature properties of equiatomic FeAl with ternary additions  
[NASA-TM-86938] p 73 N85-19072  
Alloys based on NiAl for high temperature applications  
[NASA-TM-86976] p 75 N85-21322

## VEERABHADRA RAO, P.

- Spherical microglass particle impingement studies of thermoplastic materials at normal incidence p 79 A85-11072  
A unified relation for cavitation erosion p 109 A85-24445

## VENTRES, C. S.

- Turbofan noise generation. Volume 2: Computer programs  
[NASA-CR-167952] p 175 N85-11791

## VENUGOPALAN, M.

- Analysis of glow discharges for understanding the process of film formation  
[NASA-TM-83750] p 62 N85-10138

## VERDON, J. M.

- A linearized unsteady aerodynamic analysis for transonic cascades p 3 A85-20744

## VERSAW, E. F.

- Study of advanced fuel system concepts for commercial aircraft and engines  
[NASA-CR-174752] p 93 N85-19176

## VERZWEVELT, S. A.

- Long life nickel electrodes for a nickel-hydrogen cell. III - Results of an accelerated test and failure analyses p 156 A85-45391  
The failure mechanism of a nickel electrode in a nickel-hydrogen cell p 105 N85-31408

## VICKERS, E. C.

- Flow modifying device  
[NASA-CASE-LEW-13562-2] p 33 N85-35195

## VINET, P.

- Aluminum work function: Effect of oxidation, mechanical scraping and ion bombardment  
[NASA-TM-87079] p 78 N85-34265

## VINOPAL, T. J.

- Vehicle/engine integration p 37 N85-17008

## VONGLAHN, U. H.

- Preliminary analysis of tone-excited two-stream jet velocity decay  
[NASA-TM-86951] p 8 N85-21114

## VONTIENENHAUSEN, G.

- Report of the Constellations Panel p 131 N85-20368

## W

## WAGNER, R. C.

- Effects of silver and group 2 fluorides addition to plasma sprayed chromium carbide high temperature solid lubricant for foil gas bearing to 650 deg C  
[NASA-TM-86895] p 84 N85-14928

- Experimental test program for evaluation of solid lubricant coating as applied to compliant foil gas bearings to 315 deg C  
[NASA-CR-174837] p 85 N85-15895

## WALKER, K. P.

- A survey of unified constitutive theories p 150 N85-31531

## WALLACE, J. F.

- Effect of reduction of strategic Columbium addition in 718 Alloy on the structure and properties  
[NASA-CR-174841] p 75 N85-21320

## WALTON, E. K.

- Adaptive antenna arrays for satellite communications: Design and testing  
[NASA-CR-176162] p 100 N85-34329

## WANG, C. L.

- Develop and test fuel cell powered on-site integrated total energy systems. Phase 3: Full-scale power plant development  
[NASA-CR-174887] p 161 N85-25941  
Develop and test fuel cell powered on-site integrated total energy systems. Phase 3: Full-scale power plant development  
[NASA-CR-168338] p 164 N85-30483

## WANG, C.-H.

- Multibus-based parallel processor for simulation p 169 A85-28613

## WANG, S. Y.

- Primary propulsion of electrothermal, ion and chemical systems for space-based radar orbit transfer  
[NASA-TM-87043] p 51 N85-27972

## WANG, T.

- Heat transfer and fluid mechanics measurements in transitional boundary layer flows p 118 N85-31439

## WARK, C.

- Development of a temperature measurement system with application to a jet in a cross flow experiment  
[NASA-CR-174896] p 27 N85-25262

## WARNER, J. D.

- Plasma deposited hydrogenated carbon on GaAs and InP p 182 A85-40386  
Plasma deposited diamondlike carbon on GaAs and InP p 183 N85-10844  
Optical properties of hydrogenated amorphous carbon films grown from methane plasma  
[NASA-TM-86995] p 183 N85-26406  
Calibration stability of some hot-cathode ion gauges p 122 A85-41634

## WASSERBAUER, C. A.

- Static jet noise test results of four 0.35 scale-model QCGAT mixer nozzles  
[NASA-TM-86871] p 175 N85-13551

## WASSERBAUER, J. F.

- Performance and surge limits of a TF30-P-3 turbofan engine/axisymmetric mixed-compression inlet propulsion system at Mach 2.5  
[NASA-TP-2461] p 27 N85-25261

## WATSON, G. K.

- Effect of hot isostatic pressing on reaction-bonded silicon nitride p 79 A85-15195  
Effect of hot isostatic pressing on the properties of sintered alpha silicon carbide p 83 A85-48757

## WATSON, J. W.

- Deposition stress effects on the life of thermal barrier coatings on burner rigs p 79 A85-19086

## WAYNE, S. F.

- Iron rich low cost superalloys  
[NASA-CR-174900] p 76 N85-26962

## WAYNERT, J.

- A rotating superconducting solenoid for 100 kWh energy storage p 44 A85-33144

## WEAR, J. D.

- Combustion gas properties I-ASTM jet A fuel and dry air  
[NASA-TP-2359] p 17 N85-10064  
Combustion system for radiation investigations p 21 N85-10986

- Combustion gas properties. 2: Natural gas fuel and dry air  
[NASA-TP-2435] p 26 N85-21168

- Combustion gas properties. Part 3: Hydrogen gas fuel and dry air  
[NASA-TP-2477] p 32 N85-31058

## WEHNER, G. K.

- Cone formation as a result of whisker growth on ion bombarded metal surfaces p 182 A85-41635

## WEINBERG, I.

- Theory of the high base resistivity  $n(+)$ pp $(+)$  silicon solar cell and its application to radiation damage effects p 154 A85-32639

- Radiation damage and defect behavior in ion-implanted, lithium counterdoped silicon solar cells p 182 A85-35698

- Lithium counterdoped silicon solar cell  
[NASA-CASE-LEW-14177-1] p 160 N85-20535

- The effects of lithium counterdoping on radiation damage and annealing in  $n(+)$ p silicon solar cells p 50 N85-22586

## WEISS, J. S.

- A design methodology for robust failure detection and isolation p 171 A85-47794

## WEIZER, V. G.

- Applicability of the Meyer-Neldel rule to solar cells p 154 A85-19948  
Effect of solar-cell junction geometry on open-circuit voltage p 154 A85-29080  
Voltage controlling mechanisms in low resistivity silicon solar cells - A unified approach p 155 A85-35617  
The effect of diffusion induced lattice stress on the open-circuit voltage in silicon solar cells p 181 A85-35620

- The high voltage silicon cell: A comparative analysis p 49 N85-22569

## WELDON, V. A.

- Vehicle/engine integration p 37 N85-17008

## WELGE, H. R.

- Low-speed aerodynamic test of an axisymmetric supersonic inlet with variable cowl slot  
[AIAA PAPER 85-1210] p 5 A85-40819

- Low-speed aerodynamic test of an axisymmetric supersonic inlet with variable cowl slot  
[NASA-TM-87039] p 28 N85-26710

## WENGER, N. C.

- HOST instrumentation R and D program overview p 19 N85-10957

## WERTH, J.

- Develop and test fuel cell powered on-site integrated total energy systems. Phase 3: Full-scale power plant development  
[NASA-CR-174887] p 161 N85-25941

- Develop and test fuel cell powered on-site integrated total energy systems. Phase 3: Full-scale power plant development  
[NASA-CR-168338] p 164 N85-30483
- WERTHEN, J. G.**  
Magnesium doping of efficient GaAs and Ga(0.75)In(0.25)As solar cells grown by metalorganic chemical vapor deposition p 180 A85-11486
- WESTFALL, L. J.**  
Arc spray fabrication of metal matrix composite monolayer  
[NASA-CASE-LEW-13828-1] p 58 N85-30027
- WHALEN, M. V.**  
Vacuum chamber pressure effects on thrust measurements of low Reynolds number nozzles  
[NASA-TM-86955] p 49 N85-21259  
Compatibility experiments of facilities, materials, and propellants for electrothermal thrusters  
[NASA-TM-86956] p 49 N85-21260
- WHEATON, M. L.**  
Heat treatment of bulk gallium arsenide using a phosphosilicate glass cap p 181 A85-32636
- WHEELER, R. L., III**  
Nested subcritical flows within supercritical systems  
[NASA-TM-86980] p 115 N85-21574
- WHELAN, J. A.**  
Develop and test fuel cell powered on-site integrated total energy systems. Phase 3: Full-scale power plant development  
[NASA-CR-174887] p 161 N85-25941  
Develop and test fuel cell powered on-site integrated total energy systems. Phase 3: Full-scale power plant development  
[NASA-CR-168338] p 164 N85-30483
- WHITE, B. E.**  
A frequency-routed satellite system concept using multiple orthogonally-polarized beams for frequency reuse p 97 A85-34470
- WHITE, C. D.**  
Experiments in dilution jet mixing - Effects of multiple rows and non-circular orifices  
[AIAA PAPER 85-1104] p 15 A85-39606  
Experiments in dilution jet mixing effects of multiple rows and non-circular orifices  
[NASA-TM-86996] p 28 N85-25266
- WHITEHAIR, S.**  
Experiments with a microwave electrothermal thruster concept p 42 A85-16441
- WHITTLE, D. P.**  
Effects of SO<sub>2</sub> and SO<sub>3</sub> on the Na<sub>2</sub>SO<sub>4</sub> induced corrosion of nickel p 65 A85-15603
- WHITTLESEY, A.**  
Design guidelines for assessing and controlling spacecraft charging effects p 40 N85-22500
- WHYTE, W.**  
On the subjective evaluation of the interference protection ratios' measurements for co-channel FM-TV signals p 96 A85-28241
- WHYTE, W. A.**  
The subjective effect of multiple co-channel frequency modulated television interference p 96 A85-28234
- WHYTE, W. A., JR.**  
Experimental results supporting the determination of service quality objectives for DBS systems p 96 A85-29611
- WILKINSON, C. L.**  
Space station propulsion options  
[AIAA PAPER 85-1155] p 45 A85-43975
- WILLENBERG, H. J.**  
Applicability of 100kW-class of space reactor power systems to NASA manned space station missions  
[NASA-CR-174696] p 177 N85-35728
- WILLIAMS, F.**  
Report of the Constellations Panel p 131 N85-20368
- WILLIAMS, G. C.**  
Interply layer degradation effects on composite structural response  
[AIAA PAPER 84-0849] p 54 A85-16096  
Interply layer degradation effects on composite structural response p 55 A85-39215
- WILLIAMS, J. H., JR.**  
Stress waves in an isotropic elastic plate excited by a circular transducer  
[NASA-CR-3877] p 138 N85-20390  
Application of homomorphic signal processing to stress wave factor analysis  
[NAS 1.26:174871] p 138 N85-21673  
Ultrasonic testing of plates containing edge cracks  
[NASA-CR-3904] p 138 N85-29307
- WILLIAMS, J. J.**  
Flow modifying device  
[NASA-CASE-LEW-13562-2] p 33 N85-35195
- WILLIAMSON, W. S.**  
Characterization of 8-cm engineering model thruster  
[NASA-CR-174673] p 46 N85-11131
- WILLIE, R.**  
Development of a lithium secondary battery separator p 104 N85-31378
- WILLISKY, A. S.**  
A design methodology for robust failure detection and isolation p 171 A85-47794
- WILREKER, V. F.**  
Measured effects of wind turbine generation at the Block Island Power Company p 153 A85-10652
- WILSON, R. B.**  
3-D inelastic analysis methods for hot section components (base program)  
[NASA-CR-174700] p 145 N85-21686
- WILSON, S. G.**  
Four-dimensional modulation and coding - An alternate to frequency-reuse p 97 A85-36653
- WINEGAR, S. R.**  
Interdisciplinary design analysis of a precision spacecraft antenna  
[AIAA PAPER 85-0804] p 38 A85-30303
- WINEMILLER, J. R.**  
Structural analysis and cost estimate of an eight-leg space frame as a support structure for horizontal axis wind turbines  
[NASA-TM-83470] p 150 N85-30361
- WINSOR, N. K.**  
Investigation of a pulsed electrothermal thruster system  
[NASA-CR-174768] p 46 N85-11132
- WIRSCHING, P. H.**  
Creep-rupture reliability analysis p 143 A85-42566  
Reliability considerations for the total strain range version of strainrange partitioning  
[NASA-CR-174757] p 144 N85-11380
- WITZELL, W. E.**  
Effect of low temperature on fatigue and fracture properties of Ti-5Al-2.5Sn(EL) for use in engine components p 70 A85-47972
- WOLAK, J.**  
Metallurgical and mechanical phenomena due to rubbing of titanium against sintered powder Nichrome p 127 A85-22281  
An experimental investigation and numerical prediction of thermomechanical phenomena in high speed rotor tip rubbing p 14 A85-25442
- WONG, R. S.**  
An experimental study of three-dimensional shock wave/turbulent boundary layer interactions in a supersonic flow  
[AIAA PAPER 85-1566] p 5 A85-40691
- WOOLLAM, J. A.**  
Dielectric properties of 'diamondlike' carbon prepared by RF plasma deposition p 182 A85-38192  
'Diamondlike' carbon films - Optical absorption, dielectric properties, and hardness dependence on deposition parameters p 82 A85-40383
- WOOTEN, W. H.**  
Altitude testing of a flight weight, self-cooled, 2D thrust vectoring exhaust nozzle  
[SAE PAPER 841557] p 14 A85-25984
- WORRELL, W. L.**  
The reactions of cobalt, iron and nickel in SO<sub>2</sub> atmospheres: Similarities and differences  
[NASA-TM-86868] p 70 N85-11217
- WU, J. M.**  
Flow control in a diffusing S-Duct  
[AIAA PAPER 85-0524] p 3 A85-25928
- WU, Y. T.**  
Reliability considerations for the total strain range version of strainrange partitioning  
[NASA-CR-174757] p 144 N85-11380
- WYNVEEN, R. A.**  
Engineering model system study for a regenerative fuel cell: Study report  
[NASA-CR-174801] p 158 N85-16292
- X**
- XUE, W.-M.**  
On the existence and stability conditions for mixed-hybrid finite element solutions based on Reissner's variational principle p 142 A85-33847
- Y**
- YAMAMOTO, K.**  
Experimental investigation of shock-cell noise reduction for dual-stream nozzles in simulated flight  
[NASA-CR-3846] p 175 N85-13549  
Experimental investigation of shock-cell noise reduction for single stream nozzles in simulated flight  
[NASA-CR-3845] p 175 N85-13550
- YAMAMOTO, O.**  
Inviscid analysis of advanced turboprop propeller flow fields  
[AIAA PAPER 85-1263] p 6 A85-43977
- YAMAURA, Y.**  
Engineering calculations for communications satellite systems planning  
[NASA-CR-175552] p 37 N85-21233
- YANG, K.**  
Electron yields from spacecraft materials p 40 N85-22512
- YEE, S. T.**  
Structural analysis and cost estimate of an eight-leg space frame as a support structure for horizontal axis wind turbines  
[NASA-TM-83470] p 150 N85-30361
- YEH, F. C.**  
Heat transfer results and operational characteristics of the NASA Lewis Research Center Hot Section Cascade Test Facility  
[NASA-TM-86890] p 114 N85-15133
- Z**
- ZACHARY, A.**  
Cryogenic upper stage test bed engine  
[AIAA PAPER 85-1339] p 44 A85-39733
- ZAFRAN, S.**  
Electrothermal thruster diagnostics p 42 A85-16440
- ZANA, L. M.**  
Rail accelerator technology and applications  
[NASA-TM-86947] p 48 N85-21258
- ZANNETTI, L.**  
Time dependent computation of the Euler equations for designing 2-D cascades, including the case of transonic shock free design p 5 A85-41814  
Inverse design technique for cascades  
[NASA-CR-3836] p 7 N85-12008
- ZARETSKY, E. V.**  
Fatigue criterion to system design, life and reliability  
[AIAA PAPER 85-1140] p 143 A85-40814  
Effect of five lubricants on life of AISI 52100 spur gears  
[NASA-TP-2419] p 123 N85-16099  
Lubrication and performance of high-speed rolling-element bearings  
[NASA-TM-86958] p 131 N85-21658  
Fatigue criterion to system design, life and reliability  
[NASA-TM-87017] p 132 N85-27226  
Operating characteristics of a 0.87 kW-hr flywheel energy storage module  
[NASA-TM-87038] p 133 N85-28371  
Lubricant and additive effects on spur gear fatigue life  
[NASA-TM-87044] p 133 N85-28373  
Effect of speed and press fit on fatigue life of roller-bearing inner-race contact  
[NASA-TP-2496] p 134 N85-31511  
Design and lubrication of high-speed rolling-element bearings  
[NASA-TM-87107] p 137 N85-34409
- ZEIDAN, F. Y.**  
Internal hysteresis experienced on a high pressure syn gas compressor p 131 N85-14122
- ZEISSER, M. H.**  
Energy efficient engine combustor test hardware detailed design report  
[NASA-CR-167945] p 18 N85-10950
- ZELAHY, J. W.**  
Advanced blade tip seal system, volume 2  
[NASA-CR-167851] p 23 N85-10999
- ZELEZNIK, F. J.**  
Computer program for calculation of complex chemical equilibrium compositions and applications. Supplement 1: Transport properties  
[NASA-TM-86885] p 184 N85-16663  
Modeling the internal combustion engine  
[NASA-RP-1094] p 172 N85-19733  
Ideal gas thermodynamic properties for the phenyl, phenoxy, and o-biphenyl radicals  
[NASA-TM-83800] p 184 N85-22204
- ZELLER, J.**  
The role of modern control theory in the design of controls for aircraft turbine engines p 13 A85-13627
- ZENAS, R.**  
Metallurgical and mechanical phenomena due to rubbing of titanium against sintered powder Nichrome p 127 A85-22281
- ZHANG, Q.-F.**  
Structure of particle-laden jets - Measurements and predictions p 109 A85-25137  
Structure of ducted particle-laden turbulent jets p 110 A85-38999  
Measurements and predictions of the structure of evaporating sprays p 112 A85-46484  
Structure of nonevaporating sprays. I - Initial conditions and mean properties p 112 A85-48538



**ZHONG, W. F.**

Fundamentals of microcrack nucleation mechanics  
[NASA-CR-3851] p 137 N85-16195

**ZIEGLER, K. R.**

Effect of reduction of strategic Columbium addition in  
718 Alloy on the structure and properties  
[NASA-CR-174841] p 75 N85-21320

**ZIERKE, W. C.**

The boundary layer on compressor cascade blades  
[NASA-CR-174369] p 114 N85-18292

**ZINOLABEDINI, R.**

Graphite fiber intercalation: Dynamics of the bromine  
intercalation process  
[NASA-TM-87015] p 53 N85-26921

**ZIZELMAN, J.**

Dilution jet configurations in a reverse flow combustor  
[NASA-CR-174888] p 27 N85-22392

**ZOPFF, D.**

Solids mixing in a three phase fluidized bed containing  
spherically shaped-porous solid particles  
[PB85-187961] p 120 N85-33453

**ZRIBI, G.**

Substrate-induced orientational order in the isotropic  
phase of liquid crystals p 181 A85-24649

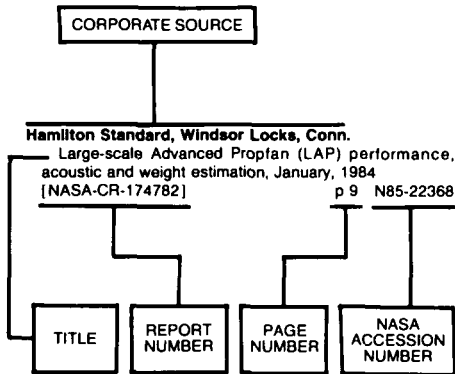
**ZUMWALT, G. W.**

Icing tunnel tests of Electro-Impulse De-Icing of an  
engine inlet and high-speed wings  
[AIAA PAPER 85-0466] p 10 A85-20872

Electro-impulse de-icing of a turbofan engine inlet  
[AIAA PAPER 85-1118] p 12 A85-40811

# CORPORATE SOURCE INDEX

## Typical Corporate Source Index Listing



Listings in this index are arranged alphabetically by corporate source. The title of the document provides the user with a brief description of the subject matter. The report number helps to indicate the type of document cited (e.g., NASA report, translation, NASA contractor report). The NASA accession number denotes the number by which the citation is identified. The titles are arranged under each corporate source in ascending accession number order.

## A

### Aerodyne Research, Inc., Billerica, Mass.

An approach for automated analysis of particle holograms p 120 A85-10034

### Aerojet Techsystems Co., Sacramento, Calif.

Progress report - Advanced cryogenic OTV engine technology [AIAA PAPER 85-1341] p 44 A85-39735

### Aerometrics, Inc., Mountain View, Calif.

Phase/doppler spray analyzer for simultaneous measurements of drop size and velocity distributions p 120 A85-10035

### Air Force Aero Propulsion Lab., Wright-Patterson AFB, Ohio.

Vibrations of twisted cantilevered plates - Summary of previous and current studies p 140 A85-22069

Vibrations of twisted cantilever plates - A comparison of theoretical results p 144 A85-47626

### Air Force Flight Dynamics Lab., Wright-Patterson AFB, Ohio.

Structural optimization using optimality criteria methods p 144 A85-48703

### Air Force Geophysics Lab., Hanscom AFB, Mass.

Spacecraft Environmental Interactions Technology, 1983 [NASA-CP-2359] p 39 N85-22470

### Akron Univ., Ohio.

An analysis of temperature effect in a finite journal bearing with spatial tilt and viscous dissipation p 126 A85-11074

Extension of constrained incremental Newton-Raphson scheme to generalized loading fields p 139 A85-13942

Progress in development of a Navier-Stokes solver for evaluation of iced airfoil performance [AIAA PAPER 85-0410] p 3 A85-19731

On the development of hierarchical solution strategies for nonlinear finite element formulations p 171 A85-21979

Plastic flow of plasma sprayed ceramics p 80 A85-24161

Pantographing self adaptive gap elements p 142 A85-37440

Quasi-static solution algorithms for kinematically/materially nonlinear thermomechanical problems p 143 A85-41983

Viscoplastic constitutive relationships with dependence on thermomechanical history [NASA-CR-174836] p 146 N85-21691

On thermomechanical testing in support of constitutive equation development for high temperature alloys [NASA-CR-174879] p 147 N85-25894

Some advances in experimentation supporting development of viscoplastic constitutive models [NASA-CR-174855] p 147 N85-27260

Thermomechanical deformation in the presence of metallurgical changes p 150 N85-31533

Some advances in experimentation supporting development of viscoplastic constitutive models p 151 N85-31545

Results of an interlaboratory fatigue test program conducted on alloy 800H at room and elevated temperatures

[NASA-CR-174940] p 152 N85-32340

A continuous damage model based on stepwise-stress creep rupture tests [NASA-CR-174941] p 152 N85-32341

Measurement and correlation of jet fuel viscosities at low temperatures [NASA-CR-174911] p 94 N85-34295

### Alabama Univ., Huntsville.

Experiments in charge control at geosynchronous orbit - ATS-5 and ATS-6 p 39 A85-35379

### ALPHATECH, Inc., Burlington, Mass.

A design methodology for robust failure detection and isolation p 171 A85-47794

### Analex Corp., Cleveland, Ohio.

Interdisciplinary design analysis of a precision spacecraft antenna [AIAA PAPER 85-0804] p 38 A85-30303

Computer program for the calculation of multicomponent convective diffusion deposition rates from chemically frozen boundary layer theory [NASA-CR-168329] p 116 N85-27164

### Applied Medical Technology, Inc., Brecksville, Ohio.

Percutaneous connectors [NASA-CR-175627] p 168 N85-27508

### Arizona State Univ., Tempe.

Multibus-based parallel processor for simulation p 169 A85-28613

Jet characteristics in confined swirling flow p 112 A85-45282

Density effects on jet characteristics in confined swirling flow p 112 A85-45283

Behavior of turbulent gas jets in an axisymmetric confinement [NASA-CR-174829] p 28 N85-25265

### Arizona Univ., Phoenix.

Creep-rupture reliability analysis p 143 A85-42566

### Arizona Univ., Tucson.

Effect of airfoil mean loading on convected gust interaction noise [AIAA PAPER 84-2324] p 173 A85-13955

Noise produced by the interaction of a rotor wake with a swept stator blade [AIAA PAPER 84-2326] p 173 A85-13956

The linear two-dimensional stability of inviscid vortex streets of finite-cored vortices [AD-A153032] p 107 A85-14241

Interply layer degradation effects on composite structural response [AIAA PAPER 84-0849] p 54 A85-16096

Reliability considerations for the total strain range version of strainrange partitioning [NASA-CR-174757] p 144 N85-11380

### Army Armament Research and Development Command, Dover, N. J.

Automatic sphericity interferometer for testing lens radii [AD-A155736] p 125 N85-33457

### Army Aviation Research and Development Command, Cleveland, Ohio.

Mechanical properties of SiC fiber-reinforced reaction-bonded Si3N4 composites [NASA-TM-87085] p 59 N85-34223

Generated spiral bevel gears: Optimal machine-tool settings and tooth contact analysis [NASA-TM-87075] p 136 N85-34405

Thermal stress analysis of a new turbine shroud seal concept [NASA-TM-87082] p 136 N85-34406

### Army Propulsion Lab., Cleveland, Ohio.

Comparison of icing cloud instruments for 1982-1983 icing season flight program [AIAA PAPER 84-0020] p 13 A85-16098

Hydrodynamic lubrication of rigid nonconformal contacts in combined rolling and normal motion [ASME PAPER 84-TRIB-13] p 127 A85-21280

A note on blade wake interaction influence on compressor stator row aerodynamic performance p 4 A85-32965

A computer aided design procedure for generating gear teeth [ASME PAPER 84-DET-184] p 128 A85-33779

Dynamic analysis of straight and involute tooth forms [ASME PAPER 84-DET-226] p 128 A85-33780

Temperature distortion generator for turboshaft engine testing [SAE PAPER 841541] p 15 A85-39065

High-temperature erosion of plasma-sprayed, yttria-stabilized zirconia in a simulated turbine environment [AIAA PAPER 85-1219] p 82 A85-39662

Rotor wake characteristics of a transonic axial flow fan [AIAA PAPER 85-1133] p 6 A85-43974

### Army Research and Technology Labs., Cleveland, Ohio.

Predicted turbine stage performance using quasi-three-dimensional and boundary-layer analyses p 15 A85-34013

Future fundamental combustion research for aeropropulsion systems [AIAA PAPER 85-1398] p 16 A85-42671

High-temperature erosion of plasma-sprayed, yttria-stabilized zirconia in a simulated turbine environment [NASA-TP-2406] p 84 N85-13045

Low cycle fatigue of MAR-M 200 single crystals at 760 and 870 deg C [NASA-TM-86933] p 74 N85-19074

Transmission efficiency measurements and correlations with physical characteristics of the lubricant p 89 N85-23781

Environmental effects on the tensile strength of chemically vapor deposited silicon carbide fibers [NASA-TM-86981] p 89 N85-24000

Multiaxial and thermomechanical fatigue considerations in damage tolerant design [NASA-TM-87022] p 76 N85-26964

DEAN: A program for dynamic engine analysis [NASA-TM-87033] p 30 N85-28945

### Avco Lycoming Div., Stratford, Conn.

Application of Runge Kutta time marching scheme for the computation of transonic flows in turbomachines [AIAA PAPER 85-1332] p 5 A85-39728

## B

### Babcock and Wilcox Co., Akron, Ohio.

Quasi-static solution algorithms for kinematically/materially nonlinear thermomechanical problems p 143 A85-41983

### Babcock and Wilcox Co., Alliance, Ohio.

High-temperature fiber optic pressure sensor p 123 A85-46607

### Babcock and Wilcox Co., New York, N.Y.

Extension of constrained incremental Newton-Raphson scheme to generalized loading fields p 139 A85-13942

**Ball Aerospace Systems Div., Boulder, Colo.**  
Fracture toughness of hot-pressed beryllium  
p 66 A85-25835

**Banaras Hindu Univ., Varanasi (India).**  
Hydrodynamic lubrication of rigid nonconformal contacts in combined rolling and normal motion  
[ASME PAPER 84-TRIB-13] p 127 A85-21280  
Thermal elastohydrodynamic lubrication of line contacts  
p 128 A85-31202

**Battelle Columbus Labs., Ohio.**  
A history dependent damage model for low cycle fatigue  
[ASME PAPER 84-PVP-112] p 140 A85-18795  
Preliminary analysis of space mission applications for electromagnetic launchers  
[NASA-CR-174067] p 35 N85-12071  
Composite loads spectra for select space propulsion structural components: Probabilistic load model development  
p 148 N85-27954

**Bell Telephone Labs., Inc., Allentown, Pa.**  
Optical linear algebra processors - Noise and error-source modeling  
p 169 A85-36727

**Bell Telephone Labs., Inc., Whippany, N. J.**  
A fast time domain digital simulation technique for power converters - Application to a buck converter with feedforward compensation  
p 101 A85-20900

**Boeing Aerospace Co., Seattle, Wash.**  
Space station propulsion options  
[AIAA PAPER 85-1155] p 45 A85-43975  
High voltage requirements and issues for the 1990's  
p 46 A85-45429

Applicability of 100kWe-class of space reactor power systems to NASA manned space station missions  
[NASA-CR-174696] p 177 N85-35728  
**Boeing Commercial Airplane Co., Seattle, Wash.**  
Detailed studies of aviation fuel flowability  
[NASA-CR-174938] p 94 N85-31308

**Boeing Vertol Co., Philadelphia, Pa.**  
Performance degradation of helicopter rotor in forward flight due to ice  
p 11 A85-42937

**Bolt, Beranek, and Newman, Inc., Cambridge, Mass.**  
Turbofan noise generation. Volume 2: Computer programs  
[NASA-CR-167952] p 175 N85-11791

**Bonneville Power Administration, Portland, Ore.**  
Government review of the Mod-2 wind turbine (as-built)  
[NASA-TM-86983] p 162 N85-29365

**Braun (Willis H.), Berea, Ohio.**  
Unsteady flow in a supersonic cascade with two in-passage shocks  
[NASA-CR-3925] p 10 N85-35158

## C

**California Inst. of Tech., Pasadena.**  
The linear two-dimensional stability of inviscid vortex streets of finite-cored vortices  
[AD-A153032] p 107 A85-14241  
Vortex induced lift on a flat plate with a curved forward-facing flap  
p 4 A85-30175  
Growth of a diffusion flame in the field of a vortex  
p 61 A85-47320  
Free-surface phenomena under low- and zero-gravity conditions  
[NASA-CR-175835] p 116 N85-27168

**California State Univ., Long Beach.**  
Into mesh lubrication of spur gears with arbitrary offset oil jet. I - For jet velocity less than or equal to gear velocity  
p 128 A85-24497  
Lubricant jet flow phenomena in spur and helical gears with modified center distances and/or addendums - For out-of-mesh conditions  
[ASME PAPER 84-DET-96] p 129 A85-35049

**California Univ., Berkeley.**  
Effects of SO<sub>2</sub> and SO<sub>3</sub> on the Na<sub>2</sub>SO<sub>4</sub> induced corrosion of nickel  
p 65 A85-15603  
Recent advances in methods for numerical solution of O.D.E. initial value problems  
p 171 A85-21370  
Properties of coated and modified surfaces  
p 53 A85-36694

**California Univ., Berkeley. Lawrence Berkeley Lab.**  
Knock syndrome: Its cures and its victims  
[NASA-CR-174395] p 93 N85-19185

**California Univ., Irvine.**  
A two-equation turbulence model for two-phase jets  
p 107 A85-14376  
Prism-coupled light emission from tunnel junctions  
p 181 A85-21425  
Substrate-induced orientational order in the isotropic phase of liquid crystals  
p 181 A85-24649

**California Univ., Los Angeles.**  
The response of Helmholtz resonators to external excitation. I - Single resonators  
p 174 A85-26915

Data flow methods for dynamic system simulation - A CSSL-IV microcomputer network interface  
p 170 A85-28614

A functional language approach in high-speed digital simulation  
p 170 A85-28615  
General approaches for achieving high speed computations  
p 169 A85-28628  
Functional language and data flow architectures  
p 170 A85-28629

Vortex modeling of single and multiple dilution jet mixing in a crossflow  
[AIAA PAPER 85-1580] p 111 A85-40701

**Carnegie-Mellon Univ., Pittsburgh, Pa.**  
Effects of friction dampers on aerodynamically unstable rotor stages  
p 14 A85-21866  
Optical linear algebra processors - Noise and error-source modeling  
p 169 A85-36727

**Case Western Reserve Univ., Cleveland, Ohio.**  
An analysis of temperature effect in a finite journal bearing with spatial tilt and viscous dissipation  
p 126 A85-11074

Statistics and thermodynamics of fracture  
p 140 A85-19433  
Flame flashback in a premixed dump combustor  
[AIAA PAPER 85-0145] p 60 A85-19550

The effect of plasma on solar cell array arc characteristics  
[AIAA PAPER 85-0384] p 43 A85-19713  
Circular waveguide bifurcation for asymmetric modes  
p 101 A85-20170

Dual-mode coaxial feed with low crosspolarisation  
p 101 A85-20171  
Plastic flow of plasma sprayed ceramics  
p 80 A85-24161

Elevated temperature creep-rupture behavior of the single crystal nickel-base superalloy NASAIR 100  
p 66 A85-27812

A procedure for obtaining explicit solutions to a class of Fredholm integral equations  
p 171 A85-28006  
Influence of composition on the microstructure and mechanical properties of a nickel-base superalloy single crystal  
p 66 A85-32387

Factors which influence directional coarsening of gamma-prime during creep in nickel-base superalloy single crystals  
p 67 A85-32388  
Dendritic solidification. I - Analysis of current theories and models. II - A model for dendritic growth under an imposed thermal gradient  
p 182 A85-38019

A new interpretation of internal heat transfer coefficients of porous media  
[ASME PAPER 84-WA/HT-51] p 110 A85-39894  
Dopant effect of yttrium and the growth and adherence of alumina on nickel-aluminum alloys  
p 82 A85-40973

Mechanism for chelated sulfate formation from SO<sub>2</sub> and bis (triphenylphosphine) platinum  
p 62 A85-48493  
Mechanism for forming hydrogen chloride and sodium sulfate from sulfur trioxide, water, and sodium chloride  
p 62 A85-48513

The transient oxidation of single crystal NiAl+Zr  
[NASA-CR-174756] p 70 N85-11221  
Analysis techniques for tracer studies of oxidation  
[NASA-CR-174796] p 84 N85-12162

Experimental test program for evaluation of solid lubricant coating as applied to compliant foil gas bearings to 315 deg C  
[NASA-CR-174837] p 85 N85-15895  
Effect of reduction of strategic Columbium addition in 718 Alloy on the structure and properties  
[NASA-CR-174841] p 75 N85-21320

Translational and extensional energy release rates (the J- and M-integrals) for a crack layer in thermoelasticity  
[NASA-CR-174872] p 145 N85-21685  
Dilution jet configurations in a reverse flow combustor  
[NASA-CR-174888] p 27 N85-22392

Electron yields from spacecraft materials  
p 40 N85-22512  
Study of Kapton under simulated shuttle environment  
[NASA-CR-176003] p 41 N85-29997

Why CO bonds side-on at low coverage and both side-on and upright at high coverage on the Cr(110) surface  
[NASA-CR-176071] p 77 N85-32173  
Molecular orbital studies in oxidation: Sulfate formation and metal-metal oxide adhesion  
[NASA-CR-176070] p 77 N85-32174

Adsorption of O<sub>2</sub>, SO<sub>2</sub>, and SO<sub>3</sub> on nickel oxide. Mechanism for sulfate formation  
[NASA-CR-176072] p 77 N85-32175  
CO adsorption on (111) and (100) surfaces of the Pt sub 3 Ti alloy. Evidence for parallel binding and strong activation of CO  
[NASA-CR-176077] p 77 N85-32176

Perturbation-iteration theory for analyzing microwave striplines  
[NASA-CR-176189] p 100 N85-35321

**CBS Labs., Stamford, Conn.**  
Experimental results supporting the determination of service quality objectives for DBS systems  
p 96 A85-29611

**Chevron Oil Field Research Co., La Habra, Calif.**  
The linear two-dimensional stability of inviscid vortex streets of finite-cored vortices  
[AD-A153032] p 107 A85-14241

**Chronos Research Labs., Inc., Olivehain, Calif.**  
Pyroelectric conversion in space  
p 45 A85-45377

**Cincinnati Univ., Ohio.**  
Computation of internal flows: Methods and applications; Proceedings of the Energy Sources Technology Conference, New Orleans, LA, February 12-16, 1984  
p 106 A85-11630

Two-dimensional internal compressible viscous flows using semi-elliptic analysis  
p 106 A85-11640  
A study of fatigue damage mechanisms in Waspaloy from 25 to 800 C  
p 65 A85-12098

High-voltage solar-cell chip  
p 154 A85-24668  
A computer aided design procedure for generating gear teeth  
[ASME PAPER 84-DET-184] p 128 A85-33779

Dynamic analysis of straight and involute tooth forms  
[ASME PAPER 84-DET-226] p 128 A85-33780  
The three-dimensional compressible flow in a radial inflow turbine scroll  
p 6 A85-41826

Finite element analysis of notch behavior using a state variable constitutive equation  
p 152 N85-31548  
**Clarkson Coll. of Technology, Potsdam, N.Y.**  
Electroanalysis of fuel cell reactions: Investigation of alternate electrolytes  
[NASA-CR-174753] p 157 N85-11455

**Clemson Univ., S.C.**  
Heat transfer and fluid mechanics measurements in transitional boundary layer flows  
p 118 N85-31439

**Cleveland State Univ., Ohio.**  
Control algorithms and computer simulation of a stand-alone photovoltaic village power system  
p 153 A85-11345  
Near-optimum design of GaAs-based concentrator space solar cells for 80 C operation  
p 153 A85-15800

Applicability of the Meyer-Neldel rule to solar cells  
p 154 A85-19948  
A unified relation for cavitation erosion  
p 109 A85-24445

The subjective effect of multiple co-channel frequency modulated television interference  
p 96 A85-28234  
On the subjective evaluation of the interference protection ratios' measurements for co-channel FM-TV signals  
p 96 A85-28241

Theory of the high base resistivity n(+)/pp(+)-silicon solar cell and its application to radiation damage effects  
p 154 A85-32639  
Gear mesh stiffness and load sharing in planetary gearing  
[ASME PAPER 84-DET-229] p 129 A85-33781

Incident beam polarization for laser Doppler velocimetry employing a sapphire cylindrical window  
p 122 A85-39835  
Combined influence of unsteady free stream velocity and free stream turbulence on stagnation point heat transfer  
p 112 A85-41782

Preliminary design of a 10 kW thermophotovoltaic system for space applications  
p 45 A85-45371  
Manual of phosphoric acid fuel cell power plant optimization model and computer program  
[NASA-CR-174721] p 157 N85-10445

Manual of phosphoric acid fuel cell stack three-dimensional model and computer program  
[NASA-CR-174722] p 157 N85-10447  
Phosphoric acid fuel cell power plant system performance model and computer program  
[NASA-CR-174638] p 157 N85-11456

A historical overview of the electrical power systems in the US manned and some US unmanned spacecraft  
[NASA-CR-174806] p 47 N85-13910  
Investigation on experimental techniques to detect, locate and quantify gear noise in helicopter transmissions  
[NASA-CR-3847] p 176 N85-17667

Conceptual design of a fixed-pitch wind turbine generator system rated at 400 kilowatts  
[NASA-CR-174877] p 162 N85-29363

**College of William and Mary, Williamsburg, Va.**  
The use of Ada in distributed simulations  
p 169 A85-28612

Moving target, distributed, real-time simulation using Ada  
p 170 A85-34131

**Colorado School of Mines, Golden.**  
Jet fuel instability mechanisms  
[NASA-CR-175856] p 93 N85-28127

**Colorado State Univ., Fort Collins.**  
Ion flow experiments in a multipole discharge chamber  
p 178 A85-12705

- Theory of ion acceleration with closed electron drift  
p 41 A85-15512
- Efficient solution of the Euler and Navier-Stokes equations with a vectorized multiple-grid algorithm  
p 2 A85-18679
- Columbia Univ., New York.**  
Modeling of gamma/gamma-prime phase equilibrium in the nickel-aluminum system  
p 65 A85-14959  
Effects of cobalt on the hot workability of nickel-base superalloys  
p 67 A85-32412
- Concordia Univ., Montreal (Quebec).**  
Recent advances in methods for numerical solution of O.D.E. initial value problems  
p 171 A85-21370
- Connecticut Univ., Storrs.**  
Mass and momentum turbulent transport experiments with confined coaxial jets  
p 107 A85-14399  
Biaxial constitutive equation development for single crystals  
[NASA-CR-174056]  
p 183 A85-11862  
Iron rich low cost superalloys  
[NASA-CR-174900]  
p 76 A85-26962  
Elevated temperature biaxial fatigue  
[NASA-CR-175795]  
p 148 A85-27263
- Control Data Corp., Minneapolis, Minn.**  
GASP cloud encounter statistics - Implications for laminar flow control flight  
p 166 A85-11979  
A comparison of NMC and GWC analysis field temperatures with aircraft measurements  
p 166 A85-21140  
Variability of cloudiness at airline cruise altitudes from GASP measurements  
p 166 A85-31199
- Cornell Univ., Ithaca, N.Y.**  
Combustion efficiency of a premixed continuous flow combustor  
p 61 A85-42571  
A theory of post-stall transients in multistage axial compression systems  
[NASA-CR-3878]  
p 8 A85-21117
- Creare, Inc., Hanover, N.H.**  
An experimental investigation of rubbing interaction in labyrinth seals at cryogenic temperature  
p 129 A85-39938  
Analytical and experimental investigation of rubbing interaction in labyrinth seals for a liquid hydrogen fuel pump  
[NASA-CR-174657]  
p 48 A85-18084
- Cummins Engine Co., Inc., Columbus, Ind.**  
Advanced automotive diesel assessment program  
[NASA-CR-168285]  
p 130 A85-13235
- ## D
- Dartmouth Coll., Hanover, N.H.**  
Thermal and thermomechanical effects in dry sliding  
p 127 A85-23838  
An experimental investigation of rubbing interaction in labyrinth seals at cryogenic temperature  
p 129 A85-39938
- Defence Metallurgical Research Lab., Hyderabad (India).**  
Deformation and fracture behavior of Ni-Mo-Al(gamma/gamma prime-alpha) in situ composite  
p 64 A85-11058
- Delaware Univ., Newark.**  
New eutectic alloys and their heats of transformation  
p 66 A85-27808
- Department of Communications, Ottawa (Ontario).**  
Development and use of the computer software package for planning the 12 GHz broadcasting-satellite service at RARC '83  
p 96 A85-29605  
Experimental results supporting the determination of service quality objectives for DBS systems  
p 96 A85-29611
- Department of Energy, Washington, D. C.**  
Apparatus and method for identification of matrix materials in which transuranic elements are embedded using thermal neutron capture gamma-ray emission  
[DE85-011659]  
p 125 A85-33454  
Manufacturing process to reduce large grain growth in zirconium alloys  
[DE85-011649]  
p 78 A85-34267
- Detroit Diesel Allison, Indianapolis, Ind.**  
Analytical fuel property effects--small combustors  
[NASA-CR-174738]  
p 28 A85-26709  
Advanced Gas Turbine (AGT) technology project  
[NASA-CR-174798]  
p 31 A85-29961
- Douglas Aircraft Co., Inc., Long Beach, Calif.**  
Calculation of compressible flow about three-dimensional inlets with auxiliary inlets, slats and vanes by means of a panel method  
[AIAA PAPER 85-1196]  
p 5 A85-40817  
Low-speed aerodynamic test of an axisymmetric supersonic inlet with variable cowl slot  
[AIAA PAPER 85-1210]  
p 5 A85-40819

- Calculation of compressible flow about three-dimensional inlets with auxiliary inlets, slats and vanes by means of a panel method  
[NASA-CR-174975]  
p 10 A85-35162
- Draper (Charles Stark) Lab., Inc., Cambridge, Mass.**  
First-order ball-bearing kinematics  
p 128 A85-31203
- Drexel Univ., Philadelphia, Pa.**  
Use of static indentation laws in the impact analysis of laminated composite plates  
p 55 A85-29133
- Duke Univ., Durham, N. C.**  
A space-marching method for incompressible Navier-Stokes equations  
[AIAA PAPER 85-0170]  
p 108 A85-19564

## E

- EIC, Inc., Norwood, Mass.**  
Moderate temperature sodium cells. V - Discharge reactions and rechargeability of NiS and NiS<sub>2</sub> positive electrodes in molten NaAlCl<sub>4</sub>  
p 59 A85-11892
- Electrotek Concepts, Inc., Knoxville, Tenn.**  
Experimental investigation of a variable speed constant frequency electric generating system from a utility perspective  
[NASA-CR-174950]  
p 105 A85-32251
- Enertech Corp., Norwich, Vt.**  
Measured effects of wind turbine generation at the Block Island Power Company  
p 153 A85-10652
- Engelhard Industries, Inc., Edison, N.J.**  
Develop and test fuel cell powered on-site integrated total energy systems. Phase 3: Full-scale power plant development  
[NASA-CR-174887]  
p 161 A85-25941  
Develop and test fuel cell powered on-site integrated total energy systems. Phase 3: Full-scale power plant development  
[NASA-CR-168338]  
p 164 A85-30483
- Environmental Research Inst. of Michigan, Ann Arbor.**  
Comparison of atmospheric correction algorithms for the Coastal Zone Color Scanner  
p 153 A85-10244
- Exxon Research and Engineering Co., Linden, N.J.**  
Jet fuel property changes and their effect on producibility and cost in the U.S., Canada, and Europe  
[NASA-CR-174840]  
p 93 A85-27012

## F

- Florida State Univ., Tallahassee.**  
A multiple-scales model of the shock-cell structure of imperfectly expanded supersonic jets  
p 113 A85-49354
- Flow Research, Inc., Kent, Wash.**  
Direct numerical simulations of a reacting mixing layer with chemical heat release  
[AIAA PAPER 85-0143]  
p 60 A85-19548  
Direct simulations of chemically reacting turbulent mixing layers  
[AIAA PAPER 85-0321]  
p 60 A85-19666
- Ford Aerospace and Communications Corp., Palo Alto, Calif.**  
The 20 GHz proof-of-concept test model results for a multiple scan beam dual reflector antenna  
[NASA-CR-174268]  
p 98 A85-15944
- Ford Motor Co., Dearborn, Mich.**  
Fracture of yttria-doped, sintered reaction-bonded silicon nitride  
[ACS PAPER 7-J3-84]  
p 82 A85-42797
- Foster Wheeler Corp., Houston, Tex.**  
Advanced technology cogeneration system conceptual design study: Closed cycle gas turbines  
[NASA-CR-168222]  
p 159 A85-16300

## G

- Garrett Turbine Engine Co., Phoenix, Ariz.**  
Ceramic component development for the AGT101 gas turbine engine  
p 126 A85-15972  
Life modeling of atmospheric and low pressure plasma-sprayed thermal-barrier coating  
p 81 A85-29728  
Development of coated single-crystal superalloy systems for gas turbine applications  
p 68 A85-32440  
Progress in the utilization of an oxide-dispersion-strengthened alloy for small engine turbine blades  
[SAE PAPER 841512]  
p 68 A85-39284  
Experiments in dilution jet mixing - Effects of multiple rows and non-circular orifices  
[AIAA PAPER 85-1104]  
p 15 A85-39606  
Creep-rupture reliability analysis  
p 143 A85-42566  
Advanced technology cogeneration system conceptual design study: Closed cycle gas turbines  
[NASA-CR-168222]  
p 159 A85-16300

- Advanced Gas Turbine (AGT) powertrain system development for automotive applications  
[NASA-CR-174809]  
p 185 A85-18831
- General Dynamics/Convair, San Diego, Calif.**  
Effect of low temperature on fatigue and fracture properties of Ti-5Al-2.5Sn(ELI) for use in engine components  
p 70 A85-47972
- General Electric Co., Cincinnati, Ohio.**  
Comparison of scaled model data to full size energy efficient engine test results  
[AIAA PAPER 84-2281]  
p 13 A85-13953  
Measurement and prediction of Energy Efficient Engine noise  
[AIAA PAPER 84-2284]  
p 13 A85-13954  
Considerations for damage analysis of gas turbine hot section components  
[ASME PAPER 84-PVP-77]  
p 14 A85-18792  
Altitude testing of a flight weight, self-cooled, 2D thrust vectoring exhaust nozzle  
[SAE PAPER 841557]  
p 14 A85-25984  
Life modeling of atmospheric and low pressure plasma-sprayed thermal-barrier coating  
p 81 A85-29728
- Unified constitutive material models for nonlinear finite-element structural analysis  
[AIAA PAPER 85-1418]  
p 142 A85-39769  
Stall recovery control strategy methodology and results  
[AIAA PAPER 85-1433]  
p 16 A85-40841  
Energy efficient engine component development and integration program  
[NASA-CR-169496]  
p 22 A85-10989  
Energy efficient engine component development and integration program  
[NASA-CR-170034]  
p 22 A85-10990  
Energy efficient engine ICLS Nacelle detail design report  
[NASA-CR-167870]  
p 22 A85-10993  
Energy efficient engine. Low pressure turbine test hardware detailed design report  
[NASA-CR-167956]  
p 22 A85-10994  
Energy efficient engine high pressure turbine test hardware detailed design report  
[NASA-CR-167955]  
p 23 A85-10995  
Energy efficient engine high pressure turbine ceramic shroud support technology report  
[NASA-CR-168036]  
p 23 A85-10996  
Energy efficient engine ICLS engine bearings, drives and configuration: Detail design report  
[NASA-CR-167871]  
p 23 A85-10997  
Energy efficient engine. High pressure compressor detail design report  
[NASA-CR-165558]  
p 23 A85-10998  
Advanced blade tip seal system, volume 2  
[NASA-CR-167851]  
p 23 A85-10999  
Materials for advanced turbine engines. Project 2: Rene 150 directionally solidified superalloy turbine blades, volume 2  
[NASA-CR-167993]  
p 23 A85-12059  
Experimental investigation of shock-cell noise reduction for dual-stream nozzles in simulated flight  
[NASA-CR-3846]  
p 175 A85-13549  
Experimental investigation of shock-cell noise reduction for single stream nozzles in simulated flight  
[NASA-CR-3845]  
p 175 A85-13550  
Study of advanced fuel system concepts for commercial aircraft  
[NASA-CR-174751]  
p 12 A85-19978  
Development of a rotor wake-vortex model, volume 1  
[NASA-CR-174849]  
p 9 A85-26668  
Effects of surface chemistry on hot corrosion life  
[NASA-CR-174915]  
p 28 A85-26711  
Component-specific modeling  
[NASA-CR-174765]  
p 147 A85-27261  
Energy Efficient Engine (E3) controls and accessories detail design report  
[NASA-CR-168017]  
p 31 A85-29957  
Component-specific modeling  
[NASA-CR-174925]  
p 32 A85-32119  
A review of path-independent integrals in elastic-plastic fracture mechanics, task 4  
[NASA-CR-174956]  
p 152 A85-33541  
High pressure compressor component performance report  
[NASA-CR-168245]  
p 33 A85-34138  
Component-specific modeling  
[NASA-CR-174765]  
p 33 A85-34140  
Energy efficient engine. Fan and quarter-stage component performance report  
[NASA-CR-168070]  
p 33 A85-34141  
Flow modifying device  
[NASA-CASE-LEW-13562-2]  
p 33 A85-35195  
Energy efficient engine, high pressure turbine thermal barrier coating. Support technology report  
[NASA-CR-168037]  
p 34 A85-35199

**General Electric Co., Lynn, Mass.**

- Contingency power concepts for helicopter turboshaft engine p 15 A85-32005  
 TF34 convertible engine control system design p 15 A85-32006  
 Analytical fuel property effects: Small combustors, phase 2 [NASA-CR-174848] p 93 N85-19175

**General Electric Co., Philadelphia, Pa.**

- Advanced multi-megawatt wind turbine design for utility application p 157 A85-45517  
 Transformation toughened ceramics for the heavy duty diesel engine technology program [NASA-CR-174689] p 185 N85-16698

**General Electric Co., Schenectady, N. Y.**

- Prediction of an axisymmetric combustor flow p 59 A85-12713  
 Laser balancing system for high material removal rates [NASA-CR-174731] p 126 N85-12341  
 Effects of vane/blade ratio and spacing on fan noise, volume 1 [NASA-CR-174664] p 176 N85-19791  
 Effects of vane/blade ratio and spacing on fan noise. Volume 2: Data supplement [NASA-CR-174665] p 176 N85-19792  
 Advanced smoke meter development survey and analysis [NASA-CR-168287] p 124 N85-25792  
 Parametric study of potential early commercial power plants Task 3-A MHD cost analysis [NASA-CR-175839] p 161 N85-27377  
 Manufacturing process to reduce large grain growth in zirconium alloys [DE85-011649] p 78 N85-34267

**General Electric Co., Syracuse, N. Y.**

- Configuration study for a 30 GHz monolithic receive array: Technical assessment [NASA-CR-174697] p 98 N85-18238  
 Configuration study for a 30 GHz monolithic receive array, volume 1 [NASA-CR-174697-VOL-1] p 98 N85-18239  
 Configuration study for a 30 GHz monolithic receive array, volume 2 [NASA-CR-174697-VOL-2] p 99 N85-18240

**General Motors Corp., Indianapolis, Ind.**

- Ceramic components for gas turbine engines p 127 A85-15973  
 Photoacoustic microscopy of ceramic turbine blades p 83 A85-43930  
 An investigation of enhanced capability thermal barrier coating systems for diesel engine components [NASA-CR-174820] p 86 N85-18154  
 Ceramic applications in turbine engines [NASA-CR-174715] p 91 N85-28109
- General Motors Research Labs., Warren, Mich.**  
 Drop-turbulence interactions in a diffusion flame [AIAA PAPER 85-0319] p 60 A85-19665  
 Development and testing of stable, invariant, isoparametric curvilinear 2- and 3-D hybrid-stress elements p 140 A85-19899

**Georgia Inst. of Tech., Atlanta.**

- A study of fatigue damage mechanisms in Waspalloy from 25 to 800 C p 65 A85-12098  
 Hybrid stress finite elements for large deformations of inelastic solids p 139 A85-15894  
 Development and testing of stable, invariant, isoparametric curvilinear 2- and 3-D hybrid-stress elements p 140 A85-19899  
 The effect of microstructure, temperature, and hold-time on low-cycle fatigue of As HIP P/M Rene 95 p 67 A85-32399

- On the existence and stability conditions for mixed-hybrid finite element solutions based on Reissner's variational principle p 142 A85-33847

- Thermodynamically consistent constitutive equations for nonisothermal large strain, elasto-plastic, creep behavior [AIAA PAPER 85-0621] p 142 A85-38425  
 Constitutive modeling and computational implementation for finite strain plasticity p 143 A85-40910

- Technology for satellite power conversion [NASA-CR-174335] p 159 N85-18451  
 Study of the effects of implantation on the high Fe-Ni-Cr and Ni-Cr-Al alloys [NASA-CR-175625] p 76 N85-22661

- Analysis of shell type structures subjected to time dependent mechanical and thermal loading [NASA-CR-175747] p 147 N85-25896  
 Dynamic creep buckling: Analysis of shell structures subjected to time-dependent mechanical and thermal loading p 149 N85-27959

**Georgia Tech Research Inst., Atlanta.**

- Infrared technology for satellite power conversion [NASA-CR-174266] p 159 N85-16293

**Gibbs and Hill, Inc., New York.**

- Advanced technology cogeneration system conceptual design study: Closed cycle gas turbines [NASA-CR-168222] p 159 N85-16300

**Giner, Inc., Waltham, Mass.**

- Development of electrodes for the NASA iron/chromium [NASA-CR-174724] p 165 N85-35471

**GMAF, Inc., Freeport, N. Y.**

- Inverse design technique for cascades [NASA-CR-3836] p 7 N85-12008

**Goodrich (B. F.) Co., Akron, Ohio.**

- Pantographing self adaptive gap elements p 142 A85-37440

**Grumman Aerospace Corp., Bethpage, N. Y.**

- The computation of viscous/inviscid interaction on airfoils with separated flow p 6 A85-42954

**GT-Devices, Alexandria, Va.**

- Investigation of a pulsed electrothermal thruster system [NASA-CR-174768] p 46 N85-11132

**H****Hamilton Standard, Windsor Locks, Conn.**

- Large-scale Advanced Propfan (LAP) performance, acoustic and weight estimation, January, 1984 [NASA-CR-174782] p 9 N85-22368  
 Multi-mesh gear dynamics program evaluation and enhancements [NASA-CR-174747] p 133 N85-28372
- Hamilton Standard Div., United Aircraft Corp., Windsor Locks, Conn.**  
 Large-scale advanced propfan (LAP) program progress report [AIAA PAPER 85-1187] p 17 A85-47021

**Hiroshima Univ. (Japan).**

- A unified relation for cavitation erosion p 109 A85-24445

**Honeywell, Inc., Lexington, Mass.**

- Mosaic Infrared Sensor for Space Astronomy (MIRSSA) [NASA-CR-176154] p 125 N85-33456

**Hughes Aircraft Co., El Segundo, Calif.**

- Environmentally-induced voltage limitations in large space power systems p 43 A85-18584  
 Advanced nickel-hydrogen cell configuration study [NASA-CR-174775] p 157 N85-10444

**Hughes Aircraft Co., Torrance, Calif.**

- A 20 GHz, 75 watt, helix TWT for space communications p 101 A85-14433  
 Sixty GHz IMPATT diode development [NASA-CR-174969] p 105 N85-33293

**Hughes Research Labs., Malibu, Calif.**

- IAPS (8-cm) ion thruster cyclic endurance test p 42 A85-16406  
 Ion propulsion for communications satellites p 42 A85-16412  
 Ring-cusp ion thrusters p 42 A85-16438  
 Long life nickel electrodes for a nickel-hydrogen cell. III - Results of an accelerated test and failure analyses p 156 A85-45391  
 Characterization of 8-cm engineering model thruster [NASA-CR-174673] p 46 N85-11131  
 Ion thruster system (8-cm) cyclic endurance test [NASA-CR-174745] p 47 N85-12937  
 Extended performance technology study 30-cm thruster [NASA-CR-168259] p 48 N85-15806  
 The failure mechanism of a nickel electrode in a nickel-hydrogen cell p 105 N85-31408

**IBM Watson Research Center, Yorktown Heights, N. Y.**

- Substrate-induced orientational order in the isotropic phase of liquid crystals p 181 A85-24649

**IIT Research Inst., Chicago, Ill.**

- Creep-rupture behavior of iron superalloys in high-pressure hydrogen [NASA-CR-174411] p 74 N85-19078

**Illinois Univ., Urbana.**

- Plot of modal field distribution in rectangular and circular waveguides p 101 A85-25170  
 The influence of temperature on the lubricating effectiveness of MoS<sub>2</sub> dispersed in mineral oils [ASLE PREPRINT 84-LC-2A-2] p 80 A85-25963  
 On the calculation of the directivity of planar array feeds for satellite reflector applications p 97 A85-32249  
 Rapid solidification and dynamic compaction of Ni-base superalloy powders p 67 A85-32414  
 Properties of coated and modified surfaces p 53 A85-36694  
 Focal shifts in parabolic reflectors p 97 A85-39356

- MMIC devices for active phased array antennas [NASA-CR-174281] p 98 N85-15943  
 Behavior of the lean methane-air flame at zero-gravity [NASA-CR-175586] p 62 N85-21283  
 Numerical methods for analyzing electromagnetic scattering [NASA-CR-175507] p 99 N85-21438  
 Normal modes in an overmoded circular waveguide coated with lossy material p 100 N85-35320  
 Characterization of microstrip discontinuities in the time and frequency domains [NASA-CR-176190] p 106 N85-35342  
 The use of a laser Doppler velocimeter in a standard flammability tube [NASA-CR-174960] p 125 N85-35389

**Illinois Univ., Urbana-Champaign.**

- The mechanisms of flame holding in the wake of a bluff body [NASA-CR-174058] p 62 N85-11149  
 The study of microstrip antenna arrays and related problems [NASA-CR-174054] p 97 N85-11265  
 The mechanisms of flame holding in the wake of a bluff body [NASA-CR-3866] p 26 N85-21166

**Imperial Coll. of Science and Technology, London (England).**

- Assessment of discretization schemes to reduce numerical diffusion in the calculation of complex flows [AIAA PAPER 85-0441] p 108 A85-19751

**Indian Inst. of Tech., Madras.**

- Natural frequencies of twisted rotating plates p 141 A85-32343

**Integral Technologies, Inc., Westmont, Ill.**

- Methods for heat transfer and temperature field analysis of the insulated diesel [NASA-CR-174783] p 185 N85-16699

**Iowa State Univ. of Science and Technology, Ames.**

- A note on blade wake interaction influence on compressor stator row aerodynamic performance p 4 A85-32965

**Iowa Univ., Iowa City.**

- Development of finite analytic method for unsteady three-dimensional Navier-Stokes equation p 106 A85-11647  
 Effects of chemical releases by the STS 3 orbiter on the ionosphere p 166 A85-29538  
 DE-1 measurements of AKR wave directions p 166 A85-37717  
 Suprathermal plasma observed on STS-3 Mission by plasma diagnostics package p 179 N85-22472

**J****Jet Propulsion Lab., California Inst. of Tech., Pasadena.**

- An evaluation of oxygen/hydrogen propulsion systems for the Space Station [AIAA PAPER 85-1156] p 45 A85-43976  
 Feasibility demonstration of a novel, flat-belt, continuously variable transmission or automotive and electric-hybrid vehicle application [NASA-CR-174430] p 185 N85-19894  
 An evaluation of oxygen-hydrogen propulsion systems for the Space Station [NASA-TM-87059] p 52 N85-28971

**John Carroll Univ., Cleveland, Ohio.**

- Remote displacement measurements using a laser diode p 121 A85-24464

**John Deere Technologies International, Inc., Wood-Ridge, N. J.**

- Stratified charge rotary aircraft engine technology enablement program [NASA-CR-174812] p 25 N85-21163

**K****Kansas Univ., Lawrence.**

- Numerical simulations of positively-biased probes and dielectric-conductor disks in a plasma p 179 A85-17262  
 Numerical simulation of positive-potential conductors in the presence of a plasma and a secondary-emitting dielectric p 102 A85-35306

**Kentucky Univ., Lexington.**

- Gravitational effects on flames spreading over thick solid surfaces [IAF PAPER 84-154] p 59 A85-13092  
 Solids mixing in a three phase fluidized bed containing spherically shaped-porous solid particles [PB85-187961] p 120 N85-33453

**Kumm (Emerson L.), Tempe, Ariz.**

Feasibility demonstration of a novel, flat-belt, continuously variable transmission or automotive and electric-hybrid vehicle application  
[NASA-CR-174430] p 185 N85-19894

**L****Life Systems, Inc., Cleveland, Ohio.**

Engineering model system study for a regenerative fuel cell: Study report  
[NASA-CR-174801] p 158 N85-16292

**Little (Arthur D.), Inc., Cambridge, Mass.**

Preliminary evaluation of a liquid belt radiator for space applications  
[NASA-CR-174807] p 47 N85-15804

**Little (Arthur D.), Inc., Santa Monica, Calif.**

Advanced technology cogeneration system conceptual design study: Closed cycle gas turbines  
[NASA-CR-168222] p 159 N85-16300

**Lockheed-California Co., Burbank.**

Effect of low temperature on fatigue and fracture properties of Ti-5Al-2.5Sn(ELI) for use in engine components  
[NASA-CR-174752] p 70 A85-47972

Study of advanced fuel system concepts for commercial aircraft and engines  
[NASA-CR-174752] p 93 N85-19176

**Lockheed-Georgia Co., Marietta.**

An experimental study of tone excited heated jets  
[AIAA PAPER 84-2341] p 172 A85-10882

Some unique experiments on receptivity  
[AIAA PAPER 85-0533] p 174 A85-25932

Acoustic control of free jet mixing  
[AIAA PAPER 85-0569] p 109 A85-25951

**Loral Electro-Optical Systems, Inc., Pasadena, Calif.**

Inert gas test of two 12-cm magnetostatic thrusters  
p 43 A85-29310

**Louisiana State Univ., Baton Rouge.**

Systematic optimization of a detailed kinetic model using a methane ignition example  
p 59 A85-12890

Transferring data oscilloscope to an IBM using an Apple II+  
[NASA-CR-174880] p 63 N85-25444

**Lulea Univ. (Sweden).**

Elastohydrodynamic lubrication of line contacts  
p 126 A85-11069

**M****MARC Analysis Research Corp., Palo Alto, Calif.**

Probabilistic finite element development  
p 149 N85-27956

**Martin Marietta Aerospace, Denver, Colo.**

Main propulsion system design recommendations for an advanced Orbit Transfer Vehicle  
[AIAA PAPER 85-1336] p 36 A85-39730

Technology requirements to be addressed by the NASA Lewis Research Center Cryogenic Fluid Management Facility program  
[AIAA PAPER 85-1229] p 94 A85-47024

Fiberglass epoxy laminate fatigue properties at 300 and 20 K  
p 56 A85-47970

**Massachusetts Inst. of Tech., Cambridge.**

Rational approach for assumed stress finite elements  
p 139 A85-12029

Flutter and forced response of mistuned rotors using standing wave analysis  
p 139 A85-12721

Hybrid Semiloof elements for plates and shells based upon a modified Hu-Washizu principle  
p 139 A85-15893

A numerical study of the steady scalar convective diffusion equation for small viscosity  
p 107 A85-16533

Three-dimensional inviscid flow analysis of turbulent forced mixers  
[AIAA PAPER 85-0086] p 2 A85-19510

Methanol as a soot reducer in a turbulent swirling burner  
[ASME PAPER 84-JPGC-GT-2] p 61 A85-23192

Evolution of assumed stress hybrid finite element  
p 142 A85-35046

Axisymmetric solid elements by a rational hybrid stress method  
p 143 A85-41109

Rotor wake characteristics of a transonic axial flow fan  
[AIAA PAPER 85-1133] p 6 A85-43974

Thermal-mechanical fatigue crack growth in Inconel X-750  
[NASA-CR-174740] p 72 N85-15877

Metal vapor arc switch electromagnetic accelerator technology  
[NASA-CR-174380] p 103 N85-18259

Researched applied to transonic compressors in numerical fluid mechanics of inviscid flow and viscous flow  
[NASA-CR-174353] p 114 N85-18291

Stress waves in an isotropic elastic plate excited by a circular transducer  
[NASA-CR-3877] p 138 N85-20390

A theory of post-stall transients in multistage axial compression systems  
[NASA-CR-3878] p 8 N85-21117

Advanced stress analysis methods applicable to turbine engine structures  
[NASA-CR-175573] p 26 N85-21165

Application of homomorphic signal processing to stress wave factor analysis  
[NAS 1.26:174871] p 138 N85-21673

Recent advances in hybrid/mixed finite elements  
[NASA-CR-175574] p 145 N85-21687

Structural response of a rotating bladed disk to rotor whirl  
[NASA-CR-175605] p 27 N85-22391

On Hybrid and mixed finite element methods  
[NASA-CR-175551] p 146 N85-23096

Ultrasonic testing of plates containing edge cracks  
[NASA-CR-3904] p 138 N85-29307

Structural characteristics of high temperature composites  
[NASA-CR-175998] p 58 N85-30037

**Materials Research Lab., Inc., Glenwood, Ill.**

Fracture of composite-adhesive-composite systems  
p 141 A85-27935

**Max-Planck-Inst. fuer Metallforschung, Stuttgart (West Germany).**

A study of fatigue damage mechanisms in Waspalloy from 25 to 800 C  
p 65 A85-12098

**Mechanical Technology, Inc., Latham, N. Y.**

Mod II engine and technology development  
p 129 A85-45473

Automotive Stirling engine systems development  
p 130 A85-45474

Development of gas-lubricated pistons for heavy duty diesel engine technology program  
[NASA-CR-174746] p 184 N85-12808

Development of a multiplane multispeed balancing system for turbine systems  
[NASA-CR-174750] p 35 N85-22400

Free-piston Stirling engine/linear alternator 1000-hour endurance test  
[NASA-CR-174771] p 163 N85-30481

**Michigan State Univ., East Lansing.**

Experiments with a microwave electrothermal thruster concept  
p 42 A85-16441

Measurements of energy distribution in microwave plasmas of N<sub>2</sub> and He and comparisons with results for H<sub>2</sub>  
p 178 A85-16443

The energetics of hydrogen atom recombination - Analysis, experiments, and modeling  
p 179 A85-16444

Recent work on a microwave ion source  
p 179 A85-16455

Closed-loop strain controlled testing at elevated temperatures with a non-contacting gage  
p 121 A85-29562

Experimental performance of a microwave cavity plasma disk ion source  
p 179 A85-43552

Improved models for increasing wind penetration, economics and operating reliability  
[NASA-CR-175538] p 160 N85-20545

Development of a temperature measurement system with application to a jet in a cross flow experiment  
[NASA-CR-174896] p 27 N85-25262

A comparison of smooth specimen and analytical simulation techniques for notched members at elevated temperatures  
p 151 N85-31546

**Michigan Technological Univ., Houghton.**

The mechanisms of formation and prevention of channel segregation during alloy solidification  
p 180 A85-18082

Cyclic oxidation behavior of beta+gamma overlay coatings on gamma and gamma+gamma-prime alloys  
p 68 A85-32431

The effect of tantalum and carbon on the structure/properties of a single crystal nickel-base superalloy  
[NASA-CR-174779] p 71 N85-11223

The effect of tantalum on the structure/properties of two polycrystalline nickel-base superalloys: B-1900 + Hf MAR-M247  
[NASA-CR-174847] p 73 N85-18127

Effects of MAR-M247 substrate (modified) composition on coating oxidation coating/substrate interdiffusion  
[NASA-CR-174851] p 73 N85-19073

A study of interdiffusion in beta + gamma/gamma + gamma prime Ni-Cr-Al  
[NASA-CR-174852] p 74 N85-20041

Raman structural studies of the nickel electrode  
[NASA-CR-175619] p 183 N85-23414

**Michigan Univ., Ann Arbor.**

Integrating chemical kinetic rate equations by selective use of stiff and nonstiff methods  
[AIAA PAPER 85-0237] p 60 A85-19607

High temperature oxidation of propene  
p 61 A85-33570

Practical aspects of photovoltaic technology, applications and cost (revised)  
[NASA-CR-174963] p 165 N85-35472

**Minnesota Univ., Minneapolis.**

Acoustic structure and propagation in highly porous, layered, fibrous materials  
p 173 A85-12301

Cone formation as a result of whisker growth on ion bombarded metal surfaces  
p 182 A85-41635

Holographic optical system for aberration corrections in laser Doppler velocimetry  
p 123 A85-48659

**Missouri Univ., Rolla.**

Modelling of wind tunnel wall effects on the radiation characteristics of acoustic sources  
[AIAA PAPER 84-2364] p 174 A85-16104

**Mitre Corp., Bedford, Mass.**

A frequency-routed satellite system concept using multiple orthogonally-polarized beams for frequency reuse  
p 97 A85-34470

**Motorola, Inc., Scottsdale, Ariz.**

Satellite baseband processor test performance summary  
p 95 A85-14434

**N****Nanjing Aeronautical Inst. (China).**

Structure of particle-laden jets - Measurements and predictions  
p 109 A85-25137

Structure of ducted particle-laden turbulent jets  
p 110 A85-38999

**National Aeronautics and Space Administration, Washington, D.C.**

Status of NASA's multibeam communications technology program  
p 100 A85-14432

Effects of chemical releases by the STS 3 orbiter on the ionosphere  
p 166 A85-29538

The NASA photovoltaic technology program  
p 155 A85-35604

Suprathermal plasma observed on STS-3 Mission by plasma diagnostics package  
p 179 N85-22472

Electron and ion density depletions measured in the STS-3 orbiter wake  
p 39 N85-22474

**National Aeronautics and Space Administration, Langley Research Center, Hampton, Va.**

GASP cloud encounter statistics - Implications for laminar flow control flight  
p 166 A85-11979

A numerical study of the steady scalar convective diffusion equation for small viscosity  
p 107 A85-16533

Variability of cloudiness at airline cruise altitudes from GASP measurements  
p 166 A85-31199

A three-dimensional boundary-layer analysis including heat-transfer and blade-rotation effects  
p 6 A85-42988

A multiple-scales model of the shock-cell structure of imperfectly expanded supersonic jets  
p 113 A85-49354

**National Bureau of Standards, Gaithersburg, Md.**

Advanced thin film thermocouples  
[NASA-CR-175541] p 124 N85-21607

Convective influence on the stability of a cylindrical solid-liquid interface  
p 109 A85-26911

**Naval Research Lab., Washington, D. C.**

Effects of 1 MeV electrons and 10 MeV protons on the performance and reflectance of thin BSR cells  
p 182 A85-35699

The J3 SCR model applied to resonant converter simulation  
p 102 A85-42156

**Nebraska Univ., Lincoln.**

Dielectric properties of 'diamondlike' carbon prepared by RF plasma deposition  
p 182 A85-38192

'Diamondlike' carbon films - Optical absorption, dielectric properties, and hardness dependence on deposition parameters  
p 82 A85-40383

**Negev Univ., Beersheva (Israel).**

RF-sputtered silicon and hafnium nitrides - Properties and adhesion to 440C stainless steel  
p 81 A85-36240

Surface hardening of steel by boriding in a cold rf plasma  
p 68 A85-40275

**Nevada Univ., Reno.**

Oscillatory conductive heat transfer for a fiber in an ideal gas  
p 109 A85-26077

## Northwestern Univ., Evanston, Ill.

- Deposition stress effects on the life of thermal barrier coatings on burner rigs p 79 A85-19086  
On stress field near a stationary crack tip [AD-A152863] p 141 A85-24532  
Probabilistic finite element: Variational theory p 149 N85-27957

## Notre Dame Univ., Ind.

- Feedback in separated flows over symmetric airfoils [AIAA PAPER 84-2297] p 3 A85-28899  
Alternatives for jet engine control [NASA-CR-175831] p 29 N85-26713  
Alternatives for jet engine control [NASA-CR-175832] p 29 N85-26714  
Alternatives for jet engine control [NASA-CR-175833] p 29 N85-26715

## O

## O'Donnell and Associates, Inc., Pittsburgh, Pa.

- Simplified design and life prediction of rocket thrust chambers p 44 A85-29314

## Oak Ridge National Lab., Tenn.

- Dispersed metal-toughened ceramics and ceramic brazing [NASA-CR-174284] p 86 N85-15916  
Dispersed-metal-toughened alumina [NASA-CR-174687] p 89 N85-22758

## Oberlin Coll., Ohio.

- The infinite line pressure probe p 122 A85-37704

## Ohio State Univ., Cleveland.

- Vibrations of twisted cantilevered plates - Summary of previous and current studies p 140 A85-22069

## Ohio State Univ., Columbus.

- Ultrasonic wave propagation in two-phase media - Spherical inclusions p 54 A85-11926  
Optical computer switching network p 178 A85-23134  
Predicting rime ice accretion on airfoils p 3 A85-25135

- Vibrations of twisted cantilever plates - A comparison of theoretical results p 144 A85-47626  
Design and wind tunnel evaluation of a symmetric airfoil series for large wind turbine applications [NASA-CR-174764] p 7 N85-10919

- Fundamentals of microcrack nucleation mechanics [NASA-CR-3851] p 137 N85-16195  
Adaptive antenna arrays for weak interfering signals [NASA-CR-174336] p 98 N85-17258  
Engineering calculations for communications satellite systems planning [NASA-CR-175552] p 37 N85-21233

- Analysis of the electromagnetic scattering from an inlet geometry with lossy walls [NASA-CR-175743] p 99 N85-25686  
A study of internal and distributed damping for vibrating turbomachinery blades [NASA-CR-175901] p 30 N85-27868

- Diffusion welding of Cassegrainian concentrator cell stack assemblies [NASA-CR-176104] p 164 N85-33566  
Adaptive antenna arrays for satellite communications: Design and testing [NASA-CR-176162] p 100 N85-34329

- The design and analysis of single flank transmission error test for loaded gears [NASA-CR-176163] p 136 N85-34404

## Oklahoma State Univ., Stillwater.

- Flow visualization of lateral jet injection into swirling crossflow [AIAA PAPER 85-0059] p 2 A85-19490

- Swirling flows in typical combustor geometries [AIAA PAPER 85-0184] p 108 A85-19574  
Turbulence measurements of lateral jet injection into confined tubular crossflow [AIAA PAPER 85-1102] p 110 A85-39604

- Investigation of flowfields found in typical combustor geometries [NASA-CR-3869] p 26 N85-21167  
Deflected jet experiments in a turbulent combustor flowfield [NASA-CR-174863] p 26 N85-22390

- Confined turbulent swirling recirculating flow predictions [NASA-CR-174917] p 29 N85-26716  
Turbulence characteristics of swirling flowfields [NASA-CR-174918] p 29 N85-26717

- Predictions and measurements of isothermal flowfields in axisymmetric combustor geometries [NASA-CR-174916] p 29 N85-27867

## Opco, Inc., Santa Ana, Calif.

- Fiber optic, Fabry-Perot high temperature sensor [NASA-CR-174712] p 178 N85-31594

## P

## Pennsylvania State Univ., State College.

- The boundary layer on compressor cascade blades [NASA-CR-174369] p 114 N85-18292

## Pennsylvania State Univ., University Park.

- Computation of viscous flows in turbomachinery cascades p 106 A85-11631  
Computation and turbulence closure models for shear flows in rotating curved bodies p 107 A85-14349

- A space-marching method for incompressible Navier-Stokes equations [AIAA PAPER 85-0170] p 108 A85-19564  
Drop-turbulence interactions in a diffusion flame [AIAA PAPER 85-0319] p 60 A85-19665

- A morphological study of silicon carbide prepared by chemical vapor deposition p 79 A85-20938  
Effects of friction dampers on aerodynamically unstable rotor stages p 14 A85-21866

- Structure of particle-laden jets - Measurements and predictions p 109 A85-25137  
Acoustic control of free jet mixing [AIAA PAPER 85-0569] p 109 A85-25951

- Computation of three-dimensional viscous flows using a space-marching method p 4 A85-29259  
The scattering of ultrasonic third sound from substrate surface defects p 174 A85-36047

- Structure of ducted particle-laden turbulent jets p 110 A85-38999  
Turbulence modelling for complex shear flows [AIAA PAPER 85-1652] p 111 A85-40752

- The performance of jet noise suppression devices for industrial applications p 175 A85-42563  
Measurements and predictions of the structure of evaporating sprays p 112 A85-46484

- Structure of nonevaporating sprays. I - Initial conditions and mean properties p 112 A85-48538  
The structure of dilute combustor sprays [NASA-CR-174838] p 24 N85-15728

- Mass analysis of neutral particles and ions released during electrical breakdowns on spacecraft surfaces [NASA-CR-175585] p 39 N85-21250  
Mass spectra of neutral particles released during electrical breakdown of thin polymer films p 88 N85-22511

## Perkin-Elmer Corp., Norwalk, Conn.

- Electrical characterization of plasma-grown oxides on gallium arsenide p 181 A85-32635

## Politecnico di Torino (Italy).

- Time dependent computation of the Euler equations for designing 2-D cascades, including the case of transonic shock free design p 5 A85-41814

## Pontificia Univ. Catolica do Rio de Janeiro (Brazil).

- Heat transfer and turbulence measurements of a film-cooled flow over a convexly curved surface p 112 A85-41787

## Pratt and Whitney Aircraft, East Hartford, Conn.

- Energy efficient engine. Volume 1: Component development and integration program [NASA-CR-173084] p 22 N85-10992

- Hot isostatically pressed manufacture of high strength MERL 76 disk and seal shapes [NASA-CR-165550] p 71 N85-11225  
3-D inelastic analysis methods for hot section components (base program) [NASA-CR-174700] p 145 N85-21686

- Error reduction program [NASA-CR-174776] p 172 N85-27584  
Energy efficient engine component development and integration program [NASA-CR-172846] p 31 N85-29958

- Creep fatigue life prediction for engine hot section materials (isotropic) [NASA-CR-168228] p 32 N85-31057  
Energy Efficient Engine Program technology benefit/cost study, volume 1 [NASA-CR-174766-VOL-1] p 33 N85-35197

- Energy Efficient Engine Program technology benefit/cost study, volume 2 [NASA-CR-174766-VOL-2] p 33 N85-35198  
Development of advanced high-temperature heat flux sensors. Phase 2: Verification testing [NASA-CR-174973] p 126 N85-35391

## Pratt and Whitney Aircraft, West Palm Beach, Fla.

- Design and analysis report for the RL10-2B breadboard low thrust engine [NASA-CR-174857] p 48 N85-19020

- Convulsed nozzle design for the RL10 derivative 2B engine [NASA-CR-174953] p 32 N85-29965

## Pratt and Whitney Aircraft Group, East Hartford, Conn.

- Assessment of discretization schemes to reduce numerical diffusion in the calculation of complex flows [AIAA PAPER 85-0441] p 108 A85-19751

- Finite element engine blade structural optimization [AIAA PAPER 85-0645] p 141 A85-30313  
Application of two creep fatigue life models for the prediction of elevated temperature crack initiation of a nickel base alloy [AIAA PAPER 85-1420] p 69 A85-43979

- Study of controlled diffusion stator blading [NASA-CR-167995] p 25 N85-18058  
Energy efficient engine high-pressure turbine component rig performance test report [NASA-CR-168189] p 30 N85-29955

- Energy efficient engine integrated core/low spool test hardware design report [NASA-CR-168137] p 31 N85-29956

## PRC Planning and Economics, Inc., Lake Success, N.Y.

- Comparative analysis of operational forecasts versus actual weather conditions in airline flight planning, volume 1 [NASA-CR-167862] p 167 N85-35534

- Comparative analysis of operational forecasts versus actual weather conditions in airline flight planning, volume 2 [NASA-CR-167863] p 167 N85-35535

- Comparative analysis of operational forecasts versus actual weather conditions in airline flight planning, volume 3 [NASA-CR-167864] p 167 N85-35536

- Comparative analysis of operational forecasts versus actual weather conditions in airline flight planning, volume 4 [NASA-CR-167865] p 167 N85-35537

- Comparative analysis of operational forecasts versus actual weather conditions in airline flight planning: Summary report [NASA-CR-167866] p 168 N85-35538

## Princeton Univ., N. J.

- The role of surface generated radicals in catalytic combustion p 30 N85-27869

## Purdue Univ., West Lafayette, Ind.

- A stagnation pressure probe for droplet-laden air flow [AIAA PAPER 85-0330] p 108 A85-19672  
Use of static indentation laws in the impact analysis of laminated composite plates p 55 A85-29133

- The effect of aerodynamic and structural detuning on turbomachine supersonic unstalled torsional flutter [AIAA PAPER 85-0761] p 14 A85-30378  
Noise constraints affecting optimal propeller designs [SAE PAPER 850871] p 7 A85-50106

- Effects of cobalt, boron, and zirconium on the microstructure of Udmet 738 [NASA-CR-174762] p 70 N85-10166

## Purdue Univ. School of Science at Indianapolis, Ind.

- A finite element solution of three-dimensional inviscid rotational flows through curved ducts p 107 A85-11648

## R

## Rensselaer Polytechnic Inst., Troy, N.Y.

- Topological reaction rate measurements related to scuffing p 64 A85-11070  
Convective influence on the stability of a cylindrical solid-liquid interface p 109 A85-26911

- The influence of hold times on LCF and FCG behavior in a P/M Ni-base superalloy p 67 A85-32400  
Electrical characterization of plasma-grown oxides on gallium arsenide p 181 A85-32635

- Heat treatment of bulk gallium arsenide using a phosphosilicate glass cap p 181 A85-32636  
Fabrication of p(+)-n junction GaAs solar cells by a novel method p 181 A85-33645

- Heat transfer investigation in the junction region of circular cylinder normal to a flat plate at 90 deg location [ASME PAPER 84-WA/HT-70] p 111 A85-39898  
Research on gallium arsenide diffused junction solar cells [NASA-CR-174057] p 158 N85-11457

- Development of a lithium secondary battery separator p 104 N85-31378

## Rice Univ., Houston, Tex.

- Oscillator response to nonstationary excitation [ASME PAPER 84-WA/APM-38] p 140 A85-17039

## Rocket Research Corp., Redmond, Wash.

- Performance characterization tests of a 1-kW resistojet using hydrogen, nitrogen and ammonia as propellants [AIAA PAPER 85-1159] p 44 A85-39628

## Rockwell International Corp., Canoga Park, Calif.

- The effect of microstructure, temperature, and hold-time on low-cycle fatigue of As HIP P/M Rene 95 p 67 A85-32399  
Reusable rocket engine turbopump condition monitoring [SAE PAPER 841619] p 44 A85-39267

- Cryogenic upper stage test bed engine



- [AIAA PAPER 85-1339] p 44 A85-39733  
Small centrifugal pumps for low thrust rockets
- [AIAA PAPER 85-1302] p 45 A85-43978  
Electric power - Photovoltaic or solar dynamic?
- p 46 A85-47042  
Reusable rocket engine turbopump condition monitoring
- p 51 N85-26907  
Composite loads spectra for select space propulsion structural components
- p 148 N85-27953  
Feasibility of mapping velocity field flows in SSME powerhead by laser anemometry techniques
- p 41 N85-27971
- Rockwell International Corp., Columbus, Ohio.**  
Application of computational fluid dynamics to complex inlet ducts
- [AIAA PAPER 85-1213] p 6 A85-47023

## S

- Sandia National Labs., Albuquerque, N. Mex.**  
Properties of coated and modified surfaces
- p 53 A85-36694
- Scientific Research Associates, Inc., Glastonbury, Conn.**  
Analytical modeling of circuit aerodynamics in the new NASA Lewis Altitude Wind Tunnel
- [AIAA PAPER 85-0380] p 3 A85-26389
- Scientific Systems, Inc., Cambridge, Mass.**  
Nonlinear global stability analysis of compressor stall phenomena
- [NASA-CR-174908] p 31 N85-29960
- Signatron, Inc., Lexington, Mass.**  
A frequency-routed satellite system concept using multiple orthogonally-polarized beams for frequency reuse
- p 97 A85-34470
- SKF Engineering and Research Centre, Nieuwegein (Netherlands).**  
Fast numerical calculations of EHD sliding traction forces
- Application to rolling bearings
- [ASME PAPER 84-TRIB-26] p 127 A85-21289
- SKF Industries, Inc., King of Prussia, Pa.**  
Planetary-gear-support bearing test rig design
- [NASA-CR-174927] p 12 N85-35185
- South Carolina State Coll., Orangeburg.**  
On local total strain redistribution using a simplified cyclic inelastic analysis based on an elastic solution
- [AIAA PAPER 85-1419] p 142 A85-39770
- Southwest Research Inst., San Antonio, Tex.**  
Unified constitutive material models for nonlinear finite-element structural analysis
- [AIAA PAPER 85-1418] p 142 A85-39769
- Constitutive modeling and computational implementation for finite strain plasticity
- p 143 A85-40910
- Sliding seal materials for adiabatic engines
- [NASA-CR-174893] p 89 N85-22757
- Probabilistic structural analysis theory development
- p 148 N85-27955
- A survey of unified constitutive theories
- p 150 N85-31531
- Spectron Development Labs., Inc., Costa Mesa, Calif.**  
Spray characterization with a noninvasive technique using absolute scattered light
- p 120 A85-10036
- Noninvasive optical single-particle counter for measuring the size and velocity of droplets in a spray
- p 120 A85-16794
- Research study of droplet sizing technology leading to the development of an advanced droplet sizing system
- [NASA-CR-174839] p 123 N85-21604
- Spring Arbor Coll., Mich.**  
Chemical and electrochemical behavior of the Cr(III)/Cr(II) half-cell in the iron-chromium redox energy storage system
- p 61 A85-33785
- SRI International Corp., Menlo Park, Calif.**  
Chemistry of fuel deposits and sediments and their precursors
- [NASA-CR-174778] p 92 N85-10209
- Standard Oil Co., Cleveland, Ohio.**  
Control algorithms and computer simulation of a stand-alone photovoltaic village power system
- p 153 A85-11345
- Stanford Univ., Calif.**  
Velocity visualization in gas flows using laser-induced phosphorescence of biacetyl
- p 121 A85-21695
- Optical computer switching network
- p 178 A85-23134
- Fast laser-induced aerosol formation for visualization of gas flows
- p 121 A85-31113
- Two-frequency laser-induced fluorescence technique for rapid velocity-field measurements in gas flows
- p 121 A85-32294
- Heat transfer and turbulence measurements of a film-cooled flow over a convexly curved surface

- Augmented weak forms and element-by-element preconditioners: Efficient iterative strategies for structural finite elements. A preliminary study
- p 144 N85-10384
- Free-surface phenomena under low- and zero-gravity conditions
- [NASA-CR-175885] p 36 N85-27922
- Stanford Univ., Palo Alto, Calif.**  
Velocity visualization in gaseous flows
- [NASA-CR-174954] p 119 N85-31445
- Stanitz (John D.), University Heights, Ohio.**  
General design method for 3-dimensional, potential flow fields. Part 2: Computer program DIN3D1 for simple, unbranched ducts
- [NASA-CR-3926] p 10 N85-35159
- State Univ. of New York, Albany.**  
Plasma deposited hydrogenated carbon on GaAs and InP
- p 182 A85-40386
- State Univ. of New York, Stony Brook.**  
Failure during thermal cycling of plasma-sprayed thermal barrier coatings
- p 81 A85-36246
- Stonehart Associates, Inc., Madison, Conn.**  
Electrocatalyst advances for hydrogen oxidation in phosphoric acid fuel cells
- p 60 A85-15614
- Preparation and evaluation of advanced catalysts for phosphoric acid fuel cells
- [NASA-CR-168223] p 160 N85-19511
- Sverdrup Technology, Inc., Arnold Air Force Station, Tenn.**  
Gear mesh stiffness and load sharing in planetary gearing
- [ASME PAPER 84-DET-229] p 129 A85-33781
- Sverdrup Technology, Inc., Cleveland, Ohio.**  
Flame flashback in a premixed dump combustor
- [AIAA PAPER 85-0145] p 60 A85-19550
- System Science and Software, San Diego, Calif.**  
Computer simulation of plasma electron collection by PIX-II
- [AIAA PAPER 85-0386] p 43 A85-19715
- Systems Science and Software, La Jolla, Calif.**  
Surface interactions and high-voltage current collection
- p 40 N85-22493

## T

- Technion - Israel Inst. of Tech., Haifa.**  
High temperature oxidation of propene
- p 61 A85-33570
- Electronic heterodyne readout of fringes in moiré deflectometry
- p 122 A85-36726
- Thermodynamically consistent constitutive equations for nonisothermal large strain, elasto-plastic, creep behavior
- [AIAA PAPER 85-0621] p 142 A85-38425
- Tennessee Univ. Space Inst., Tullahoma.**  
Flow control in a diffusing S-Duct
- [AIAA PAPER 85-0524] p 3 A85-25928
- Texas A&M Univ., College Station.**  
Analytical determination of propeller performance degradation due to ice accretion
- [AIAA PAPER 85-0339] p 14 A85-20867
- Experimental aerodynamic characteristics of an NACA 0012 airfoil with simulated ice
- p 12 A85-21844
- Heat transfer enhancement in channels with turbulence promoters
- [ASME PAPER 84-WA/HT-72] p 111 A85-39900
- Rotordynamic coefficients for compressible flow in tapered annular seals
- p 129 A85-42573
- Performance degradation of helicopter rotor in forward flight due to ice
- p 11 A85-42937
- On the use of internal state variables in thermoviscoplastic constitutive equations
- p 150 N85-31536
- Numerical considerations in the development and implementation of constitutive models
- p 151 N85-31541
- Texas Technological Univ., Lubbock.**  
Flow visualization of lateral jet injection into swirling crossflow
- [AIAA PAPER 85-0059] p 2 A85-19490
- Turbulence measurements of lateral jet injection into confined tubular crossflow
- [AIAA PAPER 85-1102] p 110 A85-39604
- Texas Univ., Austin.**  
Analysis of hourglass instabilities and control in underintegrated finite element methods
- p 139 A85-11125
- Stability, accuracy, and efficiency of some underintegrated methods in finite element computations
- p 172 A85-50073
- Interaction of finite-amplitude sound with air-filled porous materials
- [NASA-CR-174885] p 177 N85-27637
- Textron Bell Aerospace Co., Buffalo, N. Y.**  
Convolute nozzle design for the RL10 derivative 2B engine

- [NASA-CR-174953] p 32 N85-29965
- Tokai Univ., Hiratsuka (Japan).**  
Flow visualization of lateral jet injection into swirling crossflow
- [AIAA PAPER 85-0059] p 2 A85-19490
- Toledo Univ., Ohio.**  
An allpass filter design for luminance and chrominance separation of NTSC signals
- p 102 A85-28230
- Modeling of NASA's 30/20 GHz satellite communications system
- p 38 A85-36663
- Small-signal model for the series resonant converter
- p 102 A85-39453
- Thermal-stress analysis for a wood composite blade
- [NASA-CR-174794] p 159 N85-17421
- Wake effects on the aerodynamic performance of horizontal axis wind turbines
- [NASA-CR-174920] p 162 N85-29364
- Aerodynamic analysis of a horizontal axis wind turbine by use of helical vortex theory. Volume 1: Theory
- [NASA-CR-168054] p 9 N85-29916
- Transmission Research, Inc., Cleveland, Ohio.**  
Thermal traction contact performance evaluation under fully flooded and starved conditions
- [NASA-CR-168173] p 132 N85-25848
- Rolling, slip and traction measurements on low modulus materials
- [NASA-CR-174909] p 135 N85-33491
- TriSolar Corp., Bedford, Mass.**  
Microprocessor control of photovoltaic systems
- p 156 A85-45408
- TRW Electronic Systems Group, Redondo Beach, Calif.**  
The 30 GHz solid state amplifier for low cost low data rate ground terminals
- [NASA-CR-174795] p 102 N85-12300
- TRW, Inc., Cleveland, Ohio.**  
Energy efficient engine. Volume 2. Appendix A: Component development and integration program
- [NASA-CR-173085] p 22 N85-10991
- TRW, Inc., Redondo Beach, Calif.**  
Advanced 30/20 GHz multiple beam antenna for future communications satellites
- p 96 A85-14436
- Electrothermal thruster diagnostics
- p 42 A85-16440
- An experimental study of three-dimensional shock wave/turbulent boundary layer interactions in a supersonic flow
- [AIAA PAPER 85-1566] p 5 A85-40691
- Electric power - Photovoltaic or solar dynamic?
- p 46 A85-47042
- TRW Space Technology Labs., Redondo Beach, Calif.**  
High frequency plasma generator for ion thrusters
- [NASA-CR-174772] p 48 N85-17023
- Tuskegee Inst., Ala.**  
Friction in rail guns
- p 101 A85-16424
- An improved computer model for prediction of axial gas turbine performance losses
- [NASA-CR-174246] p 24 N85-15724
- Arc-driven rail gun research
- [NASA-CR-174816] p 132 N85-21662

## U

- United Technologies Corp., East Hartford, Conn.**  
Finite difference methods for reducing numerical diffusion in TEACH-type calculations
- [AIAA PAPER 85-0057] p 108 A85-19488
- Calculation of confined swirling flows
- [AIAA PAPER 85-0060] p 108 A85-19491
- A linearized unsteady aerodynamic analysis for transonic cascades
- p 3 A85-20744
- Energy efficient engine flight propulsion system preliminary analysis and design report
- [NASA-CR-174701] p 18 N85-10947
- Energy efficient engine combustor test hardware detailed design report
- [NASA-CR-167945] p 18 N85-10950
- United Technologies Corp., South Windsor, Conn.**  
Regenerative fuel cell energy storage system for a low Earth orbit space station
- [NASA-CR-174802] p 158 N85-13371
- Electric utility acid fuel cell stack technology advancement
- [NASA-CR-174804] p 159 N85-17422
- Long-life high performance fuel cell program
- [NASA-CR-174874] p 50 N85-25384
- United Technologies Research Center, East Hartford, Conn.**  
Mass and momentum turbulent transport experiments with confined coaxial jets
- p 107 A85-14399
- Finite difference methods for reducing numerical diffusion in TEACH-type calculations
- [AIAA PAPER 85-0057] p 108 A85-19488
- Three-dimensional inviscid flow analysis of turbofan forced mixers

- [AIAA PAPER 85-0086] p 2 A85-19510  
Fiber optic temperature sensor p 121 A85-29563  
The scattering of ultrasonic third sound from substrate surface defects p 174 A85-36047  
High temperature static strain sensor development program p 19 N85-10959  
External fuel vaporization study, phase 2 [NASA-CR-174079] p 92 N85-11252  
High-temperature optically activated GaAs power switching for aircraft digital electronic control [NASA-CR-174711] p 34 N85-12901  
Imide modified epoxy matrix resins [NASA-CR-174695] p 85 N85-15892  
Turbulent transport and length scale measurement experiments with confined coaxial jets [NASA-CR-174831] p 117 N85-30245  
**Universities Space Research Association, Columbia, Md.**  
Design and performance of a fixed, nonaccelerating guide vane cascade that operates over an inlet flow angle range of 60 deg [ASME PAPER 84-GT-75] p 4 A85-32964  
**University of Southern California, Los Angeles.**  
Focal shifts in parabolic reflectors p 97 A85-39356

## V

- Varian Associates, Palo Alto, Calif.**  
Magnesium doping of efficient GaAs and Ga(0.75)In(0.25)As solar cells grown by metalorganic chemical vapor deposition p 180 A85-11466  
Design of low loss helix circuits for interference fitted and brazed circuits [NASA-CR-168313] p 103 N85-19328  
**Virginia Polytechnic Inst. and State Univ., Blacksburg.**  
The influence of combustion liner holes on noise production by ducted burners [AIAA PAPER 84-2322] p 172 A85-10869  
Bipolar-FET combinational power transistors for power conversion applications p 100 A85-12669  
A fast time domain digital simulation technique for power converters - Application to a buck converter with feedforward compensation p 101 A85-20900  
New eutectic alloys and their heats of transformation p 66 A85-27808  
Vortex induced lift on a flat plate with a curved forward-facing flap p 4 A85-30175  
The J3 SCR model applied to resonant converter simulation p 102 A85-42156  
Optimization of cascade blade mistuning. I - Equations of motion and basic inherent properties p 16 A85-42365  
Optimization of cascade blade mistuning. II - Global optimum and numerical optimization p 16 A85-45715  
Geometrically nonlinear analysis of laminated elastic structures [NASA-CR-175609] p 146 N85-21720  
Thermodynamic evaluation of transonic compressor rotors using the finite volume approach [NASA-CR-175811] p 29 N85-26712  
A study of the stress wave factor technique for the characterization of composite materials [NASA-CR-174870] p 58 N85-30035  
**Virginia Univ., Charlottesville.**  
Four-dimensional modulation and coding - An alternate to frequency-reuse p 97 A85-36653

## W

- Washington Univ., Seattle.**  
Direct numerical simulations of a reacting mixing layer with chemical heat release [AIAA PAPER 85-0143] p 60 A85-19548  
Direct simulations of chemically reacting turbulent mixing layers [AIAA PAPER 85-0321] p 60 A85-19666  
Recent advances in methods for numerical solution of O.D.E. initial value problems p 171 A85-21370  
Metallurgical and mechanical phenomena due to rubbing of titanium against sintered powder Nichrome p 127 A85-22281  
An experimental investigation and numerical prediction of thermomechanical phenomena in high speed rotor tip rubbing p 14 A85-25442  
An experimental study of three-dimensional shock wave/turbulent boundary layer interactions in a supersonic flow [AIAA PAPER 85-1566] p 5 A85-40691  
An interactive computer code for calculation of gas-phase chemical equilibrium (EQLBRM) [NASA-CR-168337] p 18 N85-10948  
**Western Union Telegraph Co., McLean, Va.**  
Satellite provided customer promises services, a

- forecast of potential domestic demand through the year 2000. Volume 4: Sensitivity analysis [NASA-CR-174662] p 99 N85-27092  
**Westinghouse Electric Corp., Pittsburgh, Pa.**  
Measured effects of wind turbine generation at the Block Island Power Company p 153 A85-10652  
Fuel cell power plant economic and operational considerations [ASME PAPER 84-AES-7] p 154 A85-21297  
Gas cooled fuel cell systems technology development [NASA-CR-174732] p 158 N85-16291  
**Westinghouse Research Labs., Pittsburgh, Pa.**  
Breakway friction and dynamic friction/wear measurements of various ceramic materials from 25 C (75 F) to 650 C (1200 F) [NASA-CR-174803] p 90 N85-26994  
**Wichita State Univ., Kans.**  
Icing tunnel tests of Electro-Impulse De-Icing of an engine inlet and high-speed wings [AIAA PAPER 85-0466] p 10 A85-20872  
Electro-impulse de-icing of a turbofan engine inlet [AIAA PAPER 85-1118] p 12 A85-40811  
**Wisconsin Univ., Madison.**  
A rotating superconducting solenoid for 100 kWh energy storage p 44 A85-33144  
**Wisconsin Univ., Milwaukee.**  
A study of Reynolds-stress closure model [NASA-CR-174342] p 114 N85-17324  
**Wyle Labs., Inc., Huntsville, Ala.**  
Flow dynamic environment data base development for the SSME p 147 N85-26885

## X

- Xerox Electro-Optical Systems, Pasadena, Calif.**  
Development of a large insert gas ion thruster p 45 A85-42922

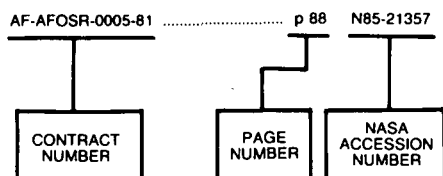
## Y

- Yale Univ., New Haven, Conn.**  
Polarization (ellipsometric) measurements of liquid condensate deposition and evaporation rates and dew points in flowing salt/ash-containing combustion gases p 123 A85-46925  
Computer program for the calculation of multicomponent convective diffusion deposition rates from chemically frozen boundary layer theory [NASA-CR-168329] p 116 N85-27164

8

# CONTRACT NUMBER INDEX

## Typical Contract Number Index Listing



Listings in this index are arranged alphanumerically by contract number. Under each contract number the NASA accession numbers denoting documents that have been produced as a result of research done under that contract are arranged in ascending order. The NASA accession number denotes the number by which the citation is identified.

AF-AFOSR-0005-81	p 88	N85-21357	DE-AI01-80CS-5019	p 186	N85-32043	NAG3-156	p 96	A85-28234
AF-AFOSR-79-0091	p 169	A85-36727	DE-AI01-80ET-17088	p 158	N85-16698	NAG3-157	p 96	A85-28241
AF-AFOSR-80-0265	p 61	A85-47320		p 161	N85-25941	NAG3-159	p 38	A85-36663
AF-AFOSR-81-0005	p 64	A85-11070	DE-AI04-80AL-12726	p 61	A85-33785		p 2	A85-19490
AF-AFOSR-84-0034	p 123	A85-46925		p 158	N85-12465	NAG3-160	p 37	N85-21233
DA PROJ. 1L1-61101-AH-45	p 74	N85-19074	DE-AI05-82OR-1005	p 162	N85-27387		p 148	N85-27263
DAAE07-80-C-9115	p 134	N85-29295	DE-AI21-80ET-17088	p 164	N85-34443	NAG3-161	p 173	A85-12301
DAAG24-83-K-0058	p 88	N85-21357		p 165	N85-35471	NAG3-164	p 81	A85-36246
DAAG29-82-K-0147	p 141	A85-24532		p 185	N85-27769	NAG3-172	p 58	N85-30035
DE-AC03-76SF-00098	p 65	A85-15603		p 157	N85-10445	NAG3-175	p 181	A85-32635
	p 171	A85-21370	DE-FG22-80PC-30247	p 157	N85-10447	NAG3-176	p 107	A85-14376
	p 93	N85-19185	DE-FG22-80PC-30303	p 157	N85-11455	NAG3-177	p 79	A85-20938
DE-AC03-78ET-15365	p 77	N85-32176	DEN3-153	p 157	N85-11456	NAG3-179	p 107	A85-14241
DE-AC05-84OR-21400	p 60	A85-15614	DEN3-167	p 159	N85-17422		p 4	A85-30175
	p 86	N85-15916		p 160	N85-19511	NAG3-181	p 129	A85-42573
DE-AC12-76SN-00052	p 89	N85-22758	DEN3-168	p 168	A85-24526	NAG3-182	p 113	A85-49354
DE-AE01-77CS-51040	p 78	N85-34267	DEN3-176	p 107	A85-14376	NAG3-185	p 165	N85-35472
DE-AI-01-80ET-17088	p 31	N85-29961	DEN3-17	p 157	A85-45517	NAG3-186	p 129	A85-33781
DE-AI01-76ET-20320	p 164	N85-30483		p 126	A85-15972	NAG3-188	p 181	A85-32636
	p 7	N85-10919		p 82	A85-42797		p 181	A85-33645
	p 158	N85-11458	DEN3-244	p 185	N85-18831	NAG3-190	p 158	N85-11457
	p 159	N85-16299	DEN3-261	p 127	A85-15973		p 60	A85-19665
	p 161	N85-23242	DEN3-275	p 31	N85-29961		p 109	A85-25137
	p 161	N85-27385	DEN3-290	p 60	A85-15614		p 110	A85-38999
	p 162	N85-29364	DEN3-303	p 160	N85-19511		p 112	A85-46484
	p 162	N85-29365	DEN3-309	p 83	A85-43930		p 112	A85-48538
	p 9	N85-29916	DEN3-310	p 91	N85-28109	NAG3-194	p 24	N85-15728
	p 150	N85-30361	DEN3-326	p 159	N85-17422	NAG3-197	p 106	A85-11640
	p 162	N85-30476	DEN3-32	p 159	N85-16300	NAG3-199	p 93	N85-28127
	p 163	N85-30477	DEN3-333	p 161	N85-25941	NAG3-200	p 104	N85-31378
	p 163	N85-30478	DEN3-339	p 164	N85-30483	NAG3-201	p 27	N85-22391
	p 163	N85-30479	DEN3-342	p 161	N85-27377	NAG3-201	p 116	N85-27164
	p 105	N85-32251	DEN3-346	p 130	N85-13235	NAG3-208	p 146	N85-21720
DE-AI01-77CS-1040	p 79	A85-15195	DEN3-352	p 165	N85-35471	NAG3-210	p 140	A85-17039
DE-AI01-77CS-51040	p 83	A85-48757	DEN3-354	p 185	N85-19894	NAG3-214	p 139	A85-12721
	p 72	N85-13007	DEN3-35	p 153	N85-10652	NAG3-216	p 68	A85-32431
	p 53	N85-14864		p 154	A85-21297		p 71	N85-11223
	p 185	N85-19895	DEN3-390	p 74	N85-19078		p 73	N85-18127
DE-AI01-77ET-13111	p 91	N85-28109	DOT-FA78WAI-893	p 184	N85-12808	NAG3-220	p 73	N85-19073
DE-AI01-79ET-20320	p 159	N85-16300	F19628-82-C-0081	p 156	A85-45408	NAG3-223	p 101	A85-20900
	p 159	N85-17421		p 86	N85-18154		p 140	A85-19433
	p 162	N85-29363	F33615-78-C-2401	p 129	A85-45473	NAG3-227	p 145	N85-21685
	p 165	N85-34444	F33615-83-K-5016	p 130	A85-45474	NAG3-22	p 171	A85-21370
DE-AI01-79ET-20485	p 103	N85-13157	F49620-83-C-0060	p 163	N85-30481	NAG3-22	p 67	A85-32400
DE-AI01-80CS-50194	p 184	N85-12808		p 185	N85-16699	NAG3-231	p 14	A85-21686
	p 84	N85-14928	F49620-83-K-0004	p 185	N85-16699	NAG3-232	p 169	A85-28612
	p 85	N85-15895		p 90	N85-26994		p 170	A85-34131
	p 185	N85-16699	F49620-83-K-0023	p 89	N85-22757	NAG3-238	p 157	N85-11455
	p 86	N85-18154	JPL-956602	p 153	A85-10652	NAG3-242	p 14	A85-20867
	p 89	N85-22757	NAG3-10	p 132	N85-25848		p 12	A85-21844
	p 90	N85-26994	NAG3-112	p 135	N85-33491	NAG3-244	p 11	A85-42937
			NAG3-124	p 158	N85-16291		p 68	A85-32431
			NAG3-132	p 167	N85-21872	NAG3-245	p 74	N85-20041
				p 40	N85-22486		p 27	N85-25262
				p 108	A85-19672	NAG3-250	p 181	A85-24649
				p 142	A85-35046	NAG3-255	p 76	N85-22661
				p 120	A85-10036	NAG3-256	p 5	A85-40891
				p 120	A85-16794	NAG3-258	p 59	A85-13092
				p 121	A85-21695	NAG3-260	p 112	A85-45282
				p 121	A85-31113		p 112	A85-45283
				p 121	A85-32294	NAG3-268	p 28	N85-25265
				p 4	A85-32965		p 75	N85-21320
				p 185	N85-19894	NAG3-26	p 6	A85-41826
				p 166	A85-37717	NAG3-271	p 76	N85-26962
				p 169	A85-28613	NAG3-277	p 18	N85-10948
				p 172	A85-10869	NAG3-280	p 72	N85-15877
				p 170	A85-28614	NAG3-282	p 159	N85-16293
				p 169	A85-28628		p 159	N85-18451
				p 170	A85-28629	NAG3-283	p 103	N85-18259
				p 93	N85-19185	NAG3-284	p 10	A85-20872
				p 141	A85-24532		p 12	A85-40811
				p 93	N85-19185	NAG3-285	p 121	A85-21695
				p 97	A85-36653		p 121	A85-31113
				p 61	A85-33570	NAG3-286	p 118	N85-31439
				p 17	N85-10065	NAG3-28	p 3	A85-25135
				p 17	N85-10068	NAG3-290	p 60	A85-19550
				p 25	N85-21162	NAG3-292	p 111	A85-39898
				p 80	A85-25963	NAG3-294	p 61	A85-33570
				p 182	A85-38192	NAG3-305	p 17	N85-10065
				p 82	A85-40383	NAG3-311	p 42	A85-16441
						NAG3-315	p 111	A85-39900
							p 176	N85-17667

## NAG3-319

## CONTRACT NUMBER INDEX

NAG3-319	p 144	N85-10384	NAG3-54	p 139	A85-13942	NAS3-22250	p 5	A85-40817
NAG3-324	p 84	N85-12162		p 142	A85-37440		p 10	N85-35162
NAG3-325	p 67	A85-32414		p 143	A85-41983	NAS3-22253	p 47	N85-15804
NAG3-328	p 138	N85-20390	NAG3-557	p 36	N85-27922	NAS3-22342	p 101	A85-20170
	p 138	N85-29307	NAG3-560	p 180	A85-18082		p 101	A85-20171
NAG3-329	p 139	A85-11125	NAG3-57	p 65	A85-14959	NAS3-22441	p 103	N85-19328
	p 172	A85-50073		p 67	A85-32412	NAS3-22444	p 45	A85-42922
NAG3-330	p 7	N85-10919	NAG3-58	p 70	N85-11221	NAS3-22473	p 48	N85-17023
NAG3-333	p 109	A85-26911	NAG3-593	p 29	N85-26712	NAS3-22498	p 98	N85-15944
NAG3-33	p 139	A85-12029	NAG3-59	p 70	N85-10166	NAS3-22499	p 96	A85-14436
	p 139	A85-15893	NAG3-5	p 169	A85-36727	NAS3-22502	p 95	A85-14434
	p 142	A85-35046	NAG3-60	p 62	N85-11149	NAS3-22510	p 92	N85-10209
	p 142	A85-35048		p 26	N85-21166	NAS3-22514	p 175	N85-13550
	p 143	A85-41109	NAG3-62	p 108	A85-19672	NAS3-22525	p 141	A85-30313
	p 26	N85-21165	NAG3-70	p 61	A85-47320	NAS3-22534	p 14	A85-18792
	p 145	N85-21687	NAG3-74	p 108	A85-19574	NAS3-22535	p 34	N85-12901
	p 146	N85-23096		p 26	N85-21167	NAS3-22654	p 168	N85-27508
NAG3-340	p 54	A85-11926		p 29	N85-26716	NAS3-2266C	p 125	N85-35389
	p 137	N85-16195		p 29	N85-26717	NAS3-2271	p 117	N85-30245
NAG3-341	p 82	A85-40973		p 29	N85-27867	NAS3-22748	p 167	N85-35534
	p 62	A85-48493	NAG3-76	p 101	A85-16424		p 167	N85-35535
	p 62	A85-48513		p 132	N85-21662		p 167	N85-35536
	p 77	N85-32173	NAG3-7	p 127	A85-22281		p 167	N85-35537
	p 77	N85-32174		p 14	A85-25442		p 168	N85-35538
	p 77	N85-32175	NAG3-80	p 154	A85-24668	NAS3-22752	p 15	A85-32006
	p 77	N85-32176	NAG3-95	p 82	A85-40383	NAS3-22769	p 93	N85-27012
NAG3-346	p 140	A85-19899	NAG3-97	p 110	A85-39894	NAS3-22771	p 107	A85-14399
	p 142	A85-33847	NAG3-9	p 107	A85-16533	NAS3-22772	p 5	A85-41814
	p 143	A85-40910		p 114	N85-18291		p 7	N85-12008
NAG3-347	p 16	A85-42365	NASA ORDER C-49029-D	p 97	A85-34470	NAS3-22814	p 126	N85-12341
	p 16	A85-45715	NASA ORDER C-54715-D	p 124	N85-21607	NAS3-22825	p 140	A85-18795
NAG3-34	p 8	N85-21117	NASA ORDER C-72801-D	p 86	N85-15916	NAS3-22829	p 93	N85-19175
NAG3-353	p 30	N85-27869		p 89	N85-22758	NAS3-22876	p 43	A85-29310
NAG3-356	p 4	A85-32965	NASA ORDER C-74148-D	p 86	N85-15916	NAS3-22892	p 153	A85-10244
NAG3-357	p 173	A85-13955	NASA ORDER DSB-5710-2-79	p 161	N85-23243	NAS3-22902	p 32	N85-29965
	p 173	A85-13956	NASW-3688	p 125	N85-33456	NAS3-23039	p 2	A85-19510
NAG3-359	p 44	A85-33144	NASI-16147	p 28	N85-26710	NAS3-23051	p 9	N85-22368
NAG3-364	p 3	A85-25928	NASI-17070	p 107	A85-16533	NAS3-23052	p 45	A85-45377
NAG3-373	p 159	N85-17421		p 168	N85-21990	NAS3-23056	p 25	N85-21163
NAG3-377	p 58	N85-30037	NASI-17130	p 107	A85-16533	NAS3-23058	p 40	N85-22493
NAG3-379	p 146	N85-21691	NAS3-18896	p 70	A85-47972	NAS3-23164	p 45	A85-43978
	p 147	N85-25894	NAS3-19779	p 130	N85-13233	NAS3-23165	p 28	N85-26709
	p 147	N85-27260	NAS3-20072	p 71	N85-11225	NAS3-23166	p 175	N85-13549
	p 150	N85-31533	NAS3-20073	p 68	A85-32440	NAS3-23169	p 19	N85-10959
	p 151	N85-31545		p 68	A85-39284	NAS3-23245	p 56	A85-47970
	p 152	N85-32340	NAS3-20074	p 23	N85-10999	NAS3-23253	p 105	N85-33293
	p 152	N85-32341		p 23	N85-12059	NAS3-23255	p 99	N85-27092
NAG3-38	p 139	A85-15894	NAS3-20609	p 35	N85-22400	NAS3-23258	p 42	A85-16412
NAG3-399	p 160	N85-20545	NAS3-20643	p 13	A85-13953	NAS3-23265	p 42	A85-16440
NAG3-3	p 112	A85-41787		p 22	N85-10989	NAS3-23266	p 102	N85-12300
NAG3-40	p 100	A85-12669		p 22	N85-10990	NAS3-23267	p 12	N85-19978
NAG3-416	p 3	A85-19731		p 22	N85-10993	NAS3-23271	p 93	N85-19176
NAG3-417	p 69	A85-44703		p 22	N85-10994	NAS3-23276	p 129	A85-39938
NAG3-418	p 97	N85-11265		p 23	N85-10995		p 48	N85-18084
NAG3-419	p 97	A85-32249		p 23	N85-10996	NAS3-23286	p 174	A85-25932
	p 97	A85-39356		p 23	N85-10997	NAS3-23288	p 69	A85-43979
	p 143	A85-42566		p 23	N85-10998		p 32	N85-31057
NAG3-41	p 144	N85-11380		p 31	N85-29957	NAS3-23293	p 116	N85-27164
NAG3-424	p 30	N85-27868		p 33	N85-34138	NAS3-23349	p 44	A85-39267
NAG3-425	p 102	A85-42156		p 33	N85-34141		p 51	N85-26907
NAG3-426	p 41	N85-29997		p 34	N85-35199	NAS3-23351	p 101	A85-14433
NAG3-42	p 102	A85-28230	NAS3-20646	p 18	N85-10947	NAS3-23353	p 45	A85-43975
NAG3-448	p 164	N85-33566		p 18	N85-10950	NAS3-23354	p 35	N85-12071
NAG3-449	p 166	A85-29538		p 22	N85-10991	NAS3-23522	p 178	N85-13594
	p 179	N85-22472		p 22	N85-10992	NAS3-23525	p 59	A85-12713
	p 39	N85-22474		p 30	N85-29955	NAS3-23528	p 85	N85-15892
NAG3-466	p 116	N85-27168		p 31	N85-29956	NAS3-23531	p 60	A85-19666
NAG3-475	p 101	A85-25170		p 31	N85-29958	NAS3-23532	p 124	N85-25792
	p 99	N85-21438		p 33	N85-35197	NAS3-23538	p 120	A85-10036
	p 100	N85-35320		p 33	N85-35198		p 120	A85-16794
NAG3-476	p 99	N85-25686	NAS3-21036	p 46	N85-11131		p 123	N85-21604
NAG3-477	p 59	A85-12890	NAS3-21249	p 166	A85-21140	NAS3-23540	p 16	A85-40841
	p 168	A85-24526	NAS3-21252	p 175	N85-11791	NAS3-23542	p 168	A85-24526
	p 63	N85-25444	NAS3-21287	p 158	N85-16292	NAS3-235924	p 108	A85-19491
NAG3-488	p 94	N85-34295	NAS3-21358	p 46	N85-11131	NAS3-23681	p 9	N85-26668
NAG3-491	p 150	N85-31536	NAS3-21509	p 103	N85-19328	NAS3-23684	p 120	A85-10035
	p 151	N85-31541	NAS3-21726	p 59	A85-11892	NAS3-23686	p 108	A85-19491
NAG3-511	p 152	N85-31548	NAS3-21741	p 42	A85-16406		p 172	N85-27584
NAG3-512	p 183	N85-11862		p 47	N85-12937	NAS3-23687	p 147	N85-27261
NAG3-519	p 183	N85-23414	NAS3-21824	p 141	A85-27935		p 32	N85-32119
NAG3-51	p 121	A85-29562	NAS3-21841	p 121	A85-29563		p 33	N85-34140
	p 151	N85-31546	NAS3-21943	p 42	A85-16438	NAS3-2368	p 108	A85-19488
NAG3-524	p 181	A85-21425		p 48	N85-15806		p 108	A85-19751
NAG3-52	p 6	A85-41826	NAS3-21971	p 92	N85-11252	NAS3-23696	p 3	A85-20744
NAG3-534	p 142	A85-38425	NAS3-21991	p 10	N85-35159	NAS3-23697	p 145	N85-21688
	p 147	N85-25896	NAS3-22008	p 25	N85-18058	NAS3-23698	p 152	N85-31548
	p 149	N85-27959	NAS3-22062	p 176	N85-19791	NAS3-23702	p 12	N85-35185
NAG3-535	p 149	N85-27957		p 176	N85-19792	NAS3-23705	p 15	A85-32005
NAG3-536	p 98	N85-17258	NAS3-22133	p 126	N85-35391	NAS3-23708	p 172	A85-10882
	p 100	N85-34329	NAS3-22229	p 182	A85-35699		p 109	A85-25951
NAG3-541	p 136	N85-34404	NAS3-22232	p 180	A85-11466	NAS3-23712	p 123	A85-46607
NAG3-543	p 111	A85-40701	NAS3-22234	p 158	N85-13371	NAS3-23716	p 6	A85-42988
NAG3-546	p 114	N85-17324		p 50	N85-25384	NAS3-23772	p 44	A85-39735
NAG3-547	p 47	N85-13910	NAS3-22238	p 156	A85-45391	NAS3-23773	p 44	A85-39733
NAG3-549	p 110	A85-39604	NAS3-22249	p 105	N85-31408	NAS3-23780	p 98	N85-18238
	p 26	N85-22390		p 157	N85-10444		p 98	N85-18239

CONTRACT NUMBER INDEX

505-55-52

NAS3-23858	p 99	N85-18240	p 4	A85-29259	p 57	N85-21273
NAS3-23865	p 36	A85-39730	p 111	A85-40752	p 84	N85-13045
NAS3-23866	p 177	N85-35728	p 102	A85-39453	p 57	N85-14882
NAS3-23868	p 46	N85-11132	p 171	A85-21979	p 176	N85-22109
NAS3-23869	p 44	A85-39628	p 179	A85-17262	p 71	N85-11223
NAS3-23881	p 43	A85-18584	p 102	A85-35306	p 73	N85-18127
NAS3-23925	p 43	A85-19715	p 107	A85-11648	p 86	N85-18153
NAS3-23926	p 150	N85-31531	p 24	N85-15724	p 73	N85-19072
NAS3-23927	p 28	N85-26711	p 178	A85-16443	p 73	N85-19073
NAS3-23928	p 152	N85-31548	p 179	A85-16444	p 74	N85-19076
NAS3-23940	p 133	N85-28372	p 179	A85-16455	p 74	N85-20041
NAS3-24078	p 152	N85-33541	p 179	A85-43552	p 75	N85-20043
NAS3-24081	p 171	A85-47794	p 39	N85-21250	p 75	N85-21323
NAS3-24082	p 94	N85-31308	p 88	N85-22511	p 88	N85-21357
NAS3-24089	p 6	A85-42954	p 178	A85-23134	p 131	N85-21657
NAS3-24094	p 31	N85-29960	p 106	A85-11647	p 62	N85-22644
NAS3-24100	p 120	A85-10034	p 66	A85-32387	p 76	N85-26963
NAS3-24105	p 10	N85-35158	p 138	N85-21673	p 117	N85-30242
	p 6	A85-43977	p 136	N85-34405	p 134	N85-30342
	p 32	N85-31058	p 177	N85-27637	p 77	N85-31283
	p 105	N85-32251	p 127	A85-23838	p 77	N85-31284
NAS3-24229	p 60	A85-19548	p 177	N85-27637	p 58	N85-32148
NAS3-24238	p 48	N85-19020	p 121	A85-29563	p 135	N85-32331
NAS3-24356	p 41	N85-27971	p 68	A85-40275	p 78	N85-34266
NAS3-24382	p 148	N85-27953	p 86	N85-15916	p 137	N85-34408
	p 148	N85-27954	p 147	N85-27260	p 57	N85-15823
NAS3-24389	p 148	N85-27955	p 151	N85-31545	p 145	N85-18375
	p 149	N85-27956	p 125	N85-33454	p 58	N85-27978
NAS3-285	p 119	N85-31445	p 162	N85-27387	p 133	N85-28371
NAS5-23481	p 39	A85-35379	p 38	N85-34150	p 144	N85-15184
NAS8-32807	p 166	A85-29538	p 52	N85-34176	p 132	N85-25847
NAS8-33727	p 180	A85-18082	p 49	N85-21259	p 133	N85-29292
NAS8-33982	p 39	A85-35379	p 47	N85-11133	p 152	N85-34427
NCC3-15	p 61	A85-23192	p 50	N85-25386	p 144	N85-16205
NCC3-16	p 153	A85-11345	p 58	N85-30034	p 72	N85-18124
NCC3-17	p 157	N85-10445	p 175	N85-13549	p 73	N85-18125
	p 157	N85-10447	p 133	N85-28373	p 74	N85-19074
	p 157	N85-11456	p 7	N85-12036	p 131	N85-21658
NCC3-21	p 65	A85-11935	p 7	N85-12008	p 145	N85-21685
NCC3-29	p 100	N85-35321	p 113	N85-10306	p 134	N85-31511
NCC3-30	p 85	N85-15895	p 7	N85-14798	p 137	N85-34409
	p 135	N85-32330	p 24	N85-14840	p 132	N85-27226
NCC3-35	p 62	N85-21283	p 115	N85-20269	p 135	N85-32333
NCC3-38	p 98	N85-15943	p 26	N85-21164	p 70	N85-11221
	p 106	N85-35342	p 27	N85-25263	p 58	N85-30035
NCC3-3	p 112	A85-41782	p 28	N85-25265	p 123	N85-16100
NCC3-43	p 71	N85-11224	p 63	N85-25444	p 30	N85-28945
NCC3-5	p 162	N85-29364	p 115	N85-25760	p 125	N85-32302
	p 9	N85-29916	p 116	N85-25761	p 24	N85-15727
NCC3-6	p 162	N85-29363	p 124	N85-25794	p 94	N85-31308
NSERC-A-9265	p 171	A85-21370	p 30	N85-27870	p 94	N85-34295
NSF CME-79-13389	p 110	A85-39894	p 63	N85-28983	p 130	N85-13233
NSF CPE-81-15163	p 171	A85-21370	p 63	N85-31244	p 130	N85-13234
NSF CPF-81-15163	p 93	N85-19185	p 119	N85-31445	p 176	N85-17667
NSF DMR-79-23647	p 70	N85-11217	p 64	N85-32156	p 17	N85-10067
NSF DMR-82-06195	p 65	A85-14959	p 8	N85-15689	p 7	N85-12039
NSF DMR-82-12115	p 180	A85-18082	p 175	N85-13550	p 25	N85-18057
NSF ECS-79-10269	p 101	A85-20170	p 175	N85-13551	p 114	N85-19363
	p 101	A85-20171	p 175	N85-10788	p 114	N85-19364
NSF ECS-81-20305	p 97	A85-39356	p 17	N85-10065	p 169	N85-10659
NSF ENG-78-17782	p 110	A85-39894	p 17	N85-10068	p 178	N85-13594
NSF MCS-83-01844	p 171	A85-28006	p 18	N85-10069	p 25	N85-21163
NSF MEA-80-06806	p 111	A85-39898	p 92	N85-10209	p 178	N85-28786
NSF MEA-80-1136	p 173	A85-12301	p 113	N85-10303	p 8	N85-15688
NSG-3011	p 178	A85-12705	p 18	N85-10948	p 24	N85-15725
	p 41	A85-15512	p 18	N85-10949	p 35	N85-15758
NSG-3012	p 111	A85-40752	p 92	N85-12183	p 171	N85-17596
NSG-3019	p 61	A85-42571	p 92	N85-13066	p 35	N85-18067
NSG-3040	p 110	A85-39894	p 24	N85-15728	p 177	N85-30770
NSG-3041	p 182	A85-41635	p 184	N85-16663	p 1	N85-23685
NSG-3048	p 29	N85-26713	p 184	N85-22204	p 8	N85-21114
	p 29	N85-26714	p 93	N85-27012	p 63	N85-23941
	p 29	N85-26715	p 30	N85-27869	p 113	N85-11317
NSG-3147	p 67	A85-32399	p 119	N85-33435	p 113	N85-12314
NSG-3150	p 39	A85-35379	p 124	N85-25792	p 136	N85-34406
NSG-3169	p 123	A85-46925	p 24	N85-15726	p 123	N85-16099
NSG-3180	p 64	A85-11070	p 131	N85-14116	p 133	N85-27227
NSG-3184	p 66	A85-27808	p 113	N85-14078	p 133	N85-28372
NSG-3185	p 55	A85-29133	p 116	N85-27165	p 136	N85-34405
NSG-3188	p 128	A85-33779	p 1	N85-15658	p 136	N85-34407
	p 128	A85-33780	p 172	N85-19733	p 170	N85-17576
NSG-3197	p 40	N85-22512	p 70	N85-10165	p 170	N85-10683
NSG-3198	p 109	A85-26077	p 71	N85-12129	p 26	N85-21168
	p 177	N85-27637	p 84	N85-12162	p 27	N85-25261
NSG-3206	p 27	N85-22392	p 74	N85-20042	p 28	N85-26710
NSG-3208	p 8	N85-21117	p 75	N85-21322	p 32	N85-31058
NSG-3212	p 111	A85-40752	p 76	N85-22660	p 11	N85-27839
NSG-3236	p 174	A85-26915	p 86	N85-15897	p 11	N85-15702
NSG-3246	p 67	A85-32388	p 76	N85-26962	p 12	N85-18049
	p 70	N85-10165	p 90	N85-26993	p 8	N85-19923
NSG-3253	p 127	A85-23838	p 134	N85-32329	p 176	N85-22108
NSG-3263	p 65	A85-12098	p 144	N85-11380	p 9	N85-29925
NSG-3264	p 114	N85-18292	p 23	N85-13798	p 30	N85-28944
NSG-3266	p 106	A85-11631	p 85	N85-14929	p 137	N85-16195
	p 107	A85-14349	p 146	N85-25893	p 94	N85-11261
	p 108	A85-19564	p 57	N85-15822	p 157	N85-10444
NSG-3281						
NSG-3283						
NSG-3290						
NSG-3294						
NSG-3295						
NSG-3299						
NSG-3301						
NSG-3302						
NSG-3305						
NSG-330						
NSG-3328						
NSG3-48						
N00014-75-C-0867						
N00014-81-K-0090						
N00014-84-K-0574						
N00163-81-C-0071						
USIBSF-2813/82						
W-7405-ENG-26						
W-7405-ENG-36						
141-20-17						
146-20-1A						
384-55-62						
481-01-02						
481-59-12						
482-50-22						
485-49-02						
501-31-3B						
505-23-72						
505-31-OA						
505-31-OA						
505-31-04						
505-33-52						
505-33-53						
505-33-62						
505-33-7A						
505-33-7B						
505-33-7C						
505-33-72						
505-33-78						
505-36-12						
505-36-22						
505-40-1B						
505-40-14						
505-40-22						
505-40-42						
505-40-5A						
505-40-5B						
505-40-68						
505-40-74						
505-40-84						
505-40-90						
505-41-32						
505-42-92						
505-42-94						
505-43-3						
505-43-4						
505-43-52						
505-45-12						
505-45-45						
505-45-54						
505-45-58						
505-45-72						
505-53-1A						
505-53-1B						
505-55-52						

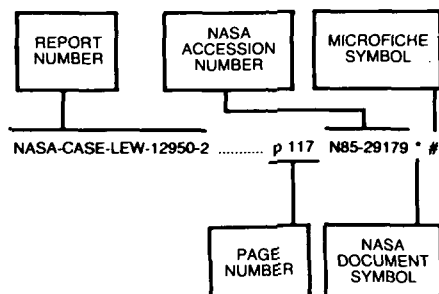
## 505-90-22

## CONTRACT NUMBER INDEX

505-90-22 .....	p 10	N85-35158	p 86	N85-19136
506-36-22 .....	p 117	N85-30246	p 87	N85-20127
506-53-1A .....	p 137	N85-10371	p 88	N85-21356
	p 137	N85-20389	p 138	N85-21674
	p 138	N85-21673	p 89	N85-24000
	p 138	N85-29307	p 53	N85-30011
	p 138	N85-32337	p 91	N85-30135
506-53-1B .....	p 83	N85-10186	p 59	N85-34223
	p 72	N85-12132	p 92	N85-34284
	p 72	N85-13006	p 147	N85-27260
	p 84	N85-13044	p 9	N85-22368
	p 131	N85-15168	p 32	N85-29964
	p 85	N85-15893	p 27	N85-22392
	p 74	N85-19075	p 9	N85-26670
	p 53	N85-21264	p 8	N85-21115
	p 87	N85-21355	p 27	N85-25264
	p 88	N85-21359	p 46	N85-11131
	p 132	N85-23085	p 164	N85-34443
	p 183	N85-24961	p 51	N85-27941
	p 90	N85-26991	p 100	N85-31348
	p 78	N85-34265	p 97	N85-15099
506-53-18 .....	p 95	N85-29085	p 161	N85-23242
506-55-22 .....	p 48	N85-21258	p 162	N85-29365
	p 49	N85-21263	p 158	N85-11458
	p 132	N85-21662	p 159	N85-16299
	p 51	N85-27972	p 161	N85-27385
	p 52	N85-34177	p 150	N85-30361
	p 52	N85-34178	p 162	N85-30476
	p 52	N85-34179	p 163	N85-30478
506-55-24 .....	p 49	N85-21260	p 165	N85-34444
506-55-42 .....	p 49	N85-21261	p 161	N85-23243
506-55-52 .....	p 50	N85-25384	p 165	N85-35472
	p 162	N85-28444	p 158	N85-12465
	p 163	N85-30480	p 159	N85-17422
506-55-62 .....	p 51	N85-26912	p 130	N85-13235
506-55-72 .....	p 53	N85-10105	p 84	N85-14928
	p 84	N85-10187	p 186	N85-32043
	p 47	N85-13910	p 72	N85-13007
	p 39	N85-14858	p 53	N85-14864
	p 103	N85-20246	p 185	N85-19895
	p 89	N85-25521		
	p 53	N85-26921		
	p 90	N85-26992		
	p 91	N85-28110		
	p 104	N85-28222		
	p 91	N85-30137		
	p 91	N85-30138		
	p 178	N85-34631		
506-55-8A .....	p 115	N85-24245		
506-55-82A .....	p 47	N85-15804		
506-58-22 .....	p 97	N85-10234		
	p 183	N85-10844		
	p 38	N85-15779		
	p 99	N85-20224		
	p 183	N85-26406		
	p 105	N85-33293		
506-60-12 .....	p 145	N85-20396		
	p 37	N85-21231		
	p 88	N85-22755		
	p 89	N85-22756		
	p 50	N85-23926		
	p 146	N85-24339		
506-60-22 .....	p 52	N85-28971		
506-60-42 .....	p 36	N85-21228		
	p 115	N85-21574		
	p 50	N85-25385		
	p 52	N85-35225		
506-62-42 .....	p 38	N85-29987		
533-04-1A .....	p 18	N85-10951		
	p 123	N85-16096		
	p 124	N85-21605		
	p 145	N85-21686		
	p 26	N85-22390		
	p 146	N85-24338		
	p 28	N85-25266		
	p 29	N85-26716		
	p 29	N85-26717		
	p 29	N85-27867		
	p 125	N85-30288		
	p 32	N85-32119		
	p 33	N85-34140		
533-04-1B .....	p 71	N85-12131		
533-04-1C .....	p 84	N85-10191		
	p 70	N85-11217		
	p 88	N85-21358		
533-04-1E .....	p 70	N85-10168		
	p 71	N85-11224		
533-04-12 .....	p 73	N85-18126		
	p 75	N85-21321		
	p 146	N85-21691		
	p 27	N85-25262		
	p 147	N85-25894		
	p 148	N85-27264		
	p 152	N85-32340		
	p 152	N85-32341		
533-05-12 .....	p 56	N85-12095		

# REPORT/ACCESSION NUMBER INDEX

## Typical Report Number Index Listing



Listings in this index are arranged alphanumerically by report number. The NASA accession number denotes the number by which the citation is identified. An asterisk (\*) indicates that the item is a NASA report. A pound sign (#) indicates that the item is available on microfiche.

AAE-85-2 ..... p 62 N85-21283 \* #  
ACS PAPER 130-13-84 ..... p 80 A85-25271 \* #  
ACS PAPER 19-B-84P ..... p 83 A85-45302 \* #  
ACS PAPER 7-J3-84 ..... p 82 A85-42797 \* #

AD-A146051 ..... p 12 N85-12887 \* #  
AD-A152863 ..... p 141 A85-24532 \* #  
AD-A153032 ..... p 107 A85-14241 \* #  
AD-A153479 ..... p 134 N85-29295 \* #  
AD-A153977 ..... p 26 N85-21164 \* #  
AD-A155736 ..... p 125 N85-33457 \* #  
AD-A157111 ..... p 89 N85-24000 \* #  
AD-A157112 ..... p 76 N85-26964 \* #  
AD-A157113 ..... p 7 N85-14798 \* #

AD-E401352 ..... p 125 N85-33457 #

AEDC-TR-84-10 ..... p 12 N85-12887 \* #

AFGL-TR-85-0018 ..... p 39 N85-22470 \* #

AIAA PAPER 83-2658 ..... p 78 A85-10675 \* #  
AIAA PAPER 84-0020 ..... p 13 A85-16098 \* #  
AIAA PAPER 84-0105 ..... p 10 A85-10653 \* #  
AIAA PAPER 84-0849 ..... p 54 A85-16096 \* #  
AIAA PAPER 84-0974 ..... p 54 A85-16094 \* #  
AIAA PAPER 84-0991 ..... p 139 A85-16095 \* #  
AIAA PAPER 84-1452 ..... p 13 A85-16097 \* #  
AIAA PAPER 84-2278 ..... p 173 A85-16099 \* #  
AIAA PAPER 84-2281 ..... p 13 A85-13953 \* #  
AIAA PAPER 84-2284 ..... p 13 A85-13954 \* #  
AIAA PAPER 84-2285 ..... p 173 A85-16102 \* #  
AIAA PAPER 84-2297 ..... p 3 A85-28899 \* #  
AIAA PAPER 84-2322 ..... p 172 A85-10869 \* #  
AIAA PAPER 84-2323 ..... p 173 A85-16103 \* #  
AIAA PAPER 84-2324 ..... p 173 A85-13955 \* #  
AIAA PAPER 84-2325 ..... p 2 A85-10870 \* #  
AIAA PAPER 84-2326 ..... p 173 A85-13956 \* #  
AIAA PAPER 84-2341 ..... p 172 A85-10882 \* #  
AIAA PAPER 84-2364 ..... p 174 A85-16104 \* #  
AIAA PAPER 85-0057 ..... p 108 A85-19488 \* #  
AIAA PAPER 85-0058 ..... p 2 A85-19489 \* #  
AIAA PAPER 85-0059 ..... p 2 A85-19490 \* #  
AIAA PAPER 85-0060 ..... p 108 A85-19491 \* #  
AIAA PAPER 85-0083 ..... p 14 A85-19509 \* #  
AIAA PAPER 85-0086 ..... p 2 A85-19510 \* #  
AIAA PAPER 85-0090 ..... p 35 A85-26381 \* #  
AIAA PAPER 85-0143 ..... p 60 A85-19548 \* #  
AIAA PAPER 85-0145 ..... p 60 A85-19550 \* #  
AIAA PAPER 85-0170 ..... p 108 A85-19564 \* #  
AIAA PAPER 85-0184 ..... p 108 A85-19574 \* #  
AIAA PAPER 85-0237 ..... p 60 A85-19607 \* #  
AIAA PAPER 85-0314 ..... p 34 A85-19661 \* #  
AIAA PAPER 85-0319 ..... p 60 A85-19665 \* #

AIAA PAPER 85-0321 ..... p 60 A85-19666 \* #  
AIAA PAPER 85-0330 ..... p 108 A85-19672 \* #  
AIAA PAPER 85-0338 ..... p 11 A85-28898 \* #  
AIAA PAPER 85-0339 ..... p 14 A85-20867 \* #  
AIAA PAPER 85-0379 ..... p 34 A85-19709 \* #  
AIAA PAPER 85-0380 ..... p 3 A85-26389 \* #  
AIAA PAPER 85-0384 ..... p 43 A85-19713 \* #  
AIAA PAPER 85-0386 ..... p 43 A85-19715 \* #  
AIAA PAPER 85-0410 ..... p 3 A85-19731 \* #  
AIAA PAPER 85-0441 ..... p 108 A85-19751 \* #  
AIAA PAPER 85-0466 ..... p 10 A85-20872 \* #  
AIAA PAPER 85-0468 ..... p 11 A85-30192 \* #  
AIAA PAPER 85-0524 ..... p 3 A85-25928 \* #  
AIAA PAPER 85-0533 ..... p 174 A85-25932 \* #  
AIAA PAPER 85-0569 ..... p 109 A85-25951 \* #  
AIAA PAPER 85-0621 ..... p 142 A85-38425 \* #  
AIAA PAPER 85-0645 ..... p 141 A85-30313 \* #  
AIAA PAPER 85-0761 ..... p 14 A85-30378 \* #  
AIAA PAPER 85-0804 ..... p 38 A85-30303 \* #  
AIAA PAPER 85-1102 ..... p 110 A85-39604 \* #  
AIAA PAPER 85-1104 ..... p 15 A85-39606 \* #  
AIAA PAPER 85-1118 ..... p 12 A85-40811 \* #  
AIAA PAPER 85-1133 ..... p 6 A85-43974 \* #  
AIAA PAPER 85-1140 ..... p 143 A85-40814 \* #  
AIAA PAPER 85-1154 ..... p 44 A85-39626 \* #  
AIAA PAPER 85-1155 ..... p 45 A85-43975 \* #  
AIAA PAPER 85-1156 ..... p 45 A85-43976 \* #  
AIAA PAPER 85-1159 ..... p 44 A85-39628 \* #  
AIAA PAPER 85-1187 ..... p 17 A85-47021 \* #  
AIAA PAPER 85-1196 ..... p 5 A85-40817 \* #  
AIAA PAPER 85-1198 ..... p 56 A85-47022 \* #  
AIAA PAPER 85-1210 ..... p 5 A85-40819 \* #  
AIAA PAPER 85-1213 ..... p 6 A85-47023 \* #  
AIAA PAPER 85-1219 ..... p 82 A85-39662 \* #  
AIAA PAPER 85-1229 ..... p 94 A85-47024 \* #  
AIAA PAPER 85-1259 ..... p 6 A85-47025 \* #  
AIAA PAPER 85-1263 ..... p 6 A85-43977 \* #  
AIAA PAPER 85-1290 ..... p 15 A85-39703 \* #  
AIAA PAPER 85-1302 ..... p 45 A85-43978 \* #  
AIAA PAPER 85-1312 ..... p 16 A85-39717 \* #  
AIAA PAPER 85-1332 ..... p 5 A85-39728 \* #  
AIAA PAPER 85-1336 ..... p 36 A85-39730 \* #  
AIAA PAPER 85-1339 ..... p 44 A85-39733 \* #  
AIAA PAPER 85-1341 ..... p 44 A85-39735 \* #  
AIAA PAPER 85-1398 ..... p 16 A85-42671 \* #  
AIAA PAPER 85-1408 ..... p 5 A85-39767 \* #  
AIAA PAPER 85-1418 ..... p 142 A85-39769 \* #  
AIAA PAPER 85-1419 ..... p 142 A85-39770 \* #  
AIAA PAPER 85-1420 ..... p 69 A85-43979 \* #  
AIAA PAPER 85-1433 ..... p 16 A85-40841 \* #  
AIAA PAPER 85-1441 ..... p 110 A85-39780 \* #  
AIAA PAPER 85-1471 ..... p 122 A85-39796 \* #  
AIAA PAPER 85-1566 ..... p 5 A85-40691 \* #  
AIAA PAPER 85-1580 ..... p 111 A85-40701 \* #  
AIAA PAPER 85-1650 ..... p 111 A85-40750 \* #  
AIAA PAPER 85-1652 ..... p 111 A85-40752 \* #

AIAA-85-0090 ..... p 35 N85-15758 \* #  
AIAA-85-0237 ..... p 24 N85-15726 \* #  
AIAA-85-0314 ..... p 35 N85-18067 \* #  
AIAA-85-0338 ..... p 11 N85-15702 \* #  
AIAA-85-0379 ..... p 35 N85-15757 \* #  
AIAA-85-0380 ..... p 8 N85-15688 \* #  
AIAA-85-0468 ..... p 12 N85-18049 \* #  
AIAA-85-1187 ..... p 32 N85-29964 \* #  
AIAA-85-1213 ..... p 118 N85-30247 \* #  
AIAA-85-1229 ..... p 38 N85-29967 \* #  
AIAA-85-1259 ..... p 9 N85-29925 \* #  
AIAA-85-1398 ..... p 30 N85-27870 \* #

AR-1 ..... p 168 N85-27508 \* #  
AR-1 ..... p 32 N85-31057 \* #  
AR-2 ..... p 28 N85-26711 \* #

ARL-TR-85-15 ..... p 177 N85-27637 \* #

ARPAD-TR-85001 ..... p 125 N85-33457 #

ASLE PREPRINT 84-LC-2A-2 ..... p 80 A85-25963 \* #

ASLE PREPRINT 84-LC-4A-4 ..... p 168 A85-38444 \* #

ASME PAPER 84-AES-7 ..... p 154 A85-21297 \* #

ASME PAPER 84-DET-184 ..... p 128 A85-33779 \* #

ASME PAPER 84-DET-226 ..... p 128 A85-33780 \* #  
ASME PAPER 84-DET-229 ..... p 129 A85-33781 \* #  
ASME PAPER 84-DET-96 ..... p 129 A85-35049 \* #  
ASME PAPER 84-GT-138 ..... p 141 A85-32962 \* #  
ASME PAPER 84-GT-187 ..... p 4 A85-32961 \* #  
ASME PAPER 84-GT-191 ..... p 141 A85-23150 \* #  
ASME PAPER 84-GT-199 ..... p 4 A85-32963 \* #  
ASME PAPER 84-GT-75 ..... p 4 A85-32964 \* #  
ASME PAPER 84-JPGG-GT-2 ..... p 61 A85-23192 \* #  
ASME PAPER 84-PVP-112 ..... p 140 A85-18795 \* #  
ASME PAPER 84-PVP-77 ..... p 14 A85-18792 \* #  
ASME PAPER 84-TRIB-13 ..... p 127 A85-21280 \* #  
ASME PAPER 84-TRIB-26 ..... p 127 A85-21289 \* #  
ASME PAPER 84-TRIB-7 ..... p 128 A85-32960 \* #  
ASME PAPER 84-WA/APM-38 ..... p 140 A85-17039 \* #  
ASME PAPER 84-WA/APM-41 ..... p 140 A85-17040 \* #  
ASME PAPER 84-WA/HT-51 ..... p 110 A85-39894 \* #  
ASME PAPER 84-WA/HT-70 ..... p 111 A85-39898 \* #  
ASME PAPER 84-WA/HT-72 ..... p 111 A85-39900 \* #  
ASME PAPER 84-WA/NCA-11 ..... p 174 A85-39909 \* #

ASR-1 ..... p 145 N85-21686 \* #  
ASR-1 ..... p 147 N85-27261 \* #  
ASR-1 ..... p 33 N85-34140 \* #  
ASR-2 ..... p 32 N85-32119 \* #

AT85T004 ..... p 12 N85-35185 \* #

AVSCOM-TR-84-C-14 ..... p 28 N85-26709 \* #  
AVSCOM-TR-84-C-17 ..... p 84 N85-13045 \* #

BBN-4770 ..... p 175 N85-11791 \* #

CCMS-84-13 ..... p 58 N85-30035 \* #

CONF-831142-3 ..... p 86 N85-15916 \* #  
CONF-8410138-1 ..... p 93 N85-19185 \* #

CR-R-84041 ..... p 28 N85-25265 \* #

CREARE-TN-371 ..... p 48 N85-18084 \* #

CTR-0747-84003 ..... p 130 N85-13235 \* #

D-1998 ..... p 171 N85-17596 \* #

DE84-016884 ..... p 93 N85-19185 \* #  
DE85-000865 ..... p 160 N85-20545 \* #  
DE85-001552 ..... p 86 N85-15916 \* #  
DE85-011649 ..... p 78 N85-34267 \* #  
DE85-011659 ..... p 125 N85-33454 \* #

DOE/CS-54209/20 ..... p 185 N85-19894 \* #

DOE/NASA/0005-1 ..... p 162 N85-29364 \* #  
DOE/NASA/0005-1 ..... p 9 N85-29916 \* #  
DOE/NASA/0006-1 ..... p 162 N85-29363 \* #  
DOE/NASA/0017-3 ..... p 157 N85-11456 \* #  
DOE/NASA/0017-4 ..... p 157 N85-10445 \* #  
DOE/NASA/0017-4 ..... p 157 N85-10447 \* #  
DOE/NASA/0017-6 ..... p 91 N85-28109 \* #  
DOE/NASA/0030-1 ..... p 85 N85-15895 \* #  
DOE/NASA/0168-8 ..... p 185 N85-18831 \* #  
DOE/NASA/0168-8 ..... p 31 N85-29961 \* #  
DOE/NASA/0191-1 ..... p 159 N85-17422 \* #  
DOE/NASA/0215-1 ..... p 159 N85-16300 \* #  
DOE/NASA/0238-1 ..... p 157 N85-11455 \* #  
DOE/NASA/0241-11 ..... p 164 N85-30483 \* #  
DOE/NASA/0241-14 ..... p 161 N85-25941 \* #  
DOE/NASA/0261-1 ..... p 130 N85-13235 \* #  
DOE/NASA/0262-1 ..... p 165 N85-35471 \* #  
DOE/NASA/0290-1 ..... p 158 N85-16291 \* #  
DOE/NASA/0326-1 ..... p 86 N85-18154 \* #  
DOE/NASA/0330-1 ..... p 7 N85-10919 \* #  
DOE/NASA/0333-1 ..... p 163 N85-30481 \* #  
DOE/NASA/0339-1 ..... p 185 N85-16698 \* #  
DOE/NASA/0342-1 ..... p 185 N85-16699 \* #  
DOE/NASA/0346-1 ..... p 90 N85-26994 \* #  
DOE/NASA/0352-1 ..... p 89 N85-22757 \* #  
DOE/NASA/0373-1 ..... p 159 N85-17421 \* #  
DOE/NASA/1005-5 ..... p 185 N85-27769 \* #  
DOE/NASA/12726-25 ..... p 162 N85-27387 \* #  
DOE/NASA/12726-26 ..... p 164 N85-34443 \* #



DOE/NASA/20320-49	p 150	N85-30361 * #	E-2315	p 169	N85-10659 * #	E-2463	p 115	N85-21570 * #
DOE/NASA/20320-50	p 162	N85-30476 * #	E-2316-1	p 178	N85-28786 * #	E-2464	p 138	N85-21674 * #
DOE/NASA/20320-51	p 163	N85-30477 * #	E-2317	p 84	N85-14928 * #	E-2465	p 36	N85-21228 * #
DOE/NASA/20320-52	p 163	N85-30478 * #	E-2319	p 57	N85-15823 * #	E-2466	p 48	N85-21258 * #
DOE/NASA/20320-55	p 163	N85-30479 * #	E-2320	p 75	N85-21323 * #	E-2469	p 99	N85-20223 * #
DOE/NASA/20320-60	p 158	N85-11458 * #	E-2321	p 53	N85-10105 * #	E-2470	p 137	N85-20389 * #
DOE/NASA/20320-61	p 159	N85-16299 * #	E-2322	p 84	N85-10187 * #	E-2471	p 161	N85-23242 * #
DOE/NASA/20320-62	p 161	N85-23242 * #	E-2324	p 1	N85-17935 * #	E-2473	p 8	N85-21114 * #
DOE/NASA/20320-63	p 162	N85-29365 * #	E-2325-1	p 92	N85-34284 * #	E-2475	p 8	N85-21115 * #
DOE/NASA/20320-64	p 161	N85-27385 * #	E-2327	p 18	N85-10949 * #	E-2476	p 134	N85-31511 * #
DOE/NASA/20320-65	p 165	N85-34444 * #	E-2328	p 84	N85-10191 * #	E-2478	p 131	N85-21657 * #
DOE/NASA/20485-17	p 103	N85-13157 * #	E-2329	p 71	N85-12129 * #	E-2479	p 49	N85-21260 * #
DOE/NASA/2801-1	p 89	N85-22758 * #	E-2330	p 158	N85-11458 * #	E-2480	p 103	N85-20246 * #
DOE/NASA/4105-1	p 105	N85-32251 * #	E-2331	p 70	N85-11217 * #	E-2482	p 133	N85-28373 * #
DOE/NASA/50194-40	p 84	N85-14928 * #	E-2332	p 183	N85-10844 * #	E-2483	p 90	N85-26991 * #
DOE/NASA/50194-41	p 184	N85-13692 * #	E-2333	p 175	N85-13551 * #	E-2484	p 75	N85-21321 * #
DOE/NASA/50194-43	p 186	N85-32043 * #	E-2334	p 92	N85-13066 * #	E-2485	p 49	N85-21261 * #
DOE/NASA/51040-57	p 72	N85-13007 * #	E-2335	p 75	N85-20043 * #	E-2487	p 132	N85-23085 * #
DOE/NASA/51040-58	p 185	N85-19895 * #	E-2336	p 185	N85-19895 * #	E-2489	p 99	N85-20224 * #
DOE/NASA/51040-59	p 53	N85-14864 * #	E-2337	p 137	N85-10371 * #	E-2490	p 26	N85-21164 * #
DOE/NBM-1077	p 160	N85-20545 * #	E-2339	p 56	N85-12095 * #	E-2491	p 77	N85-31284 * #
DOUGLAS-PAPER-7551	p 28	N85-26710 * #	E-2341	p 113	N85-10306 * #	E-2493	p 53	N85-21264 * #
DS-3-VOL-2	p 176	N85-19792 * #	E-2343	p 25	N85-18057 * #	E-2495	p 37	N85-21231 * #
D180-28461-1	p 177	N85-35728 * #	E-2344	p 167	N85-21872 * #	E-2496	p 161	N85-23243 * #
D6-52996	p 94	N85-31308 * #	E-2346	p 113	N85-11317 * #	E-2501	p 124	N85-25794 * #
E-1458	p 18	N85-10951 * #	E-2347	p 119	N85-33435 * #	E-2502	p 124	N85-21605 * #
E-1529	p 150	N85-30361 * #	E-2348	p 184	N85-16663 * #	E-2503	p 117	N85-30246 * #
E-1611	p 57	N85-14882 * #	E-2348	p 72	N85-18124 * #	E-2506	p 178	N85-34631 * #
E-1786	p 162	N85-30476 * #	E-2351	p 47	N85-11133 * #	E-2507	p 91	N85-30135 * #
E-1798	p 163	N85-30478 * #	E-2352	p 72	N85-13007 * #	E-2512	p 53	N85-30011 * #
E-1865	p 163	N85-30479 * #	E-2354	p 72	N85-12132 * #	E-2513	p 75	N85-21322 * #
E-1935	p 11	N85-27839 * #	E-2357	p 114	N85-15133 * #	E-2514	p 76	N85-26964 * #
E-1971	p 116	N85-27164 * #	E-2358	p 144	N85-15184 * #	E-2515	p 132	N85-25847 * #
E-1979	p 113	N85-14078 * #	E-2359	p 49	N85-21263 * #	E-2517	p 116	N85-25761 * #
E-1980	p 116	N85-27165 * #	E-2361	p 88	N85-21359 * #	E-2518	p 115	N85-21574 * #
E-1988	p 25	N85-21162 * #	E-2362	p 131	N85-21658 * #	E-2519	p 89	N85-24000 * #
E-1999	p 170	N85-28610 * #	E-2365	p 123	N85-16096 * #	E-2522	p 41	N85-23904 * #
E-2042	p 130	N85-13234 * #	E-2366	p 23	N85-13798 * #	E-2523	p 135	N85-32330 * #
E-2049-1	p 74	N85-19075 * #	E-2367	p 97	N85-15099 * #	E-2524	p 134	N85-32329 * #
E-2055	p 24	N85-14840 * #	E-2368	p 150	N85-31530 * #	E-2525	p 76	N85-22660 * #
E-2088	p 85	N85-15896 * #	E-2369	p 24	N85-15725 * #	E-2526	p 162	N85-29365 * #
E-2125	p 158	N85-12465 * #	E-2371	p 73	N85-18126 * #	E-2527	p 9	N85-23711 * #
E-2127	p 130	N85-13233 * #	E-2372	p 56	N85-14878 * #	E-2529	p 146	N85-24338 * #
E-2129	p 10	N85-35158 * #	E-2373	p 145	N85-20396 * #	E-2530	p 161	N85-27385 * #
E-2147	p 113	N85-12314 * #	E-2376	p 93	N85-31307 * #	E-2531	p 134	N85-30342 * #
E-2149	p 17	N85-10065 * #	E-2380	p 85	N85-14929 * #	E-2533	p 27	N85-25264 * #
E-2151	p 184	N85-22255 * #	E-2386	p 85	N85-15893 * #	E-2534	p 146	N85-24339 * #
E-2156	p 70	N85-10165 * #	E-2387	p 7	N85-14798 * #	E-2535	p 133	N85-28371 * #
E-2171	p 37	N85-16989 * #	E-2388	p 10	N85-35159 * #	E-2538	p 88	N85-22755 * #
E-2172	p 170	N85-17576 * #	E-2389	p 53	N85-14864 * #	E-2539	p 89	N85-22756 * #
E-2176	p 17	N85-10068 * #	E-2393	p 145	N85-18375 * #	E-2540	p 50	N85-23926 * #
E-2183	p 123	N85-16099 * #	E-2394	p 72	N85-15878 * #	E-2541	p 183	N85-26406 * #
E-2184	p 72	N85-13006 * #	E-2395	p 12	N85-18049 * #	E-2542	p 28	N85-25266 * #
E-2186	p 39	N85-22470 * #	E-2396	p 38	N85-15779 * #	E-2544	p 50	N85-25386 * #
E-2194	p 18	N85-10069 * #	E-2397	p 76	N85-26963 * #	E-2545	p 32	N85-31058 * #
E-2196	p 186	N85-32043 * #	E-2398	p 144	N85-16205 * #	E-2546	p 9	N85-26670 * #
E-2197	p 1	N85-15658 * #	E-2399	p 88	N85-21356 * #	E-2547	p 63	N85-23941 * #
E-2201	p 57	N85-15822 * #	E-2400	p 183	N85-24961 * #	E-2548	p 27	N85-25263 * #
E-2214	p 131	N85-14116 * #	E-2404	p 24	N85-15727 * #	E-2549	p 133	N85-27227 * #
E-2219	p 84	N85-13044 * #	E-2405	p 8	N85-15688 * #	E-2550	p 138	N85-29307 * #
E-2231	p 62	N85-10138 * #	E-2406	p 145	N85-21690 * #	E-2552	p 115	N85-24245 * #
E-2238	p 94	N85-11261 * #	E-2408	p 8	N85-15689 * #	E-2553	p 1	N85-23685 * #
E-2239	p 39	N85-14858 * #	E-2410	p 159	N85-16299 * #	E-2554	p 51	N85-27941 * #
E-2242	p 57	N85-21273 * #	E-2412	p 27	N85-25261 * #	E-2555	p 115	N85-25760 * #
E-2254	p 131	N85-15168 * #	E-2413	p 35	N85-15757 * #	E-2556	p 184	N85-28876 * #
E-2256	p 135	N85-32331 * #	E-2414	p 35	N85-15758 * #	E-2557	p 32	N85-31060 * #
E-2258	p 7	N85-12039 * #	E-2415	p 35	N85-18067 * #	E-2559	p 133	N85-27228 * #
E-2262	p 17	N85-10067 * #	E-2416	p 85	N85-15895 * #	E-2560	p 89	N85-25521 * #
E-2271	p 84	N85-13045 * #	E-2418	p 24	N85-15726 * #	E-2562	p 132	N85-27226 * #
E-2275	p 7	N85-12008 * #	E-2419	p 88	N85-21358 * #	E-2564	p 165	N85-34444 * #
E-2279	p 170	N85-10683 * #	E-2420	p 86	N85-19136 * #	E-2570	p 50	N85-25385 * #
E-2280	p 71	N85-12131 * #	E-2421	p 11	N85-15702 * #	E-2571	p 148	N85-27264 * #
E-2282	p 175	N85-13550 * #	E-2422	p 86	N85-18153 * #	E-2572	p 51	N85-26912 * #
E-2283	p 175	N85-13549 * #	E-2423	p 91	N85-30138 * #	E-2574	p 64	N85-32156 * #
E-2286	p 103	N85-13157 * #	E-2428	p 87	N85-20127 * #	E-2580	p 90	N85-26992 * #
E-2287	p 70	N85-10168 * #	E-2430	p 115	N85-21569 * #	E-2581	p 117	N85-30242 * #
E-2289	p 74	N85-20042 * #	E-2432	p 119	N85-31443 * #	E-2582	p 91	N85-28110 * #
E-2291	p 7	N85-12036 * #	E-2433	p 62	N85-22644 * #	E-2584	p 185	N85-27769 * #
E-2294	p 176	N85-17667 * #	E-2434	p 30	N85-28944 * #	E-2585	p 162	N85-28444 * #
E-2295	p 175	N85-10788 * #	E-2435	p 26	N85-21168 * #	E-2588	p 30	N85-28945 * #
E-2296	p 137	N85-16195 * #	E-2437	p 77	N85-31283 * #	E-2590	p 162	N85-27387 * #
E-2301	p 97	N85-10234 * #	E-2439	p 73	N85-18125 * #	E-2591	p 138	N85-32337 * #
E-2302	p 123	N85-16100 * #	E-2440	p 49	N85-21259 * #	E-2592	p 90	N85-26993 * #
E-2303	p 184	N85-22204 * #	E-2441	p 53	N85-26921 * #	E-2594	p 164	N85-31646 * #
E-2305	p 47	N85-13880 * #	E-2444	p 74	N85-19074 * #	E-2595	p 28	N85-26710 * #
E-2306	p 113	N85-10303 * #	E-2448	p 176	N85-22108 * #	E-2596	p 104	N85-28222 * #
E-2308	p 92	N85-12183 * #	E-2449	p 8	N85-19923 * #	E-2598	p 152	N85-34427 * #
E-2310	p 146	N85-25893 * #	E-2450	p 115	N85-20269 * #	E-2599	p 95	N85-29085 * #
E-2311	p 83	N85-10186 * #	E-2451	p 74	N85-19076 * #	E-2601	p 63	N85-28983 * #
E-2313	p 86	N85-15897 * #	E-2452	p 73	N85-19072 * #	E-2603	p 51	N85-27972 * #
E-2314	p 71	N85-11224 * #	E-2454	p 91	N85-30137 * #	E-2604	p 63	N85-31244 * #
			E-2456	p 118	N85-31433 * #	E-2606	p 58	N85-27978 * #
			E-2457	p 114	N85-19363 * #	E-2607	p 135	N85-32333 * #
			E-2458	p 114	N85-19364 * #	E-2608	p 163	N85-30480 * #
			E-2459	p 87	N85-21355 * #	E-2609	p 125	N85-30288 * #
			E-2462	p 88	N85-21357 * #	E-2610	p 38	N85-29987 * #

## REPORT NUMBER INDEX

NAS 1.15:87034

E-2612	p 30	N85-27870 * #	MTI-84TR39	p 35	N85-22400 * #	NAS 1.15:86928	p 115	N85-21569 * #
E-2616	p 133	N85-29292 * #	MTI-84TR58	p 184	N85-12808 * #	NAS 1.15:86929	p 72	N85-18124 * #
E-2621	p 9	N85-29925 * #				NAS 1.15:86930	p 73	N85-18125 * #
E-2625	p 58	N85-30034 * #	NAS 1.15:83022	p 18	N85-10951 * #	NAS 1.15:86931	p 73	N85-18126 * #
E-2628	p 52	N85-28971 * #	NAS 1.15:83354	p 57	N85-14882 * #	NAS 1.15:86932	p 86	N85-19136 * #
E-2629	p 118	N85-30247 * #	NAS 1.15:83470	p 150	N85-30361 * #	NAS 1.15:86933	p 74	N85-19074 * #
E-2633	p 177	N85-30770 * #	NAS 1.15:83471	p 163	N85-30477 * #	NAS 1.15:86934	p 74	N85-19075 * #
E-2634	p 119	N85-31444 * #	NAS 1.15:83472	p 162	N85-30478 * #	NAS 1.15:86935	p 176	N85-22108 * #
E-2637	p 32	N85-29964 * #	NAS 1.15:83480	p 163	N85-30478 * #	NAS 1.15:86936	p 115	N85-20269 * #
E-2638	p 52	N85-35225 * #	NAS 1.15:83517	p 163	N85-30479 * #	NAS 1.15:86937	p 74	N85-19076 * #
E-2642	p 100	N85-31348 * #	NAS 1.15:83556	p 11	N85-27839 * #	NAS 1.15:86938	p 73	N85-19072 * #
E-2643	p 125	N85-32302 * #	NAS 1.15:83590	p 25	N85-21162 * #	NAS 1.15:86939	p 114	N85-19363 * #
E-2646	p 164	N85-34443 * #	NAS 1.15:83621	p 24	N85-14840 * #	NAS 1.15:86940	p 114	N85-19364 * #
E-2648	p 136	N85-34405 * #	NAS 1.15:83677	p 158	N85-12465 * #	NAS 1.15:86941	p 74	N85-20042 * #
E-2653	p 38	N85-34150 * #	NAS 1.15:83693	p 184	N85-22255 * #	NAS 1.15:86942	p 75	N85-20043 * #
E-2657	p 78	N85-34265 * #	NAS 1.15:83698	p 70	N85-10165 * #	NAS 1.15:86943	p 87	N85-20127 * #
E-2658	p 137	N85-34408 * #	NAS 1.15:83711	p 85	N85-15898 * #	NAS 1.15:86944	p 115	N85-21570 * #
E-2659	p 52	N85-34176 * #	NAS 1.15:83748	p 1	N85-15658 * #	NAS 1.15:86945	p 138	N85-21674 * #
E-2660	p 136	N85-34407 * #	NAS 1.15:83750	p 62	N85-10138 * #	NAS 1.15:86946	p 36	N85-21228 * #
E-2661	p 58	N85-32148 * #	NAS 1.15:83754	p 57	N85-21273 * #	NAS 1.15:86947	p 48	N85-21258 * #
E-2666	p 136	N85-34406 * #	NAS 1.15:83767	p 7	N85-12039 * #	NAS 1.15:86948	p 99	N85-20223 * #
E-2670	p 137	N85-34409 * #	NAS 1.15:83771	p 17	N85-10067 * #	NAS 1.15:86949	p 137	N85-20389 * #
E-2671	p 59	N85-34223 * #	NAS 1.15:83783	p 170	N85-10683 * #	NAS 1.15:86950	p 161	N85-23242 * #
E-2672	p 52	N85-34177 * #	NAS 1.15:83784	p 71	N85-12131 * #	NAS 1.15:86951	p 8	N85-21114 * #
E-2673	p 52	N85-34178 * #	NAS 1.15:83790	p 103	N85-13157 * #	NAS 1.15:86952	p 8	N85-21115 * #
E-2689	p 52	N85-34179 * #	NAS 1.15:83791	p 70	N85-10168 * #	NAS 1.15:86953	p 186	N85-32043 * #
E-2694	p 78	N85-34266 * #	NAS 1.15:83797	p 175	N85-10788 * #	NAS 1.15:86955	p 49	N85-21259 * #
E-996	p 172	N85-19733 * #	NAS 1.15:83798	p 94	N85-11261 * #	NAS 1.15:86956	p 49	N85-21260 * #
			NAS 1.15:83800	p 184	N85-22204 * #	NAS 1.15:86957	p 103	N85-20246 * #
EDR-11442	p 91	N85-28109 * #	NAS 1.15:83801	p 113	N85-10303 * #	NAS 1.15:86958	p 131	N85-21658 * #
EDR-11682	p 31	N85-29961 * #	NAS 1.15:83803	p 131	N85-15168 * #	NAS 1.15:86959	p 75	N85-21321 * #
EDR-11683	p 28	N85-26709 * #	NAS 1.15:83804	p 83	N85-10186 * #	NAS 1.15:86960	p 49	N85-21261 * #
EDR-11869	p 86	N85-18154 * #	NAS 1.15:83805	p 169	N85-10659 * #	NAS 1.15:86961	p 99	N85-20224 * #
			NAS 1.15:83806	p 17	N85-10068 * #	NAS 1.15:86962	p 87	N85-21355 * #
ER-8050-F-VOL-2-APP-A	p 22	N85-10991 * #	NAS 1.15:83807	p 92	N85-12183 * #	NAS 1.15:86963	p 26	N85-21164 * #
			NAS 1.15:86505	p 91	N85-28107 * #	NAS 1.15:86964	p 88	N85-21357 * #
ESL-713533-5	p 37	N85-21233 * #	NAS 1.15:86858	p 53	N85-10105 * #	NAS 1.15:86965	p 131	N85-21657 * #
ESL-716109	p 136	N85-34404 * #	NAS 1.15:86859	p 84	N85-10187 * #	NAS 1.15:86966	p 62	N85-22644 * #
ESL-716111-2	p 98	N85-17258 * #	NAS 1.15:86860	p 1	N85-17935 * #	NAS 1.15:86967	p 8	N85-19923 * #
ESL-716111-3	p 100	N85-34329 * #	NAS 1.15:86863	p 18	N85-10949 * #	NAS 1.15:86968	p 53	N85-21264 * #
			NAS 1.15:86864	p 84	N85-10191 * #	NAS 1.15:86969	p 37	N85-21231 * #
E9787	p 157	N85-10444 * #	NAS 1.15:86865	p 18	N85-10069 * #	NAS 1.15:86970	p 161	N85-23243 * #
			NAS 1.15:86866	p 71	N85-12129 * #	NAS 1.15:86973	p 124	N85-21605 * #
FCR-4684F	p 159	N85-17422 * #	NAS 1.15:86867	p 158	N85-14158 * #	NAS 1.15:86974	p 88	N85-21356 * #
FCR-6128	p 158	N85-13371 * #	NAS 1.15:86868	p 70	N85-11217 * #	NAS 1.15:86976	p 75	N85-21322 * #
FCR-6853	p 50	N85-25384 * #	NAS 1.15:86869	p 7	N85-12036 * #	NAS 1.15:86977	p 88	N85-21358 * #
			NAS 1.15:86870	p 183	N85-10844 * #	NAS 1.15:86978	p 132	N85-25847 * #
FR-18046-3	p 48	N85-19020 * #	NAS 1.15:86871	p 175	N85-13551 * #	NAS 1.15:86979	p 116	N85-25761 * #
			NAS 1.15:86872	p 97	N85-10234 * #	NAS 1.15:86980	p 115	N85-21574 * #
FSFL-R-85-002	p 27	N85-25262 * #	NAS 1.15:86874	p 92	N85-13066 * #	NAS 1.15:86981	p 89	N85-24000 * #
			NAS 1.15:86875	p 185	N85-19895 * #	NAS 1.15:86982	p 76	N85-22660 * #
GARRETT-31-3725(8)	p 185	N85-18831 * #	NAS 1.15:86876	p 137	N85-10371 * #	NAS 1.15:86983	p 162	N85-29365 * #
			NAS 1.15:86878	p 56	N85-12095 * #	NAS 1.15:86984	p 9	N85-23711 * #
GE-84SRD006-VOL-1	p 176	N85-19791 * #	NAS 1.15:86880	p 113	N85-10306 * #	NAS 1.15:86985	p 146	N85-24338 * #
GE-84SRD006-VOL-2	p 176	N85-19792 * #	NAS 1.15:86881	p 25	N85-18057 * #	NAS 1.15:86986	p 161	N85-27385 * #
			NAS 1.15:86882	p 71	N85-11224 * #	NAS 1.15:86987	p 76	N85-26963 * #
GTD-84-4	p 46	N85-11132 * #	NAS 1.15:86883	p 167	N85-21872 * #	NAS 1.15:86988	p 134	N85-30342 * #
			NAS 1.15:86884	p 113	N85-11317 * #	NAS 1.15:86989	p 27	N85-25264 * #
GTEC31-4773	p 159	N85-16300 * #	NAS 1.15:86885	p 184	N85-16663 * #	NAS 1.15:86990	p 146	N85-24339 * #
			NAS 1.15:86887	p 47	N85-11133 * #	NAS 1.15:86991	p 132	N85-23085 * #
H-8407-07	p 125	N85-33456 * #	NAS 1.15:86888	p 72	N85-13007 * #	NAS 1.15:86992	p 88	N85-22755 * #
			NAS 1.15:86889	p 72	N85-12132 * #	NAS 1.15:86993	p 89	N85-22756 * #
IAF PAPER 84-154	p 59	A85-13092 * #	NAS 1.15:86890	p 114	N85-15133 * #	NAS 1.15:86994	p 50	N85-23926 * #
IAF PAPER 84-156	p 61	A85-23199 * #	NAS 1.15:86891	p 144	N85-15184 * #	NAS 1.15:86995	p 183	N85-26406 * #
IAF PAPER 84-15	p 36	A85-23200 * #	NAS 1.15:86893	p 23	N85-13798 * #	NAS 1.15:86996	p 28	N85-25266 * #
			NAS 1.15:86894	p 97	N85-15099 * #	NAS 1.15:86999	p 50	N85-25386 * #
IAF-85-164	p 52	N85-35225 * #	NAS 1.15:86895	p 84	N85-14928 * #	NAS 1.15:87000	p 41	N85-23904 * #
			NAS 1.15:86896	p 24	N85-15725 * #	NAS 1.15:87001	p 9	N85-26670 * #
ICASE-85-13	p 168	N85-21990 * #	NAS 1.15:86897	p 56	N85-14878 * #	NAS 1.15:87002	p 63	N85-23941 * #
			NAS 1.15:86898	p 123	N85-16096 * #	NAS 1.15:87003	p 27	N85-25263 * #
IITRI-M06116-3	p 74	N85-19078 * #	NAS 1.15:86899	p 186	N85-17928 * #	NAS 1.15:87004	p 146	N85-25893 * #
			NAS 1.15:86900	p 119	N85-33435 * #	NAS 1.15:87005	p 124	N85-25794 * #
IMMR84-098	p 120	N85-33453 #	NAS 1.15:86901	p 184	N85-13692 * #	NAS 1.15:87006	p 133	N85-27227 * #
			NAS 1.15:86902	p 85	N85-14929 * #	NAS 1.15:87007	p 90	N85-26991 * #
IR-2	p 132	N85-25848 * #	NAS 1.15:86903	p 7	N85-14798 * #	NAS 1.15:87008	p 115	N85-24245 * #
IR-3	p 135	N85-33491 * #	NAS 1.15:86904	p 53	N85-14864 * #	NAS 1.15:87010	p 1	N85-23685 * #
			NAS 1.15:86905	p 72	N85-15878 * #	NAS 1.15:87011	p 115	N85-25760 * #
JDTI-RED-85-1	p 25	N85-21163 * #	NAS 1.15:86906	p 12	N85-18049 * #	NAS 1.15:87012	p 184	N85-28876 * #
			NAS 1.15:86907	p 38	N85-15779 * #	NAS 1.15:87013	p 32	N85-31060 * #
JM/85-6	p 29	N85-26712 * #	NAS 1.15:86908	p 144	N85-16205 * #	NAS 1.15:87014	p 133	N85-27228 * #
			NAS 1.15:86909	p 57	N85-15823 * #	NAS 1.15:87015	p 53	N85-26921 * #
JPL-9950-945	p 185	N85-19894 * #	NAS 1.15:86911	p 24	N85-15727 * #	NAS 1.15:87016	p 89	N85-25521 * #
			NAS 1.15:86912	p 8	N85-15688 * #	NAS 1.15:87017	p 132	N85-27226 * #
KI-P-1008	p 185	N85-19894 * #	NAS 1.15:86913	p 145	N85-21690 * #	NAS 1.15:87018	p 165	N85-34444 * #
			NAS 1.15:86914	p 8	N85-15689 * #	NAS 1.15:87019	p 50	N85-25385 * #
L-15861	p 176	N85-22109 * #	NAS 1.15:86915	p 85	N85-15893 * #	NAS 1.15:87020	p 77	N85-31284 * #
			NAS 1.15:86916	p 145	N85-18375 * #	NAS 1.15:87021	p 148	N85-27264 * #
LBL-18163	p 93	N85-19185 * #	NAS 1.15:86918	p 159	N85-16299 * #	NAS 1.15:87022	p 76	N85-26964 * #
			NAS 1.15:86919	p 35	N85-15757 * #	NAS 1.15:87023	p 51	N85-26912 * #
LSI-TR-376-30	p 158	N85-16292 * #	NAS 1.15:86920	p 35	N85-15758 * #	NAS 1.15:87025	p 90	N85-26992 * #
			NAS 1.15:86921	p 35	N85-18067 * #	NAS 1.15:87026	p 91	N85-28110 * #
MAI-R4	p 47	N85-13910 * #	NAS 1.15:86923	p 24	N85-15726 * #	NAS 1.15:87028	p 185	N85-27769 * #
			NAS 1.15:86924	p 57	N85-15822 * #	NAS 1.15:87029	p 162	N85-28444 * #
MDC-J3789	p 10	N85-35162 * #	NAS 1.15:86925	p 11	N85-15702 * #	NAS 1.15:87032	p 117	N85-30242 * #
			NAS 1.15:86926	p 86	N85-18153 * #	NAS 1.15:87033	p 30	N85-28945 * #
MPN-764038	p 136	N85-34404 * #	NAS 1.15:86927	p 86	N85-15897 * #	NAS 1.15:87034	p 162	N85-27387 * #

# NAS 1.15:87035

# REPORT NUMBER INDEX

NAS 1.15:87035	p 138	N85-32337	#	NAS 1.26:173085	p 22	N85-10991	#	NAS 1.26:174852	p 74	N85-20041	#
NAS 1.15:87036	p 90	N85-26993	#	NAS 1.26:174054	p 97	N85-11265	#	NAS 1.26:174855	p 147	N85-27260	#
NAS 1.15:87037	p 164	N85-31646	#	NAS 1.26:174056	p 183	N85-11862	#	NAS 1.26:174857	p 48	N85-19020	#
NAS 1.15:87038	p 133	N85-28371	#	NAS 1.26:174057	p 158	N85-11457	#	NAS 1.26:174863	p 26	N85-22390	#
NAS 1.15:87039	p 28	N85-26710	#	NAS 1.26:174058	p 62	N85-11149	#	NAS 1.26:174870	p 58	N85-30035	#
NAS 1.15:87040	p 104	N85-28222	#	NAS 1.26:174067	p 35	N85-12071	#	NAS 1.26:174871	p 138	N85-21673	#
NAS 1.15:87041	p 117	N85-30246	#	NAS 1.26:174079	p 92	N85-11252	#	NAS 1.26:174872	p 145	N85-21685	#
NAS 1.15:87042	p 63	N85-28983	#	NAS 1.26:174246	p 24	N85-15724	#	NAS 1.26:174874	p 50	N85-25384	#
NAS 1.15:87043	p 51	N85-27972	#	NAS 1.26:174266	p 159	N85-16293	#	NAS 1.26:174877	p 162	N85-29363	#
NAS 1.15:87044	p 133	N85-28373	#	NAS 1.26:174268	p 98	N85-15944	#	NAS 1.26:174879	p 147	N85-25894	#
NAS 1.15:87045	p 58	N85-27978	#	NAS 1.26:174281	p 98	N85-15943	#	NAS 1.26:174880	p 63	N85-25444	#
NAS 1.15:87047	p 125	N85-30288	#	NAS 1.26:174284	p 86	N85-15916	#	NAS 1.26:174885	p 177	N85-27637	#
NAS 1.15:87048	p 38	N85-29987	#	NAS 1.26:174335	p 159	N85-18451	#	NAS 1.26:174887	p 161	N85-25941	#
NAS 1.15:87049	p 30	N85-27870	#	NAS 1.26:174336	p 98	N85-17258	#	NAS 1.26:174888	p 27	N85-22392	#
NAS 1.15:87051	p 91	N85-30137	#	NAS 1.26:174342	p 114	N85-17324	#	NAS 1.26:174893	p 89	N85-22757	#
NAS 1.15:87052	p 91	N85-30135	#	NAS 1.26:174353	p 114	N85-18291	#	NAS 1.26:174896	p 27	N85-25262	#
NAS 1.15:87053	p 133	N85-29292	#	NAS 1.26:174369	p 114	N85-18292	#	NAS 1.26:174900	p 76	N85-26962	#
NAS 1.15:87054	p 9	N85-29925	#	NAS 1.26:174380	p 103	N85-18259	#	NAS 1.26:174908	p 31	N85-29960	#
NAS 1.15:87055	p 95	N85-29085	#	NAS 1.26:174395	p 93	N85-19185	#	NAS 1.26:174909	p 135	N85-33491	#
NAS 1.15:87056	p 91	N85-30138	#	NAS 1.26:174411	p 74	N85-19078	#	NAS 1.26:174911	p 94	N85-34295	#
NAS 1.15:87056	p 163	N85-30480	#	NAS 1.26:174430	p 185	N85-19894	#	NAS 1.26:174915	p 28	N85-26711	#
NAS 1.15:87058	p 58	N85-30034	#	NAS 1.26:174638	p 157	N85-11456	#	NAS 1.26:174916	p 29	N85-27867	#
NAS 1.15:87059	p 52	N85-28971	#	NAS 1.26:174657	p 48	N85-18084	#	NAS 1.26:174917	p 29	N85-26716	#
NAS 1.15:87060	p 118	N85-30247	#	NAS 1.26:174662	p 99	N85-27092	#	NAS 1.26:174918	p 29	N85-26717	#
NAS 1.15:87061	p 53	N85-30011	#	NAS 1.26:174664	p 176	N85-19791	#	NAS 1.26:174920	p 162	N85-29364	#
NAS 1.15:87062	p 77	N85-31283	#	NAS 1.26:174665	p 176	N85-19792	#	NAS 1.26:174925	p 32	N85-32119	#
NAS 1.15:87063	p 119	N85-31443	#	NAS 1.26:174673	p 46	N85-11131	#	NAS 1.26:174927	p 12	N85-35185	#
NAS 1.15:87064	p 178	N85-28786	#	NAS 1.26:174687	p 89	N85-22758	#	NAS 1.26:174938	p 94	N85-31308	#
NAS 1.15:87065	p 177	N85-30770	#	NAS 1.26:174689	p 185	N85-16698	#	NAS 1.26:174940	p 152	N85-32340	#
NAS 1.15:87066	p 119	N85-31444	#	NAS 1.26:174695	p 85	N85-15892	#	NAS 1.26:174941	p 152	N85-32341	#
NAS 1.15:87067	p 32	N85-29964	#	NAS 1.26:174696	p 177	N85-35728	#	NAS 1.26:174950	p 105	N85-32251	#
NAS 1.15:87068	p 64	N85-32156	#	NAS 1.26:174697-VOL-1	p 98	N85-18239	#	NAS 1.26:174953	p 32	N85-29965	#
NAS 1.15:87069	p 52	N85-35225	#	NAS 1.26:174697-VOL-2	p 99	N85-18240	#	NAS 1.26:174954	p 119	N85-31445	#
NAS 1.15:87070	p 100	N85-31348	#	NAS 1.26:174697	p 98	N85-18238	#	NAS 1.26:174956	p 152	N85-33541	#
NAS 1.15:87071	p 125	N85-32302	#	NAS 1.26:174700	p 145	N85-21686	#	NAS 1.26:174960	p 125	N85-35389	#
NAS 1.15:87074	p 164	N85-34443	#	NAS 1.26:174701	p 18	N85-10947	#	NAS 1.26:174963	p 165	N85-35472	#
NAS 1.15:87075	p 136	N85-34405	#	NAS 1.26:174711	p 34	N85-12901	#	NAS 1.26:174969	p 105	N85-33293	#
NAS 1.15:87077	p 38	N85-34150	#	NAS 1.26:174712	p 178	N85-13594	#	NAS 1.26:174973	p 126	N85-35391	#
NAS 1.15:87078	p 135	N85-32333	#	NAS 1.26:174715	p 91	N85-28109	#	NAS 1.26:174975	p 10	N85-35162	#
NAS 1.15:87079	p 78	N85-34265	#	NAS 1.26:174721	p 157	N85-10445	#	NAS 1.26:175007	p 99	N85-21438	#
NAS 1.15:87080	p 52	N85-34176	#	NAS 1.26:174722	p 157	N85-10447	#	NAS 1.26:175038	p 160	N85-20545	#
NAS 1.15:87081	p 58	N85-32148	#	NAS 1.26:174724	p 165	N85-35471	#	NAS 1.26:175541	p 124	N85-21607	#
NAS 1.15:87082	p 136	N85-34406	#	NAS 1.26:174731	p 126	N85-12341	#	NAS 1.26:175551	p 146	N85-23096	#
NAS 1.15:87083	p 178	N85-34631	#	NAS 1.26:174732	p 158	N85-16291	#	NAS 1.26:175552	p 37	N85-21233	#
NAS 1.15:87085	p 59	N85-34223	#	NAS 1.26:174738	p 28	N85-26709	#	NAS 1.26:175573	p 26	N85-21165	#
NAS 1.15:87086	p 52	N85-34177	#	NAS 1.26:174740	p 72	N85-15877	#	NAS 1.26:175574	p 145	N85-21687	#
NAS 1.15:87087	p 52	N85-34178	#	NAS 1.26:174745	p 47	N85-12937	#	NAS 1.26:175585	p 39	N85-21250	#
NAS 1.15:87092	p 92	N85-34284	#	NAS 1.26:174746	p 184	N85-12808	#	NAS 1.26:175586	p 62	N85-21283	#
NAS 1.15:87096	p 136	N85-34407	#	NAS 1.26:174747	p 133	N85-28372	#	NAS 1.26:175605	p 27	N85-22391	#
NAS 1.15:87097	p 137	N85-34408	#	NAS 1.26:174750	p 35	N85-22400	#	NAS 1.26:175609	p 146	N85-21720	#
NAS 1.15:87098	p 57	N85-34179	#	NAS 1.26:174751	p 12	N85-19978	#	NAS 1.26:175619	p 183	N85-23414	#
NAS 1.15:87100	p 78	N85-34266	#	NAS 1.26:174752	p 93	N85-19176	#	NAS 1.26:175625	p 76	N85-22661	#
NAS 1.15:87102	p 152	N85-34427	#	NAS 1.26:174753	p 157	N85-11455	#	NAS 1.26:175627	p 168	N85-27508	#
NAS 1.15:87107	p 137	N85-34409	#	NAS 1.26:174756	p 70	N85-11221	#	NAS 1.26:175743	p 99	N85-25686	#
NAS 1.15:87391	p 12	N85-12887	#	NAS 1.26:174757	p 144	N85-11380	#	NAS 1.26:175747	p 147	N85-25896	#
NAS 1.15:87483	p 134	N85-29295	#	NAS 1.26:174762	p 70	N85-10166	#	NAS 1.26:175795	p 148	N85-27263	#
NAS 1.26:165550	p 71	N85-11225	#	NAS 1.26:174764	p 7	N85-10919	#	NAS 1.26:175811	p 29	N85-26712	#
NAS 1.26:165558	p 23	N85-10998	#	NAS 1.26:174765	p 147	N85-27261	#	NAS 1.26:175831	p 29	N85-26713	#
NAS 1.26:167851	p 23	N85-10999	#	NAS 1.26:174765	p 33	N85-34140	#	NAS 1.26:175832	p 29	N85-26714	#
NAS 1.26:167862	p 167	N85-35534	#	NAS 1.26:174766-VOL-1	p 33	N85-35197	#	NAS 1.26:175833	p 29	N85-26715	#
NAS 1.26:167863	p 167	N85-35535	#	NAS 1.26:174766-VOL-2	p 33	N85-35198	#	NAS 1.26:175835	p 116	N85-27168	#
NAS 1.26:167864	p 167	N85-35536	#	NAS 1.26:174768	p 46	N85-11132	#	NAS 1.26:175839	p 161	N85-27377	#
NAS 1.26:167865	p 167	N85-35537	#	NAS 1.26:174771	p 163	N85-30481	#	NAS 1.26:175856	p 93	N85-28127	#
NAS 1.26:167866	p 168	N85-35538	#	NAS 1.26:174772	p 48	N85-17023	#	NAS 1.26:175885	p 36	N85-27922	#
NAS 1.26:167870	p 22	N85-10993	#	NAS 1.26:174775	p 157	N85-10444	#	NAS 1.26:175901	p 30	N85-27868	#
NAS 1.26:167871	p 23	N85-10997	#	NAS 1.26:174776	p 172	N85-27584	#	NAS 1.26:175998	p 58	N85-30037	#
NAS 1.26:167945	p 18	N85-10950	#	NAS 1.26:174778	p 92	N85-10209	#	NAS 1.26:176003	p 41	N85-29997	#
NAS 1.26:167952	p 175	N85-11791	#	NAS 1.26:174779	p 71	N85-11223	#	NAS 1.26:176070	p 77	N85-32174	#
NAS 1.26:167955	p 23	N85-10995	#	NAS 1.26:174782	p 9	N85-22368	#	NAS 1.26:176071	p 77	N85-32173	#
NAS 1.26:167956	p 22	N85-10994	#	NAS 1.26:174783	p 185	N85-16699	#	NAS 1.26:176072	p 77	N85-32175	#
NAS 1.26:167993	p 23	N85-12059	#	NAS 1.26:174794	p 159	N85-17421	#	NAS 1.26:176077	p 77	N85-32176	#
NAS 1.26:167995	p 25	N85-18058	#	NAS 1.26:174795	p 102	N85-12300	#	NAS 1.26:176104	p 164	N85-33566	#
NAS 1.26:168017	p 31	N85-29957	#	NAS 1.26:174796	p 84	N85-12162	#	NAS 1.26:176154	p 125	N85-33456	#
NAS 1.26:168036	p 23	N85-10996	#	NAS 1.26:174798	p 31	N85-29961	#	NAS 1.26:176162	p 100	N85-34329	#
NAS 1.26:168037	p 34	N85-35199	#	NAS 1.26:174801	p 158	N85-16292	#	NAS 1.26:176163	p 136	N85-34404	#
NAS 1.26:168054	p 9	N85-29916	#	NAS 1.26:174802	p 158	N85-13371	#	NAS 1.26:176186	p 100	N85-35320	#
NAS 1.26:168070	p 33	N85-34141	#	NAS 1.26:174803	p 90	N85-26994	#	NAS 1.26:176189	p 100	N85-35321	#
NAS 1.26:168137	p 31	N85-29956	#	NAS 1.26:174804	p 159	N85-17422	#	NAS 1.26:176190	p 106	N85-35342	#
NAS 1.26:168173	p 132	N85-25848	#	NAS 1.26:174806	p 47	N85-13910	#	NAS 1.26:176386	p 7	N85-12008	#
NAS 1.26:168189	p 30	N85-29955	#	NAS 1.26:174807	p 47	N85-15804	#	NAS 1.26:176385	p 175	N85-13550	#
NAS 1.26:168222	p 159	N85-16300	#	NAS 1.26:174809	p 185	N85-18831	#	NAS 1.26:176387	p 175	N85-13549	#
NAS 1.26:168223	p 160	N85-19511	#	NAS 1.26:174812	p 25	N85-21163	#	NAS 1.26:176388	p 176	N85-17667	#
NAS 1.26:168228	p 32	N85-31057	#	NAS 1.26:174816	p 132	N85-21662	#	NAS 1.26:176389	p 137	N85-16195	#
NAS 1.26:168245	p 33	N85-34138	#	NAS 1.26:174820	p 86	N85-18154	#	NAS 1.26:176390	p 26	N85-21166	#
NAS 1.26:168259	p 48	N85-15806	#	NAS 1.26:174829	p 28	N85-25265	#	NAS 1.26:176391	p 26	N85-21167	#
NAS 1.26:168285	p 130	N85-13235	#	NAS 1.26:174831	p 117	N85-30245	#	NAS 1.26:176397	p 138	N85-20390	#
NAS 1.26:168287	p 124	N85-25792	#	NAS 1.26:174836	p 146	N85-21691	#	NAS 1.26:176398	p 8	N85-21117	#
NAS 1.26:168313	p 103	N85-19328	#	NAS 1.26:174837	p 85	N85-15895	#	NAS 1.26:176399	p 138	N85-29307	#
NAS 1.26:168329	p 116	N85-27164	#	NAS 1.26:174838	p 24	N85-15728	#	NAS 1.26:176399	p 10	N85-35158	#

## REPORT NUMBER INDEX

NASA-CR-175835

NAS 1.55:2386	p 118	N85-31433 *	#	NASA-CR-167864	p 167	N85-35536 *	#	NASA-CR-174768	p 46	N85-11132 *	#
NAS 1.60:2359	p 17	N85-10064 *	#	NASA-CR-167865	p 167	N85-35537 *	#	NASA-CR-174771	p 163	N85-30481 *	#
NAS 1.60:2372	p 17	N85-10065 *	#	NASA-CR-167866	p 168	N85-35538 *	#	NASA-CR-174772	p 48	N85-17023 *	#
NAS 1.60:2378	p 170	N85-15756 *	#	NASA-CR-167870	p 22	N85-10993 *	#	NASA-CR-174775	p 157	N85-10444 *	#
NAS 1.60:2388	p 113	N85-12314 *	#	NASA-CR-167871	p 23	N85-10997 *	#	NASA-CR-174776	p 172	N85-27584 *	#
NAS 1.60:2390	p 113	N85-14078 *	#	NASA-CR-167945	p 18	N85-10950 *	#	NASA-CR-174778	p 92	N85-10209 *	#
NAS 1.60:2398	p 176	N85-22109 *	#	NASA-CR-167952	p 175	N85-11791 *	#	NASA-CR-174779	p 71	N85-11223 *	#
NAS 1.60:2403	p 72	N85-13006 *	#	NASA-CR-167955	p 23	N85-10995 *	#	NASA-CR-174782	p 9	N85-22368 *	#
NAS 1.60:2404	p 130	N85-13233 *	#	NASA-CR-167956	p 22	N85-10994 *	#	NASA-CR-174783	p 185	N85-16699 *	#
NAS 1.60:2405	p 84	N85-13044 *	#	NASA-CR-167993	p 23	N85-12059 *	#	NASA-CR-174794	p 159	N85-17421 *	#
NAS 1.60:2406	p 84	N85-13045 *	#	NASA-CR-167995	p 25	N85-18058 *	#	NASA-CR-174795	p 102	N85-12300 *	#
NAS 1.60:2407	p 39	N85-14858 *	#	NASA-CR-168017	p 31	N85-29957 *	#	NASA-CR-174796	p 84	N85-12162 *	#
NAS 1.60:2408	p 130	N85-13234 *	#	NASA-CR-168036	p 23	N85-10996 *	#	NASA-CR-174798	p 31	N85-29961 *	#
NAS 1.60:2419	p 123	N85-16099 *	#	NASA-CR-168037	p 34	N85-35199 *	#	NASA-CR-174801	p 158	N85-16292 *	#
NAS 1.60:2421	p 145	N85-20396 *	#	NASA-CR-168054	p 9	N85-29916 *	#	NASA-CR-174802	p 158	N85-13371 *	#
NAS 1.60:2422	p 170	N85-28610 *	#	NASA-CR-168070	p 33	N85-34141 *	#	NASA-CR-174803	p 90	N85-26994 *	#
NAS 1.60:2424	p 123	N85-16100 *	#	NASA-CR-168137	p 31	N85-29956 *	#	NASA-CR-174804	p 159	N85-17422 *	#
NAS 1.60:2426	p 171	N85-17596 *	#	NASA-CR-168173	p 132	N85-25848 *	#	NASA-CR-174806	p 47	N85-13910 *	#
NAS 1.60:2435	p 26	N85-21168 *	#	NASA-CR-168189	p 30	N85-29955 *	#	NASA-CR-174807	p 47	N85-15804 *	#
NAS 1.60:2437	p 49	N85-21263 *	#	NASA-CR-168222	p 159	N85-16300 *	#	NASA-CR-174809	p 185	N85-18831 *	#
NAS 1.60:2443	p 75	N85-21323 *	#	NASA-CR-168223	p 160	N85-19511 *	#	NASA-CR-174812	p 25	N85-21163 *	#
NAS 1.60:2449	p 88	N85-21359 *	#	NASA-CR-168228	p 32	N85-31057 *	#	NASA-CR-174816	p 132	N85-21662 *	#
NAS 1.60:2453	p 183	N85-24961 *	#	NASA-CR-168245	p 33	N85-34138 *	#	NASA-CR-174820	p 86	N85-18154 *	#
NAS 1.60:2460	p 116	N85-27165 *	#	NASA-CR-168259	p 48	N85-15806 *	#	NASA-CR-174829	p 28	N85-25265 *	#
NAS 1.60:2461	p 27	N85-25261 *	#	NASA-CR-168285	p 130	N85-13235 *	#	NASA-CR-174831	p 117	N85-30245 *	#
NAS 1.60:2463	p 30	N85-28944 *	#	NASA-CR-168287	p 124	N85-25792 *	#	NASA-CR-174836	p 146	N85-21691 *	#
NAS 1.60:2473	p 135	N85-32331 *	#	NASA-CR-168313	p 103	N85-19328 *	#	NASA-CR-174837	p 85	N85-15895 *	#
NAS 1.60:2477	p 32	N85-31058 *	#	NASA-CR-168329	p 116	N85-27164 *	#	NASA-CR-174838	p 24	N85-15728 *	#
NAS 1.60:2488	p 134	N85-32329 *	#	NASA-CR-168337	p 18	N85-10948 *	#	NASA-CR-174839	p 123	N85-21604 *	#
NAS 1.60:2495	p 93	N85-31307 *	#	NASA-CR-168338	p 164	N85-30483 *	#	NASA-CR-174840	p 93	N85-27012 *	#
NAS 1.60:2496	p 134	N85-31511 *	#	NASA-CR-169496	p 22	N85-10989 *	#	NASA-CR-174841	p 75	N85-21320 *	#
NAS 1.60:2498	p 63	N85-31244 *	#	NASA-CR-170034	p 22	N85-10990 *	#	NASA-CR-174847	p 73	N85-18127 *	#
NAS 1.60:2500	p 135	N85-32330 *	#	NASA-CR-172557	p 168	N85-21990 *	#	NASA-CR-174848	p 93	N85-19175 *	#
NAS 1.61:1094	p 172	N85-19733 *	#	NASA-CR-172846	p 31	N85-29958 *	#	NASA-CR-174849	p 9	N85-26668 *	#
NAS 1.71:LEW-13324-2	p 57	N85-21266 *	#	NASA-CR-173084	p 22	N85-10992 *	#	NASA-CR-174851	p 73	N85-19073 *	#
NAS 1.71:LEW-13414-1	p 160	N85-20530 *	#	NASA-CR-173085	p 22	N85-10991 *	#	NASA-CR-174852	p 74	N85-20041 *	#
NAS 1.71:LEW-13770-3	p 87	N85-21350 *	#	NASA-CR-174054	p 97	N85-11265 *	#	NASA-CR-174855	p 147	N85-27260 *	#
NAS 1.71:LEW-13770-4	p 87	N85-21351 *	#	NASA-CR-174056	p 183	N85-11862 *	#	NASA-CR-174857	p 48	N85-19020 *	#
NAS 1.71:LEW-13770-5	p 87	N85-21352 *	#	NASA-CR-174057	p 158	N85-11457 *	#	NASA-CR-174863	p 26	N85-22390 *	#
NAS 1.71:LEW-13827-1	p 160	N85-21768 *	#	NASA-CR-174058	p 62	N85-11149 *	#	NASA-CR-174870	p 58	N85-30035 *	#
NAS 1.71:LEW-13833-1	p 103	N85-21492 *	#	NASA-CR-174067	p 35	N85-12071 *	#	NASA-CR-174871	p 138	N85-21673 *	#
NAS 1.71:LEW-13837-2	p 57	N85-21267 *	#	NASA-CR-174079	p 92	N85-11252 *	#	NASA-CR-174872	p 145	N85-21685 *	#
NAS 1.71:LEW-13837-3	p 95	N85-20155 *	#	NASA-CR-174246	p 24	N85-15724 *	#	NASA-CR-174874	p 50	N85-25384 *	#
NAS 1.71:LEW-13881-1	p 48	N85-21256 *	#	NASA-CR-174266	p 159	N85-16293 *	#	NASA-CR-174877	p 162	N85-29363 *	#
NAS 1.71:LEW-13935-1	p 103	N85-20248 *	#	NASA-CR-174268	p 98	N85-15944 *	#	NASA-CR-174879	p 147	N85-25894 *	#
NAS 1.71:LEW-14080-1	p 95	N85-20153 *	#	NASA-CR-174281	p 98	N85-15943 *	#	NASA-CR-174880	p 63	N85-25444 *	#
NAS 1.71:LEW-14104-1	p 75	N85-21324 *	#	NASA-CR-174284	p 86	N85-15916 *	#	NASA-CR-174885	p 177	N85-27637 *	#
NAS 1.71:LEW-14108-1	p 104	N85-29149 *	#	NASA-CR-174335	p 159	N85-18451 *	#	NASA-CR-174887	p 161	N85-25941 *	#
NAS 1.71:LEW-14130-1	p 95	N85-20156 *	#	NASA-CR-174336	p 98	N85-17258 *	#	NASA-CR-174888	p 27	N85-22392 *	#
NAS 1.71:LEW-14170-1	p 131	N85-20377 *	#	NASA-CR-174342	p 114	N85-17324 *	#	NASA-CR-174893	p 89	N85-22757 *	#
NAS 1.71:LEW-14177-1	p 160	N85-20535 *	#	NASA-CR-174353	p 114	N85-18291 *	#	NASA-CR-174896	p 27	N85-25262 *	#
NASA-CASE-LEW-12950-2	p 117	N85-29179 *	#	NASA-CR-174369	p 114	N85-18292 *	#	NASA-CR-174900	p 76	N85-26962 *	#
NASA-CASE-LEW-13102-1	p 104	N85-29144 *	#	NASA-CR-174380	p 103	N85-18259 *	#	NASA-CR-174908	p 31	N85-29960 *	#
NASA-CASE-LEW-13324-2	p 57	N85-21266 *	#	NASA-CR-174395	p 93	N85-19185 *	#	NASA-CR-174909	p 135	N85-33491 *	#
NASA-CASE-LEW-13414-1	p 160	N85-20530 *	#	NASA-CR-174411	p 74	N85-19078 *	#	NASA-CR-174911	p 94	N85-34295 *	#
NASA-CASE-LEW-13506-1	p 135	N85-33490 *	#	NASA-CR-174430	p 185	N85-19894 *	#	NASA-CR-174915	p 28	N85-26711 *	#
NASA-CASE-LEW-13562-2	p 33	N85-35195 *	#	NASA-CR-174638	p 157	N85-11456 *	#	NASA-CR-174916	p 29	N85-27867 *	#
NASA-CASE-LEW-13717-1	p 134	N85-30333 *	#	NASA-CR-174657	p 48	N85-18084 *	#	NASA-CR-174917	p 29	N85-27616 *	#
NASA-CASE-LEW-13770-2	p 63	N85-28982 *	#	NASA-CR-174662	p 99	N85-27092 *	#	NASA-CR-174918	p 29	N85-26717 *	#
NASA-CASE-LEW-13770-3	p 87	N85-21350 *	#	NASA-CR-174664	p 176	N85-19791 *	#	NASA-CR-174920	p 162	N85-29364 *	#
NASA-CASE-LEW-13770-4	p 87	N85-21351 *	#	NASA-CR-174665	p 176	N85-19792 *	#	NASA-CR-174925	p 32	N85-32119 *	#
NASA-CASE-LEW-13770-5	p 87	N85-21352 *	#	NASA-CR-174673	p 46	N85-11131 *	#	NASA-CR-174927	p 12	N85-35185 *	#
NASA-CASE-LEW-13770-6	p 63	N85-30039 *	#	NASA-CR-174687	p 89	N85-22758 *	#	NASA-CR-174938	p 94	N85-31308 *	#
NASA-CASE-LEW-13827-1	p 160	N85-21768 *	#	NASA-CR-174689	p 185	N85-16698 *	#	NASA-CR-174940	p 152	N85-32340 *	#
NASA-CASE-LEW-13828-1	p 58	N85-30027 *	#	NASA-CR-174695	p 85	N85-15892 *	#	NASA-CR-174941	p 152	N85-32341 *	#
NASA-CASE-LEW-13833-1	p 103	N85-21492 *	#	NASA-CR-174696	p 177	N85-35728 *	#	NASA-CR-174950	p 105	N85-32251 *	#
NASA-CASE-LEW-13837-2	p 57	N85-21267 *	#	NASA-CR-174697-VOL-1	p 98	N85-18239 *	#	NASA-CR-174953	p 32	N85-29965 *	#
NASA-CASE-LEW-13837-3	p 95	N85-20155 *	#	NASA-CR-174697-VOL-2	p 99	N85-18240 *	#	NASA-CR-174954	p 119	N85-31445 *	#
NASA-CASE-LEW-13881-1	p 48	N85-21256 *	#	NASA-CR-174700	p 98	N85-18238 *	#	NASA-CR-174956	p 152	N85-33541 *	#
NASA-CASE-LEW-13914-1	p 135	N85-33489 *	#	NASA-CR-174701	p 145	N85-21686 *	#	NASA-CR-174960	p 125	N85-35389 *	#
NASA-CASE-LEW-13935-1	p 103	N85-20248 *	#	NASA-CR-174711	p 18	N85-10947 *	#	NASA-CR-174963	p 165	N85-35472 *	#
NASA-CASE-LEW-14039-1	p 119	N85-33433 *	#	NASA-CR-174712	p 34	N85-12901 *	#	NASA-CR-174969	p 105	N85-33293 *	#
NASA-CASE-LEW-14053-1	p 136	N85-34402 *	#	NASA-CR-174715	p 178	N85-13594 *	#	NASA-CR-174973	p 126	N85-35391 *	#
NASA-CASE-LEW-14057-1	p 59	N85-35233 *	#	NASA-CR-174721	p 91	N85-28109 *	#	NASA-CR-174975	p 10	N85-35162 *	#
NASA-CASE-LEW-14077-1	p 164	N85-34441 *	#	NASA-CR-174722	p 157	N85-10445 *	#	NASA-CR-175507	p 99	N85-21438 *	#
NASA-CASE-LEW-14080-1	p 95	N85-20153 *	#	NASA-CR-174724	p 157	N85-10447 *	#	NASA-CR-175538	p 160	N85-20545 *	#
NASA-CASE-LEW-14104-1	p 75	N85-21324 *	#	NASA-CR-174731	p 165	N85-35471 *	#	NASA-CR-175541	p 124	N85-21607 *	#
NASA-CASE-LEW-14108-1	p 104	N85-29149 *	#	NASA-CR-174732	p 126	N85-12341 *	#	NASA-CR-175551	p 146	N85-23096 *	#
NASA-CASE-LEW-14130-1	p 95	N85-20156 *	#	NASA-CR-174738	p 158	N85-16291 *	#	NASA-CR-175552	p 37	N85-21233 *	#
NASA-CASE-LEW-14170-1	p 131	N85-20377 *	#	NASA-CR-174740	p 28	N85-26709 *	#	NASA-CR-175573	p 26	N85-21165 *	#
NASA-CASE-LEW-14177-1	p 160	N85-20535 *	#	NASA-CR-174745	p 72	N85-15877 *	#	NASA-CR-175574	p 145	N85-21687 *	#
NASA-CR-165550	p 71	N85-11225 *	#	NASA-CR-174746	p 47	N85-12937 *	#	NASA-CR-175585	p 39	N85-21250 *	#
NASA-CR-165558	p 23	N85-10998 *	#	NASA-CR-174747	p 184	N85-12808 *	#	NASA-CR-175586	p 62	N85-21283 *	#
NASA-CR-167851	p 23	N85-10999 *	#	NASA-CR-174748	p 133	N85-28372 *	#	NASA-CR-175605	p 27	N85-22391 *	#
NASA-CR-167862	p 167	N85-35534 *	#	NASA-CR-174750	p 35	N85-22400 *	#	NASA-CR-175609	p 146	N85-21720 *	#
NASA-CR-167863	p 167	N85-35535 *	#	NASA-CR-174751	p 12	N85-19978 *	#	NASA-CR-175619	p 183	N85-23414 *	#
				NASA-CR-174752	p 93	N85-19176 *	#	NASA-CR-175625	p 76	N85-22661 *	#
				NASA-CR-174753	p 157	N85-11455 *	#	NASA-CR-175627	p 168	N85-27508 *	#
				NASA-CR-174756	p 70	N85-11221 *	#	NASA-CR-175743	p 99	N85-25686 *	#
				NASA-CR-174757	p 144	N85-11380 *	#	NASA-CR-175747	p 147	N85-25896 *	#
				NASA-CR-174762	p 70	N85-10166 *	#	NASA-CR-175795	p 148	N85-27263 *	#
				NASA-CR-174764	p 7	N85-10919 *	#	NASA-CR-175811	p 29	N85-26712 *	#
				NASA-CR-174765	p 147	N85-27261 *	#	NASA-CR-175831	p 29	N85-26713 *	#
				NASA-CR-174765	p 33	N85-34140 *	#	NASA-C			

NASA-CR-175839	p 161	N85-27377 * #	NASA-TM-86896	p 24	N85-15725 * #	NASA-TM-87001	p 9	N85-26670 * #
NASA-CR-175856	p 93	N85-28127 * #	NASA-TM-86897	p 56	N85-14878 * #	NASA-TM-87002	p 63	N85-23941 * #
NASA-CR-175885	p 36	N85-27922 * #	NASA-TM-86898	p 123	N85-16096 * #	NASA-TM-87003	p 27	N85-25263 * #
NASA-CR-175901	p 30	N85-27868 * #	NASA-TM-86899	p 186	N85-17928 * #	NASA-TM-87004	p 146	N85-25893 * #
NASA-CR-175998	p 58	N85-30037 * #	NASA-TM-86900	p 119	N85-33435 * #	NASA-TM-87005	p 124	N85-25794 * #
NASA-CR-176003	p 41	N85-29997 * #	NASA-TM-86901	p 184	N85-13692 * #	NASA-TM-87006	p 133	N85-27227 * #
NASA-CR-176070	p 77	N85-32174 * #	NASA-TM-86902	p 85	N85-14929 * #	NASA-TM-87007	p 90	N85-26991 * #
NASA-CR-176071	p 77	N85-32173 * #	NASA-TM-86903	p 7	N85-14798 * #	NASA-TM-87008	p 115	N85-24245 * #
NASA-CR-176072	p 77	N85-32175 * #	NASA-TM-86904	p 53	N85-14864 * #	NASA-TM-87010	p 1	N85-23685 * #
NASA-CR-176077	p 77	N85-32176 * #	NASA-TM-86905	p 72	N85-15878 * #	NASA-TM-87011	p 115	N85-25760 * #
NASA-CR-176104	p 164	N85-33566 * #	NASA-TM-86906	p 12	N85-18049 * #	NASA-TM-87012	p 184	N85-28876 * #
NASA-CR-176154	p 125	N85-33456 * #	NASA-TM-86907	p 38	N85-15779 * #	NASA-TM-87013	p 32	N85-31060 * #
NASA-CR-176162	p 100	N85-34329 * #	NASA-TM-86908	p 144	N85-16205 * #	NASA-TM-87014	p 133	N85-27228 * #
NASA-CR-176163	p 136	N85-34404 * #	NASA-TM-86909	p 57	N85-15823 * #	NASA-TM-87015	p 53	N85-26921 * #
NASA-CR-176186	p 100	N85-35320 * #	NASA-TM-86911	p 24	N85-15727 * #	NASA-TM-87016	p 89	N85-25521 * #
NASA-CR-176189	p 100	N85-35321 * #	NASA-TM-86912	p 8	N85-15688 * #	NASA-TM-87017	p 132	N85-27226 * #
NASA-CR-176190	p 106	N85-35342 * #	NASA-TM-86913	p 145	N85-21690 * #	NASA-TM-87018	p 165	N85-34444 * #
NASA-CR-3836	p 7	N85-12008 * #	NASA-TM-86914	p 8	N85-15689 * #	NASA-TM-87019	p 50	N85-25385 * #
NASA-CR-3845	p 175	N85-13550 * #	NASA-TM-86915	p 85	N85-15893 * #	NASA-TM-87020	p 77	N85-31284 * #
NASA-CR-3846	p 175	N85-13549 * #	NASA-TM-86916	p 145	N85-18375 * #	NASA-TM-87021	p 148	N85-27264 * #
NASA-CR-3847	p 176	N85-17667 * #	NASA-TM-86918	p 159	N85-16299 * #	NASA-TM-87022	p 76	N85-26964 * #
NASA-CR-3851	p 137	N85-16195 * #	NASA-TM-86919	p 35	N85-15757 * #	NASA-TM-87023	p 51	N85-26912 * #
NASA-CR-3866	p 26	N85-21166 * #	NASA-TM-86920	p 35	N85-15758 * #	NASA-TM-87025	p 90	N85-26992 * #
NASA-CR-3869	p 26	N85-21167 * #	NASA-TM-86921	p 35	N85-18067 * #	NASA-TM-87026	p 91	N85-28110 * #
NASA-CR-3877	p 138	N85-20390 * #	NASA-TM-86923	p 24	N85-15726 * #	NASA-TM-87028	p 185	N85-27769 * #
NASA-CR-3878	p 8	N85-21117 * #	NASA-TM-86924	p 57	N85-15822 * #	NASA-TM-87029	p 162	N85-28444 * #
NASA-CR-3904	p 138	N85-29307 * #	NASA-TM-86925	p 11	N85-15702 * #	NASA-TM-87032	p 117	N85-30242 * #
NASA-CR-3925	p 10	N85-35158 * #	NASA-TM-86926	p 86	N85-18153 * #	NASA-TM-87033	p 30	N85-28945 * #
NASA-CR-3926	p 10	N85-35159 * #	NASA-TM-86927	p 86	N85-15897 * #	NASA-TM-87034	p 162	N85-27387 * #
			NASA-TM-86928	p 115	N85-21569 * #	NASA-TM-87035	p 138	N85-32337 * #
NASA-RP-1094	p 172	N85-19733 * #	NASA-TM-86929	p 72	N85-18124 * #	NASA-TM-87036	p 90	N85-26993 * #
			NASA-TM-86930	p 73	N85-18125 * #	NASA-TM-87037	p 164	N85-31646 * #
NASA-TM-83022	p 18	N85-10951 * #	NASA-TM-86931	p 73	N85-18126 * #	NASA-TM-87038	p 133	N85-28371 * #
NASA-TM-83354	p 57	N85-14882 * #	NASA-TM-86932	p 86	N85-19136 * #	NASA-TM-87039	p 28	N85-26710 * #
NASA-TM-83470	p 150	N85-30361 * #	NASA-TM-86933	p 74	N85-19074 * #	NASA-TM-87040	p 104	N85-28222 * #
NASA-TM-83471	p 163	N85-30477 * #	NASA-TM-86934	p 74	N85-19075 * #	NASA-TM-87041	p 117	N85-30246 * #
NASA-TM-83472	p 162	N85-30476 * #	NASA-TM-86935	p 176	N85-22108 * #	NASA-TM-87042	p 63	N85-28983 * #
NASA-TM-83480	p 163	N85-30478 * #	NASA-TM-86936	p 115	N85-20269 * #	NASA-TM-87043	p 51	N85-27972 * #
NASA-TM-83517	p 163	N85-30479 * #	NASA-TM-86937	p 74	N85-19076 * #	NASA-TM-87044	p 133	N85-28373 * #
NASA-TM-83556	p 11	N85-27839 * #	NASA-TM-86938	p 73	N85-19072 * #	NASA-TM-87045	p 58	N85-27978 * #
NASA-TM-83590	p 25	N85-21162 * #	NASA-TM-86939	p 114	N85-19363 * #	NASA-TM-87046	p 163	N85-30480 * #
NASA-TM-83621	p 24	N85-14840 * #	NASA-TM-86940	p 114	N85-19364 * #	NASA-TM-87047	p 125	N85-30288 * #
NASA-TM-83677	p 158	N85-12465 * #	NASA-TM-86941	p 74	N85-20042 * #	NASA-TM-87048	p 38	N85-29987 * #
NASA-TM-83693	p 184	N85-22255 * #	NASA-TM-86942	p 75	N85-20043 * #	NASA-TM-87049	p 30	N85-27870 * #
NASA-TM-83698	p 70	N85-10165 * #	NASA-TM-86943	p 87	N85-20127 * #	NASA-TM-87051	p 91	N85-30137 * #
NASA-TM-83711	p 85	N85-15896 * #	NASA-TM-86944	p 115	N85-21570 * #	NASA-TM-87052	p 91	N85-30135 * #
NASA-TM-83748	p 1	N85-15658 * #	NASA-TM-86945	p 138	N85-21674 * #	NASA-TM-87053	p 133	N85-29292 * #
NASA-TM-83750	p 62	N85-10138 * #	NASA-TM-86946	p 36	N85-21228 * #	NASA-TM-87054	p 9	N85-29925 * #
NASA-TM-83754	p 57	N85-21273 * #	NASA-TM-86947	p 48	N85-21258 * #	NASA-TM-87055	p 95	N85-29085 * #
NASA-TM-83767	p 7	N85-12039 * #	NASA-TM-86948	p 99	N85-20223 * #	NASA-TM-87056	p 91	N85-30138 * #
NASA-TM-83771	p 17	N85-10067 * #	NASA-TM-86949	p 137	N85-20389 * #	NASA-TM-87058	p 58	N85-30034 * #
NASA-TM-83783	p 170	N85-10683 * #	NASA-TM-86950	p 161	N85-23242 * #	NASA-TM-87059	p 52	N85-28971 * #
NASA-TM-83784	p 71	N85-12131 * #	NASA-TM-86951	p 8	N85-21114 * #	NASA-TM-87060	p 118	N85-30247 * #
NASA-TM-83790	p 103	N85-13157 * #	NASA-TM-86952	p 8	N85-21115 * #	NASA-TM-87061	p 53	N85-30011 * #
NASA-TM-83791	p 70	N85-10168 * #	NASA-TM-86953	p 186	N85-32043 * #	NASA-TM-87062	p 77	N85-31283 * #
NASA-TM-83797	p 175	N85-10788 * #	NASA-TM-86955	p 49	N85-21259 * #	NASA-TM-87063	p 119	N85-31443 * #
NASA-TM-83798	p 94	N85-11261 * #	NASA-TM-86956	p 49	N85-21260 * #	NASA-TM-87064	p 178	N85-28786 * #
NASA-TM-83800	p 184	N85-22204 * #	NASA-TM-86957	p 103	N85-20246 * #	NASA-TM-87065	p 177	N85-30770 * #
NASA-TM-83801	p 113	N85-10303 * #	NASA-TM-86958	p 131	N85-21658 * #	NASA-TM-87066	p 119	N85-31444 * #
NASA-TM-83803	p 131	N85-15168 * #	NASA-TM-86959	p 75	N85-21321 * #	NASA-TM-87067	p 32	N85-29964 * #
NASA-TM-83804	p 83	N85-10186 * #	NASA-TM-86960	p 49	N85-21261 * #	NASA-TM-87068	p 64	N85-32156 * #
NASA-TM-83805	p 169	N85-10659 * #	NASA-TM-86961	p 99	N85-20224 * #	NASA-TM-87069	p 52	N85-35225 * #
NASA-TM-83806	p 17	N85-10068 * #	NASA-TM-86962	p 87	N85-21355 * #	NASA-TM-87070	p 100	N85-31348 * #
NASA-TM-83807	p 92	N85-12183 * #	NASA-TM-86963	p 26	N85-21164 * #	NASA-TM-87071	p 125	N85-32302 * #
NASA-TM-86505	p 91	N85-28107 * #	NASA-TM-86964	p 88	N85-21357 * #	NASA-TM-87074	p 164	N85-34443 * #
NASA-TM-86658	p 53	N85-10105 * #	NASA-TM-86965	p 131	N85-21657 * #	NASA-TM-87075	p 136	N85-34405 * #
NASA-TM-86659	p 84	N85-10187 * #	NASA-TM-86966	p 62	N85-22644 * #	NASA-TM-87077	p 38	N85-34150 * #
NASA-TM-86660	p 1	N85-17935 * #	NASA-TM-86967	p 8	N85-19923 * #	NASA-TM-87078	p 135	N85-32333 * #
NASA-TM-86663	p 18	N85-10949 * #	NASA-TM-86968	p 53	N85-21264 * #	NASA-TM-87079	p 78	N85-34265 * #
NASA-TM-86664	p 84	N85-10191 * #	NASA-TM-86969	p 37	N85-21231 * #	NASA-TM-87080	p 52	N85-34176 * #
NASA-TM-86665	p 18	N85-10069 * #	NASA-TM-86970	p 161	N85-23243 * #	NASA-TM-87081	p 58	N85-32148 * #
NASA-TM-86666	p 71	N85-12129 * #	NASA-TM-86973	p 124	N85-21605 * #	NASA-TM-87082	p 136	N85-34406 * #
NASA-TM-86667	p 158	N85-11458 * #	NASA-TM-86974	p 88	N85-21356 * #	NASA-TM-87083	p 178	N85-34631 * #
NASA-TM-86668	p 70	N85-11217 * #	NASA-TM-86976	p 75	N85-21322 * #	NASA-TM-87085	p 59	N85-34223 * #
NASA-TM-86669	p 7	N85-12036 * #	NASA-TM-86977	p 88	N85-21358 * #	NASA-TM-87086	p 52	N85-34177 * #
NASA-TM-86670	p 183	N85-10844 * #	NASA-TM-86978	p 132	N85-25847 * #	NASA-TM-87087	p 52	N85-34178 * #
NASA-TM-86671	p 175	N85-13551 * #	NASA-TM-86979	p 116	N85-25761 * #	NASA-TM-87092	p 92	N85-34284 * #
NASA-TM-86672	p 97	N85-10234 * #	NASA-TM-86980	p 115	N85-21574 * #	NASA-TM-87096	p 136	N85-34407 * #
NASA-TM-86674	p 92	N85-13066 * #	NASA-TM-86981	p 89	N85-24000 * #	NASA-TM-87097	p 137	N85-34408 * #
NASA-TM-86675	p 185	N85-19895 * #	NASA-TM-86982	p 76	N85-22660 * #	NASA-TM-87098	p 52	N85-34179 * #
NASA-TM-86676	p 137	N85-10371 * #	NASA-TM-86983	p 162	N85-29365 * #	NASA-TM-87100	p 78	N85-34266 * #
NASA-TM-86678	p 56	N85-12095 * #	NASA-TM-86984	p 9	N85-23711 * #	NASA-TM-87102	p 152	N85-34427 * #
NASA-TM-86680	p 113	N85-10306 * #	NASA-TM-86985	p 146	N85-24338 * #	NASA-TM-87107	p 137	N85-34409 * #
NASA-TM-86681	p 25	N85-18057 * #	NASA-TM-86986	p 161	N85-27385 * #	NASA-TM-87391	p 12	N85-12887 * #
NASA-TM-86682	p 71	N85-11224 * #	NASA-TM-86987	p 76	N85-26963 * #	NASA-TM-87483	p 134	N85-29295 * #
NASA-TM-86683	p 167	N85-21872 * #	NASA-TM-86988	p 134	N85-30342 * #			
NASA-TM-86684	p 113	N85-11317 * #	NASA-TM-86989	p 27	N85-25264 * #	NASA-TP-2359	p 17	N85-10064 * #
NASA-TM-86685	p 184	N85-16663 * #	NASA-TM-86990	p 146	N85-24339 * #	NASA-TP-2372	p 17	N85-10065 * #
NASA-TM-86687	p 47	N85-11133 * #	NASA-TM-86991	p 132	N85-23085 * #	NASA-TP-2378	p 170	N85-17576 * #
NASA-TM-86688	p 72	N85-13007 * #	NASA-TM-86992	p 88	N85-22755 * #	NASA-TP-2388	p 113	N85-12314 * #
NASA-TM-86689	p 72	N85-12132 * #	NASA-TM-86993	p 89	N85-22756 * #	NASA-TP-2390	p 113	N85-14078 * #
NASA-TM-86690	p 114	N85-15133 * #	NASA-TM-86994	p 50	N85-23926 * #	NASA-TP-2398	p 176	N85-22109 * #
NASA-TM-86691	p 144	N85-15184 * #	NASA-TM-86995	p 183	N85-26406 * #	NASA-TP-2403	p 72	N85-13006 * #
NASA-TM-86693	p 23	N85-13798 * #	NASA-TM-86996	p 28	N85-25266 * #	NASA-TP-2404	p 130	N85-13233 * #
NASA-TM-86694	p 97	N85-15099 * #	NASA-TM-86999	p 50	N85-25386 * #	NASA-TP-2405	p 84	N85-13044 * #
NASA-TM-86695	p 84	N85-14928 * #	NASA-TM-87000	p 41	N85-23904 * #	NASA-TP-2406	p 84	N85-13045 * #



## REPORT NUMBER INDEX

USAAVSCOM-TR-84-C-20

NASA-TP-2407	p 39	N85-14858 *	#	SAR-8	p 22	N85-10989 *	#	US-PATENT-CLASS-415-196	p 136	N85-34402 *	#
NASA-TP-2408	p 130	N85-13234 *	#	SASR-7-VOL-1	p 22	N85-10992 *	#	US-PATENT-CLASS-415-200	p 136	N85-34402 *	#
NASA-TP-2419	p 123	N85-16099 *	#	SASR-7-VOL-2-APP-A	p 22	N85-10991 *	#	US-PATENT-CLASS-416-174	p 136	N85-34402 *	#
NASA-TP-2421	p 145	N85-20396 *	#	SASR-8	p 31	N85-29958 *	#	US-PATENT-CLASS-416-97A	p 119	N85-33433 *	#
NASA-TP-2422	p 170	N85-28610 *	#					US-PATENT-CLASS-423-DIG.10	p 95	N85-20153 *	#
NASA-TP-2424	p 123	N85-16100 *	#					US-PATENT-CLASS-423-414	p 95	N85-20153 *	#
NASA-TP-2426	p 171	N85-17596 *	#	SP-06A83	p 9	N85-22368 *	#	US-PATENT-CLASS-423-445	p 95	N85-20153 *	#
NASA-TP-2435	p 26	N85-21168 *	#					US-PATENT-CLASS-423-446	p 57	N85-21267 *	#
NASA-TP-2437	p 49	N85-21263 *	#	SRI-06-7963	p 89	N85-22757 *	#	US-PATENT-CLASS-423-446	p 95	N85-20153 *	#
NASA-TP-2443	p 75	N85-21323 *	#					US-PATENT-CLASS-423-446	p 57	N85-21267 *	#
NASA-TP-2449	p 88	N85-21359 *	#	SSI-24089	p 31	N85-29960 *	#	US-PATENT-CLASS-423-449	p 95	N85-20153 *	#
NASA-TP-2453	p 183	N85-24961 *	#					US-PATENT-CLASS-423-449	p 57	N85-21267 *	#
NASA-TP-2460	p 116	N85-27165 *	#	TACOM-TR-13046	p 134	N85-29295 *	#	US-PATENT-CLASS-427-178	p 58	N85-30027 *	#
NASA-TP-2461	p 27	N85-25261 *	#					US-PATENT-CLASS-427-37	p 58	N85-30027 *	#
NASA-TP-2463	p 30	N85-28944 *	#	TIS-R82AEB403-VOL-2	p 23	N85-10999 *	#	US-PATENT-CLASS-427-39	p 57	N85-21267 *	#
NASA-TP-2473	p 135	N85-32331 *	#					US-PATENT-CLASS-427-422	p 58	N85-30027 *	#
NASA-TP-2477	p 32	N85-31058 *	#	TR-AAE-85-4	p 125	N85-35389 *	#	US-PATENT-CLASS-427-85	p 160	N85-20530 *	#
NASA-TP-2488	p 134	N85-32329 *	#					US-PATENT-CLASS-428-633	p 57	N85-21266 *	#
NASA-TP-2495	p 93	N85-31307 *	#	TR-85-8	p 100	N85-35320 *	#	US-PATENT-CLASS-428-633	p 59	N85-35233 *	#
NASA-TP-2496	p 134	N85-31511 *	#					US-PATENT-CLASS-428-656	p 57	N85-21266 *	#
NASA-TP-2498	p 63	N85-31244 *	#	UILU-ENG-85-0502	p 62	N85-21283 *	#	US-PATENT-CLASS-428-656	p 59	N85-35233 *	#
NASA-TP-2500	p 135	N85-32330 *	#	UILU-ENG-85-0504	p 125	N85-35389 *	#	US-PATENT-CLASS-428-678	p 57	N85-21266 *	#
				UILU-ENG-85-2565	p 106	N85-35342 *	#	US-PATENT-CLASS-428-678	p 59	N85-35233 *	#
NBSIR-84-2949	p 124	N85-21607 *	#					US-PATENT-CLASS-428-679	p 57	N85-21266 *	#
ORNL/TM-9518	p 89	N85-22758 *	#	US-PATENT-APPL-SN-202228	p 117	N85-29179 *	#	US-PATENT-CLASS-428-680	p 59	N85-35233 *	#
				US-PATENT-APPL-SN-282298	p 104	N85-29144 *	#	US-PATENT-CLASS-428-680	p 57	N85-21266 *	#
PB85-127173	p 146	N85-21720 *	#	US-PATENT-APPL-SN-375784	p 57	N85-21266 *	#	US-PATENT-CLASS-428-680	p 59	N85-35233 *	#
PB85-132322	p 124	N85-21607 *	#	US-PATENT-APPL-SN-375784	p 59	N85-35233 *	#	US-PATENT-CLASS-428-681	p 57	N85-21266 *	#
PB85-187961	p 120	N85-33453 *	#	US-PATENT-APPL-SN-404809	p 63	N85-28982 *	#	US-PATENT-CLASS-428-681	p 59	N85-35233 *	#
				US-PATENT-APPL-SN-463456	p 134	N85-30333 *	#	US-PATENT-CLASS-428-682	p 57	N85-21266 *	#
PR-715723	p 99	N85-25686 *	#	US-PATENT-APPL-SN-465364	p 160	N85-20530 *	#	US-PATENT-CLASS-428-682	p 59	N85-35233 *	#
				US-PATENT-APPL-SN-473498	p 48	N85-21256 *	#	US-PATENT-CLASS-428-683	p 57	N85-21266 *	#
PWA-FR-18323-2	p 32	N85-29965 *	#	US-PATENT-APPL-SN-486470	p 160	N85-21768 *	#	US-PATENT-CLASS-428-684	p 57	N85-21266 *	#
				US-PATENT-APPL-SN-486471	p 103	N85-21492 *	#	US-PATENT-CLASS-429-206	p 104	N85-29144 *	#
PWA-5574-149	p 71	N85-11225 *	#	US-PATENT-APPL-SN-495381	p 57	N85-21267 *	#	US-PATENT-CLASS-429-249	p 104	N85-29144 *	#
PWA-5594-179-VOL-1	p 22	N85-10992 *	#	US-PATENT-APPL-SN-500651	p 33	N85-35195 *	#	US-PATENT-CLASS-445-35	p 135	N85-33489 *	#
PWA-5594-179-VOL-2-APP-A	p 22	N85-10991 *	#	US-PATENT-APPL-SN-507626	p 117	N85-29179 *	#	US-PATENT-CLASS-526-204	p 63	N85-30039 *	#
PWA-5594-197	p 18	N85-10950 *	#	US-PATENT-APPL-SN-516217	p 87	N85-21350 *	#	US-PATENT-CLASS-526-217	p 87	N85-21350 *	#
PWA-5594-202	p 31	N85-29958 *	#	US-PATENT-APPL-SN-516217	p 87	N85-21351 *	#	US-PATENT-CLASS-526-217	p 63	N85-30039 *	#
PWA-5594-231	p 31	N85-29956 *	#	US-PATENT-APPL-SN-516217	p 87	N85-21352 *	#	US-PATENT-CLASS-526-262	p 87	N85-21350 *	#
PWA-5594-243	p 30	N85-29955 *	#	US-PATENT-APPL-SN-516217	p 63	N85-28982 *	#	US-PATENT-CLASS-526-262	p 87	N85-21351 *	#
PWA-5594-248	p 18	N85-10947 *	#	US-PATENT-APPL-SN-516217	p 63	N85-30039 *	#	US-PATENT-CLASS-526-262	p 87	N85-21352 *	#
PWA-5594-251-VOL-2	p 33	N85-35198 *	#	US-PATENT-APPL-SN-523297	p 57	N85-21266 *	#	US-PATENT-CLASS-526-262	p 63	N85-28982 *	#
PWA-5594-258-VOL-1	p 33	N85-35197 *	#	US-PATENT-APPL-SN-523297	p 59	N85-35233 *	#	US-PATENT-CLASS-526-262	p 63	N85-30039 *	#
PWA-5598-77	p 25	N85-18058 *	#	US-PATENT-APPL-SN-537615	p 135	N85-33489 *	#	US-PATENT-CLASS-528-229	p 87	N85-21350 *	#
PWA-5894-17	p 32	N85-31057 *	#	US-PATENT-APPL-SN-560035	p 58	N85-30027 *	#	US-PATENT-CLASS-528-229	p 87	N85-21351 *	#
PWA-5914-39	p 126	N85-35391 *	#	US-PATENT-APPL-SN-561429	p 87	N85-21351 *	#	US-PATENT-CLASS-528-229	p 87	N85-21352 *	#
PWA-5928-25	p 172	N85-27584 *	#	US-PATENT-APPL-SN-561431	p 87	N85-21350 *	#	US-PATENT-CLASS-528-314	p 63	N85-30039 *	#
PWA-5940-19	p 145	N85-21686 *	#	US-PATENT-APPL-SN-561434	p 63	N85-30039 *	#	US-PATENT-CLASS-528-315	p 87	N85-21350 *	#
				US-PATENT-APPL-SN-561435	p 87	N85-21352 *	#	US-PATENT-CLASS-528-322	p 87	N85-21350 *	#
QNR-1	p 74	N85-19078 *	#	US-PATENT-APPL-SN-580419	p 119	N85-33433 *	#	US-PATENT-CLASS-528-322	p 87	N85-21351 *	#
				US-PATENT-APPL-SN-580573	p 164	N85-34441 *	#	US-PATENT-CLASS-528-322	p 87	N85-21352 *	#
QR-11	p 164	N85-30483 *	#	US-PATENT-APPL-SN-591089	p 57	N85-21267 *	#	US-PATENT-CLASS-528-322	p 63	N85-28982 *	#
				US-PATENT-APPL-SN-596960	p 135	N85-33490 *	#	US-PATENT-CLASS-528-322	p 63	N85-30039 *	#
REPT-4-9-T-10-F	p 102	N85-12300 *	#	US-PATENT-APPL-SN-602050	p 136	N85-34402 *	#	US-PATENT-CLASS-528-336	p 87	N85-21350 *	#
REPT-84-SRD-042	p 126	N85-12341 *	#	US-PATENT-APPL-SN-628866	p 95	N85-20153 *	#	US-PATENT-CLASS-528-342	p 87	N85-21350 *	#
REPT-85-6	p 106	N85-35342 *	#	US-PATENT-APPL-SN-636659	p 78	N85-34267 *	#	US-PATENT-CLASS-528-342	p 87	N85-21351 *	#
REPT-85-9JDIESTL-R1	p 90	N85-26994 *	#	US-PATENT-APPL-SN-640712	p 59	N85-35233 *	#	US-PATENT-CLASS-528-342	p 87	N85-21352 *	#
REPT-8881-933004	p 32	N85-29965 *	#	US-PATENT-APPL-SN-659475	p 95	N85-20156 *	#	US-PATENT-CLASS-528-342	p 63	N85-28982 *	#
				US-PATENT-APPL-SN-661481	p 75	N85-21324 *	#	US-PATENT-CLASS-60-202	p 48	N85-21256 *	#
RFP763340/714952	p 137	N85-16195 *	#	US-PATENT-APPL-SN-668433	p 95	N85-20155 *	#	US-PATENT-CLASS-60-39,23	p 33	N85-35195 *	#
				US-PATENT-APPL-SN-669140	p 160	N85-20535 *	#	US-PATENT-CLASS-60-748	p 33	N85-35195 *	#
RL-1PD-85	p 93	N85-27012 *	#	US-PATENT-APPL-SN-672224	p 131	N85-20377 *	#				
				US-PATENT-APPL-SN-700255	p 103	N85-20248 *	#				
				US-PATENT-APPL-SN-732321	p 104	N85-29149 *	#				
R81-915326-5	p 92	N85-11252 *	#					US-PATENT-4,437,962	p 57	N85-21267 *	#
R81AEG284	p 23	N85-10995 *	#	US-PATENT-CLASS-136-225	p 160	N85-21768 *	#	US-PATENT-4,455,418	p 63	N85-28982 *	#
R81AEG597	p 22	N85-10994 *	#	US-PATENT-CLASS-136-246	p 160	N85-21768 *	#	US-PATENT-4,466,242	p 48	N85-21256 *	#
R81AEG700	p 22	N85-10993 *	#	US-PATENT-CLASS-136-253	p 164	N85-34441 *	#	US-PATENT-4,478,879	p 160	N85-20530 *	#
R81AEG709	p 22	N85-10990 *	#	US-PATENT-CLASS-136-255	p 103	N85-21492 *	#	US-PATENT-4,482,778	p 160	N85-21768 *	#
R81AEG710	p 23	N85-10998 *	#	US-PATENT-CLASS-136-256	p 160	N85-20530 *	#	US-PATENT-4,482,779	p 103	N85-21492 *	#
R81AEG821	p 23	N85-10997 *	#	US-PATENT-CLASS-165-104.14	p 117	N85-29179 *	#	US-PATENT-4,485,151	p 57	N85-21266 *	#
R82AEB285	p 22	N85-10989 *	#	US-PATENT-CLASS-165-32	p 117	N85-29179 *	#	US-PATENT-4,485,151	p 59	N85-35233 *	#
R82AEB293	p 34	N85-35199 *	#	US-PATENT-CLASS-204-192C	p 95	N85-20153 *	#	US-PATENT-4,490,229	p 95	N85-20153 *	#
R82AEB399	p 23	N85-10996 *	#	US-PATENT-CLASS-204-192C	p 57	N85-21267 *	#	US-PATENT-4,495,044	p 57	N85-21267 *	#
R82AEB400	p 31	N85-29957 *	#	US-PATENT-CLASS-204-192N	p 57	N85-21267 *	#	US-PATENT-4,495,339	p 63	N85-30039 *	#
R82AEB408	p 33	N85-34141 *	#	US-PATENT-CLASS-204-192R	p 95	N85-20153 *	#	US-PATENT-4,497,939	p 87	N85-21351 *	#
R82AEB437	p 33	N85-34138 *	#	US-PATENT-CLASS-204-192R	p 57	N85-21267 *	#	US-PATENT-4,497,940	p 87	N85-21352 *	#
R82AEB492	p 175	N85-13550 *	#	US-PATENT-CLASS-204-192SP	p 95	N85-20153 *	#	US-PATENT-4,497,948	p 87	N85-21350 *	#
R82AEB540-VOL-2	p 23	N85-12059 *	#	US-PATENT-CLASS-219-76.14	p 58	N85-30027 *	#	US-PATENT-4,505,998	p 104	N85-29144 *	#
R83AEB358	p 175	N85-13549 *	#	US-PATENT-CLASS-239-402.5	p 33	N85-35195 *	#	US-PATENT-4,506,183	p 117	N85-29179 *	#
R84-916161-14	p 85	N85-15892 *	#	US-PATENT-CLASS-310-306	p 117	N85-29179 *	#	US-PATENT-4,514,557	p 63	N85-28982 *	#
R85AEB014	p 93	N85-19175 *	#	US-PATENT-CLASS-310-77	p 134	N85-30333 *	#	US-PATENT-4,517,505	p 134	N85-30333 *	#
R85AEB166	p 12	N85-19978 *	#	US-PATENT-CLASS-310-93	p 134	N85-30333 *	#	US-PATENT-4,518,625	p 58	N85-30027 *	#
R85AEB307	p 28	N85-26711 *	#	US-PATENT-CLASS-315-3.5	p 135	N85-33489 *	#	US-PATENT-4,527,092	p 135	N85-33489 *	#
				US-PATENT-CLASS-315-5.38	p 135	N85-33489 *	#	US-PATENT-4,527,910	p 135	N85-33490 *	#
SAE PAPER 841512	p 68	A85-39284 *	#	US-PATENT-CLASS-318-611	p 134	N85-30333 *	#	US-PATENT-4,528,417	p 164	N85-34441 *	#
SAE PAPER 841522	p 110	A85-39257 *	#	US-PATENT-CLASS-335-100	p 134	N85-30333 *	#	US-PATENT-4,529,358	p 119	N85-33433 *	#
SAE PAPER 841541	p 15	A85-39065 *	#	US-PATENT-CLASS-357-12	p 103	N85-21492 *	#	US-PATENT-4,534,166	p 33	N85-35195 *	#
SAE PAPER 841557	p 14	A85-25984 *	#	US-PATENT-CLASS-357-30	p 103	N85-21492 *	#	US-PATENT-4,535,033	p 59	N85-35233 *	#
SAE PAPER 841619	p 44	A85-39267 *	#	US-PATENT-CLASS-357-30	p 160	N85-21768 *	#	US-PATENT-4,540,336	p 136	N85-34402 *	#
SAE PAPER 850871	p 7	A85-50106 *	#	US-PATENT-CLASS-384-101	p 135	N85-33490 *	#				
				US-PATENT-CLASS-384-99	p 135	N85-33490 *	#	USAAVSCOM-TM-84-C-2	p 114	N85-19363 *	#
SAPR-8	p 185	N85-18831 *	#	US-PATENT-CLASS-415-115	p 119	N85-33433 *	#	USAAVSCOM-TR-84-C-12	p 1	N85-15658 *	#
				US-PATENT-CLASS-415-170-R	p 136	N85-34402 *	#	USAAVSCOM-TR-84-C-18	p 24	N85-15727 *	#
SAR-7	p 22	N85-10990 *	#	US-PATENT-CLASS-415-174	p 136</						

USAAVSCOM-TR-84-C-21 .....	p 7	N85-14798 * #
USAAVSCOM-TR-84-C-4 .....	p 133	N85-27228 * #
USAAVSCOM-TR-85-C-10 .....	p 30	N85-28945 * #
USAAVSCOM-TR-85-C-11 .....	p 30	N85-27870 * #
USAAVSCOM-TR-85-C-14 .....	p 59	N85-34223 * #
USAAVSCOM-TR-85-C-16 .....	p 136	N85-34406 * #
USAAVSCOM-TR-85-C-1 .....	p 74	N85-19074 * #
USAAVSCOM-TR-85-C-3 .....	p 133	N85-27227 * #
USAAVSCOM-TR-85-C-4 .....	p 89	N85-24000 * #
USAAVSCOM-TR-85-C-5 .....	p 76	N85-26964 * #
USAAVSCOM-TR-85-C-6 .....	p 32	N85-31060 * #
USAAVSCOM-TR-85-C-9 .....	p 136	N85-34405 * #
UTRC-R83-925312-25 .....	p 34	N85-12901 * #
UTRC-R84-915540-34 .....	p 117	N85-30245 * #
VPI-E-84-36 .....	p 146	N85-21720 * #
W-45797 .....	p 105	N85-33293 * #
WGR-85-5 .....	p 100	N85-35321 * #
YU-2115 .....	p 92	N85-10209 * #



1. Report No. <b>NASA TM-87263</b>		2. Government Accession No.		3. Recipient's Catalog No.	
4. Title and Subtitle  <b>Bibliography of Lewis Research Center Technical Publications Announced in 1985</b>				5. Report Date <b>May 1986</b>	
				6. Performing Organization Code <b>None</b>	
7. Author(s)				8. Performing Organization Report No. <b>E-2960</b>	
				10. Work Unit No.	
9. Performing Organization Name and Address <b>National Aeronautics and Space Administration Lewis Research Center Cleveland, Ohio 44135</b>				11. Contract or Grant No.	
				13. Type of Report and Period Covered <b>Technical Memorandum</b>	
12. Sponsoring Agency Name and Address <b>National Aeronautics and Space Administration Washington, D.C. 20546</b>				14. Sponsoring Agency Code	
15. Supplementary Notes <b>Compiled by Technical Information Services Division, Lewis Research Center.</b>					
16. Abstract  <b>This compilation of abstracts describes and indexes the technical reporting that resulted from the scientific and engineering work performed and managed by the Lewis Research Center in 1985. All the publications were announced in the 1985 issues of STAR (Scientific and Technical Aerospace Reports) and/or IAA (International Aerospace Abstracts). Included are research reports, journal articles, conference presentations, patents and patent applications, and theses.</b>					
17. Key Words (Suggested by Author(s)) <b>Bibliographies Abstracts Documentation Indexes (Documentation)</b>			18. Distribution Statement <b>Unclassified - unlimited STAR Category 82</b>		
19. Security Classif. (of this report) <b>Unclassified</b>	20. Security Classif. (of this page) <b>Unclassified</b>		21. No. of pages <b>306</b>	22. Price* <b>A14</b>	

National Aeronautics and  
Space Administration

**Lewis Research Center**  
Cleveland, Ohio 44135

Official Business  
Penalty for Private Use \$300

**SECOND CLASS MAIL**

ADDRESS CORRECTION REQUESTED



Postage and Fees Paid  
National Aeronautics and  
Space Administration  
NASA-451

**NASA**

---